F1103

04

ACADÉMIE DE LA RÉPUBLIQUE SOCIALISTE DE ROUMANIE

66

REVUE ROUMAINE DE CHIMIE

TOME 33

N° 1

Janvier 1988

Rev. Roumaine Chim.

RRCHAX, 33, *1*, p. 1–104 (1988), Bucarest

EDITURA ACADEMIEI REPUBLICII SOCIALISTE ROMÂNIA

ACADÉMIE DE LA RÉPUBLIQUE SOCIALISTE DE ROUMANIE

COMITÉ DE RÉDACTION

Rédacteur en chef:

I. G. MURGULESCU, membre de l'Académie de la République Socialiste de Roumanie

Rédacteurs en chef adjoints:

A. T. BALABAN et V. EM. SAHINI, membres correspondants de l'Académie de la République Socialiste de Roumanie

Collège de rédaction:

EM. BRATU, ELENA CEAUŞESCU, ECATERINA CIORĂNESCU-NENITZESCU, CR. SIMIONESCU, membres de l'Académie de la République Socialiste de Roumanie; P. SPACU, membre correspondant de l'Académie de la République Socialiste de Roumanie; M. BANCIU, M. D. GHEORGHIU, I. HAIDUC, D. I. MARCHIDAN, G. NIAC et D. SĂNDULESCU

La Revue Roumaine de Chimie parait 10 fois par an. Toute commande de l'étranger sera adressée à ROMPRESFILATELIA — sectorul Export-Import Presă, P. O. Box 12—201, télex 10376 prsfi r 78104 Bucarest, Calea Griviţei nr. 64—66, Bucarest, Roumanie

Les manuscrits, les livres et les revues proposés en échange, ainsi que toute correspondance seront envoyés à la rédaction:

REVUE ROUMAINE DE CHIMIE

125, Calea Victoriei, 79717 Bucaret, Roumanie, telephone 50 76 80

EDITURA ACADEMIEI REPUBLICII SOCIALISTE ROMÂNIA
125, Calea Victoriei 79717 Bucarest, Roumanie, téléphone 50 76 80

REVUE ROUMAINE DE CHIMIE

ORSZÁGOS MŰSZAKI INFORMÁCIÓS KÖZPONT ÉS KÖNYVTÁR 1988

Tome 33, N° 1 **Janvier, 1988**

VASILE PÂRVULESCU, IOAN SĂNDULESCU, NICOLETA GRECU, CRISTIAN CONȚESCU and IOAN V. NICOLESCU, Effect of palladium concentration on the state and activity of Pd/γ-Al_2O_3 catalysts 3–11
N. DOCA and E. SEGAL, Dehydrogenation kinetics of low aliphatic alcohols on copper catalysts. IV. Analysis of structure — activity relationships . . . 13–16
M. A. ARAMENDIA, V. BORAU, C. JIMENEZ and J. M. MARINAS, Catalytic activity of Pt/$AlPO_4$ and related systems. I. Gas-phase hydrogenation of mono-alkylbenzenes 17–23
A. CĂLUȘARU and M. APOSTOL, *REDOX* and *COLHOM* quantum transitions as basic components of chemical processes 25–37
ADRIAN O. FULEA, Chemical shift nonequivalence *versus* chemical shift equivalence of geminal diastereotopic groups in prochiral assemblies and Curie's principle of symmetry. I. General analysis 39–52
C. ANDREI, I. HOGEA and V. DOBRESCU, Photodegradation and photostabilization of ethylene-vinyl acetate copolymers. II. New facts which support the scheme of photodegradation mechanism 53–58
N. CALU and N. FOCA, Complexes of Pd(II), Cu(II), Hg(I) and Hg(II) with 1-methyltriazol-diethylazoaniline (I) 59–65
I. BERDAN and I. SANDU, Complex compounds of Tl(III) with organic heterocyclic ligands. III. Infrared absorption spectra (in French) 67–74
MIHAELA BUGEANU and V. EM. SAHINI, Aniline complexes with iodine acceptor 75–81
MIRCEA D. GHEORGHIU, LUMINIȚA PÂRVULESCU, RODICA CECLAN, IOANA MANOLESCU, DOINA CONSTANTINESCU, CRISTINA FLOREA and MICHAELA STĂNESCU, A convenient synthesis for Moore's ketene precursors 83–85
GRIGORE BOZGA, JAFAR TOWFIGHI and OCTAVIAN FLOAREA, Optimal temperature profiles for propane pyrolysis in tubular reactors 87–96

BOOK REVIEWS 97–103

Rev. Roumiane Chim. 33, *1*, 1–104 (1988), Bucarest

Revue Roumaine de Chimie, 33, *1*, 3–11 (1988)

EFFECT OF PALLADIUM CONCENTRATION ON THE STATE AND ACTIVITY OF Pd/γ-Al_2O_3 CATALYSTS

VASILE PÂRVULESCU *, IOAN SĂNDULESCU *, NICOLETA GRECU **, CRISTIAN CONȚESCU *** and IOAN V. NICOLESCU *

* National Institute of Chemistry, Chair of Chemical Technology and Catalysis, Bucharest, Romania

** Institute for the Physics and Technology of Materials, Bucharest, Romania

*** Central Institute of Chemistry, Central of Physical Chemistry Bucharest, Romania

Received February 15, 1987

Hydrogen chemosorption and EPR measurements on Pd/$\gamma \cdot Al_2O_3$ catalysts have been performed in order to get a view of the way in which palladium concentration influences the metal state and the dispersion on support. From the EPR spectra Pd^{+1} clusters have been found. The relative intensities of signals change with Pd concentration in a ratio smaller than expected. The EPR and dispersion results are discussed in connection with the activity measurements.

Palladium catalysts on alumina support are widely used in hydrogenation and especially in the selective hydrogenation of acetylenes and vinylbenzenes.

The reactions develop selectively with the formation of ethylenes and alkylbenzenes respectively, the conversion depending upon the dispersion of palladium on the support, which in turn depends on palladium concentration.

In order to determine the degree of dispersion or agglomeration of palladium on the alumina support surface, various techniques were used, such as hydrogen chemosorption, [1-3] electronic microscopy, [1] magnetic measurements. [4-6]

The results obtained were correlated with the activity and selectivity of the catalysts of palladium. The practical importance of this type of correlations consists in the selection of the method for preparing the catalysts which will ensure the dispersion necessary for optimal activity and also decrease in the palladium content.

Palladium catalysts on alumina support are obtained by impregnating the porous support, drying and then reducing the palladium compounds on support with hydrogen, hydrazine and hydroxylamine.

Reduction and dispersion degree depends on the conditions under which the reduction is performed and on the reduction agent.

Literature data for palladium catalysts indicate total reduction of Pd to metal. [7]

In this paper it has been investigated dispersion and the degree of Pd reduction on γ-Al_2O_3 support and the correlation between these values and the activity data.

EXPERIMENTAL

Catalysts were prepared by impregnating γ-Al_2O_3 with an acid solution of $PdCl_2$, then dried after a program of temperatures at 110°C, ashed at 500° C for 2 h and reduced in hydrogen flow at 400° C for 4 h.

Palladium concentrations of catalysts were 0.1 %, 0.3 % and 0.5 %.

Catalysts were tested in the chromatographic pulse reaction for styrene hydrogenation.[8-9] Reduction degree of Pd in catalysts was given by EPR data. EPR measurements were made with a JES – ME(JEOL) spectrometer operating in X-band frequencies. The first derivatives of the spectra were recorded by using a 100 kHz field modulation. A DPPH probe with $g = 2.0036 \pm 0.0003$ was used as a marker to calibrate the magnetic field. EPR spectra were recorded at different temperatures in the range $-156 \div -23$°C, the temperature of the samples was controlled within ± 1° C by the temperature controlling unit attached to the spectrometer.

Palladium dispersion was determined by hydrogen chemosorption using a volumetric absorption installation. Samples were reactivated in hydrogen flow at 350° C, degasified in vacuum at 400°C in a measured cell and cooled till the working temperature. Absorption isotherms of hydrogen were traced out at the temperature of 250°C in a pressure field of 0–50 torr.

RESULTS

a) EPR spectra of Pd/γ-Al_2O_3 catalysts

Figure 1 gives the EPR spectrum of γ-Al_2O_3 support calcined at 500°C. Different kinds of lines have been noticed. The triplet of lines with

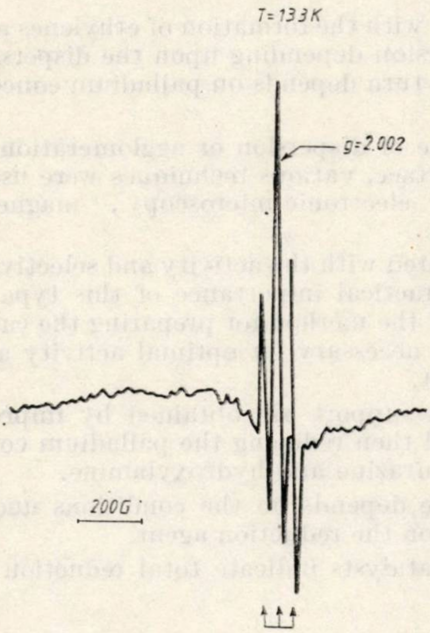

Fig. 1. — EPR spectrum of the γ-Al_2O_3 support calcined at 500 °C.

nearly equal intensities and g values of 2.037 ; 2.003 and 1.969 respectively has been as well noticed in the thermally treated alumina in an oxygen atmosphere.[12] The intensities of this spectrum increase at lower temperatures and it is associated with superficial centers which imply oxidated chemisorbed species. Likewise over EPR spectrum of alumina shows a very narrow signal with $g = 2.002$ due to mobile electrons.

The characteristic EPR spectra of (0.5 ; 0.3 and 0.1%) Pd/Al_2O_3 samples are given in Fig. 2. The large and intense signal (noted Pd) has

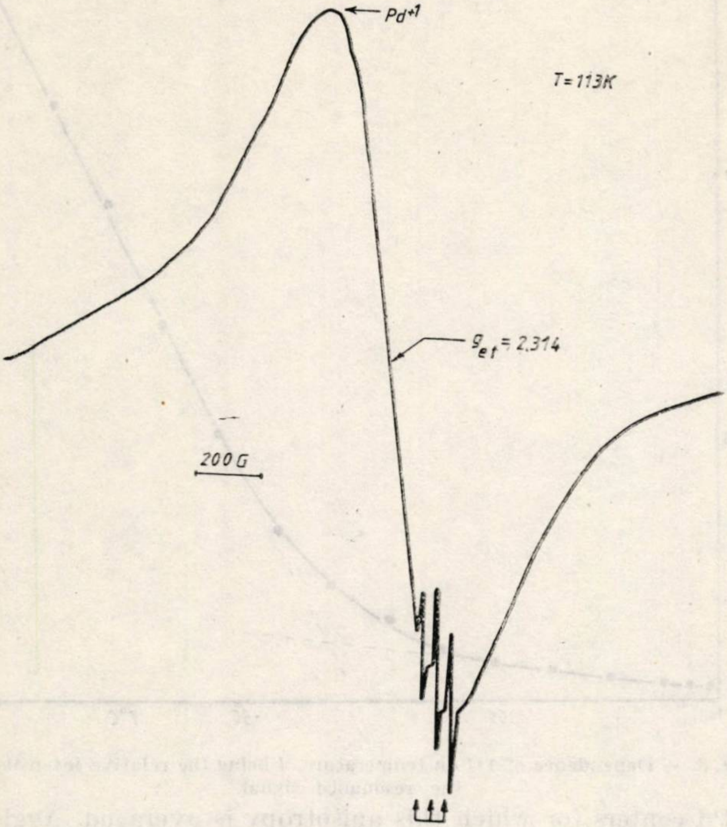

Fig. 2. — Characteristic EPR spectrum for a sample of Pd/γ-Al_2O_3 catalyst.

$g = 2.314$ and $\Delta B = 650$ G (ΔB is the line width). These parameters do not change with temperature, although changes in shape of line are observed. The line intensity undergoes also important changes by decreasing the temperature. The plot of $1/I$ versus T where I is the relative intensity for this signal is given in Fig. 3.

Due to the following arguments we assign the EPR line discussed above to the Pd^{+1} clusters. Pd^{+1} ion is a $4d^9$ and in an octahedral field with tetragonal distorsion its fundamental state is an orbital singlet. Therefore its EPR line can be observed at a temperature higher than −195°C.

The g factor has to be higher than $g_e = 2.003$ in agreement with the value determined experimentally. Moreover if isolated ions existed a marked anisotropy [13,14] should be observed, that is different principal values for g — tensor. Experimentally, the almost symmetrical line observed

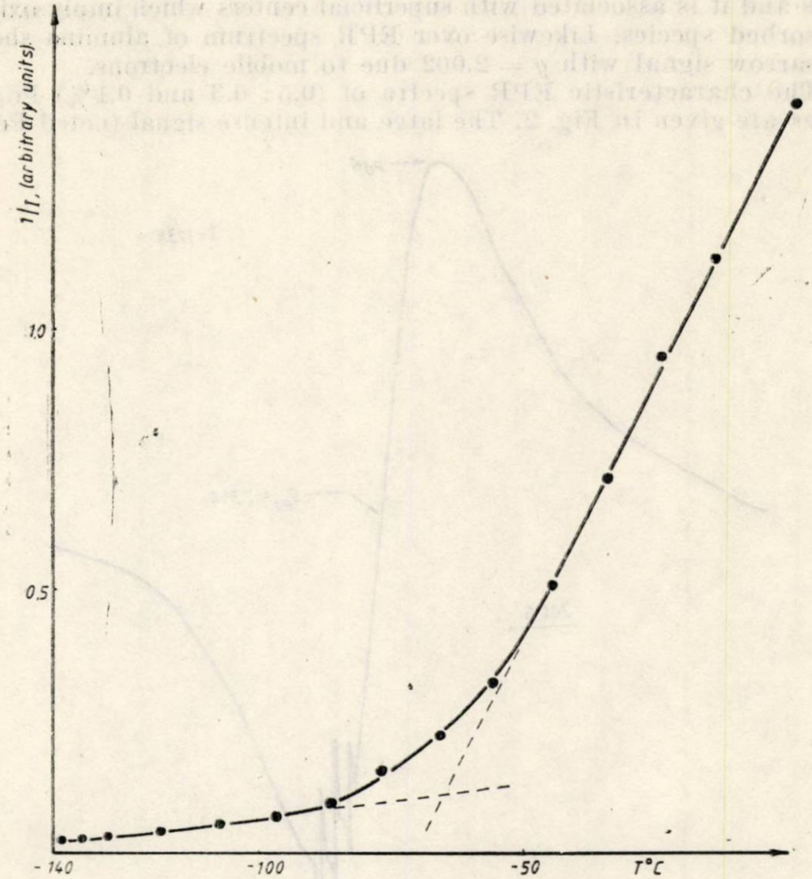

Fig. 3. — Dependence of $1/I$ on temperature, I being the relative intensity of the resonance signal.

implies Pd centers for which this anisotropy is averaged. Agglomeration of palladium ions in clusters with a pronounced internal exchange interaction explains the experimental data noticed. The rapid variation with temperature of the line intensity without any change of g_{ef} and ΔB parameters supports as well this idea.

Comparison of the signals of the three catalyst samples with different palladium concentrations shows that the relative intensities are not in 5 : 3 : 1 ratio, but approximately 2 : 1,7 : 1 respectively. This indicates that only a small part of palladium exists as paramagnetic Pd^{+1} and it decreases with the concentration of palladium. The properties of Pd^{+1} in the catalysts probably depend on the reduction temperature and time, or on the reduction agent.

b) Hydrogen chemosorption on catalysts

The results of hydrogen chemosorption on Pd/γ-Al_2O_3 catalysts confirmed the remarks given by EPR data on dispersion.

In order to calculate the diameters of palladium formations, the following formulas have been used[3]:

$$d(\text{Å}) = \frac{8.85}{(\mathrm{H/Pd})} \tag{1}$$

$$S(\mathrm{m^2/g}) = \frac{p(\mathrm{H/Pd})\,N}{100 \times A \times 1.45 \times 10^{19}} = 3.9\ \mathrm{p}\ (\mathrm{H/Pd}) \tag{2}$$

where : N — Avogadro number;
A — atomic mass;
p — Pd percent in catalyst.

The rate of H/Pd is determined experimentally by extrapolation of the dependences p_{H_2} of (H/Pd) when $p_{H_2} \to 0$ (Fig. 4).

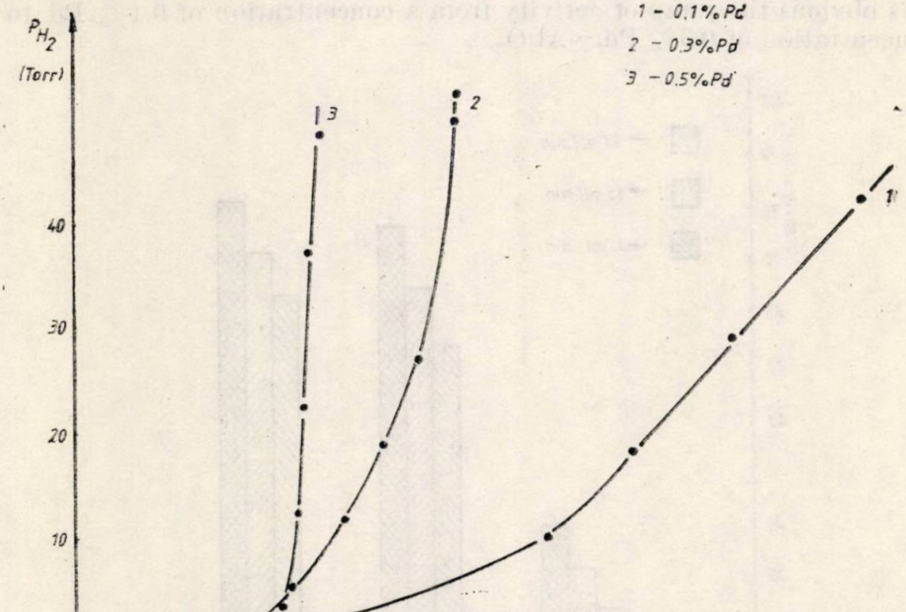

Fig. 4. — Dependence of p_{H_2} on H/Pd ratio for different concentrations of Pd/γ-Al_2O_3 catalysts.

Table 1 presents the values of three parameters resulted from (1) and (2) formulas for Pd/γ-Al_2O_3 catalysts with 0.1%, 0.3% and 0.5% concentrations. Considering that the surface occupied by Pd atom is 7.9, dispersion was calculated.

Variations of metallic formations dimensions and metallic active area with the increase of Pd concentration show a correlation between the increase of metallic aggregates with the increase of Pd concentration. It may be noticed that the values of diameters belonging to metallic formations range within a smaller domain.

Table 1

Values of the H/Pd ratio, of the active clusters diameter and of metal surface for different concentrations of $Pd/\gamma\text{-}Al_2O_3$.

Catalyst	H/Pd	D(Å)	S (m^2/g)
0.1 % $Pd/\gamma\text{-}Al_2O_3$	0.73	12	0.28
0.3 % $Pd/\gamma\text{-}Al_2O_3$	0.55	16	0.64
0.5 % $Pd/\gamma\text{-}Al_2O_3$	0.41	21	0.81

c) Catalysts activity

The results of styrene hydrogenation on studied catalysts were published.[10] The conversion to ethylbenzene depends on the Pd content. It is obvious the jump of activity from a concentration of 0.1% Pd to a concentration of 0.3% $Pd/\gamma\text{-}Al_2O_3$.

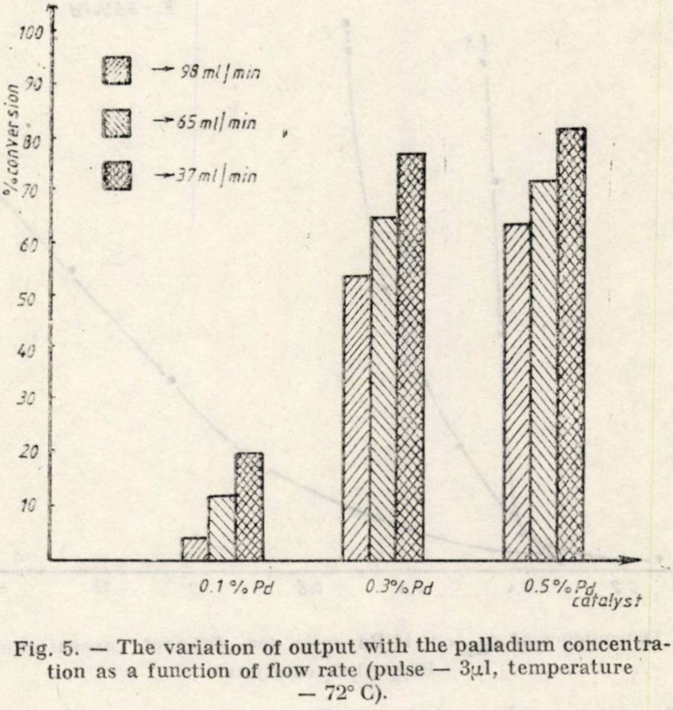

Fig. 5. — The variation of output with the palladium concentration as a function of flow rate (pulse — 3μl, temperature — 72° C).

Kinetic parameters of tested catalysts during hydrogenation were determined according to the conditions of chromatographic pulse. From the experimental data, a first order reaction kinetics has been obtained. For a first order reaction, in the conditions of reaction, the concentration distribution in the catalysts column verified the equation :

$$\frac{\partial c(x, t)}{\partial t} + u_p \frac{\partial c(x, t)}{\partial x} = -k \Gamma_A c(x, t)$$

where : c — reactant concentration in gas phase ;

$u_p = \frac{u}{1 + \Gamma_A}$ — u — linear velocity of carrier gas at x distance
— Γ_A — Henry's factor ;

k — velocity constant ;
t — time.

The apparent activation energies have been calculated from the values of velocity constants, and the adsorption heats from the values of Henry's factor. Based on these the real activation energies have been calculated. These values of these parameters depend on Pd concentration as it is shown in Fig. 6.

The values of these parameters are smaller with the increase of concentration from 0.3 to 0.5% Pd. The insignificant variation of activity has been explained by the compensation effect.

DISCUSSION

The results of the activity tests regarding the hydrogenation of styrene on Pd/γ-Al_2O_3 catalysts, in conditions of chromatographic pulse, have shown a correlation between activity data and Pd concentration on γ-Al_2O_3 support.

Correlation between the activity data and the metal content supported does not reflect the interaction between reagent and catalyst and has a formal character.

As shown in table 1, although the metallic area is almost three times bigger for catalyst with 0.5% Pd concentration in comparison with the one with 0.1 % Pd concentration, the dispersion of the active metal is approximately twice smaller on the catalyst with 0.5% Pd concentration than on that with 0.1% Pd and considering that these formations have spheric forms, approximately the same number of metallic formations supported resulted.

It can be estimated that in the conditions of the preparation method used, the main thing is not the quantity of active metal but the birth of metallic formations with a certain dimension of active aggregates. Formation of Pd aggregates in clusters form was demonstrated not only by the chemosorption measurements but also by the EPR spectra which pointed out the existence of Pd^{+1} clusters.

In atomic state, Pd has the structure $4d^{10}$ $5s^{\circ}$ and the passage from the atomic state to the metallic state is achieved as an increase of the dimensions of the metallic formations and it is shown by a movement of the "d" level so that its structure became $4d^{10-x}$ $5s^{x}$.

The interaction styrene — catalyst may be considered as an interaction of the Blyholder — Allen type, in which an electronic transfer is achieved from the molecular orbitals of organic molecules to the metallic

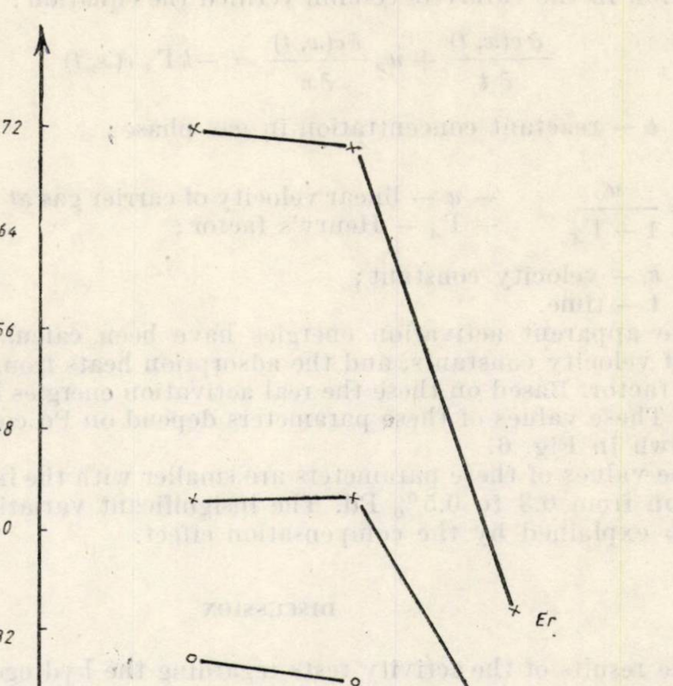

Fig. 6. — Adsorption heat (Q_{ST}), real activation energy (E_r) and apparent activation energy (E_a) for styrene on Pd/γ-Al_2O_3 catalysts.

unoccupied orbitals (especially "d") and a back donation from the metallic occupied orbitals to the unoccupied π orbitals.

Due to that mechanism the dispersion diminution with the formation of the large agglomerations which encourages a large interaction between the reacting substance and the catalyst and explains the high values of conversion obtained with 0.5% Pd/γ-Al_2O_3 catalyst and on the other hand, the correlation between the activity data with the semiconductor character and the extraction work values of the solid components in interaction on the support surface may indicate :

— the extraction work of Pd is 4.98 eV in comparison with 4.7 eV which is for γ-Al_2O_3 ;

— the presence of Pd as Pd^{+1} shows the existence of a semiconductor phase which at the concentration of the metallic component (less than 0.5% concerning the solid support) and the dimensions of the metallic formations supported (less 21 Å) had an important role in the catalyst activity ;

— γ-Al_2O_3 is an "n" type support with satisfactory accuracy and the EPR data emphasized at $g = 2.002$ the presence of the mobile electrons

From the classic theory of catalysis it is known that the relations $\chi_{Me} > \chi$ semiconductor (χ = the extraction work) emphasize the reactions which take place following the mentioned mechanism. This is another element which shows the dependence observed between the dispersion of Pd/γ-Al_2O_3 catalyst and their activity in the hydrogenation of styrene.

CONCLUSIONS

The Pd/γ-Al_2O_3 catalysts activity in the selective hydrogenation reaction of styrene increases with the increase of Pd content.

The EPR results and hydrogen chemosorption data have shown the proportion of alumina surface occupied by Pd agglomerations. These determinations lead to the detection of Pd^{+1} ions as clusters for the described catalysts. This may indicate the agglometrations formation in thermal processes supported by catalaysts before the reduction step.

A correlation was emphasized between the dispersion determinations, the oxidation state and the catalysts activity. This correlation is justified by the interaction mechanism of organic molecule with the active ensembles supported.

REFERENCES

[1] R. Gomez, S. Fuentes, F. J. Fernandez del Valle, A. Camprero and J. M. Fereira, *J. Catal.*, **38**, 47 (1975).

[2] J. J. F. Seholten, "Preparation of Catalysts" (II), Elsevier Scientific Publishing Company, Amsterdam, Oxford, New York, 1979, P. 685.

[3] P. C. Aben, *J. Catal.*, **10**, 224 (1968).

[4] M. Trzebiatowski and H. Kubicka, *Z. Chem.*, **3**, 262 (1963).

[5] H. Kubicka, *J. Catal.*, **5**, 39 (1966).

[6] L. H. Reyerson, A. Solakken and R. W. Zuehlke, *J. Phys. Chem.*, **65**, 1471 (1961).

[7] J. P. Boitiaix, J. Cosynos and S. Vasudevan, *Appl. Catal.*, **6**, 41 (1983).

[8] I. V. Nicolescu, V. Pârvulescu, Yu Yandong and I. Săndulescu, Proc. V-th Intern, Symp. Heterogeneous Catalysis, Varna, Part. I, 321 (1983).

[9] I. Săndulescu and V. Pârvulescu, *Rev. Roumaine Chim.*, **11**, 1086 (1979).

[10] I. Săndulescu, V. Pârvulescu, E. Szabo, A. Popa and I. V. Nicolescu, *Rev. Roumaine Chim.* (to be published).

[11] S. Ursu, "La Resonance Paramagnetique Electronique", Dunod, Paris, 1968.

[12] Y. Ben Tsarit, J. C. Vedine, J. F. Dutel and C. Naccache, *J. Moyn. Res.*, **31**, 251 (1978).

[13] P. A. Berger and J. F. Roth, *J. Catal.*, **4**, 717 (1965).

[14] G. Blyholder and M. C. Allen, *J. Amer. Chem. Soc.*, **91**, 3158 (1969).

Revue Roumaine de Chimie, 33, *1*, 13 – 16 (1988)

DEHYDROGENATION KINETICS OF LOW ALIPHATIC ALCOHOLS ON COPPER CATALYSTS. IV*

ANALYSIS OF STRUCTURE – ACTIVITY RELATIONSHIPS

N. DOCA[a] and E. SEGAL[b]

[a] Chemical Research Center, Blvd Mihai Viteazul 24, 1900 Timişoara, Romania
[b] Chair of Physical Chemistry and Electrochemical Technology, Faculty of Chemical Technology, Polytechnical Institute of Bucharest, Blvd Republicii 13, 7000 Bucharest, Romania

Received August 15, 1986

The apparent activation energy of dehydrogenation of ethyl, n-propyl, iso-propyl, n-butyl and 2-butyl alcohols on copper catalysts containing 0.5,1.0 and 1.5 at. % of Cr, Mn, Fe and Ni was correlated with the descriptor parameters of both reactant molecule and catalyst. The reactant molecule structure was quantitatively expressed by the Randić connectivity index and the catalyst main characteristic by the magnetic susceptibility. The dehydrogenation reaction was significantly favoured by the increase of catalyst paramagnetism; the reactant topology had a lower significance on the dehydrogenation reaction.

In our previous papers [1,2] the apparent activation energy of ethyl, n-propyl, iso-propyl, n-butyl and 2-butyl alcohols on copper catalysts containing in turn 0.5, 1.0 and 1.5 at.% of Cr, Mn, Fe or Ni was determined. The peculiar values of the apparent activation energy depended both on the reactant and catalyst nature.

In this paper we intend to describe quantitatively the dehydrogenation reaction as a simultaneous contribution of reactant and catalyst characteristics. The frame of mathematical formalism and the manner of structure – activity relationship analysis were similar to those presented in an earlier paper. [3]

PARAMETERS AND MODEL

Since the reactant molecules differ only by the alkyl radicals, the topological parameter of reactants is of interest for their numerical characteristics. We decided on the connectivity index χ_t^1 because it does not impose a priori consideration of the geometry of the surface complex.

For catalyst numerical characterisation, the magnetic susceptibility χ_m was selected due to its significant variation vs. both chemical nature and quantity of elements added on copper (as was observed in the previous papers [1,2]).

---

* Part III in : *Rev. Roumaine Chim.*, 32, 199 (1 987).

These parameters were used in the biparametric liniar model:

$$\log \hat{Y} = \alpha + \beta_1 \chi_t + \beta_2 \chi_m \tag{1}$$

were $\hat{Y}$ represents the estimated values of the measured catalytic activity i.e. the apparent activation energy and α, β_1, β_2 are the regressional coefficients obtained by the least squares method.

The statistical quality of the regressional equation (1) was characterised by means of : r — correlation coefficient, s — standard deviation, E — Fisher statistics, EV — explained variance.

RESULTS AND DISCUSSIONS

The computed values of the connectivity index for the five alcohols used as reactants are listed in table 1. The determined values of magnetic susceptibility and apparent activation energy (first presented in our papers[1,2]) are listed in tables 2 and 3 respectively.

Table 1

The Randić connectivity index of reactant molecules χ_t

Reactant	χ_t
Ethanol	1.0233
n-Propanol	1.5233
Iso-propanol	1.4128
n-Butanol	2.0233
2-Butanol	1.8790

Table 2

The magnetic susceptibility of the catalysts[1,2], χ_m

Catalyst	Added element	Amount, at. %	$\chi_m \times 10^6$
C_1	Cr	0.5	2.74
C_2		1.0	2.80
C_3		1.5	2.95
C_4	Mn	0.5	3.60
C_5		1.0	4.20
C_6		1.5	5.02
C_7	Ni	0.5	3.15
C_8		1.0	3.48
C_9		1.5	3.75
C_{10}	Fe	0.5	4.37
C_{11}		1.0	4.84
C_{12}		1.5	5.24

Table 3

Values of apparent activation energy, E_{ap}, kJ/mol [1,2]

Reactant / Catalyst	EtOH	n-Pr—OH	i-Pr—OH	n-Bu—OH	2-Bu—OH
C_1	65.7	81.2	76.8	95.1	86.5
C_2	73.9	78.8	76.4	88.8	82.5
C_3	63.8	71.7	70.0	80.0	77.5
C_4	49.3	51.2	50.8	58.4	56.0
C_5	33.5	38.6	36.9	42.5	41.2
C_6	22.2	25.4	24.5	28.4	27.6
C_7	52.4	54.0	62.8	73.0	70.0
C_8	48.4	65.0	53.0	60.6	59.0
C_9	43.0	47.9	46.0	53.7	52.2
C_{10}	30.8	35.5	34.1	39.2	37.9
C_{11}	24.4	27.6	26.8	30.8	29.9
C_{12}	20.5	22.5	21.9	25.2	24.1

With these values, the computed regressional equation was :

$$\log \hat{Y} = 2.348 + 0.105\ \chi_t - 0.221\ \chi_m \tag{2}$$

n^*	r	$r(\chi_t)$	$r(\chi_m)$	s	F	EV
60	0.997	0.347	0.978	0.0133	3867	0.995

n^* = number of data points

The statistical quality and the descriptive capability of the biparametric model are very good.

Equation (2) explains 99.5% of the experimental data variation by variations in the connectivity index and magnetic susceptibility values, but the significance and contribution of each parameter differs.

The partial correlational coefficient of the topological parameter is three times smaller than the total correlational coefficient; however, it exceeds the minimum significant value ($r_{\min} = 0.250$ for $n = 60$). The activation energy increases with the value of the connectivity index, i.e. with the number of carbon atoms in the alcohol molecule. The activation energy is smaller for the secondary alcohols (or with branched chain) than for the linear isomers.

The contribution of the reactant molecule topology on the numerical characterisation of the reaction is not so important as seen from the regressional coefficient β_1 which is less than half of β_2.

The magnetic susceptibility is the most significant parameter of the regressional equation. The apparent activation energy decreases with the increase of catalyst magnetic susceptibility, i.e. the dehydrogenation reaction is favoured by increasing the catalyst paramagnetism.

CONCLUSIONS

1. The dehydrogenation reaction of the lower aliphatic alcohols on copper catalysts was modeled by a biparametric linear free energy relationship, using the Randić connectivity index and the magnetic susceptibility as independent variables.

2. The analysis of the statistical quality of the linear equation allows a realistic assessment of the influence of each parameter on the variation of experimental data.

3. The dehydrogenation reaction was significantly favoured by the increase of catalyst paramagnetism. The reactant topology had a lower significance on the dehydrogenation reaction.

REFERENCES

[1] N. Doca and E. Segal, *Rev. Roumaine Chim.*, **30**, 949 (1985).
[2] N. Doca and E. Segal, *Rev. Roumaine Chim.*, **31**, 567 (1986).
[3] N. Doca, F. Klepp and E. Segal, *Rev.. Roumaine Chim.*, **27**, 365 (1982).
[4] M. Randić, *J. Amer. Chem. Soc.*, **97**, 6609 (1975).

Revue Roumaine de Chimie, 33, *1*, 17–23 (1988)

CATALYTIC ACTIVITY OF Pt/$AlPO_4$ AND RELATED SYSTEMS. I

GAS-PHASE HYDROGENATION OF MONO-ALKYLBENZENES

M. A. ARAMENDIA, V. BORAU, C. JIMENEZ and J. M. MARINAS
Departamento de Química Orgánica, Facultad de Ciencias, Universidad de Córdoba, Córdoba, Spain

Received July 15, 1982
Revised October 2, 1986

The gas-phase hydrogenation of benzene, toluene, ethylbenzene, iso-propylbenzene, and tert-butylbenzene on supported Pt catalysts using a pulsed microcatalytic reactor is reported. Three different materials have been used to support the metal (0.5% metal loading): $AlPO_4$, SiO_2-AlPO_4 (80/20 w/w), and γ-$Al_2O_3-AlPO_4$ (25/75 w/w). The effect of the reduction temperature of the catalysts on the catalytic activity has been monitored. In the temperature range here studied (200–500 °C), a Hammett-type correlation $\ln X/X_0 = \sigma\rho$ has been observed to exist between the electron donor strength of the substituent and the initial reduction rate of the substrate.

INTRODUCTION

In the last few years, Marinas et al. have reported the synthesis of new reduction catalysts obtained by supporting group VIII metals (Ni, Pd, Pt and Rh) on $AlPO_4$ and related systems. These catalysts have been already tested to reduce aromatic nitroderivatives by hydrogen transfer using different hydrogen donors, [1,2] as well as to reduce olefines at low hydrogen pressure, [3,4] with good yields in both cases.

In the present paper, some of these catalysts (Pt supported on $AlPO_4$, SiO_2-AlPO_4 and γ-$Al_2O_3-AlPO_4$) have been used to reduce several arenes in a pulse reactor.

Although the microcatalytic pulse technique was initially used to carry out kinetic studies in first-order reactions, [5,6] several authors [7–9] have successfully applied it to study non-first order reaction.

In our case, some kinetic results of the reduction of benzene have been already reported, [10] and in the present paper the reduction of a comprehensive series of methylbenzene derivatives is reported.

EXPERIMENTAL

(a) Catalysts

Platinum was supported on three different materials whose synthesis and textural properties have been reported elsewhere [11] : $AlPO_4$ (support B), SiO_2-AlPO_4 (90/20 w/w, support

E), and $\gamma-Al_2O_3-AlPO_4$ (25/75 w/w, support CB). The B.E.T. specific surface areas were 263, 327, and 256 $m^2 g^{-1}$, respectively.

The metallic phase was incorporated by impregnating the support with an aqueous solution (3.85×10^{-3} M) of hexachloroplatinic acid, and the reduction of the complex to yield the metallic particles was carried out in the microreactor itself, immediately before to perform the catalytic runs. In all cases, the metal loading, as measured by atomic absorption, was 0.5% weight. The catalysts were always isolated from external contaminants by flowing a continuous hydrogen stream (25 mL min^{-1}) through the catalytic bed.[12]

The average metallic particle size (Transmission Electron Microscopy) ranges from 40 to 50 Å, and no dependence of this parameter on the nature of the support was observed.

On the other hand, no sintering of the metallic crystallites in the presence of hydrogen has been observed within the temperature range studied. In the case of alumina-supported platinum, sintering of the metallic crystallites in the presence of hydrogen occurs at temperatures well above the upper limit here studied.[13]

Naming of the catalysts is as follows: Chemical symbol of the metal (Pt)-Support (E, B or CB)-reduction temperature (°C).

(b) Apparatus

Reduction experiments have been carried out in the pulse reactor shown in Fig. 1. It consists of an oven and a reactor attached to a gas chromatograph provided with a TCD to analyze the reaction products (see below). Stopcocks between the reactor and the chromatograph allow to exhaust the gas stream during reduction of the precursor, or to drive it to the GC instrument during reduction runs. Within the temperature range here studied, no diffusion phenomena and a complete lack of catalytic activity of the system was observed during blank experiments.

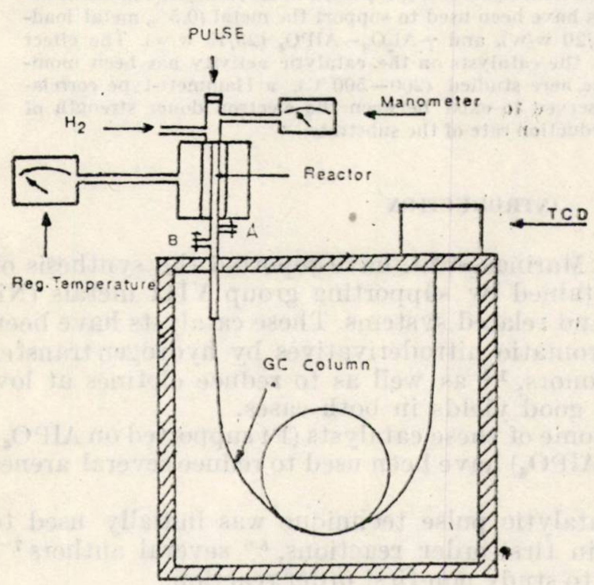

1 — Pulse reactor system.

(c) Analysis of the products

The reduction products were identified by mass spectrometry of the products collected at the exit of the gas chromatograph using a GC—MS Hewlett-Packard 5992 system. In all cases, the corresponding cycloalkane was obtained as the only reduction product.

The amount of catalyst (0.05 g), reaction temperature (120°C), and hydrogen flow (50 mL min^{-1}) were kept constant in all experiments, in order to obtain a good GC resolution of the products, using a celanese ester column (3m, 1/8″).

All chemicals were from Fluka or Merck, puriss quality.

RESULTS AND DISCUSSION

In order to assess the effect of the reduction temperature of the precursor on the activity of the final catalyst, the hydrogenation of benzene, toluene, ethylbenzene, iso-propylbenzene, and tert-butylbenzene has been studied with catalysts previously reduced at varied temperatures for one hour.

Figure 2 shows the conversion of benzene to cyclohexane (% mol) vs. injected mole.

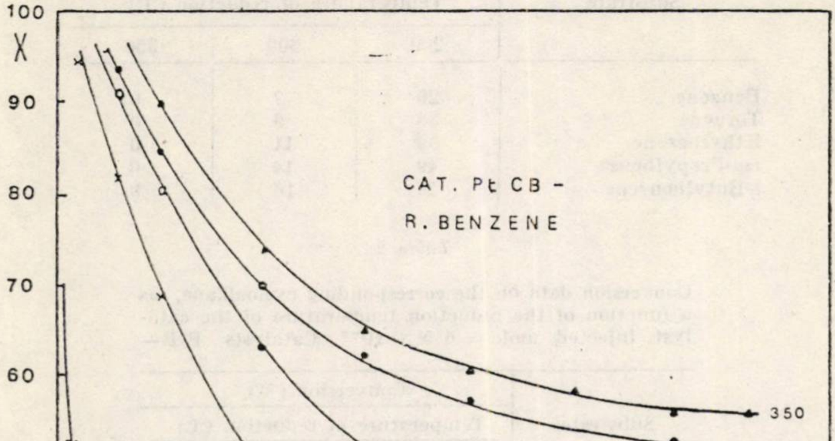

Fig. 2. — Dependence of the conversion on the amount of substrate injected.

Tables 1, 2 and 3 collect the catalytic activity values at constant conversion (6.5×10^{-5} M) for the arenes here studied, at varied reduction temperatures of the precursor. It can be seen that a maximum limit is obtained with catalysts Pt CB — and Pt B — (75 and 100% $AlPO_4$, respectively) between 300 and 350°C, whereas catalyst Pt E— (20% $AlPO_4$) shows an activity decrease from 200°C downwards.

Table 1

Conversion data on the corresponding cycloalkane, as a function of the reduction temperature of the catalyst. Injected mole$=6.5\times10^{-5}$ Catalysts PtE —

Substrate	Conversion (%)		
	Temperature of reduction (°C)		
	200	300	350
Benzene	29	7	0
Toluene	33	9	0
Ethylbezene	39	11	0
iso-Propylbenze	49	14	0
t-Butylbenzene	59	16	0

Table 2

Conversion data on the corresponding cycloalkane, as a function of the reduction temperature of the catalyst. Injected mole $= 6.5 \times 10^{-5}$. Catalysts PtB—

Substrate	Conversion (%)				
	Temperature of reduction (°C)				
	200	300	350	400	500
Benzene	17	36	30	17	0
Toluene	25	45	38	26	0
Ethylbenzene	31	49	48	39	0
iso-Propylbenzene	34	52	55	48	0
t-Butylbenzene	41	55	51	50	0

Table 3

Conversion data on the corresponding cycloalkane, as a function of the reduction temperature of the catalyst. Injected mole $= 6.5 \times 10^{-5}$. Catalysts PtCB—

Substrate	Conversion (%)				
	Temperature of reduction (°C)				
	200	300	350	400	500
Benzene	29	54	56	43	3
Toluene	32	60	68	48	6
Ethylbenzene	47	67	78	73	12
iso-Propylbenzene	61	72	86	76	10
t-Butylbenzene	62	72	80	78	6

On the other hand, if the reduction of the precursor is carried out below 200°C, the catalytic activity depends on the reduction time, whereas no dependence is observed, even after 12 h reduction, if the catalyst is reduced above this temperature. The interval error of experimental results is smaller than 1 %.

It is as well observed that the catalytic activity changes as the $AlPO_4$ content in the catalyst does, being larger for supports CB and B than for support E.

Similar results were obtained by Meriaudeau, [14] and Moss [15] in the hydrogenation of benzene on Pt/TiO_2 and Pd/SiO_2 catalysts. The workers justified the observed decay of activity when the temperature is increased, by means of different metal-support interactions or by variation of the metal surface. These variations of the catalytic properties would carry to different amounts of adsorbed benzene. The observed decay of activity cannot be explained by diminution of the dispersion of the metal. In agreement, Boudart [16] postulated that different electronic states are present in the metal when the structure of the metal is changed by the temperature. In our case, no change in metallic dispersion was observed. Thus, we can postulate that the different interaction metal-support is responsible for the results obtained.

On the other hand, the tert-butylbenzene is hydrogenated more easy than the other alkylbenzenes for all catalyst studied.

Our results agree with those previously reported by other authors for the hydrogenation of the same arenes on Ni/Al_2O_3,[17] or on Pt-catalyst non-sensitive to sulphur poisoning.[18] However, some authors observed an inverse reactivity trend when using Rh catalysts at 100 atm. in methanol solution, probably due to steric effects. [19]

In our experimental conditions, the hydrogenation rate increases as the length of the alkyl branch in the arene does, suggesting an electronic effect of the substituent instead of a steric one. In order to assess this electronic effect, our results have been fitted to Hammett's equation, [20] taking toluene as a reference :

$$\ln X/X_0 = \sigma \rho$$

where X and X_0 represent the conversion obtained for hydrogenation of arene and of toluene, respectively ; σ represents the electron donor strength of the substituent and ρ stands for the specific reaction rate constant.

Following Best's criteria,[21] toulene was chosen as a reference instead of benzene, as, according to these authors, benzene is adsorbed in a "nearly-planar" conformation on the surface of the catalyst, standing aside from Hammett's plot. The values obtained for catalysts tested at 120°C have been plotted in Figs 3, 4 and 5. In the most of the cases, a good correlation ($r > 0.98$) has been obtained, with ρ values between -0.4 and -2.0. Only tert-butylbenzene moves away from the straight line at temperatures above 350°C.

The results suggest that in the rate determining step hydrocarbon is not co-planarly adsorbed, as no steric hindrance due to the substituent is observed.

On the other hand, hydrocarbon should adsorb dissociatively on electron-deficient metal atoms. In such a way, the intermediate would be stabilized by the electronodonor ability of the substituent, that increases as the length of the alkylic chain does. Similar results are obtained by Imelik et al.[22] upon adsorption of benzene on several catalysts, assuming interactions between the hydrocarbon and surface cationic sites.

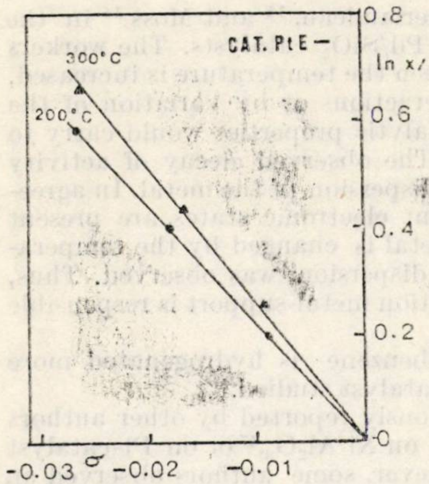

Fig. 3. — Fitting of arene reduction to Hammett's equation, for different-temperature reduced catalysts. Catalyst : Pt E-.

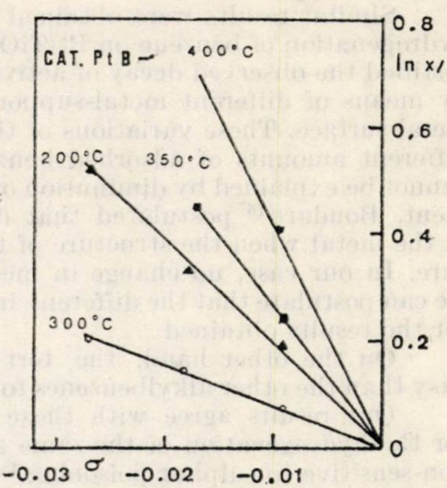

Fig. 4. — Fitting of arene reduction to Hammett's equation, for different-temperature reduced catalysts. Catalyst : Pt B—.

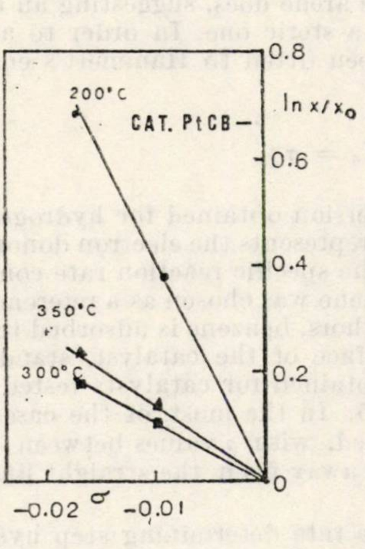

Fig. 5. — Fitting of arene reduction of Hammett's equation, for different-temperature reduced catalysts. Catalyst : Pt CB—.

REFERENCES

[1] M. A. Aramndia, M. S. Climent, C. Jimenez and J. M. Marinas, *React. Kinet. Catal. Lett.* **14**, 489 (1980).

[2] M. A. Aramendia, "Doctoral Thesis", Universidad de Córdoba, Córdoba, Spain, 1981.

[3] J. M. Campelo, D. Luna, J. M. Marinas and A. Garcia, *Afinidad*, in press.

[4] M. A. Aramendia, V. Borau, C. Jimenez and J. M. Marinas, *Acta Chim. Acad. Sci. Hung,* 1st Issue, **110**, July (1982).

[5] G. A. Gaziev, V. Y. Filinovskii and M. I. Yanovski, *Kinetica i Kataliz*, **4**, 688 (1963).

[6] G. M. Schwab and A. M. Watson, *J. Catalysis*, **4**, 570 (1965).

[7] K. Toyota and E. Echigoya, *K. Kogatu*, **32**, 1005 (1968).

[8] W. A. Blanton, C. H. Byers amd R. P. Merrill, *Ind. Eng. Chem. Fund.*, **7**, 611 (1968).

[9] A. M. Sica, E. M. Valles and C. E. Gigola, *Rev. Lat. Am. Inc. Quim. and Quim. Appl.*, **4**, 109 (1974); ibid. *J. Catalysis*, **51**, 115 (1978).

[10] M. A. Aramendia, V. Borau, C. Jimenez and J. M. Marinas, "Ist Semm. Catal. I.B.P." Rio de Janeiro, Brasil, 1981, p. 65.

[11] C. Jimenez, J. M. Marinas, R. Perez-Ossorio and J. V. Sinisterra, *Ann. Quim.*, **70**, 860 (1974); ibid. *Ann. Quim.*, **72**, 254 (1976).

[12] G. A. Somorjai, *Catal. Rev. Sci. Eng.*, **18**, 173 (1978).

[13] G. I. Straguzzi, H. R. Aduriz and C. E. Gigola, *J. Catalysis*, **63**, 1 (1980).

[14] P. Meriaudeau, B. Pommier and S. J. Teichner, *Compt. Rend.*, **389**, 395 (1979).

[15] R. L. Moss, D. Pope, B. J. Davis and B. H. Edwards, *J. Catalysis*, **58**, 206 (1979).

[16] M. Boudart, "Proceedings VIth Congress Catalysis", Vol 1, 1976 p. 1.

[17] M. Linero and J. Yves, "Proceedings Vth Symp. Ib. Am. Catal.", Vol. 2, 1978, p. 253.

[18] J. Cosyns, J. P. Franck and J. M. Gil, *Compt. Rend.*, **288**, 115 (1979).

[19] M. Freifelder, *J. Org. Chem.*, **26**, 1835 (1961).

[20] J. March, "Advanced Organic Chemistry", Mc. Graw-Hill Ed. Kogakusha, Tokio, 1977, p. 252.

[21] A. B. Best and B. W. Wojciechowski, *J. Catalysis*, **31**, 74 (1973).

[22] M. Primet, E. Garbowski, M. F. Mathieu and B. Imelik, *J. Chem. Soc. Faraday*, **76**, 1942 (1980).

M. A. Arzamendi, V. Fornés, [illegible] J. M. Montes, [illegible] Chem. [illegible] [illegible] 119, July (1983).

G. A. Ozin, [illegible] and [illegible] Tomczak, [illegible], 1, [illegible] (1980).

G. M. Crowell and A. H. Watson, J. Catalysis, 4, 375 (1965).

[illegible] and [illegible], J. [illegible], 32, 1005 (1968).

W. A. Blanton, [illegible] and R. L. Burwell, [illegible] Proc., 7, 311 (1968).

A. [illegible] F. Gómez, [illegible] 14, [illegible] and J. Catalysis, 31, 115 (1973).

M. A. Arzamendi, V. Fornés, [illegible] J. M. Montes, [illegible] Catal. [illegible] 1982, [illegible].

C. Dimitrov, L. M. Kalinov, [illegible] 70, 303 (1971); [illegible] Chem., 72, 251 (1976).

G. A. Somorjai, [illegible] Angew., 16, 12 (1979).

[illegible] and [illegible] J. Catalysis, 47, 1 (1980).

[illegible] and [illegible], J. [illegible] 385, 356 (1979).

[illegible] and [illegible], J. Catalysis, 50 [illegible].

M. [illegible], Proceedings VIII Congress Catalysis, Vol. 1, 1074 [illegible].

[illegible] and [illegible] Proceedings VIII [illegible] Catal. Vol. 2, 1976, p. 303.

[illegible] and J. M. [illegible] 296, 1 [illegible] (1979).

[illegible], [illegible] Chem., 26, 1595 (1961).

J. March, Advanced Organic Chemistry, McGraw-Hill Book Co., Tokyo, 1977, p. [illegible].

[illegible] and [illegible] J. Catalysis, 31, 71 (1973).

M. [illegible], M. [illegible] and [illegible], J. [illegible] 70, 1642 (1966).

Revue Roumaine de Chimie, **33**, *1*, 25–37(1988)

REDOX AND *COLHOM* QUANTUM TRANSITIONS AS BASIC COMPONENTS OF CHEMICAL PROCESSES

A. CĂLUȘARU * and M. APOSTOL **

* Institute of Chemical Research, Spl. Independenței 202, Bucharest, Romania
** Central Institute of Physics, Dept. of Theoretical Physics, P.O. Box 5206, Bucharest, Romania

Received July 3, 1987

By analogy with the term of REDOX-reactions, the term of COLHOM-reactions was adopted for the *col*igation-*hom*olysis processes. Both *redox* and *colhom* transformations are elementary reactions allowing to compose the operator of the four types of heterolytic reactions and, in this way, of any chemical process. Since the matrix of reaction contains no information on the direction of the chemical transformations, a quantum mechanical interpretation of both the *redox* and *colhom* reactions was discussed, on the basis of the quantum tunneling in perturbation mechanism.

The outstanding evolution of the modern computers promoted considerably the development of the present chemistry by an efficient effort focused towards the mathematical foundation of this empirical discipline. The foundation of chemistry on mathematical concepts[1] appears as a natural idea, since all known bonded systems are formed from about 100 atoms arranged in groups, called molecules or complex ions, according to a few mathematically stated combinatorial laws. In spite of the obvious suggestiveness of the classical formulas, the accumulation of an enormous set (about 7 million compounds) of experimental data, together with the fast development of computers, incited chemists to find suitable procedures for a dialogue with electron computers, the unique means that can handle such an enormous database. From the practical point of view, the problem was successfully solved by the extension of molecular structures and chemical reactions in form of graphs, the conversion of these in matrices and the drawing up of the codes of possible valence states of the elements (a review on this subject can be found in ref. [2] together with the references given herein).

Computer routines were already elaborated for about four million structures, commercially available, and adapted for the I.B.M.-type personal computers.[3] However the result is a success especially for the computer assisted chemistry. Although thus transposed in mathematical symbolism, the chemistry remains an empirical discipline, as long as it is not founded on simple principles allowing to deduce all other cases, no matter of their complexity. This desideratum was however fulfiled for the mathematical foundation of the chemical reactions only, by the finding that any matrix operator of reaction can be established by means of 2 × 2 matrices[4]: (1) one of a *redox-reaction* type and (2) the other of a *colhom-reaction* type.[5] By analogy with the synthetic term *redox*, commonly adopted from electrochemical disciplines for the *red*uction and *oxi*dation processes, in ref.[5] the term *colhom* was suggested to design *col*igation-*hom*olysis correlated reactions. The introduction of this term is justified by the fact that, together with the one-electron *redox* transformations, the *colhom* (radicalic) processes are fundamental elements, irreducible to simpler forms. A scheme was drawn up [5] for the composition matrix operators of heterolytic reactions, using *redox* and *colhom* basic components, whose sum determines the electrofugic-electrophilic or nucleofugic-nucleophilic character of a specified reaction. Further with the matrices of *redox*, *colhom* and *heterolytic* reactions one is possible to compose the matrix operator of any chemical transformation.

In this paper we show that the character of a heterolytic reaction depends on the form of the quantum potential barrier, specific for the *redox* or *colhom* processes.

1. MATRICES OF *REDOX* REACTIONS

The *redox* one-electron reactions include the following pair of processes : (1) oxidative dissociation and (2) reductive association.

The first process of one-electron oxidation follows formally the general scheme :[5]

$$^{\cdot}A_i + A_j \to A_i + {}^{\cdot}A_j \tag{1}$$

In this reaction the atomic species are labelled with the corresponding electrical charges neither before nor after the electron transfer. But, also in this form, the two species are not equivalent, owing to the electron at one of the components of the center of reaction. The nonequivalence of these species is the cause of the sensitivity of the oxidation process to the permutation operation, producing its transformation in the reverse reduction process.

When the electrical charges are taken into account, then reaction (1) reaches a multitude of forms, among which a set is shown in table 1. In matrix form, reaction (1) can be written as follows :

$$\begin{array}{c} \begin{array}{cc} i & j \end{array} \\ \begin{pmatrix} 1 & 0 \\ 0 & 0 \end{pmatrix} \end{array} + \begin{array}{c} \begin{array}{cc} i & j \end{array} \\ \begin{pmatrix} -1 & 0 \\ 0 & 1 \end{pmatrix} \end{array} = \begin{array}{cc} \begin{array}{cc} i & j \end{array} & \\ \begin{pmatrix} 0 & 0 \\ 0 & 1 \end{pmatrix} & \begin{array}{c} i \\ j \end{array} \end{array} \tag{2}$$

where the operator of reaction is noted by R_1 :

$$R_1 = \begin{array}{cc} \begin{array}{cc} i & j \end{array} & \\ \begin{pmatrix} -1 & 0 \\ 0 & 1 \end{pmatrix} & \begin{array}{c} i \\ j \end{array} \end{array} \tag{3}$$

Table 1

Schemes for one-electron redox reactions : direct sense is a reduction, the reversed one is an oxidation process

No.	Reaction scheme
1	${}^{\bullet}A_i + {}^{\bullet}A_j \rightarrow A_i^+ + \bar{A}_j^-$
2	${}^{\bullet}A_i + A_j \rightarrow A_i^+ + {}^{\bullet}A_j^-$
3	${}^{\bullet}A_i + A_j^+ \rightarrow A_i^+ + {}^{\bullet}A_j$
4	${}^{\bullet}A_i^+ + A_j \rightarrow A_i^{2+}\,{}^{\bullet}A_j^-$
5	${}^{\bullet}A_i^- + A_j \rightarrow A_i + {}^{\bullet}A_j$
6	${}^{\bullet}\bar{A}_i^- + {}^{\bullet}A_j \rightarrow \bar{A}_i + \bar{A}_j^-$
7	$\bar{A}_i^- + A_j \rightarrow {}^{\bullet}A_i + {}^{\bullet}A_j^-$
8	$\bar{A}_i^- + A_j^+ \rightarrow {}^{\bullet}A_i + {}^{\bullet}A_j$
9	$\bar{A}_i + A_j \rightarrow {}^{\bullet}A_i^+ + {}^{\bullet}A_j^-$
10	${}^{\bullet}A_i^+ + A_j \rightarrow A_i^{2+} + {}^{\bullet}A_j^-$

The reverse or permuted process of the previous one is the reductive association[5] :

$$A_i + {}^{\bullet}A_j \rightarrow {}^{\bullet}A_i + A_j \tag{4}$$

Or, in matrix form :

$$\begin{array}{cc} i & j \\ \multicolumn{2}{c}{\begin{pmatrix} 0 & 0 \\ 0 & 1 \end{pmatrix}} \end{array} + \begin{array}{cc} i & j \\ \multicolumn{2}{c}{\begin{pmatrix} 1 & 0 \\ 0 & -1 \end{pmatrix}} \end{array} = \begin{array}{ccc} i & j & \\ \multicolumn{2}{c}{\begin{pmatrix} 1 & 0 \\ 0 & 0 \end{pmatrix}} & \begin{array}{c} i \\ j \end{array} \end{array} \tag{5}$$

In this case the operator of reaction, R_2, is :

$$R_2 = \begin{array}{ccc} i & j & \\ \multicolumn{2}{c}{\begin{pmatrix} 1 & 0 \\ 0 & -1 \end{pmatrix}} & \begin{array}{c} i \\ j \end{array} \end{array} \tag{6}$$

As has been already shown,[2,4,5] R_2 is correlated with R_1 by the relation :

$$R_2 = \bar{R}_1 = -R_1 \tag{7}$$

The matrix R_2 can be deduced also by permutation of row/columns of the matrix R_1 :

$$\begin{pmatrix} -1 & 0 \\ 0 & 1 \end{pmatrix} \xrightarrow{\text{rows}} \begin{pmatrix} 0 & 1 \\ -1 & 0 \end{pmatrix} \xrightarrow{\text{columns}} \begin{pmatrix} 1 & 0 \\ 0 & -1 \end{pmatrix} \tag{8}$$

and, therefore, the relation of permutation holds too :

$$R_2 = {}^{p}R_1 \tag{9}$$

2. *COLHOM* REACTIONS[5]

Colhom (radicalic) processes refer to the dissociation reaction of the covalent bonds, termed as *homo*lysis and to the radicalic association termed as *co*ligation. In the *colhom* pairs of processes, the two specified reactions are correlated by a reverse operation, unlike to the pair of redox transformations in which the transitions are produced both by permutation and reversion operations.

For the process of radicalic dissociation (homolysis) the general schemes are :

$$A_i - A_j \rightarrow {}^{\bullet}A_i + {}^{\bullet}A_j \tag{10}$$

$$A_i = A_j \rightarrow {}^{\bullet}A_i - {}^{\bullet}A_j \tag{11}$$

$$A_i \equiv A_j \rightarrow {}^{\bullet}A_i = {}^{\bullet}A_j \tag{12}$$

As has been previously shown [2,4,5] the matrix operator of the process is :

$$R_3 = \begin{array}{cc} i & j \\ \end{array} \quad \begin{array}{c} \\ \end{array}$$

$$R_3 = \left(\begin{array}{cc|c} \multicolumn{2}{c}{} & \\ \end{array}\right)$$

$$\begin{array}{ccc} & i & j \\ i & 1 & -1 \\ j & -1 & 1 \end{array} \qquad R_3 = \begin{pmatrix} 1 & -1 \\ -1 & 1 \end{pmatrix} \tag{13}$$

The reverse transformations (10) — (12) are the general schemes for radicalic association (coligation) with the following matrix operator, R_4 :

$$\begin{array}{ccc} & i & j \\ i & -1 & 1 \\ j & 1 & -1 \end{array} \qquad R_4 = \bar{R}_3 = \begin{pmatrix} -1 & 1 \\ 1 & -1 \end{pmatrix} \tag{14}$$

Both (13) and (14) matrices are not sensitive to the permutation operations, which leaves them unchanged.

Within the principle of conservation of the electron number in the two-atom center of reaction, the matrices R_1 and R_3 (or their reversed forms) cannot be reduced to simpler forms. But, while the matrices R_1 and R_2 are permuted or reverse processes, R_3 and R_4 represent reverse processes only.

3. HETEROLYTIC REACTIONS AS SUM OF *REDOX* AND *COLHOM* TRANSFORMATIONS

An outstanding interest is presented by the possible combinations of *redox* and *colhom* reactions, by which the matrices of reactions for the four types of heterolytic reactions can be obtained : (1) electrofugic dissociation, R_7, (2) electrophilic association, R_8, (3) nucleofugic dissociation, R_9 and (4) nucleophilic association, R_{10}; the R_5 and R_6 matrices designate the two-electron *redox* reactions.[1,4,5]

By the sum of the elementary processes, the *redox* components (R_1, $-R_1$) introduce the element sensitive to permutation operation, and the *colhom* components introduce the element characteristic of reverse operation. In this way the four types of heterolytic reactions are correlated in the following form :

$$\text{reversion} \quad R_7 \rightarrow R_8 = -R_7 \tag{15}$$

$$\text{permutation} \quad R_7 \rightarrow R_9 = {}^{p}R_7 \tag{16}$$

$$\begin{array}{l}\text{permutation} \\ \text{reversion}\end{array} \quad R_7 \rightarrow R_{10} = -{}^{p}R_7 \tag{17}$$

On the other hand R^7 is deduced by the sum :[1,4,5]

$$R_7 = \bar{R}_1 + R_3 \tag{18}$$

In this way, together with the introduction of the mathematical symbolism of the chemical transformations, it has been found, starting from two basic elements, the law of the simple deduction of each among them.[1,5] One can conclude that a basis, mathematically founded, was established for the interpretation of one of the basic problems of the chemistry, namely the one of the chemical transformations.

[4. *REDOX* AND *COLHOM* QUANTUM TRANSITIONS

The mathematically established basis for the deduction of the reaction operator of any chemical transformation is based on the elementary matrices, where, however, no information is based on the sense of quantum transitions, corresponding to the elementary components. The decisive factor on the value of the probability of quantum transition in a *redox* process is represented by the charges of the reactive species (Table 1). These charges can enhance or diminish the value of the electron tunneling probability, by the change of both shape and basic parameters of the potential barrier, which must be penetrated during the process of electron tunneling. Therefore, in order to carry out estimations on these basic factors one is necessary to establish the main relationships, allowing to evaluate the penetrabilities of the quantum barriers and to apply the results for the interpretation of the *redox* and *colhom* quantum transitions.

4.1. Quantum tunneling in perturbation formalism [6]

One assumes that a voltage is applied between two media (1) and (2). The one-electron wave functions are denoted by $\varphi^{(1)}(p)$ and $\varphi^{(2)}(p)$, corresponding to the milieu (1) and (2) respectively. The variable p represents all quantum numbers that describe the one-electron state with the free energy levels $\varepsilon_p^{(1,2)}$.

The potential difference (voltage) U created by the applied electrical field displaces the energy levels occupied in the electron fundamental state in the milieu (1), whose displacement is in opposite direction as compared with the electrical field applied considering N electrons on the unit length in the milieu (1); the Fermi momentum is (the electron spin is omitted):

$$k_F^0 = \pi N \tag{19}$$

without consideration of the electrons on the other directions. The variable λ_1 of the Fermi momentum is given by the equation (Fig. 1):

$$k_{F_1}^{(1)} = k_F^0 + \lambda_1 \tag{20a}$$

$$k_{F_2}^{(1)} = k_F^0 - \lambda_1 \tag{20b}$$

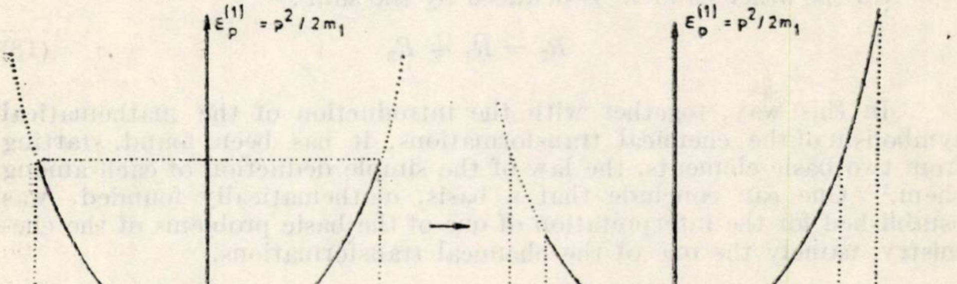

Fig. 1. — Energy levels as a function of the electron momentum. a — free electrons; b — with an applied voltage.

The energy of the fundamental state is:

$$E = \frac{1}{2\pi}\int_0^{k_{F_1}^{(1)}} \mathrm{d}k\,\frac{k^2}{2m_1} + \frac{1}{2\pi}\int_{-k_{F_2}^{(1)}}^{0} \mathrm{d}k\,\frac{k^2}{2m_1} = \frac{1}{2\pi}\int_{-k_F^0}^{k_F^0} \mathrm{d}k\,\frac{k^2}{2m_1} + NeU \tag{21}$$

from which it follows:

$$\lambda_1 = (2m_1 eU)^{1/2} \tag{22a}$$

Similarly, for the milieu (2) we obtain:

$$\lambda_2 = (2m_2 eU)^{1/2} \tag{22b}$$

where U is the potential difference (electrical voltage) at the interface.

By standard calculations[6] one found that the kinetic hamiltonian, H_0, of the system, in the second quantization, can be written in the form :

$$H_0 = \sum_p (\varepsilon_p^{(1)} a_p^+ a_p + \varepsilon_p^{(2)} b_p^+ b_p) \tag{23}$$

The symbols a_p and a_p^+ denote the annihilation and creation operators respectively of one-electron states in the milieu (1) and by b_p and b_p^+ the same operators corresponding to the milieu (2).

The presence of the interface is signified by the potential $V(x)$, a real and even function, $V(x), = V(-x) = V^x(x)$, conditions imposed evidently by the physics of the problem, in which move two kinds of electrons. Owing to the present two-component formulation of the electric field, in the (2) milieu there are no more electrons of the b type ; it results that the effect of the interface must be manifested by absorption and creation of electrons. More precisely electrons of the a type, annihilated by the interface, will be created in the (1) milieu by shutting the electrical circuit and the electrons of the b type created in the interface will be annihilated in the milieu (2) by shutting the same electrical circuit. Consequently, the current flow process through the interface must be expressed by a purely imaginary potential :

$$W(x) = iV(x) \tag{24}$$

which, as is known from the nuclear physics (the optical model)[7] is responsible for the absorption and creation of particles in a collision process. The interaction hamiltonian can be written in the second quantisation in the form :

$$H_1 = \int \mathrm{d}x\, \psi^+(x) W(x) \psi(x) = \sum_{pk} (W_k b_p^+ a_{p-k} + W_{-k} a_p^+ b_{p-b}) \tag{25}$$

where :

$$W(x) = \begin{pmatrix} 0 & W(-x) \\ W(x) & 0 \end{pmatrix} \tag{26}$$

and ψ is the electronic field, represented by a vector with two components :

$$(x) = \begin{pmatrix} \psi_1(x) \\ \psi_2(x) \end{pmatrix} \tag{27}$$

Considering the one-particle Green function, by means of the Feynman diagrams the expression of the propagator $G(p, \varepsilon)$ can be obtained :

$$G(p, \varepsilon) = \frac{\varepsilon - \varepsilon_p}{(\varepsilon - \varepsilon_p)^2 + t^2} = \frac{\varepsilon - \varepsilon_p}{(\varepsilon - \varepsilon_p + it)(\varepsilon - \varepsilon_p - it)} \tag{28}$$

where t is a parameter controlling the fraction of the "lost" electrons in inelastic "channels", when the problem is treated in the model of the inelastic scattering and p, ε and ε_p are the previously shown notations.

By further calculations, considering the propagators for the different types of electrons, and approximating $G_1^0(p, \varepsilon) = G_2^0(p, x) = G^0(p, x)$, the following equation is obtained :

$$\bar{G}(p, \varepsilon) = it\frac{G^{02}(p, \varepsilon)}{1 + t^2G^{02}(p, \varepsilon)} = it\frac{1}{(\varepsilon - \varepsilon_p)^2} =$$

$$= it\frac{1}{(\varepsilon - \varepsilon_p + it)(\varepsilon - \varepsilon_p + it)} \tag{29}$$

This relation shows that the model used allows to find an exact solution, considering the perturbation theory formalism which makes possible a more exact treatment of the problem.

Using equation (29), by a series of calculations shown in ref. [6] and considering the analytical structure of the one-particle Green function, the equation of the current I is obtained :

$$I = iet\left[\sum_{0<p<k_{F_1}} it\frac{1}{2t} - \sum_{-k_{F_1}<p<0} it\frac{1}{2t}\right] = -\frac{et}{2\pi}\lambda \tag{30}$$

Hence :

$$I = -\frac{et}{2\pi}(2meU)^{1/2} \tag{31}$$

It is interesting to emphasize that according to this model a loss of energy in time unit arises from the kinetic energy variation of the electrons of the *a* type and from the variation of the kinetic energy of the *b* type electrons (for each electron type a specific component is introduced in the general form of the interaction hamiltonian).

Equation (30) can be written in the form :

$$I = -et^2\left(\sum_{0<p<k_{F_1}}\frac{1}{2t} - \sum_{-k_{F_2}<p<0}\frac{1}{2t}\right) \tag{32}$$

The sums in brackets represent the number of states accessible for electron transition from a medium to another. It is well known that the probability of transition from the state i to the state j, under the influence of a V perturbation acting in a finite short interval is :

$$w_{me} = \frac{|V_{ij}|^2}{(E_i - E_j)^2} \tag{33}$$

or for a continuous spectrum :

$$\mathrm{d}w = 2\pi|V_{ij}|^2\delta|E_i - E_j|\mathrm{d}\nu_e \tag{34}$$

where $d\nu_e$ is the number of acceptors states and V is constant in time. V_{ij} is the matrix element of perturbation between the states i and j. By summing all available states in equations (33) and (34), including in this sum also the denominator $(E_i - E_j)^{-2}$, we can understand the meaning of equation (32). It follows that t^2 can be taken as an average value of the sum:

$$\sum_e |V_{ij}|^2 = \int dx\, |V(x)|^2 \tag{35}$$

$V(x)$ is the function in real coordinates which describes the interface barrier.

For a rectangular barrier with a width and V height, we have:

$$t^2 = Va \tag{36}$$

which is the geometrical area of the barrier having a defined form. In general, t^2 must be equated with the area S of the barrier having a particular shape. Therefore, t^2 is defined as the integral of the function describing the form of the barrier. The integration limits are located within the width of the corresponding barrier:

$$t^2 \equiv S \tag{37}$$

This interpretation of the parameter t is justified as a first approximation. A more exact calculation should take into account all the components of the interaction hamiltonian and also the reflexion terms. Such treatment of the problem appears as more advantageous in the frame of the perturbation theory, considering the inelastic collisions of the electrons on the interface barrier.

For the interpretation of transition probabilities in the case of the *redox* and *colhom* processes, the calculation of t^2 values is a tool for quantitative evaluations.

4.2. Quantum barriers in *REDOX* and *COLHOM* transitions

The transition of the electron between two species A_i and A_j of the center of reaction occurs by a tunneling process across a potential barrier. In the present section this barrier is approximated by a parabolic shape, described by the following equation:

$$V(x) = -b^2x^2 + a^2 \tag{38}$$

where a is the height of the potential $V(x)$ and $\pm a/b$ are the roots of this equation, in the coordinate system shown in Fig. 2. As has been found in the previous section, the transition rate depends essentially in the area enclosed by the parabolic potential function $V(x)$. This area can be calculated from the defined integral of (38) between the limits $-a/b$ and a/b:

$$S = \int_{-a/b}^{a/b} (-b^2x^2 + a^2)\, dx \tag{39}$$

Therefore, according to relation (37) we get:

$$I^2 = -\frac{4}{3}\frac{a^3}{b} \tag{40}$$

This is a symmetrical barrier, corresponding to electrically uncharged A_i, A_j species, forming the center of reaction, before and after the occurrence of chemical transformation. This case corresponds obviously to *colhom* processes described by (10) — (12) reactions and the corresponding reversed ones. The transition probability is strongly dependent on the height a of the potential barrier, a relatively high value for the homolysis process.

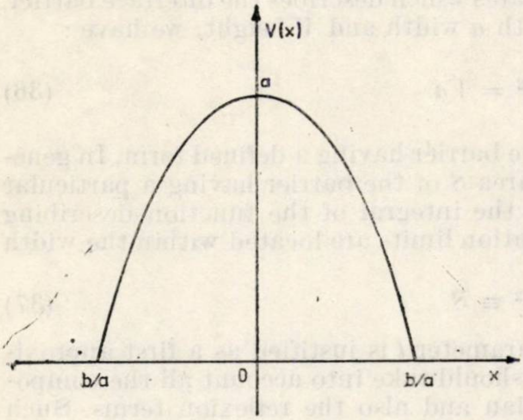

Fig. 2. — Parabolic potential barrier, with the characteristic values: $a =$ barrier height; $2\frac{b}{a} =$ barrier width.

This condition is not fulfilled by the redox reactions, where the one or both species are charged before and/or after charge transfer process. In this case the potential function must be corrected by the difference of potential E, introduced by the electrical field of the charged particles:

$$\tilde{V}(x) = V(x) + E\left(x + \frac{b}{a}\right) \tag{41}$$

In a coarse approximation that the field E is constant we obtain by integration:

$$\int_{-a/b}^{a/b}\left[V(x) + E\left(x + \frac{b}{a}\right)\right]\mathrm{d}x = -\frac{4}{3}\frac{a^3}{b} + 2E \tag{42}$$

According to relation (42) the symmetrical tunneling is more or less favoured as compared with the asymmetrical one as a function of the charge of particle between which the tunneling transition occurs, therefore depending on the sign of the potential difference E.

4.3. Double-well potential for electron transfer in *REDOX* and *COLHOM* processes

A more elaborated method to interpret the electron transitions in *redox* and *colhom* processes is represented by the model of double-well potential.

It is difficult to establish the rigorous equation describing the outline of such energetical state, but a good approximation is obtained by using a four degree equation. In order to simplify the calculation, the terms containing x^2 and x^4 only can be used. The contour given in Fig. 3 is the graphical drawing of the following potential equation :

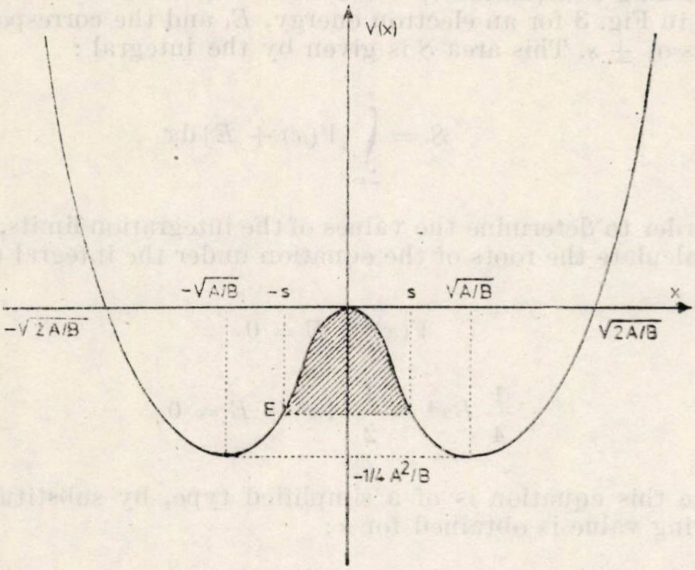

Fig. 3. — Double-well potential barrier with the characteristic values (explanations are given in text).

$$V(x) = -\frac{1}{2}Ax^2 + \frac{1}{4}Bx^4 \qquad (43)$$

The constants A and B are greater than zero. Using the equation (43) the following characteristic values can be calculated, as is shown in Fig. 3 :

$$V(x) = 0$$

$$V(x) = 0 \text{ when } x = \pm\sqrt{2A/B}$$

The derivative :

$$V'(x) = -Ax + Bx^3 = 0$$

has the following roots :

$$x = 0 \text{ and } x = \pm \sqrt{A/B}$$

showing the maxima and minima reached by $V(x)$, for the ordinate values :

$$V(\pm\sqrt{A/B}) = -\frac{1}{2}\frac{A^2}{B} + \frac{1}{4}\frac{A^2}{B} = -\frac{1}{4}A^2/B$$

According to equation (37) the tunneling is controlled by the hatched area in Fig. 3 for an electron energy, E, and the corresponding abscisa values of $\pm s$. This area S is given by the integral :

$$S = \int_{-s}^{s} [V(x) + E]\,\mathrm{d}x \tag{44}$$

In order to determine the values of the integration limits, it is necessary to calculate the roots of the equation under the integral (44), therefore :

$$V(x) + E = 0$$

$$\frac{1}{4}Bx^4 - \frac{1}{2}Ax^2 + E = 0 \tag{45}$$

Since this equation is of a simplified type, by substitution of x^2, the following value is obtained for s :

$$s = \sqrt{A/B - \sqrt{A^2/B^2 - 4\,E/B}} \tag{46}$$

This value must be substituted in the integrated (44) equation. Thus :

$$S = \int_{-s}^{s} [V(x) + E]\,\mathrm{d}x = \int_{-s}^{s} \left[\frac{1}{4}Bx^4 - \frac{1}{2}Ax^2 + E\right]\mathrm{d}x =$$

$$= \frac{1}{20}Bx^5 - \frac{1}{6}Ax^3 + Ex\,\Big|_{-s}^{s} = \frac{B}{10}s^5 - \frac{A}{3}s^3 + 2Es \tag{47}$$

where s is given by (46).

The electron transition in a symmetrical double-well potential corresponds to a homolysis process with an expense of the energy E, necessary to reach the radicalic states of the resulted species.

In the *redox* reactions the double-well potential is not more symmetrical, the lowest minima representing the stable state for the occupied electron position (reduced species) or for the free electron level (oxidised species). The potential function can be described by a more complex four degree equation, including also an x^3 term. This problem is particularly useful for the interpretation of heterolytic reaction, allowing to define the electrofugic-electrophilic and nucleofugic-nucleophilic character of these transformations. The problem of the heterolytic reactions will be studied elsewhere.

REFERENCES

[1] A. T. Balaban (Editor), "Chemical Application of Graph Theory", Academic Press, London, 1976.

[2] A. Călușaru, "Representation of Chemical Structures by Matrices and Computer Algorithms". in press.

[3] E. Garfield, "Index Chemicus goes online with graphic access to three milion new compounds. Essays of an Information Scientist : The award of Science and other Essays, Philadelphia, I.S.I.— Press, 1985, Vol. 7, p. 194—201.

[4] A. Călușaru, *Rev. Chim. (București)*, **38**, 273 (1987).

[5] A. Călușaru, *Rev. Chim. (București)*, in press.

[6] A. Călușaru and M. Apostol, *Rev. Roumaine Chim.*, **27**, 175 (1982).

[7] A. Bohr and B. Mattelson, "Nuclear Structure", vol. I, Benjamin Inc., New York, 1969.

Revue Roumaine de Chimie, **33**, *1*, 39–52 (1988)

CHEMICAL SHIFT NONEQUIVALENCE *VERSUS* CHEMICAL SHIFT EQUIVALENCE OF GEMINAL DIASTEREOTOPIC GROUPS IN PROCHIRAL ASSEMBLIES AND CURIE'S PRINCIPLE OF SYMMETRY. I

GENERAL ANALYSIS

ADRIAN O. FULEA *

Department of Physical Chemistry and Electrochemical Technology, Polytechnic Institute of Bucharest, Blvd. Republicii 13, Bucharest, Romania

Received November 3, 1986
Revised March 27, 1987

An in-depth and critical analysis of the terminologies, concepts, factors and relationships for the chemical shift nonequivalence and chemical shift equivalence of geminal groups is made, also taking into account the principle of symmetry of Curie. The concepts in force in the literature on the phenomena are proved to be essentially erroneous in many respects. Our analysis shows that the terminology : isochronism — anisochronism is, by its definition, inconsistent with the spectroscopic reality and should be abandoned. The terminology 'origin of the chemical shift nonequivalence' is ambiguous. It is logically established the complementarity relation between the origin and the necessary diastereotopic condition for the chemical shift nonequivalence, as opposed to several researchers who viewed an exclusion relationship between them. Several logical errors in the area are discussed, while the statements in the literature — essential for the understanding of the phenomenon — are corrected. On the basis of our analysis the conclusion can be reached that the principle of symmetry in Physics is in fact a consequence of the corpuscular character of matter.

INTRODUCTION

During the last thirty years or so, the chemical shift nonequivalence of geminal groups has been extensively studied by several hundreds of researchers in the NMR spectroscopy area and aroused much interest and debate. In his review on the phenomenon, Jennings shows that this spectroscopic phenomenon "often appears to have been associated with some mistique".[1]

Though an enormous research effort was made, we have found that, in fact, many confusing, erroneous or inconsistent assertions referring to the essential aspects of the phenomenon exist in the literature. Furthermore ambiguous or inconsistent terminologies are used, erroneous relationships between the factors involved in the reasoning of the rationalization of the phenomenon are considered, definitions including characteristics for a particular class of substances in the general case are claimed and even more serious logical errors were done, none of them being corrected or repudiated from the logical point of view. Essentially erroneous statements continue to be perpetuated at an even larger degree of error at present as recently, by Mislow et al.[2]

---

* Present and correspondence address : Str. Calea Plevnei 127, Bucharest, R–77103, Romania.

In our view, the situation in the literature as it stands to date may rather obfuscate than enlighten an interested reader in the understanding of the phenomena we intend to analyze in the present paper.

We think that the principal reason of the existence of this undesirable situation lies mainly in the fact that not enough attention has been paid to the reality that the geminal chemical shift nonequivalence *as well as* the geminal chemical shift equivalence of diastereotopic groups are phenomena determined by the molecular structure and not only by one of its characteristics, the symmetry.

While in progress with this work we fortunately read the general principle of symmetry in Physics about which we were previously unaware. We immediately realized that our ideas and reasoning involved in the present paper are in fact also backed by some ideas of this general principle, which, according to our knowledge, has unfortunately been completely ovelooked in the spectroscopy area up to now.

The purpose of our work is to give a correct view on the phenomena, pointing out and correcting the essentially erroneous views still admitted in the literature.

A. ON THE INCONSISTENCY OF THE TERM ANISOCHRONISM

The practice in the NMR spectroscopy has shown that there are three different kinds of equivalence of nuclei : [3]

i) chemical shift equivalent nuclei,
ii) symmetry equivalent nuclei,
iii) magnetically equivalent nuclei.

The symmetry equivalent nuclei are necessarily chemical shift equivalent.

For the phenomenon of the (geminal) chemical shift nonequivalence the term (geminal) anisochronism is increasingly used in the literature. According to Mislow et al.[4] the term anisochronous was suggested by Binsch in a private communication * to signify "magnetically nonequivalent in chemical shift" as a *counterpart* for the term isochronous signifying "magnetically equivalent in the chemical shift sense" introduced by Abragam.[6] However, Abragam,[6] as well as Pople et al.,[7] consider that only the symmetry equivalent nuclei are chemical shift equivalent, a point which is erroneous, but which unfortunately was adopted especially by Mislow and his coworkers and, in general, by workers in the area of geminal chemical shift nonequivalence.** Views such as "nuclei which are diastereotopic must have different chemical shifts in either chiral or achiral solvents"[8] or "resonances due to symmetry equivalent or nonequivalent atoms are isochronous and anisochronous, respectively" [2] are those admitted in the literature.

---

* See also ref.[5]

** See for example ref.[1]

To begin with, the above statements are in disagreement with the classification of the types of equivalent nuclei of Emsley et al.[3] If this were indeed the spectroscopic reality, the classification should include only two types of equivalent nuclei: symmetry equivalent and magnetically equivalent.

In 1972 Schiemenz and Rast published an important paper [9] on this problem. Firstly, they purposely proved experimentally, by using chemical shift reagents, that there exists cases where symmetry nonequivalent nuclei exhibit exactly the same chemical shift: previously, the literature admitted Mislow's view that it is only possible that the difference in the chemical shifts of two diastereotopic groups might be sometimes too small to be resolved by the instrument. We can add that geminal diastereotopic groups, whose chemical shift nonequivalence exhibits sign reversal with the temperature variation, are also clear-cut examples where the exact coincidence of the signals can be established without any doubt.* The above experimental findings must certainly be contrasted with the view that the difference in shieldings of two geminal protons "must persist as long as the stereochemical integrity of the environment is maintained".[8]

Secondly, Schiemenz and Rast pointed out that the terminology of anisochrony has two meanings in the literature.[9]

On the other hand it has not yet been observed that the term anisochronous, *defined as a counterpart of isochronous*, is bound to be by itself inconsistent with the spectroscopic reality too, because isochronous is inconsistent with the valid NMR classification of equivalent nuclei,[3] as we have pointed out.

Many statements that can be called to question were made in the literature with a view of coping with the NMR data by using the inconsistent terminologies isochronism — anisochronism. Thus, Mislow and his coworkers state that "the geminal protons are diastereotopic and therefore anisochronous";[4] "the geminal protons will be diastereotopic and therefore anisochronous",[4] assertions which are shown to be not necessarily true even by another statement of Mislow et al. that "two methylene protons on any one of the benzylic carbons are stereochemically** nonequivalent and might also be expected to be magnetically nonequivalent".[8]

Further Mislow and Raban state for example, that some "diastereotopic protons are not isochronous in carbon tetrachloride" *though they*

---

* There is no reason to suppose a discontinuity of the second type for the function $\Delta\nu_{12} = f(T)$, at the temperature where the sign reversal occurs.

** It might be supposed that in the above statement, Mislow et al. [8] excluded from stereochemical nonequivalent groups the enantiotopic groups; the same should be the situation in regard to some reasoning including the following statement of Waugh and Cotton [10]: "two methylene protons of the *same* methylene group are not stereochemically equivalent because of the lack of symmetry of the (non-planar) substituted sulphur atom with respect to the internal rotation about S—O—C linkage." For spatial relationships between chemical groups see Table I in ref. [11]

have the same chemical shift in the spectrum.* [11] In line with this erroneous view, Mislow and his coworkers introduce the attribute "apparent": "apparent chemical shift equivalence", "apparent isochronous" [4] and "apparent A_2 pattern which remain unsolved even at 100 MHz".[8] In the process of analysing an NMR spectrum the nuclei having the same chemical shift are chemical shift equivalent and noted with the same letter. Thus the spectrum of toluene at 60 MHz is just an A_5X_3 spectrum and not only an "apparent" A_5X_3 spectrum.

On the other hand, Brink [12] uses the attribute "nearly (nahe) isochronous" and considers as equivalent nuclei those which are either "isochronous" or "nearly isochronous", whereas Jennings uses the attribute "potentially anisochronous" [1] which would be correct if anisochronism were consistent with the spectroscopic reality; in the sense in which this terminology is used it simply means, according to Abragam,[6] potentially symmetry nonequivalent (?). In the same review, Jennings [1] also uses "sufficiently anisochronous".

Another terminology related to isochronism is "accidental isochronism". Reisse, Mislow et al. [13] understood by it the exact coincidence of the chemical shift of symmetry nonequivalent group, quoting thus the work of Schiemenz and Rast, [9] while the latter authors,[9] as well as Gorkom and Hall [14] and Jennings[1] understood by "accidental isochronism" the chemical shift coincidence of symmetry nonequivalent groups in the limit of the resolution of the instrument. Mislow and Raban call this spectroscopic phenomenon "apparent accidental coincidence of NMR signals".[11] It seems that Willen et al. [15] understand by "accidental isochronies" both the exact coincidence of the chemical shifts and the coincidence only within the limit of the instrument resolution.

Examples of such confusing, ambiguous and contradictory statements in which the authors were forced by using the inconsistent terminology isochronism — anisochronism could probably be found in other works too, but we think that the above examples show clearly enough that this terminology should be abandoned and instead, chemical shift equivalence — chemical shift nonequivalence should be used, in agreement with Emsley et al. [3] Thus the geminal diastereotopic groups can be either chemical shift equivalent or chemical shift nonequivalent, as the experimental data show, and, as we will show in the next section, it can be predicted from a better understanding of the phenomena.

Attention should be called that in all the three reviews dealing with the chemical shift nonequivalence of symmetry nonequivalent groups, existing to date in the literature [1,14,16] there are used improper terminologies allied with the phenomenon. Siddall and Stewart use "observable nonequivalence" and "magnetic nonequivalence" for the chemical shift nonequivalence, while by "nonequivalence" they mean "symmetry nonequivalence".[16] Gorkom and Hall [14] denote by "magnetic nonequivalence" both the symmetry nonequivalence and magnetic nonequivalence; in ref.[1] and ref. [14] the inconsistent terminology of anisochronism is extensively used. As a matter of fact we have found confusions in the classification of the equivalent nuclei in all the other monographs available to us, [17–19] except [3].

---

* Compare also with a statement of Jennings "Cases of accidental equivalence are very common; thus, for example, compound 13 shows nonequivalent geminal methylene protons in carbon tetrachloride solution, but not in deuteriomethanol" [1]

B. CHEMICAL SHIFT EQUIVALENCE *VERSUS* CHEMICAL SHIFT NONEQUIVALENCE OF TWO GEMINAL NUCLEI IN AN NMR SPECTRUM AND CURIE'S GENERAL PRINCIPLE OF SYMMETRY*

The screening constant of one of the two nuclei represents in fact the sum of the effects of the electrons of the molecule and the solvent.

d_1) When the two sums are unequal to such a degree that the signals appear at different chemical shifts in the NMR spectrum, the two nuclei are chemical shift nonequivalent.

d_2) If the inequality of the two sums is smaller than necessary in order that the two signals should be resolved at the resolution of the instrument the nuclei are chemical shift equivalent. In this second case it should be specified the resolution of the instrument at which the chemical shift equivalence of the two nuclei was observed.

If the sums corresponding to the two nuclei are equal, two cases should be also distinguished.

e) The first one in which each term of one of the sums is equal by symmetry reasons with a term of the second sum; this is the situation of symmetry equivalent nuclei. In the particular case of the geminal protons in a prochiral assembly this is the case when they are enantiotopic on the NMR time scale by both internal and external comparison.

d_3) It is of course also possible that the equality of the screening constants for the two protons should occur without each term from one of the sums being equal to another one in the second sum; the two protons are chemical shift equivalent.

The cases (d_1), (d_2) and (d_3) can all be envisaged for symmetry nonequivalent nuclei.

It should be emphasized that from the viewpoint of the analysing the information given in the spectrum it is irrelevant which of the cases (d_2) or (d_3) is taking place; on the other hand, because when looking at the spectrum we could not know which of the two cases occurs, in the case of symmetry nonequivalent nuclei exhibiting chemical shift equivalence it should be always noted the resolution at which the phenomenon was observed.

The conclusions of our above reasoning illustrate, in fact, in the area of NMR spectroscopy, the general principle of symmetry in Physics, formulated by Pierre Curie [20] which states: **

"When certain principles cause certain consequences, then the elements of the symmetry of the causes must manifest themselves in the area of the consequences provoked by them.

---

* The discussion in this section generally applies to any of the two nuclei.

** The author translated into English this principale from the Romanian translation [20] of the Russian original book of Sirotin and Shaskolskaia. In a footnote, the Russian authors specify that by dissymmetry should be understood, according to [21] "a defect of symmetry". However we could not find any definition for a "defect of symmetry".

When in the case of some phenomena a certain dissymmetry is manifested, the same dissymmetry has to appear also in the causes which generated it.

The assertions reciprocal to the above ones are not true, at least in practice; in other words, the consequences can have a much higher symmetry than the causes which produced them."

Thus taking into account an idea of Curie's principle, two geminal diastereotopic protons should have been expected to be either chemical shift nonequivalent or chemical shift equivalent; in the latter case the screening constants have 'additional' symmetry elements as compared to molecular structure which is their cause.

Therefore the statement of Reisse, Mislow et al.[13] that "the pairwise bonding connectedness of atoms... is fundamentally irrelevant to the question of chemical shift equivalence or nonequivalence except insofar it bears upon the magnitude of the effect" is wrong, contradicting in fact the general principle of symmetry too.

The further assertion of Mislow et al.[2,13] that "the anisochronies stem from a single source: the symmetry nonequivalence of nuclei" is also erroneous. The cause of this spectroscopic phenomenon is the molecular structure the symmetry being only one of its characteristics; the molecular symmetry can tell us *only* that it is not going to occur in the case of enantiotopic nuclei, i.e. when the phenomenon is *forbidden* by *molecular* symmetry.

Waugh and Cotton[10] and later on Reisse* made also some erroneous assertions in regard to the molecular symmetry and the potential barrier hindering in the internal rotation. Thus the statement of Reisse * that "the question what is the origin of the barrier hindering internal rotation in ethane? has only one simple answer: 'Symmetry' " is wrong, the answer to this question being the molecular structure.

The view of Waugh and Cotton[10] that "it seems unlikely that *in practice* ** the asymmetry with respect to the internal rotation required to produce magnetic nonequivalence would not also be reflected in some angular dependence of potential energy" is also at variance with the general principle of symmetry of Curie. According to it, the potential energy could very well lack, *at least in practice*, the molecular asymmetry necessarily required for chemical shift nonequivalence, and we may envisage such a situation for example for $CHDT-CH_2D$.

It is very interesting to compare the conclusions drawn by us with the conditions put down by Siddall et al.[16,23] for the chemical shift nonequivalence of two groups:

"1) There be no symmetry element between the species on NMR time scale,

2) There be a field gradient between species. The species might well be geometrically nonequivalent (condition one), but still be in so nearly the same field that the chemical shift between them is beyond the limits of the resolution of the NMR spectrometer or even the natural line width set by the uncertainty principle.

---

* See footnote (13) in ref. [22]

** Italics ours.

3) The third condition is that there be no molecular motion(s) that simulates a symmetry operation too closely."

By condition two Siddall et al. [16,23] had actually tried to eliminate the cases where there is a symmetry element *for the magnetic field* sensed by two groups even in the absence of a symmetry element of the molecular structure for the two sensor groups. By introducing the condition three, Siddall et al. [16,23] envisaged the possibility that even in the case of the existence of the gradient in the magnetic field, sometimes because of the long NMR time scale, some molecular motion(s) can still render the nuclei chemical shift equivalent.

Recently, we have shown, based on NMR data, that the conditions two and three of Siddall et al. [16,23] are in fact strongly interdependent, specifying also that the "simulation of a symmetry operation" is referring in fact *to the magnetic fields* sensed by the two groups and *not* to the molecular symmetry. [24] In the cases discussed by us [24] the librational motion around C—N bond in 4(2'-hydroxythiobenzoyl)morpholine, **5**, in acetone-d_6,* is introducing symmetry operations (at least in practice, as the 300 MHz spectrum shows), for the screening constants of the equatorial syn NCH proton in the two conformers, whereas in the *cis* isomer of 2,6-dimethyl-4-(2'-hydroxythiobenzoyl)morpholine,**4**, this libration does not have yet the necessary amplitude to introduce symmetry operations for the two screening constants up to —11°C ; still, between —33°C and —11°C it is visible that the amplitude increases and the chemical shift difference of the equatorial syn NCH proton in the two populated conformers A and C[24] decreases accordingly. We have to emphasize that the environments of the two equatorial positions remain diastereomeric, though for the screening constants there are symmetry operations for **5**.[24]

Even before Siddall, it seemed to us that Waugh and Cotton [10] and Gutowsky [27] sensed somehow the same thing as the former. Thus they made the following statements : "The asymmetry effect makes nuclei nonequivalent even though conformational populations are equal, but population differences do not lead to nonequivalence unless the molecular asymmetry is high enough" ; [27] "when the symmetry of substitution is sufficiently low, the nonequivalence of methylene protons can in principle still persist when the isomers are all accidentally of equal energy...".[10]

The correct statements in regard to the above problems would have been :

— The asymmetry makes the nuclei symmetry nonequivalent even in the case of equal conformational populations ; these nuclei will be chemical shift nonequivalent *if* the difference of the magnetic fields sensed by the two nuclei is high enough ; populations differences do not lead to the chemical shift nonequivalence if the two nuclei are symmetry equivalent (conformer populations factor usually leads to the asymmetry for the two magnetic fields sensed by the two symmetry nonequivalent nuclei).

— When the difference of the magnetic fields sensed by the two protons is sufficiently high, the nonequivalence of methylene protons still persists when the conformational isomers are all accidentally of equal free enthalpy.

---

* Our previous interpretation [25] on intramolecular proton transfer taking place when these two compounds are solved in acetone-d_6 was found to be erroneous.[26]

Taking into account our discussion above, revealing fundamental misconception in the area of geminal chemical shift nonequivalence, we will try to correct below some statements of Mislow and Raban [11] and Jennings,[1] which are essential for understanding of the phenomenon.

1° "... We may deduce from symmetry arguments that diastereotopic nuclei (or enantiotopic nuclei in chiral media) must be anisochronous..."[11].

We *cannot* deduce *only* from symmetry arguments that certain diastereotopic nuclei (or enantiotopic nuclei in chiral media) must be chemical shift nonequivalent.

2° Although symmetry principles can tell us whether or not the environment of two groups are diastereomeric, the magnitude of the difference in chemical shift of two diastereotopic groups will be influenced by the specific difference in the average environments of the two groups..."[11]

The molecular symmetry tells us whether or not the environments of two groups are diastereomeric : however, because the diastereotopic groups may exhibit in principle either chemical shift equivalence or chemical shift nonequivalence, the real alternative will be determined by the specific magnetic difference in the average environments of the two groups, sensed by the two groups.

3° "The symmetry rules discussed in section IIB enable it to be established whether geminal chemical shift nonequivalence should be observed in principle. However, these rules do not afford any guide as to whether the nonequivalence will be large enough in practice to be observed under any given condition." [1]

The symmetry principle enables one to establish whether geminal chemical shift nonequivalence is not forbidden because of molecular symmetry. In some conditions such as : a certain field of the instrument, a certain solvent or a temperature, some diastereotopic groups may exhibit geminal chemical shift equivalence ; changing some of these conditions the same diastereotopic groups may exhibit chemical shift nonequivalence in the new spectrum.

We should stress again that if in a spectrum the chemical shift equivalence is observed for some diastereotopic protons, then these nuclei are chemical shift equivalent.

It is interesting to point out that a rather similar situation can be found in fact in the area of the vibrational spectroscopy of long chain polymers. Thus the polymer studied by us [28] has as six allowed infrared fundamental bands : $(2B_{1u} + 2B_{2u} + 2B_{3u})$ and not only six "apparent" allowed infrared fundamental bands, considering instead for $n = \text{even}$, the number of allowed fundamental bands as $\left(\frac{5}{2}n + 2n + 2n - x\right)$ (see eq. (6)) [28] where $\max x = 6$ (n being the degree of polymerization). As a matter of fact the situation, as far as we can see now, presents even a higher degree of novelty. In fact the translations are *not* symmetry operations *of the space group of the macromolecule*, even extended, as they are considered to date in the literature, because no polymer is infinite (and the same should apply to any crystal). Thus the translation $T_{N/2}$ gets out of the macromolecule no less than N/2 unit cells and this situation is maintained as long as N is finite, no matter if its value increases. The symmetry of the polymer $(MgI_2)_n$ (n = odd) [28] is just C_{2v} and not that of the line group. *

The misunderstanding of the NMR spectroscopic phenomena discussed in this work was caused to a high degree by the false belief, still in force, that the geminal chemical shift nonequivalence "can be simply rationalized by combining the prochirality concept of Hanson [29] with the nomenclature of Mislow and Raban [11]".[1] The prochirality concept takes into account *only* certain *stereochemical* properties of the molecule and, though it proved helpful, it cannot account by itself for a property which is determined by the molecular structure, while a nomenclature cannot serve in the process of reasoning in any other way than to provide a means of expressing in a concise way the reasoning.

The related inconsistent statement of Balaban et al.[30,]** may be relevant in regard to the aspect pointed out above : "In CH_2Cl_2 in most cases both α-methyl- and β-protons are degenerate, but all these accidental degeneracies of ^1H—NMR α-methyl or β-ring peaks can be resolved with 0.1—0.2 moles of $Eu(fod)_3$ per mole of compound III."[30] **

The "accidental degeneracies" (in any sense this ambiguous terminology may be accepted) are not "resolved" by adding a lanthanide shift reagent ; by this proceeding a new chemical shift nonequivalence phenomenon, caused by another molecular structure, is taking place ; the work of Shiemenz and Rast [9] might have been proved of course beneficial for the understanding of what was really going on by adding $Eu(fod)_3$ in ref.[30,]***

C. ON THE AMBIGUITY OF THE TERM 'THE ORIGIN OF THE CHEMICAL SHIFT NONEQUIVALENCE'

In 1965 Roberts and his coworkers pointed out that by the origin of the geminal chemical shift nonequivalence they understood the most important factor on determining the magnitude of the chemical shift between geminal protons, in what originates the major contribution to $\nu_1 - \nu_2$. [32]

Prior to this date and afterwards, that was the meaning prevalently attributed to this term in the literature ; **** sometimes, efforts were made to assess whether the conformer preference or the intrinsic asymmetry factor is the origin of a certain chemical shift nonequivalence.

---

* We intend to discuss this topic in a more detailed form in the future, considering the Raman-Born dispute on Raman spectra of crystals and Curie's principle of symmetry.

** We wish to thank Professor A. T. Balaban (Polytechnic Institute of Bucharest) for providing us with a xerox copy of this paper, as well as for calling to our attention, immediately after its publication, the paper of Fraser and Taymaz, [31] which is somehow related to our previous work in the area.

*** The authors [30] could have correctly spoken of "resolving" only in the case that the terminology of "accidental degeneracies" had been used in the sense understood by Gorkom and Hall [14] *and* the NMR spectrum had been recorded with a higher field spectrometer, *all the other "conditions" remaining still constant.*

**** See for example refs. [33–39]

We have found in the literature reviewed by Jennings [1] allied terminologies with this primary sense of origin : "arises", "ascribed", "causes", "a consequence", "explained", "due", "lay", "is responsible".

On the other hand, Mislow et al. used the term of origin for the slow rotation around a bond, which, by becoming rapid, renders the geminal groups enantiotopic on the NMR time scale : [4] the same sense was attributed more recently by Jennings et al. [40,41] Jennings together with other coworkers used previously allied terminologies such as "arises", "attributed" in the same sense with the origin as meant by Mislow et al.[4] *

It is of course unfortunate that two meanings were attributed to the term of origin of the chemical shift nonequivalence and allied terminologies in the literature without even noting this ambiguity. Even Roberts used the term "origin" in its secondary sense [4] in one of his earlier papers,[42] while Mislow et al. [8] used "ascribed" in the primary sense of the origin.** However, this ambiguity signals here that the workers realized in a certain degree the logical connection between the two senses of origin in explaining the phenomenon, this being in fact rooted in the general principle of symmetry of Curie, as we will show.

In the light of the discussion in this paper, which explains why the diastereotopic relationship of two hydrogens is a necessary but not a sufficient requirement for them to have different chemical shifts, a fact observed by Lyle and Pridgen even since 1973,[43] and in agreement with several other works in which this topic was referred to,[13,44,45] we propose for this requirement the terminology of the necessary diastereotopic condition, while retaining the terminology of origin in its prevalently used sense, due to Whitesides, Roberts et al.[32]

D. ON THE COMPLEMENTARITY RELATION BETWEEN THE ORIGIN AND THE NECESSARY DIASTEREOTOPIC CONDITION IN EXPLAINING THE GEMINAL CHEMICAL SHIFT NONEQUIVALENCE

Sorensen stated in 1967 that "the NMR spectra showing methyl nonequivalence are generally attributed to the necessary asymmetry of the methyl groups and the presence of unequal populations of various conformers", [45] whereas Mislow and his coworkers asserted even previously that "two conditions for the observation of magnetic equivalence *** of diastereotopic protons are conceivable : (1) rapid conformational interchange of the two diastereomeric environments, i.e. the equivalent of rapid interchange of the two diastereotopic protons ; (2) and/or very small differences in the chemical shift of the protons or spin coupling constant effects".[8]

---

* Dr. W. B. Jennings stated in a private communication with us (1985), that by term origin he was referring in fact to the "basic diastereotopic relationship" in refs. [40,41]

** In [13] Reisse, Mislow et al. debated an earlier statement of Snyder, in which the latter uses the term 'origin' of the geminal chemical shift nonequivalence in the sense defined by Whitesides, Roberts et al. [32] with no notice that previously Mislow [2] used in it a completely different sense.

*** We want to point out that in this statement, Mislow himself admitted that diastereotopic protons can exhibit in NMR spectra chemical shift equivalence and not only the so-called "apparent" chemical shift equivalence, claimed later on by Mislow and his co-workers; in this statement Mislow admitted in fact the (d_2) case in our discussion in section B.

In the above statements the authors [8,45] overlooked a series of facts :

1° The presence of unequal populations is not the only possible origin of the geminal chemical shift nonequivalence as it seems from [45];

2° By condition (1)[8] the geminal protons become in fact *enantiotopic on the NMR time scale* and therefore the logical connection between conditions (1) and (2) [8] is only *or*.

However, in general, these two statements point out the valid relation between the necessary diastereotopic condition(s) and the origin of the geminal chemical shift nonequivalence. We will try to write it in the language of mathematical logic. Let us note with $d \equiv$ the necessary diastereotopic condition(s) and with $O(s) \equiv$ the origin(s) of the chemical shift nonequivalence, by origins understanding all the structural factors which make two diastereotopic protons not to have symmetry operations for screening constants.

Sorensen's above statement [45] can be written then :

$$d \wedge O(s) \tag{1}$$

while the statement of Mislow et al. [8] can be written after the above correction and letting aside spin coupling:

$$(\neg d) \vee (\neg O(s)) \equiv \neg(d \wedge O(s)) \tag{2}$$

Eqs (1) and (2) show that, from the point of view of the logical connection between the origin(s) and the necessary diastereotopic condition inside a correct rationalization of the geminal shift conequivalence, the corrected statements of Sorensen [45] and Mislow et al. [8] are identical.

In 1977 Mislow proposed a classification of pairwise relations between isomeric structures, based primarily on symmetry and only secondarily (if at all) on constitution. [46] The discussion in our paper shows that the claimings that this "new classification of topic relationship is especially well suited for the analysis of problems in spectroscopy : resonances due to symmetry equivalent and nonequivalent atoms are isochronous and anisochronous respectively" and that "these distinctions are particularly significant in NMR spectroscopy",[2] are wrong, being as a matter of fact in disagremeent with the general principle of symmetry formulated by Curie.

In spite of the logical relationships (1) and (2), many workers in the area considered that between the origin and the necessary diastereotopic conditions there is an exclusion relationship in the rationalization of the phenomenon of geminal chemical shift nonequivalence. This could be very well connected with the fact that two meanings were attributed in the literature to the term of origin. This error can be found frequently in the papers studying the geminal chemical shift nonequivalence of ortho (thio)benzamides where the necessary diastereotopic condition and the orgin were considered as "different interpretations", "alternative interpretations", [47] "different rationalizations" ,[48] "different causes" [41] for the geminal chemical shift nonequivalence. Even previously to the above assertions done while studying ortho (thio)benzamides, similar ones were claimed for other classes of substances.* Thus, Gorkom and Hall concluded their review [14] by stating that "the magnetic nonequivalence arises from quite subtle differences in average environment *or*** conformer population."

On the basis of the logical connection between the necessary diastereotopic condition and the origin***, rooted in the general principle of symmetry, we think that all the terminologies allied either with the origin or with the necessary diastereotopic condition such as "caused", "explained" etc. should either be used only if *both* the necessary diastereotopic condition(s) and the origin(s) are specified together, or if they refer only *to one* of the two categories not to be used any longer. Thus for the compounds studied by us,[39,50] a correct statement would be : the chemical shift nonequivalence of the syn NCH_2 protons is due to the slow rotation around aryl$-$C(S) bond, E_{steric},[24] and around C$-$N bond and to the conformer populations factor.

CONCLUSIONS

From the discussion presented in this paper the following can be concluded :

1. The principle of symmetry of Curie is in fact a consequence of the corpuscular character of matter, so it would be probably more adequate to call it the Curie law of spatial symmetry.****

2. Other characteristics of the molecular structure besides the symmetry could induce the same effect as a certain element of symmetry.***** This is in fact our understanding of the third part of the Curie law of symmetry.

3. The principle of Curie proved very useful in helping us to improve our present understanding of the basic phenomena from NMR spectroscopy. In our view, though simple it is one of the greatest achievements of human mind in science, and, as we have already shown in refs. [52,53] it is also very much related with another bright achievement of human knowledge : the principle of complementarity due to Bohr. It is of course unfortunate that to date Curie's law of symmetry is used only in Irreversible Thermodynamics, no attempt being made to be used in Molecular Spectroscopy when the data accumulated in this field show, at a closer analysis, a dire

---

* See for example refs.[33,49]

** Italics ours.

*** This logical connection was presented at the 4th Conference of Chemistry and Chemical Engineering of the Polytechnic Institute of Bucharest, October 18th, 1985, by the author during a communication.

**** For the definition of spatial symmetry see.[51]

***** We reached this conclusion after thinking of the question Prof. A. T. Balaban asked us on Jan. 30, 1986 : "Why could a property have a higher symmetry than its cause?"

need of it.[*] Curie's law of symmetry is according to our knowledge one of the best examples of creative work in science : providing that kind of recurrence and, therefore, the regularity in Universe — from these segments of regularity human mind plunges into understanding of the cosmos.[54]

Note added in proof: We think that it is appropriate to indicate right now the way in which the *apparent* contradiction betwen Curie's law and the symmetry properties of some screening constants we pointed out above, can be solved: briefly, this can be done by sticking to the exact definition of a phenomenon due to Bohr and using the principle of superposition of symmetry groups of the causes. It seems also important to point out here that in the case of the equality of two screening constants, they have in fact no asymmetry (no 'dissymmetry' in Curie's nomenclature) so, they have, as a matter of fact, an infinite number of symmetry elements.

REFERENCES

[1] W. B. Jennings, *Chem. Rev.*, **75**, 307 (1975).

[2] K. Mislow and J. Siegel, *J. Amer. Chem. Soc.*, **106**, 3319 (1984).

[3] J. W. Emsley, J. Feeney and L. H. Sutcliffe, "High Resolution Nuclear Magnetic Resonance Spectroscopy", Pergamon Press, Oxford, 1967, Vol. 1, p. 284.

[4] Y. Shvo, E. C. Taylor, K. Mislow and M. Raban, *J. Amer. Chem. Soc.*, **89**, 4910 (1967).

[5] G. Binsch, E. L. Eliel and H. Kessler, *Angew. Chem., Int. Ed. Engl.*, **10**, 570 (1971), cf. ref.[1]

[6] A. Abragam, "The Principles of Nuclear Magnetism", Oxford, 1961, p. 480.

[7] J. A. Pople, W. G. Schneider and H. J. Bernstein, "High Resolution Nuclear Magnetic Resonance", McGraw-Hill Book Company, Oxford, 1959, pp. 88, 110.

[8] K. Mislow, M. A. W. Glass, H. B. Hopps, E. Simon and G. H. Waal, *J. Amer. Chem. Soc.*, **86**, 1710 (1964).

[9] G. P. Schiemenz and H. Rast, *Tetrahedron Letters*, **1972**, 1697.

[10] J. S. Waugh and F. A. Cotton, *J. Phys. Chem*, **65**, 562 (1961).

[11] K. Mislow and M. Raban, *Top. Stereochem.*, **1**, 1 (1967).

[12] M. Brink, *Tetrahedron*, **27**, 143 (1971).

[13] J. Reisse, R. Ottinger, P. Bickart and K. Mislow, *J. Amer. Chem. Soc.*, **100**, 911 (1978).

[14] M. van Gorkom and G. E. Hall., *Quart. Rev.*, **22**, 14 (1968).

[15] R. Willem, H. Pepermans, C. Hoogzand, K. Hallenga and M. Gielen, *J. Amer. Chem. Soc.*, **103**, 2297 (1981).

[16] T. H. Siddall and W. E. Stewart, *Progr. in Nuclear Magnetic Resonance Spectroscopy*, **5**, 33 (1969), Editors, J. W. Emsley, J. Feeney and L. H. Sutcliffe, Pergamon Press, Oxford.

---

[*] Even worst, this very important law is not found in handbooks or dictionaries of Physics and Chemistry available to us; at the best it is given in a rather erroneous or shortened form, in spite of the fact that M. Curie and Langevin pointed out long time ago the brightness and potential use of Curie's law of symmetry. We are now in a process of introducing it in other areas of Molecular Spectroscopy[52] and also in Stereochemistry, Physical Chemistry of Polymers and Solid State Physics,[53] as well as to enlarge its content,[52,53] as to be made accountable for the new data which science reached in the last century. However one may still justifiably argue that a molecular structure having a higher symmetry than C_1, but different screening constants for two symmetry nonequivalent groups is not at all in agreement with Curie's law of symmetry; we will tackle this problem in a second paper in this series.

[17] R. M. Silvestein and G. C. Bassler, "Spectrometric Identification of Organic Compounds" 2nd Edition, John Wiley and Sons, Inc., New York, 1967, p. 119.

[18] A. Pidcock, in "Polymer Science", Editor A. D. Jenkins, North-Holland Publishing Co., 1972, p. 1395.

[19] E. Luca and V. Bărboiu, "Analiza structurală prin metode fizice", Vol. 1, Ed. Academiei, Bucharest, 1984, p. 172.

[20] I. I. Sirotin and M. P. Shaskolskaia, "Fizica cristalelor" Ed. Ştiinţifică şi Enciclopedică Bucharest, 1981, pp. 39, 209.

[21] A. V. Shubnikov, "Simmetriia i antisimmetria konechnch figur", Izd-vo AN SSSR, 1951, p. 160, cf. ref [20].

[22] G. Houshnell, L. D. Iroff, D. V. Iverson, R. J. Wroczynski and K. Mislow, *Isr. J. Chem.*, **20**, 65 (1980).

[23] T. H. Siddall, III, *J. Phys. Chem.*, **70**, 2249 (1966).

[24] A. O. Fulea, *Rev. Roumaine Chim.*, **31**, 309 (1986).

[25] A. O. Fulea and P. J. Krueger, *Spectrochim. Acta*, **A33**, 681 (1977).

[26] A. O. Fulea, *Spectrochim. Acta*, **A42**, 447 (1986).

[27] H. S. Gutowyky, *J. Chem. Phys.*, **37**, 3196 (1962).

[28] A. O. Fulea, *Rev. Roumaine Chim.*, **30**, 357 (1985).

[29] K. R. Hanson, *J. Amer. Chem. Soc.*, **88** 2731 (1966), cf. ref. [1]

[30] A. T. Balaban, C. Uncuţa, A. Dinulescu, M. Elian and F. Chiraleu, *Tetrahedron Letters*, **21**, 1553 (1980).

[31] R. R. Fraser and K. Taymaz, *Tetrahedron Letters*, 4573 (1976).

[32] G. M. Whitesides, J. J. Grocki, D. Holtz, H. Steinberg and J. D. Roberts, *J. Amer. Chem. Soc.*, **87**, 1058 (1965).

[33] E. I. Snyder, *J. Amer. Chem. Soc.*, **85**, 2624 (1963).

[34] E. I. Snyder, *J. Amer. Chem. Soc.*, **88**, 1155 (1966).

[35] E. I. Snyder, *J. Amer. Chem. Soc.*, **88**, 1165 (1966).

[36] G. M. Whitesides, D. Holtz and J. D. Roberts, *J. Amer. Chem. Soc.*, **86**, 2628 (1964).

[37] G. R. Franzen and G. Binsch, *J. Amer. Chem. Soc.*, **95**, 175 (1973).

[38] R. D. Norris and G. Binsch, *J. Amer. Chem. Soc.*, **95**, 182 (1973).

[39] A. O. Fulea and P. J. Krueger, *Tetrahedron Letters*, **1975**, 3135.

[40] W. B. Jennings and M. S. Tolley, *Tetrahedron Letters*, **1976**, 695.

[41] U. Berg, J. Sandström, W. B. Jennings and D. Randall, *J. Chem. Soc.*, Perkin II, **1980**, 949.

[42] F. Kaplan and J. D. Roberts, *J. Amer. Chem. Soc.*, **83**, 4666 (1961).

[43] R. E. Lyle and L. N. Pridgen, *J. Org. Chem.*, **3**, 1618 (1973).

[44] W. McFarlane and J. A. Nash, *Chem. Comm.*, 524 (1969).

[45] T. S. Sorensen, *Canad. J. Chem.*, **45**, 1585 (1967).

[46] K. Mislow, *Bull. Soc. chim. belges*, **86**, 595 (1977), cf. ref.[2] and *Chem. Abstr.*, **87**, 141484u.

[47] A. H. Lewin and M. Frucht, *Tetrahedron Letters*, **1970**, 1079.

[48] U. Berg and J. Sandström, *Tetrahedron Letters*, **1976**, 3179.

[49] A. Rauk, E. Buncel, R. Y. Moir and S. Wolfe *J. Amer. Chem. Soc.*, **87**, 5498 (1965), footnote (18).

[50] A. O. Fulea, *Rev. Roumaine Chim.*, **24**, 1107 (1979).

[51] J. P. Mathieu, A. Kastler and P. Fleury, "Dictionnaire de Physique", Masson, Paris, 1983.

[2] A. O. Fulea, "Curie's law of spatial symmetry in Physics and the vibrational and high resolution NMR spectra of polymers", Abstract requested to be written by Professor E. Osawa, Editor, submitted for consideration of publication of a chapter in the series "Molecular Structure and Energetics", Verlag Chemie International, Florida, USA.

[53] A. O. Fulea, accepted for publication in *Rev. Roum. Chim.*

[54] S. Arieti, in "American Handbook of Psychiatry", S. Arieti, Editor, Basic books Inc. Publishers, New York, 1967, Vol. III, pp. 737.

Revue Roumaine de Chimie, **33**, *1*, 53–58 (1988)

PHOTODEGRADATION AND PHOTOSTABILIZATION OF ETHYLENE-VINYL ACETATE COPOLYMERS. II*

NEW FACTS WHICH SUPPORT THE SCHEME OF PHOTODEGRADATION MECHANISM

C. ANDREI[a], I. HOGEA[a] and V. DOBRESCU[b]
[a] Brazi Petrochemical Plant, Research Department, 2000 Ploieşti, Romania
[b] CPMP Bucureşti, Ziduri Moşi 23, Bucureşti, Romania

Received September 8, 1986
Revised March 30, 1987

IR and UV measurements have supplied new data which support the mechanism of photodegradation of ethylene-vinyl acetate (EVA) copolymers unstabilized and stabilized with quenchers and UV absorbers. The results of quantitative measurements on low molecular weight compounds (CH_3COOH, CH_3CHO, CO_2, CO, CH_4) removed on irradiation of copolymers in atmosphere are also presented. An improved scheme of oxidative photodegradation of EVA copolymers is presented which evidences the major role of chromophoric and hydroperoxidic groups in the process.

INTRODUCTION

Previous works[1-4] presented various aspects of EVA copolymer photodegradation. The scheme advanced for the mechanism of photodegradation reaction of these copolymers evidences the decisive role of chromophoric and hydroperoxidic groups. In this contribution new evidence is given which supports the mechanism of photodegradation of EVA copolymers and new aspects of this mechanism are discussed.

EXPERIMENTAL

EVA copolymers of the Levapren 450 (Bayer AG) type with 45% vinyl acetate were purified by solving them in benzene and precipitation with methanol. The UV irradiation was effected as mentioned elsewhere [1] with a high pressure Hg lamp, type Romlux (250 W).

IR spectra were recorded with a Spekord IR–75 spectrophotometer and UV spectra with a Hitachi E P S – 3.

The analysis of degradation products was carried on a Carlo Erba C. V. chromatograph for CH_3COOH, CH_3CHO, CH_4 (copper column 1 m × 2 mm with Porapak P) and a Carlo Erba ATC/f chromatograph provided with a thermoconductivity cell (column 6 m × 4mm with active carbon) for CO and (column 3.5 m × 4 mm with Porapak P) for CO_2.

The photostabilizers utilised were *n*-butylamine-Ni-2,2′-thio-bis-4-*tert*-octyl phenolate (Cyasorb 1084) supplied by Cyanamid and 2-hydroxy-4-*n*-octyl-benzophenone (Chimassorb 81) supplied by Chimosa.

---

* Part I: *Rev. Roumaine Chim.*, **30**, 865 (1985).

RESULTS AND DISCUSSION

The role and place of chromophoric groups in the initiation of photodegradation reaction of EVA copolymers was shown in earlier works.[1,4] According to the scheme advanced, under the influence of UV irradiation the chromophoric groups may pass into an excited form through a transition state, with formation ot a six atom ring; acetic acid is thus eliminated from the copolymer and double bonds are formed. These bonds were evidenced by UV spectra obtained in nitrogen atmosphere within the 180—210 mm. To produce new evidence for this reaction we irradiated both EVA copolymers anti-UV stabilized with quenchers (Cyasorb 1084) or UV absorbers (Chimassorb 81) and unstabilized copolymers.

The protecting action of quenchers is based on deactivation of excited states (singlet or triplet) of chromophoric group:

$$>C=O \xrightarrow{h\nu} (>C=O)^{*} \xrightarrow{Q} >C=O + Q^{*} \xrightarrow{-\Delta} Q \qquad (1)$$

The results are shown in fig. 1.

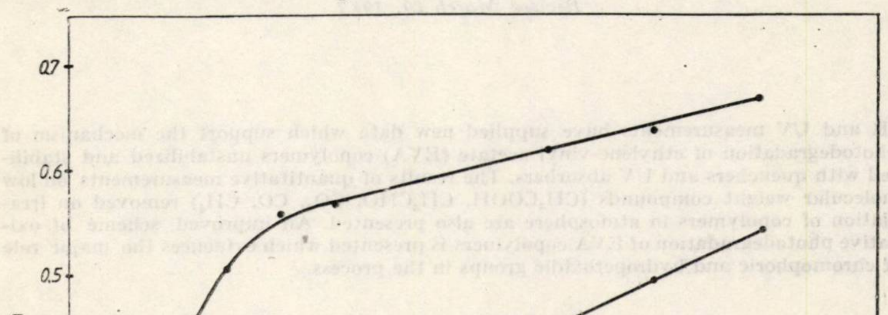

Fig. 1.— The evolution of the intensity of the band at 193.5 nm for EVA copolymer (Levapren 450) stabilized and unstabilized subjected to UV irradiation: *a* Levapren 450 unstabilized; *b* Levapren 450 stabilized with 0.5% Cyasorb 1084; *c* Levapren 450 stabilized with 0.5 % Chimassorb 81.

Examination of the behaviour of the band at 193.5 nm for stabilized and unstabilized EVA copolymer shows that the formation of double bonds is slowed down both by quenchers and UV absorbers; this fact emphasizes the role of chromophoric groups in initiation of photodegradation reaction of these copolymers.

The hypothesis that further oxidation of polymer occurs according to "ene" process [5,6]:

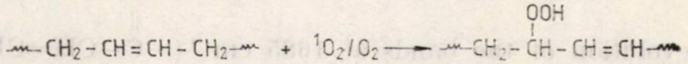

$$\sim CH_2-CH=CH-CH_2\sim + {}^1O_2/O_2 \longrightarrow \sim CH_2-\overset{OOH}{\overset{|}{C}H}-CH=CH\sim \quad (2)$$

was confirmed by the presence and evolution of the band at 3390 cm^{-1} (OOH).[4]

According to the scheme proposed the decomposition of these hydroperoxides leads to formation of conjugated ketones.

Fig. 2 shows the evolution of the absorption band in IR (1600–1800 cm^{-1}) of irradiated and unirradiated EVA copolymers.

After irradiation the copolymer was extracted with methanol to remove products of lower molecular weight (acetic acid, aldehydes, ke-

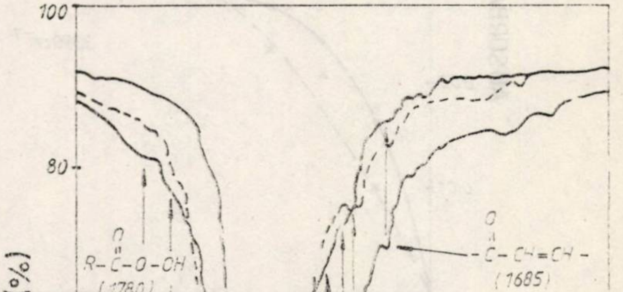

Fig.2. — The evolution o IR absorption between 1600 and 1800 cm^{-1} for EVA copolymer (Levapren 450) subjected to UV irradiation: *a* Levapren 450 unirradiated; *b* Levapren 450 irradiated with UV, 5 hours; *c* Levapren 450 irradiated with UV, 5 hours, extraction with methanol 24 hours.

tones, esters). One may notice that in the copolymer extracted the bands at 1685–1701 cm^{-1} characteristic of the formation of conjugated ketones $(-\overset{\overset{O}{\|}}{C}-CH=CH-)$ in copolymer are present.

One should note that such low molecular weight compounds are also found in the extraction methanol.

The evolution of the bands at 1685 cm^{-1} $(-\overset{\overset{O}{\|}}{C}-CH=CH-)$ and 3390 cm^{-1} (OOH) with the variation of irradiation time is shown in fig. 3.

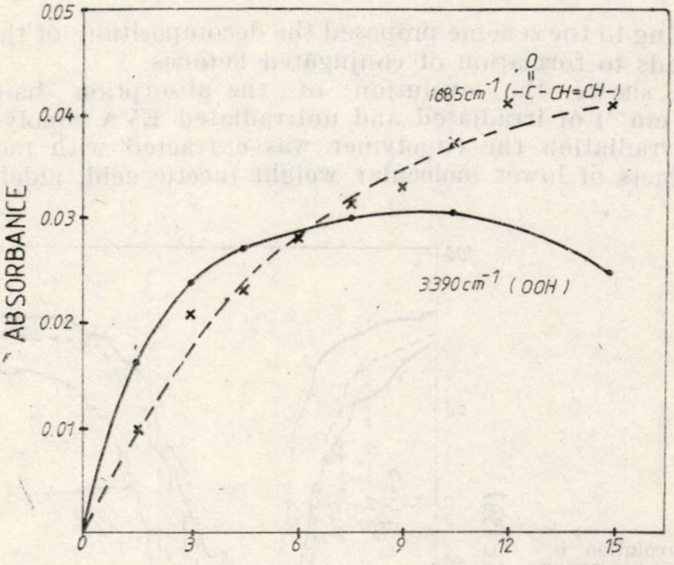

Fig. 3. – The dependence of IR absorption bands at 3390 cm^{-1} (OOH) and 1685 cm^{-1} $(-\overset{\overset{O}{\|}}{C}-CH=CH-)$ on the UV irradiation time for Levapren 450.

In establishing a reaction mechanism for photodegradation of EVA copolymers the quantitative determination of low molecular weight compounds formed during photodegradation is very useful indeed.

Buchanan and McGill [7] have effected such measurements at photodegradation of some poly(vinyl esters) in vacuum and have conceived-several possibilities of formation of degradation compounds.

Table 1 lists the composition of the mixture of low molecular weight compounds resulted from irradiation of EVA copolymer (45% vinyl acetate) in atmosphere.

It is worth noting that besides acetic acid, a relatively large amount of acetaldehyde is formed.

Table 1

Compounds resulted from irradiation of EVA copolymer (Levapren 450) at 27°C, three hours

Compound	% g ± 10 %
CH_3COOH	72.82
CH_3CHO	22.80
CO_2	0.19
CO	0.04
CH_4	4.15

The formation of acetaldehyde in the photodegradation of EVA copolymers may take place either through a type III Norrish mechanism:

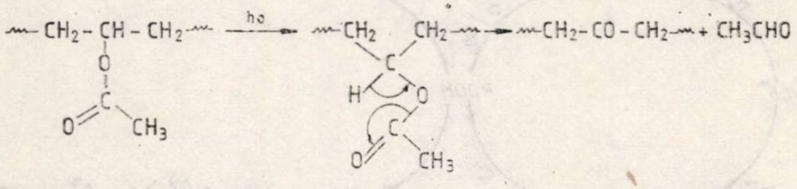

~CH₂–CH–CH₂~
hν
~CH₂
CH₂~
~CH₂–CO–CH₂~ + CH₃CHO
O
C
CH₃
H

(3)

or through a type I Norrish mechanism:

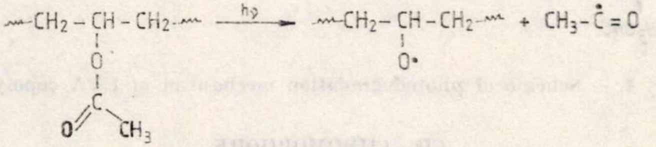

$$\sim CH_2-\underset{\substack{|\\ O\\ |\\ C(=O)CH_3}}{CH}-CH_2\sim \xrightarrow{h\nu} \sim CH_2-\underset{\substack{|\\ O\bullet}}{CH}-CH_2\sim + CH_3-\dot{C}=O \quad (4)$$

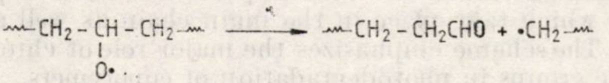

$$\sim CH_2-\underset{\substack{|\\ O\bullet}}{CH}-CH_2\sim \longrightarrow \sim CH_2-CH_2CHO+\bullet CH_2\sim \quad (5)$$

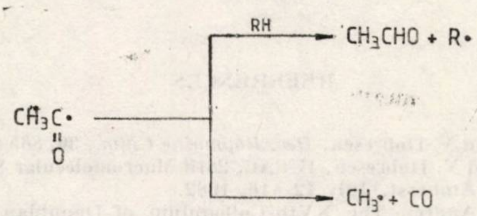

RH
CH₃CHO + R•
CH₃C•
O
CH₃• + CO

(6)

in the presence of oxygen:

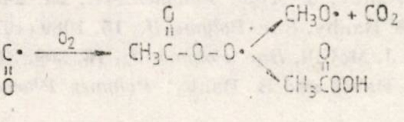

CH₃C•
O
O₂
CH₃C–O–O•
CH₃O• + CO₂
CH₃COOH

(7)

The photodegradation of copolymers through Norrish type I reactions should be accompanied by formation of compounds such as acetaldehyde, CO_2, CO and CH_4. However, part of these compounds (CO, CO_2, CH_4) could be formed through the photolysis of acetic acid which breaks off the copolymer by a type II Norrish reactions.[8]

The formation of aldehyde polymer groups according to Norrish I reaction is supported by the presence of the band at 1725 cm^{-1} in the spectrum of irradiated copolymer.

The data presented above allow the completion of the reaction mechanism scheme advanced earlier[1-4] (Fig. 4):

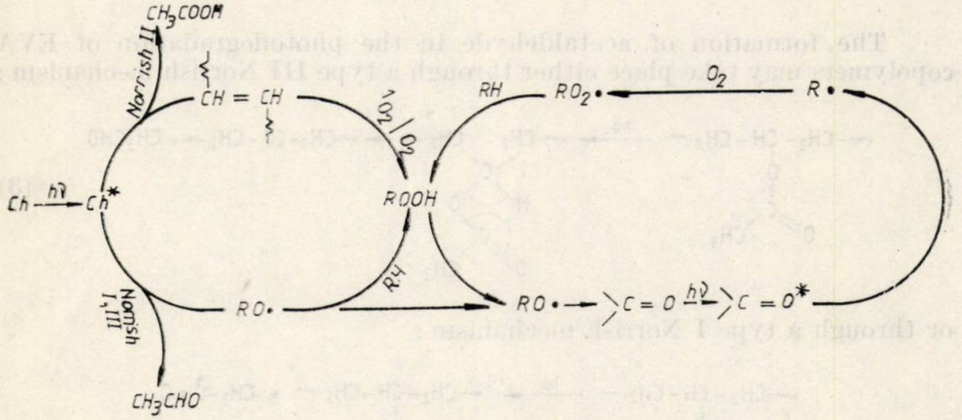

Fig. 4. — Scheme of photodegradation mechanism of EVA copolymers.

CH – CHROMOPHORE

This scheme includes the most important oxidative photodegradation reactions which take place in the main chain as well as in the side acetate group. The scheme emphasizes the major role of chromophoric and hydroperoxidic groups in photodegradation of copolymers.

REFERENCES

[1] C. Andrei, I. Hogea and V. Dobrescu, *Rev. Roumaine Chim.*, **30**, 865 (1985).

[2] C. Andrei, I. Hogea and V. Dobrescu, IUPAC, 28th Macromolecular Symposium, University of Massachusetts, Amherst, July 12—16, 1982.

[3] V. Dobrescu and C. Andrei, The XVth Colloquium of Danubian Countries for Natural and Artificial Ageing of Polymers, September 27—30, 1982, Moscow.

[4] V. Dobrescu, C. Andrei and I. Hogea, The 25th Microsymposium on Macromolecules "Processing and Long-Term Stabilities of Hydrocarbon Polymers", Prague, July 18—21, 1983.

J. F. Rabek and B. Ranby, *J. Appl. Polymer Sci.*, **23**, 2481 (1979).

[6] J. F. Rabek, J. Lucki, B. Ranby, *Eur. Polymer J.*, **15**, 1089 (1979).

[7] K. J. Buchanan and W. J. McGill, *Eur. Polymer J.*, **16**, 309, 313, 319 (1980).

[8] T. A. Skowronski, J. F. Rabek and B. Ranby, *Polymer Photochemistry*, **3**, 341 (1983).

Revue Roumaine de Chimie, **33**, *1*, 59–65 (1988)

COMPLEXES OF Pd(II), Cu(II), Hg(I) and Hg(II) WITH 1-METHYLTRIAZOL-DIETHYLAZOANILINE (I)

N. CALU and N. FOCA

Department of Chemical Technology, Polytechnic Institute, Splai Bahlui 71, Iaşi, Romania

Received May 26, 1986

The paper deals with a series of spectrophotometrical data, obtained by the study of interaction of the Pd(II), Cu(II), Hg(I) and Hg(II) ions with 1-methyltriazol diethylazoaniline. The data reported are based on the absorption spectra in the visible domain of the new complexes produced by interaction of the above-mentioned ions with azo dye. By interaction of the ligand with Pd(II), Cu(II), Hg(I) and Hg(II), the ML and ML_2 complexes can take form, detected by several spectrophotometrical methods. The stability constant was calculated for both ML and ML_2 complexes.

INTRODUCTION

The azopyrazolonic dyes, due to their structure, may work as ligands, forming complex compounds with cations of transitional metals. Three azo dyes were investigated i.e. 1-methyltriazol-diethylazoaniline (I), 3-methyl-5-pyrazolone-azobenzene (II) and 1-phenol-3-methyl-azopyrazolone (III). The qualitative studies have shown that only 1-methyl-triazodiethylazoaniline is able to form complex compounds with cations of transitional metals. This dye reacts with the Pd(II), Cu(II), Hg(I) and Hg(II) in acid medium, forming coloured complexes easy to be studied due to some important changes in electronic absorption spectra.[1]

EXPERIMENTAL

The azo dye that works as ligand is a brown powder with poor water solubility, having not solubilizant groups. This is soluble in a series of solvents such as strong mineral acids (HCL, H_2SO_4), dimethylformamide and certain organic acids as formic acid and acetic acid

In the present work the dye was employed as acetic solution, prepared by dissolution of the corresponding amount of dye in 100 cm^3 glacial acetic acid, diluted then with 0.1 N acetic acid up to one liter. The solution prepared in such a manner has pH $\approx$ 4–4.5. The concentration of the final solution was 1.10^{-3} mol.L^{-1}.

The cations of the metals were employed as solutions: $PdCl_2$ in HCl, i.e. $H_2[PdCl_4]$, pH = 1.5–2, $Cu(CH_3COO)_2$ in dimethylformamide, pH = 6, $Hg_2(NO_3)_2$ in HNO_3 20% and C_2H_5OH 80%, pH $\approx$ 3 and $HgCl_2$ in water, pH = 5. For each cation the adequate solvent was utilized. [2]

RESULTS AND DISCUSSION

The ligand with the molecular formula $C_{13}H_{18}N_6$ and the structure given below

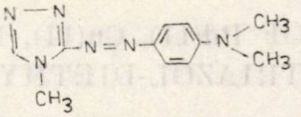

exhibits absorption bands in the UV-Visible domain, bands influenced by the solvent nature. [3]

The absorption spectra of the ligand in aqueous solution, alcohol and dimethylformamide (Fig. 1) show that the absorption band in the visible domain is influenced on both value at λ_{max} and molar absorption coefficient, ε_{max} (Fig. 1 and Table 1).

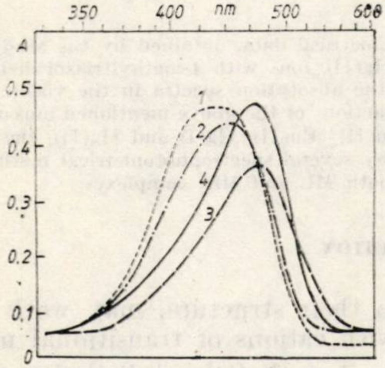

Fig. 1. — Electronic absorption spectra of the ligand (I) in ethanol, water, dimethylformamide and buffer: 1 — in DMF, $C = 1\cdot10^{-5}$ mol·L^{-1}; 2 — in ethanol, $C = 1\cdot10^{-5}$ mol·L^{-1}; 3 — in water, $C = 1\cdot10^{-5}$ mol·L^{-1}; 4 — in buffer with pH 6.25.

The spectra of figure 1 and the data set out in table 1 show that the strongest bathochromic and hyperchromic effect on I is that of buffer ($CH_3COONa + CH_3COOH$), pH = 6.25), the absorption maximum being located at 480 nm. This fact allows to choose the solvent for spectrophotometrical test of the solutions that contain the metal—ligand systems.

Table 1

Characteristics of the absorption bands in the spectra of figure 1, cell thickness 0.2 cm

Run	Medium	λ_{max} nm	ε_{max} L·mol^{-1}·cm^{-1}
1	D.M.F.	440	24.000
2	C_2H_5OH	455	29.600
3	H_2O	470	24.800
4	Buffer, pH = 6.25	480	30.500

Solutions with the Hg(I) and Hg(II) cations are colourless and present absorption bands in the UV domain only while those with Cu(II) exhibit absorption bands in both VIS and UV domain. Within VIS domain the absorption band of Cu(II) by the crystalline field type is situated towards 800—900 nm and does not apper in spectra for concentration of 1.10^{-4} mol/L and layer thickness of 0.2 cm.

In the case of solutions with Pd(II) there is the same situation. These remarks are necessary because the spectrophotometrical study of the metal-ligand systems was worked in the VIS region.

Reaction of (I) with Pd(II), Cu(II), Hg(I) and Hg(II)

The azo dye (I) that works as ligand reacts with the above-mentioned cations forming complex compounds. This fact is noticed in the changes that occur in the absorption spectrum of (I) in the visible domain.[1,3]

Reaction between ligand and the Pd(II), Cu(II), Hg(I) and Hg(II) cations is a rapid one, colour exchanges can be easily seen by formation of certain absorption bands proper to each system (Fig. 2 and Table 2).

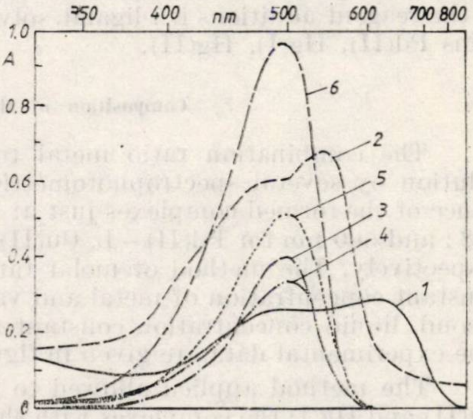

Fig. 2. — Electronic absorption spectra in the visible range of different metal-ligand systems: 1 — Pd(II) + L, 1 : 1, $C = 1 \cdot 10^{-4}$ mol.L^{-1}; 2 — Cu(II)+ +L 1 : 1, $C = 1 \cdot 10^{-4}$ mol·L^{-1}; 3 — Hg(I)+L, 1 : 1, $C = 2 \cdot 5 \times 10^{-5}$ mol·L^{-1}; 4 — Hg(I)+L, 1 : 2, $C = 1 \cdot 10^{-5}$ mol·L^{-1}; 5 — Hg(II) + L, 1 : 1, $C = 1 \cdot 10^{-4}$ mol.L^{-1}; 6 — Hg(II) + L, 1 : 2, $C = 1 \cdot 10^{-4}$ mol·L^{-1}

In the Pd(II).xL and Cu(II)—xL systems there are two absorption bands in the VIS domain. The former at 480 nm (curves 1 and 2, figure 2), proper to the ligand, and the latter is of change transfer ligand—metal type. In the case of the system Pd(II)—xL, the absorption band with charge transfer, proper to the complex, is situated at 620 nm and has the same intensity for $x = 1$ and 2, that points out the complex composition of 1 : 1, no matter whether the ligand amount is over. In the case of the Cu(II)—L, the charge transfer band, proper to the complex, is situated at 538 nm. The larger amounts of ligand modify λ_{max} with hypsochromic effects — shifting towards the bend proper to the ligand.

From the absorption spectra of different metal—ligand systems (Fig. 2) and from their characteristics given in table 2 it can be seen that in all cases, the absorption bands proper to the complexes are accompani-

Table 2

Characteristics of the absorption bands in the spectra of figure 2, cell thickness 0.2 cm

Run	System	Solvent	C, mol·L^{-1}	ε_{max} nm	λ_{max} L·mol^{-1}·cm^{-1}
1	Pd(II)—L(1 : 1)	C_2H_5OH	1.10^{-4}	620	14.500
2	Cu(II)—L(1 : 1)	C_2H_5OH	1.10^{-4}	538	23.600
3	Hg(I) —L(1 : 1)	C_2H_5OH	1.10^{-5}	500	40.000
4	Hg(I) —L(1 : 2)	C_2H_5OH	1.10^{-5}	500	60.000
5	Hg(II)—L(1 : 1)	H_2O	1.10^{-4}	505	26.000
6	Hg(II)—L(1 : 2)	H_2O	1.10^{-4}	505	49.000

nied by a batochromic effect, the largest of them being in the case of Pd(II)—L and Cu(II)—L systems. On the other hand in the case of the Hg(I)—L 1 : 1 and 1 : 2 and Hg(II)—L, 1 : 2 systems, in the absorption spectra a strong hyperchromic effect is exhibited, the value of ε_{max} being the largest one.[1]

The optimal test conditions, i.e. pH, order of adding of solutions, necessary time for spectrophotometrical determinations, were established on the basis of the above observations. This fact was necessary because for Pd(II)—L, Hg(I)—L and Hg(II)—L the reading of absorbance must be done at instant of putting reactants together; otherwise in the above-mentioned systems the complexes become solids. Consequently, the order of the reagent additions is: ligand, solvent and then the solution that contains Pd(II), Hg(I), Hg(II).

Composition of the complexes

The combination ratio metal to ligand was determined on fresh solution by several spectrophotometrical methods, measuring the absorbance of the formed complexes just at λ_{max} proper to each system, i.e. 620; 538; and 500 nm for Pd(II)—L, Cu(II)—L and Hg(I)—L, and Hg(II)—L respectively. The method of molar ratio was applied in two ways: first, constant concentration of metal and variable concentration of ligand and second, liquid concentration constant and metal concentration variable.[4] The experimental data are given in figures 3 a and 3 b.

The method applied allowed to see that in the case of Pd(II) and Cu(II) and Hg(I) the complexes with the ratio 1 : 1 are evident while in the case of Hg(II) the intercept of the straight line of different slopes proves the formation of two complexes, Hg(II)—L 1 : 1 and 1 : 2 (Figs 3a and 3b).

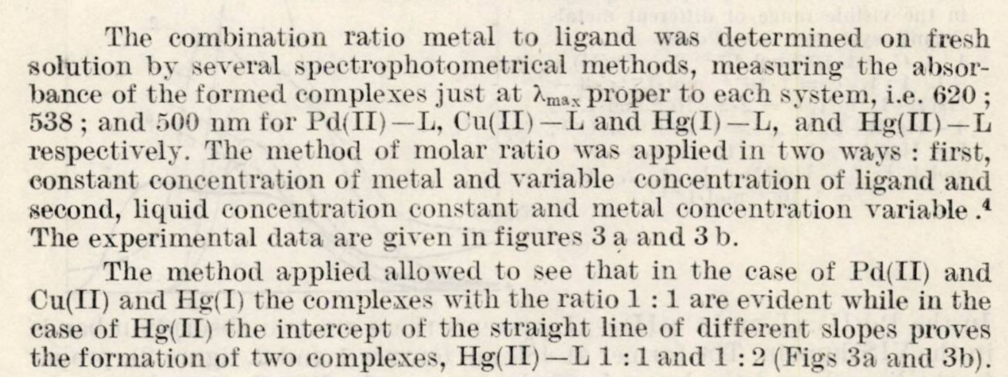

Fig. 3. — Dependence of absorbance on molar ratio: *a* — L/M; 1 — Pd(II) — L; 2 — Cu(II)— — L; 3 — Hg(II) — L; 4 — Hg(I) — L; *b* — M/L: 1 — Pd(II) — L; 2 — Cu(II) — L; 3 — — Hg(I) — L; 4 — Hg(II) — L.

Applying the Job method [5] for each system separately we got the data showing that in the case of Pd(II) and Cu(II) the complexes obtained have the metal to ligand ratio of 1 :1 while in the case of Hg(I)—L and Hg(II)—L, the method evidences formation of the complexes with the 1 M : 2 L ratio (Fig. 4).

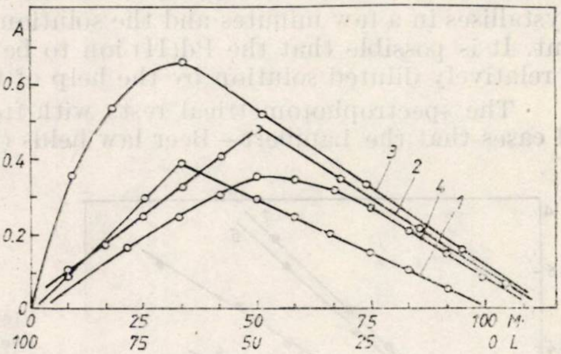

Fig. 4. — Job's curves :
1 — Cu(II) — L ; 2 — Pd(II)— L ;
3 — Hg(I) — L, 4 — Hg(II) — L

On the basis of the experimental data the following equilibriums in the complexes formation exist

$$M + L \rightleftharpoons M L$$

$$M L + L \rightleftharpoons ML_2$$

The spectrophotometrical data did not prove the step by step formation of the ML_2 complexes.

Structure of formed complexes, with the metal—ligand bond is included in the general formulation of the complexes with azo dyes ligands (L)[6-9] with a planar-square configuration and mixt ligands : X + L. The structural formulas of these complexes, for M : L equal to 1 : 1 and 1 : 2, are given below.

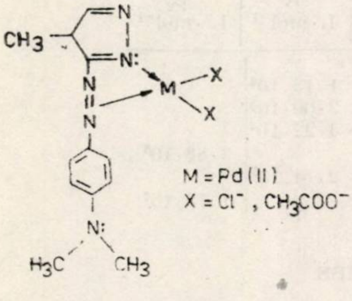

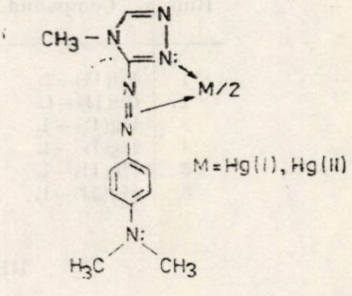

The azo group of the ligand involved in the absorption band at 455 nm participates in the metal—ligand bands, a fact proved by the pronounced batochromic displacement in the absorption spectra of the complexes. Otherwise, the coordination of such a type ligand, also by the azo group, was proved by Porter, Murray and Heck.[10-11]

In three cases, i.e. Pd(II)—L, Hg(L) and Hg(II)—L the complexes resulted are crystalline and can be separated from solution. The reaction between Pd(II) and I is a total one. In the aqueous medium the complex crystallises in a few minutes and the solution remains completely transparent. It is possible that the Pd(II) ion to be determined gravimetrically in relatively diluted solution by the help of this azo dye.

The spectrophotometrical tests with fresh solutions have shown in all cases that the Lambert—Beer law helds (Fig. 5).

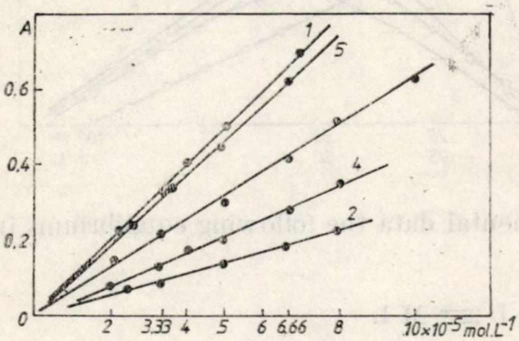

Fig. 5. — Verification of the Lambert-Beer law: 1 — Pd(II) — L; 2 — — Cu(II) — L; 3 — Hg(II) — L; 4 — — Hg(I) —L; 1 : 1; 5 — Hg(I) —L, 1 : 2.

Stability of the complexes

For the M : L complexes the stability was appreciated from the data obtained by the method of continued variation i.e. Turner—Anderson's method,[12] and for the ML_2 complexes by Turner—Anderson and Edmonds-Birnbaum's method.[13] The data obtained are presented in table 3.

Table 3

Stability constants of the studied compounds

Run	Compound	Molar	K $L \cdot mol^{-1}$	β_2 $L^2 \cdot mol^{-1}$
1	Pd(II)—L	1 : 1	$1.13.10^4$	
2	Cu(II)—L	1 : 1	$3 \cdot 00 \cdot 10^3$	
3	Hg(I) —L	1 : 1	$4 \cdot 22 \cdot 10^4$	
4	Hg(I) —L	1 : 2		$3 \cdot 88 \cdot 10^6$
5	Hg(II)—L	1 : 1	$2.\ 4.10^5$	
6	Hg(II)—L	1 : 2		$1.15.10^7$

REFERENCES

[1] I. Pogany and M . Banciu, "Metode fizice în chimia organică", Ed. Ştiinţifică, Bucharest, 1972.

[2] L. Kekedy, "Chimie analitică calitativă" Ed. Scrisul Românesc, Craiova, 1982.

[3] M. Răileanu, "Influența mediului asupra reactivității chimice", Ed. Scrisul Românesc, Craiova, 1981.

[4] J. Yoe and A. Jones, *Ind. Eng. Chem. Anal.*, **16**, 111 (1944).

[5] P. Job, *Liebigs Ann. Chem.*, **1928**, 113.

[6] A. C. Cope and R. W. Siekman, *J. Amer. Chem. Soc.*, **87**, 3272 (1965).

[7] R. F. Heck, *J. Amer. Chem. Soc.*, **90**, 313 (1968).

[8] J. P. Kleiman and M. Dubeck, *J. Amer. Chem. Soc.*, **85**, 1544 (1963).

[9] M. M. Bagga, P. L. Pauson, F. J. Preston, and R.I. Reed, *Chem. Comm.*, **543** (1965).

[10] J. J. Porter and J. L. Murray, *J. Amer. Chem. Soc.*, **87**, 1628 (1965).

[11] R. F. Heck, *J. Amer. Chem. Soc.*, **90**, 313 (1968).

[12] S. E. Turner and R. G. Anderson, *J. Amer. Chem. Soc.*, **71**, 912 (1949).

[13] S. Edmonds and N. Birnbaum, *J. Amer. Chem. Soc.*, **63**, 1471, (1941).

Revue Roumaine de Chimie, 33, *1*, 67–74 (1988)

COMBINAISONS COMPLEXES DU Tl(III) AVEC DES LIGANDS DU TYPE DES HÉTÉROCYCLES ORGANIQUES. III[1]

SPECTRES D'ABSORPTION INFRAROUGE

I. BERDAN et I. SANDU
Institut Polytechnique « Gh. Asachi », Iassy
Faculté de Technologie Chimique, Iassy, Roumanie

Reçu le 20 décembre 1986

The infrared spectra of crystalline complexes of thallium (III) halides, TlX_3, with nitrogen donors such as heterocyclic derivatives (thiazole, imidazole, pyridine, pyrazine and pyridazine) have been recorded in the frequency region 5000. . .200 cm^{-1}. From the study of the vibrational frequencies associated with the thallium-halogen and thallium-nitrogen stretching modes, definite conclusions are possible concerning the molecular structures of these species. The infrared spectrum of complexes in the low frequency region (400. . . 200 cm^{-1}) shows vibrational modes ν_{Tl-X} at sufficiently high frequencies to be attributable to cationic species such as $[TlL_2X_2]^+$ and $[TlL_3]^{3+}$.

Les auteurs présentent l'étude des spectres infrarouge (5000 . . . 200 cm^{-1}) d'une nouvelle série de combinaisons complexes des halogénures de Tl(III), TlX_3, avec des ligands du type des hétérocycles organiques ayant la fonction N-donneuse tels que : dérivés de thiazole, d'imidazole, pyridine, pyrazine et pyridazine. A partir de l'analyse des fréquences de vibration des liaisons Tl—N, Tl—X et Tl—O, on admet la formation de complexes cationiques mononucléaires.

1. PARTIE THÉORIQUE

Les halogénures de Tl(III), TlX_3 (X = Cl, Br) forment avec les ligands N-donneurs du type des hétérocycles organiques (pyridine, quinoline, pyrazine, etc.) des combinaisons complexes de compositions variables.[2–4] Les études de ces complexes n'offrent cependant pas assez d'informations pour pouvoir interpréter leur structure et, souvent, les conclusions sur ce problème sont contradictoires. Ainsi, dans une série d'études[5–6] on admet que l'ion Tl(III) des complexes avec les ligands ci-dessus mentionnés se trouve sous forme d'anion complexe, $[TlX_n]^{+3-n}$ à côté de la base protonée, $[LH]^+$, provenant du ligand L. D'autres auteurs, [7–8] en se basant sur l'étude des spectres d'absorption dans l'ultraviolet, visible infrarouge et Raman, mettent en évidence la formation de nouvelles liaisons, Tl-N, Tl-O, correspondant à des symétries différentes des complexes thalliques.

C'est en cet esprit que nous avons abordé, dans les travaux publiés antérieurement,[1,9-10] le problème de la synthèse et la caractérisation d'une nouvelle série de combinaisons complexes des halogénures de thallium TlX_3 (X = Cl, Br) avec les ligands suivants : benzthiazole (BT), amino-2-benzthiazole (ABT), benzimidazole (BI), N-benzyle-benzimidazole (BBI), l'acide benzimidazolyle-2-carboxylique (ABIC), les acides pyridinmonocarboxyliques : 1,2 (PIC) ; 1,3 (NIC) ; 1,4 (INIC), la benzocinnoline (BC) et la quinoxaline (QUIN). Les données de l'analyse élémentaire, les déterminations de masses molaires et les caractéristiques des spectres électroniques ont indiqué la formation des complexes mononucléaires, de compositions variables représentées par les formules brutes suivantes : $TlX_3 \cdot 2BT$, $TlX_3 \cdot 2ABT$, $TlX_3 \cdot 2BI$, $TlX_3 \cdot 2BBI$, $TlX_3 \cdot 2ABIC$, $TlX_3 \cdot 2PIC$, $TlX_3 \cdot 3NIC$, $TlX_3 \cdot 3INIC$, $TlX_3 \cdot 2QUIN$, $TlX_3 \cdot 2BC$.

En poursuivant ces études, dans ce travail on présente de nouvelles données concernant la structure de ces complexes, obtenues par spectroscopie d'absorption infrarouge dans le domaine 5000...200 cm^{-1}.

2. PARTIE EXPÉRIMENTALE

Les complexes ont été préparés et purifiés suivant des méthodes décrites dans un travail antérieur.[2]

Les spectres d'absorption infrarouge dans le domaine des hautes fréquences, 5000 ... ... 400 cm^{-1} ont été enregistrés à l'aide d'un spectrophotomètre du type SP–200 alors que le domaine des basses fréquences a été investigué en utilisant l'appareil du type Perkin-Elmer 325. On a utilisé également le spectrophotomètre UR–20 pour l'étude du domaine 700...400 cm^{-1}.

Dans le domaine de 5000 à 400 cm^{-1} les spectres ont été obtenus à partir d'échantillons préparés par pastillage en milieu de KBr. Dans le domaine des basses fréquences, les spectres ont été enregistrés sur des suspensions dans du Nuyol soutenues par des fenêtres de polyéthylène d'épaisseur convenable, de sorte que la déformation de celle-ci sous l'action des rayons infrarouges soit négligeable. L'utilisation des fenêtres de CsI n'a pas été possible en raison de la forte affinité du thallium vis-à-vis de l'ion iodure.

3. RÉSULTATS ET DISCUSSIONS

L'étude des spectres d'absorption infrarouge apporte des informations utiles sur le mode de coordination des ligands à l'ion Tl(III) et donc sur la structure des complexes formés. Les résultats expérimentaux nous ont permis de mettre en évidence tant l'apparition de nouveaux modèles de vibration (Tl–N, Tl–O, Tl–S, etc.) ainsi que la conservation des modes de vibration propres aux liaisons Tl–X avec les modifications dues au processus de coordination.

3.1. Etude du domaine de 5000 cm^{-1} à 400 cm^{-1}

L'étude des spectres dans le domaine infrarouge se base sur l'analyse des modifications concernant la position et l'intensité des bandes d'absorption caractéristiques aux ligands libres qui apparaissent lorsqu'il réagissent avec les halogénures de Tl(III).

En ce qui concerne les spectres des complexes avec les dérivés de thiazole, $TlX_3 \cdot 2BT$ et $TlX_3 \cdot 2ABT$, on remarque tant la conservation des bandes qui correspondent aux vibrations des noyaux aromatiques (benzéniques et thiazoliques) qu'une série de modifications des bandes associées aux vibrations $\nu_{C=N}$, ν_{NH_2} et $\nu_{C=C}$.

Ainsi, dans les spectres des complexes $TlX_3 \cdot 2BT$ (fig. 1), la bande de la vibration $\nu_{C=N}=1650$ cm^{-1} propre au ligand libre apparaît à 1658 cm^{-1} (X = Cl) respectivement 1657 cm^{-1} (X = Br). D'autre part, les vibrations $\nu_{C=S}$, (720 cm^{-1}), ν_{CH}(3100—3080 cm^{-1}), ainsi que les vibrations de déformation des cycles (1120 cm^{-1} et 880—890 cm^{-1}) ne sont pas affectées. Ce résultat vient donc confirmer le fait que la coordination des ligands à l'ion métallique central se réalise par l'atome d'azote donneur.

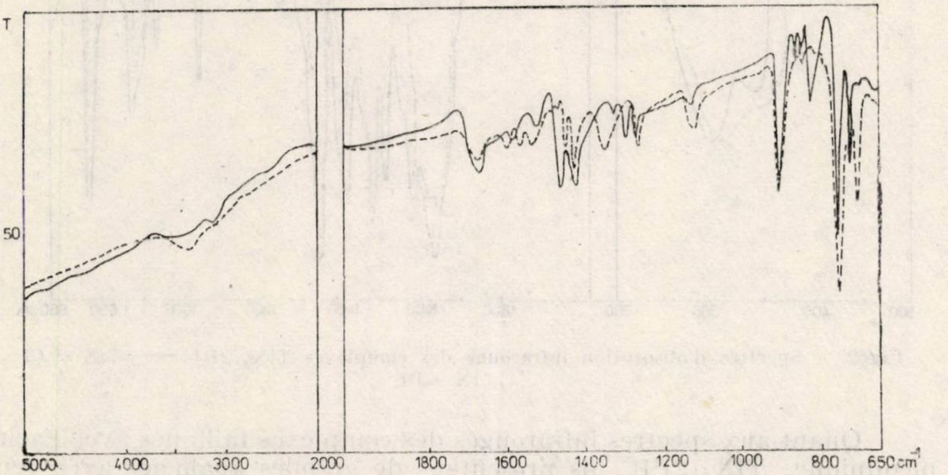

Fig. 1. — Spectres d'absorption infrarouge des complexes $TlX_3 \cdot 2BT$; ——— X = Cl ; ...... X = Br.

L'étude des spectres infrarouges des complexes avec les dérivés d'imidazole, $TlX_3 \cdot 2BI$, $TlX_3 \cdot 2BBI$ et $TlX_3 \cdot 2ABlC$, montre l'existence de trois vibrations principales des ligands libres[11] : la vibration du cycle imidazolique (700—880 cm^{-1}), $\nu_{C-C(arom.)}$(1500—1600 cm^{-1}) et $\nu_{NH(associé)}$ (2900—3200 cm^{-1}) (fig. 2). La protonation du groupement >NH de la molécule de ligand n'est pas possible car la vibration associée au mode $\nu_{[>NH_2]^+}$ n'apparaît pas dans l'intervalle attendu (2000—2800 cm^{-1}). De même, le déplacement de la fréquence de vibration $\nu_{C=N}=1630$ cm^{-1} de l'imidazole à des valeurs plus basses (1620 cm^{-1} pour X = Cl et 1622 cm^{-1} pour X = Br) prouve le caractère azote-donneur du ligand.

Les spectres des complexes $TlX_3 \cdot 2ABIC$, représentés sur la fig. 3, attestent, tout d'abord, la participation du groupement —COOH à la coordination de ABIC à l'ion Tl(III). En effet, la vibration de valence antisymétrique ν_{COO}, la plus sensible lors du processus de coordination, qui apparait dans le spectre du ligand libre à 1748 cm^{-1}, est déplacée à des fréquences beaucoup plus basses : 1640 cm^{-1} (X = Cl) respectivement 1610 cm^{-1} (X = Br). L'accroissement de la fréquence dans la série Br < Cl est corrélé avec l'augmentation du caractère covalent de la liaison Tl—O dans la structure des complexes chélates formés.

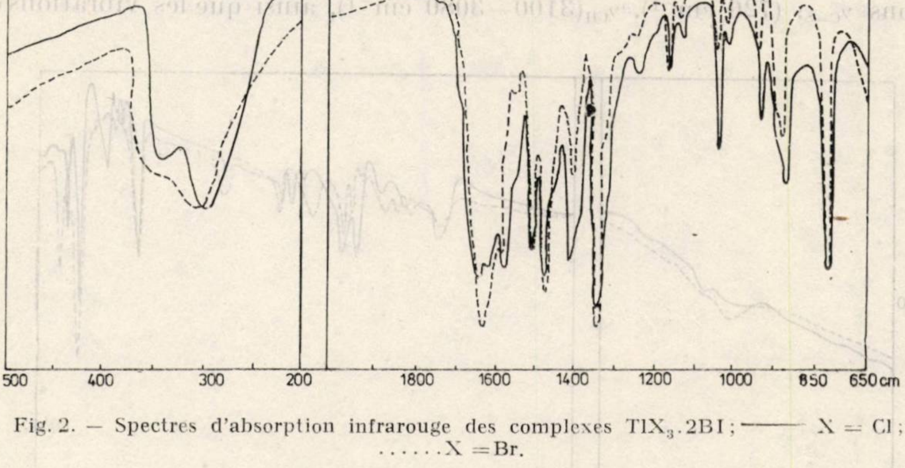

Fig. 2. — Spectres d'absorption infrarouge des complexes $TlX_3.2BI$; ——— X = Cl ; ......X = Br.

Quant aux spectres infrarouges des complexes talliques avec l'acide picolinique, $TlX_3 \cdot 2PIC$, ils présentent de grandes analogies avec ceux du type $TlX_3 \cdot 2ABIC$. Donc une structure chélatique peut être attribuée aux complexes avec le ligand PIC dont les spectres indiquent la modification de la vibration antisymétrique $\nu_{as,COO} = 1739\ cm^{-1}$; celle-ci apparaît

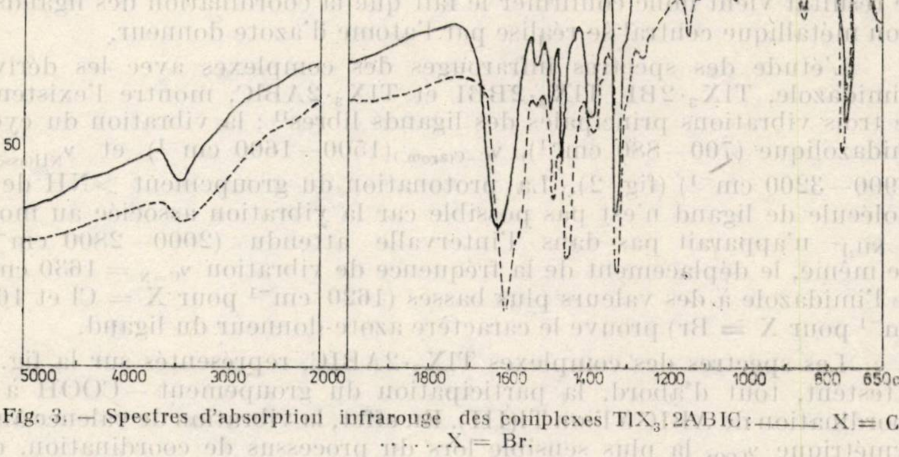

Fig. 3. — Spectres d'absorption infrarouge des complexes $TlX_3.2ABIC$: ——— X = Cl ; ......X = Br.

dans les spectres des complexes dans l'intervalle 1600—1680 cm^{-1}. De plus, la formation de la liaison Tl—O dans les molécules des complexes est indiquée par l'apparition dans les spectres infrarouges d'une bande d'absorption (430—435 cm^{-1}) associés au mode de vibration ν_{Tl-O}.

Les caractéristiques spectrales des complexes avec les dérivés de pyrazine et pyridazine, $TlX_3 \cdot 2QUIN$ et $TlX_3 \cdot 2BC$ sont données dans le tableau 1. L'interprétation de ces spectres est difficile à cause de la superposition des modes de vibration des ligands. Bien que certaines vibrations de squelette des ligands subissent des modifications lors du processus de coordination, une relation directe entre les déplacements de fréquences caractéristiques et la basicité des ligands (QUIN<BC) n'est pas évidente.

Tableau 1

Caractéristiques spectrales i.r. des complexes $TlX_3 \cdot 2QUIN$ et $TlX_3 \cdot 2BC$ et des ligands libres

Type de vibration	Fréquences caractéristiques (cm^{-1})					
	QUIN	$TlX_3 \cdot 2QUIN$		BC	$TlX_3 \cdot 2BC$	
		X = Cl	X = Br		X = Cl	X = Br
ν_{CH}	3060	—	—	—	—	—
	3120	3120	3108	3250	3280	3274
	3045	—	—	—	—	—
Vibrations de noyaux (ν)	1584	1640	1600	1606	1660	1650
	1523	—	—	1570	1568	1563
	1490	1445	1470	1450	1451	1458
	1418	1390	1395	1400	1410	1426
	1342	—	—	1373	1260	1261
β_{CH}	1232	1210	1208	1170	1187	1174
	1148	1170	1169	1120	1120	1119
	1067	1030	1053	1060	1085	1084
γ_{CH}	950	960	970	893	900	920
	804	880	879	830	820	828
	753	765	780	765	757	751

3.2. Etude du domaine de 400 cm^{-1} à 200 cm^{-1}

L'étude des spectres infrarouges des complexes thalliques dans le domaine 400. . .200 cm^{-1}, dans lequel, en général, les ligands libres ne présentent pas d'absorption, met en évidence tant la conservation des liaisons Tl—X, avec les modifications dues au processus de coordination, ainsi que l'apparition de nouveaux modèles de vibration propres aux liaisons formées, telles que : Tl—N, Tl←O. Ainsi, dans les spectres lointain infrarouge des complexes du type $TlX_3 \cdot 2BT$ (fig. 4) on remarque non seulement l'existence d'une bande d'absorption propre au ligand libre, située à 363 cm^{-1}, mais aussi d'une autre bande associée au mode de vibration ν_{Tl-X}, avec les fréquences suivantes : 300 cm^{-1} (doublet pour X=Cl) et 265 cm^{-1} (X=Br). En ce qui concerne la fréquence de vibration ν_{Tl-N}, la littérature indique un domaine assez large : 200. . .240 cm^{-1}.[12] De fait, la bande d'absorption située à 216—218 cm^{-1} peut être attribuée à la vibration ν_{Tl-N}.

Il est intéressant de noter que les fréquences de vibration symétrique ν_{Tl-X} s'accroissent lors du passage des espèces anioniques du type $[TlX_n]^{+3-n}$ aux complexes cationiques.[13] C'est pourquoi et tenant compte que les fréquences de vibration ν_{Tl-X} des complexes étudiés sont beaucoup plus élevées par rapport aux anions du type $[TlX_4]^-$ ou $[TlX_6]^{3-}$, nous admettons que l'ion Tl(III) forme avec les ligands mentionnés des complexes cationiques des types : $[TlL_2X_2]^+$ ou $[TlL_3]^{3+}$, où L=ligand bidenté.

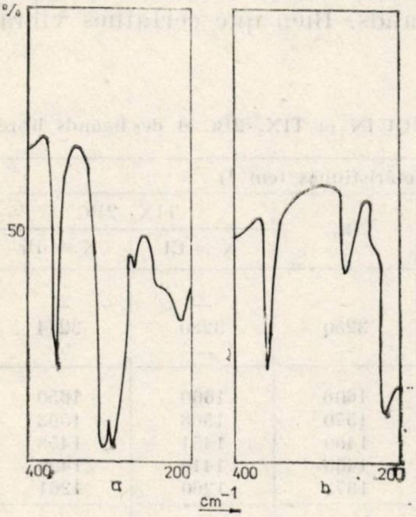

Fig. 4. — Spectres d'absorption lointain infrarouge (400. . .200 cm^{-1}) des complexes $TlX_3.2BT$; a. X = Cl ; b. X = Br.

L'étude des spectres des complexes avec les dérivés d'imidazole, dont les caractéristiques sont présentées dans le tableau 2, permet d'établir quelques corrélations. Ainsi, le décroissement de la fréquence de vibration ν_{Tl-X} avec le changement du ligand dans la série : BBI<BI<ABIC correspond à la diminution de la force de la liaison Tl—X due à l'augmentation de la force de la liaison Tl—N.[14]

Quant aux complexes thalliques avec les acides pyridine-monocarboxyliques, dont les caractéristiques sont présentées dans le tableau 3, les spectres lointain infrarouge sont parmi les plus évidents. Remarquons la forte analogie que présentent les spectres de ces complexes avec ceux du type $TlX_3\cdot2ABIC$ tant au point de vue de l'intensité qu'au point de vue de la position des bandes. Cette ressemblance confirme la formation des complexes du type : $[TlL_2X_2]^+X^-$, où L=PIC et $[TlL_3X_3]$, où L=NIC,

Tableau 2

Caractéristiques spectrales i.r. des complexes $TlX_3\cdot2BI$ et $TlX_3\cdot2BBI$

Complexe	ν_{Tl-Cl} (cm^{-1})	ν_{Tl-Br} (cm^{-1})	ν_{Tl-N} (cm^{-1})
$TlCl_3\cdot2BI$	300, 270	—	218
$TlBr_3\cdot2BI$	—	265	216
$TlCl_3\cdot2BBI$	291, 268	—	210
$TlBr_3\cdot2BBI$	—	260	212

INIC, correspondant à une symétrie octaédrique. D'autre part, les faibles différences entre les valeurs des fréquences de vibration pour les complexes avec le même ligand montrent le même type d'isomère géométrique, probablement, la configuration cis-octaédrique.[15]

Tableau 3

Caractéristiques spectrales des complexes du Tl(III) avec les acides pyridine-monocarboxyliques dans le domaine 400...200 cm^{-1}

Complexe	ν_{Tl-Cl} (cm^{-1})	ν_{Tl-Br} (cm^{-1})	ν_{Tl-N} (cm^{-1})
$TlCl_3 \cdot 2PIC$	290	—	213
$TlBr_3 \cdot 2PIC$	—	263	210
$TlCl_3 \cdot 3NIC$	291	—	208
$TlBr_3 \cdot 3NIC$	—	265	206
$TlCl_3 \cdot 3INIC$	282	—	216
$TlBr_3 \cdot 3INIC$	—	257	214

La similitude des spectres des complexes $TlX_3 \cdot 2QUIN$ et $TlX_3 \cdot 2BC$ (fig. 5), concernant les fréquences de vibration ν_{Tl-X} n'est pas en accord avec la modification de la basicité des ligands, QUIN<BC, qui devrait produire une variation inverse de la fréquence ν_{Tl-X}. Cela est dû certainement à l'existence dans la molécule des complexes $TlX_3.2BC$ à deux atomes d'azote non équivalents comme résultat de la fonction mono-dentée du ligand BC.

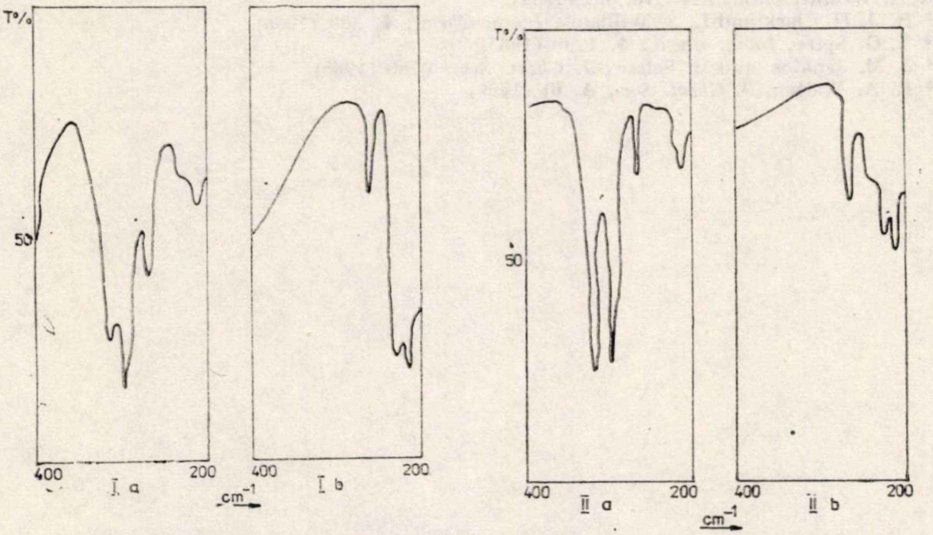

Fig. 5. — Spectres d'absorption lointain infrarouge (400 ... 200 cm^{-1}) des complexes thalliques avec les dérivés de pyrazine, $TlX_3 \cdot 2QUIN$(I) et de pyridazine, $TlX_3 \cdot 2BC$(II) : a. X = Cl ; b. X = Br.

4. CONCLUSIONS

L'étude des spectres infrarouges des complexes des halogénures de Tl(III), TlX_3 ($X=Cl$, Br), avec des ligands N-donneurs du type des hétérocycles organiques offre une série d'informations utiles concernant l'apparition de nouveaux modèles de vibration, ν_{Tl-N}, ν_{Tl-O}, mais aussi la conservation des vibrations ν_{Tl-X}. D'une manière générale, l'abaissement des fréquences de vibration ν_{Tl} au fur et à mesure que la basicité des ligands s'accroît peut constituer un critère d'évalution de l'augmentation de la force de liaison Tl—N.

BIBLIOGRAPHIE

[1] I. Berdan et N. Calu, *Bul. Inst. Politeh. Iași*, **27** (31), 1—2, p. 9 (1981).

[2] F. A. Cotton, B. F. G. Johnson et R. M. Wing, *Inorg. Chem.*, **4**, 502 (1965).

[3] B. F. G. Johnson et R. A. Walton, *Inorg. Chem.*, **5**, 49 (1966).

[4] N. S. Giel, R. N. Nutall, D. F. Scaife et D. W. A. Sharp, *J. Inorg, Nuclear Chem.*, **18**, 79 (1961).

[5] A. J. Carty. *Coord. Chem. Rev.*, **4**, 29 (1969).

[6] R. A. Walton, *J. Inorg. Nuclear. Chem.*, **32**, 2875 (1970).

[7] A. G. Lee, *J. Chem. Soc.*, A, **7** (1971).

[8] R. A. Walton, *Coord. Chem. Rev.*, **6**, 1 (1971).

[9] I. Berdan, *Bul. Inst. Politeh. Iași*, **26** (30), 3—4, 21 (1980).

[10] I. Berdan, D. Ancuța et I. Sandu, *Rev. Roumaine Chim.*, **30**, 1031 (1985).

[11]. R. Wright, *Chem. Rev.*, **48**, 397 (1951).

[12] R. J. H. Clark and L. S. Williams, *Inorg. Chem.*, **4**, 350 (1965).

[13] T. G. Spire, *Inorg. Chem.*, **4**, 1290 (1965).

[14] J. M. Jenkins and B. Schaw, *J. Chem. Soc.*, 6780 (1965).

[15] R. A. Walton, *J. Chem. Soc.*, **A**, **61** (1969).

Revue Roumaine de Chimie, **33**, *1*, 75–81 (1988)

ANILINE COMPLEXES WITH IODINE ACCEPTOR

MIHAELA BUGEANU * and V. EM. SAHINI **

*** Polytechnic Institute, Faculty of Electronics and Telecommunications, Department of Physics, Spl. Independenței 313, Bucharest, Romania**
**** Polytechnic Institute, Department of Physical Chemistry, Blvd. Republicii 13, Bucharest, Romania**

Received May 18, 1986

The present paper contributes to the elucidation of the electronic structure of the aniline-iodine charge transfer complexes. The stability constants and the dipole moments are obtained by different methods. The structural aspects of these complexes are obtained by the Mulliken analysis and EHT calculations.

INTRODUCTION

Aniline-iodine complexes have been reported in the literature since 1959, starting with Tsubomura's paper.[1] Evidence of these complexes is of great importance as it raises the problem of the way in which the corresponding amine acts as donor. In the aniline complexes with iodine the question arises of whether the orbital that contains the donated electron is located on nitrogen or on the whole ring and hence, whether amines functions as n or π donors.

The subsequent studies of Tsubomura [2] furnish evidence that the major transfer interaction is located on nitrogen with a high degree of transfer from this atom to iodine. The complexes are of medium strength. Electronic spectroscopy studies as well as those carried out by IR and NMR techniques likewise reveal this main interaction. [3-6] The polarity of the molecule in the ground state is well described by the dipole moments obtained experimentally. [7]

The present paper is an attempt to characterize iodine-aniline complexes from the viewpoint of their electronic stability and structure.

EXPERIMENTAL

Various aniline derivatives with N- or ring-substituents (Me, Ph, OMe) were used. Iodine was resublimated. The solvents "Reactivul" were distilled and dried and had the physical constants shown in the literature.

The spectra were obtained with a "Specord UV – VIS" and "Specord IR" spectrophotometer; the dielcometric measurements were performed with an "Oehme 600 RL" diescometer. The refraction index was measured with an Abbé refractometer. Concentration. used were 10^{-3} mol/L iodine and 10^{-2}/L donor for determining the stability constants-

In order to determine the dipole moments we worked within the 10^{-2} mol/L acceptor and 10^{-1} mol/L donor range.

The IR spectrum was obtained in solution in a concentration of 10^{-2} mol/L acceptor and 10^{-1} mol/L donor. The solution density was measured with a pycnometer. The solvent was carbon tetrachloride, and the working temperature 25°C.

RESULTS

Evidence of the complexes is supplied by a shoulder in the UV spectrum within the 300–400 nm range, reported in the literature.

Two methods were used for demonstrating the CT band of these complexes :

I. decrease of amine absorbance from the total absorbance ;

II. starting from the idea that the absorbance $A(\lambda)$ is a function of the wavelength and the experimental curve presents an inflection point, this was considered to be the maximum of absorption of the complex. The absorption maxima are shown in table 1.

Table 1

λ_{CT} absorption maxima of the aniline-iodine complexes

Donor	λ_{CTmax} (method I) (nm)	λ_{CTmax} (method II) (nm)
Aniline	330	332
N-Methylaniline	353	355
N,N-Dimethylaniline	363	363
p-Toluidine	341	345
o-Toluidine	338	338
p-Anisidine	372	370
o-Anisidine	334	356
Diphenylamine	420	420

Using the experimental absorption for λ_{max} CT, the stability constants can be calculated by Scott's method.[8] The values of K, complexity constant, are given in table 2.

Table 2

Stability constants for aniline iodine complexes

Donor	K L. mol^{-1}	K^3	$-\Delta G^0$ (kcal/mol)
Aniline	9.1	8.76	1.28
N-Methylaniline	20.5	20.4	1.78
N,N-Dimethylaniline	19.2		1.35
p-Toluidine	13.8	13.81	1.91
o-Toluidine	11.2	12.4	1.49
o-Anisidine	21.4		
p-Anisidine	18.5	18.0	1.71

The dipole moments are obtained by Guggenheim's method, and are shown in table 3.

Table 3

The values of dipole moments for the aniline-iodine complexes

Donor	μ_{exp} (Guggenheim)
Aniline	6.3
N-Methylaniline	6.7
N,N-Dimethylaniline	6.2
p-Toluidine	6.7
o-Toluidine	6.5
p Anisidine	7.6
o-Anisidine	6.7
Diphenylamine	1.99

The complexes can also be evidenced by IR spectroscopy. In the IR spectra of the complex changes can be observed as revealed by shifts of 20 to 60 cm^{-1} of the NH and CN stretching bands of the C—N stretching vibration (Table 4). The spectrum aso shows new bands within the 900—700 cm^{-1} region.

Table 4

Frequency shifts in IR spectrum of the aniline-iodine complexes

Complex	N—H (cm^{-1}) symmetrical	N—H (cm^{-1}) antisymmetrical	C—N (cm^{-1})
Aniline · Iodine	42	61	21
N-Methylaniline — Iodine	38	54	27
N,N′-Dimethylaniline · Iodine	25	42	25
o-Toluidine · Iodine	48	57	31
p Toluidine · Iodine	31	48	36
o-Anisidine · Iodine	52	63	41
p-Anisidine · Iodine	42	52	45

THEORETICAL RESULTS

With the view of elucidating the electronic structure of these complexes, EHT calculations were performed by measuring the charge distribution in the ground state and the values of dipole moments. A variable geometry was considered, wherein the nitrogen-to-iodine distance was varied from 2 to 3 Å. Moreover, the HNH angle received different values, the best value being that which is in keeping with the experimental data. The values of theoretically calculated dipole moments as well as the corresponding distances and angles are given in table 5.

Following the intermolecular charge transfer, the most marked charge decrease appears on the nitrogen atom. The difference between the charge on the atoms within the benzene ring in the complex and the charge in the free amine indicates how strongly the degree of transfer is influenced by the existence of the substituents in the ring or at the nitrogen atom.

Table 5

ETH study of iodine-aniline complexes

Donor	d_{N-I}	∢ HNM	μ_{calc}
Aniline	2.32	108°19′	6.32
N,N-Dimethylaniline	2.41	108°25′	6.54
o-Toluidine	2.5	108°28′	6.56
p-Toluidine	2.35	108°21′	5.42
p-Anisidine	2.56	108°22′	6.72
o-Anisidine	2.41	108°20′	6.51

Table 6 shows the charge differences between the complex and free amine, according to figure 1.

Table 6

The charge differences from the complex to free amine (numbering as in Fig. 1)

Donor/Position	N	4	5	6	7	8	9
Aniline	0.215	0.0021	0.0012	0.007	0.075	0.062	0.002
N,N-Dimethyaniline	0.222	0.0032	0.0014	0.009	0.082	0.073	0.008
p-Toluidine*	0.231	0.0045	0.0016	0.011	0.097	0.082	0.009
o-Toluidine*	0.225	0.0036	0.0013	0.085	0.093	0.075	0.011
p-Anisidine*	0.242	0.0049	0.0019	0.012	0.101	0.091	0.023
o-Anisidine*	0.238	0.0047	0.0017	0.082	0.095	0.072	0.021

* Important changes are noticed at the CH_3 and OCH_3 groups in the *ortho* and *para* positions.

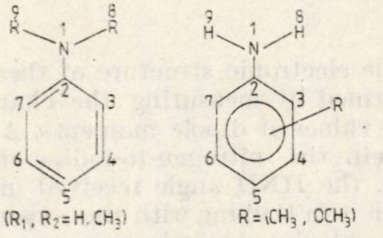

Fig. 1. — Donors considered in the study of aniline-iodine complexes.

The frequencies in the IR spectrum were used for obtaining the force constants, K_{NH}, and the valence angle, θ, according to Linett's[9] equations :

$$2\nu_s^2 = K_{\mathrm{NH}}\left(\frac{1}{m_{\mathrm{H}}} + \frac{1+\cos\theta}{m_{\mathrm{N}}}\right)$$

$$2\nu_{as}^2 = K_{\mathrm{NH}}\left(\frac{1}{m_{\mathrm{H}}} + \frac{1-\cos\theta}{m_{\mathrm{N}}}\right)$$

From the valence angle, the weight of the *s* character in the nitrogen hybride can be calculated :

$$b^2 = -\frac{\cos\theta}{1-\cos\theta}$$

The angle θ, the force constants, and the value *b* are given in table 7.

Table 7

The results of Linnett's analysis for aniline-iodine complexes

Donor	θ°	b²
Aniline	108°19′	0.2542
N-Methylaniline	108°21′	0.2611
p-Toluidine	108°25′	0.2731
o-Toluidine	108°22′	0.2652
p-Anisidine	108°28′	0.2811
o-Anisidine	108°17′	0.2622

DISCUSSION

The data presented may be used for studying the electronic structure and stability of aniline complexes with iodine.

The values of the stability constants reflect the fact that these complexes have medium stability and are intermediate between the $n-\sigma$ and $\pi-\pi$ complexes. A marked variation of the stability constants is noted with the introduction of certain electron repelling substituents. The variation of the stability constants with the basicity of the amine is given in figure 2.

On the basis of Mulliken's theory the energy curves, W_{N}, W_{E} and W_{E} for the complex were drawn (Fig. 3).

Evidence was found of the following :

1. The curve is that of a strong complex with a marked energy minimum.

2. The *CT* transition occurs between the first excited state and fundamental state.

3. The equilibrium distances do not coincide, being 2.54 Å in the excited state, as against 2.4 Å in the ground state for dimethylaniline.

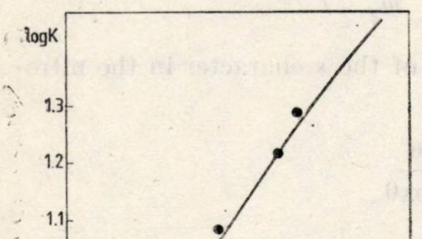

Fig. 2. — Variation of the stability of aniline-iodine complexes with donor basicity.

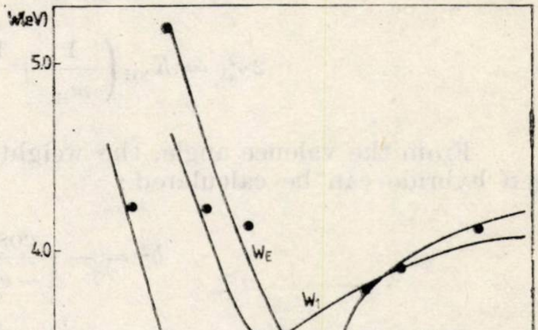

Fig. 3. — Variation of electronic energy of the complex (Dimethylaniline I_2 with the distance between donor and acceptor).

The curve of the excited state of amine is situated at a much greater distance in order to permit a locally excited transition in the complex.

Bearing in mind the electronic structure of the amine, it may be postulated that at the moment of transfer a localization of the electrical charge appears on the nitrogen atom and, therefore, a localization of the amine orbital on nitrogen. Between this "lone pair" located orbital and the σ^x orbital of iodine a strong overlap appears and hence, a corresponding force of the bond — the localization being favoured by the rotation of the CH_3 group at the nitrogen atom. Lending support to this assumption are the IR spectra (the frequency of the stretching vibration in the complex) which also furnish data on the structural changes of the amino group.

The formation of the complex is accompanied by electronic transfer from the nitrogen atom. Decrease of the electron density on this atom produced three predominant effects, the most important being the decrease of the bond force. The shift is strongly influenced by the substituent because it increases the density on nitrogen.

Evidence of the CT interaction between amines and iodine can be revealed by following up the magnitude of the charge transferred from nitrogen to iodine by the EHT method. The differences between the charge in the complex and the free amine are given in table 6.

An increase of the charge transferred with increasing electron-repelling character can be noted. This charge displacement favours the appearance of a dipole moment, characteristic of the transfer, which strongly varies with the charge transferred and with the donor power, represented by I_V^D. Linear relations are obtained. The increased dipole moment is calculated by difference between the theoretically calculated dipole for the complex, and the dipole obtained by

$$\mu_D + \mu_A.$$

Therefore, the iodine – aniline complexes characterized by their special type of donor and transfer are intermediate between $n-\sigma$ and $\pi-\pi$ CT complexes.

REFERENCES

[1] H. Tsubomura, *J. Amer. Chem. Soc.*, **82**, 41 (1960).
[2] H. Tsubomura and D. C. Mukerjee, *Trans. Faraday Soc.*, **60**, 62 (1964).
[3] M. Ciureanu and V. E. Sahini, *Rev. Roumaine Chim.*, **24**, 655 (1979).
[4] G. Lichtfaus and Z. Zugers — Huyskeurs, *Bull. Soc. chim. belges*, **82**, 123 (1973).
[5] A. Fyatiello, *J. Chem. Phys.*, **41**, 2204 (1963).
[6] J. Lauransan and J. Corset, *Ann. Chim.*, **4**, 475 (1969).
[7] M. Ciureanu, *Adv. Mol. Relax. Inter. Proc.*, **15**, 37 (1979).
[8] R. Scott, *Rec. Trav. chim.* **75** 787 (1956); *Ann. Rev. Phys. Chem.*, **20**, 126 (1969).
[9] A. Linnett, *Trans. Faraday Soc.*, **41**, 225 (1945).

Revue Roumaine de Chimie, **33**, *1*, 83–85 (1988)

A CONVENIENT SYNTHESIS FOR MOORE'S KETENE PRECURSORS

MIRCEA D. GHEORGHIU *, LUMINIȚA PÂRVULESCU, RODICA CECLAN, IOANA MANOLESCU, DOINA CONSTANTINESCU, CRISTINA FLOREA and MICHAELA STĂNESCU

Department of Organic Chemistry, Polytechnic Institute — TCH, Bucharest 16, Romania 76206

Received April 15, 1987

The phase transfer catalyzed hydrochloric acid elimination from dichlorocyclohexanediones 3a and 3b gave in high yield quinones 2a and 2b, respectively. A more convenient synthesis for triethylbenzylammonium chloride, the phase catalyst, is also provided.

t-Butylcyanoketene, *which hereafter we would like to call Moore's ketene*, has apparently the most documented chemistry in the field of ketenes.[1] Concurrently with the studies concerning cycloaddition of Moore's ketene to alkenes and alkynes,[1] we have proposed a new entry in the synthetic route developed originally by Moore,[2] having as target of the synthesis the diazido-quinone **2c**, which by thermolysis is cleanly converted into Moore's ketene **1**. Our previous proposal[3] started with hydroquinone, which was converted by alkylation with t-butanol into 2,5-di-t-butylhydroquinone. The latter compound was then converted by chlorine oxidation and chlorine addition to the dichlorocyclohexenedione **3a**. This compound was then converted, according to Moore's original route to compounds **2b**, **3b** and **2c**, respectively. The latter gave Moore's ketene by thermolysis in anhydrous benzene.

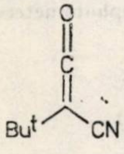

1

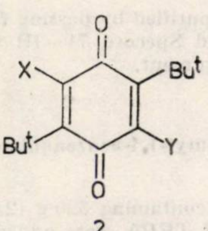

2

a: X=H, Y=Cl
b: X=Y=Cl
c: X=Y=N_3

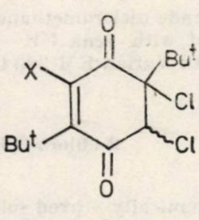

3,

a: X=H
b: X=Cl

Here we would like to propose an alternative procedure for the synthesis of 2-chloro-3,6-di-t-butyl-1,4-benzoquinone (**2a**) and 3,6-di-t-butyl-2,5-dichloro-1,4-benzoquinone (**2b**), from the dichloro precursors

3a and **3b** respectively, by hydrochloric acid elimination with potassium carbonate, phase transfer catalysis in the methylene chloride/water biphasic system.

$$\begin{matrix} \underline{2a} \\ \underline{2b} \end{matrix} \xrightarrow[\text{TEBA}]{K_2CO_3/CH_2Cl_2} \begin{matrix} \underline{3a} \\ \underline{3b} \end{matrix}$$

In the original synthetical sequence, these steps were carried out by using triethylamine in anhydrous ethyl ether.[2] In our procedure monochloroquinone **2a** and dichloroquinone **2b** respectively, were obtained in fairly high yields, 82–97% for **2a** and 60% for **2b**. In each case the products are of high purity, and could be obtained safely in batches of 200–500 g in reaction vessels not larger than 3 L.

Both reactions were run using triethylbenzylammonium chloride (TEBA), as phase transfer catalyst, in quantity not exceeding 10^{-2} moles equivalents. As mentioned above, the base was anhydrous potassium carbonate, but also sodium carbonate is a good eliminating agent.

Both were added in ca 100% molar excess in respect to chloroderivatives **2a** and **2b**, respectively. The reactions were monitored by IR and ^{1}H–NMR (see experimental part). We have estimated 45 minutes, as reaction time for conversion of **3a** → **2a**, while for **3b** → **2b** reaction, 8 hours. In the latter case, the major isomer of **3b**, presumably *trans*-dichloroderivative, (content of 68.7 – 77.7% based on ^{1}H–NMR results) eliminates hydrochloric acid much faster than the minor one.[4]

We would like to propose also a more convenient synthesis of TEBA.

According to literature, TEBA is obtained from benzylchloride and triethylamine using anhydrous acetone as solvent.[5] Our method requires a mere mixing of 1 : 3 molar ratio of benzylchloride and triethylamine, provided it is vigorously shaken.

EXPERIMENTAL PART

Reagent grade dicloromethane was purified by passing through basic alumina. IR spectra were recorded with Jena UR–20 and Specord 71–IR spectrophotometers, ^{1}H–NMR were recorded with Varian EM 360 L instrument.

2-Chloro-3,6-di-t-butyl-1,4-benzenquinone (2a)

To a mechanically stirred solution containing 320 g (2.315 mol) of anhydrous K_2CO_3, 400 mL of water and 10 g (43.9 mmol) of TEBA were added, during 45 minutes, a solution of 380 g (1.305 mol) 2,5-di-t-butyl-5,6-dichlorocyclohex-2-ene-1,4-dione **(3a)** in 900 mL of dichloromethane. During the addition the reaction mixture became slightly warm. Then the stirring was continued for an additional 45 minutes. After this period a sample monitored by IR has shown the disappearance of the strong peaks at 1700 and 1600 cm^{-1}, belonging to dichloroderivative **3a**, and the appearance of peaks at 1680 and 1660 cm^{-1} belonging to the title monochloroquinone.

The organic layer was separated. The aqueous layer was extracted with dicloromethane (2 × 100 mL). The combined organic layers were washed with water to neutral pH. After solvent removal under vacuum (100 torr), 350 g (93%), yellow oil, of 2-chloro-3,6-di-t-butyl-1,4-quinone were obtained. For the next step of chlorination, [2] no further purification was necessary.

3,6-Di-t-butyl-2,5-dichloro-1,4-benzoquinone(2b)

The procedure is identical with that described above. The following quantities were used : 320 g (2.315 mol) anhydrous K_2CO_3, 400 mL water, 10 g (43.9 mol) TEBA and 380 g (1.167 mol). of 2,5-di-t-butyl-3,5,6-trichlorocyclohex-2-ene-1,4-dione dissolved in 700 mL dichloromethane. The reaction was monitored by IR ; the disappearance of the peak at 1710 cm^{-2} and its replacement by the peak at 1660 cm^{-1} were illustrative for reaction completion. The reaction mixture worked up as described above for **2a** gave a brown semisolid. The crude reaction product was dissolved in 200 mL hot ethanol 90%. After cooling the yellow solid crystals were filtered off and washed with 200 mL chilled 90% ethanol, to give 3,6-di-t-butyl-2,5-dichloro-1,4-benzoquinone ; yield : 195–200 g (60%) ; m.p. 65–67°C (lit. 68–69°C).

Triethylbenzylammonium chloride (TEBA)

A 1 : 3 molar ratio mixture of benzylchloride and triethylamine was vigorously shaken. The solid obtained was carefully filtered off until all the oil was removed. No recrystallization of the reaction product was necessary for the next steps.

REFERENCES

[1] H. W. Moore and W. Weyler, Jr., *J. Am. Chem. Soc.*, **93**, 2812 (1971). H. W. Moore and M. D. Gheorghiu, *Chem. Soc. Rev.*, **10**, 289 (1981).

[2] W. Weyler Jr., W. G. Duncan, M. B. Liewen and H. W. Moore, *Org. Synth.* **55**, 32 (1976) and literature cited therein.

[3] M. D. Gheorghiu and M. Avram, *Org. Prep. Proc. Int.*, **6**, 231 (1974).

[4] The major isomer was isolated as a solid, by column chromatography on silicagel ; m.p. = = 57°C (uncorrected, methanol), ^1H-NMR (CCL_4/TMS) : $\delta = 4.62$ (s, 1H) ; 1.44 (s, 9H) ; 1.37 ppm (s, 9H).

[5] R. P. Widera, W. P. Weber and G. W. Goker, *Org. Synth.*, **55**, 97 (1976) and literature cited therein.

Revue Roumaine de Chimie, 33, 1, 87–96 (1988)

OPTIMAL TEMPERATURE PROFILES FOR PROPANE PYROLYSIS IN TUBULAR REACTORS

GRIGORE BOZGA[a], JAFAR TOWFIGHI[b] and OCTAVIAN FLOAREA[a]

[a] Department of Chemical Engineering, Polytechnic Institute, Polizu 1, 78126 Bucharest, Romania

[b] College of Engineering, University of Tarbiat Modarres, Teheran, Iran

The formulation and solution of a temperature profile optimization problem, for an industrial propane pyrolysis reactor, is presented. The performance index represents the ethylene yield, penalized by a term dependent on coking rate integral along the reactor. The computed optimal temperature profiles correspond to higher ethylene yields and lower propylene yields than in an industrial reference case.

In the selection of thermal conditions of pyrolysis reactors it is important to consider the effect of working temperature both on olefins yields and on secondary phenomenon of inner surface coking.

These effects are conflicting, the temperature rise favouring the ethylene yield and at the same time increasing the intensity of coking.

Therefore it is important to determine the optimal thermal conditions, i.e. those which give the best compromise between these two effects. Although they have a great economic importance, these aspects have less frequently been dealt with in the literature, especially because of the difficulties in mathematical modelling of coke rate formation, and its distribution along the reactor.

Optimal control problems of pyrolysis reactors were solved by Jackman and Aris[1] and Wilson and Bélanger, [2] but the process mathematical models were rather simplified and incomplete.

Robertson and Hanesian [3] determined the optimum temperature profiles for ethane pyrolysis reactors by extrapolation, starting from the industrial temperature profiles published in literature.

Advanced control models for pyrolysis processes were studied on a pilot plant by D'Hulster et. al.[4]

This paper presents a computation study of optimal temperature profiles for propane pyrolysis, with a performance index representing ethylene yield, penalized by a term dependent on coking rate integral along the reactor.

The computational algorithm used to determine the optimal temperature profiles is based on the first variation method.

REACTOR MODEL AND OPTIMIZATION PROBLEM

The pyrolysis tubular reactor is adequately represented by a one dimensional ideal model, assuming plug type flow of reacting mixture.[5]

The model consists of mass balance, and pressure drop equations.

The thermal balance equation is not necessary, the temperature being the control variable.

The mass balance equations are written in the structure that represents the evolution of reaction molar extent along the reactor :

$$\frac{\mathrm{d}\,\xi_{mi}}{\mathrm{d}z} = \frac{1}{Dm}\, v_{R,i}(\,\xi_{mi},\, T,\, p), \qquad i = 1, r \tag{1}$$

and the pressure drop equation :

$$\frac{\mathrm{d}p}{\mathrm{d}z} = -\,\lambda_f\,\frac{1}{d_t}\,\frac{D_m^2}{2\,\rho}\;; \quad \lambda_f = 0.184\,\mathrm{Re}^{-0.2} \tag{2}$$

The kinetic and operating data necessary for reactor modelling were taken from the detailed study reported by Sundaram and Froment.[6]

The chemical equations considered to describe propane pyrolysis and the corresponding kinetic data are shown in Table 1.

The performance index used, that combines the favourable effect of ethylene yield and the negative effect of coking rate on the profit, has the form :

$$\mathrm{I} = \eta_{\mathrm{C_2H_4}}(L) - \beta\int_0^L v_{R,C}(z)\,\mathrm{d}z \tag{3}$$

The second term represents a penalty of ethylene yield, dependent on global coking rate in industrial reactor and the proportionality constant β, which reflects the influence of coking on reactor economic efficiency. A reasonable value for β, can be obtained from the simplified yearly profit expression :

$$I' = D_m\,\eta_{\mathrm{C_2H_4}}(L)\;p_{\mathrm{C_2H_4}}(t_\theta - n_i t_i) - C_{mu} \tag{4}$$

The frequency of reactor interruptions required for decoking, n_i corresponding to a coking rate profile $v_{R,C}(z)$, is estimated from a reference run with known coking characteristics $v_{RC}^{(0)}(z)$, assuming the proportionality dependence :

$$\frac{n_i}{n_i^{(0)}} = \frac{\displaystyle\int_0^L v_{R,C}(z)\,\mathrm{d}z}{\displaystyle\int_0^L v_{R,C}^{(0)}(z)\,\mathrm{d}z}, \text{ or} \tag{5}$$

Table 1

Reaction scheme for propane craking[1]

No. (i)	Reactions	The rate expression	$k_{i(T)} = A_i \exp(-E_i/RT)$	
			A_i $[s^{-1}]$ or $[1 \cdot \text{mole}^{-1} \cdot s^{-1}]$	E_i (kcal/mole)
1	$C_3H_8 \rightarrow C_2H_4 + CH_4$	$v_{R,1} = k_1 C_{C_3H_8}$	$4.692.10^{10}$	50.6
2	$C_3H_8 \rightleftharpoons C_3H_6 + H_2$	$v_{R,2} = k_2(C_{C_3H_8} - C_{C_3H_6} C_{H_2}/K_{C_2})$	$5.888.10^{10}$	51.29
3	$C_3H_8 + C_2H_4 \rightarrow C_2H_6 + C_3H_6$	$v_{R,3} = k_3 C_{C_3H_8} C_{C_2H_4}$	$2.536.10^{13}$	59.06
4	$2C_3H_6 \rightarrow 3C_2H_4$	$v_{R,4} = k_4 C_{C_3H_6}$	$1.514.10^{11}$	55.80
5	$2C_3H_6 \rightarrow 0.5C_6 + 3CH_4$	$v_{R,5} = k_5 C_{C_3H_6}$	$1.423.10^{9}$	45.50
6	$C_3H_6 \rightleftharpoons C_2H_2 + CH_4$	$v_{R,6} = k_6(C_{C_3H_6} - C_{C_2H_2} C_{CH_4}/K_{C_6})$	$3.794.10^{11}$	59.39
7	$C_3H_6 + C_2H_6 \rightarrow C_4H_8 + CH_4$	$v_{R,7} = k_7 C_{C_3H_6} C_{C_2H_6}$	$5.553.10^{14}$	60.01
8	$C_2H_6 \rightleftharpoons C_2H_4 + H_2$	$v_{R,8} = k_8(C_{C_2H_6} - C_{C_2H_4} C_{H_2}/K_{C_8})$	$4.652.10^{13}$	65.20
9	$C_2H_4 + C_2H_2 \rightarrow C_4H_6$	$v_{R,9} = k_9 C_{C_2H_4} C_{C_2H_2}$	$1.026 .10^{12}$	41.26
10	$C_4H_8 \rightarrow C_6$	$v_{R,10} = k_{10} C_{C_4H_8}$	$6.960.10^{7}$	34.32
11	$C_3H_6 \rightarrow 3C + 3H_2$	$v_{R,11} = k_{11} C_{C_3H_6} = v_{R,C}$	$5.82.10^{14}$	73.58

$$n_i = n_i^{(0)} \frac{1}{L \cdot \bar{v}_{R,C}^{(0)}} \int_0^L v_{R,C}(z)\, dz \tag{6}$$

$\bar{v}_{R,C}^{(0)} = \frac{1}{L} \int_0^L v_{R,C}^{(0)}(z)\, dz$, being the average coking rate for the reference run.

The man power and utilities costs necessary for decoking, c_{mu}, are expressed as a fraction α, of the term representing the cost of ethylene lost, due to interruptions :

$$c_{mu} = \alpha\, D_m\, \eta_{C_2H_4}(L)\, p_{C_2H_4} \cdot n_i t_i$$

and the performance index expression becomes :

$$I' = D_m p_{C_2H_4} t_0 \left[\eta_{C_2H_4}(L) - \frac{n_i^{(0)} t_i \eta_{C_2H_4}(L)\,(1+\alpha)}{t_0\, \bar{v}_{R,C}^{(0)}\, L} \int_0^L v_{R,C}(z)\, dz \right] \tag{7}$$

so that the maximizing of the performance index I', is equivalent to the maximization of the functional (3), with :

$$\beta = \frac{n_i^{(0)} t_i \eta_{C_2H_4}(L)(1+\alpha)}{t_0\, \bar{v}_{R,C}^{(0)} L} \tag{8}$$

As reference run we selected the results of the simulation study reported by Sundaram and Froment, already quoted. Thus, the objective is to find the reaction temperature profile $T(z)$, along with the reactor, which maximizes the performance index (3), subject to constraint

$$T(z) \leqslant T_{\max}.$$

COMPUTATIONAL ALGORITHM

The problem previously defined belongs to a general class in which is required to maximize the functional

$$I = h(\mathbf{X}(L)) + \int_0^L g(\mathbf{X}(z), \mathbf{U}(z))\, dz \tag{9}$$

for the system described by vectorial state equation :

$$\frac{d\mathbf{X}}{dz} = \mathbf{F}(\mathbf{X}, \mathbf{U}) \qquad \begin{array}{l} \mathbf{X}_{(0)} = \mathbf{X}_0 \\ z \in [0, L], \end{array} \tag{10}$$

by a suitable selection of the control vector $\mathbf{U}(z)$.

There are many algorithms that can be used to solve this class of problems. We preferred the order gradient method described by Kirk [7].

In order to solve the problem, the hamiltonian functional is usually used :

$$\mathrm{H}(\mathbf{X},\mathbf{U},\mathbf{P}) = g(\mathbf{X},\mathbf{U}) + \mathrm{P}^{\mathrm{T}}\cdot \mathbf{F}(\mathbf{X},\mathbf{U}), \tag{11}$$

as well as the costate (adjoint) vectorial equation :

$$\frac{\mathrm{d}\mathbf{P}}{\mathrm{d}z} = -\frac{\partial \mathrm{H}}{\partial \mathbf{X}}\,; \quad \mathbf{P}(L) = \frac{\partial h}{\partial \mathbf{X}(L)} \tag{12}$$

The numerical procedure is iterative and consists of the following steps :

1. Initially, an approximation to control $\mathbf{U}^{(0)}(z)$, $z \in [0, L]$ is guessed and stored in the memory of the digital computer (this is done by dividing the interval $[0, L]$ into N intervals Δz of equal size, and considering the control as being piecewise—constant on each interval).

2. State equations (10) are integrated from 0 to L and performance index $I^{(i)}$ is computed for the resulted state trajectory.

3. Adjoint equations (12) are integrated backwards from $z = L$ to $z = 0$ and a new control function $\mathbf{U}(z)$ is generated :

$$\mathbf{U}^{(i+1)}(z_k) = \mathbf{U}^{(i)}(z_k) + \varepsilon \frac{\partial \mathbf{H}^{(i)}}{\partial \mathbf{U}}(z_k) \tag{13}$$

4. State equations (10) are again integrated from $z = 0$ to $z = L$, and simultaneously the performance index $I^{(i+1)}$ is evaluated for the new state.

5. A convergence test is performed. If

$$\frac{I^{(i+1)} - I^{(i)}}{I^{(i)}} \leqslant \gamma \tag{14}$$

terminate the iterative procedure and output the optimal control $\mathbf{U}^{(i+1)}(z)$. Otherwise, put $i = i + 1$ and go to step (3).

To bring the reactor model equations in the conventional form (10), the following new notations were introduced :

$$x_i = \xi_{mi},\ i = 1{,}10,\ x_{11} = p\,;\ u = T$$

$$a_1 = \frac{\pi \mathrm{d}_i^2}{4 D_m R} = \frac{1}{D_m R}\,; \quad a_2 = -\frac{0.092\, D_m^{1.8} R}{3600^{1.8}(\pi/4)^{1.8}\mathrm{d}^{4.8}} \tag{15}$$

In these notations the mass balance equations become :

$$\frac{\mathrm{d}x_1}{\mathrm{d}z} = a_1k_1(u)y_1\,\frac{x_{11}}{u} = f_1(x_1, \ldots, x_{11}, u) \tag{16}$$

$$\frac{\mathrm{d}x_2}{\mathrm{d}z} = a_1k_2(u)\,\frac{x_{11}}{u}\left(y_1 - \frac{x_{11}}{Ru}\,\frac{y_4y_5}{K_{c,2}}\right) = f_2(x_1, \ldots, u) \tag{17}$$

$$\frac{\mathrm{d}x_3}{\mathrm{d}z} = a_1k_3(u)y_1y_2\,\frac{x_{11}^2}{Ru^2} = f_3(x_1, \ldots, u) \tag{18}$$

$$\frac{\mathrm{d}x_4}{\mathrm{d}z} = a_1k_4(u)\,y_4\,\frac{x_{11}}{u} = f_5(x_1, \ldots\ u) \tag{19}$$

$$\frac{\mathrm{d}x_5}{\mathrm{d}z} = a_1k_5(u)\,y_4\,\frac{x_{11}}{u} = f_5(x_1, \ldots\ u) \tag{20}$$

$$\frac{\mathrm{d}x_6}{\mathrm{d}z} = a_1k_6(u)\,\frac{x_{11}}{u}\left(y_4 - \frac{x_{11}}{Ru}\,\frac{y_3y_8}{K_{c,6}}\right) = f_6(x_1, \ldots u) \tag{21}$$

$$\frac{\mathrm{d}x_7}{\mathrm{d}z} = a_1k_7(u)\,y_4y_6\,\frac{x_{11}^2}{Ru^2} = f_7(x_1, \ldots\ u) \tag{22}$$

$$\frac{\mathrm{d}x_8}{\mathrm{d}z} = a_1k_8(u)\,\frac{x_{11}}{u}\left(y_6 - \frac{x_{11}}{Ru}\,\frac{y_2y_5}{K_{c,8}}\right) = f_8(x_1. \ldots\ u) \tag{23}$$

$$\frac{\mathrm{d}x_9}{\mathrm{d}z} = a_1k_9(u)\,y_2y_8\,\frac{x_{11}^2}{Ru^2} = f_9(x_1, \ldots\ u) \tag{24}$$

$$\frac{\mathrm{d}x_{10}}{\mathrm{d}z} = a_1k_{10}(u)\,y_9\,\frac{x_{11}}{u} = f_{10}(x_1, \ldots\ u) \tag{25}$$

$$\frac{\mathrm{d}x_{11}}{\mathrm{d}z} = a_2\,\frac{\eta_{am}^{0.2}u}{M_{am}x_{11}} = f_{11}(x_1, \ldots\ u) \tag{26}$$

The hamiltonian functional (11) has the particular expression :

$$\mathrm{H} = -\,\beta v_{RC}(x_1, \ldots\ u) + \sum_{i=1}^{11} p_i f_i(x_1, \ldots\ u) \tag{27}$$

The costate variables are computed from the costate equations (12) whose particular form is :

$$\frac{\mathrm{d}p_i}{\mathrm{d}z} = -\,\frac{\partial \mathrm{H}}{\partial x_i} = -\sum_{j=1}^{11} p_j\,\frac{\partial f_j}{\partial x_i} - \beta\,\frac{\partial v_{RC}}{\partial x_i} \tag{28}$$

with the boundary conditions :

$$p_i(L) = \frac{\nu_{i,C_2H_4}}{g_{0,C_3H_8}} \frac{M_{C_2H_4}}{M_{C_3H_8}}, \quad i = 1,10 \tag{29}$$

$$p_{11}(L) = 0$$

Optimal temperature profile along the reactor is computed from iterative formula (13) with the hamiltonian gradient expression :

$$\frac{\partial \mathrm{H}}{\partial u} = \sum_{i=1}^{11} p_i \frac{\partial f_i(x_1, \ldots u)}{\partial u} - \beta \frac{\partial v_{RC}(x_1, \ldots u)}{\partial u} \tag{30}$$

To integrate the systems of state and costate differential equations, the fourth-order Runge-Kutta method was used. More details regarding the algorithm are presented in reference. [8]

COMPUTATIONAL RESULTS

Constructional and operating data considered in this study are given in Table 2. The physico-chemical properties of the reaction mixture were obtained from reference [9].

Table 2

Characteristics of the industrial reactor[1]

Length (L)	95 m
Diameter (d_t)	0.108 m
Overall mass flow (D_m)	2845 kg/h
Dilution factor	0.406 kg steam/kg propane
Inlet temperature (T_0)	600°C
Inlet pressure (P_0)	3 atm

To perform the necessary computations, a Fortran computer program was developed, easy adaptable to other reaction systems.

The iterative procedure was started using as initial profile $u^0(z)$, the industrial temperature profile specified in the work of Sundaram and Froment. [1]

In a first stage of the computations, the optimal temperature profiles were determined, which maximize the ethylene yield, neglecting the influence of coking ($\beta = 0$ in performance index expression).

The results showed that the ethylene yield increases accordingly, as the reaction temperature is increased. The maximum temperature increase is required on the second half of the reactor tube, to prevent ethylene degradation (Figs 1 and 2).

Such operating temperatures are not recommended for industrial reactors, because coking phenomena are intensified to an unacceptable level.

More realistic profiles are obtained, taking into account the negative influence of coking, represented through the value of parameter β. This value is strongly influenced by the specific operating conditions of the plant (i.e. the duration of decoking t_i, the cost of ethylene and utilities etc.). Figure 3 presents optimal temperature profiles computed for two

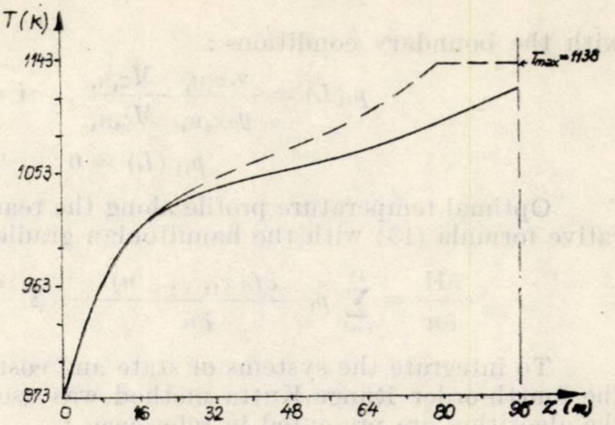

Fig. 1. — Industrial and optimal temperature profiles (β = 0) — industrial; — — — optimal profile.

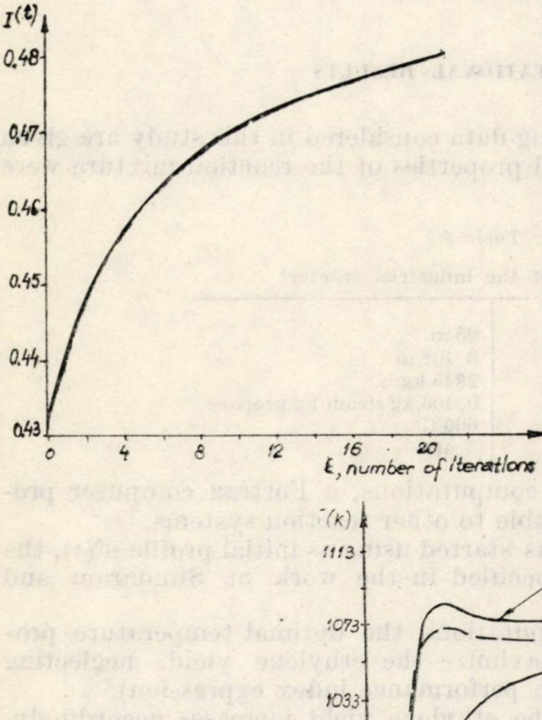

Fig. 2. — Performance index against the number of iterations (β = 0).

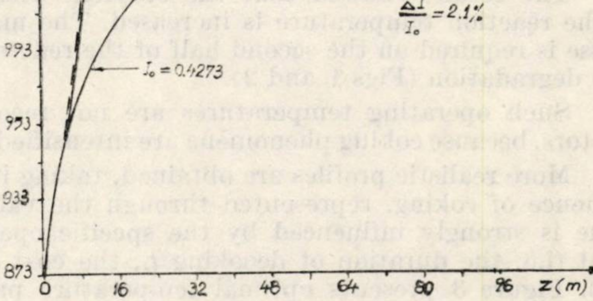

Fig. 3. — Optimal temperature profile (β ≠ 0). 1 — industrial; 2, 3 — optimal profiles.

values of parameter β. These profiles require higher values of temperature on the first half of the reactor than in industrial reference profile.

The shape of optimal temperature profile is mainly explained by the combined effects of coking and ethylene formation mechanisms. The peak on the first half appears as a consequence of lower concentration of coke precursors on this zone. Figure 4 presents the ethylene and propylene yields corresponding to the optimal run, versus the industrial reference ones. In optimal alternatives, the outlet ethylene yield is greater, and the outlet propylene is lower than in the reference case, as a consequence of an earlier appearance of propylene and its conversion into ethylene.

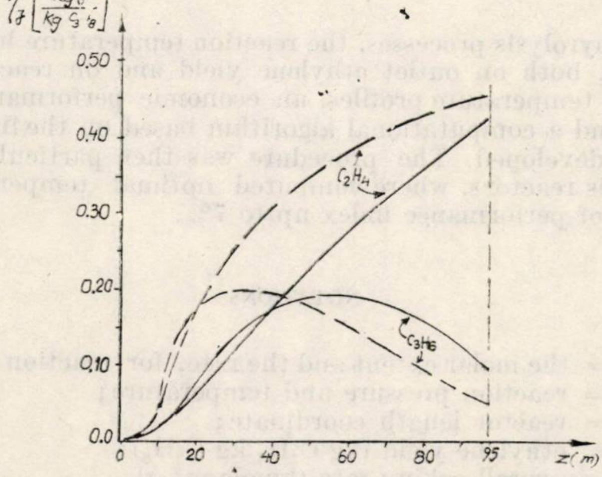

Fig. 4. — Ethylene and propylene yields along the tubular reactor. ——— industrial ; — — — — optimal profile (β = 0.025).

The computations indicated a strong dependence of optimal temperature and performance index values on the value of parameter β.

The gain of the performance index over the reference conditions is 2.1% for β = 0.03 and 7.6% for β = 0.025.

Lower values of β permit greater gains of performance index as a result of greater values in the optimal temperature profile. Figure 5

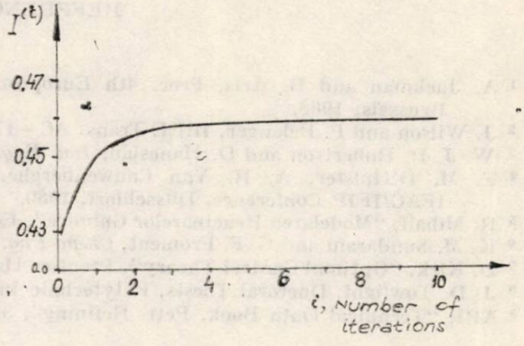

Fig. 5. — Performance index versus the number of iterations (β = 0.025).

presentes the values of performance index as a function of the number of iterations. Notice that the first three iterations increase the performance significantly, and the final seven iterations yield a very slight improvement, this illustrating a good convergence of the first variation algorithm.

CONCLUSIONS

In the pyrolysis processes, the reaction temperature has a considerable influence, both on outlet ethylene yield and on reactor coking. To find optimal temperature profiles, an economic performance index was formulated and a computational algorithm based on the first variational method was developed. The procedure was then particularized for propane pyrolysis reactors, where computed optimal temperature profiles ensure gains of performance index up to 7%.

NOTATIONS

ξ_{mi}, v_{Ri} = the molar extent and the rate, for reaction i;
p, T = reaction pressure and temperature;
z = reactor length coordinate;
$\eta_{C_2H_4}$ = ethylene yield (kg C_2H_4/kg C_3H_8);
$v_{R,C}$ = overall coking rate (kmole/m^3.s);
$D_m, \dot{D}_m$ = mass flow rate (kg/s) and specific mass flow rate (kg/m^2.s);
λ_f = friction factor;
ρ = gas mixture density;
$p_{C_2H_4}$ = cost of ethylene;
t_0 = yearly operating time;
t_i = shut down time necessary for decoking;
ε = step size in the gradient algorithm;
R = ideal gas constant;
ν_{i, C_2H_4} = stoichiometric coefficient of ethylene in reaction i;
M_j = molecular weight of j-th component;
g_{0, C_3H_8} = inlet concentration of propane (kmole/kg).

REFERENCES

[1] A. Jackman and R. Aris, Proc. 4th European Symp. Chemical Reaction Engineering, Brussels, 1968.

[2] J. Wilson and P. Belanger, IEEE Trans. AC−17, 756 (1972).

[3] W. J. R. Robertson and D. Hanesian, *Ind. Engng. Chem., Proc. Des. Dev.*, **14**, 216 (1975).

[4] F. M. D'Hulster, A. R. Van Cauwenberghe, P. S. Van Damme and G. F. Froment, IFAC/IFIP Conference, Düsseldorf, 1980.

[5] R. Mihail, "Modelarea Reactoarelor Chimice", Ed. Tehnică, Bucharest, 1976.

[6] K. M. Sundaram and G. F. Froment, *Chem. Eng. Sci.*, **34**, 635 (1979).

[7] D. Kirk, "Optimal Control Theory", Prentice Hall, 1970.

[8] J. D. Towfighi, Doctoral Thesis, Polytechnic Institute, Bucharest, 1986.

[9] API, "Technical Data Book, Petr. Refining", 3rd edition.

Revue Roumaine de Chimie, 33, *1*, 97–103 (1988)

BOOK REVIEWS

S. Torii, "Electroorganic Syntheses. Methods and Applications. Part. I : Oxidations", VCH Publishers (New York) and Verlagsgesellschaft (Weinheim), 1985, 338 pp. hardcover, 138 DM. ISBN 3–527–26 318–7

Volumes 15 and 16 in the series "Monographs in Modern Chemistry" edited by H. F. Ebel are written by S. Torii (Japan) and describe electrooxidations and electroreductions, respectively. The present book discusses electrooxidations (EOs). It is a revised translation of the book by S. Torii in Japanese version which was published in 1981 by Kodansha Ltd.

A brief overview of the chapter headings follows.

1. EO and product-selectivity
2. Electrodecarboxylation of carboxylic acids
3. EO of alkylbenzene side-chains
4. EO of aromatic nucleus
5. EO of nitrogen compounds
6. EO of sulfur compounds
7. EO of olefins
8. EO of alcohols and ethers
9. Electrohalogenation and EO of halogen compounds
10. EO of phosphorus, boron, and selenium compounds
11. Indirect EO and the use of electron carriers (mediators)
12. EO of cyclopropanes and adamantanes
13. Electrogenerated acid-catalyzed functionalizations.

The first chapter describes how after Kolbe's pioneering discovery of the electrodecarboxylation of carboxylic acids in 1849, industrial applications of organic electrochemistry appeared only in 1955–1965 : a large-scale adiponitrile plant by electroreduction and coupling of acrylonitrile (Monsanto Co., USA) and the manufacture of tetraethyl lead (Nalco Co., USA). More recently, in the seventies, organic electrochemical reactions proliferated owing to theoretical advances, product selectivity and awareness of environmental damage caused by waste chemicals, obviated when using electrochemical processes. Useful hints are given to those who are less experienced in organic electrochemistry as to apparatus, methods for adjusting and measuring potentials, choice of electrode, solvent, and supporting electrolyte. A 25-page appendix of chapter 1 serves as a formula index for the remaining chapters by directing the reader to the paragraph and page where a reaction mode is discussed, providing also information on solvent, electrolyte and electrode.

Not only is the approach highly systematic and well organized but the literature coverage is quite extensive, especially for the Japanese literature ; most literature data are pre-1980 but there exists a fair number of post-1980 references.

This book provides a wealth of useful information for organic chemists and electrochemists. No organic chemical laboratory interested in organic synthesis can afford nowadays to overlook electrosynthetic methods. The author has done a good job of selecting relevant data.

A. T. Balaban
Polytechnic Inst. Bucharest

"Inventory in Theory and Practice", Edited by Attila Chikan, Academy of Science — Budapest, 1986

The publication comprises 64 scientific papers presented at the 3rd International Symposium on Inventory Theory and Practice (Budapest, 27th — 31st August 1984), sponsored by the International Society for Inventory Research and Academy of Science — Budapest.

The scientific papers are linked together in three sections : inventories in national economy level, inventory management and control, mathematical models in inventory theory and practice with contributions in the fields of energy, extraction, financing, agriculture.

The inventory problems are approached at national economy levels, for underdeveloped countries as well as at microeconomic level. Various topics are presenting a real interest : integration of inventories with production (I. Abel, G. Kordosi), inventory forecasting (B. Agren,

S. Wandel), factors acting upon inventories in investments (A. Khican, K. Kalotai), methodological problems in inventory planning (P. Dimitrov), prices influences upon inventory (C. Gustafson, W. Stervander), information systems for production development (W. Zabel) etc.

A special attention is paid to mathematical models and informatical systems for inventory management and control (E. Barancsi), decisional problems (A. Lehtimaki), MIS systems (G. Tomek) etc.

Out of all mathematical methods presented by various authors one could underline dynamic programming (M. Bugataj), heuristical approach (S. Axsater), statistical relations (E. Buhinskaya), multilevel allocation (M. Vujosevic), games theory (R. Kalfakakou), Pontriaghin principle (S. Sethi).

The publication is dealing with very interesting problems, at a high scientific level and it is of a real interest for theoretical and practical investigations of scientists working in the field of inventory management and control.

Marin Neguț
Computer Centre — Bucharest
Ministry of Chemical Industry

Y. Takeuchi and A. P. Marchand, Editors, "Applications of NMR Spectroscopy to Problems in Stereochemistry and Conformational Analysis; Methods in Stereochemical Analysis", Volume 6, Series Editor Alan P. Marchand, Verlag Chemie, ISBN 3–527–26145–1, Deerfield Beach Florida, 1986, 221 pp. Hardcover.

The sixth volume in the series edited by professor Alan P. Marchand, Methods in Stereochemical Analysis, is again dedicated to NMR spectroscopy, the most powerful method for solving stereochemical and conformational problems of chemical compounds. The recent conquests of NMR spectroscopy (especially two-dimensional NMR) have widened considerably the field of applications to complex molecules, polymers or biopolymers which can now be routinely analysed. The editors, professors Y. Takeuchi (Tokyo) and A. P. Marchand (North Texas State University) have undertaken the difficult task (and deserve praise on the outcome) of assembling in a single volume current applications of NMR spectroscopy which are quite interdisciplinary. Well-known scientists with important contributions in NMR spectroscopy have authored six reviews on their respective fields.

In the first of these, professor I.O.Sutherland (University of Liverpool) discusses "Guest-Host Chemistry and Conformational Analysis". Although of great importance in biological systems, except for an illustrative example for the deductive powers of NMR spectroscopy on the conformational changes induced in antibiotics (vancomycin, ristocetin, avoparcin) upon complexation with peptide residues, the chapter is entirely devoted to synthetic hosts (mono- and polycyclic crown ethers and aza-analogues of crown ethers) which accomodate as guests alkylammonium cations or bisammonium dications. Emphasis is given to the dynamic behaviour of these complexes and various processes are detected (guest-host exchange, conformational changes in the complexed and uncomplexed host) and measured by means of equilibrium constants, rate constants for the formation of complexes and free energies of activation. The review has 40 pages, numerous examples are given and 18 references are cited.

The second chapter by professor P. Diehl (University of Basel) and his collaborator, professor J. Jokisaari (University of Oulu, Finland) is entitled "NMR Studies in Liquid Crystals: Determination of Solute Molecular Geometry" and is a self-consistent review of NMR determinations of molecular structures in partially oriented molecules. Since the first use of liquid crystals as solvents (Saupe and Englert, 1963) the NMR of oriented molecules has evolved both theoretically and practically, the molecular structures of more than 500 molecules were resolved, the upper limit of complexity being molecules like *p*-chlorotoluene or benzaldehyde. The method is very precise for angle measurements (precisions of a few seconds are achieved) and gives in some cases about a hundred times more accurate relative bond lengths than infrared or electron diffraction methods. The chapter which has 34 pages and 62 references includes sections in Liquid Crystals, Basic Theory, Experimental Use, Spectral Analysis, Structural Data from Spectra, Limitations to the Precision of Structure Determination and Conclusions.

Chapter 3 by professor R. Kitamaru (Kyoto University) is the largest (50 pages) and is entitled "Carbon 13 Nuclear Spin Relaxation Study as an Aid to Analysis of Chain Dynamics and Conformations of Macromolecules". It consists of two parts: Theory of magnetic relaxation by dipole-dipole interactions (the main relaxation mechanism in the ^{13}C–NMR of macromolecules) and Applications (pertaining to molecular motions and chain dynamics of macromolecules). After exemplifying the general aspect of ^{13}C spin relaxation and discussing the data for ethylene—hexene-1 copolymer, the Applications include ^{13}C-spin relaxation of α-carbons in proteins, of the sidechains in polypeptides, of rubbery polymers and rubbery components in semicrystalline polymers as well as studies in the solid state by cross polarization (CP), ^{1}H-dipolar decoupling, and magic angle sample spinning (MAS). Sixty references are cited.

In the fourth chapter professor T. Terao and Dr. F. Imashiro (Kyoto university) discuss "Stereochemical Studies in the Solid State". After a brief review on the high resolution NMR for dilute spins in solids and a listing of the recent advances, three examples are given for studies of molecular motions by means of proton relaxation times and high-resolution ^{13}C-spectra, namely, the dynamic behaviour of methanol molecules trapped in β-quinol clathrate, proton transfer in benzoic acid dimer, and in plane molecular rotation of substituted naphthalenes. The last part (which cites almost half of the 205 references) covers studies of static and dynamic properties in the solid state by means of ^{13}C-CP-MAS-NMR, especially systems involving intermolecular hydrogen bonding, complexation, etc., which could not be clearly investigated in solution (owing to dissociation or rapid equilibration), or molecular motions such as the rearrangements of the norbornyl, sec-butyl and heptamethylbenzenonium cations.

The last two chapters cover applications of two-dimensional NMR techniques. The first of these by professor K. Nagayama (University of Tokyo) is a review of 2D-techniques for determining the molecular skeleton and partial structures of organic substances. Although chronologically not the first, δ-COrrelated SpectroscopY (COSY) is viewed as the basic 2D-technique and is elegantly explained after which other techniques such as J-resolved spectroscopy, spin-echo correlated spectroscopy (SECSY), nuclear Overhauser enhancement spectroscopy, multiple quantum (MQT) filter and MQT coherence, relayed COSY, are all shown to be derived from COSY. These different techniques are considered as successive information filters for elucidating partial structures. An example is given for rotenone, a pentacyclic medium-sized molecule $C_{23}H_{22}O_6$. The molecular skeleton (carbon-carbon connectivities) is established by combining other techniques such as INADEQUATE, H—C COSY, $^{13}C—^{13}C$ DQT coherence or selective H—C 2DJ. An Appendix (which accounts for most of the 96 references) presents a brief survey of applications of 2D techniques in biological systems. These include proteins, peptides, saccharides, tRNAs, oligonucleotides and others.

Professor H. Kessler and his coworker Dr. W. Bermel (Frankfurt) authored the last chapter concerned with the conformational analysis of peptides by 2D—NMR. After cautioning on the necessity and criteria of having conformationally homogeneous peptides, the extraction of NMR parameters and hence the spectral assignments are commented. By means of COSY, relayed COSY, H—C COLOC or INADEQUATE spectra the recognition of the individual aminoacids and their sequence are systematically performed while dynamic phenomena are evidenced with NOESY spectra. A useful spectroscopic methods "menu" for analysis of peptides by NMR is given in the conclusions. The chapter has 26 pages and 101 references.

The book is endowed with carefully edited subject and author indexes with page and reference number for the reader's convenience. The book is highly recommended not only to NMR spectroscopists but also for chemists and biochemists who want to become acquainted with some of the current applications of NMR.

T.-S. Balaban
Centre of Organic Chemistry

"Ion-Selective Electrodes, 4", Edited by E. Pungor, Akadémiai Kiadó, Budapest, 1985, 765 p.

This book contains the papers originally presented at the Symposium held at Mátrafüred, Hungary, 8—12 October, 1984. The Symposium, the fourth in the series, is already a traditional meeting. Among the outstanding personalities were present professors Bates, Buck, Hopârtean, Hulanicki, Janata, Pungor, Rechnitz, Thomas, Simon and Vlasov. The papers are divided into four main chapters : plenary lectures, keynote lectures, discussion lectures and round table discussion on the problems of standards in work with ion-selective electrodes (ISEs).

The chapter of plenary lectures has four papers : "Chemical sensors mechanisms" (R. P. Buck), "Polarization studies with ion-selective electrodes" (K. Cammann and G. A. Rechnitz), "Selectivity properties of ion-selective membrane electrodes" (N. Ishibashi *et. al.*) and "Membrane technological optimization of ISEs" (W. Simon *et al.*).

Professor Buck presented a progress report on the mechanism of chemical sensors. It is based on electrochemical effects and included physical phenomena that obey electrostatic laws applicable to charged species (ions and electrons) and dipolar species (solvents, plasticizers and membrane components). The model fits to solid state sensors, liquid-membrane electrodes and biosensors.

Cammann and Rechnitz pointed out the importance of exchange current density in polarization studies with ISEs and/or membranes. The proposed theoretical approach treats all kinds of membranes of the ion-selective electrodes and allows easy explanation for all known properties of ISE, e.g. selectivity, time response, sub- and super-Nernstian slope, transient response to interfering ions etc.

Based on the theoretical treatment on the concentration variation at the interface between an electrode membrane and a sample solution, Ishibashi *et al.* clarified the condition necessary to evaluate the selectivity coefficients of the neutral carriers liquid ion exchange membrane electrodes. Sensitivities of these detectors in flow analysis are discussed in connection with their selectivity.

Simon *et al.* emphasized on the requirements (selectivity, stability, response time and life time) for a reliable monitoring of ion-activities with ion-selective solvent polymeric membranes for clinical applications in flow-through analyzers. The performances of neutral carrier based electrodes selective to hydrogen, lithium, potasium, magnesium, calcium, chloride and dicarbonate ions are discussed and compared to currently available membrane systems.

The chapter of keynote lectures contains eight papers : "Chemically modified electrode sensors" (R. A. Durst), "Chemically sensitive field effect transistors" (CHEMFETs)" (G. Janata), "Bis (crown ether) based ISEs" (K. Kimura and T. Shono), "Theoretical treatment of the dynamic behaviour of precipitate based ISEs" (E. Pungor *et al.*), "New developments and consequences of theory of ion-selective membranes" (W. E. Morf *et al.*), "Continuous analysis with ISEs" (J. D. R. Thomas), "Bis(crown ether)s for potassium ISEs" (K. Tóth *et al.*), "Ion-selective field effect transistors (ISFETs)" (Yu. G. Vlasov).

A review of the types of chemically modified electrodes, their fabrication, and some examples of their use is given by Durst. Biochemical systems which greatly extends the analytical usefulness of these devices are also presented.

Janata and Vlasov in two well-documented papers focused on CHEMFET and ISFET classification, operation and preparation as well as on problems and limitations arising in the development and application of these sensors.

Various bis(crown ether) derivatives have been used by Kimura and Shono as neutral carriers for potassium, sodium, caesium, thallium (I) and calcium ion-selective electrodes, whereas Tóth *et al.* emphasized on different bis(crown ether) ionophores with urethane linkages that have good selectivity towards potassium ions.

A simplified and more detailed quantitative description of the theoretical treatment of the dynamic behaviour of precipitate based sensors on the presence of interfering ions was proposed by Pungor *et al.*

A unified approach to the theory of ion-selective liquid membrane electrodes based on ion-exchangers and neutral carriers was presented by Morf *et al.* The results were discussed for novel sensors responsive to nitrate, chloride and enantiomeric organic ammonium ions.

Various aspects of work at University of Wales (Cardiff) on flow-injection analysis (FIA) and continuous analysis with ISEs were described by professor Thomas. They relate to uses of calcium and sulphide ISEs for monitoring primary ions, of iodide electrode for monitoring enzyme reactions and some aspects of ISEs in microcomputerised titrations.

The discussion lectures chapter has 37 papers. They include theortical studies aiming to elucidate the mechanism of ISEs working, membrane or membrane/interface phenomena, the influence of primary and interfering ions on electrode behaviour. Another class of papers deals with new type of electrodes, researches on complex forming reactions, determination of stability constants, drug and *in vivo* analyses, the use of ISEs as detectors on FIA and HPLC and environmental analyses.

The fourth chapter is devoted to round table discussions. It contains an introductory lecture on "Further studies of ionic activity scales" (R. G. Bates) and a paper on "Determination of mean activity coefficients with ISEs" (E. Pungor *et al.*). These contributions give methods of activity coefficients estimation at high ionic strength and a procedure to compute them.

This book deals, therefore, with numerous and various developments and applications of ion-selective electrodes. It emphasizes the theoretical and technological efforts towards understanding the phenomena and a more easy-to-handle instrumentation. Perhaps, it would gain in clarity if tables and figures would be fitted to the appropriate position in the text, and in

personality if the authors of questions and comments would be nominated. The book will be useful to all scientists working in ion-selective electrodes as well as to those involved in various connected fields.

Dan F. Anghel
Institute of Chemical Research,
Department of Physical Chemistry,
Bucharest, Spl. Independenței 202

J. Holló, K. J. Kaffka and J. L. Gönczy (Editors): "Near Infrared Diffuse Reflectance/ Transmittance Spectroscopy", Académiai Kiadó, Budapest, 1987, 319 pages.

Analysis of agricultural products and of foodstuffs constitutes a major problem of modern economy. The necessity of such an analysis has been raised as early as the middle of the 19th century and gradually the worked-out analysis methods have been grouped into sets of methods, each of which devoted to the systematic analysis of cereal seeds, fruits, dairy products, meat and other animal products, etc. The number and variety of these methods are very large today and many of them have already been integrated among the mandatory food-control procedures in many countries.

Originally, most of these methods were chemical methods, but the physico-chemical methods have gradually begun to compete seriously the former ones, owing especially to their sensitivity and rapidity, and also to their non-destructive character. Among the latter, the infrared spectroscopic methods, particularly in the near-infrared (NIR, the 14,000—3000 cm^{-1}) region, where overtones or combinations of the vibrations of hydrogen bonds (with C, N or O atoms) may appear, might be included. The first applications of the NIR spectroscopic methods were the determination of proteins, oils and water in cereal seeds and foods, of amino acids (particularly of lysine) in proteins, of the degree of ripeness of fruits, etc.

The most recent advances of the application of NIR spectroscopy in agriculture and food industry have formed the subject matter of an international conference which was held in Budapest in May, 1986. The book reviewed here contains the proceedings of the papers presented on that occasion. It is divided into five sections — theory, methodology, instrumentation, applicatons in agriculture, and in food industry. Overall, about 30 communications are presented *in extenso*.

Among the theoretically-oriented papers we can note those devoted to the state of water in foodstuffs (and generally in biological materials), which is really a frontier domain of research today. The field of research methodology is represented by, e.g., the application of the pattern recognition technique in NIR spectroscopy (for characterising raw materials or finished products in cereal industry), the multidimensional analysis of spectroscopic data (for analysing the components of milk), the application of Fourier transform NIR (FT—NIR) spectroscopy, the use of diffuse reflectance NIR spectroscopy (for controlling the quality and composition of batter meat, seeds or fodder), etc. The section devoted to instrumentation also contains several valuable contributions, in which the applicability of some simple NIR apparata — or their modification — for the routine analysis of a large variety of food produce is investigated.

The last two sections of the book are devoted to some problems raised by the analysis of agricultural and food products, respectively. Among the most important NIR methods approached at the conference, we may quote those for the determination of the ten essential amino acids in various high-protein products (wheat, barley, soy bean, lupin, sunflower), of cellulose, oils, gluten and starch in various seeds, for the determination of the optimal period of harvesting the fodder (as a function of the nitrogen/protein ratio and moisture), for the analysis of fats, proteins and solids in milk, of the quality of cotton fibres, of the total nitrogen content in dried vine leaves (for the early detection of some imbalances in plant nutrition), for the analysis of milk, cheese, butter and meat in various of their processing steps. Many other applications are also fully described.

The title of this collection of very valuable papers is somewhat misleading: it does not reflect the area to which the discussion on NIR spectroscopy has been restricted — agriculture and food industry. NIR spectroscopy has found today many other applications, both in structural and analytical chemistry of many compounds involved in various branches of economy, as well as in research. In spite of this superficial drawback, this book remains a precious contribution to the knowledge of modern methods of analysing foodstuffs and the corresponding raw materials. It may be extremely useful to any analyst working in quality-control laborations for seeds, fruits, forage and food products and particularly to those analysts who consider the acquisition for their laboratories of a NIR spectrometer (equipped with facilities for both transmittance and reflectance), an instrument which has proved to open new and better ways for such a control,

Dr. Alex. Butucelea
Center of Physical Chemistry

Alan P. Marchand, "Stereochemical Applications of NMR Studies in Rigid Bicyclic Systems", Volume 1 in "Methods in Stereochemical Analysis", Series Editor Alan P. Marchand, Verlag Chemie International, Deerfield Beach, Florida 1982, Hardcover, 231 pp. 280 DM.

The series "Methods in Stereochemical Analysis" edited by Professor Alan P. Marchand aims at presenting in book form timely reviews from outstanding contributors covering stereochemical applications of physical methods (i.e. spectroscopic techniques, physical techniques or applied theoretical studies). Volume 1 in this series covers Nuclear Magnetic Resonance (NMR) studies applied to rigid bicyclic systems mainly with bicyclo[2.2.1]heptane (norbornane) and bicyclo[2.2.2]octane skeletons.

As stated in the preface, only relevant stereochemical NMR analyses were considered. The truly "onerous" task of selecting the data from the ocean of published papers on such systems is admirably performed by Prof. Marchand.

In a short introduction, the mutual beneficial influences between the fields of NMR analysis and the chemistry of rigid bicyclic systems are enumerated. These include on one hand the development of synthetic skills in obtaining pure products, free of any other stereoisomers, a feat accomplished only with the advent of NMR, and on the other hand, the NMR information gained from these rigid systems with a known and predictable geometry proved to be of general applicability and paved the way for applications of NMR techniques to much more complex systems. The norbornyl and bicyclo[2.2.2]octyl systems have thus played key roles in the development of NMR analysis and these roles are followed in the three chapters of the book.

The first and shortest of these (Chapter 2) considers aromatic solvent and lanthanide induced shifts (ASIS and LIS) as well as intramolecular nuclear Overhauser effects (NOE) as aids in making spectral assignments.

The stereochemical applications of NMR chemical shifts (Chapter 3) and of NMR spin-spin coupling constants (Chapter 4) in rigid bicyclic systems cover over 190 pages, mainly in tabular form. NMR studies of $^{1}H-$, $^{13}C-$, $^{19}F-$ and other nuclei are considered. Beside norbornyl and bicyclo[2.2.2]octyl systems, aza-, phospha-analogs and other rigid polycyclic systems are included.

Almost 500 references with a useful author index make this book a reference text both for NMR spectroscopists as well as for synthetic chemists involved with the "notorious" norbornyl or other rigid bicyclic systems.

T.-S. Balaban
Centre of Organic Chemistry

J. L. Marshall "Carbon-Carbon and Carbon-Proton NMR Couplings : Applications to Organic Stereochemistry and Conformational Analysis ; Methods in Stereochemical Analysis", Volume 2, Series Editor Alan P. Marchand, Verlag Chemie, ISBN 0-89573-113-4, Deerfield Beach, Florida 1983, 241 pp, Hardcover, DM 175.

The second volume in the series "Methods in Stereochemical Analysis" edited by Professor A. P. Marchand, is a comprehensive monograph on carbon-proton ($^{13}C - {}^{1}H$) and carbon-carbon ($^{13}C - {}^{13}C$) NMR coupling constants authored by Professor J. L. Marshall (North Texas State University) whose contribution to the application of these coupling constants in stereochemical analysis was essential.

The basic idea is that long range (over more than one bond) coupling constants involving ^{13}C nuclei (J_{CX}) convey reliable and predictable stereochemical information and are suitable for a larger range of compounds than proton-proton (J_{HH}) couplings. The latter, however, have enjoyed a much wider application to stereochemical and conformational analysis firstly because proton-proton couplings are easily obtained (in contrast to carbon-proton and carbon-carbon couplings) and secondly because the dependence of the proton-proton couplings on the substrate geometry is simple and well understood (mainly through the Karplus dihedral angle relationship). The book is a first attempt for a thorough, authoratative view of the subject containing all the available (until 1982) coupling constants and even some unpublished results from the author's own work.

After the introduction which gives practical considerations on how to obtain the data (mostly by syntheses of ^{13}C-labelled compounds), Chapter 2 considers carbon-proton couplings. Chapter 3 is devoted to aliphatic vicinal ($^3J_{CC}$), carbon-carbon couplings while the more unpredictable geminal ($^2J_{CC}$) couplings are treated in Chapter 5 entitled "Special Topics", along with the determination of signs of couplings and the additivity of J_{CC} values. Chapter 4 considers C—C couplings in π systems separately for conjugated and non-conjugated systems depending on whether the ^{13}C-label is involved in the conjugation or not. The last chapter, 6, considers "Biochemical Applications of C—C Couplings" mainly as an aid in understanding biosynthetic pathways and ^{13}C-chemical shift assignments ; it tabulates the available data for saccharides, aminoacids and peptides and mentions a few heterocycles.

Each chapter, in view of the desired stereochemical analysis, considers correlations between the observed J_{CH} or J_{CC} values *versus* either the molecular structure (diehedral angle relationships, substituents to the coupling path, the presence of more than one coupling pathway or mechanism) or the more common J_{HH} values in suitably selected models.

The book has somewhat less than 200 references, a vast tabular material in which for the readers' convenience beside the coupling constants also the ^{13}C chemical shifts are given (when these were directly available), a general index and a very useful compound type index which facilitates greatly the entry to both the text and the Tables.

Although the book assumes a general knowledge of NMR spectroscopy, FT techniques and proton-proton couplings, it is self-contained. It is highly recommended to all ^{13}C-NMR spectroscopists and scientists involved with synthesis or use of ^{13}C-labelled compounds in connection with NMR analysis.

In the reviewer's opinion, however, the book haș a timing handicap being issued on the dawn of the two-dimensional NMR era which has rendered much easier the gaining of ^{13}C homo- or heteronuclear coupling constants. Although mentioned in the book's introduction as additional techniques for obtaining C—C couplings, these were seldom used ; in fact most of the values in the book result from a sometimes "ardous" synthetic effort of ^{13}C-labelled compounds, and not as a result of the new pulse sequences. In these last few years a lot of data has been gathered and the accumulation will undoubtedly continue in the next decade. It is imperative that a continuation of professor Marshall's trail, encompassing the new data, should appear in the next years. In this way it is hoped that the somewhat pathological behaviour of some C—C couplings can be accomodated in a clear and useful picture.

T.-S. Balaban
Centre of Organic Chemistry

ORSZÁGOS [illegible]
198[illegible]

NOTE POUR LES AUTEURS

La Revue Roumaine de Chimie publie des articles en anglais, français, russe, allemand ou espagnol. Les auteurs sont priés d'envoyer des articles et des comptes rendus inédits.

Les manuscrits seront dactylographiés à double interligne. La bibliographie, les tableaux et la légende des figures seront placés après le texte.

Si l'article fait partie d'une série numérotée, la partie précédente sera donnée comme première référence.

Chaque article sera précédé d'un résumé comprenant quinze lignes au maximum.

Les références bibliographiques dans le texte seront faites par des exposants sans parenthèses et paraitront à la fin de l'ouvrage.

Les publications périodiques mentionnées dans la bibliographie seront présentées suivant les prescriptions internationales : le nom de l'auteur précédé de l'initiale du prénom, le titre du périodique abrégé conformément à « Chemical Abstracts » et souligné par une ligne, le numéro du tome indiqué par des chiffres arabes et souligné par deux lignes, suivi de la première page de l'article : à la fin, l'année de la parution sera placée entre parenthèses. Le numéro de la revue ne sera pas indiqué si les pages du volume sont numérotées consécutivement.

Les textes des livres ou traités inclueront : le nom des auteurs, précédé de l'initiale du prénom, le titre du livre entre guillemets et sans être souligné, le numéro du tome précédé par l'abréviation « vol.» (ou « Bd »), le numéro de l'édition, les éditions (the publisher), la localité de la parution du livre, l'année de la parution et la page de la référence précédée par l'abréviation « p » (ou « S »).

Les brevets seront indiqués comme suit : l'auteur ou la firme, le pays et le numéro du brevet, la date de la revue (*Chem. Abstr.*). Par ex. : M. Jones (to Union Carbide Co.) Brit. Pat. 610 238,2 Sept. 1959 : cf. *Chem. Abstr.*, 54, 12808 (1960).

Si la référence n'a pas été lue en original, on indiquera aussi la revue de références consultée.

Les diagrammes seront tracés à l'encre de Chine sur papier calque. Les tableaux et les figures (en nombre strictement nécessaire), ainsi que les courbes dans les figures seront numérotés par des chiffres arabes. Leur explication sera donnée dans la légende des figures. Prière de ne pas inscrire les mêmes données dans les tableaux et les figures. Chaque tableau aura un titre. On indiquera dans le texte la place approximative des tableaux et des figures. Les formules chimiques seront incluses dans le texte ; en outre, elle seront transcrites sur papier calque, à l'encre de Chine.

Les auteurs sont priés d'indiquer les caractères italiques (en soulignant les lettres au crayon), ainsi que tout autre caractère spécial : les préfixes *ortho*, *méta*, *para*, *cis*, *trans*, etc. seront soulignés pour indiquer leurs caractères italiques, et ne seront jamais écrits avec des majuscules.

Aucune correction à la main ne sera admise sur le manuscrit. Les corrections seront frappés à la machine. Les lettres grecques ou d'autres symboles spéciaux seront insérés à la main à l'encre clairement.

Le manuscrit sera signé par l'auteur.

Le titre courant aura 50 lettres au maximum.

L'entière responsabilité du contenu des articles appartient aux auteurs.

Sur demande on peut obtenir une note plus complète.

PRINTED IN ROMANIA

1988 MAR 1 8

TRAVAUX PARUS AUX ÉDITIONS DE L'ACADÉMIE DE LA RÉPUBLIQUE SOCIALISTE DE ROUMANIE

ELENA CEAUŞESCU, **Răşini de hidrocarburi, vol. 1**, 1988, 344 p.
ELENA CEAUŞESCU, **Progrese in chimia şi tehnologia polimerilor**, 1986, 446 p.
ELENA CEAUŞESCU, **Forschungen im Bereich der Chemie und Technologie der Polymere**, 1986, 444 p.
ELENA CEAUŞESCU **Cercetări în chimia şi tehnologia polimerilor**, 1983, 520 p.
ELENA CEAUŞESCU, **Noi cercetări în domeniul compuşilor macromoleculari**, 1981, 536 p.
ELENA CEAUŞESCU, **Polimerizarea stereospecifică a izoprenului**, 1979, 307 p.
ELENA CEAUŞESCU, **Research work on synthesis and characterization of macromolecular compounds. Contributions**, 1974, 251 p.
I. G. MURGULESCU, **Introducere în chimia fizică. Vol. I. 1 Atomi, molecule, legătură chimică**, 1976, 650 p.
I. G. MURGULESCU, V. Em. SAHINI, **Introducere in chimia fizică. Vol. I, 2. Structura şi proprietăţile moleculelor**, 1978, 604 p
I. G. MURGULESCU, E. SEGAL, **Introducere în chimia fizică. Vol. II. 1. Teoria molecular cinetică a materiei**, 1979, 1036 p.
I. G. MURGULESCU, TATIANA ONCESCU, E. SEGAL, **Introducere în chimia fizică. Vol.II, 2. Cinetică chimică şi cataliză**, 1981, 1024 p.
I. G. MURGULESCU, J. PĂUN, **Introducere în chimia fizică, Vol. I.3. Nucleul atomic, reacţii nucleare, particule elementare**, 1982, 606 p.
I. G. MURGULESCU, RODICA VÎLCU, **Introducere în chimia fizică, Vol. III. Termodinamica chimică**, 1982, 624 p.
I. G. MURGULESCU, O. M. RADOVICI, **Introducere în chimia fizică, vol. IV, Electrochimia**, 1986, 416 p.
R. VÎLCU, M. LECA, **Termodinamica polimerilor prin cromatografie de gaze**, 1987, 238 p.
I. ZUGRĂVESCU, M. PETROVANU, **Cicloadiţii 3 + 2-dipolare**, 1987, 446 p.
RAUL MIHAIL, ION GROZEANU, **Estimarea secvenţială aplicată sistemelor chimice**, 1986, 406 p.
M. BREZEANU, L. PATRON, M. ANDRUH, **Combinaţii complexe polinucleare şi aplicaţiile lor**, 1986, 244 p.
A. T. BALABAN et al. **Labelled compounds and radiopharmaceuticals applied in nuclear medicine**, coédition avec J. Wiley & Sons, 1986, 742 p.
D. PURDELA, **Nomenclatura chimiei anorganice**, 1986, 454 p.
P. BUDRUGEAC, **Probleme de chimie**, 1986, 280 p.
T. ONCESCU, S. G. IONESCU, **Conversie fotochimică şi stocare de energie solară**, 1985, 272 p.
V. DRĂGUŢAN, A. T. BALABAN, M. DIMONIE, **Olefin metathesis and ring-opening polymerization of cyclo-olefins**, coédition avec John Wiley & Sons, 1985, 544 p.
N. PERESCU, **Chimia extracţiei cu solvenţi şi aplicaţii**, 1985, 212 p.
V. Em. SAHINI, M. HILLEBRAND, **Chimia cuantică în exemple şi aplicaţii**, 1985, 380 p.
GH. MARCU, **Chimia compuşilor coordinativi**, 1984, 415 p.
E. CORDOŞ, C. MANOLIU, **Spectrometria de absorbţie şi fluorescenţă atomică**, 1984, 178 p.
C. BODEA, **Tratat de biochimie vegetală, p. II, vol. 5**, 1984, 438 p.
N. ASANDEI, A. GRIGORIU, **Chimia şi structura fibrelor**, 1983, 395 p.
N. IONESCU, M. CĂLDĂRARU, **Oxidarea catalitică a olefinelor inferioare**, 1983, 178 p.
C. I. SIMIONESCU, F. DANEŞ, **Originea vieţii**, 1983, 110 p.
C. BODEA, **(editeur), Tratat de biochimie vegetală**, p. II, Vol. IV, 1982, 408 p.
ELENA JERCAN, **Analiza cromatografică**, 1982, 286 p.
I. GĂLĂŢEANU, **Procese şi metode radiochimice în energetica nucleară**, 1981, 234 p.
CR. SIMIONESCU, VALERIA GORDUZA, **Polimeri biocompatibili şi biologic activi**, 1980, 479 p.
M. FLORESCU, **Metode ştiinţifice în dezvoltarea industriei chimice moderne**, 1979, 256 p.
CONST. GH. MACAROVICI, **Analiza chimică cantitativă anorganică**, 1979, 457 p.

ISSN 0035—4090

c. 1667—I. P. INFORMAŢIA

43 426

Lei 40
$ 90 (pour un abonnement annuel)

F 1103

04

ACADÉMIE DE LA RÉPUBLIQUE SOCIALISTE DE ROUMANIE

REVUE ROUMAINE DE CHIMIE

TOME 33
N° 2
Février 1988

Rev. Roumaine Chim. RRCHAX, 33, 2, p. 105–222 (1988), Bucarest
EDITURA ACADEMIEI REPUBLICII SOCIALISTE ROMÂNIA

ACADÉMIE DE LA RÉPUBLIQUE SOCIALISTE DE ROUMANIE

COMITÉ DE RÉDACTION

Rédacteur en chef:

I. G. MURGULESCU, membre de l'Académie de la République Socialiste de Roumanie

Rédacteurs en chef adjoints:

A. T. BALABAN et V. EM. SAHINI, membres correspondants de l'Académie de la République Socialiste de Roumanie

Collège de rédaction:

EM. BRATU, ELENA CEAUŞESCU, ECATERINA CIORĂNESCU-NENITZESCU, CR. SIMIONESCU, membres de l'Académie de la République Socialiste de Roumanie ; P. SPACU, membre correspondant de l'Académie de la République Socialiste de Roumanie ; M. BANCIU, M. D. GHEORGHIU, I. HAIDUC, D. I. MARCHIDAN, G. NIAC et D. SĂNDULESCU

La Revue Roumaine de Chimie parait 10 fois par an. Toute commande de l'étranger sera adressée à ROMPRESFILATELIA — sectorul Export-Import Presă, P. O. Box 12—201, télex 10376 prsfi r 78 104 Bucarest, Calea Griviţei nr. 64—66, Bucureşti, Roumanie

Les manuscrits, les livres et les revues proposés en échange, ainsi que toute correspondance seront envoyés à la rédaction :

REVUE ROUMAINE DE CHIMIE

125, Calea Victoriei, 79717 Bucarest, Roumanie, téléphone 50 76 80

EDITURA ACADEMIEI REPUBLICII SOCIALISTE ROMÂNIA
125, Calea Victoriei, 79717 Bucarest, Roumanie, téléphone 50 76 80

REVUE ROUMAINE DE CHIMIE

ORSZÁGOS MŰSZAKI INFORMÁCIÓS KÖZPONT ÉS KÖNYVTÁR 1988

Tome 33, N° 2 **Février 1988**

RODICA VÎLCU and ANDREI DOBRESCU, Calculation of higher order Onsager's coefficients for monomolecular reactions 107–110
S. STERNBERG, A. MATEESCU, V. BRÂNZOI and L. APĂTEANU, Effect of phosphoric acid on the $PbSO_4/PbO_2$ electrode in sulphuric acid solutions 111–123
M. WOLDAN, Viscosity of some alkali halides in water–acetamide mixtures at 333.15 K 125–131
I. SILAGHI-DUMITRESCU and I. HAIDUC, Linear *versus* bent bis(diphosphine)iminium cations. A molecular orbital discussion of the bonding in $[H_3PNPH_3]^+$ and related species 133–142
MARIA BREZEANU and OTILIA COSTIȘOR, Polynuclear coordination compounds containing vanadium-tin bond 143–148
FELICIA IACOMI, ELEONORA TRIF, EVELINE POPOVICI, AURELIA VASILE, MARIA ALEXANDROAEI, M. CRUCEANU and GH. SINGUREL, Determination of the nature of iron(III) impurities in NaA zeolites 149–155
SUBAS C. PATI, ASHOK KUMAR SAHU and Y. SRIRAMULU, Kinetics and mechanism of Ru(III) chloride-catalysed oxidation of benzaldehyde and substituted benzaldehydes by trichloroisocyanuric acid in acid medium 157–166
M.M. ALY, I.M.A. AWAD and A. M. FAHMY, Photochemical bromination of anilides by benzenehexabromide 167–169
M. P. ALVAREZ MACHO, Kinetics of oxidation of some disaccharides by chromic acid in perchloric acid medium (in Spanish) 171–176
KERIMAN GÜNAYDIN and TURAN ÖZTÜRK, Photoirradiation of 1-phenylcyclopentadecene-1 177–181
AHMED M. NOUR EL-DIN, ABD EL-RAZAK M. TAWIK and RAMADAN MEKAMER, Reactions of dibenzoylacetylene with N-Alkyl nitrones, heteroaromatic-N-oxides, diazo and azoxy compounds 183–187
N. NEGOIȚĂ, J. M. HERDAN, NICOLETA GRECU and GH. IORDACHE, Transformations of aminic antioxidants in the inhibited oxidation of hydrocarbons 189–194
M. VLASSA and M. CENAN, Alkylation of phenothiazine using solid-liquid phase transfer catalysis without solvent 195–197
MARIA ENCULESCU, Hydraulic binders. I. Contribution to the processes of producing high-quality Portland and aluminous cements, noble and coloured limes and plasters out of wastes resulted from the chemical industry and other industries 199–216
BOOKS REVIEWS 217–221

Rev. Roumaine Chim. **33**, *2*, 105–222 (1988), Bucarest

Revue Roumaine de Chimie, **33**, *2*, 107–110 (1988)

CALCULATION OF HIGHER ORDER ONSAGER'S COEFFICIENTS FOR MONOMOLECULAR REACTIONS

RODICA VÎLCU and ANDREI DOBRESCU
Department of Physical Chemistry, Polytechnic Institute of Bucharest, Blvd Republicii 13, Bucharest, Romania

Received May 26, 1986

The paper deals with Onsager's coefficients of the second order for monomolecular reactions. Onsager's coefficients are expressed in terms of absolute temperature and molar fractions of the components.

The study of the particular features of the chemical reactions leads to the conclusion that generally the chemical processes are irreversible and nonlinear.

The kinetic and energetical characteristics of the chemical reactions far from equilibrium are difficult to be experimentally and theoretically established. The linear theory given by Onsager[1], Casimir [2] and Prigogine[3] was improved by Rysselberghe [4] and Gyarmati [5] in order to express the reaction rate as a function of chemical affinities for the case when the chemical reactions take place near to equilibrium. The mentioned authors have considered ideal systems in gaseous phase, the results valid for the chemical reactions near to equilibrium being completely determined by the state parameters.

The general expression for reaction rate as a function of affinities is of the form:

$$v_r = \sum L_{rs} A_s + \frac{1}{2!} \sum L_{rst} A_s A_t + \frac{1}{3!} \sum L_{rstq} A_s A_t A_q + \ldots \; (r = 1, 2, \ldots, R) \tag{1}$$

where L_{rstq} is the highest order Onsager's coefficient.

Because expression (1) represents an analytical function of affinities, it is valid for any system of chemical reactions near to or far from equilibrium. Calculation of Onsager's coefficients of different orders has been performed [5] for the ideal case above mentioned, in the vicinity of equilibrium and low affinity values.

We shall consider in this note that expression (1) is also valid for the case when the chemical reactions take place far from equilibrium. If one denotes by n'_k, n''_k the mole number of reagents and products respectively at a given moment, and by $\Delta n'_k = n'_k - n'_{ke}$, $\Delta n''_k = n''_k - n''_{ke}$ the corresponding deviations from the equilibrium values, the affinity is then given [5] by:

$$\frac{A_r}{RT} = \ln \prod_{k'} \left(1 + \frac{\Delta n'_k}{n'_{ke}}\right)^{\nu_{k'r}} - \ln \prod_{k''} \left(1 + \frac{\Delta n''_k}{n''_{ke}}\right)^{\nu_{k''r}} \tag{2}$$

$(r = 1,2, = \ldots, R)$, $\nu_{k'_r}$, $\nu_{k''_r}$ being the stoichiometric coefficients of reagents and reaction products respectively.

If one takes into account that

$$\Delta n_k = \sum_{r=1}^{R} \nu_{kr} \Delta \lambda_r \tag{3}$$

where λ_r is the evaluation degree of the reaction denoting

$$\ln \mathscr{A}_r = \frac{A_r}{RT} \tag{4}$$

we have:

$$\mathscr{A}_r(\Delta\lambda_1, \Delta\lambda_2, \ldots, \Delta\lambda_r) = \frac{\prod_{k'}{}^{k'} \left(1 + \frac{\sum \nu_{k'r} \Delta\lambda_r}{n_{k'e}}\right)^{\nu_{k'r}}}{\prod_{k''} \left(1 + \frac{\sum \nu_{k''r} \Delta\lambda_r}{n_{k''e}}\right)^{\nu_{k''r}}} \tag{5}$$

where $r = 1,2 \ldots, R$.

Similarly

$$v_r = v_r^e \left[\prod_{k'} \left(1 + \frac{\sum \nu_{k'r} \Delta\lambda_r}{n_{k'e}}\right)^{\nu_{k'r}} - \prod_{k''} \left(1 + \frac{\sum \nu_{k''r} \Delta\lambda_r}{n_{k''e}}\right)^{\nu_{k''r}}\right] \tag{6}$$

where,

$$v_r^e = k'_r \prod_{k'} \left(\frac{n_{k'e}}{n}\right)^{\nu_{k'r}} = k''_r \prod_{k''} \left(\frac{n_{k''e}}{n}\right)^{\nu_{k''r}} \tag{7}$$

From (5) and (6) one can, in principle, determine $v_r = \varphi(A_1, A_2, \ldots A_R)$ which is of form (1).

We shall determine in the present note Onsager's coefficients of the second order for the following system of chemical reactions or equivalently:

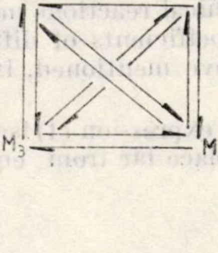

$$- M_1 + M_2 = 0$$
$$- M_2 + M_3 = 0$$
$$- M_3 + M_4 = 0$$
$$- M_4 + M_1 = 0$$
$$M_1 + M_3 = 0$$
$$- M_4 + M_2 = 0$$

The matrix of stoichiometric coefficients is

$$\nu_{kr} = \begin{pmatrix} -1 & 0 & 0 & 1 & -1 & \\ 1 & -1 & 0 & 0 & 0 & 1 \\ 0 & 1 & -1 & 0 & 1 & 0 \\ 0 & 0 & 1 & -1 & 0 & -1 \end{pmatrix}$$

One may obviously see that the six reactions are not independent. The last three reactions depend on the first ones, and therefore only three reaction rates are distinct. They can be deduced from (1) and have the form

$$v_1^x = n\,\frac{-v_4^e - v_5^e\, e^{\frac{A_3}{RT}} - v_1^{e}{}^{\frac{A_2+A_3}{rT}} + (v_1^e + v_4^e + v_5^e)\, e^{\frac{A_1+A_2+A_3}{RT}}}{n_4^e + n_3^e\, e^{\frac{A_3}{RT}} + n_2^e\, e^{\frac{A_2+A_3}{RT}} + n_1^e\, e^{\frac{A_1+A_2+A_3}{RT}}}$$

$$V_2^x = n\,\frac{-(v_4^e + v_6^e) - (v_2^e + v_5^e)\, e^{\frac{A_3}{RT}} + (v_2^e + v_6^e)\, e^{\frac{A_2+A_3}{RT}} + (v_4^e + v_5^e)\, e^{\frac{A_1+A_2+A_3}{RT}}}{n_4^e + n_3^e\, e^{\frac{A_3}{RT}} + n_2^e\, e^{\frac{A_2+A_3}{RT}} + n_1^e\, e^{\frac{A_1+A_2+A_3}{RT}}}$$

$$V_3^x = n\,\frac{-(v_3^e + v_4^e + v_5^e) + v_3^e\, e^{\frac{A_3}{RT}} + v_6^e\, e^{\frac{A_2+A_3}{RT}} + v_4^e\, e^{\frac{A_1+A_2+A_3}{RT}}}{n_4^e + n_3^e\, e^{\frac{A_3}{RT}} + n_2^e\, e^{\frac{A_2+A_3}{RT}} + n_1^e\, e^{\frac{A_1+A_2+A_3}{RT}}}$$

From expression (1) results Onsager's coefficient of the second order

$$L_{rst} = \left(\frac{\partial^2 v_r}{\partial A_s\, \partial A_t}\right) A_s = A_t = 0$$

All these coefficients given in table 1 fulfill the Gyarmaty and Ly principle of reciprocity, namely :

$$\frac{\partial v_s}{\partial A_n} = \frac{\partial v_n}{\partial A_s}$$

where v_s, v_k are the reaction rates and A_m, A_s chemical affinities.

The second order Onsager's coefficients thus obtained remain also valid for the chemical reactions far from equilibrium.

The results are summarized in Table 1.

Table 1

$$L_{111} = \frac{(v_1^e + v_2^e + v_5^e)\,(x_2^e + x_3^e + x_4^e - x_1^e)}{(RT)^2} \quad \text{where} \quad x_1^e = \frac{n_1^e}{n}$$

$$L_{211} = \frac{L_{112} + L_{121}}{2} = \frac{v_1(2x_1^e + 2x_2^e + x_3^e + x_4^e) + v_4^e(2x_2^e + x_3^e + x_4^e) + v_5^e(2x_2^e + 2x_3^e + x_4^e)}{(RT)^2}$$

$$L_{122} = \frac{(v_4^e + v_5^e)\,x_4^e}{(RT)^2}$$

$$\frac{L_{123} + L_{132}}{2} = \frac{-v_4^e(x_1^e + x_2^e + x_3^e) + x_4^e v_5^e}{(RT)^2}$$

$$L_{133} = \frac{v_4^e(x_4^e - 3x_2^e - 3x_1^e - 3x_3^e)}{(RT)^2}$$

REFERENCES

[1] L. Onsager, *Phys. Rev.*, **37**, 405 (1931); **38**, 2265 (1931).

[2] H. B. G. Casimir, *Rev. Mod. Phys.*, **17**, 343 (1945).

[3] I. Prigogine "Étude Thermodynamique des Phénomènes Irreversibles" (Thesis), Dunod : Paris, and Desoer, Liege, 1947.

[4] Van P. Rysselberghe, *Journ. Chem. Phys.*, **36**, 1329 (1962).

[5] I. Gyarmati, *Ann. Phisique*, **7**, 353 (1969).

[6] S. Lengyei and I. Gyarmati, Nonlinear thermodynamical studies of homogeneous chemical kinetic systems, Periodica Polytechnica, Chemical Engineering. Vol. 25., No 1. 1981.

Revue Roumaine de Chimie, 33, 2, 111–123 (1988)

EFFECT OF PHOSPHORIC ACID ON THE $PbSO_4/PbO_2$ ELECTRODE IN SULPHURIC ACID SOLUTIONS

S. STERNBERG[a], A. MATEESCU[b], V. BRÂNZOI[a] and L. APĂTEANU[c]

[a] Department of Physical Chemistry and Electrochemical Technology, Calea Griviței 132, Polytechnic Institute Bucharest, Romania

[b] "ACUMULATORUL" Enterprise, Blvd Biruinței 102, Bucharest, Romania

[c] Biochemical and Chemical Energetic Institute, Splaiul Independenței 206, Bucharest, Romania

Received February 3, 1986

The influence of small additions of H_3PO_4 on the polarization behaviour of the $PbSO_4/PbO_2$ electrode, in H_2SO_4 solutions of varied concentrations, was studied using the microelectrode technique and the coulometric method. The reference electrode was the $Hg/Hg_2SO_4/H_2SO_4$ electrode. The potentiograms analysis and the coulometric measurements showed that the main effect of H_3PO_4 is the drastic passivation of the electrode processes, within the potential range under study that means the +800 mV to +1 650 mV potential range. The Q_a and Q_c electricity amounts are of about 5 to 10 times smaller in the H_2SO_4 solution with H_3PO_4 addition comparatively with the H_2SO_4 solution free of H_3PO_4 addition. A high increase of the oxygen evolution overvoltage can be noticed. Taking into account the ratio between the H_3PO_4 addition amount, in % $\left(\frac{w}{o}\right)$, and the PbO_2 active mass per units surface area, from the lead acid batteries, we can conclude that the small H_3PO_4 additions do not decrease the capacity of the active mass of the battery, but they hinder the insulator films formation between the active mass and the grid.

INTRODUCTION

An efficient way used for increasing the life time of lead-sulphuric acid batteries is the addition of phosphoric acid in the electrolyte. This additive increases the functioning time of the positive plates by hindering the formation of a $PbSO_4$ unconductible layer at the active mass-grid interface.[1-6]

The electrode processes in the $PbO_2/PbSO_4$ system, using a $H_2SO_4-H_3PO_4$ electrolyte, were studied in the last years, by Bullock and co-workers.[1-3] The purpose of their papers was to get lead microelectrodes, similar to those used in the steady state conditions of functioning of the batteries.

The voltammograms were registered at very small potential scan rates (0.1÷1 mV/s) and after a preliminary potential scan of 24÷48 hours, within the investigated potential range.

The aim of the present paper is to investigate the electrode processes in conditions which deviate from reversibility. For this purpose, the voltammograms evolution during the first ten cycles was studied, using a higher potential scan rate (6.5 mV/s).

The anodic (Q_a) and cathodic (Q_c) electricity amounts were simultaneously registered by means of a digital coulometer. By this way it was possible to obtain supplementary information and new aspects related to the influence of H_3PO_4 addition.

The present paper shows the results concerning the behaviour of a pure lead electrode in a $H_2SO_4-H_3PO_4$ solution (type I). Microelectrodes obtained by successive recyclings at the potential scan within the anodic range, have been used. The results are analysed comparatively with those obtained previously,[7-9] concerning the PbO_2-PbSO_4 electrode behaviour in H_2SO_4 solutions (type II) and in 0.75 M H_3PO_4 solution (type III), respectively.

EXPERIMENTAL PART

The experiments were carried out using the linear voltammetry method of low rate (6.5 mV/s).

The working electrodes were of pure lead, the surface exposed to the electrolyte being of 50 mm^2.

A platinum net was used as counterelectrode. The potential was scanned within the (+800 ÷ +1 650) mV range vs. the $Hg/Hg_2SO_4/SO_4^{2-}$ reference electrode by means of a Model 173 Potentiostat — Galvanostat (Princeton Applied Research) with a 179 Model Digital Coulometer. The potential — current curves (the voltammograms) were registered by means of an X — Y recorder. An Orion EMG 1117/2 Low Frequency Generator was used. The Q_a and Q_c electricity amount was read by means of the digital coulometer simultaneously with the voltammograms registering.

A glass cell with a single compartment was used. The electrolytes were "pure" solutions of sulphuric acid, phosphoric acid or solutions composed of sulphuric acid and small amounts of phosphoric acid. The temperature of the cell and of the reference electrode was maintained at 25°C by means of a thermostat.

RESULTS

Figure 1 shows comparatively the voltammograms obtained on pure lead in sulphuric acid solution (type II) and in phosphoric acid solution (type III).

The shape of the voltammograms as well as the electricity amounts which characterize the anodic and cathodic processes are very different from the electrolytes used by us. Thus, on the anodic curve in figure 1a an (A) peak of PbO_2 formation appears following the increase of current on the account of the oxygen discharge reaction. At the reverse potential scan a (B) peak of reduction appears representing the lead dioxide to lead sulphate reduction. The number of the cycle as well as the characteristic electricity amounts (in C) are indicated on the figure.

The rate determining steps at the appearance of (A) and (B) peaks, as well as the variation of the electricity amounts, have been studied in detail, in [8]. The anodic capacity (Q_a) is much higher than the cathodic one because of the gaseous oxygen evolution. Thus, in figure 1(a), for the 10th cycle, $\frac{Q_a}{Q_c} \approx 20$. We may consider that the cathodic peak entirely arises from the reduction of PbO_2 formed during the anodic polarization and represents in fact the lead dioxide which forms on the electrode during the potential scan within the (+800÷1650) mV range.

From now on, the "microelectrode" capacity will be denoted by Q_c. Hence, in the potential range under study, except for the oxygen discharge the following wellknown electrode reactions occur :

$$PbO_2 + HSO_4^{2-} + 3\,H^+ + 2\,e \rightleftarrows PbSO_4 + 2\,H_2O \qquad (1)$$

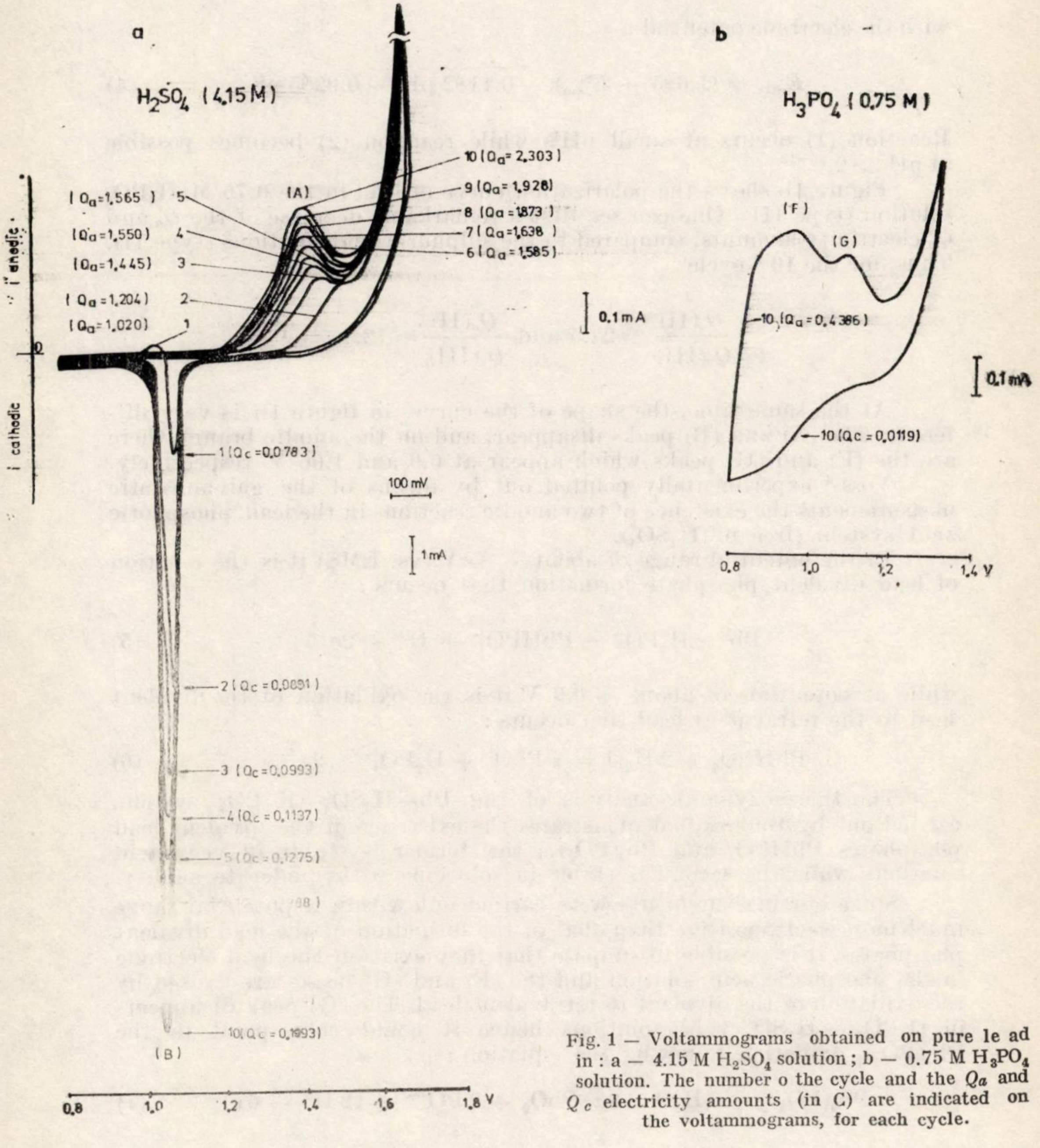

Fig. 1 — Voltammograms obtained on pure lead in : a — 4.15 M H_2SO_4 solution ; b — 0.75 M H_3PO_4 solution. The number o the cycle and the Q_a and Q_c electricity amounts (in C) are indicated on the voltammograms, for each cycle.

with the electrode potential :

$$E_{esm} = (1.628 - E^0_{esm}) - 0.0886\ pH - 0.0295\ pS \tag{2}$$

$$PbO_2 + SO_4^{-2} + 4\,H^+ + 2e^- \rightleftarrows PbSO_4 + 2\,H_2O \tag{3}$$

with the electrode potential :

$$E_{esm} = (1.685 - E^0_{esm}) - 0.1182\ pH - 0.0295\ pS \tag{4}$$

Reaction (1) occurs at small pH's while reaction (2) becomes possible at pH > 2.[10-13]

Figure 1b shows the polarization curve of lead in the 0.75 M H_3PO_4 solution (type III). One can see first a remarkable decrease of the Q_a and Q_c electricity amounts, compared to the sulphuric acid solutions (type II). Thus, for the 10th cycle

$$\frac{Q_c(\mathrm{II})}{Q_c(\mathrm{III})} = 24.5 \text{ and } \frac{Q_a(\mathrm{II})}{Q_c(\mathrm{III})} = 13.4.$$

At the same time, the shape of the curves in figure 1b is very different. The (A) and (B) peaks disappear, and on the anodic branch there are the (F) and (G) peaks which appear at 0.9 and 1.06 V respectively.

Voss [4] experimentally pointed out by means of the galvanostatic measurements the existence of two anodic reactions in the lead phosphoric acid system (free of H_2SO_4).

In the potential range of about − 85 V (vs. EMS) it is the reaction of lead divalent phosphate formation that occurs :

$$Pb + H_2PO_4^- \rightarrow PbHPO_4^- + H^+ + 2e^- \tag{5}$$

while at potentials of about + 0.9 V it is the oxidation of the divalent lead to the tetravalent lead that occurs :

$$PbHPO_4 + 2\,H_2O = \alpha\text{-}PbO_2 + H_2PO_4^- + 2\,e^- \tag{6}$$

The thermodynamic analysis of the $Pb-H_2SO_4-H_3PO_4$ system, carried out by Bullock, [3] demonstrates the existence of the divalent lead phosphates $PbHPO_4$ and $Pb_3(PO_4)_2$; the former is stable in very acid solutions while the second is stable in solutions with moderate acidity.

Since our measurements were carried out within a potential range much more electropositive than that of the formation of the lead divalent phosphates, it is possible to suppose that they exist on the lead electrode in the phosphoric acid solution and the (F) and (G) peaks are caused by the oxidation of the divalent to tetravalent lead. The (G) peak disappears in $H_3PO_4 + H_2SO_4$ acid solutions hence it could correspond to the $Pb_3(PO_4)_2$ oxidation following the equation :

$$Pb_3(PO_4)_2 + 6\,H_2O \rightarrow 3\,\alpha\text{-}PbO_2 + 2\,PO_4^{3-} + 12\,H^+ + 6\,e^- \tag{7}$$

The (F) peak corresponds to reaction (6). At the same time, following,[1-4] the action of H_3PO_4 results in the formation of a series of irreversible lead oxides, of the PbO_x type.

Voss [4] suggests the possibility of formation of tetravalent lead phosphates, too, (e.g. $Pb(HPO_4)_4$ or $Pb(HPO_4)_2 \cdot nH_2O$) as results of a prolonged electrolysis at potentials higher than +0.88 V in 3 M (or more concentrated) phosphoric acid solutions. The $\frac{Q_a}{Q_c} = 40$ ratio shows that within the (1.2 ÷ 1.65) V potential range the main electrochemical process is the gaseous oxygen evolution. But the high $Q_a(II)/Q_a(III)$ ratio, mentioned above, shows at the same time that the oxygen overpotential is higher in phosphoric acid solutions. On the cathodic branches of the voltammograms there are no well-outlined peaks. This behaviour could be explained by means of the irreversible PbO_x existence. Because of the cathodic current which is different from zero, there is probably a reduction of PbO_x oxides, but with a very high overvoltage.

Figures 2, 3 and 4 show the voltammograms obtained in sulphuric acid solutions with an addition of phosphoric acid (type I). Figures 5 and 6 show the variation of Q_a and Q_c electricity amounts, for the 10th cycle, in solutions with a constant concentration of H_2SO_4 and with a variable concentration of H_3PO_4 (Fig. 5) and in solutions of variable concentrations of H_2SO_4 and a constant concentration of 1% (w/0) H_3PO_4 (Fig. 6) respectively. Figure 2 shows the voltammograms evolution as a function of the number of successive recyclings of the lead electrode. The number of the cycles is indicated on each curve. The following differences are present, comparatively with the solutions II and III (Fig. 1) : for the example from figure 2, Q_a and Q_c for the 10th cycle are one order of magnitude smaller then in solution (II) but they are comparable with those in solution (III) although the phosphoric acid concentrations are much smaller in (I) than in (III). Apart from the solution (III), in solution (I) there are two evident peaks, (M) and (N) which appear on the cathodic branch, separated by a maximum denoted by (0). On the anodic branch starting from the 6th cycle, an (F) peak appears which exists in solution (III), too, but the (G) peak disappears in solution of type I.

In solutions (I) the evolution of the cycles is also different in comparison with that in pure sulphuric acid (solution II). Thus, in solution (II) beginning with the third cycle, the voltammograms shape becomes reproducible while in solution (I) it becomes reproducible only from the 7th cycle. The position of the (0) point is characteristic. At the first cycle it is placed in the anodic range, moving successively towards smaller and smaller anodic currents, while at the last cycles it becomes stable, within the cathodic range. Such a characteristic evolution of the voltammograms as a function of the number of cycles is obtained for all the solution of type I, for a concentration higher than 0.1% H_3PO_4.

Figure 3 shows the voltammograms obtained in solution of type (I) for the concentrations of 0.1, 0.3 and 1% H_3PO_4, and figure 4 for the concentration of 2% H_3PO_4. Q_a and Q_c were determined for other concentrations of H_3PO_4, too, and the results obtained for the 10 cycles are illustrated in figure 5. At relatively small additions of H_3PO_4 (Fig. 3 (a)), the voltammogram keeps the shape of the voltammograms from the "pure"

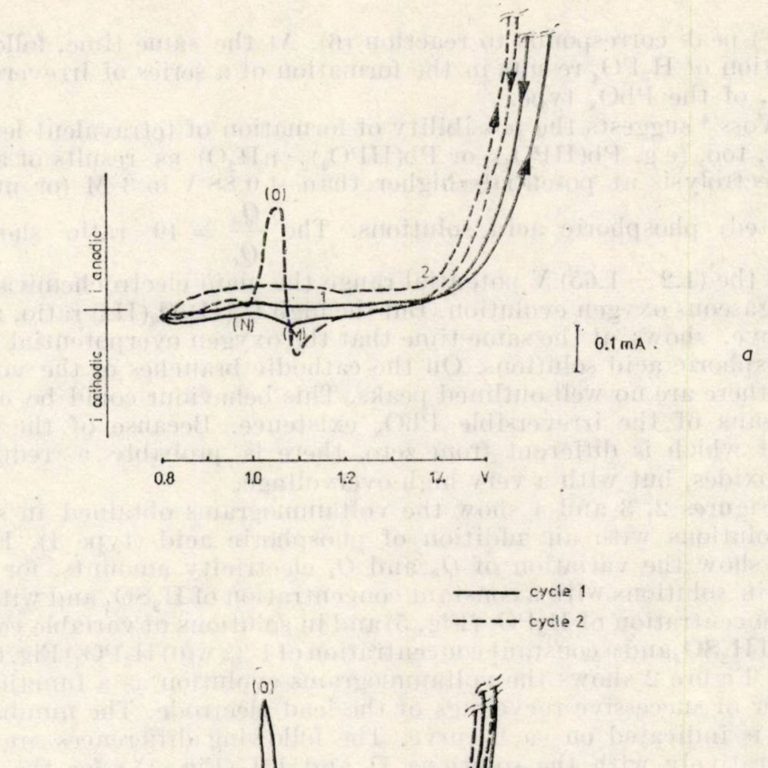

Fig. 2. — Voltammograms obtained on pure lead for the first 10 successive cycles, in 4.15 M H_2SO_4 solution containing 0.715 % $\left(\frac{w}{o}\right)$ H_3PO_4 ; a — cycles 1 and 2 ; b — cycles 3 and 4 ;

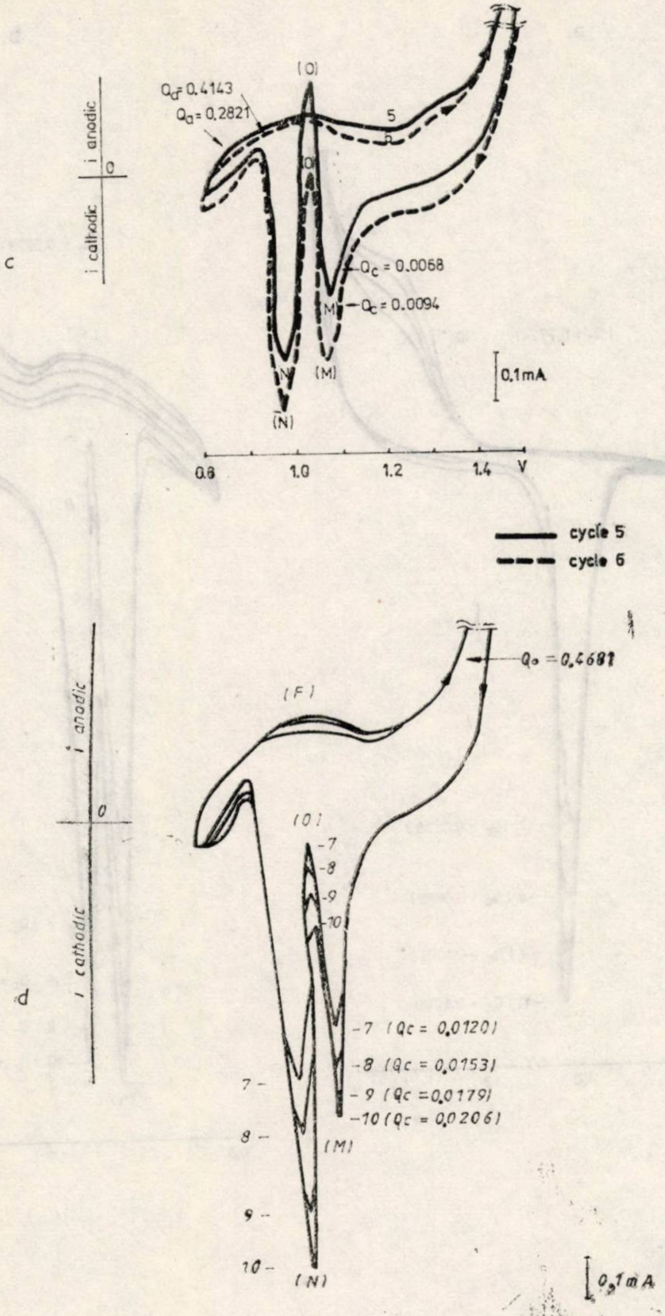

Fig. 2. — c — cycles 5 and 6 ; d — cycles 7, 8, 9 and 10.

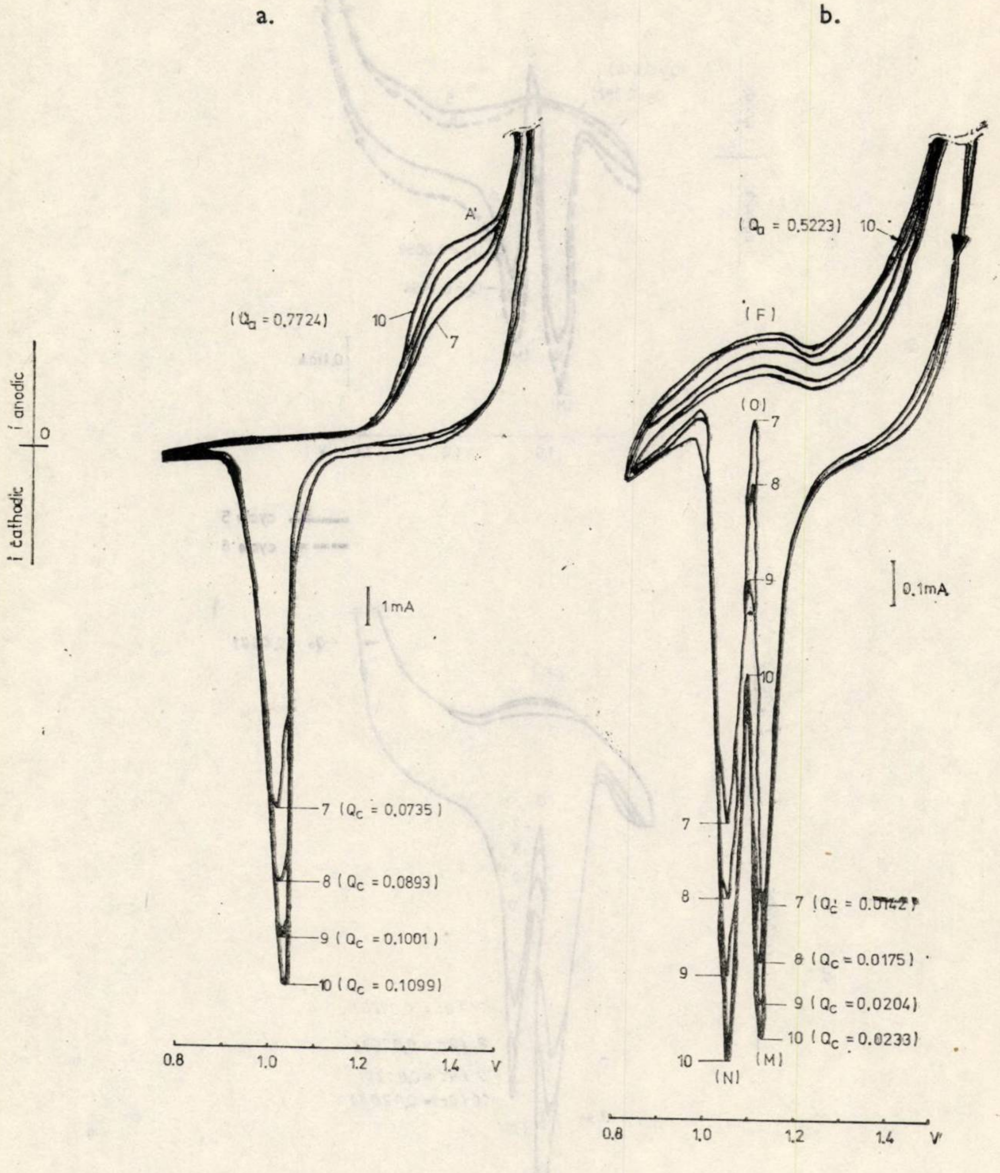

Fig. 3. — Voltammograms of the lead in 4.15 M $H_2SO_4 + x\% \left(\frac{w}{o}\right) H_3PO_4$ solutions; a — x = 0.145% b — x = 0.430%

Fig. 3. — c — x = 1.450 %

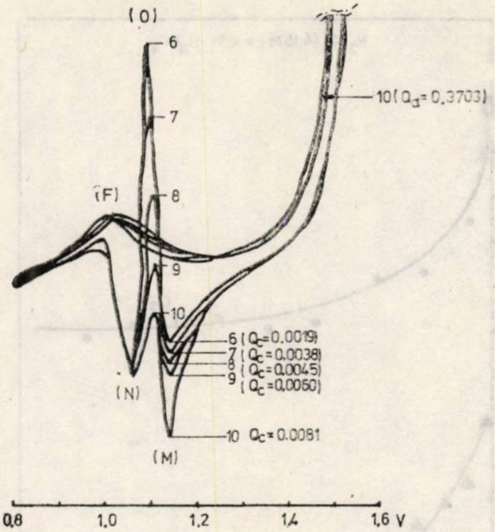

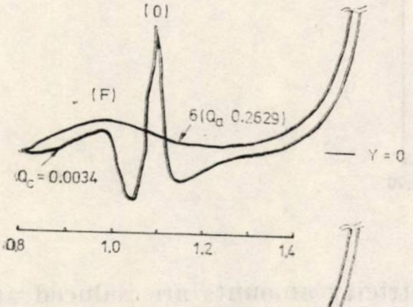

Fig. 4. — Voltammograms of pure lead in 4.15 M H_2SO_4 + 2.90 % $\left(\frac{w}{o}\right)$ H_3PO_4 solutions.

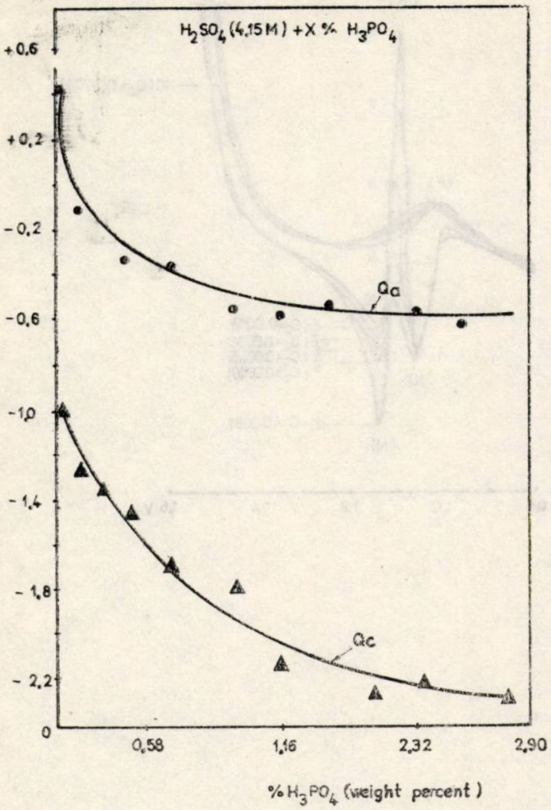

Fig. 5. — The variation of the anodic (Q_a, in C) and cathodic (Q_c, in C) electricity amounts, for the 10th cycle, in H_2SO_4 solutions of constant concentration (4.15 M) containing variable additions of phosphoric acid.

H_2SO_4 solutions, but the Q_a and Q_c electricity amounts are reduced at about a half of the initial value and instead of the (A) peak corresponding to the PbO_2 formation there appears a "shoulder" (A′). At the next concentrations the diagrams obtained are similar to those discussed above (Fig. 2) with the (F) peak on the anodic branch and with the splitting up of the cathodic branch into the (M) and (N) peaks; the Q_a and Q_c electricity amounts decrease with the increase of the H_3PO_4 concentration. In solutions with 2% H_3PO_4, Q_c is 50 times smaller than in the pure solution of H_3PO_4 (Fig. 4).

Figure 5 shows the dependence of the Q_a and Q_c amounts as a function of the H_3PO_4 concentration. At the relativelly small additions of H_3PO_4 a remarkable decrease of Q_a and Q_c takes place. Thus in the range of concentration of 0.5 — 0.6% H_3PO_4 the electricity amounts become one order of magnitude smaller than in sulphuric acid (II) solutions. At higher concentration of H_3PO_4 the decrease of Q_a and Q_c becomes slower. Figure 6 shows the variation of the anodic and cathodic electricity amounts in a solution with a constant concentration of 1% H_3PO_4, but with a variable concentration of H_2SO_4. In order to make a comparison, the results obtained in "pure" sulphuric acid were reproduced.

In an earlier paper [8] it was shown that Q_a and Q_c increase when H_2SO_4 concentration decreases.

This behaviour was explained by the increase of the range of oxygen evolution, in solutions with higher pH and by the increase of PbO_2 formation range. Thus, on the voltammograms obtained, the range of the active anodic process moves towards negative values with about 0.3 V when the concentration decreases from 5 M H_2SO_4 to 0.75 M H_2SO_4.

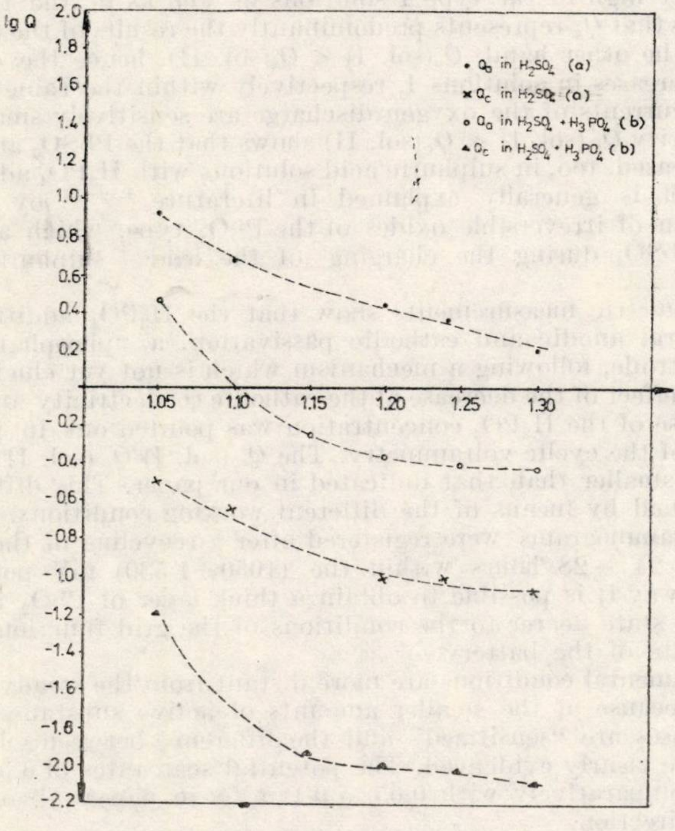

Fig. 6. — The variation of the anodic (Q_a, in C) and cathodic (Q_c, in C) electricity amounts, for the 10th cycle : a — variation of the sulphuric acid concentration ; b — variation of the sulphuric acid concentration for a constant addition of 1.45 % $\left(\frac{w}{o}\right)$ H_3PO_4.

In solutions with H_3PO_4 additions, the behaviour is the same, Q_a and Q_c decrease respectively when the H_2SO_4 concentration increases, but both these amounts are about one order of magnitude smaller in solutions I (with 1 % H_3PO_4), comparatively ith solutions II.

DISCUSSION

The results presented in this paper show that the main effect of the phosphoric acid additions in sulphuric acid solutions consists in a drastic "passivation" of the electrode processes within the (800 ÷ 1650 mV) potential range. This effect of passivation increases with the H_3PO_4 concentration, and within the range of H_3PO_4 moderate concentrations ($0.5 \div 0.6\%$), Q_a and Q_c are about $5 \div 10$ times smaller in solution (Is) comparatively with solution (II).

All the electrode processes, anodic and cathodic, as well as the oxygen discharge, are influenced by passivation. The Q_a/Q_c ratio, which all the time is very high in the type I solutions as well as in the type II solutions, shows that Q_a represents predominantly the results of the oxygen evolution. On the other hand, $Q_a(\text{sol. I}) \ll Q_a(\text{sol. II})$, hence the oxygen overvoltage increases in solutions I, respectively within the same potential range the currents of the oxygen discharge are sensitively smaller.

The quantity $Q_c\,(\text{sol. I}) \ll Q_c(\text{sol. II})$ shows that the $PbSO_4$ amounts are highly decreased, too, in sulphuric acid solutions with H_3PO_4 addition.

This effect is generally explained in literature, [1,10-12] by means of the formation of irreversible oxides of the PbO_x type, which are not reducible to $PbSO_4$ during the charging of the lead — sulphuric acid battery.

Our coulometric measurements show that the H_3PO_4 addition results in a general anodic and cathodic passivation, a "phosphatation" of the lead electrode, following a mechanism which is not yet elucidated.

The same effect of the decrease of the cathodic Q_c electricity amounts with the increase of the H_3PO_4 concentration was pointed out in paper,[1] too, by means of the cyclic voltammetry. The $Q_c\,(\text{sol. I})/Q_c\,(\text{sol. II})$ ratio reported in[1] is smaller than that indicated in our paper. This difference could be explained by means of the different working conditions. In the paper [1] the voltammograms were registered after a recycling of the electrode of about 24 — 28 hours within the ($1050 \div 1\,530$) mV potential range. By this way it is possible to obtain a thick layer of PbO_2 and to realize a steady state nearer to the conditions of the grid functioning in the positive plate of the battery.

Our experimental conditions are more distant from the steady state, but probably because of the smaller amounts of active substances, the electrode processes are "sensitized" and the difference between solutions I and II is more clearly evidenced. The potential scan rates of 6.5 mV/s in our paper comparatively with 0.05 — 0.1 mV/s in papers, [12] operate in the same direction.

Comparison of the anodic branch of the voltammograms obtained in solution I and of those obtained in solution III (Fig. 2b) shows the disappearance of the (G) peak in the $H_2SO_4 + H_3PO_4$ solutions.

Much more evident differences between solutions I and III occur on the cathodic branch of the voltammograms.

The appearance of the two (M) and (M) peaks which exist in the solutions I, when H_3PO_4 is present and do not appear in solutions III, when H_2SO_4 is absent, could be explained by means of some small amounts of reversible PbO_2 which forms only in the presence of H_2SO_4.

The splitting up of the cathodic process of the PbO_2 to $PbSO_4$ reduction in more peaks was observed by other workers, too,[14,15] mainly at the PbO_2 reduction in a HNO_3 solution in the presence of H_3PO_4.

In our paper, the (M) and (N) peaks appear only in the $H_2SO_4 + H_3PO_4$ solution. They do not appear in the H_2SO_4 solution free of additions. The presence of the two peaks was observed, too, during the reduction of PbO_2 formed on the lead electrode, in a $HNO_3 + H_3PO_4$ solution. The explanation is the following: in the $H_2SO_4 + H_3PO_4$ and $HNO_3 + H_3PO_4$ solution, α and β-PbO_2 form in small amounts and, in this case, two reduction peaks appear, corresponding to the two forms of PbO_2.

In H_2SO_4 solution free of addition, where high amounts of PbO_2 exist, the two reduction peaks overlap each other. It was pointed out, at the same time, that the potential difference between the two peaks is of 100 mV and remains constant irrespective of H_3PO_4 concentration and of the number of cycles; this is an indication of the fact that the two peaks correspond to two different mechanisms of reduction of PbO_2 to $PbSO_4$ (see equations 2 and 3).

It seems possible to correlate our results with the lead acid battery functioning, taking into account that the H_3PO_4 action increases, probably, as a function of the ratio:

$$\frac{H_3PO_4(\%) \text{ in solution}}{\text{active mass of } PbO_2 \text{ on the unit of surface}} = \eta$$

In our experiments this ratio is much higher than in the positive active mass-solution system from the battery but it is near to that from the grid — electrolyte system.

The small H_3PO_4 additions do not decrease the active mass capacity from the battery (η is small) but hinders the formation of the insulator film between the active mass and the grid. The aim of our experiments was to obtain a high η ratio, by means of a high potential scan rate and a short electrochemical activation time. By this way it becomes possible to obtain a very pronounced difference between the voltammograms obtained in the $H_2SO_4 + H_3PO_4$ solutions and in the "pure" H_2SO_4 solutions.

REFERENCES

[1] R. K. Bullock and D.H.Mc Clelland, *J. Electrochem. Soc.*, **124**, 1478 (1977).

[2] R. K. Bullock, *J. Electrochem. Soc.*, **126**, 360 (1979).

[3] R. K. Bullock, *J. Electrochem. Soc.*, **126**, 1848 (1979).

[4] E. Voss, Second International Symposium on Batteries, Bournemouth, 1960.

[5] B. K. Mahato, *J. Electrochem. Soc.*, **126**, 365 (1979).

[6] M. A. Dasoian and I. A. Aguf, "Sovremenaia Teoria svintsovogo acumuliatora", Ed. Energhia, Leningrad, 1975.

[7] S. Sternberg, A. Mateescu V. Brânzoi and L. Apăteanu *Rev. Roumaine de Chim.*, **29**, 727 (1984).

[8] S. Sternberg, A. Mateescu, V. Brânzoi and L. Apăteanu, *Rev. Roumaine Chim.* (in press).

[9] S. Sternberg and A. Mateescu, *Rev. Chim. (Bucureşti)*, **35**, 510 (1984).

[10] K. Eberts, in "Power Sources 2", D. H. Collins, Editor, Pergamon Press, New York, 1968.

[11] S. Tudor, A. Weisstuch and S. H. Davang, *Electrochem. Technol.*, **3**, 90 (1965).

[12] S. Tudor, A. Weisstuch and S. H. Davang, *Electrochem. Technol.*, **5**, 406 (1966),

[13] K. Bullock, *J. Electrochem. Soc.*, **126**, 662 (1980).

[14] H. A. Kaitinen and N. H. Watkins, *Analyt. Chem.*, **47**, 1352 (1975).

[15] H. S. Pansear, in "Power Sources 3", D. H. Collins, Editor, Oriel Press, Newcastle upon Tyne, England, 1971.

Revue Roumaine de Chimie, **33**, *2*, 125–131 (1988)

VISCOSITY OF SOME ALKALI HALIDES IN WATER–ACETAMIDE MIXTURES AT 333.15 K

M. WOLDAN

Research and Development Centre for Standard Reference Materials
WZORMAT – Branch in Lodz, 90 – 132 Lodz, Poland

Received June 9, 1986

Relative viscosities of NaCl, NaI, KCl, KBr and CsI solutions in water and water – acetamide mixtures containing 15, 30 and 50 wt% of $AcNH_2$ at 333.15 K have been determined. The value of the *A* and *B* Jones-Dole viscosity coefficients, the ionic *B* coefficients and the ionic *B* coefficients of transfer from water to water – acetamide mixtures have been calculated. The data were analyzed in terms of the effect of the constituent ions on the overall structure of the binary solvent. It is found that the addition of acetamide to water increases the solvation of ions.

INTRODUCTION

The variation of viscosity with temperature and solvent composition has been employed by many workers [1] to study the ion – solvent interaction both in aqueous and non-aqueous solutions. Although molten acetamide is a good solvent for electrolytes, [2] the investigations of electrolytes in water – acetamide mixtures are scanty. In continuation of our previous studies on the partial molal volume[3–4] and viscosity[5–6] of some salts in water – acetamide mixed solvents, we now have determined the viscosity of some alkali halides in three water – acetamide mixtures at 333.15 K. From the obtained values of relative viscosity, the ionic *B*-coefficients have been calculated and the structure-making and structure-breaking effects of ions on structure of water-acetamide mixtures is analysed.

EXPERIMENTAL SECTION

NaCl, KCl, and KBr(POCH – Gliwice, A.R.) were recrystallized from doubly distilled water and dried for a day at 383 K. NaI A.R. (POCH-Gliwice) was recrystallized from a 1 : 1 water – acetone mixture and dried under vacuum for a day at 333 K. Laboratory grade CsI(BDH) was used without further purification and dried under vacuum for a day at 333K. The method of purification of acetamide was described elsewhere. [7] The mixed solvents used for investigations were prepared by mixing the weighed amounts of acetamide with twice distilled water. All solutions were prepared by weighing. The procedure of the measurements of viscosity was described earlier. [5] The viscosity of the investigated solutions was determined at a series of concentrations covering the range 0.005 to 0.2 mol.dm^{-3}. The total uncertainty of viscosity is $(3 \pm 6) \cdot 10^{-4}$ mPa.s. Density of the investigated solutions was determined by the magnetic float densimeter with the precision 1.10^{-5} g·cm^{-3}. All measurements were made at 333.15 ± 0.02 K.

RESULTS

The relative viscosities η_r for investigated solutions were calculated from the known equation

$$\eta_r = \frac{t \cdot d}{t_0 \cdot d_0} \qquad (1)$$

where t and t_0 are the flow times of solution and solvent, d and d_0 are densities of solution and solvent, respectively. The variation of the relative viscosity of solution with concentration of the salt can be represented by the extended Jones — Dole's eq. [8,9]

$$\eta_r = 1 + Ac^{1/2} + Bc + Dc^2 \qquad (2)$$

where A, B and D are constants depending on solute, solvent, temeperature and pressure. In case of diluted solutions up to concentration 0.15 — — 0.20 mol·dm^{-3} term Dc^2 can be omitted. In the present paper A and B coefficients were calculated from Jones — Dole's equation in the form

$$(\eta_r - 1)c^{1/2} = A + Bc^{1/2} \qquad (3)$$

The values of A and B coefficients obtained for investigated electrolytes in water and water — acetamide mixtures are given in Table 1.

Table 1

Viscosity A coefficient (dm$^{3/2}$mol$^{-1/2}$) and B coefficient (dm^{3}mol^{-1}) for some alkali halides in water-acetamide mixtures at 333.15 K

Salt	Water	15wt% $AcNH_2$	30 wt% $AcNH_2$	50 wt% $AcNH_2$
		Coefficient A		
NaCl	0.006	0.006	0.005	0.004
NaI	0.006	0.006	0.005	0.005
KCl	0.005	0.005	0.005	0.004
KBr	0.005	0.005	0.004	0.003
CsI	0.005	0.004	0.004	0.003
		Coefficient B		
NaCl	0.104±0.003	0.169±0.004	0.205±0.005	0.236±0.005
NaI	0.040±0.002	0.096±0.003	0.120±0.003	0.135±0.004
KCl	0.044±0.002	0.112±0.003	0.158±0.004	0.202±0.005
KBr	0.022±0.002	0.090±0.003	0.130±0.004	0.167±0.004
CsI	−0.042±0.002	0.020±0.001	0.057±0.002	0.091±0.003

The values of A coefficient obtained in the present work are accurate to within ± 0.001 $dm^{3/2}$ $mol^{-1/2}$. The estimated deviations in the B values are given in Table 1. It is known that the B coefficient of a salt is additively built up from the individual values of the ions. From the obtained B values of the investigated salts it is possible to calculate the values of B coefficients for non-investigated salts (NaBr, Kl, CsCl and CsBr). Thus

$$B_{NaBr} = B_{NaCl} + B_{KBr} - B_{KCl}$$

$$B_{KI} = B_{KCl} + B_{NaI} - B_{NaCl} \tag{4}$$

$$B_{CsCl} = B_{CsI} + B_{NaCl} - B_{NaI}$$

$$B_{CsBr} = B_{CsI} + B_{NaBr} - B_{NaI}$$

The B coefficients for NaBr, Kl, CsCl and CsBr calculated from eq. 4 are given in Table 2.

Table 2

The values of viscosity B-coefficient (dm^3mol^{-1}) calculated from equation (4)

Salt	Water	15wt % $AcNH_2$	30 wt % $AcNH_2$	50 wt % $AcNH_2$
NaBr	0.082	0.147	0.177	0.201
KI	−0.020	0.039	0.073	0.101
CaCl	0.022	0.093	0.142	0.192
CsBr	0.000	0.071	0.114	0.157

The utility of the B coefficient of electrolyte at infinite dilution to study ion — solvent interaction lies in the additivity principle. Since it is impossible to determine the B value of a single ion, we use the convention $B_{(Cl^-)} = B_{(K^+)}$.[10,11] The values of ionic B coefficients calculated by this method are given in Table 3.

Table 3

Ionic viscosity B-coefficients ($dm^3 \cdot mol^{-1}$) in water—acetamide mixtures at 333.15 K

Ion	Water	15wt % $AcNH_2$	30 wt % $AcNH_2$	50 wt % $AcNH_2$
Na^+	0.082	0.113	0.126	0.135
K^+	0.022	0.056	0.079	0.101
Cs^+	0.000	0.037	0.063	0.091
Cl^-	0.022	0.056	0.079	0.101
Br^-	0.000	0.034	0.051	0.066
I^-	−0.042	−0.017	−0.006	0.000

DISCUSSION

It is known that Jones — Dole's B coefficient is an empirical constant which is a measure of ion — solvent interactions. Recently Krumgalz [12] has shown that B coefficient of an inorganic ion can be split into the following terms

$$B_{\text{ion}} = B_{\text{ion}}^{\text{Einst}} + B_{\text{ion}}^{\text{or}} + B_{\text{ion}}^{\text{str}} \tag{5}$$

where $B_{\text{ion}}^{\text{Einst}}$ is the positive increment arising from the shape and size of ion, $B_{\text{ion}}^{\text{or}}$ is the positive contribution due to the orientation of solvent molecules in the region of centrosymmetrical order around the ion and $B_{\text{ion}}^{\text{str}}$ is the negative contributions related to the destruction of solvent structure in the region of the ionic cosphere. It is known that structure — breaking ions (Cs^+, I^-) have negative B-coefficients in case of highly structured solvents with water as a prime example. [11] Hence, these ions in the solvents which are more structured than water would give much higher value of $B_{\text{ion}}^{\text{str}}$ which will further decrease B value relative to water. The situation is entirely different for ions with a rather high surface-charge density with Na^+ as a prime example. In any polar solvent they will orientate solvent molecules centrosymmetrically. In successive shells around the ion the degree of orientation of solvent molecules will fall off with distance from the ion until the free rotation of solvent molecules and normal strucure of solvent are reestablished. The strength of the binding of solvent molecules to each other is increased on polarization by the ionic field and they are also strongly bound to the ion. For such ions the value of $B_{\text{ion}}^{\text{or}}$ will be large and B coefficient will be positive. As can be seen from Table 3, Na^+ ion in water — acetamide mixture has the largest B_{ion} value but I^- ion has the smallest. The Na^+ ion has high charge density and therefore strongly orders solvents molecules creating a sheath of firmly attached layer. This leads to large values of $B_{\text{ion}}^{\text{or}}$ and B_{ion} values are positive. The ionic B coefficients decrease with increase in ionic size since the smaller charge density has weaker orientation effect in the solvation layer. Therefore $B_{\text{ion}}^{\text{or}}$ will be smaller and distortion of structure of water — acetamide mixture in vicinity of such ions due to competition between the ionic field and bulk structure will lead to large $B_{\text{ion}}^{\text{str}}$ value. If $B_{\text{ion}}^{\text{str}} > B_{\text{ion}}^{\text{Einst}} + B_{\text{ion}}^{\text{or}}$ the B_{ion} coefficient will be negative and in case when $B_{\text{ion}}^{\text{str}} < B_{\text{ion}}^{\text{Einst}} + B_{\text{ion}}^{\text{or}}$ the B_{ion} coefficient will be positive. The values of the B_{ion} coefficient for all ions in water — acetamide mixtures increase with increasng contents of $AcNH_2$ in the mixed solvent. If we assume that $B_{\text{ion}}^{\text{Einst}}$ does not depend on the contents of acetamide in the mixed solvent we can conclude that the acetamide causes the increase of $B_{\text{ion}}^{\text{or}}$ value or decrease $B_{\text{ion}}^{\text{str}}$ value. This leads to the conclusion that the addition of acetamide to water causes loosening of primary water structure. More information concerning interaction ion — solvent can be obtained from the analysis of the dependence of the ionic B coefficient of transfer on the composition of the mixed solvent. The ionic B coefficient of transfer, $B_{\text{ion(tr)}}$, from water to water-acetamide mixtures was calculated from the relation

$$B_{\text{ion(tr)}} = B_{\text{ion(ms)}} - B_{\text{ion(w)}} \tag{6}$$

where $B_{\text{ion(ms)}}$ and $B_{\text{ion(w)}}$ are B coefficient of a given ion in mixed solvent and water, respectively. The values of $B_{\text{ion(tr)}}$ are given in Table 4.

Table 4

Ionic *B*-coefficients of transfer, $B_{\text{ion(tr)}}$ from water to water-acetamide mixtures ($dm^3 \cdot mol^{-1}$)

Ion	15 wt% $AcNH_2$			30 wt% $AcNH_2$			50 wt% $AcNH_2$		
	298.15 K[a]	313.15 K[b]	333.15 K	298.15 K[a]	313.15 K[b]	333.15 K	298.15 K[a]	313.16 K[b]	333.15 K
Na^+	0.029	0.030	0.031	0.041	0.043	0.044	0.049	0.052	0.053
K	0.032	0.033	0.034	0.053	0.055	0.057	0.073	0.077	0.079
Cs^+	0.035	0.036	0.037	0.059	0.061	0.063	0.086	0.090	0.091
Cl^-	0.032	0.033	0.034	0.053	0.055	0.057	0.073	0.077	0.079
Br^-	0.030	0.032	0.034	0.048	0.050	0.051	0.062	0.065	0.066
I^-	0.025	0.024	0.025	0.034	0.035	0.036	0.040	0.041	0.042

a) From reference 13
b) From reference 6

On the other hand, when $B_{\text{ion}}^{\text{Einst}}$ does not depend on the composition of mixed solvent, $B_{\text{ion(tr)}}$ can be expressed as

$$B_{\text{ion(tr)}} = B_{\text{ion(ms)}}^{\text{or}} + B_{\text{ion(ms)}}^{\text{str}} - B_{\text{ion(w)}}^{\text{or}} - B_{\text{ion(w)}}^{\text{str}} \qquad (7)$$

In case of water-acetamide mixtures $B_{\text{ion(tr)}}$ is positive for all ions, therefore

$$B_{\text{ion(ms)}}^{\text{or}} - B_{\text{ion(w)}}^{\text{or}} > B_{\text{ion(w)}}^{\text{str}} - B_{\text{ion(ms)}}^{\text{str}} \qquad (8)$$

From this it follows that the water — acetamide mixtures are less structured than water and the orientation of the solvent molecules by the ions becomes larger. Table 4 shows that the values of $B_{\text{ion(tr)}}$ increase with increasing contents of acetamide in the mixture and with the increase of ionic radius for cations unlike the anions for which they decrease. It is interesting to note that the addition of acetamide to water causes the largest changes in hydratation of Cs^+ ion for cations and Cl^- ion for anions. The different behaviour of cations and anions can be explained in terms of different dipole orientation of water molecules around cations and anions. As it is seen from Table 4 the $B_{\text{ion(tr)}}$ values increase slightly with increasing temperature. According to literature [14] the effective ionic molar volume, V_e, can be obtained from the relation

$$B = 2 \cdot 5 V_e \qquad (9)$$

For electrolyte solutions, V_e can be regarded as the volume of one mole of ions together with their solvation layers. [15] Thus, we get

$$V_e = V_{\text{ion}}^0 + n_h V_{H_2O}^0 \qquad (10)$$

Table 5

The hydration number of some ions in water-acetamide mixtures

Ion	Water			15 wt% $AcNH_2$			30 wt% $AcNH_2$			50 wt% $AcNH_2$		
	298.15 K	313.15 K	333.15 K	298.15 K	313.15 K	333.15 K	298.15 K	313.15 K	333.15 K	298.15 K	313.15 K	333.15 K
Na^+	4.8	4.6	4.6	6.6	6.4	6.5	7.3	7.2	7.3	7.8	7.8	7.8
K^+	−1.3	−0.4	0.4	0.6	1.6	2.5	1.9	2.9	3.9	3.1	4.2	5.2
Cs	−4.0	−2.8	−1.8	−1.8	−0.7	0.4	−0.4	0.8	2.0	1.2	2.6	3.7
Cl	−2.7	−1.8	−0.9	−0.7	0.2	1.1	0.5	1.6	2.5	1.7	2.9	3.9
Br	−5.2	−4.0	−2.8	−3.4	−2.1	−0.8	−2.3	−1.0	0.3	−1.5	−0.1	1.2
I	−8.9	−7.5	−6.4	−7.3	−6.0	−4.9	−6.8	−5.3	−4.2	−6.4	−5.0	−3.8

where V^0_{ion} is ionic molar volume calculated from the relation $V^0_{ion} = 2.52r^3$ (r is Pauling's ionic radius), n is the hydration number and $V^0_{H_2O}$ is molar volume of water equal to $6.62 cm^3 mol^{-1}$ taking the radius of water molecule as $1.38 \cdot 10^{-10}$m. If we assume that in water-acetamide mixtures (water-rich region) the ions are only hydrated by water molecules we can calculate the values of the hydration number, n_h (see Table 5).

It is known that positive hydration numbers of ions are associated with structure-making properties and negative n_h aie associated with structure-breaking properties. Table 5 shows that the hydration of ions increases with increasing contents of acetamide in the mixed solvents. The effect of acetamide on hydration of ions increases with increasing ionic radius for cations and decreases for anions. This difference in behaviour of ions can be explained on the basis of different structural behaviour of cations and anions in water — acetamide mixtures. It is easy to note that Na^+ ion is positively hydrated in all investigated mixed solvents contrary to I^- ion which is negatively hydrated. The magnitude of hydration number suggests that the structure-breaking ability of ions in water — acetamide mixtures is in the order

$$I^- > Br^- > Cs^+ > Cl^- > K^+ > Na^+$$

The increase of temperature does not change in this order but it decreases the structure — breaking ability of ions nearly identical in water and water — acetamide mixtures.

In conclusion it can be said that the addition of acetamide to water increases the solvation of ions, and the effect of temperature on the solvation of ions in water and water — acetamide mixtures is almost identical. From this it follows that the water — acetamide interactions are close to water-water interactions.

REFERENCES

[1] R. H. Stokes and R. Mills, "International Encyclopedia of Physical Chemistry and Chemical Physics", V. 3, Pergamon Press, New York 1965.

[2] O. F. Stafford, *J. Amer. Chem. Soc.*, **55**, 3987 (1933).

[3] M. Woldan, *Acta Univ. Lodz. Folia Chimica*, **2**, 3 (1983).

[4] M. Woldan, *Acta Univ. Lodz. Folia Chimica*, **5**, 105 (1985).

[5] M. Woldan, *J. Chem. Eng. Data*, **30**, 479 (1985).

[6] M. Woldan, *Z. phys. Chem.* (in press).

[7] M. Woldan, *Thermochim. Acta*, **94**, 345 (1985).

[8] G. Jones and M. Dole, *J. Amer. Chem. Soc.*, **51**, 2950 (1929).

[9] G. Jones and K. Talley, *J. Amer. Ch . Soc.*, **55**, 4124 (1933).

[10] R. W. Gurney "Ionic Processes in Solution", McGraw-Hill, New York 1953.

[11] M. Kaminsky, *Discuss. Faraday Soc.*, **24**, 171 (1957).

[12] B. S. Krumgalz, *J. Chem. Soc. Faraday Trans*, **76**, 1275 (1980).

[13] M. Woldan, in prep.

[14] B. Breslau and F. Miller, *J. Phys. Chem.*, **74**, 1056 (1970).

[15] R. A. Robinson and R. H. Stokes, "Electrolyte Solution" Butherworths Sci. Publ. London 1959.

Revue Roumaine de Chimie, **33**, 2, 133–142 (1988)

LINEAR *VERSUS* BENT BIS(DIPHOSPHINE)IMINIUM CATIONS. A MOLECULAR ORBITAL DISCUSSION OF THE BONDING IN $[H_3PNPH_3]^+$ AND RELATED SPECIES

I. SILAGHI-DUMITRESCU and I. HAIDUC*
Chemistry Department, University of Cluj-Napoca,
R–3400 Cluj-Napoca, Romania

Received October 27, 1986

Bis(triphenylphosphine)iminium cation, $[Ph_3PNPPh_3]^+$, a versatile counterion for stabilizing unusual, air sensitive organometallic derivatives, is known to exhibit a bent (a) and a linear conformer (b). In order to get a better understanting of this situation, based upon electron distribution in this skeleton, molecular orbital calculations have been carried out at the SCF–CNDO/2 level. The bent form appears to be favored over the linear one. One of the stabilizing factors could be a quite appreciable phosphorus-phosphorus direct interaction. The calculations strongly suggest that, with an appropriate choice of electron-releasing substituents at phosphorus, cyclic structures (i or j), with possible aromatic character could exist.

INTRODUCTION

Bis(triphenylphosphine)iminium cation $[Ph_3PNPPh_3]^{\oplus}$ (PPN) is known as a very efficient counterion for isolating unusual, inorganic or organometallic anions. A wealth of data is available on this subject, but references[1–11] quote only a few of them, just to illustrate the matter. X-Ray structural examinations of several compounds containing the PPN cation revealed noteworthy structures, but in most cases the target of the determinations happened to be the anions. However, the cation is interesting also by itself, as both bent[1–6,9–11] and linear[7–8] forms have been reported. Moreover, in the crystal structure of $(PPN)_3[Na\{Mo_3(CO)_6(NO)_3(OCH_3)_3O\}_2]^{3-}$, both linear and bent PPN cations are simultaneously present in the same crystal lattice. The existence of the bent form is not unexpected, since Ph_3PCPPh_3, isoelectronic with $[Ph_3PNPPh_3]^+$ is also bent [12]. ESCA studies of the N(1s) and P(2p) binding energies [13] cannot distinguish between the linear and bent forms. For all PPN^+X^- salts, X = F, Cl, Br, J, SCN, N_3, NO_3, OCN_3, $V(CO)_6$, the binding energies were found to be the same. Since in the $PPN^+[V(CO)_6]^-$ crystals the cation is linear, it means that, either the linear form is present in all above salts or N(1s) and P(2p) binding energies are not sensitive to geometrical changes in the cation [8,13]. In order to sound the preference of this cation for linear or bent geometries, we carried out CNDO/2 type SCF molecular orbital calculations on a model, hypothetical cation, $[H_3PNPH_3]^+$.

---

* Author to whom correspondence should be addressed.

CALCULATIONS

The CNDO/2 calculations[14] were made by using a modified version[15] of PARAMOL-2.[16] Both *sp* and *spd* orbital bases on phosphorus have been used with parameters of Santry and Segal.[17] The coordinate system is shown in Fig. 1.

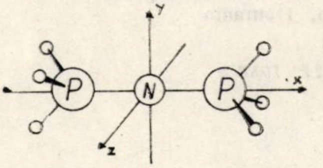

Fig. 1 — The coordinate system and the position of the atoms in the linear D_{3d} form of $[H_3PNPH_3]^{\oplus}$.

The bent form is simulated by moving down the PH_3 groups under the *xz* plane (*i.e.* by decreasing the P—N—P bond angle).

RESULTS AND DISCUSSION

In terms of Lewis electron pair bond structures the bent form of the cations could be understood as an association of two phosphonium units with a negatively charged nitrogen, resulting in a net charge + 1 :

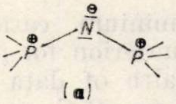

(a)

while the linear form would consist of two five-covalent four-coordinate neutral phosphorus atoms, attached to a positively charged nitrogen atom, each forming a double bond :

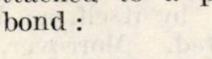

(b)

In these two conformers, not only the P—N—P bond angle would be different, but also the PN bond lengths and the electron populations at the P and N sites. Thus, it seems that MO calculations might readily explain the preference for the bent conformer, confirmed, at least statistically by the much larger number of such examples, in the X-ray diffraction structure determinations performed to date.

An alternative structure (**c**) can be written by allowing the phosphorus atom to share three electrons with the three substituents and one with the nitrogen atoms :

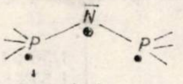

(**c**)

This counting leaves an unshared pair at the central nitrogen and two unpaired electrons, one at each of the phosphorus atoms. Structure (**c**) would imply relatively long PN bonds (classical single P—N bonds), and diradical properties. No such compounds are known so far, and their possible existence is questionable.

If the unpaired electrons of phosphorus delocalize into the PNP skeleton, structure (**d**) can be drawn :

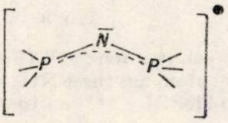

(**d**)

In (**d**), the angular shape of the PNP skeleton is still preserved due to the electron pair localized at nitrogen, but the P—N bonds should be shorter than in (**a**) or (**c**). Now, if the nitrogen lone pair is also delocalized (this is possible since the phosphorus *3d* orbitals are empty), the PNP skeleton should become linear (**b**), and even shorter than in (**d**), PN bond lengths should be displayed. As mentioned in the Introduction, both linear and bent structures have been identified by X-ray diffraction. Table 1 summarizes some of the pertinent geometrical parameters of these cations, determined by X-ray diffraction.

PN bond lengths in the bent forms are indeed significantly longer than of the linear one (1.574 Å, a mean value from various bent $[Ph_3PNPPh_3]^{\oplus}$ cations, compared to 1.539 Å).

The linear PNP system. The calculation of the total energy curve as a function of the P—N bond length, at a PNP angle of 180° yields the minimum for a PN distance of 1.85Å, when only *sp* basis is used ; inclusion of the phosphorus *3d* orbitals shortens the PN bond to about 1.65 Å, which is already comparable with the experimental values found in real compounds. A section of the energy surface is given in Figure 2.

As can be noticed, at the PNP angle of 180°, the minimum of energy is not very marked, and it is in the vicinity of a very small height barrier. This could explain why linear-bent isomerization takes place quite easily, and, depending on the counterion and on the requirements of the crystal symmetry, both linear or bent isomers can crystallize from the same $[Ph_3PNPPh_3]^+X^-$ precursors (usually $X = Cl$).

Table 1

Geometric data on $[R_3PNPR_3]^{\oplus}$ cations

No.	Radical (R)	R_{PN}	PNP	Ref.
Bent				
1	Ph	1.56 ; 1.58	137	1
2	Ph	1.572 ; 1.584	137.5	2
3	Ph*^a^	1.572	141.8	3
4	Ph*^b^	1.568	138.5	3
5	Ph	1.581 ; 1.587	134.6	4
6	Ph	1.570 ; 1.580	145	5
7	Ph	1.591 ; 1.564	139.9	6
8	Ph	—	136.3	18
9	Me	1.582	137	19
10	NH_2 ; 2Ph	1.57 ; 1.58	136	20
11	$3NH_2$ ** NH_2 ; $2NHCN_3$ **	1.539 ; 1.583	129	21
12	Cl	—	140***	22
13	Ph	1.575	142	23
Linear				
14	Ph	1.539	180	8

*a) $[Fe_2(CO)_8]^{2-}$ the counter ion ; *b) $[FeCo(CO)_8]^{2-}$ the counter ion ; **) one phosporus atom has three NH_2 substitutents, the second only one NH_2 and two $HNCH_3$; ***) on the basis of IR and Raman spectra.

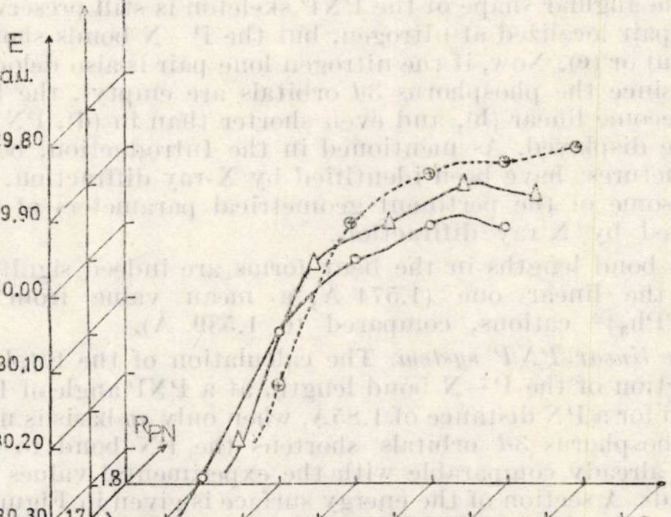

Fig. 2. — Total energy curves as a function of PNP angle for three different values of the P—N distance.

The Wiberg PN bond index of 1.80 (calculated at $R_{PN} = 1.60$ Å) is indicative of a remarkable degree of π bonding. Figure 3 shows in a qualitative manner how the atomic orbitals combine into canonical molecular orbitals in the linear D_{3d} $[H_3PNPH_3]^{\oplus}$ cation.

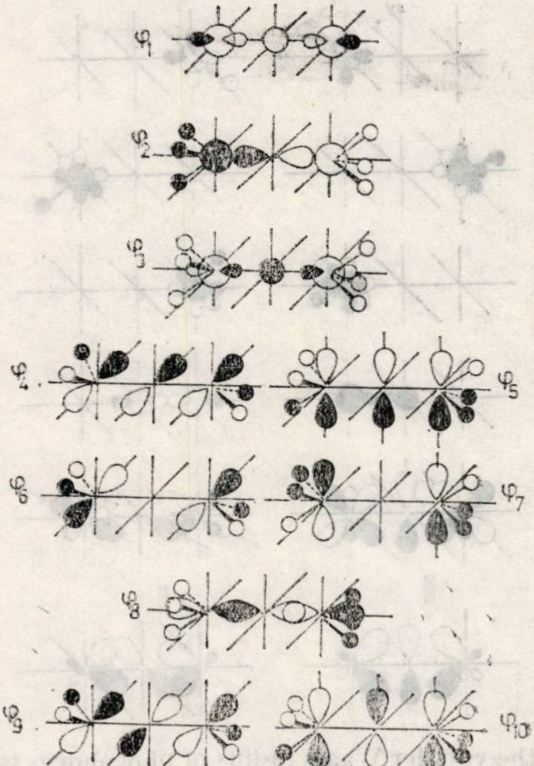

Fig. 3. — The combination of atomic orbitals in the linear $[H_3PNPH_3]^{\oplus}$ cation. The contribution of 3d orbitals is not shown explicitely.

To make the picture clearer, the contribution of *3d* orbitals was not shown explicitely. The lower three MO's ($\varphi_1 - \varphi_3$) describe the σ skeleton of the molecule. The next two form a degenerate pair which is of π symmetry. Note here a relatively important contribution from the σ orbitals of the ligands (pseudo π contribution). The highest occupied MO's ($\varphi_9 - \varphi_{10}$) also constitute a degenerate pair : they are antibonding in the PNP framework, but bonding for the PH part of molecule.

A better view on the bonding is offered, perhaps by the localized MO's obtained by the Edminston-Ruedenberg localization procedure. Figure 4 clearly shows that a system of six P—H σ-bonds is formed through hydrogen 1*s* orbitals and the proper combinations of phosphorus orbitals.

Again, excepting the π bonding, the *3d* orbitals were neglected from the picture. The two P—N σ bonds take place through mixed *s*—*p* orbitals. Two three-centered π bonding orbitals are also formed. The major contribution to these bonds, from phosphorus $3d_{xy}$ and $3d_{xz}$ orbitals is noteworthy. In addition the two phosphorus atoms are at such distance that, also, direct P ... P interactions are possible. Thus it should be noted that a P—P covalent bond has a length of about 2.20 Å, while the van der Waals radius of phosphorus is 1.90 Å. In the cation discussed, the P ... P distance (*ca.* 3.20Å) lies between that of a normal covalent P—P bond (2.20Å) and that of two weakly (van der Waals) interacting phosphorus atoms (3.80 Å). This situation is reflected in the high value of P ... P Wiberg bond index (~0.5). The partition of the total energy in diagonal (E) and non-diagonal (E_{AB}) terms [25] reveals a very marked $E_{P...P}$ component (−0.545 a.u.) which is almost half of the E_{PN} component (−1.1599 a.u.). Such interactions have already been reported in cyclic phosphorus-nitrogen rings (cyclophosphazenes),[26] but not yet in linear PNP systems.

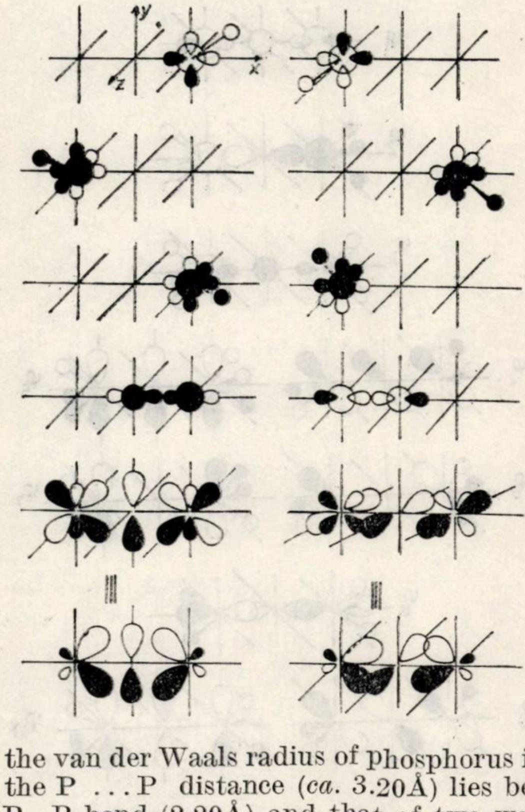

Fig. 4. — The formation of the σP—H, P—N and of the π bonding system (localized orbitals) in the linear $[H_3PNPH_3]^{\oplus}$ cation.

Bent PNP systems. Most of the bent PNP bond angles listed in Table 1 lie close to 140°. Looking at figure 2, no clear minimum of energy appears in this range. Instead of the expected minimum, at most some inflection of the potential surface is noticeable at this value of the bond angle. However, this is the part of the potential surface which could be associated with the observed bent geometries. Of course, variations of the PNP angles are due to the influence of the ligands bound to phosphorus.

A localization of the molecular orbitals shows, like for the linear form, six well defined δ P—H bonds and two σ P—N bonds. However at variance with the linear form, only one three-centered π bond is achieved **(e)**, (through p_z) orbitals) :

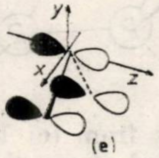

(e)

In addition, some admixture of $3d_{xz}$ orbitals does not only enhance the PN π bonds, but also makes easier a P . . . P interaction **(f)** :

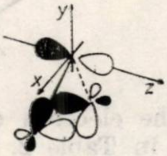

(f)

On bending the molecule, the two phosphorus atoms come closer and their orbital overlapping in *(f)* becomes more effective. Note also that φ_9 and φ_{10} of the linear form are thus stabilized because : 1) the phosphorus P_{p_z}—N_{p_z} unfavorable overlap in φ_9 is outweighed by that of P_{p_z} —N_{p_z} in phase overlap and 2) the phosphorus p_y orbitals are moved into a more favorable position for in phase overlapping either with N_{p_y} or with the other phosphorus p_y orbitals (see **g**)

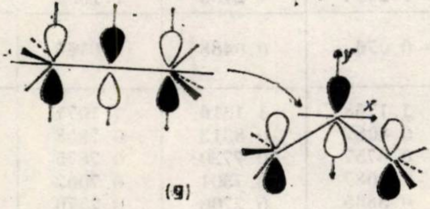

(g)

These phosphorus-phosphorus through space interactions could be responsible for the relative stability of the bent PNP forms over the linear conformers.

The ultimate bending : ring formation. A dramatic decrease in the total energy, acompanying the reduction of PNP angle to smaller than 120° is observed in Figure 2. This time a clear-cut minimum is reached at a PNP angle of *ca.* 86° ($R_{PN} = 1.60$Å), but the minimum energy molecular species (**h**) is no more an open, bent PNP cation! It is the skeleton of a new inorganic P_2N heterocycle, containing phosphorus in (+5) oxidation state.

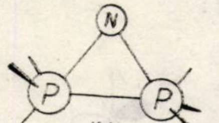

(h)

Its structure formally derives from (**c**) by letting the two phosphorus atoms to share their unpaired electrons (**i, j**)

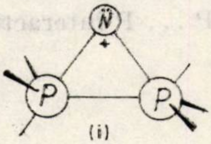

(i)

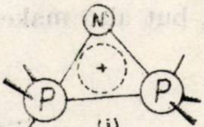

(j)

During the cyclization the electron density at each atom suffers important changes, illustrated in Table 2.

Table 2

Orbital population of N and P at various geometries of $[H_3PNPH_3]$

Orbitals	PNP bond agle			
	180°	120°	100°	80°
N s	1.3797	1.3876	1.4137	1.4474
p_y	1.2494	1.2364	1.1616	1.1088
p_x	1.1976	1.2089	1.2548	1.2693
p_z	1.2494	1.2159	1.1530	1.0489
charge	−0.076	−0.0488	0.0166	0.1254
P s	1.1768	1.1316	1.1071	1.0696
p_y	0.8087	0.8313	0.7958	0.7335
p_x	0.6757	0.7720	0.7875	0.7758
p_z	0.8087	0.7301	0.7062	0.7089
d_{xy}	0.3865	0.2700	0.2576	0.2943
d_{yz}	0.0965	0.3683	0.4765	0.5336
d_{z^2}	0.1079	0.1412	0.2114	0.3660
d_{xz}	0.3865	0.2049	0.1739	0.2036
$d_{x^2-y^2}$	0.1307	0.2272	0.2882	0.3025
charge	0.4230	0.3211	0.1934	0.0119

Note the relatively high occupation numbers of the initially empty 3*d* orbitals! This way, the phosphorus atoms gain some electron density partially from the nitrogen and partially from the ligands. Consequently the initially high positive charge on phosphorus is greatly diminished and phosphorus-phosphorus interaction is intensified (the electrostatic repulsion is reduced). The calculated P—P bond distance in this three-membered ring is *ca.* 2.24Å, *i.e.* slightly longer than a normal, single P—P bond. This may suggest some sort of P—P bent bonding, formed by an angular rather than coaxial overlap of appropriate *p* and *d* phosphorus atomic orbitals.

To the best of our knowledge no phosphorus(V)—nitrogen three-membered heterocycles have been synthesized. However, a trivalent phosphorus analogue **(k)** prepared not long ago, is known [27]:

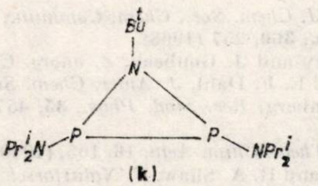

(k)

Its structure was established by X-ray diffraction and thus the existence of the P_2N ring **(k)** is well documented.[27] The P—P bond length in this ring is 2.21 Å, the P—N bond lengths are 1.698 — 1.70 Å and the PNP bons angle is 80.9°.

This three-membered ring contains eight electrons : (regardless of the exocyclic bonds and electron pairs) : six are used for σ bonding and two are probably delocalized ; it is isoelectronic, from this point of view, with the cyclopropenium cation $C_3H_3^+$ which also contains eight skeleton electrons. Structures **(i, j)** differ from **(k)** by a positive charge and by the absence of a substituent at nitrogen. The skeleton electron counting however, makes them perfectly analogous : **(i, j)** also contain eight skeleton electrons, six used for σ bonding and one delocalized, or localized at the nitrogen site. These data are encouraging and show that a NP_2 (V) ring might be isolated if some electron releasing R groups would be attached to phosphorus. These could also be bulky groups (perhaps *t*-butyl, cyclohexyl) to protect the nitrogen site, which seems to be the most labile part of the molecule.

REFERENCES

[1] L. B. Handy, J. K. Ruff and L. F. Dahl, *J. Amer. Chem. Soc.*, **92**, 7312 (1970).

[2] J. K. Ruff, R. P. White and L. F. Dahl, *J. Amer. Chem. Soc.*, **93**, 2159 (1971).

[3] H. B. Chin, M. B. Smith, R. D. Wilson and R. Bau, *J. Amer. Chem. Soc.*, **96**, 5285 (1974).

[4] S. A. Goldfield and K. N. Raymend, *Inorg. Chem.*, **13**, 770 (1971).

[5] G. Huttner and N. Gartzke, *Chem. Ber.*, **108**, 1373 (1975).

[6] A. Müller, M. Romer, H. Bögge, E. Krickemeyer and M. Zimmermann, *Z. anorg. Chem.*, **534**, 69 (1986).

[7] S. W. Kirtley, J. Chanton, R. A. Love, T. Sorrell and R. Bau, unpublished results, quoted in ref. 8.

[8] R. D. Wilson and R. Bau, *J. Amer. Chem. Soc.*, **96**, 7601 (1974).

[9] T. Chivers, A. W. Cordes, R. T. Oakley and W. T. Pennington, *Inorg. Chem.*, **22**, 2429 (1983).

[10] Y. S. Chen and J. E. Ellis, *J. Amer. Chem. Soc.*, **105**, 1689 (1983).

[11] A. Müller, W. Hellman, U. Schimanski, R. Jostes and W. E. Newton, *Z. Naturforsch.*, **38b**, 528, (1983).

[12] A. T. Vincent and P. J. Wheatley, *J. Chem. Soc., Chem. Commun.*, **1971**, 582 : *J. Chem. Soc., Dalton Trans*, **1972**, 617.

[13] W. E. Schwartz Jr., J. K. Ruff and D. M. Hercules, *J. Amer. Chem. Soc.*, **94**, 5227 (1972).

[14] J. A. Pople and G. A. Segal, *J. Chem. Phys.*, **43**, S136 (1965).

[15] In some cases, the standard technique leads to divergences. To avoid this, the method of V. C. Maslov, *Zhur. strukt. Khim.*, **20**, 761 (1979) has been implemented in the original PARAMOL-2.

[16] D. A. Zhogolev and V. B. Volkov, "Metody, Algoritmy i Programy dlya Kvantovokhimicheskih Raschetov Molekul", Kiev, Naukova Dumka, 1976.

[17] S. Santry and G. A. Segal, *J. Chem. Phys.*, **47**, 158 (1967).

[18] C. Glidewell and H. D. Holden, *J. Organometal Chem.*, **226**, 171 (1982).

[19] D. W. H. Rankin, M. D. Walkinshow and H. Schmidbaur, *J. Chem. Soc., Dalton Trans.*, **1982**, 2317.

[20] J. W. Cox and E. R. Corey, *J. Chem. Soc., Chem. Commun.*, **1969**, 205.

[21] M. L. Ziegler, *Z. anorg. Chem.*, **360**, 257 (1968).

[22] R. Baumgartner, W. Sawodny and J. Goubeau, *Z. anorg. Chem.*, **340**, 246 (1965).

[23] L. B. Handy, J. K. Ruff and L. F. Dahl, *J. Amer. Chem. Soc.*, **92**, 7327 (1970).

[24] C. Edminston and K. Ruedenberg, *Rev. Mod. Phys.*, **35**, 457 (1963). *J. Chem Phys.*, **43**, S97 (1965).

[25] H. Fischer and H. Kollmar, *Theor. Chim. Acta*, **16**, 163, (1970).

[26] J. P. Foucher, J. F. Labarre and R. A. Shaw, *F. Naturforsch.*, **31b**, 677 (1976).

[27] E. Niecke, A. Nickloweith—Lüke, R. Rüger, B. Krebs and H. Grewe, *Z. Naturforsch.*, **36b** 1566 (1981).

Revue Roumaine de Chimie, 33, 2, 143–148 (1988)

POLYNUCLEAR COORDINATION COMPOUNDS CONTAINING VANADIUM-TIN BOND

MARIA BREZEANU[1] and OTILIA COSTIŞOR[2]

[1] Polytechnic Institute of Bucharest, Inorganic Chemistry Department, 23, Dumbrava Roşie, Bucharest, Romania

[2] Chemical Research Centre Timişoara, 24, Mihai Viteazul, Timişoara, Romania 1900

Received August 30, 1986
Revised April 15, 1987

Compounds containing trichlorostannate anion as ligand and corresponding to the general formula $(NH_4)_2[VO(SnCl_3)_nCl_{4-n}]\cdot 2H_2O$ where n= 1–4, have been isolated from the $NH_4VO_3 - SnCl_2 - NH_3$ system. The compounds have been characterized by elemental analysis, electronic and IR spectra, magnetic measurements and thermodifferential analysis.

The literature describes a relatively small number of coordination compounds, especially of platinum metals [1–3] containing trichlorostannate (II) ion as ligand. However, a series of Co(II)[4,5] and copper(II) [6,7] complex compounds containing the $SnCl_3^-$ ligand have been described. In order to explain the reduction mechanism of vanadium (V) by tin(II) kinetic studies in dilute hydrochloric [8,9] or perchloric [10,11] acid solutions have been carried out but compounds containing vanadium-tin bond have not been yet described.

In the present paper we succeeded to characterize a series of complex compounds with the general formula:

$$(NH_4)_2[VO(SnCl_3)_nCl_{4-n}]\cdot 2H_2O$$

where n = 1 – 4.

RESULTS AND DISCUSSION

The results of our previous study [12] regarding the vanadium(V)–tin(II) system in concentrated hydrochloric acid were used in the preparation of oxovanadium(IV) complex compounds containing the $SnCl_3^-$ anion as ligand.[13] It was then established that the 3M hydrochloric acid concentration is optimal. By carrying out the synthesis in 3M HCl aqueous solutions at V(V) : $SnCl_2$ ratios ranging from 1 : 2 to 1 : 5 and adjusting the pH medium with ammonia to 4, the compounds of the type

$(NH_4)_2[VO(SnCl_3)_nCl_{4-n}]\cdot 2H_2O$ were obtained. The results of the chemical analysis and some of their properties are presented in Table 1.

The nature of the obtained compounds is dependent on the vanadium (V) : tin(II) ratio, the time and the temperature of the solutions containing NH_4VO_3 and $SnCl_2$.

Table 1

Complex compounds of VO^{+2} containing $SnCl_3^-$ as ligand

Complex	Colour	Elemental analyses[a] %				μ BM	$\nu_{V=0}$ cm^{-1}
		V	Sn	Cl	NH_3		
$(NH_4)_2[VO(SnCl_3)Cl_3]\cdot 2H_2O$	green	10.74 (10.82)	25.61 (25.22)	44.93 (44.25)	6.90 (7.22)	1.85	972
$(NH_4)_2[VO(SnCl_3)_2Cl_2]\cdot 2H_2O$	green	7.85 (7.71)	36.49 (35.94)	42.81 (43.01)	4.80 (5.14)	1.62	966
$(NH_4)_2[VO(SnCl_3)_3Cl]\cdot 2H_2O$	green	5.47 (5.99)	42.31 (41.85)	41.16 (41.76)	3.73 (4.00)	1.69	959
$(NH_4)_2[VO(SnCl_3)_4]\cdot 2H_2O$	grey	4.36 (4.91)	46.34 (45.89)	40.90 (41.35)	3.01 (3.28)	1.67	952

[a] Calculated values in parentheses.

The nature of the obtained compounds is dependent on the vanadium(V) : tin(II) ratio, the time and the temperature of the solutions containing NH_4VO_3 and $SnCl_2$.

The hydrochloric solutions containing NH_4VO_3 and $SnCl_2$ were investigated spectrophotometrically. The absorption spectra of hydrochloric solutions show a maximum at 760 nm assigned to VO^{2+} species. The intensity of the band at 760 nm decreases and a well developed one appears at 405 nm. The last band is assigned to the vanadium (III) species. As is shown in our previous paper, [12] the relative intensity of the observed bands is dependent on the vanadium(V) : tin(II) ratio, hydrochloric acid concentration, time and temperature. The isolation of the complexes is possible only when the vanadium(IV) species disappear in favour of the vanadium(III) ones. During the isolation, in air, vanadium (III) is oxidized to vanadium (IV).

The temperature of the solutions containing NH_4VO_3 and $SnCl_2$ is very important. Thus, at 5°C, the number of $SnCl_3^-$ ligands is strictly dependent on the V(V) : Sn(II) ratio—obviously, taking into account that, for the reduction of a mol of V(V) to V(VIII) it is necessary a mol of tin(II)—whereas at room temperature the composition is less reproducible.

In the presence of moisture the $(NH_4)_2[VO(SnCl_3)_nCl_{4-n}]\cdot 2H_2O$ compounds hydrolyse as demonstrated by the infrared spectra.

To obtain additional data on the nature, stereochemistry and thermal stability of the studied compounds, magnetic moments, electronic and IR spectra as well as thermal derivatograms have been measured.

Magnetic moments. The oxidation state of vanadium was established with the aid of magnetic moments of $(NH_4)_2$ $[VO(SnCl_3)_nCl_{4-n}]\cdot 2H_2O$ complexes, determined at room temperature. The values presented in

Table 1 show that all magnetic moments are close to the spin-only value for a d^1 configuration, 1.78 BM. The smaller values of some magnetic moments may be assigned to distortions of the octahedral environment.

Electronic spectra. As figure 1 shows, the absorption spectra, recorded on KBr discs or in nujol mulls and the reflectance spectra are identical. The reflectance spectrum of $VOSO_4 \cdot 5H_2O$ — for which the presence of $VO(H_2O)_5^{+2}$ ion was postulated — was used as reference. The spectra of the vanadium(IV)trichlorostannate(II)complexes and that of $VO-SO_4 \cdot 5H_2O$ consist of a band in about the same region in the spectrum.

Based on the energy levels diagram of the exovanadium(IV) ion in a C_{4v} ligand field, the intense band at 825 nm and the shoulder at 725 nm may be assigned to the $^2B_2 \rightarrow {}^2E$ and $^2B_2 \rightarrow {}^2B_1$ transitions respectively.

As figure 1 shows, the observed band in the $VOSO_4 \cdot 5H_2O$ spectrum appears at a greater wavelength than that of vanadium(IV)-trichlorostannate (II) complexes. This indicates that $SnCl_3^-$ anion, as well as Cl^-, stands before H_2O ligand in the spectrochemical series.

The broad band at 825 nm does not allow to distinguish the maxima as a function of the $SnCl_3^-$ ligands number. On the other hand, the width of this band can be assigned to the disappearance of degeneracy of the ^2E term as a result of some distortions.

Infrared spectra. The IR spectra of $(NH_4)_2[VO(SnCl_3)_nCl_{4-n}] \cdot 2H_2O$, where n = 1—4, are very similar. All complexes have a strong absorption band in the 950 — 980 cm^{-1} range. This indicates a high π-bond order in VO^{+2}, showing that the oxovanadium species is present as a monomeric entity, [15] and not as a polymeric chain V—O—V—.

Table 1 shows that, as the number of $SnCl_3^-$ ligands increases, the $\nu_{V=0}$ frequencies are shifted to lower values. This may be explained by the electronic configurations of vanadium(IV) and by the fact that $\nu_{V=0}$ depends on the oxygen-vanadium π-bond order. Due to the d^1 configuration of vanadium(IV) — for which a π-backbonding is not possible, the $\nu_{V=0}$ frequency is a measure of the ligand donation capacity. It is well known that the $SnCl_3^-$ ligand is a better donor than Cl^-. As the number of $SnCl_3^-$ increases the charge density at vanadium (IV) also increases and a decrease in the oxygen-vanadium bond order occurs.

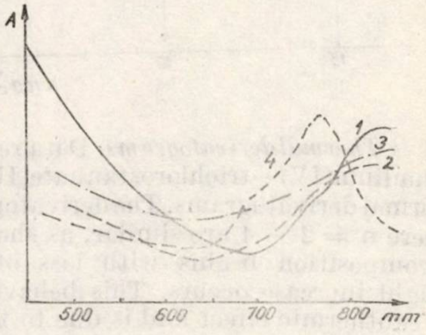

Fig. 1. — Electronic spectra of $(NH_4)_2VO(SnCl_3)_4 \cdot 2H_2O$: in nujol (1), KBr disc (2), reflectance (3) and of $VOSO_4.5H_2O$(4)

In the 250 — 400 cm^{-1} range all complexes show two relatively intense bands, at 332 and 300 cm^{-2}, assigned to the symmetrical, respectively antisymmetrical, Sn—Cl mode of the coordinated $SnCl_3^-$ anion. [16]

A large band at 3450 cm^{-1} and one at 1600 cm^{-1} are assigned to coordinated water. In the 3150 — 3450 cm^{-1} range the water bands overlap those of the ammonium ion. However, the intense band at 1400 cm^{-1} is due to the ammonium ion.

As already mentioned above, in the presence of moisture, the hydrolysis of $(NH_4)_2[VO(SnCl_3)_nCl_{4-n}] \cdot 2H_2O$ complexes occurs. This process is accompanied by a colour change from green to gray. The slight hydrolysis is suggested by the IR spectrum, as shown in figure 2 : a large intense band appears at 560 cm^{-1}. This band is assigned — according to literature data — to the δ_{Sn-OH} mode.[17] Elemental analyses data of the unhydrolysed and of the hydrolysed complexe sare the same. Thus, the hydrolysis may imply the crystallization water.

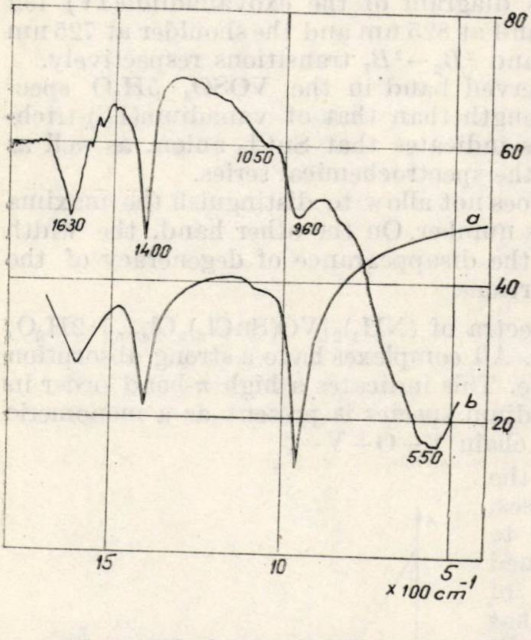

Fig. 2. — IR spectra of $(NH_4)_2VO(SnCl_3)_3Cl \cdot 2H_2O$: unhydrolysed (a) and hydrolysed (b) species

Thermal derivatograms. Data regarding the thermal stability of the oxovanadium(IV)—trichlorostannate(II) compounds, were obtained from their thermal derivatograms. The derivatograms of $(NH_4)_2[VO(SnCl_3)_nCl_{4-n}] \cdot 2H_2O$ where $n = 2 - 4$ are similar, as shown in figure 3 for $n = 2$. The thermal decomposition begins with loss of water at 135 — 140°C. At 370°C a weight increase occurs. This behaviour is exhibited on the DTA curve as an exothermic effect and is due to the vanadium oxidation.

Fig. 4 represents the thermal derivatogram of the diaquabis (ammonium) trichloro(trichlorostannato) oxovanadate (IV). It may be noticed that this is quite different from those of the above mentioned compounds : the exothermic effect does not appear at 370°C and the final weight does not correspond to residual V_2O_5 and SnO_2.

The thermal derivatogram of $(NH_4)_2[VO(SnCl_3)Cl_3] \cdot 2H_2O$ may be explained by the formation of $VOCl_2$ as a result of decomposition in the presence of air. The oxovanadium dichloride undergoes a slow decomposition at 170°C with formation of gaseous chlorine and oxovanadium(V) trichloride.[18]

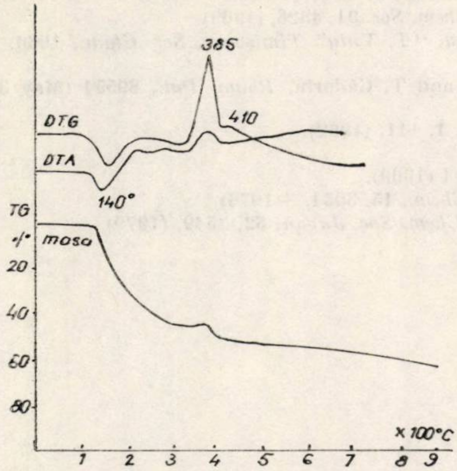

Fig. 3. — Thermal derivatogram of $(NH_4)_2VO(SnCl_3)_2Cl_2 \cdot 2H_2O$

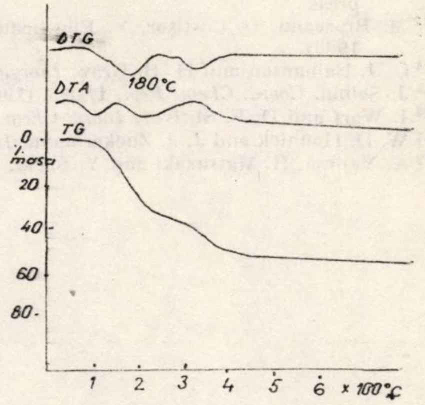

Fig. 4. — Thermal derivatogram of $(NH_4)_2VO(SnCl_3)Cl_3.2H_2O$

EXPERIMENTAL

The compounds of the general formula $(NH_4)_2[VO-(SnCl_3)_nCl_{4-n}].2H_2O$ have been obtained by procedures already described. [12]

$(NH_4)_2[VO(SnCl_3)_3Cl] \cdot 2H_2O$. A solution of 1.17 g ($10^{-2}$ mol) of NH_4VO_3 in 30 mL concentrated hydrochloric acid and 100 mL water was treated with 9.02 g(4.10^{-2} mol)$SnCl_2 \cdot 2H_2O$. The solution was kept at 5°C for 8 days. A solution of NH_4OH(25%) was added dropwise to the clear solution with vigorous stirring until pH = 3.5 when a green precipitate persisted. Filtration, after 2 hr gave 6.3g of product. This was washed with water and ethanol and then dried *in vacuo* overnight.

The same procedure, using convenient V(V) : Sn(II) ratio, is followed in the preparation of $(NH_4)_2[VO(SnCl_3)_nCl_{4-n}]. 2H_2O$, n = 1, 2, 4 complexes.

Electronic spectra were recorded at room temperature by using a Specord UV—VIS Carl Zeiss spectrophotometer.

The IR spectra were recorded with a Perkin Elmer type 457 spectrophotometer, by using KBr discs.

Magnetic susceptibility measurements were performed by Gouy method on finely powdered samples at room temperature.

Derivatograms were recorded in the 20 — 900°C range using a MOM-Budapest derivatograph. The curves were obtained in air by using calcined Al_2O_3 as standard.

REFERENCES

[1] R. D. Cramer, R. V. Lindsey, G. T. Prewitt and U. G. Stolberg, *J. Amer. Chem Soc.*, **87**, 658 (1965).

[2] J. F. Young, R. D. Gillard and G. Wilkinson, *J. Chem. Soc.*, **1964**, 5176.

[3] R. D. Cramer, *Inorg. Chem.*, **4**, 445, (1965).

[4] M. Brezeanu and L. Patron, *Anal. Univ. București, Ser. Chim.*, **21**, 71(1972).

[5] M. Brezeanu and L. Patron, *Anal. Univ. București, Ser. Chim.*, **21**, 171 (1972).

[6] J. A. Dilts and M. P. Johnson, *Inorg. Chem.*, **5**, 2079 (1966).

[7] M. Brezeanu and I. Jitaru, *Rev. Roumaine Chim.*, **17**, 1873 (1972).

[8] D. J. Drye, W. C. E. Higginson and P. J. Knowles, *J. Chem Soc.*, **1962**, 1137.

[9] W. C. E. Higginson, R. T. Leichgh and R. Nightingale, *J. Chem. Soc.* **1962**, 435.

[10] B. Schiefelbein, and N. A. Daugerty, *Inorg. Chem.*, **9**, 1716 (1970).

[11] B. Schiefelbein and N. A. Daugerty, *J. Amer. Chem. Soc.* **91**, 4328, (1969).

[12] O. Costişor and M. Brezeanu, *Bull. Polyt. Inst, "T. Vuia" Timişoara, Ser. Chim.*, 1986, in press.

[13] M. Brezeanu, O. Costişor, V. Eliu-Ceauşescu and T. Cădariu, *Roum. Pat.*, 89554 (May 30, 1986).

[14] C. J. Balhausen and H. B. Gray, *Inorg. Chem.* **1**, 111, (1962).

[15] J. Selbin, *Coord. Chem. Rev.*, **1**, 293, (1966).

[16] I. Warf and D. F. Shriver, *Inorg. Chem.*, **8**, 914 (1969).

[17] W. D. Honnick and J. J. Zuckermann, *Inorg. Chem.*, **15**, 3034, +1976).

[18] A. Yajima, R. Matsuzaki and Y. Saeki, *Bull. Chem. Soc. Japan*, **52**, 3549, (1979).

Revue Roumaine de Chimie, **33**, *2*, 149–155 (1988)

DETERMINATION OF THE NATURE OF IRON(III) IMPURITIES IN NaA ZEOLITES

FELICIA IACOMI[b], ELEONORA TRIF[c], EVELINE POPOVICI[a],
AURELIA VASILE[a], MARIA ALEXANDROAEI[a], M. CRUCEANU[a]
and GH. SINGUREL[b]

[a] Department of Chemical Technology, Polytechnic Institute, Iași, Romania
[b] Department of Physics, "Al. I. Cuza" University, Iași, Romania
[a] Department of Physics, Cluj-Napoca University, Cluj-Napoca, Romania

Received June 16, 1986
Revised March 16, 1987

EPR and IR studies of Fe^{3+} impurity in NaA zeolite show that iron can be simultaneously present in zeolite as : Fe^{3+} ions in cationic positions, and Fe_3O_4 or another Fe^{3+} compound with strong exchange spin-spin interactions precipitated on zeolite. All of these are incorporated in zeolite during its synthesis or by cation-exchange. Amount of substitutional Fe^{3+} cations in the aluminosilicate framework is negligible. EPR data show that iron can be easily removed from zeolite.

The industrial utilization of the synthetic zeolites in different ionic exchange processes,[1] in detergents conditioning,[2] in antistatization processes of the macromolecular products,[3] or in anhydrization processes of the organic solvents requires very pure zeolites, especially with a low iron content, which cannot be obtained by synthesis, because of all technical raw materials that have an increased content of Fe^{3+} ions. Establishing the ways for improving the synthetic zeolite purity implies the knowledge of the nature of Fe^{3+} retained in zeolite.

In a previous work[4] we studied the influence of Fe^{3+} ions on the NaA zeolite crystallization kinetics and their repartition during the synthesis between the zeolite solid phase which crystallizes and the liquid phase of the mother solution. For a better understanding of the way in which zeolite retains the Fe^{3+} ions originating in the raw materials (natrium aluminate and natrium silicate), it was analysed the possibility of Fe^{3+} retention in the NaA zeolite, depending on their content in the synthesis medium.

EXPERIMENTAL

A lot of NaA zeolite samples were synthesized from the raw materials : natrium aluminate (2.59 mmol Al_2O_3/mL ; 4.50 mmol Na_2O/mL ; 348.36 Fe^{3+}/mL) and natrium silicate (6.18 mmol SiO_2/mL ; 4.50 mmol Na_2O/mL ; 498 Fe^{3+}/mL). They were brought in contact under stirring and was obtained an initial mixture characterized by the following molar oxide composition :

30.23 % SiO_2 ; 14.53 % Al_2O_3 ; 55.23 % Na_2O and $H_2O/Na_2O = 50$. The hydrothermal synthesis in water bath at (368±5) K for 8 hours was performed. After filtration the products were washed with distilled water up to a pH = 9.

In order to obtain reaction mixtures with variable Fe^{3+} content, the iron removal from the materials was first performed by using repeated extractions with amines [2]. Thus reaction mixtures with a Fe^{3+} content ranging between 54.0 Fe^{3+}/mL — 366.3Fe^{3+}/mL were obtained, samples 1 — 4. Product 1 (Table 1) was subjected to an ion-exchange process with 0.1 respectively 1.0 N ferric nitrate solutions at room temperature, solid/liquid ratio being 1 : 10 (samples 6, 7). For emphasizing the effect of the thermal treatment on the retained iron in zeolite, samples 4 and 7, having a high iron content, were heated at 723 K for 2 hours (samples 5, 8). The ions of Fe^{3+} were colourimetrically dosed in the presence of orthophenanthroline. In the obtained zeolite products the molar ratio SiO_2/Al_2O_3 was 1.98 — 2.00. The diffractometric data for all the synthesized products were characteristic of NaA zeolite structure.

Table 1

Chemical analysis of products

Sample	Observation	Fe^{3+} concentration	
		Fe^{3+}/mL (reaction mixture)	Fe^{3+}/g (product)
1		54.0	400.4
2		101.0	1156.5
3		247.0	2814.9
4		366.6	7660.0
5	Thermally treated		7660.0
6	Ion-exchanged		1872.0
7	Ion-exchanged		9260.0
8	Ion-exchanged and thermally treated		9260.0

The IR spectra were recorded with a UR-20 "C. Zeiss-Jena" spectrometer and the EPR measurements were made on an X-band JES 3B spectrometer at room temperature.

RESULTS AND DISCUSSIONS

IR spectra. It is well known from the X-ray diffraction on A zeolite that most of the exchangeable cations are bonded to the negatively charged zeolite framework. These cations may influence the lattice vibration modes, so that IR spectroscopy is able to give information about cation positions. The spectra reported here are for hydrated zeolites in KBr pellets.

The IR spectra of some NaO products with different Fe^{3+} ion concentrations, obtained by synthesis or by ion-exchange, are compared in Fig. 1. The influence of Fe^{3+} ions on the relative intensities and lattice vibration frequencies is evident. The presence of Fe^{3+} cations has also a strong influence on the vibration frequencies within the ranges 440 — — 490 cm^{-1} and 540 — 590 cm^{-1}. These bands are assigned to a Si(Al)-O bending mode and double 4-ring vibrations.

Maxwell and Baks [6] studied the influence of the exchangeable cations on the zeolite lattice and found a nearly linear dependence between the absorption band frequency and the reciprocal of the sum of the cation and oxygen ionic radii ($1/r_{\text{cation}} + r_{0^{2-}}$) for the Si(Al)—O bending mode and the double ring vibrations. The influence of iron content is more emphasized for sample 7 (Fig. 1) by the shift of bands from 555 to 550 cm^{-1}, respectively from 465 to 455 cm^{-1}. We suppose that the new bands at 410 and 620 cm^{-1} are due to the cluster form (Fe_3O_4 or Fe/Al species) precipitated in the zeolite cavities. No visible change in the NaA zeolite spectra was seen for small Fe^{3+} concentrations

EPR spectra. The EPR spectra of the Fe^{3+} ions allow the investigation of the retention form of Fe^{3+} introduced in NaA by synthesis (Figs. 2 and 3) or during the ion-exchange. According to the EPR spectra the products, which have been analysed, contain Fe^{3+} ions localized in S_{II} cationic positions, near the eight-membered oxygen rings ($g = 2.05$); in S_I cationic positions, near the six-membered oxygen rings and in the aluminosilicate framework ($g = 4.30$). The broad signal in the spectrum ($g = 2.20$) is due to Fe^{3+} chaotically distributed in clusters [7,8] with strong exchange spin-spin interactions (Fig. 3).

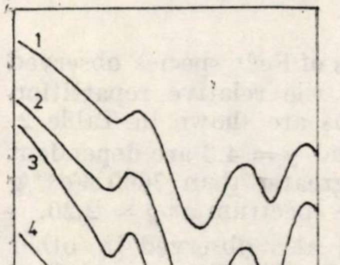

Fig. 1. — IR spectra of the NaA zeolite with different Fe^{3+} ions concentrations.

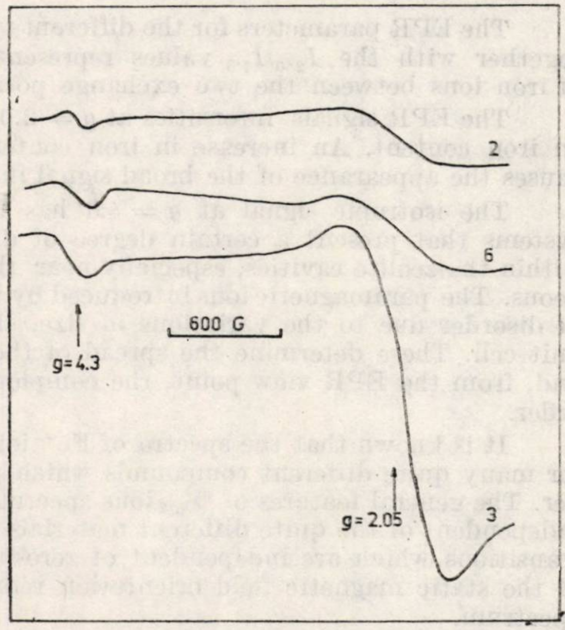

Fig. 2. — EPR spectra of Fe^{3+} ions at room temperature in NaA zeolite. Amplification: $4 \times 10^4 V/V$

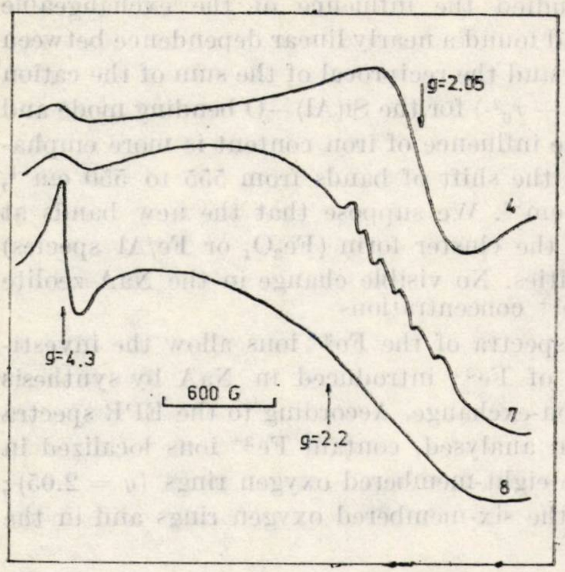

Fig. 3. — EPR spectra of Fe^{3+} ions at room temperature in NaA zeolite. Amplification : 1×10^4 V/V.

The EPR parameters for the different types of Fe^{3+} species observed together with the $I_{2 \cdot 0}/I_{4 \cdot 3}$ values representing the relative repartition of iron ions between the two exchange positions are shown in Table 2.

The EPR signals intensities at $g = 2.05$ and $g = 4.3$ are dependent on iron content. An increase in iron content greater than 7660 Fe^{3+}/g causes the appearance of the broad signal in the spectrum at $g = 2.20$.

The isotropic signal at $g = 4.3$ has been also observed in other systems that present a certain degree of disorder. [9,10] The crystal field within the zeolite cavities, especially near the cavity walls, is heterogeneous. The paramagnetic ions introduced by ion exchange feel some degree of disorder due to the variations in size, shape and composition of the unit cell. These determine the spread of the B_n^m crystal field parameters and, from the EPR view point, the complete absence of the long-range order.

It is known that the spectra of Fe^{+} ions are qualitatively the same for many quite different compounds which present some degree of disorder. The general features of $^6S_{5/2}$ ions spectra in a disordered system being independent of the quite different materials composition, only those EPR transitions which are independent of zero-field splitting parameters and of the static magnetic field orientation remain visible in the derivative spectrum.

The experimental EPR spectrum is a superposition of a great number of absorption lines, each of which described by a spin Hamiltonian of the general form :

$$\mathscr{H}_0 = \sum_{n=2,4} \sum_{m=-n}^{n} B_n^m O_n^m + g\beta HS.$$

Table 2

EPR Parameters for the different types of Fe^{3+} species

Sample	Nature	g-value (± 0.05)	Width, G (± 0.05)	$I_{2\cdot 0}/I_{4\cdot 3}$
2	$Fe^{3+}_{S_{II}}$	2.02	400.00	2.8
	$Fe^{3+}_{S_{I}}$, Fe^{3+}_{S}	4.30	100.00	
3	$Fe^{3+}_{S_{II}}$	2.05	500.00	7.9
	$Fe^{3+}_{S_{I}}$, Fe^{3+}_{S}	4.30	180.00	
4	$Fe^{3+}_{S_{II}}$	2.05	500.00	12.0
	$Fe^{3+}_{S_{I}}$, Fe^{3+}_{S}	4.30	180.00	
5	$Fe^{3+}_{S_{II}}$	2.05	500.00	3.5
	$Fe^{3+}_{S_{I}}$, Fe^{3+}_{S}	4.30	180.00	
6	$Fe^{3+}_{S_{II}}$	2.08	500.00	3.0
	$Fe^{3+}_{S_{I}}$, Fe^{3+}_{S}	4.28	180.00	
7	$Fe^{3+}_{S_{II}}$	2.05	500.00	20.0
	Fe^{3+}_{P}	2.20	1500.00	
	$Fe^{3+}_{S_{I}}$, Fe^{3+}_{S}	4.28	180.00	
8	Fe^{3+}_{P}	2.20	1600.00	1.7
	$Fe^{3+}_{S_{I}}$, Fe^{3+}_{S}	4.30	180.00	

By treating the Zeeman interaction as a perturbation on the fine structure of Hamiltonian, then the EPR transition occurs only inside the Kramers doublets which have the following eigenfunctions :

$$\psi(\pm) = \sin\alpha \sin\beta \left| \pm \frac{5}{2} \right\rangle - \cos\alpha \sin\beta \left| \pm \frac{1}{2} \right\rangle + \cos\beta \left| \mp \frac{3}{2} \right\rangle$$

The theoretical g_{eff} factors defined as : $g_{eff} = (E_+ - E_-)/\beta H$ will be :

$$g_x = 2(3\sin^2\beta\cos^2\alpha + 2\sqrt{5}\sin\beta\cos\beta\sin\alpha + 4\sqrt{2}\sin\beta\cos\beta\cos\alpha)$$

$$g_y = 2(3\sin^2\beta\cos^2\alpha + 2\sqrt{5}\sin\beta\cos\beta\sin\alpha - 4\sqrt{2}\sin\beta\cos\beta\cos\alpha)$$

$$g_z = 2(4\sin^2\beta\sin^2\alpha + 4\sin^2\beta - 6).$$

The values of the isotropic g tensor and the form of the corresponding eigenfunctions may be obtained by solving the equations :

$$|g_x| = |g_y| = |g_z|.$$

The requirement of isotropy imposed to the tensor g leads to the isotropic value $g = 30/7$ and $g = 10/3$ respectively, which are just those observed experimentally for $3d^5$ ions in disordered compounds. The isotropic spectrum at $g = 30/7$ is assigned to the Fe^{3+} ions located in the lattice or in the cationic positions having C_{3v} symmetry of neighborhood. By following the $g = 4.3$ EPR signal during zeolite heating at 723 K in air, an increase in the isotropic signal intensity at $g = 4.3$ to the prejudice of the signal at $g = 2.05$ (Fig. 3) is evidenced. This fact may be considered to be produced by the Fe^{3+} ions migration from S_{II} exchange positions to S_I exchange positions. So, one observes a decrease in $I_{2\cdot0}/I_{4\cdot3}$ ratio values presented in Table 2.

The signal at $g = 2.05$ assigned to the presence of the $Fe^{3+} - O^{-2} - Fe^{3+}$ isolated pairs in S_{II} cationic positions, involves a dominant Zeeman interaction to the prejudice of the fine structure term of the spin Hamiltonian.

The migration of exchangeable cations from S_{II} positions to S_I positions having a lower symmetry, during the heat treatment, is also evidenced by the disappearance of the characteristic signal of Mn^{2+} impurity ($g = 2.05$, Fig. 3), which was introduced in zeolite during the ion-exchange process.

CONCLUSIONS

During the NaA type zeolite synthesis Fe^{3+} ions in the reaction mixture get accumulated in zeolite, being distributed mainly in S_{II} cationic positions and also in S_I cationic positions. After the dehydration, by heat treating the samples, a migration of Fe^{3+} ions occurs towards the S_I cationic positions. The Fe^{3+} ions isomorphically substituted in the aluminosilicate framework are negligible (Fe^{3+}_S, Table 2).

At small iron concentrations the Fe^{3+} ions introduced by ionic-exchange prefer S_{II} cationic positions, but as the concentration increases they get accumulated in zeolite forming $Fe^{3+} - O^2 - Fe^{3+}$ clusters or Fe^{3+} —complexes (Fe^{3+}_P, Table 2).

The retention mode of Fe^{3+} ions in zeolite suggests different possibilities of iron removal by chemical extraction.

REFERENCES

[1] A. Bold, A. Popa, M. Cruceanu, Ev. Popovici and M. Găburici, *Rev. Chim (București)*, **6**, 554 (1985).

[2] M. Cruceanu, A. Popa, Ev. Popovici, A. Vasile and M. Alexandroaei, 1st Sympossium "Zeoliții în tehnologia modernă" Iași 1983, p. 193.

[3] M. Cruceanu, Ev. Popovici, A. Vasile and C. Iacob, Romanian Patent 80560 (1982).

[4] M. Cruceanu, A. Popa, Ev. Popovici, A. Vasile, M. Alexandroaei and F. Iacomi, *Rev. Chim. (București)*, **8**, 727 (1985)

[5] M. Cruceanu, Ev. Popovici, A. Vasile and M. Alexandroaei, Romanian Patent 85303 (1984).

[6] I. E. Maxwell and A. Baks, "Molecular Sieves" in "Adv. in Chem. Series 121", Ed. Am. Chem. Soc., Washington, 1973, p. 88.

[7] B. Wichterlova, L. Kubelkova, P. Jiru and D. Kolihova, *Coll. Czech. Chem. Comm.*, **8**, 2143 (1980).

[8] E. C. Derouane, M. Mestdach and L. Vielvoye, *J. Catal.*, **33**, 169 (1974).

[9] Th. Castner, G. S. Newell, W. C. Holton and C. P. Slichter, *J. Chem. Phys.*, **32**, 3, 668 (1960).

[10] H. H. Wickman, M. P. Klein and D. A. Shirley, *J. Chem. Phys.*, **42**, 6, 2113 (1965).

Revue Roumaine de Chimie, 33, 2, 157–166 (1988)

KINETICS AND MECHANISM OF Ru(III) CHLORIDE-CATALYSED OXIDATION OF BENZALDEHYDE AND SUBSTITUTED BENZALDEHYDES BY TRICHLOROISOCYANURIC ACID IN ACID MEDIUM

SUBAS C. PATI*, ASHOK KUMAR SAHU and Y. SRIRAMULU

Department of Chemistry, Berhampur University
Berhampur-760 007, Orissa, India

Received June 9, 1986

The kinetics of Ru(III) chloride-catalysed oxidation of benzaldehyde and substituted benzaldehydes by trichloroisocyanuric acid (TCCA) in aqueous acetic acid—perchloric acid medium is reported. The reactions are first order with respect to [substrate] and [Ru(III)]. The order with respect to [TCCA] is zero. Added [H^+] has no effect on the oxidation process. The order of reactivity is: $p-OCH_3 > p-CH_3 > p-NO_2 > m-NO_2 > H > p-Cl > p-Br$. The ρ, σ plot shows a break in the reactivity order. A mechanism involving outer sphere complexation between the substrate and Ru(III) followed by breakdown of the complex in a slow step involving hydride ion loss has been postulated for substrates having electron releasing groups. The unusual behaviour of *p*-nitrobenzaldehyde and *m*-nitrobenzaldehyde has been rationalised on the basis of an inner sphere mechanism involving rate limiting proton loss. Activation parameters have also been computed.

INTRODUCTION

Oxidation of aromatic aldehydes using various oxidants has received considerable attention. Kinetics of Os(VIII) catalysed oxidation of benzaldehydes by different oxidants like periodic acid, chloramine-T, hexacyanoferrate have already been reported.[1–3] Many investigators have also reported the Ru(III)-catalysed oxidation of benzaldehydes by various oxidants like ferricyanide, peroxy disulphate, periodic acid, sodium metaperiodate.[4–7] Recently the oxidation of different organic substrates by trichloroisocyanuric acid (TCCA) has been reported by many workers.[8–10] A survey of literature reveals that no systematic work has been done on the oxidation of benzaldehyde and some substituted benzaldehydes by TCCA in order to throw light on the catalytic role of Ru(III) and the mechanism involved in these oxidations.

---

* For correspondence.

EXPERIMENTAL

Materials and Methods

All the substrates were of Analar (BDH) grade and were used after redistillation in the case of liquid substrates and recrystallisation in the case of solid substrates. The oxidant trichloroisocyanuric acid was of Analar (Fluka) grade. The catalyst $RuCl_3$ was from Johnson Mathey (London) and its aqueous solution was standardised by the method of Horiuchi[11] et al. An electrically operated thermostatic water bath was used. The temperature fluctuation was not more than ± 0.02°C.

The progress of the reaction was monitored by estimating oxidant iodometrically at regular intervals of time. The experiments were carried out in duplicate to ensure reproducibility.

Stoichiometry and product analysis

A reaction mixture containing a known excess of [TCCA] over that of the substrate at a desired solvent composition and a definite concentration of Ru(III) was thermostated for 24 hours. It was found that one mole of substrate consumes one mole of TCCA. Thus the stoichiometry is 1 : 1.

The excess of acetic acid from the mixture was evaporated under reduced pressure and the remaining acetic acid was neutralised by sodium bicarbonate solution. Finally the reaction mixture was strongly acidified with HCl and then extracted with ether[12] repeatedly. The ether extract was washed several times with distilled water and evaporated, and the product was identified by its characteristic spot test.[13]

RESULTS AND DISCUSSION

Kinetic of the oxidation of benzaldehyde and some substituted benzaldehydes in aqueous acetic acid—perchloric acid by trichloroisocyanuric acid (TCCA) catalysed by Ru(III) chloride have been investigated.

i. Effect of varying [oxidant] on the reaction rate

The reaction is zero order in TCCA. The plots of time versus percentage of reaction (Fig. 1) in an individual run are linear up to 80% of the reaction. The zero order rate constants k_0(mole $L^{-1}s^{-1}$) are fairly constant over the TCCA concentration studied as is evident from Table 1.

ii. Effect of varying [substrate] on the reaction rate

The effect of change in substrate concentration on the reaction kinetics has been studied by varying the initial substrate concentration for a number of substrates. The zero order rate constants increase with an increase in substrate concentration. The plots of log k_0 versus log [S] are linear with unit slopes. Also the first order rate constants $k_1(k_0/[S])$ (where k_0 is the zero order rate constant and [S] is the substrate concentration) are fairly constant, confirming first order dependence on the substrate (Table 1).

iii. Effect of catalyst on the reaction rate

The effect of a change in Ru(III) chloride concentration on the reaction kinetics has been studied. The k_0 or $k_1(k_0/[S])$ values increase linearly with an increase in the concentration of Ru(III). The plots of

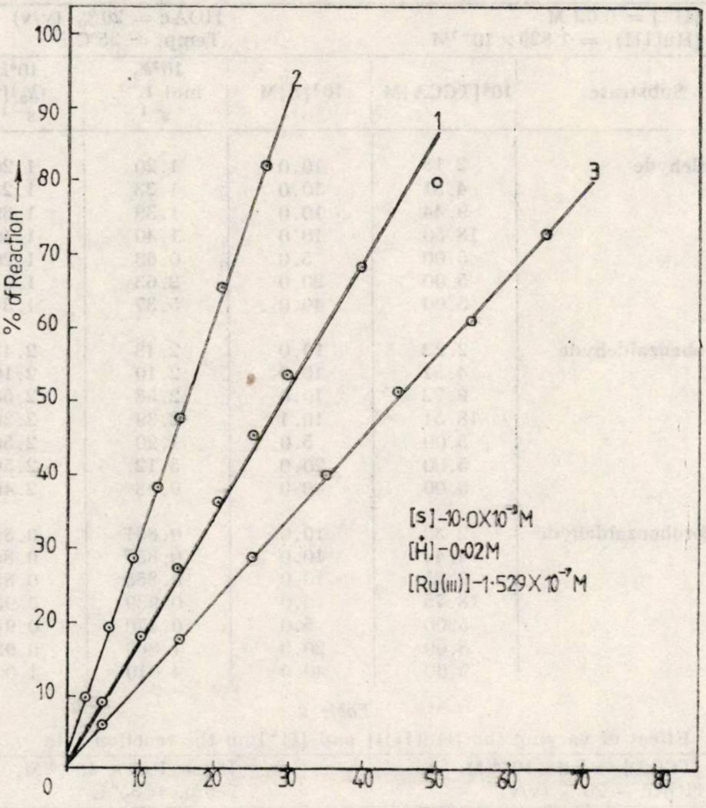

Fig. 1. — % of reaction vs time at 35°, HOAc 20 % (v/v) ; 1 — benzaldehydes ; 2 — *m*-nitrobenzaldehyde ; 3 — *p*-cholrobenzaldehyde.

log k_1 versus log [Ru(III)] are linear with unit slopes, confirming first order dependence on the catalyst, Ru(III) chloride (Table 2).

iv. Effect of [H^+] on the reaction rate

The effect of change of perchloric acid on the catalysed oxidation of different aromatic aldehydes has been studied. It has been observed that the reaction is independent of acid concentration in the range studied i.e. from 0.02 M to 0.2 M (Table 2).

v. Effect of chloride ions on the reaction rate

On addition of [KCl] the rate of reaction increases (Table 3) presumably due to formation of molecular chlorine as per the reaction.

$$H_2OCl^+ + Cl^- \rightleftharpoons Cl_2 + H_2O$$

Table 1

Effect of varying the [Oxidant] and [substrate] on the reaction rate

$[H^+] = 0.02$ M HOAc = 20 % (v/v)
$[Ru(III)] = 1.529 \times 10^{-7}$M Temp. = 35°C.

Substrate	10^4[TCCA]M	10^3[S]M	10^7k_0 mol L^{-1}. s^{-1}	10^5k_1 $(k_0/[S]$ s^{-1}
Benzaldehyde	2.18	10.0	1.20	1.20
	4.31	10.0	1.23	1.23
	9.44	10.0	1.39	1.39
	18.50	10.0	1.40	1.40
	5.00	5.0	0.63	1.20
	5.00	20.0	2.63	1.31
	5.00	40.0	5.37	1.34
m-Nitrobenzaldehyde	2.22	10.0	2.43	2.43
	4.51	10.0	2.10	2.10
	9.72	10.0	2.58	2.58
	18.51	10.1	2.39	2.39
	5.00	5.0	1.20	2.56
	5.00	20.0	5.12	2.56
	5.00	40.0	9.98	2.49
p—Chlorobenzaldehyde	2.33	10.0	0.861	0.861
	4.44	10.0	0.857	0.857
	9.25	10.0	0.855	0.855
	18.75	10.0	0.939	0.939
	5.00	5.0	0.470	0.940
	5.00	20.0	1.860	0.93
	5.00	40.0	4.010	1.00

Table 2

Effect of varying the [Ru(III)] and [H+] on the reaction rate

$[TCCA] = 5.0 \times 10^{-4}$ M, $[S] = 10.0 \times 10^{-3}$ M,
HOAc — 20 % (v/v) Temp. = 35° C

Substrate	10^7[Ru(III)]M	$[H^+]$M	10^7k_0 mole L^{-1}. s^{-1}	10^5k_1 $(k_0/[S])$ s^{-1}
Benzaldehyde	0.76	0.02	0.75	0.75
	1.52	0.02	1.23	1.23
	3.05	0.02	3.09	3.09
	6.11	0.02	5.71	5.71
	1.52	0.04	1.59	1.59
	1.52	0.1	1.50	1.50
	1.52	0.2	1.61	1.60
m-Nitrobenzaldehyde	0.76	0.02	1.32	1.32
	1.52	0.02	2.40	2.40
	3.05	0.02	5.88	5.88
	6.11	0.02	10.41	10.41
	1.52	0.04	2.51	2.51
	1.52	0.1	2.59	2.59
	1.52	0.2	2.69	2.69
p—Chlorobenzaldehyde	0.76	0.02	0.44	0.44
	1.52	0.02	0.85	0.85
	3.05	0.02	1.80	1.80
	6.11	0.02	3.80	3.80
	1.52	0.04	0.89	0.89
	1.52	0.1	0.94	0.94
	1.52	0.2	0.97	0.97

Table 3

Effect of varying [KCl] and % of acetic acid on the reaction rate

[TCCA] = 5.0×10^{-4} M, [S] = 10.0×10^{-3} M, [H$^+$] = 0.02 M
[Ru(III)] = 1.529×10^{-7} M, Temp = 35°C

Substrate	[KCl]M	% HOAc (v/v)	10^7 k_0 mole $L^{-1}s^{-1}$	$10^5 . k_1(k_0/[S])$ s^{-1}
Benzaldehyde	0.005	20	3.69	3.69
	0.01	20	8.81	8.81
	—	30	1.10	1.10
	—	40	0.88	0.88
	—	50	0.57	0.57
m-Nitrobenzaldehyde	0.005	20	5.28	5.28
	0.01	20	11.33	11.33
	—	30	2.31	2.31
	—	40	1.29	1.29
	—	50	0.89	0.89
p-Chlorobenzaldehyde	0.005	20	2.78	2.78
	0.01	20	5.57	5.57
	—	30	0.73	0.73
	—	40	0.62	0.62
	—	50	0.46	0.46

vi. Effect of solvent on the reaction rate

The effect of change in the solvent composition on the reaction kinetics has been studied by varying the amount of acetic acid in the reaction mixture. It has been found that increasing proportions of acetic acid have retarding effect on the reaction rate (Table 3). This is due to the fact that the pre-equilibrium formation of aldehyde hydrate is hindered on decreasing the content of water or increasing the proportion of acetic acid.

vii. Effect of temperature on the reaction rate

In order to investigate the effect of temperature and to evaluate the various Arrhenius activation parameters the reaction has been carried out at 35°C, 40°C, 45°C and 50°C. The plot of log k_0 versus $1/T$ is found to be linear. The rate constants at different temperatures and computed activation parameters have been recorded in Table 4. The plots of $\log_{10}A$ versus $1/\sqrt{E}$ are found to be linear indicating that both the thermodynamic parameters control the reaction. The Lefflers plot of $\Delta H^{\neq}$ versus $-\Delta S^{\neq}$ also shows a fair linearity.

Structure and reactivity

The rate constants for benzaldehyde and substituted benzaldehydes studied under identical conditions are presented in Table 5. The order of reactivity of different substituted aldehydes is :

$p-OCH_3 \rangle\ p-CH_3 \rangle\ p-NO_2 \rangle\ m-NO_2 \rangle$ Benzaldehyde $\rangle\ p-Cl \rangle\ p-$ bromobenzaldehyde

Table 4

Effect of temperature on the reaction rate and various Arrhenius activation parameters

$[TCCA] = 5.0 \times 10^{-4}$ M $[S] = 10.0 \times 10^{-3}$ M, $[H^+] = 0.02$ M,
$[Ru(III)] = 1.529 \times 10^{-7}$ M HOAc = 20% (v/v)

Substrate	$10^5\ k_1(k_0[S])\ s^{-1}$ at			
	35°C	40°C	45°C	50°C
Benzaldehyde	1.23	1.76	2.12	2.64
m-Nitrobenzaldehyde	2.40	3.23	3.88	4.56
p-Chlorobenzaldehyde	0.85	1.32	1.58	1.98
	$\Delta E^{\neq}$ KJ·mole^{-1}	$\Delta H^{\neq}$ KJ·mole^{-1}	$\log_{10}A$ s^{-1}	$-\Delta S^{\neq}$ JK^{-1}· mole^{-1}
Benzaldehyde	39.89	37.33	1.85	218.08
m-Nitrobenzaldehyde	37.23	34.67	1.69	221.16
p-Chlorobenzaldehyde	34.19	31.63	0.73	239.60

Table 5

Rate constants for different substituted benzaldehydes

$[TCCA] = 5.0 \times 10^{-4}$ M. $[S] = 10.0 \times 10^{-1}$ M $[H^+] = 0.02$ M
$[Ru(III)] = 1.529 \times 10^{-7}$ M HOAc = 20% (v/v). Temp. = 35°C

Substrate	$10^5\ k_1(k_0/[S])\ s^{-1}$	σ
Benzaldehyde	1.23	+0.0
m-Nitrobenzaldehyde	2.40	+0.71
p-Chlorobenzaldehyde	0.85	+0.28
p-Nitrobenzaldehyde	2.74	+0.78
p-Methoxybenzaldehyde	11.70	−0.27
p-Methylbenzaldehyde	7.43	−0.17
p-Bromobenzaldehyde	0.70	+0.23

The σ values were taken from H. H. Jaffe, *Chem. Rev.*, **53**, 191 (1953).

ρ,σ Relationship

The plot of $\log k_1$ versus σ values (Fig. 2) is not linear. The shape of the curve is concave indicating that electron releasing groups enhance the reaction rate and electron withdrawing groups retard the rate except for *p*-nitrobenzaldehyde and *m*-nitrobenzaldehyde.This sort of abnormality has been observed by Anantakrishnan et al. [14] in the oxidation of benzaldehydes by Cr (IV). Bakore et al. [15] in the oxidation of substituted benzyl alcohol by V(V) in acid medium and also by Pati and Mahapatro [16] in the catalysed oxidation of benzaldehydes by iodsophenyl acetate in acid medium. The anomalous concave nature of the curve is possibly a pointer to the nature of the mechanistic path involved in these oxidations. It appears that the substrates having electron releasing groups react with rate deter-

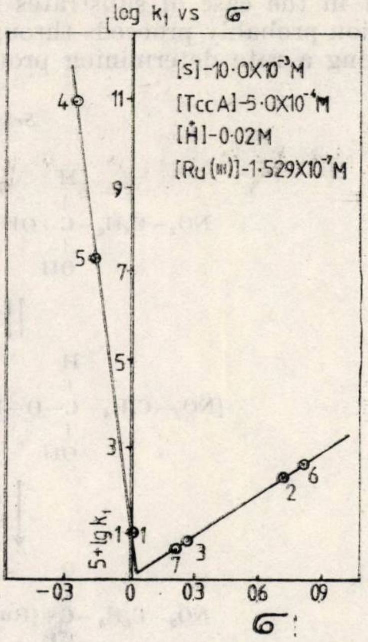

Fig. 2. — Log K_1 vs σ at 35°C HOAc 20% (v/v); 1-benzaldehyde; 2 — *m*-nitrobenzaldehyde; 3 — *p*-chlorobenzaldehyde; 4 — *p*-methoxybenzaldehyde; 5 — *p*-methylbenzaldehyde; 6 — *p*-nitrobenzaldehyde; 7 — *d*-bromobenzaldehyde.

mining step of hybride ion loss which is well supported by high negative value of $\rho = -2.5$ from the ρ, σ plot. In such cases a mechanistic pathway involving an outersphere complex might be operating (Scheme 1).

Scheme 1

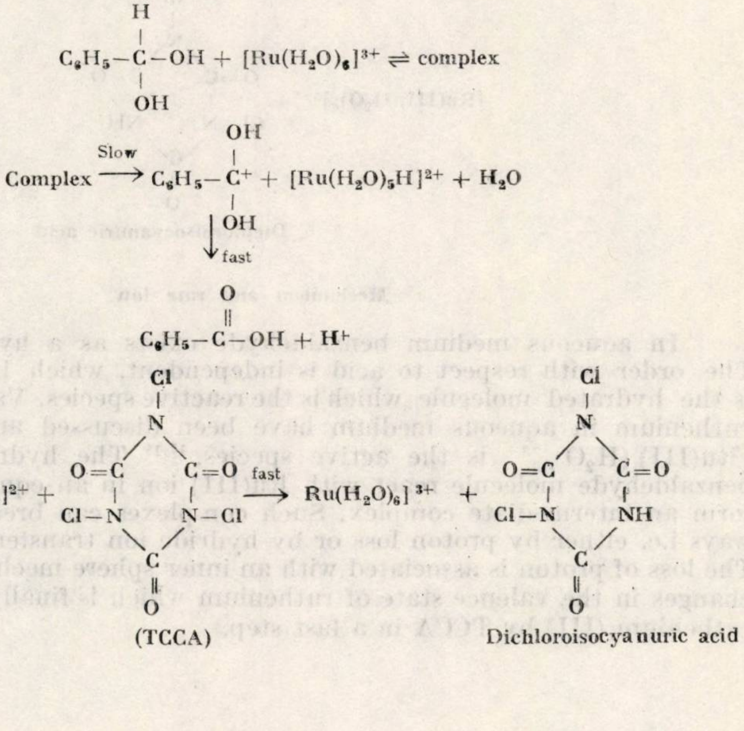

$$C_6H_5-\underset{OH}{\overset{H}{C}}-OH + [Ru(H_2O)_6]^{3+} \rightleftharpoons \text{complex}$$

$$\text{Complex} \xrightarrow{\text{Slow}} C_6H_5-\underset{OH}{\overset{OH}{C^+}} + [Ru(H_2O)_5H]^{2+} + H_2O$$

$$\downarrow \text{fast}$$

$$C_6H_5-\overset{O}{\overset{\|}{C}}-OH + H^+$$

$$[Ru(H_2O)_5H]^{2+} + \text{TCCA} \xrightarrow{\text{fast}} Ru(H_2O)_6]^{3+} + \text{Dichloroisocyanuric acid}$$

But in the case of substrates having electron withdrawing group, the reaction probably proceeds through an inner sphere complex (Scheme 2) involving a rate determining proton loss.

Scheme 2

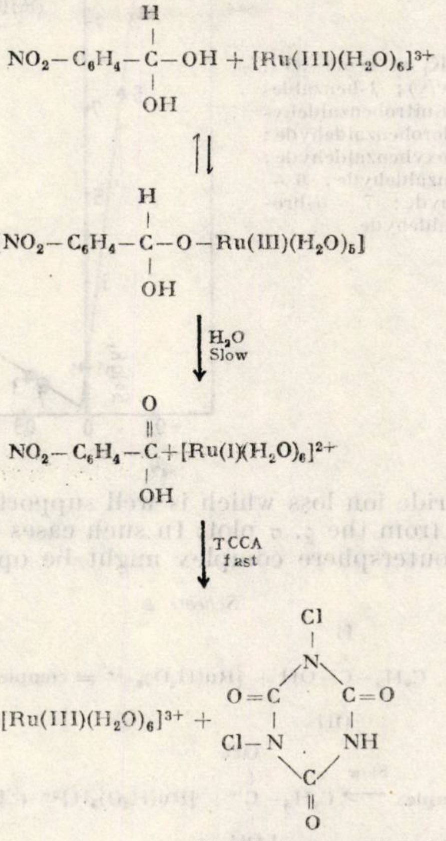

Dichloroisocyanuric acid

Mechanism and rate law

In aqueous medium benzaldehyde exists as a hydrate molecule. The order with respect to acid is independent, which indicates that it is the hydrated molecule which is the reactive species. Various species of ruthenium in aqueous medium have been discussed and out of these $[Ru(III)(H_2O)_6]^{3+}$ is the active species.[17,18] The hydrated species of benzaldehyde molecule react with Ru(III) ion in an equilibrium step to form an intermediate complex. Such complexes can break down in two ways i.e. either by proton loss or by hydride ion transfer in a slow step. The loss of proton is associated with an inner sphere mechanism involving changes in the valence state of ruthenium which is finally reconverted to ruthenium (III) by TCCA in a fast step.

In the outer sphere mechanism as suggested for electron releasing group substrates, the reaction proceeds with a rate limiting hybride ion loss without changes in valence of Ru(III) species and the resulting hydride complex breaks down in a fast step reaction with TCCA. Then in both pathways zero order dependence on [TCCA] is observed.

The detailed mechanism can be envisaged as follows:

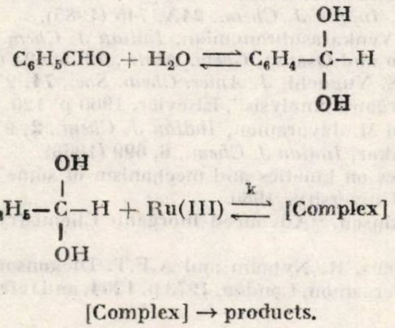

$$C_6H_5CHO + H_2O \rightleftharpoons C_6H_4-\underset{OH}{\overset{OH}{C}}-H$$

$$C_6H_5-\underset{OH}{\overset{OH}{C}}-H + Ru(III) \overset{k}{\rightleftharpoons} [Complex]$$

$$[Complex] \rightarrow products.$$

The rate of oxidation of the aromatic aldehyde would be the rate of disproportionation of the complex.

$$\frac{-d[\text{complex}]}{dt} = -\frac{d[\text{TCCA}]}{dt} = k[\text{Complex}]$$

The total ruthenium at any time would be

$$[\text{Ru(III)}]_T = [\text{Ru(III)}] + \text{complex} = [\text{Ru(III)}] + k[\text{Ru(III)}]\,[S]$$

$$[\text{Ru(III)}]_T = [\text{Ru(III)}]\,(1 + k[S])$$

$$\text{Ru(III)} = \frac{[\text{Ru(III)}]_T}{1 + k[S]}$$

$$\text{Now complex} = k[\text{Ru(III)}]\,[s]$$

Hence the rate of decomposition of TCCA would be:

$$-\frac{d[\text{TCCA}]}{dt} = k[\text{Complex}] = k[\text{Ru(III)}]\,[S]$$

The above rate law explains all the observed facts.

Acknowledgements. Our thanks are due to Prof. P.S.R. Murti for his keen interest throughout the work. One of us (A.K.S.) thanks the UG.C., New Delhi for a fellowship.

REFERENCES

[1] G. P. Panigrahi and P. K. Misra, *Indian J. Chem*, **16A**, 201 (1977).
[2] P. S. Radhakrishnamurti and B. Sahu, *Indian J. Chem.*, **15A**, 785 (1977).
[3] P. S. Radhakrishnamurti and B. Sahu, *Indian J. Chem*,. **17A**, 63 (1978).
[4] P. S. Radhakrishnamurti and B.R.K. Swamy, *Proc. Ind. Acad. Sci.*, **88a**. 163 (1979).
[5] B.R.K. Swamy "Oxidation Mechanisms", Ph. D. Thesis, Berhampur University (1979).
[6] P. S. Radhakrishnamurti and P. C. Misra, *Indian J. Chem.*, **18A**. 126 (1979).
[7] P. S. Radhakrishnamurti and P. C. Misra, *Indian J. Chem.*, **19A**, 427 (1980).
[8] P. S. Radhakrishnamurti and N. K. Rath, *Indian J. Chem.*, **24A**, 300 (1985).
[9] S. C. Pati and C. Sarangi, *Indian J. Chem.*, **24A**, 745 (1985).
[10] K. S. Vasudevan and N. Venkatasubramanian, *Indian J. Chem.*, **24A**, 304 (1985).
[11] Horiuchi, Yoshizo, Ichijyo and Osamu, *Chem. Abstr.*, **72**, 50624 (1970).
[12] Y. Ogata, A. Fukui and S. Yuguchi, *J. Amer. Chem. Soc.*, **74**, 2707 (1952).
[13] F. Feigl, "Spot Test in Organic Analysis", Elsevier, 1960 p. 120.
[14] S. V. Anantakrishnan and M. Jayaraman, *Indian J. Chem.*, **2**, 91 (1964).
[15] G. V. Bokare and R. Shankar, *Indian J. Chem.*, **6**, 699 (1968).
[16] R. C. Mahapatro, "Studies on kinetics and mechanism of some oxidation reactions", Ph. D. Thesis, Berhampur University, 1980.
[17] F. A. Cotton and G. Wilkinson, "Advanced Inorganic Chemistry", Willy Eastern, New Delhi, 1972 p. 999.
[18] J. C. Bailar, H. J. Emeleus, R. Nyholm and A.F.T. Dickonson, "Comprehensive Inorganic Chemistry", Vol. 3, Pergamon, London, 1973 p. 1204, and references cited therein.

Revue Roumaine de Chimie, 33, 2, 167–169 (1988)

PHOTOCHEMICAL BROMINATION OF ANILIDES BY BENZENEHEXABROMIDE

M. M. ALY, I. M. A. AWAD and A. M. FAHMY
Chemistry Department, Faculty of Science, Assiut University, Assiut Egypt A.R.E.

Received June 9, 1986

Benzenehexabromide was found to afford photochemical bromination of substituted acetanilide in the *p*-position. The rates of bromination were found to follow the order predicted on the basis of inductive effect of the substituents similarly to the sequence of reactivities observed for bromination of acetanilides with N-bromosuccinimide. Similar results were also obtained in the case of *p*-substituted benzanilides and the reaction shows a good Hammett correlation with the σ^+-values for the substituents with a ρ value -0.266.

1,2,3,4,5,6-Hexabromocyclohexane, commonly known as benzenhexabromide (BHB), the gamexane analogue has recently been used as a brominating agent for arenes [1] as compared with the classical brominating agent N-bromosuccinimide (NBS).[2]

In a recent work [3] it has been found that BHB can afford photochemical side-chain bromination for various *p*-substituted toluene derivatives. The relative reactivity sequence was found to follow the order of increasing inductive effect of the *p*-substituent with a Hammett reaction constant ρ-132 ($\pm$ 0.05) which agrees well with the value obtained for side-chain bromination affected by a slow stream of molecular bromine or NBS. Hence, it was concluded that bromination by BHB involves its photodegradation in the presence of any brominatable substrate furnishing bromine in a low concentration that affects side-chain bromination.

The present work is a study of nuclear photobromination of substituted anilides with BHB in dioxane solution at constant temperature (25°C) in the absence of any promotor. Solutions of BHB in dioxane were found to be photostable under the present experimental conditions.

The bromination was found to obey first order rate kinetics as concerning BHB as shown by the linearity of the plots of $\log(a-x)$ against (t), where $(a-x)$ is the change in concentration of BHB as estimated in terms of volume of standard silver nitrate solution in time (t) minutes.

The rates of *p*-bromination of different anilides Ph.NH.CO.R ($R = CH_3$, C_2H_5, n-C_3H_7, iC_3H_7 CH_2Cl, $CHCl_2$ CCl_3) were found to increase progressively by increasing + I effect of the substituents in the acyl moiety of the anilide in the order; acetanilide < propionanilide < n-butyranilide < < iso-butyranilide. Similarly, the rate decreases by increasing − I effect of the substituents in the acyl group of the anilide in the following order; acetanilide >α-chloroacetanilide> α,α-dichloracetoanilide> α,α,α,-trichloroacetanilide (Table 1).

Table 1

Bromination of acetanilides by BHB

Ph–NH–CO–R	m.p. °C	P. Bromoanilide m.p. °C	P. Bromoanilide $k \times 10^2$ (min^{-1})
a. R = CH_3	114	166	3.42
b. = C_2H_5	105	148	4.20
c. = n-C_3H_7	96	111	5.85
d. = i-C_3H_7	105	158	17.25
e. = CH_2Cl	137	180	1.62
f. = $CHCl_2$	119	147	0.35
g. = CCl_3	95	124	0.18

On the other hand, the rate of bromination for *p*-substituted benzanilides (Ph.NH–CO–$C_6H_4R(p)$) was greatly affected by the nature of R. Thus the rate has been found to vary with R in the order; $OCH_3 >$ $>$ Cl $>$ Br $>$H $>NO_2$ (Table 2). These substituent effects can generally be correlated in the usual way with the Hammett α-values. However, the best fit in all cases is obtained when σ^+-values according to Brown and Okamoto [4] were used.

Table 2

Bromination of *p*-substituted benzanilides by BHB

Ph–NH–CO–Ar	m.P. °C	k×10^2 (min.$^{-1}$)
a. Ar = C_6H_5	161–2	3.99
b. = $C_6H_4-OCH_3p$	172	5.07
c. = C_6H_4-Clp	198	3.80
d. = C_6H_4-Brp	150	3.02
e. = $C_6H_4-NO_2p$	195	3.02

The Hammett reaction constant obtained (ρ-0.266) being of negative sign implies that the reaction is favoured by high electron density at the reaction site. The observed order presumably is a reflection of the relative capacities of the substituents to release electrons to the reaction centers by a combination of inductive and resonance effects.

The fact that the rates of such radical bromination are subject to inductive and resonance influences of polar substituents which can interact electronically with the reaction center can be explained on the assumption that polar structures contribute to stabilization of the transition state. [5]

Since the relative reactivity sequences observed in BHB and NBS [6] brominations are fairly unique, this adds further support to the conclusion observed by the author [3] that both processes take place through the bromine supplied at low concentration.

EXPERIMENTAL

Melting points were obtained on a-hot-stage apparatus calibrated with known samples. All m.p.s. are uncorrected. Solvents used are analaR reagents and used without further purification. Photolyses were performed using a Hannovia 210-w low pressure mercury vapour lamp in open topped pyrex beackers.

Preparation of 1,2,3,4,5,6-hexabromocyclohexane (BHB)[7]

It was prepared from irradiation of a benzene solution of bromine (5%) by sunlight for 6 days. The solid BHB formed was filtered off and crystallized from dry xylene, m.p. 215°C. Purity of BHB was checked by thin layer chromatography (T.L.C.)

Preparation of anilides

Anilides were prepared according to literature [8] from aniline (0.1M) and the corresponding acid chloride (0.12M) with cooling. The product was washed with water and crystallized from dilute ethanol. Melting points are recorded in Tables 1 and 2.

Rate measurements

All rate measurements were carried out by mixing a solution of anilide (0.005 mol.) in dioxane (40 mL) thermostated at 25°C (± 0.05) and BHB (0.0025 mol. ; 1.4 g) was added at once with continuous stirring under incident u.v. light. The progress of the reaction was followed by withdrawing 5 mL portions of the reaction mixture at different time intervals and the amount of BHB was estimated.

The main difficulty is that BHB cannot be estimated by direct iodometry as in the case of NBS. Such difficulty was overcome by the observation that BHB can be decomposed easily in the presence of triethylamine yielding the corresponding amine hydrobromide [9] that can be easily estimated by argentimetric method.

To the 5 mL portions of the reaction mixture was added 0.2 mL trimethylamine to decompose BHB and the resulting hydrobromide was titrated with standard (0.01 N) silver nitrate solution using potassium dichromate as indicator. The volume of silver nitrate solution was taken as a measure for the amount of BHB present at any time.

Control experiment was done and corrections for the observed results were taken into consideration. At the end of the reaction (usually after 25 min.) the reaction product was poured into water, filtered, crystallized from ethanol and tested for the bromoanilides formed by t.l.c, m.p. and m.m.p. determinations as compared with authentic samples.

REFERENCES

[1] R. Bolton, M. I. Bhangar and G. H. Williams, *J. Chem. Soc. Perkin I*, **1984**, 893.

[2] N. K. Mathur and C. K. Narang, "The Determination of Organic Compounds with NBS and Allied Reagents", Academic Press, London, 1975, p. 22.

[3] M. M. Aly, R. Bolton and G. H. Williams, *J. Chem. Res.* **(S)**, **1983**, 24.

[4] H. C. Brown and Y. Okamoto, *J. Amer. Chem. Soc.*, **79**, 1913 (1947); and **80**, 4979 (1958).

[5] R. E. Lovins, L. J. Andrews and R. M. Keefer, *J. Org. Chem.*, **29**, 1616 (1964).

[6] N. Z. A. Badr, M. M. Aly, M. Fahmy, 5th IUPAC Conference on Physical Organic Chemistry, Univ. of California, Santa Cruz, U.S.A. August, 17 — 22 (1980) p. 155. Bull. Fac. Sci. Assiut University **10** 17, (1981).

[7] F. E. Matthews, *J. Chem. Soc.*, **73**, 243 (1898).

[8] A. I. Vogel, "Practical Organic Chemistry", Longmans, London, 1971, p. 362.

[9] In a similar manner to that described for NBS. in E. A. Braude and E. S. Waight, *Nature*, **164**, 241 (1949); E. A. Braude and E. S. Waight, *J. Chem. Soc.*, **1952**. 1116; M. M. Aly, A. M. Fahmy, S. A. Mahgoub and M. Z. A. Badr, unpublished results).

Revue Roumaine de Chimie, **33**, *2*, 171–176 (1988)

ESTUDIO CINETICO DE LA OXIDACION CROMICA DE DISACARIDOS EN MEDIO DE ACIDO PERCLORICO

M. P. ALVAREZ MACHO

Departamento de Química Física, Facultad de Ciencias, Universidad de Valladolid, 47005 Valladolid, España

Recibido el 23 de Mayo de 1986

Se ha realizado un estudio cinético de las reacciones de oxidación de sacarosa y de lactosa por ácido crómico en medio de ácido perclórico. Las reacciones han sido estudiadas espectrofotométricamente en un amplio rango de condiciones experimentales. Por último, se han determinado los parámetros de activación y se ha propuesto un mecanismo de reacción.

Kinetic data for the oxidation of saccharose and lactose by chromic acid are reported. The reactions have been studied spectrophotometrically over a wide range of experimental conditions. The activation parameters have been calculated and mechanism is suggested.

INTRODUCCIÓN

Los disacáridos son carbohidratos que derivan formalmente de la deshidración intramolecular entre dos molécules de monosacáridos. La unión entre ellos no es una unión etérea, sino glicosída, es decir, se establece entre el OH anomérico de un monosacárido y cualquiera de los otros OH del otro azúcar. Por ejemplo, en la sacarosa los carbonos C_1 de la glucosa y C_2 de la fructosa están implicados en la unión glicosídica (aquí se ha producido entre los OH de los carbonos anoméricos); así como, en la lactosa los carbonos implicados son el C_4 de la glucosa con el C_1 de la galactosa (en este caso el OH del carbono anomérico de la glucosa queda libre).

En la presente investigación se ha realizado el estudio cinético de las reacciones de oxidación de sacarosa y de lactosa por cromo (VI) en medio de ácido perclórico, habiéndose encontrado un orden cinético uno respecto del oxidante y del disacárido. También, se estudió la dependencia de la velocidad de reacción con la acidez del medio, observándose una relación análoga a la indicada en un trabajo precedente [1] en la oxidación crómica de hexosas, siendo las condiciones de realización de los experimentos semejantes. Esto nos ha permitido sugerir un mecanismo de oxidación de estos disacáridos muy parecido al propuesto en la oxidación de monosacáridos.

PARTE EXPERIMENTAL

Los reactivos utilizados han sido sacarosa y lactosa, Merck; y ácido perclórico, Panreac y se empleó agua bidestilada para la preparación de las disoluciones.

En todos los experimentos cinéticos la mezcla de reacción ha sido obtenida como se indica : se preparaba una disolución de dicromato potásico en disolución acuosa de ácido perclórico y se añadía un volumen adecuado de disolición de hidrato de carbono en agua, de tal forma que al final la mezcla reaccionante fuese de las concentraciones adecuadas. Además, se ha tenido la precaución de utilizar disoluciones recién preparadas para evitar en la posible los procesos de hidrólisis de los disacáridos.[2]

La cinética ha sido seguida espectrofotométricamente a 350 nm. mediante un método dinámico, con un espectrofotómetro Perkin Elmer modelo Coleman 55, y la constancia de la temperatura se consiguió con un termostáto Heto que la garantiza con un error de ± 0,05°C.

RESULTADOS CINÉTICOS

Los órdenes cinéticos de reacción se determinaron trabajando en exceso de cabohidrato y ácido perclórico, pues así estos pueden considerarse constantes en cada experimento. La existencia de correlaciones lineales entre los logaritmos de la absorbancia y el tiempo indican un orden uno respecto del Cr(VI). A partir de las pendientes de estas rectas se obtuvieron las Pseudoconstantes de la velocidad de primer orden, $k_{exp.}$, y repitiendo el proceso a diversas concentraciones de disacáridos manteniendo constantes las concentraciones de dicromato y ácido perclórico, se observó que ésta aumentaba a medida que la hacia la concentración de sacarosa tal como muestra la figura 1; un comportamiento semejante se encontró para la lactosa (figura 2). Esto mismo se realizó a distintas concentraciones de ácido perclórico, observándose que las correlaciones lineales encontradas al representar k_{exp} frente a concentración de disacárido pasaban prácticamente por el origen de coordenadas en todas las acideces del medio, por tanto, el orden cinético respecto de la sacarosa o de la lactosa es también uno.

En el estudio de la variación de la constante de velocidad de segundo orden ($k = k_{exp}/[\text{disacarido}]$), con la acidez del medio, se pretendió aplicar la hipótesis alternativa de Zucker-Hammett, [3] los criterios de Bunnett [4] y Bunnett-Olsen [5] no encontrándose resultados satisfactorios para ambos hidratos de carbono. Sin embargo, la dependencia entre k y h_0 (función de acidez de Hammett) es lineal, de pendiente positiva y ordenada negativa, cuyo ajuste por mínimos cuadrados ha permitido deducir las siguientes ecuaciones :

$$\text{Sacarosa } k = -4{,}47 \cdot 10^{-3} + 5{,}79 \cdot 10^{-3}\, h_0 \qquad (r_{xy} = 0{,}9997)$$

$$\text{Lactosa } k = -4{,}58 \cdot 10^{-3} + 6{,}52 \cdot 10^{-3}\, h_0 \qquad (r_{xy} = 0{,}9993)$$

válidas en el intervalo de acidez ($0{,}98 \leqslant h_0 \leqslant 20{,}98$) empleado a 25°C El valor negativo de la ordenada, nos hace suponer que, existe una acidez umbral, por encima de la cual la velocidad de oxidación crómica de los discáridos estudiados es distinta de cero. La magnitud de esta acidez umbral esta por debajo de las concentraciones de ácido perclórico usadas en la presente investigación.

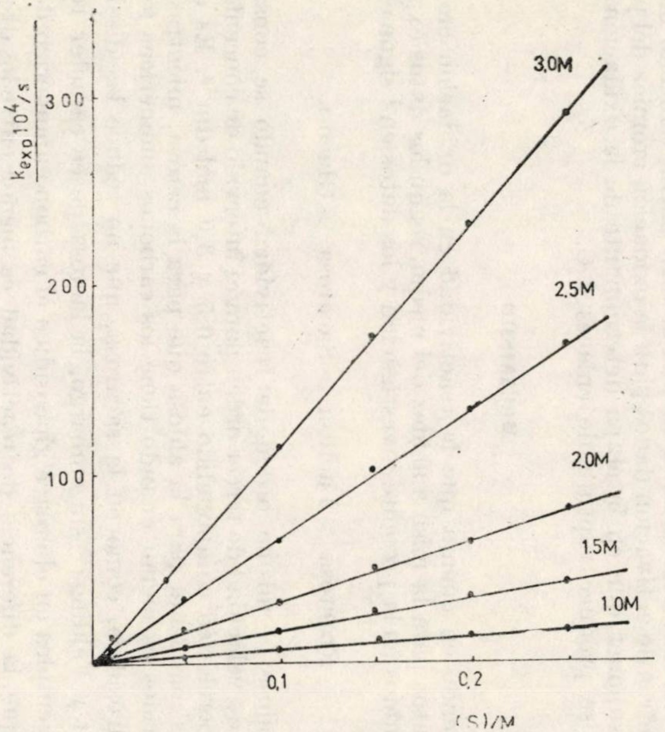

Fig. 1. — Dependencia de la constante experimental de velocidad con la concentración de sacarosa : $[K_2Cr_2O_7] = 3.10^{-4}$ mol dm^{-3}, $T = 25$ °C y a distintas concentrationes de ácido perclórico.

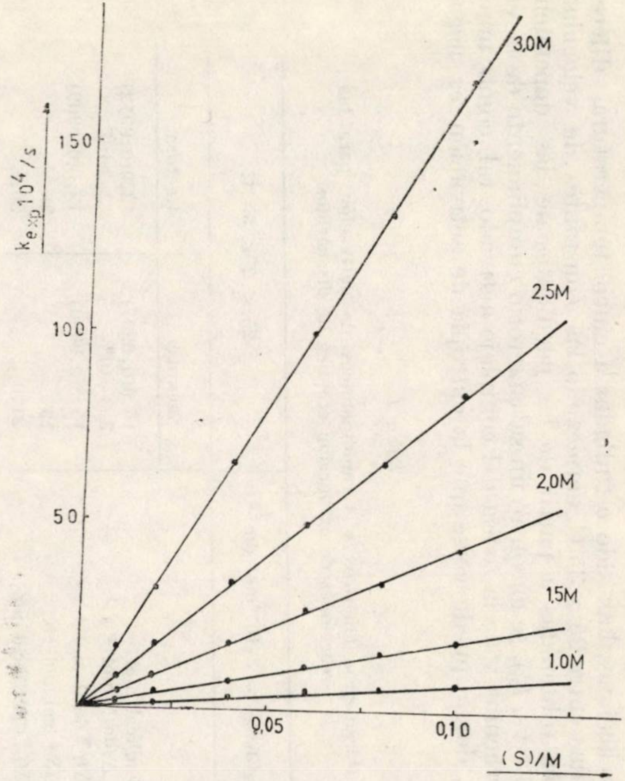

Fig. 2. — Dependencia de la constante experimental de velocidad con la concentración de lactosa : $[K_2Cr_2O_7] = 3.10^{-4}$ mol dm^{-3}, $T = 25$ °C y a distintas concentrationes de ácido perclórico.

Las reacciones han sido estudiadas a cinco temperaturas diferentes comprendidas entre 25 y 35°C, empleando las constantes de velocidad de tercer orden (obtenidas a partir de las pendientes de las dependencias lineales de k vs. h_0), se encontró un satisfactorio cumplimiento de la ecuación de Arrhenius y de la teoría del complejo activado, tal como muestra la tabla 1, donde puede verse que la entropia de activación es negativa para ambos disacáridos, de donde podemos deducir un cierto ordenamiento. Además, se observó que la energía de activación y la entropia de activación es mayor para la oxidación de la sacarosa que de la lactosa; así como, la energía libre de activación a 30°C. Por otra parte, teniendo en cuenta los parámetros de activación dados para la oxidación crómica del pinacol, [6] podemos suponer que en la etapa determinante de la oxidación de azúcares no se produce ruptura de enlaces C/C.

Tabla 1

Parámetros cinéticos y termodinámicos de activación para las reacciones de oxidacción crómica de disacáridos

$[K_2Cr_2O_7] = 3\cdot 10^{-4}$mol dm^{-3}	$25 \leqslant T \leqslant 35$ °C	
	Sacarosa	Lactosa
Ea/kcal mol^{-1}	15,9(0,9997)	12,9(0,9912)
A/dm^6 mol^{-2} s^{-1}	$2,8 \cdot 10^9$	$2,3.10^7$
$\Delta H^{\ddagger}$/kcal mol^{-1}	15,3(0,9990)	12,3(0,9909)
$\Delta S^{\ddagger}$/cal mol^{-1}K^{-1}	-19	-28
$\Delta G^{\ddagger}$(30°C)kcal mol^{-1}	21,0	20,8

MECANISMO

Teniendo en cuenta que la reactividad en la oxidación crómica de carbohidratos para la misma acidez del medio, según los datos experimentales obtenidos en la presente investigación y los datos en [1] sigue el orden :

$$\text{Fructosa} > \text{Lactosa} > \text{Sacarosa} > \text{Glucosa}$$

manteniéndose el mismo orden de reactividad cuando se considera la constante de velocidad de tercer orden para el intervalo de concentraciones de ácido perclórico comprendido entre 0,5 y 3,0 mol dm^{-3}. Es decir, la reacción es más lenta para la aldosa que para la cetosa, mientras que en los disacáridos es menor cuando tiene los carbonos anoméricos formando enlace glucosídico, como en la sacarosa, que no reduce las disoluciones de Benedit y Fehling; [7] sin embargo, la lactosa posee caracter reductor, ya que no emplea en el enlace glucosídico el carbono anomérico de la glucosa. Aunque, la diferencia de reactividad es menor entre los disacáridos estudiados que entre los monosacáridos, parece que el ataque de las especies oxidantes se realiza preferentemente sobre los grupos OH que se encuentran en los carbonos anoméricos.

Debido a que este trabajo se ha realizado en medio de ácido perclórico, se considera la existencia del equilibrio :

$$HCrO_4^- + H^+ + HClO_4 \rightleftharpoons HCrO_3ClO_4 + H_2O$$

estando las especias de Cr(VI) en medio de ácido perclórico como $HCrO_4^-$ y $HCrO_3ClO_4$ que representaremos por $HCrO_3A$. [8]

Un mecanismo que interpreta satisfactoriamente los resultados experimentales, puede expresarse como :

$$HCrO_3A + \text{disacárido} \overset{k_1}{\rightleftharpoons} X \quad (1)$$

$$X + H^+ \underset{k_{-2}}{\overset{k_2}{\rightleftharpoons}} (XH)^+ \quad (2)$$

$$(XH)^+ \xrightarrow{k_3} \text{Productos} \quad (3)$$

El equilibrio propuesto corresponde a la formación de un ester crómico, X, entre el disacárido y la especie crómica presente en el medio seguida de una etapa cinética reversible correspondiente a la formación del ester protonado, $(XH)^+$, siendo la etapa determinante de velocidad del proceso la descomposición del ester protonado. Existen referencias bibliográficas [9] de formación de un complejo semejante entre las aldosas y el Cr (VI) (formado por el grupo alcoholico del carbono anomérico y la especie oxidante Cr(VI) presente en el medio.

De acuerdo con este mecanismo, la velocidad de desaparición del Cr(VI) puede expresarse como

$$v = k_3[(XH)^+] \quad (4)$$

las concentraciones de los compuestos intermedios pueden obtenerse a partir de la aproximación del estado estacionario, expresando la concentración de protones en la escala de acidez de Hammett, h_0, y teniendo en cuenta que se ha trabajado en exceso de disacárido, la concentración del mismo se mantiene practicamente constante, con lo que se llega a la siguiente ecuación de velocidad de reacción

$$v = \frac{k_3 k_2 k_1}{k_{-2} + k_3} h_0 \ [\text{disacárido}]\,[\text{Cr(VI)}] \quad (5)$$

donde $k_3k_2k_1/(k_{-2} + k_3)$ se identifica con las constantes de valocidad de tercer orden obtenida a partir de la repesentación de k vs. h_0. Esta ecuación interpreta los ordenes cinéticos encontrados respecto de las especies oxidante y reductora; así como, la influencia de la acidez del medio sobre la velocidad de oxidación crómica de hidratos de carbono.

AGRADECIMIENTO. Quiero agradecer al Prof. Dr. L. Ferrari Alonso el asesoramiento recibido durante el transcurso de este trabajo.

BIBLIOGRAFÍA

[1] M. P. Alvarez Macho, enviado a *An. Quim.*
[2] F. A. Long y M. Paul, *Chem. Rev.*, **57**, 938 (1957).
[3] L. Zucker y L. P. Hammett, *J. Amer. Chem. Soc.*, **61**, 2791 (1939).
[4] J. F. Bunnett, *J. Amer. Chem. Soc.*, **83**, 4986 (1961).
[5] J. F. Bunnett y F. P. Olsen, *Canad. J. Chem.*, **44**, 1899 y 1917 (1966).
[6] M. P. Alvarez Macho, Enviado a *An. Quim.*
[7] L. O. Smith y S. J. Cristol, "Quimica Orgánica", Reverté, Barcelona (1970), pag. 217.
[8] D. G. Lee y R. Stewart, *J. Amer. Chem. Soc.*, **86**, 3051 (1964).
[9] K. K. Sen Gupta, S. Sen Gupta y S. N. Basu, *Carbohydr. Res.*, **71**, 75 (1979).

Revue Roumaine de Chimie, 33, 2, 177–181 (1988)

PHOTOIRRADIATION OF 1-PHENYLCYCLOPENTADECENE-1

KERIMAN GÜNAYDIN* and TURAN ÖZTÜRK

Istanbul Technical University, Faculty of Science,
Department of Chemistry, Istanbul, Turkey

Received November 16, 1986

UV Photoirradiation of the title compound in hexane causes isomerization *trans→cis*. In methanol, 3-hydroxymethyl-1-phenylcyclopentadecene-1 is obtained on irradiation.

INTRODUCTION

Photochemical behaviors of phenylcycloalkenes which have medium ring size (n : 5, . . ., 10), have been investigated. In 1969, Paul J. Kropp stated that a dimeric or polymeric (white, solid) product was obtained with rapid loss of starting material during its photolysis in methanol.[1] Later, in 1971, a mixture of phenylcyclohexane, 1-methoxy-1-phenylcyclohexane, 1-hydroxymethyl-1-phenylcyclohexane and dimer was obtained by Herbert M. Rosenberg and M. Paul Serve as products of the photolysis of 1-phenylcyclohexene in methanol.[2]

In this study, photolysis of 1-phenylcyclopentadecene-1 containing macrochain ring size has been investigated in polar and nonpolar solvents. In a previous study, isomerisation of 1-phenylcyclododecene-1 was stated during its photolysis in methanol.[3] 1-Phenylcyclopentadecene-1 was synthesised by dehydration of 1-phenylcyclopentadecanol (that was synthesised according to Grignard method) in toluene with H_3PO_4 as a catalyst.

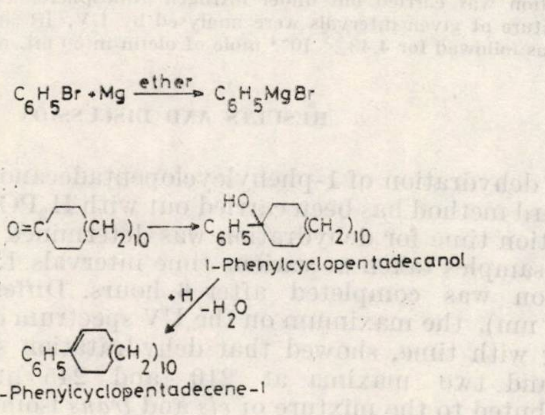
$C_6H_5Br + Mg \xrightarrow{ether} C_6H_5MgBr$
C_6H_5MBr
$(CH_2)_{10}$
HO
C_6H_5
$(CH_2)_{10}$
1-Phenylcyclopentadecanol
$+H^+$
$-H_2O$
C_6H_5
$(CH_2)_{10}$
1-Phenylcyclopentadecene-1

EXPERIMENTAL SECTION

a. Spectroscopic and Gas Chromatographic Studies

IR spectra were determined on a Schimadzu IR-400 model spectrophotometer and ^{1}H$-$NMR spectra were determined on a Varian T$-$60 instrument using TMS as an internal standard. UV spectra were obtained with a Beckman spectrophotometer. Gas chromatographic analyses were performed on a Schimadzu model GG$-$5A instrument equipped with a flame ionization detector and $1/8 \times 12$ ft stainless steel columns packed with Silicone OV-17 3%. The chromatograph was operated at a column temperature of 260°C, the injector and detector temperatures of 300°C and nitrogen carrier gas flow rate of 100 mL/min.

b. Preparation of 1-Phenylcyclopentadecanol

2.4 g (0.1 mole) of magnesium turnings, 10 mL of absolute ether and a small portion of iodine were placed into a dry 250 mL three-necked flask equipped with an addition funnel, magnetic stirrer and condenser with a calcium chloride drying tube. 5.25 mL of bromobenzene in 40 mL of absolute ether were added dropwise under stirring to magnesium turnings. Stirring was continued until almost all Mg was consumed. To the Grignard reagent, 5 g of cyclopentadecanone in 40 mL of anhydrous ether were added with constant agitation. The mixture was left overnight under stirring at room temperature and then 10 mL of 10 % HCl were added. The contents were transferred to a separatory funnel and extracted with ether, then dried over anhydrous Na_2SO_4 and the ether was evaporated. The residue was crystallised from heptane. Yield 85 %; mp. 63$-$64°C ;^{1}H$-$NMR spectrum (δ, ppm) 1.75 (CH_2, 4H), 1.65 (OH, 1H), 1.57 (CH_2, 24H), 7.2 (C_6H_5, 5H); IR spectrum 3300, 3400, 1440, 1480, 2850, 2950, 1600 cm^{-1}; λ_{max} 215 nm.

c. 1-Phenylcyclopentadecene-1

0.25 g of phenylcyclopentadecanol, 0.3 mL H_3PO_4 and 45 mL of toluene were refluxed for 1, 2, 3, 4, 5, 6 and 16 hours. The organic phase was extracted with toluene and washed successively with water, 5 % of aqueous sodium bicarbonate and water, and then dried over anhydrous sodium sulfate. After filtration and concentration the olefin was obtained. ^{1}H$-$NMR spectrum (δ, ppm) 7.2 (C_6H_5, 5H), 5.4 (C=CH, 1H), 1.8$-$2.4 (CH_2, 4H). 1.2(CH_2, 22H); IR spectrum 33000, 3100, 1640, 2850, 2950, 1600, 1590, 1440, 1490, 1335, 1280, 1080, 1020, 830, 697 cm^{-2}; λ_{max} 210, 245 nm.

d. Irradiations

A solution of 1.0×10^{-4} mole 1-phenylcyclopentadecene-1 in 75 mL of cyclohexane was placed in a double-wall water cooled immersion-well photochemical reactor. UV irradiation was applied by using a filtered (borosilicate tube) 16 W medium pressure immersion mercury lamp with peak emission at 254 nm. The apparatus was wrapped with aluminum foil. Irradiation was carried out under nitrogen atmosphere. The samples taken from the reaction mixture at given intervals were analysed by UV, IR and GLC methods. The same procedure was followed for 4.43×10^{-4} mole of olefin in 50 mL of methanol.

RESULTS AND DISCUSSION

The dehydration of 1-phenylcyclopentadecanol that was synthesised by Grignard method has been carried out with H_3PO_4 in toluene. The necessary reaction time for dehydration was determined by IR and UV analysis of the samples taken at various time intervals. IR spectra showed that dehydration was completed after 6 hours. Different from the alcohol (λ_{max} 215 nm), the maximum on the UV spectrum of the olefin at 245 nm increasing with time, showed that dehydratation started after one hour (fig. 1) and two maxima at 210 and 245 nm after dehydration were attributed to the mixture of *cis* and *trans* isomers respectively.

The amounts of the isomers were determined according to GLC and UV analysis of the samples taken in various time intervals during photolysis in cyclohexane. It was showns in Table 1 that before photolysis the ratio was determined as 20.24/79.76 and two maxima were seen on the UV spectrum (fig. 1). But after 6 hours of the photolysis, the ratio was changed as 98.79/1.21 and the maximum at 245 nm on the UV spectrum almost disappeared (Fig. 2). The transformation of the *trans* isomer into the *cis* isomer was also observed on the GLC (Table 1).

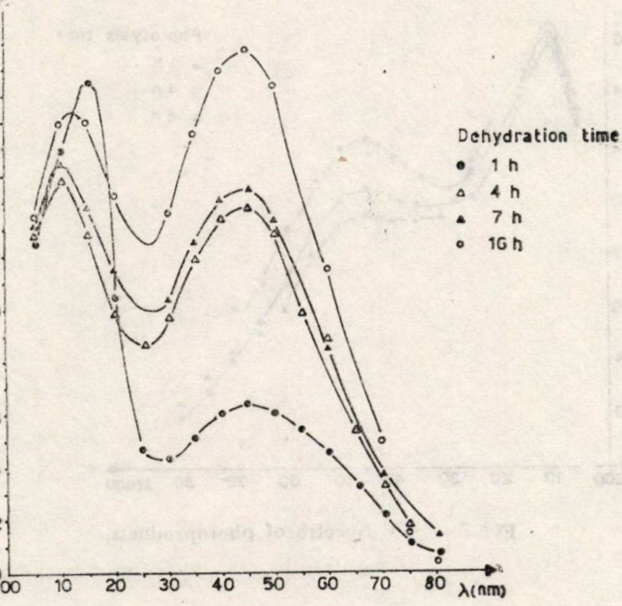

Fig. 1. — UV Spectra of dehydration products.

Table 1

Irradiation of 1-phenylcyclopentadecene-1 in cyclohexane

Photolysis time (hours)	R.T. : 2.21 min %*cis*, 210 nm	R.T. : 2.98 min %*trans*, 245 nm	Φi
0	20.24	79.76	
1/2	47.75	52.25	1.26
1	69.36	30.64	1.048
1.5	84.87	15.13	0.85
2	87.20	12.80	0.68
4	94.45	5.55	0.35
6	98.79	1.21	0.24

As shown in fig. 3, by increasing the irradiation time, *trans* isomer has been transformed into the *cis* isomer until an equilibrium is reached, and only small changes took place after 1.5 h of irradiation when the equilibrium state of the mixture may be reached. Furthermore during 90 minutes, *trans* isomers transformed to *cis* isomers.

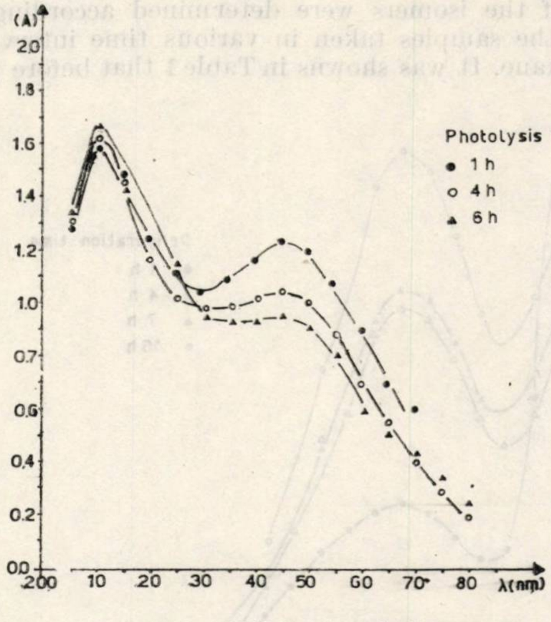

Fig. 2. — UV Spectra of photoproducts.

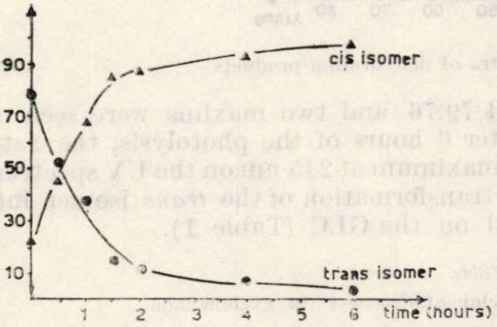

Fig. 3. — Rate of transformation of *trans* isomer to *cis* isomer.

The quantum yield for disappearance of *trans* isomer at the equilibrium state was found to be 0.85, which indicates high efficiency of photoisomerisation.

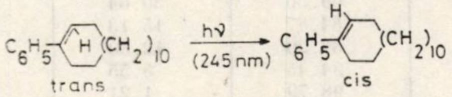

The IR values at 1640, 880 cm^{-1} and 1720, 1200, 900 cm^{-1} were attributed to specific *cis* and *trans* absorption bands respectively. In Table 1, the percentage of *cis* and *trans* isomers during various photolysis time intervals and the quantum yields have been given.

Different from nonpolar solvent cyclohexane, methanol has been used as a polar solvent for the photolysis of the olefin. In polar solvent absorption values of the isomers were changed as 210 and 235 nm because of the solvent effect. Similar to photolysis in cyclohexane, absorption of *trans* isomer at 235 nm disappeared after 6 h of irradiation, but contrary to it a white solid precipitated rapidly. Its UV spectrum showed only one absorption maximum at 210 nm and the melting point has been determined as 120°C. According to GLC analysis, it has 100% purity. IR spectrum showed specific absorption bands at 1680–1710 and 3400 cm^{-1}. ^{1}H-NMR spectrum has vinylic, 1H at 5.4 ppm; multiplet, 5H at 7.0–7.2 ppm; OH, 1H at 2.6 ppm; CH_2—OH, 2H at 2.8 ppm; singlet, 3H at 2.0 ppm; singlet 22 H at 1.4 ppm.

From two spectra considered together, the structure can be atributed as 3-hydroxymethyl-1-phenylcyclopentadecene-1. The possible reaction mechanism is shown below.

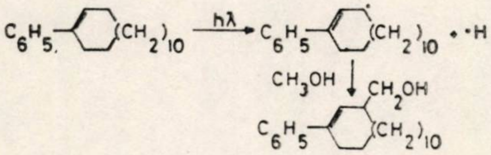

The formation of allylic radical is highly probable because of spin delocalization of radical over double bond and phenyl group. In methanol, this radical forms a methylol radical and then it bonds to the allylic carbon. As a result, if the ring is a macrochain, one product rather than a mixture has been obtained easily. When n = 7 a photoisomerisation ha occurred, but if n = 1, 2, 3 a mixture of methoxy, dimeric and polymeri product has been obtained. [1-3] Contrary to them, at allylic carbon on the macro ring (n : 15), a methylol group has formed during photolysis in methanol.

REFERENCES

[1] P. J. Kroop, *J. Amer. Chem. Soc.*, **91**, 5783 (1969).
[2] H. M. Rosenberg and M. P. Serve, *J. Org. Chem.*, **37**, 141 (1972).
[3] K. Günaydin and Ü. Oyman, *Chim. Acta Turcica*, **13**, 3 (1985).

Revue Roumaine de Chimie, **33**, 2, 183—187 (1988)

REACTIONS OF DIBENZOYLACETYLENE WITH N-ALKYL NITRONES, HETEROAROMATIC-N-OXIDES, DIAZO AND AZOXY COMPOUNDS

AHMED M. NOUR EL-DIN*, ABD EL-RAZAK M. TAWIK and RAMADAN MEKAMER
Chemistry Department, Faculty of Science, El-Minia University, El-Minia, A. R. Egypt and
Chemistry Department, Faculty of Science, Ain Shams University, Cairo, A. R. Egypt

Received May 24, 1986

Dibenzoylacetylene affords 4-oxazolines, enamines and pyrazoles by reaction with N-alkyl nitrones, heteroaromatic-N-oxides and aryl diazo compounds, respectively. However, azoxy compounds did not react with dibenzoylacetylene.

In connection with our studies on the reactions of 1,3-dipoles, azomethine N-oxides [1-5] (nitrones), heteroaromatic-N-oxides [6] and azoxy [7] compounds with the electron-deficient compounds like tetracyanoethylene (TCNE) and 1,4-benzoquinones, we have recently reported [8] that the reaction of dibenzoylacetylene (**1**) with N-aryl nitrones follows a different path from those with other alkynes. [9] 3-Anilino-1,4-diphenylbutane-1,2,4-trione and the corresponding aldehydes were obtained from the reaction of (**1**) with these N-aryl nitrones. [8] The formation of this trione by 1,3-dipolar cycloaddition reaction followed by intramolecular rearrangement and ylide decomposition has been postulated. [8] These results prompted us to extend this reaction to N-alkyl nitrones (**2a**, **b**) and other 1,3-dipoles heteroaromatic-N-oxides (**6a**, **b**), (**9**) and (**10**), diazo (**13a**—**c**) and azoxy (**15a**, **b**) compounds, to investigate the behaviour of this alkyne (**1**) towards these 1,3-dipoles.

We found that the reaction of N-alkyl nitrones (**2a**, **b**) with dipolarophile (**1**) in CH_2Cl_2 at room temperature did not give the corresponding triones (**3a**, **b**), but instead 4-oxazolines (**5a**, **b**), via the primary cycloadducts (**4a**, **b**), were obtained as sole products (Fig. 1). Structure of 4-oxazoline was assigned to these products (**5a**, **b**) on the basis of their analytical and spectroscopic data (see experimental). Observation of the methine proton signal at 5.90 and 6.10 ppm in their NMR spectra is indicative for the methine group being located between an oxygen and a nitrogen atom. [10-13] Therefore, it seems that the attachment of a phenyl group to the nitrone nitrogen atom is essential for the stabilization of the ylide intermediate and consequently for occurrence of the rearrangement to the corresponding triones.

On the other hand, the addition of (**1**) to the heteroaromatic-N-oxides (**6a, b**), (**9**) and (**11**) under the same conditions yielded solely the ring opened enamines (**8a, b**), (**10**) and (**12**), respectively (Fig. 1). The infrared spectra of these enamines (**8a, b**), (**10**) and (**12**) showed absorp-

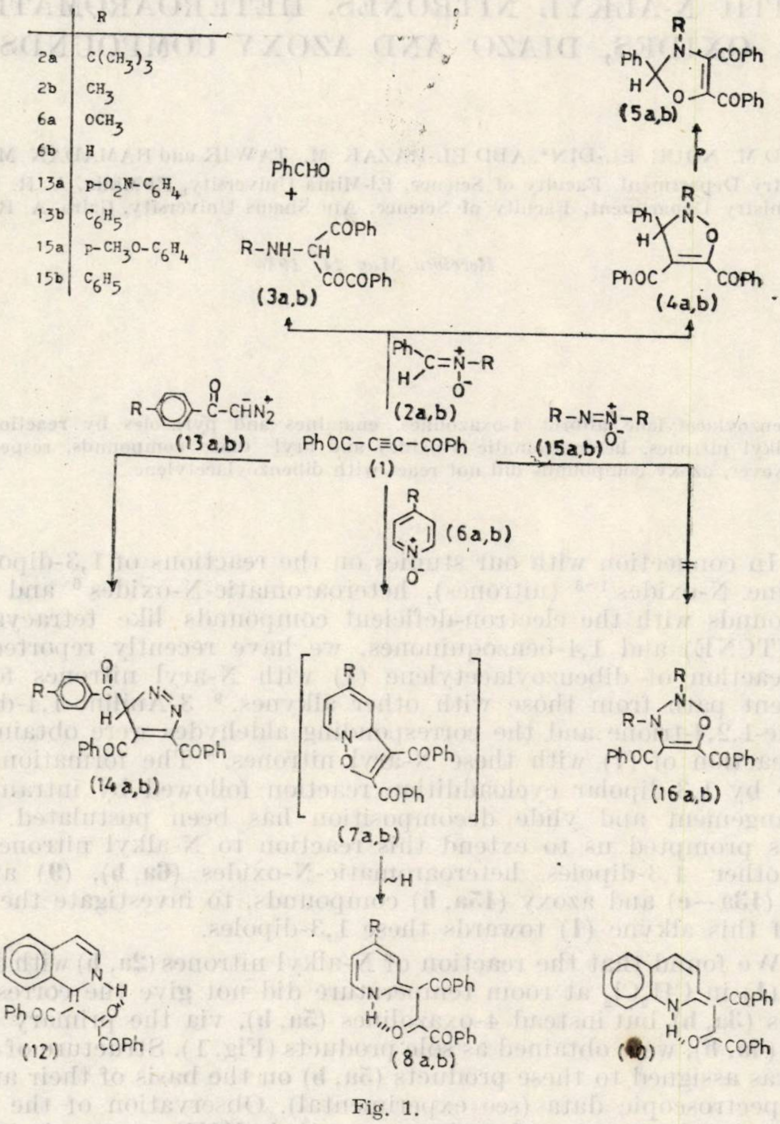
R
2a C(CH3)3
2b CH3
6a OCH3
6b H
13a p-O2N-C6H4
13b C6H5
15a p-CH3O-C6H4
15b C6H5
(5a,b)
PhCHO
+
R-NH-CH COPh COCOPh
(3a,b)
(4a,b)
(2a,b)
(13a,b)
PhOC-C≡C-COPh
(1)
(15a,b)
(6a,b)
(14a,b)
(7a,b)
(16a,b)
~H
(12)
(8a,b)
(10)

Fig. 1.

tion maxima in the amino group region 3350, 3400, 3450 and 3100 cm^{-1}, respectively. The observation of a doublet from doublet and a doublet in the NMR spectra of (8a) and (**12**) at relatively high magnetic fields (6.7 and 7.05 ppm) gives another evidence for the olefinic structure of these enamines, as compared to the chemical shifts of the pyridine and isoquinoline protons 7.1—8.5 and 7.5—8.5 ppm, respectively.[14] Moreover, the ^{13}C chemical shift values observed in the NMR spectra of (**8a**), (**10**) and (**12**) at 111.30 ÷ 117.25 ppm for olefinic carbons, further support the structure suggested (Fig. 1).

The formation of the enamines (**8a, b**), (**10**) and (**12**) may take place through an initial 1,3-dipolar cycloaddition followed by opening and 1,2-hydrogen shift (Fig. 1). This indicates that the reaction of (**1**) with heteroaromatic-N-oxides has a different reaction path; the corresponding triones were not formed. This behaviour can be ascribed to the rigid cyclic structure of the heteroaromatic-N-oxides.

While the α-diazocarbonyl compounds (**13a, b**) underwent 1,3-dipolar cycloaddition with the dipolarophile (**1**) giving the primary cycloadducts (**14a, b**), diazophosphonium salt (**13c**) did not react with (**1**), even after prolonged heating (see experimental). This behaviour can be attributed to the high stabilization of 1,3-dipole of this diazo compound (**13c**), which arises from their ionic nature (salt character).[15]

However, treatment of the aryl azoxy compounds (**15a, b**) in toluene with the electron-poor dipolarophile (**1**) did not undergo 1,3-dipolar cycloaddition reaction, even after prolonged reflux. This behaviour may be ascribed to the low-laying π-molecular orbitals of the azoxy compounds (**15a, b**).[16]

EXPERIMENTAL

Melting points, uncorrected, were determined on a Gallenkamp device. Infrared spectra were recorded on a Shimadzu-408 spectrophotometer using KBr disk. ^1H and ^{13}C-NMR spectra were obtained with Varian EM-360 (60 MHz) and Bruker WP 80 spectrometer. Mass spectra were determined on a MAT 311A spectrometer operating at (70 MeV). Elemental analyses were performed by the microanalytical unit at Cairo University. Dibenzoylacetylene (**1**),[17] nitrones[18,19] and diazo compounds (**13—c**)[15] were prepared according to the literature. The heteroaromatic-N-oxides, 4-methoxy-pyridine-N-oxide (**6a**), pyridine-N-oxide (**6b**), quinoline-N oxide (**9**) and isoquinoline-*N*-oxide (**11**), and azoxy compounds (**15a, b**) were purchased from Aldrich and used without further purification. A 1-mm layer of silica gel Merck PF_{254} on a plate 20 cm by 48 cm was employed for preparative t.l.c. and bands were detected by exposure to short-wavelength ultraviolet.

Reaction of nitrone (**2a**) *and* (**1**). A solution of 234.2 mg (1.0 mmol) of (**1**) in 2 mL of CH_2Cl_2 was added to a stirred solution of 177.2 mg (1.0 mmol) of (**2a**) in 3 mL of CH_2Cl_2. The stirring was continued for 24 h until the t.l.c. showed disappearance of the starting compounds. T.l.c. revealed only one spot. The solution was concentrated with rotary evaporator at room temperature. Upon addition of hexane and cooling colorless crystals 380 mg (92%) of 3-tert-butyl-4,5-dibenzoyl-2-phenyl-4-oxazoline (**5a**), mp 121°C, were obtained, (Found: C, 78.62; H, 6.01; N, 3.27. $C_{27}H_{25}NO_3$ requires C, 78.81; H, 6.12; N, 3.40%), ν_{max} 1668 (CO), 1615 (C=C) cm^{-1}; $\delta(CDCl_3)$ 1.25 (9H, s, $C(CH_3)_3$), 5.90 (1H, s, OCHN), 6.80 — 7.8 (15H, m, ArH).

Reaction of nitrone (**2b**) *and* (**1**). To a stirred solution of 135.2.mg (1.0 mmol) of (**2b**) in 3 mL of CH_2Cl_2, 234 mg (1.0 mmol) of (**1**) in 3 mL CH_2Cl_2 were added. The stirring was continued for 48 h and then the solution was concentrated with rotary evaporator at room temperature. The residue was then chromatographed on a t.l.c. using a mixture of benzene-ethyl acetate (10 : 1) as eluent, to give one zone ($R_f = 0.52$). Extraction with acetone and crystallization afforded 278 mg (78%) 4,5-dibenzoyl-3-methyl-2-phenyl-4-oxazoline (**5b**), as colorless crystals, mp 102 — 104 °C (ethanol-hexane) (Found: C, 77.89; H, 5.07; N, 3.65. $C_{24}H_{19}NO_3$ requires C, 78.03; H, 5.18; N, 3.79%), ν_{max} 1665 (CO) cm^{-1}; $\delta(CDCl_3)$ 1.35 (3H, s, CH_3), 6.10 (1H, s, OCHN), 6.95—7.90 (15H, m, ArH).

Reaction of heteroaromatic-N-oxides (**6a, b**), (**9**) *as well as* (**11**) *with* (**1**). *General procedure.* To a stirred solution of 1 mmol of heteroaromatic-N-oxide in 5 mL of chloroform, 1 mmol of (**1**) in 2 mL of chloroform was added. The stirring was continued for 10 — 12 h at room temperature until the t.l.c showed the disappearance of the starting compounds. The solvent then removed at room temperature with rotary evaporator and the residue was crystallized from the proper solvent to give the products (**8a, b**), (**10**) and, (**12**).

1,4-Diphenyl-3-(4-methoxy-1,2-dihydro-2-pyridylidene)-butane-1,2,4-trione (**8a**). Recrystallization from CH_2Cl_2-hexane gave pale yellow crystals 245 mg (68 %) of (8a), mp 253 — 254°C (Found : C, 73.37 ; H, 4.62 ; N, 3.68. $C_{22}H_{17}NO_4$ requires C, 73.52 ; H, 4.77 ; N, 3.90 %) ; ν_{max} 3350 (NH), 1680, 1630 (CO) ; *m/e* 359 (M^+, 9 %), 328 (5 %), 254 (100 %), 226 (5 %) ; ^1H-NMR (DMSO) δ 4.05 (3H, s, OCH_3), 6.70 (1H, dd, J = 3 Hz, *J* = 9 Hz, 5—H), 7.10 — 8.25 (13H, m, ArH and NH) ; ^{13}C—NMR 112.25 and 114.50 (olefinic carbon).

1,4-Diphenyl-3-(1,2-dihydro-2-pyridylidene)-butane-1,2,4-trione (**8b**) Recrystallization from ethanol afforded 190 mg (55 %) as yellow crystals of (**8b**) mp 137 — 139°C (Found : C, 76.32 ; H, 4.42 ; N, 4.11. $C_{21}H_{15}NO_3$ requires C, 76.58 ; 4.59 ; H, N, 4.25 %) ; ν_{max}3400 (NH), 1658 (CO).

1,4-Diphenyl-3-(1,2-dihydro-2-quinolylidene)-butane-1,2,4-trione (**10**). Recrystallization from CH_2Cl_2-hexane gave 180 mg (69 %) as yellow crystals of (**10**) mp 250 — 251°C (decomp.) (Found : C, 79.01 ; H, 4.43 ; N, 3.50. $C_{25}H_{17}NO_3$ requires C, 79.14 ; H, 4.52 ; N, 3.69 %) ν_{max} 3450 (NH), 1685 (CO) ; *m/e* 379 (M^+, 9 %), 274 (100 %), 246 (7 %) ; ^1H—NMR (DMSO) δ7.20—8.10 (15H, m, ArH and NH), 8.45 (2H, d, *J* = 6 Hz, ArH) ; ^{13}C—NMR 111.30, 114.49 and 117.25 (three olefinic carbon).

1,4-Diphenyl-3-(1,2-dihydro-1-isoquinolylidene)-butane-1,2,4-trione. (**12**). Recrystallization from $CHCl_3$-hexane gave 190 mg (73 %) as yellow crystals of (**12**) mp 210 — 211°C (decomp.) (Found : C, 79.04 ; H, 4.46 ; N, 3.51. $C_{25}H_{17}NO_3$ requires C, 79.14 ; H, 4.52 ; N, 3.69 %) ; ν_{max} 3100 (NH), 1645 (CO) ; m/e 379 (M^+, 15%), 274 (100%) 246 (25%) ; ^1H—NMR ($CDCl_3$) δ 7.05 (11H, d, *J* = 7 Hz, C=CH), 7.20 — 7.95 (15H, m, ArH and NH), 8.80 (1H, d, *J* = 7 Hz, C=CH—N) ; ^{13}C—NMR 112.65, 114.60 and 116.30 (three olefinic carbons).

3,4-Dibenzoyl-5-(4-nitrophenyl)pyrazole (**14a**) : 95.6 mg (0.5 mmol) of 4-nitrobenzoyl diazomethane (**13a**) in 3 mL of CH_2Cl_2 were added to a solution of 117 mg (0.5 mmol) of (**1**) in 3 mL of CH_2Cl_2. The mixture was stirred for 24 h until the t.l.c showed the disappearance of the starting compounds. The solvent was then removed at room temperature with rotary evaporator. The residue was recrystallized to give 180 mg (85 %) of (**14a**), as colorless crystals, mp 99 — 101°C (ethanol-hexane) (Found : C, 67.58 ; H, 3.49 ; N, 9.72.$C_{21}H_{15}N_3O_5$ requires C, 67.76 ; H, 3.55 ; N, 9.87 %) ; ν_{max} 1642 (CO) ; δ ($CDCl_3$) 7.4 — 7.9 (10H, m, ArH), 8.1 — 8.5 (5H, m, OH and ArH).

3,4,5-Tribenzoyl pyrazole (**14b**). To a stirred solution of 73 mg (0.5 mmol) of (**13b**) in 3mL CH_2Cl_2, 117 mg (0,5 mmol) of (**1**) in 3 mL CH_2Cl_2 were added. The stirring was continued for 24 h until the t.l.c. showed the disappearance of the starting compounds. T.l.c. revealed only one spot. The solvent was removed with rotary evaporator at room temperature and the residue was recrystallized from benzene-hexane to give 152 mg (80 %) of (**14b**) as colorless crystals, mp 158 — 159°C (Found : C, 75.50 ; H, 4.16 ; N, 7.22. $C_{24}H_{16}N_2O_3$ requires C, 75.58 ; H, 4.24 ; N, 7.36 ; ν_{max} 1640(CO) ; δ (DMSO) 7.2 — 8.1 (15H, m, ArH), 8.35 (1H, s, OH).

Reaction of (1-diazo-oxopropyl)triphenylphosphonium-tetrafluoroborate (**13c**) *with* (**1**) : To a stirred solution of 216 mg (0.5 mmol) of (**13c**) in 3 mL toluene, 117 mg (0.5 mmol) of (**1**) in 3 mL toluene were added. The reaction mixture was refluxed for 48 h and then the solvent was evaporated. The residue was separated on a t.l.c. plate of silica gel, using a mixture of benzene : ethyl acetate (10 : 1) as eluent, to give two zones. Extraction with acetone and rectystallization from ethanol-hexane gave the starting materials (**13c**) and (**1**).

Reaction of the azoxy compounds (**15a, b**) with (**1**). Mixture of the azoxy compound (**15a, b**) (1.0 mm01), (**1**) (1.0 mmol) and toluene (10 mL) was heated for 3 days. The solvent was evaporated and the residue was separated on t.l.c. plate of silica gel (benzene : ethyl acetate, 10 : 1). The starting materials, the azoxy compounds (**15a, b**) as well as (**1**), were recovered.

REFERENCES

[1] A. M. Nour El-Din and A. E. Mourad, *Bull. Soc. chim. belges*, **91**, 539 (1982).
[2] A. M. Nour El-Din and A. E. Mourad, *Monatsh.*, **114**, 211 (1983).
[3] A. M. Nour El-Din and A. E. Mourad, *J. prakt. chem.*, **325**, 908 (1983).
[4] A. M. Nour El-Din, *J. Chem. Fes.* (*M*) **1984**, 3019.
[5] A. M. Nour El-Din and D. Döpp, *Bull. Soc. chim. belges*, **93**, 891 (1985).
[6] A. M. Nour El-Din, *Spectrochim. Acta*, **41A**, 1101 (1985).
[7] A. M. Nour El-Din, *Gazz. Chim. Ital.*, **115**, 401 (1985).
[8] A. M. Nour El-Din, A. E. Mourad and R. Mekamer, *Heterocycles*, **23**, 1155 (1985).
[9] D. St. C. Black, R. F. Crozier and V. C. Davis, *Synthesis*, **4**, 205 (1975).
[10] A. M. Nour El-Din, Dissertation Kaiserslautern University, 1979.
[11] J. E. Baldwin, R. G. Pudussery, A. K. Qureshi and B. Sklarz, *J. Amer. Chem. Soc.*, **90**, 5325 (1968).
[12] J. W. Lown, R. K. Smalley, G. Dallas and T. W. Maloney, *Canad. J. Chem.*, **48**, 89 (1970).
[13] D. Döpp and A. M. Nour El-Din, *Tetrahedron Letters*, **17**, 1463 (1978).
[14] D. H. Williams and I. Fleming, "Spectroscopic Methods in Organic Chemistry", McGraw-Hill Book Company (UK) Limited, London, 1973.
[15] A. M. Tawfik, Dissertation, Kaiserslautern University, 1981.
[16] R. Huisgen and F. P. Gambra, *Tetrahedron Letters*, **23**, 55 (1982).
[17] E. Ziegler and W. Klementschitz, *Monatsch.*, **81**, 1113 (1950).
[18] W. Rundel, "In Methoden der Organischen Chemie" (Houben-Wely-Müller), Thieme, Stuttgart, XI4, 1968, p. 309.
[19] T. Ohkuma, Y. Kirino and T. Kwan, *Chem. Pharm. Bull.*, **29**, 25 (1981).

Revue Roumaine de Chimie, 33, 2, 189–194 (1988)

TRANSFORMATIONS OF AMINIC ANTIOXIDANTS IN THE INHIBITED OXIDATION OF HYDROCARBONS

N. NEGOIŢĂ[a], J. M. HERDAN[b]*, NICOLETA GRECU[c] and GH. IORDACHE[b]
[a] Institute of Physics and Nuclear Engineering, Măgurele, Bucharest, Romania
[b] Institute of Research, Technological Engineering and Design for Refineries,
Bd. Republicii 291 A, 2000 Ploieşti, Romania
[c] Institute of Physics and Molecular Technology, Măgurele, Bucharest, R omania

Received August 2, 1987

During the oxidation of hydrocarbons inhibited with *p,p'*-di-tert-octyldiphenylamine, a stable aminoxyl was formed by the reaction of the antioxidant with hydroperoxides. Using mixtures of *p, p'*-di-tert-octyldiphenylamine with disulfides as oxidation inhibitors, another stable radical, a tetraarylhydrazyl cation-radical was observed.

The use of antioxidants for the stabilisation of many organic materials such as synthetic polymers, lubricants and even foods is employed on a very large scale. Aminic antioxidants are a very important class of these products.

Though many data are known concerning the action mechanism of the phenolic antioxidants,[1-3] the data about the aminic ones are much less numerous.[4,5]

RESULTS AND DISCUSSION

The studied antioxidants were *p,p'*-di-tert-octyldiphenyl-amine I and *p*-tert-octylphenyl-β-naphthylamine II.

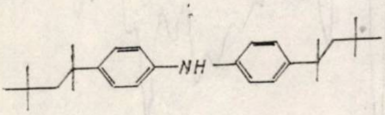

I

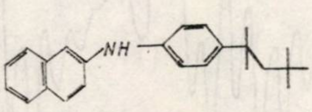

II

As oxidizable substrates we used tetraline, squalane, dodecylbenzene, decaline, white mineral oil, and chlorobenzene. The oxidation of the hydrocarbons inhibited with 1% antioxidant was performed by bubbling dry air at 90°C. To follow the transformation of the antioxidants in time the oxidation period was varied. After oxidation the samples were deaerated, sealed in glass tubes and the ESR spectra were recorded.

---

* Correspondence author

The ESR spectra of the samples containing I show the formation of a single stable radical III during the oxidation.

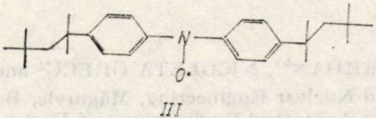

III

The structure of III was deduced by analysing the coupling constants on nitrogen and on *ortho* and *meta* protons of the *para*-substituted benzenic rings.

The ESR spectrum has three groups of lines due to the large coupling constant on nitrogen ($a_N = 10.6$ Gs) and to the small coupling constants on *ortho* ($a_{H\ ortho} = 1.1$ Gs) and *meta* ($a_{H\ meta} = 0.55$ Gs) hydrogens. The *g* factor (the spectroscopic splitting factor), relative to a Mn^{2+} salt standard, is 2.0063 indicating a nitroxide structure. Our data are similar with those of Rozantsev and coworkers,[6] who obtained the same radical III by oxidizing I with hydroperoxides.

The concentrations of the free radical III vary during the oxidation of the sample. This variation is easier to observe for the samples in tetraline. In figure 1 are presented the ESR spectra of tetraline samples containing 1% I at different oxidation times. The concentration of free radicals increases in time, reaching a maximum and then decreases.

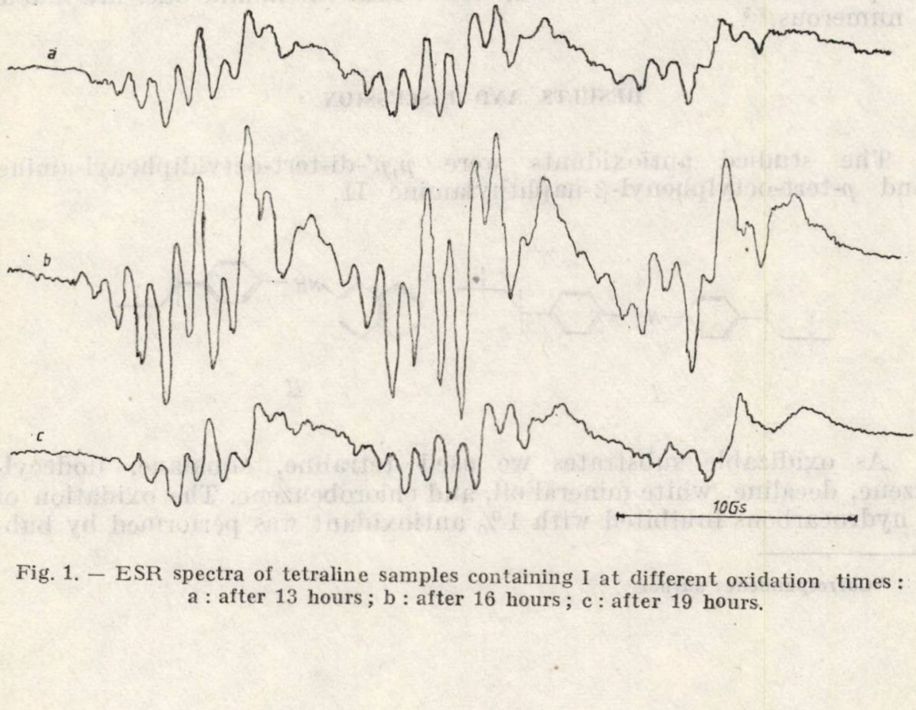

Fig. 1. — ESR spectra of tetraline samples containing I at different oxidation times: a : after 13 hours; b : after 16 hours; c : after 19 hours.

The concentration of the free radicals after the same oxidation time, in strictly identical conditions, depends of the nature of the substrate: dodecylbenzene > tetraline > white oil > decaline > squalane. With any substrate the same radical III is obtained.

These results and also literature data [4,6] permit to presume the following mechanism for the formation of nitroxide III:

$$\mathrm{R{-}H + O_2 \rightarrow R{-}OOH}$$

$$\mathrm{R{-}OOH \rightarrow R{-}O\cdot + HO\cdot}$$

$$\mathrm{R{-}O\cdot + Ar{-}NH{-}Ar \rightarrow R{-}OH + Ar{-}\dot{N}{-}Ar}$$

$$\mathrm{Ar{-}\dot{N}{-}Ar + R{-}OOH \rightarrow \underset{\textit{III}}{Ar_2N{-}O.} + R{-}OH}$$

To confirm this mechanism chlorobenzene was used as substrate for the oxidation of I. Chlorobenzene is not oxidizable, and due to the lack of hydroperoxides, stable radicals were not observed in ESR spectra.

The decrease of the concentration of III during oxidation can be explained by its partial decomposition to non-radicalic species at 90°C. At room temperature III is stable for long time.

The influence of the substrate on the concentration of radicals III is correlated with its aptitude to form hydroperoxides, as it can be seen from table 1.

Table 1

Hydroperoxide concentration in autooxidation of the substrates at 90°C for 19 hours

Substrate	ROOH mval/L
dodecylbenzene	0.267
tetraline	0.211
white oil	0.017
decaline	0.012
squalane	0.010
chlorobenzene	0.003

In the attempts to oxidize tetraline inhibited with 1% *p*-tert-octylphenyl-β-naphthylamine II, the formation of a stable radical was not observed in the ESR spectra. This fact corresponds with the results of Ingold and coworkers,[4,5] who observed that peroxy radicals prefer the attack at the naphthylic nucleus of phenyl-naphthylamine to the attack at the aminic nitrogen.

Following these experiments, attempts were made to oxidize tetraline containing 1% I and 0.5% sulfur compounds IV, V and VI. The sulfur compounds act as decomposers of hydroperoxides.

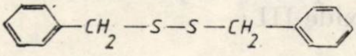

IV

$n\text{-}C_{12}H_{25}\text{—}S\text{—}S\text{—}C_{12}H_{25}\text{-}n$

V

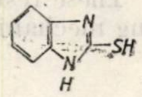

VI

The oxidation was conducted in the same conditions as indicated previously. On oxidizing tetraline containing I and VI no radicalic species were observed.

On oxidizing tetraline containing I in addition to IV or V respectively, a stable radical was observed, whose concentration increased during oxidation. The hyperfine structure of the ESR spectrum (Fig. 2) consists of five lines in 1 : 2 : 3 : 2 : 1 ratios. Based on this, we presume that the radical has two equivalent nitrogens, i.e. a hydrazyl structure VII.

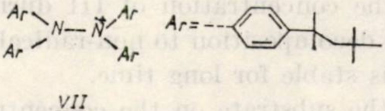

VII

Abakumov and Pomerantseva[7] obtained the cation-radical of tetra(*p*-cumyl)hydrazine, with a similar ESR spectrum, on treating the corresponding hydrazine with trichloroacetic acid. The similitude of ESR spectra of other tetraarylhydrazyls[8,9] with the ESR spectrum of VII confirms this structure.

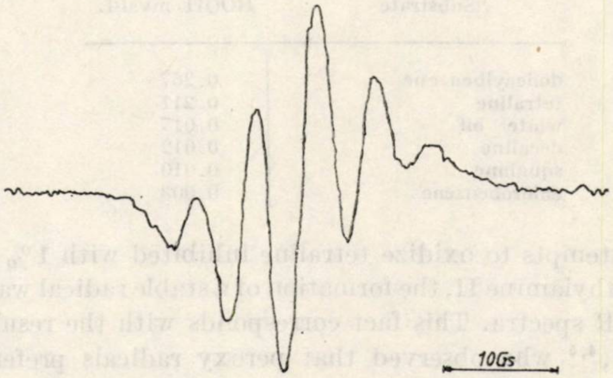

Fig. 2. — ESR spectrum of tetraline containing I + IV after 19 hours of oxidation.

For the formation of the cation-radical, the presence of a protonic acid is necessary. In this case, the protonic acid could be formed by an oxidation of the disulfide to a sulfonic acid.[10]

To explain the formation of the radical VII we must admit the oxidation of 1 to an aminyl, which dimerizes to the tetraaryl-hydrazine before reacting with the hydroperoxide to form III.

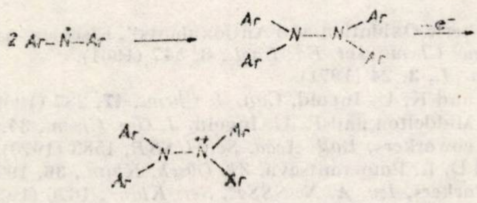

VII

The preference of the aminyl to dimerize is explained by the catalytic action of the sulfur compounds which act as hydroperoxide decomposers and decrease their concentration.

The lack of a stable radical formed in the oxidation of tetraline inhibited with I and VI can be explained as in scheme 1.

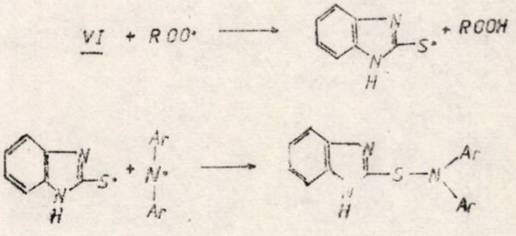

VIII

Scheme 1. — Proposed reaction sequence for explaining the lack of ESR signals in the products formed in the oxidation of tetraline inhibited by I + VI

The sulfenamides VIII are stable compounds but the S-aliphatic sulfenamides are much less stable.

From the experimental data we can conclude that during the oxidation of hydrocarbons inhibited with secondary aromatic amines, stable nitroxide radicals are formed, via hydroperoxides. The presence of sulfur compounds (acting as hydroperoxide decomposers) modifies the reaction pathway, conducting to tetraarylhydrazine cation-radicals or to non-radicalic species.

EXPERIMENTAL PART

The oxidation was performed in 50 mL flasks provided with reflux condensers. In the flasks are introduced 20 mL of sample and these are heated on an oil bath at 90°C. The oxidation is produced by bubbling dry air with a rate of 5 L/h.

The oxidation times were 10, 13, 16, 19, 22 and 23 hours. After these times the samples were sealed in glass vials and kept at room temperature till the ESR spectra were recorded.

To record the ESR spectra, 2mL of sample were introduced in glass tubes, deaerated with argon and sealed. The ESR spectra were recorded at room temperature on a JEOL M 3X spectrometer.

REFERENCES

[1] G. B. Scott, "Atmospheric Oxidation and Antioxidants", Elsevier, Amsterdam, 1965.

[2] L. M. Mahoney, *Angew. Chem., Int. Ed. Engl.*, **8**, 547 (1961).

[3] G. Scott, *Brit. Polym. J.*, **3**, 24 (1971).

[4] K. Adamic, M. Dunn and K. U. Ingold, *Can. J. Chem.*, **47**, 287 (1969).

[5] D. F. Bowman, B. S. Middelton and E. U. Ingold, *J. Org. Chem.*, **34**, 3456 (1969).

[6] E. G. Rozantsev and coworkers, *Bull. Acad. Sci. USSR*, 1583 (1970).

[7] G. A. Abakumov and D. L. Pomerantseva, *Zh. Obsch, Khim.*, **36**, 1921 (1966).,

[8] G. V. Fomin and coworkers, *Izv. A. N. SSSR, Ser. Khim.*, 1626 (1978).

[9] F. A. Neugebauer and S. Bamberger, *Chem. Ber.*, **105**, 2058 (1972).

[10] G. Scott and R. Sukarto, *Eur. Polym. J.*, **20**, 139 (1984).

Revue Roumaine de Chimie, **33**, 2, 195–197 (1988)

ALKYLATION OF PHENOTHIAZINE USING SOLID-LIQUID PHASE TRANSFER CATALYSIS WITHOUT SOLVENT

M. VLASSA and M. CENAN

Institute of Chemistry Cluj-Napoca, str. Fîntînele 30, Romania

Received November 15, 1986

N-Alkylphenothiazines were prepared by phase transfer catalytic reaction between phenothiazine and various alkylating agents without solvent, tetrabutylammonium bromide being used as the phase transfer catalyst.

The preparation of N-alkylphenothiazine derivatives was performed using the classical procedure by heating phenothiazine with alkyl iodides in a sealed tube[1] or in hexametapol in the presence of basic condensing agents [2,3] or with alkyl chlorides in various solvents[4–14] and by liquid-liquid[15–18] or liquid-solid [19] phase transfer catalysis.

It has recently been shown that acetate,[20] alkoxide,[21] fluoride,[22] indole,[23] pyrimidine and purine [24] and thioacridone [25] anions can be efficiently alkylated without solvent in the presence of catalytic amounts of quaternary ammonium salts.

We described here the alkylation of phenothiazine using phase transfer catalysis without the use of a solvent.

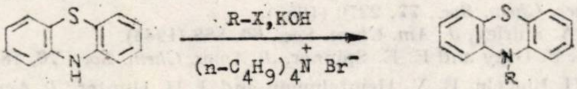

1 **2**

$X=I, R=CH_3; X=Br, R=C_2H_5,$

$n\text{-}C_3H_7, i\text{-}C_3H_7, n\text{-}C_4H_9,$

$CH_2=CH\text{-}CH_2, X=Cl, R=C_6H_5\text{-}CH_2$

The results of our experiments are shown in Table. This method allows to obtain N-alkylphenothiazines in fairly good yields.

When this manuscript was in preparation Bram and coworkers[26] reported the alkylation of 2-R-phenothiazines with halogeno alkyl amino hydrochlorides with trioctylmethylammonium chloride as catalyst.

Table

N-alkylphenothiazines obtained by phase transfer catalysis without solvent.

Comp.	R	Yield (%)	m.p. or b.p.(°C)	lit. m.p. or b.p.
2a	CH_3	70	99–100	99–100[4]
2b	C_2H_5	68	104–105	102, 5–103[6]
2c	n-C_3H_7	70	48–50	49–50[11]
2d	i-C_3H_7	60	58–60	59–60[11]
2e	n-C_4H_9	70	228–230/13mm	226–230/13mm[15]
2f	$CH_2{=}CH-CH_2$	80	190–194/1mm	187–195/1mm[8]
2g	$C_6H_5-CH_2$	40	90–92	90–90.5[6]

EXPERIMENTAL

Melting points were not corrected. A Tabor apparatus was used for shaking the reaction mixture. TLC analyses were run on plates covered with silica gel eluted with C_6H_6-EtOH (10 : 1), visualizing agent iodine (unreacted phenothiazine has a green colour and the alkylated product a brown one).

General procedure. Phenothiazine (0.1 mol) finely ground KOH (1.22 g, 0.2 mol) and tetrabutylammonium bromide (3.2 g, 0.01 mol) were well mixed. After that alkylating agent (0.2 mol) was added and the resulting mixture was shaken at room temperature for one hour, then left for 12 days at the same temperature. After that the reaction mixture was chromatographed with toluene on an alumina column, the organic solvent was removed *in vacuo* and the residue purified by recrystallization from ethanol (charcoal was added), for compounds **2a** – **2d** and **2g** or by distillation, for compounds **2e** and **2f**.

REFERENCES

[1] H. V. Bernstein and I. R. Rothstein, *J. Amer. Chem. Soc.*, **66**, 1886 (1944).
[2] H. Normant and T. Cuvigny, *Bull. Soc. Chim. France*, **1965**, 1866.
[3] H. Normant, T. Cuvigny, J. Normant and B. Angelo, *Bull. Soc. Chim. France*, **1965**, 3446.
[4] A. Burger and A. Ch. Schmolz, *J. Org. Chem.*, **19**, 1841 (1954).
[5] A. A. Levi, U. S. Pat., 2, 145, 252 ; cf. *Chem. Abstr.*, **41**, 2756 (1947).
[6] H. Gilman, R. D. Nelson and J. F. Champaigne jr., *J. Amer. Chem., Soc.*, **74**, 4205 (1952).
[7] H. Gilman, *J. Amer. Chem. Soc.*, **77**, 2270 (1955).
[8] H. Gilman and D. A. Shirley, *J. Am. Chem. Soc.*, **60**, 888 (1944).
[9] Ch. J. Cavallito, A. P. Gray and E. E. Spinner, *J. Amer. Chem. Soc.*, **76**, 1862 (1954).
[10] J. B. Wright, E. H. Lincoln, R. V. Heintelmann and J. H. Hunter, *J. Amer. Chem. Soc.*, **72**, 3536 (1950).
[11] H. Gilman, R. K. Ingham, J. F. Champaigne jr., J. W. Diehl and R. O. Ranck, *J. Org. Chem.*, **19**, 560 (1959).
[12] H. Gilman and D. W. Henberg, *J. Amer. Chem. Soc.*, **72**, 3536 (1950).
[13] Fr. Pat., 1, 167, 653 ; cf. *Chem. Abstr.*, **55**, 9436 (1961).
[14] H. E. Zangg, L. R. Swett and G. R. Stone, *J. Org. Chem.*, **23**, 1389 (1958).
[15] J. Masse, *Synthesis*, **1977**, 341.
[16] H. Wunderlich, W. Lungenheim, A. Stark and G. Detrekoei, *Pharmazie*, **21**, 57 (1966).
[17] East German Pat., 51, 642 ; cf. *Chem. Zentral.*, **14**, 1986 (1969).
[18] I. Gozaln, D. Ladkam, H. Halpern, M. Rabinovicz and D. Avnir, *J. Heteroc. Chem.*, **21**, 613 (1984).
[19] S. C. Schmolz and H. Zimmer, *Synthesis*, **1984**, 29.

[20] J. Barry, G. Bram, G. Decodts, A. Loupy, P. Pigeon and J. Sanaoulet, *Tetrahedron*, **39**, 2673 (1983).

[21] J. Barry, G. Bram, G. Decodts, A. Loupy, P. Pigeon and J. Sansoulet, *Tetrahedron*, **40**, 2945 (1984).

[22] P. Pigeon, Dissertation, Université Paris-Sud, 1984.

[23] J. Barry, G. Bram, C. Decodts, A. Loupy, P. Pigeon and J. Sansoulet, *Tetrahedron*, **39**, 2669 (1983)

[24] G. Bram, G. Decodts, Y. Bensoid, C. Combet-Farnoux, H. Galons and M. Miocque, *Synthesis*, **1985**, 543.

[25] M. Vlassa and M. Kezdi, *Org. Prep. and Proced. Int.*, in press.

[26] H. Galons, M. Miocque, C. Combet-Farnoux, Y. Bensoid and G. Bram, *Chem. and Pharm. Bull.*, **33**, 5108 (1985).

Revue Roumaine de Chimie, **33**, *2*, 199—216 (1988)

HYDRAULIC BINDERS. I

CONTRIBUTION TO THE PROCESSES OF PRODUCING HIGH-QUALITY PORTLAND AND ALUMINOUS CEMENTS, NOBLE AND COLOURED LIMES AND PLASTERS OUT OF WASTES RESULTED FROM THE CHEMICAL INDUSTRY AND OTHER INDUSTRIES

MARIA ENCULESCU
ICPILA-Bucharest, Romania

Received December 15, 1985
Revised September 25, 1987

The laboratory studies and researches on the possibilities of producing limes, plasters as well as other noble and coloured binders, based on wasters or secondary products, resulted from various industries : 1. $CaCO_3$ precipitates, wastes from chemical industry ; 2. phosphoplasters from chemical industry ; 3. ferritic, aluminatic red slimes from chemical industry ; 4. mine wastes and opening-ups from mining and oil industry ; 5. slags from metal-working and ferrons metallurgy ; 6. other wastes resulted from various industries ; The recent studies and researches centered mainly on the molar requirement of : CaO, SiO_2, Al_2O_3, Fe_2O_3 or other oxides, substances necessary to produce different types of binders.[1]

1. CONTRIBUTION TO THE KINETICS OF FORMING THE NOBLE PORTLAND AND ALUMINOUS REFRACTORY CLINKERS

The clinkerization kinetics of the raw powders for the pure mineralogical compounds specific for the Portland clinkers : $3CaO \cdot SiO_2$; $\beta 2CaO \cdot SiO_2$; $3CaO \cdot Al_2O_3$ and $4CaO \cdot Al_2O_3 \cdot Fe_2O_3$ as well as for the pure mineralogical compounds specific for the aluminous refractary clinkers : $CaO \cdot Al_2O_3$; $CaO \cdot 2Al_2O_3$; $12CaO \cdot 7Al_2O_3$; $3CaO \cdot Al_2O_3$ and $CaO \cdot 6Al_2O_3$ was studied on the apparatus ATD + ATG — MOM Hungary.

Very recently, the author established simple-molar-original formulas according to which the clinkerization kinetics of the powders takes place depending implicitly on the temperature time and burning conditions — — reducing—oxidant—as it results from appendix 1, where :

$$C_{C_3S} = \frac{3 \times 56}{1 \times 60} = 2{,}8 ; \qquad 2 \cdot 8 \times \frac{T \times t \times D \times C_F \times C_{redox}}{10^6}$$

$$\mathrm{C}_{\mathrm{C_2S}} = \frac{2 \times 56}{1 \times 60} = 1.86\,; \quad 1{\cdot}86 \times \frac{T \times t \times D \times C_{\mathrm{F}} \times C_{\mathrm{redox}}}{10^6}$$

T = burning temperature °C
t = burning time (h)
C_{F} = smoothness, degree of smoothness (R% ; cm²/g)
C_{redox} = redox conditions (%)
D = raw material hardness – Mohs

The formulas show that the basicity of the $3CaO \cdot SiO_3$ powders – with the molar ratio of 2.6 – implies a much more difficult clinkerization kinetics as compared to the $2CaO \cdot SiO_2$ powders having a more reduced basicity, that is a molar ratio of 1.86.

Hence, according to the basicity, the raw powders with a high content of $3CaO \cdot SiO_2$, will have a more difficult clinkerization kinetics depending on the difference of the molar ratios :

$$\Delta C = 2 \cdot 8 - 1.86 = 0.94$$

In the case of refractory aluminium powders, the clinkerization kinetics will occur depending on the molar ratios, according to appendix 1, where :

$$C_{\mathrm{C_3A}} = \frac{3 \times 56}{102} = 1.64\,; \quad 1.64 \times \frac{T \times t \times D \times C_{\mathrm{F}} \times C_{\mathrm{redox}}}{10^6}$$

$$C_{\mathrm{C12A_7}} = \frac{12 \times 56}{7 \times 102} = 0.97\,; \quad 0.97 \times \frac{T \times t \times D \times C_{\mathrm{F}} \times C_{\mathrm{redox}}}{10^6}$$

$$C_{\mathrm{CA}} = \frac{12 \times 56}{1 \times 102} = 0.55\,; \quad 0.55 \times \frac{T \times t \times D \times C_{\mathrm{F}} \times C_{\mathrm{redox}}}{10^6}$$

$$C_{\mathrm{CA_2}} = \frac{56}{102} = 0.27\,; \quad 0.27 \times \frac{T \times t \times D \times C_{\mathrm{F}} \times C_{\mathrm{redox}}}{10^6}$$

$$C_{\mathrm{CA_6}} = \frac{1 \times 56}{6 \times 102} = 0.91\,; \quad 0.91 \times \frac{T \times t \times D \times C_{\mathrm{F}} \times C_{\mathrm{redox}}}{10^6}$$

T = burning temperature °C
t = burning times (hrs)
D = Mohs hardness
C_{F} = smoothness conditions (R%, cm²/g)
C_{redox} = reducing, oxidant conditions

wherefrom it results that the powders with a low basicity (% CaO reduced) and a high content of Al_2O_3 (% Al_2O_3 maximum) will have a very difficult clinkerization kinetics and at high temperatures.

Likewise for the clinkerization capacity of the raw powders for the white and coloured Portland and aluminous clinkers, the author expressed very recently the formulas presented in appendix 2 and appendix 3 — where :

$$A_C \text{ total } 1 = \frac{n \times \sum_0^n C \times t \times D \times C_F \times C_{redox}}{\sum_0^n T}$$

$$A_C \text{ total } 2 = \frac{\sum_0^n T}{n \times \sum_0^n C \times t \times D \times C_F \times C_{redox}}$$

where :

C = free CaO (%)

T = temperatures at which samples for the free CaO were taken

t = burning time [hrs]

n = number of samples

C_F = smoothness (R% or cm^2/g)

C_{redox} = burning conditions — reducing — oxidant

D = Mohs hardness

1.1. *The clinkerization capacity of the white and coloured cements* — — according to Blaise — observes the following formula :

$$A_C \text{ white} = \frac{600}{C_0 + 2C_1 + 2C_2 + 3C_3 + 4C_4 + 4C_5 + 2C_6}$$

or for the white — alitic Portland clinkers, the adopted formula :

$$A_C \text{ white} = \frac{600}{3C_3 + 4C_4 + 4C_5 + 2C_6}$$

and for the coloured clinkers, the following formula is observed :

$$A_C \text{ colour} = \frac{600}{C_0 + 2C_1 + 2C_2 + 3C_3 + 4C_4 + 4C_5 + 2C_6}$$

where C_0, C_1, C_2, C_3, C_4, C_5, C_6 represent the free CaO content from the burnt masses, at temperatures of 1000°C ; 1100°C ; 1200°C ; 1300°C ; 1350°C ; 1400°C ; 1450°C.

a) The following papers present the clinkerization capacity of the raw powders, for the white Portland clinkers ; the best capacity to be observed is that of the white pegmatite clinker.

b) The following papers present the clinkerization capacity of the raw powders for the aluminous clinkers, out of which the white aluminous clinkers $CaO \cdot 2A_2O_3$ and $CaO \cdot Al_2O_3$ are noticed.

c) The following papers present the clinkerization capacity of the raw powders based in slag — from Galați, out of which the powders with a very reduced content of $3CaO \cdot SiO_2$ and very high content of $\beta 2CaO \cdot SiO_2$ are noticed.

1.2. *Formation of limes and lime-plaster mixturs*; *decarbonation kinetics*. By analysing the values of the molar ratios, one points out the fact that V_1, V_2 and V_3 increase continuously up to 1000°C, and V_4 decrease continuously: the largest decrease as a result of the decarbonation phenomenon is registered in the range of 940–1000° C.

Analysing the values of the total molar ratios for lime, the author drew up the following formulas, presented in appendix-4

$$\text{a)}\quad V_1 \text{ total} = \frac{\sum_0^n \text{active}(\text{CaO} + \text{MgO analysed})\, n \times t \times D \times C_F \times C_{\text{redox}}}{\sum_0^n T}$$

$$\text{b)}\quad V_2 \text{ total} = \frac{\sum_0^n (\%\text{CaO analysed}) \times n \times t \times D \times C_F \times C_{\text{redox}}}{\sum_0^n T}$$

$$\text{c)}\quad V_3 \text{ total} = \frac{\sum_0^n (\%\text{H}_2\text{O analysed}) \times n \times t \times D \times C_F + C_{\text{redox}}}{\sum_0^n T}$$

$$\text{d)}\quad V_4 \text{ total} = \frac{\sum_0^n (\%\text{CO}_2 \text{ analysed}) \times n \times t \times D \times C_F \times C_{\text{redox}}}{\sum_0^n T}$$

1.3. *Burning of lime — plaster mixtures*; *kinetics*. By analysing the values of the molar ratios during the burning process, the formulas CaO and the specific formulas SO_4Ca, hence V_1, V_2, V_3, V_4 and S_1 are valid (Appendix 4) where:

$$S_1 = \frac{\sum_0^n (\%\text{SO}_2\text{Ca analysed}) \times n \times t \times D \times C_F \times C_{\text{redox}}}{\sum_0^n T}$$

where:

T = temperature (°C)

D = Mohs hardness

C_F = degree of smoothness (R %), (s.cm^2/g)
t = burning temperature (hours, minutes)
n = number of tests
C_{redox} = reducing — oxidant conditions

2. REFLECTION FACTORS — WHITENING CAPACITY — COLOUR DEGREES

The raw materials — wastes of calcium carbonate, kaolins, feldspars, tuffs, alumina etc. have various whitening capacities.

2.1. The whitening capacity, the reflection factors, are within the limits of the formulas elaborated by the author (shown in appendix 5) where :

$$A_1 \text{ white} = \frac{600}{\% \ \rho \text{ white}}$$

$$A_2 \text{ white} = \frac{\% \ \rho \text{ white}}{600}$$

$$A_3 \text{ white} = \frac{1}{60} \% \ \rho \text{ white}$$

2.2. The colouring capacity in the burning process, the reflection factors — the colour degrees — are also within the limits of the formulas elaborated by the autor (appendix 5) where :

$$A_1 \text{ colouring} = \frac{60}{\% \ \rho \text{ white } (\rho \text{ blue}, \rho \text{ red}, \rho \text{ green})}$$

$$A_2 \text{ colouring} = \frac{\% \ \rho \text{ white } (\rho \text{ blue}, \rho \text{ red}, \rho \text{ green})}{6}$$

$$A_3 \text{ colouring} = \frac{\% \ \rho \text{ white } (\rho \text{ blue}, \rho \text{ red}, \rho \text{ green})}{60}$$

as it will be specified in the following papers.

3. THE PHYSICAL CHEMISTRY OF THE HYDRATION PROCESS

Prof. Solacolu[1] showed that in the hydration of the Portland cement, the following compounds may appear in the $CaO - SiO_2 - H_2O$ system :

- hillebrandite — hydrated dicalcic silicate $2CaO \cdot SiO_2 \cdot H_2O$ compound with incongruous solubility;
- afwillite — hydrated tricalcic disilicate $3CaO \cdot 2SiO_2 \cdot 3H_2O$ pyrosilicate — a compound with incongruous solubility;
- xonotlite — plombierite — hydrated monocalcic silicate $CaO \cdot SiO_2 \cdot 2H_2O$ — metasilicate — a compound with congruous solubility.

The hydration process of the Portland cements, according to Solacolu[1] is shown in the following papers where C_3A hydrates quickly, C_4AF hydrates more slowly, C_3S has a moderate hydration and C_2S has a very slow hydration.

According to the ratio of the mineralogical components of the clinker, the setting and hardening systems are different. In hydration — C_3S — releases $Ca(OH)_2$, after 28 days, only about 1/2 out of $Ca(OH)$ is released, a fact that shows the development of the reactions in time, as it results from the papers that follow.

It was found out, with the pure calcium silicates : pure $3CaO \cdot SiO_2$ and $2CaO \cdot SiO_2$, that pure $3CaO \cdot SiO_3$ shows a deeper, more accelerated hydration kinetics, being in a perfect correlation with their basicity, with the content of %CaO or more exactly correlated depending on the specific molar ratios, at it results from appendix 6, where :

$$H_1 \text{ for } 3CaO \cdot SiO_2 = \frac{3 \times 56}{1 \times 60} = 2.8 \text{ superior to}$$

$$H_2 \text{ for } 2CaO \cdot SiO = \frac{2 \times 56}{1 \times 60} = 1.86 \text{ a fact for which our}$$

own invention processes (51799 — 51805 — 57413) require the manufacture of alitic white and coloured Portland clinkers — with a content of 80 — 88% $3CaO \cdot SiO_2$ in order to reach the maximum performances of the mechanical strengths both at short terms (1, 3, 7 days) and at 28 days.

The hydration kinetics of the pure calcium silicates, $3CaO \cdot SiO_2$ and $2CaO \cdot SiO_2$, was also analysed depending on the molar theoretical ratios, the hydration, new formations and the following order was established according to the author's own process :

$$2CaO \cdot SiO_2 \cdot H_2O > 3CaO_2 \cdot 2SiO_2 \cdot 2H_2O > CaO \cdot SiO_2 \cdot 2H_2O$$

$$H = \frac{2 \times 56}{60} = 1.8 > H = \frac{3 \times 56}{2 \times 60} = 1.4 > H = \frac{56}{60} = 0.93$$

$$R\text{—Maximum} \quad > H\text{—Medium} \quad > H\text{—Minimum}$$

We also calculated the ratios of the resistances of the pure mineralogical components :

$$R_{C1} = \frac{R_1 C_3 S}{R_1 C_2 S} = \frac{150}{1} = 150$$

$$R_{C3} = \frac{R_3 C_3 S}{R_3 C_2 S} = 30$$

$$R_{C7} = \frac{R_7 C_3 S}{R_7 C_2 S} = \frac{217}{13} = 17$$

$$R_{C2} \quad \frac{R_{28} C_3 S}{R_{28} C_2 S} = \frac{226}{33} = 7$$

so that all the allitic white and coloured cements, with a high content of $3CaO \cdot SiO_2$ had the initial mechanical strengths at 24 hours and the final strengths at 28 days, superior to the cements with a lower content of $3CaO \cdot SiO_2$ and more increased in $2CaO \cdot SiO_2$, as it results from appendix 7, where :

$$RC_2S = \frac{2 \times 56}{60} \times \frac{T \times t \times W}{10^4}\ ; \quad RC_3S = \frac{3 \times 56}{60} \times \frac{T \times t \times W}{10^4}$$

4. THE HYDRATION PROCESS – THE HYDRATION KINETICS OF THE WHITE AND COLOURED ALUMINOUS CEMENTS

This process was studied similarly to the chemically pure compounds : $CaO \cdot Al_2O_3$; $CaO \cdot 2Al_2O_3$; $CaO \cdot 7Al_2O_3$; $3CaO \cdot Al_2O_3$ and $CaO \cdot 6Al_2O_3$.

The refractory aluminous cements were made of the pure compounds $CaO \cdot Al_2O_3$ – hydrated at : 30 minutes, 1 h, 6 h, and then at 1, 3, 7 and 28 days.

The difractometric and electronomicroscopic studies, show that by hydration, new formation $Al(OH)_3$; C_2AH_8 ; CAH_{10} ; C_4AH_{19} and $3CaO \cdot CaCO_3 \cdot 12H_2O$ appear immediately after some minutes of hydration, then the hydration takes place normally up to one day and accomplishes at 3, 7 and 28 days.

The hydration kinetics of the white and coloured refractory aluminous cements based on the specific mineralogical compounds : $CaO \cdot Al_2O_3$; $CaO \cdot 2Al_2O_3$; $12CaO \cdot 7Al_2O_3$; $3CaO \cdot Al_2O_3$, $CaO \cdot 6Al_2O_{33}$ will have mainly in view the law of basicity but will, at the same time, be implicitly in accordance with the complexity of the hydration, conditions, that is, mainly depending on :

C_F – degree of smoothness ($R\%$ or cm^2/g)
W – air or water humidity (%)
C – salt concentration of the sea waters, soft waters, aggressive, corrosive chemical waters (oxidant, acid, basic media, oils, petroleum, other media) (% conc.)
T – temperature (°C)
R – solar – ultraviolet – X, α, β, γ radiations, neutrons, other radiations ;
E – wind forces – winds storms, hurricanes etc.
t – hydration time (hours, days, years) included mainly in the author's original relations, from appendix 8, where :

$$H(3CaO \cdot Al_2O_3) = \frac{3 \times 56}{102} \times \frac{T \times t \times C_F \times W}{10^4} \text{ and natural factors}$$

(C, R, E)

$$H(12CaO \cdot 7Al_2O_3) = \frac{12 \times 56}{7 \times 102} \times \frac{T \times t \times C_F \times W}{10^4} \text{ and natural factors}$$

(C, R, E)

$H(CaOAl_2O_3) = \frac{56}{102} \times \frac{T \times t \times C_F \times W}{10^4}$ and natural factors (C, R, E)

$H(CaO \cdot 2Al_2O_3) = \frac{56}{2 \times 102} \times \frac{T \times t \times C_F \times W}{10^4}$ and natural factors (C, R, E)

$H(CaO \cdot 6Al_2O_3) = \frac{56}{6 \times 102} \times \frac{T \times t \times C_F \times W}{10^4}$ and natural factors (C, R, E).

Thus, the hydration kinetics of the white and coloured aluminous cements depends in fact, implicitly on a large number of factors, that contribute each separately and all together to the development of the hydration processes, from the initial phase up to the final phase — of total hydration and total carbonatation to get white and coloured carbonates, silicates and aluminates — similar to the natural ones, white and coloured natural rocks from nature.

The author analysed only the main factors that contribute to a great extent and the hydration process can be judged depending on one factor, two factors or all the factors simultaneously.

In the case of the molar ratios, the following :

— for $3CaO \cdot Al_2O_3$; $H = \frac{3 \times 56}{102} = 1.64$

— for $12CaO \cdot 7Al_2O_3$; $H = \frac{12 \times 56}{7 \times 102} = 0.97$

will require the development of the hydration processes, with speed and intensity much superior to the compounds.

— for $CaO \cdot Al_2O_3$ with $H = \frac{56}{102} = 0.55$

— for $CaO \cdot 2Al_2O_3$ with $H = \frac{56}{2 \times 102} = 0.27$

— for $CaO \cdot 6Al_2O_3$ with $H = \frac{56}{6 \times 102} = 0.091$

Hence, in the order of accomplishing the hydration processes, the hydration kinetics will be in the following relation :

$$\overset{1}{CaO \cdot Al_2O_3} > \overset{2}{CaO \cdot 2Al_2O_3} > \overset{3}{CaO \cdot 6Al_2O_3}$$

$$H = 0.55 \quad > \quad H = 0.27 \quad > \quad H = 0{,}091$$

$$\text{Maximum} > \text{Medium} > \text{Minimum}$$

Based on our own results referring to the new formations and their intensity and particularly based on the molar ratios of the hydration new formations, the following rule will be observed :

$$4CaO \cdot Al_2O_3 \cdot 19H_2O > 3CaO \cdot CaCO_3 \cdot 12H_2O > CaO \cdot Al_2O_3 \cdot 10H_2O$$

$$H = \frac{4 \times 56}{102} = 2.2 \quad > \quad - \quad > H = \frac{56}{102} = 0.55$$

$$\text{Maximum} - H = 2.2 > \quad - \quad > \text{Minimum} - H = 0.55$$

$$\text{Maximum} - 19H_2O \quad > \quad \text{Medium} - 12H_2O \quad > \text{Minimum} - 10H_2O$$

The hydration law of the calcium aluminates, the formation kinetics of the hydration compounds, the hydration new formations depend obviously on the basicity, the content of %CaO, similarly to the calcium silicates as it results from the papers that follow.

The mechanical stengths of the pure mineralogical compounds point out superior maximum values of $CaO \cdot Al_2O_3$ — quickly cooled in water, as it result from the data written down in the following papers and appendices 7 and 8.

The mechanical strengths of $CaO \cdot Al_2O_3$ and $3CaO \cdot Al_2O_3$ with oxides of the transitional elements, of Fe, Mn, Cr, Co, Ni in certain percentages, generally microadditions 1%, are superior to the standards without oxides, which confirms the fact that in certain limits, the oxides contribute to the increase of the mechanical strengths, shown in the following papers.

The mechanical strengths of the $CaO \cdot Al_2O_3$ white and a coloured luminous cements are superior to the normal aluminous cements and are in the limits of 400 — 550 daN/cm^2 at 1 day and 600 — 700 daN/cm^2 at 28 days as shown in the following papers.

One can also notice that the coloured, aluminous refractory cements, based on $CaO \cdot Al_2O_3$ and with additions of 0.5%; 2%, 4%, and 8% microadditions of iron, manganese, chromium, cobalt, nickel, oxides — can have the mechanical strengths, superior to the white aluminous cements, without colouring oxides, with about 110 — 150 daN/cm^2, a fact for which they are estimated to be superior both from the point of view of the coloures and pure and bright hues and of the performances of the mechanical strengths.

The refractoriness of the white and coloured aluminous cements, coloured with 0.5%, 2%, 4% and 8% colouring oxides obviously diminishes, depending on the quantity and quality of the metallic oxides.

The order of the results of the refractoriness test is the same as of the white aluminous, refractory cements : $CaO \cdot 6Al_2O_3 > CaO \cdot 2Al_2O_3 > 12CaO \cdot 7Al_2O_3 > 3CaO \cdot Al_2O_3$: 1600 — 1700°C > 1500 — 1600°C > 1400 — 1500°C > 3100 — 1400°C.

Air shrinkage and water swelling of the white and coloured — refractory aluminous cements was below 1 mm/m.

The wear resistance of the white and coloured refractory aluminous cements was superior.

5. THE EVOLUTION OF THE MECHANICAL STRENGTHS OF THE BINDERS OUT OF METALLURGICAL AND FERROUS METALLURGY SLAGS, SILICAL, POWDERS, MINE WASTES, OPENING-UPS, WASTES, ASHES, SLIMES, OTHER WASTES OF INORGANIC SECONDARY PRODUCTS

The binders resulted from metallurgical, ferrous metallurgy slags, wastes, silica powders, mine wastes, opening-ups, ashes, slimes, other types of wastes of inorganic secondary products with a high content of hydraulically activated oxides : CaO, SiO_2, Al_2O_3, Fe_2O_3 or mineralogical compounds : C_3S, C_2S, C_3A, C_2F, C_4AF, C_6A_2F, CA, CA_2, C_3A, $C_{12}A_7$; CA_6, or their solid solutions as results from the industrial processes : metallurgical, siderurgical, chemical, mining, oil thermoenergetical and other industries. Considering only the active oxides, they can be mainly, in the quaternary system $CaO-SiO_2-Al_2O_3-Fe_2O_3$ and will observe the conditions specific for the Portland cements, according to Solacolu :[1]

$$CaO + SiO_2 + Al_2O_3 + Fe_2O_3 = 100; \quad MAl = \frac{Al_2O_3}{Fe_2O_3}$$

$$MSi = \frac{SiO_2}{Al_2O_3 + Fe_2O_3}; \; S_K = \frac{\%CaO}{2.8\%\ SiO_2 + 1.1\%\ Al_2O_3 + 0.7\%\ Fe_2O_3}$$

When, in the respective binders, the main active component is $CaO \cdot SiO_2$, the author's relation :

$$S_{C_3S} = \frac{3\,\%CaO}{\%\ SiO_2}$$

will be valid which points out the correlation between the content of $3CaO \cdot SiO_2$ and the mechanical strengths, obtained at short terms (1—3 — 7 days) and also at long terms (28 — 90 — 180 days).

When, in the respective binders, the main active component is $\beta_2CaO \cdot SiO_2$ the author's relation :

$$S_{\beta C_2S} = \frac{2\,\%CaO}{SiO_2}$$

will be valid which points out the correlation between the preceding contents of $\beta 2CaO \cdot SiO_2$ from the siderurgical, metallurgical, slags from the belite wastes or other wastes and mechanical strengths at long terms (28 — 90 — 180 days).

When the main active components is $3CaO \cdot Al_2O_3$, the author's relation :

$$SC_3A = \frac{3\,\%CaO}{\%Al_2O_3}$$

will be valid, and the binders will be characterized by the rapid setting and very high mechanical strengths at short terms (1, 3, 7 days).

When the main active component is $4CaO \cdot Al_2O_3 \cdot Fe_2O_3$ the author's relationship :

$$SC_4AF = \frac{4\% \; CaO}{\% Al_2O_3 + \% Fe_2O_3}$$

will be valid, by which it is pointed out the correlations between the content of $4CaO \cdot Al_2O_3 \cdot Fe_2O_3$ from slags, slimes, wastes or ferritic secondary products and the mechanical strengths at short terms (1, 3, 7 days) an at long terms (28, 90, 180 days).

When in the binders resulted from slags, wastes, ashes, slimes etc., the aluminates will have the precedence, the relations of Solacolu [1] specific for the aluminous cements will be valid :

$$\% \; CaO + \% \; SiO_2 + \% \; Al_2O_3 + \% \; Fe_2O_3 = 100$$

$$M_{Al} = \frac{\% Al_2O_3}{\% SiO_2}$$

$$M_{Fe} = \frac{\% Al_2O_3}{\% Fe_2O_3}$$

$$SK = \frac{\% CaO}{1.8\% \; SiO_2 + 0.55\% \; Al_2O_3 + 1\% \; Fe_2O_3}$$

When the main active component is $CaO \cdot Al_2O_3$, the author's relation

$$S_{CA} = \frac{\% CaO}{\% Al_2O_3} \quad \text{will be valid.}$$

The content of spinels CA, MgA, MnA, CrA, CuA, NiA, CoA TiA, PbA, BaA, SrA, etc., from slags, ashes, slimes, spinelic wastes gives to the respective mortars, concretes, superior mechanical strengths at 1,3 and 7 days, that is at short terms.

When the main active components are $CaO \cdot 2Al_2O_3$; $12CaO \cdot 7Al_2O_3$, and $CaO \cdot 6Al_2O_3$, the author's relations :

$$S_{CA_2} = \frac{\% CaO}{2\% \; Al_2O_3}$$

$$S_{C_{12}A_7} = \frac{12\% \; CaO}{7\% \; Al_2O_3}$$

$$S_{CA_6} = \frac{\% CaO}{6\% \; Al_2O_3}$$

will be valid.

The following papers show the compression strength of the pure mineralogical components, according to Prof. Solacolu, where the essential part of the main component is pointed out.

From the hydraulic standpoint the $3CaO \cdot SiO_2$ content particularly at short terms, 1 – 3 – 7 days, but also at 28 days, is the most important as it results from the following papers where the ratios :

$$K_1 = \frac{R28}{R3}; \quad K_2 = \frac{R28}{R7}; \quad K_3 = \frac{R28}{R_{90}}; \quad K_4 = \frac{R28}{R180}$$

are given

a) the ratio $RC - C_3S$

b) the author's ratios concerning the mechanical strengths, on plastic mortars of the cements with slag as raw material, depending on the contents of the main component $3CaO \cdot SiO_2$ – and the ratios

$$K_1 = \frac{R28}{R3} \text{ and } K_2 = \frac{R28}{R7}$$

c) the ratios of the mechanical strengths on the plastic mortars of the cements with slag as raw material and with slag additions, are pointed out

d) the ratios of the mechanical strengths on the plastic mortars, obtained at slags with $\sim 40\%$ $2\,CaO \cdot SiO_2$, experimentally calculated and determined, are presented here.

e) the ratios of the strengths at short terms 1 – 3 – 7 days and at long terms 28 – 90 days, depending on the A/C ratios of the cement concretes with high strengths are shown here

f) the mechanical strength ratios of the cement concretes, with high strength are shown here.

Thus it comes out that, depending on the contents of the active mineralogical compounds – roentgenographically and microscopically determined – one can obtain mechanical strengths determined by the same sizes as the calculated ones at all terms – this succeeding to apply to mortars, concretes and prefabricated – the original theoretical relations of the author.

CONCLUSIONS

The laboratory studies and researches pointed out the possibilites to obtain various types of binders : Portland and white and coloured aluminous cements, white and coloured limes and plasters, as well as other white and coloured binders, of high quality and great technical-economic efficiency based on wasters or secondary products, resulted from various industries, $CaCO_3$ precipitates, wastes from chemical industry, phosphoplasters, wastes from opening-ups, mine waste from mining and oil industry, slimes, ferritic rocks from chemical industry, mine waste from the mining industry, slags from siderurgical and metallurgical industries as well as other wastes, slimes, mine waste that bring the necessary molar of : %CaO ; $\%SiO_2$; $\%Al_2O_3$; $\%Fe_2O_3$ or other oxides — substances necessary to produce different types of binders that can be used in various application fields, with great technical-economic efficiency.

ACKNOWLEDGEMENTS : The author thanks the specialists from ICPILA, Bucharest : Valerian Mihai, Nicolae Butucescu, Irina Stamate, Ruxandra Bănescu, Sorina Popescu and G. Leizarovici.

APPENDIX 1

Formulas — clinkerization kinetics (elaborated by the author)

I. Mineralogical compounds specific for the Portland cement

$$C_{C_3S} = \frac{3 \times 56}{1 \times 60} = 2.8; \quad 2.8 \times \frac{T \times t \times D \times C_F \times C_{redox}}{10^6}$$

$$C_{C_2S} = \frac{2 \times 56}{1 \times 60} = 1.86; \quad 1.86 \times \frac{T \times t \times D \times C_F \times C_{redox}}{10^6}$$

$$C_{C_2F} = 0.7 \times \frac{T \times t \times D \times C_F \times C_{redox}}{10^6}$$

$$C_{C_4AF} = 0.95 \times \frac{T \times t \times D \times C_F \times C_{redox}}{10^6}$$

$$\Delta C = 2.8 - 1.86 = 0.94$$

II. Mineralogical compounds specific for the aluminous cements

$$C_{C_3A} = \frac{3 \times 56}{102} = 1.64; \quad 1.64 \times \frac{T \times t \times D \times C_F \times C_{redox}}{10^6}$$

$$C_{C_{12}A_7} = \frac{12 \times 56}{7 \times 102} = 0.97; \quad 0.97 \times \frac{T \times t \times D \times C_F \times C_{redox}}{10^6}$$

$$C_{CA} = \frac{1 \times 56}{1 \times 102} = 0.55; \quad 0.55 \times \frac{T \times t \times D \times C_F \times C_{redox}}{10^6}$$

$$C_{CA_2} = \frac{1 \times 56}{2 \times 102} = 0.27; \quad 0.27 \times \frac{T \times t \times D \times C_F \times C_{redox}}{10^6}$$

$$C_{CA_6} = \frac{1 \times 56}{6 \times 102} = 0.091; \quad 0.091 \times \frac{T \times t \times D \times C_F \times C_{redox}}{10^6}$$

where :

T — maximum clinkerization temperature (°C)
t = burning time (hours, minutes)
C_{redox} — reducing oxidant conditions
D — Mohs hardness

APPENDIX 2

Formulas — clinkerization capacity of the raw powders for the Portland and aluminous clinkers (elaborated by the author)

$$AC\text{ total }1 = \frac{\sum_{0}^{n} C \times n \times t \times D \times C_F \times C_{\text{redox}}}{\sum_{0}^{n} T}$$

$$AC\text{ total }2 = \frac{\sum_{0}^{n} T}{\sum_{0}^{n} C \times n \times t \times D \times C_F \times C_{\text{redox}}}$$

where c — free CaO(%)
T — temperatures at which samples for the free CaO where taken (°C)
t — burning time (hours)
n — number of samples
D — Mohs hardness
C_F — degree of smoothness (R % or cm^2/g)
C_{redox} — reducing — oxidant conditions

Blaise's formula — clinkerization capacity of the white and coloured cements

$$AC_{\text{white}} = \frac{600}{\text{Co} + 2C_1 + 2C_2 + 3C_3 + 4C_4 + 4C_5 + 2C_6}$$

$$AC_{\text{colour}} = \frac{600}{\text{Co} + 2\text{C}_1 + 2\text{C}_2 + 3\text{C}_3 + 4\text{C}_4 + 4\text{C}_5 + 2\text{C}_6}$$

where : Co, C_1, C_2, C_3, C_4, C_5, C_6 are the free CaO content from the burnt masses at temperatures of 1000°C, 1100°C, 1200°C, 1300°C, 1350°C, 1400°C, 1450°C.

APPENDIX 3

Formulas — burning capacity of the raw materials necessary to obtain various types of binders (elaborated by the author)

$$A_{\text{burning},1} = \frac{\sum_{0}^{n} \text{MeO} \times n \times t \times D \times C_F \times C_{\text{redox}}}{\sum_{0}^{n} T}$$

$$A_{\text{burning},2} = \frac{\sum_{0}^{n} T}{\sum_{0}^{n} \text{MeO} \times n \times t \times D \times C_F \times C_{\text{redox}}}$$

where : MeO — metallic oxide resulted after dehydration, decarbonization of the type CaO, MgO, BaO, SrO etc.
n — number of samples
T — clinkerization temperature (°C)

t — burning time (hours)
D — Mohs hardness
C_F — degree of smoothness (cm^2/g)
C_{redox} — burning — reducing — oxidant conditions

APPENDIX 4

Formulas — decarbonization kinetics when burning the carbonates (elaborated by the author

$$V_{1_{total}} = \frac{\sum_{0}^{n} \%(\mathrm{Ca,Mg,Sr,Ba})\mathrm{O}\ \text{active analysed} \times n \times t \times D \times C_F \times C_{redox}}{\sum_{0}^{n} T}$$

$$V_{2total} = \frac{\sum_{0}^{n} \%(\mathrm{Ca,Mg,Sr,Ba})\mathrm{O}\ \text{total analysed} \times n \times t \times D \times C_F \times C_{redox}}{\sum_{0}^{n} T}$$

$$V_{3total} = \frac{\sum_{0}^{n} (\%\mathrm{H_2O}\ \text{analysed}) \times n \times t \times D \times C_F \times C_{redox}}{\sum_{0}^{n} T}$$

$$V_{4total} = \frac{\sum_{0}^{n} (\%\mathrm{CO_2}\ \text{analysed} \times n \times t \times D \times C_F \times C_{redox}}{\sum_{0}^{n} T}$$

Formula — burning kinetics of the sulphate mixtures elaborated by the author

$$S_1 = \frac{\sum_{0}^{n} \%(\mathrm{Ca,Mg,Sr,Ba})\mathrm{SO_4}\ \text{analysed} \times n \times t \times D \times C_F \times C_{redox}}{T}$$

where

n — number of samples
T — clinkerization, temperature (°C)
t — time (hours, minutes)
C_F — degree of smoothness (R % or cm^2/g)
C_{redox} — reducing — oxidant conditions
D — Mohs hardness

APPENDIX 5

Formulas — white capacities — reflection factors whitenesses (elaborated by the author)

$$A_{1\text{white}} = \frac{600}{\%\ \rho\ \text{white}}$$

$$A_{2\text{white}} = \frac{1}{6}\ \%\ \rho\ \text{white}$$

$$A_{3\text{white}} = \frac{1}{60}\ \%\ \rho\ \text{white}$$

Formulas — colouring capacities — reflection factors with blue, green, red filters — colouring degrees (elaborated by the author)

$$A_{1\text{colouring}} = \frac{600}{\%\ \rho\ \text{white (blue, red, green)}}$$

$$A_{2\text{colouring}} = \frac{\%\ \rho\ \text{white (blue, red. green)}}{6}$$

$$A_{3\text{colouring}} = \frac{\%\ \rho\ \text{white (blue, red, green)}}{60}$$

ρ white = white
ρ blue = with blue filter
ρ red = with red filter
ρ green — with green filter

APPENDIX 6

Formulas — hydration kinetics of the Portland and white and coloured aluminous cements (elaborated by the author)

I. Hydration of mineralogical compounds specific for the white and coloured Portland cements

$$H_{C_3S} = \frac{3 \times 56}{60} \times T \times t \times C_F \times W$$

$$H_{C_2S} = \frac{2 \times 56}{60} \times T \times t \times C_F \times W$$

and natural factors (C. R, E)

$$H_{C_2F} = \frac{2 \times 56}{159} \times T \times t \times C_F \times W$$

and natural factors (C, R, E)

$$H_{C_4AF} = \frac{4 \times 56}{102 + 159} \times T \times t \times C_F \times W$$

and natural factors (C, R, E)

II. Hydration of mineralogical compounds specific for the white and coloured aluminous cements

$$H_{C_3A} = \frac{3 \times 56}{102} \times T \times t \times C_F \times W$$

and natural factors (C, R, E)

$$H_{C_{12}A_7} = \frac{12 \times 56}{7 \times 102} \times T \times t \times C_F \times W$$

and natural factors (C, R, E)

$$H_{CA} = \frac{56}{102} \times T \times t \times C_F \times W$$

and natural factors (*C*, *R*, *E*)

$$H_{CA_2} = \frac{56}{2 \times 102} \times T \times t \times C_F \times W$$

and natural factors (*C*, *R*. *E*)

$$H_{CA_6} = \frac{56}{6 \times 102} \times T \times t + C_F \times W$$

and natural factors (*C*, *R*, *E*

T = temperature (°C)
t = hydration time (hours, days, years)
W = air or water humidity (%)
C = concentration in salts, acids, bases, oils, petroleum, etc.(%)
R = solar rays, ultraviolet X, α, β, γ neutrons
E = wind forces, winds, storms,
C_F = specific surface (cm²/g)

APPENDIX 7

Formulas — mechanical strength factors of the Portland and aluminous cements (elaborated by the author)

I. Mechanical strengths of the pure compound — based on white and coloured Portland cements :

$$R_{C_3S} = \frac{3 \times 56}{60} \times Rag \times T \times t \times C_F \times W$$

and the natural factors (*C*, *R*, *E*)

$$R_{C_2S} = \frac{2 \times 56}{60} \times Rag \times T \times t \times C_F \times W$$

and the natural factors (*C*, *R*, *E*)

$$R_{C_4AF} = \frac{4 \times 56}{102 + 159} 9.5 \times Rag \times T \times t \times C_F \times W$$

and the natural factors (*C*, *R*, *E*)
where :
Rag = proper mechanical strength of the aggregates (daN/cm²)
T = temperature (°C)

t = hydration time (hours, days, years)
C_F = degree of smoothness (%R or cm^2/g)
W = air, water humidity conditions (%)
C = concentration in salts, acids, bases, oils, petroleum etc. (%)
R — solar rays, ultraviolet X, α, β, γ, neutrons
E = wind forces, winds, strems, hurricanes

APPENDIX 8

II. Mechanical strength factors of the pure compound-based white and coloured aluminous cements (elaborated by the author)

$$R_{C_3A} = \frac{3 \times 56}{102} \times Rag \times T \times t \times C_F \times W$$

and the natural factors (C,R, E)

$$R_{C_{12}A_7} = \frac{12 \times 56}{7 \times 102} \times Rag \times T \times t \times C_F \times W$$

and the natural factors (C, R, E)

$$R_{CA} = \frac{56}{102} \times Rag \times T \times t \times C_F \times W$$

$$R_{CA_2} = \frac{56}{2 \times 102} \times Rag \times T \times t \times C_F \times W$$

and the natural factors (C, R, E)

$$R_{CA_6} = \frac{56}{6 \times 102} \times Rag \times T \times t \times C_F = W$$

and the natural factors (C, R, E)

Rag — mechanical strength of the aggregate (daN/cm^2)
T — temperature (°C)
t — hydration time (hours, days, years)
C_F — degree of smoothness (R % or the specific surface cm^2/g)
W — air or water humidity (%)
C — concentration in salts, acids, bases, oils, petroleum etc. (%)
R — solar rays, ultraviolet, x, α, β, γ, neutrons
E — wind forces, wind, storms, hurricanes

REFERENCE

[1] S. Solacolu, "Physical Chemistry of the Technical Silicates" (in Romanian), Ed. Tehnică, Bucharest, 1968.

Revue Roumaine de Chimie, 33, 2, 217–221 (1988)

COMPTES RENDUS

P. F. Gordon and P. Gregory, "Organic Chemistry in Colour", Springer Verlag, Berlin, 1987. Soft cover, 322 pp, ISBN 3–540–17260–2, DM 58

The Springer Study Edition is a reprint of the original hard cover edition (Springer Verlag, Berlin, 1983). The two authors are associated with dyestuffs research at the ICI Company in Birmingham. They produced a delightful book addressed to mainstream organic chemists, describing all problems pertinent to colour.

The first chapter (The Development of Dyes) is a historical introduction which starts by enumerating the natural dyes (only indigo and the black Logwood are still in use); then Perkin's serendipitous discovery of Mauvein is described, followed by the fast development of the German dyestuffs industry based upon the work of Kekulé, Hofmann, Caro, Martius, Baeyer, Fischer, Böhn, Graebe and Liebermann. At present the market is dominated by USA and Japan followed by Britain, West Germany and Switzerland. In less than a century, the natural dyestuffs have been almost completely superseded by synthetic products: more than 7000 substances are produced nowadays for dyeing textiles and for printing, with world sales of more than two billion dollars. The present-day chromogens, which often have better fastness properties than natural dyes, include azo dyes, sulphur dyes, vat dyes based mainly on anthraquinones, phthalocyanines. With the introduction of semisynthetic and synthetic fibres, corresponding dyestuffs have been developed. The dyestuffs industry was the first organic chemical manufacturing industry, and thus it is no coincidence that the major dyestuffs companies such as BASF or ICI had successful pharmaceutical, agrochemical and other organic chemistry intensive divisions.

The second and the most substantial chapter (Classification and Synthesis of Dyes) describes the main classes of dyes according to their structure. Then the synthesis of dye intermediates (carbocyclic and heterocyclic aromatics) and of dyes is described with a thorough discussion, including electronic effects and reaction mechanisms. Thus the paragraph on the synthesis of azo dyes starts with an in-depth kinetic dscription of the diazo condensation reaction depending on the pH of the solution, then the coupling reaction is similarly detailed.

Chapters 3 (Azo Dyes) and 4 (Anthraquinone Dyes) are structured analogously and constitute together a third of the book. They have sections on the structure of these dyes, on their tautomerism and metal complexes, and on relationships between colour and constitution. The last sections are highly interesting, as they start with the early theories based upon empirical findings, and one sees how by gradual accumulation of knowledge the theories became more precise. The best predictions on the basis of VB and MO theories so far have been obtained by means of the Roothaan equations solved semiempirically according to the Pariser-Parr-Pople model. Thus not only the colour (λ_{max}) but also the tinctorial strength (calculated oscillator strength) may be quantitatively predicted.

Chapter 5 is entitled Miscellaneous Dyes, and presents vat dyes (indanthrones, benzanthrones and sulphur-containing vat dyes), indigoid dyes, phthalocyanines, polymethine dyes (oxonols, cyanines, merocyanines, hemicyanines), di- and tri-aryl carbonium dyes, and nitro/nitroso dyes. Within each group, a discussion is included on relationships between colour and constitution. The authors indicate why some of the dyes with poor fastness are still in use: the reason is cost-effectiveness, i.e. cheap dyes for paper in contrast to expensive dyes for curtains, furnishings or carpets. Interesting hints are given on the discovery of phthalocyanines by chemists of Scottish Dyes Ltd. (now part of ICI) from phthalic anhydride and ammonia in iron vessels when a deep blue contaminant of phthalimide resulted. Its structure (iron phthalocyanine) was elucidated chemically by R. P. Linstead, and confirmed by X-ray diffraction by Robertson. The authors give a detailed account of the reason why the indigoid chromogen is so bathochromic (actually, in non-polar solvents or in the vapour state indigo is red).

The last (6th) chapter is entitled: Application and Fastnees Properties of Dyes. It starts by describing textile fibres: natural, semisynthetic and synthetic (polyamides, polyester and polyacrylonitrile). The five broad types of dye-fibre interaction (physical adsorption, solid solution, insoluble aggregates within the fibre, ionic bonds, covalent bonds) are reviewed. As application, various dyeing processes result, e.g. for polyesters the carrier, or high-temperature, or pad-dry heat processes; for cotton, the introduction of reactive dyes (by ICI in

1956) based on 1,3,5-triazines (later Bayer extended reactive dyes to pyramidine derivatives). The light fastness of dyes is discussed in detail indicating how a Hammett plot may distinguish for azo dyes between reductive fading and oxidative fading. The fastness is a function of nucleophilic displacements of halogen bonded to both fibre and dye. Alkylaminoanthraquinones fade by dealkylation; this mechanism can also operate for azo dyes.

The phototendering of fibres is mentioned and explained by two possible mechanisms: formation of singlet oxygen, or hydrogen abstraction from the fibre by triplet sensitized dye. Also, the heat fastness and bleach fastness of dyes are described.

Each chapter is followed by a few bibliographic general references. An appendix indicates about 30 references on colour, its measurement and perception, as well as books on MO theory. A second appendix mentions the Colour Index (3rd Edition). The book has a Colour Map on the internal side of the back cover. Author and subject indexes provide substantial help.

The book is excellently produced and illustrated with numerous carefully drawn formulas, tables (59) and figures (52). Although it assumes familiarity with organic chemistry, it is self-consistent providing much of the background for understanding how and why organic reactions take place, by including details on steric and electronic effects. Therefore the book is of interest to all organic chemists, to those wishing to know about progress in dyestuffs research, and to the historians of organic chemistry, from student level to research worker or teaching staff.

In the preface, the authors state in a footnote that they did not include a chapter on photographic dyes because of space reasons. A highly readable chapter on this topic, like the other six chapters, would be a welcome addition in a future new edition of this book.

Alexandru T. Balaban
Polytechnic Institute, Bucharest

W. P. Duncan and A. B. Susan (eds.), "Synthesis and Applications of Isotopically Labeled Compounds", Proc. Internat. Symposium held in Kansas City, Missouri, 6—11 June 1982, 508 pp, hard cover, Dfl. 275, ISBN 0—444—42152—1 (Elsevier Sci. Publ. Co., POB 211, Amsterdam, or POB 1663, Grand Central Station, New York, NY 10163), 1983.

The importance of isotopically labeled compounds for medicine, biology, environmental sciences and chemistry hardly needs to be stressed. The advent of multinuclear NMR spectroscopy further increased the interest in stable isotope labeling. The 1st symposium in this area was sponsored by the Midwest Research Institute in Kansas City, and supervised by an international scientific committee of ten scientists (one of whom was the present reviewer) from USA, England, France, Switzerland and Roumania; 330 participantes from 18 countries attended the symposium which was held in the Hyatt Regency Hotel, Kansas City, MO.

The plenary lectures were held by E. A. Evans (Synthesis and applications of tritium-labeled compounds), L. Pichat (Applications and synthesis of ^{14}C-labeled compounds), J. S. Fowler and A. P Wolf (Short-lived positron emitter labeled radiotracers — present status), J. A. Elvidge (Tritium NMR spectroscopy and its applications). A. Benakis (Radioactive labeled compounds in drug metabolism studies), W. R. Waterfield (Quality control of radio-labeled chemicals), and E. Buncel (Catalysis and specificity of hydrogen-deuterium exchange).

The numbers of communications are listed below for each of the 15 scientific sessions, some of which were followed by panel discussions (PD):

1 — Stable and radioactive isotopes in pharmacology and toxicology (4+PD)
2 — Low level radioactivity waste disposal (3 + PD)
3 — Isotopic carbon (4 + PD)
4 — Synthesis and applications of ^{10}B-labeled compounds for ^{10}B-neutron capture therapy (7)
5 — Synthesis and applications of isotopically labeled compounds other than ^{2}H and ^{3}H (including also ^{14}C, ^{13}C, ^{32}P, ^{36}Cl, ^{82}Br, ^{125}I) (11)
6 — High performance liquid chromatography (including detection, analytical and preparative HPLC, radio-HPLC) (5)
7 — Isotopes in organic and bioorganic chemistry (6)
8 — Stable isotopes in biomedical research (7)
9 — Tritium NMR spectroscopy and applications (6)
10 — Isotopes in pharmacology and drug metabolism research (5 + PD)

11 — Labeled compounds in environmental and industrial reasearch (9)
12 — Separation of isotopes (7)
13 — Synthesis and applications of organic compounds labeled with isotopic hydrogen (10)
14 — Radiochemical analysis, purification and storage (5)
15 — Recent developments and future trends (4)

The book ends with Dr. A. B. Susan's closing remarks, the titles of the posters (30 + + 25 in two sessions), and an author index.

It will be impossible to highlight all the important papers presented at the symposium, so that the following ones reflect the subjective interest of the reviewer. For uniformity, all authors were requested to submit camera-ready manuscripts on pre-lined paper supplied by the publisher : ten pages for a plenary lecture, six pages for a section lecture, and two pages for a communication. The reviewer's section lecture was entitled "Steric *versus* electronic effects of deuterium".

In the panel discussion of section 1, chaired by T. A. Baillie, it was mentioned by W.J.A. Vandenheuvel, who had delivered the section lecture, that 2-deutero-3-fluoro-D-alanine, developed by Merck, Sharp and Dohme, was a promising therapeutic drug (an antagonist of alanine whose deuteration retards its biodegradation).

In the section 3, the section lecture was delivered by G. D. Mateescu : Synthesis and high resolution ^{13}C-and ^{15}N-NMR of visual pigments and related systems.

The conclusion of the communications held in section 4 is the hope that the advent of monoclonal antibodies may allow the achievement of a suitable boron differential between normal and malignant cells to attain selective destruction of the latter by the nuclear reaction $^{10}B(n, \alpha)^{7}Li$. One of the second generation compounds is $Na_2B_{12}H_{11}SH$ used in Japan for glioblastoma therapy, and third-generation compounds are targeted specifically to neoplastic cells. The boron-loaded tumor-associated antibodies are discussed by Wellum, Zamenhof and Tolpin. 17,α-Carboranyltestosterone acetate was synthesized for neutron capture therapy of cancers of the female and male reproductive systems.

In section 7, C.C. Lee described the use of ^{14}C and ^{13}C in mechanistic studies with vinyl cations, where the isotopes gave evidence for automerizations (degenerate rearrangements) of triarylvinyl cations.

Interesting communications were presented in section 9, based on the most sensitive nuclide for NMR : tritium NMR spectroscopy was developed by J.R. Jones and J. A. Elvidge at the University of Surrey in England.

The panel discussion of section 10 was entitled "Applications of stable isotopes to bioavailability, bioequivalence and human drug interaction studies". The consensus of the panel's opinion was that stable isotopes can be used in humans with fewer restrictions than radioisotopes ; there is a tendency away from using multiple deuterium labels to avoid kinetic isotope effects, and use instead a single ^{13}C or ^{15}N label in a metabolically stable position.

In section 12, Gauthier, Hackett and Wills reported that one installation may effect a CO_2 laser separation of ^{13}C with high productivity by irradiating $CHClF_2$ at 100 Torr pressure in a 2 m long cell with photons of 1041.3 cm^{-1} : the resulting C_2F_4 contains 50 % ^{13}C ; in a scaling-up using a 3-liter cell. a five-minutes irradiation reacted 40 % of the ^{13}C in the cell, which corresponds to 2 % of the world production of 5 kg per year via low-temperature CO distillation.

J. I. Garnett and M. A. Long presented in section 14 new developments in one-step catalytic methods for ^{2}H and ^{3}H labeling of organic compounds using homogeneous Group VIII transition metals (Ir, Rh, Ru), Lewis acids, or zeolites.

The high-level tritium facility at the Lawrence Berkeley Laboratory, California, designed to handle up to 20kCi of gaseous T_2 and 6 kCi of HTO, prepared labeled endorphin and other biological compounds with specific activities of 100 kCi/mole, as shown by W. R. Erwin, C. T. Peng and R. M. Lemmon.

The last section contains two contributions on the relative merits of stable and radioactive isotopes in biomedical research : one by Matwiyoff et al., and the other by C.T. Peng and A. B. Susan. In addition, Van Etten and Risley reported on the ^{18}O-isotope shifts in ^{13}C-and ^{15}N-NMR spectroscopy ; G. D. Mateescu with G. M. Benedikt and M. P. Kelly contributed a paper on new dimensions in ^{17}O-NMR spectroscopy.

The volume is produced in excellent conditions and provides a wealth of data on all areas in which labeled compounds are used, giving also numerous references to the literature. Far from being a drawback, the direct reproduction of authors' manuscripts offers an error-free and rapidly printed volume.

A.T. Balaban
Polytechnic Institute, Bucharest

T. H. Pierce and B. A. Hohne (eds.) "Artificial Intelligence Applications in Chemistry", Am. Chem. Soc. Symposium Series No. 306, ACS, Washington D. C., 1986. Clothbound, 394 pp., ISBN 0-8412-0966-9, 71.95 US $ (export price)

The editors state in their preface that chemistry is an ideal field for applications for artificial intelligence (AI), and thus is one of the leading areas in these applications. Whereas computer applications developed from theoretical chemistry tend to be algorithmic and numerical, AI applications tend to be heuristic and symbolic by nature.

The initial chapter is "Artificial intelligence : the technology of expert systems" by D. H. Smith. The aim of this chapter is to demystify the technology of expert systems, i.e.of a special kind of software. Two provocative statements of the author are : (i) knowledge engineering is the technology base of the "Second Computer Age"; (ii) What's on the horizon is not just the Second Computer Age, it's the important one. The basic idea is that KNOWLEDGE IS POWER. Therefore, for fusing expertise of several fields or for preserving the organizational memory in a competitive branch, expert systems were developed in various areas such as chemical synthesis and analysis, medical dignosis, genetic engineering, computer assisted design. Discussed examples are biological reactors, communications satellites, and space stations.

The 27 communications presented at the Symposium are grouped into five sections : Expert systems, Computer algebra, Handling molecular structures, Organic synthesis, and Analytical chemistry. Author and subject indexes are appended.

Among the expert systems described in the first section, we mention two communications by J.D. Stuart and coworkers based on a general-purpose software package (Rule Master) for building and delivering expert systems, applied for diagnosing faults in large transformers (based on GLC analysis of the insulating oil), for quality control and quality assurance, or for choosing the best suited protection glove material for various solvents. Two other communications describe (i) a real-time expert system for process control by Hawkinson et al., providing intelligent alarming and process diagnosis, control and optimization, and (ii) the formulation of agricultural chemicals by Hohne and Houghton.

The first communication in the second section discusses the MACSYMA computer algebra system which operates with symbols, numbers, or graphics ; it can solve equations without specifically designed algorithms. A. L. Smith describes the high-level computer language TK ! Solver for solving sets of algebraic equations. Chemical kinetics problems are discussed by Edelson. Finally, Cornelius, Cabrol and Cachet describe the computer program GEORGE which is a "problem-solving partner" for freshmen in chemistry.

Wipke and Hahn describe in the first paper of the third section the AIMB algorithm which builds quickly 3-D molecular models much faster than the MM2 (molecular mechanics-2) procedure, mimicking the manual procedures used by chemists using methods of expert systems. T. E. Klein, C. Hansch and their coworkers present the KARMA system for drug receptor mapping analysis, with beautifully colored reproductions of the enzyme-ligand complex formed by alcohol dehydrogenase with a substituted pyrazole. An interesting intelligent sketch pad, described by Trindle, manipulates chemical graphs in LISP, and derives (from a crude sketch of the structure), atom coordinates suitable for MM programs or for *ab-initio* quantum chemical calculations ; in addition, it derives various properties (bond strengths, electronic, IR, and NMR spectra). S. H. Bertz and W. C. Herndon, in their communication (The similarity of graphs or molecules) give a new definition of molecular similarity which provides a new way to measure molecular complexity.

In the section on Organic Synthesis, Wipke and Dolata discuss a multivalent logic predicate calculus approach to synthesis planning. This paper has wider philosophical implications about the question whether chemical theories and chemical knowledge can be axiomatized, or not yet. Along with the three main programs already existing in this area, namely Wipke's SECS, Corey's LHASA, and Gelernter's SYNCHEM, a new program, QED, is presented, which is able to infer a synthesis plan in high-level terms without reference to reactions.

Moseley et al. present grammar-based expert-system rules for Diels-Alder reactions using the Wiswesser Line Notation to produce valid synthons, and frontier MO's for verifying the disconnections (heteroatoms are possible).

Wang et al. describe an expert system for organic synthesis which uses a resolution-based theorem prover as its reasoning component, and which can make use of large databases (Institute for Scientific Information or Chemical Abstracts).

Gasteiger et al., describe in the paper "Acquisition and representation of knowledge for expert systems in organic chemistry" the system EROS which considers electronegativities, polarizabilities, inductive and resonance efects, in predicting the outcome of chemical reaction and is able to design organic syntheses.

In the last section, which includes seven papers, we mention expert systems for HPLC, ultracentrifugation, interpretation of IR spectra, mass spectra and organic structure determination on the basis of IR and mass spectra.

The book is reproduced by photoprinting from authors' manuscripts, and is thus error-free. It contains contributions of some of the most active scientists in this field. As already mentioned, some of the authors give not only a narrow technical description but a wider, more philosophical outlook. The book is an excellent introduction for all research-oriented chemists interested in artificial intelligence.

Alexandru T. Balaban
Polytechnic Institute, Bucharest

Attila Veres and Istvan Kiss, "Nuclear Chemistry", Akadémiai Kiadó, Budapest, and Elsevier Scientific Publ., Amsterdam, 1987, ISBN 963-05-4063-0, 619 pp, hard cover.

The twelve chapters of the comprehensive monograph are the following :

1. Basic properties of the atomic nucleus (20 pp)
2. Nuclear reactions (15 pp)
3. Radioactive decay (44 pp)
4. Interaction of nuclear radiation with matter (55 pp)
5. Investigation methods of chemical structure based on the interaction of nuclear radiation with matter (110 pp)
6. Radioactive tracing (10 pp)
7. The chemistry of ultra-low concentrations (11 pp)
8. Hot atom chemistry (51 pp)
9. Radiation chemistry (51 pp)
10. Isotope effects (81 pp)
11. Isotope enrichment (37 pp)
12. Nuclear reactors (42 pp)

It can be seen that the book discusses all the important aspects of the large area known as "Nuclear Chemistry". It is true that chapter 5 is quite large with respect to all other chapters, and that chapters 6 and 7 are rather small. The book is written by two well-known nuclear chemists and its orientation is towards the traditional areas of inorganic nuclear and radiochemistry.

A specially valuable asset of the book is constituted by the exercises (provided with answers) and the references at the end of each chapter; in addition to references cited in the text, relevant monographs are listed separately.

Especially attractive and extensive treatments can be observed for positronium and muonium, muonium spin resonance, and other exotic atoms. Among the methods based upon the interaction of nuclear radiation with matter, the Mössbauer spectroscopy and the tracer Mössbauer spectroscopy can also be highlighted for the clear and comprehensive treatment.

In a future edition of this valuable book one would like to see more applications directed, towards the organic and biological areas of nuclear chemistry such as radioimmunoassay methods the production of grafted (not "injected") polymers, food irradiation, radiation polymerization of various monomers (e.g. styrene, not "styrol").

The book has an extensive appendix (over 60 pages) with tables of physical constants; stable nuclides, important radionuclides; transuranium elements (for element 104 both the name Unnilquadrium, Unq, and Kurchatovium are to be found in the book); the natural radioactive series; binding energies for orbital electrons; mass attenuation coefficients for photons of various energies and 27 common elements.

The book will be of interest to students, research workers and teaching staff in all disciplines using isotopes.

A. T. Balaban
Polytechnic Institute Bucharest

polarizabilities, inductive and resonance effects in predicting the outcome of chemical reaction and its use in design organic syntheses.

In the last section, which includes seven papers, we mention expert systems for ESR, ultracentrifugation, interpretation of 13C spectra, mass spectra and organic structure determination on the basis of IR and mass spectra.

The book is reproduced by photo-offseting from authors' manuscripts, and is thus cheaper. It contains contributions of some of the most active scientists in this field. As already mentioned, some of the authors give not only a narrow technical description but a wider, more philosophical outlook. The book is an excellent introduction for all research-oriented chemists interested in artificial intelligence.

Alexandru T. Balaban
Polytechnic Institute, Bucharest

Attila Vértes and István Kiss: "Nuclear Chemistry". Akadémiai Kiadó, Budapest, and Elsevier Scientific Publ. Amsterdam, 1987. ISBN 963 05 4065 0. 410 pp. hard cover.

The twelve chapters of the comprehensive monograph are the following:

1. Basic properties of the atomic nucleus (23 pp)
2. Nuclear reactions (18 pp)
3. Radioactive decay (44 pp)
4. Interaction of nuclear radiation with matter (55 pp)
5. Investigation methods of chemical structure based on the interaction of nuclear radiation with matter (110 pp)
6. Radioactive isotopes (15 pp)
7. The chemistry of ultra-low concentrations (14 pp)
8. Hot atom chemistry (24 pp)
9. Radiation chemistry (31 pp)
10. Isotope effects (31 pp)
11. Isotope techniques (37 pp)
12. Nuclear reactors (42 pp)

It can be seen that the book discusses all the important aspects of the large area known as "Nuclear Chemistry". It is true that chapter 5 is quite large with respect to all other chapters, and that chapters 6 and 7 are rather small. The book is written by two well-known Hungarian chemists and its orientation is towards the traditional areas of inorganic, nuclear and radiochemistry.

A specially valuable asset of the book is constituted by the exercises (provided with answers) and the references at the end of each chapter; in addition to references cited in the text, relevant monographs are listed separately.

Especially informative and extensive treatment can be observed for positronium and muonium, nuclear spin resonance and other exotic atoms. Among the methods based upon the interaction of nuclear radiation with matter, the Mössbauer spectroscopy and the tracer Mössbauer spectroscopy can also be highlighted for the clear and comprehensive treatment.

In a future edition of this valuable book one would like to see more applications directed towards the organic and biological areas of nuclear chemistry such as radiation processes and for the production of grafted and "tailored" polymers, food irradiation, radiation polymerization of various monomers (e.g. styrene, methyl styrol).

The book has an extensive appendix (over 40 pages) with tables of physical constants, nuclide tables, important radionuclides, transuranium elements (for which both the name [illegible] and Kurchatovium are to be found in the tables), the natural radioactive series, binding energies for orbital electrons, mass attenuation coefficients for photons of various energies and 27 common elements.

The book will be of interest to students, research workers and teaching staff in all disciplines using isotopes.

A. T. Balaban
Polytechnic Institute, Bucharest

NOTE POUR LES AUTEURS

La Revue Roumaine de Chimie publie des articles en anglais, français, russe, allemand ou espagnol. Les auteurs sont priés d'envoyer des articles et des comptes rendus inédits.

Les manuscrits seron dactylographiés à double interligne. La bibliographie, les tableaux et la légende des figures seront placés après le texte.

Si l'article fait partie d'une série numérotée, la partie précédente sera donnée comme première référence.

Chaque article sera précédé d'un résumé comprenant quinze lignes au maximum.

Les références bibliographiques dans le texte seront faites par des exposants sans parenthèses et paraitront à la fin de l'ouvrage.

Les publications périodiques mentionnées dans la bibliographie seront présentés suivant les prescriptions internationales : le nom de l'auteur précédé de l'initiale du prénom, le titre du périodique abrégé conformément à « Chemical Abstracts » et souligné par une ligne, le numéro du tome indiqué par des chiffres arabes et souligné par deux lignes, suivi de la première page de l'article ; à la fin, l'année de la parution sera placée entre parenthèses. Le numéro de la revue ne sera pas indiqué si les pages du volume sont numérotés consécutivement.

Les textes des livres ou traités inclueront : le nom des auteurs, l'initiale du prénom, le titre du livre entre guillemets et sans être souligné, le numéro du tome précédé par l'abréviation « vol. » (ou « Bd. »), le numéro de l'édition, les éditions (the publisher), la localité de la parution du livre, l'année de la parution et la page de la référence précédée(s) par l'abréviation « p. » (ou « S ».)

Les brevets seront indiqués comme suit : l'auteur ou la firme, le pays et le numéro du brevet, la date et la revue (*Chem. Abstr.*) Par ex. : M. Jones (to Union Carbide Co.), Brit. Pat. 601 2238, 2 Sept. 1959 ; cf. *Chem. Abstr.*, **54**, 12808 (1960).

Si la référence n'a pas été lue en original, on indiquera aussi la revue de référence consultée.

Les diagrammes seront tracés à l'encre de Chine sur papier calque. Les tableaux et les figures (en nombre strictement nécessaire) ainsi que les courbes dans les figures seront numérotés par des chiffres arabes. Leur explication sera donnée dans la légende des figures. Prière de ne pas inscrire les mêmes données dans les tableaux et les figures. Chaque tableau aura un titre. On indiquera dans le texte la place approximative des tableaux et des figures. Les formules chimiques seront incluses dans le texte : en outre, elles seront transcrites sur papier calque, à l'encre de Chine.

Les auteurs sont priés d'indiquer les caractères italiques (en soulignant les lettres au crayon), ainsi que tout autre caractère spécial ; les préfixes *ortho*, *meta*, *para*, *cis*, *trans*, etc. seront soulignés pour indiquer leurs caractères italiques et ne seront jamais écrits avec des majuscules.

Aucune correction à la main ne sera admise sur le manuscrit. Les corrections seront tapées à la machine. Les lettres grecques ou d'autres sysmboles spéciaux seront insérés à la main à l'encre clairement.

Le manuscrit sera signé par l'auteur.

Le titre courant aura 50 lettres au maximum.

L'entière responsabilité du contenu des articles apartient aux auteurs.

Sur demande on peut obtenir une note plus complète.

PRINTED IN ROMANIA

NOTE POUR LES AUTEURS

La Revue [illegible] de Chimie publie des articles en anglais, français, russe, allemand et [illegible]. Les auteurs sont priés d'envoyer des articles et des comptes rendus [illegible].

Les manuscrits seront dactylographiés à double interligne. La bibliographie, les tableaux et la légende des figures seront placés après le texte.

Si l'article fait partie d'une série numérotée, la partie précédente sera donnée comme première référence.

Chaque article sera précédé d'un résumé comprenant [illegible] lignes au maximum.

Les références bibliographiques dans le texte seront faites par des exposants [illegible] et [illegible] à la fin de l'ouvrage.

Les publications périodiques mentionnées dans la bibliographie seront présentées suivant les prescriptions internationales : le nom de l'auteur précédé de l'initiale du prénom, le titre du périodique abrégé conformément aux Chemical Abstracts et souligné par une ligne, le numéro du volume indiqué par des chiffres arabes et souligné par deux lignes, suivi de la première page de l'article [illegible] la fin, l'année de la parution sera placée entre parenthèses. Le numéro de la revue ne sera pas indiqué si les pages du volume sont numérotées consécutivement.

Les textes des livres ou traités indiqueront le nom des auteurs, l'initial du prénom, le titre du livre [illegible], le numéro du tome précédé par l'abréviation «vol.» [illegible], le numéro de l'édition, les éditions (the publisher), la localité de la parution [illegible], l'année de la parution et la page de la référence précédée par l'abréviation [illegible] (ou «pp.»).

Les brevets seront indiqués comme suit : l'auteur ou la firme, le pays et le numéro du brevet, la date et la revue (Chem. Abstr.) [illegible] M. Jones (to [illegible] Carbide [illegible]) [illegible] Pat. 807 [illegible]; Chem. Abstr., 57, 1208 [illegible].

Si la référence n'a pas été lue en original on indiquera aussi la revue de référence consultée.

Les diagrammes seront tracés à l'encre de Chine sur papier calque. Les tableaux et les figures [illegible] strictement nécessaires ainsi que les courbes dans les figures seront numérotés par des chiffres arabes. Leur explication sera donnée dans la légende des figures. Prière de ne pas inscrire les mêmes données dans les tableaux et les figures. Chaque tableau aura un titre. On indiquera dans le texte la place approximative des tableaux et des figures. Les formules chimiques seront incluses dans le texte; en marge, elles seront [illegible] au crayon, à l'encre de Chine.

Les auteurs sont priés d'indiquer les caractères italiques en soulignant les lettres au [illegible] ainsi que [illegible] avec des majuscules.

Aucune correction [illegible] ne sera admise sur le manuscrit. Les corrections seront [illegible] les lettres grecques ou d'autres caractères spéciaux seront [illegible].

[illegible] envoyé par l'éditeur.

Le texte [illegible].

[illegible] responsabilité du contenu des articles appartient aux auteurs.

[illegible] une [illegible] plus complète.

[illegible]

CENTRALA INDUSTRIEI LINII
BUCURESTI

CENTRAL OF WOOL INDUSTRY

is the main producer of wool and wool-type fabrics in Romania. Its specialized enterprises produce a wide range of cloth, blankets and carpets with a large display of patterns and colours. An increasing place in our production is held by chemical fibres (cellofibre, polyester, PNA) obtained by modern technologies and superior treatment which endow the wool-type fabrics with important characteristics :

- wear and light resistance ;
- high dyeing affinity ;
- good wrinkle resistance ;
- moth resistance ;
- good thermal protection ;
- soft touch and excellent resiliency.

The high quality of our products makes them appreciated by specialists and customers in Romania and abroad. They are used for ready-made clothes and for furnishing and decoration of houses, institutions (laboratories, hotels, etc.).

ORSZÁGOS MŰSZAKI INFORMÁCIÓS KÖZPONT ÉS KÖNYVTÁR

1988 MAR 2 5

TRAVAUX PARUS AUX ÉDITIONS DE L'ACADÉMIE DE LA RÉPUBLIQUE SOCIALISTE DE ROUMANIE

ELENA CAUŞESCU, **Răşini de hidrocarburi vol. 1**, 1988, 344 p.

ELENA CEAUŞESCU, **Progrese în chimia şi tehnologia polimerilor**, 1986, 446 p.

ELENA CEAUŞESCU, **Forschungen im Bereich der Chemie und Technologie der Polymere**, 1986, 444 p.

ELENA CEAUŞESCU, **Cercetări în chimia şi tehnologia polimerilor**, 1983, 520 p.

ELENA CEAUŞESCU, **Noi cercetări în domeniul compuşilor macromoleculari**, 1981, 536 p.

ELENA CEAUŞESCU, **Polimerizarea stereospecifică a izoprenului**, 1979, 307 p.

ELENA CEAUŞESCU, **Research work on synthesis and characterization of macromolecular compounds. Contributions**, 1974, 251 p.

I. G. MURGULESCU, **Introducere în chimia fizică, Vol. I. 1. Atom, molecule, legătură chimică**, 1976, 560 p.

I. G. MURGULESCU, V. EM. SAHINI, **Introducere în chimia fizică, Vol. I, 2. Structura şi proprietăţile moleculelor**, 1979, 601 p.

I. G. MURGULESCU, E. SEGAL, **Introducere în chimia fizică, Vol. II 1. Teoria molecular-cinetică a materiei**, 1979, 1036 p.

I. G. MURGULESCU, TATIANA ONCESCU, E. SEGAL, **Introducere în chimia fizică. Vol. II. 2. Cinematică chimică şi cataliză**, 1981, 1024 p.

I. G. MURGULESCU, J. PĂUN, **Introducere în chimia fizică, Vol. I. 3, Nucleul atomic, reacţii nucleare, particule elementare**, 1982, 606 p.

I. G. MURGULESCU, RODICA VÎLCU, **Introducerea în chimia fizică, Vol. III. Termodinamica chimică**, 1982, 624 p.

I. G. MURGULESCU, O. M. RADOVICI, **Introducere în chimia fizică, vol. IV, Electrochimia**, 1986, 410 p.

R. VÎLCU, M. LECA, **Termodinamica polimerilor prin cromatografie de gaze**, 1987, 238 p.

I. ZUGRĂVESCU, M. PETROVANU, **Cicloadiţii 3+2-dipolare**, 1987, 446 p.

RAUL MIHAIL, ION GROZEANU, **Estimarea secvenţială aplicată sistemelor chimice**, 1986, 406 p.

M. BREZEANU, L. PATRON, M. ANDRUH, **Combinaţii complexe polinucleare şi aplicaţiile lor**, 1986, 244 p.

A. T. BALABAN et al., **Labelled compounds and radiopharmaceuticals applied in nuclear medicine**, coédition avec John Wiley and Sons, 1986, 742 p.

D. PURDELA, **Nomenclatura chimiei organice — IUPAC**, 1986, 454 p.

PETRU BUDRUGEAC, **Probleme de chimie**, 1986, 280 p.

T. ONCESCU, S. G. IONESCU, **Conversie fotochimică şi stocare de energie**, 1985, 272 p.

V. DRĂGUŢAN, A. T. BALABAN, M. DIMONIE, **Olefin Metathesis and Ring-Opening Polymerization of Cyclo-Olefins**, coédition avec John Wiley and Sons, 1985, 544 p.

C. LITEANU, I. RICĂ, **Optimizarea proceselor analitice**, 1985, 360 p.

N. PERESCU, **Chimia extracţiei cu solvenţi şi aplicaţii**, 1985, 212 p.

V. E. SAHINI, M. HILLEBRAND, **Chimie cuantică în exemple şi aplicaţii**, 1984, 378 p.

GH. MARCU, **Chimia compuşilor coordinativi**, 1984, 415 p.

E. CORDOS, C. MANOLIU, **Spectrometria de absorbţie şi fluorescenţă atomică**, 1984, 178 p.

C. BODEA, **Tratat de biochimie vegetală p. II, t. 5**, 1984, 438 p.

N. ASANDEI, A. GRIGORIU, **Chimia şi structura fibrelor**, 1983, 395 p.

N. IONESCU, M. CĂLDĂRARU, **Oxidarea catalitică a olefinelor inferioare**, 1983, 178 p.

C. CAŞCAVAL, **Studiul polimerilor prin piroliză şi cromatografie de gaze**, 1983, 220 p.

C. I. SIMIONESCU, F. DANES, **Originea vieţii**, 1983, 110 p.

C. BODEA, **Tratat de biochimie vegetală, p. II. t. IV**, 1982, 480 p.

I. GĂLĂŢEANU, **Procese şi metode radiochimice în energetica nucleară**, 1981, 234 p.

CR. SIMIONESCU, VALERIA GORDUZA, **Polimeri biocompatibili şi biologic activi**, 1980, 479 p.

M. FLORESCU, **Metode ştiinţifice în dezvoltarea industriei chimice moderne**, 1979, 256 p.

C. GH. MACAROVICI, **Analiza chimică cantitativă anorganică**, 1979, 457 p.

I. ZUGRĂVESCU, MAGDA PETROVANU, **N-ylid chemistry**, coédition avec McGraw-Hill International Book Company U.S.A., 1977, 386 p.

ISSN 0035–3930

I. P. Informaţia c. 1684

43 426

Lei 40

$ 90 (pour un abonnement annuel)

F 1103

ACADÉMIE DE LA RÉPUBLIQUE SOCIALISTE DE ROUMANIE

REVUE ROUMAINE DE CHIMIE

TOME 33
N° 3
Mars 1988

Rev. Roumaine Chim.

RRCHAX, 33, 3, p. 223–348 (1988), Bucarest

EDITURA ACADEMIEI REPUBLICII SOCIALISTE ROMÂNIA

ACADÉMIE DE LA RÉPUBLIQUE SOCIALISTE DE ROUMANIE

COMITÉ DE RÉDACTION

Rédacteur en chef :

I. G. MURGULESCU, membre de l'Académie de la République Socialiste de Roumanie

Rédacteurs en chef adjoints :

A. T. BALABAN et V. EM. SAHINI, membres correspondants de l'Académie de la République Socialiste de Roumanie

Collège de rédaction :

EM. BRATU, ELENA CEAUŞESCU, ECATERINA CIORĂNESCU-NENITZESCU, CR. SIMIONESCU, membres de l'Académie de la République Socialiste de Roumanie; P. SPACU, membre correspondant de l'Académie de la République Socialiste de Roumanie; M. BANCIU, M. D. GHEORGHIU, I. HAIDUC, D. I MARCHIDAN, G. NIAC et D. SĂNDULESCU.

La Revue Roumaine de Chimie paraît 10 fois par an. Toute commande de l'étranger sera adressée à ROMPRESFILATELIA — sectorul Export-Import Presă, P.O. Box 12—201, télex 10376, prsfi r 78 104, 64—66, Calea Griviței, Bucarest, Roumanie

Les manuscrits, les livres et les revues proposés en échange, ainsi que toute correspondance seront envoyés à la rédaction

REVUE ROUMAINE DE CHIMIE

125, Calea Victoriei, 79717 Bucarest, Roumanie, téléphone 50 76 80

EDITURA ACADEMIEI REPUBLICII SOCIALISTE ROMÂNIA
125, Calea Victoriei 79717 Bucarest, Roumanie, téléphone 50 76 80

REVUE ROUMAINE DE CHIMIE

ORSZÁGOS MŰSZAKI

Tome 33, N° 3 **Mars, 1988**

A. C. BANCIU, Electronic spectra and magnetic moments of Ni(II) complexes synthesized with ligands from the class of substituted 1-methyl-2-carbethoxy-glyoxalanil-(1)-phenylhydrazones-(2). The square-planar — tetrahedral isomerism of these complexes . . . . 225—236

ORTANSA LANDAUER, CORNELIA MATEESCU, OLGA IULIAN and DAN GEANĂ, Experimental determination of liquid-vapour equilibrium curves and correlation by different activity models for the cyclohexane-monochlorocyclohexane and cyclohexane-water systems (in French) . . . . 237—251

JEAN-LOUIS BRISSET, Thermodynamics of some iron complexes in water-pyridine mixtures . . . . 253—262

Z. FINTA, J. ZSAKÓ and CS. VÁRHELYI, Kinetics and mechanism of substitution reactions of complexes. LIX. Influence of pH upon the aquation kinetics of iodo-aquo-bis-dimethylglyoximato-cobalt(III) . . . . 263—269

C. FERNANDEZ-SANCHEZ, Mª T. GANDASEGUI, R. BARAJAS and J. Mª MARINAS, The effect of using aluminium phosphate-γ-alumina and aluminium phosphate-silica on the synthesis of organic esters (in Spanish) . . . . . 271—275

B. S. HOLLA, B. KALLURAYA and K. R. SRIDHAR, Studies on nitrofuran heterocycles. Part I. Synthesis and antibacterial activity of 7H, 6-(5-nitro-2-furyl)-*s*-triazolo[3,4-*b*]-1,3,4-thiadiazines . . . . 277—282

I. POP, I. CIUPE, MIOARA BUTAN, L. TEREC, L. FEY and I. BÂLDEA, Quantitative dialkylation of aromatic amines under a minimum excess of alkylation agent . . . . 283—290

A. K. EL-SHAFEI and A. M. EL-SAYED, Studies on the nucleophilic reactivity of sulphur and nitrogen in 2-mercapto-4(3H)quinazolinone under solid-liquid phase transfer catalysis conditions. . . . . 291—293

NIZAMUDDIN and D. N. PUROHIT, Infrared spectral studies of 3-hydroxy-3-methyl-1-phenyl-triazene derivatives . . . . 205—303

R. P. VARMA, B. B. BHATNAGAR and ANURADHA SINGH, Studies on physical properties of some organochloro pesticides in methanol . . . . 305—311

ROBERT SCHWARTZ and ANIKÓ SCHWARTZ, 17α-Substituted derivatives of B-nor-5-androstene-3β-ol-17-one and 5-androstene-3β-ol-17-one . . . 313—319

JAMIL AHMAD and K. BRIAN ASTIN, Correlation of reduction potentials of cyanine dyes with their orbital energies . . . . 321—324

M. SURPĂŢEANU, A. DUCA, G. SURPĂŢEANU and M. GĂBURICI, The potentiometric determination of mixtures of alkylphosphates, orthophosphoric and hydrochloric acids . . . . 325—329

FRANCISC A. GOTHARD, Predicting fluid phase equilibria by a model of equilibrium of interactions in restrained molecular systems . . . . 331—345

BOOK REVIEWS . . . . 347—348

Rev. Roumaine Chim. **33**, *3*, 223—348 (1988), Bucarest

Revue Roumaine de Chimie, **33**, *3*, 225–236 (1988)

ELECTRONIC SPECTRA AND MAGNETIC MOMENTS OF Ni(II) COMPLEXES SYNTHESIZED WITH LIGANDS FROM THE CLASS OF SUBSTITUTED 1-METHYL-2-CARBETHOXY-GLYOXALANIL-(1)-PHENYLHYDRAZONES-(2). THE SQUARE-PLANAR – TETRAHEDRAL ISOMERISM OF THESE COMPLEXES

A. C. BANCIU
ICECHIM – Centre of Physical Chemistry,
79611 – Bucharest, Spl. Independenţei 202, Romania

Received December 8, 1986

The study of electronic spectra and magnetic moments of the Ni(II) complexes synthesized with ligands from the class of substituted 1-methyl-2-carbethoxy-glyoxalanil-(1)-phenylhydrazones-(2) shows that only few of these complexes possess a whole tetrahedral or whole square-planar structure. In solid state most of these complexes are mixtures of both isomers; in some of them (almost diamagnetic) prevails the square-planar isomer while in the others (paramagnetic) the tetrahedral isomer is predominant. For all complexes the dissolution in acetone entails the conversion of the square-planar isomers into tetrahedral ones. The tetrahedral isomers exhibit a β_{35} value of approximately 0.83, i.e. a low to medium covalency degree for the Ni(II)–N chemical bonds.

I. INTRODUCTION

Structurally and chemically related to the well known formazane chelate ligands ($Ar-NH-N=C(R)-N=N-Ar'$; Ar, Ar' = substituted aryl groups; $R = -CH_3$, $-COOC_2H_5$, $-COCH_3$, $-COAr$, etc.[1]) the compounds from the class of substituted 1-methyl-2-carbethoxy-glyoxalanil-(1)-phenylhydrazones-(2), **IA**, [2-7]

I, A, B

I A: $Y = H$; $X =$ a: H;
b: $p-CH_3$; c: $m-CH_3$;
d: $p-CH_3O$; e: $m-CH_3O$;
f: $p-NO_2$; g: $m-NO_2$;
h: $p-Cl$; i: $m-Cl$;
j: $p-Br$; k: $m-Br$;

I B: a: $X = Y = p-CH_3$;
b: $X = Y = p-CH_3O$;
c: $X = p-NO_2$; $Y = p-CH_3O$;

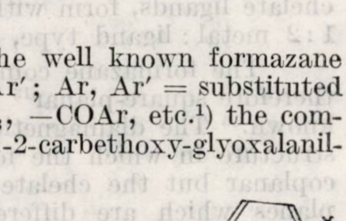

I A, B

behave as true chelate ligands which form complexes of 1 :2 metal : ligand type [2–14] with the Co(II),[2–7] Ni(II) [2,8–12] and Cu(II) [13,14] ions.

In the **I A, B** compounds, exactly as in the corresponding formazanes, the hydrogen atom of the imino-group has no acidic properties. However, in presence of bases (as triethylamine) it may dissociate so that the **I A, B** compounds yield the corresponding monovalent conjugated anions **II A, B** :

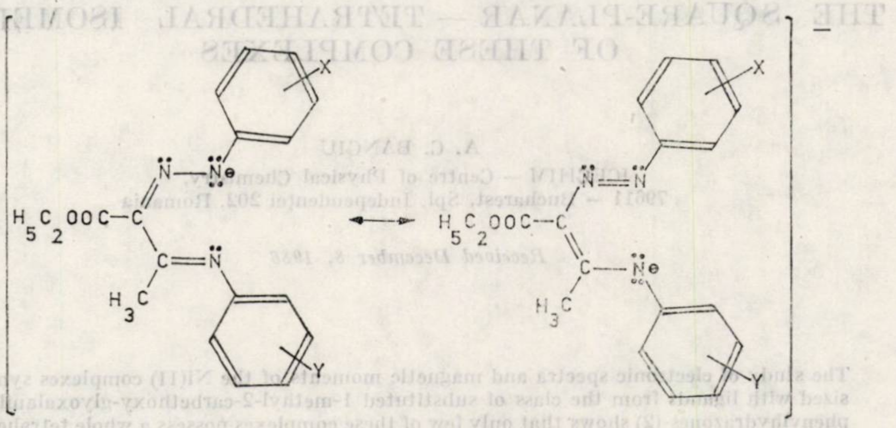

II, A, B

where the substituents X and Y have the same meanings as in the protonated ligands **I A, B** above.

The conjugated anions **II A, B** are the true chelatic complexation agents for the transition metal ions. Thus, the anions **II A, B**, as didentate chelate ligands, form with the Ni(II) ions tetracoordinated complexes of 1 : 2 metal : ligand type, i.e. Ni[II A, B]$_2$.

The formazane complexes of Ni(II) are generally diamagnetic and therefore square-planar[15] yet tetrahedral complexes of this class are also known.[15] The diamagnetic ones certainly adopt a stepped square-planar structure in which the four Ni(II)—N chemical bonds are rigorously coplanar but the chelate rings (as well as the aryl substituents) lie in planes which are different from those of the Ni(II)—N$_4$ chromophore.[15, 16]

The Ni[II A, B]$_2$ complexes are expected to assume a similar structure. Indeed, in the series of 11 complexes of Ni[II A]$_2$ type almost all are, in a first approximation, diamagnetic : they exhibit only a weak residual paramagnetism. The only exception, the Ni[II A—g]$_2$ complex, is strongly paramagnetic and assumes a distorted tetrahedral structure.[17]

To continue these investigations we started the synthesis of new **I B** type chelate ligands substituted at both aromatic rings, and of the Co(II), Ni(II) and Cu(II) complexes synthesized with these ligands ; we have also started a study of electronic spectra and magnetic moments of the new complexes.

This paper deals first with the study of the new complex Ni[II B—a]$_2$ whose spectral and magnetic properties differ from those of the Ni[II A]$_2$ complexes. Then the comparison of the electronic spectra and magnetic moments of the new complex with those of other Ni[II A, B]$_2$ complexes supplies an explanation of the unusual structure of most of Ni(II) complexes from this class and suggests corrections of some spectral band assignments in our previous papers; [10–12] those assignments were based on poorer experimental evidence.

II. EXPERIMENTAL

All reagents used were of p.a. grade.

The synthesis of the new ligand I B-a. The acetylacetic ester was condensed with *p*-toluidine to the corresponding anil, $H_5C_2COO-CH=C(CH_3)-NH-C_6H_4-p-CH_3$, in concentrated etheric solution, at room temperature, according to a previously described procedure [18] (regarding the condensation of the acetylacetic ester with aniline). The obtained anil was a light red-brown oil. *Yield*: 85% of the theoretical one. The new ligand was synthesized from this anil by azoic coupling reaction with diazotized *p*-toluidine. The anil (72 mmoles) was solved in a mixture of 200 mL ethanol and 300 mL methanol, then 86 mmoles of anhydrous sodium acetate were added and the obtained solution (which contained the sodium salt of the anil) was vigorously stirred and cooled to about 5°; into this solution was dropped an aqueous solution of *p*-tolyl-diazonium chloride [19] (freshly prepared from 72 mmoles *p*-toluidine and 75 mmoles sodium nitrite), cooled to about 5° and buffered, by addition of anhydrous sodium acetate to pH = 2—3. During dropping from the liquid reaction mixture the new ligand started to separate as a solidified oil, strongly impurified with dark red secondary reaction products. However, cooling and stirring were extended one hour more, then the reaction products were allowed to settle and separate. After drying on a porous plate, two washings with cold methanol in a Büchner funnel, recrystallization from hot methanol in presence of active charcoal, the new ligand I B-a was obtained as bright yellow-orange needle crystals whose m.p. was 79—83°. *Yield*: 19 mmoles (26% of theoretical one). Before elemental chemical analysis a sample of the compound was dried in a vacuum desiccator over P_4O_{10}.

Chemical analysis: Calculated for $C_{20}H_{23}O_2N_3$: C 71.2%; H 6.9%. Found: C 70.8%; H 7.2%.

The synthesis of the new complex Ni [II B-a]$_2$. 10 mmoles pure ligand I B-a, 6 mmoles $NiCl_2 \cdot 6H_2O$ dissolved in 35 mL cold methanol and 10 mmoles triethylamine were added to 200—220 mL hot methanol. The resulted solution was refluxed on water bath for 80 min. From the hot liquid dark violet, almost black microcrystals of complex have separated. After filtering the complex was washed at 35—40° three times with a 3% acetic acid solution; each acidic washing was followed by washing with cold methanol. The complex was finally washed in suspension with about 70 mL hot methanol and then dried, first in atmosphere then in a vacuum desiccator over P_4O_{10}. *Yield*: 3.15 mmoles (61% of the theoretical one). M.p. 196—199°. *Chemical analysis*: Calculated for $NiC_{40}H_{44}O_4N_6$: C 65.7%; H 6.0%; Ni 8.0%. Found: C 65.3%; H 6.4%; Ni 8.1%.

The elemental chemical analyses were performed by usual micromethods.

The electronic diffuse reflectance spectra were recorded with a VSU—2 Carl Zeiss (Jena) spectrophotometer within the 220—1150 nm range and with a Beckman DK—2 spectrophotometer within the 220—1400 nm range, using MgO as standard.

The electronic absorption spectra were recorded with a VSU—2 Carl Zeiss (Jena) spectrophotometer within the 350—1150 nm range, in acetone solutions of concentration $0.5 \times 10^{-4} \ldots$ $\ldots 5.0 \times 10^{-4}$ mole. L^{-1}.

The magnetic susceptibility of the solid complex was determined at room temperature, by the Faraday method, with $Hg[Co(SCN)_4]$ as standard. *The magnetic moment* was calculated by formula

$$\mu_{\mathrm{eff}} = 2.828 \sqrt{\chi'_M T} \ \mathrm{BM}$$

where T is the absolute temperature and $\chi'_M = \chi_M - \chi_{\mathrm{dia}}$ is the molar susceptibility corrected for diamagnetism. The diamagnetic correction, calculated by the Pascal constants, was $-313 \times$ $\times 10^{-6}$ c.g.s.u. mol^{-1}.

III. RESULTS AND DISCUSSIONS

The elemental chemical analysis shows that the new complex is of 1 : 2 metal : ligand type. However, one can not assume with certainty that it is tetracoordinated, i.e. square-planar or tetrahedral. Thus, there are Ni(II) complexes of this type in whose crystal lattice (and, partially, in solutions too) one may achieve the hexacoordination of the Ni(II) ions, through a process of association which yields oligomeric species.[20] However, these complexes are all light coloured (in octahedral Ni(II) complexes there are no strong transitions in the visible range) while Ni[II B—a]$_2$ is dark, almost black. Likewise, there are some complexes of this type in whose crystal lattice the Ni(II) ions are pentacoordinated, e.g. bis(3-carbethoxy-1,5-di-*o*-anisyl-formazyl)Ni(II).[21] These pentacoordinated complexes are strongly coloured, like Ni[II B—a]$_2$, but they exhibit an electronic spectrum which *characterizes them* and is radically *different* from that of all tetracoordinated (square-planar or tetrahedral) complexes of Ni(II).

The optical data (colour, spectra) rule out an octahedral or pentacoordinated structure of the new complex and show that it is, as all the Ni[II A]$_2$ complexes, tetracoordinated.

The establishing of the geometrical structure adopted by the complex within the tetracoordination is more difficult. It implies too the study of the magnetic susceptibility of the complex, of its electronic spectrum in solution and the thorough comparison of these properties with those already known for the Ni[II A]$_2$ complexes as well as with those of some complexes not yet described in literature, as, e.g., Ni[II B—b]$_2$ and Ni[II B—c]$_2$ which I intent to study in more detail in another paper.

The electronic diffuse reflectance spectrum of the Ni[II B—a]$_2$ complex in solid state is shown in Fig. 1.

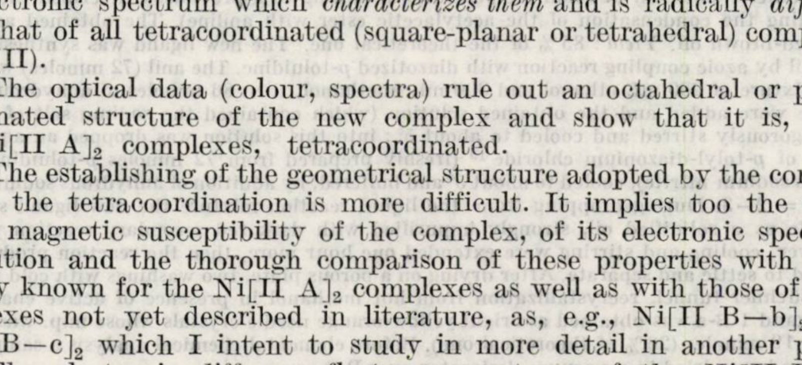

Fig. 1. — Electronic diffuse reflectance spectrum of the new complex Ni[II B-a]$_2$.

This band-rich spectrum is summarized in Table 1, together with the spectra of other similar complexes of the Ni[II A]$_2$ and Ni[II B]$_2$ type. (*Note 1*: The spectra of other Ni[II A]$_2$ complexes not included in Table 1 are similar to those of the Ni[II A—a]$_2$ and Ni[II A—b]$_2$ complexes). Table 1 also lists the spectra of the corresponding free ligands as well as the magnetic moments of the solid complexes.

At the time we carried out our previous works [2,8-12] only the complexes of the Ni[II A]$_2$ type were known and of these only one, Ni[II A-g]$_2$ is strongly paramagnetic ($\mu_{eff} = 3.15$ B.M.) i.e. (distorted) tetrahedral.[17] All the other complexes of the Ni[II A]$_2$ type which exhibit at most a weak residual paramagnetism were considered diamagnetic and implicitly square-planar. Therefore the bands in their spectra at 600 nm and about 1150 nm were assigned to some *d-d* transitions in the square-planar ligand field. Now, the discovery of the new complex Ni[II B—a]$_2$ and the study of its spectral and magnetic properties have proved that the above-mentioned bands assignments [10-12] were erroneous.

The new complex Ni[II B—a]$_2$ exhibits spectral and magnetic properties different from all the other complexes listed in Table 1. It is spectrally very much like the almost diamagnetic complexes, yet is strongly paramagnetic, its μ_{eff} being of 2.80 B.M. which practically coincides with the spin-only value for two unpaired electrons (2.83 B.M.) and is very close to that of the tetrahedral complex Ni[II A—g]$_2$ ($\mu_{eff} = 3.15$ B.M.).

One has to rule out the possibility that the new complex is square-planar and paramagnetic. Although this possibility stands from a theoretical viewpoint,[22] no such complex has been detected so far. Moreover, in case that such a complex exists, it should exhibit an electronic spectrum different from that of the other square-planar diamagnetic complexes (due to the different, i.e. high-spin, distribution of the *d* electrons). But the spectrum of Ni[II B—a]$_2$ is very much like the spectrum of the mentioned complexes (Table 1).

Following the exclusion of the mentioned structures (octahedral, pentacoordinated and high-spin square-planar) there is only one structural alternative left: *in solid state* the new complex Ni[II B—a]$_2$ is, in fact, *a mixture* of easily detectable (only by means of electronic spectra and magnetic moments measurements) amounts of *tetrahedral* and *square-planar* species; the former ones account for the high paramagnetism and the absorption in near I.R. while the latter account for a certain decrease of the paramagnetism and, to a large extent, for the pronounced spectral similarity with the square-planar diamagnetic complexes. Thus one has to do with the phenomenon of *allogony* [23]; the structural equilibrium square-planar ⇌ tetrahedral is not established only after dissolution of complexes but when *both geometrical isomers* coexist already in the *crystalline state* of the complexes, due to a minimal free energy difference between them.

I consider that all experimental (spectral and magnetic) data on the new complex Ni[II B—a]$_2$, on all complexes of the Ni[II A]$_2$ type and on the other complexes of the Ni[II B]$_2$ type (see Table 1) support

Table

The electronic diffuse reflectance spectra of the free organic ligands I, A, B and of the corres
and the magnetic moments

No	Compounds (free ligands and corresponding Ni(II) complexes)	Substituents (X; Y)	Maxima of the corresponding			
1	I A-a	X = H; Y = H			360	
2	Ni[II A-a]$_2$	X = H; Y = H	sh* ~295		365	
3	I A-b	X = p-CH$_3$; Y = H			370	
4	Ni[II A-b]$_2$	X = p-CH$_3$; Y = H	sh ~285	sh 310	365	
5	I A—f	X = p-NO$_2$; Y = H			383	
6	Ni[II A—f]$_2$	X = p-NO$_2$; Y = H				430
7	I A—g	X = m-NO$_2$; Y = H		335		
8	Ni II[A—g]$_2$	X = m-NO$_2$; Y = H			sh ~350	
9	I B-a	X = p-CH$_3$; Y = p-CH$_3$	290		380	
10	Ni[II B-a]$_2$	X = p-CH$_3$; Y = p-CH$_3$			370	405
11	I B—b	X = p-CH$_3$O; Y = p-CH$_3$O	300			400
12	Ni[II B—b]$_2$	X = p-CH$_3$O; Y = p-CH$_3$O	315		380	
13	I B—c	X = p-NO$_2$; Y = p-CH$_3$O	300			400
14	Ni[II B—c]$_2$	X = p-NO$_2$; Y = p-CH$_3$O		335		415

[x] sh = Shoulder; [a] between 900...1100 nm a very weak absorption; [b] at 800...1100 nm
tion; [d] between 950...1100 nm a weak absorption; [e] at 720 nm ceases any absorption; [f] at

convincingly this conclusion. Moreover, one may conclude (see below) that the allogony is present (although it is not too obvious) in most of the Ni[II) complexes of this class.

Thus, comparison of the electronic spectra of the solid complexes (Table 1) with those in Fig. 2 and Table 2 (for complexes in solutions), shows that the only spectra in *excellent agreement* (with respect to *all four bands* within the 500—1150 nm range) are those of the complex Ni[II A-g]$_2$, both in solid state and in solution.

This is the only purely tetrahedral complex in solid state and it results that it retains its structure in solution. It is worth to mention here that the new complex Ni[II B—a]$_2$, as well as *all complexes of the* Ni[II A]$_2$ *type* in Table 2 exhibit in solution electronic absorption spectra *almost similar* to those of this *tetrahedral* complex. E.g., one may notice in Fig. 2 that the two spectra coincide over large domains and all the bands located at ~500, ~600 and ~1150 nm are strong. It results that all electronic spectra from Table 2 for the complexes in solution are due exclusively to some *tetrahedral* species of Ni(II) complexes, which means that in all complexes in Table 2, even in those which are predominantly square-planar (diamagnetic) in solid state (see Table 1), the square-planar species turn upon dissolution into tetrahedral ones, the latter being the only species existing in solution. (*Note 2*: Were the tetrahedral complexes in Table 2 impurified with square-planar species

1

ponding Ni[II, A, B]$_2$ complexes recorded on the solid compounds in the 285...1150 nm range of the Ni(II) complexes

absorption bands [nm]									μ_{eff}[B.M.] and observations about electronic spectra
		540			sh ~ 715				~0.4 [a]
		540		sh 600	sh ~ 700				~0.5 [b]
		535		620	sh 740	sh 800		~1050	~1.0 [c]
	500			600			sh ~ 910	1150	3.15
		535		sh 600	sh 715		sh ~ 900	1150	2.80
sh 460			sh 550						
440		530		sh 590	sh 710		sh ~ 900		~0.9 [d]
455				580					[e]
sh 450		sh 540		580		sh ~ 800			diamagnetic [f]

a weak absorption; [c] measured between 350...1150 nm; between 850...1100 a weak absorp-
920 nm ceases any absorption.

Table 2

Absorption spectra of the Ni[II A, B]$_2$ complexes recorded in the 350...1150 nm range on acetone solutions (concentration $0.5 \times 10^{-4} \ldots 5.0 \times 10^{-4}$ mole $\cdot$ L^{-1})

No.	Ni(II, A, B]$_2$ complex compound	Substituents (X; Y)	λ_{max}[nm]					
1	Ni[II A-a]$_2$	X = Y = H	370		sh 500	sh 600	sh 950	1140
2	Ni[II A–b]$_2$	X = p-CH$_3$; Y = H	382		sh 500	sh 600	960	1100
3	Ni[II A–f]$_2$	X = p-NO$_2$; Y = H	410		sh broad	520...620	sh 1000	1150
4	Ni[II A–g]$_2$	X = m-NO$_2$; Y = H	360		sh 525	sh 600	sh 1020	1160
5	Ni[II B-a]$_2$	X = Y = = p-CH$_3$	380	sh 405	sh 500	sh 600	940	1100

sh = shoulder.

(which do not absorb at all within the range in question), they could not yield the same high value, $\varepsilon = 70$ l.mol^{-1}.cm^{-1} as the pure *tetrahedral* complex Ni[II A–g]$_2$ for the band at 1150 nm; see Figure 2).

The spectral feature of the *tetrahedral* species is the set of four consecutive bands located at 500 ; 600 ; 900 – 950 and ~ 1150 nm and present in *all* complexes *in solution*, and for the strongly paramagnetic complex Ni[II A – g]$_2$ in *solid state* as well.

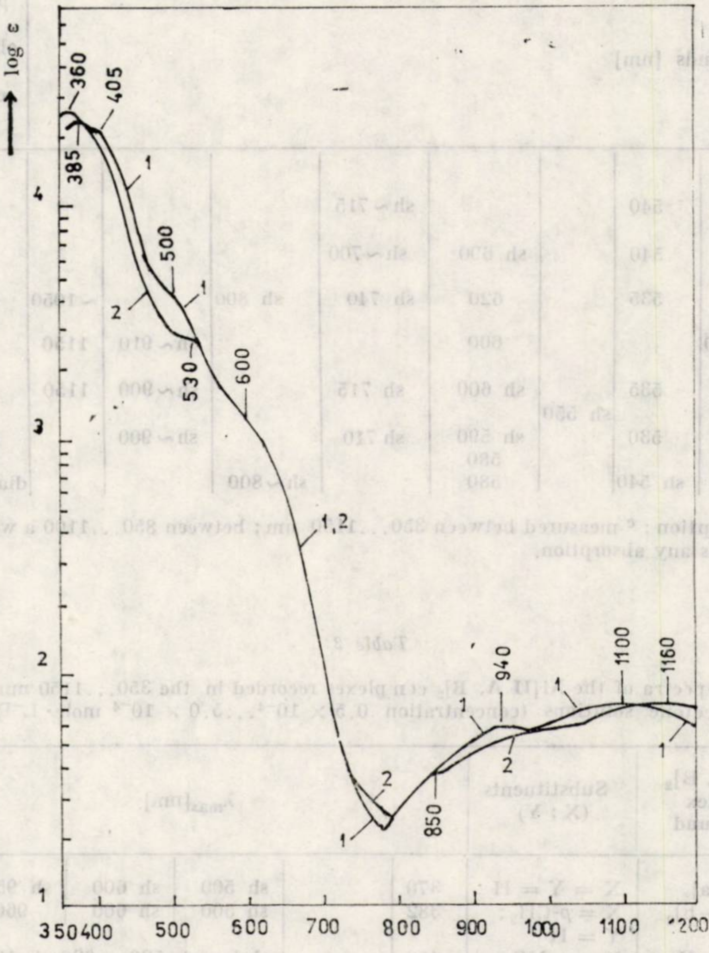

Fig. 2. — Electronic absorption spectra of the Ni(II) complexes : 1 — the new complex Ni[B-a]$_2$; 2 — the tetrahedral complex Ni[II A – g]$_2$.

Among these bands, those at 600 nm and ~ 1150 nm stand for the well known spin-allowed *d-d* transitions $\nu_3[{}^3T_1(F) \rightarrow {}^3T_1(P)]$ and $\nu_2[{}^3T_1(F) \rightarrow {}^3A_2]$ of the tetrahedral Ni(II) complexes, while the band at ~ 950 nm represents, most likely, a spin-forbidden *d-d* transition. The very strong band at 500 nm (Figure 2) certainly represents the first allowed charge transfer (CT) transition of the tetrahedral Ni(II) complexes.

The *square-planar* species of complexes are evidenced in this series *only* in the *solid compounds* (Table 1) through the diamagnetism and in the spectra through the bands at ~ 535 nm and ~ 715 nm (these bands are absent in the spectra of the tetrahedral Ni[II A—g]$_2$ complex) as well as through the *absence* of *any absorption* at wavelengths larger than 950 nm. The band at ~ 715 nm represents a spin-allowed *d-d* transition; this band is relatively weak because it does not alter the dark violet colour of the complexes; yet it is strong enough to show up in the spectra, although it is partly overlapping the strong band centered at 600 nm, due to the ν_3 transition of the tetrahedral Ni(II) complexes.

The very strong band at ~ 535 nm certainly represents the first allowed charge transfer (CT) transition of the square-planar Ni(II) complexes. It accounts for the dark indigo-violet color of the solid diamagnetic complexes. (*Note 3*: Another CT band of the square-planar complexes is probably present in the 310—340 nm range. In Table 1 this band is mentioned only for the complexes Ni[II A—b]$_2$ and Ni[II B-c]$_2$ because in the other complexes it overlaps the stronger intra-ligands transitions).

The absence of any absorption at wavelengths larger than 900—1000 nm characterizes the square-planar Ni(II) complexes; this is the case of the complex Ni[II B-c]$_2$. This is the only complex in Table 1 whose magnetic (diamagnetism) and spectral (absorption ceases at 920 nm) data point to an exclusively square-planar structure of the solid complex.

Obviously, to the fact that this complex assumes exclusively the square-planar structure contribute the particular substituents existing in the molecule, i.e. $X=p-NO_2$ and $Y=p-CH_3O$, which exhibit *very* strong and *opposite* electronic effects. Thus, the substituent constant σ^+-Brown is +0.777 for the —M and —I effects in the $p-NO_2$-substituent and —0.764 for the $+M > -I$ effects in the $p-CH_3O$-substituent.[24] The accumulation of these effects causes the strength of the square-planar ligand field to become so high that the complex adopts exclusively the square-planar structure. The accumulation of the same strong and opposite electronic effects of the substituents X and Y makes the electronic spectrum of this complex in the visible range be bathochromically shifted with respect to all the other complexes : the first CT band appears at 580 nm and the *d-d* band at ~ 800 nm.

The fact that most complexes in Table 1, which exhibit at most a residual paramagnetism ($\mu_{eff} \lesssim 1$ B.M.) and are therefore predominantly square-planar, exhibit in their spectra the bands which are characteristic for tetrahedral species is obviously due to the existence of these latter species but also to the absence of transitions (except the weak *d-d* one at 715 nm) in the major square-planar species of the complex in the occurrence range of the tetrahedral transitions (600—1150 nm).

Accidentally, the CT band at ~ 535 nm of the Ni(II) square-planar complexes from this class lies in the same range as that at 500 nm of the Ni(II) tetrahedral complexes. This contributes to the spectral similitude between the square-planar and tetrahedral complexes, and may, at the same time, cause confusions. Thus, at the first sight, the band at 535 nm seems to undergo only a small hypsochromic shift (of about 35 nm = 1300 cm^{-1}) on dissolution of the square-planar complexes. In fact we have to do with the complete disappearance of the CT band of the square-planar complexes and its replacement by the CT band of the tetrahedral Ni(II) complexes.

Leaving out the two extreme cases, i.e. the tetrahedral Ni[II A-g]$_2$ and the stepped square-planar Ni[II B-c]$_2$ complexes, one may find out that not only the new complex, Ni[II B-a]$_2$, but all the other solid complexes in Table 1 exhibit allogony, too. In the new complex, Ni[II B-a]$_2$, ($\mu_{\text{eff}} = 2.80$ B.M.) the paramagnetic tetrahedral species predominate while in all the other complexes ($\mu_{\text{eff}} \lesssim 1$ B.M.) the diamagnetic square-planar species are predominant. Upon dissolution of complexes (which practically causes the complete square-planar → tetrahedral conversion) their electronic spectrum loses the transitions characterizing the square-planar complexes (the band at 715 nm vanishes and that at 535 nm *is replaced* by one at 500 nm; see above) while the electronic spectrum has only the transitions characteristic for the tetrahedral complexes: the bands at ~ 600 nm, ~ 910 nm and ~ 1150 nm (see Table 2).

A rough estimation of the relative weights of isomers in the solid complexes is easy to do for the new complex Ni[II B-a]$_2$. If we assign to the tetrahedral species a magnetic moment of 3.20 B.M. (as for the tetrahedral complex Ni[II A-g]$_2$) from the value of 2.80 B.M. for the complex in question we deduce that it contains about 87% tetrahedral and about 13% square-planar species. This evaluation is not possible for the approximately diamagnetic complexes in Table 1 (*Note 4*: The measurements of small magnetic moments have been affected by a large error, of ± 0.4 . . . ± 0.6 B.M. Therefore the magnetic moment measurements carried out do not allow us to establish whether these complexes are strictly diamagnetic or if they exhibit a residual diamagnetism. On the other hand, in the strongly paramagnetic complexes as Ni[II B-a]$_2$ the measurement error is "normal" (i.e. smaller), of ± 0.2 B.M., so that the paramagnetism is accurately measured). The fact that these complexes possess a residual paramagnetism (they are impurified with tetrahedral paramagnetic species) is indicated by the electronic diffuse reflectance spectra (see above). Anyhow, in these complexes the minor species (the tetrahedral ones) have a low relative weight (it is difficult to detect them in the electronic spectra and they are undetectable in the results of magnetic measurements).

In the new complex Ni[II B-a]$_2$ considering in calculations the values of the *d-d* spin-allowed tetrahedral transitions ν_2 and ν_3 from the electronic spectra (Fig. 2) recorded on acetone solutions (in which only the tetrahedral species are noticed) i.e.:

$$\nu_2[{}^3T_1(F) \rightarrow {}^3A_2] = 9090 \text{ cm}^{-1} \text{ (1100 nm)},$$

$$\nu_3[{}^3T_1(F) \rightarrow {}^3T_1(P)] = 16670 \text{ cm}^{-1} \text{ (600 nm)}$$

where the involved spectral terms are[25]:

$${}^3T_1(F): \ 7.5\ B - 3\ Dq - \frac{1}{2}[225\ B^2 + 100\ Dq^2 + 180\ Dq\ B]^{1/2}$$

$${}^3T_1(P): \ 7.5\ B - 3\ Dq + \frac{1}{2}[225\ B^2 + 100\ Dq^2 + 180\ Dq\ B]^{1/2}$$

$${}^3A_2: + 12Dq$$

and solving the transition energy expression yields the orbital splitting parameter

$$\Delta = 10Dq = 4780 \text{ cm}^{-1}$$

as well as the B Racah parameter

$$B = 886 \text{ cm}^{-1}.$$

The latter parameter and its value in the case of the free Ni(II) ion, i.e. $B_0 = 1060$ cm^{-1} (the average value of 1040 cm^{-1} [25] and 1080 cm^{-1} [26]) allows the calculation of the nephelauxetic ratio

$$\beta_{35} = \frac{B}{B_0} = \frac{880}{1060} = 0.83$$

This value points to a weak to medium covalence degree of the Ni(II)—N chemical bonds in the discussed tetrahedral complex species. Similar β_{35} values were obtained for all tetrahedral species of Ni(II) complexes from this class; this indicates approximately the same weak to medium covalence degree.

IV. CONCLUSIONS

1. In the series of tetracoordinated Ni(II) complexes synthesized with chelate ligands from the class of substituted 1-methyl-2-carbethoxy-glyoxalanil-(1)-phenylhydrazones-(2) only a few complexes adopt an exclusively tetrahedral or square-planar structure.

2. Most complexes from this class are, in solid state, a mixture of both geometric isomers; in some of them predominates the square-planar isomer whereas in other the tetrahedral isomer is predominant.

3. The *tetrahedral* isomers are characterized by paramagnetism ($\mu_{eff} \sim 3.2$ B.M.) and in the electronic spectra by the bands situated at ~500 nm (CT); 600 nm (*d-d*); ~ 930 nm (forbidden *d-d*) and ~1150 nm (*d-d*).

4. The *square-planar* isomers are characterized by diamagnetism and in the electronic spectra by the bands situated at ~ 500 nm (CT) and 715 nm (*d-d*) as well as by the absence of any absorption at wavelengths larger than 950 nm.

5. The dissolution of the solid complexes in acetone is accompanied by a practically total conversion of the square-planar isomers into tetrahedral ones, regardless of the relative weight the former ones have in the solid complexes.

6. The tetrahedral isomers show a weak to medium covalence degree of the Ni(II)—N chemical bonds ($\beta_{35} \sim 0.83$).

ACKNOWLEDGEMENT. The author is grateful to lecturer Dr. V. Mincu from the Polytechnic Institute of Bucharest for the magnetic susceptibility measurements.

REFERENCES

[1] C. D. Nenițescu, "Chimie organică", vol. 2, Ed. Tehnică, București, 1980, p. 77.
[2] P. Spacu, A. C. Banciu and C.I. Lepădatu, *Rev. Roumaine Chim.*, **18**, 1143 (1973).
[3] A. C. Banciu and P. Spacu, *Rev. Roumaine Chim.*, **19**, 1019 (1974).
[4] A. C. Banciu and P. Spacu, *Rev. Roumaine Chim.*, **19**, 1169 (1974).
[5] A. C. Banciu and P. Spacu, *Rev. Roumaine Chim.*, **21**, 1487 (1976).
[6] A. C. Baciu, *Rev. Roumaine Chim.*, **23**, 707 (1978).
[7] A. C. Banciu and V. Mincu, *Rev. Roumaine Chim.*, **25**, 513 (1980).
[8] A. C. Banciu and P. Spacu, *Rev. Roumaine Chim.*, **19**, 817 (1974).
[9] A. C. Banciu and P. Spacu, *Rev Roumaine Chim.*, **19**, 1307 (1974).
[10] A. C. Banciu and C. I. Lepădatu, *Z. phys. Chem. (Frankfurt)*, **97**, 197 (1975).
[11] A. C. Banciu, *Rev. Roumaine Chim.*, **23**, 1251 (1978).
[12] A. C. Banciu, *Rev. Roumaine Chim.*, **24**, 1137 (1979).
[13] A. C. Banciu and P. Spacu, *Rev. Roumaine Chim.*, **21**, 1331 (1976).
[14] A. C. Banciu, O. Constantinescu and P. Spacu, *Rev. Roumaine Chim.*, **23**, 215 (1978).
[15] R. H. Holm and M. J. O'Connor, "Progress in Inorganic Chemistry" vol. 14, Wiley, New York, 1971, p. 286.
[16] D. Dale, *J. Chem. Soc.*, A **1967**, 278.
[17] A. C. Banciu, *Rev. Roumaine Chim.*, **22**, 1181 (1977).
[18] 7. Conrad and L. Lipach, *Ber. dtsch. chem. Ges.*, **20**, 944 (1887).
[19] L. Gattermann, "Die Praxis des organischen Chemikers", Walter de Gruyter, Berlin, 1958, p. 252.
[20] F. A. Cotton and G. Willkinson, "Advanced Inorganic Chemistry", Interscience, London, 1966, p. 887.
[21] A. C. Banciu, unpublished results.
[22] L. Saconi, "Transition Metal Chemistry", vol. 4, Edvard Arnold, London, 1968, p. 199–298.
[23] F. A. Cotton and G. Willkinson, ibid., p. 889.
[24] F. Badea, "Mecanisme de reacție în chimia organică", Ed. Științifică. București, 1971, p. 101.
[25] A. B. P. Lever, "Inorganic Electronic Spectroscopy", Elsevier, Amsterdam, 1968, chap. 8–9.
[26] J. S. Griffith, "The Theory of Transition-Metal Ions", Univ. Press., Cambridge, 1964, p. 437.

Revue Roumaine de Chimie, **33**, *3*, 237–251 (1988)

LA DÉTERMINATION EXPÉRIMENTALE DES COURBES D'ÉQUILIBRE LIQUIDE–VAPEURS ET LA CORRÉLATION DES DONNÉES PAR DES MODÈLES D'ACTIVITÉ POUR LES SYSTÈMES CYCLOHEXANE–MONOCHLORCYCLOHEXANE ET CYCLOHEXANE–EAU

ORTANSA LANDAUER, CORNELIA MATEESCU, OLGA IULIAN et DAN GEANĂ
Chaire de Chimie physique, Institut Polytechnique, Calea Griviţei 132, Bucarest, Roumanie

Reçu le 3 novembre 1986

Dans cet article sont présentées des déterminations expérimentales d'équilibre liquide–vapeurs pour les systèmes cyclohexane–monochlorcyclohexane et cyclohexane–eau. On a déterminé la courbe de la pression de vapeurs du monochlorcyclohexane et on a établi par régression l'équation correspondante pour le domaine de température 30–85 °C. On a effectué la corrélation des données expérimentales liquide–vapeurs pour les systèmes cyclohexane–monochlorcyclohexane et cyclohexane–eau avec des modèles d'activité (Wilson, NRTL/H et LEMF) suivant des programmes d'ordinateur. On a obtenu les diagrammes des phases calculés pour le domaine entier de la composition des systèmes.

Liquid–vapour equilibrium data for the mixture cyclohexane–monochlorocyclohexane and cyclohexane–water are presented. For monochlorocyclohexane the vapour pressure equation (Antoine) was obtained for the temperature range between 30 and 85 °C. The data were correlated by activity models. The parameters of Wilson, NRTL/H and LEMF equations were obtained by a least square procedure, thus permitting the computation of the liquid–vapor and liquid–liquid–vapor phase diagrams of the above systems.

I. INTRODUCTION

Les installations de distillation et rectification occupent une place importante dans l'industrie chimique. Le modèle des équilibres des phases (thermodynamiques) liquide–vapeurs constitue une base de calcul généralement utilisée pour l'étude et l'exploitation de ces installations. Pour utiliser ce modèle, des déterminations expérimentales pression–température–compositions des phases sont nécessaires, relatives aux mélanges qui seront soumis aux opérations de séparation. Les données expérimentales qui sont obtenues dans le cas des systèmes (mélanges) binaires sont de deux types :

a) des données isothermes : pression totale–composition des phases, c'est-à-dire P–X–Y pour T = constante.

b) des données isobares : température–composition des phases c'est-à-dire T–X–Y pour P = constante.

Certes, si les domaines de pression et de température sont suffisamment larges, il est possible de transformer un type de données dans l'autre, mais il est recommandable de faire cette transformation par des procédés analytiques plutôt que graphiques.

Généralement le type de données (a) est obtenu par des méthodes appelées statiques et le type (b) par des méthodes dynamiques.[1]

Dans le cas des données du type (a) il est possible de limiter les mesurages à la composition de la phase liquide (X), la composition des vapeurs étant calculée.

Il faut mentionner que les données expérimentales de n'importe quel type sont interprétées à présent conformément aux algorithmes proposés par la littérature et implémentés sur des ordinateurs numériques. Cette interprétation appelée aussi corrélation des équilibres L—V est faite pour apprécier la qualité (les erreurs) des données mesurées et pour représenter quantitativement les écarts par rapport à l'idéalité des deux phases. Les différentes variantes de calcul, les méthodes numériques ou analytiques) utilisées et d'autres détails visant le calcul des équilibres iquide—vapeurs sont présentés dans la littérature.[2-5]

II. DÉTERMINATIONS EXPÉRIMENTALES.

On a effectué dans cette étude des déterminations expérimentales relatives à l'équilibre liquide—vapeurs dans le système cyclohexane—monochlorcyclohexane et cyclohexane—eau. Pour les deux systèmes on a fait des mesurages par la méthode statique dans une installation isoténiscopique. Dans cette installation on obtient les valeurs de la pression totale en fonction de la composition de la phase liquide (P — X) à une température constante. Les données expérimentales sont interprétées conformément à une méthode du type Barker[2,4], pour calculer la composition de la phase des vapeurs et des paramètres d'une modèle de coefficient d'activité (ou d'enthalpie libre d'excès).

Le programme de l'ordinateur nommé COBELV,[6] est décrit dans la section suivante (COBELV — la corrélation des équilibres binaires). Certes, la méthode isoténiscopique ne peut être utilisée que de pair avec le programme COBELV.

Pour le système cyclohexane — eau on a obtenu expérimentalement par la méthode statique, les pressions correspondant à l'hétéroazéotrope, pour $t = 30\,°C$, à quelques compositions globales.

Les substances utilisées pour des mesurages ont été purifiées par rectification dans une colonne de laborateur.

Le monochlorcyclohexane a été synthétisé de cyclohexanol et d'acide chlorhydrique, [7] purifié par lavement avec acide sulphurique concentré et par rectification dans la colonne avec remplissage de verre.

La pureté de la substance obtenue a été vérifiée par spectroscopie I.R., chromatographie et par des indices de réfraction.

On a réalisé une pureté de plus de 99% masse.

Les déterminations analytiques ont été effectuées conformément au mesurage de l'indice de réfraction. Les courbes d'étalonnage ont été obtenues dans des conditions de thermostatagee ($t = 23\,°C$) et les données ont été représentées par une fonction de régression ayant la forme :

$$n = a_0 + a_1x + a_2x^2\ ;\ x = x_1$$

Les coefficients de régression a_0, a_1, a_2 ont été obtenus par la méthode de la régression multilinéaire, étant présentés plus loin.

III. LA MÉTHODE DE CORRÉLATION ET LE PROGRAMME COBELV

La méthode de corrélation des données limitées P—T—X, d'équilibre liquide—vapeurs dans des systèmes binaires est fondée sur un modèle du coefficient d'activité à 2 ou plusieurs paramètres. On calcule les valeurs de ces paramètres qui minimisent l'expression :

$$\min Q_p = \sum_{k=1}^{N} \frac{(P_k^{exp} - P_k^{calc})^2}{\sigma^2_{P_k}}$$

où P représente la pression totale expérimentale respectivement calculée, $\sigma^2_{P_k}$ — la variance standard de la pression mesurée, N — le nombre des points expérimentaux.

La pression est calculée conformément aux équations d'équilibre thermodynamique :

$$P^{calc} = Y_1P + Y_2P = \frac{\gamma_1 X_1 f_1^0}{\varphi_1} + \frac{\gamma_2 X_2 f_2^0}{\varphi_2}$$

où : Y_1Y_2 — fractions molaires dans la phase vapeurs
X_1X_2 — fractions molaires dans la phase liquide
$\gamma_1\gamma_2$ — coefficients d'activité
$\varphi_1\varphi_2$ — coefficients de fugacité
f_1^0, f_2^0 — fugacités de référence (standard)

La minimisation de la fonction Q_p constitue un problème de programmation non-linéaire (ou optimisation). Il y a beaucoup d'algorithmes pour la solution de ce type de problèmes ; on en a choisi celui de Powell[8] (dans une version primitive on a utilisé aussi l'algorithme Hooke-Jeeves) et respectivement un algorithme adapté aux programmes d'estimation non-linéaire des paramètres, nommé Gauss.[9] Il faut mentionner que, simultanément avec le calcul des paramètres optimaux on obtient aussi la fraction molaire Y_1 représentant la composition de la phase vapeurs. Suivant la méthode Gauss il est possible d'établir la signification des paramètres, de l'unicité et de leur corrélation.[2,9] Sans entrer en détail, nous mentionnons que ces éléments sont obtenus à l'aide de la matrice de covariance (cov). Cette matrice résulte au cours de la dernière étape, pendant le processus itératif de calcul des paramètres optimaux. Les éléments diagonaux de la matrice de covariance approximent les variances (écarts) des paramètres étant une mesure de leur incertitude. Les éléments non-diagonaux de la matrice de covariance représentent les covariances des paramètres. De ceux-ci on calcule la matrice des coefficients de corrélation. La valeur de l'élément ρ_{12} exprime la dépendance des paramètres. Si les paramètres sont tout à fait indépendants $\rho_{12} \to 0$ et si la valeur $\rho_{12} \to \pm 1$, les paramètres sont tout à fait corrélatifs.

La procédure de minimisation constitue un segment du programme COBELV décrit dans une autre étude.[6] Ce programme contient une série de sous-routines pour le calcul des coefficients d'activité, des coefficients de fugacité à l'aide d'une équation d'état (par exemple virial second) et de la fugacité de référence.

Le calcul de la pression est un calcul « Bubble-P ».[2,6]

IV. LE SYSTÈME CYCLOHEXANE–MONOCHLORCYCLOHEXANE

Pour ce système, l'analyse de la phase liquide a été faite par des mesurages de l'indice de réfraction. On présente dans le tableau 1 les données utilisées pour obtenir la courbe d'étalonnage. La fonction des régressions determinée est :

$$n = 1,461593 - 0,0339125\, X_1 - 2,77165 \cdot 10^{-3} X_1^2$$

avec la variance $\sigma^2 = 3,781 \cdot 10^{-8}$ et le coefficient de corrélation $\rho = 0,9989$.

Ces valeurs montrent une très bonne représentation des données, ce qui est aussi relevé en comparant les valeurs n calculées avec celles expérimentales (tableau 1).

Tableau 1

Les valeurs de l'indice de réfraction déterminé expérimentalement et calculé pour le système cyclohexane (1) — monochlorcyclohexane (2)

X_1	n_{exp}	n_{calc}
0	1,4618	1,46159
0,06812	1,4592	1,45927
0,13542	1,4568	1,45695
0,26766	1,4521	1,45232
0,39682	1,4478	1,44770
0,52301	1,4432	1,44309
0,64632	1,4388	1,43851
0,76686	1,4338	1,43396
0,88473	1,4292	1,42942
0,94268	1,4272	1,42716
1	1,4250	1,42491

Vu que, pour le monochlorcyclohexane, on n'a pas trouvé une expression pour la pression des vapeurs, on a effectué des déterminations par la méthode statique. Dans le tableau 2 sont présentés les résultats expérimentaux.

Tableau 2

Données expérimentales de pression de vapeurs pour le monochlorcyclohexane

t°, C	30	45	60	75	84
P, mm Hg	22	38	62,5	107,5	145

Ces données ont été mises en relation avec une équation ayant la forme :

$$\ln P = A + \frac{B}{t + 230}, \quad P, \text{ mm Hg}, \; t, \; °C$$

Pour le cyclohexane on a utilisé l'équation du type Antoine [10]

$$\ln P^0 = 15{,}7527 - \frac{2766{,}63}{T - 50{,}5}$$

Les données expérimentales d'équilibre liquide—vapeurs (P—X) à une température de 30°C sont présentées dans les tableaux 3 et 4. On a effectué la corrélation des données conformément au modèle Wilson (tableau 3) et respectivement au nouveau modèle du type NRTL (non random two liquids), nommé NRTL/H (tableau 4) et proposé par nous.[11] Le modèle Wilson [12] est donné par les expressions :

$$\frac{G^E}{RT} = -X_1 \ln(X_1 + \Lambda_{12}X_2) - X_2 \ln(X_2 + \Lambda_{21}X_1)$$

$$\ln \gamma_1 = -\ln(X_1 + \Lambda_{12}X_2) + X_2\left(\frac{\Lambda_{12}}{X_1 + \Lambda_{12}X_2} - \frac{\Lambda_{21}}{\Lambda_{21}X_1 + X_2}\right)$$

$$\ln \gamma_2 = -\ln(X_2 + \Lambda_{21}X_1) - X_1\left(\frac{\Lambda_{12}}{X_1 + \Lambda_{12}X_2} - \frac{\Lambda_{21}}{\Lambda_{21}X_1 + X_2}\right)$$

où X_1X_2 — fractions molaires des composants
G^E — enthalpie libre molaire d'excès
γ_1, γ_2 — coefficients d'activité

$$\Lambda_{ij} = \frac{V_j^L}{V_i^L} \exp\left[-\frac{\lambda_{ij} - \lambda_{ii}}{RT}\right], \qquad i \neq j = 1, 2$$

Les paramètres du modèle sont $\lambda_{ij} - \lambda_{ii}$ qui constituent des termes énergétiques déterminés par la différence entre l'énergie d'interaction de la paire i — j et celle de la paire i — i. Pour le système binaire ceux-là sont 2 paramètres notés $\lambda_{12} - \lambda_{11}$ et $\lambda_{12} - \lambda_{22}$. Le comportement idéal correspond à la situation $\Lambda_{12} = \Lambda_{21} = 1$. Le modèle NRTL/H est donné par les équations :

$$\frac{G^E}{RT} = X_1X_2\left(\frac{\tau_{21}\,\theta_{21}}{X_1 + X_2\theta_{21}} + \frac{\tau_{12}\,\theta_{12}}{X_2 + X_1\theta_{12}}\right)$$

$$\ln \gamma_1 = X_2^2\left[\tau_{21}\left(\frac{\theta_{21}}{X_1 + X_2\theta_{21}}\right)^2 + \tau_{12}\frac{\theta_{12}}{(X_2 + X_1\theta_{12})^2}\right]$$

$$\ln \gamma_2 = X_1^2\left[\tau_{12}\left(\frac{\theta_{12}}{X_2 + X_1\theta_{12}}\right)^2 + \tau_{21}\frac{\theta_{21}}{(X_1 + X_2\theta_{21})^2}\right]$$

Tableau 3

Données d'équilibre liquide—vapeurs pour le système cyclohexane (1) — monochlorcyclohexane (2) pour $t = 30\,°C$. Corrélation avec le modèle Wilson. $P_1^0 = 121{,}78$; $P_2^0 = 22$ mm Hg ; $V_1 = 108{,}04$ cm³/mol ; $V_2 = 118{,}61$ cm³/mol

X_1	P_{exp} mm Hg	Y_1^{calc}	P_{calc} mm Hg	γ_1	γ_2	ΔP, mm Hg
0,093	36	0,465	37,43	1,538	1,002	1,43
0,125	44	0,543	42,35	1,512	1,005	−1,65
0,254	60	0,721	60,29	1,406	1,022	0,29
0,394	76	0,815	76,52	1,299	1,062	0,52
0,520	87	0,865	88,59	1,210	1,127	1,59
0,639	102	0,900	98,16	1,135	1,233	−3,84
0,745	105	0,926	105,53	1,077	1,389	0,53
0,752	110	0,927	105,93	1,073	1,403	−4,01
0,851	109	0,952	112,28	1,031	1,656	3,28
0,862	109	0,954	112,97	1,027	1,695	3,97
0,936	115	0,976	117,62	1,007	2,030	2,62

$$\lambda_{12} - \lambda_{11} = -\ 62{,}42 \pm 111{,}74 \qquad Q_p = 72{,}1726$$

$$\lambda_{12} - \lambda_{22} = 627{,}02 \pm 204{,}33 \qquad \sigma^2 = 8{,}019$$

$$\text{cov} = \begin{pmatrix} 12486 & -22076 \\ & 41750 \end{pmatrix}$$

$$\rho = \begin{pmatrix} 1 & -0{,}967 \\ & 1 \end{pmatrix}$$

où

$$\tau_{12} = \ln \frac{P_{12}}{P_1^0}\ ; \quad \tau_{21} = \ln \frac{P_{12}}{P_2^0}$$

$$\theta_{12} = \exp\left(\frac{\Delta^v H_{12} - \Delta^v H_2}{RT}\right); \quad \theta_{21} = \exp\left(\frac{\Delta^v H_{12} - \Delta^v H_1}{RT}\right)$$

$\Delta^v H_1$, $\Delta^v H_2$ — les enthalpies de vaporisation des composants purs, P_1^0, P_2^0 — les pressions de vapeurs des composants purs. Les paramètres du modèle sont P_{12} et $\Delta^v H_{12}$ qui sont obtenus des données expérimentales.

Dans les tableaux 3 et 4 sont présentés les résultats des corrélations conformément aux deux modèles ci-dessus. Il faut remarquer que les résultats calculés sont pratiquement identiques dans les deux corrélations.

Les paramètres Wilson présentent, comme on peut le voir, de très grandes covariances (écarts), respectivement un grand nombre de valeurs dans l'intervalle donné conformément aux données expérimentales. La valeur $\rho_{12} = -0{,}967$ montre que les deux paramètres sont étroitement liés. Du point de vue physique le modèle n'est pas satisfaisant.

Les paramètres du modèle NRTL/H présentent des covariances (écarts) limitées et un coefficient de corrélation $\rho_{12} = -0{,}393$ réduit, ce qui recommande le modèle comme étant plus adéquat pour représenter

Tableau 4

Données d'équilibre liquide–vapeurs pour le système cyclohexane (1) – monocyclohexane (2) pour t = 30 °C. Corrélation avec le modèle NRTL/H.
$P_1^0 = 121{,}78$; $P_2^0 = 22$ mm Hg ; $\Delta^V H_1 = 7914{,}5$ cal/mol ; $\Delta^V H_2 = 7691{,}3$ cal/mol

X_1	P^{exp} mm Hg	Y_1^{calc}	P^{calc} mm Hg	γ_1	γ_2	ΔP, mm Hg
0,0934	36	0,455	36,58	1,470	0,99896	0,58
0,125	44	0,538	41,62	1,471	0,99894	−2,38
0,254	60	0,727	60,57	1,424	1,007	0,57
0,394	76	0,820	77,40	1,323	1,045	1,40
0,520	87	0,868	89,17	1,222	1,118	2,17
0,639	102	0,899	98,12	1,134	1,239	−3,88
0,745	105	0,924	105,08	1,071	1,411	0,08
0,752	110	0,926	105,52	1,067	1,425	−4,47
0,851	109	0,950	111,79	1,026	1,676	2,79
0,862	109	0,954	112,49	1,022	1,710	3,49
0,936	115	0,976	117,36	1,005	1,991	2,36

$P_{12} = 69{,}5 \pm 2{,}6$ mm Hg $\qquad Q_p = 73{,}688$

$\Delta^V H_{12} = 7555{,}4 \pm 100{,}6$ cal/mol $\qquad \sigma^2 = 8{,}187$

$$\mathrm{cov} = \begin{pmatrix} 6{,}81 & -103{,}2 \\ & 10130{,}9 \end{pmatrix}$$

$$\rho = \begin{pmatrix} 1 & -0{,}393 \\ & 1 \end{pmatrix}$$

le système. Vu que $\sigma_{pk} = 1$ mm Hg, la valeur de la variance totale (σ) donne l'erreur moyenne des déterminations. Les deux modèles donnent des valeurs rapprochées $\sigma^2 = 8{,}019$ (Wilson) et 8,187 (NRTL/H).

Dans les tableaux 5 et 6 sont présentés les résultats expérimentaux et les valeurs calculées relatives au même système pour t = 45°C. Il faut remarquer les mêmes particularités des deux modèles déterminées par les écarts des paramètres, respectivement la confidence de ceux-ci. Le modèle NRTL/H se montre de nouveau plus adéquat pour représenter le système donné.

Dans les tableaux 3 et 6, les écarts par rapport au comportement idéal sont représentés par les coefficients d'activité qui montrent que ces écarts sont modérés. La précision des déterminations et de la corrélation peut aussi être appréciée en tenant compte des écarts absolus $\Delta P = p^c - p^{ex}$. Les valeurs réduites de ces écarts témoignent d'une bonne qualité des données.

V. LE SYSTÈME CYCLOHEXANE–EAU

Ce système binaire présente un hétéroazéotrope, et les liquides conjugués sont chacun très riches en un des composants. De plus les phases liquides en équilibre avec les vapeurs présentent les mêmes particularités.

Tableau 5

Données d'équilibre liquide—vapeurs pour le système cyclohexane (1) — monochlorcyclohexane (2) pour t = 45 °C. Corrélation avec le modèle Wilson.
$P_1^0 = 224{,}97$ mm Hg ; $P_2^0 = 38$ mm Hg ; $V_1 = 108{,}04$ cm³/mol ; $V_2 = 118{,}61$ cm³/mol

X_1	P_{exp} mm Hg	Y_1^{calc}	P_{calc} mm Hg	γ_1	γ_2	ΔP, mm Hg
0,093	58	0,458	63,78	1,398	1,002	5,78
0,125	74	0,537	72,16	1,379	1,003	−1,84
0,254	105	0,721	103,45	1,306	1,016	−1,55
0,394	135	0,818	133,02	1,228	1,047	−1,98
0,520	152	0,872	156,03	1,162	1,097	4,03
0,639	178	0,907	175,03	1,105	1,178	−2,97
0,745	190	0,934	190,22	1,060	1,294	0,22
0,752	196	0,936	191,18	1,057	1,304	−4,22
0,851	200	0,959	204,47	1,024	1,487	4,47
0,862	201	0,961	205,93	1,021	1,513	4,93
0,936	217	0,980	215,89	1,005	1,743	−1,11

$\lambda_{12} - \lambda_{11} = -110{,}9 \pm 106{,}9$ cal/mol $\qquad Q_p = 136{,}975$

$\lambda_{12} - \lambda_{22} = 589{,}3 \pm 191{,}9$ cal/mol $\qquad \sigma^2 = 15{,}22$

$$\mathrm{cov} = \begin{pmatrix} 11435 & -20050 \\ & 36823 \end{pmatrix}$$

$$\rho = \begin{pmatrix} 1 & -0{,}977 \\ & 1 \end{pmatrix}$$

Tableau 6

Données d'équilibre liquide—vapeurs pour le système cyclohexane (1) — monochlorcyclohexane (2) pour t = 45 °C. Corrélation avec le modèle NRTL/H.
$P_1^0 = 224{,}97$ mm Hg ; $P_2^0 = 38$ mm Hg ; $\Delta^V H_1 = 7767{,}4$ cal/mol ; $\Delta^V H_2 = 7572{,}8$ cal/mol

X_1	P^{exp} mm Hg	Y_1^{calc}	P^{calc} mm Hg	γ_1	γ_2	ΔP, mm Hg
0,093	58	0,448	62,39	1,337	0,999	4,39
0,125	74	0,532	70,89	1,340	0,998	−3,11
0,254	105	0,725	103,64	1,316	1,003	−1,36
0,394	135	0,823	134,28	1,247	1,030	−0,72
0,520	152	0,873	157	1,173	1,086	−5,00
0,639	178	0,907	175,12	1,106	1,178	−2,88
0,745	190	0,933	189,67	1,056	1,308	−0,33
0,752	196	0,935	190,61	1,053	1,318	−5,39
0,851	200	0,958	203,82	1,020	1,500	3,82
0,862	201	0,961	205,31	1,017	1,524	4,31
0,936	217	0,980	215,58	1,004	1,719	−1,42

$P_{12} = 113{,}7 \pm 2{,}83$ mm Hg $\qquad Q_p = 129{,}012$

$\Delta^V H_{12} = 7478 \pm 68{,}8$ cal/mol $\qquad \sigma^2 = 14{,}33$

$$\mathrm{cov} = \begin{pmatrix} 8{,}02 & -5{,}52 \\ & 4740{,}2 \end{pmatrix}$$

$$\rho = \begin{pmatrix} 1 & -0{,}028 \\ & 1 \end{pmatrix}$$

C'est pourquoi les déterminations expérimentales relatives à l'analyse chimique des phases liquides se trouvent devant de grandes difficultés. On présente dans la littérature une série de résultats des déterminations d'équilibre liquide—liquide mais seulement pour la phase riche en hydrocarbure.[13,14] Ces données sont présentées dans le tableaux 7 et 8.

Tableau 7

La solubilité de l'eau en cyclohexane[13]

t, °C	% masse H_2O
14	0,005
19	0,01
28,5	0,015
32,5	0,02
38	0,031
53	0,05

Tableau 8

La solubilité de l'eau en cyclohexane[14]

t, °C	% masse H_2O
10	0,0067
20	0,0122
30	0,0194
40	0,0317
50	0,049

Dans une autre étude[15] on rapporte pour $t = 20°C$ la solubilité du cyclohexane en eau comme fraction molaire $X_{C_6H_{12}}$ (en H_2O) $= 1,2 \cdot 10^{-5}$. Tenant compte de ces données et supposant le modèle LEMF[4] comme applicable pour le coefficient d'activité, on peut obtenir par les solubilités présentées, les paramètres du modèle.

Les expressions pour le modèle LEMF sont :

$$\frac{G^E}{RT} = X_1X_2\left[\frac{\tau_{21}G_{21}}{X_1 + X_2G_{21}} + \frac{\tau_{12}G_{12}}{X_2 + X_1\,G_{12}}\right]$$

$$\ln \gamma_1 = X_2^2\left[\tau_{21}\left(\frac{G_{21}}{X_1 + X_2G_{21}}\right)^2 + \frac{\tau_{12}G_{12}}{(X_2 + X_1G_{12})^2}\right]$$

$$\ln \gamma_2 = X_1^2\left[\tau_{12}\left(\frac{G_{12}}{X_2 + X_1G_{12}}\right)^2 + \frac{\tau_{21}G_{21}}{(X_1 + X_2G_{21})^2}\right]$$

où G^E — enthalpie libre molaire d'excès
X_1X_2 — fractions molaires

$$\tau_{12} = \frac{\Delta g_{12}}{RT} \qquad \tau_{21} = \frac{\Delta g_{12}}{RT}$$

$$G_{12} = e^{\tau_{12}} \quad G_{21} = e^{\tau_{21}}$$

Les paramètres du modèle qui doivent être déterminés des données expérimentales sont Δg_{12} et respectivement Δg_{21} qui ont des dimensions d'énergie et peuvent être attribués aux interactions binaires entre les composants du mélange relativement à celles des composants purs :

$$\Delta g_{ij} = g_{ij} - g_{ii} \text{ avec } i,\ j = 1{,}2\ ;\ i \neq j$$

Pour le système liquide–liquide à 2 composants, les conditions d'équilibre de phases sont, pour T et P constantes :

$$(X_1\gamma_1)^{L_1} = (X_1\gamma_1)^{L_2}$$

$$[(1 - X_1)\gamma_2]^{L_1} = [(1 - X_1)\gamma_2]^{L_2}$$

Conformément à la théorie des équilibres de phases fondée sur la programmation géométrique,[16,17] ces équations peuvent se transformer ainsi :

$$\frac{1}{\gamma_1^{L_1}} Z_1 + \frac{1}{\gamma_2^{L_1}} Z_2 = 1$$

$$\frac{1}{\gamma_1^{L_2}} Z_1 + \frac{1}{\gamma_2^{L_2}} Z_2 = 1$$

avec les inconnues auxiliaires Z_1, Z_2 qui ont le sens physique d'activités thermodynamiques. Les équations ci-dessus représentent un système linéaire qui est solutionné pour Z_1 et Z_2.

Les compositions des phases en résultent :

$$X_1^{L_1} = Z_1/\gamma_1^{L_1}; \quad X_1^{L_2} = Z_1/\gamma_1^{L_2}$$

Vu que γ_i sont des fonctions de la composition des phases, la solution du système linéaire est faite d'une manière itérative :

a) on choisit des valeurs initiales $X_1^{L_1}$, $X_1^{L_2}$;

b) on calcule $\gamma_1^{L_1}$, $\gamma_2^{L_1}$, $\gamma_1^{L_2}$, $\gamma_2^{L_2}$ à l'aide d'un modèle adéquat (par exemple LEMF) ;

c) on résout le système linéaire en trouvant Z_1, Z_2 ;

d) on calcule de nouvelles valeurs $X_1^{L_1}$, $X_1^{L_2}$;

e) on effectue un test de convergence, par exemple : $|X_i^{\text{nouvelles}} - X_i^{\text{antérieures}}| < \varepsilon$. Si le test est vérifié, le calcul s'achève, sinon, il est repris de l'étape (b).

Pour déterminer les paramètres Δg_{12} et Δg_{21} dans le cas du système cyclohexane–eau, l'algorithme ci-dessus (a–e) a été implémenté dans une procédure d'estimation non-linéaire des paramètres.[9,10]

La fonction but a été :

$$S = \sum_{i=1}^{N1} (X_{1,i}^{c} - X_{1,i}^{ex})_{L_1}^2 + \sum_{i=1}^{N2} (X_{1,i}^{c} - X_{1,i}^{ex})_{L2}^2$$

où $X_{1,i}^{c}$ sont les compositions calculées à l'aide de l'algorithme décrit (a–e) ;

$X_{1,i}^{ex}$ sont les compositions expérimentales (on a utilisé les données du tableau 8) ;

N_1, N_2 — le nombre des points expérimentaux relatifs aux phases L_1, L_2.

On a obtenu les paramètres du modèle LEMF qui réalisent

$$\min S = 2{,}956 \cdot 10^{-9}$$

dans Δg_{12}, Δg_{21} respectivement $\Delta g_{12} = 4012{,}5$ et $\Delta g_{21} = 3462{,}5$ J/mol.

Dans le tableau 9 on présente les résultats obtenus.

Tableau 9

Les compositions des phases en équilibre L—L pour le système cyclohexane (1)—eau (2)

t, °C	$X_1^{L_1}$ (exp)	$X_1^{L_1}$ (calc)	$X_1^{L_2}$ (exp)	$X_1^{L_2}$ (calc)
10	0,999687	0,999693	—	$1{,}958 \cdot 10^{-5}$
20	0,999430	0,999447	$1{,}2 \cdot 10^{-5}$	$4{,}735 \cdot 10^{-5}$
30	0,999094	0,999068	—	$1{,}021 \cdot 10^{-4}$
40	0,998521	0,998515	—	$2{,}004 \cdot 10^{-4}$
50	0,997715	0,997740	—	$3{,}637 \cdot 10^{-4}$

Tenant compte de ces données et utilisant les valeurs des paramètres du modèle LEMF ainsi obtenues, on peut calculer les diagrammes des phases pression—compositions des phases (P—X—Y) pour des températures diverses.

Conformément à la théorie fondée sur la programmation géométrique,[16,17] le calcul est fait en résolvant d'une manière itérative le système linéaire d'équations :

$$\frac{1}{\gamma_1 P_1^0} Z_1 + \frac{1}{\gamma_2 P_2^0} Z_2 = 1$$

$$\frac{1}{P} Z_1 + \frac{1}{P} Z_2 = 1$$

pour T = constante, où P_1^0 et P_2^0 sont les pressions de vapeurs des composants purs, et P est la pression totale. Z_1, Z_2 sont les inconnues auxiliaires qui sont liées aux compositions des phases—liquide (X_1) respectivement vapeurs (Y_1).

$$X_1 = Z_1/\gamma_1 P_1^0; \quad Y_1 = Z_1/P$$

Pour l'eau on a utilisé une équation Antoine[10] :

$$\ln P^0 = 18{,}3036 - \frac{3816{,}44}{T - 46{,}13}, \text{ P, mm Hg}$$

$$T \in 284 - 441 \text{ K}$$

Vu que $\gamma_1 \gamma_2$ sont des fonctions des compositions de la phase liquide, le système ci-dessus est résolu d'une manière itérative conformément à l'algorithme (pour T et P données) :

a) on choisit les valeurs initiales X, Y ;
b) on calcule γ_1, γ_2 à l'aide des équations LEMF et les paramètres connus tenant compte des données L—L ;
c) on résout le système linéaire en trouvant Z_1, Z_2 ;
d) on calcule de nouvelles valeurs X, Y ;
e) on effectue un test de convergence, par exemple :

$$|X_1^{\text{nouveau}} - X_1^{\text{antérieur}}| < \varepsilon_1 \text{ et } |Y_1^{\text{nouveau}} - Y_1^{\text{antérieur}}| < \varepsilon_2$$

Si le test est satisfait, le calcul s'achève, sinon il est repris de l'étape (b).

En utilisant cette procédure on a obtenu les données (les diagrammes des phases) des tableaux 10 et 11 pour les températures de 30°C et respectivement de 50°C, du domaine pour lequel ont existé les données liquide—liquide.

Tableau 10

Données d'équilibre liquide—vapeurs pour le système cyclohexane (1) — eau (2) t = 30 °C. $P_1^0 = 121,78$; $P_2^0 = 31,65$. Les coefficients d'activité exprimés par le modèle LEMF.

Branche cyclohexane

P, mm Hg	X_1	Y_1	γ_1	γ_2
125	0,999908	0,97418	1	1113,2
130	0,999764	0,93658	1	1106,2
135	0,999619	0,90176	1	1099,2
140	0,999471	0,86943	1	1092,2
145	0,999321	0,83933	1	1085,2
150	0,999170	0,81123	1	1078,1
153	0,999078	0,79525	1	1073,8

Branche eau

P, mm Hg	X_1	Y_1	γ_1	γ_2
35	$2,788 \cdot 10^{-6}$	0,09566	9859,4	1
45	$1,112 \cdot 10^{-5}$	0,29663	9853,0	1
55	$1,947 \cdot 10^{-5}$	0,42452	9846,7	1
75	$3,619 \cdot 10^{-5}$	0,57799	9833,9	1
95	$5,296 \cdot 10^{-5}$	0,66684	9821,1	1
115	$6,978 \cdot 10^{-5}$	0,72478	9808,3	1
135	$8,663 \cdot 10^{-5}$	0,76556	9795,5	1
153	$1,018 \cdot 10^{-4}$	0,79315	9783,9	1

Dans le tableau 12 sont presentées les pressions correspondant à l'hétéroazéotrope pour t = 30°C, obtenues expérimentalement par la méthode statique pour deux compositions globales.

On remarque une bonne concordance entre la valeur calculée (153 mm Hg, tableau 10) et celle expérimentale.

Tableau 11

Données d'équilibre liquide—vapeurs pour le système cyclohexane (1) — eau (2) pour t = 50 °C. $P_1^0 = 271,92$; $P_2^0 = 92,46$. Les coefficients d'activité exprimés par le modèle LEMF.

Branche cyclohexane

P, mm Hg	X_1	Y_1	γ_1	γ_2
280	0,999815	0,97097	1	474,9
290	0,999582	0,93727	1	471,2
300	0,999346	0,90582	1	467,4
310	0,999106	0,87639	1	463,6
320	0,998862	0,84881	1	459,7
330	0,998613	0,82289	1	455,7
340	0,998360	0,79849	1	451,7
350	0,998102	0,77549	1	447,8
360	0,997840	0,75376	1	443,9
364	0,997734	0,74541	1	442,4
364,387	0,997723	0,74461	1	442,05

Branche eau

P, mmHg	X_1	Y_1	γ_1	γ_2
100	$9,89 \cdot 10^{-6}$	0,07536	2801,9	1
130	$4,939 \cdot 10^{-5}$	0,28876	2795,3	1
160	$8,907 \cdot 10^{-5}$	0,42214	2788,7	1
190	$1,289 \cdot 10^{-4}$	0,51340	2782,0	1
220	$1,690 \cdot 10^{-4}$	0,57977	2775,4	1
250	$2,092 \cdot 10^{-4}$	0,63021	2768,7	1
280	$2,497 \cdot 10^{-4}$	0,66985	2762,0	1
310	$2,903 \cdot 10^{-4}$	0,70181	2755,4	1
340	$3,312 \cdot 10^{-4}$	0,72813	2748,6	1
364	$3,642 \cdot 10^{-4}$	0,74607	2742,2	1
364,387	$3,647 \cdot 10^{-4}$	0,74633	2742,1	1

Tableau 12

Données d'équilibre pour l'hétéroazéotrope cyclohexane (1)—eau (2) à t = 30°C.

Fraction molaire globale, X_1	Pression hétéroazéotrope, mm Hg
0,3	155
0,7	148,5

On a essayé aussi une extrapolation, en calculant le diagramme des phases pour la température de 69°C. Les résultats sont présentés dans le tableau 13. Pour cette température la composition expérimentale du hétéroazéotrope est $X_{H_2O}^{ex} = 0,316$ pour P = 1 atm. On remarque

Tableau 13

Données d'équilibre liquide—vapeurs pour le système cyclohexane (1) — eau (2) pour $t = 69\,°C$. $P_1^0 = 526,667$; $P_2^0 = 223,876$. Les coefficients d'activité exprimés par le modèle LEMF.

Branche cyclohexane

P, mm Hg	X_1	Y_1	γ_1	γ_2
530	0,999940	0,99365	1	249,7
550	0,999574	0,95717	1	247,1
570	0,999201	0,92325	1	244,6
590	0,998819	0,89162	1	241,9
610	0,998429	0,86206	1	239,2
630	0,998030	0,83438	1	236,6
650	0,997622	0,80839	1	233,9
670	0,997203	0,78395	1	231,2
690	0,996775	0,76093	1	228,5
710	0,996335	0,73920	1	225,7
730	0,995885	0,71866	1	222,9
750	0,995422	0,69921	1	220,1

Branche eau

P, mm Hg	X_1	Y_1	γ_1	γ_2
230	$1,063 \cdot 10^{-5}$	0,02664	1093,8	1
250	$4,544 \cdot 10^{-5}$	0,10453	1091,9	1
300	$1,329 \cdot 10^{-4}$	0,2538	1087,4	1
350	$2,212 \cdot 10^{-4}$	0,36049	1082,8	1
400	$3,102 \cdot 10^{-4}$	0,44048	1078,2	1
450	$4,001 \cdot 10^{-4}$	0,50269	1073,5	1
500	$4,907 \cdot 10^{-4}$	0,55246	1068,9	1
550	$5,821 \cdot 10^{-4}$	0,59318	1064,2	1
600	$6,743 \cdot 10^{-4}$	0,62712	1059,5	1
650	$7,673 \cdot 10^{-4}$	0,65583	1054,9	1
700	$8,612 \cdot 10^{-4}$	0,68044	1050,1	1
750	$9,559 \cdot 10^{-4}$	0,70177	1045,4	1

une concordance satisfaisante, la valeur calculée étant $X^c_{H_2O} = 0,316$ au $P = 750$ mm Hg.

VI. CONCLUSIONS

1. On a effectué des déterminations expérimentales d'équilibre liquide—vapeurs pour les systèmes cyclohexane—monochlorcyclohexane et cyclohexane—eau.

2. On a déterminé la courbe de la pression de vapeurs du monochlorcyclohexane et on a établi par régression l'équation correspondante pour le domaine de température 30—85°C.

3. On a effectué la corrélation des données expérimentales liquide—vapeurs pour les systèmes cyclohexane—monochlorcyclohexane et cyclo-

hexane—eau avec des modèles d'activité (Wilson, NRTL/H et LEMF) suivant des programmes d'ordinateur. On a obtenu ainsi les diagrammes des phases calculés pour le domaine entier de la composition des systèmes.

BIBLIOGRAPHIE

[1] E. Hala, J. Pick, V. Fried et O. Vilim, « Vapor-Liquid Equilibrium », Pergamon, Oxford, 1967.

[2] J. M. Prausnitz, « Computer Calculations for Multicomponent Vapor-Liquid and Liquid-Liquid Equilibria », Prentice-Hall, N. J., 1980.

[3] J. M. Prausnitz, « Molecular Thermodynamics of Fluid Phase Equilibria », Prentice-Hall, N.J., 1969.

[4] F. A. Gothard, « Echilibre lichid-vapori », Ed. Academiei, București, 1975.

[5] C. Strătulă, V. Marinoiu et Gh. Sorescu, « Metode și programe de calcul al proceselor de distilare, fracționare și absorbție », Ed. Tehnică, București, 1976.

[6] D. Geană, *Rev. Chimie (București)*, **32**, 337 (1981).

[7] A. Vogel, « Textbook of Practical Organic Chemistry », Longman, p. 384, London, 1978.

[8] V. Dumitru, « Programare neliniară », Ed. Academiei, București, 1975.

[9] Y. Bard, « Nonlinear Parameter Estimation », Academic Press, New York, 1974.

[10] R. C. Reid, J. M. Prausnitz et T. K. Sherwood, « The Properties of Gases and Liquids », 3rd edition, McGraw-Hill, New York, 1977.

[11] O. Landauer, C. Mateescu, D. Geană et O. Iulian, communiqué à la Conférence de chimie et d'ingénierie chimique, București, oct. 1985.

[12] G. M. Wilson, *J.A.C.S.*, **86** 127 (1964).

[13] D. N. Tarassenkov et E. N. Poloshinzewa, *Ber. dtsch. Chem. Ges.*, **65**, 184, 1932.

[14] B. A. Englin, *Chim Technol. Topliv Masel*, **1965**, p. 42, 9.

[15] A. G. Moracevskii, N. A. Smirnova, I. M. Balashova et I. B. Pukinski, « Termodinamik razbavlenykh rastvorov neelectrolitov », Khimia, Leningrad, 1982.

[16] D. Geană, *Rev. Roumaine Chim.*, **26**, 363 (1981).

[17] D. Geană, *Rev. Roumaine Chim.*, **29**, 395 (1984).

Revue Roumaine de Chimie, **33**, *3*, 253–262 (1988)

THERMODYNAMICS OF SOME IRON COMPLEXES IN WATER-PYRIDINE MIXTURES

JEAN-LOUIS BRISSET
Laboratoire des Réacteurs Chimiques en phase plasma,
École Normale Supérieure de Chimie et Physique, 11, rue P. & M. Curie, 75005 Paris, France

Received November 17, 1986

The spectrophotometric and electrochemical studies of iron derivatives (i.e. tris 1,10-phenanthroline iron (II), tris 2,2-dipyridyl iron (II), hexacyanoferrates (II) and (III), ferrocene) have been undertaken in a series of buffered water-pyridine mixtures (fraction x of amine comprised between 0 and 68.2% by weight) to gather data on their stoechiometry, stability, solubility and electrochemical behaviour. Evidence is given of the limited influence of the solvent. Stoechiometry remains 1 : 3, the same as in water for the phenanthroline and related complexes. The changes in the solvent composition do not affect significantly the stability constants for $48.2 > x > 9.2$ % while the oxidation-reduction potentials are generally stabilized ax x increases in the mixture.

The water-pyridine mixtures may be considered as good examples of solvents characterized with both Bronsted and Lewis acid-base properties. The proton exchange equilibria have been carefully examined[1, 2] in these media, so that numerous calibrated buffers are now available which cover the full range of the autoprotolysis product for a large variety of solvent composition (i.e. $0 < x < 98$; x: amine percent by weight in the mixture). In addition the acidity scales pS^+ thus determined in each mixture were discussed[3] with respect to various classical extrathermodynamic assumptions and compared to the aqueous pH scale.

We concentrate in this matching paper on the Lewis acid/base properties of the relevant mixtures, which may be expected from the occurrence of an electron pair on the pyridine N atom. We selected various iron derivatives as solutes (i.e. tris 1,10-phenanthroline iron (II), tris 2,2′-dipyridyl iron (II), potassium hexacyanoferrates (II) and (III) and bis cyclopentadienyl iron (ferrocene)) for which the close environment of the metal ion may be strongly affected by pyridine.

Spectrophotometry and voltammetry were the two independent techniques used to gather informations on the stoechiometry, stability, solubility and electrochemical behaviour of the considered complexes in a large range of solvent composition.

Literature reports a limited number of similar works:[4–8] only particular aspects have been investigated in the papers which generally concern mixtures different from those considered here. For example Co(II), Ni(II) and Cu(II) complexes with monoethylamine have been examined in aqueous solutions of methanol, dioxane, acetonitrile or dimethylformamide.[8] The acidity constants of some ligands (e.g. 2,2′-dipyridyl and related compounds) were determined in selected mixtures,[9-10] or the effect of acidity on the electrochemical behaviour of the relevant iron complexes has been reported.[11-12]

EXPERIMENTAL

A — Spectrophotometric measurements

A Beckman Acta III UV—Vis spectrophotometer thermostated at 20 °C and fitted with 1 cm quartz cells was used for all the spectrophotometric measurements, except for kinetic experiments which were performed on a Durrum-Gibson Stopped flow device (also thermostated 20 °C). The general procedure for solubility measurements has been reported.[13]

B — Electrochemical measurements

The general device was a 3-electrodes set previously described.[14] The rotating platinum electrode was a Tacussel EDI—2 fitted with a Tacussel Controvit speed control unit. The ionic strength of the tested solutions was fixed at 0.1 M by addition of KNO_3 when necessary; the non-aqueous buffers were previously calibrated.[2]

C — Chemicals

Pyridine was distilled[2] and water bidistilled. Most of the inorganic chemicals were analytical grade commercially available and used without further purification. Ferrocene was recrystallized from petroleum ether. Phenanthroline and dipyridyl were purchased from Aldrich and used without purification. The relevant FeX_3 complexes were synthesized according to the literature procedures; $Co(NH_3)_6Cl_3$ was prepared following known methods.[15] All complexes analyzed satisfactorily.

RESULTS AND DISCUSSION

C — Spectrophotometric studies

The spectrophotometric techniques have been intensively used in this work. They led to informations of various kinds, such as stoechiometry and stability of the complexes as well as solubility data in various mixtures or the kinetics of formation.

1) — *Stoechiometry*

Shilt's pertinent analysis[16] reports that Fe(II) ion and bidentate ligands such as Dipyridyl or Phenanthroline undergo association reactions to form 1 :1 or 1 :3 complexes in water or in a variety of non-aqueous media. However it has been claimed that 1 :2 complexes were stable in water-hydrazine mixtures.[6] To elucidate the question, we determined the stoechiometry of the relevant complexes in the considered solvents.

Starting from freshly prepared aqueous solutions of Fe(II) (pH : 2) and pyridine solution of complexing agent to prepare the convenient mixture, we found that only 1 :3 complexes were formed in the mixtures investigated ($19.2 < x < 68.2$). Two independant methods were used, i.e. Job's method[17] and the mole ratio method[18] and gave the same results for the stoechiometry as illustrated by Fig. 1. The spectrophotometric measurements were performed in each mixture at the absorption peaks which are independent of the solvent composition and the same as in water (respectively 510 and 525 nm for Fe $Phen_3$ and $FeDipy_3$). This indicates that no solvatochromic effect occurs in the water-pyridine mixtures.

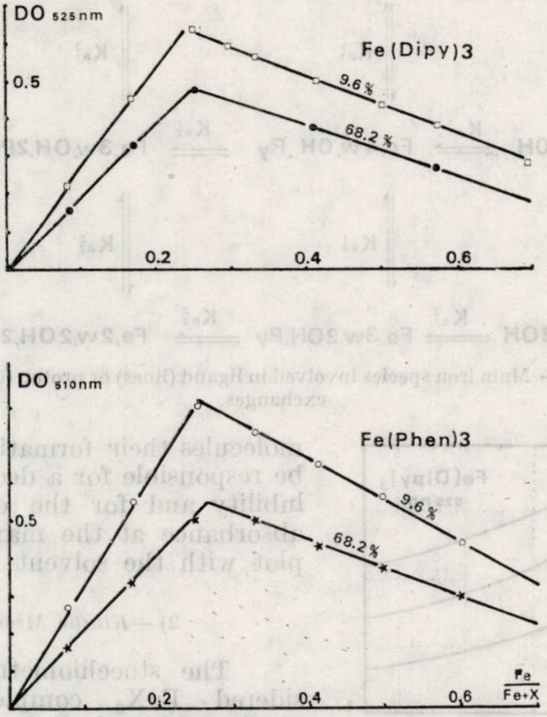

Fig. 1. — Job's plots for $Fe(II)Dipy_3$ and Fe(II) $Phen_3$ complexes.

In addition the maximum of Job's plots lowers as x increases. This shows that either the molar absorptivity ε is affected by the solvent composition (which involves solvation processes) or more likely the Fe(II) ions are in part masked to the complexing agents. The latter character may be connected with the acid/base properties of the hexaaquoiron (II) in pyridine solutions : one can reasonably assume that ligand exchanges occur and are governed by a difference in the Lewis base character of water and pyridine, e.g. :

$$Fe(H_2O)_6^{++} + Py = Fe(H_2O)_5Py^{++} + H_2O$$

or by a classical Bronsted acid/base character, e.g. :

$$Fe(H_2O)_6^{++} + Py = Fe(H_2O)_5OH^+ + PyH^+$$

A generalized scheme presented on Fig. 2 is limited to the consideration of uncharged species involving two hydroxy groups as ligands. Since uncharged species undergo no charge/dipole interactions with the solvent molecules their formation should then be responsible for a decreasing iron solubility and for the evolution of the absorbance at the maximum of Job's plot with the solvent composition.

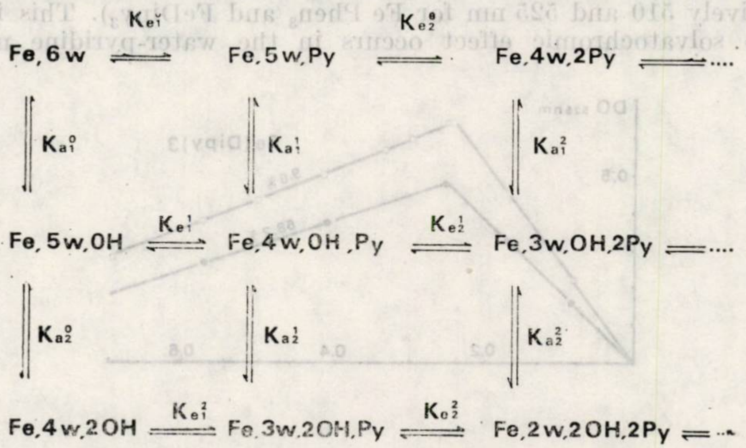

Fig. 2. — Main iron species involved in ligand (lines) or proton (columns) exchanges.

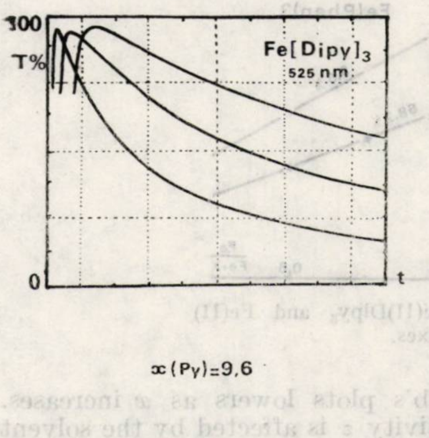

Fig. 3. — Typical stopped flow experiments giving evidence that only the 3rd step can be considered.

2) — *Kinetic Measurements*

The stoechiometry of the considered FeX_3 complexes could be confirmed kinetically by means of stopped flow experiments. We started from an aqueous solution of Iron(II) at pH : 2 and a pyridine solution of the ligand which were mixed such as the final solution had the required composition x in pyridine and a ligand to metal ratio of 3. The formation of the FeX_3 complexes was followed at their absorption peaks and exhibited three separate steps for any solvent composition. The first one is very fast and partly masked by the mixing of the solutions and corresponds (Fig. 3) to the formation of strongly absorbing compounds. The second step is also too fast to be considered for accurate kinetic data and corresponds to the disappearance of the relevant compounds. The third step can be observed more conveniently since the half-life time was found in the range 50—125 ms : it slightly depends on the the solvent composition and slowers as x increases. Our purpose was not to investigate the reaction mechanism ; we will limit to show that it is complicated and involves several steps. We can only suggest that the observed steps do not correspond to the successive formation of the 1 :1, 1 :2 and 1 ;3 complexes since the 1 :1 complexes absorb in UV and our experiments were performed in the visible range. In addition the formation under the considered experimental conditions (i.e. in the presence of a great excess of pyridine which acts as a matching complexing agent, and in alkaline media referred to the aqueous pH scale) of compounds which exhibit the same absorption spectra as FeX_3 in aqueous solutions prevents to consider the side formation of pseudo-base species (e.g. FeX_3OH) similar to those studied by Gillard [19-20] and Burgess [21,22] in water or in hydro-alcoholic mixtures.

3) — *Stability of the complexes*

We were then concerned with the stability of the considered FeX_3 complexes and thus we determined first their molar absorptivity at the absorption peaks wavelengths, which are not affected by the solvent composition.

Starting from a pyridine solution of the ligand and from an aqueous 0.1 M solution of Fe(II) which was previously acidified to prevent hydrolysis [23] we prepared synthetic solutions of the complexes having alway ligand excesses in the desired solvent mixture and measured their absorp^{s}tion at the convenient wavelength. For various solvent compositions-(i.e. $9.6 < x < 68.2$), the molar absorptivities were found respectively $1.15\ 10^5\ mol^{-1}\ dm^2$ at 510 nm and $86350\ mol^{-1}\ dm^2$ at 525 nm for the Dipy and Phen complexes.

We were then able to determine the stability constants from absorbance measurements of synthetic solutions whose compositions were close to stoechiometry :

$$K_{\text{diss}} = \frac{C(Fe)\cdot C(X)^3}{C(FeX_3)} = \frac{(Co(Fe) - C(FeX_3))\cdot(Co'(X) - 3C(FeX_3))^3}{C(FeX_3)}$$

K_{diss} is a formal constant since it involves concentration instead of activity terms.

Besides C(Fe) refers to the total concentration of solvated Fe(II) (i.e. $Fe(H_2O)_n(Ph)_{6-n}$ and related hydroxylated species) while X and FeX_3 are assumed to exist only in one form.

The dissociation constant K_{diss} may be expressed by means of the various ligand exchange constants Ke_j^i and the acidity constants Ka_j^i (see Fig. 2). Its expression can be simplified if we assume that the prominent equilibria involve :

— the hexaaquoiron(II) ion noted Few_6 as the main acid species, so that only Ka_1^0 and Ka_2^0 are to be considered.

— the $Fe(H_2O)_{6-n}Py_n$ ions are the main species undertaking ligand exchange equilibria, so that only the Ke_i^0 should be considered. This assumption is strongly backed up by the difference in the labile character of the ligands OH^- and H_2O.

Then :

$$C(Fe) = C(Few_6) + C(Few_5OH) + C(Few_4(OH)_2) + C(Few_5Py) + \\ + C(Few_4Py_2)$$

If we define K_0 as

$$K_0 = C(Few_6) \cdot C(X)^3 / C(FeX_3)$$

the ratio K_{diss}/K_0 may be expressed as the sum of a function of the acidity, $\alpha(1/C(S^+))$, and a function of the solvent composition, $\sigma(C(Py)/C(w))$:

$$K_{diss}/K_0 = 1 + Ka_1/C(S^+) + Ka_1 \cdot Ka_2/C(S^+)^2 + \\ + Ke_1 C(Py)/C(w) + Ke_1 \cdot Ke_2 C(Py)^2/C(w)^2$$

In a given solvent mixture the σ function takes a constant value and the ratio K_{diss}/K_0 depends only on the acidity terms $C(S^+)$. Then it may be expected that the plot $-\log K_{diss}$ *vs* $-\log C(S^+)$ exhibit linear parts with slopes 0, -1 or -2. In addition the effect of the solvent composition may be appreciated when α is constant, i.e. for a slope 0 of the considered plot.

Our experimental results are reported on Fig. 4. Each plot consists in two linear parts with slopes 0 and -2, which confirms our assumptions

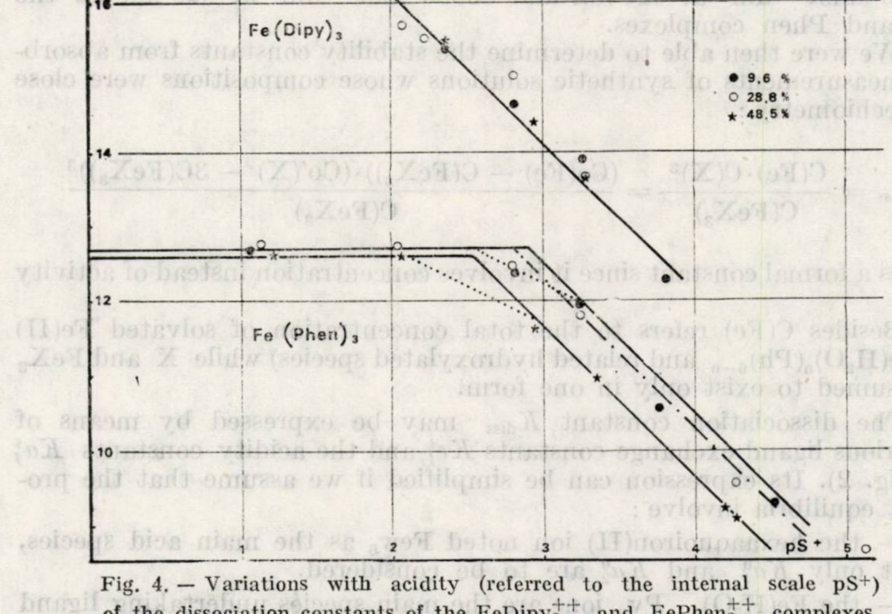

Fig. 4. — Variations with acidity (referred to the internal scale pS^+) of the dissociation constants of the $FeDipy_3^{++}$ and $FePhen_3^{++}$ complexes. The plots are relevant to the mixtures $x = 9.6$; 28.8 and 48.5.

and shows that the acidity constants Ka_1 and Ka_2 are separated by less than 2 pK units in any considered mixture.

The solvent effect on the stability of the complexes may be neglected in the considered mixtures, as evident from the position of the horizontal parts of the plots. This leads to consider that the σ function may be neglected in the ratio K_{diss}/K_0 or otherwise, that solvation phenomena do not drastically affect the complexes in the composition range $9.6 < x < 48.5$. This might be an argument favouring the choice of one of these complexes as a partner of a reference couple for the study of non aqueous media.

4) — *Solubility measurements*

The solubilities of potassium hexacyanoferrate (III) and biscyclopentadienyliron (ferrocene) were determined spectrophotometrically in a series of water-pyridine mixtures. The relevant data are reported in Table 1 : they can be used [3] to calibrate an acidity scale in each mixture (i.e. the pS^+ scale) with respect to the acidity scale in pure water, the pH scale. The solubility of $Co(NH_3)_6Cl_3$ could not be measured in the considered solvents because ligand exchange reactions occur. The pyridine molecules take the place of NH_3 as the solubility equilibrium is reached.

Table 1

Solubilities ($-\log C_{sat}$ (i) in the molar scale) in water-pyridine mixtures at 20 °C

x	0	9.6	19.2	28.8	38.8	48.5	58.5	68.2	78.4	88.4	100
$Fe(CN)_6K_3$	0.02	0.05	0.13	0.30	0.45	0.70	1.15	3.42			
Ferrocene	4.47	3.54	3.09	2.65	2.23	2.00	1.68	1.37	0.97	0.45	0.08

B — Electrochemical studies

1) — *Voltamperometry of potassium hexacyanoferrate*

In spite of the high electric charges involved, the ferri/ferrocyanide system has been studied in numerous non-aqueous solvents and data on the oxidation-reduction potentials are available in the literature, but we found no information on the behaviour of this system in the water-pyridine mixtures.

Solutions of potassium ferrocyanide were found unstable in most of the investigated mixtures : spontaneous oxidation occurs which may be due to the supporting electrolyte KNO_3 (ionic strength fixed at 0.1) so that only reduction of potassium ferricyanide could be examined in a large range of solvent composition ($19.2 < x < 68.2$). For a given solvent the reduction curves at the rotating platinum electrode of buffered solutions of ferricyanide are single monoelectronic waves which verify the usual criteria of reversibility at the polarographic scale. The half-wave potentials are constant for neutral or basic media, i.e. for $pS^+ > 3$ in the acidity scale relevant to the considered solvent (Fig. 5) and the redox system may be characterized by the plateau value $E^*_{1/2}$. These $E^*_{1/2}$ values depend on the solvent composition : as illustrated on Fig. 6, $E^*_{1/2}$ is a decreasing function of x. Besides the limiting current of the voltamperometric wave is lowered as x increases, which gives evidence of a progressive modification of the diffusion coefficients and may be correlated to the solubility measurements.

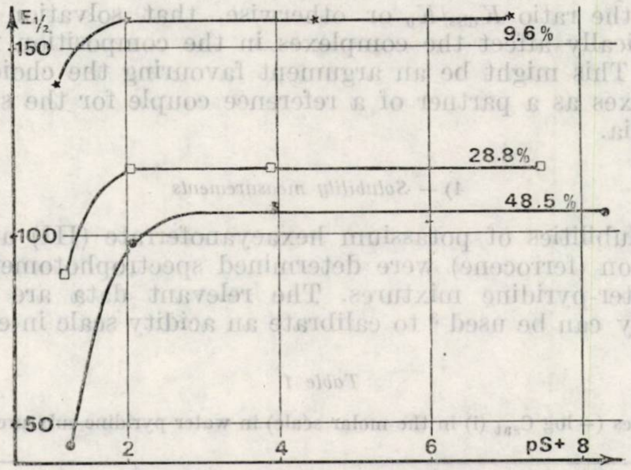

Fig. 5. — Variations of the reduction half-wave potential of $Fe(CN)_6K_3$ (referred to aq. SCE) for various water-pyridine mixtures.

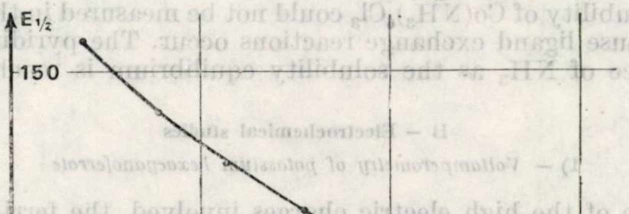

Fig. 6. — Stabilization of the $E^*_{1/2}$ (mV, *vs.* aq. SCE) with the solvent composition for the reduction of potassium hexacyanoferrate (III).

2) — 1.10-*Phenanthroline and 2.2'-Dypyridyl Fe(II) complexes*

The spectrophotometric study has given evidence that the stability of the complexes is unaffected by the solvent composition provided we consider only the plateau region, i.e. the "acidic" media. To carry on our investigations of the solvent effects we developed an electrochemical study and determined the oxidation-reduction potentials of the involved systems and concentrated on the plateau region.

For various "acidic" media ($pS^+ < 1.5$ and $x < 48.5$), the $FeDipy_3$ complex shows single oxidation curves close to the solvent oxidation walls : the characteristic half-wave potentials cannot then be determined with sufficient accuracy. The same technique was applied to the oxidation of $FePhen_3$ complex. The one-electron oxidation waves satisfy the reversibility criteria (on the polarographic scale) and the half-wave potentials are independant of the acidity ($pS^+ > 2$) for a given mixture and increase with x (Table 2).

Table 2

Half-wave oxidation or reduction potentials (E^* plateau for hexacyanoferrate (III)), mV/aq. NHE

x	0	9.6	19.2	28.8	38.8	48.5	58.5	68.2	78.4	88.4
$FePhen_3$:	1092	1162	1187	1202	1220	1234	1257	1274	1312	1362
Ferrocene	392	410	435	460	484	507	533	559	611	677
$Fe^{III}(CN)_6$:	410	405	390	373	360	352	341	341		
$Co^{III}(NH_3)_6$:	−26	−373	−371	−353	−328	−298	−263	−233	−178	

3) — *Ferricenium/ferrocene system*

Oxidation of ferrocene has been followed on the whole range of solvent composition, and found independent of the acidity. The half-wave potentials in a given solvent were used to determine the transfer activity coefficient of the proton on the basis of a very popular extrathermodynamic assumption.[3]

4) — *Hexamminecobalt (III) chloride*

The electrochemical behaviour of the title compound was also examined in the water-pyridine mixtures. We selected hexamminecobalt (III) chloride as a matching example of octahedral complex in which all the ligands have a strong donnor character. It was expected that the pyridine molecules of the solvent would not undergo exchange reactions with ammonia. In fact this exchange may partly occur and be responsible for the limited reproducibility of the voltamperometric curves. The half-wave reduction potentials are reported in Table 2 only for information purposes and indicate that the $E_{1/2}$ *bs.* x present a minimum. The electrochemical behaviour of the cobalt complex is then intermediate between those of iron phenanthroline and cyanide complexes.

REFERENCES

[1] J. M. Nigretto and M. Josefowicz, "The Chemistry of Non-aqueous Solvents", J. J. Lagowski Ed., Vol. VA, Academic, New York, 1978, pp. 179—250.

[2] J. L. Brusset, R. Gaboriaud and R. Schaal, *J. Chim. phys.*, **68**, 1506 (1971).

[3] J. L. Brisset, *J. Sol. Chem.*, **5**, 587 (1976).

[4] M. Bigois, J. C. Touller and B. Tremillon, *Bull. Soc. chim. France*, **1847**, 1965.
[5] J. C. Touller, M. Grall, M. Bigois and N. Tremillon, *Bull. Soc. chim. France*, **1853, 1965.**
[6] D. Bauer, *Bull. Soc. chim. France*, **2631**, 1966.
[7] N. Rayen-Baldy and M. Machtinger, *Bull. Soc. chim. France*, **2221**, 1968.
[8] M. S. Masoud and A. A. Abdallah, *J. Chem. Eng. Data*, **27**, 60 (1982).
[9] D. K. Hazra and S. C. Lahiri, *J. Indian Chem. Soc.*, **53**, 567 (1976).
[10] D. K. Ram, A. K. Mandal and S. C. Lahiri, *J. prakt. Chemie*, Band **319**, Heft 5, 719 (1977).
[11] D. P. Poe and A. D. Eppen, *Talanta*, **27**, 1007 (1980).
[12] D. P. Poe and J. A. Adamczak, *Talanta*, **27**, 1012 (1980).
[13] J. L. Brisset, *J. Chem. Eng. Data*, **27**, 153 (1983).
[14] J. L. Brisset, *J. Electroanal. Chem. Interfac. Electrochem.*, **51**, 133 (1974).
[15] G. Brauer, "Handbook of Preparative Inorganic Chemistry", Vol. 2, 2nd Ed. Academic, New York, 1963, p. 1531.
[16] A. A. Schilt, "Analytical Applications of 1,10-Phenanthroline and Related Compounds", Pergamon, New York, 1969.
[17] P. Job, *Ann. Chimie*, **9**, 113 (1928).
[18] A. E. Harvey and D. L. Manning, *J. Amer. Chem. Soc.*, **72**, 4488 (1950).
[19] R. D. Gillard, *Coord. Chem. Rev.*, **16**, 67 (19 5).
[20] R. D. Gillard, L. A. P. Kane-Maguire and P. A. Williams, *J. Chem. Soc.*, **1972**, **1977.**
[21] J. Burgess and R. H. Prince, *J. Chem. Soc.*, **4697**, 1965.
[22] J. Burgess and C. D. Hubbard, *J. Amer. Chem. Soc.* **106**, 1717 (1984).
[23] C. M. Flynn, *Chem. Rev.*, **85**, 31 (1984).

Revue Roumaine de Chimie, **33**, *3*, 263–269 (1988)

KINETICS AND MECHANISM OF SUBSTITUTION REACTIONS OF COMPLEXES. LIX*

INFLUENCE OF pH UPON THE AQUATION KINETICS OF IODO-AQUO-BIS-DIMETHYLGLYOXIMATO-COBALT(III)

Z. FINTA †, J. ZSAKÓ and CS. VÁRHELYI
Faculty of Chemical Technology, University of Cluj-Napoca, str. Arany János 11, 3400 – Cluj-Napoca, Romania

Received September 15, 1986
Revised April 2, 1987

Aquation kinetics of the $[Co(DH)_2(H_2O)I]$ complex (DH_2 = dimethylglyoxime) was studied within a pH range between 3 and about 13.3. The strong influence of pH upon the aquation rate was explained on the basis of protolytic pre-equilibria. With the aid of the proposed reaction scheme acidity constants, rate constants and activation parameters were derived for several conjugated species. The results are discussed in terms of electronic effects and of other possible reaction pathways.

INTRODUCTION

In bis-dimethylglyoximato-complexes of Co(III) two short hydrogen bridges ensure the stability of the $Co(DH)_2$ equatorial plane.[1] Thus in aqueous solutions, aquation reactions occur only with the two axial ligands.

The aquation kinetics is highly influenced by the pH of the solutions.[2-13] This behaviour is assigned to the following protolytic equilibria:

$$\underset{\mathbf{1}}{[Co(DH_2)XY]} \xrightleftharpoons{K_1} \underset{\mathbf{2}}{[Co(DH_2)(DH)XY]} \xrightleftharpoons{K_2} \underset{\mathbf{3}}{[Co(DH)_2XY]} \xrightleftharpoons{K_3}$$

$$\xrightleftharpoons{K_3} \underset{\mathbf{4}}{[Co(DH)(D)XY]} \xrightleftharpoons{K_4} \underset{\mathbf{5}}{[Co(D)_2XY]} \qquad (1)$$

where K_i represents the acidity constant of the species i. K_2 is of 10^{-3} – 10^{-2}.[4,14] K_3 is of about 10^{-12} – 10^{-13}.[6-8,10,12-16]

---

* Part LVIII. J. Zsakó, J. Demeter-Vodnár, I. Bâldea and Cs. Varhelyi, *Rev. Roumaine Chim.*, **31**, 443 (1986).

† Deceased.

The species **5** appears only in strongly alkaline solutions, allowing the obtention of bis-dimethylglyoximatocomplexes of *cis*-configuration.[17-19]

Frequently, also the axial ligands can be protonated or deprotonated. Thus, the co-ordinated NO_2 ion being protonated [20,21] its corresponding acidity constant is of $2 \cdot 3 \times 10^{-2}$ at 50°C.[4]

The co-ordinated H_2O molecule becomes a weak acid with an acidity constant of about $10^{-7} - 10^{-8}$. [6,12,22-24]

For the aquation of $[Co(DH)_2(H_2O)I]$ in acid solutions first order kinetics was found, [25,26] but for alkaline solutions a second order one. [9]

In the present paper the aquation kinetics of this complex was studied in a large pH range.

EXPERIMENTAL

Synthesis of $[Co(DH)_2(H_2O)I]$ was performed according to literature data. [25]

Kinetic measurements. Samples were quickly dissolved in a preheated solution containing buffer mixtures (0.2 N acetic acid — 0.2 N sodium acetate, or 1/15 M KH_2PO_4 — 1/15 M Na_2HPO_4); different amounts of NaOH in order to ensure the wanted pH, as well as the necessary amount of $NaNO_3$ ensuring an ionic strength of 1.0 M. were added. The temperature was maintained at different constant values with an accuracy of ±0.01 °C.

The concentration of the I^- anions liberated was followed potentiometrically, [27] by using improved AgI electrodes. [26]

RESULTS AND DISCUSSIONS

The experimental electrode potential values transformed into free I^- ion concentrations allowed us to obtain good linear first order plots and to derive apparent first order rate constants, denoted as K_{exp}. Their values, representing the arithmetical mean of 3—5 individual data, are given in Table 1.

Table 1

Overall first order aquation rate constants of the $[Co(DH)_2(H_2O)I]$ complex at $\mu = 1.0$ M

pH	$k_{exp} \times 10^4$, s^{-1}				
	25°	30°	35°	40°	
3.0	0.0112	0.0254	0.0565	0.112	
5.0	0.0496	—	—	—	
6.0	1.86	3.41	6.39	11.9	
6.1	2.31	4.01	8.00	14.6	
6.3	3.23	5.74	11.2	23.1	
6.5	4.42	7.97	15.3	31.1	
6.7	5.57	10.1	19.7	38.6	
7.0	11.5	16.9	28.7	52.7	
$[OH^-] \times 10^2$	18°	20°	23°	25°	28°
2.9	17.0	21.1	29.5	37.0	51.8
3.9	20.8	26.5	36.8	44.5	62.8
4.9	24.9	30.9	42.6	53.4	74.8
6.9	32.5	40.7	56.2	69.3	90.2
9.9	39.6	51.2	71.1	88.7	119
14.9	53.8	64.5	87.3	114	171
19.9	63.8	80.9	114	133	199

As seen from this Table, at pH > 4, the overall rate constant increases rapidly with increasing pH. Since the acidity constant of the species **2** is of about 5×10^{-3}, at pH $= 3$ over 80 % of the complex must be present in the form of species **3**. Consequently, in the range investigated, the following protolytic equilibria might be considered :

$$\underset{a}{[Co(DH)_2(H_2O)I]} \overset{K_a}{\rightleftarrows} \underset{b}{[Co(DH)_2(OH)I]^-} \overset{K_b}{\rightleftarrows} \underset{c}{[Co(DH)(D)(OH)I]^{2-}} \quad (2)$$

The first order aquation of these species may be described as :

$$[Co(DH)_2(H_2O)I] + H_2O \xrightarrow{K_a} [Co(DH)_2(H_2O)_2]^+ + I^- \quad (3)$$

$$[Co(DH)_2\,(OH)I]^- + H_2O \xrightarrow{K_b} [Co(DH)_2(OH)(H_2O) + I^- \quad (4)$$

$$[Co(DH)(D)(OH)I]^{2-} + H_2O \xrightarrow{K_c} [Co(DH)(D)(OH)(H_2O)]^- + I^- \quad (5)$$

Presumably, after formation the hydroxo-aquo species undergoes a very rapid deprotonation in the alkaline region, viz. :

$$[Co(DH)(D)(OH)(H_2O)]^- \rightarrow [Co(DH)(D)(OH)_2]^{2-} + H^+ \quad (6)$$

If reactions (3), (4) and (5) occur according to an SN_1 type dissociation mechanism, the leaving of the I^- anion is favoured by the negative charge of species *b* and especially of that of the species *c*. Consequently, an important increase of the rate constants in the order $k_a < k_b < k_c$ can be expected, which seems to be consistent with our experimental data.

By adopting the above scheme as working hypothesis and by taking into account that the acidity constants of the species *a*, *b* and *c* differ very much from each other, one may presume that in the samples practically only two species are present, viz. *a* and *b* up to pH $= 7$, and only *b* and *c* in the alkaline region investigated.

Consequently, the overall reaction rate will be

$$-d[I_0^-]/dt = k_x c_x + k_y c_y = k_{\exp} c \quad (7)$$

where k_x, k_y, c_x, c_y stand for the aquation rate constant and for the molar concentration of the protonated (x) and for the deprotonated (y) species, respectively, and $x_x + c_y = c$. Since

$$K_x = (S^+]c_y)/c_x \quad (8)$$

Eq. (7) may be written as

$$-d[I^-]/dt = K_x(k_y - k_x)/(K_x + [H^+]) + k_x c \quad (9)$$

After rearrangement, Eqs. (7) and (9) yield

$$\frac{1}{k_{\text{exp}} - k_x} = \frac{1}{K_x(k_x - k_y)}[\text{H}^+] + \frac{1}{k_y - k_x} \tag{10}$$

Eq. (10) allows us to derive from the experimental k_{exp} and $[\text{H}^+]$ values both K_x and k_y, if k is known, by performing a plot of the left hand side *vs.* $[\text{H}^+]$.

Since at pH $= 3$ one may consider in a good approximation species a to be present alone, the k value obtained at this pH can be taken for k_x, i.e. for k_x in Eq. (10).

The linearization performed according to Eq. (10) is given in Fig. 1.

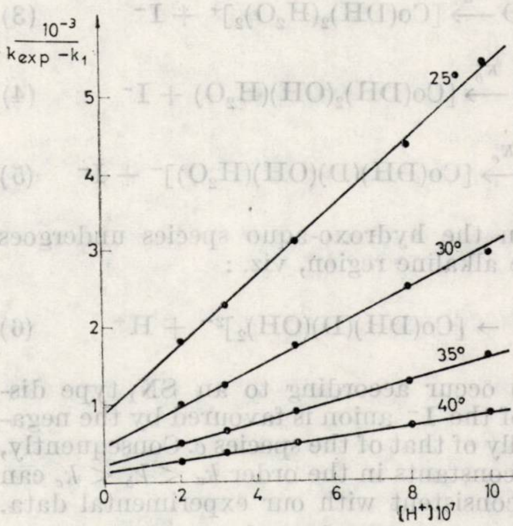

Fig. 1. — Deriviation of k_a and k_b values.

As seen, the linearization is rather good, allowing us to derive the parameters of the straight lines by using a linear regression method and to calculate the K_a and k_b values given in Table 2.

Table 2

Acidity constants (K_n) and aquation rate constants (k_n) of several conjugated specia of the $[\text{Co(DH)}_2\text{aH}_2\text{O)I}]$ complex, at $\mu = 1.0$ M

t°C	$K_1 \times 10^7$	$k_2 \times 10^{14}$	$k_1 \times 10^5$	$k_2 \times 10^4$	$k_3 \times 10^4$
18	—	1.72	—	—	166
20	—	1.77	—	—	228
23	—	2.15	—	—	322
25	1.94	2.45	0.110	11.5	403
28	—	2.76	—	—	609
30	1.90	—	0.254	20.8	—
35	1.92	—	0.565	40.0	—
40	1.82	—	1.12	76.9	—

The k_b value obtained was used in working up our data obtained in the alkaline region. By taking k_b for k_x in Eq. (10) a similar linearization was performed, allowing us to derive the K_b and k_c values presented in the same Table 2.

The acidity constant K_a of the co-ordinated water is in good agreement with the literature data concerning similar complexes.[6,12,22-24]

Concerning the acidity constant K , it is interesting to compare the values obtained with the corresponding constants of other $[Co(DH)_2XY]$ type complexes. These constants are given for 25°C in Table 3 after literature data. If the corresponding papers did not report data for this temperature, an extrapolation of the published data was performed. These extrapolated values are given in parantheses.

Table 3

Acidity constants of $[Co(DH)_2XY]$ type complexes at 25°C (K_3 in the scheme (1))

X	Y	$K_3 \times 10^{13}$	Ref.
NO_2	NH_3	(79.0)	13
NO_2	NO_2	57.8	6
NO_2	CN	(50.7)	10
NO_2	OH	9.13	6
NCS	OH	1.47	8
NCSe	OH	0.977	7
I	OH	0.245	this paper

As seen, if both X and Y contain π-bonds, i.e. they allow the Co to form retrodative type π-bonds, leading to the diminution of the electron density at the level of the central atom, the acidity is relatively high, due to the increased electrophilic character of Co, which entails the proton to be more weakly bonded. If $Y = OH$, the acidic character is weaker and decreases as a function of X in the order : $NO_2 > NCS > NCSe > I$, which is approximately the order of decreasing tendency to form retrodative π-bonds. The behaviour of the NH_3 complex is very surprising. Its acidity constant is about ten times higher than one might expect on the basis of the above considerations. In our view the constant reported cannot be K_3, but K_2, corresponding to the deprotonation of the co-ordinated NH_3, which obtains acid properties, like the co-ordinated water molecule. Thus, the real equilibrium is the following :

$$[Co(DH)_2(NO)_2(NH_3)] \xrightleftharpoons{K_2} [Co(DH)_2(NO_2)(NH_2)]^- + H^+ \qquad (12)$$

The rate constants reported in Table 2 allow us to derive activation enthalpy $\Delta H^{\neq}$ and activation entropy $\Delta S^{\neq}$ values by performing a plot of log (k/T) *vs.* $(1/T)$ and by calculating the parameters of the straight lines obtained, by means of a linear regression method. The activation parameters derived are presented in Table 4. The same Table contains also literature data concerning the aquation of other iodo-bis-dimethylglyoximato-Co(III) — complexes.

Table 4

Activation parameters of the aquation of [Co(DH)ZXI] type complexes

Z	X	ΔH^* kcal/mole	ΔS^* cal/*K* mole	Ref.
DH	NH_3	30.1	6.0	28
DH	H_2O	27.8 ± 0.2	7.9	this paper
DH	N_3	27.2 ± 0.4	6.3	29
DH	I	25.9 ± 0.3	5.3	26
DH	CN	25.7 ± 0.3	-3.1	30
DH	NO_2	25.3 ± 0.3	2.8	31
DH	OH	21.7 ± 0.4	1.3	this paper
D	OH	21.5 ± 0.3	7.3	this paper

Inspection of this table shows that our hypothesis concerning the dissociation mechanism seems to be likely, the positive activation entropy values (with a single exception) are consistent with an SN_1 pathway. In this case the activation enthalpy can be expected to decrease in the same order as the strength of the Co — I bond does. The latter must be strongest in the case of non-electrolyte type complexes, as observed indeed with $X = NH_3$, H_2O. Presumably in the complex anions this bond is weaker and its strength decreases if the tendency of $Co \rightarrow X$ type retrodative π — bond formation increases. The $\Delta H^{\neq}$ values decreasing in the order $N_3 > I > CN > NO_2$ are in perfect agreement with this presumption. The very low $\Delta H^{\neq}$ value obtained in the present paper for $X = OH$ is rather surprising. Similarly, the activation enthalpy obtained for the aquation of $[Co(DH)(D)(OH)I]^{2-}$ seems to be too high, as compared to the analogous anion $[Co(DH)_2(OH)I]^-$ with a single negative charge.

Consequently, in the alkaline region the other possible pathway, viz. the direct substitution of I^- for OH^-—ion, accordingly to an SN_2 mechanism, must be taken into account. Since in our experiments the concentration of OH^- ions is much larger than the concentration of the complex studied, the first order kinetics observed is not in disagreement with this possibility. In this case of the olation reactions

$$[Co(DH)_2(OH)I]^- + OH^- \xrightarrow{k_b'} [Co(DH)_2(OH)_2]^- + I^- \qquad (4')$$

$$[Co(DH)(D)(OH)I]^{2-} + OH^- \xrightarrow{k_c'} [Co(DH)(D)(OH)_2]^{2-} + I^- \qquad (5')$$

the condition $k_b' > k_c'$ could be expected, due to the large negative charge of *c*, making the formation of the dimolecular transition state more difficult.

The reaction rate can be given as

$$-d[I^-]/dt = k_b'c_b[OH^-] + k_c'c_c[OH^-] = k_{exp}c[OH^-] \qquad (12)$$

leading to the expression

$$\frac{k_{exp}}{[OH^-]} = k_b' + \frac{(k_c' - k_b')K_b}{K_x + K_b[OH^-]}[OH^-] \qquad (13)$$

where K stands for the ionic product of the water. By using data presented in Table 1, the plot of the ratio $k_{exp}/[OH^-]$ vs. $[OH^-]$ gives curve of a shape, which is consistent with Eq. (13). Theoretically, it would be possible to derive K_b, k_b' and k' values from the experimental data, e.g. by using a curve fitting method. For this purpose very accurate apparent rate constant values are needed, presumably in the range comprised between 9 and 12. Unfortunately, our attempts to obtain reproducible results in this range were not successful.

REFERENCES

[1] R. Blinc and D. Hadzi, *J. Chem. Soc.*, **1958**, 4536 ; *Spectrochim. Acta*, **16**, 853 (1968).
[2] A. V. Ablov and D. M. Palade, *Doklady Akad. Nauk S.S.S.R.*, **144**, 341 (1962).
[3] S. C. Chan, C. Y Cheang and F. Leh, *J. Chem. Soc. (A)*., **1967**, 1586.
[4] J. Zsakó, Z. Finta and Cs. Várhelyi, *Proc.* 3*rd Symp. Coord. Chem.* Debrecen, Hungary, T. 1., p. 333, 1970.
[5] Cs. Várhelyi, J. Zsakó and T. Finta, *Stud. Univ. Babeș-Bolyai, Chem.*, **15**, (2) 27 (1970).
[6] J. Zsakó, Z. Finta and Cs. Várhelyi, *J. Inorg. Nuclear Chem.*, **34**, 2887 (1972).
[7] C. Zsakó, Z. Finta and Cs. Várhelyi, *J. Inorg. Nuclear Chem.*, **35**, 2839 (1973).
[8] Z. Finta, Cs. Várhelyi and J. Zsakó, *Rev. Roumaine Chim.*, **18**, 417 (1973).
[9] N. M. Samush, T. S. Lukyanetz and A. V. Ablov. *Zhur. neorg. Khim.*, **19**, 2221 (1974).
[10] R. Ripan, Z. Finta and Cs. Várhelyi, *Rev. Roumaine Chim.*, **19**, 37 (1974).
[11] Cs. Várhelyi, Z. Finta and S. Kiss, *Monatsh. Chem.*, **106**, 1325 (1975).
[12] J. Zsakó. Cs. Várhelyi, Z. Finta and J. Kiss-Jakab, *Z. Naturforsch.* **30b**, 393 (1975).
[13] Z. Finta, Cs. Várhelyi and E. Dakó, *J. Inorg. Nuclear Chem.*, **38**, 2261 (1976).
[14] J. Zsakó, Z. Finta and Cs. Várhelyi, *Stud. Univ. Babeș-Bolyai Chem.*, **14**, (2), 14 (1969).
[15] J. P. Birk, P. B. Chook and J. Halpern, *J. Amer. Chem. Soc.*, **90**, 6959 (1968).
[16] V. R. Vijaryarghavan and M. Satrappa, *J. Inorg. Nuclear Cehm.*, **35**, 3035 (1973).
[17] A. V. Ablov, N. M. Samush, *Dokl. Akad. Nauk S.S.S.R.*, **113**, 1265 (1957).
[18] A. V. Ablov, N. M. Samush and O. A. Bologa, *Zhur. Neorg. Khim.*, **8**, 860 (1963).
[19] A. V. Ablov, O. A. Bologa and N. M. Samush, *Zhur. Neorg. Khim.*, **11**, 2632 (1966) ; **13**, 3169 (1968).
[20] P. J. Staples, *J. Chem. Soc.*, **1964**, 2534 ; **1965**, 7320 ; (*A*) **1967**, 45.
[21] P. J. Staples and A. Thompson, *J. Chem. Soc.* (*A*)., **1969**, 1058.
[22] D. M. Palade, T. N. Voloh, N.•A. Breslavskaya and T. N. Golyshina, *Zhur. Neorg. Khim.*, **15**, 2698 (1970).
[23] Cs. Várhelyi, J. Zsakó and M. Zsigmond, *Studia Univ. Babeș-Bolyai, Chem.*, **16**, (2), 52 (1971).
[24] B. A. Bovykin, *Zhur. Neorg. Khim.*, **17**, 169 (1972).
[25] A. Ya. Sychev, A. V. Ablov and V. A. Zarinski, *Zhur. Neorg. Khim.*, **6**, 825 (1961).
[26] Z. Finta, J. Csakó and Cs. Várhelyi, *Z. physik. Chem. (Leipzig)*, **242**, 200 (1969).
[27] J. Selbin and J. C. Bailar Jr., *J. Amer. Chem. Soc.*, **79**, 4285 (1957).
[28] Cs. Várhelyi, J. Zsakó and Z. Finta, *Z. anorg. Chem.*, **397**, 83 (1973).
[29] Z. Finta and Cs. Várhelyi, *J. Inorg. Nuclear Chem.*, **36**, 2199 (1974).
[30] Z. Finta and Cs. Várhelyi, *Acta Chim. Aacad. Sci. Hung.*, **83**, 281 (1974).

Revue Roumaine de Chimie, 33, 3, 271–275 (1988)

INFLUENCIA EJERCIDA EN SINTESIS DE ESTERES ORGANICOS POR LA UTILIZACION DE FOSFATO DE ALUMINIO-γ-ALUMINIA Y FOSFATO DE ALUMINIO SILICE

C. FERNANDEZ-SANCHEZ, Mª T. GANDASEGUI, R. BARAJAS y J. Mª MARINAS[a]
Departamento de Química Orgánica, Facultad de Ciencias. Universidad de Alcalá de Henares, Madrid — España
[a]Departamento de Química Orgánica, Facultad de Ciencias. Universidad de Córdoba, Córdoba — España

Recibido el 16 de Junio de 1986

Sintetizados por diferentes métodos los sistemas cataliticos binarios CF, FIA y FIB en este trabajo se estudia su aplicación a reacciones de esterificación en fase líquida y gaseosa. De los resultados obtenidos, al comparar el comportamiento de los tres sistemas estudiados, se puede deducir que el factor gobernante del proceso es la acidez del sistema catalitico. Asi como, que la esterificación transcurre sin ausencia de procesos contaminantes cuando se realiza en fase liquida.

This paper studies the application of the CF, FIA and FIB binary catalytic systems, synthesized by various methods, to esterification reactions in the liquid and gas phase. It may be deduced from the results obtained, comparing the behaviour of the three systems studied, that the governing factor of the process is the acidity of the catalytic system, and also that esterification occurs in the absence of contaminating processes when effected in the liquid phase.

INTRODUCCIÓN

Numerosos autores se han ocupado del estudio de esteres orgánicos tanto desde el punto de vista sintético, como de su cinética de reacción utilizando catalizadores homógeneos [1] y heterogéneos [2], tales como alúminas, fosfatos de aluminio, etc.

Uno de los compuestos más usados en la industria de plásticos, cosméticos, etc. es el acetato de n-pentilo, de ahí el interés que puede presentar la optimización de su proceso sintético.

En el presente trabajo se emplean en la reacción de esterificación, los sistemas catalíticos binarios : $AlPO_4$-γ-alúmina y $AlPO_4$ — silice previamente utilizados en otras reacciones químico orgánicas que transcurren vía catión carbonio y cuyos resultados se comparan con los obtenidos con otros catalizadores como por ejemplo $AlPO_4$ tipo Kearby.[3]

METODOLOGÍA EXPERIMENTAL

Los catalizadores que hemos utilizado ortofosfato de aluminio-γ-alumina (CF) y ortofosfato de aluminio-silice (FIA y FIB) cuyas caracteristicas fisico-quimicas se indican en la Tabla 1. El sistema de reacción tanto en fase liquida como en fase gaseosa son semejantes al utilizado en trabajos precedentes.[3,4]

En las experiencias en fase líquida se utilizan un mol de alcohol, 0,2 moles del correspondiente ácido y cantidades de catalizador correspondientes entre 3,5 y 7 g (4,2 y 9, m.e.q. de acidez frente a p-dimetilaminoazobenceno), p-DMAAB). La temperatura es de 95°±2°C, y la agitación constante a 600 r.p.m.

A intervalos de una hora, se extraen muestras del bruto de reacción, que son sometidas a valoración ácido-base o análisis cromatográfico de gases, con lo que se sigue el progreso de la misma.

Las experiencias en fase gaseosa se realizan a temperaturas entre 200 y 400°C, se define una nueva magnitud, W/F, siendo W = Peso del catalizador en el lecho catalítico (g) y F = caudal de alimentacion (moles de reactante/hora).

Las cantidades reaccionantes corresponden a las variables de tiempo espacial (entre 140 a 20) y relacion molar, ácido/alcohol (5/1 a 1/5).

RESULTADOS Y DISCUSIÓN

Los catalizadores binarios CF, FIA y FIB, cuyas caracteristicas fisicoquímicas se describen en la tabla 1, su aplicación a la sintesis de esteres con interes desde el punto de vista industrial, ha sido altamente satisfactoria

Tabla 1

Caracteristicas estructurales de los sistemas catalitícos

Catalizador	S_{esp} m²/g	$\sum V_p$ ml/g	$\overline{d}^0_A$	m.e.g. acidez		
				R. N.	p-DMAAB	p-AAB
F	150	0,40	36,3	0,95	0,80	0,72
B	316	0,20	24,9	1,20	0,94	0,76
CF	306	0,42	29,6	1,13	0,90	0,74
FIA	230	—	15—50	0,89	0,61	0,60
FIB	210	—	10—45	1,10	0,70	0,65

Estos resultados se comparan a los obtenidos cuando se emplean los catalizadores B ó F en los mismos sistemas de reacción.

1. Fase Líquida

En esta parte del trabajo se estudia la influencia ejercida sobra la conversión en ester, de factores como : cantidad de catalizador relación molar ácido/alcohol y velocidad de agitación.

En la tabla 2, aparecen recogidos los resultados obtenidos al variar la proporción de catalizador empleado observandose que el optimo corresponde para todos los sistemas a 6,3 m.e.q.

El análisis realizado variando la velocidad de agitación, entre 400 — 900 r.p.m. de manera que se reduzcan al máximo los procesos de difusión, nos manifiesta que las experiencias deben realizarse con una agitación constante alrededor de 600 r.p.m.

Tabla 2

Variación de la conversión en función de la cantidad de catalizador. Fase líquida

Cat. m.e.q. / t(h)	1,8 m.e.q.			3 m.e.q.			4,2 m.e.q.			6,3 m.e.q.			8,4 m.e.q.		
	CF	FIA	FIB	CF	FIA	FIB	CF	FIA	FIB	CF	FIA	FIB	CF	FIA	FIB
1	45	—	—	—	—	10	6	2	12	—	4	14	10	2	6
2	11	—	10	—	28	11	2	12	17	4	14	23	2	14	
3	14	6	—	16	6	32	13	8	15	19	4	20	28	8	24
4	15	8	14	18	26	26	6	16	21	28	8	28	32	9	32
5	19	10	14	20	16	38	29	20	24	33	12	32	39	20	36
6	20	15	16	22	18	40	35	24	28	38	24	36	44	42	37
7	36	19	20	24	20	52	38	28	40	47	26	40	48	48	38
8	38	20	21	28	21	54	46	30	48	67	32	48	55	50	40
9	41	24	26	50	24	54	52	32	52	72	33	49	63	52	46
10	43	28	32	53	30	54	68	36	54	75	36	54	66	54	49
11	50	36	42	61	38	54	50	46	56	83	44	58	67	54	54
12	59	42	44	68	48	54	72	46	56	86	56	58	69	54	54

Por otra parte, si comparamos sistemas catailticos binarios con los mismos componentes, come el FI. Una vez filtrado y seco, sometido a diferentes tratamientos proporciona catalizadores cuyas características estructurales son distintas (FIA y FIB), lo que nos va a permitir poner d relieve que la propiedad que más va a influir en este tipo de procesos, es la acidez del sistema catalitico. Asi, cuando utilizamos el sistema catalitico FIB, obtenemos una conversión del 50 % rendimento superior al registrado con FIA de menor acidez.

Tabla 3

Variación de la conversión en función de la relación molar. Fase liquida

ácido/alcohol / t(h)	1/4,5			1/2,5			1/1			2,5/1			4,5/1		
	CF	FIA	FIB	CF	FIA	FIB	CF	FIA	FIB	CF	FIA	FIB	CF	FIA	FIB
1	7	3	4	2,5	1	1,7	1	1	1	5	2	3	22	10	16
2	12	7	9	6	3	2	4	2	3	11	6	7	22	12	17
3	18	12	15	8	4	4		ö‾	ö9	15	9	10	23	15	18
4	37	21	27	9	6	7	36	22	27	20	16	18	24	18	19
5	45	33	39	12	8	9	41	31	39	25	19	21	27	21	22
6	64	48	57	13	9	10	50	40	43	31	23	27	34	26	27
7	68	50	63	16	10	12	53	42	47	43	27	29	35	28	31
8	82	54	67	31	12	19	58	45	51	48	27	34	35	28	31
9	86	59	71	33	ö‾	4	63	48	55	50	32	47	35	28	31
10	89	69	80	36	20	28	68	50	59	50,5	36	47	35	28	31
11	92	78	85	38	26	31	73	55	62	51	38	47	35	29	21
12	96	84	90	45	33	39	79	59	68	51	38	47	35	29	31

Temperatura de reacción = 95°C ; cat = 6,3 m.e.q. y 600 r.p.m.

En la Tabla 3 se recoge el tercer factor objeto de estudio la variación de R_M, resultando máximo el rendimiento para la relación ácido/alcohol = 1/4,5.

2. Fase Gaseosa

Las condiciones óptimas de la reacción, cuando se realiza el proceso en fase gaseosa, se determinan mediante una serie de experiencias en las que se van variando la temperatura de reacción la relación molar y el tiempo espacial W/F.

La variación de la conversión total a diferentes temperaturas entre 200 y 450°C para $W/F = 100$ y $R_M = 1/2$, se mantienen constantes para los tres sistemas cataliticos seleccionados; encontrandose que el máximo de conversión en ester se encuentra a 220°C y 240°C respectivamente. A altas temperaturas los productos resultantes son en su mayoría debidos a procesos térmicos y no catalíticos, aumentando la conversión total, aúnque el rendimiento en acetato de n-pentilo disminuye, apareciendo junto a él los productos de deshidratación del alcohol, isomerización etc. (Tabla 4).

Tabla 4

Variación de la conversión en función de la temperatura de reacción. Fase gaseosa

Temperatura °C	W/F	R_M	R % CF	FIA	FIB
200	100	1/2	75	65	69
240	100	1/2	92	80	88
280	100	1/2	84	75	78
320	100	1/2	78	70	75
360	100	1/2	71	56	70
400	100	1/2	58	44	48

A temperatura constante para tiempos espaciales variables se observa, para los tres sistemas cataliticos que el máximo rendimiento se alcanza para un $W/F = 1000$ (Tabla 5).

Tabla 5

Variación de la conversión en función del tiempo espacial (W/F). Fase gaseosa

Temperatura (°C)	W/F	R_M	R % CF	FIA	FIB
240	140	1/2	73	60	61
240	120	1/2	85	51	64
240	100	1/2	92	80	88
240	80	1/2	61	38	42
240	60	1/2	52	35	50
240	40	1/2	47	30	42
240	20	1/2	41	29	38

Tabla 6

Variación de la conversión en función de la relación molar (R_M) ácido/alcohol. Fase gaseosa

Temperatura (°C)	W/F	R_M	R% CF	FIA	FIB
240	100	5/1	25	12	14
240	100	4/1	30	13	17
240	100	3/1	39	17	26
240	100	2/1	48	30	39
240	100	1/1	74	31	37
240	100	1/2	95	80	88
240	100	1/3	88	69	81
240	100	1/4	80	68	75
240	100	1/5	74	65	70

Para relaciones molares variables ambos catalizadores conducen a resultados semejantes en conversión y componentes de la mezcla (Tabla 6).

Por tanto las condiciones óptimas para estos procesos aúnque se utilice distintos catalizadores son: 220°C, W/F = 100 y R = 1/2 para el sistema CF y 240°C, W/F = 100 y R = 1/2 para FIA y FIO.

Al haber estudiado estos procesos con dos catalizadores de igual composición pero de distintas propiedades fisicoquímicas, los resultados obtenidos nos proporcionan una idea clara de la influencia de estas propiedades sobre la reacción de esterificación. Pues observamos que el catalizador FIB que aunque posee una superficie de 210 m^2/g menor que la de FIA, 230 m^2/g, como su acidez es mayor conduce a mayores conversiones totales; y a diferencia de los resultodos a los que se llega con los otros catalizadores, el proceso en fase gaseosa conduce a mejores conversiones que en fase liquida.

Para comprovar experimentalmente, si el factor predominante es la acidez del catalizador, se procedio a realizar el proceso con la adición de compuestos básicos que actuan como venenos del sistema catalitico, tales como piridina, observandose que el rendimiento en ester disminuye, mientras que si se añaden trazas de fenol, sustancia ácida, el rendimiento en ester, sufre un ligero aumento, lo que pone de manifiesto que el rendimiento está en función de la densidad de centros ácidos que posee el catalizador.

Si realizamos el estudio comparativo entre los resultados obtenidos con estos sistemas y los rendidos por los sistemas catalíticos F y B utilizados en trabajos anteriores, [3] se observa nuevamente la dependencia de la conversión del proceso con la acidez del catalizador. Asi como, que la reacción de esterificación transcurre sin contaminación de reacciones secundarias y en condiciones óptimas, cuando se realiza en fase líquida, salvo cuando se utilizá el sistema FIB que conduce a mejores rendimientos en ester.

En las condiciones de trabajo, el tanto por ciento de carbonización fué inferior al 2%.

BIBLIOGRAFÍA

[1] G Doleschall y K. Lempert; *Tetrahedron Letters*, **1963**, 1195; M. Smith and all, *J. Amer. Chem. Soc.*, **80**, 6204 (1958).

[2] R. Tartarelli, G. Stopatto, F. Morelli, A. Luchessi y M. Giorgint; *J Catal.*, **13**, 108 (1969); *Ibid*, **18**, 219 (1070).

[3] A. Alberola, C. Fernández y J. M. Marinas, *An. Quim.*, **68** (12), 1399 (1972).

[4] C. Fernández, J. M. Marinas, R. Pérez Ossorio; *Revista Portuguesa de Quim.* **2**, 155 (1979)

Revue Roumaine de Chimie, **33**, *3*, 277—282 (1988)

STUDIES ON NITROFURAN HETEROCYCLES. PART I

SYNTHESIS AND ANTIBACTERIAL ACTIVITY OF 7H, 6-(5-NITRO-2-FURYL)-*s*-TRIAZOLO[3,4-*b*]-1,3,4-THIADIAZINES

B. S. HOLLA[a], B. KALLURAYA[a] and K. R. SRIDHAR[b]

[a] Department of Post-graduate Studies and Research in Chemistry
[b] Department of Post-graduate Studies and Research in Bio-Sciences Mangalore University,
Mangalagangothri — 574199, India

Received July 19, 1986

The preparation of thirteen new 7H, 6-(5-nitro-2-furyl)-*s*-triazolo [3,4-*b*]-1,3,4-thiadiazines is described. The compounds are evaluated for antibacterial activity against both gram-positive and gram-negative bacteria. The results of the screening indicate the highest activity for compound carrying aryl substituents at [illegible].

Various 1,2,4-triazole derivatives are found to be associated with diverse pharmacological activities such as analgesic, antiasthmatic, diuretic, antihypertensive, anticholinergic, antibacterial antifungal and antiinflammatory properties.[1-8] A number of nitrofuryl 1,2,4-triazoles have been synthesized and investigated for antibacterial activity in urinary tract infections.[9] Herbert *et. al.*[10-15] in a series of patents have described the synthesis and antibacterial activity of various nitrofuryl-*s*-triazolo[4,3-b]pyridazines and have established that nitrofurans directly attached to condensed heterocycles possess excellent antibacterial activity.

Prompted by these observations and as a part of our general search[16,17] for pharmacologically active nitrofuran heterocycles we wish to report in this present paper the syntheses and biological activities of various substituted 7H-6-(5-nitro-2-furyl)-*s*-triazolo[3,4-*b*]-1,3,4-thiadiazines.

During the present work 4-amino-5-mercapto-1,2,4-triazoles(I) were obtained according to the methods described by Pujari *et. al.*[18] and Heindel *et al.*[19] 5-Nitro-2-furanacyl bromide (II) was obtained by the bromination of 5-nitro-2-acetylfuran.[20] The triazoles (I), when condensed with (II) in the presence of aq. sodium acetate in alcohol media gave moderate to good yields of the title compounds (III) (scheme I). The compounds are described in Table 1. However when sodium acetate was replaced by ammonium hydroxide or triethylamine, the reaction mixture turned greenish and all our attempts to isolate the title compounds were unsuccessful.

Table 1

Characterisation data of 7H, 6-5-(nitro-2-furyl)-s-triazolo[3,4-*b*]-1,3,4-triadiazines(III)

Compound No.	R=	Yield % m.p. °C	Colour and crystal form	Molecular formula	Analysis % Found (Calculated)		
					C	H	N
IIIa	H	80 191	Red micro needles	$C_8H_5N_5SO_3$	38 .48 (38.24)	2.13 (1.99)	27.51 (27.88)
IIIb	methyl	68 220—22^b	Pale yellow flakes	$C_9H_7N_5SO_3$	40.98 (40.75)	2.71 (2.64)	26.23 (26.41)
IIIc	ethyl	71 185—7^a	Pale yellow cubes	$C_{10}H_9N_5SO_3$	43.25 (43.01)	3.07 (3.22)	25.28 (25.08)
IIId	propyl	49 142—3^a	Yellow stout cubes	$C_{11}H_{11}N_5SO_3$	44.86 (45.05)	3.68 (3.75)	24.04 (23.89)
IIIe	phenyl	79 163—5^c	Yellow micro crystals	$C_{14}H_9N_5SO_3$	51.00 (51.37)	2.84 (2.75)	21.62 (21.40)
IIIf	*o*-hydroxy phenyl	87 229^a	Yellow micro crystals	$C_{14}H_9N_5SO_4$	49.10 (48.98)	2.70 (2.62)	20.10 (20.40)
IIIg	*o*-chloro phenyl	80 199—201^a	Pale brown micro crystals	$C_{14}H_8ClN_5SO_3$	46.40 (46.47)	2.35 (3.21)	19.53 (19.36)
IIIh	*p*-chloro phenyl	88 223—4^a	Yellow micro needles	$C_{14}H_5ClN_5SO_3$	46.70 (46.47)	2.31 (2.21)	19.12 (19.36)
IIIi	*o*-tolyl	82 104—6	Brown yellowish crystals	$C_{15}H_{11}N_5SO_3$	53.10 (52.78)	2.91 (3.22)	20.75 (20.52)
IIIj	*p*-tolyl	84 228—29	Yellow micro crystals	$C_{15}H_{11}N_5SO_3$	53.20 (52.78)	2.87 (3.22)	20.31 (20.52)
IIIk	*p*-anisyl	80 184—4	Greyish micro crystals	$C_{15}H_{11}N_5SO_4$	50.16 (50.42)	(2.93 (3.08)	19.95 (19.60)
IIIl	*p*-nitro phenyl	40 343	Greyish micro crystals	$C_{14}H_8N_6SO_5$	45.30 (45.16)	2.15 2 06	22.41 22.58
IIIm	benzyl	52 151—3^d	Brownish yellow crystals	$C_{15}H_{11}N_5SO_3$	51.80 (52.78)	2.93 (3.22)	20.62 (20.52)

Solvent of crystallization: ^{a}Dimethyl formamide; ^{b}Ethanol; ^{c}Benzene; ^{d}Acetic acid.

As a part of structure activity studies 1,2,4-triazoles (I) substituted at position 3 by alkyl, aryl and benzyl groups were taken for the present investigation.

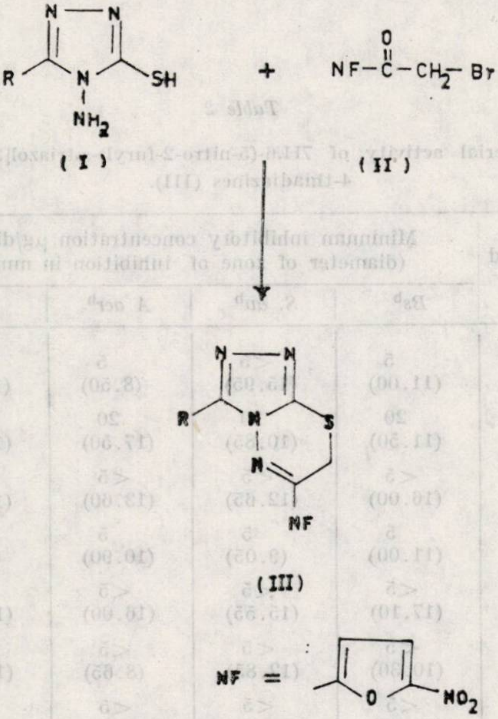

SCHEME - I

The structure of the title compounds (III) was confirmed by elemental analysis, IR and ^1H-NMR spectral data. The characteristic N−H absorptions in IR spectra of triazoles (I) around 3100−3300 cm^{-1} disappeared in the IR spectra of condensed products, thus suggesting the cyclic structure (III) for these products. The ^1H-NMR spectrum of (IIIc, $R=C_2H_5$) showed a sharp singlet at δ, 4.1 ppm integrating for two protons which confirmed the presence of $S-CH_2-\overset{|}{C}=N-$ grouping in this compound. The signal due to nitrofuryl β protons appeared as two doublets centered at δ, 7.4 and 7.55 ppm ($J = 4.5$ Hz).

The nitrofuryl triazolothiadiazines (III) prepared in the present investigation were screened for antibacterial activity against *B. Substilis*, *S. Aures*, *A. Aerogenes* and *E. Coli*, employing the disk-diffusion method [21] and the results are reported in Table 2. Nitrofurazone [22] was used as a standard drug. Most of the compunds showed moderate to good antibacterial activity against all the microorganisms at less than 5μg/mL dilution. In some cases the activity was higher than that of nitrofurazone.

Compounds (IIIe-k) carrying aryl substituents showed higher activity than III a-d and III m carrying alkyl and bezyl substituents. Substitution of nitro group in the aryl moiety however reduced the antibacterial activity significantly.

Table 2

Antibacterial activity of 7H,6-(5-nitro-2-furyl)-*s*-triazol[3,4-*b*]-1,3,4-thiadiazines (III).

Compound No.	Minimum inhibitory concentration µg/disk[a] (diameter of zone of inhibition in mm).			
	Bs[b]	*S. au*[b]	*A aer*[b]	*Es*[b]
IIIa	5 (11.00)	<5 (15.95)	5 (8.50)	<5 (13.50)
IIIb	20 (11.50)	20 (10.85)	20 (17.50)	20 (11.25)
IIIc	<5 (16.00)	<5 (12.65)	<5 (13.60)	<5 (15.85)
IIId	5 (11.00)	5 (9.05)	5 (10.90)	5 (9.35)
IIIe	<5 (17.10)	<5 (15.55)	<5 (16.00)	<5 (15.25)
IIIf	<5 (10.30)	<5 (12.85)	<5 (8.65)	5 (10.95)
IIIg	<5 (16.35)	<5 (16.85)	<5 (14.15)	5< (13.50)
IIIh	<5 (20.30)	<5 (21.60)	<5 (19.85)	<5 (21.25)
IIIi	<5 (18.45)	<5 (17.85)	<5 (18.70)	<5 (16.85)
IIIj	<5 (20.15)	<5 (20.75)	<5 (19.35)	<5 (22.75)
IIIk	<5 (18.20)	<5 (20.80)	<5 (17.75)	<5 (18.15)
IIIl	15 (11.15)	15 (9.55)	15 (10.90)	10 (10.10)
IIIm	<5 (12.45)	<5 (10.85)	<5 (11.95)	<5 (12.45)
Nitro-furazone	<5 (12.65)	<5 (14.45)	5 (10.20)	<5 (11.25)

[a] minimum inhibitory concentration is the lowest concentration of the compound that prevents visible growth after 24 hours of incubation.

[b] *Bs*: *Bacillus subtilis*; *S. au*: *Staphylococcus aureus*. *A. aer*: *Aerobacter aerogenes*; *Es*: *Escherichia coli*.

EXPERIMENTAL[23]

5-Nitro-2-furanacylbromide (II) was obtained by nitration of 2-acetylfuran[24] and subsequent bromination.[20] 3-Alkyl-4-amino-5-mercapto-1,2,4-triazoles (Ia-d) were prepared starting from aliphatic acids and thiocarbohydrazide[18]; while 3-aryl-4-amino-5-mercapto-1,2,4-triazoles (Ie-1) and 3-benzyl-4-amino-5-mercapto-1,2,4-triazole (Im) were prepared from the corresponding hydrazides following the procedure of Heindel *et. al.*[19]

General method of synthesis of 7-H, 6-(5-nitro-2-furyl)-s-triazolo(3,4-b)-1,3,4-thiadiazines(IIIa-m)

A mixture of triazole (I.0.01 mole) and 5-nitro-2-furancyl bromide (II, 0.01 mole) in absolute ethanol (25 mL) was heated under reflux for two to four hours. The reaction mixture was cooled to room temperature and neutralized with sodium acetate solution (10%). The precipitated triazolot hiadiazines (III) were collected by filtration, washed with water and recrystallized from a suitable solvent. The colour, yield, melting point and analytical data of these compounds are given in Table 1.

Evaluation of antibacterial activity of 7H-6-(5-nitro-2-furyl)-s-triazolo(3,4-b)-1,3,4-thiadiazines III a-m)

Antibacterial activities of the title compounds (III a-n) were determined against *B. Subtilis, S. Aures, A. Aerogenes* and *E. Coli* by the disk-diffusion method.[21] The disks measuring 6.25 mm in diameter were punched from Whatman No. 1 filter paper. Batches of 100 disks were dispensed to each screw capped bottle and sterilized by heating at 140° for one hour. The solutions of the test compounds were prepared in different concentrations using dimethylformamide. One mL containing 100 times the amount of the chemical required for each disk was added to each bottle containing 100 disks. The disk of each concentration was placed in triplicate on nutrient agar medium seeded with fresh bacterial culture separately. The incubation was carried out at 37°C for twenty four hours. Nitrofurazone[22] was used as standard drug and solvent control was kept. The minimum inhibitory concentrations for each compound was determined and the results are tabulated in Table 2. The diameter of the zone of inhibition was also determined for each compound and are included in Table 2 as figures in parenthesis.

ACKNOWLEDGEMENTS. We thank Prof. M. R. Gajendragad and Prof. M. Abdul Rahman for their interest in our work. One of us (B.K.) is grateful to Mangalore University for a Research Fellowship. We are also thankful to Head, R.S.I.C., Lucknow and Head, R.S.I.C., I.I.T. Madras for elemental analysis and ^{1}H-NMR spectra respectively.

REFERENCES

[1] B. N. Goswami, J. C. S. Kataky and J. N. Baruah, *J. Heteropyclic Chem.*, **21**, 1225 (1984).

[2] P. J. Kothari, M. A. Mehlhoff, S. P. Singh, S. S. Parmar and V. I. Stenberg, *J. Heterocyclic Chem.*, **17**, 1369 (1980).

[3] P. J. Kothari, S. P. Singh, S. S. Parmar and V. I. Stenberg, *J. Heterocyclic Chem.*, **17**, 1393 (1980).

[4] A. K. Sengupta and H. K. Misra, *J. Indian. Chem. Soc.*, **58**, 508 (1981).

[5] S. C. Sharamah and S. C. Bahel, *J. Indian. Chem. Soc.*, **59**, 877 (1982).

[6] H. L. Yale and J. J. Piala, *J. Med. Chem.*, **9**, 42 (1966).

[7] K. Shirakawa, T. Tsujiwawa and T. Tsuda, *U.S. Pat.*, 3, 041, 339 (1062); *Chem. Abstr.*, **57**, 13774 (1962.

[8] A. K. Bhat, R. P. Bhamaria, R. A. Bellare and C. V. Deliwala, *Indian. J. Chem.*, **5**, 397 (1967).

[9] E. Akerblom and D. E. S. Campbell, *J. Med. Chem.* **16**, 312 (1973).

[10] B. Herbert, G. Rudi, M. Hartmut, S. Kurt, S. Winfriede and V. Wolfgang, *Ger. Offen*, **2**, 004, 713 (1070); *Chem. Abstr.*, **75**, 118388f (1971).

[11] B. Herbert, G. Rudi, M. Hartmut, S. Kurt, S. Winfriede and V. Wolfgang, *Ger. Offen*, 2,030, 218 (1970); *Chem. Abstr.*, **76**, 72536w (1972).

[12] B Herbert, G. Rudi, M. Hartmut, V. Wolfgang and S. Winfriede, *Ger. Offen*, 2, 113, 438 (1971); *Chem. Abstr.*, **78**, 16204r (1973).

[13] B. Herbert, G. Rudi, M. Hartmut, S. Kurt and S. Winffriede, *Ger. Offen*, 2, 109, 570 (1971); *Chem. Abstr.*, **78**, 84431n (1973).

[14] B. Herbert, G. Rudi, T. Max, V. Wolfgang and S. Winfriede, *Ger. Offen*, 2, 202, 745 (1972); *Chem. Abstr.*, **79**, 105268c (1973).

[15] B. Herbert, G. Rudi, T. Max, V. Wolfgang and S. Winfriede, *Ger. Offen*, 2, 202, 744 (1972); *Chem. Abstr.*, **79**, 105269d (1973).

[16] B. S. Holla, B. Kalluraya and K. R. Sridhar, *Current Sci.* **55**, 73 (1986).

[17] B. S. Holla, B. Kalluraya snd K. R. Srudhar, *Current Sci*, **55**, in press (1986).

[18] K. S. Dhaka, J. Mohan, V. K. Chadha and H. K. Pujari, *Indian J. Chem.*, **12.** 288 (1974).

[19] K. R. Reid and N. D. Heindel, *J. Heterocyclic. Chem.*, **13**, 925 (1976).

[20] M. Portelli and G. Bartolini, *Ann. Chim.*, **53**, 1180,(1963); *Chem. Abstr.*, **60**, 8011b (1964).

[21] R. Gruickshank, J. P. Duguid, B. P. Morinion and R. H. A. Swain, "Medicinal Microbiology" Vol. II, 2nd Ed., Churchill-Livingstone, New-York, 1975, p. 190.

[22] "The Merk Index", 9th Ed., Merck and Co Inc., Rahway, New-Jersey, 1976, p. 6422.

[23] All melting points are taken in open capillary and are uncorrected.

[24] B. S. Holla, *Ph. D. Thesis*, University of Mysore, 1979, p, 223.

Revue Roumaine de Chimie, **33**, *3*, 283–290 (1988)

QUANTITATIVE DIALKYLATION OF AROMATIC AMINES UNDER A MINIMUM EXCESS OF ALKYLATION AGENT

I. POP[a], I. CIUPE[a], MIOARA BUTAN[a], L. TEREC[a], L. FEY[a] and I. BÂLDEA[b]
[a] Institute of Chemical and Pharmaceutical Research, Cluj-Napoca, Romania
[b] University of Cluj-Napoca, Department of Chemistry, Cluj-Napoca, Romania

Received May 22, 1986

The reaction of dialkylation of aromatic primary amines has been studied using diethyl sulphate as alkylation agent. The process was followed by chrpmatographical methods, determining the amounts of unalkylated amine, mono- and bi-alkylated products. In order to establish the optimum conditions, a set of experimental parameters has been investigated: temperature, molar ratio of reactants, solvent, alkalinity and feasibility of product separation. The best results were obtained with sylene as solvent, in a suspension of sodium hydrogen carbonate to remove sulphuric acd formed during the process, within the temperature range of 135–145°. The maximum molar excesses of diethyl sulphate of 0.6 for aniline and *meta*-toluidine and of 0.8 for *ortho*-toluidine are sufficient to yield almost quantitative dialkylation (above 95 %). Some kinetical measurements have been carried out on *meta*-toluidine + diethyl sulphate system. Both the first and the second alkylation were second order. Rate constants for the consecutive processes weie evaluated.

The papers dealing with the dialkylation of aromatic amines contain various examples of such processes, using alkylation agents as alkenes, acetaldehyde, alkyl phosphates and phosphites, alcohols dialkyl sulphates, alkyl halides, either in the presence of some catalysts as: BF_3, I_2, $KHFe(CO)_4$, salicylic acid, HI, HBr, H_3PO_4, H_2SO_4, NaBr, $CaCl_2$, $CuCl_2$, $AlCl_3$, etc, or not. The reaction mixture contains some alkaline agents such as Na_2CO_3, $NaHCO_3$ $Ca(OH)_2$.[1–15] Among the alkylation agents, the most available are alcohols and alkyl sulphates. Using alcohols, the alkylation process requires high temperature and pressure, the degree of conversion to dialkyl derivative is not too high, and a separation of mono- and di-substituted amines should be performed.

The purpose of the present paper is to realize the dialkylation process with dialkyl sulphates, which ensures a quite quantitative transformation. This process may be performed at an industrial scale.

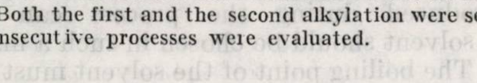

(1)

High degree of conversion was obtained by Huning,[4] who used $Ca(OH)_2$ as alkaline agent, $(C_2H_5O)_2SO_2$ as alkylation agent, within a molar excess of 0.4, carrying out the reaction at 110—115° in a first stage, and accomplished it at 145°. Various degrees of conversion in the absence of an alkaline agent were obtained by Fahim,[1] with a relatively large excess of diethyl sulphate (1.2 molar excess), depending on toluidine isomers. Yields of 35, 80 and 91% were reached for *ortho-*, *meta-* and *para-*isomers respectively. Lushina[14] used an aqueous solution of $NaHCO_3$ at room temperature in order to produce *ortho*-diethyltoluidine with a 52% yield.

In the methods described in the literature, there are some difficulties in the product separation when $Ca(OH)_2$ is used as akaline agent due to: the precipitate formed during reaction, a poor temperature control of reaction mixture where solvent is not present and a large consumption of reactants. We attempted to avoid such disadvantages by choosing optimal conditions in order to gain a high purity and yield of dialkyl derivate and a small consumption of alkylation agent.

1. THE CHOICE OF REACTION MEDIUM

All reactions described in the literature, dealing with dialkylation of aromatic amines do not use any solvent. The reaction requires a temperature around 120° and it is quite exothermic. When an alkaline solid compound is used, some difficulties arise, concerning the stirring of the reaction mixture and temperature control. To ensure an optimal and uniform temperature we have chosen a synthesis in which a solvent is present. Because the water produced during the process can decompose the alkylation agent, the solvent should be chosen in such a manner to remove water as it is formed. The boiling point of the solvent must be at least 120°. Another condition for the reaction medium is to be inert towards the alkylation agent. Xylene satisfied these conditions. Some experiments were done using benzene (b.p. ~ 80°) and toluene (b.p. 111°). As shown in tables 1 and 2, the reaction time and the consumption of alkylation agent are increased because the systems were maintained at 80 and 111°, respectively.

Table 1

Dialkylation of *m*-toluidine in benzene as solvent

Reaction time	Moles of $(C_2H_5O)_2SO_2$	Percentage concentration of		
		m-toluidine	N-ethyl-*m*-toluidine	N, N-diethyl-*m*-toluidine
2	0.25	50	42	8
4	0.50	44	45	11
6	0.50	19	57	24
8	0.80	7	45	48
10	1.20	4	33	63
12	1.57	2	29	69
14	1.70	1	22	77
16	1.80	—	16	84
18	1.90	—	9	91
20	2.10	—	1	99

Table 2

Dialkylation of *m*-toluidine in toluene solvent

Reaction time	Moles of $(C_2H_5O)_2SO_2$	Percentage concentration of *m*-toluidine	N-ethyl-*m*-toluidine	N,N-diethyl-*m*-toluidine
2	0.25	73.0	24.0	3.0
4	0.50	47.0	43.0	10.0
6	0.74	25.0	49.0	26.0
8	1.00	12.0	48.0	40.0
10	1.25	6.5	44.5	49.0
12	1.50	1.0	27.0	72.0
14	1.50	1.0	26.0	73.0
16	1.70	—	15.0	85.0
18	1.90	—	3.5	96.5
20	1.90	—	1.0	99.0

2. CHOICE OF ALKALINE AGENT

Calcium hydroxide gave good results concerning the reaction yield, when a small molar excess of diethyl sulphate was used, but some problems arose when the final product had to be isolated. When CaO played the role of basic agent, the reaction started with a high rate and the mixture got hotter partly because of the reaction exothermicity and partly because of the secondary reaction between CaO and formed water.

Sodium salts gave similar yields but sodium sulphate could be separated from the reaction mixture by water extraction, before the product distillation. Sodium carbonate manifested a too strong alkalinity and therefore a part of diethyl sulphate was hydrolysed. Sodium hydrogen carbonate suited nicely with our purposes, leading to a good yield and only a small consumption of diethyl sulphate. Table 3 presents the results for different alkaline agents.

Table 3

Yields of N,N-diethyl-*m*-toluidine with different bases

Alkaline agent	Molar ratio diethyl sulphate : *m*-toluidine	Content in N-ethyl-*m*-toluidine %	Yield in N.N,-diethyl-*m*-toluidine %
$Ca(OH)_2$	1.4:1	7	81.3
$Ca(OH)_2$	1.5:1	1	86.6
CaO	1.6:1	absent	83.6
Na_2CO_3	1.6:1	11	64.7
$NaHCO_3$	1.6:1	0.9	90.2
$NaHCO_3$	1.5:1	absent	91.6

3. MOLAR RATIO OF DIETHYL SULPHATE-AMINE

Starting with the ratios given in the literature, we have carried out a series of syntheses, following the degree of conversion of *m*-toluidine to N,N-diethyl-*m*-toluidine as a function of diethyl sulphate amount added to the mixture. Because such syntheses could be affected by initial loading we used a reaction vessel with the whole mass of amine dissolved, the basic agent suspended in xylene and then feeding with ethyl sulphate at such a rate that the heat released could be adequately removed without elevation of the mixture temperature. Table 4 presents these results. As table 4 shows, the process of diethylation takes place from the beginning, at temperature of 120°. The period of time when the alkylation agent is steadily added is very important. A large excess — until mono-alkyl derivate. decreased below 10% — is not useful because of its decomposition. A small excess becomes necessary at low concentration of monoalkylated compound. A molar excess of 1.4—1.6 ensures the decrease in percentage of mono-ethyl toluidine below 1%, which permits the use of the product without further purification. Optimal conditions led to good yields (above 90%) of diethyl derivative for *o*-toluidine and aniline using a molar excess of 0.8 and 0.5 respectively, figures below those mentioned in the literature.

Table 4

Degree of transformation as a function of molar ratio and reaction time *

Moles of diethyl sulphate to one mole of amine	Reaction time hours*	Degree of tiansformation		
		unreacted *m*-toluidine %	N-ethyl-*m*-toluidine %	N,N -diethyl-*m*-toluidine %
0.575:1	4	27	51	22
0.15:1	8	absent	38	62
1.40:1	12	absent	9	91
1.40:1	12+2	absent	9	91
1.50:1	16+1	absent	4	96
1.50:1	16+2	absent	2	98
1.60:1	18	absent	0.9	99.1
1.60:1	18+1	absent	absent	100

* first value represents time of alkyl sulphate feeding; the secon done, the extra-time to accomplish the process.

4. SEPARATION OF THE PRODUCT

The separation of diethyl-*m*-toluidine from xylene solution, after Na_2SO_4 was removed by water extraction, was possible either by chemical or by physical means. By simple distillation, the mixture of xylene and N,N-diethyl-*m*-toluidine is not separable. When a rectification column (Vigreux) was used, xylene distilled with a maximum 0.3% of the reaction product. That which remained in the still could be vacuum distilled, obtaining a 76.5% yield. The decrease in the product amount is due to its decay during the process of distillation. To avoid such a loss, we extracted the diethyl-*m*-toluidine by a hydrochloric acid solution. The chlorhydrate salt can be crystallised or used to obtain the free base.

5. ANALYTICAL CONTROL OF DIETHYLATION PROCESS

The progress of reaction was followed chromatographically using a chrom-2 Model. James [16] showed the possibility of separation of the above three compounds on the basis of their different retention volumes. He used three types of stationary phases. The separation is poor on the polar column, but quite satisfactory on nonpolar column.

We have succeeded to analyse the mixture of unreacted *m*-toluidine, mono- and di-ethylated compounds in xylene using methyl-phenyl-silicone having a nonpolar character and a good capacity of separation for aromatic compunds. Solvent has not interfered. Table 5 contains the retention times for the four species involved.

Table 5

Retention time for compounds to be analysed

Compound	Retention time
Xylene	0.4
m-Toluidine	1.0
N-Ethyl-*m*-toluidine	1.7
N,N-Diethyl-*m*-toluidine	2.3

The following data present the working conditions: Column: Stationary phase: Silicon oil 550 — 20%, Stearic acid; Support: Chromosorb 80/100 mesh; Length: 85 cm; Diameter 0.6 cm; Material: stainless steel; Temperature: 160°; Carrier gas: nitrogen 0.4 atm.; Detector: F.I.D.; Sensibility: 1 : 50000 — 1 : 100000; Sample volume: $0.2-0.4_1$ μL of xylene solution.

The final product has been determined by acid titration using $HClO_4$ in CH_3COOH in a standard procedure.

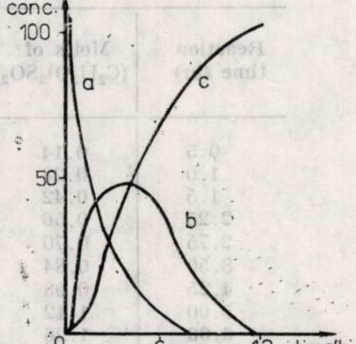

Fig. 1. — Variation of concetration in time during the amine alkylation process: a—unalkylated amine; b—monoalkylated amine; c—dialkylated amine.

Some results are presented in figures 1 and 2 and tables 6 and 7. Figure 1 shows the aspect of a chromatogram of our experiments. Figure 2 presents the evolution of relative concentration for the species involved in the process.

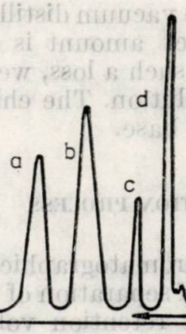

Fig. 2 — Gas-chromatogram of *m*-toluidine alkylation after about 6 hours: a — dialkylated amine (35 %); b — monoalkylated amine (48 %); c— unalkylated amine (17 %); d — solvent.

Tables 6 and 7 contain data concerning the syntheses in the presence of $Ca(OH)_2$ and $NaHCO_3$ as bases respectively, as determined chromatographically.

Table 6

Gas chromatographic evolution of the *m*-toluidine alkylation in the presence of $Ca(OH)_2$

Reaction time (hr)	Moles of $(C_2H_5)_2SO_2$	Percentage concentration of N-ethyl-*m*-toluidine
2.5	1.4	33.0
4	1.4	30.0
6	1.4	20.8
8	1.4	10.0
10	1.4	8.0
12	1.6	7.0
14	—	1.0

Table 7

Gas chromatographic evolution of *m*-toluidine alkylation in the presence of $NaHCO_3$

Reaction time (hr)	Moles of $(C_2H_5O)_2SO_2$	Percentage concentration of		
		m-toluidine	N-ethyl-*m*-toluidine	N, N-diethyl-*m*-toluidine
0.5	0.14	73.0	26	1.0
1.0	0.28	56.4	38	5.6
1.5	0.42	42.0	45	13.0
2.25	0.56	39.0	43	18.0
2.75	0.70	30.0	47	24.0
3.50	0.84	17.0	48	35.0
4.25	0.98	10.0	44	46.0
5.00	1.12	6.0	39	55.0
6.00	1.26	2.0	33	65.0
7.00	1.40	0.5	19	80.5
8.00	1.40	—	16	84.0
9.00	1.50	—	9	91.0
10.00	1.500	—	4	96.0
11.00	1.60	—	2	98.0
12.00	1.60	—	1	99.0

6. KINETICS

Some attempts have been made to appreciate the rate constants of the process. The reaction scheme is quite complicated containing consecutive and parallell steps :

$$\begin{gathered}
C_6H_5-NH_2 + (C_2H_5O)_2SO_2 \xrightarrow{k_1} C_6H_5NH(C_2H_5)\cdot SO_2(C_2H_5O)OH \\
C_6H_5-NH(C_2H_5) + (C_2H_5O)_2SO_2 \xrightarrow{k_2} C_6H_5N(C_2H_5)_2\cdot (SO_2OH)_2 \\
C_6H_5-NH_2 + (C_2H_5O)SO_3H \xrightarrow{k_3} C_6H_5-NH(C_2H_5)\cdot SO_2(OH)_2 \\
C_6H_5-NH(C_2H_5) + (C_2H_5O)SO_3H \xrightarrow{k_4} C_6H_5N(C_2H_5)_2\cdot SO_2(OH)_2 \qquad (2) \\
(C_2H_5O)_2SO_2 + 2H_2O \xrightarrow{base} 2C_2H_5OH + H_2SO_4 \\
C_6H_5-NH(C_2H_5)\cdot SO_2(C_2H_5O)OH \xrightarrow[H_2O]{base} C_6H_5-NH(C_2H_5) + \\
+ C_2H_5OH + H_2SO_4 \\
C_6H_5-N(C_2H_5)_2\cdot SO_4H_2 \xrightarrow{base} C_6H_5-N(C_2H_5)_2 + H_2SO_4
\end{gathered}$$

In the initial stages of the process, the involvement of $C_2H_5OSO_3H$ can be neglected because of its low concentration, and the reaction can be treated as a consecutive second-order system :

$$\begin{aligned}
A + B &\rightarrow M + P \qquad k_1 \\
M + B &\rightarrow D + P \qquad k_2
\end{aligned} \qquad (3)$$

where A stands for amine, M and D for mono- and di-substituted derivatives respectively. It is clear from the reaction mass balance that $C_2H_5OSO_3H(C_2H_5OSO_3)$ should be involved in the substitution in the latter stages of reaction.

Measurements were carried out adding a small amount of diethyl sulphate (substrate : alkylation agent ratio of about 10 : 1) to the reaction mixture, and the first constant was calculated. Two series of data gave relative close values of $k_1 = (2.0 \pm 0.3)\times 10^{-2}$ M^{-1}min^{-1}, only for early stages of reaction. When amine was fully consumed, a new small portion of diethyl sulphate was added and the reaction was further followed. A mean value of $k_2 = (1.8 \pm 0.2)\times 10^{-3}$ M^{-1}min^{-1} has been calculated for the second process. At longer times, both k_1 and k_2 calculated as second-order rate constants diminished because of subsequent processes effectiveness.

From the above simplified reaction scheme, using the method of elimination of time from rate expressions for the three species, the concentration of intermediate M may be written after Capellos[17]:

$$[M] = \frac{[A]}{k-1}\left[1 - \left(\frac{(A)}{(A)_0}\right)^{k-1}\right] \tag{4}$$

where $k = k_2/k_1$. Using the form

$$1 \equiv \frac{[A]}{(M)}\,\frac{1}{(k-1)}\left[1 - \left(\frac{(A)}{(A)_0}\right)^{k-1}\right] \tag{5}$$

and inserting the data for the initial stages of the process, k values-numerically calculated-range between 0.08 and 0.1, even for the data in table 7, when the alkylation agent was steadily added. This fact supports the rate constants calculated by separation of the two steps of the reaction.

CONCLUSION

This study has led to the conclusion that aromatic amines could be dialkylated using an inert solvent, $NaHCO_3$ as basic agent and diethyl sulphate as alkylating agent at 120—130° within a molar excess of 0.4—0.8. Good yields and a high purity of the final product, separated as chlorhydrate, were obtained.

REFERENCES

[1] H. A. Fahim and M. Fleifel, *J. Chem. Soc.*, **1951**, 2761.
[2] D. Hill, *J. Ind. Eng. Chem.* **12**, 636 (1920); **13**, 504 (1921).
[3] M. De Godon, *Compt. rend.*, **172**, 1418 (1921).
[4] S. Hunning, *Ber. dtsch. chem. Ges.*, **85**, 1056 (1952).
[5] H. E. Fierz-David, "Farben Chemie" Springer Verlag, Wien, 1952, p. 129.
[6] J. Reilly and W. J. Hickinbottom, *J. Chem. Soc.*, **113**, 974, 985 (1918).
[7] E. Knoevenagel, *J. prakt. Chem.*, **89**, 30 (1914).
[8] R. J. Morley and J. S. Abel, *Ann. Chem. Pharm.*, **93**, 315 (1855).
[9] A. Riche and P. Berard, *Ann. Chem. Pharm.*, **129**, 77 (1864).
[10] H. J. Szymanski and T. Dockner, Ger. Offen., 2338418 (1975).
[11] A. K. Bhattacharyya and D. K. Naidi, *Ind. Eng. Chem.*, *Prod. Res. Des.*, **14**, 162 (1975).
[12] T. Dockner and H. Krug, Ger. Offen., 2335906 (1975).
[13] J. B. Dickey and J. G. McNally, U.S.Pat., 2391139 (1945).
[14] O. T. Lushina and T. V. Fomina, *Metody Poluch. Khim. Reactiv. Prep.*, **22**, 89 (1970).
[15] S. Hashimoto and I. Furukawa, Japan Pat. 70, 32411.
[16] A. T. James, *Analyt. Chem.*, **28**, 1564 (1956).
[17] C. Capellos and B. H. J. Bielski, "Kinetic systems", J. Wiley, New York, 1972, p. 100.

Revue Roumaine de Chimie, **33**, *3*, 291–293 (1988)

STUDIES ON THE NUCLEOPHILIC REACTIVITY OF SULPHUR AND NITROGEN IN 2-MERCAPTO-4(3H)QUINAZOLINONE UNDER SOLID-LIQUID PHASE TRANSFER CATALYSIS CONDITIONS

A. K. EL-SHAFEI and A. M. EL-SAYED
Chemistry Department, Faculty of Science, Sohag, Egypt

Received November 3, 1986

Some new condensed heterocyclic systems were obtained by reacting 2-mercapto-4(3H) quinazolinone with some mono- or dichloroaliphatic or aromatic moieties. Addition to benzylidenemalononitrile was found to proceed effectively under the applied PTC conditions.

In connection with our previous work [1-4] on phase transfer catalysis we tried to apply this simple and rapid method to obtain some new heterocycles. Thus 2-mercapto4(3H)quinazolinone **1a** was reacted with ethylchloroacetate, chloroacetonitrile, chloroacetyl chloride, benzylidenemalononitrile, 2,3-dichloroquinoxaline, 2,3-dichloroquinoxaline-1,4-N, N-dioxide, 2,3-dichloro-1,4-napthoquinone or chloranil. The reaction was performed in solid-liquid two phase system, organic reactants in aprotic solvent (benzene) form the organic phase in which solid potassium carbonate is suspended. The reaction was catalyzed with tetrabutylammonium bromide (TAB) which is unable to transfer carbonate anions (CO_3^{2-}) into the organic phase,[5] thus solid-liquid phase transfer phenomena are probably not involved here. It is more plausible that the first step, namely proton abstraction, takes place on the surface of solid carbonate. The anion formed then migrates into the organic phase as ion pair with the catalyst cation. In our substrate two anionic poles S^- and N^- were available, and dianionic ambident species was reacted forming a new ring through two step mechanism (c.f. Scheme); however, in competitive substitution reactions and also in some intances, the reaction stops at S-substitution step. Thus, with ethyl chloroacetate the reaction gave the S-substituted ester **1b** which was gradually converted into the corresponding acid **1c** as the reaction proceeds. With chloroacetonitrile the reaction gave the S-cyanomethyl derivative **1b**. The S-acetyl derivative. **1e** was obtained on reaction with chloroacetyl chloride probably through initial formation of ketene according to the following mechanism :

$$ClCH_2COCl \rightarrow CH_2{=}C{=}O$$

$$\text{Het}-\text{S}-\text{H} + \text{CH}_2=\text{C}=\text{O} \xrightarrow{\text{fast}} \text{Het}-\text{S}^- + \text{CH}_2=\overset{+}{\text{C}}-\text{OH} \xrightarrow{\text{slow}}$$

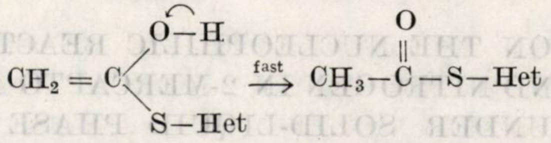

$$\text{CH}_2=\text{C}\begin{matrix}\text{O}-\text{H}\\ \\ \text{S}-\text{Het}\end{matrix} \xrightarrow{\text{fast}} \text{CH}_3-\overset{\overset{\text{O}}{\|}}{\text{C}}-\text{S}-\text{Het}$$

With benzylidenemalonitrile the reaction gave the corresponding cyano addition product **1f**.

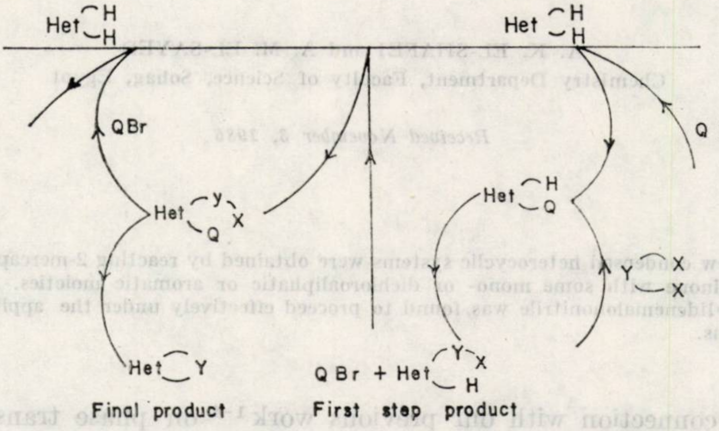
Het H H
Het H H
QBr
Q Br
Het Y X Q
Het H Q
Y X X
Het Y
Q Br + Het Y X H
Final product
First step product

Two Catalytic Solid – Liquid PTC cycle

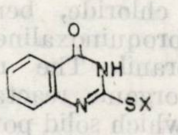

(1)

a x = H
b x = $CH_2COOC_2H_5$
c x = CH_2COOH
d x = CH_2CN
e x = $COCH_3$

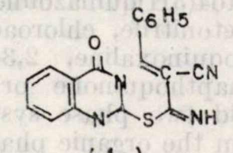

(1f)

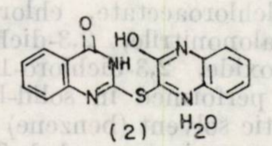

(2) H_2O

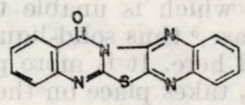

(3)

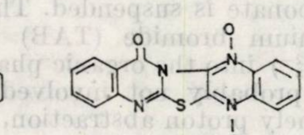

(4) 2 H_2O

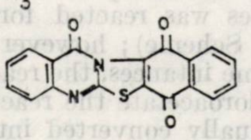

(5)

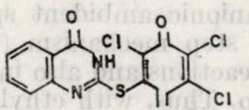

(6)

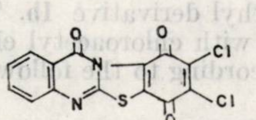

(7)

Under the applied conditions the reaction between compund **1a** and 2,3-dichloroquinoxaline failed to proceed, however when it was conducted in liquid-liquid PT conditions (30% NaOH/benezene/TOAB), it gave compound **(2)** along with a low yield of the cyclized product **(3)** (10%). The reaction with 2,3 dichloroquinoxaline-N,N-dioxide or 2,3-dichloronaphthoquinone, went well and afforded the desired cyclized products **(4)** and **(5)**, respectively. With half molar ratio of chloranil, the reaction with compound **1a** stopped at the S-substituted step and the obtained derivative **(6)** was further cyclized only under conventional method *i.e.* by boiling in benzene/ TEA for 10 minutes.

PHYSICAL AND ANALYTICAL DATA

Compound **1a** is commercially available (ALDRICH). All elemental analyses are in accordance with the structures proposed. NMR spectra were measured on VARIAN-EM 360A 60 MHZ using DMSO-d6 as a solvent and TMS as internal reference. **1b**, mp 181°C, ^{1}H-NMR 8.2—7.4 (4H, m, H_6, H_6, H_7, H_8); 4.4—41. (3H, m, CH_2 + NH); 3.45 (2H, S, CH_2 ester); 1.5 — 1.2 (3H, m, CH_3); **1c**, mp 216°C, ^{1}H-NMR; 11.25 (1HS, COOH), 8.3 — 7.5 (4H, m, H_5, H_6, H_7, H_8); 4.25 (1H, S, NH); 4.0—3.5 (2H, m, CH_2); **1d**, mp 190°C, ^{1}H-NMR; 8.15—7.35 (4H, m, H_5, H_6, H_7, H_8); 4.3 (1H, S, NH); 4.2 (2H, s, CH_2); **1e**, mp 269′C, ^{1}H-NMR; 8.25—7.4 (4H, m, H_5, H_6, H_7, H_8); 4.25 (1H, S, NH); 3.12 (3H, S. CH_3); **1f**, mp 262°C, ^{1}H-NMR; 8.07—7.3(10H, m, H_5, H_6, H_7, H_8; C_6H_5, = CH); 3.6 (2H, S, NH); **(2)**, mp 203°C, ^{1}H-NMR; 8.25—7.35 (8H, m, aromatic); 4.2. (1H, S, NH); 3.15 (1H, S, OH); **(3)** mp 208—309°C, ^{1}H-NMR; 8.3—7.8 (8H, m, aromatic); **(4)**, mp 139°C, ^{1}H-NMR; 8.2—7.9 (8H, m, aromatic); **(5)**, mp 267°C, H-NMR; 8.4—7.4 (8H, m, aromatic); **(6)**, mp, 235 °C, ^{1}H-NMR ; 8.15—7.25 (4H, m, H_5, H_6, H_7, H_8) ; 4.15 (1H, S, NH) ; **(7)**, mp 121 3°C, ^{21}H-NMR ; 8.35—8.20 (4H, m, H_5, H_6, H_7, H_8).

REFERENCES

[1] A. K. El-Shafei, G. Vernin and J. Metzger, *Gazz. chim. Ital.*, **111**, 413 (1981).

[2] G. Vernin, H. Domlog, Ch. Siv, J. Metzger and A. K. El-Shafei, *J. Heterocyclic Chem.*, **18**, 85 (1981).

[3] A. K. El-Shafei, A. Sultan and G. Vernin, *Heterocycles*, **19**, 333 (1982).

[4] A. K. El-Shafei, A. M. El-Sayed and A. A. Khalaf, *Bull. Chem. Soc. Japan*, **56**, 918 (1983)

[5] M. Fedroynski, K. Wojciechowski, Z. Matacz and M. Makosza, *J. Org. Chem.*, **43**, 4682 (1987).

Revue Roumaine de Chimie, **33**, *3*, 295–303 (1988)

INFRARED SPECTRAL STUDIES OF 3-HYDROXY-3-METHYL-1-PHENYL-TRIAZENE DERIVATIVES

NIZAMUDDIN[a] and D. N. PUROHIT[b]
[a] Department of Chemistry, B. N. College, Udaipur
[b] Department of Chemistry, Sukhadia University, Udaipur, India

Received October 27, 1986

Infrared absorbtion characteristics of 3-hydroxy-3-methyl-1-phenyl-triazene and eighteen of its derivatives (having CH_3, Cl, COOH, NO_2, OCH_3 di-substituents in different positions in the benzene nucleus) have been reported.

Applications of hydroxytriazenes as potentially useful chelating agents in the estimation of several metal ions have been reported in the literature.[1-5] The present communication deals with infrared spectral characteristics of nineteen hydroxytriazenes of 3-hydroxy-3-methyl-1-phenyl triazene series.

EXPERIMENTAL

All the above compounds were prepared following the established methods. [6,7] The infrared spectra of all the compounds were taked in nujol mull on Carl Zeiss Infracord Model No. UR 10. The infrared spectral bands are reported in Tables 1 to 6.

DISCUSSION

Recently, Purohit [8], has discussed the hydrogen bonding and tautomerism in 3-hydroxy-1,3-diphenyltriazene on the basis of infrared spectral studies. On the basis of these studies he suggested that there is a contribution of both hydroxytriazene form (structure I) and triazene oxide form (structure II) towards the final structure of hydroxytriazene (structure III).

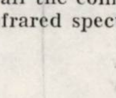
(I)

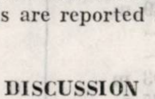
(II)

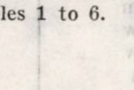
(III)

In the case of 3-hydroxy-1,3-diphenyltriazene the band at 3480 cm^{-1} (in KBr) was assigned as νOH by Purohit *et al.*,[9] whereas the band at 3250 cm^{-1} (in nujol) was established as νNH by Mitsuhashi *et al.*[10]

Table 1 *

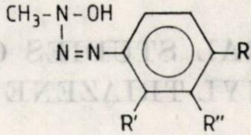

$R'=R''=R'''=H$	$R'=CH_3$, $R''=R'''=H$	$R'=R'''=H$; $R''=CH_3$	$R'=R''=H$; $R'''=CH_3$
3241 m b	3279 m	3225 m	—
—	—	—	3188 m
2930 b	2960 s	2958 s	2966 sh
2929 s	—	2927 s	2941 s
2841 s	2841 s	2858 s	2862 s
—	2755 w	—	—
2366 w	—	2378 w	—
—	1920 w	—	1920 w
1858 w	1875 w	—	1870 w
1612 s	1612 m	1612 m	1620 s
—	1596 s	1596 m	1592 m
—	1530 sh	1530 sh	1540 s
1510 s	1500 s	1500 s	1483 s
1458 s	1466 s	1462 s	1422 sh
1404 w	1416 s	1400 w	1408 m
1375 s	1383 s	1379 m	1379 m
1350 m	1358 s	1341 m	1345 s
1312 w	1306 m	—	—
—	—	1287 w	1284 m
—	—	1250 m	—
1233 m	1229 s	1229 w	1221 s
1186 w	1186 m	1154 m	—
—	1113 m	1116 w	1125 w
1075 m	1079 m	1076 w	1080 s
1037 w	—	—	1042 w
1004 w	—	1000 w	—
983 s	993 m	982 w	—
—	975 s	979 w	979 s
—	937 w	937 w	936 sh
900 m	896 w	896 w	—
842 w	854 m	870 w	842 m
—	796 sh	796 m	817 s
778 s	779 s	—	—
763 m	763 w	765 w	763 m
750 s	756 m	750 m	758 m
730 w	—	722 w	725 m
694 s	—	694 m	672 m b
669 w	665 m	658 w b	650 w
642 m	—	631 w b	628 m
620 sh	617 w	—	—
582 m	592 w	592 w b	583 w
—	544 m	556 w	558 m
—	521 s	—	—
504 m	505 s	506 w	504 m

* b = broad; m = medium; s = strong; v = very; sh = shoulder; w = weak.

Table 2

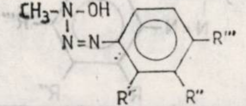

R′=Cl; R″=R‴=H	R′=R‴=H; R″=Cl	R′=R″=H; R‴=Cl	R′=R″=; R‴=**Br**
3183 m	3229 s	3200 s	—
3145 m b	—	—	3125 s b
3058 m b	—	—	3033 w
2958 s b	2958 s b	2965 s b	2963 s b
—	2929 s	—	2922 s
2862 s b	2858 s b	2854 s b	2858 s b
2750 w	—	—	—
—	—	2375 m	—
—	—	2342 w	—
1942 w	1950 w	—	—
—	1867 w	—	1867 w
1675 w	1650 w	1660 w	1633 w
1604 s	1608 s	1605 s	1600 m
1589 sh	1589 sh	1579 vw	—
a513 s	1525 w	1522 m	1521 m
1500 s	1491 s	1490 w	1500 s
1462 s	1468 w	1467 s	1465 s
1455 w	1450 s	—	—
1412 m	1404 w	1416 w	1429 w
1383 s	1383 w	2383 s	1401 m
1372 sh	—	—	1375 m
1354 m	1362 w	—	1350 m
—	1338 s	1330 w	—
1300 w	1312 w	1300 w	1305 m
1283 w	1279 w	1287 w	1283 w
1229 s	1237 s	1256 w	1233 s
1204 sh	1210 sb	1215 sh	—
—	1195 w	1195 s	—
1179 w	1185 w	1178 s	1183 m
—	1167 w	1158 s	1158 w
—	1125 sh	—	1123 w
1087 m	—	1095 w	1083 w
1058 s	1075 m	1076 w	1075 m
1037 s	—	—	—
—	1000 s	1008 w	1012 w
983 s	—	982 m	983 m
895 w	908 w	900 m	—
842 w	858 m	842 s	846 w
793 s	792 s	787 sh	—
763 m	760 w	772 m	760 w
756 m	756 m	757 w	750 w
733 m	—	735 w	—
724 m	729 m	—	726 w
—	711 m	706 w	710 w
—	685 m	—	681 w
654 m	650 w b	670 w	—
—	633 w b	633 w b	638 w b
605 w	593 w	600 w b	610 w
585 w	560 w	579 w	581 w
547 m	—	548 w	—
517 m	508 w	517 w	517 m
488 m	438 w	458 w	447 m
421 m	417 w	422 w	417 w

Table 3

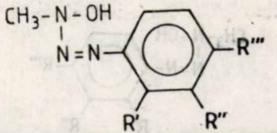

R′=COOH; R″=R‴=H	R″=COOH; R′=R‴=H	R‴=COOH; R′=R″=H
—	3583 w	3583 w
—	3566 w	3562 w
3209 m b	3150 w	3196 s
2979 s b	2975 sb	2977 s v b
2854 s b	2858 sb	2850 s b
2780 w	—	2766 w
2733 w	2733 w	2740 w
2610 w	2608 w	—
—	2370 w	2375 w
—	2258 w	—
—	2123 m	—
1958 w	—	—
1920 w	1920 w	1927 w
—	1700 m b	1725 w
1679 s	1675 m b	1665 w
1614 w	1608 m	1623 s
1591 s	1579 w	1591 w
1525 s	1545 w	1537 s
—	1512 w	1498 m
1467 s	1467 s	1470 s
1420 m	1427 sh	1420 sh
1397 s	—	—
1379 s	1383 s	1383 s
1358 w	1333 w	1333 m
—	—	1365 sh
1316 w	1312 m	1304 m
1283 s	1287 m	1287 m
1252 s	—	1262 w
1208 s	—	1216 sh
1185 sh	1187 w	1195 s
1170 s	1173 w	1178 s
1151 m	1142 w	1158 s
—	1120 w	—
1096 m	—	1075 m
1056 m	—	1045 w
1030 w	1020 w	1018 w
979 s	945 m	988 s
894 w	—	900 s
875 w	850 m	833 s
836 w	823 w	825 m
793 s	—	—
779 s	—	—
764 m	762 m	762 w
760 s	734 m	—
725 m	725 w	—
—	723 w	722 m
698 s	683 w	706 m
768 m	—	—
627 w	629 w	617 s
582 w	—	589 s
554 w b	550 m	551 w
523 w	529 w	533 w
475 w	492 w	512 w
414 w	423 w	418 w

Table 4

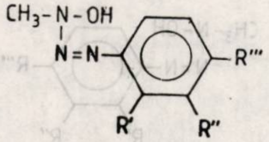

$R'=NO_2$; $R''=R'''=H$	$R''=NO_2$; $R'=R'''=H$	$R'''=NO_2$; $R'=R'=R''=H$
3279 m	3229 s	3299 w
—	3120 w	3140 w b
2958 s b	2958 s b	2965 s b
—	2929 s b	—
2850 s b	2856 s b	2842 s b
2733 w	—	2733 w
2675 w	—	2662 w
2358 w	2345 w b	—
1614 s	1629 s	1612 s
1583 m	1583 m	—
1514 s	1516 s	1523 s
—	—	1480 s b
1400 m	1419 s	1416 w
1383 s	1379 w	1383 s
1347 s	1358 s	1350 s
1320 s		1329 s
—	1295 m	1306 s
1279 m	1233 m b	1225 m
1160 w	—	1162 m
1122 sh	1122 sh	1125 sh
—	—	1112 m
1070 w	1075 w	1083 m
1055 w	1004 w	1010 w
983 m	994 m	991 m
875 w	895 w	—
842 w	862 w	842 w
—	829 m	823 w
794 w	800	810 s
778 m	771 s	876 m
764 w	750 w	742 w
687 w	693 w	689 m
648 w	670 m b	646 w
600 w	606 w b	614 w b
585 w	574 w	573 w
485 w	479 w	487 w
416 w	421 w	429 w

Table 5

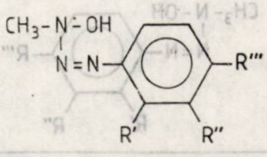

R′=OCH$_3$: R″R‴=H	R″=OCH$_3$; R′=R‴	R‴=OCH$_3$: R′=R″=H
3314 w	—	—
—	3225 s	3192 m b
2945 s b	2991 s b	2985 s b
2866 s b	2862 s b	2841 s b
—	—	2737 w
2108 w	2060 w	2058 w
1608 s	1612 s	1620 w
1550 sh	—	
1525 s	1520 s b	1529 s
1470 s	1466 s b	1472 s b
1441 s	—	—
1425 s	—	—
1412 s	1404 w	1416 w
1380 w	1383 w	1383 s
1358 m	1341 s	1350 m
1325 sh	—	1316 w
1289 w	1266 s	1300 m
1354 m	—	1248 m
1219 m	1204 s	1208 w
1179 w	1170 m	1183 w
—	1156 s	—
1116 m	1141 m	1120 w
1083 w	1083 m	1083 m
1045 w	1047 m	1039 s
983 m	1008 m	987 s
927 w b	945 sh	933 w
854 w b	841 m	839 s
—	801 sh	808 w
777 s	783 w	775 m
764 sh	762 sh	762 s
733 w	750 m	731 m
—	693 s	—
662 w b	664 m b	656 w
—	645 m	627 m b
612 w b	608 m	590 w
—	583 m	580 m
535 m b	554 s	—
514 s	514 s	524 w
445 m	454 m	449 w
425 w	422 w	421 w

A perusal of Tables 1—6 reveals that in case of *m*- and *p*-carboxy, *o*-methoxy, *m*-acetyl and *p*-sulphonyl compounds weak bands appear at 3583 cm^{-1} and 3566 cm^{-1}, 3589 cm^{-1} and 3562 cm^{-1}, 3314 cm^{-1}, 3662 cm^{-1} and 3633 cm^{-1}, 3650 cm^{-1} and 3604 cm^{-1} respectively. These bands may be assigned as νOH. The lack νOH band in fourteen hydroxytriazenes out of nineteen (parent, *o*, *m* and *p*-methyl; *o*, *m* and *p*-chloro and *p*-bromo substituted derivatives) may be interpreted to mean that there is a very

Table 6

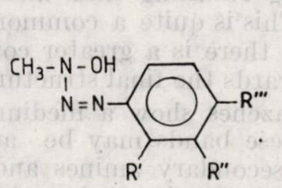

$R''=COCH_3$; $R'=R'''=H$	$R'''=SO_3Na$; $R''=R'''=H$
3662 w	3650 w
3633 w	3604 w
3233 s b	3258 m
3214 s	—
—	3150 w b
2976 s b	3003 sh
2933 s	—
2856 sh	—
2847 s	2841 sh
—	2725 s b
—	2379 w
—	1920 w
1679 s	1675 w
1605 w	1608 s
1585 m	1579 m
1552 sh	1550 m
1516 m	1512 w
1466 s b	1462 s b
1442 sh	—
1408 w	1413 w
1380 s	1383 s
1368 s	—
1347 m	1345 s
1300 w	1304 m
1270 s	—
1235 w	1229 s
1200 w	1192 s
1154 w	1139 s
1115 w	1110 sh
1083 m	1082 m
1037 w	1058 s
1029 w	1013 m
983 m	983 s
958 w	—
895 w	900 w
775 m	775 w
745 m	750 s
728 w	720 s
683 m	655 s
641 w	—
627 w	627 s
604 w	—
583 w	577 sh
—	564 sh
512 m	512 m
462 w	421 w
422 w	

strong hydrogen bonding resulting into more diffused -OH band and thus difficult to locate. This is quite a common phenomenon. Alternatively it can also mean that there is a greater contribution of form (II) as compared to form (I) towards the final structure (III).

All the hydroxytriazenes show a medium to strong band between 3100 and 3300 cm^{-1}. These bands may be assigned as νNH. The NH stretching frequency in secondary amines and imines[11,12] is assigned in the range $3300-3500$ cm^{-1}. The low value of N–H stretching frequency in hydroxytriazenes indicates the existence of hydrogen bonding.

A medium to strong band is observed at 1528 ± 18 cm^{-1} in the IR spectra of all the hydroxytriazenes, which may be assigned to δNH. This band disappears too on complex formation (removal of H), thus confirming the proposed assignment. Furthermore, Kubler *et al.*[13] identified δ NH in the same range at 1522 cm^{-1} in the case of diazoamino benzene i.e. 1,3-diphenyltriazene $C_6H_5\text{-}NH-N=N-C_6H_5$.

All these compounds show a weak to strong band at 1425 ± 15 cm^{-1}. This band may tentatively be assigned to the asymmetric stretching of $>N-N=N\rightarrow O$ or mainly $-N=N$. These compounds also exhibit a band at 1335 ± 15 cm^{-1}, which may be assigned to the symmetric stretching of $N-N=N\rightarrow O$ or mainly $N\rightarrow O$ stretch. A similar assignment in the case of azoxy compounds ($-N=N-$) in these ranges (asymmetric $1450-1480$ cm^{-1} and symmetric $1335-1315$ cm^{-1}) has been made by various workers.[14-16]

All the investigated hydroxytriazenes exhibit a band at 1080 ± 15 cm^{-1} which may tentatively be assigned to δ NOH. Appearance of this deformation band in those compounds also, where νOH was not observed, indicates that although the form (II) predominates, there is a definite contribution of form (I).

All the hydroxytriazenes except nitro derivatives show a variable intensity (weak to strong) band at 1185 ± 20 cm^{-1} which may be assigned as -N-N-stretch and another band at 1227 ± 15 cm^{-1} which may be assigned to C-N-stretching. Similar assignments have been made by Kubler *et al.*[13] in the case of $C_6H_5N=N-NHC_6H_5$ at 1202 cm^{-1} (N–N) and 1248 cm^{-1} (Phenyl-N) using ^{15}N substitution studies.

All these compounds (except in carboxy and *o* and *p*-nitro derivatives) show a band of variable intensity (weak to strong) at 970 ± 10 cm^{-1}, which may be assigned to $\nu N \rightarrow O$. The $N \rightarrow O$ stretching band in the case of tertiary amine oxides has been reported by Mathis *et al.*[17] to be between 950 and 970 cm^{-1}.

All the hydroxytriazenes (bearing *p*-methyl; *p*-nitro; *p*-bromo and *m*-carboxy) also show a weak to strong band at 890 ± 10 cm^{-1}. This may be assigned to $\nu N-O$ of $-N-OH$ group in hydroxytriazenes. A similar assignment of N–O at 900 cm^{-1} in the case of hydroxamic acid (R–CO–NHOH) has been made by Hadzi and Prevorsek[18] and near 930 cm^{-1} in the case of oximes ($>C=N-OH$) by other workers.[19-21]

From the above discussion it can be seen that all these compounds exhibit bands corresponding to νNH, ρNH, δNOH, $\delta N \rightarrow O$ and $\nu N-O$ (of NOH). The appearance of these bands is a definite indication of the fact that both the structures (I) and (II) contribute to the final structure (III) of hydroxytriazenes.

REFERENCES

[1] D. N. Purohit, *Talania*, **14**, 353 (1967).
[2] D. Chakraborti and A. K. Majumdar, *J. Indian Chem. Soc.*, **54**, 258 (1977).
[3] D. N. Purohit, Nizamuddin and A. M. Golwalkar, *Revs. Anal. Chem.*, **8**, 73 (1985).
[4] R. L. Datta and Ramdhar Sharma, *J. Indian Chem. Soc.*, **57**, 1792 (1980), *ibid*, 58, 807 (1981); *J. Inorg. Nuclear Chem.*, **43**, 1062 (1981).
[5] N. R. Biswas, B. C. Ray and S. Iahiry, *J. Indian Chem. Soc.*, **60**, 775 (1983).
[6] N. C. Sogani and S. C. Bhattacharya, *J. Indian Chem. Soc.* **360**, 563 (1959).
[7] D. N. Purohit and Nizamuddin, *J. Indian Chem. Soc.*, **60**, 712 (1983).
[8] D. N. Purohit, *Spectrochim. Acta*, **41A**, 873 (1985).
[9] D. N. Purohit, S. M. Dugar and N. C. Sogani, *Z. Naturforsch.*, **B20**, 853 (1965).
[10] T. Mitsuhasi and O. Simamura, *Tetrahedron Letters*, **30**, 2593 (1965).
[11] I. J. Bellamy, "The Infrared Spectra of the Complex Molecules", p. 348, Methuen, London, 1958
[12] C. N. R. Rao, "Chemical Applications of Infrared Spectroscopy", p 245, Academic Press, New York, 1963.
[13] R. Kubler, W. Luttke and S. Weckherlin, *Z. Elektrochem.*, **64**, 650 (1960).
[14] W. Maier and G. Englert, *Z. Elektrochem.*, **62**, 1020 (1958).
[15] B. Witkop and H. M. Kissman, *J. Amer. Chem. Soc.*, **75**, 1975 (1953).
[16] J. Jander and R. N. Haszeldine, *J. Chem. Soc.*, **1954**, 919.
[17] R. Mathis, R. Wilf and W. Galliais, *Compt. rend.*, **242**, 1973 (1956).
[18] D. Hadzi and D. Prevorsek, *Spectrochim. Acta*, **10**, 38 (1957).
[19] J. F. Brown Jr., *J. Amer. Chem. Soc.*, **77**, 6341 (1955).
[20] A. Paim and H. Weakin, *Canad. J. Chem.*, **32**, 858 (1954).
[21] D. Hadzi, J. *Chem. Soc.*, **1956**, 2725.

Revue Roumaine de Chimie, **33**, *3*, 305–311 (1988)

STUDIES ON PHYSICAL PROPERTIES OF SOME ORGANOCHLORO PESTICIDES IN METHANOL

R. P. VARMA, B. B. BHATNAGAR and ANURADHA SINGH
Department of Chemistry, D.A.V. College, Muzaffarnagar-251001, India

Received September 20, 1986

Several physical properties, viz. solubility, density and viscosity of organochloro pesticides in methanol, have been determined at different temperatures (35 – 50°C). Apparent heat of solutions of pesticides has been calculated from solubility data which are found in the order: DDT$<$Endosulphan$<$BHC. Viscosity and density data have been analysed using various equations and it has been concluded that solute-solvent interaction occurs in pesticide solution in methanol. The effects of temperature and concentration of pesticide on the fluidity of pesticide solutions have been discussed in the light of Arrhenius and Eyring equations and activation parameters of viscous flow viz. ΔH^*, ΔS^* and ΔG^* have been calculated. The non-linear variation of ΔG^* with concentration of pesticide confirms the observation of solute-solvent interaction.

INTRODUCTION

In our previous communication,[1] the ultrasonic velocity of these pesticides has been studied and several parameters such as acoustic impedance, intermolecular free length, hydration number etc. have been evaluated in methanol at different temperatures. The present paper deals with the study of various physical properties such as solubility density and viscosity of these pesticides in methanol in order to have better understanding of these solutions.

EXPERIMENTAL

The organochloro pesticides were obtained from Hindustan Insecticides Ltd., Gurgaon (Haryana), India and purified by recrystallization in methanol. The melting points of pesticides are: DDT (108 – 110°C), benzene hexachloride (109 – 112°C) and endosulphan (80 – 90°C). Methanol (BDH) was distilled before its use.

The apparatus and procedure of solubility and viscosity measurements were the same as reported earlier.[2,3] Densities of solutions were measured by a pyrex dilatometer. The capacity of the reservoir was about 15 cm^3. The measuring section was in the form of a precisely bored graduated capillary tube. The apparatus was calibrated with conductivity water and the accuracy of results was checked by using test solutions of known density at 35°C.

The reproductibility of the solubility, density and viscosity data are ±0.5 %, ±0.0002 mg and 0.3 %, respectively. All the measurements were made at a constant temperature (±0.05°C) in a thermostat.

RESULTS AND DISCUSSION

Solubility. Solubility of pesticides increases with increase in temperature. The plots of solubility of pesticides *vs*. temperature (Fig. 1) show that the solubility of BHC increases linearly with increase in temperature.

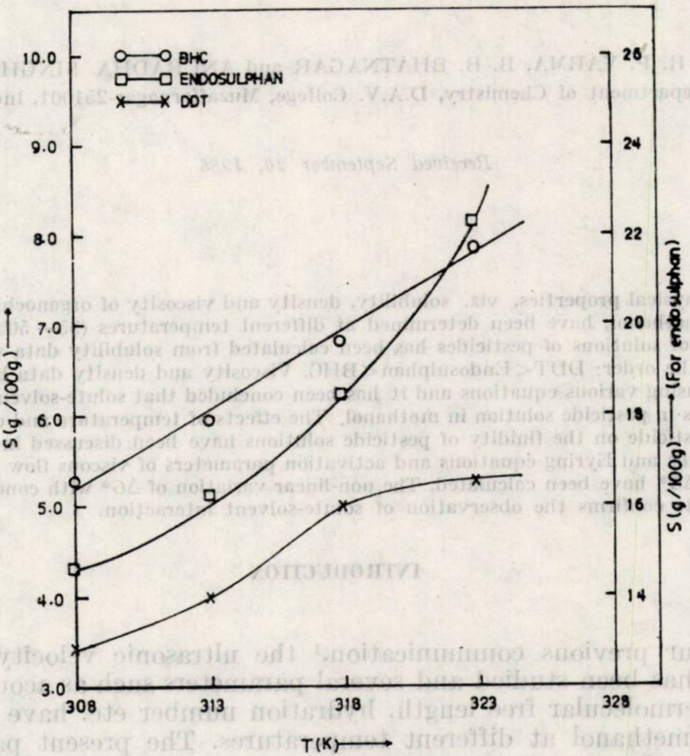

Fig. 1. — Plots of solubility S (g/100 g) *vs*. temperature (K) of DDT, BHC and endosulphan.

The solubility of endosulphan goes on increasing non-linearly with increase in temperature whereas DDT shows an abrupt change at 40°C.

The apparent heat of solution, $-\Delta H_{\text{sol}}$ has been calculated [3] and the values found were: 26.78, 22.95 and 30.60 kJ mol^{-1}, respectively for DDT, BHC and endosulphan.

Since this process can be considered as an isothermal equilibrium reaction, the free energy, ΔG_{sol} is equal to zero. Therefore, the entropy of solution ΔS_{sol} can be calculated as follows:

$$\Delta S_{\text{sol}} = \frac{\Delta H_{\text{sol}}}{T} \tag{1}$$

The values of $-\Delta S_{\text{sol}}$ are 86, 74 and 99 JK^{-1} mol^{-1}, respectively, for DDT, BHC and endosulphan.

Density. Density (g/cm^3) of pesticides increases with increase in concentration and the temperature of the solution. The plots of density *vs*. concentration are linear. The density data have been analysed using Roots' equation [4] which is represented as

$$d = d_0 + AC - BC^{3/2} \tag{2}$$

where A is a measure of solute-solvent interaction and B refers to solute-solute interaction. The values of A and B have been obtained from the intercepts and slopes of the linear plots (Fig. 2) and are given in Table 1.

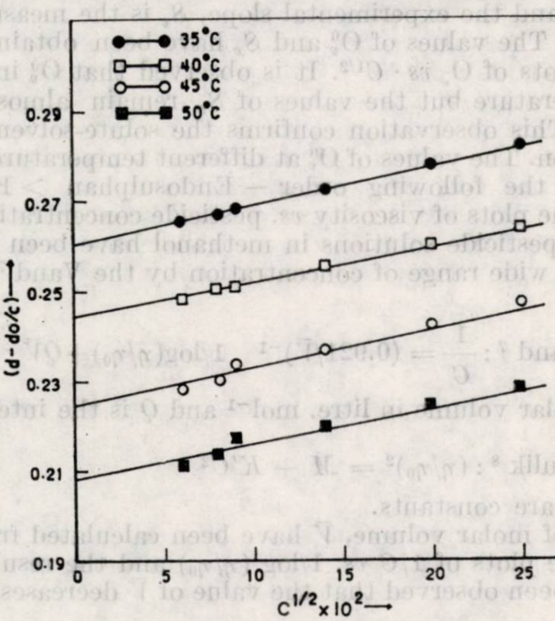

Fig. 2. — Plots of $\left(\frac{d-d_0}{c}\right)$ *vs*. $\sqrt{c}$ of DDT at different temperatures (35°−50°C).

Table 1

Values of A, B, $Ø_v^0$ and S_v of pesticides in methanol

Pesticide	Temp. (K)	A	B	$Ø_v^0$	S_v
DDT	308	0.26	0.08	122	120
	313	0.24	0.08	143	120
	318	0.22	0.08	172	120
	323	0.21	0.08	192	120
BHC	308	0.15	0.17	190	200
	313	0.14	0.17	194	200
	318	0.12	0.17	228	200
	323	0.08	0.18	278	233
Endosulphan	308	0.21	0.10	250	133
	313	0.19	0.10	278	133
	318	0.17	0.13	306	160
	323	0.16	0.12	323	160

Constant A decreases whereas B remains unchanged with increase in temperature in all the three pesticides. This clearly indicates the solute-solvent interaction in the pesticide solution which decreases due to thermal effects on increasing temperature.

Apparent molar volume, $\varnothing_v$ has been calculated and is found to obey the following equation [6]

$$\varnothing_v = \varnothing_v^0 + S_v C^{1/2} \tag{3}$$

Here $\varnothing_v^0$, the limiting apparent molar volume, is a measure of solute-solvent interaction and the experimental slope, S_v is the measure of solute-solute interaction. The values of $\varnothing_v^0$ and S_v have been obtained (Table 1) from the linear plots of $\varnothing_v$ *vs* $\cdot$ $C^{1/2}$. It is observed that $\varnothing_v^0$ increases with increases in temperature but the values of S_v remain almost unaffected by temperature. This observation confirms the solute-solvent interaction in pesticide solution. The values of $\varnothing_v^0$ at different temperatures for various pesticides are in the following order — Endosulphan > BHC > DDT.

Viscosity. The plots of viscosity *vs*. pesticide concentration are linear. Viscosity data of pesticide solutions in methanol have been satisfactorily represented in the wide range of concentration by the Vand [7] and Moulik [8] equations.

$$\text{Vand}^{\,7}: \frac{1}{C} = (0.921/\bar{V})^{-1} \quad 1/\log(\eta/\eta_0) + Q\bar{V} \tag{4}$$

where $\bar{V}$ is the molar volume in litre. mol^{-1} and Q is the interaction coefficient.

$$\text{Moulik}^{\,8}: (\eta/\eta_0)^2 = M + K'C^2 \tag{5}$$

where M and K' are constants.

The values of molar volume, $\bar{V}$ have been calculated from the slope ($= \bar{V}/0.921$) of the plots of $1/C$ *vs*. $1/\log(\eta/\eta_0)$ and the results are given in Table 2. It has been observed that the value of $\bar{V}$ decreases with increasing temperature.

Table 2
Viscosity parameters for organochloro pesticides in methanol

Temp. (K)	Tested conc. limit	Valid zone	$\bar{V}$	Q	M	K'
DDT						
308	.004—.06	.04—.06	1.84	−4.34	1.20	65.0
323	.004—.06	.04—.06	1.22	−3.29	1.16	65.0
318	.004—.06	.04—.06	1.03	+1.94	1.14	65.0
323	.004—.06	.04—.06	0.75	+5.43	1.11	65.0
BHC						
308	.02—.12	.08—.12	0.44	−6.44	1.11	7.7
313	.02—.12	.08—1.2	0.37	−4.34	1.10	7.7
318	.02—.12	.08—.12	0.33	−3.62	1.08	7.7
323	.02—.12	.08—.12	0.25	−1.04	1.07	6.3
Endosulphan						
308	.02—.12	.06—.12	0.32	−7.58	1.06	6.8
313	.02—.12	.06—.12	0.28	−5.71	1.05	6.8
318	.02—.12	.06—.12	0.25	−4.79	1.04	6.4
323	.02—.12	.06—.12	0.24	+4.94	1.03	6.1

A comparison of data shows that the values of $\bar{V}$ are in the following order : DDT > BHC > Endosulphan.

The interaction coefficient Q, calculated from the intercept $(=Q\bar{V})$ increases with increasing temperature.

It may be mentioned that Vand's equation contains perfectly defined parameters, $\bar{V}$ and the interaction coefficient, Q is only approximately obtained.[9] It appears that most probably Q is a specific property of a solute and it is not the general property.[10]

Constant M decreases whereas K' is found to be independent of temperature.

Jones-Dole equation [11] :

$$\eta_{sp}/C^{1/2} = A + BC^{1/2} \qquad (6)$$

Coefficients A and B refer to the solute-solute and solute-solvent interaction, respectively. The slope B increases slightly with increase in temperature in case of DDT whereas the slope remains almost unchanged with increase in temperature (Table 3).

Table 3

Values of constant B of pesticides in methanol at different temperatures obtained from Jones-Dole equation

Temperature (K)	DDT	BHC	Endosulphan
308	2.40	0.60	0.53
313	2.90	0.70	0.53
318	3.10	0.70	0.60
323	3.60	0.70	0.67

Plotting log η *vs.* $1/T$, straight lineas are obtained which show that the viscosity temperature function can be expressed by the Arrhenius equation :

$$1/\eta = Ae^{E_{\Phi}/RT} \qquad (7)$$

where A and $E_{\emptyset}$ are the Arrhenius coefficient and activation energy of viscous flow.

The values $E_{\emptyset}(=\Delta H^*)$ have been calculated from the linear plots of $-\log \eta$ *vs.* $1/T$. It is observed that activation energy of viscous flow increases with increase in pesticide concentration, it may be pointed out that ΔH^* measures energy barrier to fluid motion and the increase in ΔH^* with concentration indicates less fluidity. The values of ΔH^* are in the following order :

DDT < BHC < Endosulphan.

The temperature dependence of $1/\eta$ (fluidity) has also been evaluated according to the theory of absolute reaction rates in terms of the Eyring equation.[12]

$$1/\eta = (V/hN) \exp\left(-\Delta H^*/RT\right) \exp\left(\Delta G^*/R\right) \qquad (8)$$

where V is the molar volume of the solvent, R is the gas constant in cal. $\text{deg}^{-1} \cdot \text{mol}^{-1}$, T is the absolute temperature and η is the viscosity in poise. N and h are the Avogadro number and Planck's constant respectively. ΔS^* and ΔG^* are the activation entropy and free energy of viscous flow, respectively. ΔG^* is calculated from Gibbs equation at 35°C.

The variation of ΔS^* and ΔG^* are almost similar. Since ΔG^* controls the rate of flow in the fluid process, the non-linear variation of ΔG^* with concentration of added pesticide becomes the indicative of the formation of solute-solvent aggregate [13] as the principle kinetic entity. Thus, the non-linear behaviour of ΔG^* (Fig. 3) confirms the solute-solvent interaction in the pesticide solutions in methanol.

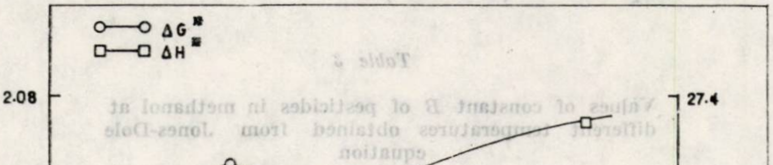

Fig. 3. — Plots of ΔH^* and ΔG^* *vs.* concentration of DDT at 35°C.

Table 4

Density and viscosity values of DDT in methanol

Conc.	Density		Viscosity	
	308 K	318 K	308 K	318 K
.004	.7787	.7719	4.842	4.320
.006	.7792	.7724	4.869	4.343
.008	.7798	.7729	4.898	4.360
.02	.7831	.7758	5.095	4.507
.04	.7887	.7807	5.431	4.769
.06	.7945	.7858	5.693	5.019

ACKNOWLEDGEMENT. The authors would like to thank college authorities for providing the laboratory facilities. One of the authors (AS) is thankful to University Grants Commission, New Delhi for the award of Junior Research Fellowship.

REFERENCES

[1] R P. Varma, B. B. Bhatnagar and A. Singh, *Acoustica* (Germany) Communicated.

[2] R. P. Varma and A. K. Virmani, *Rev. Roumaine Chim.*, **27**, 1109 (1982).

[3] R. P. Varma and P. Bahadur, *Cellulose Chem. Technol.*, **9**, 393 (1975).

[4] W. C. Roots, *J. Amer. Chem. Soc.*, **55**, 850 (1933).

[5] E. S. Harned and B. B. Owen, "Physical Chemistry of Electrolytic Solutions", D. C. Reinhold.

[6] D. C. Masson, *Phil Mag.*, **8**, 218 (1929).

[7] V. Vand, *Phys. Colloid. Chem.*, **25**, 277 (1948).

[8] S. P. Moulik. *J. Phys. Chem.*, **72**, 4682 (1986).

[9] "International Encyclopedia of Physical Chemistry and Chemical Physics". Topic 16, Vol. 3, Pergamon Press, Oxford, p. 4f (1965).

[10] S. P. Moulik, *J. Indian Chem. Soc.*, **49**, 383 (1972).

[11] G. Jones and M. Dole, *J. Amer. Chem. Soc.*, **51**, 2950 (1929).

[12] S. Glasstone, K. J. Laider and H. Eyring, "Theory of Rate Process". Mc Graw-Hill, New York, Chap. 9, p. 477, 1941.

[13] J. C. MacDonald, J. Serphillips and J. J. Guerrera, *J. Phys. Chem.*, **77**, 370 (1973

Revue Roumaine de Chimie, **33**, *3*, 313–319 (1988)

17α-SUBSTITUTED DERIVATIVES OF B-NOR-5-ANDROSTENE-3β-OL-17-ONE AND 5-ANDROSTENE-3β-OL-17-ONE

ROBERT SCHWARTZ and ANIKÓ SCHWARTZ
Chemical and Farmaceutics Research Institute
Str. Fabricii, 126, 3400 Cluj-Napoca, Romania

Received November 17, 1986

The syntheses of some 17α-substituted derivatives of B-nor-5-androstene-3β-ol-17-one and 5-androstene-3β-ol-17-one are reported. The compounds were characterized on the basis of elemental analysis and spectroscopic behaviour (IR, ^{1}H-NMR and MS). Some chemical observations and the MS data suggest that the investigated 17α-substituted derivatives of B-nor-5-androstene-3β-ol-17-one are hygroscopic.

INTRODUCTION

In the present paper some 17α-substituted derivatives of B-nor-5-androstene-3β-ol-17-one **2** and 5-androstene-3β-ol-17-one **2′** are presented. We prepared these derivatives in order to study the possible differences which can occur in their biological behaviour and in their oxidation (Oppenauer kind) with Al_2O_3 [1,2] owing to the elimination of the C_6-methylene group from ring B.

PREPARATIONS

17α-Methyl-, ethyl- and the allyl-derivatives (**2a, c, e** and **2′a, c, e**) were prepared in the usual way (Scheme 1), through the action of the corresponding Grignard reagent on the 17-carbonyl group of **1**. The

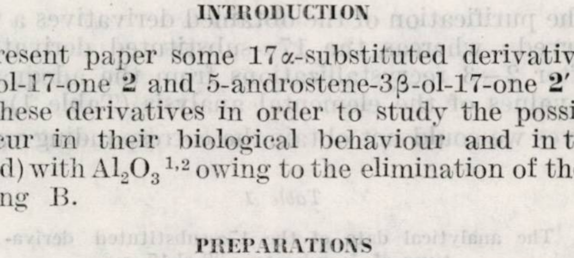

a) R : H ; R′ : CH_3 c) R : H ; R′ : C_2H_5 f) R : H ; R′ : C ≡ CH
b) R ; Ac ; R′ : CH_3 d) R : Ac ; R′ : C_2H_5 g) R : Ac ; R′ : C ≡ CH
e) R : H ; R′ : $CH_2{-}CH{=}CH_2$

required amount of magnesium in anhydrous ether was treated with methyl iodide or ethyl, respectively allyl bromide. The solution of the obtained Grignard reagent was dropped in the stirred benzene solution of the corresponding steroid. The end point of the reaction was visualised by TLC. The reaction mixture was worked up in the usual manner.

A more difficult problem was the preparation of the 17α-ethynyl derivatives **2f** and **2′f**. There is only one reference[3] in the specialty literature regarding the ethynylation of the B-nor-steroids. According to these authors the ethynylation is accomplished preparing potassium *i*-butylate which is transformed into potassium acetylide. We used for the preparation of the 17α-ethynyl-derivatives both an analogous method to the mentioned (the potassium acetylide being prepared by means of potassium *i*-propylate) as well as the method elaborated by Toth *et al.*[4] adapted to our reasons. The yields of ethynylation using the first method were 73–75%, while using naphthalene-sodium complex they were 85–90%.

RESULTS AND DISCUSSION

During the purification of the obtained derivatives a very interesting fact was observed: whereas the 17α-substituted derivatives of natural series gave, after 2–3 recrystallizations from the adequate solvent, the corresponding values of the elemental analysis (Table 1), in the case of B-nor-derivatives we could not obtain the corresponding values even using a high number of crystallizations and purifications (which lead to chromatographically pure substances). The carbon content showed an almost constant difference with 2–3% less than the calculated value (Table 2).

Table 1

The analytical data of the 17α-substituted derivatives of 5-androstene-3β-ol-17-one

No. comp.	m.p. °C	$[\alpha]_D^{20}$	Elemental analysis calc./found	
			C %	H %
2′a	203–204	−75.8 (1% $CHCl_3$)	78.89 78.61	10.60 11.04
2′c	196–198	−80.8 (1% Diox.)	79.19 79.31	10.76 11.06
2′e	150–153	−95.8 (1% Diox.)	79.94 79.63	10.36 10.12
2′f	245–246	−118.5 (1% $CHCl_3$)	80.20 80.33	9.62 10.19

This observation suggests the necessity to synthesize the 17α-substituted B-nor-derivatives by an "indirect" way starting with the corresponding 17α-substituted derivative of the androstene series (with corresponding elemental analysis and other analytical data) and removing the C_8-methylene group from this, according to the sequence 2′ → 2.

Table 2

The analytical data of the 17α-substituted derivatives of B-nor-5-androstene-3β-ol-17-one

No. comp.	m.p. °C	$[\alpha]_D^{20}$	Elemental analysis calc./calc./found C%	H%
2a	199−200	−141.4 (1% E×OH)	78.57 73.98* 73.74	10.41 10.45* 10.85
2c	200−202	−118.0 (1% MeOH)	78.89 74.49* 74.54	10.59 10.62* 10.55
2e	150−153	−103.4 (1% MeOH)	79.68 75.40* 75.18	10.19 10.24* 10.08
2f	167−168	−170.0 (0.5% EtOH)	79.95 75.43* 75.76	9.39 9.49* 10.04
2b	145−147	−131.0 (1% $CHCl_3$)	75.85 75.83	9.70 9.74
2d	144−146	−109.0 (1% $CHCl_3$)	76.25 75.97	9.89 10.04
2g	145−146	−157.0 (1% $CHCl_3$)	77.15 77.32	8.83 9.01

* the values calculated with one molecule of water

This indirect method presented in Scheme 2 and detailed in the Experimental part was necessary in order to ascertain that the desired

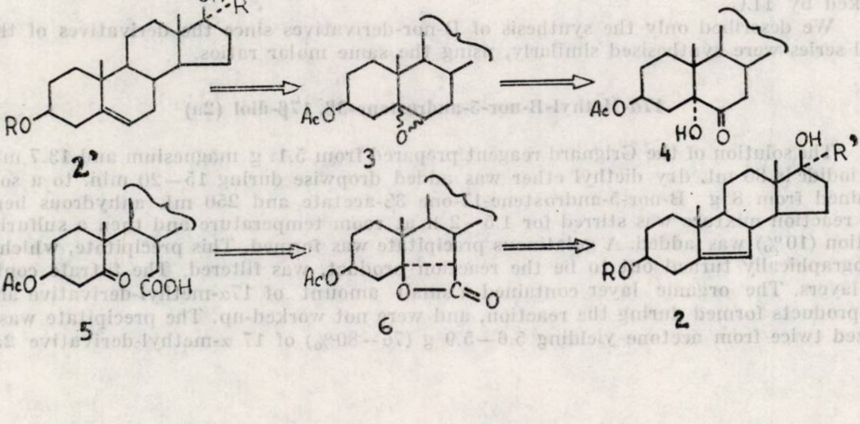

derivative has been obtained since the literature[5] mentions only the melting point of 17α-methyl-B-nor-5-androstene-3β, 17β-diol(**2a**). We found no description of 17α-allyl-B-nor-5-androstene-3β, 17β-diol(**2e**).

The 17α-substituted B-nor-5-androstene-3β, 17β-diol 3β-acetates **2b, c, g** were ascertained by elemental analysis (Table 2). The elemental analysis of the obtained derivatives after hydrolysis **2a, c, f** showed again the above-mentioned differences. The dihydroxy-derivatives **2a, c, f** obtained by the "direct" method were selectively acylated at C_3 giving the same derivatives as those obtained indirectly as shown by the corresponding elemental analysis.

These results suggested that the dihydroxy-derivatives **2a, c, e, f** either contain solvent molecule in their crystal grating or are hygroscopic. This assumption was confirmed by mass-spectra of 17α-ethynyl-**2f** and 17α-ethyl-**2c** derivatives. These spectra confirmed the molecular weight (m/e : 300 M^+, I : 100% resp. m/e : 304 M^+, I : 100%) and showed the presence of the fragments m/e : 17, I : 20% resp. 23,5% and m/e : 18, I : 152.8% resp. 156%, according to the presence of hygroscopic water in the sample which could not be removed by the usual methods. These fragments also appear with a much smaller percentage (2–5%) in the mass-spectra of the corresponding derivatives of the natural series resulting from the fragmentation of the hydroxyl-groups of the molecule.

The thymolitic activity of the synthesised substances was tested[6]. The obtained data indicated that the treatment with both the natural[2] and the B-nor-steroids gives no measurable changes of body weight of the treated animals (immature male Wistar rats) as compared with the control group. The 17α-methyl-(**2'a**) and the 17α-ethyl-(2'c) derivative from the natural series have the highest thymolitic activity, while the activities of the derivatives **2'f** and **2'e** are similarly reduced. The thymolitic activities of all derivatives of the B-nor-series are lower than that of the compound **2'a**.

EXPERIMENTAL

All melting points are uncorrected. Specific rotations were determined on Polamat-C. Zeiss Jena. IR spectra were obtained on a Specord 75-IR C. Zeiss Jena (KBr and $CHCl_3$), spectrophotometer. ^1H-NMR spectra were determined in $CDCl_3$ on a Varian XL-100 spectrometer with TMS as internal standard at 55–60°C. Mass-spectra were determined on a Varian MAT-SM-1 spectrometer.

The completion of the reactions and the purity of the prepared compounds were checked by TLC.

We described only the synthesis of B-nor-derivatives since the derivatives of the natural series were synthesised similarly, using the same molar ratios.

17α-Methyl-B-nor-5-androstene-3β, 17β-diol (2a)

The solution of the Grignard reagent prepared from 5.1. g magnesium and 13.7 mL methyl iodide in 80 mL dry diethyl ether was added dropwise during 15–20 min. to a solution obtained from 8 g B-nor-5-androstene-17-one 3β-acetate and 250 mL anhydrous benzene. The reaction mixture was stirred for 1.5–2 h at room temperature and then a sulfuric acid solution (10%) was added. A gelatinous precipitate was formed. This precipitate, which chromatographically turned out to be the reaction product, was filtered. The filtrate contained two layers. The organic layer contained a small amount of 17α-methyl-derivative and the side-products formed during the reaction, and were not worked-up. The precipitate was crystallized twice from acetone yielding 5.6–5.9 g (76–80%) of 17 α-methyl-derivative **2a**.

17α-Ethyl-B-nor-5-androstene-3β, 17β-diol 2c

The same method as in the case of 17 α-methyl-derivative was used. 8 g B-nor-5-Androstene-17-one 3β-acetate were solved in 250 mL of anhydrous benzene, 5.1 g magnesium in 80 mL of dry ether and 15.8 mL of ethyl bromide were added.

The crude product was purified from methanol to yield 5.4—5.7 g (70—75%) of 17α-ethyl-derivative **2c**.

17α-Allyl-B-nor-5-androstene-3β, 17β-diol 2e

Allyl magnesium bromide was prepared from 2.8 g magnesium, 10.3 mL allyl bromide and 50 mL dry ether. The reaction was induced with 2—3 drops of ethylene bromide. The solution of the Grignard reagent was added dropwise during 15—20 min. to a solution of 5 g B-nor-5-androsterone-17-one 3β-acetate in 100 mL of anhydrous benzene, under stirring and cooling. The reaction mixture was stirred for 1—1.5 h at room temperature and then ammonium chloride solution (10%) was added, forming a gelatinous precipitate. The mixture was worked up as described above.

After crystallization of the crude product from aqueous acetone, 3.7—3.9 g (74—78%) of 17α-allyl-derivative **2e** were obtained.

17α-Ethynyl-B-nor-5-androstene-3β, 17β-diol 2f

62 g Naphthalene were dissolved in 300 mL of anhydrous THF. To this solution 12 g of sodium were added at 20—25°C during 1.5—2 h obtaining a dark-green solution. Purified and dried acetylene was bubbled through the solution. The mixture was converted into a white-yellow gelatinous suspension and a solution of B-nor-5-androstene-3 β-ol-17-one **(1)** in 200 mL of anhydrous THF was dropped in under stirring. The reaction mixture was stirred at room temperature for 2.5—3 h, acetylene being bubbled through the solution. The mixture was then treated with an ammonium chloride solution (10%). The separated organic layer was washed with saturated sodium chloride solution to pH: 7 and distilled off. The naphthalene and its derivatives formed in the course of ethynylation were removed with petroleum ether and *n*-hexane. A quantity 29.4 (89%) of 17 α-ethynyl-derivative **2f** was obtained.

17α-Methyl/-ethyl-5,6-oxido-androstane-3β, 17β-diol 3β-acetate (3)

To a suspension containing 10 g/10 g (0.028/0.027 mol) of 17 α-methyl- / -ethyl-5-androstene-3 β, 17 β-diol 3 β-acetate **2'**, 2.4 g (0.029 mol) of sodium acetate and 60 mL of chloroform, 37.4 mL of peracetic acid (15%) were added dropwise at —5 — 0°C. The reaction was completed in 24 h at 5—10C°. The mixture was worked-up, washed with sodium hydrogen carbonate solution then with water. The evaporation of the dried chloroformic solution gave the crude mixture of 5α,6 α-and 5 β, 6β-epoxides **3**. Recrystallization from methanol afforded 9.3—9.5 (89—91%) of 17 α-methyl-5,6-oxido-derivative **3**, R': CH_3, m.p.: 157—159°C, $[\alpha]_D^{20}$: —78.5° resp. 9.4—9.7 g (90—93%) of 17α-ethyl-5,6-oxido-derivative **3** R': C_2H_5 m.p.: 148—154°C, $[\alpha]_D^{20}$: —60.5° (1% $CHCl_3$).

17α-Methyl/-ethyl-androstane-6-keto-3β, 5α, 17β-triol 3β-acetate (4)

To a solution of 9.5 g/9.7 g (0.026/0.025 mol) of **3** in 97 mL of acetone 7.2 g (0.072 mol) of chromic anhydride dissolved in 9.3 mL of water were added in such a way that the mixture was maintained under a slow reflux. The reaction was completed in 30 min. The mixture was diluted with 420 mL of cold water. The solid product was filtered, washed with water and recrystallized from methanol to give 8.5—8.7 g (86—88%) of 17 α-methyl-6-keto-derivative **4** R': CH_3 m.p.: 190—192°C, $[\alpha]^{20}$: 69.7° resp. 8.4—8.7 g (83—86%) of 17α-ethyl-6-keto-derivative **4** R : C_2H_5 m.p.: 266—270°C, $[\alpha]^{20}$: — 78° (1% $CHCl_3$).

17α-Methyl-/-ethyl-androstane-5-keto-5,6-seco-3β, 17β-diol-6-oic acid 3β-acetate (5)

To a solution of 8.7 g/8.7 g (0.023 mol) of **4** in 30 mL of chloroform 14.7 mL of peracetic acid (15%) were added under stirring and cooling in a water-bath. After working up (washing with water and evaporation of the dried chloroformic solution) a colourless oil was obtained. In the case of the 17α-methyl-derivative **5** R': CH_3 the crystallization of this oil failed, the

Table 3

The characteristic IR vibrations (cm^{-1}) of some 17α-substituted B-nor-derivatives

No. comp.	νOH	ν=CH_2 (allyl)	ν=C–H	skeletal	νC≡C	νC=C	ν CO	νC–O–C	ν≡C–H
2d	3600 3460	—	3020	2940 2862	—	1632	1722	1246	—
2g	3500 3300	—	3040	2940 2920 2170	2098	1615	1748	1290	3300
2f	3516 3428	—	3020	2983 2929 2850	2100	1633	—	—	3316
2c	3458 3241	—	3033	2960 2941 2916 2866	—	1641	—	—	—
2a	3441 3218	—	3025	2983 2940 2908 2858	—	1633	—	—	
2e	3441	3083	3033	2933 2915 2866	—	1650	—	—	—

Table 4

The ^1H-NMR (ppm) chemical shifts of some 17α-substituted B-nor-derivatives

No. comp.	$^{18}CH_3$	$^{19}CH_3$	CH_3CO	≡CH	≡CH	$^{20}CH_3$	$CH_2-^{21}CH_3$	^3CH	^{17}OH	^3OH
2g	0.83	0.90	1.95	5.48	2.54	—	—	4.58	3.41	—
2f	0.78	0.83	—	5.35	2.68	—	—	3.4	3.4	4.9
2d	0.88	0.88	1.98	5.33	—	—	0.96	4.56	—	—
2c	0.82	0.82	—	5.35	—	—	0.90	3.38	3.5	4.67
2b	0.85	0.90	2.06	5.40	—	1.22	—	4.64	—	—
2a	0.88	0.90	—	5.30	—	1.20	—	3.48	3.50	4.36

Table 5

The mass-spectral data of 17α-ethyl-B-nor-5-androstene-3 β,17β-diol(**2c**) and 17α-ethynyl-B-nor-5-androstene-3β, 17β-diol(**2f**)

No. comp.	Mass-spectra									
2c	m/e:	304	17	18	199	214	217	232		257	271
	%:	100	23.5	156	24	12.2	67	54		12	21.5
	m/e:	275	286	289							
	%:	7	8	8.5							
2f	m/e:	300	17	18	91	131	199	214	217	230	232
	%:	100	20	152.8	60	42.5	30	12.5	35	27.5	15
	m/e:	267	282	285							
	%:	55	26	40							

yield was 7.3—7.5 g, (81—83 %). In the case of the 17α-ethyl-derivative **5** R': C_2H_5 this crystallization was possible from acetone, resulting 6.7—6.9 g (75—77 %) of acid m.p.: 162—165°C, $[\alpha]_D^{20}$: +58.6° (1 % $CHCl_3$).

17α-Methyl- / -ethyl-B-nor-androstane-5α, 3β, 17β-triol-6β-carboxylic acid lactoane 3β-acetate (6)

7.5. g/6.9. g (0.019 mol) of acid **5** were dissolved in 16 mL of pyridine. To this solution 16.2 mL (0.139 mol) of benzoyl chloride were added and the mixture was allowed to stand at room temperature for 20 h. The mixture was poured into 500 mL of water, an oily substance separated which crystallized on standing and was filtered. The solid product was recrystallized from diethyl ether to give 2.6—2.8 g (37—40 %) of 17α-methyl-lactone **6** R': CH_3 m.p.: 146—150°C, $[\alpha]_D^{20}$ +25.3° resp. 4.4—4.5 g (68—70 %) of 17α-ethyl-lactone **6** R': C_2H_5 m.p.: 152—153°C, $[\alpha]_D^{20}$: 33.6° (1 % $CHCl_3$).

17α-Methyl- / -ethyl-B-nor-5-androstene-3β, 17β-diol 3β-acetate (2)

Lactone **6** (2.8 g/4.5 g; 0.007/0.011 mol) was pyrolized at 180°C for 30 min. The crude product recrystallized from methanol gave 1.9—2.1 g (80—85 %) of 17α-methyl-B-nor-derivative **2** R': CH_3 resp. 3.1—3.2 g (79—81 %) of 17α-ethyl-B-ondr-erivative **2**R': C_2H_5.

ACKNOWLEDGEMENTS. We express our thanks to Dr Gy. Horváth for ^1H-NMR and mass-spectra as well as for helpful discussions.

REFERENCES

[1] A. Bodor, R. Schwartz and D. Breazu, *Rev. Chim. (București)*, **27** 929 (1976).
[2] R. Schwartz and A. Juhász, *Rev. Roumaine Chim.*, **31**, 131 (1986).
[3] J. Joska, A. A. Achrem, J. Fajkos and F. Sorm, *Coll. Czech. Chem. Comm.*, **26**, 2050 (1961).
[4] E. Tóth M. Kovatsits and S. Gorog, *Ger. Patent*, 1, 668, 615 (1973), cf. *Chem. Abstr.*, **79**, 79059 (1973).
[5] J. F. Kerwin, *U.S. Patent*, 3, 072, 681 (1963), cf. *Chem. Abstr.*, **59**, 1723 (1963).
[6] J. Madar and M. Párdi, unpublished experiments.

Revue Roumaine de Chimie, **33**, *3*, 321–324 (1988)

CORRELATION OF REDUCTION POTENTIALS OF CYANINE DYES WITH THEIR ORBITAL ENERGIES

JAMIL AHMAD and K. BRIAN ASTIN
Chemistry Department, University College, P. O. Box 1082, Manama, Bahrain

Received July 19, 1986

Cyclic voltammograms have been obtained for a series of thiocyanine dyes. The observed one-electron reduction potentials correlate well with orbital energies calculated by the particle-in-a-box, simple Hückel and MNDO methods.

The class of cyanine dyes respresents an interesting series of substrates for experimental and theoretical study. Class members differ only in the numbers of conjugated double bonds, rendering them amenable to study by simple theoretical models. Theoretical results may be then correlated with experimental quantities such as ionisation energies measured by photoelectron spectroscopy (PES),[1] electron affinities obtained by electron transmission spectroscopy (ETS) [2] and electrochemically determined reduction potentials.[3]

In the present study we have carried out cyclic voltammetric experiments on a series of four thiacyanine dyes hereafter referred to as Dye(0)

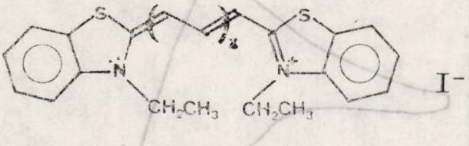

to Dye(3) corresponding to the value of x which is 0, 1, 2 or 3. The purpose of the study was to investigate the relationship between reduction potential and quantum mechanically calculated electron affinities, using the particle-in-a-box, simple Hückel molecular orbital and MNDO [4] methods. In the former two models electron affinities are equated with the energy of the lowest unoccupied molecular orbital (LUMO) in accord with Koopmans' theorem.[5] With SCF methods the correlation between the first virtual orbital energy and electron affinity is often poorly described [6] so our MNDO results are calculated as zeroth order ionization potential i.e. the ionization potential of the singly occupied molecular orbital (SOMO) of the reduced species producing electron affinities of a more realistic magnitude.

EXPERIMENTAL

The cyclic voltammograms were obtained using an approximately 10^{-4}M solution of each dye in propylene carbonate (PC) at 25°C, which had 1 M $LiClO_4$ as the background electrolyte using a Metrohm 506 Polaricord with 3 electrode system. The reference electrode was Ag/AgCl/LiCl(CH_3CN) (sat'd). The auxiliary electrode was made of a Pt wire, and a glassy carbon working electrode was used. The voltammogram was traced on an X–Y recorder. The dyes were obtained from K & K Labs, New York and used without further purification.

Nitrogen was bubbled through the solution for 10 minutes prior to recording the voltammogram to remove oxygen. The voltammogram was reversible in all the cases when PC was used as the solvent. With acetonitrile as the solvent, the return anodic peak disappeared suggesting that the radical formed on reduction had reacted with the solvent or with water that is inevitably present in it.

RESULTS AND DISCUSSION

The cathodic and anodic peak potentials (E_{pc} and E_{pa}) were read from the voltammogram and their average taken to get the value of the half wave potential, $E_{1/2}$. This half curve potential corresponds to the thermodynamic redox potential, E° if the diffusion coefficients of the oxidized and reduced form are taken to be equal.

Fig. 1 gives the voltammogram for dye(3) in PC. The traces for the other dyes are similar. The fact that it is a one-electron reduction was ascertained from the values of the peak potentials using the formula which holds under the Nernst condition [7]

$$E_p = (56.5/n)\ \text{mV},$$

where E_p is the difference in the anodic and cathodic peak potentials and n is the number of electrons.

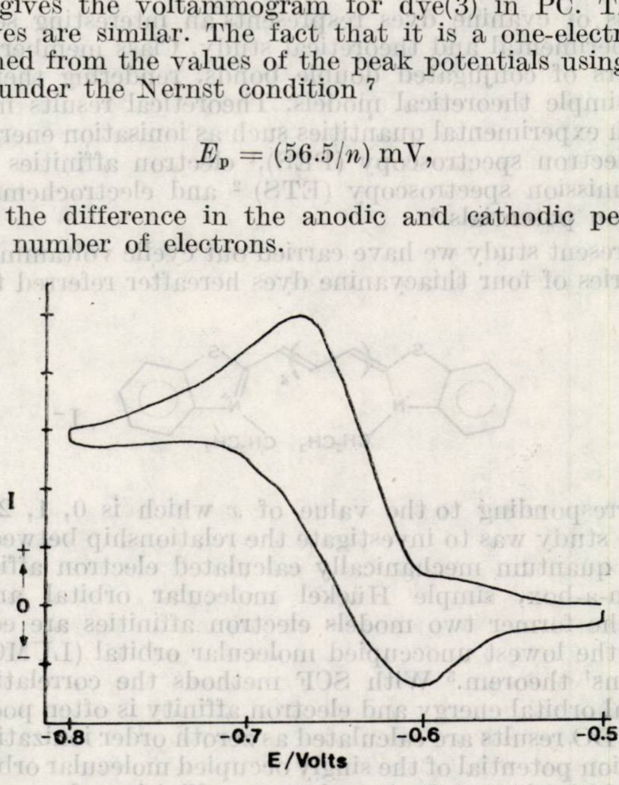

Fig. 1. — Cyclic voltammogram of Dye(3) in PC at 25°C. Background electrolyte is 1M $LiClO_4$. Scan rate 10 mV/s.

Table 1 summarizes the experimental $E_{1/2}$ values as well as the calculated values of the electron affinities using each of the approaches; the particle-in-a-box and the Hückel method reported by other workers[8] as well as the MNDO calculations done by us.

Table 1

Observed $E_{1/2}$ values and calculated energies

Dye	$E_{1/2}$V	E(Part-in-box)/eV[a]	E(Hückel)$-\alpha/\beta$[b]	E(MNDO)/eV[c]
x=0	−1.335	12.45	−0.609	−2.60
x=1	−0.974	9.93	−0.448	−3.05
x=2	−0.781	8.65	−0.353	−3.34
x=3	−0.637	7.88	−0.276	−3.54

[a] box length N−N distance + 1 bond length, ref. 8.

[b] ref 8.

[c] Energy of SOMO in reduced species calculated by the half-electron method within MNDO approximation, ref. 4.

The experimental results compare well with the polarographic values reported by Large.[9] However, the present study has established the reversibility and one electron nature of the reduction. The values reported for the particle-in-a-box method had an error in that the box length (L in the well known formula $E_n = n^2h^2/[8\ \mathrm{m}L^2]$) was not correctly taken. The correct length should have been (p + 2)l and not (p + 3)l, where p is the number of C atoms in the polyene chain and l is the average bond distance in the chain. The box is assumed to extend half a bond length beyond each nitrogen atom.

For the Hückel calculation the entire system was taken into account. Using the usual assumptions of the Hückel model, the secular matrix (which is 19 × 19 for Dye(0)) was set up and solved to get 19 energy states which were all nondegenerate. The 22 electrons in Dye(0) fill up 11 energy states, making E(12) the lowest unoccupied molecular orbital (LUMO). The value of LUMO is obtained in terms of α and β which are standard parameters for carbon.

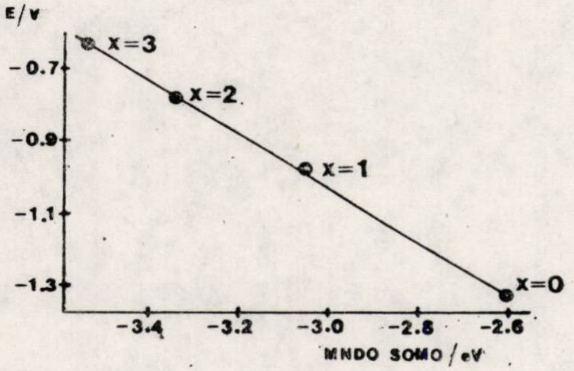

Fig. 2. — $E_{1/2}$/V against SOMO/eV for the series.

The MNDO calculations were carried out on the polyene fragment of the dye to calculate the energy of SOMO of the radical formed by the reduction of the cation, using the half-electron method.[10] All the bond lengths were optimised and the standard bond angles were assumed.

Excellent correlation is obtained between $E_{1/2}$ and the calculated energies by all methods. The linear least squares correlation coefficients are better than 0.998 for all the methods, see e.g. Fig. 2.

REFERENCES

[1] e.g. A. D. Baker, *Acc. Chem. Res.*, **3**, 17 (1970).
[2] e.g. K. D. Jordan and P. D Burrow, *Acc. Chem. Res.*, **11**, 341 (1978).
[3] e.g. G. J. Hoijtink, *Rec. Trav. Chim. Pays-Bas*, **74**, 1525 (1955).
[4] M. J. S. Dewar and W. Thiel, *J. Amer. Chem. Soc.*, **99**, 4899 (1977).
[5] T. Koopmans, *Physica*, **1**, 204 (1933).
[6] A. Szabo and N. S. Ostlund, "Modern Quantum Chemistry", Macmillan, 1982, 194.
[7] J. Heinze, *Angew. Chem. Int. Ed.*, **11**, 831 (1984).
[8] J. F. Farrell *J. Chem. Educ.*, **62**, 351 (1985).
[9] T. H. James ed., "The Theory of the Photographic Process", (4th ed.), Macmillan, New York, 1977, p. 203.
[10] M. J. S. Dewar, J. A. Hashmall and C. G. Verrier, *J. Amer. Chem. Soc.*, **90**, 1953 (1968).

Revue Roumaine de Chimie, **33**, *3*, 325–329 (1988)

THE POTENTIOMETRIC DETERMINATION OF MIXTURES OF ALKYLPHOSPHATES, ORTHOPHOSPHORIC AND HYDROCHLORIC ACIDS

M. SURPĂȚEANU, A. DUCA, G. SURPĂȚEANU and M. GĂBURICI
Department of Chemistry, Polytechnic Institute, Iași, Romania, 6600

Received December 29, 1986

A potentiometric determination of the mixture of mono- and dialkylphosphates, orthophsphoric acid and hydrochloric acid coupling the titration with natrium hydroxide solution in the presence and absence of $LaCl_3$ and the determination of Cl^- been developed.

The analytical control of organic phosphates in the process of their synthesis raises special problems.

The literature data show the possibility of determination of mono- and dialkylphosphates free or in the mixture by potentiometric measurements in the organic solvents,[1] by titration with the cation-active substances [2] or by various techniques.[3]

Previously it was reported the possibility of determination of mono- and dialkylphosphates in the presence of hydrochloric acid [4] or orthophosphoric acid.[5,6]

EXPERIMENTAL

Taking into consideration the necessity to characterize the obtaining products in the synthesis of trialkylphosphate from phosphoroxychloride and ethanol, in the present paper the analysis of the synthetic mixture containing mono- and dialkylpshosphates and orthophosphoric acid in the presence of hydrochloric acid has been realized. These compounds as by products in the synthesis of trialkylphosphates in phosphoroxychloride and alcohols may be formed[7]:

$$POCl_3+ROH=POCl_2OR+HCl \qquad (1)$$

$$POCl_2OR+ROH=POCl(OR)_2+HCl \qquad (2)$$

$$POCl(OR)_2+ROH=PO(OR)_3+HCl \qquad (3)$$

$$PO(OR)_3+HCl=RCl+PO(OR)_2OH \qquad (4)$$

$$PO(OR)_2OH+HCl=RCl+PO(OR)(OH)_2 \qquad (5)$$

$$PO(OR)(PH)_2+HCl=RCl+PO(OH)_3 \qquad (6)$$

Above, only a part of the reactions which take place in the reaction system oxychloride-alcohol has been announced.

In the presence of water, the involved reagents may be formed like mono- and dialkylphosphates. It is not exclusively the formation of polyphosphoric esters in the condensation reaction between phosphorhalogen compounds and alkyl-esters of orthophosphoric acid.

In order to realize the analytical control of this reaction mixture, the determination of mono- and dialkylphosphates in the presence of hydrochloric and phosphoric acids has been improved.

The characterization of tetracomponent mixture has been realized by coupling the potentiometric titration with aqueous natrium hydroxide solution and chloride determination using a selective electrode or silver nitrate titration.

Reagents

1) *Monoethylphosphate* (MEP), 1% solution in dimethylformamide. For the synthesis of monoethylphosphate, 28 g $(P_2O_5)_2$ were treated with 70 mL dry ethylic ether. Then 50 mL mixture of dry ethylic alcohol and dry ethylic ether 1:1 (v/v) were added gradually, by shaking, at low temperature.[8]

In the reaction between phosphoric anhydride and ethylic alcohol a mixture of mono- and diethylphosphates is always obtained.[9] Next it is necessary to isolate these compounds by column chromatography.

As stationary phase and as eluent the powder silicagel and dry acetone respectively were used.

The control of the separation by potentiometric titration with aqueous natrium hydroxide solution was realized.

The pure monoethylphosphate was characterized by phosphorus elemental analysis.

2) *Dimethylphosphate* (DMP), 1% aqueous solution.

Dimethylphosphate (natrium salt) was obtained after Benton's method[10] by warming at elbing way of the mixture formed from: 18.6 g trimethylphosphate, 20 g natrium iodide and 100 mL acetone. From the homogeneous reaction mixture, after about 15 minutes dimethylphosphate (natrium salt) is separated as white, bright thin plates. The precipitate was filtered and washed with acetone until complete removal of iodide ions. Then the washed precipitate was dried at 160°C up to constant weight.

The free dimethylphosphate was obtained by ionic exchange on Dowex 50 W× 4, H^+ form.

3) Hydrochloric and phosphoric acids as standard aqueous solutions were used.

Procedure

The synthetic mixtures were obtained mixing the four components in different ratios.

First, hydrochloric acid with selective chloride electrode was determined using the standard curve. Then, the solution with aqueous natrium hydroxyde was titrated (Fig. 1).

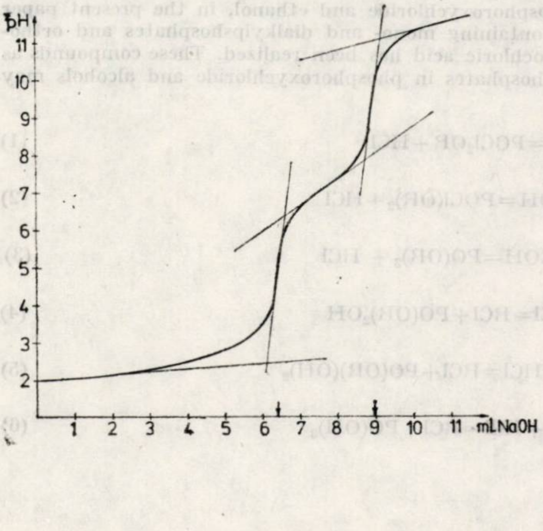

Fig. 1. — The titration curve of tetracomponent mixture with natrium hydroxide.

The obtained data for hydrochloric acid determination using a selective chloride electrode were proved with the Volhard method (it is necessary to remove the AgCl precipitate).

In a similar mixture, an aqueous solution of $LaCl_3$ 2% is added for the total precipitation of phosphoric acid.

Next, the potentiometric titration with aqueous natrium hydroxide was realized (Fig. 2).

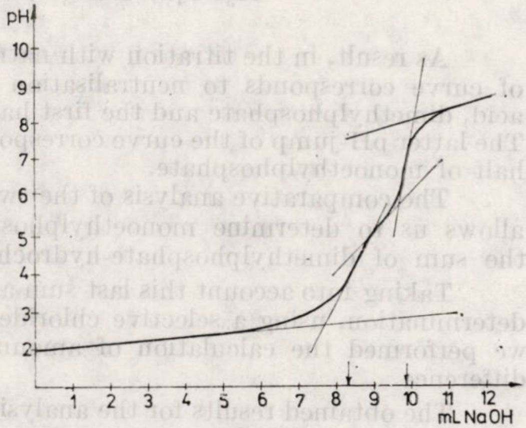

Fig. 2. — The titration curve of tetracomponent mixture with natrium hydroxide in the presence of lanthanum chloride.

The pH measurements were made with pH-meter PYE model 78.

The experiments were carried out using a glass indicator electrode and as reference, a saturated calomel electrode.

RESULTS AND DISCUSSION

Taking into account the literature data on the chemical properties of mono- and di-phosphoric esters as di- and mono-acids respectively,[1,4,5] the synthetic mixture behaviour of monoethyl- and dimethylphosphates, hydrochloric and phosphoric acids have been studied. As investigation method, the potentiometric titration with aqueous natrium hydroxide solution of the above four components system in the presence or absence of $LaCl_3$ has been used.

In this case up to the first equivalence point (Fig. 1) the following reactions occur :

$$HCl + NaOH = NaCl + H_2O \qquad (7)$$

$$H_3PO_4 + NaOH = NaH_2PO_4 + H_2O \qquad (8)$$

$$PO(OCH_3)_2OH + NaOH = PO(OCH_3)_2ONa + H_2O \qquad (9)$$

$$PO(OC_2H_5)(OH)_2 + NaOH = PO(OC_2H_5)(OH)ONa + H_2O \qquad (10)$$

Up to the second equivalence point, the next two reactions occur :

$$NaH_2PO_4 + NaOH = Na_2HPO_4 + H_2O \qquad (11)$$

$$PO(OC_2H_5)(OH)ONa + NaOH = PO(OC_2H_5)(ONa)_2 + H_2O \qquad (12)$$

The addition of lanthanum chloride in the second sample of the mixture determines the precipitation of lanthanum phosphate and the formation of an equivalent quantity of hydrochloric acid :

$$H_3PO_4 + LaCl_3 = LaPO_4 + 3HCl \tag{13}$$

As result, in the titration with natrium hydroxide, the first pH-jump of curve corresponds to neutralisation of hydrochloric acid, phosphoric acid, dimethylphosphate and the first half of monoethylphosphate (Fig. 2). The latter pH-jump of the curve corresponds to neutralisation of the second half of monoethylphosphate.

The comparative analysis of the two titration curves in Figs 1 and 2 allows us to determine monoethylphosphate, orthophosphoric acid and the sum of dimethylphosphate-hydrochloric acid.

Taking into account this last sum and the previous hydrochloric acid determination, using a selective chloride electrode or by Volhard method we performed the calculation of amount of dimethylphosphate as their difference.

The obtained results for the analysis of three pairs of parallel samples are presented in Table 1.

Table 1

The results of analysis of tetracomponent system

Compound	Added (mg)	Found (mg)	Relative standard deviation (%)
H_3PO_4	10.48	10.76	2.67
	10.22	10.46	2.35
	20.95	21.11	0.76
HCl	10.94	10.68	2.56
	10.10	10.32	2.18
	13.47	13.72	1.82
MEP	23.73	24.29	2.36
	20.16	19.69	2.33
	18.61	18.92	1.67
DMP	28.39	29.12	2.57
	21.40	20.94	2.15
	14.27	13.95	2.24

CONCLUSIONS

1. The potentiometric determination of the mixture of mono- and dialkylphosphates, orthophosphoric acid and hydrochloric acid by titration with natrium hydroxide solution of two parallel samples in the presence and absence of $LaCl_3$ coupling with the determination of Cl^- may represent a good analytical method. This procedure could be used with the best results in the characterization of all the products obtained in the

synthesis of organic phosphoric esters from phosphoroxychloride and alcohols.

2. The presence of trialkylphosphates in the synthetic mixture keeps unchanged the aspect of the titration curve. Thus, it is possible the determination of trialkylphosphates in a pentacomponent mixture by difference.

3. The purity of trialkylphosphates obtained in the reaction between phosphoroxychloride and alcohols may be controlled by polarographic method.

4. The absence of the second pH-jump in the titration curve (Fig. 2) indicates the absence of the monoalkylphosphate in the mixture.

5. The determinations may be realized with pretreated platinum electrode instead of the glass indicator electrode.

6. The potentiometric study of the individual component sample points out that the esterification takes place in inverse orders of pK_α.

7. For the water insoluble phosphoric esters, a suitable solvent is indicated and the titration of the mixture must be performed with alcoholic kalium hydroxide.

REFERENCES

V. V. Rublev, and Yu. A. Bulatova, *Zhur. analit. Khim.*, **24**, 1106 (1969).

[2] L. Daradics, *Rev. chim.*, (București), **25**, 60 (1974).

[3] V. V. Rublev, *Zhur. analit. Khim.*, **35**, 1008, (1980).

[4] V. P. Komissarenko, L. A. Molot A. G. Yarnykh and Yu. G. Titarenko *Zhur. analit. Khim.* **30**, 29 (1975).

[5] D. P. Stognushko, V. N. Ivanov, G. A. Tember, B. E. Chistyakov, G. C. Balakhonov, D. D. Schchetimina and Yu. I. Usatenko, *Zhur. analit. Khim.*, **33**, 142 (1978).

[6] H. Frind and R. Hensel, *Fres. Z. Anal. Chem.*, **307**, 283 (1981).

[7] D. Purdelea and R. Vilceanu, "Chimia compușilor organici ai fosforului și ai acizilor lui", Ed. Academiei, Bucharest, 1965.

[8] Houben Weyl, "Organische Phosphor verbindungen", Akademie Verlag, 219, 1964.

[9] V. Balasubramaniyan, V. G. Bhatia and S. B. Wagh, *Tetrahedron*, **39**, 1475 (1983).

[10] C. A. Bunton, M. M. Mhola, K. G. Oldham and C. A. Vernon, *J. Chem. Soc.*, **8**, 3293 (1960).

Revue Roumaine de Chimie, **33**, *3*, 331 – 345 (1988)

PREDICTING FLUID PHASE EQUILIBRIA BY A MODEL OF EQUILIBRIUM OF INTERACTIONS IN RESTRAINED MOLECULAR SYSTEMS

FRANCISC A. GOTHARD
Institute for Research, Design and Development for Oil Refineries (ICITPR) Blvd. Republicii 291, Ploiești 2000, Romania

Received September 25, 1986

The principles considered in the new approach leading to the model of the equilibrium of interactions in restrained molecular systems in the theory of nonelectrolyte solutions as well as the correlations derived therefrom are reviewed. The comparisons of the performances in correlating and predicting liquid-vapor and liquid-liquid equilibrium data in binary and ternary mixtures by use of the new model and equations given by Wilson, respectively by Renon and Prausnitz are summarized starting from an extended versions of the reference data sets recommended by CODATA TASK GROUP.

One of the most attractive areas of fundamental research in the field of chemical thermodynamics is the predicting liquid-vapor and liquid-liquid equilibria by models for nonelectrolyte solutions.

Since 1964 when Wilson introduced the local concentration concept[1] in the model of polymeric solutions given by Flory and Prausnitz[2] as well as by Huggins [3] and published his famous equation for Gibbs excess energy,

$$g^e/RT = 1 - \ln\Big(\sum_j x_j \Lambda_{ij}\Big) - \sum_k \frac{x_k \Lambda_{ki}}{\sum_j x_j \Lambda_{kj}} \tag{1}$$

including temperature dependent parameters

$$\Lambda_{ij} = \frac{v_j}{v_i} \cdot \exp\left(-\frac{\lambda_{ij} - \lambda_{ii}}{RT}\right) \tag{2}$$

the idea has been further promoted by the Berkeley school (led by J. M. Prausnitz) where several other correlations based on the local concentration concept have been developed. By including consequences of the two-liquid theory of Scott,[4] Renon and Prausnitz obtained the well-known NRTL (*N*on *R*andom *T*wo *L*iquid) model [5] to give

$$g^e/RT = \sum_i x_j \frac{\sum_j r_{ji} G_{ji} x_j}{\sum_j G_{ki} x_k} \tag{3}$$

where

$$G_{ji} = \exp(-a_{ij} \cdot r_{ji}),\ r_{ji} = (g_{ji} - g_{jj})/RT \tag{4}$$

which is suitable for predicting also liquid-liquid equilibrium data.

Outstanding results were obtained in the theories based on the local concentration concept, when combinatorial and intermolecular interaction ("residual") contributions to the activity coefficients were separated by Abrams and Prausnitz,[6] to obtain the UNIQUAC equation (1975) :

$$g^e/RT = (g^e/RT)_\rho + (g^e/RT)_r =$$

$$= \sum_k x_k \cdot \ln \frac{\Phi_k}{x_k} + \frac{z}{2} q_k x_k - \ln \frac{\theta_k}{\Phi_k} - \sum_k q_k x_k \cdot \ln(\sum_k \theta_j r_{jk}) \tag{5}$$

where

$$r_{ji} = \exp(-(u_{ij} - u_{ii})/RT) \tag{6}$$

$$l_i = \frac{z}{2}(r_j - q_j) - (r_j - 1)\,;\ z = 10 \tag{7}$$

$$\theta_i = \frac{q_i x_i}{\sum_j q_j x_j}\,;\ \Phi_i = \frac{r_i x_i}{\sum_j r_j x_j} \tag{8}$$

The separation of combinatorial and residual contributions, including shape and size effects in this model, allowed Fredenslund and coworkers to develop the group-contribution form of this model, well known and widely used as the UNIFAC method for predicting liquid-vapor, liquid-liquid equilibrium and solubility data.[7]

The excellent results obtained in the correlation of large experimental data sets[8] and in predicting multicomponent data by use of the above equations, encouraged various attempts to obtain improved correlations in this field, but especially to overcome some very unbearable drawbacks, inherent in all equations belonging to this family : impossibility of predicting simultaneously liquid-vapor and liquid-liquid equilibria as well as excess enthalpy by a unique set of binary parameters. Various modifications of the equations have been published and analysed in this order in some hundreds of papers in the last 20 years.

It should be considered again the merit of Prausnitz, who pointed out recently (I heard it from him at the Kühlungsborn meeting on thermodynamics in 1985[9]) that there are no means to overcome the limits of the local concentration concept, so he recommended us : "it is time to forget Wilson, N.R.T.L., UNIQUAC and other equations derived from the local concentration concept; don't waste time for improving their performances, but spend more attention to new approaches, use new ideas required for further progress in the field".

Indeed, perhaps as a consequence of the successful treatment of various problems in chemical thermodynamics starting from the statistical mechanical approach, all thinking in this field was governed almost only by the ideas of the Guggenheim school. Here interactions between the molecules of the pure component and between unlike molecules appear in the parameters of the models derived and this viewpoint is still preserved in the models based on the local concentration concept, although it is internally inconsistent with selection of the interaction energy differences as adjustable parameters. This may be in the background of the limitations of the wellknown equations especially of the limitations pointed out in the excellent analysis given by Kemény.[10]

Examining in some historical perspective how new ideas emerge to solve basic problems of science, we found that the key uses to be in some answer of Nature to a question, in its own language, provided we are able to understand the answer... Nature's language is made up by the most general laws governing the field in question. One of the laws governing all what happens in mixtures, up to chemical reactions, is, no doubt, the mass action law. This was earlier considered by Dolezalek as successful for predicting liquid-vapor equilibria in various mixtures at low temperatures.[11] The positive answer of Nature was understood even more clearly by Becker, Kiefer, Rhensius and Spörner many years later.[12,13] According to the results obtained it seems that it was not consequently followed taking into account all consequences : this leads too far from the recognized procedures of the art, as we shall see.

To be consistent with the mass action law one should recognize that analytical concentrations cannot be used as such, merely some powers of concentrations should be considered as extensive variables in the phenomenological treatment of the equilibrium of interactions, the exponents being numbers of equivalents effective for exhibiting the excess property we are interested in. These equivalents may be different for various excess properties, a concept which allows the use of various values of the same parameter in predicting various properties, without inconsistency with the basic thermodynamic correlations, provided there are sound correlations between the parameters involved. So ask Nature, how many terms (of interacting bodies) n_i should be considered in the phenomenological treatment of equilibrium by the wellknown correlation used in the form $I = x_i^{n_i} \cdot I_i$ to give at equilibrium ($\mathrm{d}I = 0$)

$$\sum_i x_i^{n_i} \cdot \mathrm{d}I_i = 0 \tag{9}$$

where I may be an intensive variable of the process e.g. interaction energy differences if one analyses the consequences of equation (9) in the framework of any wellknown model and results of the reduction of experimental data.

Never have I been more surprised than when discovering that the numbers n are related to the Gibbs excess energy for equimolar mixtures by the very simple correlation[14]

$$n = 2 \,.\, (A \,.\, \exp(g^e/RT)^B) \tag{10}$$

with $A = 4$, for several hundreds of binary data sets. In the framework of a model where n are the numbers of molecules whose interactions are effective for exhibiting the deviation from ideal behaviour g^e/RT, in ideal solutions ($g^e/RT = 0$) that is also in pure components, $n = 2$, one equivalent interaction working between pairs of molecules may be considered in the treatment of nonideal mixtures (one interaction, equivalent with one which is working between unlike molecules in nonideal solutions to give $g^e/RT \neq 0$). If so, to give a "Stoichiometric mixture" in analogy with stoichiometric reaction product, involving equal amounts of equivalents of components A and B, as the amount A—B of "reaction product" appears where the mixture exhibits the largest deviation from ideal behaviour), the identical amounts of interactions A—A and B—B pairs must vanish:

$$\frac{1}{2}(\mathrm{A{-}A}) + \frac{1}{2}(\mathrm{B{-}B}) = (\mathrm{A{-}B}) \tag{11}$$

By taking into account what Arrhenius obtained for chemical reactions, and replacing $(\mathrm{A{-}A}) = (\mathrm{B{-}B}) = N$, the mass action law leads to

$$\frac{N^{\frac{1}{2}} \cdot N^{\frac{1}{2}}}{(\mathrm{A} - \mathrm{B})} = K = \exp(g/RT) \tag{12}$$

Repeating the ways for giving an ideal solution and logarithmation one obtains

$$\ln N - \ln(\mathrm{A{-}B}) = g/RT \tag{13}$$

$$\ln 1 - 1\beta(\mathrm{A{-}B}) = g^*/RT \tag{14}$$

By subtracting, one obtains

$$g^e/RT = \ln N$$

For N in a first approach the number of combination pairs between n bodies should be considered, consequently, $N = n(n-1)/2$, and taking into account the value of the preexponential term of equation (10) one obtains:

$$g^e/RT = \frac{1}{4} \cdot \ln \frac{n(n-1)}{2} \tag{15}$$

For obtaining correlations between n and the concentrations of the components, the concentrations of the equivalent interactions N_i around each molecule of the mixture must be balanced.

If N_i equivalent interactions are around each molecule (i) at analytical concentration x_i, the numbers of equivalent interactions around the molecules (i) in one mole of mixture are $N_i x_i$ and those effective for the excess property $(N_i - 1)x_i$ because one should be considered for existing in the pure component. When n_{ji} molecules (j) are interacting in the surrounding of one molecule (i), in one mole of binary mixture there are $x_j \cdot n_{ji}$ interactions equivalent to $(N_i - 1)x_i$, thus

$$(N_i - 1) \cdot x_i = n_{ji} \cdot x_j \tag{16}$$

In the multicomponent mixture similar terms to the right hand side of equation (16) should be added, to give

$$(N_i - 1) \cdot x_i = \sum_{j=1}^{N} n_{ji} \cdot x_j \tag{17}$$

One interaction belongs to two of the n interacting molecules working each between one of the molecules (i) and (j), consequently

$$\frac{2}{n} = \frac{1}{N_i} + \frac{1}{N_j} \tag{18}$$

(the $1/N_i$-th part of the equivalent interactions around the molecule (i) is engaged in one related to the $1/n$-th part of interactions between n nearest interacting molecules). In the N component mixture, equation (18) was extended to give

$$\frac{2}{n} = \sum_{i=1}^{N} \frac{1}{N_i} \tag{19}$$

By expressing N_i from equation (16) for a binary mixture and replacing it in equation (18) one obtains

$$\frac{2}{n} = \frac{x_1}{x_1 + n_{12}x_2} + \frac{x_2}{x_2 + n_{21}x_1} \tag{20}$$

which, together with equation (15), gives the analytical form of the model for Gibbs excess energy.

Similarly, in multicomponent systems

$$\frac{2}{n} = \sum_{i=1}^{N} \frac{x_i}{\sum\limits_{j=1}^{N} n_{ij}x_j} \tag{21}$$

Using the correlation given by van Ness,[12] one obtains for activity coefficients in multicomponent systems

$$\ln \gamma_i = \frac{1}{4} \cdot \ln \frac{n(n-1)}{2} - \frac{n(2n-1)}{8(n-1)} \left\{ \frac{1}{\sum\limits_{k=1}^{N} n_{ik}x_k} - \sum_{j=1}^{N} \frac{n_{ji}x_j}{\left(\sum\limits_{k=1}^{N} n_{jk}x_k\right)^2} - \left[\sum_{k=1}^{N} \frac{x_k}{\sum\limits_{j=1}^{N} n_{kj}x_j} - \sum_{k=1}^{N} \frac{n_{jk}xx_k}{\left(\sum\limits_{k=1}^{N} n_{jk}x_k\right)^2} \right] \right\} \tag{22}$$

The parameters of this equation depend on temperature according to [16]:

$$n_{ij} = n^0_{ij}\cdot\exp\left(1 - \frac{T}{T^*_{ij}}\right)^{E_{ij}} \tag{23}$$

where $T^*_{ij} = T^s_c$ is the temperature of critical miscibility, n^0_{ij} and E_{ij} two adjustable parameters for correlation of mutual solubility data in binary systems. By correlating liquid-vapor equilibrium data $E_{ij} = 1$, two adjustable parameters remain in equation (23), for each component, that is four for a binary, n^0_{ij} and T^*_{ij}. Liquid-vapor equilibria may be predicted by use of the parameters obtained by reduction of liquid-liquid equilibrium data, taking into account that $n^{0LL}_{ij} = n^{0LV}_{ij} - 1$ and vice-versa; this fact may be considered for predicting liquid-liquid equilibrium data for systems with miscibility gap, when the parameters from reduction of the liquid-vapor equilibrium data are available. In the reduction of isothermal data and even isobaric data where the boiling points are inside a range up to 30 K, the temperature dependence of the parameters may be neglected. In this case the model requires two adjustable parameters for a binary.

For excess enthalpy in binary mixtures, the Gibbs-Helmholtz equation leads according to this model to

$$h^e = \frac{x_1x_2RT^2(2n-1)n}{8(n-1)}\left[\frac{n_{12}}{(x_1 + n_{12}x_2)^2T^*_{12}} + \frac{n_{21}}{(x_2 + n_{21}x_1)^2T^*_{21}}\right] \tag{24}$$

The correlating and predicting performances of the equations derived from the new model were analysed comparatively with the equations given by Wilson [1] using liquid-vapor equilibrium data on systems without miscibility gap, as well as with the equation given by Renon and Prausnitz [5] including systems with miscibility gap.

For 126 of the 155 binary liquid-vapor equilibrium data sets considered in a first analysis [17] smaller deviations of the dimensionless Gibbs excess energy were obtained using the new model, even neglecting the temperature dependence of the parameters, as by use of the Wilson equation. In the remaining cases the deviations were smaller for the Wilson model, but the difference between the two models was statistically without significance according to the Fischer test. In 43 cases (data sets) analysed, the improvement by the new model was significant. For systems with miscibility gap also better results were obtained by the new model than using the Renon-Prausnitz equation. In this paper the data reductions were performed by minimizing the sum of squares of the deviations of the dimensionless Gibbs excess energy.

Analysing the predicting performances of the new model comparatively with the equation given by Wilson [1] on 6 ternary systems, in 4 cases smaller deviations were obtained by use of the new correlation, therefrom in 3 cases the deviations were significantly smaller than when using the Wilson equation.

The analysis of the predicting performances of the new model was extended to the 52 binary reference data sets recommended by CODATA TASK GROUP in 1984 for critical evaluation of models for nonelectrolyte solutions. The reduction of the data to the parameters of the models compared was performed by the maximum likelihood method in the form given by Panaitescu.[18] Presented at the First CODATA Symposium on Critical Evaluation and Prediction of Phase Equilibria in Multicomponent Systems in Zaborów, Poland,[19] the results show that in 35 cases the new model leads to smaller deviations than the equations given by Wilson [1] and by Renon and Prausnitz [5] and in most cases the improvement obtained by use of the new correlation was significant according to the Fischer test. The reference data on mutual solubility for hexane and methanol as well as for cyclohexane and methanol were correlated by the use of the new model with smaller deviations than possible even with the best of the correlations known up to 1983 and given by Stryjek,[22] where a larger number of parameters are required. The parameters n_{ij} obtained in the reduction of the reference mutual solubility data and of the liquid-vapor equilibrium data recommended are presented in figure 1 in the range of temperatures where the data were available. A very good agreement with the data predicted by equations (15),[20] with parameters [23] and the rule $n_{ij}^{0LL} = n_{ij}^{0LV} - 1$ may be observed.

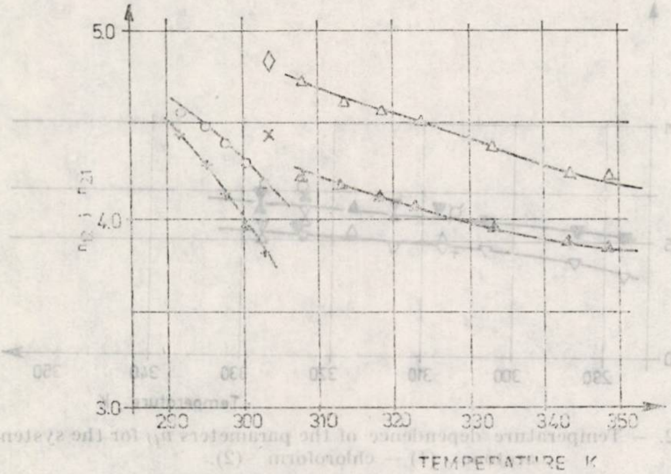

Fig. 1. — The temperature dependence of the parameters n_{ij} for the system hexane-methanol.

Legend:	n_{12}	n_{21}
From mutual solubilities given by Schmidt et al (1969);	+	O
From liquid-vapor equilibrium data given by Wolff and Höppel (1968);	▲	△
by Goral et al. (1983)	×	◇

No significant differences between predicting ternary data recommended as reference for the systems acetone — chloroform — methanol and cyclohexane — hexane — methanol were observed using the three models compared. Similar results were reported by predicting excess enthalpies, but the large differences between the recommended experimental data and the values predicted using the Gibbs-Helmholtz equation do not allow at this point relevant conclusions.

Figure 2 also gives the parameters n_{ij} obtained by reduction of the recommended reference data for the system acetone-chloroform *vs.* temperature.[19] In Table 1 the constants in eq. (23) of the parameters n_{ij} obtained from the reliable data sets of mutual solubility of hexane and methanol, and cyclohexane and methanol are given and the r.m.s. deviations of the mutual solubility data from the predicted values are compared with those obtained by the use of the correlation given by Stryjek.[22] The constants in equation (23) and r.m.s. deviations are included also for the cyclohexane — methanol and acetone — chloroform reference data.[19] As it was shown in table 1, always only the author of the considered experimental data is mentioned, the full literature references being in the cited papers.

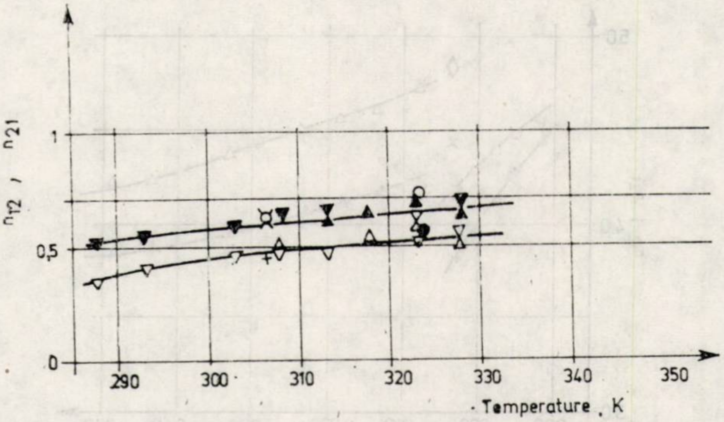

Fig. 2. — Temperature dependence of the parameters n_{ij} for the system acetone (1) — chloroform (2).

Legend: From liquid-vapor equilibrium data n_{12} n_{21}
given by Röck and Schröder (1957); Zawidski ▽ ▲
(1900); Reiders, DeMinjer (1947); Kudryavtseva and × ○
Susarev (1963). ● ○
△ ▲

The results of the comparisons of various models on a revised and extended reference data set proposed to the Kühlungsborn WAT * Seminar on Thermodynamics in April 1985,[20] were presented to the Second CODATA Symposium on Critical Evaluation and Prediction of Phase Equilibria in Multicomponent Systems held in Paris, September 1985.[16] Additional liquid vapor and also ternary liquid-liquid equilibrium data were included, for the mixtures acetonitrile — ethanol — water, ethanol — benzene — water and methyl-ethyl-ketone — heptane — toluene. Some of the results, very similar to those reported on the original CODATA reference systems, obtained on the additional reference data, are repro-

---

* Working Association for Thermodynamics

Table 1

The results of the reduction to temperature dependent parameters (23) in equations (15,20) of mutual solubility and liquid-vapor equilibrium data recommended in broad temperature range by the CODATA TASK GROUP

System	Experimental data for	Given by	n_{12}	n_{21}	E_{12}	E_{21}	T_{12}^* K	T_{21}^* K	R.m.s. deviations x_1 eq (23),	Stryjek
Hexane (1)	Mutual solubility	Sovini et al. (1965)	3.7225	3.3106	0.5031	0.4701	$306.88 = T_c^s$		0.038	
Methanol (2)		Schmidt et al. (1969)	3.6077	3.4364	0.4850	0.4938	$306.67 = T_c^s$		0.043	
	Total pressure	Wolff, Hoppel (1968)	4.723	4.31	1.0	1.0	306.86	306.85		
Cyclohexane (1)	Mutual solubility	Jones, Amstell (1930)	3.474	3.444	0.4672	0.3739	$318.75 = T_c^s$		0.020	0.02
Methanol (2)		Eekfeldt (1943)	3.273	3.756	0.5009	0.5487	$318.38 = T_c^s$		0.034	0.005
	Total pressure	Marinicev, Susarev (1965)	4.47	4.445	1.0	1.0	318.29	346.29		*
Acetone (1) Chloroform (2)	Liquid-vapor equilibria	Röck, Schröder, (1957)	0.0104	0.0088	1.0	1.0	96.2	359.0		

* By use of the equation given by Stryjek[22] one obtains also deviations of 1.2 respectively 0.31 K in temperature in the two data sets.

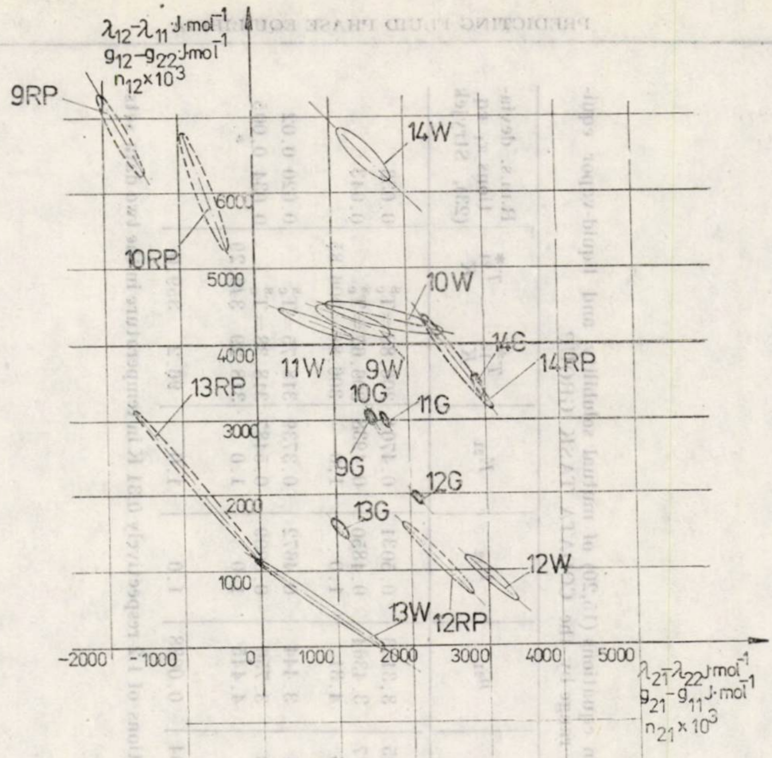

$\lambda_{12}-\lambda_{11}$ J·mol^{-1}
$g_{12}-g_{22}$ J·mol^{-1}
$n_{12}\times10^3$
9RP
10RP
14W
10W
14G
14RP
11W
9W
10G
11G
13RP
9G
12G
13G
12W
13W
12RP
6000
5000
4000
3000
2000
1000
-2000
-1000
0
1000
2000
3000
4000
5000
$\lambda_{21}-\lambda_{22}$ J·mol^{-1}
$g_{21}-g_{11}$ J·mol^{-1}
$n_{21}\times10^3$

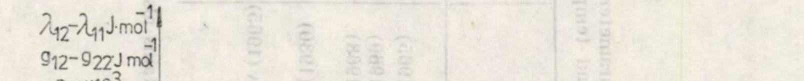

$\lambda_{12}-\lambda_{11}$ J·mol^{-1}
$g_{12}-g_{22}$ J mol^{-1}
$n_{12}\times10^3$
6000
5000
4000
3000
2000
1000
-1000
6RP
4RP
3RP
5RP
6G
8G
7RP
4G
7G
3G
5G
1G
15RP
2RP
15G
2G
15W
2W
1W
7W
5W
4W
8W
6W
3W
0
1000
2000
3000
5000
6000
7000
$\lambda_{21}-\lambda_{22}$ J·mol^{-1}
$g_{21}-g_{11}$ J·mol^{-1}
$n_{21}\times10^3$

duced in figure 3. The confidence ellipses represented in this figure, related to the significance level 0.05, are the smallest for the new model in a reference scale where the areas may be compared (about 500 J $\cdot$mole^{-1} for one unit in n_{ij}) and also the ratios of the semiaxes of the parameters of the new model are the smallest, because the parameters of the Wilson and NRTL equations are more correlated (more information may be included in the parameters of the new model).

A summary of the results of comparisons made on all selected reference liquid vapor binary data is reproduced [19] in table 2. For comparing the performances of the three models in predicting ternary liquid—vapor equilibrium data, the parameter pairs inside the confidence ellipses were selected, which leads to the smallest deviations of total pressure in the case of isothermal data, respectively of the dimensionless Gibbs excess energy in the case of isobaric experimental data. The results of this analysis are given in table 3.

The performances in predicting ternary liquid—liquid equilibrium data for the ethanol — benzene — water system of the Renon — Prausnitz equation [5] and of the new model are compared in table 4, on several experimental data sets. In all cases, the new model leads to significant improvement of the correlation, according to the Fischer test.

Comparative analysis of the equation given by Wilson [1] and of the new model in two-parameter form was published by Suărăşanu et

---

Fig. 3. — The confidence ellipses of the parameters in the equations given by Wilson (1964), Renon and Prausnitz (1968) respectively by Gothard (1981) to the significance level 0.05, as obtained on the additional reference data sets.

Legend:

No	System	References	Conditions
1.	Acetonitrile-ethanol	S. R. Wilson et al. (1979)	323.15 K
2.	Methylethylketone-toluene	H. H. Steinhauser, R. H. White (1949)	101.3 kPa
3.	Ethanol-benzene	S.R. M. Ellis, M. B. Clark, (1961)	92.07 kPa
4.	Ethanol-benzene	V. V. Udovenko, L. G. Fatkulina (1952)	333.15 K
5.	Ethanol-benzene	A. C. Jimenez, L. G. Zurbano (1967)	93.2 kPa
6.	Ethanol-benzene	V. V. Udovenko, L. G. Fatkulina (1952)	313.15 K
7.	Ethanol-benzene	S. R. M. Ellis, J. M. Thwaites (1955)	101.325 kPa
8.	Ethanol-benzene	V. V. Udovenko, L. G. Fatkulina (1952)	323.15 K
9.	Ethanol-water	H. Otsuki, F. C. Williams (1953)	101.32 kPa
10.	Ethanol-water	J. M. Willock, M. van Winkle (1975)	101.32 kPa
11.	Ethanol-water	S. R. Wilson et al. (1979)	323.15 K
12.	Methylethylketone-heptane	H. H. Steinhauser, R.R. White (1849)	101.32 kPa
13.	Heptane-toluene	H. Katayama, I. Watanabe	53.3 kPa
14.	Acetonitrile-water	D. F. Othmer, S. Josefowitz (1947)	101.32 kPa
15.	Heptane-toluene	H. H. Steinhauser, R. H. White (1949)	101.32 kPa

Table 2

The numbers of the best results obtained for various models in the reduction of the binary liquid-vapor equilibrium data from the revised and extended reference data set[20]

Correlation procedure	Criteria of comparison	The models compared		
		Wilson	Renon-Prausnitz	Gothard
Maximum likelihood	ρ	14	14	45
	R.m.s. deviation of g^e/RT	30	15	28
Minimization of $\Sigma(g^e/RT)_{\exp} - (g^e/RT)_{(\text{pred})})^2$		20	16	37

Table 3

The performances in predicting the ternary liquid-vapor reference equilibrium data by use of the best* binary parameters

Ternary system	References	*T* or *P*	Deviation compared	The models compared		
				Wilson	Renon-Prausnitz	Gothard
Ethanol Benzene Water	Morachevski Belousov (1958)	308.15 K 318.15 K 337.15 K	Total pressure %		8−12 5−14 9−23	5−10 5− 8 6−12
Methylethylketone Heptane Toluene	Steinhauser White (1949)	101.3 kPa	R.m.s. of g^e/RT	0.04	0.05	0.02
Acetone Chloroform Methanol	Tochigi & al. (1984)	101.3 kPa	R.m.s. of g^e/RT	0.007	0.01	0.03
Acetonitrile Ethanol Water	Wilson & al. (1979)	323.15 K	Total pressure %	3−6	5−15	2−7

* obtained by selection of parameter pairs inside the confidence ellipses given in figure 2 to obtain the smallest deviations.

al.[21] using the maximum likelihood method in the form recommended by Panaitescu.[18] For more than 3/4 of the 162 experimental data sets consideres in this case, smaller deviations were obtained by use of the new model and therefrom in about 1/4 the correlation was significantly improved by use of the new model in the data reduction.

Similar results were reported [24] by correlating all available liquid—vapor equilibrium data [25] for the system butanol — butyl acetate. In this case the temperature dependence of the Gibbs excess energy computed

Table 4

The results of the correlation of the selected liquid-liquid equilibrium data for the system ethanol(1)-benzene(2)-water(3)

Reference	Washburn (1931) Morachevski, Belousov (1958)					
Model	Temperature, K		298.15	308.15	318.15	328.15	337.15
Renon-Prausnitz (1968)	Parameters	r_{12}	1.2743	1.2961	1.4645	1.5018	0.7715
		r_{13}	5.6996	2.2144	1.7316	6.3934	1.9728
		r_{21}	5.4983	2.9194	2.4515	0.6872	1.9912
		r_{23}	1.3547	1.5698	2.3384	0.7155	1.8110
		r_{31}	3.2442	2.3527	2.0724	3.5334	0.8902
		r_{32}	2.3120	2.7202	2.8247	1.9086	4.3643
	Deviations	F_s	9.71	187.8	41.2	6.5 7	75.5
Gothard (1981)	Parameters	n_{12}	4.1904	2.1811	2.0514	2.1423	2.8361
		n_{13}	5.0724	2.2506	2.0556	1.8279	2.3704
		n_{21}	2.8133	2.0570	1.4231	1.8854	2.2250
		n_{23}	5.5302	4.6741	4.8040	4.7392	4.8952
		n_{31}	1.5476	1.0415	1.1907	1.5413	2.0075
		n_{32}	6.6869	4.8238	5.3413	5.9585	6.3309
	Deviations	F_s	1.22	13.2	4.81	3.86	6.00

$F_s = \Sigma(\gamma_i' \cdot x_i' - \gamma_i'' \cdot x_i'')^2$

from the isothermal data given by Figurski and von Weber[23] at four temperatures between 60 and 120°C, is in agreement with the excess enthalpies published by Kehlen and Fuhrmann[26] and the predicting of excess enthalpies by various models from the results of the reduction of liquid-vapor equilibrium data may be analysed. The results obtained show that there are no significant differences between the three models compared in predicting excess enthalpies, in this case.

In order to avoid influences of programming and computations on conclusions, extensive comparisons were performed between the new model and various other models by use of the computer programs published by Prausnitz and coworkers[3] and by Hála and coworkers,[27] after imbedding the correlations derived from the new model. Very similar results obtained were reported in various papers related to CODATA activities.

In several communications the use of the new model was qualified as successful in connection with development of separation processes and purification of acetic acid,[28] vinyl acetate[29] and butyl acetate.[30] Several comparisons of the new model and reference models were presented also as the author's own experimental data.[31–37]

CONCLUSIONS

A new approach, based on the mass action law consequences in the phenomenological treatment of the mixing to reach equilibrium of interactions in restrained molecular systems, was successful in describing deviations from ideal behaviour in nonelectrolyte solutions.

The correlations derived from the new model allow prediction of liquid-vapor equilibrium data in binary systems with as small average deviations as possible by the use of the equations given by Wilson [1] and by Renon and Prausnitz,[5] all in two-parameter form. Multicomponent data are predicted by the use of binary parameters by at least the same accuracy as possible by the use of the reference models. Mutual solubility data are predicted with as small deviations as possible by the use of the correlation given by Stryjek [22] which requires more adjustable parameters, and ternary liquid-liquid equilibrium data are predicted with significantly smaller deviations by the use of the NRTL equation.

The model derived from the new approach exhibits no limitations similar to those well known for the models derived from the local concentration concept. Liquid-vapor and liquid-liquid equilibrium data as well as excess enthalpies may be predicted by a unique set of binary parameters taking into account correlations between constants in the equation expressing the temperature dependence of the parameters, although no restraint concerning the uniqueness of parameters of the analytical form of the correlations related to various excess properties follows from the approach.

In all correlations derived from the basic concepts considered to develop the model, only the first approach of the correlation between the number of equivalent interactions acting between the number of the nearest neighbour molecules in restrained molecular systems was considered so in its further development the model is open to improvement.

ACKNOWLEDGEMENTS. The authors is gratefully recognizing the contributions of all coworkers, especially of G. Panaitescu, software eng. I. Burlacu, I. Dumitru, for programming, Stefania Popescu and Ilenuţa Gavrilă for handling the data banks created using the data offered generously in collections by J. Gmehling, U. Onken, A. Maczyński, S. Hemény G. Chikány, as well as of Victoria Săvescu, Ioana Ionescu, Daniela Gurgui, Luminiţa Simoiu and Viorica Trache, whose tedious experimental work and critical selection of the data obtained was the motivation of my own efforts in the last years.

REFERENCES

[1] G. M. Wilson, *J. Amer. Chem. Soc.*, **86**, 127 (1964).

[2] E. W. Flory and J. M. Prausnitz, *Ind. Eng. Chem.*, **62**, 9, 8 (1942).

[3] H. Huggins, *Ann. New York Acad. Sci.*, **43**, 1(1942).

[4] R. L. Scott, *J. Chem. Phys.*, **25**, 193 (1956).

[5] H. Renon and J. M. Prausnitz, *A.I.Ch.E.J.*, **14**, 135 (1968); *Ind. Eng. Chem. Peoc. Des. Dev.*, **8**, 413 (1969).

[6] D.S.Abrams and J.M. Prausnitz *A.I.Ch.E.J.* **21**, 116 (1975).

[7] A. Fredenslund, J. Gmehling and P. Rassmussen, "Vapor-Liquid Equilibria Using UNIFAC. (a Group Contribution Method)", Elsevier, Amsterdam. 1977.

[8] J. Gmehling and U. Onken, "Vapor-Liquid Equilibrium Data Collection", J. Behrens, R. Eckermann Editors, Dechema, 1982.

[9] J. M. Prausnitz, Communication to the 15-th WAT Seminar on Thermodynamics, Kühlungsborn, GDR, April 1985.

[10] S. Kemény, *Kémiai Közl.*, **51**, 311–44, 201–33 (1979).

[11] F. Dolezalek, *Z. phys. Chem.*, **69**, 727 (1908); *ibid.*, **73**, 191 (1910).

[12] F. Becker, H. Kiefer and P. Rhensius, *Z. Naturforsch.*, **27**, 1611 (1972).

[13] F. Becker, H. Kiefer, P. Rhensius and A. Spörner, *Polish J. Chem.*, **54**, 1937 (1980).

[14] F. A. Gothard, The 6-th IUPAC Conference on Thermodynamics, Merseburg, GDR, 1980, Poster Session Paper 61, *Ind. Eng. Cghem. Fundamentals*, **24**, 300—3 (1981).

[15] M. C. van Ness, "Classical Thermodynamics of Nonelectrolyte Solutions" Pergamon Press, New York, 1964.

[16] F. A. Gothard, "Predicting Performances of Various Models for Nonelectrolyte Solutions Compared on a Revised and Extended Reference Data Set", Report 3-RP-3 to the Second CODATA Symposium on Critical Evaluation and Prediction of Phase Equilibria in Multicomponent Systems Paris, 11—13 September 1985.

[17] F. A. Gothard, Communication to the V-th IUPAC Conference for Mixtures of Nonelectrolytes and Intermolecular Interactions, Halle, GDR, 1983, *Ind. Eng. Chem. Fundamentals*, **24**, 300—9 (1985).

[18] G. Panaitescu, *Rev. Chim. (Bucureşti)*, **33**, 1110 (1982).

[19] F. A. Gothard, V. Suărăşanu, G. Panaitescu, I. Cheţa and I. Dumitru, "Critical Evaluation of Liquid-Vapor Equilibrium Data and Models by Correlation Using the Maximum Likelihood Method", Lecture to the 1-st CODATA Meeting for Critical Evaluation and Prediction of Phase Equilibria in Multicomponent Systems, Zaborow, Poland, 1984.

[20] F. A. Gothard, "Referenz-Phasengleichewichtsdaten zur vergleichsmässigen Untersuchungen an Modellen für Nichtelektrolytlosungen" Invited Lecture to the 15-th WAT Seminar on Themodynamics, Kühlungsborn, GDR, April 1985.

[21] V. Suărăşanu, G. Panaitescu and I. Dumitru, *Rev. Chim. (Bucureşti)*, **34**, 1004—8 (1093).

[22] R. Stryjek, "Data for Science and Technology", P. Glaser Ed., 1983.

[23] G. Figurski and U. von Weber, Wiss. Z. "Wilhelm Pieck" Univ. Rostock Math. *Naturwiss. Reihe*, **26**, 7, 785 (1977).

[24] F. A. Gothard, G. Figurski and V. Trache, Communication to the Meeting of CODATA TASK GROUP members and experts, Warsaw, April 1986, *Polish. J. Chemistry*, in press.

[25] A. Maczyński and coworkers, "Verified Liquid-Vapor Equilibrium Data", Data for Science and Technology, Polish. Acad. Sci., Warszaw, 1978—85.

[26] H. Kehlen and E. Fuhrmann, *Z. phys. Chem. (Leipzig)*, **259**, 373—6 (1978).

[27] E. Hála, K. Aim et al., "Rovnováha kapalina-pára za normálnich a nizkých tlakù", Academia, Praha, 1982.

[28] I. Ionescu, G. Mocioacă and V. Săvescu, Communication to the 9-th Scientific Session of C.C. Rîmnicu-Vîlcea, Voineasa, 1983.

[29] I. Ionescu and V. Săvescu, The 12-th Scientific Session of Chemical Works Rîmnicu Vîlcea, Călimăneşti 1986, Poster session paper.

[30] G. Mocioacă, I. Ionescu and V. Ciorolanu, The 12-th Scientific Session of Chemical Works Rîmnicu Vîlcea, Călimăneşti 1986, Poster session paper.

[31] V. Săvescu, G. Mocioacă, V Ciorolanu, I. Ionescu and F. A. Gothard, Communication to the 9-th Scientific Session of Chemical Works Rîmnicu Vîlcea, Voineasa, 1983.

[32] M. Cerghiţescu, G. Panaitescu and V. Săvescu, Communication to the Symposium for Modern Processes in Oil Refining, Ploieşti, 1985.

[33] D. Gurgui and V. Săvescu, Communication to the 11-th Meeting on Phase Equilibria, Bucharest, 1986.

[34] I. Ionescu, I. Doca, D. Ciorolanu and V. Săvescu, Communication to the 11-th Scientific Session of Chemical Works Rîmnicu Vîlcea, Călimăneşti, 1985.

[35] I. Ionescu, G. Mocioacă, D. Gurgui, V. Săvescu, M. Băniceru and F. A. Gothard, Communication to the 9-th Scientific Session of Chemical Works Rîmnicu Vîlcea, Voineasa, 1983.

[36] V. Săvescu, G. Mocioacă, D. Gurgui and L. Simoiu, The 11-th Scientific Session of Chemical Works Rîmnicu Vîlcea, Călimăneşti 1985, Poster Session Paper.

[37] G. Mocioacă, I. Ionescu and V. Săvescu, The 11—th Scientific Session of Chemical Works Rîmnicu Vîlcea, Călimăneşti, 1985, Poster session paper.

Revue Roumaine de Chimie, **33**, *3*, 347—348 (1988)

COMPTES RENDUS

G. Pólya and R. C. Read, "Combinatorial Enumeration of Groups, Graphs, and Chemical Compounds", Springer Verlag, New York, Berlin, 1987. Hard cover, DM 68, 148 pp., ISBN 3-540-96413-4 (Berlin), ISBN 0-387-96413-4 (New York).

The book consists of two parts. The former (95 pages) is the first English translation of the famous paper by George Pólya *(Acta Mathematica*, 1937, **68**, 146—254) entitled: "Kombinatorische Anzahlbestimmungen für Gruppen, Graphen und chemische Verbindungen". George Pólya, the well-known Hungarian-born mathematician, who died in 1985 at the age of 97, had for some years (1934—1937) made use of his famous theorem for enumerating various classes of objects. In 1937, in his classical paper which can now be read for the first time in English, he made a detailed account of the uses of this theorem, based upon a powerful technique, namely the use of generating functions. Pólya's paper has an introduction and four sections: groups; graphs; chemical compounds; asymptotic evaluation of the number of combinations.

Professor R. C. Read from the Department of Combinatorics and Optimization, University of Waterloo, Canada, recalls in his preface how, as a student, he was amply rewarded for having worked painfully through the German text; indeed, his subsequent research proved that. This classical landmark paper in mathematics is now available in D. Aeppli's English translation.

In the second part of the book (52 pages), Prof. R. C. Read surveys the research, including his own, that stemmed from Pólya's paper. With 230 references, this survey starts with discussing the general idea of Pólya's theorem, illustrated by an example: we have a set of boxes, assumed for the time being to be distinguishable from one another. In addition, we have a store of objects (figures) from which we put exactly one into each box (the same figure may be put into several boxes). Pólya's theorem allows the enumeration of the various "configurations" i.e. set of boxes, each containing a figure.

Read then reviews briefly Pólya's pre-1937 papers in this area, and the so-called Burnside Lemma (which could actually be called the Cauchy-Frobenius theorem). Next, the early expositions and uses of Pólya's theorem by mathematicians are reviewed, till the end of the sixties. During the seventies, this theorem appeared in mathematical textbooks for undergraduate courses, and was extensively used by chemists. The enumeration of trees and alkanes is surveyed in detail, with the various restrictions and refinements. Next the generalizations and extensions of Pólya's theorem are discussed: de Bruijn's theorem; Gian-Carlo Rota's theory of Möbius inversion; Read's superposition theorem, Harary and Palmer's work encompassing the essence of Pólya's and de Bruijn's theorems. Then applications to graphical enumeration are summarized. A special section discusses Redfield's long neglected work, which adumbrates much of Pólya's theorem; this unique paper published by J. H. Redfield during his lifetime in 1927 (not quoted by Pólya, probably unknown to him) was excavated by Harary. It is shown in this context how R. W. Robinson on one hand and Read on another hand used the theorem for further graphical enumerations. In the section entitled "Applications to chemical enumeration" some papers on computer programs are cited. Enumerations by means of compound cycle indices, or permutational isomerizations are also discussed. Ruch's double coset formalism is equivalent to the superposition theorem, and is reducible to Redfield's approach.

The last three sections are entitled "Back to Burnside", "Asymptotics", and "Miscellaneous applications of Pólya's theorem"; in the first of these, further chemical enumerations are discussed, e.g. the necklace problem with adjacency restrictions, rooted polyhexes, chiral or diastereomeric compounds.

The book is a "must" for all chemists interested in topological and combinatorial aspects of isomerism. It is also of interest to all mathematicians working in areas such as group theory, graph theory, and combinatorics.

A. T. Balaban
Polytechnic Institute Bucharest

P. Hellmold and D. Schnurpfeil, "Acetylenchemie. Carbid und Acetylen. Herstellung und Reaktionen", VEB Deutscher Verlag für Grundstoffindustrie, Leipzig, 1986. Hard cover, 36 M, 128 pp., ISBN 3-342-00078-3.

Professor Dr. Hellmold from the Technical University "Carl Schorlemmer" Leuna-Merseburg, and Doz. Dr. Schnurpfeil from the Buna Chemical Works produced a useful book for chemists, students and teaching staff. The development of calcium carbide (CaC_2) production followed an interesting trend with gradual increase during 1920—1950, followed by a 2.9-fold increase in the 1960's, then a steep decrease in the 1970's when the gradual increase resumed; at present the yearly world production of CaC_2 is over 6 megatons.

More than half of the acetylene is produced via CaC_2, and about 40% is produced pyrolytically or by the arc process.

After a brief historical introductory chapter 1, the next two chapters describe the properties, the fabrication, and the chemical reactions of CaC_2. Technical and economical details are given in substantial detail on 42 pages.

Chapter 4 describes on seven pages petrochemical processes for acetylene production.

The last chapter presents on 57 pages the reactions of acetylene. Unlike Reppe's system of discussing acetylene reactions (vinylation, ethinylation, cyclopolymerization, and carbonylation), in this book the classification is according to electrophilic or nucleophilic addition (of alcohols, amines or carboxamides) to acetylene, cycloadditions, nucleophilic additions of acetylides to carbanions, and reactions catalysed by coordination compounds. The last category which is the most important for practical applications, contains hydrogenations, linear di- and trimerisations, addition of hydrogen cyanide, addition of carbonyl compounds, ethinylation of carbonyl derivatives, carbonylation of acetylene, cyclopolymerizations, and linear polymerizations. More than 150 literature references are cited (the references are listed after each chapter). A chart (fig. 1.1) printed on the reverse side of the jacket summarizes all acetylene reactions.

The book is a well written and concise review of the fabrication procedures for many important chemicals. Although at present petrochemical procedures are favored, the coal-based acetylene production is surely important in the future. The authors state honestly that though the acetylene hydration to acetaldehyde is a morally obsolete process in comparison with the Wacker reaction, owing to the fact that in the GDR large plants exist, the acetylene-based acetaldehyde is still produced despite the high toxicity of Hg(II) compounds. Of substantial interest are the energetic and economic details of the various processes. The book will find an audience in all chemists interested in the basic technical processes.

A. T. Balaban
Polytechnic Institute Bucharest

NOTE POUR LES AUTEURS

La Revue Roumaine de Chimie publie des articles en anglais, français, russe, allemand ou espagnol. Les auteurs sont priés d'envoyer des articles et des comptes rendus inédits.

Les manuscrits seront dactylographiés à double interligne. La bibliographie, les tableaux et la légende des figures seront placés après le texte.

Si l'article fait partie d'une série numérotée, la partie précédente sera donnée comme première référence.

Chaque article sera précédé d'un résumé comprenant quinze lignes au maximum.

Les références bibliographiques dans le texte seront faites par des exposants sans parenthèses et paraîtront à la fin de l'ouvrage.

Les publications périodiques mentionnées dans la bibliographie seront présentées suivant les prescriptions internationales: le nom de l'auteur précédé de l'initiale du prénom, le titre du périodique abrégé conformément à « Chemical Abstracts » et souligné par une ligne, le numéro du tome indiqué par des chiffres arabes et souligné par deux lignes, suivi de la première page de l'article; à la fin, l'année de la parution sera placée entre parenthèses. Le numéro de la revue ne sera pas indiqué si les pages du volume sont numérotées consécutivement.

Les textes des livres ou traités inclueront: le nom des auteurs, l'initiale du prénom, le titre du livre entre guillemets et sans être souligné, le numéro du tome précédé par l'abréviation « vol. » (ou « Bd. »), le numéro de l'édition (the publisher), la localité de la parution du livre, l'année de la parution et la page de la référence précédée(s) par l'abréviation « p. » (ou « S. »).

Les brevets seront indiqués comme suit: l'auteur ou la firme, le pays et le numéro du brevet, la date et la revue *(Chem. Abstr.)*. Par ex.: M. Jones (to Union Carbide Co), Brit. Pat. 601 238, 2 Sept. 1959; cf. *Chem. Abstr.*, **54**, 12808 (1980).

Si la référence n'a pas été lue en original, on indiquera aussi la revue de référence consultée.

Les diagrammes seront tracés à l'encre de Chine sur papier calque. Les tableaux et les figures (en nombre strictement nécessaire) ainsi que les courbes dans les figures seront numérotés par des chiffres arabes. Leur explication sera donnée dans la légende des figures. Prière de ne pas inscrire les mêmes données dans les tableaux et les figures. Chaque tableau aura un titre. On indiquera dans le texte la place approximative des tableaux et des figures. Les formules chimiques seront incluses dans le texte; en outre elles seront transcrites sur papier calque, à l'encre de Chine.

Les auteurs sont priés d'indiquer les caractères italiques (en soulignant les lettres au crayon), ainsi que tout autre caractère spécial; les préfixes *ortho*, *meta*, *para*, *cis*, *trans*, etc. seront soulignés pour indiquer leurs caractères italiques et ne seront jamais écrits avec des majuscules.

Aucune correction à la main ne sera admise sur le manuscrit. Les corrections seront tapées à la machine. Les lettres grecques ou d'autres symboles spéciaux seront insérés à la main à l'encre clairement.

Le manuscrit sera signé par l'auteur.

Le titre-courant aura 50 lettres au maximum.

L'entière responsabilité du contenu des article appartient aux auteurs.

Sur demande on peut obtenir une note plus complète.

PRINTED IN ROMANIA

ORSZÁGOS MŰSZAKI INFORM
KÖZPONT ÉS KÖNY
1883

1988 MAJ 6

TRAVAUX PARUS AUX ÉDITIONS DE L'ACADÉMIE DE LA RÉPUBLIQUE SOCIALISTE DE ROUMANIE

ELENA CEAUȘESCU, **Rășini de hidrocarburi**, vol. 1, 1987, 344 p.
ELENA CEAUȘESCU, **Progrese în chimia și tehnologia polimerilor**, 1986, 446 p.
ELENA CEAUȘESCU, **Forschungen im Bereich der Chemie und Technologie der Polymere**, 1986, 444 p.
ELENA CEAUȘESCU, **Cercetări în chimia și tehnologia polimerilor**, 1983, 520 p.
ELENA CEAUȘESCU, **Noi cercetări în domeniul compușilor macromoleculari**, 1981, 536 p.
ELENA CEAUȘESCU, **Polimerizarea stereospecifică a izoprenului**, 1979, 307 p.
ELENA CEAUȘESCU, **Research work on synthesis and characterization of macromolecular compounds. Contributions**, 1974, 251 p.
I. G. MURGULESCU, **Introducere în chimia fizică**, vol. I. 1. **Atomi, molecule, legătură chimică**, 1976, 560 p.
I. G. MURGULESCU, V. EM. SAHINI, **Introducere în chimia fizică**, Vol. I, 2. **Structura și proprietățile moleculelor**, 1979, 604 p.
I. G. MURGULESCU, E. SEGAL, **Introducere în chimia fizică**, Vol. II. 1. **Teoria molecular-cinetică a materiei**, 1979, 1036 p.
I. G. MURGULESCU, TATIANA ONCESCU, E. SEGAL, **Introducere în chimia fizică**, Vol. II. 2. **Cinetică chimică și cataliză**, 1981, 1024 p.
I. G. MURGULESCU, J. PĂUN, **Introducere în chimia fizică**, Vol. I, 3. **Nucleul atomic, reacții nucleare, particule elementare**, 1982, 606 p.
I. G. MURGULESCU, RODICA VÎLCU, **Introducere în chimia fizică**. Vol. III. **Termodinamica chimică**, 1982, 624 p.
I. G. MURGULESCU, O. M. RADOVICI, **Introducere în chimia fizică**, vol, VI, **Electrochimia**, 1986, 410 p.
R. VÎLCU, M. LECA, **Termodinamica polimerilor prin cromatografie de gaze**, 1987, 238 p.
I. ZUGRĂVESCU, M. PETROVANU, **Cicloadiții 3+2 dipolare**, 1987, 446 p.
RAUL MIHAIL, ION GROZEANU, **Estimarea secvențială aplicată sistemelor chimice**, 1986, 406 p.
M. BREZEANU, I. PATRON, M. ANDRUH, **Combinații complexe polinucleare și aplicațiile lor**, 1986, 244 p.
A. T. BALABAN et al., **Labelled Compounds and Radiopharmaceuticals Applied in Nuclear Medicine**, coédition avec John Wiley and Sons, 1986, 742 p.
D. PURDELA, **Nomenclatura chimiei organice — IUPAC**, 1986, 451 p.
PETRU BUDRUGEAC, **Probleme de chimie**, 1986, 280 p.
T. ONCESCU, S. G. IONESCU, **Conversie fotochimică și stocare de energie**, 1985, 272 p.
V. DRĂGUȚAN, A. T. BALABAN, M. DIMONIE, **Olefin Metathesis and Ring-Opening Polymerization of Cyclo-Olefins**, coédition avec John Wiley and Sons, 1985, 544 p.
C. LITEANU, I. RÎCĂ, **Optimizarea proceselor analitice**, 1985, 360 p.
N. PETRESCU, **Chimia extracției cu solvenți și aplicații**, 1985, 212 p.
V. E. SAHINI, M. HILLEBRAND, **Chimie cuantică în exemple și aplicații**, 1984, 378 p.
GH. MARCU, **Chimia compușilor coordinativi**, 1984, 415 p.
E. CORDOȘ, C. MANOLIU, **Spectrometria de absorbție și florescența atomică**, 1984, 178 p.
C. BODEA, **Tratat de biochimie vegetală, p. II, t. V**, 1984, 438 p.
N. ASANDEI, A. GRIGORIU, **Chimia și structura fibrelor**, 1983, 395 p.
N. IONESCU, M. CĂLDĂRARU, **Oxidarea catalitică a olefinelor inferioare**, 1983, 178 p.
C. CAȘCAVAL, **Studiul polimerilor prin piroliză și cromatografie de gaze**, 1983, 220 p.
C. I. SIMIONESCU, F. DANEȘ, **Originea vieții** 1983, 110 p.
C. BODEA, **Tratat de biochimie vegetală, p. II, t. IV**, 1982, 408 p.
I. GĂLĂȚEANU, **Procese și metode radiochimice în energetica nucleară**, 1931, 234 p.
CR. SIMIONESCU, VALERIA GORDUZA, **Polimeri biocompatibili și biologic activi**, 1980, 479 p.
C. GH. MACAROVICI, **Analiza chimică cantitativă anorganică**, 1979, 457 p.
I. ZUGRĂVESCU, MAGDA PETROVANU, **N-ylid chemistry,** coédition avec McGraw-Hill International Book Company U.S.A., 1977, 396 p.

ISSN 0035—3930

I. P. INFORMAȚIA, c. 1741

43 426

Lei 40

F 1103

04

ACADÉMIE DE LA RÉPUBLIQUE SOCIALISTE DE ROUMANIE

REVUE ROUMAINE DE CHIMIE

TOME 33
N° 4
Avril 1988

EDITURA ACADEMIEI REPUBLICII SOCIALISTE ROMÂNIA

Rev. Roumaine Chim.

RRCHAX, 33, *4*, p. 349–434 (1988), Bucarest

ACADÉMIE DE LA RÉPUBLIQUE SOCIALISTE DE ROUMANIE

COMITÉ DE RÉDACTION

Rédacteur en chef:

I. G. MURGULESCU, membre de l'Académie de la République Socialiste de Roumanie

Rédacteurs en chef adjoints:

A. T. BALABAN et V. EM. SAHINI, membres correspondants de l'Académie de la République Socialiste de Roumanie

Collège de rédaction:

EM. BRATU, ELENA CEAUȘESCU, ECATERINA CIORĂNESCU-NENITZESCU, CR. SIMIONESCU, membres de l'Académie de la République Socialiste de Roumanie; P. SPACU, membre correspondant de l'Académie de la République Socialiste de Roumanie; M. BANCIU, M. D. GHEORGHIU, I. HAIDUC, D. I. MARCHIDAN, G. NIAC et D. SĂNDULESCU

La Revue Roumaine de Chimie paraît 10 fois par an. Toute commande de l'étranger sera adressée à ROMPRESFILATELIA — sectorul Export-Import Presă, P. O. Box 12—201, télex 10376 prsfi r 78 104 Bucarest, Calea Griviței nr. 64—66, București, Roumanie

Les manuscrits, les livres et les revues proposés en échange, ainsi que toute correspondance seront envoyés à la rédaction :

REVUE ROUMAINE DE CHIMIE
125, Calea Victoriei, 79717 Bucarest, Roumanie, téléphone 50 76 80

EDITURA ACADEMIEI REPUBLICII SOCIALISTE ROMÂNIA
125, Calea Victoriei, 79717 Bucarest, Roumanie, téléphone 50 76 80

REVUE ROUMAINE DE CHIMIE

ORSZÁGOS MŰSZAKI INFORMÁCIÓS KÖZPONT ÉS KÖNYVTÁR 1983

Tome 33, N° 4 **Avril 1988**

RODICA VÎLCU and ST. PERIŞANU, Estimation of nonpolar gas solubilities in polar solvents 351–358
ALEXANDRU T. BALABAN, On a 3-connected carbon net (infinite tridimensional lattice of sp^2-hybridized carbon atoms) and congeneric systems 359–362
CRISTIAN KISSLING, Method for determining the phase composition in multicomponent polyphasic systems 363–369
L. DAGNINO and E. CORTÉS, Ortho effects of substituents in oximes, hydrazones and azines derived from benzaldehydes by electron impact . 371–376
ALEXANDRU T. BALABAN and CHOI IL, Reactions of pyrylium salts with nucleophiles. XX.[1] Synthesis of 4-(N-pyridinium)-4′-dialkylaminoazobenzene and 4-(4-dialkylaminophenylazo)-4′-(N-pyridinium)-biphenyl derivatives 377–383
F. J. GARCÍA, R. CRUZ, O. COLLERA and J. L. SÁNCHEZ, Mass spectrometry of diterpenic compounds with a glycol function at $C_{16}-C_{17}$ 385–392
NOSRAT MUSTAFA ABED, ABDEL-GHANI ALI ELAGAMEY, SALAH ZAKI SOWELLIM and ABDEL-FATTAH ALI HARB, Some reactions of α,β-unsaturated acyl isothiocyanates 393–398
V. DOBRESCU, G. ANDREI, A. CÎMPEANU and C. ANDREI, Some properties of linear low density polyethylene and branched low density polyethylene 399–403
N. BIÇAK, N. TAN and Ö. BEKÂROǦLU, A novel spectrophotometric method for determination of nitrite ions 405–412
D. N. PUROHIT and R. S. CHAUHAN, Spectrophotometric studies of lanthanides with 3-hydroxy-3-phenyl-1-*o*-carboxy phenyltriazene 413–417
I. BERDAN, Al. CAŞCAVAL and A. SCORŢEANU, Complex compounds of Co(II) with Schiff-base ligands (in French) 419–425

BOOK REVIEWS 427–433

Rev. Roumaine Chim. **33**, *4*, 349–434 (1988), Bucarest

Revue Roumaine de Chimie, **33**, *4*, 351–358 (1988)

ESTIMATION OF NONPOLAR GAS SOLUBILITIES IN POLAR SOLVENTS

RODICA VÎLCU and ST. PERIȘANU

Laboratory of Physical Chemistry, Polytechnic Institute of Bucharest, 13 Blvd. Republicii,
Bucharest, Romania

Received February 3, 1986

The activity coefficients of the ideal diluted solutions of gases in polar liquids were calculated by means of a modified regular solution equation, which takes into account the influence of the dipole moment of the solvent and the polarizability of the gas molecule. The agreement between the experimental solubilities and those calculated with the above mentioned activity coefficients was better than in the case of other equations proposed for such systems. The greatest discrepancies occur in the case of carbon dioxide and are considerable also for strongly polar solvents.

Some methods were proposed for the calculation of solubilities of nonpolar gases in polar liquids, deriving from the theories of solubility in nonpolar solvents. The scaled particle theory was applied to a large number of systems, including polar gases and liquids (e.g. references [1–6]).

The deviations between experimental and calculated solubilities obtained by this method are considerable. The performance of the scaled particle theory is analyzed in three papers [7–9] and the conclusion is drawn that less than a half of the calculated values differ by less than 15% from the experimental ones (although most of the systems under consideration were nonpolar). For weakly polar solvents the mean deviation exceeds 20%.

Another theory applicable to a wide range of liquid-gas systems was proposed by Kuznetsova.[10–12] It takes into consideration some molecular and macroscopic parameters of the two components (polarizability, dipole moment, surface tension a.s.o). The agreement between the predicted and experimental solubilities is poorer than in the case of the scaled particle theory.

The applicability of the regular solution theory, to solutions of nonpolar gases in polar liquids, was tested by Gjaldbaeck and Anderson,[13] who concluded that the deviations are function of the dipole moment of the solvent and the electronic polarization of the gas. Gjaldbaeck and Nieman [14] tried an analytical correlation, in which the solubility parameter of the solvent is replaced by an adjusted one. The latter is a function of the dielectric constant of the solvent and the polarizability of the gas. Yen and Mc. Ketta [15] introduced the Stockmayer potential in the formalism of the regular solution theory. For normal nonpolar gases and moderately polar solvents, it was shown that a single additional parameter must be introduced, which depends only of the radial distribution function, the dipole moment and the molar volume of the solvent. None of the above mentioned modifications of the regular solution theory was able to predict accurate values of solubilities of gases in a wide range of polar solvents.

The aim of this paper has been to test the applicability of an equation proposed in a previous one,[16] to a wide range of systems of nonpolar gases and polar solvents :

$$\delta^* = \delta_1 - (\varepsilon_1 - 1)(0.0559 - 4.12 \cdot 10^{21}\alpha_2) \tag{1}$$

δ^* — the corrected solubility parameter — depending on the dielectric constant of the solvent (ε_1) and the polarizability of the gas (α_2) — was used in the equation for the activity coefficient :

$$\ln \gamma_2 = \frac{\bar{V}_2}{RT}(\delta^* - \delta_2)^2 \tag{1'}$$

The activity coefficients, obtained with equations (1) and (1′), were introduced in the generalized Raoult law :

$$x_2 = \frac{P_2}{f_2^{\mathrm{ol}} \cdot \gamma_2^{\mathrm{l}}} \tag{2}$$

We tried to use the most reliable values for the parameters of equations (1)—(2). δ_1 was calculated by means of its definition relation :

$$\delta = \sqrt{\frac{\Delta E_v}{V}} \simeq \sqrt{\frac{\Delta H_v - RT}{V}} \tag{3}$$

We used enthalpies of vaporization recommended in the books by Stull, Westrum and Sinke[17] and Cox and Pilcher.[18] We obtained, for some solvents, values of the solubility parameter differing by about 0.2 cal$^{1/2} \cdot$ cm$^{-3/2}$ from those of Wilhelm and Battino[19] (see table 1).

Table 1

Improved solubility parameters of some polar solvents

Solvent	Iodo-benzene	Bromo-benzene	Methyl acetate	Nitro-benzene
ΔH_v^0(cal/mol)	114.00	104.70	76.00	136.30
V_1(cm^3/mol)	111.06	105.10	79.40	102.60
δ_1(cal$^{1/2}$.cm$^{-3/2}$)	9.86	9.69	9.39	11.3

For the calculation of the reference fugacities of the hypothetic liquids "2" (f_2^{ol}), we used equations with specific coefficients for each compound, recommended in the book by Prausnitz.[20] The accuracy of the equation for f_2^{ol} is extremely important, especially for highly supercritic compounds.

As regards the parameters δ_2 and $\bar{V}_2^{ol}$, it was necessary to adjust their values so they should correlate correctly the most recent data of solubilities for nonpolar systems (Table 2).

Table 2

Gas parameters used in equations (1) and (1′)

Gas	f_2^{ol}(298K)/atm	$\bar{V}_2^{ol}$(cm^3/mol)	δ_2(cal$^{1/2}\cdot$ $\cdot$cm$^{-3/2}$)	$\alpha_2 \cdot 10^{25}$
Ar	248.6	57.2	5.20	16.3
Kr	115	61	5.80	24.6
Xe	38.6	65	6.60	40.1
H_2	630	29	3.10	8.1
N_2	203.2	40	3.20	17.6
O_2	250.9	47	4.70	15.7
CO	202.1	33	3.13	19.3
CH_4	105	29.5	3.58	26
C_2H_6	26.1	69	6.30	44.7
C_2H_4	37.6	60	6.25	37.0
CO_2	40.7	35	5.20	26.5

With the above mentioned optimized values of parameters, we have calculated the solubilities of 11 gases in polar solvents. The calculated values of solubilities are given in tables 3–6, together with the experimental ones (taken from references [13,19,21,22]), at 298 K.

By examining the data of tables 3–6, some conclusions may be drawn:

— The deviations between experimental and calculated values for weakly and moderately polar solvents are generally less than 10%.

— For strongly polar solvents the same deviations are somewhat greater, exceeding 20% in the case of nitromethane.

— Great discrepancies were observed in the case of CO_2. Moderately and strongly polar solvents solve much more CO_2 than the quantity predicted by most theories.[23]

Acetone is a partially associated solvent, so that Gjaldbaeck and Anderson [13] proposed to be used, for this compound, a mean molecular weight of 75.

The temperature dependence of gas solubilities is satisfactorily predicted by equations (1) and (2) for systems with increasing solubility, as well as for those with decreasing one. In table 7, experimental and calculated solubilities of nitrogen and ethane in chlorbenzene are given for the range 273–353 K.

Table 3

Experimental and calculated solubilities of nonpolar gases in weakly polar solvents

First line — δ^*; second line — γ_2^1; third line — $x^1_{2\mathrm{calc}} \cdot 10^2$; fourth line — $x^1_{2\mathrm{exp}} \cdot 10^2$

Solvent δ_1 ε_1 Gas	Toluene 8.91 2.38	Diethylether 7.53 4.30	Iodobenzene 9.9 4.63	1,2-dibromo-ethane 10.5 4.70	Chloroform 9.21 4.72
Ar	8.84 3.59 0.112 0.109	—	9.72 7.18 0.0560 0.0501	—	—
Kr	8.85 2.605 0.334 0.335	—	9.73 4.90 0.177 0.168	—	—
Xe	8.86 1.751 1.480 1.461	—	9.76 2.99 0.866 0.881	—	—
H_2	8.83 4.99 0.0318 0.0317	—		—	—
N_2	8.84 8.56 0.0575 0.0574	7.36 3.28 0.152 0.161		—	—
O_2	8.84 3.89 0.1023 0.0928	—	9.72 7.38 0.0540 0.0510	—	—
CO	8.84 6.14 0.0806 0.0802	—		10.32 17.80 0.028 0.030	9.03 6.95 0.071 0.068
CH_4	0.85 3.98 0.239 0.243	7.38 2.05 4.64 4.55	—	—	—
C_2H_4	8.85 1.98 1.343 1.463	—	—	—	9.04 4.18 2.46 2.77 (243.2K)
Mean deviation(%)	2.8	3.8	6.2	6.7	7.8

Table 4

Experimental and calculated solubilities of nonpolar gases in moderately polar solvents

First line — δ^*; second line — γ_2^1; third line — $x^1_{2\text{calc}} \cdot 10^2$; fourth line — $x^1_{2\text{exp}} \cdot 10^2$

Solvent δ_1 ε_1 / Gas	Bromobenzene 9.7 5.40	Methylacetate 9.30 6.68	Chlorbenzene 9.42 5.62	Pyridine 10.5 12.3
Ar	9.48 5.86 0.0686 0.0680	—	9.19 4.65 0.0865 0.0861	—
Kr	9.49 4.06 0.214 0.228	—	9.20 3.29 0.265 0.273	—
Xe	9.53 2.57 1.010 1.082	—	9.24 2.15 1.206 1.232	—
H_2	—	—	9.17 6.07 0.0262 0.0261	—
N_2	—	9.11 10.57 0.047 0.059	9.19 11.27 0.0437 0.0438	9.95 21.65 0.023 0.025
O_2	9.48 6.12 0.0651 0.0748	9.11 4.68 0.085 0.089	9.19 4.95 0.0805 0.0791	9.94 8.83 0.045 0.046
CO	—	9.12 7.38 0.067 0.085	0.19 7.73 0.0640 0.0647	9.96 13.43 0.037 0.039
CH_4	—	9.13 4.63 0.205 0.194	9.21 4.84 0.197 0.204	—
C_2H_6	—	—	9.24 2.74 1.400 1.465	—
C_2H_4	—	—	9.23 2.46 1.08 1.18	—
Mean deviation (%)	6.7	12.9	2.5	5.1

Table 5

Experimental and calculated solubilities of nonpolar gases in strongly polar solvents
First line — δ^* ; second line — γ_2^1 ; third line — $x^1_{2calc} \cdot 10^2$: fourth line — $x^1_{2exp} \cdot 10^2$

Solvent δ_1 ε_1 / Gas	Acetone M = 58 9.57 20.7	Acetone M = 75 9.57 20.7	Nitrobenzene 11.6 34.75	DMSO 12.8 37.5	Nitromethane 12.4 38.6
Ar	8.60	8.60	9.94	11.00	10.55
	3.05	3.05	8.75	25.71	15.84
	0.132	0.132	0.0460	0.0156	0.0254
	0.0907	0.114	0.0448	0.0154	0.0320
Kr			10.05	11.12	10,67
			6.42	18.42	11.49
			0.1354	0.0472	0.0756
			0.1383	0.0446	0.0837
Xe			10.27	11.36	10.92
			4.38	12.01	7.74
			0.591	0.216	0.335
			0.584	0.170	0.251
H_2	8.53	8.53		10.88	
	4.23	4.23		19.34	
	0.0375	0.0375		0.00821	
	0.0299	0.0387		0.00761	
N_2	8.61	8.61		11.02	10.57
	7.21	7.21		62.02	39.90
	0.0707	0.0707		0.00793	0.013
	0.0540	0.0698		0.00833	0.020
O_2	8.59	8.59	9.93	10.99	
	3.32	3.32	8.755	23.06	
	0.1200	0.120	0.0455	0.0173	
	0.0838	0.108	0.0495	0.0157	
CO	8.62	8.62	9.98		
	5.36	5.36	13.46		
	0.0923	0.0923	0.0363		
	0.0772	0.0998	0.0372		
CH_4	8.67	8.67		11.15	
	3.65	3.65	—	17.33	—
	0.261	0.261	—	0.0550	
	0.1835	0.237		0.0386	
C_2H_6	8.83	8.83		11.43	
	2.11	2.11		21.42	
	1.818	1.818	—	0.179	—
	0.963	1.242		0.178	
C_2H_4	8.76	8.76			
	1.89	1.89			
	1.408	1.408	—	—	—
	1.091	1.406			
Mean deviation (%)	35.6	11.9	3.5	12.5	24.7

Table 6

Experimental and calculated solubilities of CO_2 in polar solvents at 298 K

Solvent	δ^*	γ_2^1	$x^1_{2calc} \cdot 10^2$	$x^1_{2exp} \cdot 10^2$
Toluene $\delta_1 = 8.91$ $\varepsilon_1 = 2.38$	8.85	2.200	1.119	1.029
$CF_2Cl-CCl_2F$ $\delta_1 = 7.06$ $\varepsilon_1 = 3.5$	6.95	1.218	2.02	1.81
Chloroform $\delta_1 = 9.21$ $\varepsilon_1 = 4.72$	9.04	2.389	1.03	1.28
n-Propyl-acetate $\delta_1 = 8.69$ $\varepsilon_1 = 5.60$	8.49	2.053	1.20	2.45
Chlorbenzene $\delta_1 = 9.42$ $\varepsilon_1 = 5.62$	9.21	2.585	0.950	0.981
Methylacetate $\delta_1 = 9.39$ $\varepsilon_1 = 6.68$	9.13	2.49	0.987	2.26
Aniline $\delta_1 = 11.7$ $\varepsilon_1 = 6.99$	11.45	9.90	0.248	0.491
Piridine $\delta_1 = 10.5$ $\varepsilon_1 = 12.3$	9.99	3.88	0.634	1.21
Acetone M = 58 $\delta_1 = 9.57$ $\varepsilon_1 = 20.7$	8.68	2.045	1.201	1.853
Propionitrile $\delta_1 = 10.6$ $\varepsilon_1 = 27.7$	9.40	2.83	0.867	1.69
Nitrobenzene $\delta_1 = 11.6$ $\varepsilon_1 = 34{,}5$	10.08	4.08	0.602	0.998
DMSO $\delta_1 = 12.8$ $\varepsilon_1 = 37.5$	11.16	8.15	0.302	0.908

Table 7

Experimental and calculated solubilities of nitrogen and ethane in chlorobenzene in the range 273–353 K

$T(K)$	$N_2 = 9.19$			$C_2H_6 = 9.24$		
	γ_2^1	$x_{2calc} \cdot 10^4$	$x_{2exp} \cdot 10^4$	γ_2^1	$x_{2calc} \cdot 10^2$	$x_{2exp} \cdot 10^2$
273.2	14.06	3.75	3.90	3.00	1.97	2.15
293.2	11.74	4.24	4.22	2.78	1.455	1.562
298.2	11.27	4.37	4.38	2.74	1.400	1.465
313.2	10.03	4.78	4.50	2.61	1.195	1.190
333.2	8.74	5.38	4.80	2.46	1.015	0.960
353.2	7.73	6.02	5.18	2.34	0.908	0.790

REFERENCES

[1] R. A. Pierotti, *J. Phys. Chem.*, **67**, 1840 (1963).

[2] R. A. Pierotti, *J. Phys. Chem.*, **69**, 281 (1965).

[3] E. Wilhelm and R. Battino, *J. Chem. Phys.*, **56**, 563 (1972).

[4] R. L. Field et al., *J. Chem. Thermodyn.*, **6**, 237 (1974).

[5] R. J. Wilcock et al., *J. Chem. Thermodyn.*, **10**, 817 (1978).

[6] L. Patyi et al., *Zhur. prikl. Khim.*, **51**, 1296 (1978).

[7] J. P. Montfort, J. R. Varela Ham and J. L. Perez Meseguer, *J. Chim. Phys. Phys.-Chim. Biol.*, **74**, 409 (1977).

[8] C. L. de Ligny and N. G. van der Veen, *Chem. Eng. Sci.*, **27**, 391 (1972).

[9] L. Patyi et al., Proc. Conf. Appl. Chem., Unit. Oper. Processes, 3rd, Budapest, 1977, p.107.

[10] E. M. Kuznetsova, *Zhur. fiz. Khim.*, **47**, 231 (1973) ; **47**, 2002 (1973).

[11] E. M. Kuznetsova, *Zhur. fiz. Khim.*, **49**, 1316 (1975).

[12] E. M. Kuznetsova and D. Sh. Rashidova, *Zhur. fiz. Khim.*, **51**, 3061 (1977).

[13] J. C. Gjaldbaeck and E. K. Anderson, *Acta Chem. Scand.*, **8**, 1389 (1954).

[14] J. C. Gjaldbaeck and H. Nieman, *Acta Chem. Scand.*, **12**, 1015 (1958).

[15] L. C. Yen and J. J. Mc. Ketta, *AIChE Journal*, **8**, 501 (1962).

[16] Rodica Vilcu and St. Perişanu, *Polish J. Chem.*, **54**, 2043 (1980).

[17] D. R. Stull, G. C. Sinke and E. F. Westrum Jr., "The Chemical Thermodynamics of Organic Compounds", J. Willey, New York, 1969.

[18] J. D. Cox and G. Pilcher, "Thermochemistry of Organic and Organometallic Compounds", Acad. Press, London, 1970.

[19] E. Wilhelm and R. Battino, *Chem. Revs.*, **73**, 1(1973).

[20] J. M. Prausnitz et al., "Computer Calculations for Multicomponent Vapor-Liquid and Liquid-Liquid Equilibria", Prentice-Hall, Englewood Cliffs, 1980.

[21] J. A. Waters, G. A. Mortimer and H. E. Clements, *J. Chem and Eng. Data*, **15**, 174 (1974).

[22] J. M. Prausnitz et al., "Computer Calculations for Multicomponent Vapor-Liquid Equilibria", Prentice-Hall Inc., Englewood Cliffs, 1967.

[23] T. Katayama, M. Tomosaburo and T. Nitta, *Kagaku Kogaku* **31**, 559(1967).

Revue Roumaine de Chimie, 33, 4, 359–362 (1988)

ON A 3-CONNECTED CARBON NET (INFINITE TRIDIMENSIONAL LATTICE OF sp^2-HYBRIDIZED CARBON ATOMS) AND CONGENERIC SYSTEMS

ALEXANDRU T. BALABAN
Polytechnic Institute, Department of Organic Chemistry,
Splaiul Independenţei 313, 76206 Bucharest, Romania

Received November 16, 1987

A new infinite tridimensional lattice of sp^2-hybridized carbon atoms is described. It possesses 8- and 9-membered puckered rings, and has large cavities with six 8-membered faces and eight 9-membered faces. In addition, there are smaller cavities whose faces are tub-shaped 8-membered rings. Congeneric systems patterned on the large cavity are a $(C = C)_{12}O_{24}$ polyhedral molecule, a carbon cluster C_{48} which might accommodate a metal atom or ion inside, and heterocyclic systems derived from the C_{48} cluster.

INTRODUCTION

The present paper continues previous work on hypothetical crystalline modifications of elemental carbon in which we examined lattices formed from sp^3-hybridized or sp^2-hybridized carbon atoms (3-connected nets)[1,2] or from both such types carbon atoms (3,4-connected nets with possible metallic properties).[3] Congeneric systems were also discussed.[4,5] In addition to enabling the understanding of experimentally-detected defects in the diamond or graphite lattices,[6] such considerations are interesting because amorphous carbon was shown experimentally to consist about 50–50% in sp^2 and sp^3 hybridized carbon atoms ;[7] crystalline forms with such mixed hybridization often have metallic energy band structures.

Reviews on real and hypothetical carbon lattices have been published.[2,8]

A 3-CONNECTED CARBON NET

In the present section a 3-connected carbon net is described : sp^2-hybridized carbon atoms form a three-dimensional infinite lattice with girth 8 (i.e. with 8-membered rings as the smallest circuits). It has large cavities that are quasi-spherical, and smaller cavities that are quasi-cylindrical (stout cylinders).

In order to visualize the large cavity one has to start from the truncated octahedron which has 24 vertices and 36 edges (Fig. 1), and which constituted the unit cell of a 4-connected carbon net examined earlier.[1]

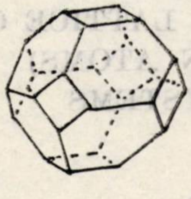

Fig. 1. — The truncated octahedron (one of the 13 semiregular polyhedra).

At every vertex three edges meet; they belong to two hexagons and one square. By replacing all edges that are common to a square and a hexagon by a C—C—C chain, one obtains the large cavity (Fig. 2). It has six puckered octagons in crown conformation whose average planes are parallel to the faces of a cube, and eight puckered 9-gons whose average planes are parallel to the faces of an octahedron. Each octagonal face is surrounded by four 9-gons, and each 9-gon is surrounded by three puckered octagons and three 9-gons (Fig. 2). The structure conserves the symmetry of the truncated octahedron.

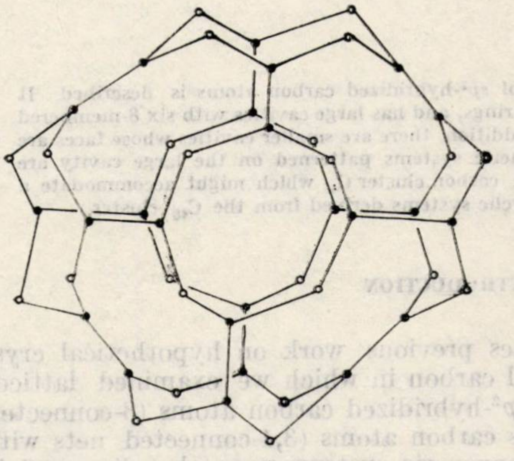

Fig. 2. — The large cavity: the 24 points of degree four are indicated by closed circles ●, and the 24 points of degree two are indicated by open circles ○.

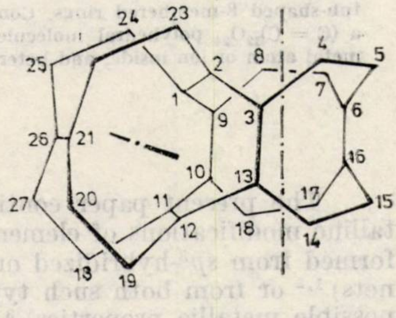

Fig. 3. — Two adjacent small cavities with vertices numbered 1—18, and 1—3, 9—13, 19—28, respectively; the non intersecting ternary axes are mutually orthogonal (— · — ·).

The small cavity (Fig. 3) has D_3 symmetry: the bases of the cylinder are puckered 9-gons, and three tub-shaped octagons sharing one edge pairwise form the circular wall of the cylinder. The bases of the cylinder are connected by three parallel edges (C=C bonds). Small cavities fit into one another as indicated in Fig. 3: each small cavity with its threefold axis is contiguous to three other small cavities whose threefold axes are in an orthogonal plane to the former axis. In addition, each small cavity is contiguous to five large cavities : two on the bases of the quasi-cylinder, and three laterally.

In the net, adjacent large cavities share their crown-shaped octagonal faces. The "free spaces" at the corners of the cubical unit cells circumscribing the large cavities form the small cavities.

As mentioned earlier, octagons are the smallest circuits. They are of two kinds : crown-shaped for the faces shared by two adjacent large cavities, and tub-shaped for small cavities. All 9-gons have the same puckered conformation with ternary symmetry.

CONGENERIC SYSTEMS

We shall describe here three congeneric systems which are derived from the large cavity. They constitute hypothetical molecules with 48 atoms, unlike the infinite lattice described so far.

1. The large cavity with its 48 vertices as such is an interesting chemical species. If the vertices of degree four are considered to be carbon atoms and the vertices of degree two are oxygen atoms, then the large cavity becomes $(C = C)_{12}O_{24}$, i.e. $C_{24}O_{24}$. Bond angles at the oxygen heteroatoms may be too large, leading to angle strain.

2. It is difficult to estimate the energy of a C_{48} cluster of sp^2-hybridized carbon atoms, similar to the much discussed buckminsterfullerane (footballene) which has 6- and 5-gonal planar faces. Like the latter, the present C_{48} cluster might accommodate a metallic atom within the cavity.

3. If some of the vertices of degree three from the large cavity are B or N atoms, the rest being CH groups, and vertices of degree two are O or S atoms, one obtains a series of tridimensional heterocycles. It is interesting to consider also the case when all pairs of vertices with degree three correspond to B = N doubly-bonded coordinative bonds. Assuming that all other vertices of degree two are oxygen atoms, among all isomers of $(BN)_{12}O_{24}$, the most interesting is that with regularly alternating $(-B-O-N-O-)_2$ bonds in all eight-membered rings; then the nine-membered rings have the structure $(-B-O-N-)_3$.

OTHER POLYHEDRAL OXIDES OF CARBON OR NITROGEN

It is easy to conceive other possible polyhedral carbon oxides. Fig. 4A depicts prismatic compounds $(CO)_{2n}$, e.g. with $n = 4$ we obtain C_8O_8 which contains four tub-shaped 1,4-dioxinic rings as the faces of the square prism, and two puckered C_4O_4 eight-membered rings as bases of the prism (Fig. 4B). With higher n values, the dihedral angles of the folded 1,4-dioxinic rings become larger; in Fig. 4B, these dihedral angles are 90°.

If the vertices of a tetrahedron, cube or pentagonal dodecahedron are nitrogen atoms, and if on every edge of these regular polyhedra one places an oxygen atom, one obtains three polyhedral nitrogen oxides : N_4O_6 with the adamantane skeleton (Fig. 4C), N_8O_{12} with a cubic framework, and the dodecahedral $N_{20}O_{30}$, respectively.

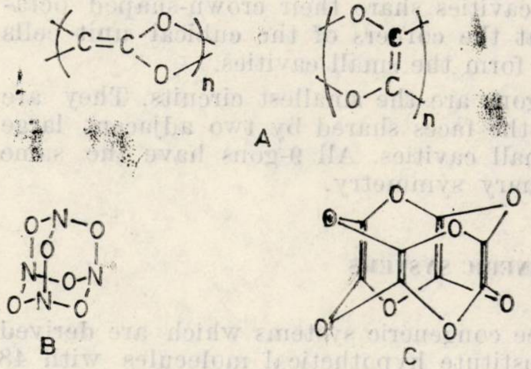

Fig. 4. — A, Polyhedral oxides of carbon ; B, one of the three polyhedral nitrogen oxides ; C, one carbon oxide with n = 4.

REFERENCES

[1] A. T. Balaban, C. C. Renţia and E. Ciupitu, *Rev. Roumaine Chim.*, **13**, 231 (1968) erratum, *ibrid.*, p. 1233.

[2] A. T. Balaban, *Computers and Math. with Applications* (in press) ; see also idem, *ibid.*, **12B**, 999 (1986) reprinted in "Symmetry Unifying Human Understanding" (ed. I. Hargittai), Pergamon Press, Oxford, 1986, p. 999.

[3] K. M. Merz Jr., R. Hoffmann and A. T. Balaban, *J. Amer. Chem. Soc.*, **109**, 6742 (1987).

[4] R. Hoffmann, O. Eisenstein and A. T. Balaban, *Proc. Natl. Acad. Sci. USA*, **77**, 5588(1980).

[5] R. Hoffmann, T. Hughbanks and M. Kertesz, *J. Amer. Chem. Soc.*, **105**, 4831 (1983).

[6] J. R. Platt, *Z. Cryst.*, **109**, 226 (1957) ; J. R. Dias, *Carbon*, **22**, 107 (1984) ; V. M. Melnichenko, Yu. N. Nikulin and A. M. Sladkov, *Dokl. Akad. Nauk SSSR*, **267**, 1150 (1982), and further references therein.

[7] R. H. Jarman et al., *Appl. Phys. Lett.*, **49**, 1065 (1986).

[8] I. V. Stankevich, M. V. Nikerov and D. A. Bochvar, *Uspekhi Khim.*, **53**, 1101 (1984) ; *Russ. Chem. Rev.*, **53**, 640 (1984).

Revue Roumaine de Chimie, **33**, *4*, 363–369 (1988)

METHOD FOR DETERMINING THE PHASE COMPOSITION IN MULTICOMPONENT POLYPHASIC SYSTEMS

CRISTIAN KISSLING

Geochemical Section, State Enterprise for Geological and Geophysical Prospectings,
Bucharest, Caransebeş st., 1, Ro-78344, Romania

Received February 22, 1987

This paper gives a general solution [to the problem of determining the equilibrium phase composition in multicomponent polyphasic systems by means of a method based on calculus and physico-chemical determinations. The quantitative chemical composition is correlated with the phase composition through a linear and nonhomogeneous system of equations, derived from thermodynamic reasons. This single solution system is also used as a criterion for the correct determination of the phase qualitative composition. At the same time, the accurate formulae of the phases subjected to continuous isomorphous substitutions are computed. The results obtained by this method, and those obtained by other methods are compared with a good concordance by using two examples. The results are derived with the aid of an IBM-360 computer on the basis of an original FORTRAN programme.

INTRODUCTION

Physical and chemical properties of a solid material and thus its domains of utilization depend on its chemical composition, which in given thermodynamic conditions leads to a certain phase composition.

The determination of phase composition of some heterogenecus solids is very useful in several domains : glass and ceramics industry, mineralogy, petrography.

Different authors have dealt with this topic giving various resolutions based on physico-chemical methods of determination such as X-ray diffraction, thermal analysis or based on calculus. [1-6]

However, these methods have some inevitable limitations because of the microcrystalline structure, of the lack of calibration curves required in X-ray quantitative determinations, or of the complex chemical composition of phases (in most cases subjected to the continuous isomorphous substitutions), especially when the phases are numerous. The methods based on calculus give a phase composition that is generally different from the real one. In this method, the difficulties are eliminated and there are possibilities of computing not only the phase composition but also accurate chemical formulae of phases.

THEORY

Let a polyphasic system be at equilibrium and assumed to be diathermically isolated.[7]

The mass of each component distributed between different phases must keep a constant value in accordance with the mass conservation law.

In order to characterize the heterogeneous system it is adequate to to know its pressure, its temperature and its chemical composition. By modifying the equilibrium a certain component (k_i) may be subjected to a transfer from a phase into another.

Considering $\varphi_1, \varphi_2, \ldots, \varphi_j, \ldots, \varphi_n$, the phases of the system and $k_1, k_2, \ldots, k_i, \ldots, k_m$ its components, m equations can be written, showing that for each k_i component found in j number of phases $(j = 1, 2, \ldots, n)$ the sum of weight variation for the whole system is 0, thus :

$$\sum_{j=1}^{n} \mathrm{d}x_{k_i}^{\varphi_j} = 0 ; \quad i = 1,\ 2,\ \ldots,\ m \tag{1}$$

where $x_{k_i}^{\varphi_j}$ represents the amount of the k_i component in the φ_j phase.

The component chemical analysis of the assumed heterogeneous system can be expressed by a set of m functions (Γ_i) of n variables whose values depend on the quantitative signals * of each component in each phase, therefore on the total amount of each component.

The Γ_i functions ($i = 1,\ 2,\ \ldots,\ m$) have the independent variables χ_j ($j = 1,\ 2, \ldots, n$), where χ_j represents the unknown concentrations of the n distinct phases in the studied physical system.

We can write these functions in the following manner :

$$\Gamma_i = \Gamma_i(\chi_1, \chi_2, \ldots, \chi_j, \ldots, \chi_n) ; \ i = 1,\ 2,\ \ldots,\ m \tag{2}$$

and thus we obtain a set of simultaneous equations, which correlate the phase quantitative composition with the amounts of the components in the system.

In order to make explicit the dependence between the Γ_i and χ_j quantities, we have to take into account that as the k_i component is in one or more phases out of the n phases, the total amount of the k_i component will be given by the sum of its amounts in each phase, and will be proportional to the concentrations of phases, the relations (2) becoming :

$$\Gamma_i = c_{i1}\chi_1 + c_{i2}\chi_2 + \ldots + c_{in}\chi_n ; \quad i = 1, 2, \ldots, m \tag{3}$$

where c_{ij} are proportionality coefficients.

The amount of the k_i component in the φ_j phase is proportional to the ratio of molecular masses of the k_i component and of the φ_j phase

---

* which can also be any other values proportional to the chemical analysis and are direct proportional to the amounts of components expressed in molar ratios, weight percentage, etc.

(m_i and M_j), multiplied by a_{ij} coefificient (which signifies the stoechiometrical coefficient of the contribution of the k_i component in the φ_j phase):

$$x^{\varphi_j}_{k_i} \sim a_{ij} \cdot \frac{m_i}{M_j} = c_{ij};\ i = 1, 2, \ldots, m;\ j = 1, 2, \ldots, n \tag{4}$$

With the significance of c_{ij} coefficients given above, relations (3) become:

$$\Gamma_i = a_{i1} \cdot \frac{m_i}{M_1} \cdot \chi_1 + a_{i2} \cdot \frac{m_i}{M_2} \cdot \chi_2 + \ldots + a_{in} \cdot \frac{m_i}{M_n} \cdot \chi_n;$$

$$i = 1, 2, \ldots, m \tag{5}$$

where Γ_i, a_{ij}, m_i, and M_j are known, but χ_j must be found.

Differentiating (5) relations we obtain:

$$\mathrm{d} \sum_{j=1}^{n} a_{ij} \cdot \frac{m_i}{M_j} \chi_j = \sum_{j=1}^{n} \mathrm{d} \left(a_{ij} \cdot \frac{m_i}{M_j} \cdot \chi_j \right) = \left(\sum_{j=1}^{n} \mathrm{d}x^{\varphi_j}_{k_i} \right) = \mathrm{d}\Gamma_i = 0$$

$$i = 1, 2, \ldots, m \tag{6}$$

and thus the conditions initially imposed are found again.

Knowing the component quantitative composition of the heterogeneous system as well as the phase qualitative composition, then there are sufficient data for computing the accurate phase quantitative composition of the heterogeneous system at equilibrium by solving the simultaneous equations (5). The linear and nonhomogeneous algebraic system (5) is the mathematical model of a real physical system, so it must always be compatible. An incompatibility of the system (5) points out an error in establishing the phase qualitative composition, or in quantitatively determining the components, thus relations (5) are the criterion of a correct determination of the two above-mentioned parameters.

Nevertheless, the quantitative determination of components is affected by random errors which cannot be eliminated. In qualitative determination of phases, errors could be also introduced by crystallo-chemical formulae, (fluctuating between sometimes large limits) which are assigned to phases, in the natural paragenesis mineral phases being frequently affected by isomorphous chemical substitutions.

Therefore, the criterion-equations (5) have to be cautiously used, a certain limit should be imposed from which the system is to be considered incompatible*, in most cases a rough solving of the system (5) being preferred.[8,9] In this case, we shall apply the least square method transforming the system (5) into the following compatible one :

---

* this limit separates random errors from mistakes.

$$\frac{\partial}{\partial \chi_j} \sum_{i=1}^{m} \left[\Gamma^i - \sum_{k=1}^{n} a_{ik} \cdot \frac{m_i}{M_k} \cdot \chi_k \right]^2 = 0 ; \; j = 1, 2, \ldots, n \qquad (7)$$

Finally we have to emphasize that the nonhomogeneous and linear algebraic system (5) is always uniquely determined. According to the mineralogic phase principle, m (the number of components of the system) will be greater or at least equal to n (the number of phases) because the highest number of crystalline phases which may coexist in rocks at stable equilibrium, is equal to the number of components, so that we have always sufficient independent equations to solve the system (5).

Moreover, applying relations (7), superabundance of equations is reduced, the result being a system of a number of equations equal to the number of unknown quantities. In case of simple natural systems at equilibrium the qualitative phase composition may be approximately established out of thermodynamic conditions by means of binary and polinary phase diagrams or ACF facies diagrams.[10] For open systems, with "mosaic" equilibrium, or in those partially equilibrated, the phase composition is complex and unpredictable. In this case, having a system of systems, we resort to experimental determination of phases.

As for the isomorphous chemical substitutions, the resulting difficulties are eliminated by taking into account the extremes of the series as independent phases and then recalculating the percentage amount of the unitary phase, together with its precise chemical formula, which is difficult to obtain by other means.

Since neither thermodynamical conditions of the system formation process nor the small reaction rate in the solid phase are known, the components of system are considered the oxides of the elements forming the phases. A determination of these conditions would decrease the number of components and of equations (5).[6]

APPLICATIONS

In order to illustrate the application of the described method, two examples were chosen, consisting of a rock (orthoamphibolite) and a refractory material (syntherized magnesite). In Table 1, the chemical composition (in oxides) of the orthoamphibolite and magnesite are shown in weight percentages.

Since the sum of chemical analysis data yielded a percentage of under 100%, the sum was arbitrary considered 100% and the concentrations of individual components were recomputed on this basis.

The phases (minerals) are shown in Table 2.[11] For syntherized magnesite they were determined by X-ray diffraction, and microscopically for orthoamphibolite (in thin sections). Ten planimetrical measurements[12-14] were also made on thin sections, the average of which is shown in Table 3.

With these data, by means of standard densities of minerals, the weight percentage of each mineral was calculated. From optical constants of minerals we have determined isomorphous substitutions which appear, without exactly defining the substitution degree.

Table 1

Chemical composition in oxides, weight %

Components	Orthoamphibolite	Syntherized magnesite
SiO_2	47.41	4.59
TiO_2	1.24	—
Al_2O_3	14.77	1.15
Fe_2O_3	3.47	1.13
FeO	5.30	—
MnO	0.208	—
MgO	9.78	92.45
CaO	9.37	0.68
K_2O	0.12	—
Na_2O	4.79	—
P_2O_5	0.364	—
CO_2	1.66	—
H_2O +105°C	1.518	—

Table 2

Chemical formulae of phases (minerals)

Minerals	Chemical formulae
Biotite	$K(Fe_{0.7120}Mg_{0.2880})_3[AlSi_3O_{10}\|(OH)_2]$
Calcite	$CaCO_3$
Ore Ilmenite	$FeTiO_3$
Magnetite	$FeO.Fe_2O_3$
Clinochlore	$5MgO.Al_2O_3.3SiO_2.4H_2O$
Apatite	$10CaO.3P_2O_5.H_2O$
Zoisite	$4(Ca_{0.6052}Mn_{0.3948})O.3Al_2O_3.6SiO_2.H_2O$
Plagioclase (7.63% An)	$12.15\ (Na_2O.Al_2O_3.6SiO_2) + 2CaO.2Al_2O_3.4SiO_2$
Hornblende	$0.6Na_2O.3.7CaO.8.5(Mg_{0.8746}Fe_{0.1254})O.2.2Al_2O_3.13SiO_2.2H_2O$
Periclase	MgO
Magnesioferrite	$MgO.Fe_2O_3$
Spinel	$MgO.Al_2O_3$
Monticellite	$CaO.MgO.SiO_2$
Forsterite	$2MgO.SiO_2$

By this method we estimated that plagioclase has approximately 10% anorthite (7.63% with our method). Using the FORTRAN programme [15,16] the chemical analysis from Table 1 and the identification of the phases, we obtained both the phase composition and the accurate formulae of the phases at the same time.

A good agreement is noted between the two methods used, with some limitations of the classical planimetric method. The qualitative phase composition being simple and known from thermodynamic data, when the refractory materials are studied, the advantage of the FORTRAN programme is obvious because the minerals percentages are listed by the computer, and depend on the chemical composition.

Table 3

Quantitative phase composition, surface % and weight %

Minerals (Phases)	Orthoamphibolite			Syntherized magnesite
	Surface a), %	Weight b), %	Weight c), %	Weight c), %
Biotite	—	—	1.29	—
Calcite	4.20	3.50	3.78	—
Ore: Ilmenite	4.50	7.10	2.35	—
Ore: Magnetite			5.03	
Clinochlore	3.20	2.50	2.83	—
Apatite	0.80	0.80	0.86	—
Zoisite	1.50	1.60	1.72	—
Plagioclase	38.60	33.90	34.07	—
Hornblende	47.20	50.60	48.07	—
Periclase	—	—	—	86.13
Magnesioferrite	—	—	—	1.42
Spinel	—	—	—	1.60
Monticellite	—	—	—	1.90
Forsterite	—	—	—	8.95

a) determined by planimetry
b) calculated from % surface
c) calculated from chemical composition, by proposed method.

CONCLUSIONS

This method offers an efficient and rapid means of determining the quantitative phase composition, eliminating a series of inexactities of other possibilities. It can also be used for other types of physical systems such as organical systems in liquid phase at equilibrium where there are no specific methods of phase determination or if previous separation of the phases is absolutely necessary.

ACKNOWLEDGEMENTS. The author thanks Dr. Al. Kissling for his valuable suggestions and discussions in mineralogical questions. Gratitude is expressed to Dr. J. Fazakas for his help.

REFERENCES

[1] A. Bezjak and I. Jelenic, "2nd International Symposium on Autoclaved Calcium Silicate Building Materials", Hannover, 1969.
[2] A. Bozjak, *Analy t·Chem.*, **47**, 790 (1975).

[3] L. E. Copeland and R. M. Bragg, *Analyt. Chem.*, **30**, 196, (1958).

[4] E. Szadeczky-Kardoss, *Acta Geologica Hungarica*, **X**, 69 (1966).

[5] M. Teichgräber, *Faserforsch. Textiltch.*, **18**, 359, (1967).

[6] D. Korjinskii, "Fizico-himiceskie osnoby analiza paragenezisov mineralov", Moscow, Izd. Akad. Nauk, SSSR, 1957.

[7] G. Joos, "Lehrbuch der Theoretischen Physik, Leipzig", Akad. Verlagsges., 1964.

[8] B. Carnahan, H. A. Luther and J. O. Wilkes, "Applied Numerical Methods", New York, Wiley, 1969.

[9] B. J. Scarborough, "Numerical Mathematical Analysis", Baltimore, The Johns Hopkins Press, 1966.

[10] V. I. Posypaiko, V. N. Pervikova and F. S. Veselova, *Zhur. neorg. Khim.*, **20**, 1050 (1975).

[11] M. Fleícher, "Glossary of Mineral Species", 1975.

[12] H. Freund, "Handbuch der Mikroscopie in der Technik", Band IV, Teil 1, Frankfurt/Main Umschau Verlag, 1955.

[13] F. Chayes, *Amer. Min.*, **40**, 126 (1955).

[14] F. Chayes, *Econ. Geol.*, **41**, 749 (1946).

[15] Fr. Stuart, "FORTRAN Programming", New York, John Wiley, 1969.

[16] M. L. James, "Applied Methods for Digital Computation with FORTRAN", Scranton-Pennsylvania, International Textbook Company, 1970.

Revue Roumaine de Chimie, **33**, *4*, 371–376 (1988)

ORTHO EFFECTS OF SUBSTITUENTS IN OXIMES, HYDRAZONES AND AZINES DERIVED FROM BENZALDEHYDES BY ELECTRON IMPACT

L. DAGNINO[a] and E. CORTÉS *
Instituto de Química, Universidad Nacional Autónoma de México
Circuito Exterior, Cd. Universitaria, Coyoacán, 04510 México, D. F.
[a]Escuela de Ciencias Químicas, Universidad Autónoma del Estado de México

Received November 3, 1986

The mass spectra of deuterated and non-deuterated oximes, hydrazones and azines derived from *ortho*-substituted benzaldehydes were studied ; their fragmentation pathways were found to be under the influence of the *ortho* effect of the substituents. The proposed fragmentation mechanisms and patterns were confirmed by the spectra recorded from the deuterium labelled derivatives and from the measurement of the metastable peaks.

Previous studies about the electron impact fragmentation of *ortho* substituted benzaldoximes have reported the loss of single fragments.[1–5] It has also been noted that benzaldazine undergoes a rather simple fragmentation pathway due to the lack of substituents on the aromatic rings.[6]

In this paper we wish to report the mass spectral fragmentation patterns of oximes (Ia, Ib), hydrazones (II) and azines (III) derived from *ortho*-substituted benzaldehydes (Scheme 1), as well as the effect of such

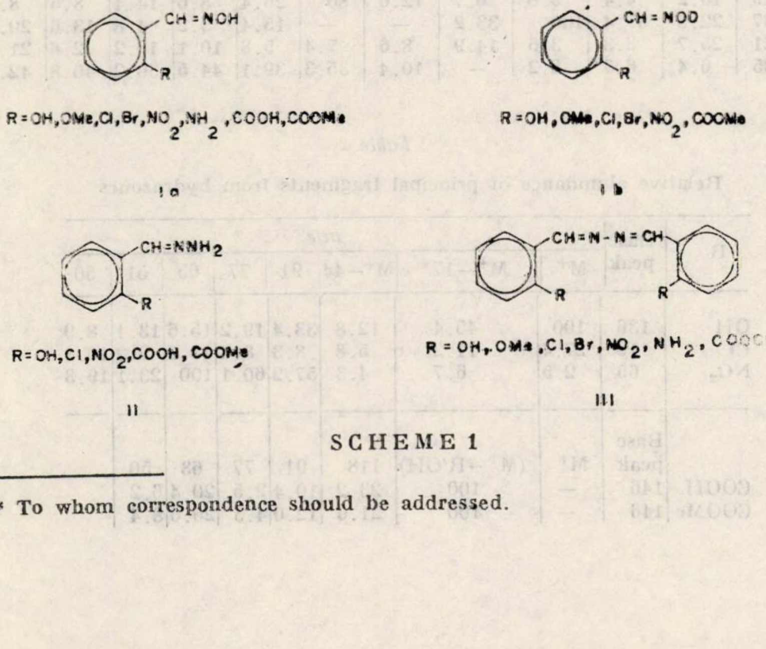
CH = NOH
R
R = OH, OMe, Cl, Br, NO2, NH2, COOH, COOMe
I a
CH = NOD
R
R = OH, OMe, Cl, Br, NO2, COOMe
I b
CH=NNH2
R
R = OH, Cl, NO2, COOH, COOMe
II
CH=N - N = CH
R
R
R = OH, OMe, Cl, Br, NO2, NH2, COOC
III

SCHEME 1

---

* To whom correspondence should be addressed.

substituents on their overall fragmentation pathway. The relative abundances of the observed ions are shown in Tables 1a, 1b, 2 and 3 and the proposed fragmentation patterns in Schemes 2 to 8.

Table 1a

Relative abundance of principal fragments from oximes

R	Base peak	*m/e*										
		M^+	M^+-17	M^+-18	M^+-44	M^+-45	91	77	65	63	51	50
OH	91	35.5	10.6	27.4	5.0	20.8	100	11.5	38.3	9.7	18.1	10.4
OCH_3	119	54.5	37.6	48.4	13.3	18.6	80.2	40.1	17.6	27.4	24.2	15.7
Cl	137	60.4	54.5	100	31.9	—	6.2	11.4	11.8	8.3	11.6	16.7
Br	120	59.8	5.4	—	14.7	6.2	9.4	9.1	37.3	15.2	6.2	20.7
NH_2	118	55.2	56.3	100	24.9	53.8	53.6	7.2	26.4	15.2	6.7	4.4
NO_2	135	10.4	19.3	28.2	—	13.7	34.5	35.9	71.2	40.5	75.6	73.2
	Base peak	M^+	(M^+-HR')	$(M^+-R'OH)$	133	104	90	77	66	51	50	39
COOH	104	—	84.3	20.2	31.8	100	7.3	30.2	4.5	10.6	30.3	8.0
COOMe	104	—	84.1	19.7	29.5	100	9.3	32.4	5.7	12.0	34.2	7.3

Table 1b

Relative abundance of principal fragments from deuterium-labelled oximes

R	Base peak	*m/e*											
		M^+	M^+-17	M^+-18	M^+-44	M^+-45	91	77	65	63	51	50	39
OH	91	21.3	27.2	56.4	7.3	27.6	100	7.5	20.1	38.4	10.8	8.3	22.6
OCH_3	119	15.2	4.4	3.8	16.7	12.6	80	26.4	8.6	14.4	8.5	8.0	4.2
Cl	137	22.8	37.4	100	33.2	—	—	15.4	3.2	4.8	13.6	20.2	5.8
Br	121	25.7	3.3	3.6	14.9	8.6	7.4	5.8	10.1	10.2	2.6	21.2	—
NO_2	135	6.4	6.7	8.2	—	10.4	35.3	39.1	44.5	30.2	46.8	42.3	31.4

Table 2

Relative abundance of principal fragments from hydrazones

R	Base peak	*m/e*							
		M^+	M^+-17	M^+-44	91	77	65	51	50
OH	136	100	45.4	12.8	33.4	19.2	15.6	13.1	8.9
Cl	119	27.4	11.2	5.8	8.3	8.4	13.9	9.2	10.1
NO_2	65	2.5	6.7	4.3	57.2	60.1	100	23.1	19.3
	Base peak	M^+	$(M^+-R'OH)$	118	91	77	63	50	
COOH	146	—	100	23.2	10.4	2.5	20.4	6.2	
COOMe	146	—	100	21.6	12.0	4.3	25.6	8.4	

Table 3

Relative abundance of principal fragments from azines

R	Base peak	m/e							
		M^+	M^+-R	M^+-2R	$M^+/2$	102	77	65	51
OH	240	100	46.2	13.1	22.7	13.2	—	8.1	6.4
OCH_3	119	21.3	60.4	18.7	19.4	10.6	48.5	8.7	17.6
Cl	206	14.5	93.7	100	14.3	42.1	13.7	3.4	9.4
Br	206	2.3	44.5	100	23.6	30.6	12.6	5.6	6.8
NH_2	65	88.4	65.1	10.1	81.2	15.7	42.5	100	12.3
NO_2	77	2.6	—	8.4	32.2	22.4	100	7.6	32.1
$COOCH_3$	130	7.7	50.3	14.6	10.0	60.5	37.5	5.0	5.0

Oximes I experience two initial losses from the molecular ion ; the first one involves the OH radical from the $-CH=N-OH$ group and leads to the fragment at *m/e* (M^+-17) [*m/e* (M^+-18) for the corresponding deuterium labelled derivatives]. The second loss stands for a water molecule, which yields the ion at *m/e* (M^+-18) [*m/e* (M^+-19) for deuterated compounds]. The fragments at *m/e* (75+R) and *m/e* (76+R) arise from a loss of HCN from the two ions described above. The derivatives substituted with OH, NH_2 and NO_2 follows the fragmentation patterns characteristic of such groups.

However, it is interesting to note that oximes substituted by $-COOH$ and $-COOCH_3$ groups have a completely different fragmentation pathway. Firstly, there is a loss of the hydrogen atom bonded to the oxygen of the $=N-OH$ group together with the group attached to the carboxylic oxygen, leading to an ion at *m/e* (M^+-HR'), which subsequently loses NO, giving rise to the fragment at *m/e* 133, as shown on Scheme 2.

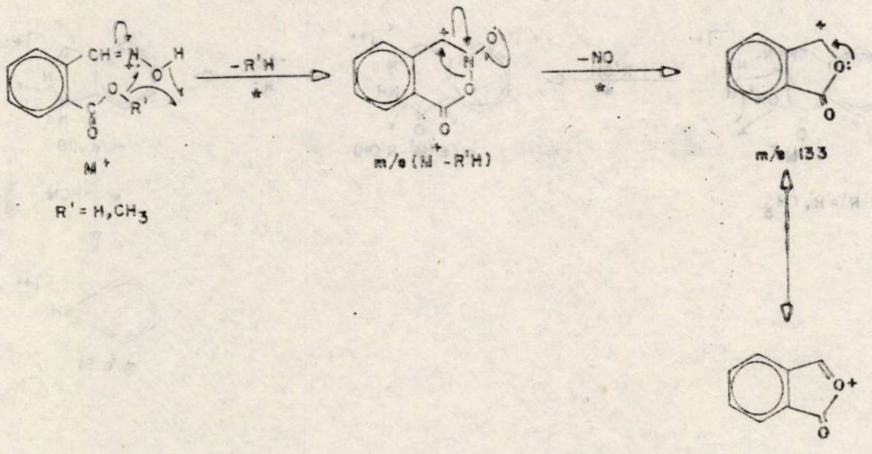

SCHEME 2

Another loss from the molecular ion is observed for these derivatives, which corresponds to the group borne by the carboxylic oxygen and the oxime OH radical, yielding a fragment containing a six-membered additional ring at m/e ($M^+ - R'OH$) (Scheme 3).

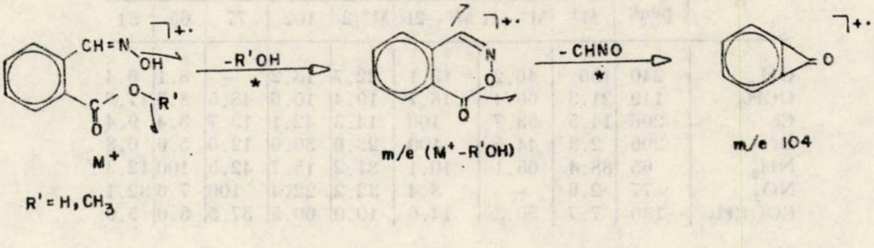

SCHEME 3

The fragmentation pattern exhibited by hydrazones II is very similar to that of oximes. In this series, the starting point is the loss of NH_3 from the molecular ion, giving rise to the fragment at m/e ($M^+ - 17$); the latter leads to an ion at m/e ($75 + R$) by losing HCN.

As it was seen for oximes, molecules substituted with OH and NO_2 groups tend to fragment according to the influence of such substituents upon them.

For these derivatives, once again the $-COOH$ and $-COOCH_3$ substituents affect greatly the fragmentation pathway of the molecule that bears them. There is an initial loss of one of the hydrogen atoms of the hydrazone NH_2 group, simultaneously to that of the $-OR'$ radical attached to the carboxyl group, on the *ortho* position, giving rise to the fragment at m/e ($M^+ - R'OH$), which afterwards undergoes the loss of CO, leading to an ion at m/e 118; the latter yields the fragment at m/e 91 by losing HCN, in the way pointed out on Scheme 4.

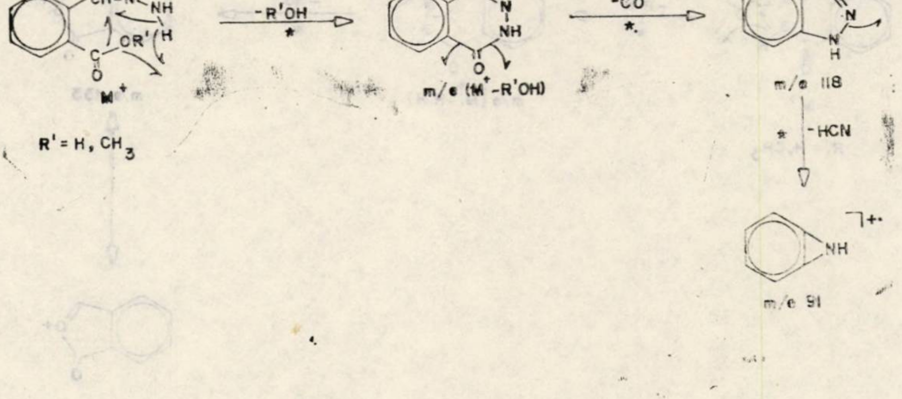

SCHEME 4

Azines III have a fragmentation pathway followed by all the members of the series and it includes the loss of one or both substituents from the molecular ion, to yield the fragments at *m/e* (M^+-R) and (M^+-2R); this second fragment undergoes the loss of C_7H_5N, producing an ion at *m/e* 102 whose structure is proposed to be similar to that of benzonitrile (Scheme 5). Furthermore, an ion at *m/e* ($M^+/2$) arises from the rupture of the N—N bond of the molecular ion, upon the loss of a portion of the molecule corresponding to C_7H_5NR (Scheme 6).

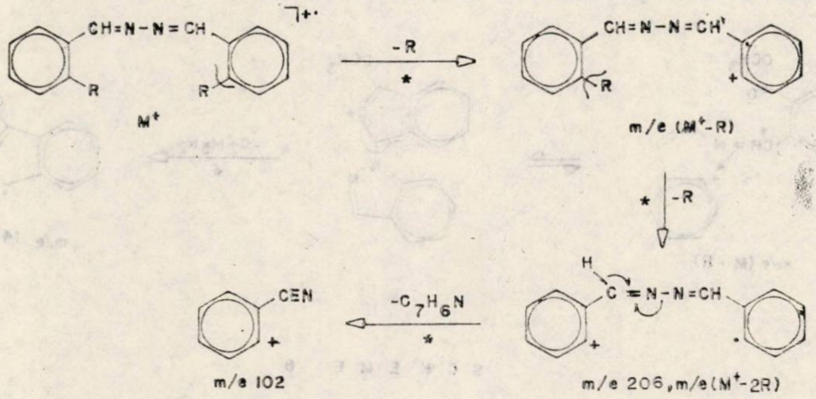
CH=N-N=CH
R
R
M+
-R
*
CH=N-N=CH'
R
+
m/e (M+-R)
*
-R
H
C=N-N=CH
+
m/e 206, m/e(M+-2R)
-C7H6N
*
CEN
+
m/e 102

SCHEME 5

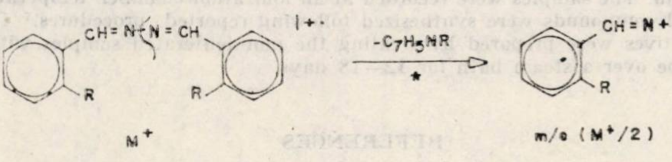
CH=N-N=CH
R
R
M+
-C7H5NR
*
CH=N+
R
m/e (M+/2)

SCHEME 6

With such substituents as NH_2 and OH, there is an ion at *m/e* ($103+X$) [$X=O$, NH] with a high relative abundance, which is formed once again by the N—N bond rupture and the subsequent cyclization of the remaining fragment, as shown on Scheme 7.

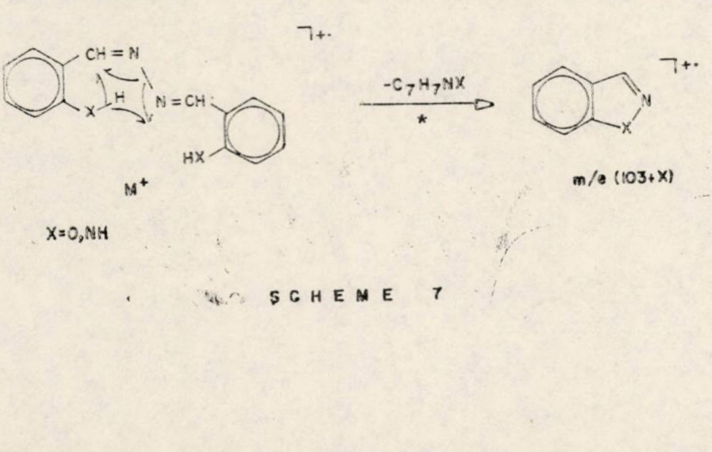
CH=N
H
X
N=CH
HX
M+
X=O,NH
-C7H7NX
*
N
X
m/e (103+X)

SCHEME 7

When the $-COOCH_3$ group is present, the ion at *m/e* ($M^+ - R$) undergoes a rearrangement where the carboxylic oxygen atom plays an important role, causing a "double cyclization" of the fragment, which loses readily $C_7H_5N_2$ to generate an ion at *m/e* 148.

The proposed mechanism that accounts for this loss is shown on Scheme 8. The characteristic fragments of substituents such as NO_2, NH_2 and OH are also present for these derivatives.

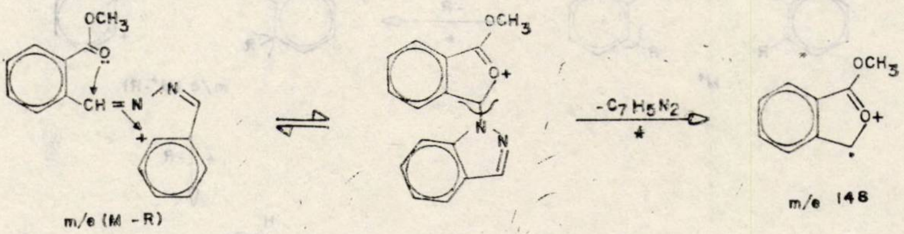

SCHEME 8

EXPERIMENTAL

The mass spectra were measured on a Hitachi Perkin-Elmer RMU-7H double focus mass spectrometer and on a Hewlett-Packard 5985A quadrupole mass spectrometer, using the direct inlet system. The samples were recorded at an ionization chamber temperature of 195°C. Non-deuterated compounds were synthesized following reported procedures.[7] The deuterium labelled derivatives were prepared by treating the non-deuterated samples with D_2O-MeOD in a sealed tube over a steam bath for 12—18 days.

REFERENCES

[1] P. Vijfhuizen, W. Heerma, and G. Dijkstra, *Org. Mass Spectrom.*, **10**, 919 (1975).
[2] P. Vijfhuizen and J. Terlow, *Org. Mass. Spectrom.*, **11**, 888 (1976).
[3] P. Vijfhuizen *et al.*, *Org. Mass Spectrom.*, **11**, 1198 (1976).
[4] P. Vijfhuizen, W. Heerma and N. Nibbering, *Org. Mass Spectrom.*, **11**, 787 (1976).
[5] P. Vijfhuizen and J. Terlow, *Org. Mass Spectrom.*, **12**, 63 (1977).
[6] B. Zeeh and R. Beutler, *Org. Mass Spectrom.*, **1**, 791 (1968).
[7] R. Shriner, "The Systematic Identification of Organic Compounds", John Wiley, New York, 1976 p. 254.

Revue Roumaine de Chimie, **33**, *4*, 377–383 (1988)

REACTIONS OF PYRYLIUM SALTS WITH NUCLEOPHILES. XX.[1]

SYNTHESIS OF 4-(N-PYRIDINIUM)-4′-DIALKYLAMINOAZOBENZENE AND OF 4-(4-DIALKYLAMINOPHENYLAZO)-4′-(N-PYRIDINIUM)-BIPHENYL DERIVATIVES *

ALEXANDRU T. BALABAN and CHOI IL

Polytechnic Institute, Organic Chemistry Department, Splaiul Independenţei 313,
76206 Bucharest, Romania

Received October 5, 1987

The reaction of 2,4,6-trisubstituted pyrylium salts with primary aromatic diamines in molar ratio 1 :1 yields N-arylpyridinium salts possessing one diazotizable amino group. On coupling the corresponding diazonium salts with N,N-dialkylanilines, cationic azo-derivatives result. They are yellow-to orange-coloured, but become violet in acid medium. Structures are proved by IR and ^{1}H-NMR spectroscopy. The cationic azoderivatives present good tinctorial and fastness properties on polyacrylonitrilic fibres.

INTRODUCTION

A previous part in this series [1] reported that 2,4,6-trisubstituted pyrylium salts reacted with *p*-phenylenediamine and its derivatives forming 1,4-phenylene-bis-pyridinium salts ; a few such compounds had been described earlier.[2–5] However, when the benzene ring carried also bulky or electronegative substituents, only one of the two amino groups was converted into a pyridinium ring.[1]

In the present paper we show such pyridinium salts obtained from *m*- or *p*-phenylenediamines, 1,4-naphthalenediamine or benzidine are converted by reacting with pyrylium salts into N-substituted pyridinium salts possessing a primary aromatic amino group. Subsequent diazotization and coupling with N,N-dialkylanilines affords new cationic azo dyes possessing a pyridinium ring.

---

* Paper based on the Ph. D. thesis submitted at the Polytechnic Institute of Bucharest, 1987 by Choi Il (previous name Lyu Yong Uk).

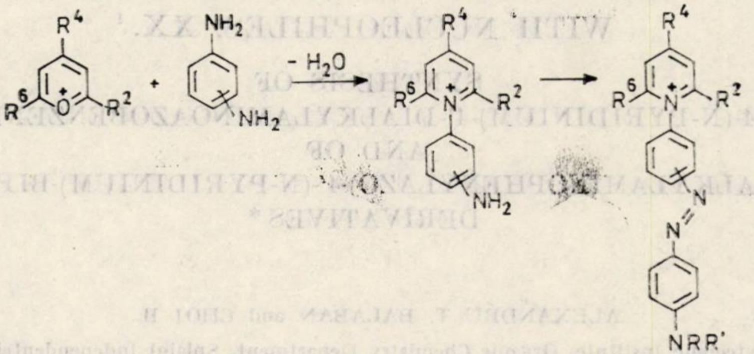

The literature on cationic heterocyclic azo dyes contains numerous references to pyridinium systems.[5–8] These have been prepared by quaternization of pyridines, and therefore they cannot contain an $\overset{+}{N}$-aryl bond. Such pyridinium salts are liable to undergo fragmentation of the exocyclic bond to the pyridinium ring, as shown by Susan and Balaban [9] and by Katritzky et al. for N-alkyl-2,4,6-triarylpyridinium salts.[10] By contrast, the systems described in the present paper are N-arylpyridinium salts with stronger bonds to the nitrogen heteroatom, and they are prepared by a new method.

One should stress that 2,4,6-trisubstituted pyrylium salts are readily available from simple starting materials. The most convenient method for synthesizing a large variety of 2,4,6-trialkylpyrylium salts consists in the diacylation of alkenes in the presence of Lewis or Brönsted acids.

In the present paper we report the preparation of pyridinium salts which have the perchlorate anion (starting from pyrylium perchlorates), but other anions which cause no danger of explosion (e.g. BF_4) or which lead to higher solubilities (e.g. sulfoacetate, halides) can be used. One starts either from pyrylium salts with other anions [11,12] or one converts the pyridinium perchlorates (which are convenient to manipulate and purify in small-scale laboratory work) into other salts by anion exchange. This exchange can be performed by taking advantage of the low solubility of potassium perchlorate, or by anion exchange resins.

SYNTHESIS OF N-(AMINOARYL)-PYRIDINIUM SALTS

The reaction between 2,4,6-trisubstituted pyrylium salts **1 a-c** and *p*-phenylenediamine **2** (molar ratio 1 :1) affords crystalline pyridinium perchlorates **3** possessing a *p*-phenyleneamino group (yields 75–85%). A longer reaction time was necessary for obtaining compound **3b** (5 hrs' refluxing in ethanol, instead of 2–3 hrs).

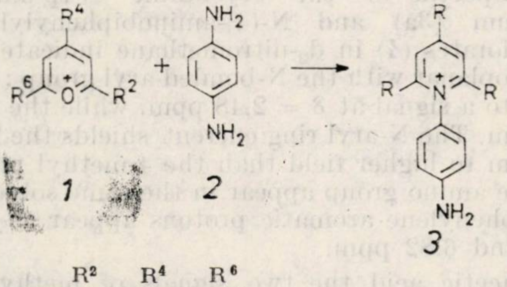

	R²	R⁴	R⁶
a	Me	Me	Me
b	Ph	Me	Ph
c	Me	Ph	Ph
d	Ph	Ph	Ph

With the sulfoacetate anion,[12] the reaction of **1a** occurs also, but no crystalline salts **3** could be obtained.

Perchlorate **1a** reacts more easily with benzidine than with **2** affording in high yield (95–98%) the corresponding crystalline 1-(4-aminobiphenylene-4')-2,4,6-trimethylpyridinium perchlorate, **4**.

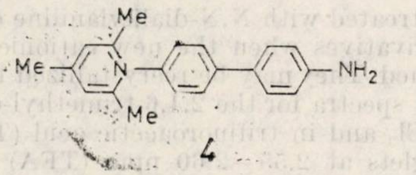

4

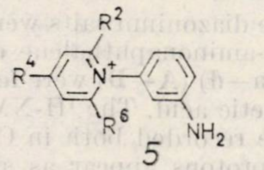

5

The perchlorates **5** obtained from pyrylium salts **1a-c** with *m*-phenylenediamine were used without separation or purification because they were not obtained in crystalline form.

In all the above cases one must employ equimolar ratios of diamine and pyrylium salt in order to avoid the formation of bispyridinium salts. In the following cases, only monopyridinium salts **6** and **7** result at any molar ratio, as it was shown earlier,[1] on treating 1,4-diamino-2,5-dichlorobenzene or 2,5-diaminobenzenesulfonic acid, respectively, with 2,4,6-trimethylpyrylium salts **1a**.

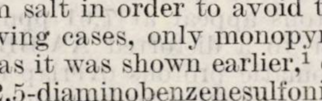

6

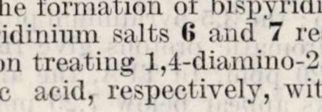

7

IR Spectra of all these salts **3**–**7** attest the presence of the amino group by N–H stretching bands in the range 3350–3400 cm^{-1}, and of the perchlorate anion by the characteristic strong bands at 625 and 1100 cm^{-1}.

^1H–NMR Spectra of the crystalline N-(p-aminophenyl)-2,4,6-trimethylpyridinium (**3a**) and N-(4′-aminobiphenylyl)-2,4,6-trimethylpyridinium perchlorates (**4**) in d_3-nitromethane indicate that the pyridinium ring is not coplanar with the N-bonded aryl group : the 2,6-dimethyl protons give rise to a signal at $\delta = 2.48$ ppm, while the 4-methyl protons appear at 2.67 ppm. The N-aryl ring current shields the 2,6-dimethyl protons, shifting them to higher field than the 4-methyl proton.[13] The NH_2 protons of the free amino group appear in the same solvent at 2.80–2.85 ppm, and the *p*-phenylene aromatic protons appear as an AA′BB′ quadruplet at 6.70 and 6.82 ppm.

In trifluoroacetic acid the two signals of methyl protons for **3a** appear at 2.53 (6H) and 2.72 (3H) ppm, and the NH_2 protons are not visible owing to rapid exchange with the solvent.

SYNTHESIS OF THE NEW HETEROCYCLIC CATIONIC AZO DYES

The pyridinium salts **3**–**6** are soluble in aqueous hydrochloric acid and the solutions have violet colour. By diazotization at 0°–5° for one hour in aqueous or acetic acid medium with aqueous sodium nitrite, the diazonium salts are formed ; although in several cases they formed crystalline solids, these were not isolated but coupled in the same solution.

The diazonium salts were treated with N,N-dialkylaniline or N,N-dimethyl-1-aminonaphthalene derivatives when the new cationic azo dyes (**8**–**13**) (**a**–**d**) (**A**–**D**) were formed. They may be recrystallized from ethanol or acetic acid. The ^1H-NMR spectra for the 2,4,6-trimethyl-derivative **8aA** were recorded both in $CDCl_3$ and in trifluoroacetic acid (TFA). The 2,6-Me_2 protons appear as singlets at 2.55–2.60 ppm (TFA) or 2.37–2.40 ppm ($CDCl_3$), while the 4-Me protons appear at 2.73 ppm (TFA) or 2.58–2.60 ppm ($CDCl_3$) ; owing to the ring current of the N-aryl group, the 2,6-methyl protons are shielded and appear at higher field than the 4-methyl proprotons. The dimethylamino protons appear at 3.08 ppm ($CDCl_3$) and 3.60 (TFA). In $CDCl_3$ and AA′BB′ quadruplet at 6.70 and 7.49 ppm is due to the aromatic protons *ortho* and *meta* to the dimethylamino group ; the 3,5-pyridinium protons appear at 7.61 ppm, while the remaining aromatic protons give rise to a distorted AA′BB′ system at 7.77 and 8.20 ppm. In TFA, the aromatic protons overlap considerably but all peaks appear below 7.25 ppm indicating protonation of the molecule, as will be discussed in the following Section. The colour of the TFA solution is bright red, but in $CDCl_3$ it is orange-yellow. The TFA solutions present blue fluorescence.

The ^1H-NMR spectrum of **8aB** in $CDCl_3$ shows similarly the 2,6-Me_2 protons at 2.37 ppm (6H), the 4-Me protons at 2.59 ppm (3H), the CH_2 protons (NEt_2) at 3.47 ppm (4H) and the CH_3 groups (NEt_2) at 1.23 ppm (6H) ; in TFA the same groups give peaks at 2.50 (6H), 2.70 (3H), 3.93q (4H) and 1.50t (6H). The aromatic protons in $CDCl_3$ appear at 6.63 (2H)

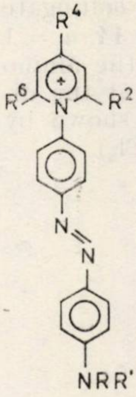

8

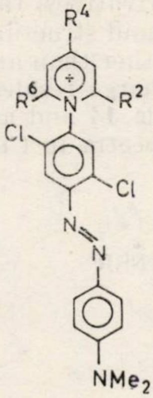

9

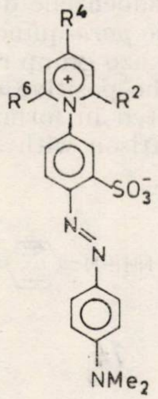

10

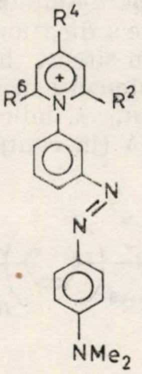

11

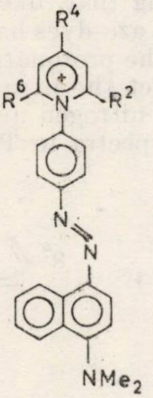

12

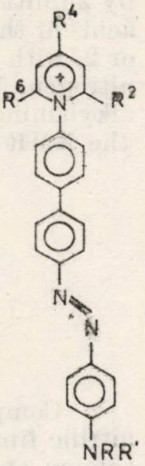

13

	A	B	C	D
R	Me	Et	Et	Et
R'	Me	Et	CH_2CH_2OH	CH_2CH_2CN

	R^2	R^4	R^6
a	Me	Me	Me
b	Ph	Me	Ph
c	Me	Ph	Ph
d	Ph	Ph	Ph

and 7.27 (2H) ppm (diethylaminophenyl), 7.57 (2H) ppm for pyridinium protons, 7.96 (2H) and 7.83 (2H) for the *p*-phenylene protons. In TFA, the pyridinium protons appear at 7.73 ppm.

Similar NMR spectra are obtained also for **8bA** and **8bB** : in TFA the 4-methyl protons appear at 2.90 ppm, the NMe_2 protons at 3.62 ppm, the NEt_2 protons at 3.92q and 1.47t and the pyridinium protons at 8.01 ppm. Also similar NMR spectra were obtained with azoderivatives **11** from the amine **5**.

The NMR spectra of **8aC** and **8aD** agree with the structure but there is considerable overlap of alkyl group protons.

The solutions of azoderivatives **12** with the benzidine moiety present an intense blue colour in trifluoroacetic acid ; NMR spectra confirm the structures.

ELECTRONIC ABSORPTION SPECTRA AND DYEING PROPERTIES

The longest-wavelength absorption band of the new dyes in methanolic solution appears at 440 – 460 nm ; all compounds **8 – 13** are yellow-orange or orange-coloured.

A marked bathochromic effect is observed on adding a strong mineral acid to the methanolic solution of compounds **8 – 12** ; the wavelength of maximum absorbance is shifted to 530 – 556 nm, with a shoulder around 650 nm, and the solution is violet-coloured. For compounds **13** the solution in acids is ink-blue. We interpret this bathochromic shift by admitting that, like *para*-aminoazobenzene derivatives, the conjugate acids of the azo-dyes have a dicationic *para*-quinonoid structure **14**, $n = 1$ or 2, with the protonation site at the azo group rather than at the amino nitrogen. Yet the main density of the positive charge resides at the dialkylamino nitrogen atom, as indicated in formula **14** and as shown by the NMR spectra in TFA (in comparison with spectra in $CDCl_3$).

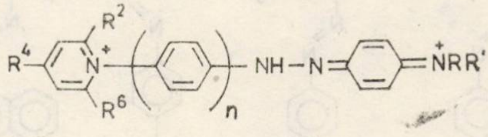

14

Compound **8aA** was tested for tinctorial properties on polyacrylonitrilic fibres, and was found to possess high light and wet fastness. The colours of the dyed fibres are yellow or orange.

EXPERIMENTAL PART

The electronic adsorption spectra were determined with a Specord UV-VIS (Jena) with methanolic $10^{-4}-10^{-5}$ M solutions. Vibrational spectra were determined with a Specord 71-IR (Jena) in potassium bromide pellets. ^{1}H-NMR spectra were recorded with 60 MHz Varian A-60A and EM-360 L instruments.

Reaction of pyrylium salts with p-phenylenediamine. To 10.5 g (100 mmol) *p*-phenylenediamine in 300 mL ethanol under reflux and mechanical stirring, 20 g (90 mmol) of 2,4,6-trimethylpyrylium perchlorate were added gradually, then the heating was continued for three hours. To the violet solution, a few mL of conc. aqueous ammonia were added for converting any unreacted pyrylium salt into *s*-collidine and the solution was cooled to room temperature. The deposited crystals were filtered off and recrystallized from methanol – ethyl ether : colourless product **3a**, 80% yield.

Reaction of pyrylium salts with m-phenylenediamine. Proceeding similarly with *m*-phenylenediamine, an oily lower layer was obtained on cooling the reaction mixture. It was separated, washed with ethyl ether, and used directly in the diazotization.

Reaction of pyrylium salts with benzidine. To a hot solution of 29.5 g (160 mmol) of benzidine in 200 mL ethanol, 2,4,6-trimethylpyrylium perchlorate (33.4 g, 150 mmol) was added and the solution was refluxed. After 3 – 5 minutes a clear solution results, then the pyridinium perchlorate **4a** crystallizes from the hot solution; treatment with ammonia, cooling, filtration and recrystallization from acetic acid affords the product **4a** in 88% yield.

Similar procedures were employed for 2-methyl-4,6-diphenyl-pyridinium, 4-methyl-2,6-diphenylpyridinium and 2,4,6-triphenyl-pyridinium derivatives : with *p*-phenylenediamine, colourless crystalline N-(*p*-aminophenyl)-pyridinium monoperchlorates are formed; they may be recrystallized from acetic acid.

Reaction of pyrylium salts with 2,5-diaminobenzenesulfonic acid. The acid (4 g, 21 mmol) was dissolved in a warm solution of 1.8 g (21 mmol) sodium hydrogen carbonate in 25 mL water, then 4.8 g (21 mmol) of 2,4,6-trimethylpyrylium perchlorate was added and the mixture was refluxed for 30 minutes. Then the solution was worked up in the usual manner.

Synthesis of azo dyes **8.** The pyridinium perchlorate **3a** (4 g, 13 mmol) was introduced into a solution of 5 mL conc. hydrochloric acid in 25 mL water; the cooled solution (0 – 5°) was treated with a concentrated aqueous solution of 0.9 g (13 mmol) sodium nitrite during 10 min., then the suspension was stirred for 2 hrs. The diazoderivative is obtained as a suspension. The coupling component is a solution of 1.7 g (14 mmol) dimethylaniline in 28 mL aqueous hydrochloric acid 0.72 N. After mixing the two reagents, crushed ice is added, then 8 g of crystalline sodium acetate hydrate is added and the mixture is stirred mechanically. The azoderivative crystallizes during 2 hrs at 10°, is filtered off, then washed successively with water, ethanol and ethyl ether for rapid drying, and recrystallized from ethanol. Yield 95%.

When the aromatic tertiary amine or the pyridinium salt are less soluble, the coupling component solution is prepared in aqueous acetic acid.

Elemental analyses of the new cationic dyes are presented in Table 1. Melting points are higher than 300°C.

Table 1

Structures and elemental analyses of the new cationic dyes

Comp.	NRR′	R^2	R^4	R^6	Formula	N%	
						Calc.	Found
8aA	Me_2N	Me	Me	Me	$C_{22}H_{25}N_4^+ClO_4^-$	12.59	12.60
8aB	Et_2N	Me	Me	Me	$C_{24}H_{29}N_4^+ClO_4^-$	11.85	11.73
8aC	$EtNCH_2CH_2OH$	Me	Me	Me	$C_{24}H_{29}H_4O_4^+ClO_4^-$	11.80	11.46
8aD	$EtNCH_2CH_2CN$	Me	Me	Me	$C_{25}H_{28}N_5^+ClO_4^-$	14.07	1.15
8bA	Me_2N	Ph	Me	Ph	$C_{32}H_{29}N_4^+ClO_4^-$	9.85	9.90
8bB	Et_2N	Ph	Me	Pu	$C_{34}H_{33}N_4^+ClO_4^-$	9.78	9.67
8cA	Me_2N	Me	Ph	Ph	$C_{32}H_{29}N_4^+ClO_4^-$	9.85	9.50
11aA	Me_2N	Me	Me	Me	$C_{22}H_{25}N_4^+ClO_4^-$	12.59	12.40
12aA	Me_2N	Me	Me	Me	$C_{32}H_{31}N_4^+ClO_4^-$	9.82	9.95
13aA	Me_2N	Me	Me	Me	$C_{28}H_{29}N_4^+ClO_4^-$	10.76	10.60
13aB	Et_2N	Me	Me	Me	$C_{30}H_{33}N_4^+ClO_4^-$	10.20	10.27
13aC	$EtNCH_2CH_2OH$	Me	Me	Me	$C_{30}H_{33}N_4O^+ClO_4^-$	9.92	9.95

ACKNOWLEDGEMENTS. Thanks are addressed to Dr. M. D. Gheorghiu and Mr. T. S. Balaban for ^1H-NMR spectra, to Prof. I. Pogany for electronic spectra, to Mrs. V. Mateescu for IR spectra, and to Mrs. A. Mihai for fastness determinations.

REFERENCES

[1] A. T. Balaban and E. Stepan, *Rev. Roum. Chim.*, **32**, 155 (1987).

[2] R. Neidlein and P. Witerzens, *Monatsh. Chem.*, **106**, 643 (1975).

[3] C. Toma and A. T. Balaban, *Tetrahedron*, Suppl. **7**, 9 (1966); G. N. Dorofeenko, Yu. P. Andreichikov, E. A. Zvezdina, V. A. Bren, G. E. Trukhova, V. V. Derbenev and A. N. Popova, *Khim. Geterotsikl. Soed.*, **1974**, 1349.

[4] E. Stepan and A. T. Balaban, *Rev. Roum. Chim.*, **28**, 707 (1983).

[5] W. Steinemann (to Sandoz Ltd.), French Pat. 1,501,256 (10 Nov. 1967), *Chem. Abstr.*, **70**, 48610 (1969).

[6] W. Bossard, J. Voltz and F. Favre (to J. R. Geigy A. G.), U. S. Pat. 2,864,813 (16 Dec. 1958), *Chem. Abstr.*, **53**, 8645 (1959).

[7] S. M. Tsang, C. E. Lewis and A. P. Paul (to American Cyanamid Co.), U. S. Pat. 2,893,816 (7 July 1959), *Chem. Abstr.*, **54**, 1868 (1960).

[8] C. W. Greenhalgh (to ICI Ltd.), Germ. Pat., 1,914,328 (2 Oct. 1969), *Chem. Abstr.*, **72**, 80343 (1970); corresponding to French Pat. 2,004,694 and to Brit. Pat. 1,249,468 (25 March 1968), *J. Soc. Dyers Colourists*, **88**, 39 (1972).

[9] A. B. Susan and A. T. Balaban, *Rev. Roum. Chim.*, **14**, 111 (1969).

[10] A. R. Katritzky, *Tetrahedron*, **36**, 679 (1980); A. R. Katritzky and C. M. Marson, *Angew. Chem. Int. Ed. Engl.*, **23**, 420 (1984); A. R. Katritzky and G. Musumarra, *Chem. Soc. Rev.*, **13**, 47 (1984).

[11] A. T. Balaban and A. J. Boulton, *Org. Synth.* Coll. Vol. **5**, 1112 (1979).

[12] A. Dinculescu and A. T. Balaban, *Org. Prep. Proc. Internat.*, **14**, 39 (1982).

[13] A. Dinculescu and A. T. Balaban, *Rev. Roum. Chim.*, **25**, 1505 (1980).

Revue Roumaine de Chimie, **33**, 4, 385–392 (1988)

MASS SPECTROMETRY OF DITERPENIC COMPOUNDS WITH A GLYCOL FUNCTION AT C_{16}—C_{17}

F. J. GARCÍA, R. CRUZ, O. COLLERA and J. L. SÁNCHEZ
Instituto de Química, Universidad Nacional Autónoma de México,
Circuito Exterior, Ciudad Universitaria, Coyoacán, 04510 México, D.F.

Received December 20, 1986

Mass spectrometric scrutiny of corymbol (**1**), 16,17,19-kaurantriol (**2**), cafestol (**3**), kahweol(**4**) and tetrahydrocafestol (**5**) reveals a common fragmentation involving C_{16}-C_{17} bound with the elimination of the hydroxymethylene group. This reaction competes with thermal dehydration of the glycol moiety which depends on the temperature of the ionization chamber.

INTRODUCTION

Tetracyclic diterpenes have a relatively rigid structure in which even small changes in substituents can modify steric interactions and hence intermolecular reactions which occur during decomposition after electronic impact. This characteristic renders them as an interesting target for the study of fragmentation paths in mass spectrometry, which are commonly postulated after the examination of results in simpler molecules.

The present research is directed to study the mass spectral fragmentation of some tetracyclic diterpene molecules having a common glycol functionality at $C_{16}-C_{17}$. There are some previous studies about the mass spectrometric degradation of kaurene derivatives,[1,2] as well as a general study on diterpenes [3] in which some tetracyclic diterpenes are included. However, there is no detailed study of diterpenes with the glycol functionality at $C_{16}-C_{17}$. The comparative examination of molecules having this common functionality may allow the observation of common fragmentation routes along with some peculiar fragments associated with the remaining functional groups. In the present paper we compare the mass spectrometric fragmentation of corymbol (**1**), 16,17,19-kaurantriol (**2**), cafestol (**3**), kahweol (**4**) and tetrahydrocafestol (**5**) (Fig. 1).

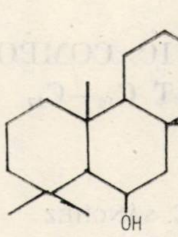

1

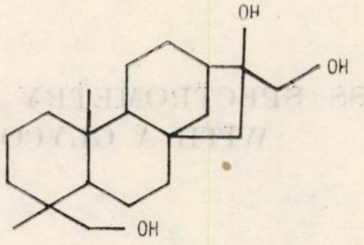

2

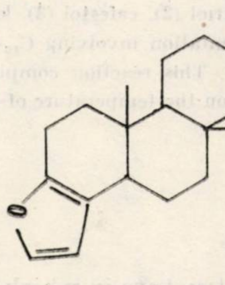

3

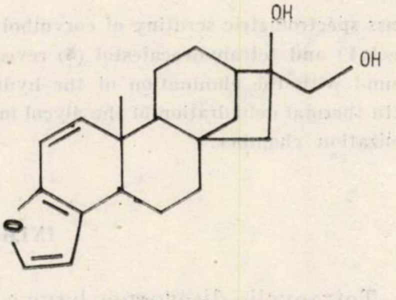

4

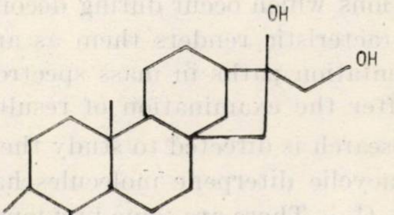

5

Fig. 1

RESULTS AND DISCUSSION

In all of the compounds studied we have been able to observe a fragmentation which is characteristic of the glycol functionality. This common fragmentation route leads to a protonated carbonyl at C_{16}, which is a rather stable fragment in all of the mass spectra examined. This particular fragmentation occurs simultaneously with a thermally sensitive dehydration of the hydroxy group at C_{16} leading to the enol of an aldehyde at C_{17} which is further decomposed. For instance, in the case of corymbol (Fig. 2) when one compares the mass spectrum of this compound with

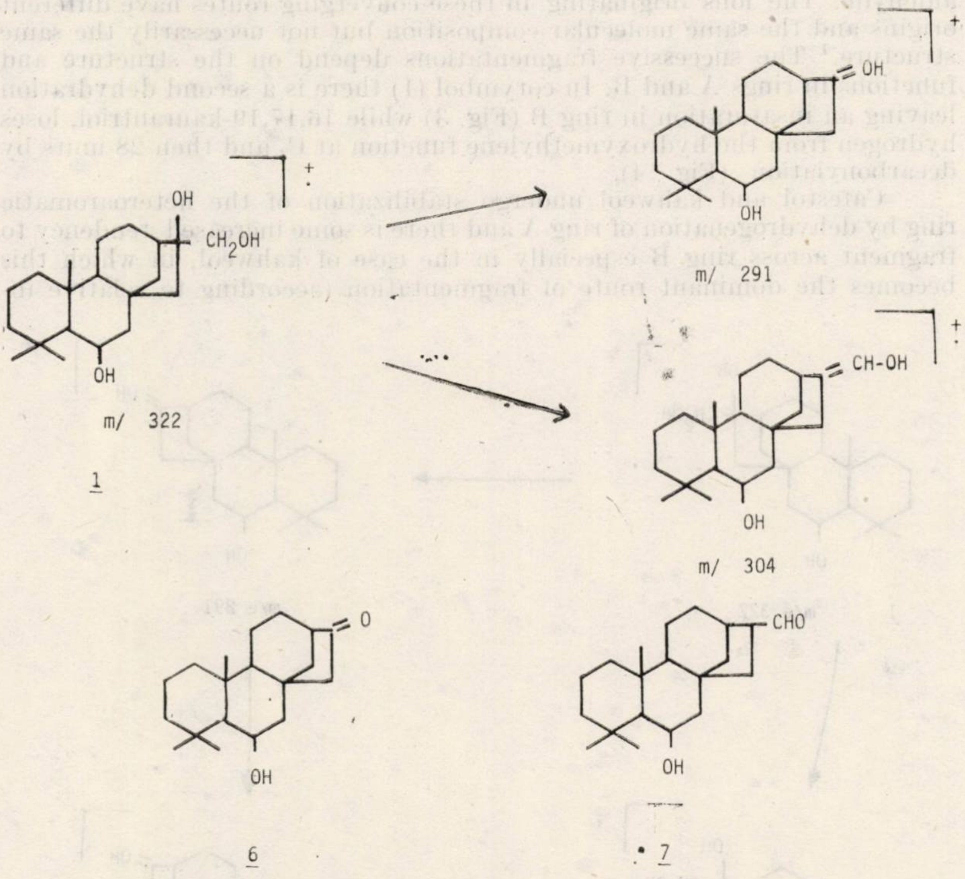

Fig. 2. — Main fragmentations pathways of corymbol **1**.

that of 6-hydroxykauran-16-one (**6**) and that of 6-hydroxykauran-17-al (**7**), the spectrum of corymbol is practically a combination of both in allmost every detail. Since dehydration is a temperature sensitive reaction, it is possible to modify its contribution by changing the ionization source temperature from 200° to 50° (in 25° intervals). A series of spectra of (1) was obtained in which the resemblance to that of 6-hydroxykauran-16-one (6) is greater when going to lower temperatures. In all of the compounds studied there is a similar competition between these two fragmentation pathways, that is to say, glycol rupture and C_{16} dehydration, but in general and especially at low ionization source temperature the loss of 31 mass units becomes dominant with the production of a protonated C_{16}

carbonyl function and the mass spectrum is very similar to that of the 17-norketone which is obtained from chemical oxidation with periodic acid.

During the study of these spectra it was possible to observe some converging fragmentation routes. These converging routes were found mainly during dehydration and glycol rupture reactions, and loss of formaldehyde. The ions originating in these converging routes have different origins and the same molecular composition but not necessarily the same structure.[4] The successive fragmentations depend on the structure and functions in rings A and B. In corymbol (1) there is a second dehydration leaving an insaturation in ring B (Fig. 3) while 16,17,19-kaurantriol, loses hydrogen from the hydroxymethylene function at C_4 and then 28 units by decarbonylation (Fig. 4).

Cafestol and kahweol undergo stabilization of the heteroaromatic ring by dehydrogenation of ring A and there is some increased tendency to fragment across ring B especially in the case of kahweol, in which this becomes the dominant route of fragmentation (according to relative intensity of the ions produced, Fig. 5), giving rise to fragments at *m/e* 132 and *m/e* 146. These fragments are accompanied by other intense fragments corresponding to the loss of hydrogen and with a structure which is possibly of the furotropilium type.[5] Cafestol and tetrahydrocafestol also show ions corresponding to this fragmentation route with two and four hydro-

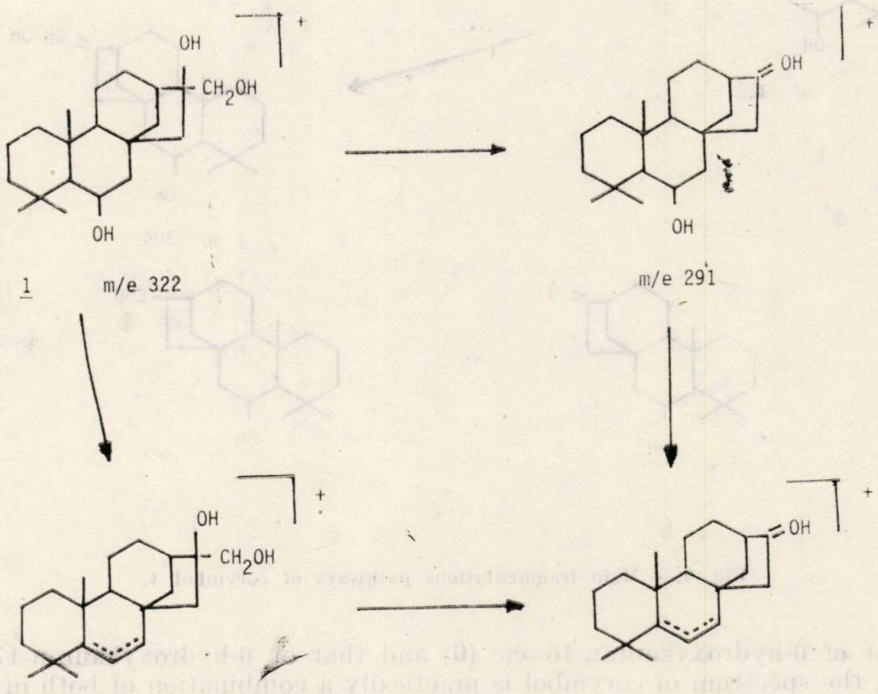

Fig. 3. — Alternative fragmentations pathways of corymbol 1.

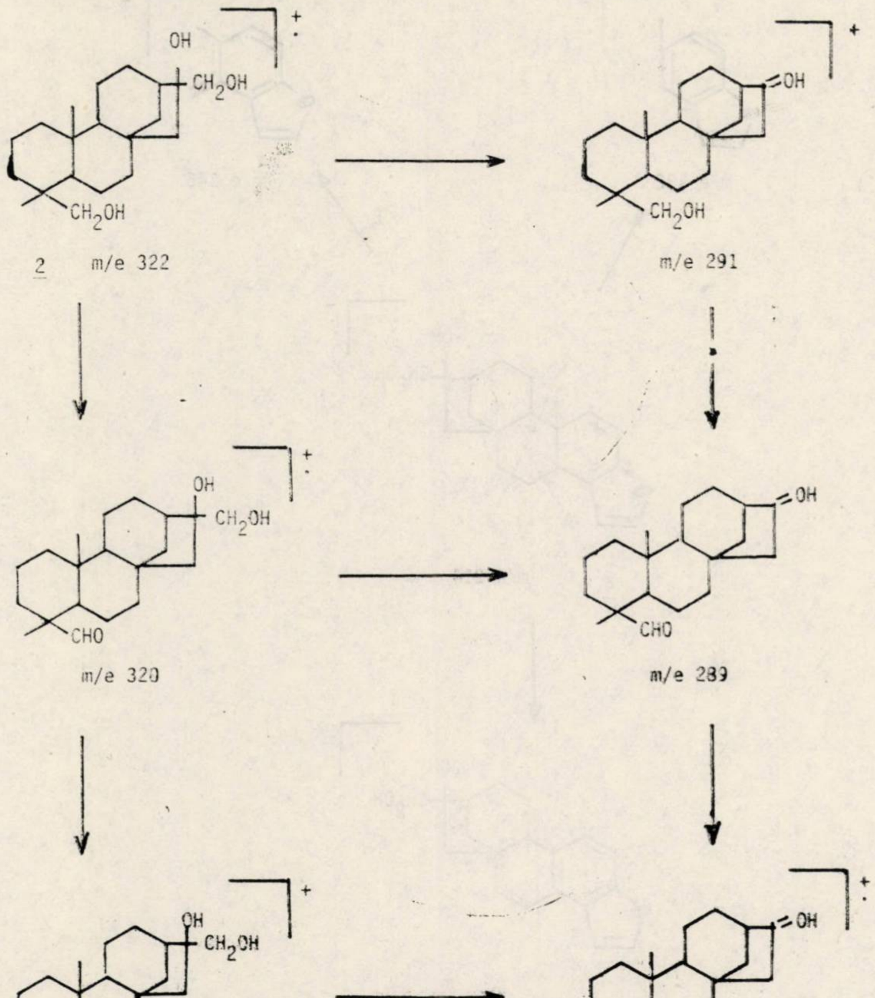

Fig. 4. — Fragmentation pattern of 16,17,19-kaurantriol 2.

gens more respectively (*m/e* 148, 134 and 150, 136 respectively) though with a much reduced relative intensity. This tendency agrees with a progressive weakening of C_5—C_6 and C_9—C_{10} bonds as they become allylic bonds.

In the spectra of kahweol there is an overall stabilization of the whole molecule evident through a much increased stability of the molecular ion. This spectra also shows a peculiar behaviour with respect to tetra-

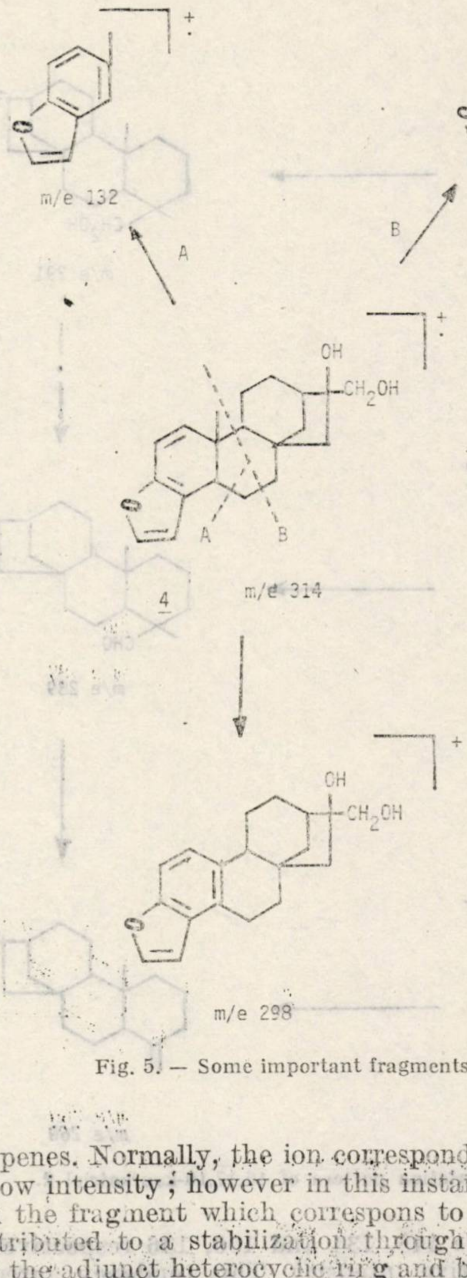

Fig. 5. — Some important fragments of kahweol 4.

cyclic diterpenes. Normally, the ion corresponding to the loss of methane is of very low intensity; however in this instance this fragment is much larger than the fragment which correspons to the loss of 15 units. This may be attributed to a stabilization through aromatization of ring A, induced by the adjunct heterocyclic ring and by the double bond in ring A (Fig. 5). In the mass spectrum of cafestol there is this type of fragmentation also, which shows an ion at *m/e* 300 by the loss of methane and another at *m/e* 298 originated by the loss of methane and hydrogen; however this route requires more energy than in the case of kahweol and gives ions of low intensity (Fig. 6).

In tetrahydrocafestol the fragments containing the heterocycle and retaining the charge are not very stable, and there are more intense fragments originating from ring A, as well as from the heterocyclic ring. As an example we can mention the fragment at *m/e* 276 that corresponds to the loss of C_2H_4O.[6]

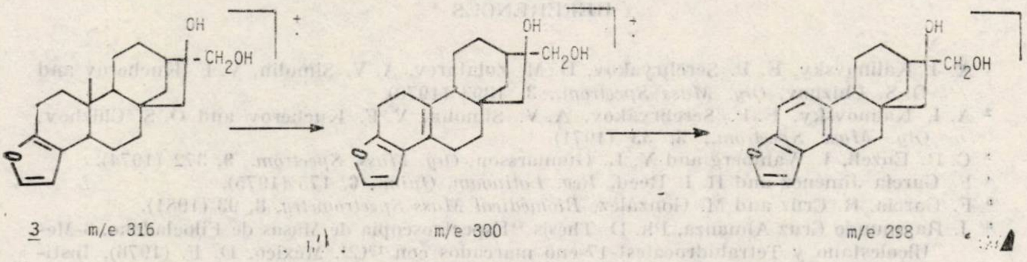

Fig. 6. — Postulated origin for fragments *m/e* 300 and *m/e* 298 of cafestol **3.**

EXPERIMENTAL

The mass spectra were obtained by H. Bojórquez at Instituto de Química, Universidad Nacional Autónoma de México, using a Hitachi-Perkin Elmer RMU-7H double focussing mass spectrometer. Samples were introduced directly to the ionization chamber. The ionization current was held at 80 μA and the ionization voltage at 70 eV. The experiments with the ionization chamber at various temperatures were carried in an AEI-MS 902s double focussing instrument with an ionization current of 100 μA and at 70 eV at the Chemistry Department of Glasgow University, thanks to the kindness of Dr. R. I. Reed.

Isolation of cafestol and kahweol. The isolation procedure is a modification of the method described by Slotta and Neisser.[7,8] Five kilograms of green Bourbon coffee from Fortín de las Flores, Veracruz, México, were ground. The finely ground coffee was extracted with chloroform in a flask protected from light and after the addition of 0.1% of 2,6 diterbuthyl-p-hydroxytoluene as antioxidant. The chloroformic extract was distilled and to the remaining oil one part of ether was added and filtered discarting the solids. Finally the ether was distilled and 0.1% more of antioxidant was added. The remaining oil was saponified according to Slotta and Neisser. The extract from the unsaponifiable fraction was purified by column chromatography in silica gel using ethyl acetate-hexane 1 :1 as eluant. The column was protected from light with black paper board ; the fractions were also protected from light with aluminum paper. The crystalline fractions were collected and extracted in a Soxhlet with hexane yielding white crystalls. Pure cafestol was obtained after reduction of the kahweol in the sample by established procedures.[9] Pure kahweol was obtained from the more polar fractions by rechromatography and crystallization from ethyl acetate. Tetrahydro cafestol was obtained from cafestol by total hydrogenation.[7] Corymbol is of synthetic origin [10] and 16,17,19-kauranetriol was obtained by enzymatic hydrolysis of corymbositine.[11]

Mass spectral data for fragments which are discussed in the text are as follows :

Corymbol *m/e* (rel. int.) ; 322 (1), 304 (3.3), 291 (82.6), 289 (15), 286 (15.3), 273 (100), 255 (19), 123 (39), 121 (64), 119 (40). Metastable transitions : 322 → 291 (263.0), 304 → 273 (245.2), 291 → 273 (256.1).

16,17,19-Kaurantriol *m/e* (rel. int.) : 322 (0.9), 320 (0.3), 304 (3), 291 (97.0), 289 (70), 275 (85.0), 273 (18.6), 260 (27), 255 (34.5), 135 (47.9), 123 (100), 121 (57.2). Metastable transitions : 322 → 291 (263.0), 322 → 320 (287.0), 320 → 291 (264.6), 320 → 289 (261), 291 → → 289 (287.0), 291 → 260 (232.3), 289 → 260 (233.9).

Kahweol *m/e* (rel. int.) ; 314 (100), 299 (3.4), 298 (6.7), 296 (0.9), 283 (13.5), 147 (62.9), 146 (33.7), 132 (40.5), 131 (49.5). Metastable transitions : 314 → 283 (255.0), 314 → 298 (282.8), 314 → 146 (67.9), 314 → 132 (55.5), 296 → 146 (72.0), 296 → 132 (58.9), 283 → 146 (75.3), 283 → 132 (61.5).

Cafestol m/e (rel. int.) : 316 (1.5), 301 (1.5), 300 (1.0), 298 (1.7), 285 (7.7), 149 (2.4), 148 (6.9), 134 (2.8), 133 (3.6), 57 (100). Metastable transitions : 316 → 285 (257.0), 316 → 300 (284.8), 300 → 298 (296.0).

Tetrahydrocafestol m/e (rel. int.) : 320 (0.5), 312 (1), 289 (25.0), 276 (2.0), 275 (5.0), 271 (3.5), 263 (17.8), 262 (21.3), 261 (100), 245 (10.6), 151 (14.2), 150 (6.3), 136 (5.0), 135 (12.5). Metastable transition : 320 → 289 (261.0).

REFERENCES

[1] A. I. Kalinovsky, E. P. Serebryakov, B. M. Zolatarev, A. V. Simolin, V. F. Kucherov and O. S. Chizhov, *Org. Mass Spectrom.*, **3**, 1393 (1970).

[2] A. I. Kalinovsky, E. P. Serebryakov, A. V. Simolin, V. F. Kucherov and O. S. Chizhov, *Org. Mass Spectrom.*, **5**, 33 (1971).

[3] C. R. Enzell, I. Wahlberg and Y. L. Gunnarsson, *Org. Mass. Spectrom.*, **9**, 372 (1974).

[4] F. García Jiménez and R. I. Reed, *Rev. Latinoam. Quim.*, **6**, 175 (1975).

[5] F. García, R. Cruz and M. González, *Biomedical Mass Spectrometry*, **8**, 93 (1981).

[6] J. Raymundo Cruz Almanza, Ph. D. Thesis "Espectroscopia de Masas de Filocladeno, 3-Metilcolestano y Tetrahidrocafest-17-eno marcados con ^{13}C", México, D. F. (1976), Instituto de Química, U.N.A.M.

[7] K. H. Slotta and K. Neisser, *Ber.*, **71**, 1991 (1938).

[8] P. N. Chakravorty, M. M. Wesner and R. H. Levin, *J. Am. Chem. Soc.*, **65**, 929 (1943).

[9] A. Wettstein, M. Spillmann and K. Miescher, *Helv. Chim. Acta*, **28**, 1004 (1945).

[10] M. C. Perezamador and F. García, *Tetrahedron*, **22**, 1937 (1966).

[11] F. García, O. Collera, G. Larios, J. Taboada and M. C. Perezamador, *Rev. Latinoam. Quim.*, **10**, 181 (1979).

Revue Roumaine de Chimie, **33**, *4*, 393—398 (1988)

SOME REACTIONS OF α,β-UNSATURATED ACYL ISOTHIOCYANATES

NOSRAT MUSTAFA ABED[a], ABDEL-GHANI ALI ELAGAMEY[b] *, SALAH ZAKI SOWELLIM[b] and ABDEL-FATTAH ALI HARB[c]

[a] Department of Chemistry, Faculty of Science, Cairo University, Giza. A.R. Egypt
[b] Faculty of Science (Damietta), Mansoura University, A. R. Egypt
[c] Faculty of Science, Qena University, A. R. Egypt

Received September 15, 1986

Nucleophilic addition reactions of α, β-unsaturated acyl isothiocyanates **1** with aromatic and heteroaromatic amines have been studied. Compound **12** was also prepared and afforded pyrazolo[1,5-a]-*s*-triazine, coumarine and pyrazolo[1,5-c]-*as*-triazine derivatives on treatment with potassium hydroxide, salicylaldehyde and diazotised aminopyrazole respectively.

RESULTS AND DISCUSSION

Aroyl and acyl isothiocyanates are versatile reagents and their chemistry has received considerable recent interest.[1–4] These reagents can react with a variety of polyfunctional molecules either *via* addition followed by cyclisation or *via* cycloaddition to yield a variety of heterocyclic derivatives. In the present study, we investigated additions of aromatic and heteroaromatic amines to α,β-unsaturated acyl isothiocyanates with the aim to obtain intermediates suitable for further cyclisation. Thus, treatment of **1a,b** with 4-aminoantipyrine has resulted in the formation of the corresponding thiourea derivatives **2a,b** in high yield. Similarly, 4-aminopyridine and 2-aminopyrimidine reacted smoothly with **1c** to afford the expected adducts **3** and **4** respectively. On the other hand, 3-amino-1,2,4-triazole (**5**) and 2-aminothiazole (**6**) reacted with **1a,c** to yield the acyl amino derivatives **7** and **8** respectively. The same products could be also obtained from the reaction of each of the amines **5** or **6** and the appropriate acid chloride in dry pyridine (Chart 1).

The formation of **8** from the reaction of **1** with **6** is assumed to proceed *via* intermediate formation of adduct **9**, which readily decompose to give **8** *via* HCNS elimination. Also, compound **7** may be formed under a similar mechanism (Chart 1).

In contrast, the experiments indicate that in the case of aromatic compounds carrying both a thiol and an amino group, a preferential attack

---

* Correspondence author A. A. Elagamey

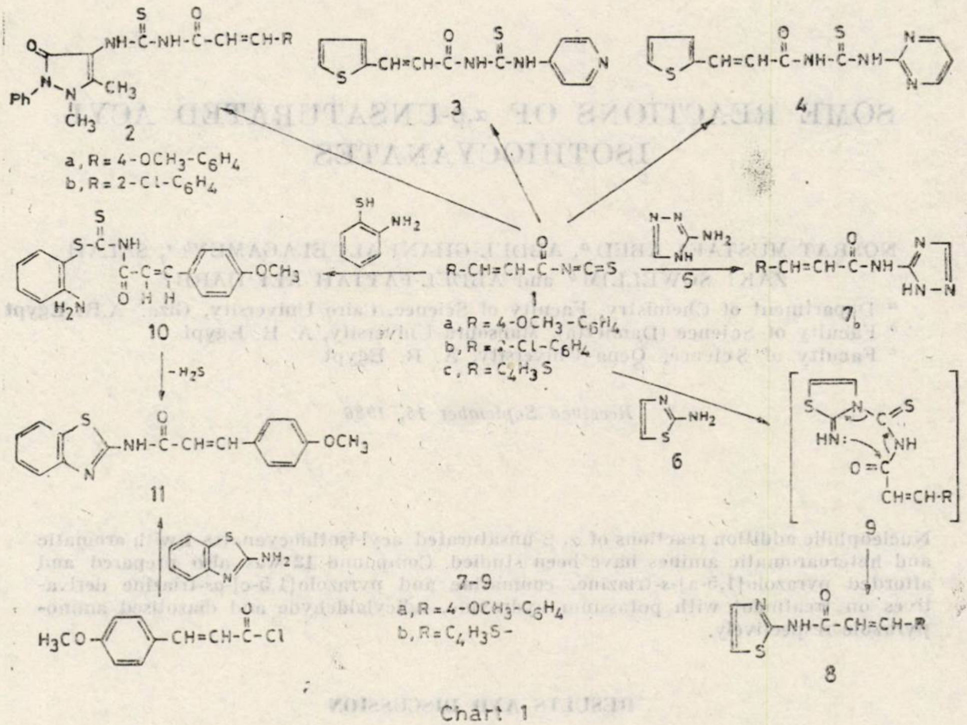

Chart 1

occurs on the thiol group. Thus, by mixing acetone solution of **1a** and *o*-aminothiophenol in equimolecular proportions, a rapid exothermic reaction takes place, and solid product **10** separates which readily losses H_2S upon crystallization to afford 2-acylaminobenzothiazole **11**; the latter product can be also obtained directly from the reaction of 2-aminobenzothiazole and *p*-methoxycinnamoyl chloride (Chart 1).

2-Cyanoethanoic acid hydrazide reacted with **1c** to yield a product which may be formulated either as **12** or as isomeric compound **13**. Structure **12** could be established for the reaction product based on IR spectrum. Since the obtained product is insufficiently soluble in the commonly used ^{1}H-NMR solvents, another evidences for the structure could be inferred from its chemical behaviour.

Similarly to a recent report,[5] compound **12** could be also cyclized into the pyrazolo[1,5-a]-*s*-triazine derivative **14** upon treatment with 5% aqueous potassium hydroxide solution (Chart 2).

Compound **12** condensed readily with aromatic aldehydes to afford the corresponding arylidene derivatives **15a, b** and with salicylaldehyde to give the coumarine derivative **16**.

Compound **12** was also coupled with aromatic diazonium salts to yield coupling products for which the hydrozone structure **17** was established based on the presence of a conjugated -CN group in the IR spectra of the products.

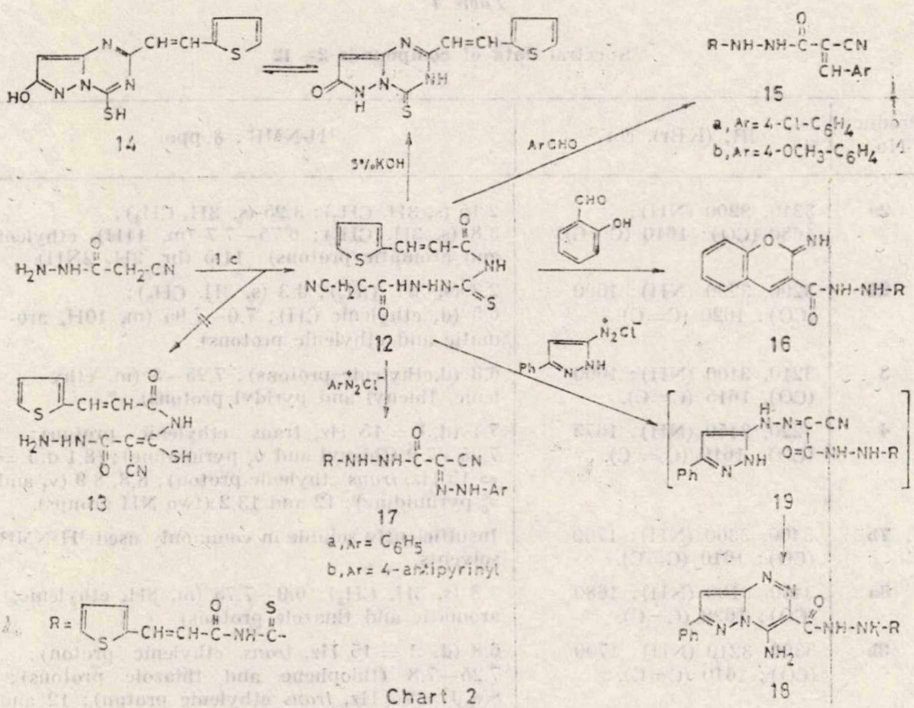

Chart 2

Similarly, compound **12** could be coupled with diazotised aminopyrazole to afford the corresponding pyrazolo[1,5-c]-*as*-triazine derivative **18**. The formation of the cyclic product **18** is assumed to proceed *via* formation of the acyclic hydrazones **19** which cyclize readily under the reaction condition. Trials to isolate the acyclic hydrazone **19** were unsuccessful. The direct isolation of triazines on coupling **12** with heterocyclic diazonium salts find parallelism to Tisler's finding as he reported isolation of triazines[6] on attempted coupling of diazotized aminoheterocycles with similar systems.

EXPERIMENTAL

All melting points are uncorrected. IR spectra were recorded on a Pye-Unicam SP-1100 spectrophotometer. ^{1}H-NMR spectra were recorded on a Varian EM-390-spectrometer using TMS as internal standard; chemical shifts are expressed in ppm as δ values (Table 1). Analytical data were obtained from Analytical Unit from Cairo University. No attempt has been made to optimize the yields of the described reactions.

The acyl isothiacyanates **1a-c** used in the described reactions were prepared by literature methods. [7]

Reactions of amines with isothiocyanates. General procedure. To a solution of **1**(0.12 mol) in 150 mL of dry acetone, a solution of the appropriate amine (0.1 mol) in dry acetone (50 mL) was added. The reaction mixture was refluxed for 3 hrs and then evaporated *in vacuo.* The remaining solid product was filtered off, washed with water and crystallized from the appropriate solvent (cf. Table 2).

Table 1

Spectral data of compounds **2**—**12**

Product No.	IR, (KBr), cm^{-1}	^{1}H-NMR ; δ ppm
2a	3310, 3200 (NH) ; 1680 (CO) ; 1610 (C=C).	2.15 (s, 3H, CH_3) ; 3.25 (s, 3H, CH_3) ; 3.8 (s, 3H, CH_3) ; 6.75—7.7 (m, 11H), ethylenic and aromatic protons) ; 11.5 (br. 2H, 2NH).
2b	3290, 3230 (NH) ; 1690 (CO) ; 1620 (C=C).	2.3 (s, 3H, CH_3) ; 3.3 (s, 3H, CH_3) ; 6.5 (d, ethylenic CH) ; 7.0—7.95 (m, 10H, aromatic and ethylenic protons).
3	3210, 3100 (NH) ; 1690 (CO), 1615 (C=C).	6.3 (d,ethylenic protons) ; 7.25—8 (m, ethylenic, thienyl and pyridyl protons).
4	3220, 3150 (NH) ; 1675 (CO) ; 1610 (C = C).	7.1 (d, J = 15 Hz, trans ethylenic proton) ; 7.25—7.9 (thienyl and ν_5 pyrimidine) ; (8.1 d, J = = 15 Hz, *trans* ethylenic proton) ; 8.8, 8.9 (ν_4 and ν_6 pyrimidine) ; 12 and 13.2 (two NH groups).
7b	3400, 3300 (NH) ; 1700 (CO) ; 1610 (C=C).	Insufficiently soluble in commonly used ^{1}H-NMR solvents.
8a	3450, 3100 (NH) ; 1680 (CO) ; 1620 (C=C).	3.8 (s, 3H, CH_3) ; 6.9—7.75 (m, 8H, ethylenic, aromatic and thiazole protons)
8b	3360, 3210 (NH) ; 1700 (CO) ; 1610 (C=C).	6.8 (d, J = 15 Hz, *trans* ethylenic proton) ; 7.25—7.8 (thiophene and thiazole protons) ; 8(d, J = 15 Hz, *trans* ethylenic proton) ; 12 and 12.8 (two NH groups).
11	3450, 3200 (NH) ; 1680 (CO) ; 1620 (C = C).	3.8 (s, 3H, CH_3) ; 6.7—7.95 (m. 10H, aromatic and ethylenic protons).
12	3450, 3340, 3210 (NH, NH_2) ; 1690 (CO) ; 1620 (C=C).	Insufficiently soluble in commonly used ^{1}H-NMR solvents.

Reactions of amines with acid halides : To a solution of each of **5**,**6** or 2-aminobenzothiazole (0.01 mol) in dry pyridine (20 mL) the equivalent quantity of the appropriate acid halide was added (Chart 1). The reaction mixture was heated on a water bath for 15 min., left to cool and the formed solid product was collected by filtration to give **7**,**8** and **11**, respectively, which proved to be identical with those obtained from the above procedure.

6-Hydroxy-2-(thien-2′-ylvinyl)-4-mercapto-pyrazolo[1,5-a]-1,3,5-triazine(**14**) : A solution of **12** (0.01 mol) in potassium hydroxide solution (30 mL, 5%), was refluxed for two hours, left to cool then acidified with dilute hydrochloric acid. The precipitated material was filtered off, washed with water and crystallized from DMF. Compound **14** formed colourless crystals, m.p.> >300°C, yield 55%, IR : 3300—2400 (NH and OH dimer), 1680 (CO), 1640(C=N), 1610 cm^{-1} (C = C).

$C_{11}H_2N_4OS_2$(276.33) calcd. C, 47.12 ; H, 2.90, N, 20.28,

Found C, 47.27 ; H, 2.85 ; N, 20.42%.

Condensation of compound **12** *with aromatic aldehydes* : A solution of **12** (0.01 mol) and (0.01 mol) of the appropriate aldehyde in 20 mL of absolute ethanol containing the catalytic amount of piperidine was heated at reflux for 3 hours. The solid product, so formed, on cooling was filtered off, washed with ethanol, dried and crystallized from DMF.

Compound **15a** formed brown crystals in 82% yield ; m.p. 253°C, IR : 3300—3100 (NH) ; 2200 (conjugated CN), 1680 (C=O), 1610 cm^{-1} (C=C).

$C_{18}H_{13}N_4O_2S_2Cl$(416.88) calcd. C, 51.86, H, 3.14 ; N, 13.44 ; S, 15.38 ; Found C, 52.21 ; H, 2.95 ; N, 13.35 ; S, 15.36%.

Table 2

Physical and analytical data of compounds **2**−**12**

Product No.	Cryst. solvent	Yield [%]	M.P. [°C]	Formula	Analysis Calcd./Found			
					C	H	N	S
2a	dioxane	78	204	$C_{22}H_{22}N_4O_3S$	62.54	5.24	13.27	7.59
					62.70	5.10	13.15	7.63
2b	ethanol	72	205	$C_{21}H_{19}N_4O_2SCl$	59.07	4.49	13.12	7.51
					59.20	4.20	12.91	7.49
3	ethanol/ chloroform	76	258	$C_{13}H_{11}N_3OS_2$	53.96	3.83	14.52	22.16
					54.27	3.59	14.23	22.31
4	ethanol/ chloroform	75	184	$C_{12}H_{10}N_4OS_2$	49.64	3.47	19.29	22.08
					49.91	3.5	19.10	22.19
7b*	ethanol	65	213	$C_9H_{10}N_4OS$	49.08	3.66	25.44	14.56
					49.38	3.78	25.32	14.72
8a*	dioxane	70	212	$C_{13}H_{12}N_2O_2S$	59.98	4.65	10.76	12.31
					59.85	4.46	10.71	12.25
8b*	dioxane	65	236	$C_{10}H_8N_2OS_2$	50.83	3.41	11.85	27.13
					50.81	3.63	11.62	27.43
11*	dioxane	75	260	$C_{17}H_{14}N_2O_2S$	65.79	4.55	9.03	10.33
					66.01	4.42	9.23	10.51
12	DMF	80	240	$C_{11}H_{10}N_4O_2S_2$	44.35	3.53	18.79	21.56
					44.88	3.42	19.03	21.8

* Recorded yields corresponding to the products of reaction of amines with acid chlorides.

Compound **15b** formed yellow crystals in 75% yield, m.p. 245°C; IR: 3400−3050 (NH); 2200 (conjugated CN); 1680 (C=O), 1620 cm^{-1} (C=C).
$C_{19}H_{16}N_4O_3S$(412.5) calcd. C, 55.32; H, 3.9; N, 13.58;
Found C, 55.12; H, 3.72; N, 13.52%.

Compound **16** formed yellow crystals in 62% yield, m.p. 215°C; IR: 3400, 3060 (NH); 1680(CO); 1640 (C = N); 1610 cm^{-1} (C=C).
$C_{18}H_{14}N_4O_3S_2$(398.4) calcd. C, 54.3; H, 3.54; N, 14.06,
Found C, 54.22; H, 3.42; N, 14.32%.

Coupling of diazotised amines with compound **12**: A solution of the appropriate diazonium salt (0.01 mol) was added to a cold solution of compound **12** in ethanol (30 mL) in the presence of sodium acetate (3 g) with stirring. The reaction mixture was left in a refrigerator for two hours. The precipitated product was filtered off, washed with water, dried and crystallized from the appropriate solvent.

Compound **17a** formed red crystals from DMF in 65% yield, m.p. 179°C, IR: 3500−3050 (NH); 2220 (conjugated CN); 1670 (C=O); 1630 cm^{-1} (C=C).
$C_{17}H_{14}N_6O_2S_2$ (398.47) calcd. C, 51.24; H, 3.54; N, 21.09;
Found C,51.40; H, 3.41; N, 20.88%.

Compound **17b** formed brown crystals from acetic acid in 72% yield, m.p. 205°C; IR: 3450−3050(NH); 2200 (CN); 1680 (exocyclic CO); 1660 (antipyrinyl CO); 1610 cm^{-1} (C=C).
$C_{22}H_{20}N_8O_3S_2$(508·59) calcd., C 51.95; H, 3.96; N, 22.03
Found C, 52.13; H, 4.22; N 22.34%.

Compound **18** formed brown crystals from DMF in 67% yield, m.p. > 300°C, IR: 3450−300 (NH); 1680 (C=O); 1610 cm^{-1} (C=C).
$C_{20}H_{16}N_8O_2S_2$ (464.54) calcd. C, 51.71; H, 3.47; N, 24.12;
Found C, 51.57; H, 3.56; N, 24.53%.

REFERENCES

[1] M. H. Elnagdi, M. R. H. Elmoghayar, D. H. Fleita, E. Hafez and Fahmey, S. M., *J. Org. Chem.*, **41**, 3781 (1976).

[2] M. H. Elnagdi, E. M. Zayed, E. M. Kandeed, and S. M. Fahmy, *Z. Naturforsch.*, **32b**, 430 (1977); *J. Heterocyclic Chem.*, **16**, 61 (1979).

[3] B. Koren, B. Stanovnik and M. Tisler, *J. Heterocyclic Chem.*, **14**, 621 (1977).

[4] J. Becher and E. G. Grandsen, *Tetrahedron*, **33**, 341 (1977).

[5] M.R.H Elmoghayar, E. A. Gali, M.M.M. Ramiz and M. H. Elnagdi, *Liebigs Ann. Chem.*, (1985).

[6] M. Tisler and Stanovnik B., *Khim. Geterotsikl. Soedin.*, **5**, 379 (1980), *Chem. Abstr.*, **93**, 150139 (1980).

[7] A. E. Dixon and J. Tayler, *J. Chem. Soc.*, **93**, 684 (1908).

Revue Roumaine de Chimie, **33**, *4*, 399–403 (1988)

SOME PROPERTIES OF LINEAR LOW DENSITY POLYETHYLENE AND BRANCHED LOW DENSITY POLYETHYLENE

V. DOBRESCU[a], G. ANDREI[b], A. CÎMPEANU[b] and C. ANDREI[b]
[a]CIPMP – Bucharest, Ziduri Moşi 23, Bucharest
[b]Brazi Petrochemical Plant, Research Department, 2000 Ploieşti, Romania

Received November 3, 1986

Properties of linear low density polyethylene (LLDPE) compared to those of branched low density polyethylene (LDPE) have been studied. The mechanical properties of LLDPE are better than those of LDPE. The flow curves, the degrees of crystallinity and melting behaviour are presented. The differences in the physico-mechanical and rheological properties are determined by the structure of polyethylene chains.

INTRODUCTION

A new generation of polyethylene has been recently obtained – the linear low density polyethylene (LLDPE) – whose physico-mechanical properties differ from those of conventional low density polyethylene (LDPE) produced under high pressure in autoclave or tubular reactors.[1-4]

The higher performances of LLDPE are due to its structure. While LDPE assumes a strongly branched "tree-like" structure, in which long branches predominate, the LLDPE has only short branches whose number determines the values of crystallinity and density of the polymer.

This paper presents some properties of LLDPE compared to those of branched low density polyethylene (LDPE).

EXPERIMENTAL

LDPE was a high pressure polymer from Brazi Petrochemical Plant (Ropol 121), obtained in an autoclave type reactor. LLDPE was a Dow Chem. Co. polymer (Dowlex 2045)[5]. Extruded films, (IDDON extruder) 0.04–0.115 mm thick, were employed in determination of physico-mechanical properties, according to ASTM D 1238–73 and ASTM D 638–76.

The degrees of crystallinity and the melting behaviour were studied by DSC, using a Du Pont 990 Instrument.

The flow curves, in the temperature range 190–290° were measured using an INSTRON 3211 capillary rheometer.

RESULTS AND DISCUSSION

The properties of extruded films are listed in table 1, while in Fig. 1 and Fig. 2, the dependence of Dart impact strength and tear strength are presented.

Table 1

Physico-mechanical properties of LDPE and LLDPE

Properties	LDPE			LLDPE		
	Film thickness, mm					
	0.04	0.07	0.11	0.04	0.075	0.115
Melt flow index (g/10 min)	0.273			0.840		
Density (g/cm^3)	0.920			0.920		
Melting point (°)	113			123		
Ultimate tensile strength (kgf/cm^2)						
MD	150.5	161.5	199.5	254.6	277.8	290.9
CD	158.3	175.3	220.0	254.6	293.9	324.6
Elongation at break (%)						
MD	497	535	560	700	698	755
CD	561	562	646	757	814	845
Haze (%)	4.5	4.9	6.2	16.9	25.7	26.5

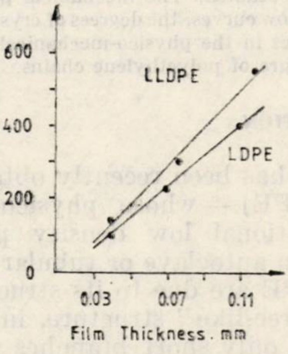

Fig. 1.—Dart impact strength *vs.* film thickness (MD — Machine Direction, CD — Cross Direction).

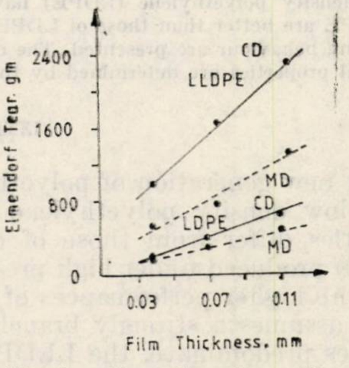

Fig. 2. — Tear strength *vs.* film thickness.

The examination of data shows that the mechanical properties of LLDPE are better than those of LDPE, the LLDPE films retaining their properties even at low thickness.

Fig. 3 and Fig. 4 give the flow curves of LDPE and LLDPE. The nonnewtonian behaviour of LDPE is more pronounced and the activation energy is higher, as can be observed in Fig. 5, where the temperature dependence of viscosity at constant shear stress ($5 \cdot 10^2$ dyne/cm^2) is presented for three polyethylene samples — LDPE, LLDPE and one high density polyethylene (HDPE) sample. It is evident that the temperature dependence (and the activation energy for viscous flow) of LLDPE is similar to that of the linear HDPE.

The degrees of crystallinity and the temperatures of the melting peaks are presented in table 2.

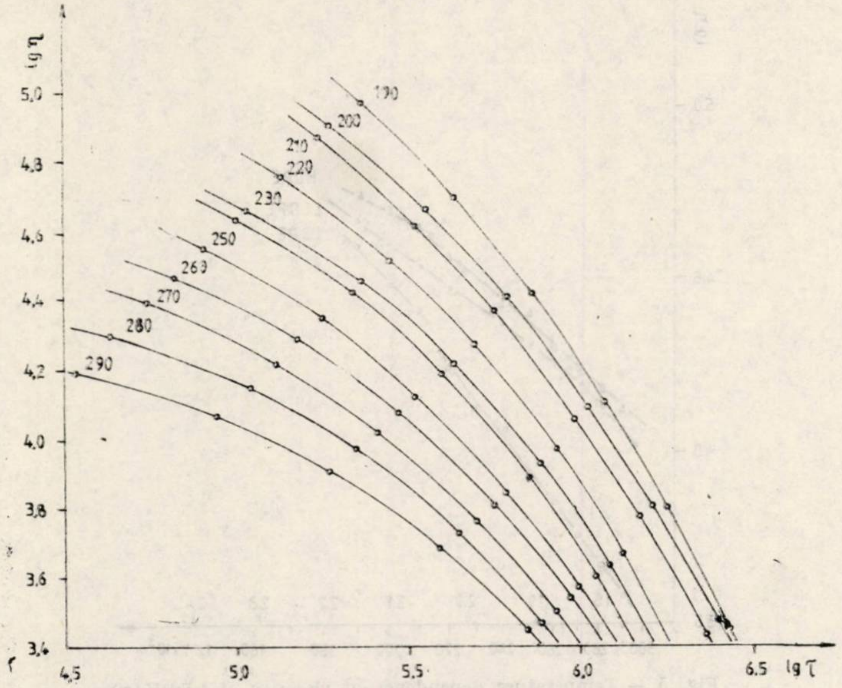

Fig. 3. — Melt flow curves for LDPE in the temperature range 190 — 290°.

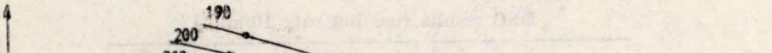

Fig. 4. — Melt flow curves for LLDPE in the temperature range 190—290°.

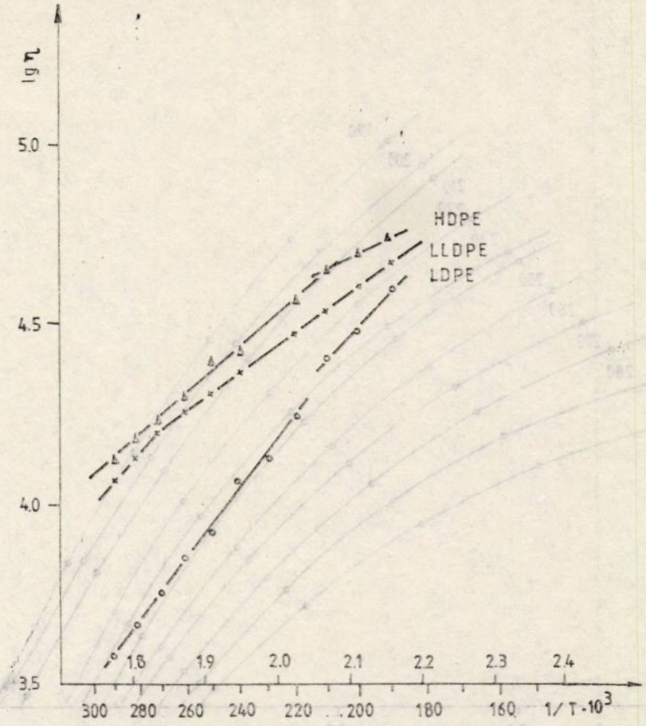

Fig. 5. — Temperature dependence of viscosity of LDPE (o), LLDPE (x) and HDPE (Δ) at $\eta = 5.10^5$ dyne/cm^2.

Table 2

DSC results (heating rate 10°/min)

Sample	Crystallinity (%)	T_m (°)
LDPE	49.0	113
LLDPE	50.0	108 118 125

The thermograms, obtained at a heating rate of 10°/min, are given in Fig. 6.

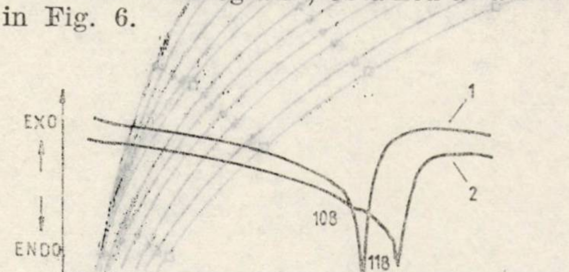

Fig. 6. — DSC thermograms for LDPE (1) and LLDPE (2).

The shape of the thermograms does not change as a function of heating rate, however the temperatures of the peaks are slightly increasing with the increase of the heating rate from 5°/min to 50°/min.

A very interesting feature of LLDPE is the complex melting behaviour, already observed in the case of blends of LDPE and HDPE.[6]

The differences in the physico-mechanical and rheological properties are determined by the structure of polyethylene chains.

REFERENCES

[1] N. Platzer, IUPAC 28th Macromolecular Symposium, Massachusetts, Amherst, July 12–16, 221 (1981).

[2] C. Andrei, G. Andrei and V. Dobrescu, *Mat. Plastice* (*București*), **19**, 207 (1982).

[3] V. Dobrescu, G. Andrei, V. Tomescu, A. Cîmpeanu, C. Andrei and C. Boborodea, IUPAC 29th Macromolecular Symposium, Bucharest, Section IV, September 5–9, 629 (1983).

[4] C. Andrei, "Developments in Polyolefins", Lecture presented at the Academy of Economic Sciences Seminar, Bucharest, May 9–10, 1986.

[5] * * * Dowlex Polyethylene Resins, Dow Chemical Company, Form No. 305–608, 1979.

[6] V. Dobrescu, "Polymer Blends Investigation of Structure and Properties", Lecture presented at the 1st Seminar Freiburg — Iași, Freiburg, March, 1981.

The shape of the thermograms does not change as a function of heating rate, however the temperatures of the peaks are slightly increasing with the increase of the heating rate from 5°/min to 20°/min.

A very interesting feature of LLDPE is the complex melting behaviour, already observed in the case of blends of LDPE and HDPE.[7]

The differences in the physico-mechanical and rheological properties are determined by the structure of polyethylene chains.

REFERENCES

[1] N. Pelzer, IUPAC 28th Macromolecular Symposium, Massachusetts, Amherst, July 12–16, 321 (1982).

[2] G. Andrei, C. Andrei and V. Dobrescu, Mat. Plastice (Bucureşti), 19, 207 (1982).

[3] V. Dobrescu, G. Andrei, V. Ionescu, A. Cimpeanu, C. Andrei and C. Poborodea, IUPAC 29th Macromolecular Symposium, Bucharest, Section IV, September 5–9, 629 (1983).

[4] G. Andrei, "Developments in Polyolefins", Lecture presented at the Academy of Economic Sciences Seminar, Bucharest, May 8–10, 1986.

[5] * , Dowlex Polyethylene Resins, Dow Chemical Company, Form No. 305–098, 1979.

[6] V. Dobrescu, "Polymer Blends Investigation of Structure and Properties", Lecture presented at the 1st Seminar Freiburg – ins. Freiburg, March, 1981.

Revue Roumaine de Chimie, **33**, *4*, 405–412 (1988)

A NOVEL SPECTROPHOTOMETRIC METHOD FOR DETERMINATION OF NITRITE IONS

N. BIÇAK *, N. TAN and Ö. BEKÂROĞLU
Department of Chemistry, Technical University of Istanbul
Y. Levent, Istanbul, Turkey

Received December 13, 1986

2,7-Dihydroxynaphthalene can be used as a reagent for rapid and reliable determination of nitrite ions in microgram amounts, in drinking water and urine. The present method is based on the formation of a nitroso compound by the reaction between 2,7-dihydroxynaphthalene and nitrite ions in acidic media. It has been shown that determination of the nitroso derivative can be performed in the presence of various ions, due to its characteristic absorption band at 440 nm.

It is well known that the detection and the determination of nitrite ions in urine, in spring water and in food has a great importance on the human health point of view, i.e. its presence in urine indicates colibacillus. There are a lot of methods in the literature for the determination of nitrite ions. One of them is based on the formation of coloured nitroso compounds. The reagents, which are most frequently used for this purpose are N,N-dimethylaniline,[1] 2,6-xylenol,[2] thioglycolic acid [3] and indole.[4] In the published methods, optimum conditions and interferences of foreign ions have been studied in detail and the main problem has appeared to be the side reactions which lead to by-products.[2]

In this study, 2,7-dihydroxy naphthalene (DHN) was used as a reagent because of its great reactivity at 1 and 8 positions. It reacts easily with nitrite ions to form the corresponding mono-nitroso derivative in acidic media according to the following reaction.

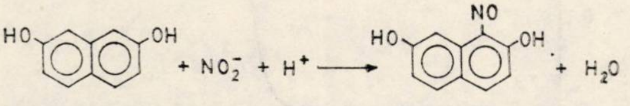

(1)

2,7-Dihydroxy-naphthalene (DHN)

1-nitroso 2,7-dihydroxy naphthalene

It seemed to be convenient for the determination of nitrite ions by this reaction. The pH, time and concentration dependences of the reaction were studied and the effects of the ions of many inorganic salts were also tested. The disturbing effects of NH_4^+ and urea have been prevented by adjusting the pH between 2.9–3.4 and to avoid the interference of the characteristic colour reaction of Fe^{3+} with DHN, trisodium citrate has been added to the sample solution as a complexing agent.

EXPERIMENTAL

Reagents and apparatus. All chemicals used were of analytical grade (Merck). 2,7-Dihydroxy naphthalene (Merck) was recrystallized from ethanol (m.p. 190°). 1-Nitroso 2,7-dihydroxy naphthalene was synthesized as described before.[5] Varian -634 UV-Visible Spectrophotometer was used for the measurements. All measurements were made at room temperature.

UV-Visible spectra. There are two new broad bands in the case of nitroso derivative ($\lambda_{max}(H_2O)$ 440 nm (ϵ 4800 $dm^3\ mol^{-1}\ cm^{-1}$), 380 nm (ϵ 5100)) which differs from that of DHN. DHN does not show any absorption in the visible region (Fig. 1 and Fig. 2). These bands also appear in the spectra of the acidified (pH 2.7) solutions of DHN and NO_2^- as shown in Fig. 3. Thus, the new band at 440 nm can be used for spectrophotometric determination of nitrite ions. In Fig. 3, the different band exhibiting at 330 nm may be attributed to an intermediate state of nitrosation reaction and this was not studied further.

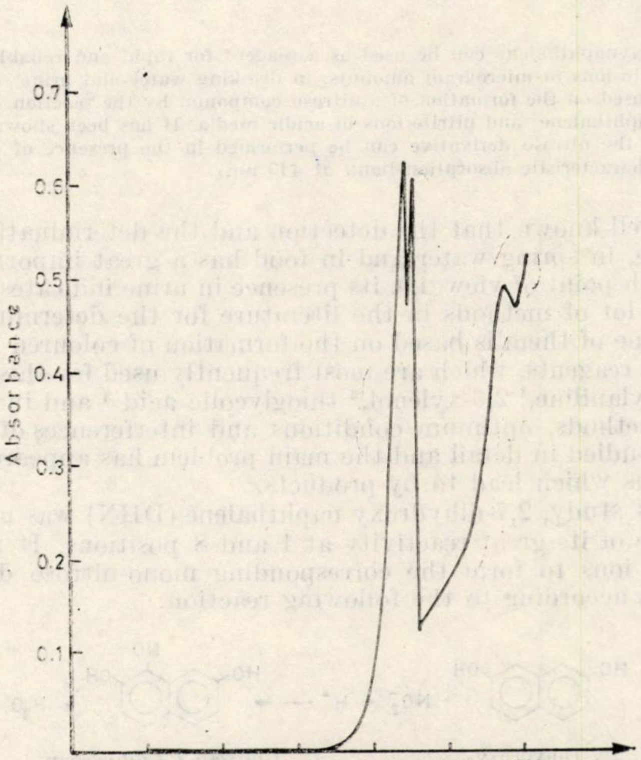

Fig. 1. — UV-Visible spectrum of 2,7-dihydroxy naphthalene (10^{-4}M in H_2O).

Variation of absorbances with pH, concentration and time. In order to find the pH dependence of the absorption maximum at 440 nm the two solutions containing $2 \cdot 10^{-4}$M DHN, $2 \cdot 10^{-4}$M $NaNO_2$ and $10 \cdot 10^{-4}$ M DHN, $2 \cdot 10^{-4}$M $NaNO_2$ were prepared properly. Each solution was divided into equal parts, each one is to be 50 mL. pH values of each part were adjusted by dropping concentrated HCl solution. After 7 minutes of acidification, the absorbances at 440 nm were measured and plotted against pH as shown in Fig. 4A and Fig. 4B.

The time dependence of nitroso formation was followed by measuring absorbances at different time intervals for the solution containing $2 \cdot 10^{-4}$ M DHN and $2 \cdot 10^{-4}$ M $NaNO_2$ at pH 2.3 (Fig. 5). However in the same conditions if DHN is present in one hundred times greater than the former, no change in absorbance (at 440 nm) is observed with time.

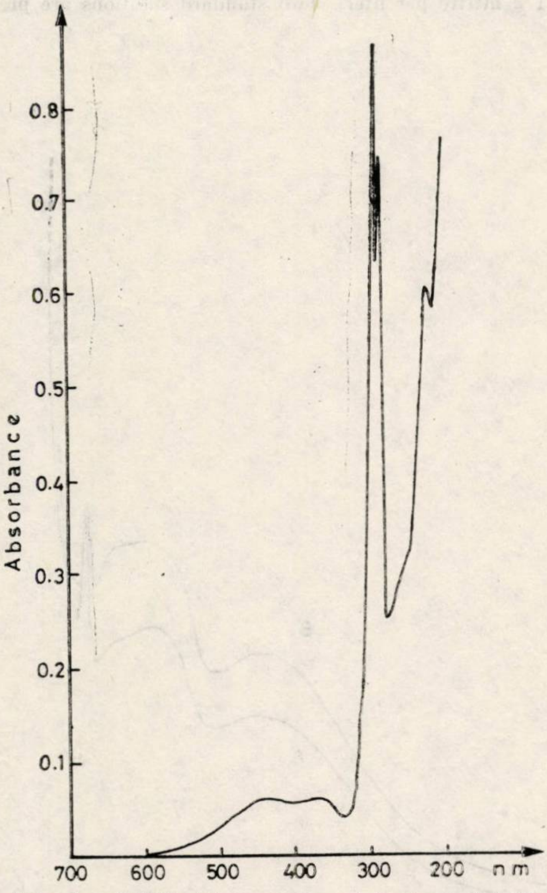

Fig. 2. — UV-Visible spectrum of 1-nitroso 2,7-dihydroxynaphthalene (10^{-4} M in H_2O).

Being proportional to the reagent concentration, the excess of DHN was used in the procedure. In order to prevent the disturbing effects of some metal ions such as Fe (III), 0.25 M trisodium citrate solution was added to the sample solutions as a complexing agent. Otherwise, in the absence of the complexing agent, the absorbances due to the reaction of Fe (III) with DHN involve the one given by nitrite ions as shown in Fig. 6. Trisodium citrate also provides buffer effect (pH 2.9—3.4).

On the other hand, in order to apply the method on the analysis of urine, the pH values of the medium should be kept above 2.5 not to cause decomposition of nitrite ions by reacting with urea. According to these considerations, the following way has been found convenient for practice.

Preparation of the reagent solution. 250 mL of 2M HCl solution were added to the solution of 2.4 g ($1.5 \cdot 10^{-2}$ mole) DHN in 250 mL water (more concentrated solutions of DHN are not suitable because of its precipitation). Hence, in the reagent solution DHN and HCl are in 0.03 M and 1M concentrations respectively.

Trisodium citrate solution (0.25 M). 44.64 g (0.5 mole) of $Na_3C_6H_5O_7 \cdot 5H_2O$ were dissolved and diluted with distilled water to 500 mL.

Preparation of nitrite solutions. 1.5 g of anhydrous $NaNO_2$(Merck) were dissolved and diluted to 1.0 liter (1 g nitrite per liter). Two standard solutions are prepared by diluting 10 mL and 100 mL of this stock solution to 1.0 liter with distilled water. The first standard contains 10 mg nitrite per liter whereas the second contains 100 mg nitrite per liter.

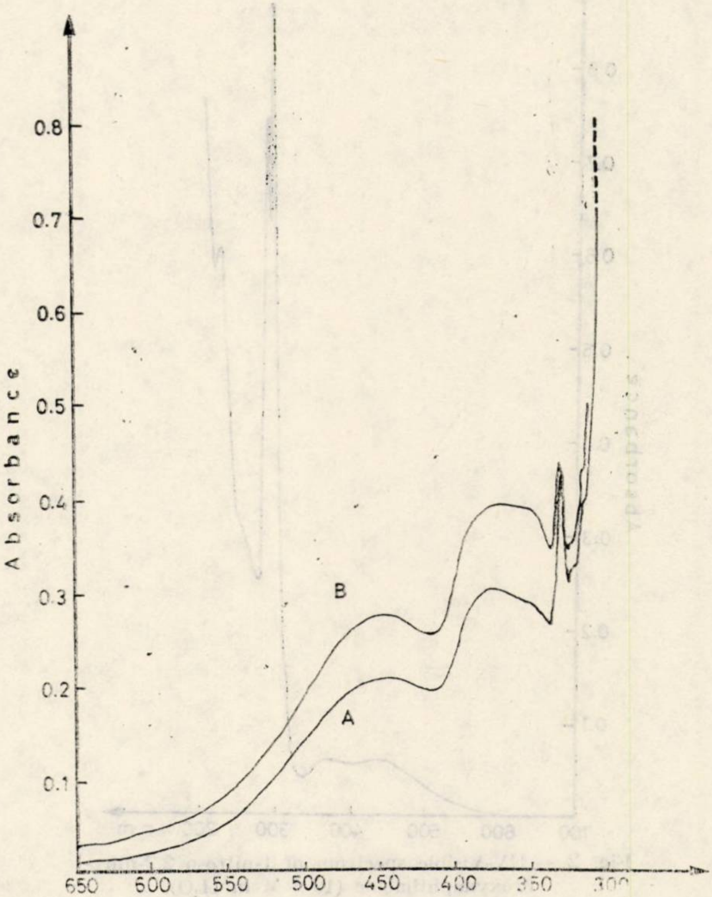

Fig. 3. — UV-Visible spectrum of the solution containing
(*A*) $2 \cdot 10^{-3}$ M. DHN and $2 \cdot 10^{-3}$M $NaNO_2$, and
(B) $2.75.10^{-3}$ M DHN and $2.75.10^{-3}$ M $NaNO_2$ (pH 2.7 in H_2O).

Procedure. A series of nitrite solutions was prepared in the concentration range from 1.0 to 100 mg per liter by diluting certain volumes of the two standard solutions. 10 mL of 0.25 M trisodium citrate solution and 10 mL of the reagent solution were added to 10 milliliters of these nitrite solutions. At room temperature, pH values of the mixtures are constant at 3.1 and colour development is sufficiently rapid and stable. About 3 minutes after mixing the equilibrium is established.

Absorbances were measured at 440 nm against that of the blank containing distilled water, trisodium citrate and reagent solutions (each one is to be 10 mL). Absorbance-concentra-

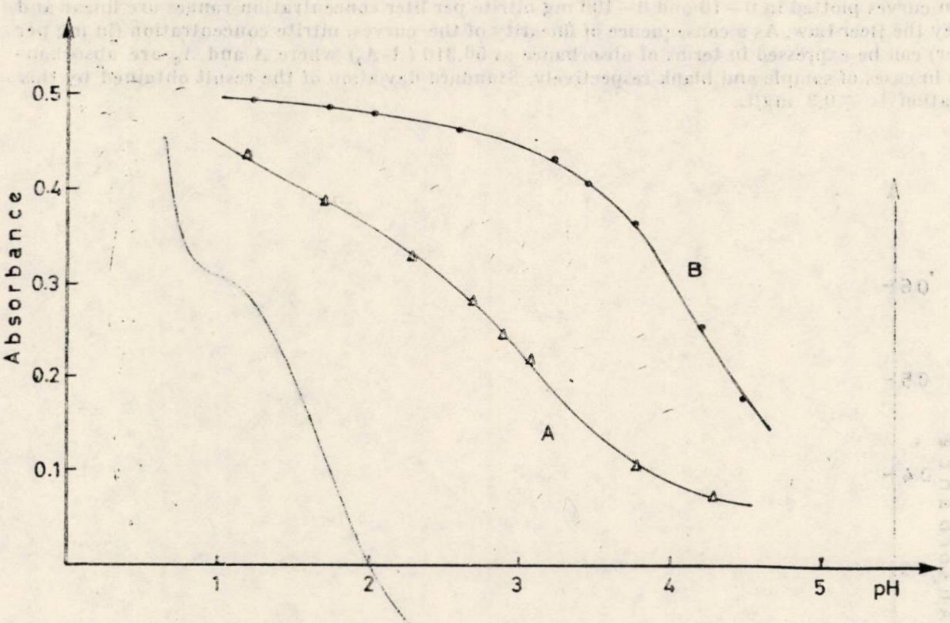

Fig. 4. — Variation of absorbance at 440 nm with pH for the solutions containing (A) 10^{-3} M DHN and $2\text{-}10^{-4}$ M $NaNO_2$. (*B*) 10^{-3} M DHN and $2 \cdot 10^{-4}$ M $NaNO_2$.

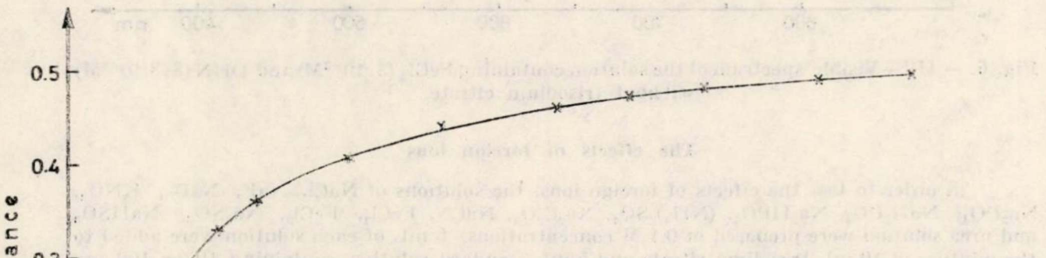

Fig. 5. — Variation of absorbance at 440 nm with time (DHN and $NaNO_2$ are in $2 \cdot 10^{-4}$M concentrations pH 2.3).

tion curves plotted in 0—10 and 0—100 mg nitrite per liter concentration ranges are linear and obey the Beer Law. As a consequence of linearity of the curves, nitrite concentration (in mg per liter) can be expressed in terms of absorbance as 56.310 (A-A_0) where A and A_0 are absorbances in cases of sample and blank respectively. Standard deviation of the result obtained by this relation is ∓0.3 mg/L.

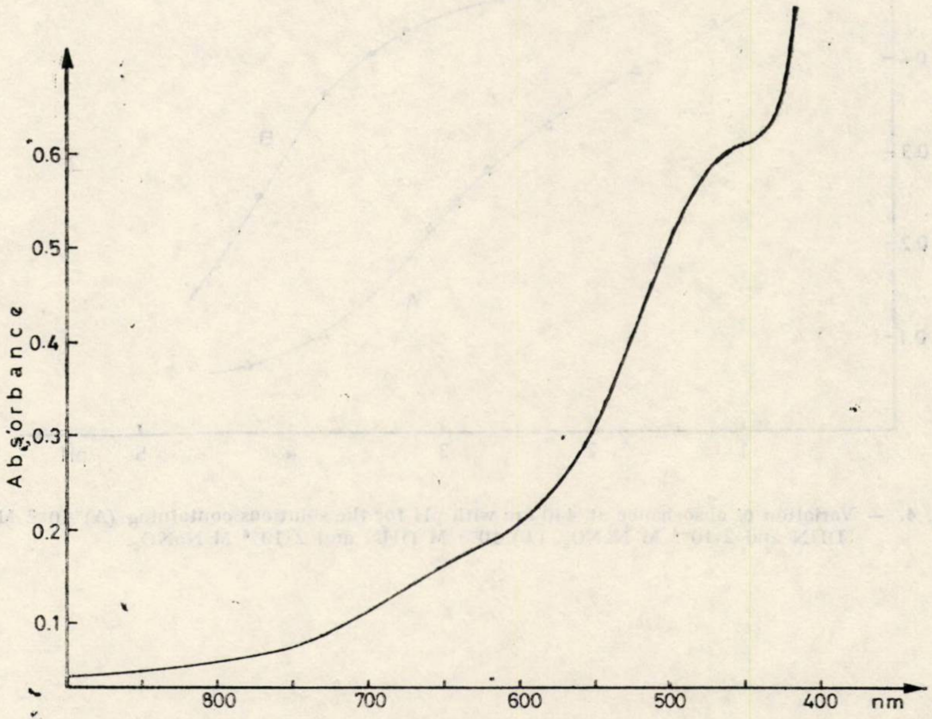

Fig. 6. — UV—Visible spectrum of the solution containing $FeCl_3$ (5.10^{-3}M) and DHN ($8.3.10^{-3}$M) without trisodium citrate.

The effects of foreign ions

In order to test the effects of foreign ions, the solutions of NaCl, NaF, NaBr, KNO_3, Na_3PO_4, NaH_2PO_4, Na_2HPO_4, $(NH_4)_2SO_4$, $Na_2C_2O_4$, NaCN, $FeCl_2$, $FeCl_3$, Na_2SO_3, $NaHSO_3$ and urea solution were prepared in 0.1 M concentrations. 5 mL of each solution were added to the mixture of 10 mL trisodium citrate and 5 mL standard solution containing 10 or 100 mg nitrite per liter. Then 10 milliliters of the reagent solution were added to these mixtures. (The solutions of foreign ions were deliberately added after the addition of citrate solution. to avoid undesired and probable interaction of foreign ions at the beginning). The absorbances at 440 nm were measured and compared with the results observed before. No changes in absorbances were observed except in the cases of SO_3^{2-} and HSO_3^- ions. Sulphide and bisulphide ions even when present in 0.01 M concentrations lead to considerable decreases (about 10 %) in the absorbances. This situation can be attributed to the reduction of the nitroso derivative of DHN to the corresponding amine as described in the literature.[6] However in 0.001 M concentrations, these ions de not affect the results practically.

Application on urine. This procedure was applied on urine in the same manner. Nitrite containing urine stock was obtained synthetically by dissolving and diluting 75 mg $NaNO_2$ to 50 mL (1 g nitrite per liter) with a fresh urine (pH 6.3). Two standards were prepared by diluting 0.5 and 5 mL of the stock solution to 50 mL with urine. Urine samples containing different amounts of nitrite were prepared by diluting the two standards with urine, so that each part to be contained 1,2,...10 and 10 ; 20 ;...100 mg nitrite per liter.

5 mililiters of these test samples were mixed with 5 mL of trisodium citrate solution and 5 mL of the reagent solution. After shaking a few minutes (pH 3.4), absorbances were measured against the reference which consists of urine, trisodium citrate and 1M HCl solutions' each one is to be 5 mL. The absorbance-concentration curves plotted in the ranges 0—10 and 0—100 mg nitrite per liter are also linear. According to these curves, the amount of nitrite in mg per liter can be written as

$$34.38\ (A - A_r)$$

where A and A_r are the absorbances of the mixture and reference respectively. Standard deviation of the result obtained by this relation is 0.3 mg/L.

RESULTS AND DISCUSSION

The present paper points out that the great reactivity of DHN toward nitrite ions can be used for detection and quantitative determination of nitrite ions.

The comparison of UV-Visible spectrum of 1-nitroso 2,7-dihydroxy naphthalene with the spectrum of the coloured solution of DHN and nitrite ions in acidic medium (Fig. 2 and Fig. 3) indicates that the colour reaction can be attributed to the formation of the corresponding nitroso derivative.

In the procedure, the equilibrium is established rapidly by using excess of DHN. At room temperature, the absorbances measured at 440 nm are a linear function of nitrite concentrations in the range of 0—100 mg per liter.

The reactions of disturbing ions which may be present in urine and in water samples can be summarized as follows.

$$NH_4^+ + NO_2^- \rightarrow N_2 + 2H_2O \qquad (2)$$

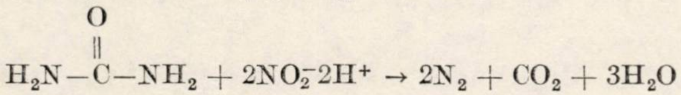

$$H_2N-\overset{\overset{\displaystyle O}{\|}}{C}-NH_2 + 2NO_2^- 2H^+ \rightarrow 2N_2 + CO_2 + 3H_2O \qquad (3)$$

$$\text{Amino acids} + NO_2^+ + H^+ \rightarrow N_2 \text{ evolution} \qquad (4)$$

$$NO_3^- + H^+ + \text{DHN} \rightarrow \text{Nitro products of DHN} \qquad (5)$$

$$2Fe^{2+}NO_2^- + 2H^+ \rightarrow Fe^{3+} + Fe(NO) + H_2O \qquad (6)$$

$$SO_3^{2-} + \text{1-nitroso 2,7-dihydroxy naphthalene} \rightarrow \text{1-amino 2,7-dihydroxy naphthalene.} \qquad (7)$$

The first five reactions take place only in concentrated acidic ($pH < 2$) solutions. These side reactions have been prevented by adjusting pH at 3.1—3.4 range in the procedure. This situation allows us to extend the procedure to urine samples. The interferences of Fe^{3+} ions[7] and some other metal ions have been prevented by masking with trisodium citrate. However SO_3^{2-}, HSO_3^- and also strong oxidizing and reducing ions should be absent in the sample.

Consequently, the new proposed method is rapid, specific and sensitive to concentration levels of 1 ppm even in the presence of foreign ions including NO_3^-. On the other hand, the simplicity of the procedure and stability of colour are distinct advantages.

REFERENCES

[1] E. H. Miller, *Analyst.*, **37**, 345 (1912).
[2] A. M. Hartley and R. I. Asai, *Analyt. Chem.*, **35**, 1214 (1963).
[3] M. Ziegler and O. Glemser, *Z. Analit. Chem.*, **144**, 187 (1955).
[4] S. A. Rahim, N. A. Fakhri and W. A. Bashir, *Microchem. J.*, **3**, 28, 479 (1983).
[5] M. D. Soffer, et al., *J. Amer. Chem. Soc.*, **70**, 3704 (1950).
[6] S. V. Bogdanov and Z. V. Todres-Selector, *Zhur. Vseosyuz. Khim. Obshch.* im. D. I. Mendeleeva **6**, 584 (1961).
[7] I. I. Trudui, Leningrad Khim-Tekhnol. Inst. No 1, 116 (1934) (in German).

Revue Roumaine de Chimie, 33, 4, 413—417 (1988)

SPECTROPHOTOMETRIC STUDIES OF LANTHANIDES WITH 3-HYDROXY-3-PHENYL-1-*o*-CARBOXY PHENYLTRIAZENE

D. N. PUROHIT and R. S. CHAUHAN
Department of Chemistry, College of Science, Sukhadia University, Udaipur — 313001, India

Received November 15, 1986

3-Hydroxy-3-phenyl-1-*o*-carboxy phenyltriazene has been used as spectrophotometric reagent for the determination of ten lanthanide (III) ions. Spectral characteristics of complexes have been studied and wavelength of maximum absorption in each case has been determined. The molar composition of each lanthanide (III) complex was investigated and it was found to be M : R = 1 : 1 for all the ten lanthanides. Stability constants and free energy of formation were calculated. Sandell's sensitivities have been determined and the results were compared with the other reagents.

Hydroxytriazenes, whose complexing ability was first examined by Elkins and Hunter,[1] has now come up as potential chelating agents. Since the evolution of analytical applications of hydroxytriazenes by Sogani and Bhattacharya,[2] two reviews have been published regarding the same topic; first by Purohit [3] in 1967 and second by Chakraborti and Majumdar[4] in 1977. These reviews reveal that a number of hydroxytriazenes have been used as spectrophotometric reagents for various metal ions.

However, no hydroxytriazene has so far been used for spectrophotometric determination of lanthanides. The 3-hydroxy-3-phenyl-1-*o*-carboxy phenyltriazene has been used for spectrophotometric determination of Fe(III), Ti(IV), and V(V)[5]; Ni(II), Cu(II) and Pb(II).[6]

In the present investigation 3-hydroxy-3-phenyl-1-*o*-carboxy phenyltriazene has been employed in spectrophotometric studies of ten lanthanide(III) ions.

EXPERIMENTAL

Reagent (hydroxytriazene) solution. The reagent 3-hydroxy-3-phenyl-1-*o*-carboxy phenyltriazene was prepared following the method suggested by Majumdar and Saha. [5] The compound was obtained as shining light yellow crystals (m.p. 165°C). A 1.0×10^{-3}M stock solution of the reagent was prepared in ethanol. Weaker solutions were prepared by appropriate dilution. Due to the decomposing tendency of hydroxytriazenes in solution on storing, fresh solutions were prepared from time to time.

Lanthanide (III) nitrate solutions. For preparing 1×10^{-3}M stock solution of rare earth nitrate, the required quantities of oxides of spectral purity (from K § K Laboratories, Inc. U.S.A.) were dissolved in minimum quantity of nitric acid and were diluted appropriately with distilled water. The solutions were standardised complexometrically with EDTA using xylenol orange as an indicator.[7]

Instruments. Carl Zeiss — 'Spekol' spectrophotometer with matched 1.0 cm quartz cuvettes and Systronics pH meter 324 were used in spectrophotometric studies.

Spectral characteristics of complexes. Absorption spectra with 1 : 5 metal (2.0×10^{-5}M) to reagent (1.0×10^{-4}M) molar ratio and pH around 6.0 (adjusted with urotropine) were determined in wavelength range 390—500 nm. In every case λ_{max} was found at 395 nm. However, at λ_{max} reagent absorption was considerably high. Therefore, 405 nm where reagent absorption was comparatively less was chosen as working wavelength. All absorption measurements were made taking reagent blank. With the same metal to reagent ratio of 1 : 5, absorption spectra were taken at different pH values. With all the lanthanides, absorption maxima remained the same. This suggested that every lanthanide (III) ion formed only one type of complex with reagent.

Effect of pH. The absorptions of solutions containing 2×10^{-5}M lanthanide(III) anl five fold excess of reagent were determined at different pH values. Absorptions were measured at 405 nm. The pH range of maximum and constant absorbance of all lanthanides fall between 5.4 and 6.7.

Colour development and its stability. All lanthanide(III) ions gave instantaneous yellowish green colour with 3-hydroxy-3-phenyl-1-*o*-carboxy phenyltriazene in pH range 5.5—6.3. The colour in each case was found to be stable and absorbance values were found to be the same for over 24 hours.

Formula of the complex. The composition of the complex in every case was determined in the usual way, by Job's method, [8] mole ratio method[9] and slope ratio method [10] (details of data obtained have been avoided for the sake of brevity). However, as determined by these methods, the composition of each complex was found to be M.R.

Beer's law. Under the established optimum conditions the validity of Beer's law was studied at 405 nm. For this purpose the concentration range studied for each lanthanide(III) ion was 1×10^{-5} M to 1×10^{-4}M with five fold excess of reagent. It is observed that Beer's law is obeyed in the entire concentration range studied for all the ten lanthanide(III) complexes.

Sensitivities. The molar absorptivities of the complexes were determined from Beer's law curves and Sandell's speectrophotometric sensitivities were calculated for all the lanthanide(III) complexes with 3-hydroxy-3-phenyl-1-*o*-carboxy phenyltriazene. The results obtained are given in Table 1.

Table 1

Sensitivities and molar absorption coefficients for lanthanide (III) 3-hydroxy-3-phenyl-1-*o*-carboxy phenyltriazene complexes

Lanthanide (III) ion	ε	Sandell's sensitivity (μg/cm²)
La(III)	7.35×10^3	0.0188
Ce(III)	7.41×10^3	0.0189
Pr(III)	7.49×10^3	0.0188
Nd(III)	7.60×10^3	0.0189
Sm(III)	8.00×10^3	0.0187
Gd(III)	8.10×10^3	0.0194
Tb(III)	8.20×10^3	0.0193
Ho(III)	8.41×10^3	0.0196
Eu(III)	8.52×10^3	0.0196
Lu(III)	9.00×10^3	0.0194

Determination of stability constants. Stability constants (at 25°C) were determined following Harvey and Manning's method.[10] The nature of mole ratio curves indicates that lanthanide complexes formed, dissociated partially which can be represented as

$$\mathrm{MR} \rightleftharpoons \mathrm{M(III)} + \mathrm{R}$$

$$c(1-\alpha) \qquad c\alpha \qquad c\alpha \quad \text{Equilibrium concentration}$$

For this type of dissociation relevant equations for the determination of stability constants are as given below:

$$\alpha = \frac{E_M - E_S}{E_M} \tag{1}$$

$$K_{\text{inst}} = \frac{c\alpha^2}{(1-\alpha)} \tag{2}$$

$$\beta = \frac{1}{k_{\text{inst.}}} \tag{3}$$

The standard free energy of formation of lanthanide(III) complex with reagent in each case was calculated using the following equation:

$$\Delta G^\circ = -RT \ln \beta \qquad (4$$

Since the chelating moiety and composition of all lanthanide(III) complexes with 3-hydroxy-3-phenyl-1-*o*-carboxy phenyltriazene is the same, the above-mentioned equations are applicable for all the ten complexes. The terms used in the above equations have their usual significance. The values of E_M and E_S were found from the mole ratio curves. These values along with the values of α, c, $\log \beta$ and ΔG° are given in Table 2.

Table 2

Studies of lanthanide(III) complexes with 3-hydroxy-3-phenyl-1-*o*-carboxy phenyltriazene

Lanthanide (III)	Concentration in mole/litre C	E_m	E_s	α	Stability constant β	$\log \beta$	ΔG° in K_{cal}
La(III)	4.0×10^{-5}	0.315	0.160	0.4920	5.2470×10^{4}	4.7199	−6.4796
Ce(III)	4.0×10^{-5}	0.310	0.170	0.4516	6.7224×10^{4}	4.8272	−6.6274
Pr(III)	4.0×10^{-5}	0.315	0.180	0.4287	7.7718×10^{4}	4.8905	−6.7137
Nd(III)	4.0×10^{-5}	0.320	0.185	0.4218	8.1247×10^{4}	4.9098	−6.7402
Sm(III)	4.0×10^{-5}	0.330	0.195	0.4090	8.8331×10^{4}	4.9461	−6.7900
Gd(III)	4.0×10^{-5}	0.330	0.21	0.3636	12.034×10^{4}	5.0802	−6.9741
Tb(III)	4.0×10^{-5}	0.350	0.225	0.3571	12.6039×10^{4}	5.1004	−7.0019
Ho(III)	4.0×10^{-5}	0.345	0.229	0.3362	14.6821×10^{4}	5.1668	−7.0930
Eu(III)	4.0×10^{-5}	0.350	0.232	0.3371	$14.5857\times10_{4}$	5.1638	−7.0889
Lu(III)	4.0×10^{-5}	0.360	0.240	0.3333	15.0000×10^{4}	5.1761	−7.1058

DISCUSSION

Composition of lanthanide (III) complexes with 3-hydroxy-3-phenyl-1-*o*-carboxy phenyltriazene was determined following Job's method, slope ratio method and mole ratio method. In each case, the composition of the complex was established to be as MR. The hydroxytriazene acts as tri-dentate ligand. This indicates that the remaining coordination positions of a lanthanide (II) ion could be satisfied by either OH^- or H_2O. However, no attempt has been made to isolate the complexes formed during their spectrophotometric studies.

As is clear from Table 2 stability constants of lanthanide complexes with the reagent regularly increase with the increase in atomic number. Similar increase has been reported for number of reagents such as iminodiacetic acid, EDTA, DCTA etc.

The sensitivities of the reagents commonly used and some of the reagents recently proposed for lanthanides are given below in Table 3. For the sake of comparison the sensitivity of 3-hydroxy-3-phenyl-1-*o*-carboxy phenyltriazene has also been given.

Table 3

Sensitivities of some calorimetric methods for lanthanides

Reagent	Sandell's sensitivity µg/cm²	Working wavelength
1. Boron-disulphophenyl fluorone complex[11]	0.00409	515 nm (For Nd)
2. Alizarine red-S[12]	0.0052	520 to 530 nm (For Ho)
3. Chlorophosphonazo-III[13]	0.003606 (For Nd)	680 nm
4. 4-(2-Pyridylazo)resorcinol[14]	0.056 to 0.025	515 nm
5. Beryllon-II : 3-(8-hydroxy-3,6-disulpho-1-naphthylazo chromotropic acid[15]	0.00603 (La) 0.01118 (Pr) 0.00695 (Nd)	610 nm 610 nm
6. Methylxylenol blue[16]	0.0037 to 0.0054	568 nm to 576 nm
7. Diethylenetriamine penta acetic acid[17]	0.0233	298 nm
8. *Ortho*-anilino-K : 3-(2-carboxy phenylazo)-6-(2-sulpho-phenylazo) chromotropic acid[18]	0.00514 to 0.00788 (for La, Ce, Pr § Nd)	600 nm to 670 nm
9. Morin[19]	0.03205	470 nm
10. Chlorosulphophenol-S: 3-6, bis(5-chloro-2-hydroxy-3-sulphophenyl azo) chromotropic acid[20]	0.006 (For Nd)	645 nm
11. 4-Benzoyl-3-methyl-1-phenyl-3-pyrazolin-5-one[21]	0.0257 (For Nd)	578 nm
12. 3-Hydroxy-3-phenyl-1-*o*-carboxyphenyltriazene	0.0187 to 0.0198	405 nm

A comparison reveals that though the sensitivity of the triazene is less than most of reagents but is more than 4-(2-pyridylazo resorcinol, diethylenetriamine-pentaacetic acid, orthoanilinic K for (Tm, Yb, Lu) morin and 4-benzoyl-3-methyl-phenyl-2-pyrazoline-5-one. However, ease of preparation of the reagent, and easy method for direct spectrophotometric determination of lanthanides are advantageous over many other reagents and therefore this compound is one more good addition to the list of spectrophotometric reagents for determination of lanthanides. Further, the work embodied here is the first report on the utility of hydroxytriazenes in the spectrophotometric determination of lanthanides.

ACKNOWLEDGEMENT. The present work was carried out under University Grants Commission's Scheme entitled "Identification and selective determination of rare earth with hydroxytriazenes". The financial assistance received is gratefully acknowledged.

REFERENCES

[1] M. Elkins and L. Hunter, *J. Chem. Soc.*, **1938**, 1346.
[2] N. C. Sogani and S. C. Bhattacharya, *Analyt. Chem.*, **28**, 81 (1956).
[3] D. N. Purohit, *Talanta*, (1967), **14**, 353.
[4] D. Chakraborti and A. K. Majumdar, *J. Indian Chem. Soc.*, **54**, 258, (1977).
[5] A. K. Majumdar and S. C. Saha, *Anal. Chim. Acta*, **40**, 299, (1968).
[6] A. K. Majumdar and S. C. Saha, *Z. Analyt. Chem.*, **257**, 33, (1971).
[7] J. Kinnunen and B. Wennerstrand, *Chemist, Analyst*, **46**, 92, (1957).
[8] P. Job, *Ann. Chim.*, **9**, 113 (1928).
[9] E. H. Yoe and A. L. Tones, *Ing. Eng. Chem. Anal. Ed.*, **16**, 111 (1944).
[10] A. E. Harvey and D. L. Manning, *J. Am. Chem. Soc.*, **72**, 4488 (1950).
[11] L. S. Serdyuk, U. F. Goloborodiko and V. W. Bliznyuk, *Zhur. analit. Khim.*, **26**, 506 (1971).
[12] L. S. Berdyuk and V. I. Dovgal, *Izv. Vyssh, Ucheb. Zaved Khim. Tekhnol.*, **14**, 1974 (1971).
[13] A. M. Lukin, V. F. Luk'Yanov, I. V. Nikol'skaya and T. V. Chernysheva., *Khim. Reakt Asobo Chist. Khim. Veschchstu*, **32**, 7 (1970).
[14] N. Munshi Kailash and Day, Arun K., *Mikrochim. Acta*, **5**, 751 (1971).
[15] I. L. Bogbonyl and N. Rustamov, *Dokl. Akad. Nauk. Azerb. SSR.*, **28**, 42 (1972).
[16] J. Veda, *J. Chem. Soc. Japan*, **21**, 724 (1973).
[17] A. I. Kirillov, L. A. Turkina and N.A. Vlasov, *Zhur. analit. Khim.*, **29**, 1225 (1974).
[18] A. I. Kirillov, L. P. Shaulina and N. A. Vlasov, *Izv. Vyss. Ucheb. Zaved. Khim. Tekhnol.*, **18**, 551 (1975).
[19] A. B. Blank and L. E. Pelenko, *Zhur. analit. Khim.*, **31**, 703 (1976).
[20] Ishikura, Fumiko and Tonosaki Koich, *Sci. Rep. Hirosaki Univ.*, **26**, 123 (1979).
[21] A. K. Nurtauva, I. P. Efinov and V. M. Peshkova, *Zhanalit. Khim.*, **32**, 1735 (1977).

Revue Roumaine de Chimie, **33**, *4*, 419–425 (1988)

COMBINAISONS COMPLEXES DU Co(II) AVEC DES LIGANDS DU TYPE DES BASES SCHIFF

I. BERDAN, AL. CAȘCAVAL et A. SCORȚEANU
Institut Polytechnique « Gh. Asachi » Jassy
Faculté de Technologie Chimique, Roumanie

Reçu le 20 décembre 1986
Revisé le 30 octobre 1987

L'ion Co(II) forme avec le bis-1,5 (hydroxyphénil-2)diazo-2,4 hexadiène-1,4 (SALM) une combinaison complexe du type chélate dont la structure correspond á une symétrie plan-carrée. La composition du complexe déterminée par des méthodes spectrophotométriques est représentée par la formule générale ML, où : M = Co(II) et L = ligand (SALM). Cette espèce complexe, avec une stabilité moyenne ($K_{stab.} = 1,3 \cdot 10^2$ L.mol^{-1}) peut constituer un modèle d'étude pour les transporteurs synthétiques d'oxygène.

Interaction between Co(II) ions (M) and 1,5-bis-(2-hydroxyphenyl)-2,4-diaza-1,4-hexadiene (L) was studied by spectrophotometric methods. On the basis of the physical measurements, the formation of ML complex with global constant of stability $K = 1.3 \cdot 10^2$L.mol^{-1} was found. The complex which has square planar structure may be employed as model for the study of synthetic oxygen carriers.

1. INTRODUCTION

Les combinaisons complexes du Co(II), bien que moins stables que celles du Co(III), présentent un grand intérêt pratique et théorique car la réactivité assez élevée explique leur aptitude de participer dans de nombreux processus physico-chimiques.[1] En ce sens, on remarque la propriété des complexes de l'ion Co^{2+} avec les bases Schiff de fixer réversiblement l'oxygène moléculaire.[2]

En vu d'approfondir les connaissances sur la formation, la stabilité et la structure des complexes du Co(II) ayant la fonction transportrice d'oxygène, dans ce travail on présente les résultats obtenus concernant l'étude du système de réaction Co(II) — bis-1,5-(hydroxyphénil-2)-diazo-2,4 hexadiène —1,4 (SALM).

2. PARTIE EXPÉRIMENTALE

D'une manière générale, les bases Schiff utilisées comme ligands sont des bases faibles dont les molécules contiennent l'atome d'azote donneur á l'état d'hybridation sp^2 et des groupements —OH ionisables. En effet, de tels ligands seront préférés par les acides Lewis de classe « b » (Co^{2+}, Fe^{3+} etc.).[3]

Le ligand SALM se prépare par condensation de l'aldéhyde salicylique avec l'ammoniac en présence de l'aldéhyde formique, selon la réaction [4] :

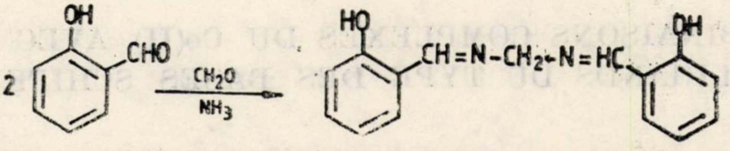

Le ligand, bis-1,6-(hydroxyphénil-2)-diazo-2,5-hexadiène-1,5 (SALEN), utilisé comme référence, a été préparé par une méthode analogue en faisant la condensation de l'aldéhyde salicylique avec l'éthylèndiamine.

L'ion Co^{2+} a été utilisé sous forme de $CoCl_2.6H_2O$. Dans la réaction entre l'ion Co^{2+} et les ligands SALM et SALEN, en solution de $C_2H_5OH-H_2O$, 1 :1, à l'abri d'oxygène, se forment des complexes solubles, colorés. Les complexes séparent à l'état solide en chauffant les mélanges de réaction, sous refluxation à 60—70°C, en atmosphère inerte. On obtient des cristaux bruns (Co^{2+} — SALEN) respectivement brun-ouverts (Co^{2+}—SALM), sensibles à l'air, qui sont purifiés par recristallisation.

Les deux systèmes de réaction ont été étudiés par des méthodes chimiques et physiques telles que : pH-métrie, spectrophotométrie (dans l'ultra-violet, visible et infra-rouge) et magnétochimie.

Les ligands (SALM et SALEN) et l'ion Co^{2+} ont été utilisés sous forme de solutions en milieu alcool éthylique—eau, 1 :1.

Les constantes d'acidité de deux ligands ont été déterminées par une méthode pH-métrique, les mesures de pH étant faites avec l'appareil de type MV-87 (R.D.A.).

Les spectres électroniques des solutions des ligands et des complexes ont été obtenus à l'aide d'un spectrophotomètre du type SPEKORD UV-VIS (Carl Zeiss-Jena, R.D.G.). Le domaine infra-rouge du spectre d'absorption a été étudié sur des pastilles de complexe en KBr, en utilisant le spectrophotomètre SPEKORD IR-71.

Les moments magnétiques des complexes ont été déterminés avec une balance Gouy en utilisant Hg $[Co(SCN)_4]$ comme référence. [5]

3. RÉSULTATS ET DISCUSSIONS

3.1. Les propriétés acido-basiques des ligands

Les propriétés acido-basiques des ligands SALEN et SALM ont été étudiées par voie pH-métrique, en titrant un volume de solution (20 cm³) de ligand avec une solution aqueuse d'acide chlorhydrique $0{,}5.10^{-1}$m ; la concentration de la solution de ligand est $0{,}5.10^{-2}$ m. Sur les graphes des fonctions $pH = f(V_{HCl})$ on observe que les deux ligands se comportent comme dibases ; figures 1 et 2.

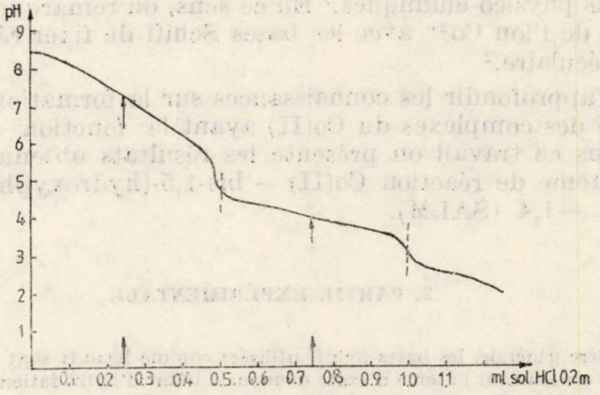

Fig. 1. — Titrage pH-métrique du SALEN avec une solution d'acide chlorhydrique.

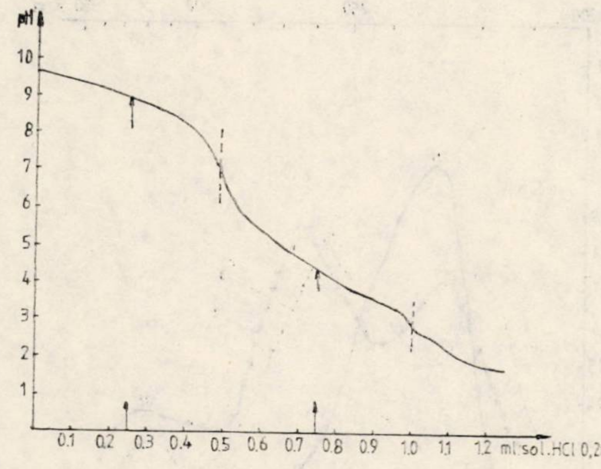

Fig. 2. — Titrage pH-métrique du SALM avec une solution d'acide chlorhydrique.

En sachant que l'addition de $V_{éq.}/2$ ($V_{éq.}$ étant le volume équivalent de solution de HCl) cm^3 de solution d'acide chlorhydrique correspond à la formation d'un mélange tampon, on calcule les grandeurs pK_{a_i} et pK_{b_i} dont les valeurs sont portées dans le tableau 1.

Tableau 1

Les valeurs pK_{a_i} et pK_{b_i} des ligands

Ligand	pK_{a_1}	pK_{a_2}	pK_{b_1}	pK_{b_2}
SALEN	7,3	4,0	6,7	10,0
SALM	8,8	4,4	5,2	9,6

La basicité un peu plus grande du SALM est due, probablement, aux groupements alchiliques qui modifient la densité électronique de l'atome d'azote donneur.

3.2. L'étude des complexes en solution

La formation, la stabilité et la structure des complexes solubles des systèmes de réaction Co(II) — bases Schiff ont été suivies par voie spectrophotométrique. Dans les figures 3a et 3b on présente les spectres électroniques des solutions de $CoCl_2.6H_2O$, des ligands (SALEN et SALM) et des complexes de rapport molaire 1 :1 (en milieu $C_2H_5OH-H_2O$, 1 :1).

L'ion $[Co(H_2O)_6]^{2+}$, en solution $C_2H_5OH-H_2O$ (1 :1), présente trois bandes d'absorption avec les maximum situés à : 229 nm, 523 nm respectivement, 648 nm, caractéristiques au cas d^7 dans la symétrie octaédrique

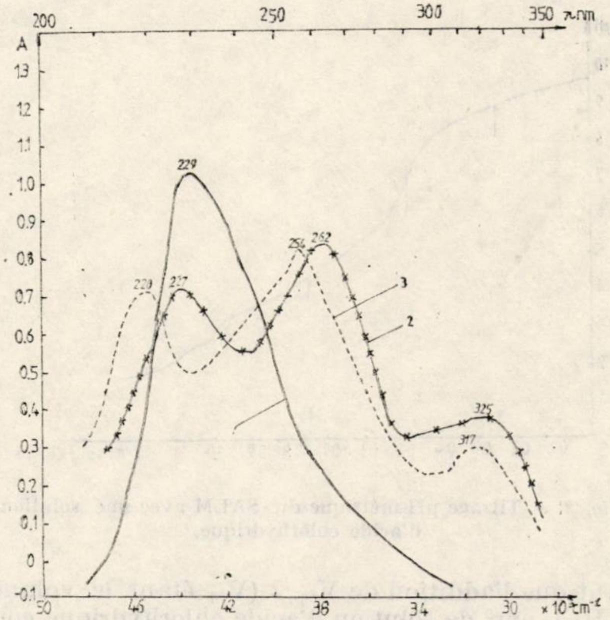

Fig. 3*a*. — Spectres d'absorption dans l'ultra-violet de l'ion Co(II) et des ligands, SALEN et SALM : 1 — $CoCl_2 \cdot 6H_2O$, $c = 2 \cdot 10^{-4}$m, en milieu $C_2H_5OH-H_2O$ (1 :1) ; 2 — SALEN, $c = 2 \cdot 10^{-4}$ m, en C_2H_5OH ; 3 — SALM, $c = 2 \cdot 10^{-4}$ m, en C_2H_5OH ; cuve : 0,5 cm.

(O_h). La bande avec le maximum situé à $\lambda = 648$ nm correspond à la transition ${}^4A_{2g} \rightarrow {}^4T_{1g}$. La même transition est associée avec la bande d'absorption de $\lambda_{max.} = 625$ nm, mais dans une solution aqueuse. Les deux ligands présentent des bandes d'absorption caractéristiques, surtout dans le domaine ultra-violet. Dans les spectres des mélanges de réaction Co(II) — base Schiff on constate que la bande de l'ion Co^{2+}, située à 648 nm est retrouvée sous forme d'épaulement à 650 nm (pour SALEN) respectivement 646 nm (pour SALM). Cette modification de l'allure de la bande de l'ion libre est due à la coordination des ligands à l'ion métallique et par conséquent serait utilisée, par la suite, pour déterminer la composition et la stabilité des complexes.

Dans les figures 4 et 5 on présente les données concernant la détermination du rapport molaire de combinaison et de la stabilité des complexes par la méthode de variations continues (Job).[6]

Pour deux concentrations différentes, le point d'intersection de deux droites, obtenues en représentant les fonctions Absorbance = f(composition du mélange), correspond au rapport molaire Co(II)/ligand = 1 :1. En outre, les données expérimentales obtenues par la methode Job nous a permis de déterminer les constantes de stabilité des complexes en utilisant la variante dite Turner-Anderson. [7] De fait, dans les points a et b, déterminés pas l'intersection de la parallèle P avec les deux droites (fig. 4

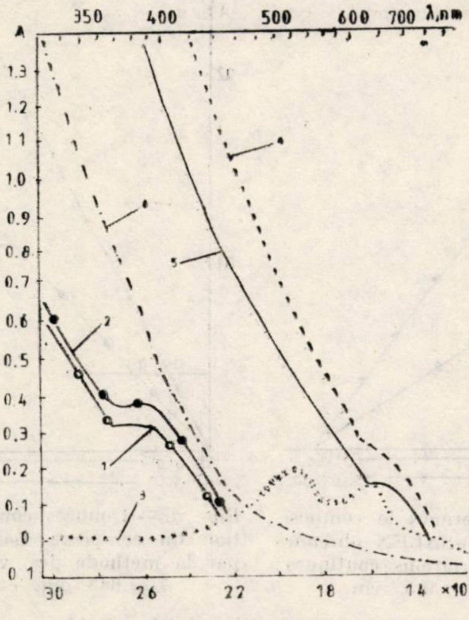

Fig. 3b. — Spectres d'absorption dans le domaine visible de l'ion Co (II) et des mélanges Co(II) — Ligand de rapport molaire 1 :1 ; 1 — SALEN, $c = 5 \cdot 10^{-3}$ m solution alcoolique ; 2 — SALM, $c = 5 \cdot 10^{-3}$, m solution alcoolique ; 3 — $CoCl_2 \cdot 6H_2O$, $c = 10^{-2}$ m, en solution $C_2H_5OH-H_2O$,1 :1 ; 4 — Co(II)-SALM (1 :1), $C_{Co(II)} = 10^{-2}$ m, en solution $C_2H_5OH-H_2O$ (1 :1) ; 5 — Co(II)-SALEN(1 :1), $C_{Co(II)} = 10^{-2}$ m, en solution $C_2H_5OH-H_2O$ (1 :1) ; 6 — Co(II)-SALM(1 :1), $C_{Co(II)} = 7{,}5 \cdot 10^{-3}$ m, en solution $C_2H_5OH-H_2O$ (1 :1) ; cuve : 0,5 cm.

et 5), les quantités de complexes formés sont égales : $X_1 = X_2 = X$. Dans ces conditions, les relations suivantes sont valables :

$$X = \frac{a_1 \cdot b_1 - a_2 \cdot b_2}{(a_1 + b_1) - (a_2 + b_2)} \text{ et } K_{stab.} = \frac{X}{(a - X)(b - X)},$$

où : a_i et b_i sont les concentrations molaires du Co(II) et du ligand dans les points a et b ; $K_{stab.}$ = constante de stabilité du complexe. Ainsi, on obtient pour $K_{stab.}$ les valeurs suivantes :

$$K_{(Co^{2+}-SALEN)} = 0{,}8.10^2 \text{ L.mol}^{-1} \text{ et}$$

$$K_{(Co^{2+}-SALM)} = 1{,}3.10^2 \text{ L.mol}^{-1}$$

La stabilité un peu plus grande du complexe avec SALM est corrélée avec la valeur correspondante de la constante de basicité du ligand.

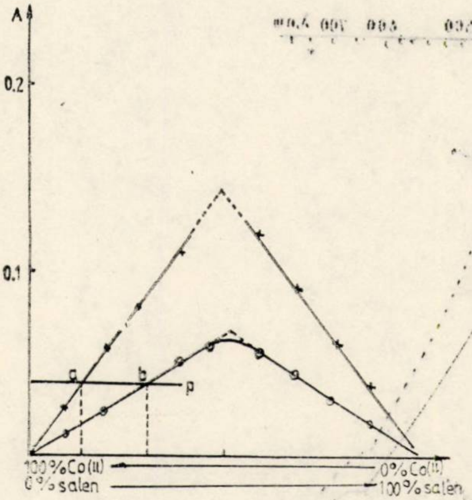

Fig. 4. — Données concernant la composition du complexe Co(II)-SALEN obtenues par la méthode des variations continues ; λ = 650 nm, cuve : 0,5 cm.

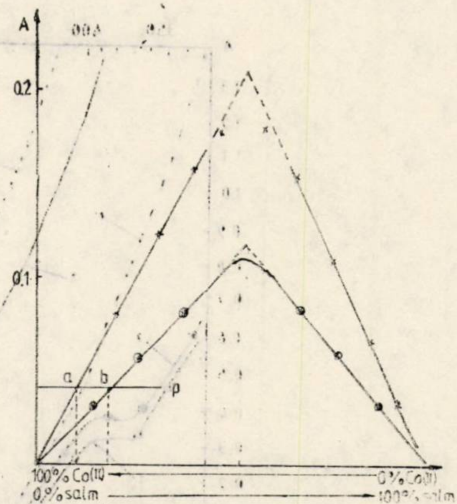

Fig. 5. — Données concernant la composition du complexe Co(II)-SALM obtenues par la méthode des variations continues ; λ = 646 nm, cuve : 0,5 cm.

3.3. L'étude des complexes à l'état solide

Les complexes à l'état solide ont été étudiés par spectroscopie d'absorption en infra-rouge et par magnétochimie.

Dans la figure 6 on présente les spectres I.R. du ligand SALM et du complexe Co(II)-SALM de rapport molaire 1 : 1. Ainsi, on observe que

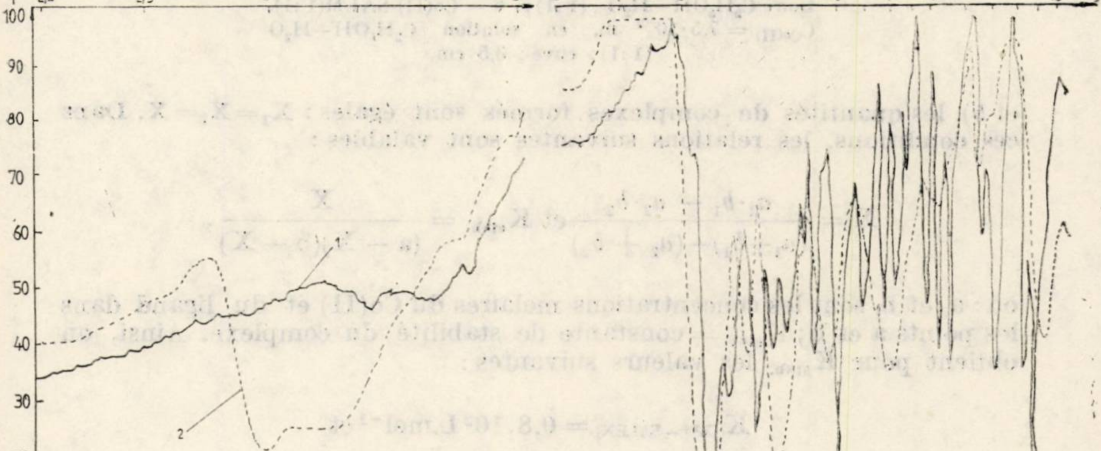

Fig. 6. — Spectres d'absorption en infra-rouge : 1 — Co(II)-SALM (1 :1) ; 2 — SALM.

la vibration de valence $\nu_{C=N}$ qui apparaît dans le spectre de la molécule de ligand libre à 1630 cm^{-1}, d'intensité moyenne, est retrouvée dans le spectre du complexe à 1615 cm^{-1}, d'intensité plus faible. Cette modification est due à l'implication de l'atome d'azote donneur du groupement C=N dans le processus de coordination du ligand à l'atome central. De même, l'affaiblissement de l'intensité de la bande d'absorption du groupement —OH phénolique (3000—3400 cm^{-1}) du ligand libre prouve qu'il y a aussi une participation de la part de celui-ci par le deuxième point basique (—OH) au processus de coordination. Ces deux observations nous permettent de conclure que la structure du complexe comporte tant des liaisons $=N \rightarrow Co$ que des liaisons covalentes, simples, —O —Co, ce qui correspond à la formation d'un chélate du type complexe interne.

La détermination de la susceptibilité magnétique, avec la balance Gouy, a permis le calcul du moment magnétique du complexe à l'état solide, à 25°C, dont la valeur est $\mu = 2{,}02$ M.B. Cette valeur indique la formation d'un complexe avec une configuration plan-carrée dans lequel les sept électrons de l'ion central se placent sur les niveaux énergétiques comme suit : $(d_{xy})^2\ (d_{zy})^2\ (d_{z^2})^2\ (d_{x^2-y^2})^1$; le paramagnétisme du complexe correspond donc à un électron non-apparié. L'écart de la valeur du $\mu_{exp.}$ par rapport à la valeur $\mu_{(spin\ pure)}$ (1,83 M.B.) montre la formation de liaisons à caractère covalent.

La détermination du moment magnétique du complexe a été considérée comme critère de base à l'appui de la symétrie plan-carrée ; les complexes tetraédriques du Co(II), dans les champs faibles de ligands, ont des valeurs $\mu_{mag.}$ comprises dans l'intervalle 3,8...4,5 M.B. Les spectres électroniques peuvent être, aussi, utilisés en vue de différencier les configurations tetraédriques (T_d) de celles plan-carrées (D_{4h}), mais la bande caractéristique du complexe de symétrie D_{4h} est située dans l'intervalle 1150—1180 nm (8400—8600 cm^{-1})[8] qui ne peut être déterminé avec les appareils que nous avons utilisées.

4. CONCLUSIONS

Dans la réaction de l'ion Co(II) avec le ligand(L) : bis-1,5-(hydroxyphénil-2)-diazo-2,4-hexadiène-1,4 (SALM) se forme un chélate de type complexe interne avec une symétrie plan-carrée. Les déterminations du rapport molaire Co(II)/SALM et de la stabilité du complexe montrent la formation de l'espèce complexe de composition Co(II) : SALM = 1 :1 avec la constante de stabilité $K_{stab.} = 1{,}3 \cdot 10^2$ $L.mol^{-1}$. Le complexe peut constituer un modèle d'étude pour les transporteurs synthétiques d'oxygène.

BIBLIOGRAPHIE

[1] E. C. Niederhoffer, J. H. Timmons et A. E. Martell, *Chem. Rev.*, **84**, 137 (1984).

[2] T. Tsumachi, *Bull. Chem. Soc. Japan*, **13**, 252 (1938).

[3] S. Ahrland, J. Chatt et N. R. Davies, *Quart. Rev.*, **12**, 265 (1958).

[4] Al. Caşcaval, Brévet R. S. de Roumanie, n° 89 358/1985.

[5] W. Haberditzl, « Magnetochemie », Academic-Verlag, Berlin, 1968.

[6] P. Job, *Ann. Chim. (France)*, **9**, 113 (1928).

[7] S. E. Turner et R. C. Anderson, *J. Amer. Chem. Soc.*, **71**, 932 (1949).

[8] A.B.P. Lever, « Inorganic Electronic Spectroscopy », Elsevier, Amsterdam, 1968.

la vibration de valeur $\nu_{C=N}$ qui apparaît dans le spectre de la molécule du ligand libre à 1630 cm^{-1}, d'intensité moyenne, est retrouvée dans le spectre du complexe à 1615 cm^{-1}, d'intensité plus faible. Cette modification est due à l'implication de l'atome d'azote donneur du groupement C=N dans le processus de coordination du ligand à l'atome central. De même, l'affaiblissement de l'intensité de la bande d'absorption du groupement –OH phénolique (3000–3100 cm^{-1}) du ligand libre prouve qu'il y a aussi une participation de la part de celui-ci par le deuxième point, c'est-à-dire (–OH) au processus de coordination. Les deux observations nous permettent de conclure que la structure du complexe contient tant des liaisons $\geq N \rightarrow Co$ que des liaisons covalentes, simples, $-O-Co$, ce qui correspond à la formation d'un chélate du type complexe interne.

La détermination de la susceptibilité magnétique, avec la balance Gouy, a permis le calcul du moment magnétique du complexe à l'état solide, à 20°C, dont la valeur est $\mu = 2{,}02$ M.B. Cette valeur indique la formation d'un complexe avec une configuration plan-carrée dans lequel les sept électrons de l'ion central se placent sur les niveaux énergétiques comme suit : $(d_{xz}, d_{yz})^4 (d_{z^2})^2 (d_{xy})^1 (d_{x^2-y^2})^0$; le paramagnétisme du complexe correspond donc à un électron non-apparié. L'écart de la valeur du μ_{eff} par rapport à la valeur $\mu_{spin\text{-}only}$ (1,83 M.B.) montre la formation de liaison à caractère covalent.

La détermination du moment magnétique du complexe a été considérée comme critère de base à l'appui de la symétrie plan-carrée ; les complexes tétraédriques du Co(II), dans les champs faibles de ligands, ont des valeurs μ_{eff} comprises dans l'intervalle 3,8 – 4,5 M.B. Les spectres électroniques peuvent être aussi utilisés en vue de différencier les configurations tétraédriques (T_d) de celles plan-carrées (D_{4h}), mais la bande caractéristique du complexe de symétrie D_{4h} est située dans l'intervalle (Réf. 8) 1100 – 2000 nm (5000 – 9000 cm^{-1}) et ne peut être déterminée avec les appareils que nous avons utilisés.

CONCLUSIONS

Dans la réaction de l'ion Co(II) avec le ligand (L) : bis-1,5-(hydroxyphényl)-2,4-diaza-2,4-hexadiène-1,1 (SALM) se forme un chélate de type complexe interne avec une symétrie plan-carrée. Les déterminations du rapport molaire Co(II) : SALM et de la stabilité du complexe montrent la formation de l'espèce complexe de composition Co(II) : SALM = 1 : 1 avec la constante de stabilité $K_{stab} = 1{,}8 \cdot 10^{[illegible]}$ l·mol^{-1}. Le complexe peut constituer un modèle [illegible] pour les porteurs synthétiques d'oxygène.

BIBLIOGRAPHIE

1 [illegible], L. B. Timmons et A. E. Martell, Chem. Rev., 54, 137 (1954).
2 C. [illegible], Bull. Chem. Soc. Japan, 13, 252 (1938).
3 S. [illegible] et N. S. [illegible], [illegible], 12, 253 (1958).
4 M. [illegible], [illegible], B. [illegible] de Roumanie, nr 89638/1968.
5 A. Haberditzl, Magnetochemie, Akademie Verlag, Berlin, 1968.
6 [illegible], Ann. Chim. (France), 9, 111 (1964).
7 S. E. [illegible] et K. C. Anderson, J. Amer. Chem. Soc., 74, 632 (1952).
8 A. B. P. Lever, Inorganic Electronic Spectroscopy, Elsevier, Amsterdam, 1968.

Revue Roumaine de Chimie, **33**, *4*, 427–433 (1988)

COMPTES RENDUS

E. Buncel and C. C. Lee (eds.), "Isotopes in Organic Chemistry". Vol. 7, "Secondary and Solvent Isotope Effects", Elsevier Sci. Publ., POB 211, Amsterdam (or POB 1663, Grand Central Station, New York, NY 10163), 1987. Hard cover, 500 pp, 330 Dfl, ISBN 0–444–42770–8 (or for all volumes 0–444–41742–7)

Volume 7 of the series contains six chapters.

All authors of this volume have adopted a uniform notation and all make extensive use of fractionation factors φ : if n is the atom fraction of D in a mixture of H_2O and D_2O, and X_{Di}, X_{Hi} are atom fractions of D and H, respectively, at site i in the molecule, then $\varphi_i = (X_{Di}/X_{Hi})/\ [n/(1-n)]$. The fractionation factor of the hydronium ion is 0.69 indicating preference for protium relative to a bulk water site, because of weaker binding in H^-O^+ relative to H–O. Vice-versa hydroxide has a tighter binding leading to $\varphi = 1.25$ (preference for deuterium), and if solvation is considered one obtains for OH^- : $\varphi = 1.25\ (0.74)^3 = 0.5$. Indeed-$H_2O$ is $1/(0.69)^3(0.5) = 6$ time more dissociated than D_2O by autoprotolysis.

The first chapter is entitled "Mechanistic deductions from solvent isotope effects" by by F. J. Alvarez and R. L. Schowen. The authors present the developments since 1972, when Schowen had published in *Prog. Phys. Org. Chem.* a review based, like the present one, on the idea of proton inventory. The latter author advocates the use of proton inventory plots for a range of concentrations with various atom fractions of deuterium in H_2O-D_2O mixtures. From the shape of the proton-inventory plot over a range of solvent compositions, conclusions are drawn relative to mechanisms of general acid/base catalysis, mechanisms of reactions catalyzed by hydrolytic enzymes, and the number of sites involved in the process. The applications which are discussed include protolytic catalysis. Charts and tables illustrate a host of reactions, among which the so-called "water reactions" are discussed in terms of the "immature hydronium ion model". Methanolyses in alkaline methanol, catalyses by hydrolytic enzymes, reactions involving aprotic solvents, cosolvent effects, the influence of salts or heterogenous phases are also discussed. Thus the mutarotation of tetramethylglucose catalyzed by deuterated 2-pyridone shows a "solvent isotope effect" in benzene and the proton inventory plot indicates two sites in the transition state; however, in aqueous acetonitrile the reaction appears to be one-site with respect to 2-pyridone which behaves as a general base at H_2O-D_2O concentrations above 5M. A final section discusses displacement reactions at saturated carbon, unsaturated carbon (e.g. methanolysis of 1-chloro-2,4-dinitrobenzene which shows an inverse solvent isotope effect, larger in pure CH_3OH/CH_3OD than in CH_3CN–methanol), and at silicon and tin. Some of the observations have not yet been satisfactorily explained.

The second chapter, by W. W. Cleland, is entitled "Secondary isotope effects on enzymatic reactions". After an introductory part on nomenclature and methodology, various enzymatic reactions are reviewed and their isotope effects are discussed : heavy atom isotope effects β-secondary deuterium isotope effects, and (with the most numerous examples) α-secondary isotope effects. From these data the structures of the transition state are inferred. Thus the ratio o the maximum velocity to the Michaelis constant for protonated *versus* deuterated systems in the hydrolysis of 4-methoxyphenyl formate by chymotripsin appears to be intermediate between sp^2 and sp^3 structures.

J. J. Gajewski's chapter is entitled "Hydrogen isotope effects in pericyclic reactions". The kinetic isotope effect for 1,1,6,6-D_4-2,5-diphenyl-1,5-hexadiene is 1.57^{-1} while for 3,3-dicyano-1,2-diethyl-6,6-D_2-hexadiene it is only 1.06^{-1}. This is interpreted as indicating a variety of transition states ranging from a 1,4-cyclohexanediyl biradical to a pair of allyl radicals. After sigmatropic shifts cycloadditions are reviewed. The α-secondary deuterium isotope effects in the Diels-Alder reaction are small but measurable. The concerted transition state appears to be symmetrical. Electrocyclic and ene reactions are also discussed. Two appendices indicate for [3,3]sigmatropic shifts the Conrad-type linear correlations and fractionation factors per D atom.

Kresge, More O'Ferrall and Powell wrote the 4th chapter entitled "Solvent isotope effects, fractionation factors and mechanisms of proton transfer reactions". They surveyed both pure D_2O and mixtures D_2O-H_2O, using mainly Albery and Davies analysis for the latter mixtures; these authors suggested that one rate or equilibrium measurement at the molar fraction $x = 0.5$ is sufficient (unlike Schowen's proton inventory method). The hydronium and hydroxide ions are associated with a strong solvent isotope effect upon transfer from H_2O to

D_2O ; critical discussions follow on the contribution of the medium effect to the solvent isotope effects of these two ions. Amplified kinetic isotope effects as large as 50 are seen in reactions proceeding through a common intermediate in exchange and elimination reactions. The chapter concludes with a compilation of fractionation factors (FF) for isotopic hydrogen bound to carbon and separately to other atoms. Among the methods used for determining FF values the NMR method is simple when the exchange with solvent is slow; for OH or NH bonds Saunders found that deuteration modifies by 7—20 Hz the chemical shift of the carbon atom bonded to the O or N atom; this leads to a convenient measurement technique.

Chapter 5 by Westaway is entitled "Secondary H—D isotope effects and transition state structure in S_N2 processes". The hyperconjugative secondary kinetic isotope effects (KIE) are normal or positive i.e. $\log (k_H/k_D) > 0$, owing to the fact that the undeuterated transition state is more stable due to the higher electron-donating ability of $C_\beta-H$ bonds than $C_\beta-D$ bonds. A strong angular dependence is observed for the angles between the C—H(D) bond and the direction of the leaving group. Indeed, most KIE's reported for carbocation S_N reactions are large and normal (in the range $1.10 \pm 0.05/\beta$-D). The steric secondary KIE's, on the other hand, due to the shorter C-D than C-H bonds, are inverse. A literature survey indicates that the case for electron-releasing inductive effect of C-D versus C-H bond, which would lead to inverse KIE's, is much less clear, although there are documented instances of such inverse KIE's in the absence of hyperconjugative or steric factors. Secondary H-D equilibrium isotope effects are also discussed, again with debatable conclusions. A hyperconjugative KIE is greater than the steric and inductive secondary KIE, and this makes it difficult to ascertain the role inductive effects in a secondary KIE observed in S_N2 reactions.

The secondary KIE's can be used as a criterion for determining the mechanism of S_N reactions: both for α-and β-deuterium, a KIE $\geqslant 1.07$/D is evidence for S_N1 while KIE $\leqslant 1.05$/D is considered evidence for an S_N2 mechanism. All factors (substitution or conjugation at the alpha carbon, bulky leaving groups, ion pairing, changes in the transition state structure, complexing effects between the nucleophile and the substrate) are considered separately. The final sections discuss the use of secondary H-D KIE's to elucidate the structure of S_N2 transition states, and the use of solvent and base KIE's for obtaining information on S_N2 reactions. Although this is one of the best written chapters and the exposition is most systematic, it is regrettable that some of the literature relevant to this topic is missing.

The last chapter is entitled "Model calculations of secondary isotope effects". The author, D. J. McLennan, starts from the Bigeleisen equation showing that vibrational zero-point energy differences are the most important factor in H-D isotope effects. Force field calculations are accurate enough to reproduce fractionation factors. The author reviews calculations using various theoretical methods (both *ab initio* and semiempirical such as MNDO) for mechanistic studies in: nucleophilic aliphatic substitutions, eliminations, nitroalkane deprotonations, carbonyl group reactions, and radical or pericyclic reactions.

The volume is prepared by photoprinting author's manuscripts, and has a subject index. The high quality of the reviews makes this volume a "must" for all those interested in secondary isotope effects.

Alexandru T. Balaban
Polytechnic Institute Bucharest

A. Nickon and E. F. Silversmith, "Organic Chemistry: the Name Game. Modern Coined Terms and Their Origins", Pergamon Press, Oxford, 1987. 347 pp, hard cover, £ 45.00, ISBN 0—08—034481X; flexicover, £ 18.00, ISBN 0—08—351573

It will be impossible to summarize adequately this delightful book. One has to enjoy reading if for the pleasure of being entertained and enlightened at the same time. The authors state in the preface that their aim was to present modern coined names in organic chemistry by contacting directly their originators. Thus a permanent record of information will be present even after our current generation of chemists is gone. The book is not a dictionary, nor are the authors lexicographers in quest of solemn definitions. The authors are practising organic chemists and they write in a light vein on a variety of terms, recounting the history of their origin, the stimuli that gave rise to the ideas, and sometimes the demise of these terms.

One is struck by the encyclopedic array of topics covered by the book: names of phenomena or compounds derived from animals or plants; from mechanical tools; from headgear; from houses; from food; from numbers or letters; from names of persons, towns, countries or continents; etc.

In order to avoid misunderstandings, this is not a book on organic name reactions, or on compounds named according to a person's name. There are quite a few exceptions to the last point, however. Thus we do not find Nenitzescu's hydrocarbon, Michler's ketone, Bindschedler's green or Homolka's base, but we do find Galvin Coppinger's radical under the name galvinoxyl (with details about who was the godfather); we learn that "friedelin" was baptized by C. Istrati and A. Ostrogovitch of the University of Bucharest in 1899 (and we see its structure established by Ruzicka and Corey independently in 1955).

Actually, a whole chapter entitled "Our colleagues and some other folks" describes how names such as kekulene, bullvalene or barbaralone came about. This chapter ends up with a brilliantly funny account of acronyms.

The chapter "Chemistry is no flask in the pan" contains the humorous facsimile of a 4-page fictitious paper in *Tetrahedron Letters* format written by C. Djerassi's friends on the occasion of the 1000th paper by C. D. Also reproduced in the chapter "Elements, my dear Watson! " are Metanomski's posters on record-breaking in *Chem. Abstr.* data base.

Fluency in English allows the reader to grasp all puns. Of course, jokes that have to be explained lose their charm. The book may prove to be (i) an incentive for self-study of English by organic chemists; (ii) a splendid textbook for classes of English with chemistry students.

The book has 20 chapters and six appendixes. The chapters are simply collector bags for funny or interesting stories about names in organic chemistry, and each bag has a distinguishing mark to connect loosely these stories. Even so, the last chapter's title is "Leftovers".

In the first chapter one learns about the professor's cat who authored two scientific papers and who almost seduced the professor's wife. Each chapter is thoroughly documented by a serious and rich bibliography.

The six appendixes are: A, Brief etymology of some traditional chemical names (16 pages of alphabetically ordered chemical names; e.g. veronal, gulose, ninhydrin, mesitylene, gallium, chalcone, anomer, have each an interesting story in the background); B, Origin of element names (briefly, in table format); C, Latin and Greek terms for numbers; D, Numerical prefixes in chemical words; E, Greek alphabet; and F, Nobel prizes in the sciences. The alphabetical subject index is quite detailed (in such a book, an author index would have helped).

For both teachers and students of organic chemistry this book will be a continuous source of pleasantly-obtained information. It will surely enrich the personal libraries of many lovers of chemistry.

A. T. Balaban
Polytechnic Institute Bucharest

J. R. Dias, "Handbook of Polycyclic Hydrocarbons, Part A, Benzenoid Hydrocarbons", Elsevier, Amsterdam, 1987, hard cover, 388 pp, ISBN 0–444–42802–X

Volume 30 in the series "Physical Sciences Data" is a reference book on benzenoid polycyclic aromatic hydrocarbons (PAH), intended to supplement and update E. Clar's well-known two-volume treatise "Polycyclic Hydrocarbons" published by Academic Press in 1964. Two thirds of this book are comprised of a tabular survey of about 500 PAH's (two per page in standard format including recent references and brief chemical, theoretical, carcinogenicity, and spectral data). Not only the known PAH's, but also some of the yet unreported ones are included when theoretical data (HOMO or E_π) were calculated, or when the PAH is considered to present some interest.

The first part of the book (120 pages) is divided into four chapters plus a 3-page introduction. As stated in this introduction the basic idea of this book is the author's "formula periodic table" for benzenoid PAH's having even numbers of carbon atoms, which is presented in detail in chapter 2. Chapter 1 is a brief survey of existing proposals for the nomenclature of PAH's; in the tables, the *Chem. Abstr.* – IUPAC nomenclature is used.

Graph-theoretical definitions are presented at the beginning of chapter 2. The formula periodic table has on the ordinate the number of internal (third-degree or 3-connected) carbon atoms in the PAH, and on the abscissa the "net disconnection" parameter $d_s = k - r - 1 = = p_3 - q_1 - 1 = N_{Pc} - r$; both parameters are positive or null integers (d_s may also have negative integer values). In the boxes of the periodic table, we have molecular formulas of PAH's. Many interesting relationships of graph invariants are listed by the author for the number of 3rd degree internal/peripheral vertices (N_{Ic} and N_{Pc}, respectively), the number of internal C–C bonds (q_I), the number of rings (r), the number of vertices having degree 3 (p_3), the number k of graph components, etc.

Chaper 3 is entitled "Benzenoid isomer enumeration". It starts with the exposition of the cata-condensed benzenoid PAH's on the basis of the dualistic graphs introduced by Balaban and Harary. Then peri-condensed benzenoid PAH's are enumerated by using the excised internal structure concept, with amply illustrated examples (28 pages of formulas).

Chapter 4, entitled "Spectroscopy of benzenoid hydrocarbons" discusses UV, photoelectron, infrared and NMR spectroscopy of PAH's. Then theoretical correlations are briefly presented. In more detail the author shows how to determine select eigenvalues (0, ± 1, etc.) by topological inspection, either by using the excised internal structure concept, or by embedding smaller alternant polyenes on PAH skeletons. For instance eigenvalues ± 1 are present in those PAH's which have a selective lineation.

The book is photoprinted from the author's manuscript, and thus practically error-free; there are some missing formulas in the tables for helicenes, but the structure is evident from the name.

For all chemists who are interested in theoretical or biological problems connected with benzenoid PAH's this book will be a precious source of information.

Alexandru T. Balaban
Polytechnic Institute Bucharest

R. R. Muccino (ed.), "Synthesis and Applications of Isotopically Labeled Compounds, 1985" (Proceedings of the Second International Symposium, Kansas City, Missouri Sept., 3–6 1985), Elsevier, Amsterdam, 1986. Hard cover, xxxiv + 558 pages, US $ 129.75, ISBN 0–444–42612–4

This Symposium was attended by 337 scientists from 19 countries including Hungary and the Soviet Union. No one from Roumania participated, although the present reviewer was a member of the International Scientific Committee (13 members from 8 countries) and submitted a review entitled "Vistas opened by Fourier-transform NMR in the area of compounds labeled with isotopes of hydrogen, carbon, nitrogen and oxygen" which is included in the present volume.

In the opening address presente dby the Chairman of the International Scientific Committee, who is also the Editor of the volume, Dr. Muccino, stressed the interdisciplinary nature of the symposium. The focus was on new applications of labeled compounds.

Professor Melvin Calvin gave the banquet speech and award address, in the spirit of his quotation: "The synthesis of a really new conception requires some sort of union in one mind of the pertinent aspects of several disciplines". This address recalls the incentive he had from E. O. Lawrence to start preparing ^{14}C-labeled compounds, which culminated in elucidating the path of carbon in photosynthesis.

The plenary lecturers and the titles of their papers are: S. C. Wang and M. T. Hua, Background and present status of isotope applications in China; K. Kumazawa, Use of ^{15}N in the field of agricultural science in Japan; A. P. Wolf and J. S. Fowler, Recent advances in the chemistry of positron emitters (this lecture concentrated on ^{11}C-and ^{18}F-labeled compounds); E. Buncel and J. R. Jones, Homogeneous catalysis of hydrogen isotope exchange; J. P. Coghlan et al, Hybridization histochemistry — locating gene expression; P. Osinsky, Analytical control of technetium-diphosphonate complexes for radiodiagnostic applications: review and recent progress.

The remaining 100 oral presentations are grouped as invited and contributed papers in the following sections (number of papers in brackets):

1. Mechanistic studies using isotopes in drug metabolism (5).
2. Isotopes in organic and bioorganic reaction mechanisms (7).
3. Chemical applications of NMR imaging (3).
4. The synthesis and use of radioligands in binding studies (5).
5. The synthesis and applications of organic compounds labeled with isotopic hydrogen (9).
6. Isotopically labeled compounds in recombinant DNA research (4).
7. Contemporary approaches to the synthesis of isotopically labeled compounds (5).
8. Applications of ^{2}H and ^{15}N NMR spectroscopy (5).
9. Isotopes in clinical pharmacology: the use of deuterated analogs of drugs as medicinal agents (4 papers plus a summary of the panel discussion on this topic).
10. Synthesis and application of organic compounds labeled with isotopes other than those of hydrogen (two separate sections with 8 + 11 papers).
11. Synthesis and applications of labeled peptides (4).

12. Applications of isotopes in clinical research (5).
13. Applications of tritium NMR spectroscopy (8).
14. Isotopically labeled compounds in medical chemical defense and related research (5).
15. State of the art in the instrumentation for analysis of isotopically labeled compounds (7).
16. Trends in the synthesis of isotopically labeled compounds (6).

The volume is concluded by the list of the 70 poster titles, and by an authors and subject index. The high-quality paper and manuscripts contribute to the pleasant reading of this volume.

It will be impossible to highlight all the significant contributions, therefore a rather subjective enumeration follows. In section 1, Farmer, Bird and Shuker describe deuterium labeling studies of protein and DNA alkylation: nitrosamines transfer alkyl groups to guanine residues in DNA or RNA, and phosphoramide mustards alkylate via aziridinium ions.

In section 2, Ahlberg et al. demonstrate that large ($k_H/k_D \cong 90$) deuterium kinetic isotope effects (KIE) may be due to reaction branching (multiplication of two or more isotope effects) rather than tunneling. On the other hand, Saunders et al. review secondary beta-tritium isotope effects in E2 reactions on the basis of tunneling. Shine et al. discuss anew the benzidine rearrangement on the baisis of heavy-atom (^{13}C, ^{14}C, ^{15}N, ^{18}O) KIE.

In the invited lecture of section 4, Pichat reviews tritium labeling of radioligands for receptor binding studies. Srivastava et al. describe the adoptation of Bodor's method for introducing radioiodinated pyridinium compounds across the blood-barrier, via the dihydro-derivative.

In section 5, Myasoedov reviews the synthesis of tritiated biologically active compounds in USSR: nucleic acid components, aminoacids and peptides, postaglandins, lipids.

In section 6, Hirschberg describes the use of radioactively labeled compounds in recombinant DNA research: both ^{32}P as in Sanger's initial method for polynucleotide sequencing and the newer use of ^{32}S-labeled nucleotide analogs led to fast and reliable methods. A second paper on the topic of ^{35}S nucleotides in Sanger dideoxy sequencing is presented by Kashdan and Ornstein. Phillips, Smith and Hahn describe the use of hypersensitization, a technique currently used by astronomers, for increasing 2- to 8-fold the detection capability of autoradiographic film.

In section 7, the amidocarbonylation is described by Ajami et al. as a method of choice for obtaining kg-amounts of ^{15}N and ^{13}C labeled amino acids, starting from [^{15}N]acetamide or ^{13}CO. Coates et al. describe the use of supertritide ($LiEt_3BT$) for synthesizing chiral methyl groups ($-CHDT$) by ring opening of stereospecifically 2-deuterated styrene oxide. Srivastava et al. reviewed the incorporation of radiohalogens (F, Br, I) via organometallic intermediates (B, Tl, Hg, Sn). Organoborane chemistry can provide convenient synthetic routes to labeled compounds as shown by Kabalka.

In section 8, Van Etten reported on the ^{18}O-isotopic shift in ^{13}C- and ^{15}N-NMR for studying bioorganic reaction mechanisms.

In section 11, Veres et al. describe labeling and separation methods for diagnostic agents in Hungary, including a sublimation generator for ^{99m}Tc from titanium molybdate as target material. Also from Hungary, Banfi and Mlinko presented in a talk and a poster a convenient method for synthesizing isotopically labeled alkali cyanides.

Summing up, the volume provides an in-depth summary of the current state of research in the field of labeled compounds. The next symposium is to be held in 1988 in Innsbruck, Austria.

A. T. Balaban
Polytechnic Institute Bucharest

E. Fitzer (ed), "Carbon Fibres and Their Composites", Springer-Verlag, Berlin, 1985. Hard cover, 300 pp, DM 128. ISBN 3-540-15804-9

The proceedings of the International Conference on Carbon Fibre Applications held on 5—9 December 1983 at Sao José dos Campos (Brazil) under the sponsorship of the U. N. Industrial Development Organization and the U. N. Financing System for Science and Technology for Development appeared in a typeset volume. The carbon-fibre project at the Centro Tecnico Aerospacial in Sao José dos Campos (SA) and in Camaçari (BA) in Brazil was financed by UNFSSTD and involved the production of the carbon fibre on pilot and then industrial scale. At the international conference participated with lectures 14 experts from universities (Wyoming Univ., Rensselaer Polytechnic Institute, and Lowell University, USA; Universität Karlsruhe, FRG; Chung-Nam University, South Korea), research institutes

(Polymer Research Institute, Zhengshan, China ; Institut für Strukturmechanik, Braunschweig, FRG ; Medical Institute, Stoke-on-Trent, Britain), and industry (CIBA-Geigy, Cambridge, Britain ; Celanese Research Company, Summit, New Jersey, USA ; Messerschmidt-Bolkow-Bohm GmbH, München, and Technochemie GmbH, Dossenheim, FRG). Their 21 papers are grouped into 7 chapters as follows (No. of papers in brackets):

1. Fibres for reinforcement of advanced composites (3)
2. Polymer matrices (3)
3. Fabrication and design of carbon fibres with polymer matrix (CFRPs) (3)
4. Testing and fracture behaviour of CFRPs (2)
5. Application of CFRPs in aerospace (3)
6. Further applications of CFRPs (non aerospace) (4)
7. Carbon fibres activities in Brazil, People's Republic of China, India and South Korea (3)

E. Fitzer (Karlsruhe), in the first paper of chapter 1 discusses in detail carbon fibres (CFs). These thin fibres (6—10 μm diametr) have much higher specific tensile strength and specific modulus than steel or aluminum, lower thermal expansion, better fatigue resistance and corrosion resistance. They are made either from mesophase pitch, or from polyacrylonitrile (PAN) fibres and consist of 99.9% chemically pure graphitic layers (visible by transmission electron microscopy). The prestretched thinly spun PAN or pitch fibres are thermoset (stabilized) at 200—300°, carbonized in N_2 al 1400°, then graphitized around 2000° ; oxidative surface treatment (in gas or liquid phase by chemical or electrochemical means) is followed by epoxy sizing and spinning. Incorporation into a thermoset polymer matrix leads to the carbon fibre reinforced polymer (CFRP), a "miracle material" that caused a revolution in material science due to its low density, high strength and durability.

The polymer matrices are examined in chapter 2 by B. J. Hayes (CIBA-Geigy) and by H. D. Stenzenberger (Technochemie). The latter paper is extremely informative on the chemistry of thermosetting resins (phenolic, epoxy, polyimide, etc.) and of the curing procedures.

In chapter 6, G. W. Hastings (Stoke-on-Tent, UK) describes the biomedical applications of composites based on the excellent compatibility of CFRPs with human tissues (artificial limbs, dental implants, hip joints, etc.)

Applications in aerospace and transport (especially car industry) are the most numerous ; they are described in three papers of chapter 5 for USA, FRG, and for UK and France. In chapter 6 the development of CFRPs in Brazil, China and South Korea is briefly sketched.

The assistance of UNDP and UNFSSTD, and in particular of Prof. E. Fitzer for starting research and development in CFRPs in Brazil and Korea in the 1980s is acknowledged in the book.

For engineers, research workers and teaching staff interested in materials science, polymer chemistry, and mechanical engineering of advanced composites this book is a "must". It is excellently illustrated and contains details on the testing of materials, and on the expected performance.

A. T. Balaban
Polytechnic Institute Bucharest

"Chromatography'84", Proceedings of the Advances in Liquid Chromatography Conference, September 10—14, 1984, Szeged, Hungary. H. Kalasz and L. S. Ettre (Eds.) Akadémiai Kiado, Budapet 1986.

The book edited in 1986 by the Hungarian Academy of Sciences contains the communications presented at the Conference "Advances in Liquid Chromatography" held on September 1984 in Szeged (Hungary). This Conference, the second in a series of meetings of the research workers in the field of liquid chromatography organized in this town (the first took place in 1981), contains the works of some specialists from 12 countries, among them Romania.

The communications were systematized into : papers of general character ; stationary phases for liquid chromatography ; analysis of drugs, metabolites and biologically active compounds ; separation of amino acids, polypeptides and nucleotides ; separation of substances belonging to different classes.

Among the papers of general interest, studies concerning the optimization of separation processes should be mentioned. A theoretical model for the description of chromatographic analysis is presented, with the experimental data obtained by liquid chromatography interpreted by means of the computer. A group of research workers of the Estonian Academy of Science

(Tallin, S.S.R. Estonia USSR) presented a study concerning the determination of some anions (F^-, Cl^-, NO_3^- NO_2^- PO_4^{3-} SO_4^{2-}) in natural waters at the ppm and ppb level by means of ion chromatographic techniques using a liquid chromatograph with a self-made conductometric detector. The ion chromatography which appeared in 1975, has known a spectacular development and its performance is being favourably compared with that of absorption spectrometry. In the case of inorganic and organic anions of relatively small size, the performance is even better than that of other known methods.

The communications devoted to the stationary phases used in liquid chromatography contained aspects regarding the synthesis of new types of packings with chemically bonded functional groups, such as heterocyclic sulphur for the separation of fluorene and dibenzothiophene, cyclodextrine for the separation of some amino acids and enantiomers.

Data concerning the influence of substituents on the retention in normal phase liquid chromatography, the dependence of retention time with temperature in normal and reversed phase liquid chromatography, the importance of the mobile phase choice in size exclusion chromatography were presented.

Other papers in this chapter deal with the characterization of packings used in reversed phase liquid chromatography as well as of stationary phases with linear adsorption isotherms used in preparative chromatography.

The communications of analytical character presented at this Conference treated problems regarding the analysis of drugs, metabolites, biologically active compounds, amino acids, polypeptides and nucleotides. It is worth mentioning the utility of liquid chromatography for the characterization of psychotropic compounds, neurotoxines, porphyrin isomers, steroids, carbohydrates, alkaloids, amino acids derivatized with phthalic aldehyde, peptides and nucleotides.

Most of the studies have been achieved using reversed or ion pairs liquid chromatographic techniques.

The chapter containing the separations of some compounds from different classes aims at the determination of plasticizers used in plastic industry, the characterization of reaction products of nitromethane with formaldehyde, as well as a study made by a research team of Timișoara (Romania) which has applied with good results liquid chromatography for the separation of some substituted triazines.

The book appeared in good graphical conditions and is intended to the specialists who apply liquid chromatographic methods for the separation and determination of various compounds with biological and pharmaceutical action.

V. A. Ilie

NOTE POUR LES AUTEURS

La Revue Roumaine de Chimie publie des articles en anglais, français, russe, allemand ou espagnol. Les auteurs sont priés d'envoyer des articles et des comptes rendus inédits.

Les manuscrits seront dactylographiés à double interligne. La bibliographie, les tableaux et la légende des figures seront placés après le texte.

Si l'article fait partie d'une série numérotée, la partie précédente sera donnée comme première référence.

Chaque article sera précédé d'un résumé comprenant quinze lignes au maximum.

Les références bibliographiques dans le texte seront faites par des exposants sans parenthèses et paraîtront à la fin de l'ouvrage.

Les publications périodiques mentionnées dans la bibliographie seront présentées suivant les prescriptions internationales : le nom de l'auteur précédé de l'initiale du prénom, le titre du périodique abrégé conformément à « Chemical Abstracts » et souligné par une ligne, le numéro du tome indiqué par des chiffres arabes et souligné par deux lignes, suivi de la première page de l'article : à la fin, l'année de la parution sera entre parenthèses. Le numéro de la revue ne sera pas indiqué si les pages du volume sont numérotées consécutivement.

Les textes des livres ou traités inclueront : le nom des auteurs, l'initiale du prénom, le titre du livre entre guillemets et sans être souligné, le numéro du tome précédé par l'abréviation « vol. » (ou « Bd. »), le numéro de l'édition, les éditions (the publisher), la localité de la parution du livre, l'année de la parution et la page de la référence précédée(s) par l'abréviation « p. » (ou S. »).

Les brevets seront indiqués comme suit : l'auteur ou la firme, le pays et le numéro du brevet, la date et la revue *(Chem. Abstr.)*. Par ex. : M. Jones (to Union Carbide Co), Brit. Pat. 601 238, 2 Sept. 1959 ; cf. *Chem. Abstr.*, **54**, 12808 (1960).

Si la référence n'a pas été lue en original, on indiquera aussi la revue de référence consultée.

Les diagrammes seront tracés à l'encre de Chine sur papier calque. Les tableaux et les figures (en nombre strictement nécessaire) ainsi que les courbes dans les figures seront numérotés par des chiffres arabes. Leur explication sera donnée dans la légende des figures. Prière de ne pas inscrire les mêmes données dans les tableaux et les figures. Chaque tableau aura un titre. On indiquera dans le texte la place approximative des tableaux et des figures. Les formules chimiques seront incluses dans le texte ; en outre, elles seront transcrites sur papier calque, à l'encre de Chine.

Les auteurs sont priés d'indiquer les caractères italiques (en soulignant les lettres au *crayon*), ainsi que tout autre caractère spécial : les préfixes *ortho*, *meta*, *para*, *cis*, *trans*, etc. seront soulignés pour indiquer leurs caractères italiques et ne seront jamais écrits avec des majuscules.

Aucune correction à la main ne sera admise sur le manuscrit. Les corrections seront tapées à la machine. Les lettres grecques ou d'autres symboles spéciaux seront insérés à la main à l'encre clairement.

Le manuscrit sera signé par l'auteur.

Le titre-courant aura 50 lettres au maximum.

L'entière responsabilité du contenu des articles appartient aux auteurs.

Sur demande ou peut obtenir une note plus complète.

PRINTED IN ROMANIA

NOTE POUR LES AUTEURS

La Revue roumaine de Chimie publie des articles en anglais, français, russe, allemand ou espagnol. Les auteurs sont priés d'envoyer des articles et des comptes rendus inédits.

Les manuscrits seront dactylographiés à double interligne. La bibliographie, les tableaux et la légende des figures seront placés après le texte.

Si l'article fait partie d'une série numérotée, la partie précédente sera donnée comme première référence.

Chaque article sera précédé d'un résumé comprenant onze lignes au maximum.

Les références bibliographiques dans le texte seront faites par des exposants sans parenthèses et paraîtront à la fin de l'ouvrage.

Les publications périodiques mentionnées dans la bibliographie seront présentées suivant les prescriptions internationales : le nom de l'auteur précédé de l'initiale du prénom, le titre du périodique abrégé conformément à « Chemical Abstracts » et souligné par une ligne, le numéro du tome indiqué par des chiffres arabes et souligné par deux lignes, suivi de la première page de l'article ; l'année de la parution sera entre parenthèses. Le numéro de la revue ne sera pas indiqué si les pages du volume sont numérotées consécutivement.

Les titres des livres ou traités incluront : le nom des auteurs, l'initiale du prénom, le titre du livre entre guillemets et sans être souligné, le numéro du tome précédé par l'abréviation « vol. » (ou « Bd »), le numéro de l'édition, les éditions (the publishers), la localité de la parution du livre, l'année de la parution et la page de la référence précédée par l'abréviation « p. » (ou S.).

Les brevets seront indiqués comme suit : l'auteur ou la firme, le pays et le numéro du brevet, la date et la revue (Chem. Abstr.). Par ex. : M. Jones (to Union Carbide Corp.) Brit. Pat. 601 238, 2 Sept. 1968; cf. Chem. Abstr., 54, 1286 (1969).

Si la référence n'a pas été lue en original, on indiquera aussi la revue de référence consultée.

Les diagrammes seront tracés à l'encre de Chine sur papier calque. Les tableaux et les figures (en nombre strictement nécessaire) ainsi que les courbes dans les figures seront numérotés par des chiffres arabes. Leur explication sera donnée dans la légende des figures. Prière de ne pas inscrire les mêmes données dans les tableaux et les figures. Chaque tableau aura un titre. On indiquera dans le texte la place approximative des tableaux et des figures. Les formules chimiques seront incluses dans le texte ; au cas contraire, elles seront tracées sur papier calque à l'encre de Chine.

Les auteurs sont priés d'indiquer les caractères italiques (en soulignant les lettres au crayon), ainsi que tout autre caractère spécial ; les préfixes ortho, méta, para, cis, trans, etc. seront soulignés pour indiquer leurs caractères italiques et ne seront jamais écrits avec des majuscules.

Aucune correction à la main ne sera admise sur le manuscrit. Les corrections seront tapées à la machine. Les lettres grecques ou d'autres symboles spéciaux seront insérés à la main à l'encre clairement.

Le manuscrit sera signé par l'auteur.

Le titre courant aura 50 lettres au maximum.

L'entière responsabilité du contenu des articles appartient aux auteurs.

Sur demande on peut obtenir une épreuve complète.

ORSZÁGOS MŰSZAKI INFORMÁCIÓS KÖZPONT ÉS KÖNYVTÁR
1983

1988 MAJ 28

TRAVAUX PARUS AUX ÉDITIONS DE L'ACADÉMIE DE LA RÉPUBLIQUE SOCIALISTE DE ROUMANIE

ELENA CEAUŞESCU, **Răşini de hidrocarburi**, vol. 1, 1988, 344 p.
ELENA CEAUŞESCU, **Progrese în chimia şi tehnologia polimerilor**, 1986, 446 p.
ELENA CEAUŞESCU, **Forschungen im Bereich der Chimie und Technologie der Polymere**, 1986, 444 p.
ELENA CEAUŞESCU, **Cercetări în chimia şi tehnologia polimerilor**, 1983, 520 p.
ELENA CEAUŞESCU, **Noi cercetări în domeniul compuşilor macromoleculari**, 1981, 536 p.
ELENA CEAUŞESCU, **Polimerizarea stereospecifică a izoprenului**, 1979, 307 p.
ELENA CEAUŞESCU, **Research work on synthesis and characterization of macromolecular compounds. Contributions**, 1974, 251 p.
I.G. MURGULESCU, **Introducere în chimia fizică, Vol. I. 1. Atomi, molecule, legătură chimică**, 1976, 560 p.
I. G. MURGULESCU, V. EM. SAHINI, **Introducere în chimia fizică, Vol. I, 2. Structura şi proprietăţile moleculelor**, 1979, 604 p.
I. G. MURGULESCU, E. SEGAL, **Introducere în chimia fizică, Vol. II. 1. Teoria molecular-cinetică a materiei**, 1979, 1036 p.
I. G. MURGULESCU, TATIANA ONCESCU, E. SEGAL, **Introducere în chimia fizică, Vol.II. 2. Cinetică chimică şi cataliză**, 1981, 1024 p.
I. G. MURGULESCU, J. PĂUN, **Introducere în chimia fizică, Vol. I, 3. Nucleul atomic, reacţii nucleare, particule elementare**, 1982, 606 p.
I. G. MURGULESCU, RODICA VÎLCU, **Introducerea în chimia fizică. Vol. III. Termodinamica chimică**, 1982, 624 p.
I. G. MURGULESCU, O. M. RADOVICI, **Introducere în chimia fizică. Vol. IV. Electrochimia**, 1986, 410 p.
R. VÎLCU, M. LECA, **Termodinamica polimerilor prin cromatografie de gaze**, 1987, 238 p.
I. ZUGRĂVESCU, M. PETROVANU, **Cicloadiţii 3+2 dipolare**, 1987, 446 p.
RAUL MIHAIL, ION GROZEANU, **Estimarea secvenţială aplicată sistemelor chimice**, 1986, 406 p.
M. BREZEANU, I. PATRON, M. ANDRUH, **Combinaţii complexe polinucleare şi aplicaţiile lor**, 1986, 244 p.
A. T. BALABAN et. al., **Labelled Compounds and Radiopharmaceuticals Applied in Nuclear Medicine**, coédition avec John Wiley and Sons, 1986, 742 p.
D. PURDELA, **Nomenclatura chimiei organice — IUPAC**, 1986, 451 p.
PETRU BURDRUGEAC, **Probleme de chimie**, 1986, 280 p.
T. ONCESCU, S. G. IONESCU, **Conversie fotochimică şi stocare de energie**, 1985, 272 p.
V. DRĂGUŢAN, A. T. BALABAN, M. DIMONIE, **Olefin Metathesis and Ring-Opening Polymerization of Cyclo-Olefins**, coédition avec John Wiley and Sons, 1985, 544 p.
C. LITEANU, I. RÎCĂ, **Optimizarea proceselor analitice**, 1985, 360 p.
N. PERESCU, **Chimia extracţiei cu solvenţi şi aplicaţii**, 1985, 212 p.
V. E. SAHINI, N. HILLEBRAND, **Chimie cuantică în exemple şi aplicaţii**, 1984, 378 p.
GH. MARCU, **Chimia compuşilor coordonativi**, 1984, 415 p.
E. CORDOS, C. MANOLIU, **Spectrometria de absorbţie şi florescenţa atomică**, 1984, 178 p.
C. BODEA, **Tratat de biochimie vegetală, p. II, t. V**, 1984, 438 p.
N. ASANDEI, A. GRIGORIU, **Chimia şi structura fibrelor**, 1983, 395 p.
N. IONESCU, M. CALDARARU, **Oxidarea catalitică a olefinelor inferioare**, 1983, 178 p.
C. CAŞCAVAL, **Studiul polimerilor prin piroliză şi cromatografie de gaze**, 1983, 220 p.
C. I. SIMIONESCU, F. DANES, **Originea vieţii**, 1983, 110 p.
C. BODEA, **Tratat de biochimie vegetală, p. II, t. IV**, 1982, 408 p.
I. GĂLĂŢEANU, **Procese şi metode radiochimice în energetica nucleară**, 1981, 234 p.
CR. SIMIONESCU, VALERIA GORDUZA, **Polimeri biocompatibili şi biologic activi**, 1980, 479 p.
C. GH. MACAROVICI, **Analiza chimică cantitativă anorganică**, 1979, 457 p.
I. ZUGRĂVESCU, MAGDA PETROVANU, **N-ylid chemistry**, coédition avec McGraw-Hill International Book Company U.S.A., 1977, 396 p.

ISSN 0035—3930

I. P. INFORMAŢIA c. 1804

43 426

Lei 40

F 1103
04
6b

ACADÉMIE DE LA RÉPUBLIQUE SOCIALISTE DE ROUMANIE

REVUE ROUMAINE DE CHIMIE

TOME 33

N° 5

Mai 1988

EDITURA ACADEMIEI REPUBLICII SOCIALISTE ROMÂNIA

Rev. Roumaine Chim. RRCHAX, 33, 5, p. 435–566 (1988), Bucarest

ACADÉMIE DE LA RÉPUBLIQUE SOCIALISTE DE ROUMANIE

COMITÉ DE RÉDACTION

Rédacteur en chef:

I. G. MURGULESCU, membre de l'Académie de la République Socialiste de Roumanie

Rédacteurs en chef adjoints:

A. T. BALABAN et V. EM. SAHINI, membres correspondants de l'Académie de la République Socialiste de Roumanie

Collège de rédaction:

EM. BRATU, ELENA CEAUŞESCU, ECATERINA CIORĂNESCU-NENITZESCU, CR. SIMIONESCU, membres de l'Académie de la République Socialiste de Roumanie; P. SPACU, membre correspondant de l'Académie de la République Socialiste de Roumanie; M. BANCIU, M. D. GHEORGHIU, I. HAIDUC, D. I. MARCHIDAN, G. NIAC et D. SĂNDULESCU

La Revue Roumaine de Chimie paraît 10 fois par an. Toute commande de l'étranger sera adressée à ROMPRESFILATELIA — sectorul Export-Import Presă, P. O. Box 12—201, télex 10376 prsfi r 78104 Bucarest, Calea Griviţei nr. 64—66, Bucarest, Roumanie

Les manuscrits, les livres et les revues proposés en échange, ainsi que toute correspondance seront envoyés à la rédaction:

REVUE ROUMAINE DE CHIMIE

125, Calea Victoriei, 79717 Bucarest, Roumanie, telephone 50 76 80

EDITURA ACADEMIEI REPUBLICII SOCIALISTE ROMÂNIA
125, Calea Victoriei 79717 Bucarest, Roumanie, téléphone 50 76 80

REVUE ROUMAINE DE CHIMIE

INFORMÁCIÓS KÖNYVTÁR

Tome 33, N° 5 **Mai 1988**

GHEORGHE SURPĂŢEANU, CRISTINA LUCHIAN, MIRCEA CONSTANTINESCU, MAGDA PETROVANU, A. LABLACHE-COMBIER and PIERRE GRANDCLAUDON, Theoretical and experimental study of the cycloaddition between 4-(*p*-tolyl)-1,2,4-triazolium *N*-(*p*-nitrophenacylide) and methyl *trans*-cinnamate (in French) 437–443

O. M. O. HABIB, I. I. ABD EL-GAWAD, E. M. KANDEEL and D. S. BADAWY, Synthesis and reactions of some new 3-oxo-fluoren-2-carboxanilide derivatives 445–453

MARIA MIOSCU, IOVANCA HAIDUC, D. C. CÖRMÖS and JANA RUSU, Potentiometric determination of some semisynthetic penicillins and their parent compounds using a Cu^{2+}-sensitive electrode 455–461

R. L. MITAL, POONAM TANEJA, VINEETA KHATRI and LALIT PRAKASH, Studies in the synthesis of some new fluoro-substituted mesoionic heterocycles 463–465

IOAN MUNTEAN, JEAN MICHEL HERDAN and GABRIELA VĂLEANU, IR analysis of amines, carboxylic acids, alcohols, phenols and mercaptans after derivatization with *n*-butylisocyanate 467–471

J. EPPERLEIN and B. BLAU, The UV-VIS-spectral behaviour of arylazo compounds. I. General remarks 473–481

ELIZA-MANUELA VASILESCU, MIRCEA IOVU and DUMITRU SĂNDULESCU, Molecular compounds with some alkyl aryl ethers. II. Hydrogen bond complexes 483–488

DAN CARTIANU, A study of the stability of realistic models of oscillating chemical reactions by using concepts derived from the rules for flow graphs 489–524

AHMED M. G. NASSAR, MOHAMED A. KHARABA and ABDEL-HAMID A. YOUSSEF, A correlation of the reactivity of some substituted phenoxide ions 525–532

SURESH K. AGARWAL and D. R. TUTLANI, Synthesis and structural characterization of Cr(III) and cobalt (III) complexes with terephthalic acid hydrazide Schiff bases 533–536

R. K. AGARWAL and GYANENDRA SINGH, Synthesis and characterization of some oxovanadium (IV) complexes of octamethyl-pyrophosphoramide and nonamethylimido-diphosphoramide 537–545

G. V. SARADAMBA, K. RAMAKRISHNA, K. N. RAJU and P. V. SUBBA RAO, Kinetics of oxidation of thiourea by iron(III) in the presence of 2,2′-bipyridyl 547–554

A. SEZAI SARAÇ and AYTEN GÖÇMEN, Kinetics of the cerium(IV) oxidation of malonic acid in $H_2SO_4 - HClO_4$ media 555–563

BOOK REVIEWS 565–566

| Rev. Roumaine Chim. | **33**, *5*, 435–566 (1988), Bucares

Revue Roumaine de Chimie, **33**, *5*, 437–443 (1988)

ÉTUDE THÉORIQUE ET EXPÉRIMENTALE DE LA RÉACTION DE CYCLOADDITION DE 4-(*p*-TOLYL)TRIAZOLIUM-1,2,4 *N*-(*p*-NITRO)-PHÉNACYLURE SUR LE *TRANS*-CINNAMATE DE MÉTHYLE

GHEORGHE SURPĂȚEANU[a], CRISTINA LUCHIAN[a], MIRCEA CONSTANTINESCU[a], MAGDA PETROVANU[a], A. LABLACHE-COMBIER[b] et PIERRE GRANDCLAUDON[b]

[a] Institut Polytechnique « Gh. Asachi », Laboratoire de Chimie Organique, Jassy, 71, Splai Bahlui, Roumanie

[b] Université de Lille, Laboratoire de Chimie Organique Physique, France

Reçu le 10 janvier, 1987

On a effectué une étude théorique concernant la réaction de cycloaddition de triazolium phénacylure V sur le *trans* cinnamate de méthyle. Selon les énergies totales, calculées par la méthode CNDO/2, l'isomère VE est plus stable. Le diagramme de corrélation interorbitalaire frontière montre que la réaction de cycloaddition découle d'une manière stéréo- et régiospécifique. Les données théoriques sont vérifiées par voie expérimentale. La structure de l'adduit cyclique VII a été établie principalement à l'aide des spectres RMN ^1H et ^{13}C et des spectres de corrélation.

A theoretical study on the cycloaddition reaction of triazolium phenacylide V to methyl cinnamate is made. The frontier orbital energies, calculated by CNDO/2 method, show that the isomer VE is more stable. The frontier orbital correlation diagrams indicate a stereo- and regiospecific sense of the cycloaddition. The theoretical data are experimentally checked. The structure of the cycloadduct VII has been established by ^1H- and ^{13}C–NMR spectra and correlation spectra.

I. INTRODUCTION

Dans une Note antérieure[1] on a montré que certains cyclo-immonium-ylures peuvent exister en formes isomères E et Z et que les barrières d'énergie pour la transformation réciproque des isomères ont une valeur de 16–20 kcal/mol.

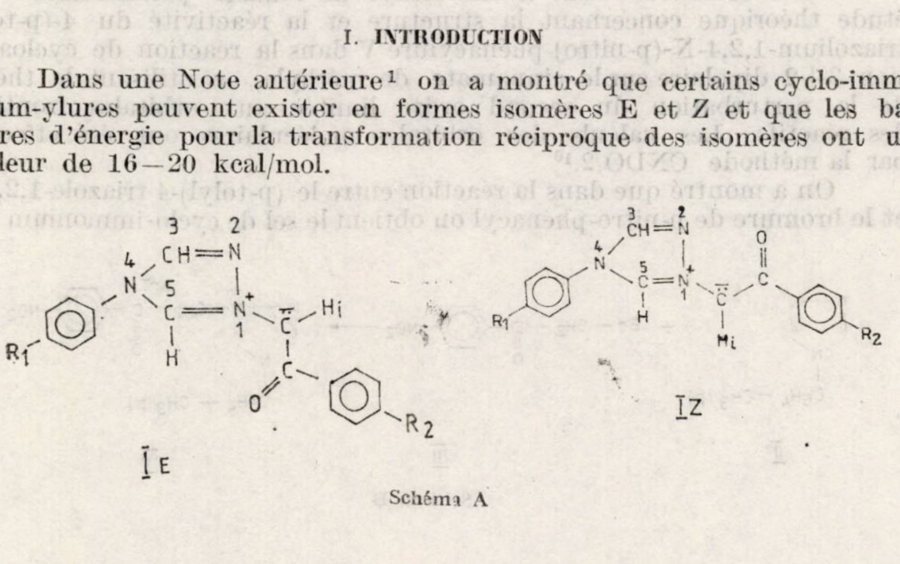

Schéma A

La mise en évidence de ces deux isomères a été due surtout aux spectres RMN ^{1}H de ces produits, enregistrés dans des solvants différents et à des températures différentes, à l'aide d'un appareil Bruker de 80 MHz.

Le proton lié à l'atome de carbone C_3 résonne à la même place dans les deux isomères. Les protons H_5 résonnent dans deux régions différentes. Le proton H_5 dans les isomères E est le plus déblindé, grâce à son voisinage avec le groupement carbonylique. Les différences entre les déplacements chimiques δ de ces protons H_5 dans les deux isomères atteignent parfois des valeurs de 1,5 ppm. Les différences entre les déplacements chimiques δ des protons yluriques H_5 dans les deux isomères, sont beaucoup plus petites. Elles ne dépassent pas 0,12 ppm.

On constate aussi des modifications importantes dans les spectres IR des ylures du type I. Systématiquement, dans les isomères E, la bande d'absorption $\nu_{C=O}$ est située à des valeurs proches de 1600 cm^{-1}. Dans les isomères du type Z, la bande $\nu_{C=O}$ est située à des valeurs comprises entre 1645–1600 cm^{-1}.

Du point de vue chimique, le comportement des ylures dans les réactions de cycloaddition est intéressant, compte tenu qu'ils peuvent participer à ces réactions comme isomères E ou Z.[2,3,4] En plus, connaissant la structure de l'isomère qui participe à la réaction, on peut mettre d'accord les diagrammes de corrélation interorbitalaires avec la structure des produits de réaction obtenus.[5,6,7]

Expérimentalement, les triazolium-ylures du type I sont stables. On les obtient à partir des sels de cyclo-immonium correspondants traités par des bases.

Dans les réactions de cycloaddition les ylures du type I sont générés *in situ* en présence du dipolarophile. On obtient directement l'adduit cyclique.[8,9]

II. RÉSULTATS ET DISCUSSIONS

Dans ce travail nous avons essayé de réaliser premièrement une étude théorique concernant la structure et la réactivité du 4-(p-tolyl) triazolium-1,2,4-N-(p-nitro)-phénacylure V dans la réaction de cycloaddition 3+2 dipolaire sur le cinnamate de méthyle, en utilisant la théorie de la perturbation du second ordre limitée aux orbitales frontières des réactifs. Les calculs des orbitales moléculaires ont été effectués par la méthode CNDO/2.[10]

On a montré que dans la réaction entre le (p-tolyl)-4 triazole-1,2,4 II et le bromure de p-nitro-phénacyl on obtient le sel de cyclo-immonium IV.[8]

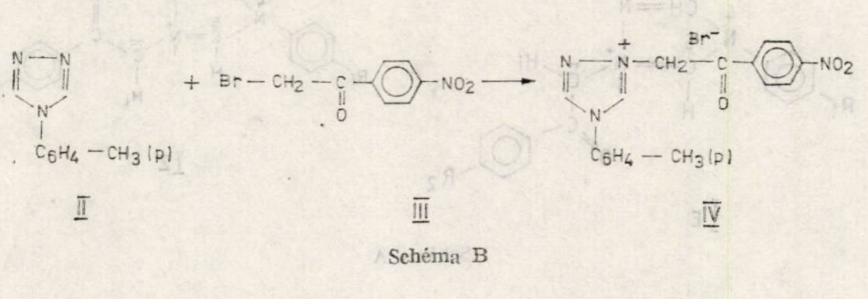

II III IV

Schéma B

Le sel IV, en milieu basique, conduit à l'ylure V qui peut exister en deux formes isomères E et Z :

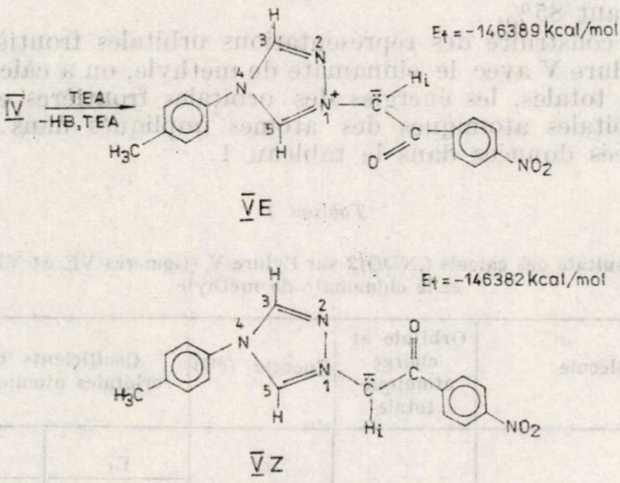

Schéma II

La transformation de l'isomère VE en isomère VZ a lieu par l'intermédiaire de la forme Va qui possède le plus haut niveau énergétique ayant un angle dièdre de 90° entre le plan de l'hétérocycle et celui du carbanion :

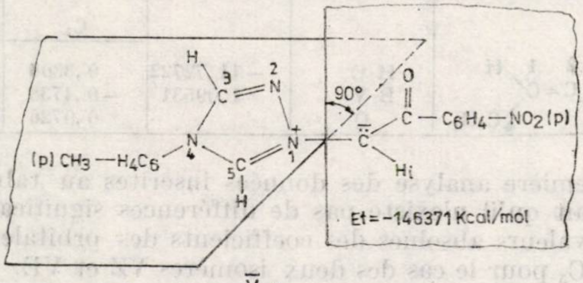

$\overline{V}a$

Schéma III

La géometrie de système moléculaire du type ylurique utilisée dans les calculs a été décrite dans un travail antérieur,[3] celle du cinnamate de méthyle a été approximée en utilisant les distances et les angles interatomiques standard. Les valeurs des énergies totales calculées pour les structures VE, VZ et Va sont présentées à côté des formules structurales (Schémas II et III). On peut observer que la barrière d'énergie lors de la transformation E—Z par l'intermédiaire de la forme Va est de 16 kcal/mol.

Ceci signifie qu'il n'existe pas de rotation libre autour de la liaison ylurique $N^+ - C^-$ et que, dans la synthèse de l'ylure V à partir du sel de cyclo-immonium correspondant, il est possible d'obtenir les deux isomères en mélange. Tous ces faits ont été vérifiés par voie expériementale.[1]

On a constaté que dans le cas de l'ylure V, obtenu à partir du sel de cyclo-immonium IV et de la triéthylamine en solution chloroformique, le spectre RMN ^1H indique l'existence de l'isomère VE dans une concentration dépassant 85%.

Afin de construire des représentations orbitales frontières pour la réaction de l'ylure V avec le cinnamate de méthyle, on a calculé les charges atomiques totales, les énergies des orbitales frontières et les coefficients des orbitales atomiques des atomes impliqués dans la réaction. On présente ces données dans le tableau 1.

Tableau 1

Résultats des calculs CNDO/2 sur l'ylure V (isomères VE et VZ) et le cinnamate de méthyle

Molécule	Orbitale et charge atomique totale	Energie (eV)	Coefficients des orbitales atomiques p_z	
			C_{ℓ}	C_5
VE	H O	−8,62655	−0,7091	0,3573
	B V	1,44002	−0,0446	0,3138
	Q		−0,2600	0,0324
VZ	H O	−8,45335	−0,7079	0,3663
	B V	1,37004	−0,0237	−0,3752
	Q		−0,2687	0,0166
			C_1	C_2
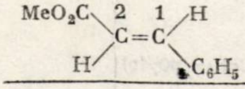	H O	−11,72722	0,3306	0,4695
	B V	1,09531	−0,4738	0,4232
	Q		0,0726	−0,1121

Une première analyse des données inscrites au tableau 1 met en évidence le fait qu'il n'existe pas de différences significatives en ce qui concerne les valeurs absolues des coefficients des orbitales atomiques des atomes C_{ℓ} et C_5 pour le cas des deux isomères VZ et VE.

Selon les différences entre les énergies des orbitales moléculaires frontières HO (la plus haute orbitale moléculaire occupée) de l'ylure VE — BV (la plus basse orbitale moléculaire vacante) de cinnamate de méthyle = 9,72186 eV et HO de cinnamate de méthyle — BV de l'ylure VE = = 13,16724 eV, il résulte que la réaction de cycloaddition entre l'ylure VE et le cinnamate de méthyle est HO contrôlée par rapport à l'ylure.

Par conséquent, l'analyse des signaux et des valeurs des coefficients des orbitales atomiques des atomes centres de réaction des orbitales HO-ylure VE et BV-cinnamate de méthyle, permet la construction du diagramme de corrélation représenté dans la figure 1.

La figure 1 indique l'interaction la plus probable entre l'ylure V et le cinnamate de méthyle, pour le cas dans lequel la cycloaddition est une réaction péricyclique et le rapprochement des réactants aurait lieu des plans parrallèles.[11]

On peut donc conclure que, selon les résultats du calcul, la cycloaddition analysée est stéréo- et régiospécifique, conduisant à un seul adduit cyclique.

Dans le but de vérifier par voie expérimentale le cours de la réaction, établi théoriquement plus haut, dans la seconde partie de notre étude on a réalisé par voie expérimentale la cycloaddition de triazolium-phénacylure V sur cinnamate de méthyle. La réaction a été effectuée en milieu chloroformique, l'ylure V étant généré *in situ* à partir du sel de cyclo-immonium IV et de la triéthylamine. On a obtenu le produit tétrahydropyrrolo-trizolique VII.

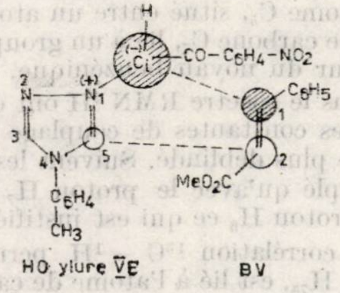

Fig. 1. — Représentation orbitale de la réaction entre le triazolium-phénacylure *VE* et le cinnamate de méthyle.

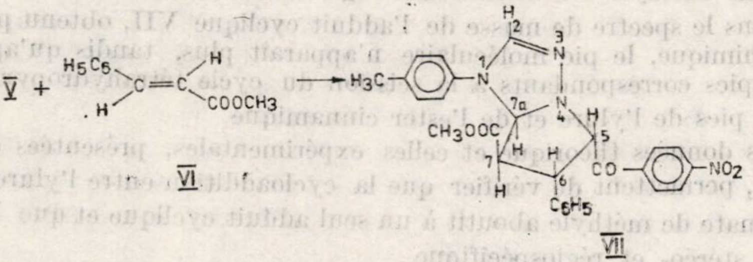

Schéma IV

Dans le produit VII apparaissent 4 atomes de carbone asymétriques, C_5, C_6, C_7 et C_{7a}. On attendait, en effet, la formation théoriquement possible, de 16 isomères de l'adduit cyclique VII. Le nombre de ces isomères est réduit si on tient compte que le système bicyclique pyrrolotriazolique est rigide, les deux cycles formant un angle dièdre et que l'atome H_{7a} est en position exo par rapport à ces deux cycles. Admettant cette position relative de l'atome d'hydrogène, H_{7a}, et que la réaction est stéréospécifique, il peut apparaître 4 isomères. Expérimentalement, on a constaté l'obtention d'un seul isomère.

La structure de cet isomère a été établie par analyses chimiques et spectrales (IR, RMN ^1H à 400,13 MHz et RMN ^{13}C à 100,62 MHz, ainsi que par un spectre de corrélation des déplacements chimiques $^{13}C-^1H$ par RMN à deux dimensions).

Le spectre IR du produit VII indique une bande d'absorption caractéristique à 1730 cm^{-1} ($\nu_{C=O\ \text{estérique}}$) et à 1685 cm^{-1} ($\nu_{C=O\ \text{cétonique}}$).

Les données les plus concluantes nécessaires à la détermination de la structure du produit VII sont celles fournies par les spectres RMN ^1H et RMN ^{13}C.

Analysant les déplacements chimiques des atomes de carbone C_5, C_6, C_7 et C_{7a} de l'adduit VII, on a constaté que l'atome C_{7a}, situé entre les deux atomes d'azote, est le plus déblindé.[12,13] Suivent, en ordre du déblindage, l'atome C_5, situé entre un atome d'azote et un groupement carbonylique, le carbone C_7, lié à un groupement estérique et, finalement l'atome C_6, porteur du noyau benzénique.

Dans le spectre RMN ^1H ont été enregistrés les déplacements chimiques et les constantes de couplage vicinales qui indiquent que le proton H_{7a} est le plus déblindé. Suivent les protons H_5, H_6 et H_7. Le proton H_{7a} n'est couplé qu'avec le proton H_7 et le proton H_5 est couplé seulement avec le proton H_6 ce qui est justifié par leur position dans le cycle.

La corrélation $^{13}C - ^1H$ permet de vérifier que le proton le plus déblindé, H_{7a}, est lié à l'atome de carbone C_{7a}, le plus déblindé. Cette relation est observée aussi en position 5. Par contre, le proton H_6 est plus blindé que le proton H_7 pendant que la situation est inversée pour les atomes de carbone correspondants.

D'après les constantes de couplage $J_{7,7a}$ et $J_{5,6}$ il résulte d'une manière plus précise que l'atome de carbone C_{7a} est voisin du carbone C_7 qui porte le cycle benzénique. La cycloaddition de l'ylure VE sur le cinnamate de méthyle est donc d'une régiosélectivité totale.

Dans le spectre de masse de l'adduit cyclique VII, obtenu par ionisation chimique, le pic moléculaire n'apparaît plus, tandis qu'apparaissent les pics correspondants à la scission du cycle tétrahydropyrrolique, donc les pics de l'ylure et de l'ester cinnamique.

Les données théorique et celles expérimentales, présentées dans ce mémoire, permettent de vérifier que la cycloaddition entre l'ylure VE et le cinnamate de méthyle aboutit à un seul adduit cyclique et que la réaction est stéréo- et régiospécifique.

PARTIE EXPÉRIMENTALE

Les calculs sont effectués par la méthode CNDO/2 avec le programme QCPE nº 141, sur un ordinateur Felix C-256.

Les spectres de RMN ^1H et ^{13}C ont été enregistrés à l'aide d'un appareil Bruker AM 400 (solvant $CDCl_3$). Les déplacements chimiques sont exprimés en ppm (TMS étalon interne) La corrélation des déplacements chimiques $^{13}C - ^1H$ par le RMN à deux dimensions a été effectuée sur un programme Bruker XH COORD. Au. La multiplicité des atomes de carbone a été déterminée par programme DEPT, les attributions ont été faites par comparaison avec les données de la littérature et par calcul des déplacements chimiques δ par la méthode des incréments dans le cas des atomes de carbone du cycle aromatique. Les spectres IR ont été enregistrés sur un spectromètre Perkin-Elmer-1310 et les spectres de masse à l'aide d'un spectromètre Ribemag 10.10.

Les points de fusion ont été mesurés sur un microscope Reichart-Thermopan et ne sont pas corrigés.

La synthèse de bromure de N-(p-nitro)-phénacyle-1(p-tolyl)-4 triazolium-1,2,4 IV a été réalisée selon les donnés de la littérature.[2]

p-Tolyl-1(p-nitro)-benzoyl-5-phényl-6 carbométhoxy-7-tétrahydropyrrolo-1,2b-triazole-1,2,4 VII

On suspend 10 mmol de sel de cyclo-immonium IV dans 50 ml de chloroforme et on ajoute 10 mmol cinnamate de méthyle *(trans)*. On refroidit le mélange avec de la glace et on laisse tomber goutte à goutte, en agitant continuellement, une solution de 1,5 ml triéthylamine dans 15 ml de chloroforme. Le mélange réactionnel est agité pendant 2 heures et ensuite abandonné pendant 24 heures à la température ambiante. La solution chloroformique est lavée trois fois à l'eau, séchée sur Na_2SO_4 anhydre. On chasse le solvant et on recristallise le résidu dans un mélange acétonitrile-méthanol. P. fus. =161—162°. Analyse : $C_{27}H_{24}N_4O_5$, calculé : C 72,05 ; H 4,95 ; N 11,57 % ; trouvé : C 72,01 ; H 4,86 ; N 11,70 %.

Spectre IR (KBr, cm^{-1}) : 1730 (C=0, estérique), 1685 (C=O cétonique), 3025, 2985, 1595, 1525, 1430, 1385, 1365, 1280, 1220, 1155, 1050, 1025, 955, 850, 835.

Spectre RMN ^1H ($CDCl_3$, δ ppm) : 2,29 (s, 3 protons CH_3) ; 3,12 (s, 3 protons $-COOCH_3$) ; 4,00 (dd, 1 proton, CH-$COOCH_3$) ; 4,25 (dd, 1 proton, $CH-C_6H_5$) ; 5,74 (d, 1 proton, $N-CH-CO$) ; 6,36 (d, 1 proton, 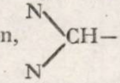 $\genfrac{}{}{0pt}{}{N}{N}\!>\!CH-$) ; 6,90 (d, 2, protons, J = 8, 4 Hz, $N-C_6H_4-CH_3$, H *ortho*/N) ; 6,95—7,15 (m, C_6H_5 et $N-C_6H_4-CH_3$, H méta/N) ; 7,37 (s, 1 proton, $N = CH-$) ; 7,73 (d, 2 protons, J = 8,8 Hz, $CO-C_6H_4-NO_2$, H *méta*/N) ; 8,06 (d, 2 protons, J = 8,8 Hz, $CO-C_6H_4-NO_2$, H *ortho*/N).

Spectre RMN ^{13}C ($CDCl_3$, δ ppm) : multiplicité déterminée par DEPT ; CH_3 : 20,59 ($CH_3-C_6H_4$) ; 51,82 ($COOCH_3$) ; CH : (en dehors de ceux appartenant au cycle tétrahydropyrrolique) : 115,54 (aromatiques, *méta*/CH_3) ; 123,35 (aromatiques, *ortho*/NO_2) ; 127,67 (aromatique, *para* dans le phényle C_6H_5) ; 127,72 (aromatiques, *ortho* dans le phényle C_6H_5) ; 128,75 (aromatiques, *méta* dans le phényle C_6H_5) ; 129,19 (aromatiques, *métha*/NO_2) ; 130,00 (aromatiques, *ortho*/CH_3) ; 139,89 (CH = N) ; *C* quaternaire : 131,91 (aromatique, lié au groupement CH_3) ; 134,74 et 135,18 (aromatiques) ; 140,58 (aromatique, lié au groupement C = O) ; 149,93 (aromatique, lié au groupement NO_2) ; 170,30 ($COOCH_3$) ; 197,82 (C=O).

Spectre moléculaire M/Z : 322 ; 162.

BIBLIOGRAPHIE

[1] M. Petrovanu, G. Surpăţeanu, M. Constantinescu et A. Lablache-Combier, *Bull. Inst. Politeh. Iaşi*, **31** **(35)** supl., s. II, 47 (1985).

[2] M. Petrovanu, C. Luchian, G. Surpăţeanu et V.Bărboiu, *Rev. Roumaine Chim.*, **24**,1053 (1979).

[3] G, Surpăţeanu, C. Luchian, M. Constantinescu, V. Bărboiu et M. Petrovanu, *Bull. Inst. Politeh. Iaşi*, **26** **(30)** s. II, 97 (1980).

[4] G. Surpăţeanu, M. Constantinescu, C. Luchian, M. Petrovanu, I. Zugrăvescu et A. Lablache-Combier, *Rev. Roumaine Chim.*, **26**, 1169 (1981).

[5] G. Surpăţeanu, M. Constantinescu, C. Luchian, M. Petrovanu, I. Zugrăvescu et A. Lablache-Combier, *Rev. Roumaine Chim.*, **28**, 933 (1983).

[6] G. Surpăţeanu, M. Constantinescu, C. Luchian, M. Petrovanu, I. Zugrăvescu et A. Lablache-Combier, *Rev. Roumaine Chim.*, **28**, 831 (1983).

[7] G. Surpăţeanu et A. Lablache-Combier, *Heterocycles*, **22**, 2079 (1984).

[8] M. Petrovanu, C. Luchian, G. Surpăţeanu et V. Bărboiu, *Tetrahedron*, **37**, 2805 (1981).

[9] M. Petrovanu, C. Luchian, G. Surpăţeanu et V. Bărboiu, *Tetrahedron*, **37**, 2811 (1981).

[10] J. A. Pople et D. L. Beveridge, "Approximate Molecular Orbital Theory", McGraw-Hill, London (1970).

[11] K. Fukui, "Theory of Orientation and Stereoselection" vol. II, Springer-Verlag, Berlin (1975).

[12] P. A. Crooks, B. Robinson et O. Meth-Cohn, *Phytochem*, **15**, 1092 (1976).

[13] S. P. Sing, R. H. Obenauf et M. Y. Albright, *J. Heterocycl. Chem.*, **14**, 407 (1977).

Revue Roumaine de Chimie, **33**, *5*, 445—453 (1988)

SYNTHESIS AND REACTIONS OF SOME NEW 3-OXO-FLUOREN-2-CARBOXANILIDE DERIVATIVES

O. M. O. HABIB, I. I. ABD EL-GAWAD, E. M. KANDEEL and D. S. BADAWY
Chemistry Department, Faculty of Science, Mansoura University, Egypt

Received December 13, 1986

Condensation of 2-arylidene-1-indanones Ia-d with acetoacetanilides gave 1,2,3-trihydro-1-aryl-3-oxo-fluoren-2-carboxanilides IIa-h. Reactions of IIa-h with hydrazine hydrate, phenylhydrazine, hydroxylamine hydrochloride, benzenediazonium chloride, polyphosphoric acid and Mannich bases were studied. Reactions of 1,2,3-trihydrofluoren [3,2-c]-pyrazol-3-ones IIIa-d with chloroacetyl chloride, benzenesulphonyl chloride piperidine and benzenediazonium chloride were also investigated.

In recent years, β-ketoanilides have been subjected to detailed investigations because of their utility as intermediates for the synthesis of various classes of biologically active products.[1-3] As continuation of our previous studies[1-4] on β-ketoanilides, we have studied in the present work the synthesis and reactions of 1,2,3-trihydro-1-aryl-3-oxo-fluoren-2-carboxanilides IIa-h. These compounds were prepared by treating 2-arylidene-1-indanones Ia—d with acetoacetanilides in the presence of potassium methoxide. Structures IIa-h were based on elemental analyses and IR spectra showing absorption bands at 1680, 1635 and 3400 cm^{-1} characteristic for the two CO and NH group, respectively.

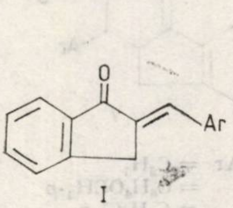

I

a, Ar $= C_6C_5$
b, $= C_6H_4-OCH_3$-*p*
c, $= C_6H_4-Cl$-*p*
d, $= C_6H_4-N(CH_3)_2$-*p*

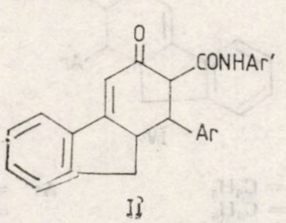

II

	Ar	Ar′
a,	$= C_6H_5$	$= C_6H_5$
b,	$- C_6H_5$	$= C_6H_4Cl$-*p*
c,	$= C_6H_4-OCH_3$-*p*	$= C_6H_5$
d,	$= C_6H_4-OCH_3$-*p*	$= C_6H_4Cl$-*p*
e,	$= C_6H_4Cl$-*p*	$= C_6H_5$
f,	$= C_6H_4Cl$-*p*	$= C_6H_4Cl$-*p*
g,	$= C_6H_4N(CH_3)_2$-*p*	$= C_6H_4Cl$
h,	$= C_6H_4N(CH_3)_2$-*p*	$= C_6H_4Cl$-*p*

Treatment of IIa—h with hydrazine hydrate in ethanol or acetic acid afforded the corresponding 1,2,3-trihydrofluoren[3,2—c]pyrazol-

3-ones IIIa-d. These products were characterised by elemental analyses and IR measurements revealing bands at 3300, 2900, 1710, and 1620 cm^{-1} assignable to the pyrazolone moiety.

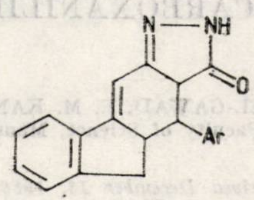

III

a, Ar $= C_6H_5$
b, $= C_6H_4OCH_3$-*p*
c, $= C_6H_4Cl$-*p*
d, $= C_6H_4N(CH_3)_2$-*p*

On the other hand, reaction of IIa-h with phenylhydrazine in ethanol gave the corresponding hydrazones IVa-h which cyclised to N-phenylpyrazolones Va-d by refluxing with acetic acid and sodium acetate. Compounds Va-d were also obtained by treating IIa-h with phenylhydrazine in the presence of acetic acid. The IR spectrum of IVc showed bands at 3300, 1650 and 1610 cm^{-1} attributable to NH, CO and C=N group, respectively. The IR spectrum of Vc revealed stretching frequencies at 1670 and 1620 cm^{-1} characteristic for the CO and C=N group. The band at 3300 cm^{-1} assignable to the NH group disappeared.

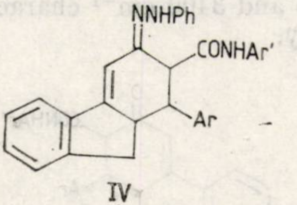

IV

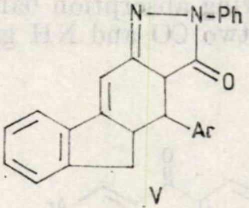

V

	Ar	Ar'
a,	$= C_6H_5$	$= C_6H_5$
b,	$= C_6H_5$	$= C_6H_4Cl$-*p*
c,	$= C_6H_4OCH_3$-*p*	$= C_6H_5$
d,	$= C_6H_4OCH_3$-*p*	$= C_6H_4Cl$-*p*
e,	$= C_6H_4Cl$-*p*	$= C_6H_5$
f,	$= C_6H_4Cl$-*p*	$= C_6H_4Cl$-*p*
g,	$= C_6H_4N(CH_3)_2$-*p*	$= C_6H_5$
h,	$= C_6H_4N(CH_3)_2$-*p*	$= C_6H_4Cl$-*p*

a, Ar $= C_6H_5$
b, $= C_6H_4OCH_3$-*p*
c, $= C_6H_4Cl$-*p*
d, $= C_6H_4N(CH_3)_2$-*p*

Treatment of IIa with hydroxylamine hydrochloride in ethanol containing few drops of piperidine afforded 1, 2, 3,-trihydro-1-aryl-fluoreno-[3,2-c]isoxazol-3-one VI. Structure of VI was established from elemental analyses and IR spectrum which showed bands at 1670 and 1620—1610 cm^{-1} assignable to CO and C=N group, respectively.

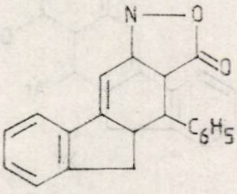

VI

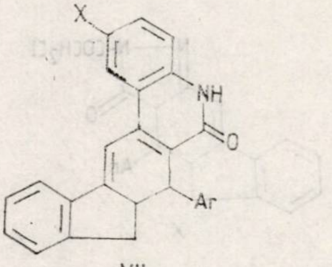

VII

a, Ar $= C_6H_5$ X $= H$
b, $= C_6H_5$ $= Cl$
c, $= C_6H_4OCH_3$-*p* $= H$
d, $= C_6H_4OCH_3$-*p* $= Cl$
e, $= C_6H_4Cl$-*p* $= H$
f, $= C_6H_4Cl$-*p* $= Cl$
g, $= C_6H_4N(CH_3)_2$-*p* $= H$
h, $= C_6H_4N(CH_3)_2$-*p* $= Cl$

Condensation of IIa-h with polyphosphoric acid gave the cyclic amides VIIa-h. The structures of these products were deduced from analytical data and IR spectra showing bands at 3100, 1660 and 1630 cm^{-1} characteristic for the NH, CONH and C=N group, respectively.

Coupling of IIa, b with benzenediazonium chloride has resulted into the coupling through the active methylene group to give 1,2,3-trihydro-1-aryl-3-oxo-2-phenylazo-2-fluorene carboxanilides VIIIa, b. The IR spectra of VIIIa, b showed bands at 3400, 3060, 1600 and 1700—1680 cm^{-1} attributable to NH, N=N and 2CO groups, respectively.

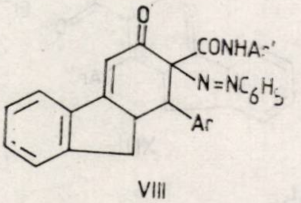

VIII

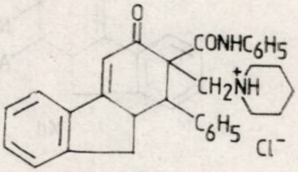

IX

a, Ar $= C_6H_5$ Ar' $= C_6H_5$
b, $= C_6H_4OCH_3$-*p* $= C_6H_5$

The Mannich reaction of II was also investigated. Thus, treatment of IIa with formaldehyde and piperidine in the presence of hydrochloric acid yielded 1,2,3-trihydro-1-aryl-3-oxo-2-piperidinomethyl-2-fluorene carboxanilide XX as hydrochloride salt.

In the present work, the behaviour of the pyrazolone derivatives IIIa-d towards chloroacetyl chloride and benzenesulphonyl chloride was also described. Thus, compounds IIIa-d reacted with chloroacetyl chloride to yield the N-acetyl chloride derivatives Xa-d. The IR spectra of Xa-d showed bands at 1660, 1695 and 1610 cm^{-1} assignable to the 2CO and C=N group, respectively.

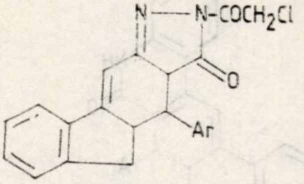

X

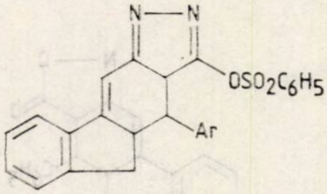

XI

a, Ar = C_6H_5
b, = $C_6H_4OCH_3$-*p*
c, = C_6H_4Cl-*p*
d, = $C_6H_4N(CH_3)_2$-*p*

a, Ar = C_6H_5
b, = $C_6H_4OCH_3$-*p*
c, = C_6H_4Cl-p
d, = $C_6H_4N(CH_3)_2$-*p*

In contrast to the action of chloroacetyl chloride, when compounds IIIa-d were treated with benzenesulphonyl chloride the O-benzenesulphonate derivatives XI were obtained. The IR spectra of XIa-d did not show any carbonyl absorption band.

On the other hand, the pyrazolones IIIa—d have been coupled with benzenediazonium chloride, and reacted with formaldehyde in methanol containing piperidine to give the corresponding arylazo XIIa-d and piperidinomethyl XIIIa-derivatives. The IR spectrum of XIIa showed bands at 3400, 1640, 1720 and 1600 cm^{-1} characteristic for the NH, C=N, CO and N=N group, respectively.

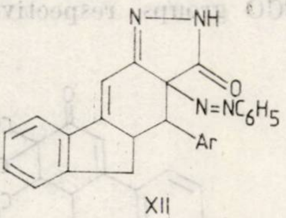

XII

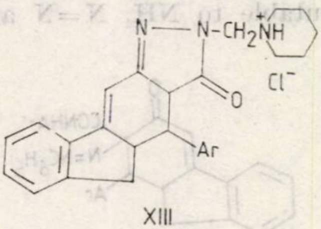

XIII

a, Ar = C_6H_5
b, = $C_6H_4OCH_3$-*p*
c, = C_6H_4Cl-*p*
d, = $C_6H_4N(CH_3)_2$-*p*

EXPERIMENTAL

Melting points are uncorrected. IR spectra were recorded on a Pye-Unicam Spectrophotometer SP-1100 using KBr wafer technique. Analytical data were determined at the Microanalytical Unit, Faculty of Science, Mansoura University, Egypt.

The 2-arylidene-1-indanones were prepared according to the general method for preparation of arylidenes.

Synthesis of 1,2,3-trihydro-1-aryl-3-oxo-2-fluoren-carboxanilides IIa-h

Acetoacetanilides (0.01 mole in each case) were added to the arylidene derivatives Ia—d (0.01 mole in each case) in potassium methoxide (0.02 mole). The reaction mixture was refluxed for 12 hours, poured onto ice-cold hydrochloric acid and the precipitated solids were recrystallised from ethanol to give IIa-b (cf. Table 1).

Table 1

1,2,3-Trihydro-1-aryl-3-oxo-3-fluoren-carboxanilides IIa-h

Compound	M.p. °C	Yield %	Formula	Analysis % C	H (Found / Calcd.)
IIa	210	70	$C_{26}H_{21}NO_2$	82.30 82.32	5.20 5.54
IIb	195	70	$C_{26}H_{20}NO_2Cl$	75,50 75.45	4.50 4.83
IIc	215	70	$C_{27}H_{23}NO_3$	78.80 79.22	5.50 5.62
IId	194	70	$C_{27}H_{22}NO_3Cl$	73.40 73.05	4.70 4.96
IIe	178	40	$C_{26}H_{20}NO_2Cl$	75.00 75.45	4.90 4.83
IIf	265	40	$C_{26}H_{19}NO_2Cl_2$	69.60 69.64	4.00 4.24
IIg	243	40	$C_{28}H_{26}N_2O_2$	79.50 79.62	6.10 6.16
IIh	255	40	$C_{28}H_{25}N_2O_2Cl$	74.10 73.60	4.90 5.47

Reaction of IIa-h with hydrazine hydrate

A. *In ethanol.* A mixture of IIa-h (0.01 mole in each case) and hydrazine hydrate (0.01 mole) in ethanol (50 mL) was refluxed for four hours. The formed solid products were filtered and recrystallised from the appropriate solvent to give the pyrazolone derivatives IIIa-d (cf. Table 2).

B. *In acetic acid.* A mixture of IIIa-h (0.01 mole in each case) and hydrazine hydrate (0.01 mole) in acetic acid (50 mL) was refluxed for three hours. Crystallisation of the obtained solids from the proper solvents gave IIIa-d, defined by melting and mixed melting points.

Table 2

1,2,3-Trihydro-1-aryl-fluoren[3,2-c]-pyrazol-3-ones IIIa-d

Compound	M.p. °C	Yield %	Formula	Analysis % C	H (Found / Calcd.)
IIIa	272	80	$C_{20}H_{16}N_2O$	79.60 80.00	4.90 5.33
IIIb	270	80	$C_{21}H_{18}N_2O_2$	76.20 76.36	5.10 5.45
IIIc	248	80	$C_{20}H_{15}N_2OCl$	72.10 71.74	4.60 4.48
IIId	256	60	$C_{22}H_{21}N_3O$	76.50 76.96	6.00 6.12

Reaction of IIa-h with phenylhydrazine

A. *In ethanol.* The same general procedure described for the reaction of IIa-h with hydrazine hydrate was used. Recrystallisation of the formed solids from the appropriate solvent afforded the hydrazone derivatives IVa-h (cf. Table 3).

Table 3

Phenylhydrazones IVa—h

Compound	M.p. °C	Yield %	Formula	Analysis % C	Analysis % H	(Found Calcd.)
IVa	145	70	$C_{32}H_{27}N_3O$	81.20 81.87	5.50 5.75	
IVb	219	70	$C_{32}H_{26}N_3OCl$	76.30 76.26	4.90 5.16	
IVc	222	70	$C_{33}H_{29}N_3O_2$	79.00 79.35	5.50 5.81	
IVd	227	70	$C_{33}H_{28}N_3O_2Cl$	73.90 74.22	4.90 5.24	
IVe	148	60	$C_{32}H_{26}N_3OCl$	76.00 76.26	5.00 5.16	
IVf	238	70	$C_{32}H_{25}N_3OCl_2$	71.50 71.37	4.60 4.64	
IVg	254	60	$C_{34}H_{32}N_4O$	80.14 79.68	6.20 6.25	
IVh	225	60	$C_{34}H_{31}N_4OCl$	74.50 74.65	5.40 5.67	

B. *In acetic acid.* The same general procedure as described for the reaction of IIa-h with hydrazine hydrate. Crystallisation of the products from acetic acid gave Va-d (cf. Table 4).

Table 4

1,2,3-Trihydro-1-aryl-fluoren[3,2—c]-N-phenyl-pyrazol-3-ones Va-d

Compound	M.p. °C	Yield %	Formula	Analysis % C	Analysis % H	(Found Calcd.)
Va	242	80	$C_{26}H_{20}N_2O$	82.90 82.97	5.00 5.32	
Vb	255	80	$C_{27}H_{22}N_2O_2$	79.60 79.80	5.30 5.41	
Vc	258	80	$C_{26}H_{19}N_2OCl$	75.70 76.00	4.60 4.62	
Vd	259	80	$C_{28}H_{25}N_3O$	80.60 80.19	6.10 5.96	

Conversion of the hydrazones IVa-h into pyrazolones Va-d

Compounds IVa-h (0.5 g in each case) were heated under reflux with acetic acid (25 mL) and sodium acetate (0.1 g). A rapid change in colour was immediately observed and the corresponding pyrazolones Va-d were obtained (melting and mixed melting points).

Reaction of IIa with hydroxylamine hydrochloride, Formation of the 1,2,3-trihydro-1-arylfluoreno [3,2—c]isoxazol-3-one VI

An ethanolic solution of IIa (0.005 mole in 10 mL ethanol), hydroxylamine hydrochloride (0.005 mole) and 0.5 mL of pyridine was refluxed for three hours. The precipitate was filtered and recrystallised from ethanol to give VI, m.p. 250°C, yield 60 %.

Analysis : $C_{20}H_{15}NO_2$ Found % : C = 80.00 ; H = 4.70 ; Calcd. % : C = 79.73 ; H = 4.98

Condensation of IIa-h with polyphosphoric acid. Formation of the corresponding cyclic amide VIIa-h

A mixture of IIIa-h (1g) and polyphosphoric acid (20 mL) was heated at 140—150°C for two hours. The reaction mixture was poured onto ice-cold water, filtered and crystallised from ethanol to give the corresponding cyclic amides VIIa-h (cf. Table 5).

Table 5

Cyclic amide derivatives VIIa-h

Compound	M.p. °C	Yield %	Formula	Analysis % C	H	(Found / Calcd.)
VIIa	112	70	$C_{26}H_{19}NO$	85.90 86.42	5.50 5.26	
VIIb	72	70	$C_{26}H_{18}NOCl$	79.00 78.88	4.60 4.55	
VIIc	85	65	$C_{27}H_{21}NO_2$	83.10 82.86	4.90 5.37	
VIId	95	70	$C_{27}H_{20}NO_2Cl$	76.60 76.14	5.00 4.70	
VIIe	207	60	$C_{26}H_{18}NOCl$	78.50 78.88	4.60 4.55	
VIIf	162	60	$C_{26}H_{17}NOCl_2$	72.40 72.55	4.00 3.96	
VIIg	115	50	$C_{28}H_{24}N_2O$	82.90 83.16	5.80 5.94	
VIIh	191	50	$C_{28}N_{23}N_2OCl$	77.10 76.62	5.00 5.24	

Reaction of IIa, b with aryldiazonium salts. Formation of 1,2, 3-trihydro-1-aryl-3-oxo-2-phenylazo-2-fluoren carboxanilides VIIIa, b

To a cold solution of IIa, b (0.01 mole in each case) in alcoholic sodium hydroxide (40 mL), 0.01 mole of benzenediazonium chloride was added. The formed solid products were filtered and recrystallised from ethanol to give the corresponding azo-dyes VIIIa, b (cf. Table 6).

Table 6

1,2,3-Trihydro-1-aryl-3-oxo-2-phenylazo-2-fluorene carboxanilides VIIIa, b

Compound	M.p. °C	Yield %	Formula	Analysis % C	H	(Found / Calcd.)
VIIIa	109	75	$C_{32}H_{25}N_3O_2$	79.38 79.50	4.86 5.17	
VIIIb	104	70	$C_{33}N_{22}N_3O_3$	77.19 77.19	3.00 3.26	

Mannich reaction of IIa. Formation of 1,2,3-trihydro-1-aryl-3-oxo-2-piperidinomethyl-2-fluoren carboxanilide IX

To 0.01 mole methanolic solution of IIa and 0.02 mole piperidine, aqueous formaldehyde (35%, 2.5 ml) and 0.5 mL hydrochloric acid were added. The reaction mixture was refluxed for eight hours, left to stand overnight at room temperature and diluted with water. The resulting solid was recrystallised from ethanol to give IX, m.p. 103 °C, yield 35%.

Analysis : $C_{32}H_{33}N_2O_2Cl$ Found % : C = 74.60 ; H = 6.30 Calcd. : C = 74.92 ; H = = 6.43

Reaction of IIIa-d with chloroacetyl chloride. Formation of 1,2,3-trihydro-1-aryl-fluoren [3,2-c]2-chloroacetyl pyrazol-3-ones Xa-d

To a solution of chloroacetyl chloride (0.03 mole) in dry benzene (15 mL), compounds IIIa—d (0.01 mole in each case) were added. The reaction mixture was refluxed for two hours and left to stand overnight at room temperature. Recrystallisation of the formed solids from the appropriate solvent afforded the chloroacetyl derivatives Xa—d (cf. Table 7).

Table 7

1, 2, 3,-Trihydro-1-aryl-fluoren[3,2—c]-2-chloroacetyl pyrazol-3-ones Xa-d

Compound	M.p. °C solvent	Yield %	Formula	Analysis % C	H (Found / Calcd.)
Xa	245 (E—B)	80	$C_{22}H_{17}N_2O_2Cl$	69.80 70.11	4.40 4.51
Xb	214 (E—B)	80	$C_{23}H_{19}N_2O_3Cl$	67.40 67.89	4.40 4.67
Xc	191 (E)	80	$C_{22}H_{16}N_2O_2Cl_2$	64.20 64.23	3.60 3.89
Xd	222 (E)	70	$C_{24}H_{22}N_3O_2Cl$	68.50	5.24

E—B = ethanol — benzene mixture ; E = ethanol

Reaction of IIIa-d with benzenesulphonyl chloride. Formation of 1,2,3-trihydro-1-aryl-fluoren [3,2—c]pyrazol-3-ol-benzene sulphonates XIa-d

Benzene sulphonyl chloride (0.01 mole) was added to IIIa-d (0.01 mole in each case) in pyridine (15 mL). The reaction mixture was refluxed for one hour, cooled and then poured onto ice-cold water. The brown solids formed were recrystallised from ethanol to give XIa-d (cf. Table 8).

Table 8

1, 2, 3-Trihydro-1-aryl-fluoren[3,2—c]pyrazol-3-ol-benzene sulphonates XIa-d

Compound	M.p. °C	Yield %	Formula	Analysis % C	H (Found / Calcd.)
XIa	195	70	$C_{26}H_{20}N_2O_3S$	70.60 70.90	4.50 4.54
XIb	218	70	$C_{27}H_{22}N_2O_4S$	68.50 68.93	4.50 4.68
XIc	194	70	$C_{26}H_{19}N_2O_3ClS$	65.50 65.75	3.90 4.00
XId	107	70	$C_{26}N_{25}N_3O_3S$	69.50 69.56	5.00 5.17

Formation of 1,2,3-trihydro-1-aryl-2-phenylazo-fluoren[3, 2—c]pyrazol-3-ones XIIa-c

To a cold solution of IIIa-c (0.01 mole in each case) in ethanolic sodium hydroxide solution (40 mL), benzenediazonium chloride (0.01 mole) was added. The formed solid products were filtered and recrystallised from ethanol to give the azo compounds XII a-c (cf. Table 9).

Table 9

1,2,3-Trihydro-1-aryl-2-phenylazo-fluoren[3,2-c]pyrazol-3-one derivatives XII a-c

Compound	M.p. °C	Yield %	Formula	Analysis %		(Found / Calcd.)
				C	H	
XIIa	123	80	$C_{26}H_{20}N_4O$	77.10	5.01	
				77.22	4.95	
XIIb	77	60	$C_{27}H_{22}N_4O_2$	74.50	6.00	
				74.65	6.06	
XIIc	99	60	$C_{26}H_{19}N_4OCl$	71.60	4.50	
				71.15	4.33	

Mannich reaction of IIIa-d. Formation of 1,2,3-trihydro-1-aryl-fluoren[3, 2-c]2-N-methyl-pyrazol-3-ones XXIIIa – d

To a methanolic solution of IIIa-d (0.01 mole in each case) and piperidine (0.02 mole) aqueous formaldehyde (2.5 mL ; 35 %) and hydrochloric acid (0.5 ml) were added. The reaction mixture was refluxed for twenty four hours and left to stand at room temperature for two days. The obtained solids were filtered and recrystallised from methanol to give XIIIa-d (cf. Table 10).

Table 10

1,2,3-Trihydro-1-aryl-fluoren[3,2-c]2-N-methylpiperidino-pyrazol-3-one derivatives XIIIa-d

Compound	M.p. °C	Yield %	Formula	Analysis %		(Found / Calcd.)
				C	H	
XIII	above 290	80	$C_{26}H_{28}N_3OCl$	71.80	6.40	
				71.97	6.45	
XIIIb	164	80	$C_{27}H_{30}N_3O_2Cl$	69.70	6.20	
				69.90	6.47	
XIIIc	95	80	$C_{26}H_{27}N_3OCl_2$	66.50	5.60	
				66.66	5.77	
XIIId	201	80	$C_{28}H_{33}N_4OCl$	69.99	6.80	
				70.51	6.92	

REFERENCES

[1] M. D. Nair, S. R. Metha and S. M. Kalbag, *Indian J. Chem.*, **5**, 464 (1967).

[2] P. A. S. Smith and Y. Ahmed, *J. Org. Chem.*, **36**, 2972 (1971).

[3] H. J. Strum and H. Armbrust, *Liebigs Annal. Chem.*, **729**, 139 (1969).

[4] I. I. Abd El-Gawad, A. M. Khalil, O.M.O. Habib and H. A. Etman, *Rev. Roumaine Chim.*, **30**, 499 (1986).

[5] O.M.O Habib, I. I. Abd El-Gawad, A. M. Khalil and H. A. Etman, *Polish J. Chem.*, in press.

Revue Roumaine de Chimie, 33, 5, 455–461 (1988)

POTENTIOMETRIC DETERMINATION OF SOME SEMISYNTHETIC PENICILLINS AND THEIR PARENT COMPOUNDS USING A Cu^{2+}-SENSITIVE ELECTRODE

MARIA MIOSCU, IOVANCA HAIDUC, D. C. CÖRMÖS and JANA RUSU
University of Cluj-Napoca, Chemistry Department and Institute of Chemico-Pharmaceutical Research, Cluj-Napoca, Romania

Received February 22, 1987

The direct titration potentiometric method was used for the determination of milligram amounts of the following aminoacids : phenylglycine, phenylalanine and *p*-hydroxyphenylglycine. The method was extended to the determination of ampicilline and its esters amoxicilline and pivampicilline. The standard solution was M/50 $CuSO_4$, the indicating electrode was a sensitive single crystal Cu^{2+} electrode. During the titration, complexes, of the CuL_2 type are formed at pH = 9 (borax buffer solution). At this pH the complexes exhibit the maximum stability. The percentage error varied between 1 and 4.5% for samples of 1.5 – 45 mg.

INTRODUCTION

The extensive development of the pharmaceutical field imposes the elaboration of increasingly rigorous analytical methods for the control of drugs.

The electrometric methods for the determination of pharmaceuticals have been scarce up to now. They possess a series of advantages as compared to the classical chemical methods : low sample size is needed, the methods are fast since the separation stages are not necessary and the subjectivity of the evaluation is avoided.

The potentiometric method is one of the simplest electrochemical methods. A modern technique of high specificity, based upon ion-sensitive electrodes can be used.

Several ion-sensitive electrodes were used in the analysis of drugs *e.g.* S^{2-},[1,2] halogen (Cl^-, Br^-, I^-)[3,4] and M^{2+} [5,6] sensitive electrodes. Liquid membrane ion sensitive electrodes were also successfully applied.[7] Enzyme-based electrodes, having a high specificity, were applied in the determination of some drugs.[8–15]

Continuing the studies[16,17] on the determination of α-aminoacids by potentiometric titration with the Cu^{2} ion, using a Cu^{2+}-sensitive single crystal electrode, we report in this paper the determination of the following aminoacids : phenylglycine, phenylalanine and *p*-hydroxyphenylglycine, as well as some drugs containing amino groups, *e.g.* ampicilline, amoxicilline and pivampicilline.

EXPERIMENTAL

Reagents and equipment

— Standard solution of M/50 $CuSO_4 \cdot 5H_2O$ (standardized against Complexone III (EDTA) using Murexide indicator).

— Buffer solution (pH = 9) obtained by disolving 19.09 g $Na_2B_4O_7 \cdot 10\,H_2O$ in 1 L doubly distilled water.

— A single crystal PbSe electrode

— Radelkis OP—208 pH-meter having a 0.1 mV sensitivity

— Magnetic stirrer

— Microburette 3—5 mL.

The sample solutions were obtained by dissolving the compound in a suitable amount of water or buffer solution.

Procedure

A volume of 10 mL aminoacid solution was transferred into a 100 mL beaker, the 5—15 mL buffer solution was added, to bring the pH to approx. 9. The solution was titrated under continuous stirring. The volume of the Cu(II) solution corresponding to the end point of the titration was determined by computation.

During the titration the e.m.f. of the following electrochemical cell was determined:

SCE	KCl saturated	Test aminoacid solution	Single crystal PbSe electrode

RESULTS AND DISCUSSION

The determination of the α-aminoacids phenylglycine, phenylalanine and *p*-hydroxyphenylglycine is based upon the formation of a CuL_2 complexe. Complexes of the same type are also formed with compounds having the following structures:

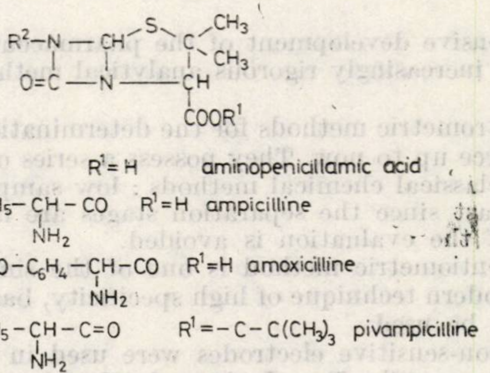

$R^2 = H$ $R^1 = H$ aminopenicillamic acid,
$R^2 = C_6H_5-CH(NH_2)-CO$ $R^1 = H$ ampicilline
$R^2 = pHO-C_6H_4-CH(NH_2)-CO$ $R^1 = H$ amoxicilline
$R^2 = C_6H_5-CH(NH_2)-C{=}O$ $R^1 = -C-C(CH_3)_3$ pivampicilline

from which by varying R_1 and R_2 the aminopenicillamic acid, amoxicilline, ampicilline and pivampicilline result.

The titration curves are shown in Figs 1—7 and they have a rather classical shape.

Phenylglycine (Fig. 1) can be titrated well under usual conditions. Regardless of sample size explicit equivalence jumps were recorded. For the phenylalanine titrations (Fig. 2) and for *p*-hydroxyphenylglycine (Fig. 3) successful titrations may be accomplished in the milligram range. For higher sample quantities a flattened curve was obtained.

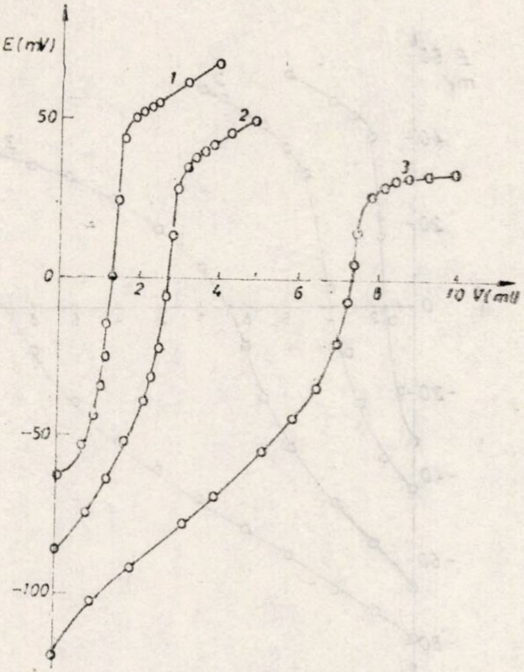

Fig. 1. — Titration of phenylglycine : 1 — 9.109 mg ; 2 — 18.218 mg ; 3 — 45.545 mg.

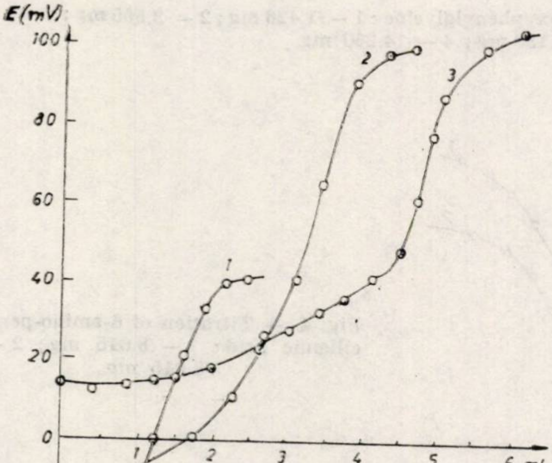

Fig. 2. — Titration of phenylalanine : 1 — 3.900 mg ; 2 — 7.938 mg : 3 — 11.970 mg.

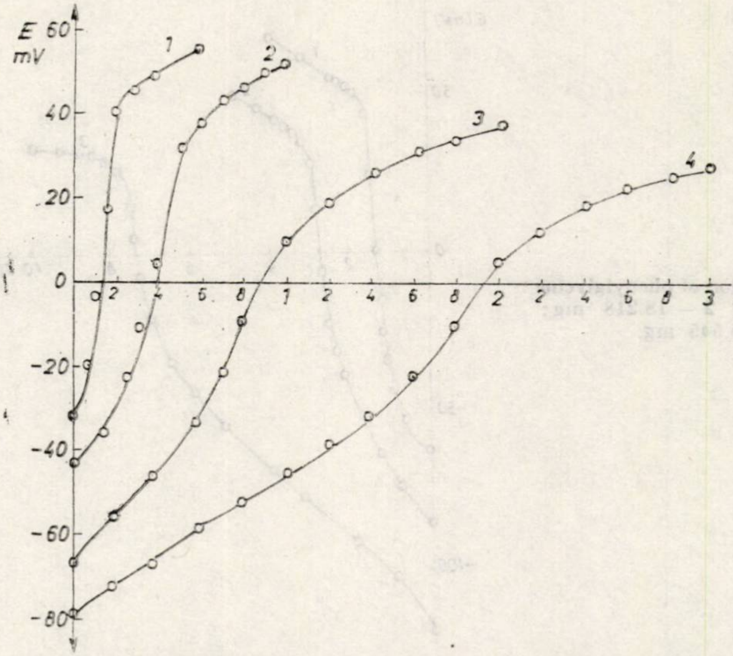

Fig. 3. — Titration of *p*-hydroxyphenylglycine : 1 — 1.426 mg ; 2 — 3.565 mg ; 3 — 7.130 mg ; 4 — 14.260 mg.

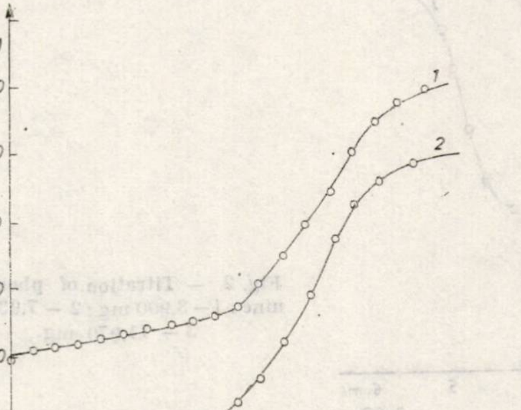

Fig. 4. — Titration of 6-amino-penicillamic acid : 1 — 8.015 mg ; 2 — 8.015 mg.

We did not find the adequate conditions for the titration of 6-amino-penicillamic acid (Fig. 4) if low sample quantities were analysed.

Ampicilline (Fig. 5), amoxicilline (Fig. 6) and pivampicilline (Fig. 7) gave good titration curves for samples below 20 mg.

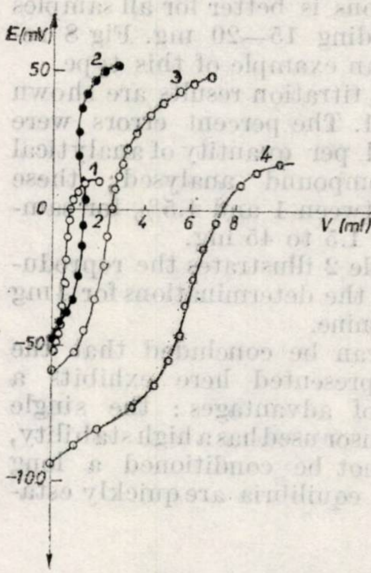

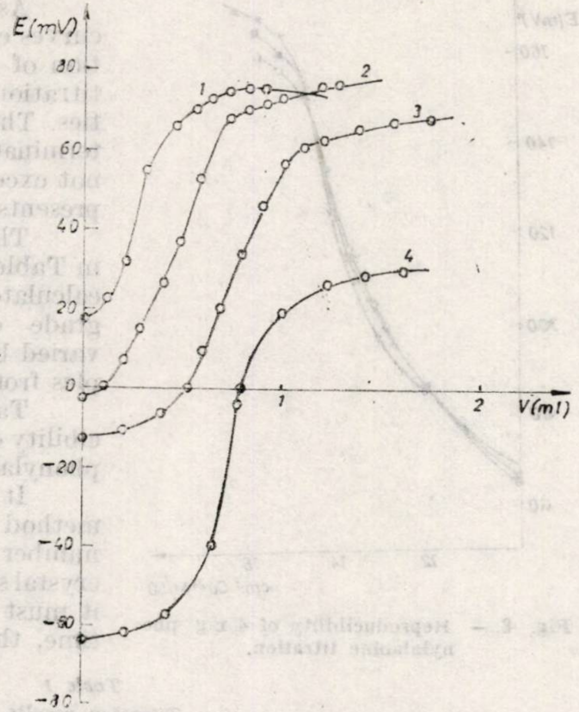

Fig. 5. — Titration of ampicilline: 1 — 3.848 mg; 2 — 9.620 mg; 3 — 19.240 mg.

Fig. 6. — Titration of amoxicilline: 1 — 3.990 mg; 2 — 7.980 mg; 3 — 10.185 mg; 4 — 11.970 mg.

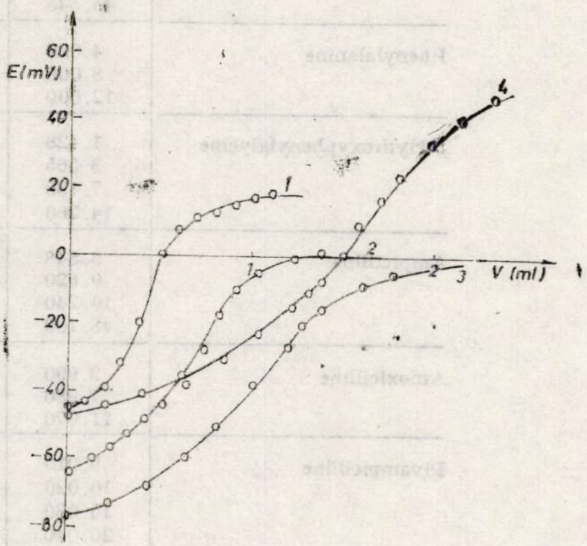

Fig. 7. — Titration of pivampicilline: 1 — 5.010 mg; 2 — 10.020 mg; 3—15.030 mg; 4 — 20.040 mg.

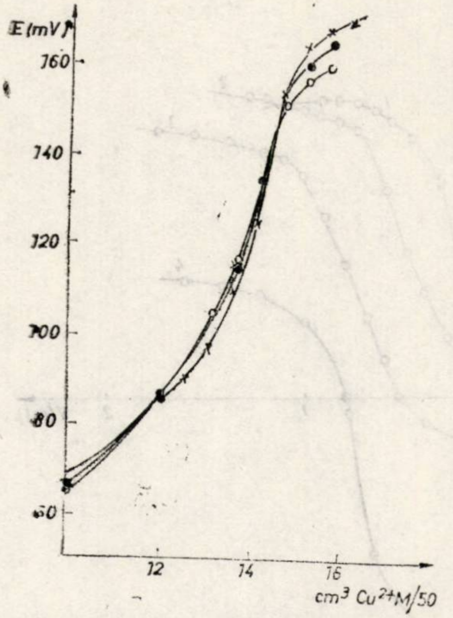

Fig. 8. — Reproducibility of 4 mg phenylalanine titration.

As a general rule the titration curves enable the more accurate location of the equivalence point in the titration, using low sample quantities. The reproducibility of the determinations is better for all samples not exceeding 15—20 mg. Fig 8 represents an example of this type.

The titration results are shown in Table 1. The percent errors were calculated per quantity of analytical grade compound analysed; these varied between 1 and 4.5% for samples from 1.5 to 45 mg.

Table 2 illustrates the reproducibility of the determinations for 4 mg phenylalanine.

It can be concluded that the method presented here exhibits a number of advantages: the single crystal sensor used has a high stability, it must not be conditioned a long time, the equilibria are quickly esta-

Table 1

Titration results

Aminoacid	Weighed (mg)	Found by titration (mg)	e %
Phenylglycine	9.100	8.720	−4.3
	18.218	17.320	−4.8
	45.545	45.070	−1.0
Phenylalanine	4.000	3.991	−0.2
	8.000	7.909	−0.6
	12.000	12.010	+0.1
p-Hydroxyphenylglycine	1.426	1.496	+5.0
	3.565	3.673	+3.0
	7.130	6.960	−2.5
	14.260	14.047	−1.5
Ampicilline	3.848	3.940	+2.5
	9.620	9.844	+2.3
	19.240	18.560	−3.5
	48.100	47.400	−1.4
Amoxicilline	3.990	3.810	−4.5
	7.980	7.975	0
	11.970	12.090	+1.0
Pivampicilline	5.010	4.865	−2.9
	10.020	9.893	−1.3
	15.030	15.560	+3.5
	20.040	20.430	+2.1

blished. Consequently, a titration can be performed in a few minutes. The standard titrating solution is a common analytical grade reagent. The equipment used is simple and available in any laboratory. The main merit of the method is its usability for the determination of very low sample quantities, thus being a semimicro method.

Table 2

Reproductibility of the determinations

Aminoacid	Weighed (mg)	Found by titration (mg)	s
Phenylalanine	4.000	3.968 3.999 3.991 3.991 3.901 3.859	1.04×10^{-2}

REFERENCES

[1] M. K. Papay, K. Toth and E. Pungor, *Analyt. Chim. Acta*, **56**, 291 (1971) ; **69, 173 (1974).**

[2] V. V. Coșofreț and A. Bunaciu, *Anal. Letters*, **12**, 677 (1979).

[3] Y. M. Dessouky, K. Toth and E. Pungor, *Analyst*, **95**, 1027 (1970).

[4] W. Selig, *Mikrochim. Acta*, **1973**, 473.

[5] S. M. Donache, G. E. Janauer and T. D. Zucconi, *Anal. Lett.*, **B 11**, 727 (1978).

[6] S. M. Saas Hassan and M. H. Eldesanski, *Talanta*, **26**, 531 (1979).

[7] C. Luca, C. Baloescu, G. Semenescu and T. Tolea, *Rev. Chim. (București)*, **30**, 72 (1979).

[8] G. G. Guilbault and J. Montalvo, *Analyt. Chem.* **41**, 1867 (1969).

[9] G. G. Guilbault and E. Hrabankova, *Analyt. Chem.*, **42**, 1779 (1970).

[10] G. G. Guilbault and G. J. Lubrano, *Analyt. Chem.*, **60**, 254 (1972).

[11] R. A. Llenado and G. A. Rechnitz, *Analyt. Chem.*, **43**, 1457 (1971).

[12] G. J. Papariello, A. K. Mukherji and C. Shearer, *Analyt. Chem.*, **45**, 790 (1973) ; **46**, 1955 (1974).

[13] L. D. Bowers and P. W. Carr, *Analyt. Chem.*, **48**, 545 A (1976).

[14] T. Yao and S. Muska, *Analyt. Chim. Acta*, **110**, 203 (1979).

[15] A. J. Blaidel and R. A. Jenkins, *Analyt. Chem.*, **48**, 1240 (1976) ; **52**, 1691 (1980).

[16] I. Haiduc, M. Mioșcu and D. C. Cörmöș, *Stud. Univ., Babeș-Bolyai, Chem.*, **2**, 59 (1979).

[17] M. Mioșcu, I. Haiduc and D. C. Cörmöș, *Rev. Roumaine Chim.*, **26**, 1487 (1981).

Revue Roumaine de Chimie, 33, 5, 463–465 (1988)

STUDIES IN THE SYNTHESIS OF SOME NEW FLUORO-SUBSTITUTED MESOIONIC HETEROCYCLES

R. L. MITAL*, POONAM TANEJA, VINEETA KHATRI and LALIT PRAKASH
Department of Chemistry, University of Rajasthan, Jaipur 302004, India

Received February 22, 1987

The synthesis of fluoro substituted 1-hydroxy-2-chloroacetyl-6-thia-10b-aza-2a-azonia-aceanthrylene hydroxide inner salt (IIa, b), 1-hydroxy-6-thia-10b-aza-2-azonia-aceanthrylene hydroxide inner salt (IIIa, b) and 1-hydroxy-2-piperidino-acetyl-6-thia-10b-aza 2a-azonia-aceanthrylene hydroxide inner salt (IVa, b) is described. The IR spectra are also included.

The literature shows that little work has been carried on the synthesis of mesoionic heterocyclic compounds.[1,2] During the last few years a growing number of useful applications of fluorinated organic compounds[3,4] has aroused our interest in the synthesis of fluoro substituted mesoionic heterocyclic compounds (II–IV) and in study of chemistry of these compounds.

In order to synthesize a new 1-hydroxy-2-chloroacetyl-6-thia-8/9-fluoro-10b-aza-2a-azonia-aceanthrylene hydroxide inner salt (IIa, b), a new 7/8-fluoro-10H-pyrido[3,2–b] [1,4]benzothiazine (Ia, b) was synthesized by Smiles rearrangement.[5]

The preparation of 1-hydroxy-2-chloroacetyl-6-thia-8/9-fluoro-10b-aza-2a-azonia-aceanthrylene hydroxide inner salt (IIa, b) was initiated by condensation of 7/8-fluoro-10H-pyrido[3,2–b] [1,4]benzothiazine (Ia, b) by chloroacetic anhydride and chloroacetic acid in dry dioxane. The product (IIa, b) on hydrolysis with a mixture of concentrated hydrochloric acid and glacial acetic acid gives 2-hydroxy-6-thia-8/9-fluoro-10b-aza-2a-azonia-aceanthrylene hydroxide inner salt (IIa, b) and on treatment with piperidine and N,N-dimethyl formamide gives 1-hydroxide-2-piperidino-acetyl-6-thia-8/9-fluoro-10b-aza-2a-azonia-aceanthrylene hydroxide inner salt (IVa, b). The structural assignments were based on elemental analysis and spectral data. The IR (KBr) spectra of Ia and Ib exhibit bands at 3320 (Ia), 3207 (Ib) (Sec.-NH-stretching vibration), 1345 (Ia), 1330 (Ib) (C–N stretching vibrations) and the bands at 1130 (Ia) and 1128 cm^{-1} (Ib) due to C–F stretching vibrations. The infrared spectrum of compound IIa and IIb lacked absorption characteristic of amine N—H stretch (3300—3500 cm^{-1}) or protonated ammonium N$^+$—H stretch (2300—2500 cm^{-1}). It was deduced that both the N—1 and the N—10 positions of the azaphenothiazine nucleus must be substituted and there must be a cationic site.

EXPERIMENTAL

1-Hydroxy-2-chloroacetyl-6-thia-9-fluoro-10b-aza-2a-azonia-aceanthrylene hydroxide inner salt (IIa ; Table 1)

A stirred mixture of 8-fluoro-10H-pyrido[3,2-b][1,4] benzothiazine (0.25 mole), chloroacetic anhydride (54.0 g, 0.32 mole), chloroacetic acid (75.0 g, 0.79 mole) in 250 mL of dry dioxane was refluxed for an hour. The hot mixture was poured into 11 mL of hot water and the precipitate was collected and washed with warm 95% ethanol until the washings were colourless. The product IIa was obtained as yellow green solid.

In a smilar manner 1-hydroxy-2-chloroacetyl-6-thia-8-fluoro-10b-aza-2a-azonia-aceanthrylene hydroxide inner salt (IIb ; Table 1) was prepared.

Table 1

Characterization data of compounds II — IV

Compound	Yield (%)	M.P. (°C)	Molecular formula	Analysis			
				Found (%)		Calculated (%)	
				C	H	C	H
IIa	52	> 300	$C_{15}H_8ClFN_2O_2S$	53.90	2.41	53.80	2.48
IIb	43	> 300	$C_{15}H_8ClFN_2O_2S$	53.72	2.32	53.80	2.48
IIIa	46	292	$C_{13}H_7FN_2OS$	60.46	2.62	60.41	2.72
IIIb	52	280	$C_{13}H_7FN_2OS$	60.37	2.81	60.41	2.72
IVa	61	> 300	$C_{20}H_{18}FN_3O_2S$	62.52	4.70	62.66	4.79
IVb	50	> 300	$C_{20}H_{18}FN_3O_2S$	62.60	4.84	62.66	4.79

1-Hydroxy-6-thia-9-fluoro-10b-aza-2-a-azonia-aceanthyrlene hydroxide inner salt (IIIa ; Table 1)

IIa was added to a mixture of concentrated hydrochloric acid (5 mL) and glacial acetic acid (15 mL) and refluxed for 15 minutes. The reaction mixture was made basic with sodium-hydroxide solution and the resultant precipitate was collected. Recrystallization from 95% ethanol yielded IIIa as a buff coloured solid.

In a similar manner 1-hydroxy-6-thia-8-fluoro-10b-aza-2a-azonia-aceanthrylene hydroxide inner salt (IIIb ; Table 1) was prepared.

41-Hydroxy-2-piperidino-acetyl-6-thia-9-fluoro-10b-aza-2a-azonia-aceanthrylene hydroxide inner salt (IVa; Table 1)

A stirred mixture of IIIa (0.07 mole), piperidine (18.8 g, 0.22 mole) and N-N-dimethylformamide was heated for one hour. After cooling overnight in a refrigerator, the resultant precipitate was collected and washed with water. The filtrate and washings were poured into 11 mL of water previously made alkaline (sodium carbonate) and the mixture filtered. The total solid collected was combined and recrystallized from propanol to yield fine yellow needle crystals of IVa.

In a similar manner 1-hydroxy-2-piperidinoacetyl-6-thia-8-fluoro-10b-aza-2a-azonia-aceanthrylene hydroxide inner salt (IVb; Table 1) was prepared.

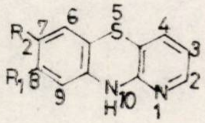
R2
7
6
5
S
4
3
R1
8
9
N
10
H
N
2
1

I

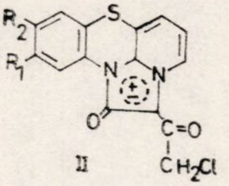
R2
S
R1
N
+
N
O
C=O
CH2Cl

II

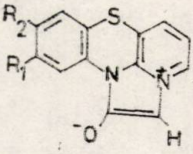

III

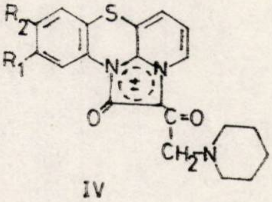
R2
S
R1
N
+
N
O
C=O
CH2
N

IV

Where I, II, III, IV a, R_1=F, R_2=H

b, R_1=H, R_2=F

REFERENCES

[1] J. W. Steele, W. K. Anderson and W. E. Trager, *Canad. J. Chem.*, **50**, 1026 (1972).

[2] V. Taneja, M. Anand, C. L. Gupta, S. B. Gupta and R. L. Mital, *J. Heterocyclic Chem.*, **21**, 1239 (1984).

[3] V. Taneja, C. L. Gupta and R. L. Mital, *Chemistry and Industry*, **1984**, 187.

[4] S. B. Tambi, M. Anand, V. Taneja, C. L. Gupta and R. L. Mital, *J. Heterocyclic Chem.*, **20**, 803 (1983).

[5] A. A. Levy, H. C. Rains and S. Smiles, *J. Chem. Soc.*, **1931**, 3264.

Revue Roumaine de Chimie, **33**, *5*, 467–471 (1988)

IR ANALYSIS OF AMINES, CARBOXYLIC ACIDS, ALCOHOLS, PHENOLS AND MERCAPTANS AFTER DERIVATIZATION WITH *n*-BUTYLISOCYANATE*

IOAN MUNTEAN, JEAN MICHEL HERDAN** and GABRIELA VĂLEANU
Research and Design Institute for Refineries, Ploieşti, Romania

Received February 22, 1987

The derivatization reaction with *n*-butylisocyanate of primary and secondary amines, carboxylic acids, alcohols, phenols and mercaptans was used for improving their identification by IR spectroscopy. The derivatization products are characterized by the stretching vibrations of the NH group at 3400–3500 cm^{-1} and C=O group at 1600–1800 cm^{-1}. Carboxyl absorptions are sensitive to electronic effects and this fact leads to the identification of the *n*-butylisocyanate derivatives using the νCO frequencies.

The IR identification of some atom groups or organic functions is sometimes difficult. The causes are both the low intensity of some absorption bands (e.g. the SH stretching), or the overlapping with other bands. A way to resolve such situations is the conversion of the difficultly recognisable groups or functions into another groups, which are easily recognisable by IR. For example, the presence of a carboxylic acid may be confirmed by its conversion into a carboxylate,[1] which is easy to perform by adding a few drops of triethylamine to the $CHCl_3$ solution.[2]

Searching other chemicals able to give good derivatives for IR analysis, *n*-butylisocyanate was selected because of its reactivity toward molecules containing active hydrogen atoms such as : amines, carboxylic acids, alcohols, phenols, mercaptans, giving the following reaction products :

$$
n\text{-}C_4H_9-N{=}C{=}O + \begin{array}{l}
R-NH_2 \rightarrow n\text{-}C_4H_9-NH-CO-NHR \\
\qquad\qquad \text{N-alkyl-N-butylureas} \\
R-COOH \rightarrow n\text{-}C_4H_9-NH-CO-O-CO-R \\
\qquad\qquad \text{mixed anhydrides} \\
R-OH \rightarrow n\text{-}C_4H_9-NH-CO-OR \\
\qquad\qquad \text{O-alkyl-N-butylurethans} \\
R-SH \rightarrow n\text{-}C_4H_9-NH-CO-SR \\
\qquad\qquad \text{S-alkyl-N-butylthiourethans}
\end{array}
$$

---

* This paper was presented at the Vth Conference of Analytical Chemistry and Quality Control, Cîmpulung-Muscel, May 16–17 1985.

** Correspondence author

Comparison of the spectra of the underivatized compounds with those of the derivatives reveals the occurrence of at least two new bands : the stretching frequencies of NH and CO groups.

Carbonyl absorption are sensitive to both chemical and physical effects. These effects are responsible for the frequencies shifts and, in our case, lead to the identification of the *n*-butylisocyanate derivatives. Bellamy[3] discusses extensively upon the frequency shifts of νCO.

Table 1

The main absorption bands of some derivatives of *n*-butylisocyanate with amines, carboxylic acids, alcohols, phenols and mercaptans (cm^{-1})

Compounds	ν NH free	νC=O main band	νC=O secondary band
n-butylamine	3490	1695	1640
isobutylamine	3485	1690	1650
sec-butylamine	3480	1690	1640
cyclohexylamine	3480	1695	1640
n-dodecylamine	3480	1690	1640
benzylamine	3480	1690	1640
aniline	3440	1700	1650
di-(*n*-butyl)amine	3465	1665	1600
di-(*i*-butyl)amine	3470	1630	1670
cyclohexylethylamine	3480	1620	1690
dicyclohexylamine	3480	1620	1670
N-methylaniline	3460	1650	1600
dibenzylamine	3450	1640	1690
diphenylamine	3440	1665	1590
propionic acid	3450	1670	1690
butyric acid	3450	1660	1690
isobutyric acid	3450	1670	1690
n-valeric acid	3450	1690	1660
benzoic acid	3450	1695	1650
n-butyl alcohol	3460	1710	
isobutyl alcohol	3460	1710	
sec-butyl-alcohol	3450	1700	
tert-butyl-alcohol	3440	1720	
1-tetradecanol	3460	1715	
phenol	3460	1740	
p-cresol	3450	1730	
nonylphenol*	3450	1730	
2,6,-di-tert-butyl-4-methylphenol	3440	1730	
cyclohexylmercaptan	3430	1680	
n-dodecylmercaptan	3440	1695	

* technical grade

Instead of *n*-butylisocyanate, other isocyanates, such as phenylisocyanate, may be used ; the former has the advantage to produce derivatives which are more soluble in chloroform and have simpler IR spectra.

Table 1 presents the main absorption bands of the reaction products between *n*-butylisocyanate and 30 organic compounds with active hydrogen atoms, respectively : seven primary amines, seven secondary amines, five carboxylic acids, five alcohols, four phenols and two mercaptans. The frequencies assignments are according to refs. [1,2,4]

Table 2 summarizes the absorption ranges of νNH and νCO frequencies of the primary and secondary amines, carboxylic acids, alcohols, phenols and mercaptans derivatives.

Table 2

Absorption ranges of νNH and νCO of *n*-butylisocyanate derivatives (cm^{-1})

Derivatives of	νN−H	νC=O,	
		main band	secondary band
$R-NH_2$	3440−3490	1690−1700	1640−1650
R_2-NH	3440−3480	1620−1665	1590−1690
R−COOH	3450	1660−1695	1650−1690
R−OH	3440−3460	1700−1720	—
Ar−OH	3440−3460	1730−1740	—
R−SH	3430−3440	1680−1695	—

Fig. 1,A−D, presents the IR spectra in 1450−1800 cm^{-1} and 3200−3600 cm^{-1} ranges for *n*-dodecylamine, dibenzylamine, valeric acid and isobutylic alcohol derivatives of *n*-butylisocyanate. The spectra of the phenol and mercaptan derivatives are similar with those of the alcohol derivatives, excepting the carbonyl frequencies.

The data in tables 1 and 2 and the examination of the spectra in figure 1 lead to the following conclusions :

1. All spectra of the studied derivatives contain a characteristic band in 3400 −3500 cm^{-1} region, assigned to ν NH stretching. When concentrated solutions are examined a new broad band appears at 3300 cm^{-1} assigned to the associated NH groups. In the case of film spectra the free band disappears and only the broad band at 3300 cm^{-1} is present.

It can be stated that only the presence of the free NH band confirm the existence of an active hydrogen atom in the starting sample.

2. The IR spectra of the *n*-butylisocyanate derivatives permit a distinction between an alcohol, phenol or mercaptan and carboxylic acid, primary and secondary amines respectively. In the case of primary amines a single band appears for CO stretching and two bands appear in the case of the secondary ones, one of them of lower intensity, called νCO secondary band (see table 1).

3. The frequency shifts of the carbonyl in the isocyanate derivatives lead to the identification of the alcohols, phenols and mercaptans. Thus, in the case of alcohols the CO band occurs at 1700−1720 cm^{-1} and at 1730−1750 cm^{-1} and 1680−1695 cm^{-1} for phenols and mercaptans respectively. The main cause of the shifts are the resonance effects to which the CO group is very sensitive.

A mention must be made for steric hindered phenols such as 2,6-di-*t*-butyl-4-methylphenol. In these cases the reaction with *n*-butylisocyanate is not complete so that in the IR spectrum the free OH band, at 3650 cm^{-1}, can be observed near the NH band at 3450 cm^{-1}.

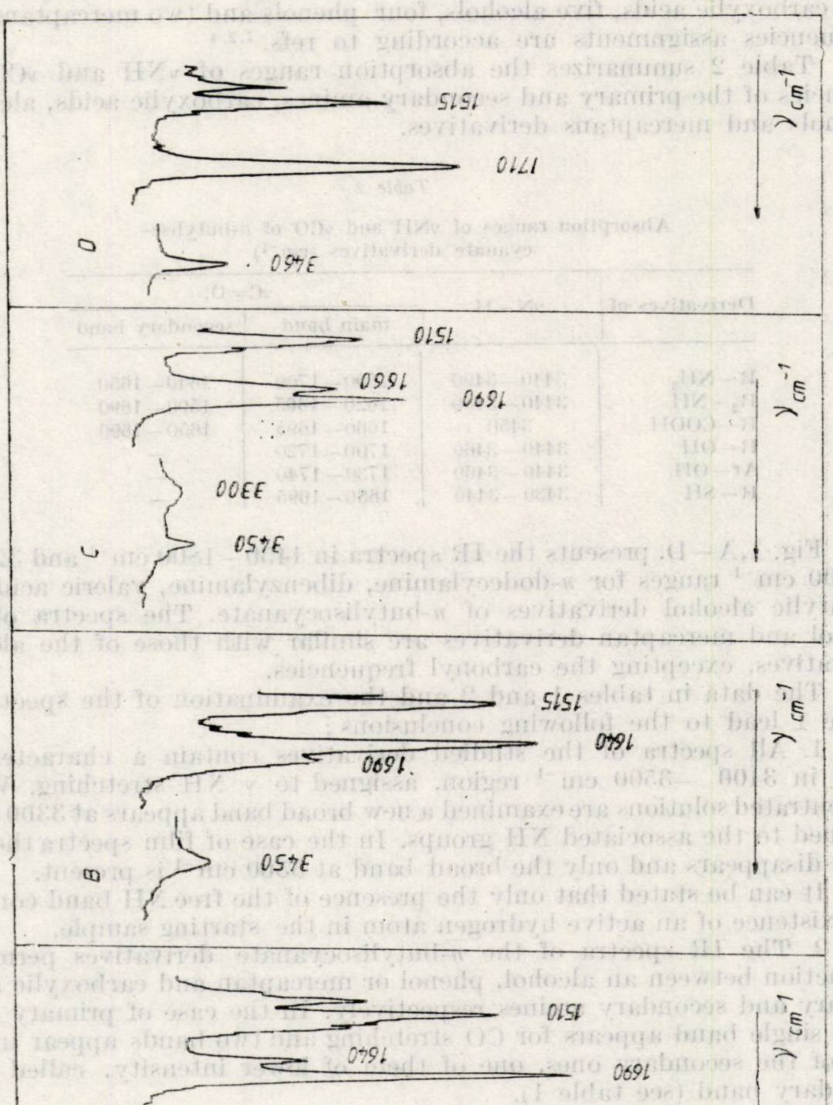

Fig. 1. — The IR spectra in 1450—1800 cm^{-1} and 3200—3600 cm^{-1} ranges of *n*-butylisocyanate derivatives with : A — *n*-dodecylamine ; B — dibenzylamine ; C — *n*-valeric acid ; D — isobutylalcohol.

4. An advantage of the derivatization with *n*-butylisocyanate is the possibility to identify a mercaptan by IR spectroscopy, because a strong band occurs at 1680—1695 cm^{-1}. Ordinarily, the SH group is difficultly observable, thus the identification of mercaptans is uncertain.

5. Using the derivatisation with *n*-butylisocyanate a distinction could be made between primary and secondary amines. The main CO band occurs at 1690—1700 cm^{-1} in the case of primary amines, and at 1620—1665 cm^{-1} in the case of secondary amines.

We can not use this method in order to make a distinction between a carboxylic acid and an amine. This fact is not a serious disadvantage because anyway the IR spectra of the carboxylic acids and of amines can not be mistaken for one another.

6. Very interesting seems to be the situation of the mixed anhydrides obtained by reaction between carboxylic acids and *n*-butylisocyanate. As known, the anhydrides are characterized by a doublet in the 1700—1850 cm^{-1} region due to coupling between the two CO stretchings. A single band, less or more split, occurs in the case of mixed anhydrides described herein. The position of this band at much lower frequencies (1660—1695 cm^{-1}), may be explained by the resonance due to the presence of the nitrogen atom :

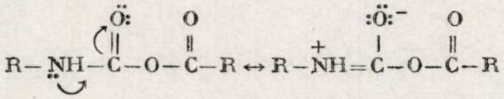

$$R-\ddot{N}H-\overset{\ddot{O}:}{\overset{\|}{C}}-O-\overset{O}{\overset{\|}{C}}-R \leftrightarrow R-\overset{+}{N}H=\overset{:\ddot{O}:^{-}}{\overset{|}{C}}-O-\overset{O}{\overset{\|}{C}}-R$$

As a result, the CO band order gets lower and the frequency decreases.

EXPERIMENTAL

Synthesis of derivatives. 0.1 g sample and 0.02 mL freshly distilled *n*-butylisocyanate were introduced in a small Claisen flask. The mixture was heated at 140° C for 3 hours. The excess isocyanate was removed by distillation under reduced pressure. In the flask were introduced 3—4 mL chloroform. The spectrum of the solution, of about 4% concentration was recorded in a 0.1 mm NaCl cell.

No special condition was necessary in order to avoid the moisture, but the sample must be anhydrous (the isocyanate reacts with water producing NN′-disubstituted ureas that can interfere).

IR spectra. The IR spectra were recorded with a C. Zeiss, Jena, SPECORD IR 75 — spectrophotometer. 0.1 mm cells were used. The sample was compensated with chloroform. Solutions of 3—4% in chloroform produce good spectra but in order to obtain a better NH band at 3400—3500 cm^{-1}, a double concentration is recommendend.

REFERENCES

[1] L. J. Bellamy, "The Infrared Spectra of Complex Molecules", Methuen, London, 1957.

[2] K. Nakanishi, "Infrared Absorption Spectroscopy — Practical", Holden-Day Inc., San-Francisco, 1962.

[3] L. J. Bellamy, "Advances in Infrared Group Frequencies", Methuen, London, 1968.

[4] M. Avram and G. D. Mateescu, " Infrared Spectroscopy. Applications in Organic Chemistry", Wiley-Interscience, New York, 1972.

Revue Roumaine de Chimie, **33**, 5, 473–481 (1988)

THE UV-VIS-SPECTRAL BEHAVIOUR OF ARYLAZO COMPOUNDS. I

GENERAL REMARKS

J. EPPERLEIN and B. BLAU
Chemistry and Material Sciences Dept., Technical University Karl-Marx-Stadt, DDR-9010 Karl-Marx-Stadt

Received October 10, 1987

Azo dyes embrace more than 50 % of the total number and of over-all tonnage produced of dye structures known to be manufactured. For some important classes of monoazo dyes semi-quantitative rules are given, describing and predicting the position of the colour-giving absorption (λ_{max}) as a function of a given substituent pattern. On the basis of rich experimental data, an incremental system is derived for calculation resp. prediction of the longest wavelength absorption maxima of substituted monoazo dyes.

INTRODUCTION

Azo dyes form the most voluminous and commercially most important class of dyes. Their present worldwide production is more than $2 \cdot 10^5$ t per year. In the London World Exhibition, 1862, the new azo dyes constituted a sensation with their colourfulness and brillance. Today the azo compounds are the basis of the most dyes and colorants for almost all purposes. Modern azo dyes are typical products of organic high-refinement chemistry.[1]

Since the 19th century knowledge and handy rules on the interdependencies between structure (subsituent pattern) and colour (absorption spectra) have been looked for. About this situation Pinnow wrote[2] at the end of the 19th century : "Zu Beignn der 80-er Jahre liessen sich aus den deutschen Patentschriften bereits 9000 mögliche Azofarbstroffe errechnen. Es galt, aus der Überfülle der Moglichkeiten die wenigen technisch wie kaufmännish wertvollen Produkte und Verfahren herauszufinden".

Only the number of imaginable azobenzenes substituted by the today available substituents for phenyl rings exceed 10^8 species. Syntheses of all these compounds is absolutely impossible and, of course, not necessary.

The present main uses of azo dyes are : a) dyeing of wool, silk, leather ; b) dyeing of synthetic fibres ; c) dyeing of polymers.

Azo dyes possess special functions (azo compounds resp. their tautomers form the image dyes) in the field of photo-and reprography like in : a) silver dye bleach materials[3] ; b) the Kodak variant of colour instant photography[4] ; c) the diazotype process. [5,6]

Other application fields of arylazo compounds are : a) liquid crystals : b) pharma ; c) photoconductors.

THE PARENT COMPOUND AZOBENZENE

Since the first spectroscopic investigation of azobenzene by Hartley[7] in 1887 this basic compound and its derivatives have been very often subject of spectroscopic studies (e.g.[8–15]). Azobenzene is iso-π-electronic with bezylidenaniline and stylbene. Beside the weak n → π^* absorption band the spectral absorption curve of *trans*-azobenzene is similar to that of *trans*-stylbene, but the longest wavelength $\pi \rightarrow \pi^*$ absorption band is situated slightly bathochromically to stylbene. The intense ($\lg\varepsilon = 4.25$) long wavelength absorption band at 318 nm (in pure ethanol) interpreted in terms of quantum chemical HMO-resp. PPP-calculations[16–20] comprises two allowed $\pi \rightarrow \pi^*$ electronic transitions. Approximately the lower energy transitions correspond to a one-electron transition from the HOMO to the LUMO, whereas the higher energy transitions are connected with the subjacent MO and the LUMO. The PPP-calculation[20] gives some hints how substituents act on the MO structure ; e.g. for the HOMO, the *para*-position is the most sensitive one against substitution (Fig. 1).

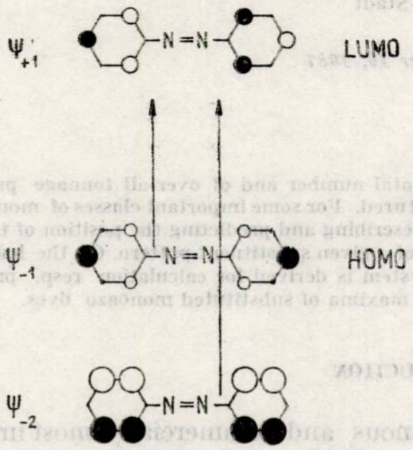

Fig. 1. — UV-VIS-Spectroscopically important molecular π-orbitals and lowest energy transitions of *trans*-azobenzene (PPP-caculation).

SUBSTITUTED AZOBENZENES

The parent compound, *trans*-azobenzene (I), allows very many variations by substitutions. *cis*-Azobenzene shows in most solvents (in ethanol, too) a lower stability in relation to the *trans*-isomer (e.g.[17]).

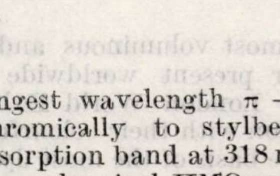

(I)

The great number of synthesized structures and hypothetical substituent pattern still increase by their latent possibilities of: a) *trans-cis*-isomerization; b) tautomerization (in *ortho*-, resp. *para*-OH- or -NHR-substituted species); c) pronotation.

A distinct demand aroused, namely to predict the colour of arylazoarenes resp. azo dyes and — if possible — to give guidelines for the synthesists; for example blue or cyano monoazo dyes for colourants or for the future colour diazotype systems[6] are to be searched.

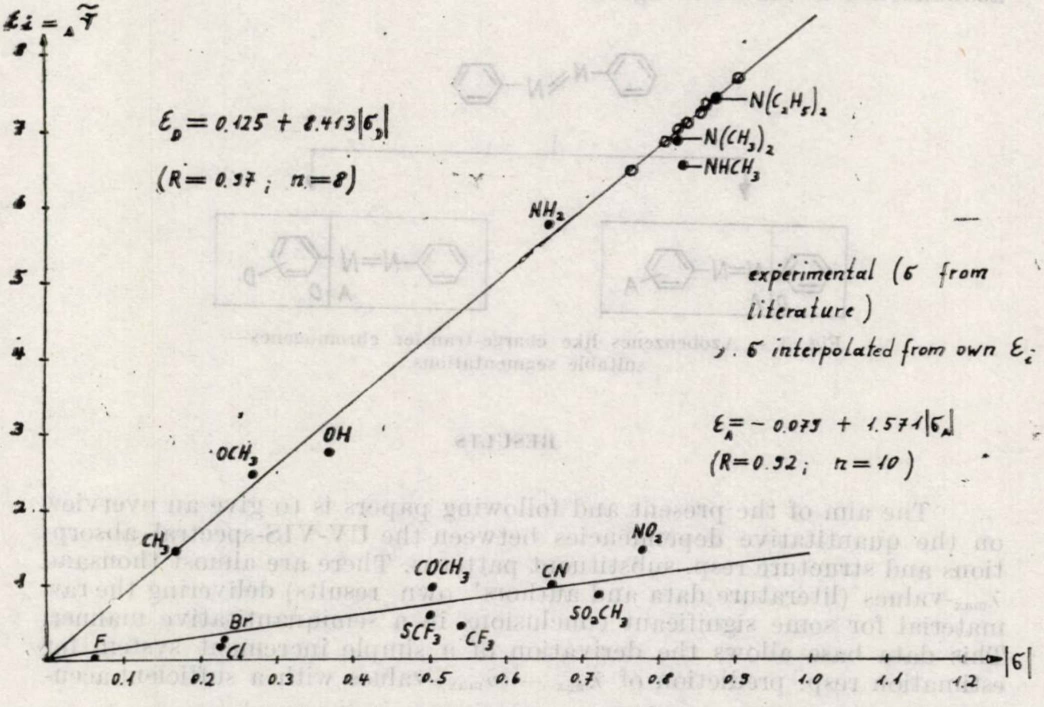

Fig. 2. — Correlations between the bathochromic shifts $\Delta\tilde{\nu}$ of *para*-substituted azobenzenes and the Hammett-σ-constants of these substituents.

At first one thinks of a quantum chemical approach, of course. Kroner and Bock[16] described the influence of substituents on the situation of the $n \rightarrow \pi^*$ — and $\pi \rightarrow \pi^*$-absorption bands in the cases of dialkylamino and nitroazobenzenes by means of a HMO-model.

Brigdeman and Peters[9] obtaines a rather satisfying correlation between the Hammett-σ-constants of the substituents of the diazo components and the λ_{max}-values of the corresponding azo dyes, too. Figure 2 illustrates the dependence $\Delta\tilde{\nu} = f(\sigma)$.

Repeatedly the higher sophisticated quantum chemical instrument of PPP—LCI—calculations has been used to calculate resp. to explain the spectral behaviour of arylazoarenes.[17-20] However the coincidence of HMO- or PPP-calculated results and experimental data is sometimes scarcely satisfying, but the expense is high. Tested parameter sets are published.[20,21]

Ago it was found that typical azo dyes do not obey well known classical colour rules; azo dyes are neither polymethines nor pure aromatic compounds or typical polyenes. Azo dyes appear in the scope of older, more phenomenological colour theories like chromogens sui generis. The very capacious triade theory of Dähne [22,23] does not regard explicitly azo dyes. Today azo dyes are well accepted following a classification given by Griffiths [21,21,25] and Fabian[19] as charge-transfer-chromogenes (conf. Mustroph and Epperlein[15], too). See also[31]. A suitable segmentation of substituted azobenzenes is shown in fig. 3.

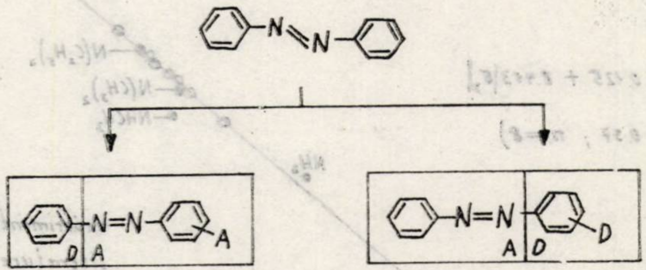

Fig. 3. — Azobenzenes like charge-transfer chromogenes— suitable segmentations.

RESULTS

The aim of the present and following papers is to give an overview on the quantitative dependencies between the UV-VIS-spectral absorptions and structure resp. substituent patterns. There are almost thousand λ_{max}-values (literature data and authors' own results) delivering the raw material for some significant conclusions in a semiquantitative manner. This data base allows the derivation of a simple increment system for estimation resp. prediction of λ_{max} — ($\tilde{\nu}_{max}$)-values with a sufficient accuracy.

Generally, aromatic azo compounds possess UV-VIS absorptions of three different types (examples are shown in Figure 4):

— bands due to localized electronic excitations in the arene rings (the so-called $\Phi \rightarrow \Phi^*$ —transitions in the range of 200 ... 300 nm),

— in non-symmetrically substituted azobenzenes a weak absorption band in the visible region, which is connected with an $n - \pi^*$-transition, relatively less sensitive for variation of substituents (lying in the range of 430 ... 470 nm, occasionally to 500 nm).

— one or two intensive, colour giving absorptions due to electronic excitation of the molecular π-system on the whole (the so-called $\pi - \pi^*$-transitions in the range of 315 ... 670 nm, in planar structures with $\lg \varepsilon = 4 \ldots 5$).

In the frame of the charge-transfer-concept (Fig. 4) one expects a decrease of excitation energy (thus a bathochromic shift):

— by decreasing "ionization potentials of the donor segment" (e.g. by means of donator substitution) or

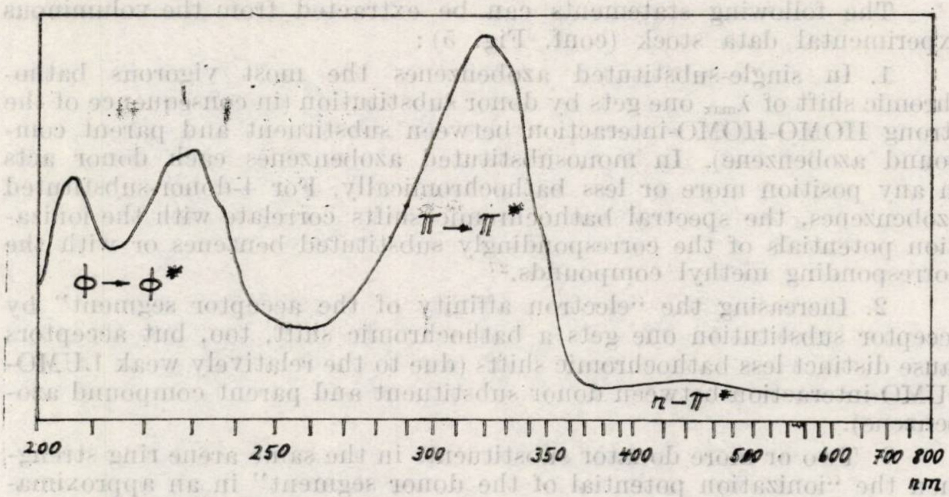

Fig. 4. — UV-VIS-absorption spectra of azobenzene in ethanol.

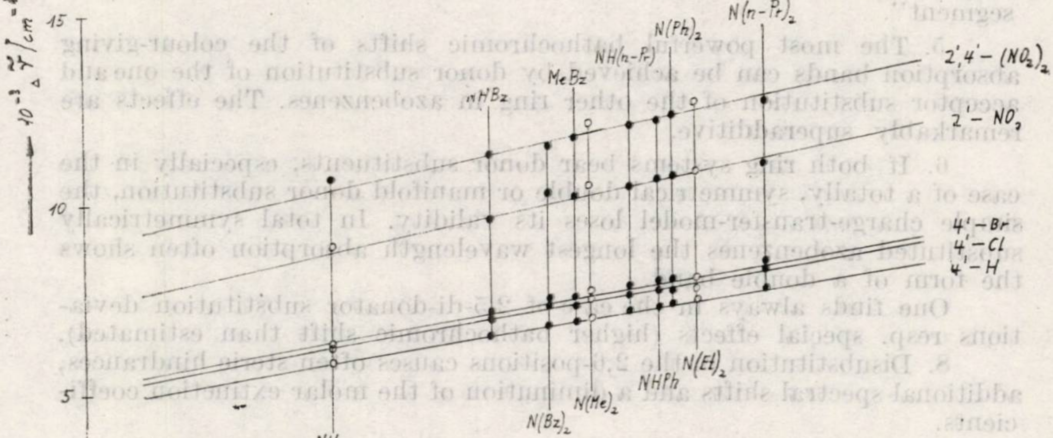

Fig. 5. — The bathochromic shifts $\Delta\tilde{\nu}$ of substituted aminoazobenzenes in dependence of the substituent — and position-specific increments ε_i.

— by increasing "electron affinity of the acceptor segment" (e.g. by means of acceptor substitution) or

— by intensification of the interaction of both segments.

The following statements can be extracted from the voluminous experimental data stock (conf. Fig. 5):

1. In single-substituted azobenzenes the most vigorous bathochromic shift of $\lambda_{\max}$ one gets by donor substitution (in consequence of the strong HOMO-HOMO-interaction between substituent and parent compound azobenzene). In monosubstituted azobenzenes each donor acts in any position more or less bathochromically. For 4-donor-substituted azobenzenes, the spectral bathochromic shifts correlate with the ionization potentials of the correspondingly substituted benzenes or with the corresponding methyl compounds.[27]

2. Increasing the "electron affinity of the acceptor segment" by acceptor substitution one gets a bathochromic shift, too, but acceptors cause distinct less bathochromic shifts (due to the relatively weak LUMO-LUMO-interaction between donor substituent and parent compound azobenzene).

3. Two or more donator substituents in the same arene ring strengthen the "ionization potential of the donor segment" in an approximately additive manner.

4. Two or more acceptor substituents in the same arene ring act equally in direction of increasing the "electron affinity of the acceptor segment".

5. The most powerful bathochromic shifts of the colour-giving absorption bands can be achieved by donor substitution of the one and acceptor substitution of the other ring in azobenzenes. The effects are remarkably superadditive.

6. If both ring systems bear donor substituents, especially in the case of a totally, symmetrical double or manifold donor substitution, the simple charge-transfer-model loses its validity. In total symmetrically substituted azobenzenes the longest wavelength absorption often shows the form of a double band.

One finds always in the case of 2,5-di-donator substitution deviations resp. special effects (higher bathochromic shift than estimated).

8. Disubstitution in the 2,6-positions causes often steric hindrances, additional spectral shifts and a diminution of the molar extinction coefficients.

AN INCREMENTAL SYSTEM

As shown in Fig. 5 almost linear correlations exist between the particular substituent series. From mono-substituted azobenzenes the substituent- and position-specific increment can be evaluated [15]:

$$\varepsilon_A = \tilde{\nu}_0 - \tilde{\nu}_A \qquad (1)$$

$\tilde{\nu}_0$ denotes the wave number corresponding to $\mu_{\max}$ of the colour giving absorption of the unsubstituted azobenzene, $\tilde{\nu}_A$ respectively the wavenumber of the A-substituted azobenzene.

The bathochromic shift of any azobenzenes subsituted with the substituents *A*, B in relation to the absorption of the parent compound azobenzene ($\tilde{\nu}_0$) can be usually expressed by a simple function of the type :

$$\Delta\tilde{\nu}_{AB} = \tilde{\nu}_0 - \tilde{\nu}_{AB} = \mathrm{f}(\varepsilon_A,\ \varepsilon_B) \tag{2}$$

An acceptor-donor-substituted azobenzene of the structure

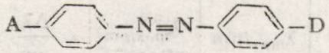

shows $\lambda_{\max}$ a value approximately corresponding to the formerly given formulae[15, 26]

$$\Delta\tilde{\nu}_{AD} = \tilde{\nu}_0 - \tilde{\nu}_{AD} \approx \varepsilon_D + 2.27\ \varepsilon_A \tag{3}$$

$$\Delta\tilde{\nu}_{AD} = \tilde{\nu}_0 - \tilde{\nu}_{AD} \approx \varepsilon_A + \varepsilon_D + c(\varepsilon_A \cdot \varepsilon_D) \tag{4}$$

Tables 1 and 2 give some examples for the power of this estimations formula (3, 4); the value for *c* was chosen $c = 1.9 \cdot 10^{-4}$ cm. These values calculated by means of the increment system of monoazo dyes, especially azobenzenes, are in good agreement with experimental results (medium deviation $\leqslant 5$ nm).[15] Formula (4) delivers a still better agreement. Note that the accuracy of the most determinations of $\lambda_{\max}$ given in the literature is not better than $\pm$ 0.5 nm.

EXPERIMENTAL

The RO-substituted azobenzenes of Table 1 were prepared by ether-syntheses after Williamson from their 4-hydroxyazobenzenes.

Table 1

Absorption maxima of some RO-substituted azobenzenes

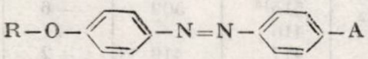

R	A	$\lambda_{\max}$/nm	$\lambda_{\max}^{\text{calc.}}$/nm after (3)	$\frac{\Delta\lambda^*}{\text{nm}}$	$\lambda_{\max}^{\text{calc.}}$/nm after (4)	$\frac{\Delta\lambda^*}{\text{nm}}$	$\frac{\varepsilon_t \cdot 10^{-3}}{\text{cm}^{-1}}$
1.1. CH_3	H	345[15]	—	—	—	—	2.46[15]
1.2. CH_3	NO_2	371	389	+18	372	+1	
1.3. Bz	H	346[29]	—	—	—	—	2.55
1.4. C_2H_5	H	347	—	—	—	—	2.63
1.5. C_2H_5	NO_2	374	392	+18	375	+1	
1.6. *n*-Pr	H	348	—	—	—	—	2.75
1.7. *n*-Pr	NO_2	376	393	+17	377	+1	
1.8. H	H	348[15]	—	—	—	—	2.75[15]
1.9 H	Cl	356[15]	355	−1	353	−3	
1.10 H	NO_2	385[15]	393	+8	377	−8	
1.11 *n*-Bu	H	348	—	—	—	—	2.75
1.12 *n*-Bu	NO_2	392	393	+1	377	−15	
1.13 *i*-Bu	H	349	—	—	—	—	2.80
1.14 *i*-Bu	NO_2	393	394	+1	378	−15	
1.15 *i*-Pr	H	351	—	—	—	—	2.96
1.16 *i*-Pr	NO_2	400	397	−3	381	−19	

* $\Delta\lambda = \lambda_{\text{calc}} - \lambda_{\max}$

Table 2

Spectral behaviour of 4-amino-substituted azobenzenes

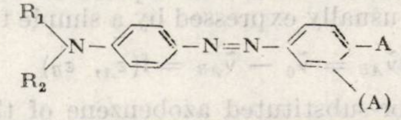

R_1	R_2	A	λ_{max}/nm	$\lambda^{calc.}_{max}$/nm after (3)	$\frac{\Delta\lambda}{nm}$	λ^{calc}_{max}/nm after (4)	$\frac{\Delta\lambda}{nm}$	$\frac{\varepsilon_i \cdot 10^{-3}}{cm^{-1}}$
2.1. H	H	H	389[15]	—	—	—	—	5.75[15]
2.2. H	H	Cl	392[28]	390	−2	396	+4	
2.3. H	H	Br	405	399	−6	398	−7	
2.4. H	H	NO_2	445[28]	446	+1	441	−4	
2.5. H	H	$(NO_2)_2$	480	481	+1	472	−8	
2.6. H	Bz	H	400[26]	—	—	—	—	6.45[26]
2.7. H	Bz	Cl	410[26]	401	−9	409	−1	
2.8. H	Bz	Br	413	410	−3	410	−3	
2.9. H	Bz	NO_2	457[26]	461	+4	459	+2	
2.10 H	Bz	$(NO_2)_2$	496[26]	498	+2	495	−1	
2.11 Bz	Bz	H	404[26]	—	—	—	—	6.70[26]
2.12 Bz	Bz	Cl	414[26]	405	−9	413	−1	
2.13 Bz	Bz	Br	418	415	−3	415	−3	
2.14 Bz	Bz	NO_2	470[26]	466	−4	466	−4	
2.15 Bz	Bz	$(NO_2)_2$	500[26]	504	+4	504	+4	
2.16 Me	Bz	H	406	—	—	—	—	6.82
2.17 Me	Bz	Cl	419	415	−4	415	−4	
2.18 Me	Bz	Br	420	417	−3	417	−3	
2.19 Me	Bz	NO_2	473	469	−4	469	−4	
2.20 Me	Bz	$(NO_2)_2$	508	507	−1	508	0	
2.21 Me	Me	H	407[15]	—	—	—	—	6.88[15]
2.22 Me	Me	Cl	417[14]	417	—	416	−1	
2.23 Me	Me	Br	419[14]	418	−1	418	−1	
2.24 Me	Me	NO_2	475[15]	470	−5	471	−4	
2.25 Me	Me	$(NO_2)_2$	515[15]	509	−6	511	−4	
2.26 H	*n*-Pr	H	410	—	—	—	—	7.06
2.27 H	*n*-Pr	Cl	417	419	+2	420	+3	
2.28 H	*n*-Pr	Br	418	421	+3	421	+3	
2.29 H	*n*-Pr	NO_2	478	474	−4	476	−2	
2.30 H	*n*-Pr	$(NO_2)_2$	518	513	−5	517	−1	
2.31 H	Ph	H	412[26]	—	—	—	—	7.18[26]
2.32 H	Ph	Cl	419[26]	413	−6	422	+3	
2.33 H	Ph	Br	426	423	−3	424	−2	
2.34 H	Ph	NO_2	478[26]	477	−1	480	+2	
2.35 H	Ph	$(NO_2)_2$	517[26]	516	−1	521	+4	
2.36 Ph	Ph	H	413[26]	—	—	—	—	7.24[26]
2.37 Ph	Ph	Cl	419[26]	414	−5	423	+4	
2.38 Ph	Ph	Br	428	424	−4	425	−3	
2.39 Ph	Ph	NO_2	480[26]	478	−2	482	+2	
2.40 Ph	Ph	$(NO_2)_2$	520[26]	518	−2	524	+4	
2.41 Et	Et	H	415[15]	—	—	—	—	7.35[15]
2.42 Et	Et	Cl	420[14]	425	+5	425	+5	
2.43 Et	Et	Br	422[15]	426	+4	426	+4	
2.44 Et	Et	NO_2	483[15]	481	−2	485	+2	
2.45 Et	Et	$(NO_2)_2$	530[15]	521	−9	529	−1	
2.46 *n*-Pr	*n*-Pr	H	420	—	—	—	—	7.64
2.47 *n*-Pr	*n*-Pr	Cl	430	430	—	431	+1	
2.48 *n*-Pr	*n*-Pr	Br	435	432	−3	432	0	
2.49 *n*-Pr	*n*-Pr	NO_2	490	487	−3	494	+4	
2.50 *n*-Pr	*n*-Pr	$(NO_2)_2$	531	529	−2	540	+9	

The compounds from table 2 were obtained by conventional diazotisation and coupling techniques.[30]

The electronic spectra were recorded on a Specord — Carl Zeiss apparatus. All the spectra were recorded in ethanol.

REFERENCES

[1] D. Merkel, Zwischenprodukte für Azofarbstoffe. MBI. Chem. Ges. DDR, **32**, 98 (1985).

[2] H. Pinnow, Werksgeschichte Farbenfabriken vorm. F. Bayer & Co. München 1938, p. **45.**

[3] A. Meyer, *Phot. Sci. Engng.*, **18**, 540 (1974) : *Chimia*, **30**, 547 (1976).

[4] W. T. Hanson, *J. phot. Sci.*, **25**, 189 (1977).

[5] R. A. Michitarov, M. M. Orešin, T. A. Gordina and A. M. Platoskin, *Usp. nauon. fotogr.*, **21**, 5 (1978).

[6] J. Marx, J. Epperlein and F. Walkow, *J. Signalaufzeichnungsmater*, **11**, 83 (1983) ; Epperlein J., H.G.O. Becker, F. Walkow and J. Marx, *J. Signalaufzeichnungsmater*, **11**, 403 (1983).

[7] W. N. Hartley, *J. Chem. Soc.*, **51**, 152 (1887).

[8] L. M. Jagupolskij et al., *Z. obšč. chim.*, **33**, 2301 (1963 ; **35**, 1252 (1965) ; **37**, 2101 (1967) ; *Ukr. chim. Z.*, **31**, 1301 (1965) ; **41**, 61 (1975).

[9] I. Bridgeman and A. Peters, *J. Soc. Dyers Colour*, **86**, 519 (1970).

[10] E. Sawicki, *J. Org. Chem.*, **22**, 323 (1957).

[11] J. B. Dickey et al., *J. Org. Chem.*, **24**, 187 (1959); *J. Soc. Dyers Colour*, **74**, 123 (1958); *Amer. Dyest. Rep.*, **1965**, 596.

[12] G. Hallas et al., *J. Chem. Soc.* (B) **1971**, 793 ; *J. Soc. Dyers Colour.*, **90**, 121 (1974) ; **93**, 284 (1977).

[13] W. Thiel, R. Mayer, E.-A. Jauner, H. Modrow and H. Dost, *J. prakt. Chem.*, **328**, 497 (1986).

[14] H. Mustroph, *Z. Chem.*, **25**, 385 (1985) ; *J. prakt. Chem.*, **329**, 157 (1987) ; C. Haessner and H. Mustroph, *J. prakt. Chem.*, **328**, 113 (1986).

[15] H. Mustroph, J. Epperlein and D. Ebert, *J. Signalaufzeichnungsmat.*, **5**, 439 (1977) ; H. Mustroph and J. Epperlein, *J. prakt. Chem.*, **323**, 755 (1981).

[16] J. Kroner and H. Bock, *Chem. Ber.*, **101**, 922 (1968).

[17] J. Fabian and H. Hartmann, "Light Absorption of Organic Colorants", Springer-Verlag, Berlin-Heidelberg-Wien 1980, Chapter VII "Azo Dyes" and the literature cited therein.

[18] J. Griffiths, *Dyes and Pigments*, **3**, 211 (1982).

[19] J. Fabian, *Chimia*, **32**, 323 (1978).

[20] H. Mustroph and J. Epperlein, *Z. phys. Chem. (Leipzig)*, **261**, 158 (1980).

[21] J. Griffiths, "Recent Developments in the Colour and Constitution of Organic Dyes", *Rev. Progr. Coloration*, **11**, 37 (1981).

[22] S. Dähne and S. Kulpe, *J. Prakt. Chem.*, **320**, 395 (1978).

[23] S. Dähne, *Science (Washington)*, **199**, 1163 (1978) ; *Wiss. Ztschr. TU Dresden*, **29**, 101 (1980) ; *Z. Chem.*, **21**, 58 (1981).

[24] J. Griffiths "Colours and Constitution of Organic Molecules", Academic Press, London 1976.

[25] J. Griffiths, "The Historical Development of Modern Colour and Constitution Theory", in *Rev. Progr. Coloration*, **14**, 21 (1981).

[26] J. Epperlein and B. Blau, *Z. Chem.*, **27**, 75 (1987).

[27] H. Mustroph and J. Epperlein, *J. prakt. Chem.*, **322**, 49 (1980).

[28] J. Havlik and C. Csunderlik, *Rev. Roumaine Chim.*, **28**, 903 (1983).

[29] M. Iovu and St. Radu, *Rev. Roumaine Chim.*, **32**, 509 (1987).

[30] H. E. Fierz-David and L. Blangey, "Grundlegende Operazionen der Farbenchemie", Wien, Springer-Verlag, 1943, p. 220.

[31] P. F. Gordon and P. Gregory, "Organic Chemistry in Colour", Springer-Verlag, Berlin, 1983.

Revue Roumaine de Chimie, **33**, *5*, 483–488 (1988)

MOLECULAR COMPOUNDS WITH SOME ALKYL ARYL ETHERS. II*

HYDROGEN BOND COMPLEXES

ELIZA-MANUELA VASILESCU[a], MIRCEA IOVU[b] and DUMITRU SĂNDULESCU[a]
[a]Petroleum and Gas Institute, Ploiești, Blvd. București, no. 39, Romania
[b]Faculty of Pharmacy, Bucharest, str. Traian Vuia no. 6, Romania

Received March 2, 1987

We investigated the capacity of some alkyl aryl ethers to accept protons by the formation of hydrogen bond complexes in comparison with the electron-donating properties of the same compounds, in the CT complexes. The correlation between the two phenomena is proved experimentally by linear relationships between ionization potentials I_D (UV spectra of CT complexes) and ν_{OH} shifts (IR spectra of hydrogen bond complexes).

1. INTRODUCTION

Alkyl aryl ethers can establish two simultaneous equilibria with proton donors: one by hydrogen bonds with participation of unshared electrons of oxygen atom (OH ... O) and another by hydrogen bonds with participation of π electrons of one of the aromatic rings (OH ... π).

Seidel and his co-workers[1,2] report that the OH ... O bonds are stronger than OH ... π bonds; for example, 20–25% phenol forms hydrogen bonds with aromatic nucleus of anisol and 70–75% phenol participates in the formation of hydrogen bonds with oxygen atom; $K_{OH\ldots\pi}/K_{OH\ldots O}$ ratio is 1/3–1/4.

Several authors [3-7] also reported that the strength of hydrogen bonds is a function of the number and nature of conformational effects. Pola and his co-workers [8] established that the polarizability influences the formation of OH ... O bonds. Some empirical relationships between the acidity constant of proton donor, pK_a, and the value of shifts of OH band, $\Delta\nu$, in IR spectra of acceptors, or between ΔH characteristic of the complex and the value $\Delta\nu$ have been reported. [9-11]

---

* Part. I in ref. 18

2. EXPERIMENTAL

a) The ethers whose IR basicity was measured in this work, were prepared in Organic Chemistry Laboratory, Pharmacy Department, IMF Bucharest.[12,14] The alkyl aryl ethers (AAE) which have been studied belong to the following groups :

A.

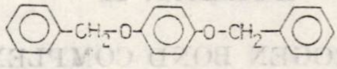

B.

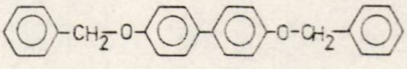

C.

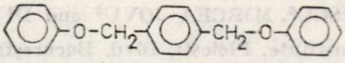

D.

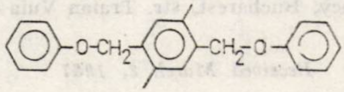

In each group, the compounds differ by the position and number of the substituents. Their purity and identity was checked and confirmed by the melting point, the elemental analysis as well as IR,[15] UV[16] and ^1H-NMR spectra. [17]

We used phenol as proton donor ; the solutions were prepared in CCl_4 (spectral purity) with concentrations (0.03 mol/L) under the limit of self-association.

b) The formation of hydrogen bonds was followed by the magnitude of the shift of the band ν_{OH} of phenol in the presence of different AAE, in the 3700—3200 cm^{-1} region of IR spectra.

The IR spectra were recorded on a 71-IR spectrophotometer (Carl Zeiss Jena, DDR) with accuracy of ± 3 cm^{-1}, in a 0.1 cm thick cell. The compensation was made with a solution of phenol in CCl_4 ; the concentration of phenol was the same in the two cells.

c) As we pointed out above, compounds similar to AAE can participate as proton acceptors at two equilibria by hydrogen bods. [1,2] The IR spectrum of (phenol + AAE) solution presented in the region 3700—3200 cm^{-1} three absorption bands ; a strong, sharp band with constant position (3609 cm^{-1}) and two other broad sharp bands, with variable positions at smaller wavenumbers. By comparison with the IR spectra of solutions in CCl_4 of (1. phenol ; 2. phenol + benzene ; 3. phenol + amylic alcohol) the three bands are assigned as follows :

I	3609 cm^{-1}	ν_{OH} phenol unassociated
II	3561—3536 cm^{-1}	$-OH \ldots \pi$ bond (small intensity)
III	3473—3437 cm^{-1}	$-OH \ldots O$ bond (larger intensity)

The existence of three aromatic nuclei in the molecules of AAE (the central ring with another substitution toward the terminal (rings) should have given the splitting the band assigned to the OH . . . π bonds which is not the case.

It is possible that the band characteristic of the complex formed with the central ring was not observed at the used concentrations ; the formation of this complex is not favoured by the presence of two bulky substituents, which hinder the approach of the molecule of phenol. Also, the participation of AAE's to the OH ... O equilibrium is more important then their participation to the OH ... π echilibrium.

3. RESULTS AND DISCUSSION

a) The influence of the structure of proton acceptor

Tables 1 and 2 give the shifts of ν_{OH} band of phenol. The number and the nature of substituents affect the strength of the hydrogen bond, when the etheric oxygen is adjacent to aromatic ring. On the contrary, the ν_{OH} shifts of phenol with different ethers of A group are the same, since the electronic effects of the substituents are not transmitted through a methylene group. The changes in the position of ν_{C-O-C} band in the IR spectra are the same,[15] contrary to the shifts in ^1H-NMR spectra[17] and contrary to the positions of CT bands[18] which are affected by the substitution even for the A group ethers.

Table 1

The ν_{OH} shifts and ΔH^0 values of phenols with different alkyl aryl esthers (AAE)

Ether *	(cm^{-1}) OH... O	OH ... π	ΔH⁰(kcal/mol) ± 0.5 kcal/mol	
			OH... O	OH... π
$A_1(-)$	172	64	3.40	1.70
$A_2(m)$	172	67		
$A_3(p)$	172	66		
$A_4(o, o)$	172	73		
$B_1(-)$	140	—	2.90	
$C_1(-)$	158	62	3.20	1.60
$D_2(pCl)$	148	56	3.00	1.50
$D_3(pNO_2)$	136	48	2.80	1.40
$D_4(o, m)$	170	70		
$D_5(o, p)$	172	70		
$D_1(-)$	159	62	3.20	1.60
$D_2(m)$	167	67	3.30	1.70
$D_3(o, m)$	170	113	3.40	1.80
$D_4(o, p)$	173	71	3.40	1.80
$D_5(m, p)$	176	72	3.50	1.80
$D_6(m, m)$	176	72		

* — The methyl substituents are situated on the terminal aromatic rings in the indicated positions.

Table 2

The ν_{OH} shifts of solutions of phenol with different ethers as a function of conjugation

	Ether	$\Delta\nu_{OH...O}$ (cm^{-1})
M_1	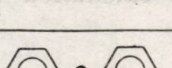	123
B_1	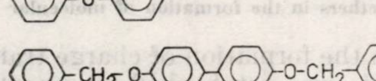	140
C_1	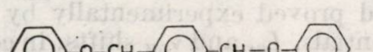	162
A_1	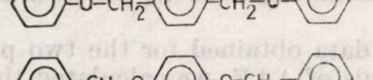	177
M_2	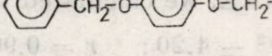	233
M_3	$C_5H_{11}-O-C_5H_{11}$	292

Generally, the position of the substituents has no influence upon $\Delta\nu$ values; an exception is observed for the *ortho*-substituents, for ether D_5 (*meta*, *para* CH_3) and D_6 (*meta*, *meta* CH_3) is 176 cm^{-1} and for D_3 (*ortho*, *ortho* CH_3) is 170 cm^{-1}. The difference for the compounds with two substituents adjoining oxygen, signaled by different authors[6,19] is ascribed to steric hindrance effects.

The value of ν_{OH} shifts are affected by the electronic effects of substituents, expressed by Hammett's constant. Thus, the methyl groups ($\tau = -0.169$) have increasing effects upon $\Delta\nu$, and chlorine atom ($\tau = 0.226$) or nitro group ($\tau = 0.778$) give a lower shift. We pointed out the discrepancy for the value of $\Delta\nu$ shifts in the case of methoxy group. This exception might be explained by the $p-\pi$ conjugation, which gives less freedom to unshared electrons of oxygen in comparison with $\Delta\nu$ shifts for unsubstitued ethers listed in Table 2. These values indicate the connection between $p-\pi$ conjugation and the number of oxygen atoms and the number of adjacent benzene rings. We give in table 2 also the $\Delta\nu$ shifts for aromatic or aliphatic ethers, M_1-M_3. The experimental values for alkyl aryl ethers, AAE, are situated between the shifts of symmetric ethers as expected.

b) The calculation of the enthalpy changes

The low solubillity of AAE in organic solvents does not allow the experimental determination of equilibrium constant for hydrogen bond complexes, and consequently not even the determination of thermodynamic data. We used the correlation proposed by Badger-Bauer[11] for related compounds:

$$-\Delta H = 0.016\,\Delta\nu + 0.6 \qquad \pm 0.5 \text{ kcal} \qquad (1)$$

This equation is checked for systems such as phenol and aromatic hydrocarbons by Szczepaniak[5] and Basila[6].

We calculated the values $-\Delta H$, with experimental shifts $\Delta\nu$, for AAE (OH...O bands), as well as for other compounds, for which the ΔH values were previously reported.[5,6] The calculated values ΔH agree with those experimentally found (Table 1).

c) Participation of alkyl aryl ethers in the formation of molecular complexes

The correlation between the formation of charge transfer complexes, which are related phenomena, was established by quantum calculations of Puranik and Kumar,[20] and proved experimentally by linear relationships between ionization potentials, I_D, and ν_{OH} shifts, in complex systems with alkenes or arenes.[5,7]

With the experimental data obtained for the two properties, specific to the molecular compounds of AAE, we calculated the equation (2):

$$I_{D(eV)} = 0.65\,(\nu_E/\Delta\nu)^{1/2} - 4.20\,; \quad r = 0.90 \qquad (2)$$

The ionization potentials (b) were calculated from the values of transition energies of charge transfer complexes, reported in the previous paper.[18]

Equation (3) calculated from the reported data of Szczepaniak[5] for aromatic hydrocarbons is similar to the equation (2).

$$I_{D(\mathrm{eV})} = 0.41(\nu_F\Delta\nu)^{1/2} - 6.01\,; \qquad r = 0.99 \qquad (3)$$

From this fact, we can draw the conclusion that in the formation of molecular compounds, AAE's behave in the same way as methyl benzenes.

Figure 1 shows the data used for calculation of the two equations.

Fig. 1. — The correlation between I_D values of CT bands and $\Delta\nu F/$: X — methyl benzenes ; o — AAE ; ⊙ — anisol.

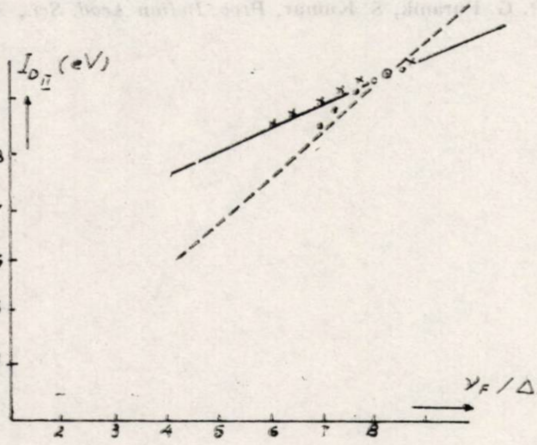

The bigger slope for equation (2) might be explained by the increase of the donor capacity of aromatic nucleus by the substitution of a hydrogen with methoxy group. The same difference in the electron accepting properties for two compounds corresponds to larger electron donating properties of ethers than those of aromatic hydrocarbons.

The related mechanism of formation of molecular compounds by AAE's either by hydrogen bond or by charge tansfer, is also proved by the influence of steric hindrance of the substituents ; the strength of the two types of complexes is decreased by the *ortho* substituents, adjoining methoxy group.

The value determined for ΔH, for the two kinds of complexes, points out a more significant participation of AAE's in formation of the CT complexes than their participation in the formation of hydrogen bond complexes.

REFERENCES

[1] H. Seidel, C. Ritter and J. Fruwert, *Spectrochim. Acta,* **32 A,** 705 (1976).
[2] H. Seidel, C. Bayer and J. Fruwert, *Z. Phys. Chem. (Leipzig).* **259,** 629 (1978).
[3] Z. Yoshida, *J. Amer. Chem. Soc.,* **87,** 1467 (1965).
[4] Z. Yoshida, *J. Amer. Chem. Soc.,* **88,** 4019 (1966).
[5] K. Szczepaniak, *Acta Phys. Pol.,* **36,** 421 (1968).
[6] M. Basila, *J. Amer. Chem. Soc.,* **87,** 1665 (1965).
[7] J. P. Seguin, *Adv. Mol. Relaxation Interact. Processes,* **11,** 143 (1977).
[8] J. Pola, and M. Jakoulikova, *Coll. Czech. Chem. Commun.,* **43,** 760 (1978).

[9] R. J. Abraham, *Mol. Phys.*, **4**, 399 (1961).

[10] Z. Yoshida, *Bull. Soc. Japan.*, **42**, 3254 (1969).

[11] R. M. Badger, and J. M. Bauer, *J. Amer. Chem. Soc.*, **84**, 3817 (1962).

[12] M. Iovu and F. Ispas, *Rev. Chim.*, *(București)*, **30**, 841 (1979).

[13] M. Iovu, *Rev. Roumaine Chim.*, **17**, 1261 (1972).

[14] M. Iovu, *Rev. Roumaine Chim.*, **16**, 1223 (1971).

[15] M. Iovu and E. M. Vasilescu, *Rev. Roumaine Chim.*, **27**. 629 (1982).

[16] E. M. Vasilescu, Ph. D. Thesis, Petroleum and Gas Institute, Ploiești.

[17] M. Iovu, F. Chirleu and E. M. Vasilescu, *Rev. Roumaine Chim.*, **25**, 1383 (1980).

[18] D. Săndulescu and E. M. Vasilescu, *Rev. Roumaine Chim.*, **31**, 605 (1986) (Part I).

[19] Z. Yoshida, *Bull. Soc. Japan.*, **42**, 3263 (1969).

[20] P. G. Puranik, S. Kumar, *Proc. Indian Acad. Sci.*, **A 58**, 327 (1963).

Revue Roumaine de Chimie, **33**, *5*, 489–524 (1988)

A STUDY OF THE STABILITY OF REALISTIC MODELS OF OSCILLATING CHEMICAL REACTIONS BY USING CONCEPTS DERIVED FROM THE RULES FOR FLOW GRAPHS

DAN CARTIANU

Center for Physical Chemistry, Splaiul Independenţei 202, Bucureşti, Romania

Received February 3, 1987

A computational flow-graph-theoretical method is devised for determining the necessary condition for realistic polynomial chemical kinetic models to exhibit oscillations or multiple steady states. The valuations of the graph stand for the elements of the linearized matrix of the kinetic equations or the products of the stoechiometric and reaction order matrices. It is proved that the Routh-Hurwitz linearized stability criterion leads to a necessary condition for instability: the presence of cycles in this flow graph. By decomposing the steady states in a basis of extreme steady states a more detailed description is given of the instability for all kinetic constants, the instability being determined by the presence of cycles on the diagram of the extreme steady state with greatest weight. Algorithms for this decomposition as well as for finding all the cycles in a digraph are devised and applied to several realistic kinetic models of oscillating chemical reactions. The diagrammatic representation of the Hurwitz determinants and its connection with the rules of solving systems of linear algebraic equations diagrammatically by flow graphs permits a study of the sensitivity of the stability property of kinetic systems.

1. INTRODUCTION

The present paper elaborates a computational graph-theoretical method for determining the necessary conditions for a realistic chemical model to oscillate or to exhibit multiple steady states.

Firstly a flow graph (i.e. a valuated directed graph) is associated to a polynomial kinetic model, the valuations standing for the elements of the linearized kinetic matrix or the products of the stoechiometric and reaction order matrices. It is demonstrated that the Routh-Hurwitz linearized stability criterion leads to a necessary condition for instability: the presence of cycles in this flow graph. A more precise description of the stability property for all kinetic constants is provided by a decomposition of the steady states according to a set of extreme steady states. The instability for a certain set of kinetic parameters is determined by the presence of cycles in the extreme steady state with greatest weight in this decomposition. Computer algorithms both for the determination of the extremal steady states and for the cycles in directed graphs are elaborated and are illustrated on several realistic models of oscillating reactions,[1-3] the Oregonator model, the Field-Körös-Noyes model, the modified Lotka-Volterra model, the modified Oregonator model, the reversible Brusselator model (all for the Belousov-Zhabotinskii reaction), the Lotka-Volterra type model of the hypercycle, and the kinetic model of the Bray-Liebhafsky reaction. The connection is established between the method of derivation of the necessary linearized stability criterion and the demonstration of the rules of Mason and Coates for flow graphs.

2. THE REPRESENTATION BY CONVEX PARAMETERS OF THE STEADY STATES OF THE POLYNOMIAL KINETIC MODELS

A kinetic model with polynomial kinetics is described by the system of differential equations

$$\frac{dc}{\mathrm{d}t} = \nu \cdot \mathbf{v}, \quad v_j = k_j \prod_{i=1}^{n} c_i^{\varkappa_{ij}}, \varkappa_{ij} \in \{1, 2\} \tag{2.1}$$

where $\varkappa$ is the matrix of the reaction orders and ν is the matrix of the stoechiometric coefficients. The steady state of this stoechiometric system is given by the equation

$$\nu \cdot \mathbf{v}^\circ(\mathbf{c}^\circ, \mathbf{k}) = 0, \tag{2.2}$$

and is represented in terms of the convex parameters $\mathbf{j}$ and of the matrix $\mathbf{E}$ by the equation

$$\mathbf{v}^\circ = \mathbf{E} \cdot \mathbf{j} \tag{2.3}$$

The set of all steady states $\mathbf{v}^\circ$ or currents is $\mathscr{C}_\nu = \{\mathbf{v}^\circ \in \bar{R}_+^r \mid \nu \cdot \mathbf{v}^\circ = 0\}$ and can be expressed in a barycentric representation $\mathscr{C}_\nu = \{\mathbf{E} \cdot \mathbf{j} \mid \mathbf{j} \in \bar{R}_+^f\}$ where $\mathbf{E}$ is a $r \times f$ matrix. They must satisfy $\mathbf{v}^\circ \geqslant 0$.

The basis of steady states or currents is composed of the column vectors E_i of the matrix $\mathbf{E}$, called extreme currents. The extreme currents satisfy the equation derived from (2.2) and (2.3) :

$$\nu \cdot \mathbf{E} = 0 \tag{2.4}$$

Thus the basis of steady states is in the kernel of the stoechiometric matrix. Which one of the steady states is realized is determined by the kinetic constants and the initial species concentrations. The kinetic constants can be modified by using equivalent species e.g. for the malonic acid.

A stoechiometric kinetic system is denoted by $(\nu, \varkappa)$ and an extreme stoechiometric system by $(\nu^{(i)}, \varkappa)$ where :

$$\nu^{(i)} = \nu \cdot (\mathrm{diag}\ E_i) \tag{2.5}$$

$(\mathrm{diag}\ E_i)$ being the matrix which has on the diagonal the elements of the vector E_i and otherwise 0.

The matrix of the kinetic equation (2.1) linearized around the steady state (current) $\mathbf{v}^\circ$ is :

$$\mathbf{V} = \nu \cdot \varkappa \tag{2.6}$$

An asymptotic stability criterion for the stoechiometric system $(\nu, \varkappa)$ is that the extreme systems $(\nu^{(i)}, \varkappa)$ satisfy the condition that all the eigenvalues of the matrix $\nu^{(i)}\varkappa^T + \varkappa \cdot \nu^{(i)T}$ be $\leqslant 0$, where T denotes the transpose matrix.

The stable currents $\mathbf{v}^\circ$ constitute a subpolyhedron in the polyhedron spanned by the extreme currents.

A useful mathematical relation is the orthogonality of the degrees of advancement of the reactions ξ on the currents $\mathbf{v}^\circ$:

$$\xi^T \cdot \mathbf{v}^\circ = 0, \tag{2.7}$$

equivalent with the theorem of Tellegen of orthogonality between the tensions and currents and which expresses the topological duality of the current cycles and of the voltage cocyles.

Be q the lowest positive integer such that $q|\nu_{ij}| \geqslant \varkappa_{ij}$ for all i, j. The reaction R_j can be written :

$$\sum_{i=1}^{n} [\varkappa_{ij} H(\nu_{ij}) - q\nu_{ij} H(-\nu_{ij})]\, X_i \to \sum_{i=1}^{n} [\varkappa_{ij} H(\nu_{ij}) + q\nu_{ij} H(\nu_{ij})] X_i, \tag{2.8}$$

where H is the Heaviside function : $H(x) = 1$ if $x \geqslant 0$ and $H(x) = 0$ if $x < 0$.

By using e.g. the matrices :

$$\nu = \begin{pmatrix} 1 & -1 & 1 & -2 & 0 & -1 & 1 & -1 & 2 & 0 \\ -1 & -1 & 0 & 0 & 1 & 1 & 1 & 0 & 0 & -1 \\ 0 & 0 & 2 & 0 & -2 & 0 & 0 & -2 & 0 & 2 \end{pmatrix}, \tag{2.9}$$

$$\varkappa = \begin{pmatrix} 0 & 1 & 1 & 2 & 0 & 1 & 0 & 2 & 0 & 0 \\ 1 & 1 & 0 & 0 & 0 & 0 & 0 & 0 & 0 & 1 \\ 0 & 0 & 0 & 0 & 1 & 0 & 0 & 1 & 0 & 0 \end{pmatrix}$$

corresponding to the reversible Oregonator model[5] where the rows correspond to the species $X_1 = X = \mathrm{HBrO_2}$, $X_2 = Y = \mathrm{Br^-}$, $X_3 = Z = 2\mathrm{Ce(IV)}$, and the first half of the columns are the direct reactions and the last half the inverse reactions, one obtains the chemical notation of the reactions of the Oregonator model or pseudoreactions expressing only the relation between the intermediate species :

$$R_1 : \quad \mathrm{Y} \to \mathrm{X}, \quad R_2 : \ \mathrm{X} + \mathrm{Y} \to, \quad R_3 : \ \mathrm{X} \to 2\mathrm{X} + 2\mathrm{Z}, \quad R_4 : 2\mathrm{X} \to,$$

$$\mathrm{R}_5 : \ 2\mathrm{Z} \to \mathrm{Y}, \tag{2.10}$$

The reaction R_j will be represented diagrammatically as an arrow from the reactants to the products. The total number of barbs or feathers of the arrow R_j at the point X_i will be the coefficient of X_i in (2.8). $\varkappa_{ij}$ feathers will be drawn to the left and the remaining to the right, i.e. $(q|\nu_{ij}| - \varkappa_{ij})\, H(-\nu_{ij})$. The matrices ν and $\varkappa$ can be read directly from such a current diagram.

If ν satisfies the relation

$$\nu \cdot \mathbf{e} = 0 \tag{2.11}$$

$\mathbf{e} = (1,1, \ldots, 1)^T$, the diagram represents a possible steady state current and the relative quantity of the reactant X_i produced (respectively consumed) by the reaction R_j in this steady state is equal to the number of barbs (respectively feathers) on the arrow that represents the reaction R_j. When ν satisfies $\nu \cdot \mathbf{e} = 0$, ν is called the stoechiometric current matrix. The algorithm which generates **E** is such that each $\nu^{(i)}$ is a stoechiometric current matrix, hence the extremal currents $(\nu^{(i)}, \varkappa)$ can be represented by f extreme current diagrams.

3. FLOW GRAPHS ASSOCIATED WITH THE POLYNOMIAL KINETIC MODELS

We will associate a flow graph[6] to the reaction system in the following way. We distinguish by σ if a certain node is at the beginning $(\sigma = -1)$ or at the tail $(\sigma = 1)$ of a directed arrow in the digraph. We define $f : T \to \bar{R}_+$ by

$$f(t) = \sigma \nu_{ij} \tag{3.1}$$

where T is the set of the ends of the edges of the digraph and i, j are chosen so that R_j is the reaction associated with the respective edge and X_i is the species associated with the respective node on the edge. We notice that $f(t) \geqslant 0$ wherever the species X_i is placed. In order to extend the definition of f to autocatalytic reactions as e.g. $R_1 : X_1 + X_2 \to 2X_1 + X_3$, for arbitrary α, we associate $\nu_{11} + \alpha$ with X_1 at the right of the edge and α with X_1 at the left. The graph valuation will be :

$$f_{ma}(t) = \alpha_{ij} + H(\sigma \nu_{ij})\, \sigma \nu_{ij} \tag{3.2}$$

where $\alpha_{ij} \geqslant 0$ is arbitrary and $H(x)$ is Heaviside's function. We will choose α_{ij} equal to the stoechiometry of X_i on the side of the reaction where $\sigma\nu_{ij} < 0$, and $\alpha_{ij} + \sigma\nu_{ij}$ will be the stoechiometry of X_i on the opposite side.

A stoechiometric flow graph with power law kinetics and autocatalysis is described by the function $f_{pl} : T \to R^2$ defined by

$$f_{pl}(t) = (\alpha_{ij} + H(\sigma\nu_{ij})\sigma\nu_{ij},\ H(-\sigma)\varkappa_{ij}) \tag{3.3}$$

For a stoechiometric graph we define :

$$f_v(t) = (f_{ma}(t),\ \ H(-\sigma)v_j(X, k)), \tag{3.4}$$

where v_j is the rate of reaction R_j.

The linearized stability problem depends on $\mathbf{v}(\mathbf{X}, \boldsymbol{\varkappa})$ only through first order derivatives evaluated in the steady state hence leads to a flow graph with the valuation

$$f_{gl}(t) = (f_{ma}(t),\quad H(-\sigma)\varkappa_{ij}(p)) \tag{3.5}$$

In the representation of the reaction diagram described above the number of barbs of the arrow is

$$B(X_i, A_j) = \alpha_{ij} + H(\nu_{ij})\nu_{ij} \tag{3.6}$$

and the number of feathers of the arrow is

$$T(X_i, A_j) = \alpha_{ij} - H(-\nu_{ij})\nu_{ij} \tag{3.7}$$

from which

$$L(X_i, A_j) = \varkappa_{ij} \tag{3.8}$$

are drawn to the left.

The stoechiometric coefficient of X_i is the total number of feathers and the order of the kinetics of X_i is equal to the number of feathers to the left side of the arrow if α_{ij} is adequately chosen in the autocatalytic case and if $\alpha_{ij} = 0$ when R_j is not autocatalytic. The reaction stoechiometries can always be multipled by a positive constant such that $T \geqslant L$, or $|\nu_{ij}| > \varkappa_{ij}$ for every i, j.

For the Oregonator model the reaction diagram is drawn in Fig. 1.

In the flow graph of the currents the matrix $\mathbf{E}$ is an incidence matrix edges (reactions)-sections (extreme currents) just as one can establish incidence matrices edges (reactions) — nodes (species) and edges (reactions)-cycles.

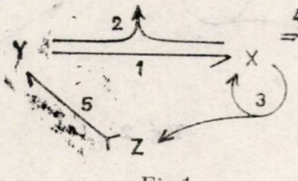

Fig. 1

We will now give a precise meaning to the notion of current diagram which will be a reaction diagram with the property

$$\sum_{j=1}^{r} B(X_i,\ A_j) = \sum_{j=1}^{r} T(X_i, A_j) \tag{3.9}$$

By using (3.6—3.8) in (3.9) results

$$\sum_{j=1}^{r} \nu_{ij} = 0 \tag{3.10}$$

hence $\nu \cdot \mathbf{e} = 0$. Thus $\mathbf{e}$ is a steady-state vector iff the reaction diagram is a current diagram.

The stoechiometric current matrix is defined by

$$\nu^* = \nu \cdot \operatorname{diag} \mathbf{v}^\circ \tag{3.11}$$

From $\nu \cdot \mathbf{v}^\circ = 0$ one derives $\nu^* \cdot \mathbf{e} = 0$ so that every diagram with the stoechiometric matrix ν^* has the steady state $\mathbf{e}$. In the study of a current in a reaction diagram one can assume that $\mathbf{e} = \mathbf{E} \cdot \mathbf{j}$ and that $\nu \cdot \mathbf{e} = 0$.

The extreme current diagram is determined by $\nu^* = \nu \cdot \operatorname{diag}(E_i)$. The current diagrams for the Oregonator model are respectively E^1 for $\mathbf{j} = (1,0)^T$ and E^2 for $\mathbf{j} = (0,1)^T$ and are represented in Fig. 2. Their sum corresponding to $\mathbf{j} = (1,1)^T$ is represented in Fig. 3.

One defines the matrix diagrams of the currents to represent the matrix of the linearized kinetic system:

$$-\mathbf{V}(\mathbf{j}) \operatorname{diag} \mathbf{h}, \text{ where } \mathbf{h} = 1/\mathbf{X} \text{ and } \mathbf{V}(\mathbf{j}) = -\nu \cdot (\operatorname{diag} \mathbf{E} \cdot \mathbf{j})\varkappa^T \tag{3.12}$$

For the current diagrams $\mathbf{v} = \mathbf{E} \cdot \mathbf{j}$ hence:

$$-\mathbf{V}(\mathbf{j}) = \nu^* \cdot \varkappa^T \tag{3.13}$$

The rules for the graphical representation of $-\mathbf{V}(\mathbf{j})$ are the following:
1. The arrow $X_j \to X_i$ represents the sign of $-V_{ij}(\mathbf{j})$ when $V_{ij}(\mathbf{j}) \neq 0$. The number of barbs of the arrow corresponds to $|V_{ij}(\mathbf{j})|$.

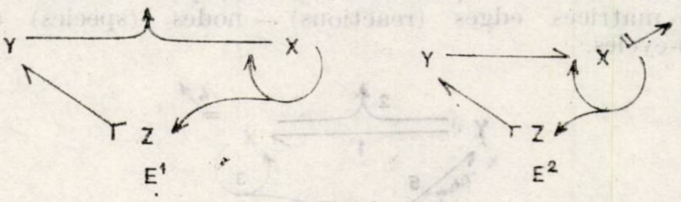

Fig. 2

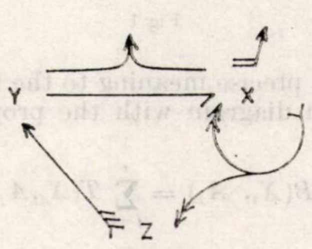

Fig. 3

2. In place of the point that stands for species X_i one writes the symbol which represents the inverse of the steady state concentration of X_i in the vector $\mathbf{h}$.

3. The matrix reaction diagrams have pointed loops at almost every species. These are omitted and one writes in front of the parameter chosen at step two the value of the diagonal element of $\mathbf{V}(\mathbf{j})$.

The current matrix diagrams of the Oregonator model are drawn in Fig. 4.

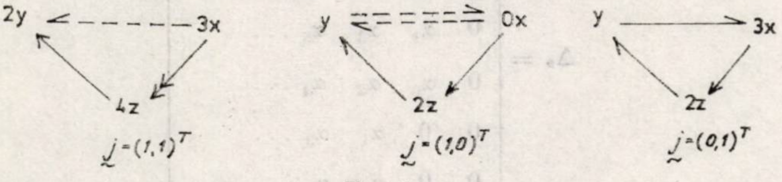
2y
3x
4z
$\underset{\sim}{j} = (1,1)^T$
y
0x
2z
$\underset{\sim}{j} = (1,0)^T$
y
3x
2z
$\underset{\sim}{j} = (0,1)^T$

Fig. 4

The pointed lines stand for inhibition and the full lines for promotion of the species. The coefficient $V_{ii}(\mathbf{j})$ is given by :

$$V_{ii}(\mathbf{j}) = \sum_{k=1}^{r} (T(X_i, A_k) - B(X_i, A_k))L(X_i, A_k) \tag{3.14}$$

The terms BL are different from zero iff there is autocatalysis ($B(X_i, A_k) \neq 0$) and have a destabilization effect.

When $\nu_{ij} > 0$, R_k contributes to $(\nu \cdot \varkappa^T)_{ij}$ with

$$b_{ijk} = \nu_{ik}\varkappa_{jk} = L(X_j, A_k)B(X_i, A_k) \tag{3.15}$$

This quantity is represented by a full line with b_{ijk} barbs directed from the species X_j of the reaction R_k to the product X_i of R_k. When $\nu_{ij} < 0$, R_k contributes with :

$$b_{\bar{i}jk} = \nu_{ik}\varkappa_{jk} = -L(X_j, A_k)T(X_i, A_k), \tag{3.16}$$

which is represented by a pointed arrow with $b_{\bar{i}jk}$ barbs directed from the reactant X_j to the reactant X_i of R_k.

On the current matrix diagrams one can make graphical simplifications (the algebraic sum of the arrows and the combination of 1-cycles with the coefficients).

4. THE ROUTH-HURWITZ CRITERION FOR THE LINEARIZED STABILITY OF THE SYSTEMS OF KINETIC DIFFERENTIAL EQUATIONS AND ITS REPRESENTATION THROUGH HYPERGRAPHS

The linearized stability of the system of kinetic equations is determined in the criterion of Routh-Hurwitz by the sign of the coefficients α_i of the secular equation which determines the eigenvalues of the linearized kinetic equation and by the sign of the Hurwitz determinants Δ_i composed of the coefficients α_i thus:

$$\Delta_n = \begin{vmatrix} \alpha_1 & \alpha_3 & \alpha_5 & \alpha_7 \ldots \alpha_{2n+1} \\ \alpha_0 & \alpha_2 & \alpha_4 & \alpha_6 \ldots \alpha_{2n} \\ 0 & \alpha_1 & \alpha_3 & \alpha_5 \ldots \\ 0 & \alpha_0 & \alpha_2 & \alpha_4 \ldots \\ 0 & 0 & \alpha_1 & \alpha_3 \ldots \\ 0 & 0 & \alpha_0 & \alpha_2 \ldots \end{vmatrix} \tag{4.1}$$

The inequality $\Delta_i > 0$ is valid in stable kinetic systems.

The secular equation is:

$$\det |\lambda \mathbf{I} + \mathbf{V}(\mathbf{j}) \cdot \operatorname{diag} \mathbf{h}| = 0 \tag{4.2}$$

and α_i is the coefficient of λ^{n-i} in this equation. The general form is

$$\alpha_i(\mathbf{h}, \mathbf{j}) = \sum_{\delta \in A(n, i)} h_{\delta(1)} \ldots h_{\delta(1)} \beta_i(\delta, \mathbf{j}) \tag{4.3}$$

the sum being over the C_n^i ways of choosing i indices out of n indices and:

$$\beta_i(\delta, \mathbf{j}) = \begin{vmatrix} V_{\delta(1)\delta(1)}(\mathbf{j}) & \ldots & V_{\delta(1)\delta(i)}(\mathbf{j}) \\ . \ . \ . & . \ . \ . & . \ . \\ V_{\delta(i)\delta(1)}(\mathbf{j}) & \ldots & V_{\delta(i)\delta(i)}(\mathbf{j}) \end{vmatrix} \tag{4.4}$$

When

$$\alpha_i(\mathbf{p}) > 0, \quad i = 1, \ldots, d, \tag{4.5}$$

only half of the Hurwitz determinants must be examined as results from the Liénard-Chipart criterion which states that if all the functions from the following four sets:

$$\begin{aligned} F_1 &= \{\Delta_i(\mathbf{p}), \alpha_d(\mathbf{p}), \alpha_j(\mathbf{p}) \mid \ i \text{ even}, \ j \text{ odd}\} \\ F_2 &= \{\Delta_i(\mathbf{p}), \alpha_d(\mathbf{p}), \alpha_j(\mathbf{p}) \mid \ i \text{ odd}, \ j \text{ even}\} \\ F_3 &= \{\Delta_i(\mathbf{p}), \alpha_d(\mathbf{p}), \alpha_j(\mathbf{p}) \mid \ i \text{ even}, \ j \text{ even}\} \\ F_4 &= \{\Delta_j(\mathbf{p}), \alpha_d(\mathbf{p}), \alpha_j(\mathbf{p}) \mid \ i \text{ odd}, \ j \text{ odd}\} \end{aligned} \tag{4.6}$$

are positive then the system is linearly asymptotically stable.

The coefficients $\alpha_i(\mathbf{p}) > 0$ for stability, what is a necessary condition, in the convention that the secular equation is written : $\det(\lambda\mathbf{I}-\mathbf{M}) = 0$, $\alpha_0 = 1$. The theorem of Routh-Hurwitz states that the number of eigenvalues λ_i with Re $\lambda_i > 0$ is equal to the sum of the number of sign changes in the sequences :

$$\begin{gathered} 1,\ \Delta_1(\mathbf{p}),\ \Delta_3(\mathbf{p}),\ \Delta_5(\mathbf{p}),\ \ldots \\ 1,\ \Delta_2(\mathbf{p}),\ \Delta_4(\mathbf{p}),\ \Delta_6(\mathbf{p}),\ \ldots \end{gathered} \tag{4.7}$$

A necessary condition of instability is that $\beta_i(\delta, \mathbf{j}) < 0$, for a certain $(\delta, \mathbf{j})$. The system is then exponentially unstable.

We will develop a diagrammatic representation of β_i or of $\det \mathbf{V}$ which will be valid also for every β_i :

$$\det \mathbf{V} = \sum_{\delta \in P} \operatorname{sgn}(\delta) V_{1\delta(1)} V_{2\delta(2)} \ldots V_{n\delta(n)} \tag{4.8}$$

where P is the set of all $n!$ permutations of the integers $1, \ldots, n$. Every permutation can be written as a product of cyclic permutations and every cyclic permutation of n objects can be written as a product of $i - 1$ transpositions. Hence the factor sign $\delta = (-1)^{n-i} = (-1)^{n+i}$ and one can associate a sign of (-1) with every factor V_{ij} and with every cycle. Then :

$$\det \mathbf{V} = \sum_{\delta \in P,\ \delta = m, n, p} C(\mathbf{m}) C(\mathbf{n}) C(\mathbf{p}) \ldots \tag{4.9}$$

$$C(\mathbf{m}) = -(-V_{m(1)m(2)})(-V_{m(2)m(3)}) \ldots (-V_{m(k)m(1)}) \tag{4.10}$$

This is just the idea in the demonstration of the topological rules of Mason and Coates for flow graphs.

The diagrammatic interpretation is that $C(\mathbf{m})$ corresponds on the current matrix diagram to a cycle. Thus the Routh-Hurwitz instability criterion is transposed in a condition for the existence of cycles in the extreme currents graphs. 2-cycles with positive feedback are drawn with a full segment, a negative 2-cycle is drawn by pointed lines. A positive 2-cycle consisting of 2 pointed arrows is drawn as a full, dashed segment.

The feedback is positive (negative) if there exists an even (odd) number of pointed edges.

The numbers in front of every species (V_{ii} at X_i) on the current matrix diagram are represented as a large point if $C(\mathbf{m}) = V_{m(1)m(1)} > 0$, and as a small point if $C(\mathrm{m}) < 0$. They are called positive viz. negative stabilizers. A negative stabilizer is called a destabilizer and results from the autocatalytic cycles.

The product $C(\mathbf{m})\, C(\mathbf{n}) C(\mathbf{p}) \ldots$ is represented diagrammatically by a diagram of the stabilizers and polygons. The product of cycles is < 0 iff the sum of the number of the destabilizers and of the number of polygons with an even number of pointed edges is odd, because these contribute with the sign (-1) to the product $C(\mathbf{m})\,C(\mathbf{n})\,C(\mathbf{p})$ . .

In order to build up the coefficients β_i for every system, one draws the diagram of the stabilizers and polygons. The factors with negative sign appear in the terms of β_i only from the destabilizers (which are absent in the Oregonator model of the Belousov-Zhabotinskii reaction, and also in every other realistic chemical mechanism) and from the polygons with 0, 2, 4, . . ., pointed edges.

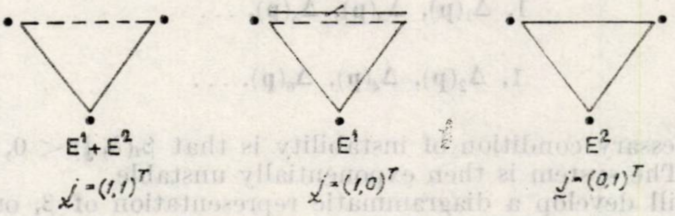

Fig. 5

For the Oregonator model the diagrams for the stabilizers and polygons are drawn in Fig. 5. The determinant β_i is represented by the sum of the diagrams of the stabilizers and polygons over the points $\delta(1)$, ..., $\delta(i)$. The types of terms in this sum can be represented by hypergraphs, with implicit summation over all equivalent diagrams. The star in Fig. 5 represents a stabilizer or a destabilizer, and the full polygons represent polygons with all types of edges as in Fig. 6.

The hypergraphs [7] are unoriented graphs whose nodes are substituted by graphs. Each edge represents a subset of the of vertexes of the total simple graph, just as in the Dyson diagrams from quantum field theory an edge represents the sum of a series of diagrams.

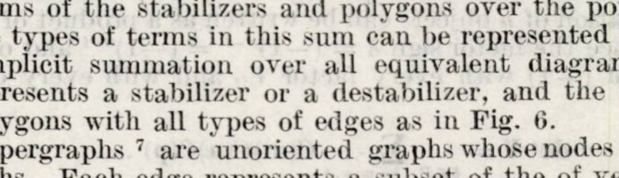

Fig. 6

The expansion of the stability polynomials of the extreme current E^2 of the Oregonator model is written diagrammatically as a sum of diagrams of the stabilizers and polygons. The available stabilizers and polygons are represented in Fig. 7. In order to determine their algebraic values, one examines the current matrix diagram of Fig. 4.

The Hurwitz determinants can be expressed by using symbolic computing programs for algebraic simplification or by using graphical simplification as in Fig. 8. The Hurwitz determinants would contain otherwise a huge number of terms which grows exponentially with the number of current parameters as illustrated in Tables 1 and 2.

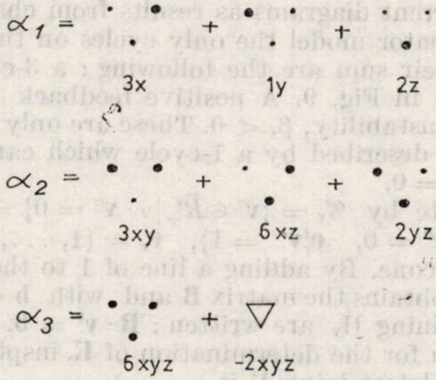

Fig. 7

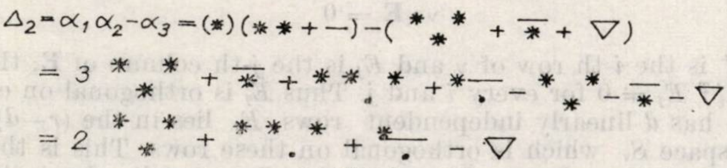

Fig 8

Table 1

The decimal logarithm of the sum of the number of terms in all the polynomials α_i (**h**, **j**) for $i = 1, \ldots, n$. The species number is n and the number of current parameters is g. The values are for the worst case, when $n=d$ (there are no conservation relations)

$n=d$	$h=1$	$g=2$	$g=3$	$g=4$	$g=5$	$g=6$
1	0	0.3	0.5	0.6	0.7	0.8
2	0.3	1.1	1.6	1.9	2.2	2.4
3	1.0	2.3	3.2	3.9	4.4	4.8
4	2.0	4.1	5.4	6.4	7.3	7.9
5	3.4	6.3	8.2	9.6	10.8	11.8
6	5.2	8.9	11.4	13.3	14.9	16.2

Table 2

The decimal logarithm of the number of terms in Δ_{n-1}(**h**, **j**) as a function of g and n $(n=d)$

$n=d$	$g=1$	$g=2$	$g=3$	$g=4$	$g=5$	$g=6$
2	0.3	0.6	0.8	0.9	1.0	1.1
3	1.0	1.6	2.0	2.3	2.5	2.8
4	1.9	2.8	3.4	3.9	4.3	4.6
5	3.0	4.0	4.8	5.5	6.0	6.5
6	4.2	5.4	6.3	7.1	7.8	8.4

5. NECESSARY CRITERION FOR THE STABILITY OF THE STEADY STATE. ALGORITHMS FOR THE DETERMINATION OF THE BASIS OF EXTREME STEADY STATES AND OF THE CYCLES IN THE GRAPHS OF THE EXTREME CURRENTS

A necessary criterion for the exponential instabilities is the presence of cycles in the current diagrams as results from chapter 4.

In the Oregonator model the only cycles on the three extreme diagrams including their sum are the following: a 3-cycle on $E^1 + E^2$ and a 1-cycle as drawn in Fig. 9. A positive feedback just as autocatalysis can determine the instability, $\beta_i < 0$. These are only necessary conditions. The autocatalysis is described by a 1-cycle which can be strong if $\beta_1 < 0$ and critical if $\beta_1 = 0$.

Let us denote by $\mathscr{C}_\nu = \{\mathbf{v}^\circ \in \bar{R}^r_+ \mid \nu \cdot \mathbf{v}^\circ = 0\} = \{\lambda \mathbf{v}^\circ \mid \mathbf{v}^\circ \in \Pi_\nu,\ \lambda \geqslant 0\}$ $\Pi_\nu = \{\mathbf{v}^\circ \in \bar{R}^r_+ \mid \nu \cdot \mathbf{v}^\circ = 0,\quad \mathbf{e}^t_r \mathbf{v}^r = 1\}$, $\mathbf{e}_r = (1, \ldots, 1)^T \in R^r$. $\mathscr{C}_\nu$ is a convex polyhedral cone. By adding a line of 1 to the d independent lines chosen from ν, one obtains the matrix $\mathbf{B}$ and with $\mathbf{b} = (0, \ldots 0, 1) \in R^{d+1}$, the restrictions defining Π_ν are written: $\mathbf{B} \cdot \mathbf{v}^\circ = \mathbf{b}$.

The algorithm for the determination of $\mathbf{E}$, inspired by [8] is the following. The equation determining $\mathbf{E}$ is:

$$\nu \cdot \mathbf{E} = 0 \tag{5.1}$$

If ν^+_i is the i-th row of ν and E_j is the j-th column of $\mathbf{E}$, the scalar product $\nu^{+T}_i E_j = 0$ for every i and j. Thus E_j is orthogonal on each row of ν. As ν has d linearly independent rows, E_j lies in the $(r-d)$-dimensional subspace S_ν which is orthogonal on these rows. This is the kernel of ν. The restriction of $\mathbf{v}^\circ$ to $\bar{R}^r_+$ means that E_j must lie also in the positive closed orthant. Thus $E_j \in S_\nu \cap \bar{R}^r_+$. If $S_\nu \cap \bar{R}^r_+ = \emptyset$ there are reactions which have zero velocity for all steady states. Thus one can assume that $S_\nu \cap R^r_+ \neq 0$. As R^r_+ is open, $\mathscr{C}_\nu$ containing $\mathbf{v}^\circ$ must have the same dimension as S_ν hence $\dim \mathscr{C}_\nu = r - d$. A cone with this dimension cannot be spanned by less than $r-d$ vectors hence $f \geqslant r - d$.

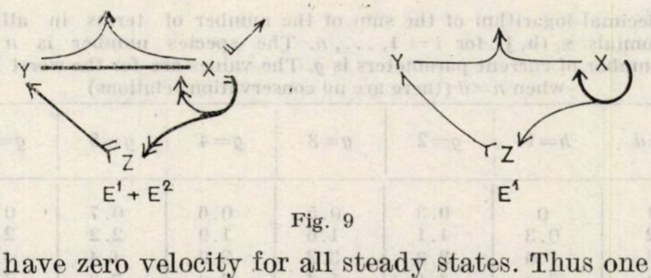

Fig. 9

Looking from within S_ν, $\mathscr{C}_\nu$ has no other boundary than the boundary of $\bar{R}^r_+$, consisting of the hyperplanes $v^0_i = 0$, $i = 1, \ldots, r$. If $\mathscr{C}_\nu$ intersects the hyperplane i in another point than the origin one can describe this intersection by putting $v^0_1 = 0$ in $\nu \cdot \mathbf{v}^\circ(\mathbf{X}, \mathbf{k}) = 0$. The resultant equations combined with $v_i(\mathbf{X}, \mathbf{k}) \geqslant 0$ are satisfied on a cone $\mathscr{C}_{v_2}$ which is a face of $\mathscr{C}_\nu$. This cone is placed in the subspace $S_{v_2} = S_\nu \cap \{\mathbf{v}^\circ \in \bar{R}^r_+ \mid v_i = 0\}$ and is $(r - d - 1)$-dimensional.

If $\mathscr{C}_{v_2}$ lies entirely on the coordinate hyperplanes of a certain v_j $j \neq i$, one can drop the respective variables and we get a r_2-dimensional subspace containing S_{v_2} and $\mathscr{C}_{v_2}$ (which are still $(r - d - 1)$-dimensional).

Looking from within the subspace S_{v_2}, $\mathscr{C}_{v_2}$ has no another boundaries than the boundary of $\overline{R}{}^{r}_{+}$ which consists of the remaining coordinate hyperplanes. That is one drops $v_i^0 = 0$ and those already dropped because they contain $\mathscr{C}_{v_2}$. If $\mathscr{C}_{v_2}$ intersects the j-th hyperplane in a point different from the origin we study this intersection just as for $\mathscr{C}_{\nu}$ by putting $v_j^0 = 0$ in order to obtain S_{v_3} and $\mathscr{C}_{v_3}$, etc., until we obtain a cone which does not intersect the coordinate hyperplanes in a point different from the origin. The cone $\mathscr{C}_{v_k}$ has the dimension $r-d-k+1$. If the dimension of $\mathscr{C}_{v_k}$ is >1, S_{v_k} must intersect a coordinate axis and the sequence can be continued. When $k = r - d$, $\mathscr{C}_{v_k}$ is a unidimensional cone or a halfline and after dropping of the v_i^0 which contain halflines, S_{r-d} will not intersect the coordinate hyperplanes of every remaining component in a point different from the origin. This halfline is a frame-vector of $\mathscr{C}_{\nu}$ and every point $\mathbf{v}^\circ \neq 0$ on it is an extreme current. The matrix **B** built above has the rank $d+1$ in order that $\mathbf{e}_r^T\mathbf{v}^\circ = 1$ but every linear combination of the other lines satisfies $\mathbf{e}_r^T\mathbf{v}^\circ = 0$. In order to find an extreme current one chooses $d+1$ columns of **B** and one builds a square matrix that is being inversed to obtain $\mathbf{v}^\circ$. All exterme currents are obtained by choosing $d+1$ columns in all possible ways and then keeping only the solutions satisfying $v_i(\mathbf{X}, \mathbf{k}) \geqslant 0$. The algorithm is concisely programmable in the computer language APL.

For example when $\nu = (1, 1, -1, -1,)$, **B** is a 2×4 matrix and two columns can be chosen in six ways. Two of these are positive and two are negative and thus give unphysical solutions. The other four choices give :

$$\mathbf{E} = \begin{pmatrix} 1 & 1 & 0 & 0 \\ 0 & 0 & 1 & 1 \\ 0 & 1 & 1 & 0 \\ 1 & 0 & 0 & 1 \end{pmatrix} \tag{5.2}$$

$\mathscr{C}_{\nu}$ is a 3-dimensional cone of pyramidal shape with square section.

For the Oregonator model the rows of ν are independent hence $d = \operatorname{rank} \nu = 3$, $r = 5$, $n = 3$, $\dim \Pi_{\nu} = r - d - 1$. There are thus two extreme currents. The matrix **B** is :

$$\mathbf{B} = \begin{pmatrix} 1 & -1 & 1 & -2 & 0 \\ -1 & -1 & 0 & 0 & 1 \\ 0 & 0 & 2 & 0 & -2 \\ 1 & 1 & 1 & 1 & 1 \end{pmatrix} \tag{5.3}$$

One can choose four columns in five ways but only two solutions of the equations $\mathbf{B}\mathbf{v}^\circ = \mathbf{b}$ will be nonnegative. It results :

$$\mathbf{E} = \begin{pmatrix} 0 & 1 & 1 & 0 & 1 \\ 1 & 0 & 1 & 1 & 1 \end{pmatrix}^T \tag{5.4}$$

In order to consider the reverse reactions the solutions with $v_i^0 < 0$ are considered realistic and are interpreted as positive velocities for the reverse reactions.

In the following an algorithm will be given for finding the simple cycles in a finite digraph, inspired by [9–11]. A cycle is simple if it meets a vertex two times and no other vertex more than one time. The algorithm prints the cycles only once, without repetitions. The cycles are found when the path followed is found cyclic or by combining parts of the cycles found earlier with the path being processed, what also requires a large storage volume.

One drops from the graphs the vertices in which no arc ends and the arcs that have their origin at these vertices. Then one drops all the vertices on which no arc originates and the arcs that end on these vertices. The algorithm then chooses one of the remaining vertices as a starting point and examines the paths that start from this vertex. Each path is explored until one meets a vertex that has been examined before, which hence cannot be on a simple cycle (Fig. 10). The algorithm then returns to the last branching point from which at least an arc originates that has not been explored. By choosing such an arc the algorithm starts in a new direction. If there does not exist such a vertex one chooses as a new starting point a vertex that has not been met before. If all the vertices have been examined the algorithm stops. The arcs and the vertices met are being stored on a list called T that represents a path through the graph from the starting point to the element examined. When the algorithm returns along the path it drops from T the arcs and vertices through which it passes. When the algorithm meets a vertex which has been examined, before returning along the path it verifies if any combination of arcs which it has examined form a cycle which has not been found before. If the vertex is still on the list T there will exist exactly one such cycle: it will consist of the vertex together with the arc of T with respect to this vertex.

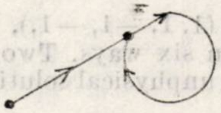
Fig. 10

If the vertex no more lies on T these cycles can exist if one or more cycles that contain the vertex have been previously found. Then a recursive routine is called that looks for the paths that originate from the reencountered vertex and end at a vertex that is still on T. It can be rigorously deduced that every such a path is either a tail of a cycle discovered previously either can be decomposed in one or several ways in several such tail subpaths. For each path found by the subroutine one forms a new cycle by the concatenation of the tail subpath of T with the path.

For example the cycle $C_1 = v_1a_2v_2a_1v_1$, $C_2 = v_2a_3v_3a_4v_2$ have been already found and with $T = v_1a_5$ the algorithm rejoins a_3. Then by the concatenation of the subtails v_1a_5 of T, $v_3a_4v_2$ of C_2 and a_1v_1 of C_1 a new cycle results $v_1a_5v_3a_4v_2a_1v_1$ (Fig. 11).

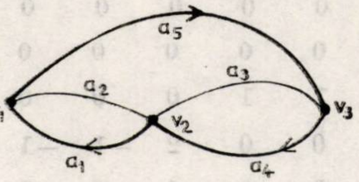

Fig. 11

The directed graphs, the linked lists and trees are new data types that can be defined for processing on a computer by the symbolic programming languages *SNOBOL*-4,[12] *LISP*[13] and other universal languages as the fourth generation programming language *FORTH*.[14]

The topology of the currents diagrams and the necessary criterion for instability can be used in establishing viz. improving the kinetic models of the oscillating reactions. By solving on a computer the systems of differential equations e.g. by the Gear algorithm, specific for these stiff systems, one must reproduce the concentration oscillations of the chemical species.

6. THE DETERMINATION OF THE BASIS OF EXTREME STEADY STATES AND OF THE NECESSARY STABILITY CRITERION FOR REALISTIC MODELS OF THE OSCILLATING REACTIONS

6.1. THE FIELD-KÖRÖS-NOYES MODEL OF THE BELOUSOV-ZHABOTINSKII REACTION

This model[15–17] consists of 11 reactions represented on the reaction diagram of Fig. 12, on which the species constant in time are omitted ($CH_2(COOH)_2$, BrO_3^-, H^+, CO_2, H_2O). The reverse reactions are omitted, what leaves undetermined certain steady state concentrations.

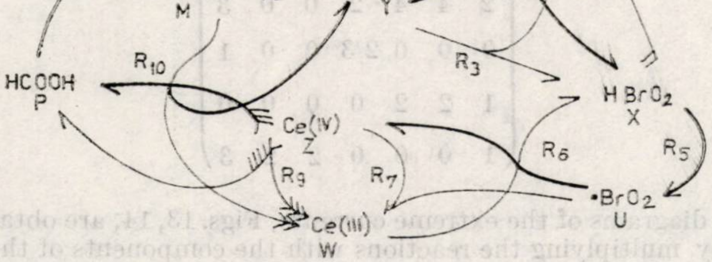

Fig. 12

The stoechiometric matrix is:

$$\nu = \begin{pmatrix} 1 & 0 & 0 & 0 & 0 & 0 & 0 & 0 & 1 & 0 & -1 & 0 \\ 0 & 0 & 0 & 0 & 0 & 0 & 0 & 0 & 0 & 1 & 1 & -1 \\ -1 & -1 & 2 & 1 & 1 & 0 & 0 & 0 & 0 & 0 & 0 & -1 \\ 0 & 0 & 0 & 0 & 0 & 2 & -1 & -1 & 0 & 0 & 0 & 0 \\ 0 & 1 & 0 & 0 & 0 & 0 & 0 & 0 & -1 & 0 & 0 & 0 \\ 0 & 0 & 0 & 0 & 0 & 0 & -1 & 1 & 0 & 6 & 4 & 0 \\ 0 & 0 & -2 & 1 & -2 & -1 & 1 & 0 & 0 & 0 & 0 & 0 \\ 0 & -1 & -1 & -1 & 0 & 0 & 0 & 0 & 1 & 0 & 1 & 1 \\ 0 & 0 & 0 & 0 & 0 & 0 & 1 & -1 & 0 & -6 & -4 & 0 \end{pmatrix} \tag{6.1}$$

Practically there are only 4 dynamically independent concentrations: $\mathbf{X} = (T, W, X, Y)$ and the reactions $\mathbf{v} = (v_1, v_2, v_3, v_4, v_5, v_9, v_{10}$ $v_{11})$. The stoechiometric matrix for these reactions is:

$$\nu = \begin{pmatrix} -1 & 2 & 1 & 1 & 0 & 0 & 0 & -1 \\ 0 & 0 & 0 & 0 & -2 & 6 & 4 & 0 \\ 0 & -1 & 1 & -2 & 1 & 0 & 0 & 0 \\ 0 & -1 & -1 & 0 & 0 & 0 & 1 & 1 \end{pmatrix} \tag{6.2}$$

The matrix $\mathbb{E}$ whose columns contain the extreme currents results:

$$\mathbb{E} = \begin{pmatrix} 3 & 5 & 5 & 1 & 1 & 1 & 3 \\ 2 & 2 & 0 & 0 & 0 & 1 & 3 \\ 0 & 0 & 2 & 0 & 2 & 1 & 0 \\ 0 & 1 & 3 & 1 & 1 & 0 & 0 \\ 2 & 4 & 4 & 2 & 0 & 0 & 3 \\ 0 & 0 & 0 & 2/3 & 0 & 0 & 1 \\ 1 & 2 & 2 & 0 & 0 & 0 & 0 \\ 1 & 0 & 0 & 0 & 2 & 2 & 3 \end{pmatrix} \tag{6.3}$$

The diagrams of the extreme currents, Figs. 13, 14, are obtained from Fig. 12 by multiplying the reactions with the components of the extreme currents. As this changes the stoechiometry but not the kinetics, all feathers are added to the right of the arrows. The current matrix diagrams are also drawn, which express the linearizied matrix of the reaction kinetics equations. The extreme currents diagrams that show cycles permit a refinement of the necessary criterion for oscillations. Their weight within this criterion is determined by the value of the kinetic constants.

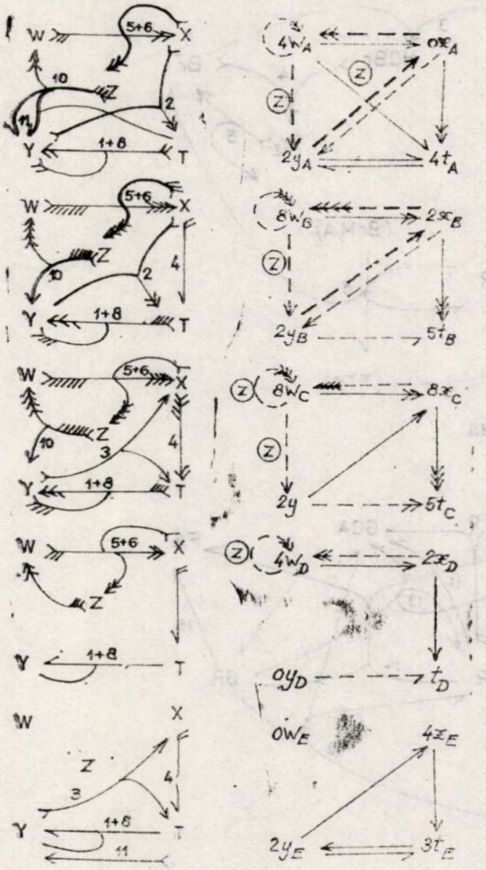
W
X
Y
T
Z
5+6
10
11
2
1+8
4
3
$4w_A$
$0x_A$
$2y_A$
$4t_A$
$8w_B$
$2x_B$
$2y_B$
$5t_B$
$8w_C$
$8x_C$
$2y$
$5t_C$
$4w_D$
$2x_D$
$0y_D$
t_D
$0w_E$
$4x_E$
$2y_E$
$3t_E$
Z

Fig. 13

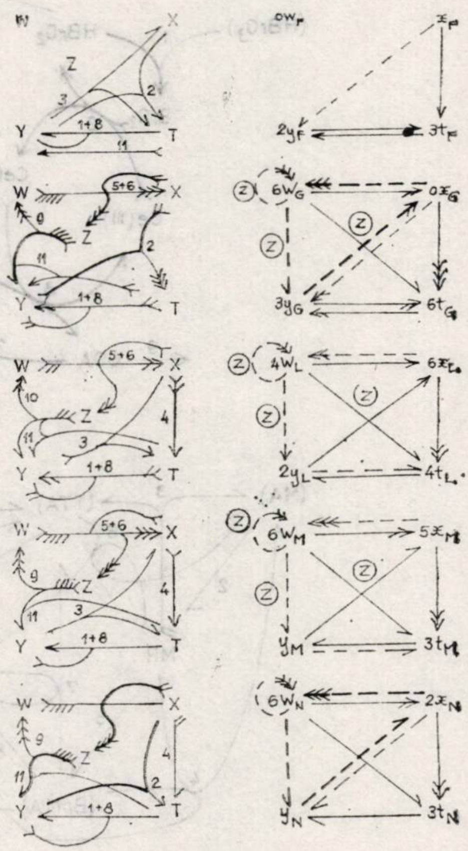
W
X
Y
T
Z
5+6
9
11
2
1+8
4
3
$0w_F$
x_F
$2y_F$
$3t_F$
$6w_G$
$0x_G$
$3y_G$
$6t_G$
$4w_L$
$6x_L$
$2y_L$
$4t_L$
$6w_M$
$5x_M$
y_M
$3t_M$
$6w_N$
$2x_N$
y_N
$3t_N$
Z

Fig. 14

The diagrams A, L, M, N correspond to the extreme currents in the case of steady state P species (formic acid). One notices that positive feedback cycles (drawn by heavy lines) exist only on the currents diagrams A, B, G, N. In the currents B and N the oscillatory cycle passes through the reactants with nonzero self-vertexes. These vertices dominate the cycle and the instability does not happen. In the currents A and G the cycle passes through a self-vertex at X that has been included in the coefficient of the inverse of the concentration of the species X and hence the cycle has a destabilizing effect.

6.2. THE KINETIC MODEL OF THE ORGANIC PART OF THE BELOUSOV-ZHABOTINSKII REACTION

The complete model of the Belousov-Zhabotinskii reaction contains an inorganic part coupled with a part of organic reactions[18] by means of only few common species. The reaction diagrams are drawn in Figs. 15—16, where GOA = glyoxylic acid, TTA = tartronic acid, TR = tar-

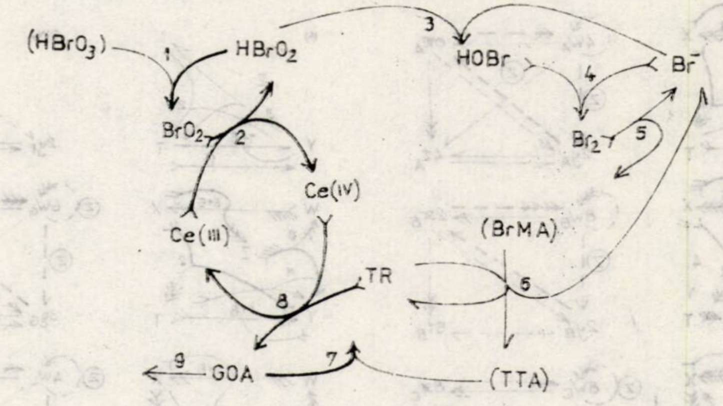

Fig. 15

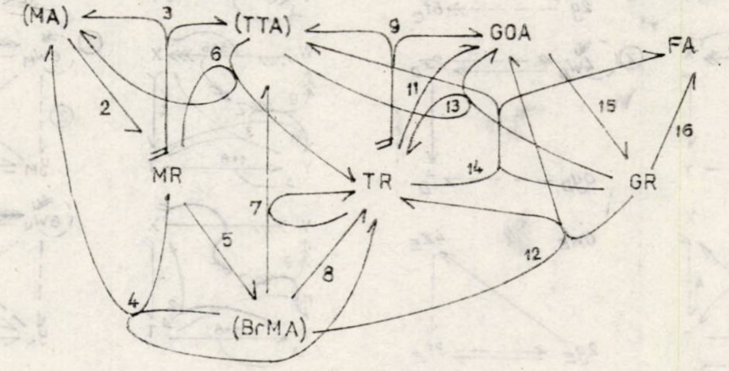

Fig. 16

tronyl radical, $BrMA$ = bromomalonic acid, MR = malonyl radical, FA = formic acid, GR = radical of the glyoxylic acid, $MA = \mathrm{CH_2(COOH)_2}$ $TTA = \mathrm{HOCH(COOH)_2}$, $GOA = \mathrm{OHCCOOH}$, $FA = \mathrm{HCOOH}$, $BrMA = \mathrm{CHBr(COOH)_2}$, $MR = \mathrm{HC(COOH)_2}$, $TR = \mathrm{OCH(COOH)_2}$, $GR = \mathrm{OC(COOH)_2}$.

In the inorganic part two cycles that determine redox instabilities are connected in tandem by the couple of catalyzing ions Ce(III)/Ce(IV) (whose sum of concentrations is constant). The two cycles are drawn by heavy lines on the reaction diagram of Fig. 15.

In the organic part (Fig. 16) the species on the first row are stable, have an even number of valence electrons and those on the second row are very reactive free radicals (they have an odd number of electrons). The oxidation numbers grow or decrease in steps equal to one, from left to the right in the order $(MA) \rightarrow (MR) \rightarrow (TTA) \rightarrow (TR) \rightarrow$ etc. The diagram explains the origin of the electrons in the Belousov-Zhabotinskii reaction. The production or addition of Br^- can be deduced from the diagram. All reactions that do not have the symmetry imposed by the conservation of electrons are redox reactions that imply Ce(IV)/Ce(III).

In order to find all the extreme currents of the organic part of the mechanism that are compatible with the reaction that describes the effect of the unstable extreme current of the inorganic part on Br^- and Ce : $R_1:\ 2\mathrm{Ce(III)} + \mathrm{Br}^- \rightarrow 2\,\mathrm{Ce(IV)}$, one starts from the stoechiometric matrix :

$$\nu =$$

$$= \begin{array}{l}\boldsymbol{Ce}(\mathrm{IV})\\ \boldsymbol{MR}\\ \boldsymbol{TR}\\ \boldsymbol{GOA}\\ \boldsymbol{GR}\\ \boldsymbol{Br}\end{array}\begin{pmatrix} 2 & -1 & 0 & 0 & -1 & 0 & 0 & -1 & 0 & 0 & -1 & 0 & 0 & 0 & -1 & -1\\ 0 & 1 & -2 & -1 & -1 & -1 & 0 & 0 & 0 & 0 & 0 & 0 & 0 & 0 & 0 & 0\\ 0 & 0 & 0 & 1 & 0 & 1 & 0 & 1 & -2 & 2 & -1 & 1 & 1 & -1 & 0 & 0\\ 0 & 0 & 0 & 0 & 0 & 0 & 0 & 0 & 1 & -1 & 1 & 1 & 1 & 0 & -1 & 0\\ 0 & 0 & 0 & 0 & 0 & 0 & 0 & 0 & 0 & 0 & 0 & -1 & -1 & -1 & -1 & -1\\ -1 & 0 & 0 & 1 & -1 & 0 & 1 & 1 & 0 & 0 & 0 & 1 & 0 & 0 & 0 & 0\end{pmatrix} \tag{6.4}$$

The extreme currents matrix has the dimension 16 × 32 (16 reactions described by the stoechiometric matrix and 32 extreme currents :

$$\mathbf{E} = \begin{pmatrix} 6&3&2&2&3&2&2&3&2&2&1&5&2&2&2&5&5&2&2&2&2&2&2&2&2&2&2&2&2&2&2&2\\ 2&5&2&2&2&0&0&2&0&0&1&7&3&1&2&1&1&3&2&2&1&1&1&0&0&0&0&0&0&0&0&0\\ 1&1&0&0&1&0&0&1&0&0&1&0&0&0&0&0&0&0&0&0&0&0&0&0&0&0&0&0&0&0&0&0\\ 0&3&2&2&0&0&0&0&0&0&0&6&2&1&2&0&0&0&0&0&0&0&0&0&0&0&0&0&0&0&0&0\\ 0&0&0&0&0&0&0&0&0&0&1&1&0&0&0&1&1&0&0&0&0&0&0&0&0&0&0&0&0&0&0&0\\ 0&0&0&0&0&0&0&0&0&0&0&0&1&0&0&0&0&3&2&2&1&1&1&0&0&0&0&0&0&0&0&0\\ 1&0&0&0&0&0&0&0&0&0&2&0&0&1&0&0&0&2&2&2&2&0&0&1&2&2&2&1&-2&2&0&0\\ 0&0&0&0&3&2&2&0&0&0&0&0&0&0&0&6&0&0&0&0&0&2&0&1&0&0&0&0&0&0&2&0\\ 0&1&1&0&1&1&0&1&1&0&0&2&1&0&1&2&2&1&1&0&0&1&1&0&1&1&0&0&0&0&1&1\\ 0&0&0&0&0&0&0&0&0&0&0&0&0&0&0&0&0&0&0&0&0&0&0&0&0&0&2&0&0&0&0&0\\ 0&0&0&1&0&0&1&0&0&1&0&0&0&1&0&0&0&0&0&1&1&0&0&1&0&0&3&1&1&1&0&0\\ 0&0&0&0&0&0&0&3&2&2&0&0&0&0&0&0&6&0&0&0&0&0&2&0&0&0&0&1&0&0&0&2\\ 0&0&0&0&0&0&0&0&0&0&0&0&0&1&0&0&0&0&0&0&0&0&0&0&3&2&0&0&2&1&1&1\\ 0&1&0&1&1&0&1&1&0&1&0&2&1&0&1&2&2&1&0&1&0&1&1&0&1&0&1&0&1&0&1&1\\ 0&1&1&1&1&1&1&4&3&3&0&2&1&1&2&2&8&1&1&1&1&1&3&1&4&3&1&2&3&2&2&4\\ 0&0&1&0&0&1&0&0&1&0&0&0&0&1&0&0&0&0&1&0&1&0&0&1&0&1&0&1&0&1&0&0 \end{pmatrix} \tag{6.5}$$

Only 6 extreme currents have critical cycles. These have the diagrams drawn in Fig. 17.

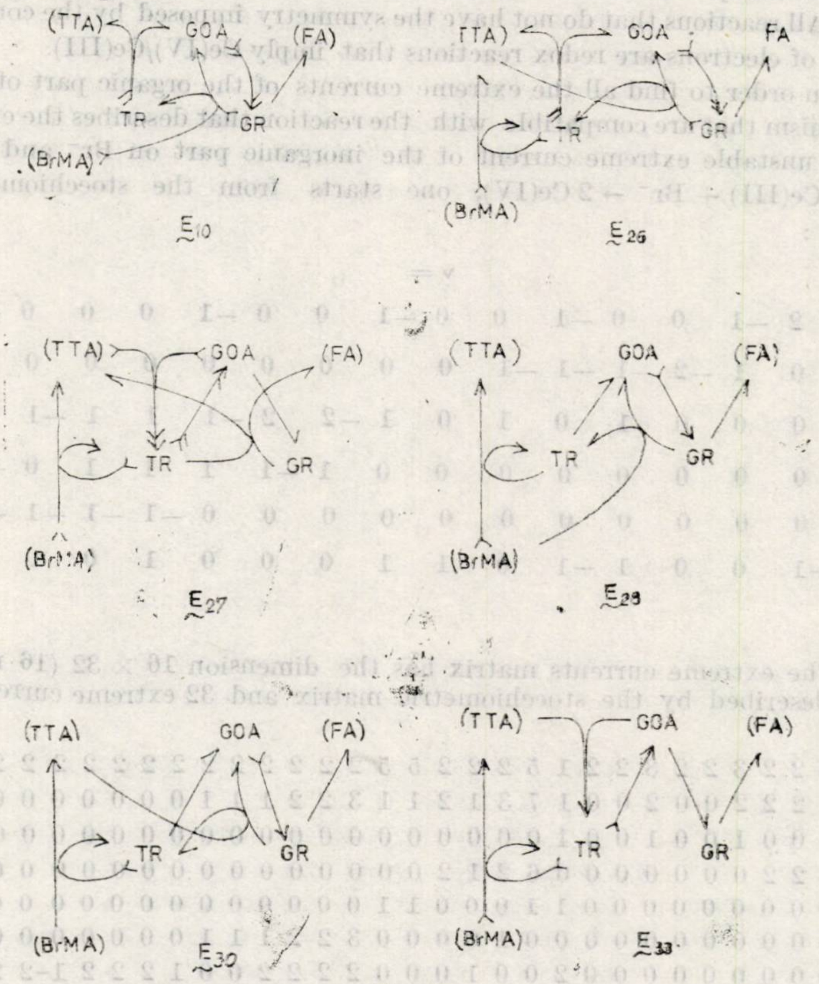

$\underset{\sim}{E}_{10}$ $\underset{\sim}{E}_{25}$ $\underset{\sim}{E}_{27}$ $\underset{\sim}{E}_{28}$ $\underset{\sim}{E}_{30}$ $\underset{\sim}{E}_{33}$

Fig. 17

6.3. THE MODIFIED LOTKA-VOLTERRA MODEL FOR THE BELOUSOV-ZHABOTINSKII REACTION

Another model of the Belousov-Zhabotinskii system is the four-variable Lotka-Volterra model.[19] This model does not assume a determinant role for the Br^- ions in the appearance of the oscillations, for the explanation of the origin of Br^- ions necessitates complex developments such as the model of the organic part of the Belousov-Zhabotinskii reaction.

For *BZ* oscillations with mixed substrate of oxalic acid-acetone in place of malonic acid, the kinetics is described by a Lotka-Voltera model

$$[A] + X \to 2X; \quad X + Y \to 2Y; \quad [D] + Y \to [B] \qquad (6.6)$$

where $[A] = [3H^+ + BrO_3^-] - [H_2O]$, $[B] = [CH_2BrCOCH_3 + H_2O)]$, $X = HBrO_2$, $Y = HOBr$, $[D] = [CH_3COCH_3]$. The first two reactions are catalyzed by transforming Ce^{3+} into Ce^{4+} and the reduction of Ce^{4+} is achieved by the reaction $(COOH)_2 \rightarrow 2H^+ + 2CO_2$

The four-variable Lotka-Volterra model is composed of the reactions (6.6) with intermediates: $W = Br_2O_4$, $Z = Br_2O_2$, and two auxiliary reactions where $C = (CCOH)_2$:

$$[A] + X \rightarrow W \rightarrow 2X; \; X + Y \rightarrow Z \rightarrow 2Y; \; [D] + Y \rightarrow [B];$$

$$[A] + [C] \rightarrow X; \; X + [C] \rightarrow Y \tag{6.7}$$

By omitting one of the new intermediates from the four-variable Lotka-Volterra model (*FLV*) one can establish two three-variable Lotka-Volterra (*TLV*) models:

$$[A] + X \rightarrow 2X; \quad X + Y \rightarrow Z \rightarrow 2Y; \quad [D] + Y \rightarrow [B], \quad \text{(model "}Z\text{")}$$

$$[A] + X \rightarrow W \rightarrow 2X; \quad X + Y \rightarrow 2Y; \quad [D] + Y \rightarrow [B], \quad \text{(model "}W\text{")} \tag{6.8}$$

The model "*W*" is always stable for positive values of the rate constants and model "*Z*" is always unstable. The model "*Z*" can be combined with one or both auxiliary reactions, resulting in three different models that each exhibits a limit cycle:

$$[A] + [C] \rightarrow X; \; [A] + X \rightarrow 2X; \; X + Y \rightarrow Z \rightarrow 2Y;$$
$$[D] + Y \rightarrow [B] \; \text{(model "}Z1\text{")}$$

$$[A] + X \rightarrow 2X; \; [C] + X \rightarrow Y; \; X + Y \rightarrow Z \rightarrow 2Y; \; [D] + Y \rightarrow [B']$$
$$\text{(model "}Z2\text{")} \tag{6.9}$$

$$[A] + [C] \rightarrow X; \; [A] + X \rightarrow 2X; \; [C] + X \rightarrow Y; \; X + Y \rightarrow Z \rightarrow 2Y;$$
$$[D] + Y \rightarrow [B] \; \text{(model "}Z3\text{")}$$

The model "*Z3*" contains the models "*Z1*" and "*Z2*" as particular cases.

The Lotka-Voltera mechanism exhibits conservative oscillations and is structurally unstable. By introducing a third intermediate in the reaction scheme one obtains the Explodator model. In order to obtain limit cycle oscillations one must add at least a reaction which limits the concentrations of the species. Kernels of the Explodator type, containing two autocatalytic consecutive reactions can be established in various ways, among them being also the hypercycle model.

The Explodator model with trajectories spiralling to the infinity, is described by the three-variable Lotka-Volterra scheme. It can be transformed in a limit cycle system by adding to the reactions $E1-E4$ one of the reactions $L1-L4$:

$$[A]+X\to(1+\alpha)X,\ (E1);\quad X+Y\to Z,\quad (E2);\quad Z\to(1+\beta)Y,\ (E3);$$
$$Y\to[B],\quad (E4)\qquad (6.10)$$

$$2X\to 1/3\,Z,\ (L1);\quad [A]\to X,\ (L2);\quad X\to 1/3Z,\quad (L3);\quad [B]\to Y,\quad (L4)$$

This model has antagonistic positive and negative feedback loops, shifted in the variable X.

For the BZ reaction with substrate malonic acid, the Oregonator model is described by the equations:

$$[B]+Y\to X;\quad X+Y\to[P];\quad [A]+X\to 2X+Z;$$
$$X+X\to[Q],\quad Z\to fY\qquad (6.11)$$

The stoechiometric factor f is of a great theoretical relevance. The difference between the two types of models is that species Z is formed serially from X in the Lotka-Volterra Explodator model and is formed in parallel with X in the Oregonator model as results from Figures 18 and 19.

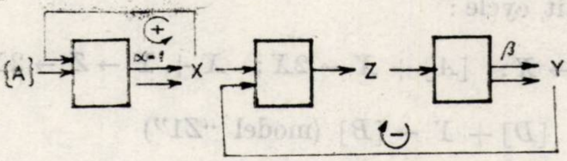

Fig. 18

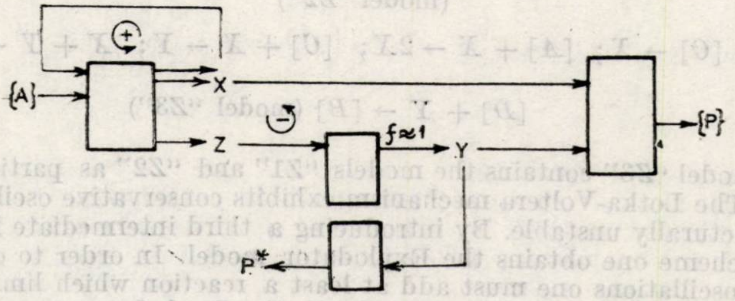

Fig. 19

The conservative Lotka-Volterra model is at the boundary between the globally stable and the explosive mechanisms.

The parallel oscillatory Oregonator model has the scheme of Fig. 20.

A Lotka-Volterra model with a reaction that limits the stoechiometric explosion to a limit cycle is the *BZ* oscillator with oxalic acid substrate in which Br^- is removed by a flow of gaseous Br_2. The kinetic scheme is shown in Fig. 21, where the notations are : $A = HBrO_3$, $X = HBrO_2$, $Z = 3HOBr$, $Y = Br$, in solution and $B = Br_2(g)$ in gaseous phase, in the Explodator model.

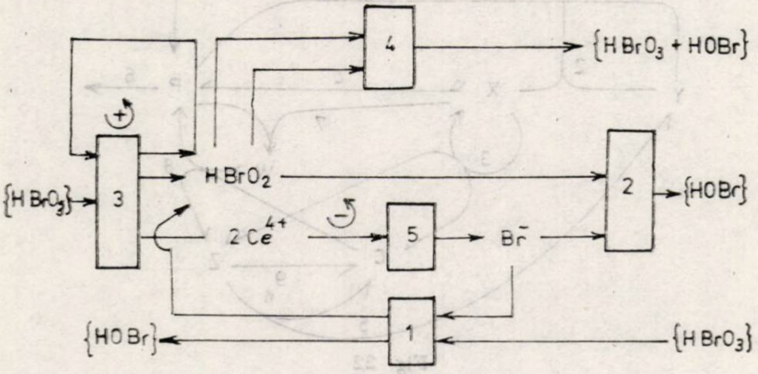

Fig. 20

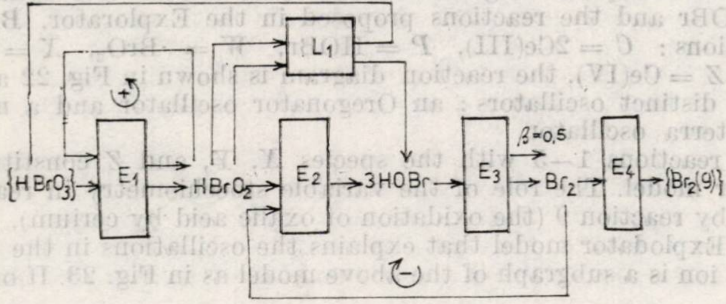

Fig. 21

6.4. THE OREGONATOR MODEL REVISED BY THE INCLUSION OF THE MODIFIED LOTKA-VOLTERRA MODEL, FOR THE BELOUSOV-ZHABOTINSKII REACTION. THE SYNCHRONIZATION PHENOMENON OF THE OSCILLATIONS OF THE TWO KINETIC SUBSCHEMES

The Oregonator model contains an autocatalytic stage and three intermediate species : $HBrO_2$, Br^- and Ce^{4+}. It contains a fifth unrealistic stage $2Ce^{4+} \rightarrow f\,Br^-$, $f \approx 1$.

A revised Oregonator model[21] must take into account that the oscillations are determined by the oxidation states of bromine ($HBrO_2$, $HOBr$, Br_2 and Br^-) and that HOBr cannot be ignored. The new model has three intermediates ($X = HBrO_2$, $Y = Br^-$, $P = HOBr$) and a second autocatalytic stage :

$$HBrO_2 + Br^- \rightarrow 2HOBr \rightarrow 2Br^- \text{ or } X + Y \rightarrow 2P \rightarrow 2Y.$$

Both the Explodator and the revised Oregonator models consider the oxidation states of bromine ($HBrO_2$, HOBr, Br_2, Br^-) as intermediates and both contain a second autocatalytic stage.

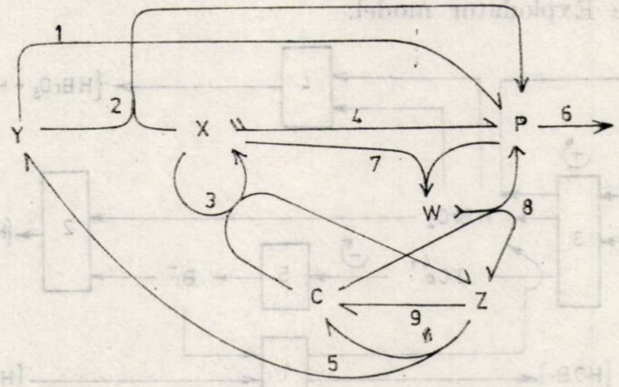

Fig. 22

We will study an Oregonator model that includes the dynamics of species HOBr and the reactions proposed in the Explorator. By using the notations: $C = 2Ce(III)$, $P = HOBr$, $W = \cdot BrO_2$, $X = HBrO_2$, $Y = Br^-$, $Z = Ce(IV)$, the reaction diagram is shown in Fig. 22 and contains two distinct oscillators: an Oregonator oscillator and a modified Lotka-Volterra oscillator.

The reactions 1–5 with the species X, Y, and Z constitute the Oregonator model. The role of the variable stoechiometry in reaction 5 in played by reaction 9 (the oxidation of oxalic acid by cerium).

The Explodator model that explains the oscillations in the absence of the Br^- ion is a subgraph of the above model as in Fig. 23. If one omits

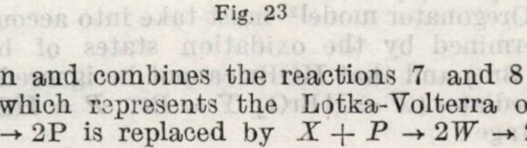

Fig. 23

the species cerium and combines the reactions 7 and 8 the diagram in Fig. 24 results, which represents the Lotka-Volterra oscillator. If the reaction $X + P \to 2P$ is replaced by $X + P \to 2W \to 2P$, the system has a limit cycle in place of a center.

A model that combines two oscillators can exhibit synchronization states [1–3] or chaotic dynamics. For example combining the LV oscillator from above with the scheme in Fig. 25, which represents an unstable competition between X and Z, results the system in Fig. 26, which has chaotic dynamics.

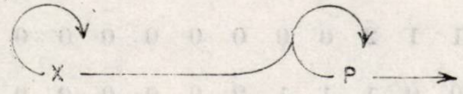

Fig. 24

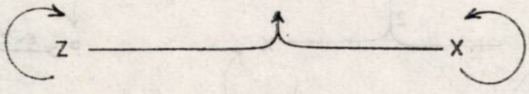

Fig. 25

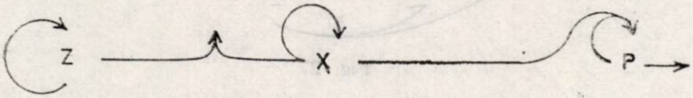

Fig. 26

The Oregonator +Explodator model has thus 6 intermediate species considered in alphabetical order, 9 direct reactions and 9 inverse reactions. The stoechiometric and the reaction order matrix are :

$$\nu = \begin{pmatrix} 0 & 0 & -1 & 0 & 1 & 0 & 0 & -1 & 1 & 0 & 0 & 1 & 0 & -1 & 0 & 0 & 1 & -1 \\ 1 & 2 & 0 & 1 & 0 & -1 & -1 & 2 & 0 & -1 & -2 & 0 & -1 & 0 & 1 & 1 & -2 & 0 \\ 0 & 0 & 0 & 0 & 0 & 0 & 2 & -2 & 0 & 0 & 0 & 0 & 0 & 0 & 0 & -2 & 2 & 0 \\ 1 & -1 & 1 & -2 & 0 & 0 & -1 & 0 & 0 & -1 & 1 & -1 & 2 & 0 & 0 & 1 & 0 & 0 \\ -1 & -1 & 0 & 0 & 1 & 0 & 0 & 0 & 0 & 1 & 1 & 0 & 0 & -1 & 0 & 0 & 0 & 0 \\ 0 & 0 & 1 & 0 & -1 & 0 & 0 & 1 & -1 & 0 & 0 & -1 & 0 & 1 & 0 & 0 & -1 & 1 \end{pmatrix} \tag{6.12}$$

$$\varkappa = \begin{pmatrix} 0 & 0 & 1 & 0 & 0 & 0 & 0 & 1 & 0 & 0 & 0 & 0 & 0 & 1 & 0 & 0 & 0 & 1 \\ 0 & 0 & 0 & 0 & 0 & 1 & 1 & 0 & 0 & 1 & 2 & 0 & 1 & 0 & 0 & 0 & 1 & 0 \\ 0 & 0 & 0 & 0 & 0 & 0 & 0 & 1 & 0 & 0 & 0 & 0 & 0 & 0 & 0 & 2 & 0 & 0 \\ 0 & 1 & 1 & 2 & 0 & 0 & 1 & 0 & 0 & 1 & 0 & 2 & 0 & 0 & 0 & 0 & 0 & 0 \\ 1 & 1 & 0 & 0 & 0 & 0 & 0 & 0 & 0 & 0 & 0 & 0 & 0 & 1 & 0 & 0 & 0 & 0 \\ 0 & 0 & 0 & 0 & 1 & 0 & 0 & 0 & 1 & 0 & 0 & 1 & 0 & 0 & 0 & 0 & 1 & 0 \end{pmatrix} \tag{6.13}$$

The extreme currents matrix E has 59 columns (extreme currents) of which only three are significant :

$$E = \begin{pmatrix} 0 & 1 & 1 & 0 & 1 & 2 & 0 & 0 & 0 & 0 & 0 & 0 & 0 & 0 & 0 & 0 & 0 & 0 \\ 1 & 0 & 1 & 1 & 1 & 2 & 0 & 0 & 0 & 0 & 0 & 0 & 0 & 0 & 0 & 0 & 0 & 0 \\ 0 & 0 & 1 & 0 & 0 & 1 & 1 & 1 & 2 & 0 & 0 & 0 & 0 & 0 & 0 & 0 & 0 & 0 \end{pmatrix} \quad (6.14)$$

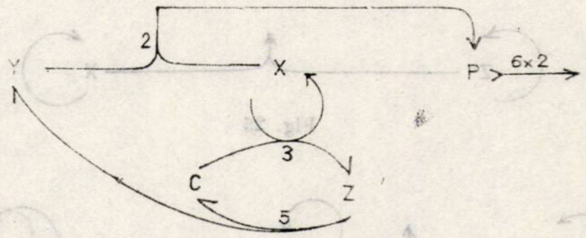

Fig. 27

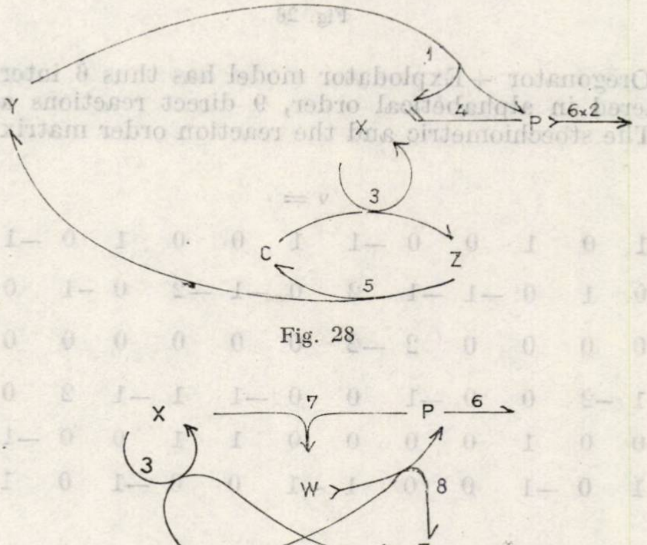

Fig. 28

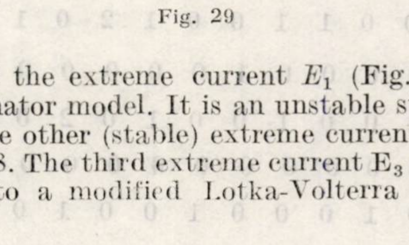

Fig. 29

The diagram of the extreme current E_1 (Fig. 27) is the extreme current of the Oregonator model. It is an unstable steady state that produces oscillations. The other (stable) extreme current E_2 of the Oregonator model is on Fig. 28. The third extreme current E_3 is an unstable steady state corresponding to a modified Lotka-Volterra (Explodator) model (Fig. 29).

6.5. THE LOTKA-VOLTERRA TYPE MODEL OF THE HYPERCYCLE

A model with several autocatalytic cycles in series is the hypercycle model[22] that describes the prebiotic evolution.

The reaction diagram (Fig. 30) contains reactions of the form $X_i \to$ $\to X_i + Y_k$. The mathematical model consists in the equations :

$$\dot{x}_i = x_i(k_i x_{i-1} - \Phi), \quad i = 1, \ldots, n, \quad \Phi = \sum_{i=1}^{n} k_i x_i x_{i-1} \tag{6.15}$$

and admits a Hopf bifurcation for $n \geqslant 4$.

The interaction of the oscillators which are present in the modified Oregonator model can be represented for hypercycles in Fig. 31.

The instability could originate in a possible feedback cycle between V and Y which would appear by a perturbation, which would determine a stoechiometric explosion of one and the extinction of the other hypercycle.

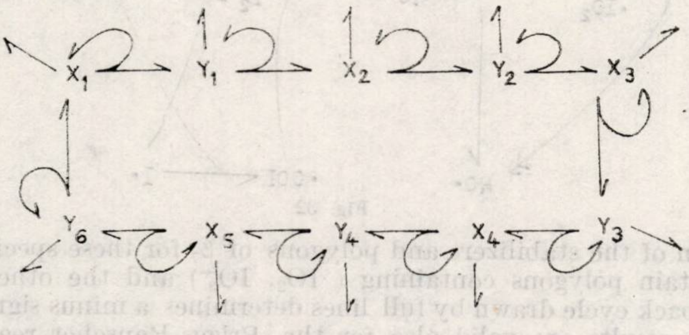

Fig. 30

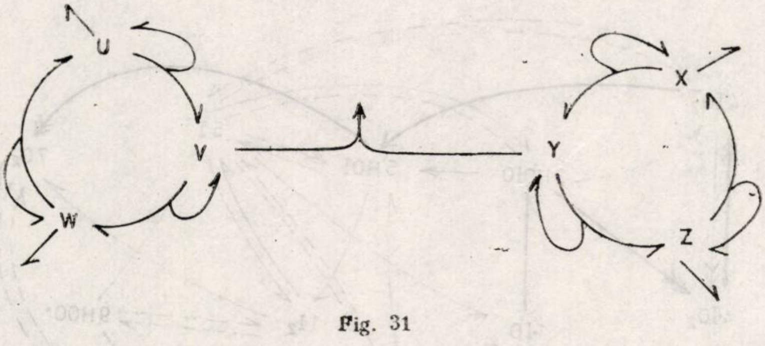

Fig. 31

6.6. THE KINETIC MODEL OF THE BRAY-LIEBHAFSKY REACTION

The Bray-Liebhafsky oscillatory reaction [23-25]: $2H_2O_2 \to 2H_2O +$ $+ O_2$ catalyzed by oxyiodate species has an extreme current drawn in Fig. 32. The only cycle on this current diagram is the 2-cycle between $\cdot IO_2$ and IO_3^-.

The current matrix diagram (Fig. 33) exhibits a positive feedback cycle through the species $\cdot IO_2$, IO_3^-, HOI, O_2, ·OOI, ·IO and HOIO. Since this cycle passes through $(\cdot IO_2, IO_3^-)$ for which $\beta_2 = 0$ (the stability determinant β_2) the only diagrams that must be evaluated in the expansion of the stabilizers and polygons of β_7 for these species are those that contain polygons containing $(\cdot IO_2, IO_3^-)$ and the other 5 species. The feedback cycle drawn by full lines determines a minus sign of β_7 (<0).

The results are valid also for the Briggs-Rauscher reaction which is a mixture of the *BL* and *BZ* compositions.

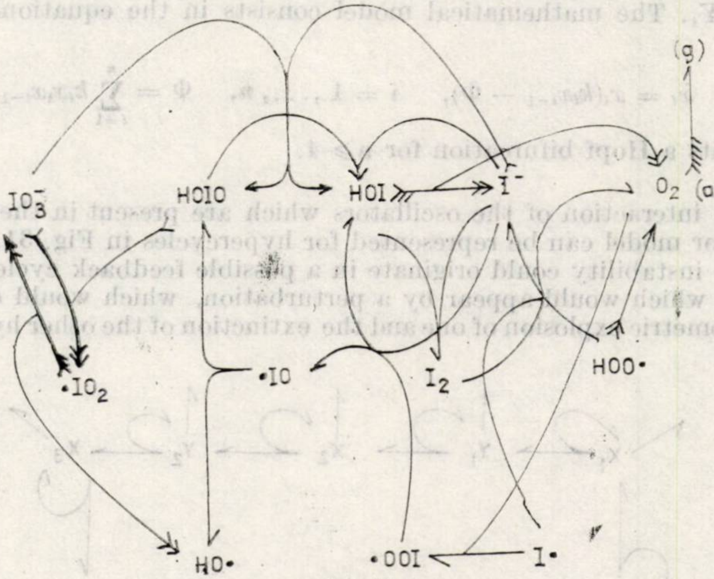
(g)
IO_3^-
HOIO
HOI
I^-
O_2 (aq)
$\cdot IO_2$
·IO
I_2
HOO·
HO·
·OOI
I·

Fig. 32

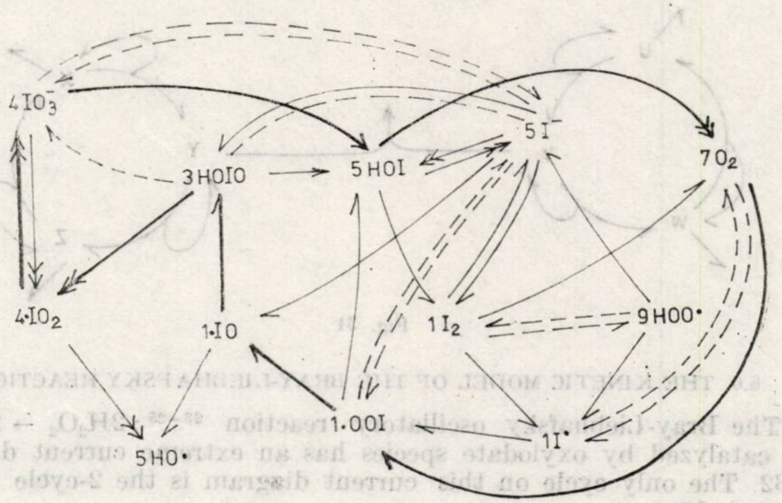
$4IO_3^-$
3HOIO
5HOI
$5I^-$
$7O_2$
$4\cdot IO_2$
1·IO
$1I_2$
9HOO·
1·OOI
1I·
5HO·

Fig. 33

6.7. THE REVERSIBLE BRUSSELATOR MODEL. THE COMPARISON WITH THE REVERSIBLE LOTKA-VOLTERRA MODEL

Recently experimental examples have been published for cubic autocatalysis like that in the Brusselator model of the Belousov-Zhabotinskii reaction. The Brusselator model consists of the following reversible reactions :

$$A \rightleftarrows X;\quad 2X + Y \leftrightarrows 3X;\quad X \leftrightarrows Y + D;\quad X \leftrightarrows E, \qquad (6.16)$$

in which A, D, E are superabundant species with concentrations constant in time. The pseudoreactions of the Brusselator model are :

$$\overset{1}{\underset{4}{\leftrightarrows}} X;\quad 2X + Y \overset{2}{\underset{5}{\leftrightarrows}} 3X;\quad X \overset{3}{\underset{6}{\leftrightarrows}} Y, \qquad (6.17)$$

The stoechiometric matrix has a column for each reaction and a row for the species X and Y :

$$\nu = \begin{pmatrix} 1 & 1 & -1 & -1 & -1 & 1 \\ 0 & -1 & 1 & 0 & 1 & -1 \end{pmatrix} \qquad (6.18)$$

The extreme current matrix is :

$$\mathbf{E} = \begin{pmatrix} 0 & 1 & 0 & 0 & 0 \\ 1 & 0 & 1 & 0 & 0 \\ 1 & 0 & 0 & 1 & 0 \\ 0 & 1 & 0 & 0 & 0 \\ 0 & 0 & 1 & 0 & 1 \\ 0 & 0 & 0 & 1 & 1 \end{pmatrix} \qquad (6.19)$$

The diagram of the extreme currents for the reversible Brusselator model is shown in Fig. 34 and is composed of two diagrams of the currents for the Brusselator model with irreversible reactions (Fig. 35). The extreme currents for the reversible Brusselator model are shown in Fig. 36.

In parallel let us show the current diagrams and the extreme current diagrams for the reversible Lotka-Volterra model :

$$A + 2X \rightarrow 3X;\; X + Y \rightarrow 2\,Y;\; Y \rightarrow B, \qquad (6.20)$$

The current diagram is in Fig. 37, and the extreme currents are in Fig. 38.

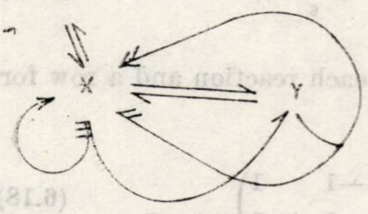

Fig .34

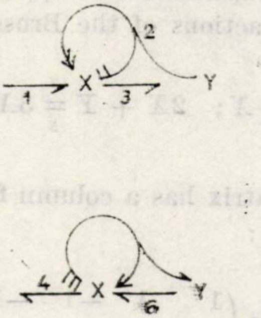

Fig. 35

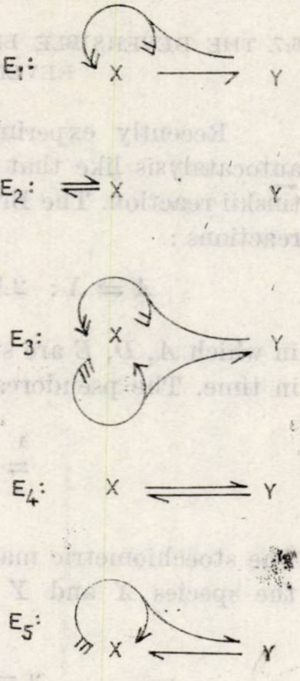
E1:
X
Y
E2:
X
Y
E3:
X
Y
E4:
X
Y
E5:
X
Y

Fig. 36

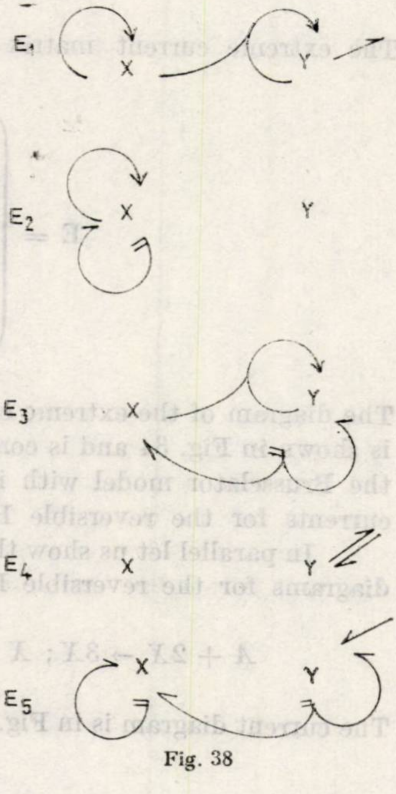
E1
X
Y
E2
X
Y
E3
X
Y
E4
X
Y
E5
X
Y

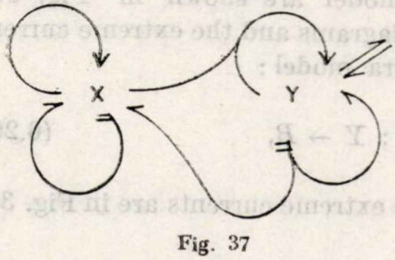

Fig. 37

Fig. 38

7. THE CONNECTION BETWEEN THE METHODS OF DEDUCTION OF THE NECESSARY LINEARIZED STABILITY CRITERION OF THE KINETIC POLYNOMIAL MODELS AND THE DEMONSTRATION OF THE RULES OF MASON AND COATES ON FLOW GRAPHS

As has been mentioned above the method utilized for establishing the topological Routh-Hurwitz stability criterion : the presence of cycles on the current diagrams is used also in the demonstration of the rules of Mason and Coates for solving systems of linear algebraic equations represented by flow graphs.[26] The equivalent valuation which represents the solution of the linear system is expressed by determinants formed by the valuations of the edges and loops of the flow graphs.

The changes in the form of the linear equations correspond to flow graph transfiguration and the solution of the system of linear algebraic equations is done by successive transfigurations of the flow graph or by the rules of Mason and Coates, without using directly Cramer's rules. Cramer's rules appear however in the demonstration of the validity of these rules. Similarly in the kinetic stoechiometric systems it is of interest not to solve directly the linearized equations but to express the coefficients of the secular equations and the Hurwitz determinants.

A system of algebraic equations with n unknowns :

$$\sum_{j=1}^{n} a_{ij}x_j = b_i, \quad i = 1, \ldots, m \tag{7.1}$$

can be written :

$$b_i x_0 - \sum_{j=1}^{n} a_{ij}x_j = 0, \quad i = 1, \ldots, m$$

where $x_0 = 1$ is called an independent entrance variabile. By introducing a zero variable $N_i = 0$ for each equation the system becomes :

$$N_i = \sum_{j=1}^{n} t_{ji}x_j, \quad i = 1, \ldots, m \tag{7.2}$$

where $t_{0i}x_0 = b_i$, $t_{ji} = -a_{ij}\,(i = 1, \ldots, m)$. The system of equations is equivalent to : $N_i = 0$, $i = 1, \ldots, m$ and is represented by a bipartite flow graph of type N (Fig. 39). These graphs correspond also to the interconnected energetic systems, REI,[27] with synchronous generators at x_i and the loads on the edges between the variables tension x_i, and the nodes N_i. The relation $N_i = 0$ expresses the current Kirchhoff's rule.

The graphs of the stoechiometric kinetic systems resemble another type of flow graphs, those of type C which derive from the type N graphs by superposing each exit node N_i over an entrance node x_j corresponding to an unknown, so that the superposition of the pairs exhausts all nodes excepting the entrance node x_0. One can obtain thus $n\,!$ graphs C from a given N-graph but usually one superposes the nodes with the same index.

A C-graph contains a single source node x_0 and n double transit nodes $x_j \leftrightarrow N_j$. In general to each transit node corresponds a self-loop of valuation t_{jj}. The linear system is reordered as:

$$\sum_{j=1}^{n} t_{ji} x_j = 0, \quad i = 1, \ldots, m \tag{7.3}$$

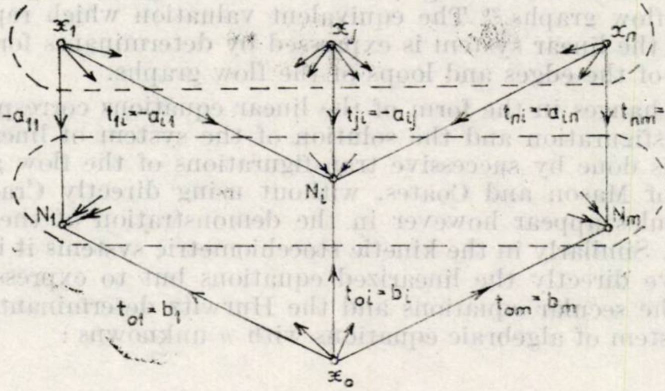

x_1
x_j
x_n
$t_{11}=-a_{11}$
$t_{1i}=-a_{i1}$
$t_{ji}=-a_{ij}$
$t_{ni}=-a_{in}$
$t_{nm}=-a_{mn}$
N_i
N_1
N_m
$t_{0i}=b_i$
$t_{01}=b_1$
$t_{0m}=b_m$
x_0

Fig. 39

where $x_0 = 1$ is the independent entrance variable, x_j the unknowns and the valuations $t_{0i}x_0 = b_i$, $t_{ji} = -a_{ij}$. The C-graphs is drawn in Fig. 40. The nodes x_j and N_j that compose a double node n_j are only superposed. A double node reduces to a simple node if one removes the eigenvaluation

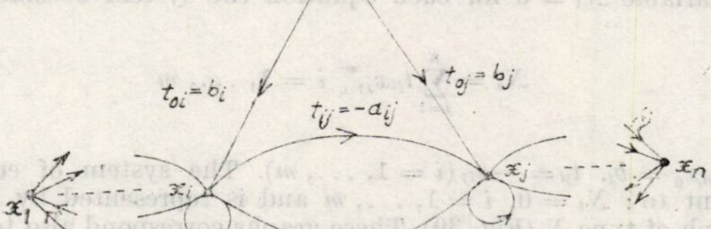

x_0
$t_{0i}=b_i$
$t_{0j}=b_j$
$t_{ij}=-a_{ij}$
x_1
x_i
x_j
x_n
$t_{ii}=-a_{ii}$
$t_{ji}=-a_{ij}$
$t_{jj}=-a_{jj}$

Fig. 40

of the node and divides the valuations of all the other branches that enter in the node with $(-t_{ii})$ what is equivalent with expliciting the equation i of the system with respect to the variable x_i:

$$N_i = t_{ii}x_i + \sum_{j=0,\, j\neq i}^{n} t_{ji}x_j = 0, \quad x_i = \sum_{j=0\, j\neq i}^{n} \left(-\frac{t_{ji}}{t_{ii}}\right) x_j \tag{7.4}$$

A C-graph can be solved by transfiguration to the form in Fig. 41 for which the unknowns result directly: $x_i = T_{0i} x_0$, $i = 1, \ldots, n$ where T_{0i} is called the equivalent valuation from the node x_0 to the node x_i.

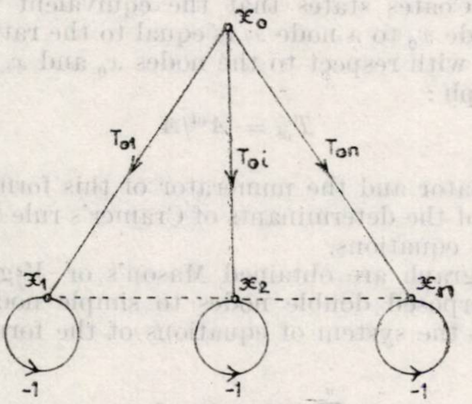

Fig. 41

The topological formula of Coates uses the following notions: The cyclic covering a_j $(j = 1, \ldots)$ of a C-graph is a set of disjoint loops that contain all the nodes except the source node. The valuation of a cyclic covering of a C-graph is equal to the product of the cyclic valuations of the loops that compose it

$$A_j = \prod_{b_h \in a_j} \bar{B}_h = (-1)^{n_j} \prod_{b_h \in a_j} B_h = (-1)^{n_j} \prod_{l_k \in a_j} t_k \tag{7.5}$$

where n_j is the number of loops that compose the cyclic covering. The cyclic valuation of a C-graph is equal to the sum of the valuations of all its cyclic coverings:

$$A = \sum_{a_j \in \{a|c\}} A_j \tag{7.6}$$

where $\{a|c\}$ is the set of cyclic coverings.

A covering a_{lj}^{0i} $(l = 1, \ldots, j = 1, \ldots)$ of a C graph based on a path C_l^{0i} is composed of the path C_l^{0i} $(l = 1, \ldots)$ from node x_0 to the node x_i and of a set of loops disjoint between them and with respect to the path, which contain together with the path all the nodes of the graph. The valuation of a covering of a C-graph based on a path, denoted A_{lj}^{0i} is equal to the product between the valuation of the path and the cyclic valuation of the loops that compose it:

$$A_{lj}^{0i} = C_l^{0i} \prod_{b_h \in a_{lj}^{0i}} \bar{B}_h = (-1)^{n_j} C_l^{0i} \prod_{b_h \in a_{lj}^{0i}} B_h \tag{7.7}$$

The valuation of a graph with respect to a path C_l^{0i} is equal to the sum of the valuations of all coverings of the graph based on the respective path.

The valuation of a C-graph with respect to the nodes x_0 and x_i is equal to the sum of the valuations of the graph with respect to all paths from the node x_0 to the node x_i.

The rule of Coates states that the equivalent valuation T_{0i} of a C-graph from a node x_0 to a node x_i is equal to the ratio between the valuation of a graph with respect to the nodes x_0 and x_i and the cyclic valuation of the graph :

$$T_{0i} = A^{0i}/A \tag{7.8}$$

The denominator and the numerator of this formula give the topological expression of the determinants of Cramer's rule for solving systems of linear algebraic equations.

Out of a C-graph are obtained Mason's or M-graphs by transforming all the superposed double nodes to simple nodes. The M-graphs (Fig. 42) represent the system of equations of the form :

$$x_j = \sum_{i=1}^{n} t_{ij} x_i, \quad j = 1, \ldots, n \tag{7.9}$$

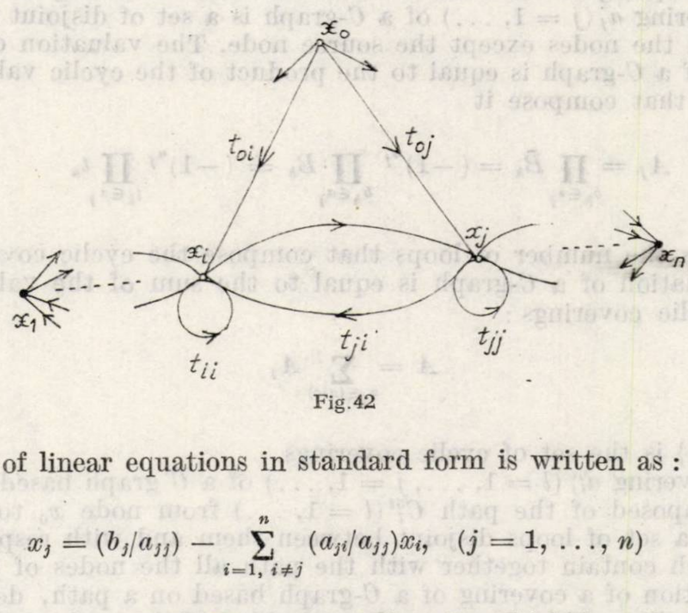

Fig.42

A system of linear equations in standard form is written as :

$$x_j = (b_j/a_{jj}) - \sum_{i=1,\ i\neq j}^{n} (a_{ji}/a_{jj}) x_i, \quad (j = 1, \ldots, n) \tag{7.10}$$

a form that leads to the M-graph of Fig. 43, which has the advantage that it does not contain self-loops, or to the M-graph of Fig. 44 which represents the system written in the form :

$$x_j = b_j + (1 - a_{jj}) x_j - \sum_{i=1,\ i\neq j}^{n} a_{ji} x_i, \quad j = 1, \ldots, n \tag{7.11}$$

The rule of Mason is formulated just as the rule of Coates, denoting the valuations of the graph by D^{oi}, what leads to topological expressions for the determinants from Cramer's rule, and is proved just as the topological formulas for the Hurwitz determinants. The number of terms can greatly exceed that for *C*-graphs but becomes equal to this by removing all self loops.

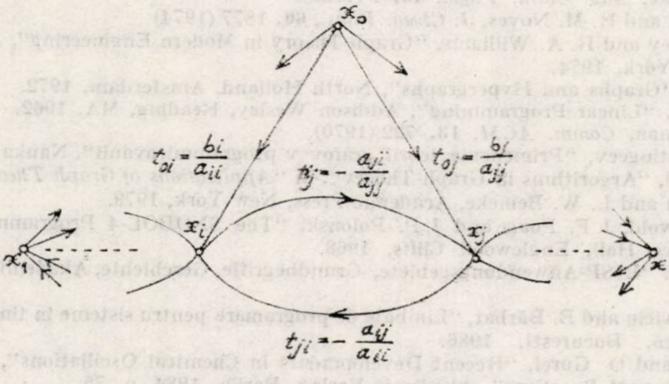
x_o
$t_{oi} = \frac{b_i}{a_{ii}}$
$t_{oj} = \frac{b_j}{a_{jj}}$
$t_{ij} = -\frac{a_{ji}}{a_{jj}}$
x_i
x_j
x_1
x_n
$t_{ji} = -\frac{a_{ij}}{a_{ii}}$

Fig. 43

The use of the *C* and *M* flow graphs has the advantage that it dodges the calculation of the nul terms of the expansion of the determinants of Cramer's rule.

The implementation of the rules of Mason and Coates on a computer is done by using the algorithm of generation of cycles in digraphs proposed above. This method can lead also to the determination of the trees of a graph by the ordered formation of the loops and their opening with restrictions, or by the alternative method of the algebra of structural numbers.

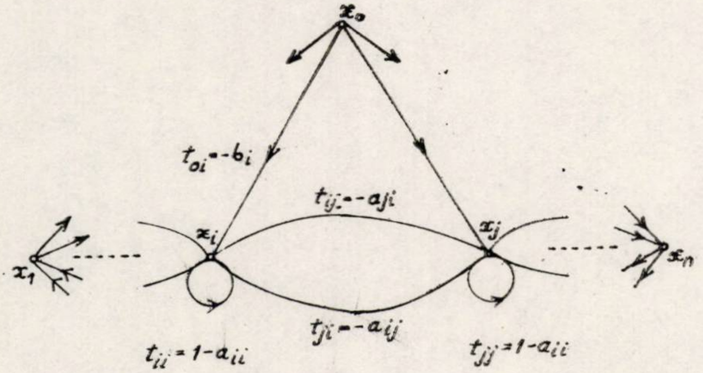
x_o
$t_{oi} = -b_i$
$t_{ij} = -a_{ji}$
x_i
x_j
x_1
x_n
$t_{ji} = -a_{ij}$
$t_{ii} = 1 - a_{ii}$
$t_{jj} = 1 - a_{ii}$

Fig. 44

The flow graph method also permits the description of the sensitivities of the circuit functions with respect to any parameter of the circuit and hence also the sensitivity of the stability property of chemical systems.

REFERENCES

[1] D. Cartianu, "Synchronization Phenomena in Reaction-Diffusion Systems", *Teubner Texte zur Physik*, Vol. 8, B. G. Teubner Verlagsgesellschaft, Leipzig, 1986, 283 p.

[2] D. Cartianu, *Rev. Roumaine Chim.*, **31**, 175 (1986).

[3] D. Cartianu, *Rev. Roumaine Chim.*, **32**, 369 (1987).

[4] B. L. Clarke, *Adv. Chem. Phys.*, **43**, 1 (1980).

[5] R. J. Field and R. M. Noyes, *J. Chem. Phys.*, **60**, 1877 (1974)

[6] E. J. Henley and R. A. Williams, "Graph Theory in Modern Engineering", Academic Press, New York, 1974.

[7] C. Berge, "Graphs and Hypergraphs", North Holland, Amsterdam, 1972.

[8] G. Hadley, "Linear Programming", Addison Wesley, Reading, MA, 1962.

[9] J. C. Tiernan, *Comm. ACM*, **13**, 722 (1970).

[10] V. A. Evstingeev, "Primenenie teorii grafov v programmirovanii", Nauka, Moscow, 1985.

[11] R. C. Read, "Argorithms in Graph Theory", in "*Applications of Graph Theory*", eds., R. J. Wilson and L. W. Beineke, Academic Press, New York, 1979.

[12] R. E. Griswold, J. F. Poage and I. P. Polonski "The SNOBOL-4 Programming Language", Prentice Hall, Englewood Cliffs, 1968.

[13] H. Stoyan. "LISP-Anwendungsgebiete, Grundbegriffe, Geschichte, Akademie-Verlag, Berlin 1980.

[14] A. Davidoviciu and B. Bărbat, "Limbaje de programare pentru sisteme în timp real" Editura Tehnică, București, 1986.

[15] D. Gurel and O Gurel, "Recent Developments in Chemical Oscillations", in "*Oscillations in Chemical Reactions*", Akademie-Verlag, Berlin, 1984, p. 75.

[16] O. Gurel and D. Gurel, "Types of Oscillations in Chemical Reactions", Ibid., p. 1.

[17] R. J. Field, E. Körös and R. M. Noyes, *J. Amer. Chem. Soc.*, **94**, 8649 (1972).

[18] J. J. Iwo and R. M. Noyes, *J. Amer. Chem. Soc.*, **97**, 5422, 5431 (1975).

[19] H. Farkas and Z. Noszticius, *J. Chem. Soc. Faraday Trans.* II, **81**, 1487 (1985).

[20] A. Lotka, *J. Phys. Chem.*, **14**, 271 (1910).

[21] R. M. Noyes, *J. Chem. Phys.*, **80**, 6071 (1984).

[22] M. Eigen and P. Schuster, "The Hypercycle, A Principle of Natural Selforganization", Springer, Wien 1979.

[23] W. C. Bray, *J. Amer. Chem. Soc.*, **43**, 1262 (1921).

[24] H. A. Liebhafsky, *J. Amer. Chem. Soc.*, **53**, 896, 2074 (1931).

[25] K. R. Sharma and R. M. Noyes, *J. Amer. Chem. Soc.*, **97**, 202 (1975), **98**, 4345 (1976).

[26] M. N. S. Swamy and K. Thulasiraman, "Grafy, seti i algoritmy", Mir, Moscow, 1984.

[27] P. Dimo, "Nodal Analysis of Power Systems", Abacus Press, Tunbridge Wells, Kent, 1975.

Revue Roumaine de Chimie, **33**, *5*, 525–532 (1988)

A CORRELATION OF THE REACTIVITY OF SOME SUBSTITUTED PHENOXIDE IONS*

AHMED M. G. NASSAR, MOHAMED A. KHARABA and ABDEL-HAMID A. YOUSSEF
Department of Chemistry, Faculty of Science, Alexandria University, A. R. Egypt

Received December 13, 1986

The reaction of fourteen different mono- and disubstituted phenoxide ions with 1-chloro-2,4-dinitrobenzene, in methanol was investigated. A satisfactory correlation between the nucleophilicity of the phenoxides and their substituent constants was found. Values of $\bar{r}$ were used to interpret the results.

INTRODUCTION

The intermediate complex mechanism for activated aromatic nucleophilic substitution reactions is well reviewed and documented.[1] All previous works on aromatic nucleophilic substitution reactions of phenoxide ions with halogeno-aromatic compounds were those with one substituent on the phenoxide rings. Thus, Ryan and Humffray [2] studied the reaction of picryl chloride with some *o*- and *p*-substituted phenoxide anions and anilines. They reported that with electron withdrawing substituents in the *p*-position, the usual Hammett σ-values do not correlate well with the rate of the aromatic substitution, although with *m*-substitution they do. The correlation with *p*-substituents was improved, however, by using the Yukawa-Tsuno equation [3] in the appropriate form as:

$$\log k/k_0 = \rho[\sigma + r^-(\sigma^- - \sigma)] \qquad (1)$$

The quantity r^- is the reaction constant measuring the magnitude of the negative charge stabilised at the transition state. Ryan et al.,[2] reported values of 0.2 and 0.3 for r^- in the alkaline hydrolysis of aryl acetates and benzoates, respectively, indicating only a small extent of bound breaking (release of phenoxide ion), in the transition state. On the other hand, values of 0.94 and 0.68 were reported for r^- in the reaction of picryl chloride with phenoxide ions and anilines, respectively, which suggest that considerable bond formation has occurred in the transition state. To the best of our knowledge, there has been no investigation of the effect of disubstituted phenols on the nucleophilicity of the ions derived from them.

---

* Presented at the Second EUCHEM Conference on Correlation Analysis in Organic Chemistry, held at the University of Hull, England, July, 1982.

In this work, we have investigated the nucleophilicity of different mono- and disubstituted phenoxides including substituents in the *ortho*-position towards 1-chloro-2,4-dinitrobenzene. It is the purpose of this study to find a satisfactory correlation between the nucleophilicity of the differently substituted phenoxides with Hammett σ-values derived from the linear combination of substituents parameters.

In other words, a study of the additivity of substitutent effects in these reactions [4] will be examined. An attempt will also be made to correlate σ-values for *ortho* substituents.[5]

EXPERIMENTAL

M.ps are uncorected, IR spectra were recorded on a Pye-Unicam SP 1100 spectrophotometer, and UV spectra on a Unicam SP 1805 program controller instrument. The NMR spectra of the compounds used in this work were recorded on a Varian 90 spectrometer. The microanalyses were done at Cairo University Microanalytical Laboratoires.

a) Preparation of Materials

i) 1-Chloro-2,4-dinitrobenzene : The pure BDN compound was recrystallised from methanol to a constant m.p. 54°.

ii) Phenol and its mono-, and disubstituted derivatives are BDH quality and were either fractionally distilled under reduced pressure to a constant b.p. or crystallised from the appropriate solvent to a constant m.p.

iii) Methanol : A.R. grade of methanol was purified by the standard methods.[6]

b) Kinetic Measurements

The kinetic runs were carried out using equimolar quantities of the nitroaromatic compound and the phenoxide ions, together with a tenfold excess of the corresponding free phenol The reactions were followed potentiometrically by monitoring the chloride ion formed.[7] Rate constants were measured at three different temperatures over a range of 30—45° for each compound. At least two to three runs were conducted until reproducible results were obtained. The values of k_2 and the Arrhenius parameters were computed using the Computer facilities of Brunel University (England) to whom we express our gratitude.

c) Reaction Products

The sole products obtained in more than 90 % yield, from the reaction of 1-chloro-2,4-dinitrobenzene with the appropriate phenoxide ions, were the corresponding monosubstituted phenyl-2,4-dinitrophenyl ethers identified by spectroscopic methods [8] and elemental analyses. The following procedure is adopted for the reaction products : 1-chloro-2,4-dinitrobenzene, (10 mmoles), in 10 mL of methanol was added to equimolar amounts of the appropriate phenoxide (prepared from the phenol and KOH) in 20 mL methanol and refluxed for 10 hours. Addition of water to the reaction mixture precipitated the ether, which was washed with dilute KOH solution to free it from excess phenol, filtered and crystallised from the appropriate solvent.

Table 1 lists the physical constants of the isolated ethers and the elemental analyses of the new ones.

Table 1

The physical properities and analyses of the new substituted phenyl-2,4-dinitrophenyl ethers

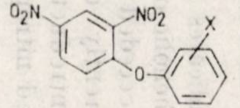	[1] m.p.	UV (in Ethanol)		IR(cm^{-1})			^1H—NMR. (in $CDCl_3$)		Analyses		
		λ_{nm}	ε	ν_{CH}	ν_{NO_2}	ν_{C-O-C}	[2] δ_H	δ_{CH_3}	% C calcd. 48.90	% H 2.82	% N 13.16
X =											
2-NO_2-3-CH_3	155	213 233 278	37,216 29,241 23,393	3100	1550 1355	1280	7.6	1.3	48.7	2.50	12.7
2-NO_2-4-CH_3	179	213 250 278	13,426 9,304 7,841	3100	1545 1350	1280	7.5	1.05	48.9	2.70	12.9
2-NO_2-5-CH_3	158	218 269	32,354 28,001	3120	1525 1360	1281	7.65	1.51	48.9	2.80	12.7
4-NO_2-3-CH_3	128	210 285	58,483 46,786	2110	1540 1355	1265	7.65	1.55	48.7	2.60	12.6

[1] Crystallised from ethanol-benzene. [2] For the most (deshielded) proton on the aromatic nucleus.

RESULTS AND DISCUSSION

The rate constants for the reaction of a total of fourteen differently substituted phenoxide ions with 1-chloro-2,4-dinitrobenzene in methanol were determined by following potentiometrically the liberation of the chloride ion. The reaction showed reproducible second order kinetics and the rate constants are unchanged on increasing the proportion of the phenol. Table 2 lists the computed reaction rate constants as well as the activation parameters.

The Monosubstituted Series. Inspection of the results shows that nuclear substituents on the aromatic ring have a pronounced effect on the nucleophilicity of the phenoxides. As expected, the introduction of an electron releasing substituent increases the rate, whereas an electron withdrawing one decreases the rate. The former substituent increases the electron density on the oxygen of the phenoxide ion, whereas the latter decreases the electron density (cf. Table 2).

Thus, a methyl group in the *o*-, or *p*-position almost doubles the rate, due to the +I and +T effects. A nitro group, on the other hand causes a large decrease in the rate especially in the *p*-position due to the strong resonance interaction between the nitro group and the negative charge on the oxygen. Thus, the unsubstituted phenoxide ion is $\simeq 500$ times faster than the *p*-nitro derivative and 2 times as fast as the *m*-substituted one. A similar rate ratio was reported earlier by Ryan and Humffray, for the reaction of *p*- and *m*-nitro phenoxides with picryl chloride.[2] The rate with *p*-halogeno substituents (Cl or Br) is 0.4 and 0.3 times the rate of the unsubstituted member due to the contribution of the -I effect.

With the mono-substituted phenoxide ions, the ordinary Hammett σ-relationship[9] was found to describe satisfactorily the behaviour of *m*-substituents used in this study with the exception of the *p*-nitro group (Fig. 1). The use of the exalted value $(\sigma)^-$ for the nitro-substituent, however, is necessary and accordingly it lies on the correlation line. The justification for the use of σ- is clearly seen from the fact that the calculated values of r^- from the Yukawa-Tsuno equation,[3] eqn. 1(with $\rho = -2.08$, slope of the plot obtained from the *m*- and electron releasing *p*-substituents) vs. log k_2 are found to be r^- 1.02 and 0.99 for the *p*-nitro and *o*-nitro-substituents, respectively.

A large value of the coefficient r^- indicates that in the transition state the formation of the bond from the phenolic oxygen to the activated nuclear carbon of the substrate has preceded to a marked extent.

The Disubstituted Series: Four differently disubstituted phenols were chosen to study the effect of further introduction of a methyl group on the nucleophilicity of the already studied nitrophenoxides. The com-

Table 2

Rate constants and activation parameters for the reaction between substituted phenoxide ions and 2,4-dinitrochlorobenzene in methanol

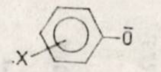	10^4 $k_2$dm^{3}mole^{-1} s^{-1}				10^4k_2 303.15	*Ea* kJ mole^{-1}	log *A*	ΔH^* kJ mole^{-1}	$-\Delta S^*$ kJ mole^{-1}	ΔF^* kJ mole^{-1}	C.C
	30.2°	35.2°	40.2°	45.2°							
X =											
H	27.20	41.60	668.40		42.63	72.77	9.96	70.21	62.72	84.54	0.99852
$2-CH_3$	43.60	73.50	118.60		72.46	79.02	11.25	76.46	38.03	88.18	0.99988
$3-CH_3$	32.60	53.40	41.30		54.19	81.28	11.51	78.72	33.10	88.93	0.99945
$4-CH_3$	55.20	83.00	144.50		87.19	75.91	10.80	73.34	46.59	87.76	0.99530
$2-Cl$	2.03	3.64	5.86		3.51	84.02	10.78	81.45	47.00	95.94	0.99867
$4-Cl$	9.79	16.70	27.40		16.49	81.22	10.98	78.66	43.20	91.97	0.99995
$2-Br$	2.02	3.64	5.86		3.51	84.02	10.78	81.54	47.00	95.93	0.99867
$4-Br$	7.39	12.85	22.45		12.87	87.75	11.98	85.18	24.09	92.60	0.99995
$2-NO_2$		0.124	0.191	0.276	0.12	65.26	6.16	62.70	135.62	104.49	0.99934
$3-NO_2$		2.051	3.051	4.441	2.043	63.02	6.99	60.45	119.63	97.32	0.99980
$4-NO_2$		0.091	0.147	0.212	0.092	69.00	6.66	66.43	125.99	105.24	0.99763
$2-NO_2-3-CH_3$		0.455	0.858	1.240	0.472	81.85	9.55	74.29	70.70	101.07	0.98981
$2-NO_2-5-CH_3$		0.187	0.354	0.537	0.192	86.10	9.88	83.54	64.38	103.37	0.99378
$2-NO_2-4-CH_3$		0.314	0.564	0.884	0.318	84.45	9.82	81.39	65.55	102.08	0.99777
$4-NO_2-3-CH_3$		0.225	0.425	0.723	0.227	95.22	11.49	92.65	33.42	102.95	0.99910

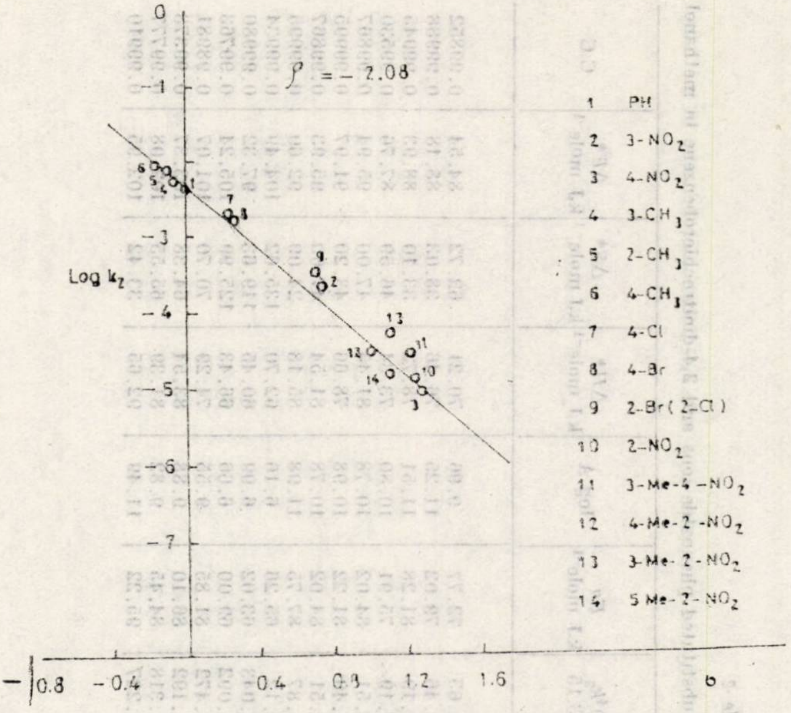

Fig. 1. — The Hammett plot.

pounds chosen include 2-nitro-3-methyl, 2-nitro-4-methyl, 2-nitro-5-methyl and 4-nitro-3-methyl-phenoxide (Scheme 1).

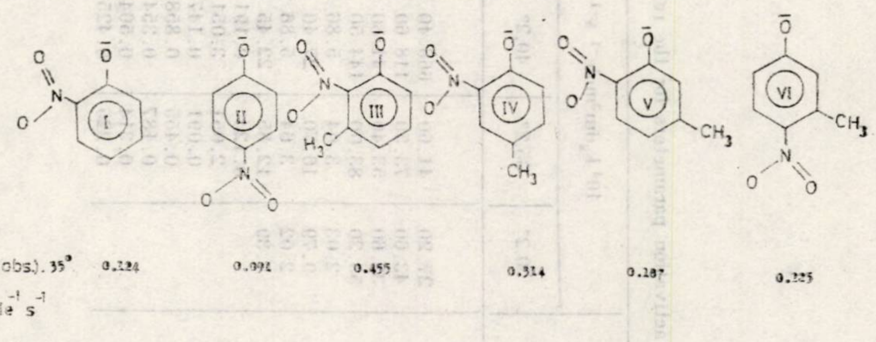

	I	II	III	IV	V	VI
$10^4 . k_2$(obs.). 35° $dm^3\ mole^{-1}\ s^{-1}$	0.224	0.092	0.455	0.314	0.187	0.225
$10^4 . k_2$ (calc.) $dm^3\ mole^{-1}\ s^{-1}$			0.173	0.279	0.173	0.163
Value of r^-	0.990	1.020	0.520	0.930	0.950	0.780
$k_{obs.} / k_{calc.}$			2.6	1.1	1.1	1.4

SCHEME 1

The r^- values calculated for the *o*-nitro-, and *p*-nitrophenoxide are 0.99 and 1.02 respectively, which suggest a large resonance interaction between the nitro group and the O^- of the phenoxide as a result of complete coplanarity of the nitro group and the benzene ring. The introduction of the methyl group at the 3-position in the 2-nitrophenoxide ion (III) causes a 3.8 times increase in rate. This is apparantely due to the inhibition of resonance of the nitro group at the 2-position with the ring, and thus, a more localised negative charge on the oxygen leading to an increase in the nucleophilicity and hence in the rate. A less increase in rate is observed, however, (2.5 times), when the methyl group is in the 4-position, presumably for the same reasoning for compound (IV). With a methyl group in position 5-, (V), only an increase of 1.5 times is observed due to a possible interaction between the *p*-methyl and the nitro group. In the case of 4-nitro-3-methyl substituent (VI), one observes an increase of 2.5 times in rate which is less than that observed with 2-nitro-3-methyl derivative (III), presumably due to greater interaction between the *p*-nitro group and the negative oxygen of the phenoxide ion.

The observed increase in rates with the four disubstitutes phenoxides can be readily inferred by the inspection of the corresponding r^- values (Scheme 1), that reflect the degree of resonance interaction between the nitro group and the phenoxide oxygen, and accordingly the reactivity of the phenoxide. The lowest value of $r^- = 0.52$ is observed with (III), where, the nitro group is sterically hindered[10] with the methyl group and cannot attain coplanarity with the ring and hence the highest value of $k_{obs.}/k_{calc.}$ (2.6). The r^- value for the 2-nitro-4-methyl compound, (IV) and 2-nitro-5-methylphenoxide, (V), are 0.93 and 0.95 respectively indicating that the nitro group in these cases is nearly exerting its full influence and hence, the observed k_2 is about the same as the calculated, (c. f. Table 1). The r^- is 0.78 for the 4-nitro-3-methylphenoxide, (VI), indicating a decreased resonance interaction between the 4-nitro group and the phenoxide oxygen due to the presence of the 3-methyl substituent.

Activation Parameters

The computed values of the activation parameters are tabulated in table 2. The activation energies are between 95—63 KJ.mole^{-1}, entropies of activation are negative as would be expected for the bimolecular reactions.

The reactiones of 4-, 3- or 2-nitrophenoxides are unusual for their more negative activation entropies 126, 119.5 and 135.6 J mole^{-1} K^{-1} respectively. These phenoxides are different from the others, since the formal negative charge on the oxygen of the phenoxide anions may be delocalised over a greater part of the ion than is the case of the other ions. Thus, solvation of the ions is reduced and there is less freeing of the solvent in the passage from the reactant to the transition state. The activation entropies are therefore more negative than for the other ions.

REFERENCES

[1] J. F. Bunnett, *Quart. Rev.*, **12**, 1, (1958); J. F. Bunnett, *Ann. Rev. Phys. Chem.*, **14**, 271 (1963).

[2] J. J. Ryan and A. A. Huffray, *J. Chem. Soc.*, **1967**; 1300, *ibid.*, **1967**, 468.

[3] a) Y. Tsuno, T. Isabata and Y. Yukawa, *Bull. Chem., Soc. Japan*, **32**, 965, 969, 971 (1959).
b) Y. Yukawa, Y. Tsuno and M. Sawada, *Bull. Chem. Soc. Japan*, **39**, 2274 (1966).

[4] J. Shorter in "Correlation Analysis in Chemistry Recent Advances", Edited by N. B. Champman and J. Shorter, Plenum Press, New York, 1978.

[5] J. Clark and P. O. Perrin, *Quart. Rev.*, **18**, 295 (1964).

[6] A. I. Vogel, "Practical Organic Chemistry", Longmans, 1959.

[7] M. A. Kharaba, M. Sc. Thesis, Alexandria University, 1982.

[8] P. P. A. Lehmann, *Anal. Chim. Acta*, **54**, 321 (1971).

[9] L. P. Hammett, "Physical Organic Chemistry". McGraw-Hill, New York, 1971.

[10] A. M. G. Nassar and R. Tawfik, *Egypt J. Chem.*, **18**, 361 (1973).

Revue Roumaine de Chimie, **33**, *5*, 533–536 (1988)

SYNTHESIS AND STRUCTURAL CHARACTERIZATION OF Cr(III) AND COBALT (III) COMPLEXES WITH TEREPHTHALIC ACID HYDRAZIDE SCHIFF BASES

SURESH K. AGARWAL* and D. R. TUTLANI
Chemistry Department, L.R. Post-Graduate College, Sahibabad (Ghaziabad), India

Received November 24, 1986

Polymeric 1 : 1 complexes of Cr(III) and Co(III) with terephthalic acid hydrazide-bis-salicylidene (THBS), terephthalic acid hydrazide-bis-2,3,4-trihydroxy phenacylidene (THTP) and terephthalic acid hydrazide-bis-2-hydroxy-5-carboxy phenacylidene (THHCP) have been synthesized. Based on elemental analysis, molar conductivity and reflectance and infrared spectral data, distorted octahedral and octahedral structure have been assigned to Cr(III) and (Co(III) complexes respectively. The values of 10 Dq, β, β and L.F.S.E. have also been calculated.

INTRODUCTION

Complexes of 2-thiooratic acid with Cr(III) have been prepared by Pandey, Nigam and Agarwal.[1] The ternary complexes of chromium nitrilo triacetate with acetylacetone, phenanthroline, dipyridyl oxalate, halide ions,[2-4] amino acids[5] and heterocyclic amines[6] have been synthesised and studied on the basis of physico-chemical methods. The co-ordination chemistry of trivalent ions viz. Cr(III) and Co(III) involving multidentate ligands has received limited attention. In the present paper we report the Cr(III) and Co(III) chelates of terephthalic acid hydrazide Schiff bases.

EXPERIMENTAL

All the reagents used were of AR Grade. Solvents were purified before use.

Synthesis and isolation of Cr(III) complexes with terephthalic acid hydrazide-bis-salicylidene terephthalic acid hydrazide-bis-2, 3, 4-trihydroxy phenacylidene and terephthalic acid hydrazide-bis-2-hydroxy, 5-carboxy phenacylidene

The preparation of ligands has been communicated elsewhere.[7]

The complexes were synthesised by refluxing Cr(III) chloride with the ligand in 1 : 1 molar ratio in an ethanolic medium for 45 min. at 60 – 70°C. On cooling dark black precipitates were obtained. All the compounds were washed with water and ether and dried under vacuum (yield 42 – 45 %).

---

* for correspondence : III-E-7/9, Nehru Nagar, Ghaziabad, INDIA.

Synthesis of Co(III) complexes with THBS, THTP and THHCP

The compounds were prepared by refluxing the mixed solution of Co(III) chloride obtained by the oxidation of $CoCl_2$ with H_2O_2 and the ligand, in ethanol medium (1 : 1 molar ratio) for 30 min. The pH of the solution was maintained at 6.8 by the addition of sodium acetate buffer. The orange yellow precipitates, separated on cooling, were washed with water and ethanol and dried over fused $CaCl_2$.

RESULTS AND DISCUSSION

All the complexes of Cr(III) and Co(III) are nonhygroscopic and stable at room temperature. The compounds are insoluble in common organic solvents. They are nonelectrolytes in nature as evidenced by their low conductivity in DMSO. On adding alcoholic silver nitrate, no precipitate appeared, indicating the participation of chlorine in coordination sphere. All the compounds start to decompose above 120°C. The mass loss observed at 125° C was corresponding to the elimination of one water molecule, indicating the presence of co-ordinated water. Analytical data of the complexes reported in Table 1 correspond to the formulae $ML\,Cl.H_2O$.

Table 1

Analytical and conductivity data of Cr(III) and Co(III) complexes with THBS, THTP and THHCP

Compounds	Found (Calcd.) %					Colour	Conductivity Δ_M $(Ohm^{-1}cm^2mol^{-1})$
	Metal	C	H	N	Halogen		
$Cr\,L\,Cl.H_2O$	10.08 (10.28)	50.03 (52.22)	3.41 (3.56)	10.82 (11.07)	7.01 (7.02)	Black	2.8
$Cr\,L'Cl.H_2O$	8.61 (8.70)	46.99 (48.20)	3.42 (3.68	9.19 (9.37)	5.91 (5.94)	Black	2.6
$Cr\,L''Cl.H_2O$	8.06 (8.36	48.29 (50.20)	3.61 (3.53)	9.20 (9.01)	5.80 (5.71)	Black	3.4
$Co\,L\,Cl.H_2O$	11.48) (11.50)	49.36) (51.51)	3.48 (3.51)	10.38 (10.92)	6.63 (6.92	Orange yellow	2.3
$Co\,L'\,Cl.H_2O$	10.13 (9.74)	48.36 (47.64)	3.73 (3.63)	9.88 (9.26)	5.98 (5.87)	Orange yellow	2.6
$Co\,L''\,Cl.H_2O$	9.20 (9.38)	47.14 (49.64)	3.56 (3.50)	9.10 (8.91)	5.29 (5.64)	Orange yellow	2.2

$L = C_{22}H_{16}N_4O_4$, $L' = C_{24}H_{20}N_4O_8$, $L'' = C_{26}H_{20}N_4O_8$

Magnetic and Reflectance Spectral Studies

Cr(III) Complexes

The present Cr(III) complexes showed magnetic moments 3.78 3.94 and 3.80 B.M., suggesting on octahedral stereochemistry for these complexes.[8,9]

The reflectance spectra of the present complexes showed bands around 21,400, 15,350 cm^{-1} with a shoulder at about 20,100 cm^{-1}. The two bands may be assigned to $^1A_{2g} \rightarrow {}^1T_{1g}$ and $^1A_{2g} \rightarrow {}^1T_{2g}$ transitions respectively. The shoulder around 20,100 cm^{-1} may be due to tetragonal distortion.[10] The values of 10 Dq, β, β, LFSE are calculated and reported in Table 2. Based on spectral data, the complexes are assumed to possess distorted octahedral stereochemistry.

Table 2

Reflectance spectral data and ligand field parameters of Cr(III) and Co(III) complexes with THBS, THTP and THHCP

Compounds	Observed bands	10 Dq (cm^{-1})	β (cm^{-1})	β	L.F.S.E. (kcal/mole)
Cr L Cl. H_2O	21,380 15,360 20,120	21,380	872.65	0.84	73.30
Cr L′ Cl. H_2O	21,400 15,350 20,100	21,400	873.46	0.84	73.37
Cr L″Cl. H_2O	21,420 15,340 20.100	21,420	874.28	0.85	73.44
Co L Cl. H_2O	20,680 23,300	20,680	517,00	0.37	23.63
Co L′ Cl. H_2O	20,700 28,310	20,700	517,50	0.36	23.65
Co L″Cl. H_2O	20,700 28,290	20,700	517.50	0.36	23.65

Co(III) Complexes

The room temperature magnetic moments of all the complexes are found to be in the 0.49–0.51 B.M. range. Low values of magnetic moments are due to low symmetry component.

The reflectance spectra of the complexes exhibit two bands at around 20,700 and 28,300 cm^{-1} due to spin-allowed transitions : $^1A_{1g} \rightarrow 1T_{1g}$ and $^1A_{1g} \rightarrow {}^1T_{2g}$ respectively.[11] On the basis of the position of the bands, octahedral geometry is suggested for these complexes.

IR STUDIES

The main frequency bands observed in the spectrum of the complexes are tabulated in Table 3.

A broad band observed in the range 3520–3460 cm^{-1} in the ligands gets disappeared on complexation, suggesting the replacement of hydrogen of the OH group by the metal ion. This is further verified by the appearance of non-ligand band in the region 375–360 cm^{-1}, assignable to ν(M–O). The involvement of azomethine nitrogens in co-ordination is evidenced by a negative shift (25–35 cm^{-1}) in ν(C=N), appeared in spectra of ligands (1620–1625 cm^{-1}). νM – N band is supported by the appearance of a new band in the region 445–430 cm^{-1}. The frequencies due to νC=O and ν N–H (1645 – 1660, 3300 – 3320 cm^{-1}), observed in the spectrum of ligands, remain almost unchanged in the spectrum of the complexes, indicating non-involvement of these groups in co-ordination. The low frequency band appearing in the range 310–300 cm^{-1}, in the complexes is tentatively assigned to ν(M–Cl) mode. The bands due to ν OH, δ OH and ρ(H_2O) appeared in the region 3475–3500, 1600 – 1620 and 725–730 cm^{-1}, characteristic of coordinated water.

Table 3

IR absorption frequencies (cm^{-1}) of Cr(III) and Co(III) complexes with THBS, THTP and THHCP

Compound	νC=N	νC=O	νN=H	νM–O	νM–N	νCl	νOH	δ_2OH (H_2O)	P(H_2O)
Cr L Cl.H_2O	1595	1665s	3315w	370	440	300m, br	3500	1610	725
Cr L′ Cl.H_2O	1590	1650s	3305w	365	430	305m	3480	1615	730
Cr L″ Cl.H_2O	1595	1660s	3310w	375	445	310m,	3475	1620	725
Co L Cl.H_2O	1590	1640s	3315w	375	440	305m, br	3500	1610	725
Co L′ Cl.H_2O	1595	1660s	3312w	360	430	300m, br	3475	1600	730
Co L″ Cl.H_2O	1585	1650s	3305w	365	435	310m, br	3480	1620	725

s = strong, w = weak, m = medium and br = broad.

REFERENCES

[1] G. S. Pandey, P. C. Nigam and V. Agarwal, *Indian J. Chem.*, **17A**, 74 (1979).
[2] Y. Fuju, E. Kyuno and R. Tsuchiya, *Bull. Chem. Soc. Japan*, **42**, 1301 (1969).
[3] A. Vehara, E. Kyuno and R. Tsuchiya, *Bull. Chem. Soc. Japan*, **40**, 1301 (1967).
[4] A. Vehara, E. Kyuno and R. Tsuchiya, *Bull. Chem. Soc. Japan*, **40**, 2322 (1967).
[5] C. L. Sharma, P. K. Jain and T. K. De *J. Inorg. Nuclear Chem.*, **42**, 168 (1980).
[6] C. L. Sharma, T. K. De and P. K. Jain *Chemica Scripta*, **18**, 79 (1981).
[7] S. K. Agarwal and D. R. Tutlani, *Oriental J. Chem.*, 1986 (in press).
[8] J. Lewis and A. Earnshaw, *Nature*, **181**, 1621 (1958).
[9] B. N. Figgis and J. Lewis, "Modern Co-ordination Chemistry", edited by J. Lewis and R. G. Wilkinson Interscience, New York, 1960, p. 427.
[10] A. B. P. Lever, "Inorganic Electronic Spectroscopy", Elsevier, New York, 1968, p. 275.
[11] F. A. Cotton and R. G. Wilkinson, "Avdanced Inorganic Chemistry", Second Edition, Wiley Eastern Pvt. Ltd., 1966, p. 874.

Revue Roumaine de Chimie, **33**, *5*, 537–545 (1988)

SYNTHESIS AND CHARACTERIZATION OF SOME OXOVANADIUM(IV) COMPLEXES OF OCTAMETHYLPYROPHOSPHORAMIDE AND NONAMETHYLIMIDODIPHOSPHORAMIDE

R. K. AGARWAL* and GYANENDRA SINGH

Department of Chemistry, Lajpat Rai (Post Graduate) College, Sahibabad-201005 (Ghaziabad), India

Received July 19, 1986
Revised November 23, 1987

A series of new complexes of VO(IV) with octamethyl-pyrophosphoramide (OMPA) and nonamethylimido-phosphoramide (NIPA) with the general composition $VOX_2.L$ (L = OMPA or NIPA ; X = Cl, Br, I, NO_3, NCS or 0.5 C_2O_4) and $VO(ClO_4)_2.2L$ (L = = OMPA or NIPA) have been isolated in non-aqueous media. Conductance, molecular weight, magnetic moments, infrared and electronic spectra of the complexes have been reported. IR reveals that the metal is linked to the ligands via O—O chelation.

INTRODUCTION

In the last two decades a number of workers have reported a number of oxovanadium(IV) complexes of neutral oxygen donor ligands.[1-11] Comparatively very little is known about the oxovanadium(IV) complexes with phoshoryl donor ligands such as triphenyl phosphine oxide[1] and hexamethyl phosphoramide.[5] In this view, we wish to report the coordinating abilities of octamethylpyrophosphoramide (OMPA) (I) and nonamethylimido-phosphoramide (NIPA) (II) towards oxovanadium(IV) cations.

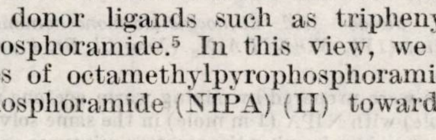

$$(CH_3)_2N-\overset{\overset{O}{\|}}{\underset{\underset{N(CH_3)_2}{|}}{P}}-O-\overset{\overset{O}{\|}}{\underset{\underset{N(CH_3)_2}{|}}{P}}-N(CH_3)_2$$

Octamethyl-pyrophosphoramide (I)

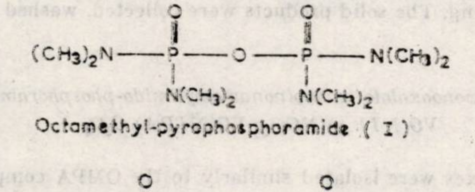

$$(CH_3)_2N-\overset{\overset{O}{\|}}{\underset{\underset{N(CH_3)_2}{|}}{P}}-\underset{\underset{CH_3}{|}}{N}-\overset{\overset{O}{\|}}{\underset{\underset{N(CH_3)_2}{|}}{P}}-N(CH_3)_2$$

Nonamethylimido-phosphoramide (II)

---

* Author to whom all correspondence should be addressed.

EXPERIMENTAL

Materials

Various oxovanadium(IV) salts were prepared using the literature methods.[10-12] Oxovanadium (IV) nitrate was prepared by treating $VOCl_2$ with silver nitrate and the blue solution obtained was used directly for synthesis. The ligand OMPA was obtained from Koch and Light and was used as received, while, the ligand NIPA was prepared by the reported methods.[13-14]

Preparation of the Complexes

(a) *Dichloro-dibromo and diiodomono(octamethyl-pyrophoshoramide)oxovanadium(IV),*
$VO(OMPA)Cl_2$, $VO(OMPA)Br_2$ and $VO(OMPA)I_2$

These complexes were prepared by the following general procedure. The ligand (1 mmole) dissolved in acetone (25 mL) was added to the freshly prepared metal salt (1 m mole in 20 mL of acetone). A dehydrating agent 2,2′-dimethoxypropane (10 mL) was added in each case. The mixture was refluxed for about an hour before concentrating it to half of its volume. On cooling, gren crystals obtained were recrystallized from acetone.

(b) *Dithiocyanato and dinitratomono-(octamethyl-pyrophosphoramide)oxovanadium(IV),*
$VO(OMPA)(NCS)_2$, $VO(OMPA)C_2O_4$ and $VO(OMPA)(NO_3)_2$

The corresponding oxovanadium(IV) salt (1 mmole) dissolved in acetone (25 mL) was mixed with the hot solution of OMPA (1 mmole) in acetone (30 mL). 2,2′-Dimethoxypropane (10 mL) was added to the reaction mixture to remove water. The reaction contents were refluxed for about 0.5 hr. The mixture was concentrated to one half of its volume and on cooling its green crystals were obtained. These crystals were dried in vacuo over P_4O_{10}.

(c) *Diperchlorato bis(octamethyl-pyrophosphoramide)oxovanadium(IV), $VO(OMPA)_2(ClO_4)_2$*

Oxovanadium(IV) perchlorate (1 mmole) dissolved in acetone (10 mL) was mixed with the ligand (2 mmole in 10 mL) and the mixture was refluxed for about 0.5 hr in the presence of 2,2′-dimethoxypropane (5 mL). The complex was isolated by the method outlined in (a). It was dried over P_4O_{10} in vacuo.

(d) *Dichloro-, dibromo-, diiodo- and dithiocyanato-mono(nonamethylimido-phosphoramide)*
oxovanadium(IV), $VO(NIPA)X_2$ ($X = Cl, Br, I$ or NCS)

All these complexes were prepared by mixing warm acetone solution (20 mL) of oxovanadium (IV) salts (1 m mole) with NIPA (1 m mole) in the same solvent (20 mL). The precipitation of the complexes occurred on keeping the reaction mixtures on water bath for 10 minutes under vigorous stirring. The solid products were collected, washed with ether and dried in vacuo over P_4O_{10}.

(e) *Dinitrato and monooxalato mono(nonamethylimido-phosphoramide)oxovanadium(IV),*
$VO(NIPA)(NO_3)_2$, $VO(NIPA)C_2O_4$

Both the complexes were isolated similarly to the OMPA complexes.

(f) *Diperchlorato bis(nonamethylimido-phosphoramide)oxovanadium(IV), $VO(NIPA)_2(ClO_4)_2$*

Oxovanadium(IV) perchlorato (1 mmole) was dissolved in acetone (10 mL) and 2,2′(dimethoxypropane (5 mL) and then mixed with NIPA (2 mmole) in acetone. The reaction mixture was refluxed about 0.5 hr. Crystallization took place upon cooling in ice. The crystals were finally washed thoroughly with anhydrous diethyl ether and dried in vacuo over P_4O_{10}.

Analytical Procedures

Vanadium metal in all the complexes was determined by igniting the complexes in air and determining the metal as V_2O_5. The halides in the complexes were determined by Volhard's method. Perchlorate was determined by the method of Kurz et al.[15] The electrical conductance of the complexes was measured with a Toshniwal conductivity bridge at room temperature and their molecular weights were determined cryoscopically in freezing $PhNO_2$. Magnetic susceptibility measurements on powder form of the complexes were made at room temperature using Gouy's balance at *ca.* 11000 gauss. All other physico-chemical studies of the complexes were made as reported earlier.[16]

RESULTS AND DISCUSSION

The analytical data (Table 1) indicate a 1 : 1 and 1 : 2 (for perchlorate) stoichiometry for these complexes. Accordingly, these complexes

Table 1

Analytical, conductivity (Ω_M), molecular weight and magnetic values (μ_{eff}) of oxovanadium(IV) complexes of OMPA and NIPA

Compound	Analysis Found (Calcd.) %				Ω_M ohm^{-1} cm^2·mole^{-1}	Mol. Wt. Found (Calcd.)	µ eff B.M.
	Metal	P	N	Anion			
$VO(OMPA)Cl_2$	11.89 (12.02)	14.73 (14.62)	13.27 (13.20)	16.66 (16.74)	4.3	418 (424)	1.71
$VO(OMPA)Br_2$	9.82 (9.94)	12.04 (12.08)	11.00 (10.91)	31.09 (31.18)	5.2	509 (513)	1.69
$VO(OMPA)I_2$	8.29) (8.40)	10.26 (10.21)	9.28 (9.22)	41.72 (41.84)	5.3	603 (607)	1.74
$VO(OMPA)(NCS)_2$	10.79 (10.87)	13.27 (13.21)	17.98 (17.91)	24.62 (24.73)	4.62	463 (469)	1.73
$VO(OMPA)(NO_3)_2$	(10.61 (10.69)	13.08 (12.99)	17.69 (17.61)	—	4.76	472 (477)	1.70
$VO(OMPA)C_2O_4$	11.48 (11.56)	14.11 (14.05)	12.76 (12.69)	—	3.2	437 (441)	1.69
$VO(OMPA)_2(ClO_4)_2$	6.01 (6.08)	14.86 (14.79)	13.42 (13.36)	23.65 (23.74)	51.8	276 (838)	1.74
$VO(NIPA)Cl_2$	11.59 (11.67)	14.24 (14.18)	16.10 (16.01)	16.16 (16.24)	4.3	429 (437)	1.76
$VO(NIPA)Br_2$	9.62 (9.69)	11.86 (11.78)	13.38 (13.30)	30.32 (30.41)	4.9	520 (526)	1.72
$VO(NIPA)I_2$	8.13 (8.22)	10.06 (10.00)	11.21 (11.29)	40.82 (40.96)	5.2	613 (620)	1.70
$VO(NIPA)(NCS)_2$	10.49 (10.58)	12.81 (12.86)	20.41 (20.33)	23.92 (24.06)	4.3	476 (482)	1.76
$VO(NIPA)(NO_3)_2$	10.31 (10.40)	12.60 (12.65)	20.06 (20.00)	—	4.6	484 (490)	1.70
$VO(NIPA)C_2O_4$	11.17 (11.23)	13.69 (13.65)	15.48 15.41)	—	3.3	449 (454)	1.68
$VO(NIPA)_2(ClO_4)_2$	5.81 (5.90)	14.41 (14.35)	16.28 (16.20)	22.96 (23.03)	50.8	284 (864)	1.66

may be formulated as $VO(L)X_2$ (L=OMPA or NIPA; X = Cl, Br, I, NO_3, NCS or 0.5 C_2O_4) and $VO(L)_2(ClO_4)_2$ respectively. The complexes are soluble in common organic solvents. Molar conductances of the complexes in nitrobenzene indicate nonelectrolytic halo, nitrato, thiocyanato and oxalato complexes. The molar conductance of perchlorato complex shows it to be a 1 : 2 electrolyte. The molecular weights in freezing nitrobenzene (determined cryoscopically) also support the similar electrolytic behaviour of the complexes.

Magnetic moments

The room temperature (305 K) magnetic moments of the complexes lie in the range 1.69—1.76 B.M. These values correspond to one unpaired spin per vanadium atom, demonstrating the presence of vanadium (IV) in these complexes and the absence of metal-metal interactions between vanadium atoms.[17]

Infrared spectra

OMPA complexes

Detailed infrared spectra of the free ligand have been reported by Joesten et al.[18,19] Table 2 summarizes the position of the IR bands of P=O, P—O—P and P—N. The shift of the P=O stretch in all cases is in the direction of lower frequency and longer wavelength. This is indicative of bond weakening and decrease in double bound character of P=O with electron density being drawn away by interaction with the metal ion.[18,19] The relative strength of the interaction is indicated by the magnitude of the shift. This in itself is an evidence for the use of phosphoryl donor sites, but to establish the chelate structure the study of P—O—P

Table 2

Infrared absorption frequencies (cm^{-1}) of oxovanadium(IV) complexes of OMPA

Compound	ν(P=O)	ν(P—O—P)	ν(P—N_1)	ν(P—N_2)	ν(V—O)
OMPA	1235s	915s	990s	755m	—
$VO(OMPA)Cl_2$	1185s	940s	1010s	795w 785w	400m
$VO(OMPA)Br_2$	1190s	935s	1005s	790w	390m
$VO(OMPA)I_2$	1195s	940s	1010s	795w	350w
$VO(OMPA)(NCS)_2$	1185 s	937s	1015s	790w 780w	370m
$VO(OMPA)(NO_3)_2$	1180s	935s	1010s	795w 775w	380w
$VO(OMPA)_2(ClO_4)_2$	1190s	930s	1015s	795w 790w	390m
$VO(OMPA)C_2O_4$	1182s	935s	1010s	790w	360m

stretch is essential. The frequency shift of the P—O—P stretch in all cases is in the direction of higher frequency, which indicates a stronger bond or higher bond order. Thus in all the complexes studied herein formed the chelate structure. Hence the polarization effect of the VO^{2+} ion will tend to decrease the double bound character of P=O and at the same time draw the electron pairs from the P—O—P oxygen into $p_\pi - d_\pi$ overlap with phosphorus. The overall effect is to decrease the P=O stretching frequency and increase the P—O—P stretching frequency. Further evidence for coordination through the phosphoryl oxygen is found by looking at the P—N stretching frequency which shifts to higher frequencies in all cases.[18-20] The decrease in the P=O bond order that occurs when the metal ion coordinates to the phosphoryl oxygen can cause the lone pair on nitrogen to delocalize into the d_π-orbitals on the phosphorus.[18-20] This would increase the P—N bond order. In far IR region ν(V—O) has been identified in 400—360 cm^{-1} region.

NIPA complexes

Joesten[21,22] and the Bolster[23] have reported the detailed IR studied of NIPA. Pertinent IR data are summarized in Table 3. The authors have compared the IR spectra of NIPA and its complexes with OMPA (vide supra) and with some previous works on NIPA complexes.[21-23]

Table 3

Infrared absortion frequencies (cm^{-1}) of oxovanadium(IV) complexes of NIPA

Compound	ν(P=O)	ν(P—N—P)	ν(PNC)	ν(PNC)	N—P—N bending	P—O bending	ν(V—O)
NIPA	1203s	885s	975m	745w	598w 443w	508m,sh	—
$VO(NIPA)Cl_2$	1185s	885m	990m 980m	750w	610w 450m	520m	385m
$VO(NIPA)Br_2$	1200s 1180m	900m	988m 980sh	755w	612w 455m	522m	380m
$VO(NIPA)I_2$	1200s 1180s	890m	990m 980sh	758w	622w 455m	520m	375m
$VO(NIPA)(NCS)_2$	1195s 1180s	895m	980m	760w	620w 458w	518m	390m
$VO(NIPA)(NO_3)_2$	1185s 1175sh	890m	985m	755w	615w 455w	520m	400m
$VO(NIPA)_2(ClO_4)_2$	1190s 1170m	885m	988m 980sh	758w	618w 458w	522m	400m
$VO(NIPA)C_2O_4$	1195m 1170m	890m	990m 985m	750w	612w 455w	520m	390m

The PNP stretch has been assigned to the peak at 885 cm^{-1} while the PNC stretchings have been assigned to 975 cm^{-1} and 745 cm^{-1}. Both the PNP and PNC stretching frequencies for complexes of NIPA are shifted towards higher frequencies. The P=O stretch, a broad band in the IR spectra of the free ligand has appeared at *ca.* 1203 cm^{-1} split into a sharp strong band at *ca.* 1195 cm^{-1} and a sharp medium intensity peak at *ca.* 1180 cm^{-1} in the spectra of all the VO^{++} complexes of NIPA. According to Joesten *et al.*[21,22] this effect is attributed to coupling between two P—O vibrations via the metal atom to which they are both coordinated. It is further noted that in all NIPA complexes the P—O bending vibration is shifted towards higher energy; the magnitude and direction of this shift indicates that coordination occurs via the oxygen atoms of the ligand.[23]

Some new medium or weak bands observed in the range 410—370 cm^{-1} in these complexes are tentatively assigned as $\nu(V-O)$.

It would not be possible to assign a $V{=}O$ (oxocation) stretching frequency, since this occurs in the same region as $\nu(P-N_1)$ (1000—900 cm^{-1} in OMPA complexes) and $\nu(PNC)$ (1000—950 cm^{-1} in NIPA complexes).

Anions

The presence of numerous bands in the spectra of OMPA and NIPA complexes of VO^{++} complicates the identification of the nature of coordination of the perchlorate, oxalate, nitrate and thiocyanate groups. However, a close comparison of the spectra makes some inference possible.

In both the perchlorato complexes the presence of the ν_3(1090—1085 cm^{-1}) and ν_4(625—620 cm^{-1}) bands indicates that the T_d symmetry of ClO_4^- is maintained in both the complexes. This therefore suggests the presence of ClO_4^- ions outside the coordination sphere of the complexes[3,7,11]. In thiocyanato complexes, the three fundamental absorptions C—N stretch (ν_1) (2080—2075 cm^{-1}), C—S stretch (ν_3) (8050—845 cm^{-1}) and N—C—S bending (ν_2) (470 cm^{-1}) are identified. These frequencies are associated with the terminal N-bonded isothiocyanate ions.[24] In nitro complexes the absence of the ν_3 band of ionic nitrate (D_{3h}) around 1360 cm^{-1} and the occurrence of two strong bands at (1510—1505 cm^{-1}) (ν_4) and (1310 cm^{-1}) (ν_1) due to the split ν_3 mode in the lower symmetry indicate a coordinated nitrato group.[27,26] If the ($\nu_4 - \nu_1$) difference is taken as an approximate measure of the covalency of the nitrate group, a value of *ca.*200 cm^{-1} for the complexes studied suggests strong covalency for the metal-nitrate bonding. The bands at 1030—1025 cm^{-1} (ν_2), 820—810 cm^{-1} (ν_6), 730—725 cm^{-1} (ν_3/ν_5) have also been observed in these complexes. By applying the Lever separation method[27] the two combination bands ($\nu_1 + \nu_4$) appeared at 1760 and 1745 cm^{-1}; a separation of 15 cm^{-1} in these bands indicates the monodentate nitrate coordination. In $VO(L)C_2O_4$ the characteristic bands attributable to the oxalato group occur at 1725—1720 cm^{-1} (ν_2), 1665—1660 cm^{-1} (ν_1), 1620 cm^{-1} (ν_a) and

3120 cm^{-1} (ν_s). The increase of asymmetric stretching (ν_a) and lowering of symmetric (ν_s) stretching frequencies clearly indicate the chelation of the oxalate to vanadium (IV).[2]

Electronic spectra

The electronic spectra of the complexes closely resemble the data published for comparable compounds.[17] In most cases three ligand fields bands were observed in the spectra (Table 4). In other cases the third band was obscured by charge-transfer band. The first shoulder is assigned to an unresolved band resulting from the $d_{xy} \rightarrow d_{xz}$, d_{yz}($^2B_2 \rightarrow {}^2E$) transition, the second band is attributed to the $d_{xy} \rightarrow d_{x^2-y^2}$($^2B_2 \rightarrow {}^2B_1$) transition and the third band may either be assigned to the $d_{xy} \rightarrow d_{z^2}$($^2B_2 \rightarrow {}^2A_1$) transition or to low energy charge-transfer.

Table 4

Electronic spectral bands (cm^{-1}) of oxovanadium(IV) complexes of OMPA and NIPA

Compound	$d_{xy} \rightarrow d_{xz}, d_{yz}$	$d_{xy} \rightarrow d_{x^2-y^2}$	$d_{xy} \rightarrow d_{z^2}$
$VO(OMPA)Cl_2$	13,210	15,250	22,750
$VO(OMPA)Br_2$	12,980	15,400	—
$VO(OMPA)I_2$	12,820	15,800	21,740
$VO(OMPA)(NCS)_2$	12,900	15,200	21,700
$VO(OMPA)(NO_3)_2$	13,150	15,950	—
$VO(OMPA)C_2O_4$	12,800	15,300	22,500
$VO(OMPA)_2(ClO_4)_2$	13,120	15,250	22,100
$VO(NIPA)Cl_2$	13,050	15,450	22,350
$VO(NIPA)Br_2$	12,850	15,600	—
$VO(NIPA)I_2$	12,950	15,720	21,900
$VO(NIPA)(NCS)_2$	12,870	15,500	22,100
$VO(NIPA)(NO_3)_2$	12,920	15,800	21,850
$VO(NIPA)C_2O_4$	12,950	15,350	—
$VO(NIPA)_2(ClO_4)_2$	12,600	15,200	21,700

Thus, on the basis of these studies, it is concluded that in all these complexes the coordination number of vanadium is five. These pentacoordinated oxovanadium(IV) complexes could have a tetragonal pyramidal structure.[2,11] The probable structures of the present complexes may be shown as :

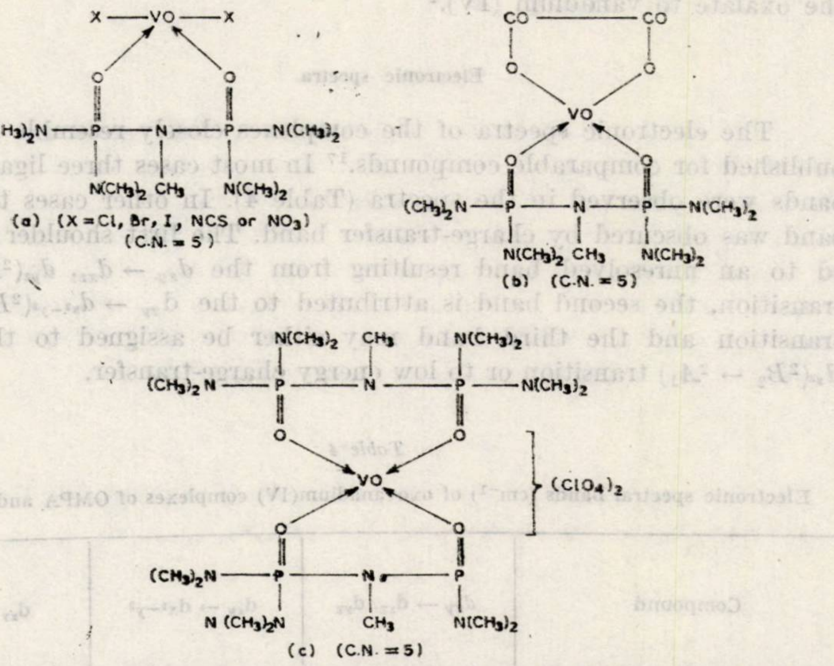
(a) (X = Cl, Br, I, NCS or NO₃)
(C.N. = 5)
(b) (C.N. = 5)
(ClO₄)₂
(c) (C.N. = 5)

Fig. 1. — Structures of oxovanadium (IV) complexes of ocramethyl pyrophosphoramide

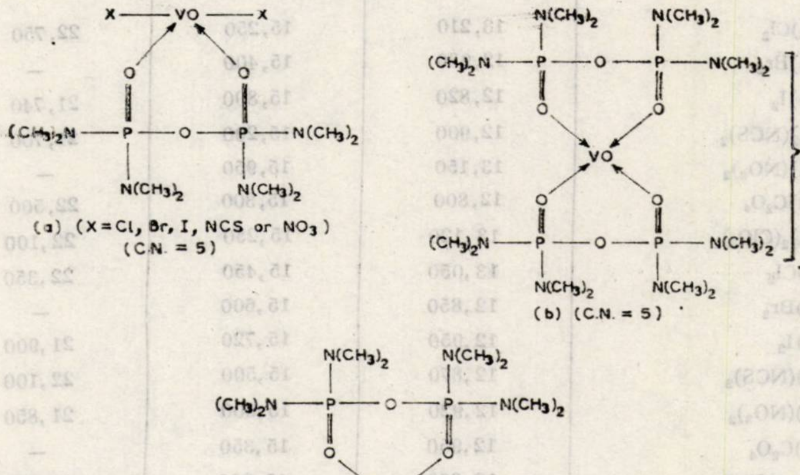
(a) (X = Cl, Br, I, NCS or NO₃)
(C.N. = 5)
(b) (C.N. = 5)
(ClO₄)₂
(c) (C.N. = 5)

Fig. 2. — Structures of oxovanadium (IV) complexes of nonamethylimido phosph oramide

REFERENCES

[1] S. M. Horner, S. Y. Tyrll (Jr.) and D. L. Vlneszky, *Inorg. Chem.*, **1**, 844 (1962).
[2] D. N. Sathyanarayana and C. C. Patel, *J. Inorg. Nucl. Chem.*, **28**, 2277 (1966).
[3] S. K. Madan and A. M. Donohus, *J. Inorg. Nucl. Chem.*, **28**, 1303 (1966).
[4] D. N. Sathyanarayana and C. C. Patel, *Indian J. Chem.*, **5**, 360 (1967).
[5] J. G. H. Du-Preeze and F. G. Sadie, *Inorg. Chim. Acta*, **1**, 202 (1967).
[6] A. K. Majumdar and R. G. Bhattacharya, *Science and Culture*, **35**, 271 (1969).
[7] V. V. Savant and C. C. Patel, *J. Inorg. Nucl. Chem.*, **31**, 2319 (1969).
[8] V. V. Savant and C. C. Patel, *J. Inorg. Nucl. Chem.*, **34**, 1462 (1972).
[9] G. Durgaprasad and C. C. Patel, *Indian J. Chem.*, **11**, 1300 (1973).
[10] G. Durgaprasad and C. C. Patel, *Indian J. Chem.*, **12**, 840 (1974).
[11] R. K. Agarwal and Gyanendra Singh, *Thermochim. Acta*, **99**, 349 (1986).
[12] D. N. Sathyanarayana and C. C. Patel, *Indian J. Chem.*, **3**, 486 (1965).
[13] H. Rudy and A. Debo, *Chem. Abstr.*, **55**, 142a (1961).
[14] K. P. Lannort and M. D. Joeston, *Inorg. Chem.*, **7**, 2048 (1968).
[15] E. Kurz, G. Kober and M. Berl, *Annal. Chem.*, **30**, 1983 (1958).
[16] R. K. Agarwal, A. K. Srivastava and T. N. Srivastava, *Transtion Met. Chem.*, **5**, 95 (1980).
[17] J. Selbin, *Chem. Rev.*, **65**, 153 (1965).
[18] M. D. Joesten and K. M. Nykerk, *Inorg. Chem.*, **3**, 548 (1964).
[19] M. D. Joesten, *Inorg. Chem.*, **6**, 1598 (1967).
[20] S. C. Rastogi, "Studies on the stereochemistry of high coordination compounds of oxozirconium (IV), dioxouranium (VI) and thorium (IV) involving some oxygen and nitrogen donor ligands", Ph. D. Thesis, Meerut University (1985).
[21] K. P. Lannert and M. D. Joesten, *Inorg. Chem.*, **7**, 2048 (1968).
[22] M. D. Joesten, R. C. Koch, T. W. Martin and J. H. Venable (Jr.), *J. Amer. Chem. Soc.* **93**, 1138 (1971).
[23] M. W. G. de Bolster, "The coordination chemistry of aminophosphine oxides and related compounds", Ph. D. Thesis, Leiden (1972).
[24] J. L. Burmeister, *Coord. Chem. Rev.*, **3**, 225 (1968).
[25] J. R. Ferraro, *J. Mol. Spectra*, **4**, 99 (1960).
[26] C. C. Addison and N. Logan, *Adv. Inorg. Chem. and Radiochem.*, **6**, 95 (1964).
[27] A. B. P. Lever, E. Mantiovani and B. S. Ramaswamy, *Canad. J. Chem.*, **49**, 1957 (1971).

Revue Roumaine de Chimie, **33**, 5, 547–554 (1988)

KINETICS OF OXIDATION OF THIOUREA BY IRON(III) IN THE PRESENCE OF 2,2′-BIPYRIDYL

G. V. SARADAMBA, K. RAMAKRISHNA, K. N. RAJU and P. V. SUBBA RAO*
School of Chemistry, Andhra University, Visakhapatnam 530003, India

Received November 17, 1986

The kinetics of oxidation of thiourea by iron (III) in the presence of bipyridyl have been investigated under the pseudo-first order conditions, [Thiourea], [HBipy$^+$], [H$^+$] $\gg$ [Fe(III)]. The reaction is first order in iron(III) and thiourea. Plots of $1/k'$ versus $1/[\mathrm{HBipy}^+]^2$ and $[\mathrm{H}^+]^2$ were found to be linear with a positive intercept on the $1/k'$ axis in each case. The rate constant of the slow step, k, calculated from the above relations was found to decrease with increase in methanol content. There was no correlation between log k and D^{-1}. The free energies of transfer of the initial state and transition state were calculated. The results show greater stabilisation of the initial state relative to the transition state leading to greater free energy of activation and consequent inhibition by methanol.

INTRODUCTION

Iron(III), though a mild oxidant, oxidises mercury(I),[1] cobalt(II)[2] and vanadium (IV)[3] in the presence of 2,2′-bipyridyl,[1-3] because the oxidation potentials of these reductants decrease in the presence of excess of this ligand. In all these cases 1 : 2 complex of iron (III) and bipyridyl was shown to be the active oxidizing species. This brown complex[1-3] (obtained by direct mixing of iron(III) and the ligand) is different from tris (bipyridyl) iron(III) which is not formed by direct mixing, but by oxidation of the corresponding tris complex of iron(II). It is interesting to investigate the kinetic pattern of the oxidation of thio compounds by this brown complex. In this paper the authors report the results of kinetic study of oxidation of thiourea by this brown complex in methanol-water mixtures.

EXPERIMENTAL

Materials and Methods

Iron(III) perchlorate was prepared by the method described elsewhere.[4] Thiourea was used after recrystallization. Methanol was purified by distillation before use. The course of the reaction was followed by measuring the absorbance due to the product tris-bipyridil iron (II) at 510 nm at different time intervals. At this wavelength all the other materials concerned have negligible absorption. All the kinetic runs were carried out keeping the ionic strength constant with sodium perchlorate. The source of the hydrogen ions was perchloric acid. In each kinetic run the hydrogen ion concentration was adjusted to required value (with the help of an expanded scale pH meter) with standard dilute perchloric acid.

The uncatalysed reaction between iron(III) and thiourea was investigated by Pustelnik et al.[5] who found simple first order kinetics with respect to each of the reactants. To compare the catalytic effectiveness of bipyridyl on the iron(III)-thiourea reaction, the rate constants of the uncatalysed reaction were determined (under the same conditions as employed in the catalysed reaction). The pseudo-first order rate constant, k' for the uncatalysed reaction was 1.2×10^{-5} s^{-1} whereas for the catalysed reaction in the presence of a 4.0×10^{-3} mol dm^{-3} bipyridyl, under the same conditions, (*i. e.*), [Thiourea] $= 4.0 \times 10^{-3}$ mol dm^{-3}, [Fe(III)] $= 7.52 = 10^{-5}$ mol dm^{-3}, [HClO$_4$] $= 1.79 \times 10^{-2}$ mol dm^{-3}, $\mu = 0.26$ mol dm^{-3} methanol (v/v) = 24% and temp. 25.0 ± 0.1°C, k' was found to be $5 = 10^{-4}$ s^{-1}. Hence the uncatalysed reaction can be neglected while analysing the kinetic data of the catalysed reaction.

Product Analysis

The product of the reaction was prepared by mixing thiourea with an excess of iron(III) and 2,2′-bipyridyl to an acidic solution of thiourea (0.1M $HClO_4$). After keeping the reaction mixture for 24 hours to ensure the completion of the reaction, the reaction mixture was shaken with ether. On concentrating the ethereal extract, crystals of product separated which were repeatedly washed with alcohol and dried in vacuum. The IR spectrum was scanned. An authentic sample of this disulphide was prepared by mixing thiourea and 1 : 1 hydrogen peroxide solution[6] and the IR spectrum of this crystalline product was found to be identical with that obtained in the present reaction. Thus the product of oxidation of thiourea is the formamidine disulphide.

RESULTS AND DISCUSSION

All the kinetic runs were carried out under the pseudofirst order conditions (viz) [Thiourea], [HBipy$^+$) $\gg$ [Fe(III)]. Under these conditions, plot of $\log(A_\infty - A_t)$ versus time (where A_t and A_∞ are the absorbance at time 't' and after the completion of the reaction respectively) were linear, showing first order kinetics with respect to Fe(III). The pseudo-first order rate constants, k', were calculated from the slopes of these plots. k' was found to be directly proportional to [thiourea], showing first order dependence of rate on thiourea also (Table 1). The data of k' determined at different [HBipy$^+$)] but at constant ([H$^+$] (Table 2) show that a plot of $1/k'$ versus $1/[\text{HBipy}^+]^2$ is linear with a positive intercept

Table 1

Effect of thiourea on oxidation of thiourea by
Fe(III) — 2,2′-bipyridyl complex
[HBipy$^+$] $= 8.0 \times 10^{-3}$ mol dm^{-3},
Methanol = 24% (v/v)
[Fe(III)] $= 7.52 \times 10^{-5}$ mol dm^{-3},
$\mu = 0.26$ mol dm^{-3}
[HClO$_4$] $= 1.79 \times 10^{-2}$ mol dm^{-3},
Temp. = 25.0 ± 0.1°C

[Thiourea] × 10^3 mol dm^{-3}	k' rate constant s^{-1}
4.0	2.45
8.0	4.90
12.0	7.90
16.0	10.00
20.0	12.50
24.0	15.20

on $1/k'$ axis, showing the formation of 1 : 2 complex between iron(III), and bipyridyl, which acts as the active oxidising species.

The reaction is inhibited by $[H^+]$ and the type of dependence of rate on $[H^+]$ (Table 3) is indicated by the linearity of $1/k'$ versus $[H^+]^2$ with a positive intercept on the $1/k'$ axis. All these kinetic results can be summarized in the empirical rate law,

$$\text{Rate} = \frac{a[\text{Fe(III)}][\text{HBipy}^+]^2[\text{Thiourea}]}{b[\text{H}^+]^2 + c[\text{HBipy}^+]^2}$$

Table 2

Effect of bipyridyl on oxidation of thiourea by Fe(II)-2,2'-bipyridyl complex
[Thiourea] = 4.0×10^{-3} mol dm^{-3} ;
[Fe(III)] = 7.52×10^{-5} mol dm^{-3}
[HClO$_4$] = 1.79×10^{-2} mol dm^{-3};
$\mu = 0.26$ mol dm^{-3},
Temp = 25.0 ± 0.1°C
Methanol = 24% (v/v)

[HBipy$^+$] × 10^3 mol dm^{-3}	Rate constant $k' \times 10^4$ s^{-1}
12.0	5.95
16.0	9.79
24.0	11.00
40.0	14.50
48.0	14.80

Table 3

Effect of HClO$_4$ on oxidation of thiourea by Fe(III)-2,2'-bipyridyl complex
[Thiourea] = 4.0×10^{-3} mol dm^{-3},
[Fe(III)] = 7.52×10^{-5} mol dm^{-3}
[HBipy] = 8.0×10^{-3} mol dm^{-3},
Methanol = 24% (v/v), $\mu = 0.26$ mol dm^{-3},
Temp. = 25.0 ± 0.1° C

[H$^+$] × 10^2 mol dm^{-3}	$k' \times 10^4$ s^{-1}
1.59	3.03
2.19	1.78
2.39	1.34
2.99	1.00
3.39	0.77
3.79	0.63
4.19	0.53
4.59	0.44

The reaction kinetics were investigated in the range of hydrogen ion concentration 0.0159–0.045 mol dm^{-3}. Since only very low concentrations of iron (III) were employed ($=10^{-5}$M), the dimeric form of iron(III) can be neglected. Since the hydrolysis constant of iron (III)[7] has a value of. 5 1 $\times 10^{-3}$, the concentration of the hydrolysed form is very small even at the lowest hydrogen ion concentration employed. Its contribution to the rate also appears to be negligible. If the hydrolysed form also has appreciable contribution to the rate, the type of hydrogen ion dependence of rate would have been different from the observed pattern (plot of $1/k'$ versus $[H^+]^2$ being linear with a positive intercept). The pK value of bipyridyl[8] is in the order of 10^{-4} and hence all bipyridyl can be assumed to be in the protonated form, $HBipy^+$, at the acid concentrations employed Thiourea[9] has a pK value of -1.0, and even at the highest concentration of $[H^+]$ employed (0.045 mol dm^{-3}) only 0.5% of thiourea exists in the protonated form. Only unprotonated form of thiourea need be considered.

The authours propose the following mechanism to explain their kinetic results.

$$\underset{}{Fe^{3+}} + 2HBipy^+ \overset{K}{\rightleftharpoons} \underset{(X)}{Fe(bipy)_2^{3+}} + 2H^+ \tag{1}$$

$$(X) + \underset{(Thiourea)}{RS} \xrightarrow[slow]{k} Fe(bipy)_2^{2+} + [RS]^{\bullet} \tag{2}$$

$$2RS^{\bullet} \xrightarrow{fast} RSSR. \tag{3}$$

$$Fe(bipy)_2^{2+} + HBipy^+ \xrightarrow{fast} Fe(bipy)_3^{2+} + H^+ \tag{4}$$

where $R = (NH_2)_2C$
The above scheme leads to the rate-law

$$-\frac{d[Fe(III)]}{dt} = \frac{kK[Fe(III)][HBipy^+]^2[Thiourea]}{[H^+]^2 + K[HBipy^+]^2} \tag{I}$$

Under the pseudo-first order conditions,
[Thiourea] $\gg$ [Fe(III)],

$$k' = \frac{kK[HBipy^+]^2[Thiourea]}{[H^+]^2 + K[HBipy^+]^2} \tag{II}$$

The rate-law requires that the plots of $1/k'$ versus $1/[HBipy^+]^2$ and $1/k'$ versus $[H^+]^2$ should be linear with positive intercepts which have been observed (Figs. 1 and 2). Further, the rate-law requires that the values of the intercepts obtained from these plots must be of nearly the same magnitude which has also been observed. From both these plots, using their intercepts and slopes, the rate constant of the rate-determining step 'k' and the equilibrium constant 'K' were calculated (Table 4). The values of the rate constant, 'k', of the rate-determining step, and equilibrium constant, 'K', of the equilibrium preceding the rate-determining step were determined in water as well as different compositions of methanol-water mixtures by determining k' at different [HBipy$^+$] in each of these media and using equation II. The results are presented in Table 4. The results indicate that k decreases with increasing methanol-content in the medium. However, a plot of log k versus $1/D$ where D is the dielectric constant of the medium was not linear.

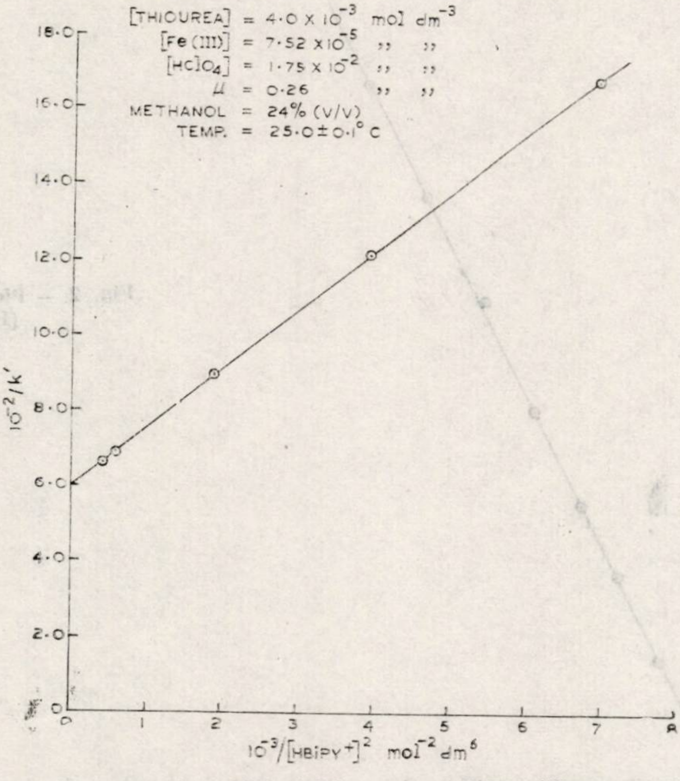

Fig. 1. — Plot of $1/k'$ versus $1/[\mathrm{HBipy}^+]^2$.

Using the values of specific rate constant, k, of the rate-limiting step and the equilibrium constant, K, of the equilibrium (I) an attempt has been made to separate the overall solvent effect into solvent effects on the initial and transition states. Since the rate-limiting step contains one molecule each of iron(III)-bipyridyl complex and thiourea, the effect of solvent on the initial state can be equated to the sum of the transfer free energies, $\delta\mu_t^{\ominus}$, of these reactants and the transfer free energy of the transition state, $\delta_t^{\neq}$, can be calculated from the equation III,

$$\delta\Delta G_t^{\neq} = \delta\mu_t^{\neq\ominus} - \Delta\mu_t^{\ominus}(\mathrm{Fe(bipy)}_2^{3+}) - \Delta\mu_t(\mathrm{Thiourea}) \qquad \mathrm{III}$$

where $\delta\Delta G^{\neq}$ is the difference in the free energy of activation in each of the solvent mixtures and water, $\Delta G^{\neq}$ was calculated using the equation

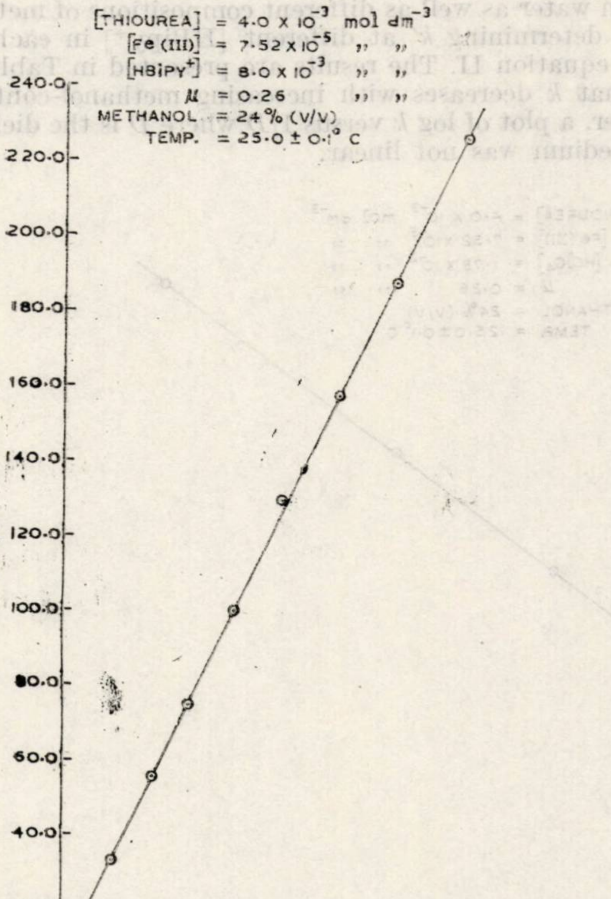

Fig. 2. — Plot of $1/k'$ versus $[H^+]^2$.

Table 4

Effect of solvent composition on k and K

$[\text{Thiourea}] = 4.0 \times 10^{-3}$ mol dm^{-3},
$[\text{Fe(III)}] = 7.52 \times 10^{-5}$ mol dm^{-3}
$\mu = 0.26$ mol dm^{-3},
$[\text{HClO}_4] = 1.79 \times 10^{-2}$ mol dm^{-3},
Temp. = 25.0 ± 0.1° C

Percentage of methanol (v/v)	Specific rate constant, ks^{-1}mol^{-1}dm^3	Equilibrium constant, K
0	0.46	1.16
24	0.42	1.26
28	0.38	1.65
40	0.30	2.25
56	0.21	3.35
60	0.13	7.84

$k = \frac{KT}{h} e^{-\Delta G^{\neq}/RT}$. To calculate $\Delta\mu_t^{\ominus}$ (Fe(bipy)$_2^{3+}$), the values of the equilibrium constant, K, of the equilibrium (I) determined in water and each of the solvent mixtures were used (Tabele 4). ΔG of the equilibrium (I) is related to K by the equation IV.

$$\Delta G = \Delta G(\text{Fe(bipy)}_2^{3+}) + 2\Delta G(H^+) - \Delta G(\text{Fe}^{3+}) - 2\Delta G(\text{HBipy}^+) = -RT \ln K \qquad \text{IVa}$$

$$\Delta G(\text{solvent}) - \Delta G(\text{water}) = \delta\mu_t^{\ominus}(\text{Fe(bipy)}_2^{3+}) + 2\delta\mu_t^{\ominus}(\text{H}^+) - \delta\mu_t^{\ominus}(\text{Fe}^{3+}) - 2\delta\mu_t^{\ominus}(\text{HBipy}^+) = RT \ln\left(\frac{K_{\text{water}}}{K_{\text{solvent}}}\right) \qquad \text{IVb}$$

where K_{water} and K_{solvent} are the constants of the equilibrium (1) in water and a given methanol-water mixture respectively (Table 4).

The $\delta\mu_t^{\ominus}$ (Fe^{3+}) was calculated using the Born equation, assuming the radius of Fe^{3+}(aq) to be 2.05 Å.[10] The $\delta\mu_t^{\ominus}$(HBipy$^+$) was computed using the method described by Bandyopadhy et al.[11] The $\delta\mu_t^{\ominus}$ (HBipy$^+$), the free energy change of trnsfer, from a pure solvent to any other medium for the reaction, HBipy$^+ \rightleftharpoons$ H$^+$ + Bipy, may be written as

$$\delta\mu_t(\text{HBipy}^+) = \delta\mu_t^{\ominus}(\text{H}^+) + \delta\mu_t^{\ominus}(\text{Bipy}) - \Delta G^{\circ}(\text{HBipy}^+) \qquad \text{V}$$

The ΔG values of the equilibrium HBipy$^+ \rightleftharpoons$ H$^+$ + Bipy, required for the calculation of $\delta\mu_t^{\ominus}$(HBipy$^+$), were those reported by Bandyopadhay et al.[11] The values of $\delta\mu_t^{\ominus}$(Bipy) were calculated using the solubility data of 2,2′-bipyridyl reported by Burgess et al.[12] in water and different water-methanol mixtures. The ΔG_t(H$^+$) were taken from the data quoted by Franks.[13] Using these data $\Delta\mu$ (Fe(bipy)$^{3+}$) was calculated making use of the equation IVa and IVb. $\delta\mu_t^{\ominus}$ (Thiourea) was computed from the determined values of solubility in water and methanol-water mixture, using the equation $\delta\mu_t^{\ominus}$ (thiourea) $= RT \ln\left(\frac{S(W)}{S(X)}\right)$ where $S(X)$ and $S(W)$ are the solubilities of thiourea in solvent mixtures and water respectively. The transfer free energies, from water to solvent mixtures, of the initial state is then equated to the sum of the transfer free energies $\Delta\mu_t$(Fe(bipy)$_2^{3+}$ and $\Delta\mu_t$(Thiourea). The transfer free energies of the transition state under the same condition was then calculated using eq. III. These values represent the effects of solvent in initial and final states (Table 5). A more negative $\Delta\mu_t$ of initial state compared to the transition state points to the possibility of greater stabilisation of the initial state compared to the transition state with increasing methanol content, resulting in greater free energy of activation and consequent inhibition by methanol.

Table 5

Ionic strength, $\mu = 0.26$ mol dm^{-3}, Temp. = 25.0 ± 0.1°C

Percentage of methanol (v/v)	$\delta\Delta G^{\neq}$ KJ mol^{-1}	$\Delta\mu_t^{\ominus}(\mathrm{Fe(bipy)_2^{3+}})$ KJ mol^{-1}	$\delta\mu_t^{\ominus}$(thiourea) KJ mol^{-1}	$\delta\mu^{\ominus}_{t(\mathrm{Activated})}$ complex KJ mol^{-1}	$\Delta\mu_{t(\mathrm{Initial})}$ KJ mol^{-1}	Solubility of thiourea gms/mL
24%	0.26	1.76	−0.38	1.6	1.38	0.15
28%	0.49	−1.02	−0.48	− 1.0	−1.50	0.16
40%	1.05	−8.24	−0.62	− 7.8	−8.86	0.17
56%	1.98	−14.34	−0.77	−13.1	−15.11	0.18
60%	3.18	−17.57	−0.80	−15.1	−18.37	0.19
0%						0.13

REFERENCES

[1] P. V. Subba Rao, M. Suryanarayana, K. V. Subbaiah and P. S. N. Murty, *J. Inorg. Nucl. Chem.*, **42**, 1181 (1980).

[2] K. V. Subbaiah, K. Srinivas and P. V. Subba Rao, *Ind. J. Chem.*, **20A** 399 (1981).

[3] P. V. Subba Rao, K. V. Subbaiah and K. Srinivas, *Ind. J. Chem.*, **19A**, 1130 (1980).

[4] J. J. Lingane, "Analytical Chemistry of Selected Metallic Elements", Reinhold, London, 1965, p. 58.

[5] N. Pustelnik and R. Soloniewicze (Inst. Ger. Chem ; Tech. Univ. Lodz., Lodz, Pol.) Monatshchem 1975, 106(3) 673—8 (Ger), *C.A.*, 83, 137469t.

[6] Michael Heffmann and John O Edwards, *Inorg. Chem.*, **16**, 3333 (1977).

[7] A. S. Wilson and Taube, *J. Am. Chem. Soc.*, **74**, 3509 (1952).

[8] D. H. Buissan and R. J. Irwing, *J. Chem. Soc. Far.*, (I) **(1977)**, 157.

[9] G. Charlot and B. Temilion, "Chemical Rections in Solvents and Melts", Pergamon, London, 1969, p. 78.

[10] F. Basolo and R. G. Pearson, "Mechanisms of Inorganic Reactions", Wiley, New York, 1958, 307.

[11] S. Bandyopadhyay, A. K. Mandal and S. Aditya, *J. Indian. Chem. Soc.*, **58**, 467 (1981).

[12] John Burgess and Robert Haines, *Chem. Ind.* (London), **(1980)** 289.

[13] F. Franks, "Physico Chemical Processes in Mixed Aqueous Solvents" Hinemann Education Ltd, London 1967, p. 77.

Revue Roumaine de Chimie, **33**, *5*, 555–563 (1988)

KINETICS OF THE CERIUM(IV) OXIDATION OF MALONIC ACID IN H_2SO_4–$HClO_4$ MEDIA

A. SEZAI SARAÇ and AYTEN GÖÇMEN

Technical University of Istanbul, Department of Chemistry, Maslak, Istanbul-Turkey

Received February 22, 1987

The kinetics of oxidation of malonic acid by cerium(IV) has been studied spectrophotometrically in H_2SO_4-$HClO_4$ media at 25° C and ionic strength of 2.0 M. The data may be interpreted in terms of a mechanism which involves fast preequilibrium complexation steps between malonic acid and cerium(IV) sulfato species and complexation is followed by rate-determining decarboxylation to an intermediate free radical, $^{\bullet}CH(CO_2H)_2$. Products of formation constants for the complexes ($K\alpha_i$) and rate constants for the intramolecular redox reactions ($K\alpha_i$) have been determined.

INTRODUCTION

The reaction kinetics of transition – metal ions with organic acids have been the subject of recent studies. Especially the kinetics of cerium(IV) oxidation of organic compounds such as polyaminocarboxylic,[1] aliphatic dicarboxylic,[2] and hydroxy carboxylic acids [3] has become increasingly important in the several media. Since cerium(IV) oxidation kinetics of such compounds are mainly dependent on the type of cerium(IV) species which are involved in the reaction steps, we have studied the kinetics of malonic acid by cerium(IV) at constant ionic strength as a continuation of our previous investigation in Na_2SO_4 – $NaClO_4$ – $HClO_4$ and H_2SO_4 – $HClO_4$ media[4], even though the cerium(IV) – malonic acid reaction has been studied in sulfuric[5] and perchloric acid media.[6]

EXPERIMENTAL

Materials

Ceric sulfate, $Ce(SO_4)_2 \cdot 4H_2O$ (Merck), malonic acid (Fluka), ferrous ammonium sulfate (Merck) and the inorganic acids and salts used were reagent grade and were used without further purification.

Acrylamide (Eastman Organic Chemicals) was used for the polymerization test which is indicative of the formation of intermediate free radicals in the reaction mixtures.

Solutions

Solutions of ceric sulfate were prepared by direct weighing, and for the very dilute solutions, by dilution of standardized solutions. Ionic strength of solution was kept at 2,0 M by adding calculated amounts of $HClO_4$ and H_2SO_4 solutions. Calculation of H^+, HSO_4^- and $SO_4^=$

concentrations was made according to equation of Lindstrom and Wirth.[7] The primary standard used was reagent-grade ferrous ammonium sulfate (Mohr's salt, $FeSO_4 \cdot (NH_4)_2SO_4 \cdot 6H_2O$) and the indicator was N-phenylanthranilic acid prepared according to standard methods.

Kinetics

The rates of cerium(IV)-malonic acid reaction were followed spectrophotometrically at 395 nm by following the consumption of cerium(IV) (Fig. 1) using a Carl Zeiss — Jena Specol spectrophotometer. The 5 cm cells were used in a thermostated cell — attachment of the spectrophotometer, and the temperature was regulated by a circulating B. Broun Melsungen thermostat, and was maintained at 25° C at better than ± 0.05° C.

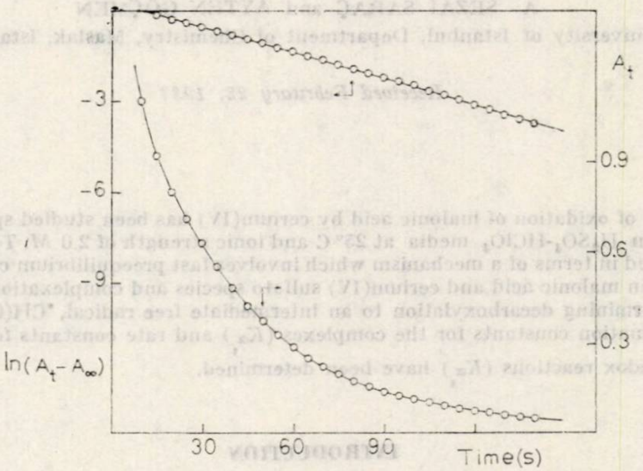

Fig. 1. — Plots of first order kinetics of malonic acid with cerium(IV) and absorbance versus time (in seconds).

The initial concentrations of cerium(IV) and malonic acid in the reaction mixture were 2.5×10^{-4} *M* (Ce(IV) and 2.5×10^{-2} *M* malonic acid for all of the studies.

The observed pseudo first-order rate constants, in s^{-1}, were calculated according to eq. (1)

$$k^{I}_{obs} t = \ln(A_0 - A_\infty) - \ln(A_t - A_\infty) \tag{1}$$

by least-squares analysis, from absorbance data; A_t, A_0 and A_∞ refer to the absorbances at time *t*, at the start of reaction, and at infinity, respectively.

RESULTS AND DISCUSSIONS

Stoichiometry

The stoichiometry of the reaction was determined from the absorbance decrease of cerium(IV) under conditions similar to those established for kinetic measurements. Absorbance measurements indicated that 6 equivalents of cerium(IV) are reduced for one mole of malonic acid at 25°C which corresponds to the following stoichiometric equation,

$$CH_2(COOH)_2 + 6Ce(IV) + 2H_2O \rightarrow 6Ce(III) + HCOOH + 2CO_2 + 6H^+$$

Kinetics

Linearity of the plots of $\ln(A_t - A_\infty)$ versus time t (Fig. 1) indicates that the cerium(IV) — malonic acid reaction is first order with respect to cerium(IV). Variation of concentration of malonic acid also showed that the order with respect to substrate is also one. These plots yielded very good straight lines and regression coefficients were very close to 1. At constant ionic strength and nearly constant hydrogen ion concentration the plot of $1/k^I_{obs}$ versus 1/[malonic acid] yields straight line with positive intercept and its magnitute depending on the $[H^+]$ and $[HSO_4^-]$ (Fig. 2). These indications suggest that the oxidation reaction involves an intermediate complex formation between the malonic acid and the reactive cerium(IV) species.

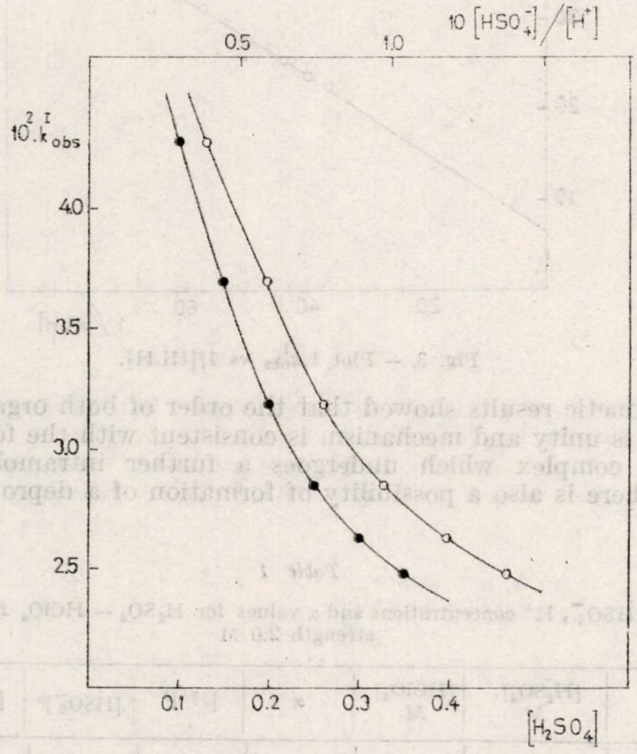

Fig. 2. — Effect of sulfuric acid concentration or $[HSO_4^-]/[H^+]$ on the reaction of malonic acid with cerium(IV) at 25°C. Initial cerium (IV) concentration : 2.5×10^{-4} *M*. Initial organic acid concentration : 2.5×10^{-2}. ● Plot of k^I_{obs} against $[H_2SO_4]$; Plot of k^I_{obs} against $[HSO_4^-]/[H^+]$.

Slope and intercept values of the plot of $1/k^{\mathrm{I}}_{\mathrm{obs}}$ vs 1/[malonic acid] (Fig. 3) are found to be 0.43 and 6.34 respectively by using least squares technique, at 1.98 M hydrogen ion concentration.

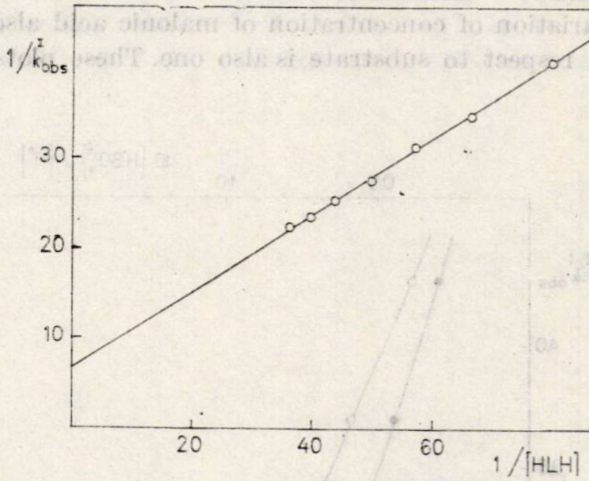

Fig. 3. — Plot $1/k^{\mathrm{I}}_{\mathrm{obs}}$ vs 1/[HLH].

The kinetic results showed that the order of both organic acid and cerium(IV) is unity and mechanism is consistent with the formation of a protonated complex which undergoes a further intramolecular redox reaction. There is also a possibility of formation of a deprotonated com-

Table 1

Calculated HSO_4^-, H^+ concentrations and α values for $H_2SO_4 - HClO_4$ media at ionic strength 2.0 M

Run no.	$[H_2SO_4]$, M	$[HClO_4]$ M	α	$[H^+]^a$	$[HSO_4^-]^b$	$[HSO_4^-]/[H^+]$
1	0.10	1.85	0.231	1.98	0.08	0.039
2	0.15	1.78	0.232	1.97	0.12	0.059
3	0.20	1.71	0.233	1.95	0.15	0.078
4	0.25	1.63	0.234	1.94	0.19	0.098
5	0.30	1.56	0.235	1.93	0.23	0.119
6	0.35	1.49	0.237	1.92	0.27	0.136

[a] Calculated according to eq. (Refs. 4 and 7)

$$[H^+] = [H_2SO_4](1+\alpha) + [HClO_4]$$

[b] Calculated according to eq.

$$[HSO_4^-] = [H_2SO_4](1-\alpha)$$

Relation of $k^{\mathrm{I}}_{\mathrm{obs}}$ and H_2SO_4 concentration or calculated amounts of H^+ and HSO_4^- concentrations are shown in Fig. 2.

plex, but in the [HSO_4^-] and [H^+] range used the concentration of the deprotonated complex would be very low (Table 1). Under the experimental conditions, malonic acid will be essentially undissociated ($K_{a1} = 1.4 \times 10^{-3}$M), assuming that only H_2L (malonic acid) are reactive, and that the mono, di, and trisulfate complexes of cerium(IV) all participate in the reaction, the scheme in equations (2) — (4) is consistent with our results in H_2SO_4 — $HClO_4$ media (Table 2).

Table 2

Dependence of k^{I}_{obs} upon the malonic acid concentration[a]

$10^4 \times$ [Ce(IV)], *M*	$10^3 \times$ [malonic acid], *M*	$10^2 \times k^{I}_{obs}$ (s^{-1}).
2.5	12.5	2.45
2.5	15.0	2.87
2.5	17.5	3.19
2.5	20.0	3.65
2.5	22.5	3.96
2.5	25.0	4.28
2.5	27.5	4.46

[a] The concentration of sulfuric acid was 0.10 *M* and of perchloric acid was 1.85 *M* for all runs. λ = 395 nm, $t = 25°C$, $I = 2.0$ *M*

$$CeX_i + HLH \overset{K_{\alpha i}}{\rightleftharpoons} [CeX_i(HLH)] \qquad (2)$$

$$[CeX_i(HLH)] \xrightarrow{K_{\alpha i}} Ce(III) + H^+ + HlL. \qquad (3)$$

$$CeX_i + HL \xrightarrow{H_2O} Ce(III) + product(s)\ (fast) \qquad (4)$$

where i is 1, 2 and 3 and [CeX_i(HL)] represents the corresponding complexes and Ce(III) represents the corresponding Ce(III)X_i species.

Appropriate combination of the above steps yields the rate law,

$$-d[Ce(IV)]_T/dt = k^{I}_{obs}[Ce(IV)]_T =$$

$$= 6\{k_{\alpha1}K_{\alpha1}[CeSO_4^{2+}] + k_{\alpha2}K_{\alpha2}[Ce(SO_4)_2] +$$

$$+ k_{\alpha3}K_{\alpha3}\ [Ce(SO_4)_3^{2-}]\}[HLH] \qquad (5)$$

where K_α is equilibrium constant for the formation of the protonated complex, and k_α is complex disproportionation constant. By using the respective equilibrium expressions for sulfato — complexes of cerium (IV)* we obtain the following equations,

$$[\mathrm{Ce(IV)}]_T = \sum_{\mathrm{i}} [\mathrm{CeX_i}] + \sum_{\mathrm{i}} [\mathrm{CeX_i(HLH)}] \tag{6}$$

$$K_{\alpha\mathrm{i}} = [\mathrm{CeX_i(HLH)}]/[\mathrm{CeX_i}][\mathrm{HLH}] \tag{7}$$

$$k^{\mathrm{I}}_{\mathrm{obs}} = 6\Big(\sum_{\mathrm{i}} k_{\alpha\mathrm{i}} K_{\alpha\mathrm{i}} [\mathrm{CeX_i}]\Big) \frac{[\mathrm{HLH}]}{[\mathrm{Ce(IV)}]_T} \tag{8}$$

or

$$k^{\mathrm{I}}_{\mathrm{obs}} = 6\{k_{\alpha1}K_{\alpha1} + k_{\alpha2}K_{\alpha2}K_{\alpha2}n + k_{\alpha3}K_{\alpha3}K_2K_2n^2\} \frac{[\mathrm{CeX_1}]}{[\mathrm{Ce(IV)}]_T} \cdot [\mathrm{HLH}] \tag{9}$$

where

$$K_2 = [\mathrm{CeX_2}]/[\mathrm{CeX_1}] \cdot \mathrm{n}$$

$$K_3[\mathrm{CeX_3}]/[\mathrm{CeX_2}] \cdot \mathrm{n}$$

and

$$n = [\mathrm{HSO_4^-}]/[\mathrm{H^+}]$$

A combination of eqs (6) and (9) and related equilibrium expressions gives eqs. (10) and (11).

$$k^{\mathrm{I}}_{\mathrm{obs}} = \frac{6(k_{\alpha1}K_{\alpha1} + k_{\alpha2}k_{\alpha2}K_2K_2n + k_{\alpha3}K_{\alpha3}K_2K_3n^2)\,[\mathrm{HLH}]}{1 + K_2n + K_2K_3n^2 + (K_{\alpha1} + K_{\alpha2}K_2n + K_{\alpha3}K_2K_3n^2).\,[\mathrm{HLH}]} \tag{10}$$

$$1/k^{\mathrm{I}}_{\mathrm{obs}} = \frac{1 + K_2n + K_2K_3n^2}{6(k_{\alpha1}K_{\alpha1} + k_{\alpha2}K_{\alpha2}K_2n + k_{\alpha3}K_{\alpha3}K_2K_3n^2)} \cdot \frac{1}{[\mathrm{HLH}]} +$$

$$+ \frac{K_{\alpha1} + K_{\alpha2}K_2n + K_{\alpha3}K_2K_3n^2}{6(k_{\alpha1}K_{\alpha1} + k_{\alpha2}K_{\alpha2}K_2n + k_{\alpha3}k_{\alpha3}K_2K_3n^2)} \tag{11}$$

After evaluating the $k_{\alpha1}k_{\alpha1}$ value from the plot of $k^{\mathrm{I}}_{\mathrm{obs}}/[\mathrm{HLH}]$ versus $[\mathrm{CeX_1}]$, and using this value in the following equation which is the rearranged form of eq. (9), and from the plot of left-hand side of eq. (12) versus n (Fig. 4), we obtain $k_{\alpha\mathrm{i}}K_{\alpha1}$ values listed in Table 4

$$\frac{k^{\mathrm{I}}_{\mathrm{obs}} \cdot [\mathrm{CeIV)}]_T/[\mathrm{CeX_1}][\mathrm{HLH}] - 6k_{\alpha1}K_{\alpha1}}{K_2n} = 6k_{\alpha2}K_{\alpha2} + 6k_{\alpha3}K_{\alpha3}K_3 \cdot n \tag{12}$$

Substitution of these values in eq. (10) yields the calculated rate constants which are shown in Table 3. The agreements with the experimental rate constants are satisfactory.

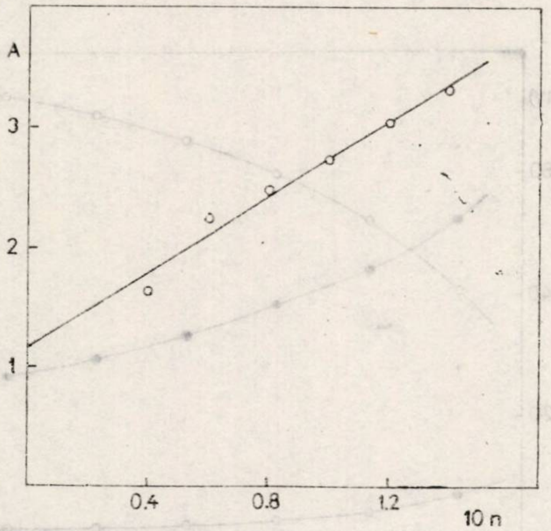

Fig. 4. — Plot of

$$\frac{k^{\mathrm{I}}_{\mathrm{obs}}[\mathrm{Ce(IV)}]_T/[\mathrm{CeX}_1][\mathrm{HLF}] - 6k_{\alpha1}K_{\alpha1}}{K_2 n} = A \text{ vs } n.$$

Table 3

Distribution of cerium(IV) sulfate complexes and first-order rate constants for Ce(IV) — malonic acid reaction in H_2SO_4 — $HClO_4$ media[a]

Run no.	$[H_2SO_4]$, M	$[HClO_4]$, M	%			$10^2 \cdot k^{\mathrm{I}}_{\mathrm{obs}}$ (s^{-1})	$10^2 \cdot k^{b}_{\mathrm{calc}}$ (s^{-1})
			C_1	C_2	C_3		
1	0.10	1.85	6.72	52.41	40.88	4.28	4.50
2	0.15	1.78	3.74	44.16	52.10	3.70	3.50
3	0.20	1.71	2.44	38.11	59.45	3.19	3.13
4	0.25	1.63	1.70	33.21	65.10	2.85	2.86
5	0.30	1.56	1.23	29.22	69.55	2.63	2.63
6	0.35	1.49	0.94	26.21	72.85	2.48	2.50

[a] $[\mathrm{Ce(IV)}]_0 = 2.5 \times 10^{-4} M$, $[\mathrm{HLH}]_0 = 2.5 \times 10^{-2} M$

$\lambda = 395$ nm, $t = 25°C$, $I = 2.0\ M$

C_1, C_2 and C_3 represents mono-, di- and tri- sulfate complexes of cerium(IV) respectively.

[b] Calculated according to eq. (10).

Relations of C_1, C_2 and C_3 with HSO_4^- concentration are shown in Fig. 5.

Inspection of eq. (11) indicates that plot of $1/k^{\mathrm{I}}_{\mathrm{obs}}$ versus $1/[\mathrm{HLH}]$ should be linear, the available data showed excellent linearity (Fig. 3) for such plot indicating the presence of intermediate complexes. The slope value of the plot of $1/k^{I}_{\mathrm{obs}}$ versus $1/[\mathrm{HLH}]$ in eq. (11) was calculated by using $k_{\alpha 1}K_{\alpha 1}$ values in Table 4, and found to be 0.57.

The $k_{\alpha 1}K_{\alpha 1}$ value may be compared with α-keto acids. The value is smaller than those for phenylglyoxylic, 2-oxobutyric acids[4] (Table 4). The decrease may be attributed to better chelation in α-keto acid case.

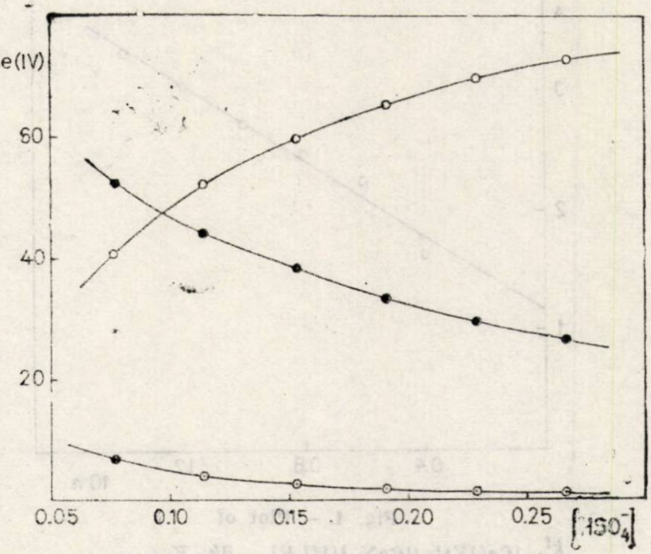

Fig. 5 — Percentage of cerium(IV) complexes versus $[\mathrm{HSO}_4^-]$ in $H_2SO_4 - HClO_4$ medium ($I = 2.0M$) : ○ CeSO_4^{2+} ; ● $\mathrm{Ce(SO_4)_2}$; ○ $\mathrm{Ce(SO_4)_3^{2-}}$

Table 4

The products of formation constant and decomposition rate constants of cerium(IV) species in $H_2SO_4 - HClO_4$ media at 25° C

MALONIC ACID	$M^{-1}.s^{-1}$
$6k_{\alpha 1}K_{\alpha 1} = 12.39$	$k_{\alpha 1}K_{\alpha 1} = 2.07$
$6k_{\alpha 2}K_{\alpha 2} = 1.17$	$k_{\alpha 1}K_{\alpha 1} = 2.07$
$6k_{\alpha 2}K_{\alpha 2} = 1.17$	$k_{\alpha 2}K_{\alpha 2} = 0.20$
$6k_{\alpha 3}K_{\alpha 3} = 0.79$	$k_{\alpha 3}K_{\alpha 3} = 0.13$
PHENYLGLYOXYLIC ACID(Ref.4)	$k_{\alpha 1}K_{\alpha 1} = 13.63$
	$k_{\alpha 2}K_{\alpha 2} = 0.34$
	$k_{\alpha 3}K_{\alpha 3} = 0.53$
2-OXOBUTYRIC ACID (Ref. 4)	$k_{\alpha 1}K_{1\alpha} = 12.70$

The stoichiometry of the reaction may be understood if malonic acid is oxidized in a one-electron step to yield a free radical which reacts further in a series of fast steps to give formic acid as product.

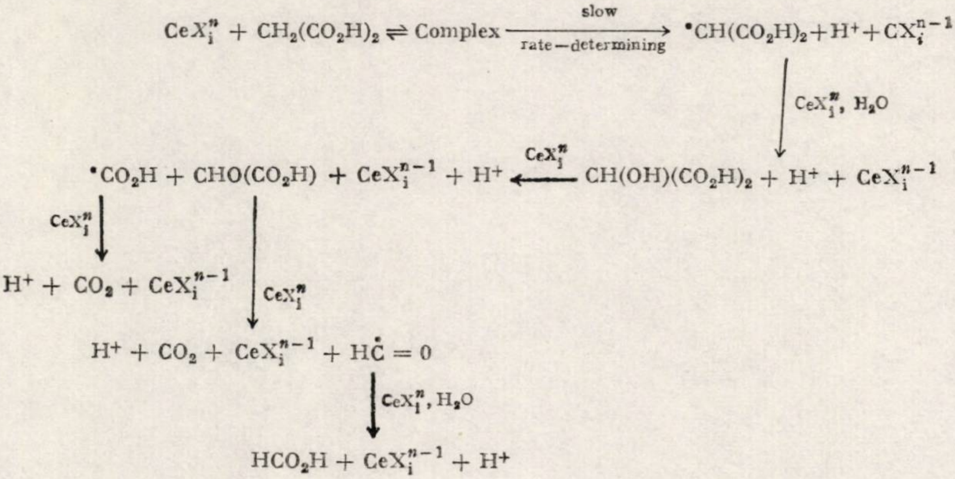

Scheme 1

REFERENCES

[1a] S. B. Hanna, S. Al-Hashimi, W. H. Webb and W. R. Carroll, *Z. Anal. Chem.*, **246**, 231 (1969).
[1b] S. B. Hanna, R. Hessley, W. H. Webb and W. R. Carroll, *Z. Anal. Chem.*, **255**, 30 (1971).
[2] B. D. Kansal, N. Singh and H. Singh, *J. Indian Chem., Soc.*, **55**, 618 (1978).
[3a] S. B. Hanna and A. S. Sarac, *J. Org. Chem.*, **12**, 2063 (1977).
[3b] Z. Amjad and A. Mc. Auley, *J. Chem. Soc., Dalton Trans.*, **1974**, 2521.
[4] A. S. Sarac, Int. *J. Chem. Kinet.*, **17**, 1333 (1985).
[5] S. Barkin, M. Bixon, and R. M. Noyes, *Int. J. Chem. Kinet.*, **10**, 619 (1978).
[6] Z. Amjad and A. Mc Auley, *J. Chem. Soc., Dalton Trans.*, **304** (1977).
[7] R. R. Lindstrom and H. E. Wirth, *J. Phys. Chem.*, **73**, 218 (1969).

Revue Roumaine de Chimie, 33, 5, 565–566 (1988)

COMPTES RENDUS

V. I. MINKIN, R. M. MINYAEV and YU. A. ZHDANOV, "Nonclassical Structures of Organic Compounds", Advances in Science and Technology in the USSR — Chemical Series, Mir Publishers, Moscow, 1987, flexicover, 311 pp.

After the review published in Uspkhi khimii by the first two authors on the same topic, this fascinating area of borderline chemistry grouping together organic, inorganic and quantum chemistry is now presented in a considerably expanded, very readable book format. The basis of the treatment involves quantum-chemical correlation diagrams, but they are presented in accessible context for organic or inorganic chemists.

After the preface and the list of symbols, the first chapter discusses molecular structure. The limitations of classical theory are pointed out, making it necessary for all chemists to become acquainted with the new data provided by the powerful *ab-initio* and semiempirical methods of quantum chemistry with the aid of modern computers. Not only the norbornyl cation, but the mono- and di-cations $(CH)_5^+$ and $(CH)_6^{2+}$, the carbenoid C_5H_4, and a host of boron or lithium organoelement compounds have structures which are at variance with the deductions of classical chemistry. The authors define chemical structure within the Born-Oppenheimer approximation as an equivalent class of molecular graphs, in agreement with ideas advocated by Bader. We quote the final paragraph of the first chapter.

"Thus the analysis of the stability of a molecular structure is closely related to the formulation of the *electron count rules* for various topological forms. This idea has proved to be very constructive in the practice of inorganic and coordination chemistry, especially in treating framework and cluster structures. Nor is it a revelation for organic chemistry either, as it is, in fact, the Hückel rule of $(4n + 2)$ that determines the stability of cyclic polyenes depending on the number, n, of π-electrons in the cycle.

This book is intended to show that simple rules of electron count can be worked up not only for planar conjugated systems, but also for a variety of complicated types of three-dimensional organic structures. These rules will assist in extending the organic chemist's structural intuition beyond the bounds of conventional typization of compounds described by the classical structural theory and by the canons of classical stereochemistry. The formulation of the electron count rules specifying the stability of nonclassical and strained structures emerges as a consequence of the generalized approach to reproduction (reconstruction) of the MO's of complex molecules from the orbitals of their adequately oriented molecular fragments."

The second capter describes orbital interactions and stability of molecular structures and presents *via* numerous examples correlation diagrams which are to be used in subsequent chapters. A strong emphasis is given to Elian and Hoffmann's isolobal fragments in organic, inorganic and organometallic systems, exemplified by the analogy between spiropentane, $Sn[Fe(CO)_4]_4$, and the bis$[Fe(CO)_4]$ complex of allene. A set of four axioms with clearly defined limitations is proposed for MO reconstruction analysis.

Non-classical structures are then analysed in the remaining six chapters: chapter 3, pyramidal structures (by far the most numerous); 4, sandwich and bipyramidal structures; 5, polyhedral and cage structures; 6, hypercoordinate hydrogen and carbon centres in organic compounds; 7, container systems and carriers (i.e. host-guest complexes involving non-classical molecules); 8, nontetrahedral tetracoordinate carbon atoms in organic compounds. The book has over 600 references and a subject index.

A special, privileged place is given to electron count rules for various topological forms, among which Hückel's rule for planar aromatic systems is the oldest and best known; thus are the 8-electron rule for pyramidal systems, the 10-electron rule for bipyramidal structures, the 14-electron rule for sandwich compounds, etc.

The richness of the documentation, the excellent illustrations, the pertinent Motto's of each chapter, and the clear exposition make the book an essential landmark in the description of non-classical structures, comparable with books on the same topic edited or authored by Bartlett, Brown and Schleyer. Nowadays that the "Non-classical Ion Problem" has been practically solved, such a review was timely. It is highly recommended to all chemists.

A. T. Balaban

Polytechnic Institute, Bucharest

VIORICA DOBRESCU and CONSTANTIN ANDREI, "Progrese în Chimia şi tehnologia poliolefinelor" (Advances in the Chemistry and Technology of Polyolefins) (in Romanian), Editura Ştiinţifică şi Enciclopedică, Bucharest, 1987, 210 p.

The remarkable achievements, both theoretical and practical, obtained in olefin polymerization allowed polyolefins to become indispensable materials for the majority of the modern industrial fields. Due to the high efficiency and quality of the obtained products along the continuous expansion of the application areas, the polyolefins represented over 55 % of the world large scale polymer production in 1985, low density polyethylene being on the first place, followed by polyvinyl chloride.

The present monograph based on both the scientific investigations carried out by the authors and the wide bibliographic material reviewed, concentrates and presents the essence of the progress made in the chemistry and technology of polyolefins revealing a vast, ordered and systematic material.

The book is structured in five chapters. The first chapter presents the main achievements and trends in low density polyethylene production, linear low density polyethylene, polypropylene, ethylene copolymers with polar monomers, as well as the new recorded ones in the field of antioxidants and photostabilizers for polyolefins.

The second chapter, after a brief historical survey, treats the complex mechanism of radical polymerization of ethylene at high pressure and examines the improvements recorded in the procedures for low density polyethylene manufacturing when autoclave or tubular type reactors are used. Further, the influence of synthesis conditions on polyethylene molecular characteristics such as molecular weight, molecular weight distribution, number, length and distribution of chain branches is outlined ; this chapter ends with the new trends in the technology of high pressure polyethylene production.

The kinetic aspects of radical copolymerization of ethylene at high pressure with polar comonomers (vinyl acetate, methyl and ethyl acrylates, acrylic and methacrylic acids, maleic anhydride) as well as the synthesis and properties inferred from the authors' own research and from the literature are examined in the next chapter.

The fourth chapter presents the spectacular results obtained in olefin polymerization in the presence of Ziegler-Natta and Phillips type catalysts, as well as a series of aspects connected with the technologies for the new types of polyolefins. As a result of the catalytic systems improvements, a new type of polyethylene was produced, i.e. linear polyethylene of low density, that actually is a copolymer of ethylene with small quantities of higher α-olefins (butene, pentene, hexene, etc.) obtained via gaseous, liquid or bulk polymerization.

Under the action of heat, light and oxygen, the polyolefins undergo degradation processes leading to a reduction of the utilization time of these materials. As a result of technological demands, the knowledge of the degradation and stabilization processes experienced during the last years has improved turning from the accumulation of practical data to the elaboration of real science in this domain, that utilizing the most sophisticated techniques of physics and chemistry. This area is presented in the last chapter of the monograph, where especially the original results of the authors in the knowledge of the mechanism of thermooxidation or photooxidation and the synergism in polyolefin stabilization are outlined.

A vast bibliography covering monographs, reviews and papers, as well as data from the various publications or patents of major firms supplements the informative material.

The book is useful to those working in the area of scientific research, the working staff of the plant laboratories, students and graduates in chemistry, physics and polymer technology.

Simion Coca
ICECHIM

ORSZÁGOS MŰSZAKI KÖNYVTÁR

NOTE POUR LES AUTEURS

La Revue Roumaine de Chimie publie des articles en anglais, français, russe, allemand ou espagnol. Les auteurs sont priés d'envoyer des articles et des comptes rendus inédits.

Les manuscrits seront dactylographiés à double interligne. La bibliographie, les tableaux et la légende des figures seront placés après le texte.

Si l'article fait partie d'une série numérotée, la partie précédente sera donnée comme première référence.

Chaque article sera précédé d'un résumé comprenant quinze lignes au maximum.

Les références bibliographiques dans le texte seront faites par des exposants sans parenthèses et paraîtront à la fin de l'ouvrage.

Les publications périodiques mentionnées dans la bibliographie seront présentées suivant les prescriptions internationales : le nom de l'auteur précédé de l'initiale du prénom, le titre du périodique abrégé conformément à « Chemical Abstracts » et souligné par une ligne, le numéro du tome indiqué par des chiffres arabes et souligné par deux lignes, suivi de la première page de l'article : à la fin, l'année de la parution sera placée entre parenthèses. Le numéro de la revue ne sera pas indiqué si les pages du volume sont numérotées consécutivement.

Les textes des livres ou traités inclueront : le nom des auteurs, précédé de l'initiale du prénom, le titre du livre entre guillemets et sans être souligné, le numéro du tome précédé par l'abréviation « vol.» (ou « Bd »), le numéro de l'édition, les éditions (the publisher), la localité de la parution du livre, l'année de la parution et la page de la référence précédée par l'abréviation « p » (ou « S »).

Les brevets seront indiqués comme suit : l'auteur ou la firme, le pays et le numéro du brevet, la date de la revue (*Chem. Abstr.*). Par ex. : M. Jones (to Union Carbide Co.) Brit. Pat. 610 238,2 Sept. 1959 : cf. *Chem. Abstr.*, **54**, 12808 (1960).

Si la référence n'a pas été lue en original, on indiquera aussi la revue de références consultée.

Les diagrammes seront tracés à l'encre de Chine sur papier calque. Les tableaux et les figures (en nombre strictement nécessaire), ainsi que les courbes dans les figures seront numérotés par des chiffres arabes. Leur explication sera donnée dans la légende des figures. Prière de ne pas inscrire les mêmes données dans les tableaux et les figures. Chaque tableau aura un titre. On indiquera dans le texte la place approximative des tableaux et des figures. Les formules chimiques seront incluses dans le texte ; en outre, elle seront transcrites sur papier calque, à l'encre de Chine.

Les auteurs sont priés d'indiquer les caractères italiques (en soulignant les lettres au crayon), ainsi que tout autre caractère spécial : les préfixes *ortho*, *méta*, *para*, *cis*, *trans*, etc. seront soulignés pour indiquer leurs caractères italiques, et ne seront jamais écrits avec des majuscules.

Aucune correction à la main ne sera admise sur le manuscrit. Les corrections seront frappés à la machine. Lès lettres grecques ou d'autres symboles spéciaux seront insérés à la main à l'encre clairement.

Le manuscrit sera signé par l'auteur.

Le titre courant aura 50 lettres au maximum.

L'entière responsabilité du contenu des articles appartient aux auteurs.

Sur demande on peut obtenir une note plus complè te.

PRINTED IN ROMANIA

TRAVAUX PARUS AUX ÉDITIONS DE L'ACADÉMIE DE LA RÉPUBLIQUE SOCIALISTE DE ROUMANIE

ELENA CEAUȘESCU, **Rășini de hidrocarburi**, 1988, 344 p.
ELENA CEAUȘESCU, **Progrese în chimia și tehnologia polimerilor**, 1986, 446 p.
ELENA CEAUȘESCU, **Forschungen im Bereich der Chemie und Technologie der Polymere**, – 1986, 444 p.
ELENA CEAUȘESCU, **Cercetări în chimia și tehnologia polimerilor**, 1983, 520 p.
ELENA CEAUȘESCU, **Noi cercetări în domeniul compușilor macromoleculari**, 1981, 536 p.
ELENA CEAUȘESCU, **Polimerizarea stereospecifică a izoprenului**, 1979, 307 p.
ELENA CEAUȘESCU, **Research work on synthesis and characterization of macromolecular compounds. Contributions**, 1974, 251 p.
I. G. MURGULESCU, **Introducere în chimia fizică, Vol. I. 1. Atom, molecule, legătură chimică**, 1976, 560 p.
I. G. MURGULESCU, V. EM. SAHINI, **Introducere în chimia fizică, Vol. I. 2. Structura și proprietățile moleculelor**, 1979, 604 p.
I. G. MURGULESCU, E. SEGAL, **Introducere în chimia fizică, Vol. II. 1. Teoria molecular-cinetică a materiei**, 1979, 1036 p.
I. G. MURGULESCU, TATIANA ONCESCU, E. SEGAL, **Introducere în chimia fizică. Vol. II. 2. Cinematică chimică și cataliză**, 1981, 1024 p.
I. G. MURGULESCU, J. PĂUN, **Introducere în chimia fizică, Vol. I. 3, Nucleul atomic, reacții nucleare, particule elementare**, 1982, 606 p.
I. G. MURGULESCU, RODICA VÎLCU, **Introducerea în chimia fizică, Vol. III. Termodinamica chimică**, 1982, 624 p.
I. G. MURGULESCU, O. M. RADOVICI, **Introducere în chimia fizică, vol. IV, Electrochimia**, 1986, 410 p.
R. VÎLCU, M. LECA, **Termodinamica polimerilor prin cromatografie de gaze**, 1987, 238 p.
I. ZUGRĂVESCU, M. PETROVANU, **Cicloadiții 3+2-dipolare**, 1987, 446 p.
RAUL MIHAIL, ION GROZEANU, **Estimarea secvențială aplicată sistemelor chimice**, 1986, 406 p.
M. BREZEANU, L. PATRON, M. ANDRUH, **Combinații complexe polinucleare și aplicațiile lor**, 1986, 244 p.
A. T. BALABAN et al., **Labelled compounds and radiopharmaceuticals applied in nuclear medicine**, coédition avec John Wiley and Sons, 1986, 742 p.
D. PURDELA, **Nomenclatura chimiei organice – IUPAC**, 1986, 454 p.
PETRU BUDRUGEAC, **Probleme de chimie**, 1986, 280 p.
T. ONCESCU, S. G. IONESCU, **Conversie fotochimică și stocare de energie**, 1985, 272 p.
V. DRĂGUȚAN, A. T. BALABAN, M. DIMONIE, **Olefin Metathesis and Ring-Opening Polymerization of Cyclo-Olefins**, coédition avec John Wiley and Sons, 1985, 544 p.
C. LITEANU, I. RICĂ, **Optimizarea proceselor analitice**, 1985, 360 p.
N. PERESCU, **Chimia extracției cu solvenți și aplicații**, 1985, 212 p.
V. E. SAHINI, M. HILLEBRAND, **Chimie cuantică în exemple și aplicații**, 1984, 378 p.
GH. MARCU, **Chimia compușilor coordinativi**, 1984, 415 p.
E. CORDOS, C. MANOLIU, **Spectrometria de absorbție și fluorescență atomică**, 1984, 178 p.
C. BODEA, **Tratat de biochimie vegetală p. II, t. 5**, 1984, 438 p.
N. ASANDEI, A. GRIGORIU, **Chimia și structura fibrelor**, 1983, 395 p.
N. IONESCU, M. CĂLDĂRARU, **Oxidarea catalitică a olefinelor inferioare**, 1983, 178 p.
C. CAȘCAVAL, **Studiul polimerilor prin piroliză și cromatografie de gaze**, 1983, 220 p.
C. I. SIMIONESCU, F. DANES, **Originea vieții**, 1983, 110 p.
C. BODEA, **Tratat de biochimie vegetală, p. II. t. IV**, 1982, 480 p.
I. GĂLĂȚEANU, **Procese și metode radiochimice în energetica nucleară**, 1981, 234 p.
CR. SIMIONESCU, VALERIA GORDUZA, **Polimeri biocompatibili și biologic activi**, 1980, 479 p.
M. FLORESCU, **Metode științifice în dezvoltarea industriei chimice moderne**, 1979, 256 p.
C. GH. MACAROVICI, **Analiza chimică cantitativă anorganică**, 1979, 457 p.
I. ZUGRĂVESCU, MAGDA PETROVANU, **N-ylid chemistry**, coédition avec McGraw-Hill International Book Company U.S.A., 1977, 386 p.

ISSN 0035–3930

I. P. Informația c. 2076

43 426

Lei 40

F 1103

ACADÉMIE DE LA RÉPUBLIQUE SOCIALISTE DE ROUMANIE

66

REVUE ROUMAINE DE CHIMIE

TOME 33
N° 6
Juin 1988

EDITURA ACADEMIEI REPUBLICII SOCIALISTE ROMÂNIA

Rev. Roumaine. Chim.

RRCHAX, 33, *6*, p. 567 - 670 (1988), Bucarest

ACADÉMIE DE LA RÉPUBLIQUE SOCIALISTE DE ROUMANIE

COMITÉ DE RÉDACTION

Rédacteur en chef:

I. G. MURGULESCU, membre de l'Académie de la République Socialiste de Roumanie

Rédacteurs en chef adjoints:

A. T. BALABAN et V. EM. SAHINI, membres correspondants de l'Académie de la République Socialiste de Roumanie

Collège de rédaction:

EM. BRATU, ELENA CEAUŞESCU, ECATERINA CIORĂNESCU-NENITZESCU, CR. SIMIONESCU, membres de l'Académie de la République Socialiste de Roumanie ; P. SPACU, membre correspondant de l'Académie de la République Socialiste de Roumanie ; M. BANCIU, M. D. GHEORGHIU, I. HAIDUC, D. I. MARCHIDAN, G. NIAC et D. SĂNDULESCU

La Revue Roumaine de Chimie paraît 10 fois par an. Toute commande de l'étranger sera adressée ı ROMPRESFILATELIA — sectorul Export-Import Presă, P. O. Box 12—201, télex 10376, prsfi r 78 104 Bucarest, Calea Griviţei nr. 64—66, Roumanie

Les manuscrits, les livres et les revues proposés en échange, ainsi que toute correspondance seront envoyés à la rédaction

REVUE ROUMAINE DE CHIMIE

125, Calea Victoriei, 79717 Bucarest, Roumanie, téléphone 50 76 80

EDITURA ACADEMIEI REPUBLICII SOCIALISTE ROMÂNIA
125, Calea Victoriei, 79717 Bucarest, Roumanie, téléphone 50 76 80

REVUE ROUMAINE DE CHIMIE

ORSZÁGOS MŰSZAKI INFORMÁCIÓS KÖZPONT ÉS KÖNYVTÁR 1883

Tome 33, N° 6 **Juin, 1988**

DUMITRU TITA, ILIE JULEAN and ZENO SIMON, Kinetic investigation of basic zinc-carbonates decomposition : $2ZnCO_3 . 3Zn(OH)_2$ (in German) . 569—577

JAVIER DOMÉNECH and JOAN MIRÓ, Ionic B coefficients in the Jones-Dole viscosity equation of halide ions in aqueous formamide solutions . . . . 579—583

O. RADU, As(III) — HCl — H_2O system. I. Homogeneous state . . . . 585—594

A. MATEESCU and D. MATEESCU, Studies on corrosion of lead acid battery grids with addition of Se, Sb and silver . . . . 595—602

V. DAVID and G. E. BAIULESCU, A UV/VIS spectrometric study of the reaction of the Pd(II)-*p*-nitrosodiphenylamine complex with carbon monoxide 603—610

P. M. SHIUNDU and S. B. JONNALAGADDA, A novel spectrophotometric method for the determination of peroxydisulphate ion using *o*-dianisidine-$S_2O_8^{2-}$ —Cu(II) indicator reaction . . . . 611—616

ABOUL-FETOUH E. MOURAD, Charge-transfer complexes of benzanilides with π-acceptors . . . . 617—622

D. PURDELA, The *Z* dependence of nuclear diamagnetic shielding constants free atoms . . . . 623—627

U.D.N. BAJPAI, ALKA JAIN and A. K. BAJPAI, Silver ion catalyzed redox polymerization of acrylamide . . . . 629—634

LIDIA POP, H. KREMPELS and F. HODOȘAN, Exo- and endohormones. XIII. Synthesis of Z-9-pentacosene . . . . 635—637

HANS-HORST GLATT, MAMADOU FOULA BARRY, CAROL CSUNDERLIK, ILSE BACALOGLU and SIMONA TIMOFEI, Imines of aminoazoles. IV. Kinetics and mechanism of benzylidene-aminoazoles hydrolysis (in German) 639—652

H. M. HASSAN and O.M.O. HABIB, Condensation of *o*- and *p*-phenylenediamine with some substituted 2-thiazolin-5-ones . . . . 653—656

O.M.O. HABIB, I. I. ABD EL-GAWAD and D. S. BADAWY, Synthesis and reactions of some new 5-arylidene-1-aryl-3-oxo-2-indane carboxanilide derivatives . . . . 657—667

BOOK REVIEWS . . . . 669—670

Revue Roumaine de Chimie, 33, 6, 569–577 (1988)

KINETISCHE UNTERSUCHUNG DER ZERSETZUNG DES BASISCHEN ZINKCARBONATS : $2ZnCO_3 \cdot 3Zn(OH)_2$

DUMITRU TITA[a], ILIE JULEAN[a] und ZENO SIMON[b]

[a] Technische Hochschule „Traian Vuia“ Timişoara, Fakultät der chemischen Technologie, Lehrstuhl für anorganische Chemie und Technologie, 1900 Timişoara, Bd. 30 Decembrie nr. 2, Rumänien

[b] Medizininstitut, Timişoara, Rumänien

Eingegangen am 16. Mai 1987

The thermal decomposition of basic zinc carbonate : $2ZnCO_3 \cdot 3Zn(OH)_2$ is studied in comparison with that of the mechanical mixture of the same composition, and the natural mineral. The kinetic study leads to concordant results as regarding the two procedures : isothermal and nonisothermal. The values of the activation energies are : isothermal : (112 ± 6) and (114 ± 8) $kJ \cdot mol^{-1}$; nonisothermal : (112 ± 6) and (110 ± 3) $kJ \cdot mol^{-1}$. The results also show that the thermal decomposition of basic zinc carbonate occurs according to a kinetic equation of the first order.

Die thermische Zersetzung des basischen Zinkcarbonats $2ZnCO_3 \cdot 3Zn(OH)_2$ wurde vergleichsweise mit der Zersetzung des mechanischen Gemisches derselben Zusammensetzung, beziehungsweise jener des natürlichen Minerals (Hydrozinkit) verfolgt. Die kinetischen Untersuchungen wurden sowohl unter isothermen als auch nichtisothermen Bedingungen durchgeführt und ergaben übereinstimmende Ergebnisse. Die Werte der Aktivierungsenergie waren : isotherm : (112 ± 6) und (114 ± 8) $kJ.mol^{-1}$; nichtisotherm : (112 ± 6) und (110 ± 3) $kJ \cdot mol^{-1}$. Ebenso konnte auf Grund der erhaltenen Ergebnisse behauptet werden, dass die thermische Zersetzung des basischen Zinkcarbonats nach einer Kinetik erster Ordnung verläuft.

1. EINLEITUNG

In einer vorangehenden Arbeit[1] wurden die Bedingungen untersucht, unter denen das basische Zinkcarbonat $2ZnCo_3 \cdot 3Zn(OH)_2$ entsteht.

Vorliegende Arbeit untersucht, im selben Zusammenhang, das thermische Verhalten der im Laboratorium erhaltenen Verbindung im Vergleich mit einem mechanischen Gemisch von derselben Zusammensetzung und dem natürlichen Mineral (Hydrozinkit). In der Fachliteratur sind diesbezüglich verhältnismässig wenig Daten aufzufinden und diese stimmen oft nicht überein. So findet man bei der Herstellung von Zinkoxid aus synthetisiertem Zinkcarbonat[2] eine einzige Zersetzungsetappe, während für die Zersetzung des natürlichen Minerals mehrere Etappen angedeutet sind[3,4,5].

Ebenso wird in vorliegender Arbeit die Kinetik der thermischen Zersetzungsreaktion untersucht, für welche wir keine Literaturangaben gefunden haben.

2. EXPERIMENTELLES

Die der thermischen Zersetzung unterworfenen Proben von basischen Zinkcarbonat gehörten zu der schon beschriebenen Versuchsreihe,[1] während $Zn(OH)_2$ und $ZnCO_3$ (für das mechanische Gemisch) im Laboratorium erhalten wurden.[5]

Die Untersuchungen wurden mit einem Derivatographen M.O.M. Budapest, Typ Paulik, Erdey, in dem Temperaturbereich 20—500°C durchgeführt, wobei als Standard α-Al_2O_3 eingesetzt wurde.

Für die isothermen Untersuchungen wurde eine Thermowaage „Ugine-Eyraud" für denselben Temperaturbereich verwendet.

3. ERGEBNISSE UND DISKUSSION

Die Zersetzung des basischen Zinkcarbonats (das im Laboratorium hergestellt wurde) verläuft in einer einzigen Etappe, im Temperaturbereich von 180—260°C, wobei die grösste Zersetzungsgeschwindigkeit bei 240°C zu verzeichnen ist. Der Massenverlust ist von einem endothermen Effekt auf dre Kurve begleitet. Die wahrscheinliche Reak tionsgleichung für die Zersetzung ist folgende :

$$2ZnCO_3 \cdot 3Zn(OH)_2 \rightarrow 5\,ZnO + 2\,CO_2 + 3\,H_2O$$

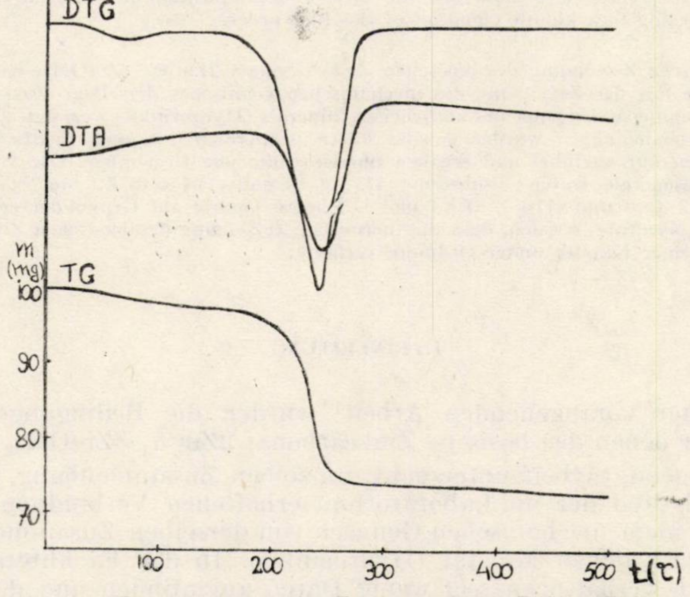

Abb. 1. — Derivatogramm der Zersetzung von $2ZnCO_3 \cdot 3Zn(OH)_2$.

Das der Zersetzung dieser Substanz entsprechende Derivatogramm ist in Abbildung 1 dargestellt.

Das der thermischen Analyse unterworfene mechanische Gemisch, bestehend aus $ZnCO_3$ und $Zn(OH)_2$ im Verhältnis 2 :3, zeigte im Vergleich zu dem synthetisirten basischen Salz ein unterschiedliches Verhalten.

Das der Zersetzung des mechanischen Gemisches von $Zn(OH)_2$ und $ZnCO_3$ entsprechende Thermogramm ist in Abbildung 2 wiedergegeben.

Auf Grund dieser Untersuchungen (vervollständigt durch chemische und röntgenostrukturelle Analysen) könnte man annehmen, dass der Unterschied im Verhalten des im Laboratorium hergestellten und des natürlichen Salzes auf ihre Entstehungsbedingungen zurückzuführen ist.

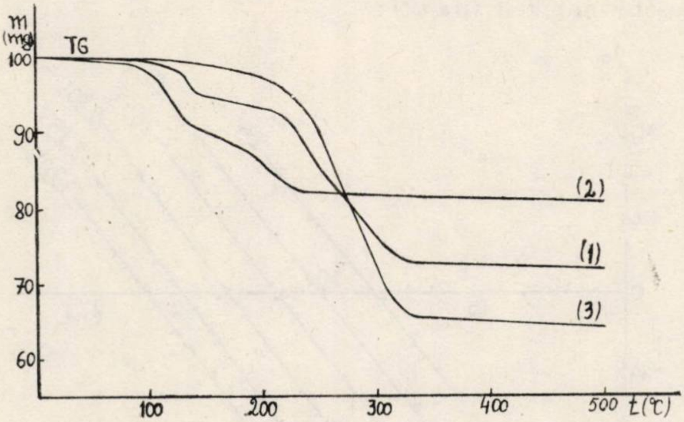

Abb. 2. — Thermogramm der Zersetzung des mechanischen Gemisches (1), $Zn(OH)_2$ (2) und $ZnCO_3$ (3).

Ein ähnliches Verhalten kann auch beim basischen Kupfercarbonat beobachtet werden.[5]

Isotherme Messungen

Der untersuchte Temperaturbereich war 220—245°C. Die entsprechende kinetische Gleichung für die Zersetzungsreaktion wurde infolge der Verifizierung einiger in der Fachliteratur[7-9] gegebenen kinetischen Gleichungen gefunden. Es wurde dabei in Betracht gezogen, dass unter isothermen Bedingungen, wenn die Geschwindigkeitskonstante unabhängig von der Zeit ist, die graphische Darstellung der kinetischen Gleichung (eine Funktion) in Abhängigkeit von der Zeit, im Falle der richtig gewählten kinetischen Gleichung eine Gerade sein müsste.

Wie zu erwarten war, handelt es sich in unserem Fall um eine Kinetik erster Ordnung, der folgende Funktion entspricht :

$$g(\alpha) = -\ln(1-\alpha) \qquad (1)$$

wobei

$$g(\alpha) = \int_0^\alpha \frac{d\alpha}{f(\alpha)} = \int_0^t k\,dt \qquad (2)$$

In Beziehung (2) stellt k die Geschwindigkeitskonstante dar :

$$k = Z \exp(-E/RT) \tag{3}$$

$f(\alpha)$ hängt vom Reaktionsmechanismus ab und charakterisiert die Reaktionsgeschwindigkeit $(d\alpha/dt)$:

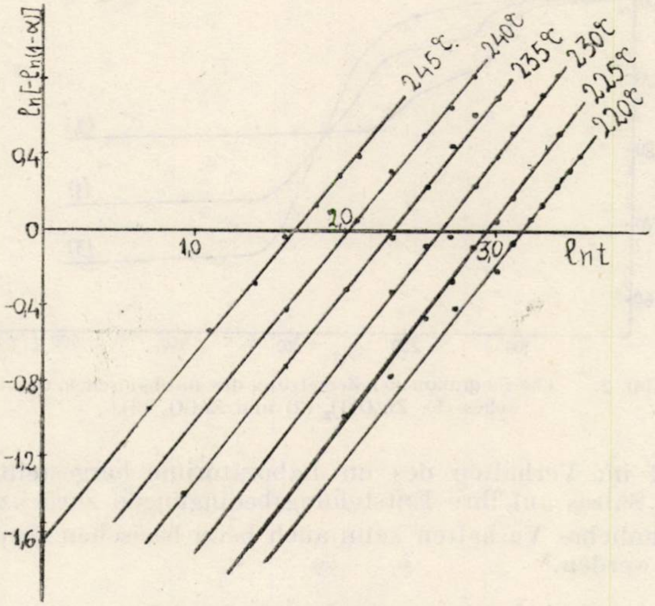

Abb. 3. — Graphische Darstellung von ln $[-\ln(1-\alpha)]$ in Abhängigkeit von ln t.

$$\frac{d\alpha}{dt} = k \cdot f(\alpha) \tag{4}$$

wobei : α die zum Zeitpunkt t zersetzte Substanzmenge darstellt (Umwandlungsgrad

Stellt man ln $[-\ln(1-\alpha)]$ in Abhängigkeit von ln t graphisch dar, kann aus der Neigung der erhaltenen Geraden die Reaktionsordnung berechnet werden. Die graphische Darstellung von ln $[-\ln(1-\alpha)]$ in Abhängigkeit von der Zeit führt zu Geraden aus deren Neigung die Geschwindigkeitskonstanten berechnet werden können. Die Darstellungen sind in den Abbildungen 3 und 4 widergegeben.

Die Werte für die Reaktionsordnung befinden sich im Bereich 0,95—1,09 ; für die Berechnungen wurde der Wert 1,00 verwendet.

Die Abbildung 5 enthält die graphische Darstellung von log k in in Abhängigkeit von 1/T. Aus der Neigung dieser Geraden $-E/2{,}3R$ kann die Aktivierungsenergie berechnet werden. Aus dem Schnittpunkt dieser Geraden mit der Ordinate kann man den preexponentiellen Faktor Z mit Hilfe der Regressionsanalyse berechnen.[10] Die Werte der Geradenparameter, mit den entsprechenden Fehlern sind: $a \pm tS_a = 8{,}9 \pm 0{,}7$; $b \pm tS_b = -5{,}9 \pm 0{,}3$ beziehungsweise $E \pm tS_E = (112 \pm 6)$ $kJ \cdot mol^{-1}$ und $Z = 8{,}32 \cdot 10^8$ sQ^{-1}

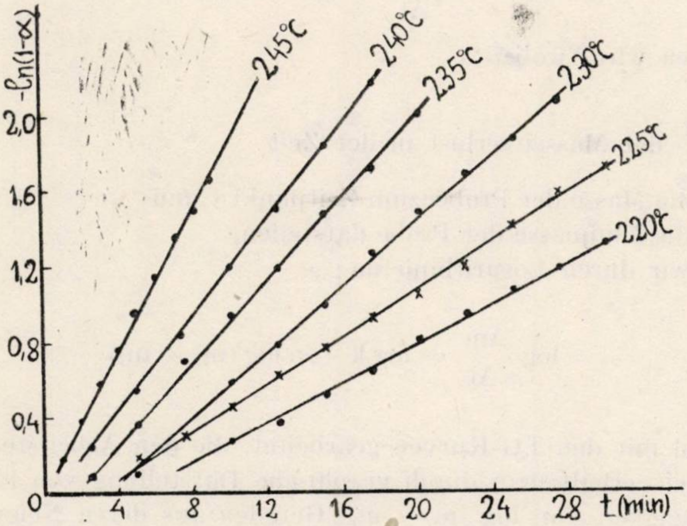

Abb. 4. — Graphische Darstellung von ln (1—α) in Abhängigkeit von der Zeit.

Zu denselben Ergebnissen gelangt man auch im Falle wenn eine Variante der Kissinger-Methode[11] angewendet wird.

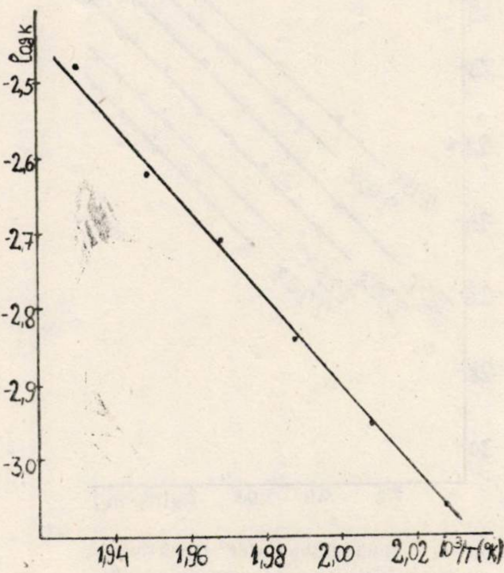

Abb. 5. — Graphische Darstellung von log k in Abhängigkeit von 1/T.

Ziehen wir in Betracht, dass die Geschwindigkeit der Zersetzungsreaktion durch die Gleichung

$$v = \frac{\Delta m}{\Delta t} = k(m_t - m_f)^n \tag{5}$$

beschrieben wird, wobei

$\frac{\Delta m}{\Delta t}$ der Massenverlust in der Zeit

m_t die Masse der Probe zum Zeitpunkt t und

m_f die Endmasse der Probe darstellen,

erhalten wir durch Logarithmieren :

$$\log \frac{\Delta m}{\Delta t} = \log k + n \log (m_t - m_f) \tag{6}$$

Wird mit den TG-Kurven gearbeitet, die den Arbeitstemperaturen entsprechen, erhält man durch graphische Darstellung von log ($\Delta m/\Delta t$) in Abhängigkeit von log ($m_t - m_f$) Geraden aus deren Neigung man n bestimmen kann, während die Ordinate zum Ursprung log k ergibt.

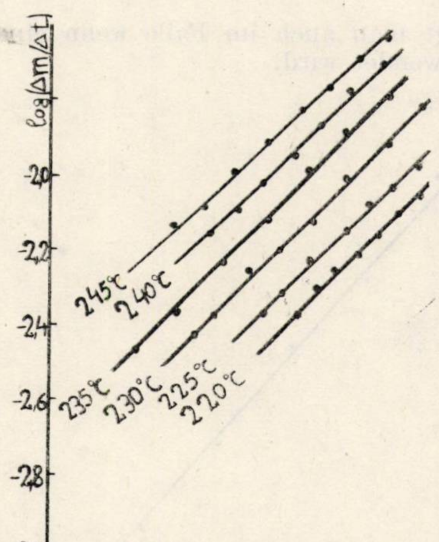

Abb. 6. — Abhängigkeit der Reaktionsgeschwindigkeit von der unzersetzten Masse.

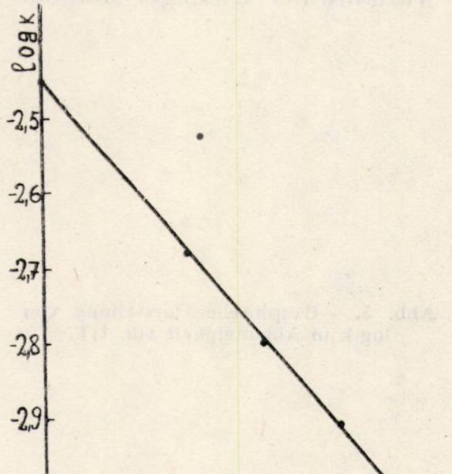

Abb. 7. — Abhängigkeit der Geschwindigkeitskonstante von der Temperatur.

Die Werte der beiden Parameter, mit den entsprechenden Fehlern, sind : bei 220°C : $n \pm tS_n = 0{,}96 \pm 0{,}03$, $k = 1{,}05 \cdot 10^{-3}$;

bei 225°C : $n \pm tS_n = 0{,}97 \pm 0{,}04$, $k = 1{,}26 \cdot 10^{-3}$;

bei 230°C : $n \pm tS_n = 0{,}99 \pm 0{,}06$; $k = 1{,}65 \cdot 10^{-3}$;

bei 235°C : $n \pm tS_n = 1{,}04 \pm 0{,}07$, $k = 2{,}69 \cdot 10^{-3}$;

bei 215°C : $n \pm tS_n = 0{,}94 \pm 0{,}02$, $k = 2{,}80.10^{-3}$.

Aus den bestimmten Geschwindigkeitskonstanten kann man nun E und Z berechnen.

Die Abbildungen 6 und 7 enthalten die graphischen Darstellungen und die Werte der Geraden- und kinetischen Parameter, mit den entsprechenden Fehlern, sind : $a \pm tS_a = 8{,}8 \pm 0{,}7$; $b \pm tS_b = -6{,}0 \pm 0{,}4$ beziegungsweise $E \pm tS_E = (114 \pm 8)$ kJ·mol^{-2}; $Z = 6{,}46.10^8$ s^{-1} ($n = 1{,}00$; der Veränderungsbereich ist 0,92 – 1,11). Die Werte der Aktivierungsenergie stimmen mit den vorher berechneten Werten gut überein.

Nichtisotherme Messungen

Die Berechnung der Aktivierungsenergie sowie anderer kinetischer Parameter auf Grund von Versuchen mit ansteigender Temperatur ist geeingneter als die Durchführung von isothermen Versuchen für eine Reihe von Temperaturen.

Es gibt einige in der nichtisothermen Kinetik öfters verwendete Berechnungsmethoden von denen die Coats-Redfern[12,13] und Fuos[12,14]-Methoden auch in unserem Fall benützt werden.

Ebenso versuchten wir auch die Freeman-Carroll-Methode[12,15] anzuwenden, obwohl diese umfangreicher ist, aber am meisten besonders für die Berechnung der Reaktionsordnung verwendet wird. Auf diese Weise fanden wir die Reaktionsordnung 1, was in Übereinstimmung war mit den Werten anderer Methoden. Nur die Werte für die Aktivierungsenergie waren etwas grösser.

Wird die Coats-Redfern-Methode angewendet, führt die graphische Darstellung von $\log\left[\frac{[1-(1-\alpha)^{1-n}}{T^2(1-n)}\right]$ und $\log\Bigg[-\left[\frac{\log(1-\alpha)}{T^2}\right]$ in Abhängigkeit von $1/T$, für $n = 1$, zu einer Geraden. Aus der Neigung dieser Geraden $b \pm tS_b = -5{,}9 \pm 0{,}3$ wurde die Aktivierungsenergie $E \pm tS_E = (112 \pm 6)$ kJ·mol^{-1} und aus der Ordinate zum Ursprung $a \pm tS_a = 5{,}6 \pm 0{,}4$ wurde $Z = 4{,}59 \cdot 10^8$ s^{-1} berechnet. Für die mit Hilfe der Bezieghung (3) berechnete Geschwindigkeitskonstante wurde der Wert $k = 1{,}74.10^{-3}$ erhalten. Die graphische Darstellung ist in Abbildung 8 widergegeben.

Das operationale Prinzip der Fouss-Methode ist in Abbildung 9 dargestellt, wobei:

m_i die aktive Masse der Probe im Inflexionspunkt,
m_{t_i} die Masse der Probe im Inflexionspunkt
m_f die Endmasse der Probe und
$\left(\frac{dm}{dT}\right)_i$ die Neigung der TG-Kurve im Inflexionspunkt sind.

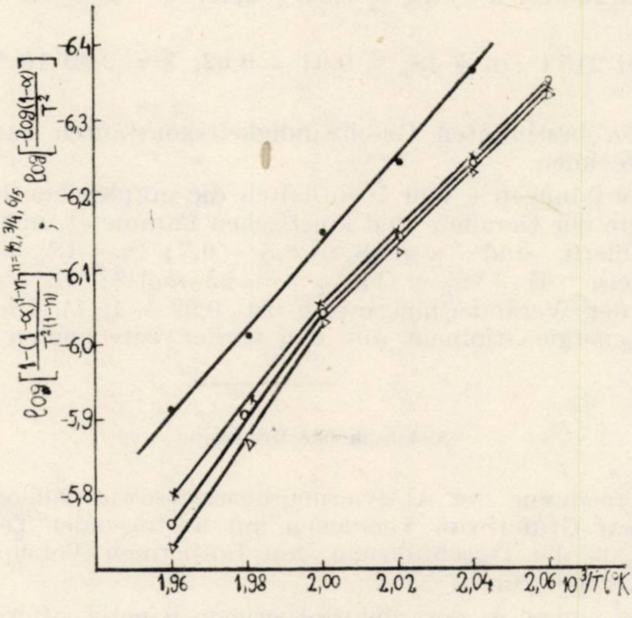

Abb. 8. — Coats-Redfern-Methode

x n = 1/2 ; o n = 3/4 ; ● n = 1 ; Δ n = 6/5

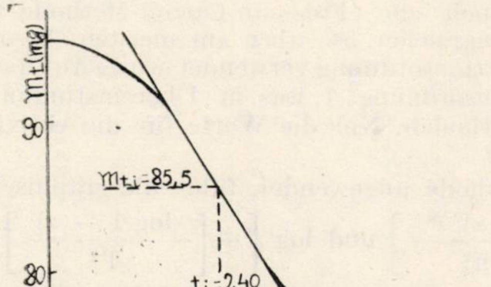

Abb. 9. — Fuoss-Methode

$$m_i = m_{t_i} - m_f = 85{,}5 - 73 = 12{,}5$$

$$T_i = 513°\,K\,;\quad \left(\frac{dm}{dT}\right)_i = \operatorname{tg}\beta = -0{,}65$$

Durch statistische Verarbeitung der Daten ($n = 3$, $t = 4{,}30$ für $P = 95\%$) wurden folgende Werte für E, Z und k erhalten : $E \pm tS_E = (110 \pm 3)$ kJ·mol^{-1}; $Z = 7{,}44 \cdot 10^8$ s^{-1} und $k = 4{,}17 \cdot 10^{-3}$.

4. SCHLUSSFOLGERUNGEN

Das im Laboratorium erhaltene Zinkcarbonat zersetzt sich in einer einzigen Etappe, während das mechanische Gemisch derselben Zusammensetzung und das natürliche Mineral sich in mehreren Etappen zersetzen.

Die durch istotherme Untersuchungen und bei ansteigender Temperatur erhaltenen Ergebnise sind übereinstimmend, was bedeutet, dass die g(α)-Funktion richtig gewählt wurde.

Die kinetischen Untersuchungen beweisen, dass die thermische Zersetzung dieser Verbindung nach einer Kinetik erster Ordnung verläuft.

LITERATURVERZEICHNIS

[1] I. Julean, R. Unc und D. Tita, *Bul. Şti. Tech. Inst. Poly. „Traian Vuia" Timişoara* (*Ser. Chimie*), **30**, 99 (1985).

[2] H. Utsugi und K. Tamiya, *Nippon Kagaku Zasshi.*, **86**, 699 (1965).

[3] G. Cocco, *Periodico Mineral*, **20**, 92 (1951) ; cf. C. A. **45** (1951) 7921 f.

[4] C. Beck, *Amer. Min.*, **35** (11—12) (1950) ; cf. D. N. Todor, „Thermal Analysis of Minerals", Abacus Press, Tunbridge Wells, Kent, 1976, p. 184.

[5] D. N. Todor, „Analiza termică a mineralelor", Editura tehnică Bucureşti, 1972, p. 200, 202 ; D. N. Todor, „Thermal Analysis of Minerals", Abacus Press, Tunbridge Wells, Kent 1976, p. 182, 184.

[6] Iu. V. Kariakin und I. I. Anghelov, "Cystye himiceskie vecestva", Moskva Izdatelstvo, "Khimia" 1974, p. 399, 403.

[7] K. N. Ninan, *Thermochim. Acta*, **98**, 221 (1986).

[8] J. Ribas, M. Serra und A. Escuer, *Thermochim. Acta*, **91**, 107 (1985).

[9] J. Ribas, M. Serra und A. Escuer, *Thermochim. Acta*, **80**, 103 (1984).

[10] D. Ceauşescu, „Utilizarea statisticii matematice în chimia analitică", Editura tehnică Bucureşti 1982, p. 208.

[11] H. E. Kissinger, *Analyt. Chem.*, **29**, 1702 (1957).

[12] E. Segal und D. Fatu, "Introducere în cinetica neizotermă", Editura Academiei R.S.R. Bucureşti,1983, cap. V, VI.

[13] A. W. Coats und J. P. Redfern, *Nature*, **201**, 69 (1964).

[14] R. M. Fuoss, I. O. Salyer und H. S. Wilson, *J. Polymer Sci.*, **2A**, 3147 (1964).

[15] E. S. Freeman und B. Carroll, *J. Phys. Chem.*, **62**, 394 (1958).

Revue Roumaine de Chimie, **33**, *6*, 579–583 (1988)

IONIC B COEFFICIENTS IN THE JONES-DOLE VISCOSITY EQUATION OF HALIDE IONS IN AQUEOUS FORMAMIDE SOLUTIONS

JAVIER DOMÉNECH [a] and JOAN MIRÓ [b]

[a] Departament de Química, Universitat Autonoma de Barcelona Bellaterra, Spain
[b] Col. legi Universitari de Girona, Pca Hospital, 62. 17071 Girona, Spain

Received March 2, 1987

The viscosities of sodium iodide solutions in formamide water mixtures have been determined at 25, 30 and 35 °C. From these data the B-coefficients of NaI in different solvent compositions have been calculated by means the Jones-Dole equation. The ionic B-coefficients of the halide ions in the range of water mole fraction 1 to 0.5, at 30 and 35°C have been determined from the known B-values of NaCl and NaBr[1,2] and the ionic B-coefficient of Na^+ reported in a previous work.[1] From these results a certain preferential hydration of the halide ions can be assumed.

INTRODUCTION

The viscosity of electrolyte solutions yields valuable information concerning ion-solvent and solvent-solvent interactions. The relative viscosity of a dilute electrolyte solution is related to the salt concentration according to the Jones-Dole equation,[3]

$$\eta_r = 1 + Ac^{1/2} + Bc$$

where the A-coefficient is a measure of ion-ion interactions and the B-coefficient, which can be expressed as a sum of the ionic contributions, depends on ion-solvent interactions. The ionic B coefficient can be considered as made up, at least of three contributions[4,5] : i) a temperature independent positive contribution due to the size and shape of the ion, related with the Einstein volume effect;[6] ii) a positive contribution from the long-range orientation of solvent molecules by the ionic field, which decreases with increasing temperature, and iii) a negative contributin due to the breaking of solvent structure produced by the ion, which increases with increasing temperature. Then, the value of the B coefficient together with its temperature dependence give an indication of the structure-making or structure breaking role of the ions on the solvent structure.

In the present work the B-coefficients of sodium iodide solutions in formamide-water mixtures have been determined at 25, 30 and 35 °C. From these data, together with those corresponding to NaCl and NaBr,[1,2] the B-coefficients of the halide ions have been obtained in a solvent composition range from 0 to 0.5 water mole fraction and are discussed in terms of ion-solvent interactions and solvent structure.

EXPERIMENTAL

The experimental techniques and procedures for the measurements of the viscosities and densities of electrolyte solutions were described in detail previously.[7]

Formamide (FA) (Fluka, analytical grade) was purified as described previously.[8] Sodium Iodide (Merck, analytical grade) was dried at 150 °C for several hours before use.

RESULTS AND DISCUSSION

The densities and viscosities of sodium iodide solutions in different FA-water mixtures have been measured at 25, 30 and 35°C. The results are reported in table 1. From these data the A and B coefficients of the Jones-Dole equation were determined by fitting $(\eta_r - 1)c^{-1/2}$ vs. $c^{1/2}$ by the least-squares method. The A values do not show practically any dependence with solvent composition and temperature, taking a mean value of 0.004 + 0.001 $dm^{3/2}$ $mol^{-1/2}$. In table 2, the B coefficients for NaI at 25, 30 and 35 °C are summarized together with the standard deviations.

In a previous paper,[1] the values of the B-coefficient for Na^+ ion in FA-water mixtures have been reported over a solvent composition range from 0 to 0.5 water mole fraction. These values were obtained assuming the equality $B_{Ph_4P^+} = B_{Ph_4B^-}$ — for temperatures higher than 30°C.[9,10]. From these values the ionic B-coefficients for Cl^-, Br^- and I^- ions at 30 and 35°C have been calculated by determining the differences between the B-coefficients of the corresponding sodium halides and that of sodium ion. The B-coefficients of NaCl and NaBr were taken from literature.[1,2] The B-values of NaCl at 30°C have been obtained by extrapolation from its temperature dependence.[2] The results are reported in table 3. The B-coefficients of the halide ions in pure FA are slightly lower than those reported by Martinus and Vincent[11] obtained from the correspondence plot between partial molar ionic entropy and the B-coefficients of Bu_4N^+ and Pe_4N^+ and the respective crystallographic radii.

From the results in table 3, it can be observed that the B-coefficients of the halide ions are low and decrease slightly with increasing temperature. In fact, it is known that the FA-water mixture shows a high degree of structuration due to the possibility of the FA molecules to form hydrogen bonds with water molecules.[2,12–14] Consequently, a certain structure breaking role for halide ions can be assumed in the FA-water mixtures. Further, the solvent becomes more structured with increasing the water mole fraction. This leads to an enhancement of the structure breaking properties of the halide ions and, consequently, to a decrease of the B-coefficients, which is the observed tendency (see table 3).

On the other hand, Finter and Hertz,[14] recently found from NMR relaxation studies, a weak tendency of selective solvation of I^- ion in FA-water by water. In this way, with adding water to FA, an increase of

Table 1

Densities and relative viscosities of NaI solutions in different FA-water mixtures at 25, 30 and 35 °C

25°C			30 °C			35°C		
c/mol dm^{-3}	d/g cm^{-3}	η_r	c/mol dm^{-3}	d/g cm^{-3}	η_r	c/mol dm^{-3}	d/g cm^{-3}	η_r
			$x_{H_2O} = 0.901$					
0.01107	1.0288	1.0004	0.01105	1.0271	1.009	0.01102	1.0244	1.0010
0.03402	1.0311	1.0013	0.03396	1.0296	1.0022	0.03385	1.0260	1.0028
0.05156	1.0329	1.0019	0.05145	1.0307	1.0031	0.05133	1.0282	1.0042
0.07295	1.0356	1.0025	0.07280	1.0334	1.0044	0.07261	1.0308	1.0059
0.09667	1.0380	1.0036	0.09642	1.0359	1.0056	0.09616	1.0331	1.0081
0.1247	1.0408	1.0044	0. 1244	1.0381	1.0072	0.1241	1.0356	1.0100
			$x_{H_2O} = 0.701$					
0.03145	1.0706	1.0050	0.03135	1.0672	1.0057	0.03125	1.0636	1.0064
0.05415	1.0735	1.0088	0.05395	1.0695	1.0095	0.05380	1.0665	1.0109
0.07670	1.0757	1.0120	0.07647	1.0723	1.0141	0.07621	1.0687	1.0147
0.09594	1.0777	1.0150	0.09561	1.0740	1.0169	0.09528	1.0703	1.0189
0.1317	1.0816	1.0209	0.1312	1.0774	1.0229	0.1308	1.0743	1.0256
			$x_{H_2O} = 0.498$					
0.01232	1.0948	1.0034	0.01227	1.0910	1.0035	0.01223	1.0868	1.0030
0.03280	1.0964	1.0085	0.03270	1.0928	1.0088	0.03257	1.0886	1.0077
0.05186	1.0986	1.0134	0.05165	1.0940	1.0131	0.05150	1.0909	1.0122
0.07544	1.1015	1.0196	0.07513	1.0970	1.0191	0.07485	1.0929	1.0175
0.1004	1.1040	1.0235	0.1000	1.0998	1.0252	0.09964	1.0955	1.0232
0.1324	1.1071	1.0331	0.1319	1.1029	1.0329	0.1314	1.0988	1 0305
			$x_{H_2O} = 0.402$					
0.01490	1.1034	1.0044	0.01484	1.0996	1.0051	0 01478	1.0951	1.0044
0.03254	1.1050	1.0090	0.03242	1.1009	1.0100	0.03230	1.0968	1.0090
0.05861	1.1079	1.0160	0.05840	1.1039	1.0174	0.05818	1.0998	1.0160
0.07727	1.1100	1.0209	0.7727	1.1053	1.0231	0.07666	1.1013	1.0208
0.1050	1.1128	1.0286	0.1046	1.1079	1.0303	0.1042	1.1045	1.0283
0.1330	1.1155	1.0366	0.1324	1.1111	1.0394	0.1319	1.1070	1.0356
			$x_{H_2O} = 0.202$					
0.01524	1.1184	1.0058	0.01519	1.1145	1.0055	0.01513	1.1099	1.0048
0.03243	1.1202	1.0116	0.03231	11.162	1.0117	0.03218	1.1116	1.0104
0.05534	1.1224	1.0203	0.05513	1.1181	1.0195	0.05493	1.1139	1.0741
0.07838	1.1246	1.0284	0.07810	1.1205	1.0276	0.07779	1.1161	1.0251
0.09877	1.1269	1.0359	0.09840	1.1226	1.0350	0.09802	1.1183	1.0323
0.1339	1.1303	1.0476	0.1334	1.1260	1.0470	0.1329	1.1218	1.0427

the solvated anion size can be expected due to the gradual entry of water molecules in the solvation shell of I^- ion. This leads to an increase of the B-coefficient which partially compensates the decrease of B due to the structure breaking effect of I^- ion. The overall effect is a slight decrease of B of I^- ion with increasing the water mole fraction. For Cl^- and Br^- ions, a more weak decrease of the respective B-coefficients with increasing the water content in the solvent is observed with regard to I^- ion. In consequence, preferential hydration of Cl^- and Br^- ions in the range of solvent compositions studied can also be suggested.

Table 2

Viscosity B coefficients for NaI in different FA-water mixtures at 25, 30 and 35 °C.

$B/dm^3\ mol^{-1}$

x_{H_2O}	25°C	30°C	35°C
1	0.0178[a]	0.014[b]	0.0315[a]
0.901	0.033±0.002	0.048±0.001	0.080±0.002
0.701	0.150±0.006	0.173±0.008	0.187±0.007
0.498	0.239±0.007	0.233±0.004	0.227±0.002
0.402	0.266±0.005	0.271±0.001	0.258±0.002
0.202	0.356±0.007	0.348±0.003	0.327±0.006
0	0.518	0.500	0.473[c]

[a] E.R. Nightingale, *J. Phys. Chem.*, **63**, 742 (1959).
[b] Ref. 8.
[c] Ref. 11.

Table 3

Ionic B coefficients for Cl^-, Br^- and I^- ions in different FA-water mixtures at 30 and 35°C

$B/dm^3\ mol^{-1}$

x_{H_2O}	30°C			35°C		
	Cl^-	Br^-	I^-	Cl^-	Br^-	I^-
0	0.12	0.11	0.07	0.11	0.11	0.06
0.20	0.12	0.09	0.05	0.12	0.09	0.04
0.40	0.09	0.08	0.03	0.08	0.07	0.02
0.50	0.09	0.07	0.02	0.08	0.07	0.02

REFERENCES

1 J. Doménech and S. Rivera, *J. Chem. Soc. Faraday Trans. I*, **80**, 1249 (1984).

2 J. M. McDowall, N. Martinus and C.A. Vincent, *J. Chem. Soc. Faraday Trans. I*, **72**, 654 (1976).

[3] G. Jones and M. Dole, *J. Amer. Chem. Soc.*, **51**, 2950 (1929).

[4] B. S. Krumgalz, *J. Chem. Soc. Faraday Trans. I*, **76**, 1275 (1980).

[5] K. G. Lawrence and A. Sacco, *J. Chem. Soc. Faraday Trans. I*, **79**, 615 (1983).

[6] A. Einstein, *Ann. Phys.*, **19**, 208 (1906).

[7] J. Doménech and J. M. Costa, *Electrochim. Acta*, **27**, 1789 (1982).

[8] J. Doménech and S. Rivera, *Z. Phys. Chem. Neue Folge*, **136**, 153 (1983).

[9] A. Sacco, A de Giglio and A. Dell' Atti, *J. Chem. Soc. Faraday Trans. I*, **77**, 2693 (1981).

[10] J. Doménech, *Minatsh. Chem.*, **114**, 1351 (1983).

[11] N. Martinus and C. A. Vincent, *J. Chem. Soc. Faraday Trans. I*, **77**, 141 (1981).

[12] P. Rohdewall and M. Moldner, *J. Phys. Chem.*, **77**, 373 (1973).

[13] M. Stockhausen, H. Utzel and E. Seitz, *Z. Phys. Chem., Neue Folge*, **133**, 69(1982).

[14] C. K. Finter and H. G. Hertz, *Z. Phys. Chem., Neue Folge*, **148**, 75 (1986).

Revue Roumaine de Chimie, 33, 6, 585–594 (1988)

As(III) — HCl — H_2O SYSTEM. I

HOMOGENEOUS STATE

O. RADU
Central Institute of Chemistry, Institute of Research and Production of Semiconductors,
Şos. Gării Căţelu No. 5, Sector 3, Bucharest, Romania

Received February 22, 1987

A general method for characterization of As(III)$-$HCl$-H_2O$ system, either multicomponent or with various phase states is presented; the system is obtained through dissolution of arsenic trioxide or trichloride in hydrochloric acid. The standard homogeneous state is studied and relations are established between the parameters of dissolution reaction of arsenic trioxide and the parameters of equilibrium state in terms of the volume increase associated to the reaction. The fact that arsenic trichloride is exclusively responsible for the volume increases has allowed the partial elucidation of liquid phase composition; a method was devised for identifying and determining arsenic trichloride in presence of other three compounds of trivalent arsenic. The same results have set the foundation of a method for preparation of liquid phases with desired concentration of arsenic trichloride.

I. HOMOGENEOUS STATE

Preparation of arsenic trichloride, the main source of arsenic for semiconductors, from arsenic trioxide and hydrochloric acid is well known. The complex molecular composition and the various phase states of the final result of this reaction have received by far a smaller share of attention. Correct values of arsenic trioxide solubility in hydrochloric acid up to concentrations of 5N at room temperature are available.[1] Attempts have been made to establish the molecular composition of homogeneous dilute phase.[2–4] A set of solubility values for arsenic trichloride in hydrochloric acid was determined and employed in calculations of activity coefficient in a restricted range of concentration for studying arsenic trichloride distillation from the hydrochloric solution of arsenic trioxide.[5–7]

The present paper (of which this is part one) presents the results of a detailed study on the product of reaction between arsenic trichloride or trioxide and aqueous solution of hydrochloric acid. A closed system As(III)$-$HCl$-H_2O$ is formed to evidence the presence of several trivalent arsenic compounds together with hydrochloric acid and water mentioned by other authors.[2–4]

1. THE METHOD OF CHARACTERIZATION

That the system is multicomponent is suggested by the succession of chemical equilibria that characterize it :

$$0.5\ As_2O_3 \overset{1{,}5H_2O}{\rightleftharpoons} As(OH)_3 \underset{H_2O}{\overset{HCl}{\rightleftharpoons}} As(OH)_2Cl \underset{H_2O}{\overset{HCl}{\rightleftharpoons}} As(OH)Cl_2 \underset{H_2O}{\overset{HCl}{\rightleftharpoons}} AsCl_3 \qquad (I-1)$$

The only stable species besides the system are As_2O_3 and $AsCl_3$. The formulation as hydrochlorides of compounds with less than three chlorine atoms is the most likely. The shift of chemical equilibria causes phase transitions. The results of the study on such transitions has allowed us to establish that :

— the diversity of physical states is caused exclusively by the displacement of chemical equilibria :

— the intervention of physical factors can perturb the chemical equilibrium ;

— the perturbing action which depends on the history of the system is intricate and hard to control so that one should avoid the interference of physical factors.

Then, all states of equilibrium of the system are univocal functions of the parameters of chemical interaction that determined the equilibrium. Considering the formation interaction as intial state and the equilibrium final state the characterization consists of establishing relations between the final and initial states whose parameters are considered known. The parameters that are specific to each state were employed *e.g.* molar concentrations of atomic and molecular species and others that are common to both states as *e.g.* the ratios of the numbers of gram atoms or moles values are constant through the transition between the states. To each final state corresponds one of the two initial states :

$$As_2O_3 + HCl + H_2O \text{ and}$$

$$AsCl_3 + HCl + H_2O.$$

The relations will be established for standard conditions (25°C and 760 mm Hg) and at boiling temperature.

2. STANDARD HOMOGENEOUS FINAL STATE

2.1. The implicit relation between states and volume increase

The molecular composition of homogenous state results from the following succession of chemical equilibria :

$$As(OH)_3 \underset{H_2O}{\overset{HCl}{\rightleftharpoons}} As(OH)_2Cl \underset{H_2O}{\overset{HCl}{\rightleftharpoons}} As(OH)Cl_2 \underset{H_2O}{\overset{HCl}{\rightleftharpoons}} AsCl_3 \qquad (I.2)$$

The arsenic compounds may be gathered under the general formula $As(OH)_{3-z}Cl_z$ where $z = 0, 1, 2, 3$; the sum of the number of moles is constant:

$$\sum_0^3 n_{As(OH)_{3-z}Cl_z} = n_{As} = \text{const.} \tag{I.3}$$

The corresponding initial state is $As_2O_3 + HCl + H_2O$. Its parameters are related by the equation:

$$\frac{R}{C_{HCl}} = \frac{V_{HCl}}{n_{As}} \tag{I.4}$$

The transition from initial to final state is associated with a volume increase *i.e.* $V_S > V_{HCl}$. This is sensed only at high concentrations and its variation with the parameters of initial state exhibits significant regularities.

The volume increase is defined by the difference:

$$\Delta V = V_s - V_{HCl} \tag{I.5}$$

where $V_s = (C_{HCl}/C_{Cl})V_{HCl}$. Eqn. (I.4) yields a first implicit relation between states:

$$\Delta V = Rn_{As}\left(\frac{1}{C_{Cl}} - \frac{1}{C_{HCl}}\right) \tag{I.6}$$

If now the volume increase is calculated for one gram atom dissolved or one mole of $As(OH)_{3-z}Cl_z$ formed one gets the molar volume increase and the general implicit relation between states:

$$\Delta V_m = R\left(\frac{1}{C_{Cl}} - \frac{1}{C_{HCl}}\right) \tag{I.7}$$

Eqn. (I.7) allows accurate calculation of molar volume increase from values of concentrations in the two states. The volume increase supplies a criterion for the equilibrium state:

$$\Delta V = \text{const.} \tag{I.8}$$

2.2. Experimental determination of volume increase

The time required by equilibrium to be reached was determined by eqn. (I.8); the maximum value is two hours.

Volume increases were determined in homogeneous state correspondig to some initial states in the range $C_{HCl} \geqslant 8$ and $R \geqslant 4$ where significant and measurable values were recorded. To do this, rapid methods were developed for the preparation of homogeneous phase through dissolution of arsenic trioxide in hydrochloric acid on boiling under reflux and heating under pressure without mass transfer from the system. A 50 mL thick wall silica vessel provided with teflon stopper and a 75 mL steel bomb lined with teflon were employed in dissolution under pressure. After dissolution the solution was cooled to room temperature and kept for two hours at 25°C. The concentration of arsenic, hydrogen and chlorine was determined in equilibrated solutions. As^{3+} ion was determined volumetrically with $KBrO_3$ 0.1N in the presence of methyl orange. Concentration of H^+ ion was determined by potentiometric titration with NaOH

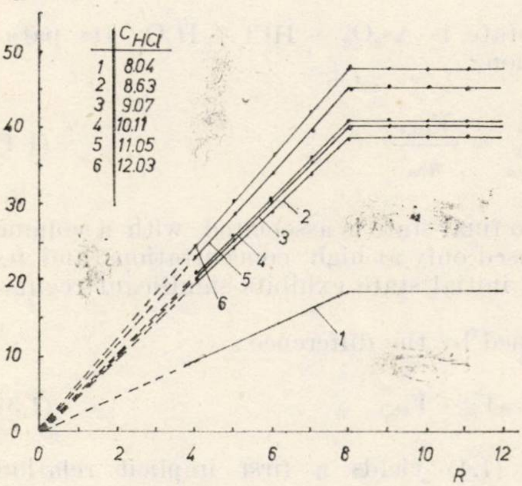

Fig. I.1. — Molar volume increase versus chlorine/arsenic atomic ratio.

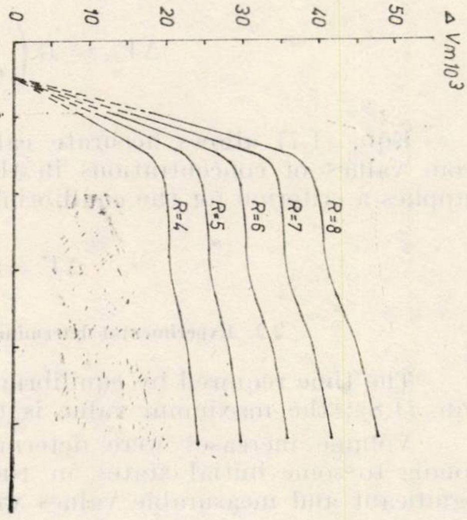

Fig. I.2. — Molar volume increase versus molar concentration of hydrochloric acid.

1N up to pH = 7. Because alkali hydrolysis frees an equal number of H^+ and Cl^- ions the same determination yields the concentration of total chlorine. For verification Cl^- ion was determined by the Volhard method.

Apriori knowledge of initial state parameters together with the determined concentration of chlorine in final state allows one to calculate the volume increase by eqn. (I.7). Examination of the plots of volume increase versus C_{HCl} and R in Figs. I.1 and I.2, respectively, shows;

— C_{HCl} increases continuously;

— at $R \simeq 8$ the change is essential;

the increase is linear in the range $R < 8$ and the values are constant at $R > 8$;

— the domain of $C_{\mathrm{HCl}} > 7.5$ is limited (the extrapolated curves ΔV_m versus C_{HCl} intersect the abscissa at 7.5);

— in liquid phase the solid liquid phase states ($R < 4$) show up as well (the extrapolated ΔV_m versus R lines meet in the origin).

2.3. Explicit elementary relation between states

The increases of molar volume determined allow one to establish relation between states for the ranges $R \leqslant 8$ and $R \geqslant 8$.

In the range $R \leqslant 8$ the concentration of chlorine in final state depends only on C_{HCl}. Fig. I.3 shows this dependence. Let us suppose that the variation is linear between points where the slope changes are recorded;

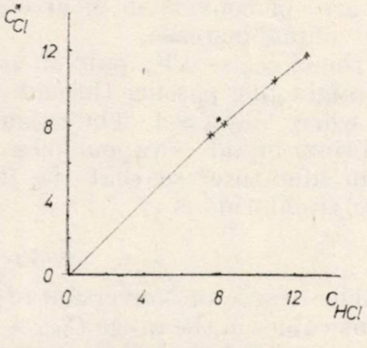

Fig. I.3. — The concentration of chlorine in final state versus the concentration of hydrochloric acid in initial state.

then the equation of straight line segments results in two sets of reciprocal linear relations between states :

$$C^*_{\mathrm{Cl}} = a_1 C_{\mathrm{HCl}} + b_1 \qquad C_{\mathrm{HCl}} = a_2 C^*_{\mathrm{Cl}} + b_2 \tag{I.9}$$

C_{HCl}	a_1	b_1	C^*_{Cl}	a_2	b_2
0 ... 7.5	1	0	0 ... 7.5	1	0
7.5 ... 8.6	0.70	2.25	7.5 ... 8.2	1.426	−3.214
8.6 ... 11	8.866	8.836	8.2 ... 10.4	1.155	0.967
11 ... 12.7	0.815	1.431	10.4 ... 11.8	1.226	1.754

In the range $R \geqslant 8$ the chloride concentration depends on C_{HCl}, R and ΔV_{m}. In this range ΔV_{m} stays constant at its value for $\mathrm{R} = 8$ and equals :

$$\Delta V_{\mathrm{m}}^{*} = \frac{8(C_{\mathrm{HCl}} - C_{\mathrm{Cl}}^{*})}{C_{\mathrm{HCl}} C_{\mathrm{Cl}}^{*}} \tag{I.10}$$

Eqs. (I.7), (I.9) and (I.10) yield the relation between states :

$$C_{\mathrm{Cl}} = \frac{R C_{\mathrm{HCl}}(a_1 C_{\mathrm{HCl}} + b_1)}{8 C_{\mathrm{HCl}} + (\mathrm{R} + 8)(a_1 C_{\mathrm{HCl}} + b_1)} \tag{I.11}$$

2.4. Relations between states and the molecular composition of homogeneous state

The volume increase is undoubtedly caused by one or more arsenic compounds formed in final states. The values and behaviour of volume increase have suggested that one compound is arsenic trichloride. The hypothesis was verified through measurements of volume increase on dissolution of arsenic trichloride in hydrochloric acid. The volumes of the two liquid components were additive for $C_{\mathrm{HCl}} \geqslant 12.7$, negative deviations from additivity were recorded for $C_{\mathrm{HCl}} < 12.7$. The absolute value of deviation rises with the decrease of C_{HCl} and approches the volume of $\mathrm{AsCl_3}$ when $C_{\mathrm{HCl_3}}$ tends to 7.5. The negative deviation from additivity of volumes is obviously a consequence of arsenic trichloride hydrolysis.

Since the hypothesis is verified it turns out that at the transition from the initial state $\mathrm{As_2O_3 + HCl + H_2O}$ to final homogeneous state the degree of conversion of arsenic to arsenic trichloride is proportional to the volume increase.

The $X_{\mathrm{AsCl_3}} - \Delta V_{\mathrm{m}}$ pair of values required in calculation of slope of the straight line passing through origin was supplied by the $C_{\mathrm{HCl}} \geqslant 12.7$ range where $X_{\mathrm{AsCl_3}} \simeq 1$. The calculated value was confirmed directly by equilibrium liquid — vapour measurements and indirectly by interpreting data in literature[2] so that the linear equation of arsenic conversion to arsenic trichloride is :

$$X_{\mathrm{AsCl_3}} = 20.42\,\Delta V_{\mathrm{m}} \tag{1.12}$$

The degree of conversion of arsenic to arsenic trichloride takes significant values in the range $C_{\mathrm{HCl}} > 7.5$. The overall conversion depends only on C_{HCl} provided that the excess of acid ($\mathrm{R} \geqslant 8$) is ensured. Otherwise ($\mathrm{R} < 8$) the conversion is not total and depends on R. Eqs. (I.7), (I.9) and (I.12) yield the equations for calculation of total specific conversion and partial nonspecific conversion as functions of initial state.

$$X'_{\mathrm{AsCl_3}} = 163.36\left(\frac{1}{a_1 C_{\mathrm{HCl}} + b_1} - \frac{1}{C_{\mathrm{HCl}}}\right)_{\mathrm{R} \geqslant 8} \tag{I.13}$$

$$X^{*}_{\mathrm{AsCl_3}} = 20.42\mathrm{R}\left(\frac{1}{a_1 C_{\mathrm{HCl}} + b_1} - \frac{1}{C_{\mathrm{HCl}}}\right)_{\mathrm{R} < 8} \tag{I.14}$$

The concentration of arsenic trichloride is calculated by the general equation :

$$C_{\mathrm{AsCl_3}} = X_{\mathrm{AsCl_3}} C_{\mathrm{As}} \tag{I.15}$$

which may by explained in terms of initial state by means of eqs. (I.13) and (I.14):

$$C^*_{\mathrm{AsCl_3}} = 20.42\,\frac{(1-a_1)C_{\mathrm{HCl}} - b_1}{\left(\dfrac{R}{8} - 1 - a_1\right)C_{\mathrm{HCl}} - b_1} \qquad R \geqslant 8 \qquad (\mathrm{I.16})$$

$$C'_{\mathrm{AsCl_3}} = 20.42\left(1 - a_1 - \frac{b_1}{C_{\mathrm{HCl}}}\right) \qquad R < 8 \qquad (\mathrm{I.17})$$

Figs. I.4 to I.7 are plots of the degree of conversion and concentration of $AsCl_3$ versus the initial state.

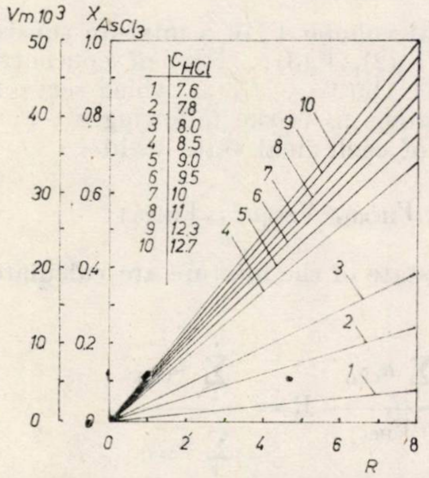

Fig. I.4. — The molar volume increase and conversion of arsenic to arsenic trichloride versus chlorine/arsenic ratio (calculated values).

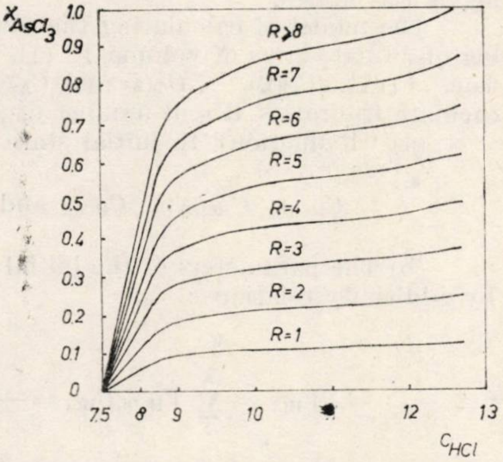

Fig. I.5. — The conversion of arsenic trichloride versus the molar concentration of hydrochloric acid (calculated values).

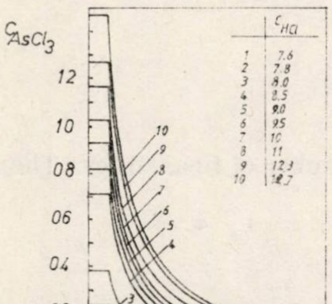

Fig. I.6. — The dependence of arsenic trichloride molar concentration on chlorine/arsenic atomic ratio.

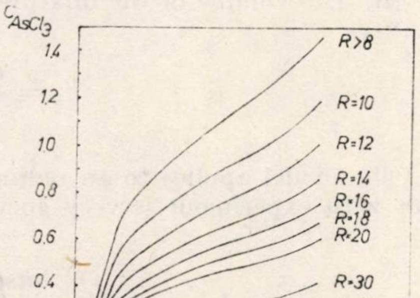

Fig. I.7. The molar concentration of arsenic trichloride versus the molar concentration of hydrochloric acid.

3. APPLICATIONS OF RECIPROCAL RELATIONS OF SUMMING UP NONADDITIVE VOLUMES

The relations of final homogeneous state make sense for liquid phases of all interphase states and will be applied to the study of these equilibria. One of these applications which requires additional mathematic modelling consists of summation of the volumes of final states of different concentrations. Because the volume increase depends on concentration it is obvious that the volumes of solutions of different concentrations are not additive. The nonadditivity of volumes of *i* different final states is removed by replacing them with the additive volumes of *i* corresponding initial states.

The model of calculating the total volume V_s of a mixture consisting of *i* final states of volume $V_s(1)$, $V_s(2)$, $V_s(3) \ldots V_s(i)$ of concentrations $C_{Cl}(1)$, $C_{Cl}(2) \ldots C_{Cl}(i)$ and $C_{As}(1)$, $C_{As}(2) \ldots C_{As}(i)$ (which serve to caculate the ratios R and number of atoms n) is the following:

(a) "Reduction" to initial state of each final state yields

$$C_{HCl(1)},\ C_{HCl(2)} \ldots C_{HCl(i)} \text{ and } V_{HCl(1)},\ V_{HCl(2)} \ldots V_{HCl(i)};$$

(b) The parameters of the initial state of the mixture are calculated by additivity relations:

$$V_{HCl} = \sum_1^i V_{HCl(i)} \qquad C_{HCl} = \frac{\sum_1^i n_{Cl(i)}}{V_{HCl}} \qquad R = \frac{\sum_1^i n_{Cl(i)}}{\sum_1^i n_{As(i)}}$$

(c) The relations between states are then utilized to calculate the concentration of chloride in the due mixture of final state;

(d) The volume of the mixture in final state results from the equation:

$$V_s = \frac{C_{HCl}}{C_{Cl}} V_{HCl}$$

The model applies to an unlimited number of final states. The agreement with experiment is very good.

DISCUSSION

The standard control of arsenic trichloride content in arsenic trioxide solutions in hydrochloric acid becomes possible by measurements of volume variations. The theoretical foundation states that arsenic trichloride is exclusively responsible for these variations. This statement may be contested by the assumption that zero or positive apparent values of volume variations represent a sum in which the other compounds of arsenic take part together with trichloride. This means that in the range $C_{HCl} < 7.5$ where the apparent volume variation is zero, the variations contributed by the other arsenic compounds cancel reciprocally in spite of permanent concentration change.

Theoretically this behaviour is not possible because it denies the partial molar character of volume variation.

The electrostriction of water about ions may not be implied because it is proper to the aqueous solution of the fully dissociated salts.

That arsenic trichloride is the only responsible for volume increase is supported by the calculation of molar volume change of trichloride. If in the sequence I.2 of chemical equilibria one admits that $X_{AsCl_3} = 1$:

$$1/2\ As + 3HCl \rightarrow AsCl_3 + 3/2\ H_2O$$

and one can calculate the volume variation of arsenic trichloride by the equation :

$$\Delta V_{AsCl_3} = V_{AsCl_3} + 1.5\ V_{H_2O} - 3\Delta V_{HCl} = 0.0497 \text{ liters}$$

where :

V_{AsCl_3} = molar volume of $AsCl_3 = 0.0843$ liters

V_{H_2O} = molar volume of $H_2O = 0.018$ liters

ΔV_{HCl} = average volume variation of HCl calculated from the variation of concentration with density = 0.0205.

The value obtained is sensitively equal to ΔV_m at $X_{AsCl_3} = 1$ (0.0490 liters). It supports the interpretation of volume increase and rules out the evetual implications of water electrostriction about ions.

The compounds of trivalent arsenic whose formation is associated with no volume increase, products of arsenic trichloride hydrolysis, are unstable outside liquid phase where they form. The practical interest for these compounds is low such that the problem of their concentration, which is the pending solution, is only of theoretical relevance. The sums of their concentration result, depending on the stability domain of $AsCl_3$ from the relations :

$$\sum_{0}^{2} C_{As(OH)3-zCl_z} = C_{As} \quad C_{Cl} < 7.5$$

$$\sum_{1}^{2} C_{As(OH)_{3-z}Cl_z} = C_{As} - C_{AsCl_3} \quad C_{Cl} > 7.5 \quad C_{As(OH)_3} = 0$$

Identification and determination of a compound from the four with common ion in the some valence state in a multiphase system is a difficult problem by itself. The experimental method is very simple while the unusual theoretical foundation is helpful and efficient. It is thus possible to exert a rigorous control of the content of arsenic trichloride, the only component of practical interest.

NOTATION

Parameters of initial state $As_2O_3 + HCl + H_2O$

$R = n_{Cs}/n_{As}$

n_{Cl} = number of gram atoms of chlorine
n_{As} = the same for arsenic
V_{HCl} = volume of HCl solution (liters)
C_{HCl} = concentration of hydrochloric acid (mole/liter)

Parameters of final homogeneous state

(liquid phase in multiphase systems)
V_s = volume of solution (liters)
C_{Cl} = concentration of chlorine (gram atoms/liter)
C_{As} = the same for arsenic
ΔV = volume increase (liters)
ΔV_m = molar increase volume (liters/gram atom for arsenic)
C^*_{Cl} = chlorine concentration independent of R (gram atoms/liter)
ΔV^*_M = molar volume increase independent of R
$X_{AsCl_3} = n_{AsCl_3}/n_{As}$ = degree of conversion of arsenic to $AsCl_3$

REFERENCES

[1] A. B. Garett, O. Holmes and A. Laube, *J. Amer. Chem. Soc.*, **62**, 2024 (1940).
[2] A. Myron, *J. Amer. Chem. Soc.*, **79**, 1865 (1957).
[3] M. Prassed, C. R. Kanekar and L. N. Mulay, *J. Chem. Phys.*, **19**, 1440 (1950).
[4] P. Floegel, *Z. Anorg. Allg. Chem.*, **389**, 188 (1972).
[5] V. V. Krapukin, I. A. Sokolov and M. M. Dorshina, *Isv. Vissh. Uceb. Zaved. Tsved. Met.*, **12**, 60 (1969).
[6] V. V. Krapuhin and I. A. Sokolov. *Isv. Vissh. Uceb. Zaved. Tsved. Met.*, **13**, 140 (1970).
[7] V. V. Krapuhin and I. A. Sokolov, *Isv. Vissh. Uceb. Zaved. Tsved. Met.*, **14**, 84 (1971).

Revue Roumaine de Chimie, **33**, *6*, 595–602 (1988)

STUDIES ON CORROSION OF LEAD ACID BATTERY GRIDS WITH ADDITION OF Se Sb AND SILVER

A. MATEESCU[a] and D. MATEESCU[b]

[a]"Acumulatorul" Enterprise, Blvd. Biruinței 98, 73 957, Bucharest, Romania
[b]Institute of Physics and Materials Technology, Bucharest, Romania

Received March 21, 1987

The effect of Sb, Ag, Se on the stationary and nonstationary anodic corrosion rates of Pb-Sb–Ag, Pb–Sb–Se and Pb–Sb alloys in H_2SO_4 has been studied. Anodic and cathodic polarization curves were plotted under potentiodynamic conditions.

This paper continues the study[1–3] on the influence of alloying elements in lead, concerning the polarization behaviours and the corrosion resistance. As in the previous papers,[4–7] we simulated in laboratory conditions the electrochemical processes that take place at the electrodes of lead-acid batteries.

The results inform on the appearance of oxides and sulphates of lead, antimony and selenium, as well as on the reduction conditions of these ones.

EXPERIMENTAL TECHNIQUE

The experiments were made using the potentiodynamic and gravimetric methods. Radelkis potentiodynamic assembly and a X–Y recorder were used. The electrochemical cell and the installation pattern were described in a previous paper.[5] A diluted aq.H_2SO_4 solution (1.05 g.cm^{-3}) was used as electrolyte. All potentials were measured in relation to the $Hg/Hg_2SO_4/SO_4^{-2}$(1 M) electrode. For quantitative evaluation of lead and the tested alloys corrosion, the gravimetric method was used,[2] the results being appreciated by:

$$K_g = \frac{m_1 - m_2}{S \cdot t} \tag{1}$$

$$P = \frac{K_g \cdot 8760}{1000 \cdot \rho} \text{ (mm/year} \tag{2}$$

m_1 = weight of the metallic sample before immersion (g)
m_2 = weight of the metallic sample after immersion (g)
s = active surface of the sample (m^2)

t = time of immersion (hours)
ρ = alloy density expressed in g/cm^3
8 760 = number of hours in a year

RESULTS

The polarization curves (potential-current) of pure lead and of lead – 2.75% antimony alloy in an aq. H_2SO_4 solution of 1.05g/cm^3 are plotted in fig. 1. The potential scanning (5 mV/s) was from –2700 mV up to + 2000 amV nd back to – 2700 mV, realizing a cycle.

For each test several cycles were made (Fig. 1) presenting the polarization curves for cycle 8.

In the anodic field, there are peaks (A) in the potential range from – 1000 to – 600 mV, corresponding to the appearance of lead sulphate ;[8,9]

$$Pb + SO_4^{-2} \rightarrow PbSO_4 + 2e \qquad (3)$$

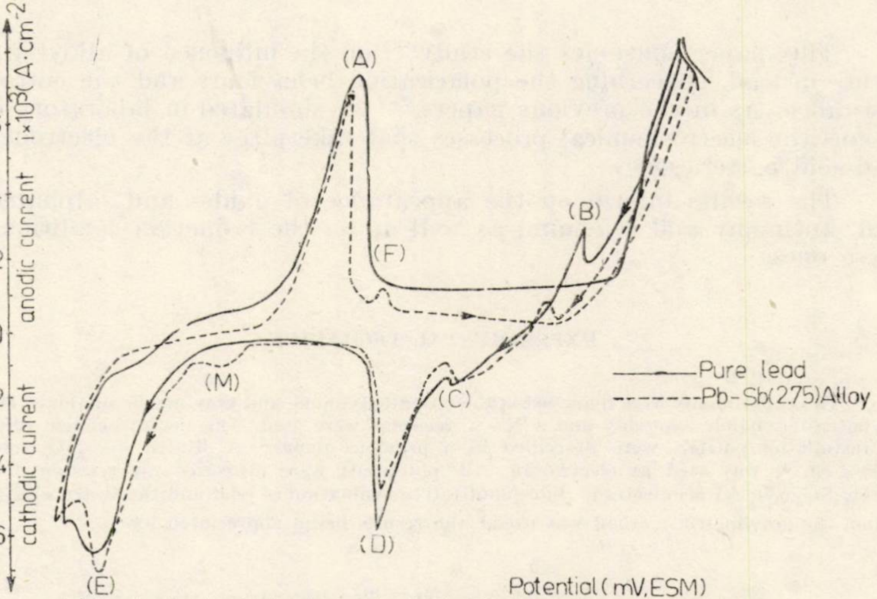

Fig. 1. – Polarization curves (cycle 8) of pure lead (solid line) and lead-antimony alloy (dotted line) in an eq. H_2SO_4 solution 1.05 g/cm^3. The potential scanning rate = 5 mVs^{-1}. Temperature 20 ± 0.1°C.

whose potential (referred to the Hg_2SO_4 electrode) is

$$E_{ESM} = -\ 970 + 0.0295 \text{ pS (V), where pS} = -\log a_{SO_4^{-2}}$$

Above + 1450 the current increase due to oxidation of lead suphate to lead dioxide, accompanied by the O_2 evolution on PbO_2 formed.

$$PbSO_4 + 2H_2O = PbO_2 + 4H^+ + SO_4^{-2} + 2e \tag{4}$$

$$2OH^- = H_2O + \frac{1}{2} O_2 + 2e \tag{5}$$

The PbO_2 production voltage resulting from eq. (4) is given by the relationship :

$$E_{ESM} = 1.467 - 0.1182 \text{ pH} - 0.0295 \text{ V}$$

When scanning back the potential, several peaks of oxidation (B) appear, followed by reduction peaks (C) and two reduction peaks (D) and (E). Oxidation peaks (B) obtained in anodic decreasing scan could be the result of remanent oxidation of the $PbSO_4$ passive layer to α-PbO_2. In the potential range of peak (B), the following redox reaction is possible :

$$3PbO \cdot PbSO_4 \cdot H_2O \rightleftharpoons Pb_2O_3 + 3SO_4^{-2} + 10H^+ + 4e \tag{6}$$

whose production voltage is $E_{ESM} = 0.876$ V. The first reduction peak (C) represents the reduction of $\alpha - PbO_2$, Pb^{+4} to Pb^{2+}.

The (D) peaks are referring to reduction of the basic lead compounds appeared under the $PbSO_4$ protective layer, while (E) peaks represent the reduction of Pb^{2+} ions to metallic lead.

Antimony present in alloys is responsible for a new peak (F), on the anodic rising curve. This oxidation peak appears in the potential range from − 450 mV to − 350 mV, and is related to the appearance of Sb_2O_3. When back scanning the potential, the appearance of another reduction peak (*H*) is observed, which corresponds to oxide reduction to metallic antimony.

In comparison with pure lead, the presence of antimony reduces the heights of (A), (B) and (D) peaks, the average anodic current and especially the density of passivation current being lower for alloys containing antimony. The lead alloys containing antimony and selenium show a different behaviour to polarization within the potential field − 2700 mV to + 2000 mV (Figs. 2, 3 and 4).

The plots for 20 ± 0.1°C temperature (Fig. 2) have also an anodic oxidation peak [5] at an average potential of + 225 mV, which may correspond to the Se oxidation to Se_2O_3. Selenium presence (1.25%) in the 2.75% antimony alloy leads to the increase of oxygen evolution overpotential with about 250 mV (see Fig. 1 and Fig. 2) in comparison with pure lead and with lead antimony alloy.

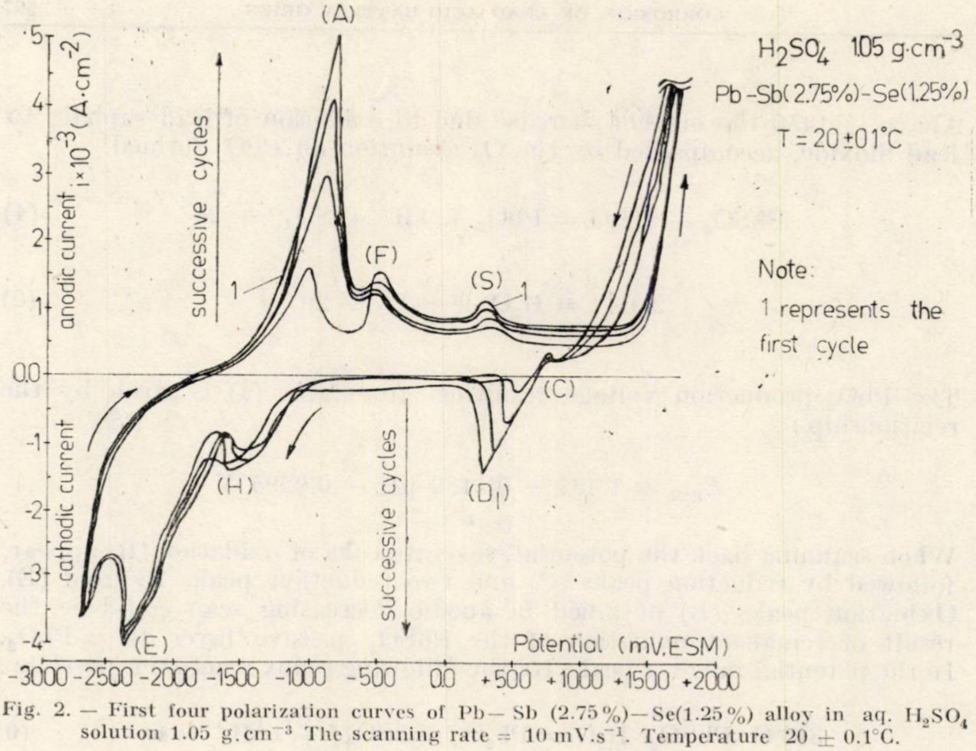

Fig. 2. — First four polarization curves of Pb—Sb (2.75%)—Se(1.25%) alloy in aq. H$_2$SO$_4$ solution 1.05 g.cm^{-3} The scanning rate = 10 mV.s^{-1}. Temperature 20 ± 0.1°C.

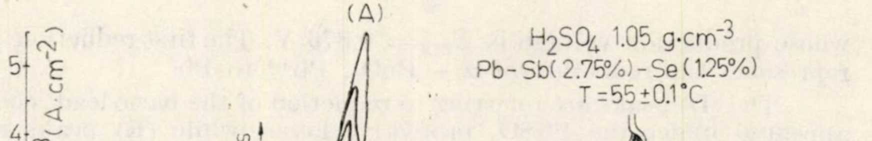

FIG. 3

Fig. 3. — Polarization curves of Pb—Sb (2.75%)—Se(1.25%) alloy in aq. H$_2$SO$_4$ solution 1.05 g/cm^3. Scanning rate = 10 mV.s^{-1}. Temperature 55 ± 0.1°C.

As concerning the cathodic slope of the polarization curves, selenium influence resembles that of silver.[1,3].

Peaks (D) are probably corresponding to some reduction reactions :

$$Pb_3O_4 + 2H_2O + 2H^+ + 2e = 3Pb(OH)_2 \qquad (7)$$

$$Ep_1 = 0.496 - 0.0591\ pH\ (V)$$

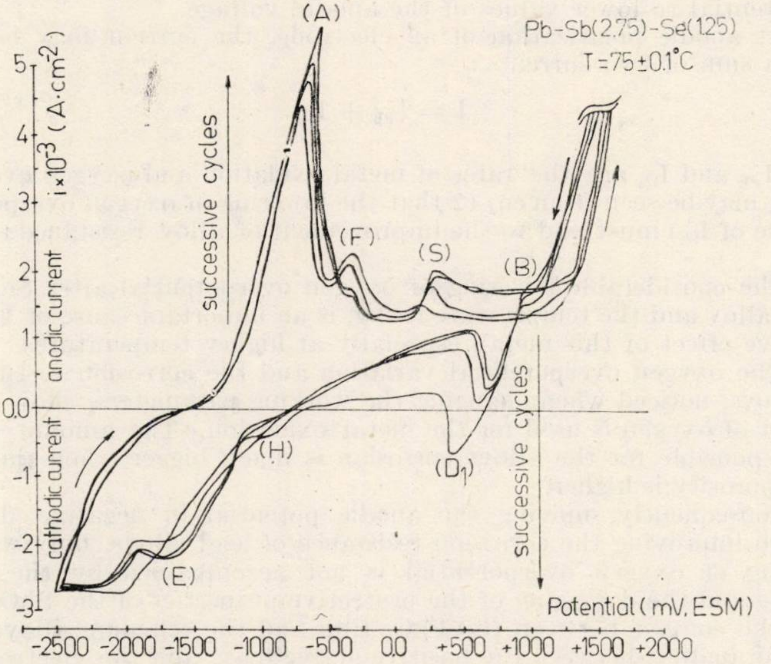

Fig. 4. — Polarization curves of Pb-Sb (2.75 %)—Se(1.25 %) alloy in aq. H_2SO_4 solution 1.05g cm^{-3}. Scanning rate = 10 mV.s^{-1}. Temperature 75 ± 0.1°C.

$$2(\beta\text{-}PbO_2) + 2H^+ + 2e = Pb_2O_3 + H_2O \qquad (8)$$

$$Ep_2 = 0.475 - 0.0591\ pH\ (V)$$

$$Pb_3O_4 + 2H^+ + 2e = 3PbO + H_2O \qquad (9)$$

$$Ep_3 = 0.461 - 0.0591\ pH\ (V)$$

$$5(\alpha\text{-}PbO_2) + 5H_2O + 10H^+ + 10e = 5PbO.2H_2O \qquad (10)$$

$$Ep_4 = 0.455\ (V)$$

The current intensity of cathodic and (especially) anodic reactions is lower when selenium is added, in comparison to Pb-Sb or Pb-Sb-Ag alloys. With temperature rising (Figs. 2 and 3) a recrystallization of anodic layer may occur[3]

$$\alpha\text{-}PbO_2 \rightleftharpoons Pb^{+4} \text{ (in solution)} \rightleftharpoons \beta\text{-}PbO_2 \qquad (11)$$

which negatively affects its protective properties.

The temperature rising is responsible for the migration of oxygen overpotential to lower values of the anodic voltage.

At anodic polarization of an electrode, the current may be considered a sum of two currents :

$$I = I_{Pb} + I_{O_2} \qquad (12)$$

where I_{Pb} and I_{O_2} are the rates of metal oxidation and oxygen evolution.

It may be seen from eq. 12 that the lowering of oxygen overpotential (the rise of I_{O_2}) must lead to the improvement of alloy resistance to corrosion.

The considerable lowering of oxygen overpotential after Se mixing in the alloy and the temperature rising, is an important cause of the anticorossive effect of this metal, especially at higher temperatures.

The oxygen overpotential variation and the corrosion resistance of the alloys, noticed when changing the working parameters, show that an amount of oxygen is used for the metal oxidation. The amount of oxygen responsible for the alloys corrosion is much bigger when the oxides layer porosity is higher.

Consequently, moving the anodic potential in negative direction leads to improving the corrosion resistance of lead alloys, only when the lowering of oxygen overpotential is not accompanied by the surface increase and the damaging of the protective properties of the PbO_2 layer.

The contact between the PbO_2 film and the selenium alloyed electrode (in reality, between the positive active mass and the electrode grill of the lead acid battery) may lead to the following type of reaction :

$$Pb + PbO_2 + 2H_2SO_4 \rightarrow 2PbSO_4 + 2H_2O \qquad (13)$$

$$Se + 5PbO_2 + 6H_2O \rightarrow (SeO)_2SO_4 + 5PbSO_4 + O_2 + 6H_2O \qquad (14)$$

Because the electrolyte has limited access to the grill, the $PbSO_4$ appearance stops the process described by the above reactions, which would lead to self-discharging of active mass.

Following the dumping of H_2SO_4 concentration the solubility of lead sulphate increases, and consequently, the rates of the above reactions increase, too.

The results of the weight losses of pure lead and lead alloys with Sb, Se and Ag are presented in Table 1.

The weight losses of lead, in both stationary and nonstationary conditions are the highest, and considering that the pure lead weight losses are 100% we may notice the following behaviour for its alloys : 2.75% Sb added reduces the stationary corrosion of the alloy to 90.5%, and the progressive additions of Se reduces it to 72% and 47%.

For a 9.74% Sb addition, the stationary corrosion is reduced to about 78%. The progressive additions of Ag reduce it to 56.5 and 34.2%.

Table 1

The values of gravimetric and penetration idices of lead and its alloys in 1.280 g/cm³ sulphuric acid solution

Alloy composition	Determining conditions			
	Stationary		Nonstationary	
	Kg (g/m²/h)	P (mm/an	Kg (g/m²/h)	P (mm/an)
Pb	0.032	0.0247	0.182	0.138
Pb-Sb (2.75 %)	0.029	0.0223	0.121	0.092
Pb-Sb (2.75 %) – Se(1.25 %)	0.015	0.0116	0.062	0.046
Pb-Sb (2.75 %)–Se(0.03 %)	0.023	0.0177	0.011	0.084
Pb-Sb (9.74 %)	0.025	0.0193	0.083	0.061
Pb-Sb (9.74 %)–Ag (0.1 %)	0 011	0.0084	0.044	0.030
Pb- Sb (9.74 %)–Ag(0.042 %)	0.018	0.0138	0.101	0.070

Under nonstationary conditions, the weight losses are higher (see Table 1), both for the pure lead case and for the studied alloys.

The alloying additives have similar effects with those mentioned above.

We may point out that weight losses are lower with the augmentation of antimony content; selenium and especially silver reduce corrosion.

CONCLUSIONS

As a result of the polarization behaviour of lead and its stibium and selenium alloys the following conclusions were drawn.

The initial stage of lead polarization is lead sulphate formation. The increase of the current density is a result of the electrode surface screening produced by the sulphate film; if the potential moves to electropositive values, the formation of Pb^{2+} and finally PbO_2 compounds becomes possible.

The character of the polarization curves at more electropositive potentials as Pb^{2+}/Pb^{4+} becomes complicated because of oxygen release, besides the lead oxidising processes.

Peaks corresponding to $PbO_2/PbSO_4$ and $PbSO_4$ system have been primarily noticed at the cathodic reduction of lead bioxide films.

Oxidizing reactions with Pb_2O_3 or Pb_3O_4 type oxides formation appear around the range of +900 mV potential (as against ESM).

The reduction peak from the potential range (−100 mV to −200 mV) is caused by Pb^{2+} compounds (PbO, $Pb(OH)_2$ or basic sulphates) occurrence.

The presence of a maximum around the −300 mV potential is observed on the polarization curve in the cycling process of a stibium lead alloy electrode, besides $PbSO_4$ and PbO_2. This maximum is considered to correspond to a stibium sulphate formation or to another composition stibium combination (probably SbO^+). The stibium introduced into the alloy reduces the oxygen over voltage on the formed lead oxide.

The anodic peak around + 224 mV potential corresponds to the selenium oxidation with Se_2O_3 probably resulting.

In sulphuric acid solutions, the pure lead has the highest corrosion rate compared to that of the studied alloys.

As resulting from this study, an important role in corrosion reduction is played by the silver, selenium and stibium additions in the battery electrode grids.

REFERENCES

[1] S. Sternberg, V. Brînzoi, L. Apăteanu and A. Mateescu, *Rev. Roumaine Chim.*, **6**, 583, (1983).

[2] S. Sternberg, A. Mateescu, V. Brînzoi and D. Mateescu, *Rev. Chim. (București)*, **35**, 1108, (1983).

[3] A. Mateescu, D. Mateescu, *Rev. Chim.* (București) (under press).

[4] S. Sternberg, A. Mateescu, V. Brinzoi and L. Apăteanu, *Rev. Roumaine Chim*, **11**, 955, (1985).

[5] A. Mateescu, *Doctoral Thesis* Polytechnic Institute Bucharest, 1986.

[6] S. Sternberg, A. Mateescu, V. Brînzoi and L. Apăteanu, *Electrochim. Acta* (under press).

[7] S. Sternberg, A. Mateescu, V. Brînzoi and L. Apăteanu, *Rev. Roumaine Chim*, **9**, 727 (1984).

[8] A. C. Simon, S. M. Caulder and J. T. Stemmle, *J. Electrochem. Soc*,. **122**, 461 (1974).

[9] J. P. Harrison and C. P. Smale, *Electrochim. Acta*, **25**, 1165 (1980).

Revue Roumaine de Chimie, **33**, *6*, 603–610 (1988)

A UV/VIS SPECTROMETRIC STUDY OF THE REACTION OF THE Pd(II)-*p*-NITROSODIPHENYLAMINE COMPLEX WITH CARBON MONOXIDE

V. DAVID[a] and G. E. BAIULESCU[b]

[a] Center for Work Protection and Hygiene, Str. Pop de Basesti 59, Sec. 2, Bucharest, Romania
[b] Department of Analytical Chemistry, National Institute of Chemistry, Spl. Independentei 202, Bucharest, Romania

Received March 21, 1987

The paper presents the UV/VIS spectrometric results obtained on the reaction of Pd(II)-*p*-nitrosodiphenylamine complex with carbon monoxide in a new reaction medium, hexamethylphosphoric triamide and water. The aim of the work was to set up a new method of determining carbon monoxide in air.

INTRODUCTION

Carbon monoxide is a chemical compound with a very weak chemical reactivity. Four classes of compounds are known today to have been used to determine CO by visible spectrometric methods : (a) salts or complexes of divalent palladium ;[1-4] (b) salts or complex salts of silver ;[5-9] (c) hemoglobin and its derivatives ; [10,11] and (d) complexes of monovalent copper.[12]

When CO reacts with Pd(II), found e.g. as a chloride, it has the notable property of reducing Pd(II) to Pd(O) ; the following reaction mechanism was proposed :[13]

$$PdCl_2 + CO \rightarrow Pd + COCl_2$$

$$COCl_2 + H_2O \rightarrow CO_2 + 2\ HCl$$

Palladium formed in this way forms a sol which finally separates and the unreduced Pd(II) can be determined by its reaction with an alkali iodide.[1] Two methods of determining CO in air based on the reduction of Pd(II) to Pd(O) have already been proposed ; in one of them, the reduced palladium converts leuco Crystal Violet in aqueous solution into Crystal Violet,[3] whereas in the other one, it converts Cacotheline into violet dihydrocacotheline.[4] Another method uses azobenzene, which is reduced by CO, in the presence of $PdCl_2$, to hydrazobenzene.[14] In the case of the reaction of CO with the complex combination of Pd(II) with *o*-phenanthroline, the first step is a reduction :

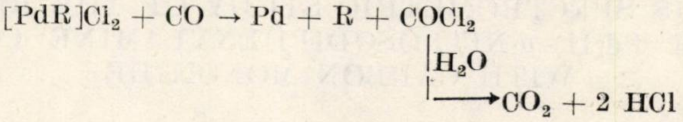

$$[PdR]Cl_2 + CO \rightarrow Pd + R + COCl_2 \quad \xrightarrow{H_2O} CO_2 + 2\ HCl$$

(R : *o*-phenanthroline)

It has been established that subsequently Pd(O) forms a carbonyl complex of the type $[Pd_2(H_2O)_4(CO)_2\ (R)_2]$[2].

In this work we present the UV/VIS spectrometric results obtained in connection with the reaction of the Pd(II)-*p*-nitrosodiphenylamine complex with carbon monoxide, as well as the use of a new reaction medium (hexamethylphosphoric triamide and water); the results are compared with the previous attempts in this field, with a view to use this complex for determining CO in air.

BACKGROUND

The trend of carbon monoxide to form carbonyl complexes is enhanced whenever the metal is in a low valency state;[15] the metals which take part in metal carbonyl formation have the following valencies :

iron — II; palladium — O or I; copper — I.

p-Nitrosodiphenylamine forms with divalent Pd a water-insoluble chelate. The molecular formulas of the ligand and of its complex with Pd(II) are the following :

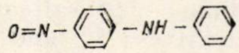

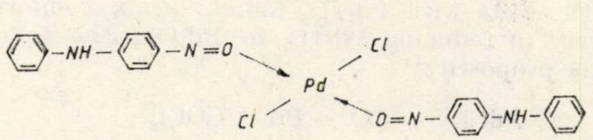

In a previous work[16] it was pointed out that a mixture of hexamethylphosphoric triamide (HMPA) and water can be used as a good solvent for the $[Pd(ONC_6H_4NHC_6H_5)_2]Cl_2$ complex. On the other hand, it was shown[17-19] that a medium containing HMPA and Cu(I) is a good absorbent for carbon monoxide.

EXPERIMENTAL

In some of the samples we worked with, the Pd(II)-*p*-nitrosodiphenylamine complex had been obtained in the reaction medium, whereas in others the complex had been previously synthesized.

(A) In order to prepare the samples needed for the reaction with CO, we used (i) a standard solution of Pd(II) in 1 vol. % HCl, containing 100 μg Pd(II)/mL, and (ii) a 0.001 % solution of *p*-nitrosodiphenylamine, prepared by dissolving the proper amount of the organic reagent in 50 mL of ethanol and diluting to 100 mL with distilled water.

(B) The $[Pd(ONC_6H_4NHC_6H_5)_2]Cl_2$ complex was synthesized as follows: first, 0.4625 g of $PdCl_2$ were dissolved in 50 mL of 1 % HCl solution and 1.0375 g of *p*-nitrosodiphenylamine were dissolved in 200 mL of ethanol; the latter solution was diluted with 200 mL of water. The complex was precipitated by adding the $PdCl_2$ solution, drop by drop, to the reagent solution, then stirring magnetically the mixture during 1 hr. to stabilize the complex. The precipitate was filtered through a fine-pore (G3-grade) sintered glass crucible, washed with ethanol and distilled water, and dried.

From this complex, a stock solution in HMPA was obtained, containing 538.8 μg $[Pd(ONC_6H_4NHC_6H_5)_2]Cl_2$/mL, or 100 μg Pd(II)/mL.

In our experiments we used HMPA and carbon monoxide of Merck quality and *p*-nitrosodiphenylamine synthesized and tested by us. The spectra were recorded with an AR Pye-Unicam Linear Recorder Spectrometer, using 1-cm cells.

RESULTS AND DISCUSSION

We showed first that Pd(O) is an important intermediate in the mechanism of the reaction of the Pd(II)-*p*-nitrosodiphenylamine complex with carbon monoxide, by carrying out two parallel experiments:

I. 0.25 mL of the 100 μg Pd(II)/mL solution, 0.75 mL of 1 % HCl and 7.5 mL of HMPA were introduced in a 25-mL volumetric flask. CO was then bubbled through the mixture; one could immediately notice the Pd formation. 2.5 mL of 0.01 % *p*-nitrosodiphenylamine solution were added and the flask was brought to the mark with distilled water.

II. 0.25 mL of 100 μg Pd(II)/mL solution, 0.75 mL of 1 % HCl, 2.5 mL of 0.01 % *p*-nitrosodiphenylamine solution and 7.5 mL of HMPA were introduced in a 25-mL volumetric flask and brought to the mark with distilled water. A few bubbles of CO were passed through the mixture, the amount of CO bubbled in the two experiments being sufficiently large to ensure that the reaction proceeds quantitatively.

The spectra of solutions I and II were recorded against a blank (consisting of 1 mL of 1 % HCl, 2.5 mL of 50% ethanol and 7.5 mL of HMPA, brought to 25 mL with distilled water), 30 and 60 minutes after bubbling CO. The spectra are identical. It results that the main intermediate which furthers the reaction is Pd(O), before this had asociated itself as a sol, $[Pd(O)]_n$, which decreases its activity). Hence, the first reaction which takes place, between the Pd(II)-*p*-nitrosodiphenylamine complex and carbon monoxide, is given by the equation

$$[Pd(ONC_6H_4NHC_6H_5)_2]Cl_2 + CO \rightarrow Pd + 2ONC_6H_4NHC_6H_5 + \underset{\displaystyle CO_2 + 2HCl}{\underset{\downarrow\, H_2O}{COCl_2}}$$

In the system containing CO, Pd(O), $ONC_6H_4NHC_6H_5$, HMPA and H_2O, the reaction proceeds henceforth in time. We give in Figure 1 the UV spectra, between 250—350 nm, obtained 5 minutes, 1 hr. and 3 hr. after passing a few bubbles of CO through a solution containing 0.25 mL of 100 μg Pd(II)/mL solution, 0.75 mL of 1 % HCl, 2.5 mL of 0.01 % *p*-nitrosodiphenylamine solution and 7.5 mL of HMPA, brought to 25 mL with distilled water. For the sake of comparison, the spectra of the organic reagent and of its complex with Pd(II) are given in Figure 2 over the same range.

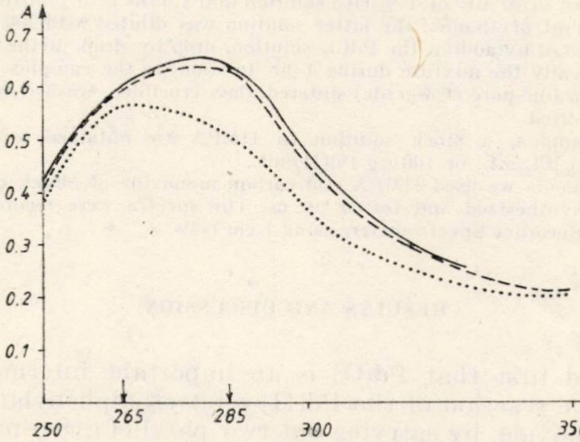

Fig. 1. — The UV spectra of the Pd(II)-*p*-nitrosodiphenylamine solution, bubbled with CO : 5 minutes (. . . . . .), 1 hr. (- - - -) and 3 hr. (— —), after bubbling CO.

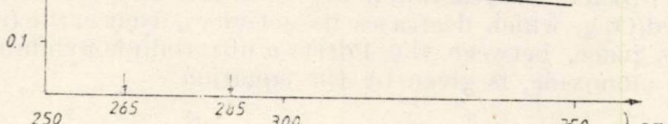

Fig. 2. — The UV spectra of the *p*-nitrospdiphenylamine solution (— —) and of the Pd(II)-*p*-nitrosodiphenylamine complex (- - -).

The spectra of *p*-nitrosodiphenylamine and of its complex with Pd(II) contain 2 maxima, located at 265 and 285 nm ; the stronger band at 265 nm can be assigned to an $n \rightarrow \pi^*$ transition. We noticed that the 265 nm band decreases in intensity after bubbling CO, whereas the 285 nm band increases its intensity. These intensities become, however, constant some 2 hr. after bubbling CO.

In the visible range, the spectrum of the solution discussed in Fig. 1 is given in Figure 3. It can be seen that it contains a band (at 450 nm) which is characteristic to the uncoordinated *p*-nitrosodiphenylamine molecules, assigned to an $n \rightarrow \pi^*$ transition. For comparison, in Figure 4 we give the visible spectra of *p*-nitrosodiphenylamine and of its complex with Pd(II). The 525 nm band in the spectrum of the $[Pd(ONC_6H_4NHC_6H_5)_2]Cl_2$ complex, assigned to a $d_{xy} \rightarrow d_{x^2-y^2}$ transition of the metal and characteristic to a coordination number of 4 of Pd(II)[20], disappears after the reaction with CO has taken place, whereas the 450 nm band, characteristic to the *p*-nitrosodiphenylamine molecules, decreases in intensity and becomes constant 2 hr. after bubbling CO. The blank solution,

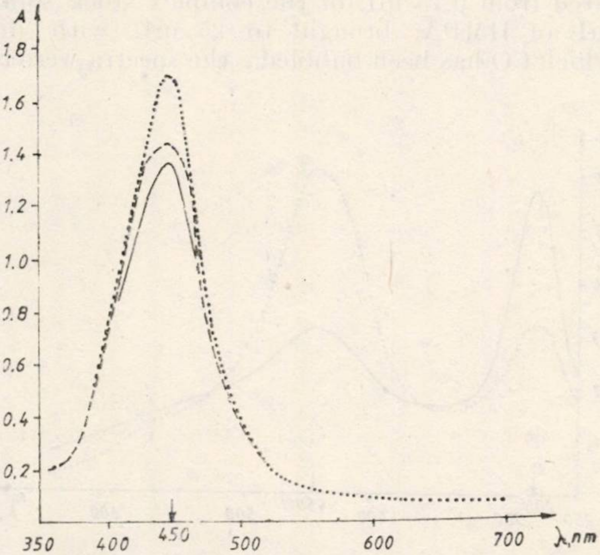

Fig. 3. — The visible spectra of the Pd(II)-*p*-nitrosodiphenylamine solution, bubbled with CO : 5 minutes (. . . . . .), 1 hr. (- - - -) and 3 hr. (— —) after bubbling CO.

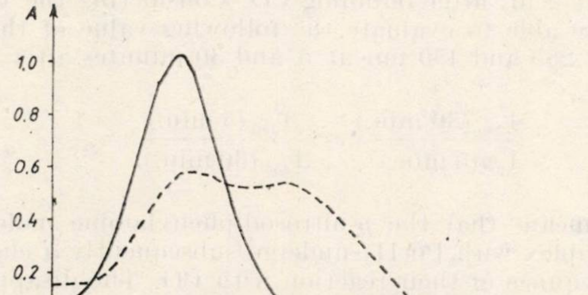

Fig. 4 — The visible spectra of the *p*-nitrosodiphenylamine solution (— —) and of the Pd(II)-*p*-nitrosodiphenylamine complex (- - -).

CO + HMPA + H_2O, does contain no spectral signals over the 250—700 nm range used in this study.

We give in the following some spectral data concerning the reaction of carbon monoxide with the synthesized $[Pd(ONC_6H_4NHC_6H_5)_2]Cl_2$ complex after it has been solubilized. Figure 5 gives the spectra of a solution prepared from 0.75 mL of the complex stock solution, 1 mL of 1% HCl, 5 mL of HMPA, brought to 25 mL with distilled water and through which CO has been bubbled : the spectra were recorded 5 and and 30 minutes after bubbling CO. Figure 6 gives the spectra of a similar solution, but which contains 5 mL of 1% HCl, at several time intervals after bubbling CO. The effect of the reaction with CO consists in the appearance of a new, very strong band at 285 nm and in the decrease in intensity of the 450 nm band, until it disappears completely from the spectrum about 2 hr. after bubbling CO. Considering the two spectra of Fig. 5, we were able to evaluate the following value of the ratio of the absorbances at 285 and 450 nm at 5 and 30 minutes after bubbling CO :

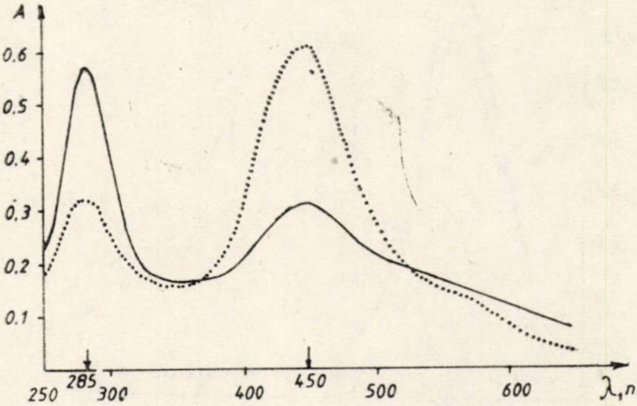

Fig. 5.—The UV/VIS spectra of the $[Pd(ONC_6H_4NHC_6H_5)_2]Cl_2$ solution, bubbled with CO : 5 minutes (. . . .) and 30 minutes (——) after bubbling CO (1 mL of 1 HCl in 25 mL of sample).

$$\frac{A_{285}\,(30\text{ min.})}{A_{285}(5\text{ min.})} = \frac{A_{450}\,(5\text{ min.})}{A_{450}\,(30\text{ min.})} = \frac{1}{2}$$

This relation means that the *p*-nitrosodiphenylamine molecules released from their complex with Pd(II) undergo subsequently a chemical conversion as a consequnce of their reaction with CO. The disappearance, 2 hr. after bubbling CO, of the 450 nm visible band, characteristic for *p*-nitrosodiphenylamine, suggests the possibility of a reduction of the nitroso group, catalyzed by Pd(O) atoms.

The spectrum of the *p*-nitrosodiphenylamine solution (consisting of 1 mL of 0.01% *p*-nitrosodiphenylamine solution, 1 mL of 1 % HCl and

5 mL of HMPA, brought 5 to 25 mL with distilled water) remains unchanged after bubbling CO; in the absence of Pd, therefore, *p*-nitrosodiphenylamine does not undergo the reaction of reduction by CO of its $-N{=}O$ group to the $-NH-OH$ group.

We noticed that by increasing the amount of 1 % HCl solution which is added to the sample, the intensities of the bands in the visible range decrease after the complex has reacted with CO, a fact which is illustrated in Fig. 6. The increase of the HMPA concentration of the reaction medium leads to a decrease of the rate of reduction of the nitroso group and to a diminished stabilization of the initial $[Pd(ONC_6H_4NHC_6H_5)_2]Cl_2$ complex in the corresponding reaction medium; we found that a concentration of 20–30% of HMPA in the reaction medium can be successfully used.

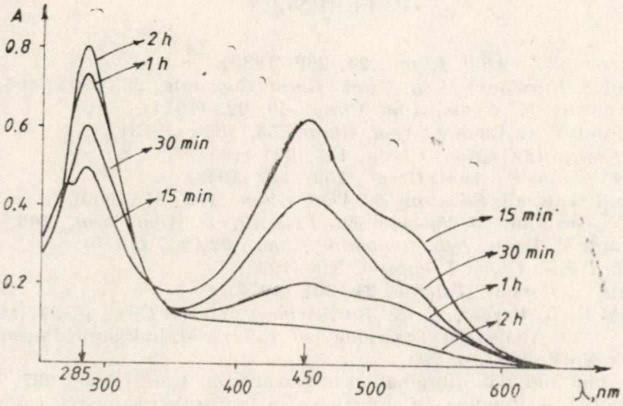

Fig. 6. — The UV/VIS spectra of the $[Pd(ONC_6H_4NHC_6H_5)_2]Cl_2$ solution, bubbled with CO, at various time intervals after bubbling CO (using 5 mL of 1 % HCl in 25 mL of sample).

Formation of a well-defined compound after the reduction of Pd(II) to Pd(O) is also proved by the observance of the Lambert-Beer law by all the samples analyzed; by taking into study increasing amounts of the $[Pd(ONC_6H_4NHC_6H_5)_2]Cl_2$ stock solution and subjecting them to the complete reaction with CO, the absorbances measured at 285 nm against a blank solution, 2 hr. after bubbling CO, have placed the measured values on a straight line, with a good correlation coefficient (0.99).

CONCLUSIONS

The complex $[Pd(ONC_6H_4NHC_6H_5)_2]Cl_2$ is the first known complex of Pd(II) with organic reagents containing the *p*-nitrosophenylamino-functional group which has been tried in the determination of carbon monoxide in air. The reaction of the Pd(II)-*p*-nitrosodiphenylamine complex with CO was investigated spectrally (in UV/VIS) in a new reaction medium, i.e. a mixture of HMPA and water. This mixture is at the same time a good absorbent for CO. The spectral data obtained during this investigation showed that the reaction of the Pd(II)-*p*-nitrosopdiphenylamine complex does not stop after the reduction to Pd(O), but proceeds further with the formation of a well-defined compound, characterized by a spectral band located at 285 nm. It was assumed that a reduction of the $-N{=}O$ group to $-NH-OH$ takes place, with the subsequent formation of a metal carbonyl which has yet to be synthesized and characterized by physico-chemical methods.

REFERENCES

[1] C. Winkler, *Fresenius'Z. Anal. Chem.*, **20**, 269 (1889).
[2] L. Burianec and J. Burianova, *Coll. Czech. Chem. Commun.*, **28**, 2895 (1963).
[3] J. L. Lambert and R. E. Wiens, *Anal. Chem.*, **46**, 929 (1974).
[4] J. L. Lambert and Y. C. Chiang, *Anal. Chem.*, **55**, 1829 (1983).
[5] G. Ciuhandu, *Fresenius'Z. Anal. Chem.*, **155**, 321 (1957).
[6] G. Ciuhandu, *Fresenius'Z. Anal. Chem.*, **158**, 345 (1948).
[7] G. Ciuhandu and G. Kroll, *Fresenius'Z. Anal. Chem.*, **172**, 81 (1960).
[8] G. Ciuhandu, V. Rusu and M. Diaconovici, *Fresenius'Z. Anal.Chem.*, **208**, 80 (1965).
[9] T. Simonescu and V. Rusu, *Rev. Roumaine Chim.*, **22**, 937 (1977).
[10] M. Micloux, *Bull. Soc. Chim. France*, **3**, 818 (1923).
[11] S. E. Mehdi and A. Corsini, *Talanta*, **24**, 291 (1977).
[12] W. P. Yant and L. B. Berger, *U. S. Bur. Mines, Miners' Circ.*, p. 34 (1963).
[13] M. B. Jacobs, "The Analytical Toxicology of Industrial Inorganic Poisons", Interscience Publ., New York, 1967, p. 703.
[14] T. V. Ramakrishna and Balasubramanian, *Fresenius'Z. Anal. Chem.*, **287**, 313 (1977).
[15] J. C. Bailard and H. J. Emeliua, "Comprehensive Inorganic Chemistry", Vol. IV, Pergamon Press, Oxford, 1975.
[16] V.David, *Anal. Lett.*, **19**, 1199 (1986).
[17] K.K. Babcock-Hitachi, *Jpn. Kokai Tokkyo Koho*, **5**, 219, 031 (1980).
[18] K.K. Babcock-Hitachi, *Jpn. Kokai Tokkyo Kohō*, **5**, 832, 005 (1981).
[19] K.K. Babcock-Hitachi, *Jpn. Kokai Tokkyo Koho*, **5**, 869, 710 (1981).
[20] A.B.P. Lever, "Inorganic Electronic Spectroscopy", Elsevier, Amsterdam, 1968.

Revue Roumaine de Chimie, 33, 6, 611–616 (1988)

A NOVEL SPECTROPHOTOMETRIC METHOD FOR THE DETERMINATION OF PEROXYDISULPHATE ION USING *o*-DIANISIDINE-$S_2O_8^{2-}$—Cu(II) INDICATOR REACTION

P. M. SHIUNDU and S. B. JONNALAGADDA

Department of Chemistry, University of Nairobi, P.O. Box 30197, Nairobi, Kenya

Received February 22, 1987

A simple spectrophotometric method for determination of peroxydisulphate ion concentration in aqueous solutions is developed, using its property of oxidation of *o*-dianisidine to a red colored compound with an absorption maxima at 450 nm. The reliability of the method is tested by determining the rate constant for the Ag(I) catalysed *n*-butylamine-$S_2O_8^{2-}$ reaction.

INTRODUCTION

Peroxydisulphate ion is a powerful oxidising agent in all acidic, alkaline and neutral media and has wider applications in different branches of chemistry.[1] A number of titrimetric[2] and instrumental methods[3–5] for determination of persulphate ion are available in literature, but most of the methods are either time consuming or tedious. The polographic methods demand removal of interfering metal ions.[5] The present communication reports a fast and simple spectrophotometric method for determination of $S_2O_8^{2-}$ in aqueous solutions, using Cu(II) catalysed oxidation reaction of *o*-dianisidine (oda) (1,1′-biphenyl-3,3′-dimethoxy-4,4′-diamine) by peroxydisulphate ion as an indicator reaction.

EXPERIMENTAL

Reagents

All the reagents used were of Analar grade or of high purity and all the solutions were prepared in deionised water. Stock solutions of oda (0.075 M) were prepared dissolving 0.018 g/100 mL into warm deionized water.

Apparatus

Pye Univam SP8-150 UV-Visible or EE1 197 visible spectrophotometer was used with 10 mm quartz cuvettes. Experiments were conducted in a thermostat (20° ± 0.1°C) or at room temperature (20 ± 2°C).

Procedure

Maintaining pseudo excess concentrations of reactants compared to peroxydisulphate ion, requisite volumes of the reagents were added to oda solution and then the reaction mixture was adjusted to desired pH, either with dilute sulphuric acid or dilute sodium hydroxide. Reaction was started with the addition of peroxydisulphate ion. Final volume of the reaction mixture was made to 10 mL. The progress of the reaction was followed by measuring the absorbance at different time intervals till a steady value was reached.

RESULTS AND DISCUSSION

The detailed kinetics and mechanism of the reaction will be reported in a separate communication.[6] The red coloured oxidation product which has an absorption peak at 450 nm is a diimine (1,1′-biphenyl-3,3′-dimethoxy-4,4′-diimine).

Effect of pH and buffers

Preliminary experiments carried out at neutral and at different acidic and alkaline pHs with oda 6.0×10^{-4} M and peroxydisulphate 1.0×10^{-4}M showed that reaction is highly pH dependent. At neutral pH, absorbance values reach a maximum in 14 minutes, while on either side, at acidic or alkaline pH conditions, reaction slowed down, consuming longer time to attain the same maximum value. Effect of buffers, acetic acid-sodium acetate buffer (1.0×10^{-4} Mto 0.1 M) and H_3PO_4- $-K_2HPO_4$ buffer (0.02 M) (after adjusting the pH to 7) were studied and it is observed that both the buffers retard the reaction. Hence all the further studies were conducted at neutral pH without buffers.

Effect of cations

To reduce the reaction time, the effect of different cations on the oxidation reaction is investigated. Fe(II), Al(III), Ce(IV) etc. up to 1.0×10^{-4}M have showed negligible influence on the reaction, while Ag(I), Cu(II), Mn(II) and Mo(VI) have exerted appreciable catalytic effect even at low concentrations. Figure 1 illustrates the positive effect of different cations on the oda$-S_2O_8^{2-}$ reaction. The curves indicate that Ag(I) precipitates in the presence of halide ions, Cu(II) is chosen as the catalyst for the reaction. Studying the reaction progress with different initial concentrations of Cu(II), 5.0×10^{-4}M is found to be the optimum concentration to hasten the reaction rate satisfactorily.

Effect of neutral salts

It is observed that the presence of KCl up to 2.0×10^{-3} M and K_2SO_4 up to 1.0×10^{-3}M exerted no appreciable effect on the reaction rate, while higher concentrations slowed down the reaction. But the presence of low concentrations of nitrate ion, 10^{-4}M interfered in the reaction decreasing both the reaction rate and maximum absorbance value.

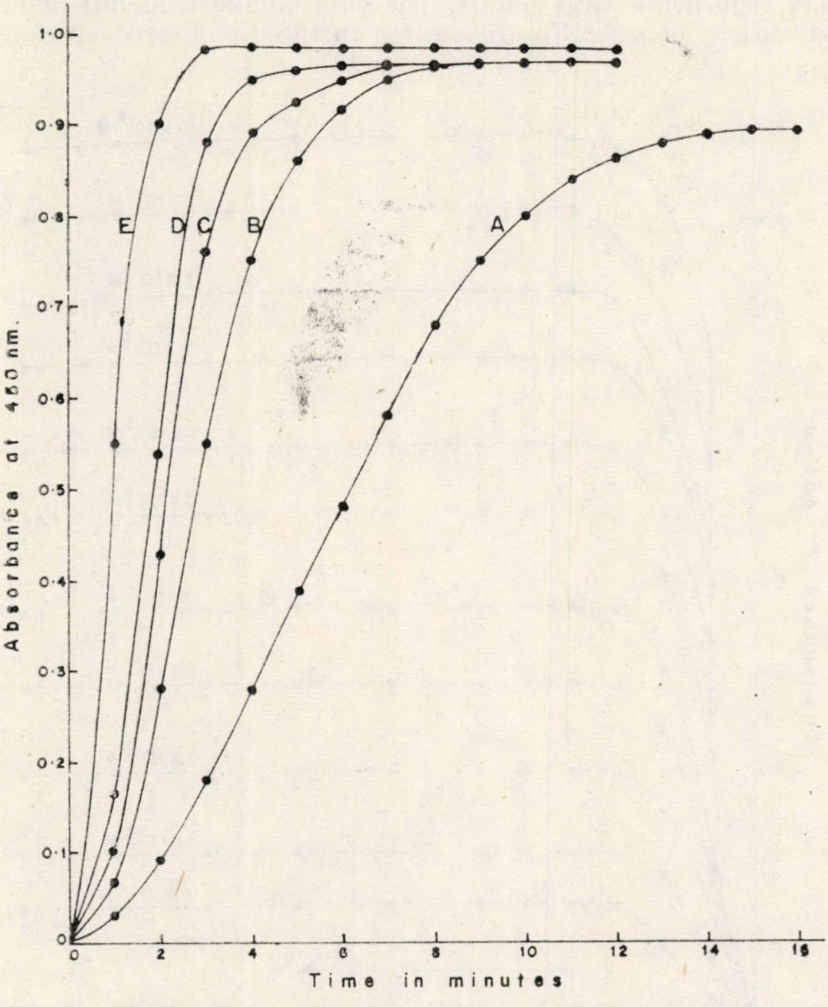

Fig. 1. — Absorbance versus time curves (at 450 nm). Effect of cations on *o*-dianisidine-peroxydisulphate reaction : [oda] 6.0 × 10^{-4}M, [$S_2O_8^{2-}$] 1.0 × 10^{-4} M. A — Uncatalysed reaction, B — [Mn(II)]10^{-5}M, C — [Mo(VI)] 10^{-5}M, D — [Cu(II)] 10^{-5}M and E — [Ag(I)] 7.0 × 10^{-7}M.

Analytical method

For the standardization of the method a number of runs of indicator reaction were studied both in a thermostat (20°C ± 0.1°) and at room temperature (20°C ± 2°) employing 8 mL of 7.5 × 10^{-4}M oda (6.0 × 10^{-4} M), 0.5 mL of 0.01 M Cu (II)SO_4(5.0 × 10^{-4}M) and requisite volumes of water to makeup the final volume to 10 mL and different initial concentrations of peroxydisulphate ion (5.0 × 10^{-2} M —1.0 × 10^{-4}M). For each experiment the absorbances were measured at 30 s or 60 s intervals for

8 minutes. The data from the thermostated and room temperature experiments yielded the same results. The data obtained for different initial concentrations of peroxydisulphate ion in three replicate experiments is

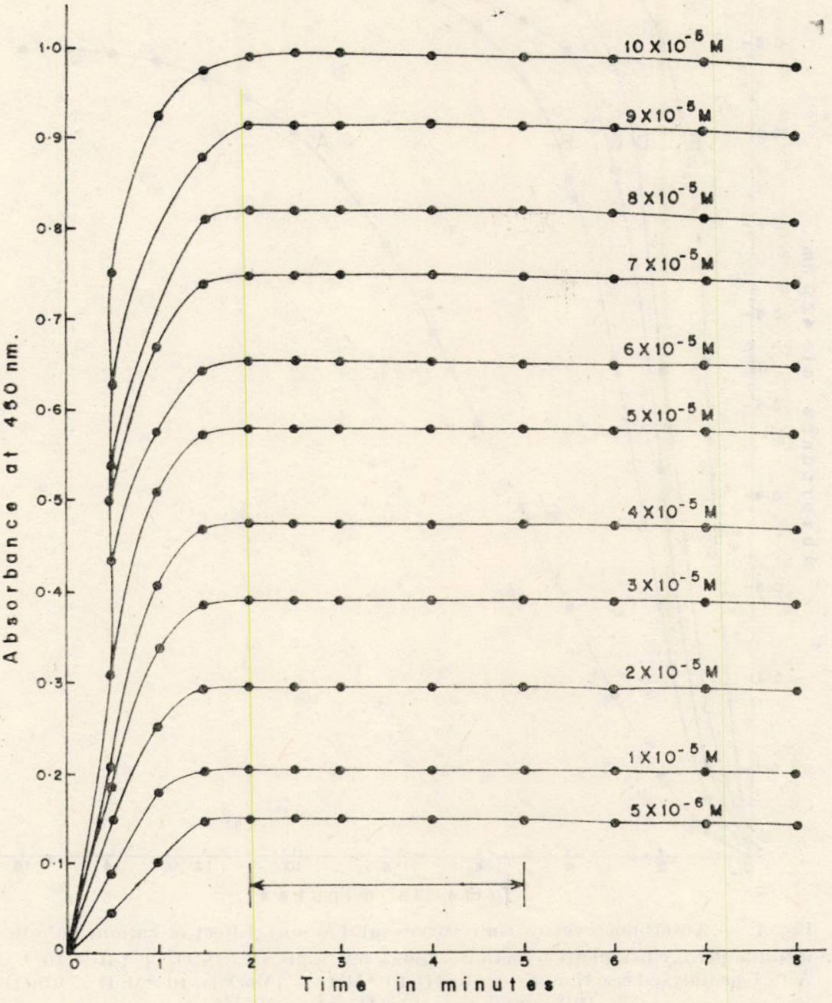

Fig. 2. — Absorbance versus time curves for different initial concentrations of peroxydisulphate ion. [oda] 6.0×10^{-4}M, [Cu(II)] 5.0×10^{-4} M.

shown as absorbance versus time curves (Figure 2). A perusal of Fig. 2 shows that in all the curves the maximum absorbance value is attained within 60 s and the value remains the same upto 300 s, although a slight decrease is observable after 300 s in some curves. Using the data presented in Fig. 2, the absorbance values (between 60 and 300 s) were plotted against peroxydisulphate ion concentration. A fairly straight line with gradient 8.8×10^3 (corr. 0.96) was obtained, if absorbance values below 0.16 are excluded, which could be used as a calibration curve for determination of peroxydisulphate ion concentration from the corresponding absorbance values.

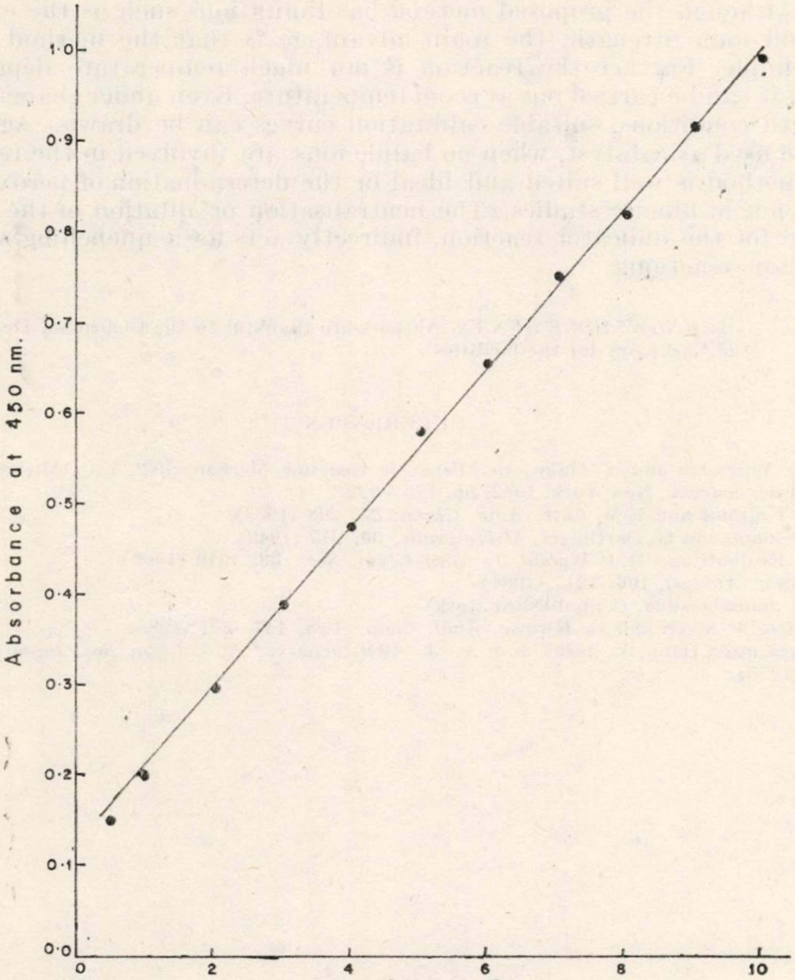

Fig. 3. — Calibration curve: Absorbance versus peroxydisulphate ion concentration. Conditions same as in Fig. 2. Entries are from three replicate experiments and values had 4% average deviation.

The validity of oda $-S_2O_8^{2-}-$Cu(II) reaction as the indicator reaction was tested by using it to monitor the kinetics of Ag(I) catalysed reaction between *n*-butylamine and potassium peroxydisulphate at 25°C. The peroxydisulphate ion concentration (Fig. 3) at fixed intervals was determined by neutralising the aliquots of reaction mixture and reading the corresponding absorbances at 450 nm after incubation for about three minutes with indicator reaction mixture. The pseudo first order rate constant for *n*-butylamine (0.20 M), peroxydisulphate (0.005 M) and Ag(I) (3.0×10^{-4}M) at 25°C determined, 5.76×10^{-3} s^{-1} agreed fairly with the literature value 5.41×10^{-3} s^{-1} .[8]

Although the proposed method has limitations such as the effect of pH and ionic strength, the main advantage is that the method is fast and simple. Further the reaction is not much temperature dependent. Hence it can be carried out at room temperature. Even under changed ionic strength conditions, suitable calibration curves can be drawn. Ag(I) can also be used as catalyst, when no halide ions are involved in the reaction. This method is well suited and ideal or the determination of peroxydisulphate ion in kinetic studies. The neutralisation or dilution of the sample needed for the indicator reaction, indirectly acts as a quenching step for the main reaction.

ACKNOWLEDGEMENTS. Authors are thankful to the Chairman, Department of Chemistry for the facilities.

REFERENCES

[1] W. K. Wilmarth and A. Haim, In "Peroxide Reaction Mechanisms", Ed. Edwards, J.O., Inter Science, New York, 1962, pp. 175–222.
[2] I. M. Kolthoff and E.M. Carr, *Anal. Chem.*, **25**, 298 (1953).
[3] W. Gelman, and H. Bartlinger, *Mikrochemie*, **30**, 217 (1942).
[4] I. M. Kolthoff and R.J. Woods, *J. Amer Chem. Soc.*, **88**, 1316 (1966).
[5] D. Amin, *Analyst*, **106**, 1217 (1981).
[6] S. B. Jonnalagadda, (Unpublished work).
[7] M. Otto, J. Stach and R. Kirmse, *Anal. Chim. Acta*, **147**, 277 (1983).
[8] J. Sreekantha Babu, V. Joshi and A. J. Bhattacharya, *Bull. Chem. Soc. Japan*, **49**, 1820 (1976).

Revue Roumaine de Chimie, **33**, *6*, 617–622 (1988)

CHARGE-TRANSFER COMPLEXES OF BENZANILIDES WITH π-ACCEPTORS

ABOUL-FETOUH E. MOURAD
Chemistry Department, Faculty of Science, El-Minia University, El-Minia, Egypt

Received May 18, 1987

A spectrophotometric study of several substituted benzanilides as electron donors with tetracyanoethylene (TCNE) and 2,3-dichloro-5,6-dicyanobenzoquinone (DDQ) as electron acceptors indicated the formation of 1 :1 charge-transfer (CT) complexes. The nature of interactions as well as the substituent effects on the CT complexation are discussed.

INTRODUCTION

Although extensive studies have been made on the CT complexes between nitrogen containing compounds with electron acceptors, there still remain some compounds whose CT complexes have not been reported. Among them, benzanilide derivatives seem to be of particular interest.

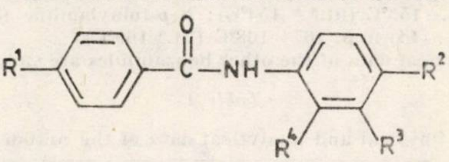

(1) $R^1 = R^3 = R^4 = H$; $R^2 = Cl$

(2) $R^1 = R^2 = R^3 = R^4 = H$

(3) $R^1 = R^3 = R^4 = H$; $R^2 = CH_3$

(4) $R^1 = R^2 = R^4 = H$; $R^3 = CH_3$

(5) $R^1 = R^2 = R^3 = H$; $R^4 = CH_3$

(6) $R^1 = R^3 = R^4 = H$; $R^2 = OCH_3$

(7) $R^1 = CH_3$; $R^2 = Cl$; $R^3 = R^4 = H$

(8) $R^1 = CH_3$; $R^2 = R^3 = R^4 = H$

(9) $R^1 = R^2 = CH_3$; $R^3 = R^4 = H$

(10) $R^1 = R^3 = CH_3$; $R^2 = R^4 = H$

(11) $R^1 = R^4 = CH_3$; $R^2 = R^3 = H$

(12) $R^1 = CH_3$; $R^2 = OCH_3$; $R^3 = R^4 = H$

(13) $R^1 = OCH_3$; $R^2 = Cl$; $R^3 = R^4 = H$

(14) $R^1 = OCH_3$; $R^2 = R^3 = R^4 = H$

(15) $R^1 = OCH_3$; $R^2 = CH_3$; $R^3 = R^4 = H$

(16) $R^1 = OCH_3$; $R^3 = CH_3$; $R^2 = R^4 = H$

(17) $R^1 = OCH_3$; $R^4 = CH_3$; $R^2 = R^3 = H$

(18) $R^1 = R^2 = OCH_3$; $R^3 = R^4 = H$

The spectroscopic properties of the CT complexes of acetamides with ICl, Br_2, I_2 and SO_2 have been discussed.[1-5] Also, the heats of formation for CT complexes of I_2 with a series of *ortho*-substituted N-methyl acetanilides have been correlated with Hammett's σ constants for the substituents.[6]

The present paper reports the results of a spectrophotometric investigation of the CT complexes formed between eighteen substituted benzanilides (**1**–**18**, Fig. 1) as electron donors and both TCNE and DDQ as π-acceptors. The role of the molecular structure of the donors **1**–**18** on the CT complexation is also discussed.

EXPERIMENTAL AND PHYSICAL MEASUREMENTS

Tetracyanoethylene (Aldrich) was recrystallized from chloroform and sublimed. 2,3-Dichloro-5,6-dicyanobenzoquinone (Aldrich) was recrystallized from benzene-chloroform (2 :3).

Methylene chloride (Merck) was purified following Organicum,[7] dried and distilled.

Benzanilide (Aldrich) was used without further purification. Substituted benzanilides were prepared according to the Schotten-Baumann method by addition of the acid chloride to the amine in 10 % aqueous sodium hydroxide solution[8]: N-benzoyl-*p*-chloroaniline (**1**) mp. 191–192°C (lit.[9] 192°C); N-benzoyl-*p*-toluidine (**3**) m.p. 158°C (lit.[8] 158°C); N-benzoyl-*m*-toluidine (**4**) m.p. 123–124°C (lit.[8] 125°C); N-benzoyl-*o*-toluidine (**5**) m.p. 144°C (lit.[8] 144°C); N-benzoyl-*p*-anisidine (**6**) m.p. 153°C (lit.[8] 154°C); N-*p*-toluylaniline (**8**) m.p. 145–146°C (lit.[8] 146°C); N-*p*-anisoylaniline (**14**) m.p. 167–168°C (lit.[8] 169°C).

Physical and analytical data of the other benzanilides are summarized in Table 1.

Table 1

Physical and analytical data of the anilides

Compd.*	m.p. (°C)	IR(KBr, cm^{-1})		Analysis, Calcd. (Found) %		
		NH	CO	C	H	N
7	205	3352	1650	68.42	4.92	5.70
				(68.40	4.80	5.60)
9	153	3350	1645	79.97	6.71	6.21
				(79.80	6.70	6.20)
10	98	3300	1650	79.87	6.71	6.21
				(80.00	6.50	6.20)
11	110	3355	1640	79.97	6.71	6.21
				(80.10	6.70	6.30)
12	161	3350	1640	74.67	6.27	5.80
				(74.40	6.30	5.70)
13	197	3345	1642	64.24	4.62	5.35
				(64.00	4.50	5.50)
15	162	3350	1645	74.67	6.27	5.80
				(74.70	6.10	5.60)
16	101	3345	1640	74.67	6.27	5.80
				(74.50	6.00	6.900)
17	159	3350	1640	74.67	6.27	5.80
				(74.70	6.10	5.70)
18	198	3330	1650	70.02	5.88	5.44
				(70.00	5.80	5.50)

* All compounds were recrystallized from ethanol/chloroform.

Association constants of formation (K) and molar extinction coefficients (ε) of the CT complexes studied were determined by the least squares method, using the Scott-modification[10] of the Benesi-Hildebrand equation.[11]

For determining the association constant and molar extinction coefficient of the CT complexes, the donor concentrations ranged from 1×10^{-2} to 4×10^{-2} mol/L, while that of the acceptors was 1×10^{-3} mol/L, However. for the determination of the stoechiometry by Job's method, stock solutions (2×10^{-3} mol/L) of donors and acceptors were prepared. Solutions of the complexes were prepared in 5mL stoppered silica cells immediately before use at 22°C. All scans covered the range from 350 to 800 nm.

The electronic spectra of the CT complexes were measured on a Beckman Model 26 recording spectrophotometer. Infrared spectra were measured on a Shimadzu-IR 408 spectrometer. The analytical data were performed by the microanalysis unit at Cairo University.

RESULTS AND DISCUSSION

The electronic spectra of solutions of either TCNE or DDQ with the donors **1—18** in methylene chloride show an extra absorption band not due to either component alone and in two cases two extra bands are observed (Table 2). These bands are attributable to the formation of donor-acceptor complexes.

Table 2

Values of the wavelengths of maximum absorption for the CT complexes of donors **1—18** with TCNE and DDQ.

Anilide	TCNE λ_{max}(nm)	DDQ λ_{max}(nm)
N-Benzoyl-*p*-chloroaniline **(1)**	565(sh)	550(sh)
Benzanilide **(2)**	575(sh)	550(sh)
N-Benzoyl-*p*-toluidine **(3)**	527	617
N-N-Benzoyl-*m*-toluidine **(4)**	509(sh)	577(sh)
N-Benzoyl-*o*-toluidine **(5)**	500(sh)	560(sh)
N-Benzoyl-*p*-anisidine **(6)**	632	579
N-(-*p*-Toluyl)-*p*-chloroaniline **(7)**	475(sh)	550(sh)
N-(-*p*-Toluyl)-aniline **(8)**	500(sh)	550(sh)
N-(*p*-Toluyl)-*p*-toluidine **(9)**	535	625
N-(*p*-Toluyl)-*m*-toluidine **(10)**	515(sh)	580(sh)
N-(*p*-Toluyl)-*o*-toluidine **(11)**	508(sh)	573(sh)
N-(*p*-Toluyl)-*p*-anisidine **(12)**	630	572
N-(*p*-Anisoyl)-*p*-chloroaniline **(13)**	410(sh), 500(sh)	450(sh)
N-(*p*-Anisoyl)-aniline **(14)**	500(sh)	550(sh)
N-(*p*-Anisoyl)-*p*-toluidine **(15)**	392, 525	620
N-(*p*-Anisoyl)-*m*-toluidine **(16)**	518(sh)	590(sh)
N-(*p*-Anisoyl)-*o*-toluidine **(17)**	515(sh)	575(sh)
N-(*p*-Anisoyl)-*p*-anisidine **(18)**	609	570

It may be concluded that introduction of an electron donating group in the *p*-position of the aroyl group (COAr) increases the Lewis basicity of the donor system studied. However, in contrast as foreseen from the data in Table 2, the CT complexes of the *p*-methylated and *p*-methoxylated anilides **7—18** show a red shift relative to the unsubstituted anilides **1—6**. In other words, the donor strengths of the *p*-substituted anilides are weaker than those of the unsubstituted donors. A plausible explanation may depend on the following facts: the stronger the electron donating character of the substituent attached to the nitrogen atom, the less is the extent of the electron delocalization of the *n* electrons of this atom. Accordingly, the *n* character of the donor will be pronounced. But as it is shown in Fig. 2 the nitrogen atom in **19** prefers to interact with its adjacent carbonyl group through its lone pair electrons, rather than with the phenyl group carrying electron donating groups.

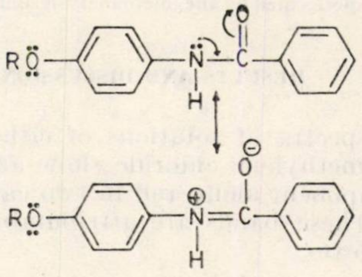

19

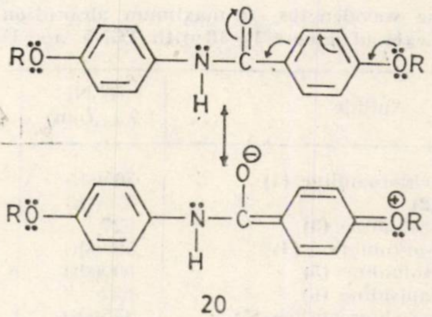

20

As a result the nitrogen lone pair electrons are not localized on the nitrogen atom, and hence the *n* character may be absent. That is to say, the interaction in the anilides **1**–**7** is suggested to be of the $\pi-\pi^*$ type.

Introduction of an electron donating group in the *p*-position of the benzoyl group results in strengthening the electron delocalization in the aroyl group (**20**). Consequently, the electron delocalization between the *n* electrons of the nitrogen atom and the carbonyl group will be inhibited. In this case one can conclude that the *n* electrons are not completely delocalized as in the case of anilides with unsubstituted aroyl group.

In conclusion, the decrease of the donor properties of the anilides in the order; benzoyl > *p*-toluyl > *p*-anisoyl may be based on the extent of the electron delocalization of the *n* electrons of the anilide nitrogen atom with the neighbouring groups, and consequently the *n* character of the nitrogen atom will follow the opposite order.

The data in Table 2 show also that the CT complexes of the benzanilides **13** and **15** with TCNE absorb at two shoulders and two maxima respectively, however the CT complexes of the other benzanilides absorb at one maximum. The lack of the values for the energy differences between the two highest occupied molecular orbitals in the literature for the donors studied makes it hard to decide quantitatively the origin of these two bands. However it may be suggested as due to either electron transition from two orbitals of the donor to the same orbital of the acceptor[12] or electron promotion from the same orbital of the donor to a different orbital of the acceptor.[13]

On the basis of the existence of the hyperconjugation and resonance effects in the *o,p*-methylated and *o,p*-methoxylated N-aryl groups, their donor strengths should be higher than their corresponding *m*-isomers. In other words, taking the long wavelength absorption band of the complex as a measure of the donor strength, the basicity decreases in the order: *para*-substituted $>$ *ortho*-substituted $>$ *meta*-substituted. But as visible in Table 2, the λ_{max}'s of the CT complexes of the *m*-substituted anilides are higher than those of the corresponding *o*-isomers. It is evident from this result that the steric factor existing in the *o*-isomers is prevailing over the electronic ones.

The values of the association constants together with the molar extinction coefficients and the energies of transition for the CT complexes of N-*p*-tolyl and *p*-anisyl anilides with TCNE and DDQ are shown in Table 3. The greater electron affinity of DDQ than TCNE[14] accounts for the higher stability of anilide-DDQ complexes. Analysis of the data in Tables 2 and 3 reveals also that the association constant values did not follow the same trend as those of both λ_{max} and ε values. That is to say that the *K* values of the CT complexes increase in the order; N-benzoyl $<$ $<$ N-toluyl $<$N-anisoyl derivatives, However as reported by Mulliken,[15] there must be a linear relationship between the the association constants and the molar extinction coefficients for the CT complexes.

Table 3

Molar extinction coefficients (ε), association constants (*K*) and transition energies (*E*) for the CT complexes with TCNE and DDQ

Donor	Acceptor	ε (L.mol^{-1}m^{-1})	K (L.mol^{-1})	E (eV)
3	TCNE	365	5.32±0.06	2.36
6	TCNE	415	8.11±0.10	1.97
9	TCNE	460	6.62±0.05	2.32
12	TCNE	290	11.02±0.03	1.97
15	TCNE	741	9.42±0.12	3.17, 2.37
18	TCNE	296	12.03±0.06	2.04
3	DDQ	485	7.45±0.11	2.02
6	DDQ	337	17.84±0.30	2.15
9	DDQ	900	12.15±0.08	1.99
12	DDQ	476	25.08±0.23	2.17
15	DDQ	612	15.94±0.35	2.01
18	DDQ	340	23.25±0.15	2.18

This abnormal correlation between *K* and ε values in the present study may be caused by steric factors in the donor system. On the other hand, with exception of 3,6-TCNE complexes, comparison of λ_{max} and ε values (Tables 2 and 3) shows that they follow the same sequence

The transition energies of the CT complexes also indicate the relative Lewis basicities of the donors studied.

The stoechiometry of all CT complexes was found to be 1 :1. This result was confirmed by application of Job's method[16] for continuous variation which gave symmetrical curves with maxima at a mole fraction 0.5.

REFERENCES

[1] R. S. Drago and D. A. Wenz, *J. Amer. Chem. Soc.*, **84**, 526 (1962).

[2] R. S. Drago, R. L. Carlson, N. J. Rose and D. A. Wenz, *J. Amer. Chem. Soc.*, **83**, 3572 (1961).

[3] R. S. Drago, D. A. Wenz and R. L. Carlson, *J. Amer. Chem. Soc.*, **84**, 1106 (1962).

[4] R. L. Carlson and R. S. Drago, *J. Amer. Chem. Soc.*, **84**, 2320 (1962).

[5] R. L. Carlson and R. S. Drago, *J. Amer. Chem. Soc.*, **85**, 505 (1963).

[6] R. S. Drago and R. L. Carlson, *J. Phys. Chem.*, **67**, 2854 (1963)

[7] "Organicum, Practical Handbook of Organic Chemistry", 1st edn. Pergamon Press, Oxford, 1973.

[8] "Vogel's Textbook of Practical Organic Chemistry", 4th edn., Longman, London, 1978.

[9] "CRC, Handbook of Tables for Organic Compound Identification", 3ed edn. CRC Press, Inc. 1980 Cranwood.

[10] R. L. Scott, *Recl. Trav. Chim.*, **75**, 787 (1965).

[11] H. A. Benesi and J. H. Hildebrand, *J. Amer. Chem. Soc.*, **71**, 2703 (1949).

[12] G. Reichenbach, S. Santini and G. G. Aloisi, *J. Chem. Soc. Faraday I*, **73**, 95 (1977).

[13] S. Iwata, J. Tanaka and S. Nagakura, *J. Amer. Chem. Soc.*, **88**, 894 (1966).

[14] R. Foster, "Organic Charge Transfer Complexes", Acdemic Press, London, 1969.

[15] R. S. Mulliken, *J. Amer. Chem. Soc.*, **74**, 811 (1952).

[16] P. Job, *Ann. Chim.*, **10**, 113 (1928).

Revue Roumaine de Chimie, **33**, *6*, 623–627 (1988)

THE *Z* DEPENDENCE OF NUCLEAR DIAMAGNETIC SHIELDING CONSTANTS FOR FREE ATOMS

D. PURDELA

Centre of Chemistry, Blvd Mihai Viteazul 24, 1900 Timişoara, Romania

Received February 22, 1987

A simple expression is presented which can be used to calculate the nuclear diamagnetic shielding constant, σ_Z^{d}, of the free atom with the atomic number Z: $\sigma_Z^{d} = b \cdot Z!/(Z-a)!$. This expression implies the convention that a is a fractional number, and not an integer. Using $a = 1.354869405$ and $b = -6.299088822 \times 10^{-6}$, the expression leads to σ_Z^{d} values which are in agreement with those obtained from Hartree-Fock calculations for light atoms and from Thomas-Fermi-Dirac calculations for heavy atoms.

INTRODUCTION

For a number of atomic and molecular calculations the value for the nuclear diamagnetic shielding constant, σ_Z^{d}, of the free atom with the atomic number Z is needed. Such a value is obtained, for example, from Hartree-Fock (HF) atomic wavefunctions or from Thomas-Fermi-Dirac (TFD) approximate statistical electron distributions. The HF equations are most largely used, especially for cases of the lighter elements, whereas the accuracy of the TFD statistical model of the atom is supposed to be best for heavy atoms. For the purpose of comparison, the HF values of σ_Z^{d} calculated by Malli and Froese[1] for $Z = 2$ to $Z = 86$ and by Dickinson[2] for $Z = 87$ to $Z = 92$ have been selected together with the corresponding TFD results obtained by Bonham and Strand[3] for $Z = 2$ to $Z = 100$.

The first approach concerning the variation with Z of σ_Z^{d} was that of Lamb,[4] who used the results of TFD calculations and proposed the approximate but simple expression:

$$\sigma_Z^{d} = 31.9 \times 10^{-6} Z^{4/3} \tag{1}$$

The most striking differences between the values obtained from eq. (1) and those computed by Bonham and Strand are for the many-electron atoms. For example, $\sigma_{90}^{d} = 12866 \times 10^{-6}$ and $\sigma_{100}^{d} = 14807 \times 10^{-6}$ instead of[3] 11025×10^{-6} and 12688×10^{-6}, respectively. Neither for the lighter atoms are the results given by eq. (1) quite satisfactory; $\sigma_2^{d} = 80.38 \times 10^{-6}$ and $\sigma_3^{d} = 138.02 \times 10^{-6}$ to be compared, in order, with[3] 89.37×10^{-6} and 143.13×10^{-6}. Moreover, $\sigma_1^{d} = 31.9 \times 10^{-6}$ from eq.

(1) is far from the correspondig theoretical value (see below). No modification of the numerical parameters of this expression accounts in a reasonable manner for all the disagreements. In fact, a reliable expression should show agreement with the HF or TFD results for light and heavy atoms, respectively. The presentation of a relation tending to accomplish such a desideratum is the purpose of this paper.

RESULTS AND DISCUSSION

In order to find a more appropriate alternative to eq. (1), the following simple observation about the possibility of expressing the ratio of two successive HF or TFD results is used :

$$\sigma_2^d/\sigma_1^d = 2/(2 - a_1),\ \sigma_3^d/\sigma_2^d = 3(3 - a_2),\ \sigma_4^d/\sigma_3^d = 4/(4 - a_3), \qquad (2)$$

and so on. As the numerical values for a_1, a_2, a_3, etc., are very close, we can use a constant value a and write a general expression as :

$$\sigma_Z^d = \sigma_1^d \frac{2 \times 3 \times 4 \times \ldots Z}{(2 - a)(3 - a)(4 - a)\ldots(Z - a)} \qquad (3)$$

The theoretical value of σ_1^d is easily calculated since the integral in the corresponding equation[5] for the case of the hydrogen atom is given by the reciprocal of the Bohr radius, $1/a_0$. Thus :

$$\sigma_1^d = e^2/3mc^2a_0 = 17.750442083 \times 10^{-6} \qquad (4)$$

using the values of a_0, e (the electronic charge), m (the rest mass of electron,) and c (the speed of light in vacuum) idicated by IUPAC.[6]

The value of the constant a can be determined by starting from one of a_1, a_2, a_3, etc., or from a mean value of these parameters computed with HF results. The chosen value is then modified by successive approximations until it leads to values of σ_Z^d, for heavy atoms, of the same magnitude as the TFD results. As a first step to the investigation of this procedure a has been evaluated to be 1.354869405, a value which in the case of the atoms with $Z \geqslant 100$ leads to the same results of σ_Z^d as those of the TFD calculations elaborated by Bonham and Strand.[7] The results for the atoms from $Z = 1$ to 100 are presented in Table 1. These results are compared with those obtained from HF[1,2] and TFD[3] calculations. In the last column of Table 1 the difference between the value of eq. (3) and the HF or TFD value, whichever is closest, is given for almost all cases. It is seen that the values of eq. (3) and HF calculations are approximately the same for the atoms $Z = 2$ to $Z = 21$. As it is to be expected, for the atoms $22 \leqslant Z \leqslant 100$ the mentioned difference is negative because both HF and TFD calculations give results which are supposed to be sightly greater than the reliable ones.

Table 1

Hartree-Fock (HF) and Thomas-Fermi-Dirac (TFD) nuclear diamagnetic shielding constants compared with those calculated from eq. (3) for free atoms with $Z = 1$ to $Z = 100$

Z	$\sigma^d_Z \times 10^6$			Δ^c
	HF[a]	TFD[b]	Eq. (3)	
1	—	—	17.75	—
2	59.90	89.37	55.03	−4.87
3	101.45	143.13	100.35	−1.10
4	149.26	205.62	151.75	2.49
5	201.99	272.10	208.15	6.16
6	260.74	341.60	268.87	8.13
7	325.47	413.80	333.40	7.93
8	395.11	488.80	401.37	6.26
9	470.71	566.50	472.50	1.79
10	552.27	646.90	546.55	−5.72
11	628.90	729.70	623.33	−5.57
12	705.60	815.00	702.66	−2.94
13	789.88	902.70	784.41	−5.47
14	874.09	992.60	868.46	−5.63
15	961.14	1085.00	954.69	−6.45
16	1050.47	1179.00	1043.02	−7.45
17	1142.64	1275.00	1133.34	−9.30
18	1237.64	1372.00	1225.59	−12.05
19	1329.36	1472.00	1319.70	−9.66
20	1422.85	1573.00	1415.60	−7.25
21	1521.35	1676.00	1513.23	−8.12
22	1622.72	1780.00	1612.53	−10.19
23	1726.62	1885.00	1713.47	−13.15
24	1833.02	1992.00	1815.99	−17.03
25	1942.10	2101.00	1920.04	−22.06
26	2052.91	2210.00	2025.60	−27.31
27	2166.38	2321.00	2132.61	−33.77
28	2282.32	2433.00	2241.05	−41.27
29	2400.71	2546.00	2350.89	−49.82
30	2521.67	2661.00	2462.08	−59.59
31	2638.57	2776.00	2574.60	−63.97
32	2757.10	2892.00	2688.43	−68.67
33	2877.18	3010.00	2803.53	−73.65
34	2998.37	3128.00	2919.89	−78.48
35	3121.19	3247.00	3037.47	−83.72
36	3245.61	3367.00	3156.26	−89.35
37	3366.80	3488.50	3276.23	−90.57
38	3489.16	—	3397.36	−91.80
39	3614.45	—	3519.63	−94.82
40	3741.61	3857.10	3643.03	−98.58
41	3870.35	—	3767.53	−102.82
42	4000.64	—	3893.11	−107.53
43	4132.52	—	4019.77	−112.75
44	4265.53	—	4147.48	−118.05
45	4400.14	4488.40	4276.23	−123.91
46	4536.25	—	4406.01	−130.24
47	4673.85	—	4536.79	−137.06
48	4813.03	—	4668.56	−144.47
49	4948.72	—	4801.32	−147.40
50	5085.55	5139.60	4935.05	−150.50
51	5223.43	—	5069.73	−153.70
52	5362.00	—	5205.36	−156.64

Table 1 (continued)

Z	$\sigma_Z^d \times 10^6$			Δ[c]
	HF[a]	TFD[b]	Eq. (3)	
53	5501.64	—	5341.92	−159.72
54	5642.32	—	5479.40	−162.92
55	5780.22	5809.90	5617.79	−162.43
56	5918.99	—	5757.07	−161.91
57	6064.83	—	5897.25	−167.58
58	6212.43	—	6038.30	−174.13
59	6361.59	—	6180.22	−181.37
60	6511.53	6499.00	6323.00	−176.00
61	6663.32	—	6466.63	—
62	6816.48	—	6611.11	—
63	6971.01	—	6756.41	—
64	7126.94	—	6902.53	—
65	7284.20	7206.60	7049.47	−157.13
66	7442.80	—	7197.22	—
67	7604.09	—	7345.77	—
68	7765.77	—	7495.10	—
69	7926.75	—	7645.22	—
70	8090.72	7932.70	7796.12	−136.58
71	8250.49	—	7947.78	—
72	8412.72	—	8100.21	—
73	8574.32	—	8253.39	—
74	8736.83	—	8407.32	—
75	8900.35	8677.40	8561.99	−115.41
76	9064.44	—	8717.40	—
77	9229.54	—	8873.54	—
78	9395.58	—	9030.40	—
79	9561.41	—	9187.97	—
80	9729.07	9440.90	9346.26	−94.64
81	9894.16	—	9505.25	—
82	10060.92	—	9664.94	—
83	10227.13	—	9825.33	—
84	10393.86	—	9986.40	—
85	10559.93	10223.00	10148.15	−74.84
86	10728.20	—	10310.60	—
87	*10800.00*	—	10473.71	—
88	*11000.00*	—	10637.48	—
89	*11100.00*	—	10801.93	—
90	*11300.00*	11025.00	10967.02	−57.98
91	*11500.00*	—	11132.78	—
92	*11600.00*	—	11299.18	—
93	—	—	11466.22	—
94	—	—	11633.91	—
95	—	11847.00	11802.23	−44.77
96	—	—	11971.18	—
97	—	—	12140.76	—
98	—	—	12310.96	—
99	—	—	12481.78	—
100	—	12688.00	12653.22	−34.78

[a] These values are from Ref. 1, except those for $Z = 87$ to $Z = 92$ which are from Ref. 2.

[b] These values are from Ref. 3.

[c] The difference between the value of Eq. (3) and the HF or TFD value, whichever is closest, in ppm.

A simple form of eq. (3) can be proposed if the nuclear diamagnetic shielding constant of the hydrogen atom is expressed by the relation :

$$\sigma_1^{\mathrm{d}} = b \frac{1}{1 - a} \tag{5}$$

where $b = -6.299088822 \times 10^{-6}$. Substituting this expression into eq. (3) and using the convention that a is a fractional number, and not an integer, we can swrite :

$$\sigma_Z^{\mathrm{d}} = b \frac{Z!}{(Z - a)!} \tag{6}$$

CONCLUSION

The comparison between eqs. (1) and (6) shows that each implies two constants, but only the latter accounts in a satisfactory manner for trends in the Z dependence of σ_Z^{d}. It is also to be pointed out that both constants of eq. (1) are empirical in character, whereas for eq. (6) this is true only for the constant a since the other, b, is derived from the theoretical parameter σ_1^{d}. Moreover, it is interesting to note that the introduction of the gamma function, $\Gamma(Z) = (Z - 1)!$, instead of $(Z - a)!$ from eq. (6) does not lead to the agreement of the obtained values with those resulted from HF and TFD calculations.

REFERENCES

[1] G. Malli and C. Froese, *Int. J. Quantum Chem.*, **1**, 95 (1967).

[2] W. C. Dickinson, *Phys. Rev.*, **80**, 563 (1950).

[3] R. A. Bonham and T. G. Strand, *J. Chem. Phys.*, **40**, 3447 (1964).

[4] W. E. Lamb, Jr., *Phys. Rev.*, **60**, 817 (1941).

[5] F. Bloch, in "NMR in Chemistry", B. Pescoe Ed., Academic Press, New York/London, 1965, p. 2.

[6] IUPAC, "Manual of Symbols and Terminology for Physicochemical Quantities and Units", Pergamon Press, Oxford, 1979, p. 35; *Pure Appl. Chem.*, **51**, 35 (1979).

[7] R. A. Bonham and T. G. Strand, *J. Chem. Phys.*, **39**, 2200 (1963).

Revue Roumaine de Chimie, **33**, *6*, 629–634 (1988)

SILVER ION CATALYZED REDOX POLYMERIZATION OF ACRYLAMIDE

U.D.N. BAJPAI, ALKA JAIN and A. K. BAJPAI
Polymer Research Laboratory, Department of Chemistry,
Rani Durgavati University, Jabalpur, M.P., India

Received March 2, 1987

Aqueous polymerization of acrylamide initiated with $K_2S_2O_8$/ascorbic acid and catalysed by A_g^+ ions has been studied in the presence of O_2 at 35 ± 0.2°C. The rate of polymerization may be expressed by the following equation: $R_p \alpha$[Persulphate]^1 [Ag+]^1 [Acrylamide].^{1} The effect of DMF and neutral salts on the rate of polymerization has been studied. The overall energy of activation is found to be 13.8 kcal/deg. in the studied range (29 – 50°C).

INTRODUCTION

Peroxydisulphate, in combination with a suitable reductant and alone also, has been found to be an effective initiator for the polymerization of vinyl monomers. Its combination with ascorbic acid has been reported to form an efficient redox system for polymerization of vinyl monomers.[1-3] The incorporation of metal ions with peroxydisulphate-ascorbic acid redox system has been proved to be a powerful tool for rapid polymerization.[4-5] In the present study Ag^+ ion has been used with $K_2S_2O_8$/ascorbic acid redox system for the polymerization of acrylamide in O_2 atmosphere. Molecular oxygen, which usually inhibits or retards the polymerization reaction acts in this system as a catalyst.

RESULTS AND DISCUSSION

The mechanism of polymerization of methacrylamide initiated by $K_2S_2O_8$/ascorbic acid was given by Misra et al.[2] and they suggested the presence of ascorbate ($AH^\bullet$) and sulphate ($SO_4^{\bullet -}$) radicals as initiating species. Similarly, Mushran and coworkers[6] showed the presence of $AH^\bullet$, $SO_4^{\bullet -}$ and $OH_4^{\bullet -}$radicals in their kinetic studies. Based on the above facts, the following tentative mechanism has been proposed for the polymerization of acrylamide initiated by persulphate-ascorbic acid – Ag^+ ion system.

(a) Formation of free radiacals

$$S_2O_8^{2-} + Ag^+ \xrightarrow{k_1} Ag^{2+} + SO_4^{--} + SO_4^{-\bullet}. \tag{1}$$

$$SO_4^{-\bullet} + AH^- \xrightarrow{k_2} SO_4^{2-} + AH^\bullet \tag{2}$$

at higher concentration of ascorbic acid

$$AH^\bullet + SO_4^{-\bullet} \xrightarrow{k_3} A + SO_4^{--} + H^+ \tag{3}$$

(b) Initiation

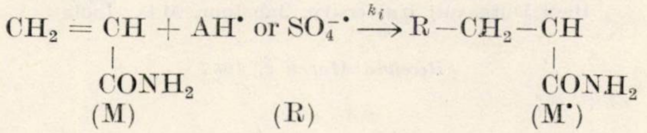

$$\underset{(M)}{\underset{CONH_2}{CH_2 = \underset{|}{CH}}} + AH^\bullet \text{ or } SO_4^{-\bullet} \xrightarrow{k_i} \underset{(R)}{R} - \underset{(M^\bullet)}{\underset{CONH_2}{CH_2 - \underset{|}{\dot{C}H}}} \tag{4}$$

(c) Propagation

$$\begin{array}{l} M^\bullet + M \xrightarrow{kp} M_1^\bullet \\ \vdots \\ M_{n-1}^\bullet + M \xrightarrow{kp} M_n^\bullet \end{array} \tag{5}$$

(d) Termination

$$M_n^\bullet \xrightarrow{kt} \text{Polymer}$$

The possibility of termination by coupling, disproportionation, primary radicals or by dissolved metal ions may also not be discorded but these processes may be negligible. By applying steady state conditions, the following rate expression has been derived.

$$R_p = \frac{k_p k_i}{k_t} [S_2O_8^{--}][Ag^+][M] \tag{7}$$

The derived rate expression is in full agreement with our experimental results.

Role of atmospheric oxygen

Molecular O_2, which tends to inhibit the persulphate initiated polymerization of acrylamide,[7] acts as a co-catalyst here and helps to reduce the induction period also.

Dependence of rate on redox components

The initial rate of polymerization and the maximum inversion increases with increase in persulphate concentrations in the range $(2.5 - -2.00) \times 10^{-3}$ mol/L (Fig. 1(a)) at fixed concentration of acrylamide, ascorbic acid an Ag^+ ions. The observed increase is due to the fact that with increasing concentration of $K_2S_2O_8$, more primary radicals are generated (Eq. 1 and 2) which in turn increase the rate. The first order dependence of rate on persulphate concentration has been determined by double logarithmic plot (Fig. 1(b)). The value 0.8 supports the unimolecular termination mechanism.

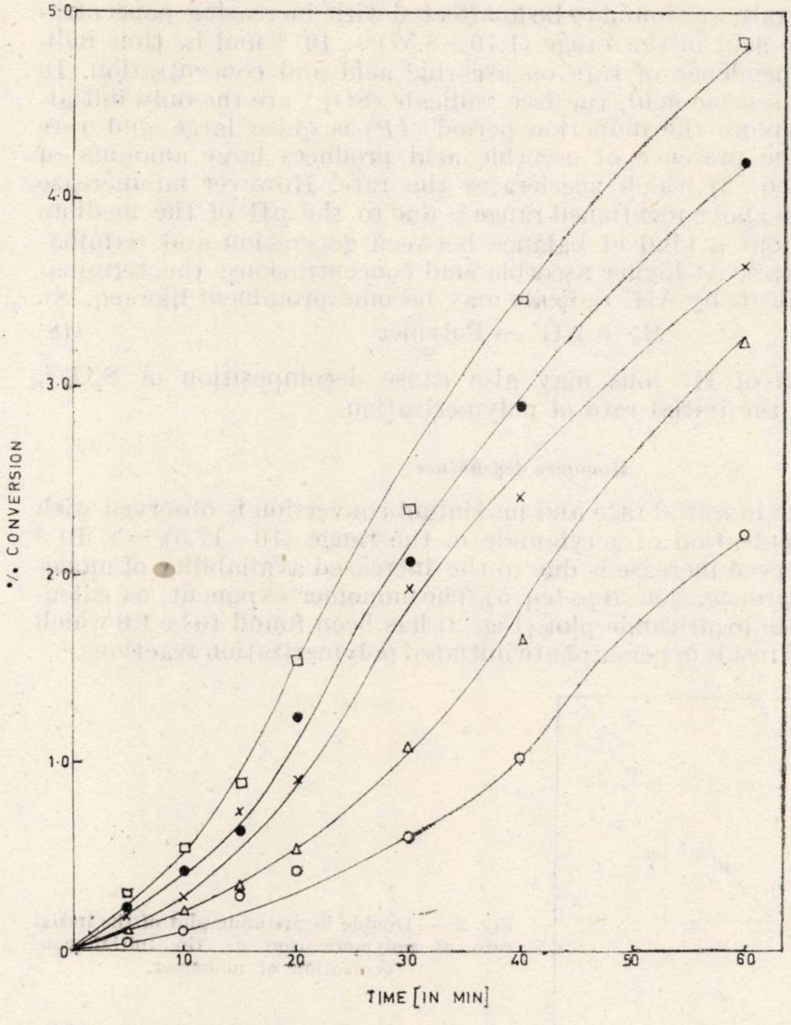

Fig. 1. (a) — Time *vs.* conversion curve for the polymerization of acrylamide with varying concentrations of potassium persulphate at fixed concentration of $AgNO_3 = 2 \times 10^{-3}$ mol/L; Acrylamide $= 10 \times 10^{-2}$ mol/L; Ascorbic acid $= 3.4 \times 10^{-3}$ mol/L; temperature — 35 ± ±0. 2°C. (○) $2.5 \times \times 10^{-3}$, (Δ) 5×10^{-3} (X) 10.0×10^{-3}, (●) 15×10^{-3}, (▭) $20 \times \times 10^{-3}$ mol/L.

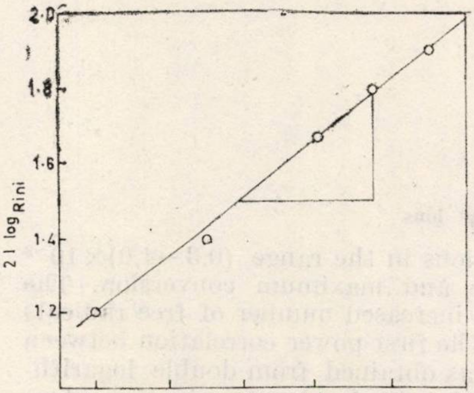

Fig. 1 (b) — Double logarithmic plot of the initial rate of polymerization *vs.* the initial concentration of persulphate.

The initial rate was found to be unaffected with increasing concentrations of ascorbic acid in the range $(1.70-8.57) \times 10^{-3}$ mol/L, thus indicating the independence of rate on ascorbic acid and concentration. In the absence of ascorbic acid, the free radicals (SO_4^-) are the only initiating species, therefore the induction period (*IP*) is quite large and rate is negligible. The presence of ascorbic acid produces large amounts of $AH^\bullet$ radicals (eq. 2) which accelerates the rate. However no increase in the rate in the above mentioned range is due to the pH of the medium which brings about a kind of balance between generation and termination of the radicals. At higher ascorbic acid concentrations, the termination of macroradicals by $AH^\bullet$ radicals may become prominent like (eq. 8).

$$M_n^\bullet + AH^\bullet \rightarrow \text{Polymer} \tag{8}$$

The excess of H^+ ions may also cause decomposition of $S_2O_8^{-2}$, thus decreasing the initial rate of polymerization.

Monomer dependence

An increase in initial rate and maximum conversion is observed with increasing concentration of acrylamide in the range $(10-17.5) = \times 10^{-2}$ mol/L. The observed increase is due to the increased availability of monomer moleculs in propagation steps (eq. 5). The monomer exponent, as calculated from double logarithmic plot (Fig. 2) has been found to be 1.0 which is a well reported result in persulphate initiated polymerization reactions.[3]

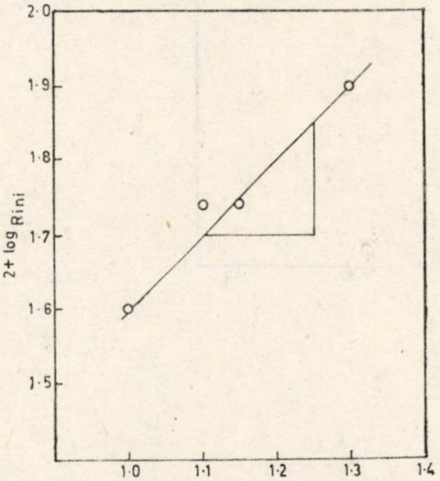

Fig. 2. — Double logarithmic plot of the initial rate of polymerization *vs.* the initial concentration of monomer.

Effect of Ag^+ ions

Increasing concentrations of Ag^+ ions in the range $(0.3-4.0)\times10^{-3}$ mol/L result in increased initial rate and maximum conversion. The observed increase is obviously due to the increased number of free radicals (eq. 1) in free radicall formation step. The first power correlation between the rate and silver ion concentration, as obtained from double logarithmic plot (Fig. 3) cleary supports the idea of unimolecular termination step.

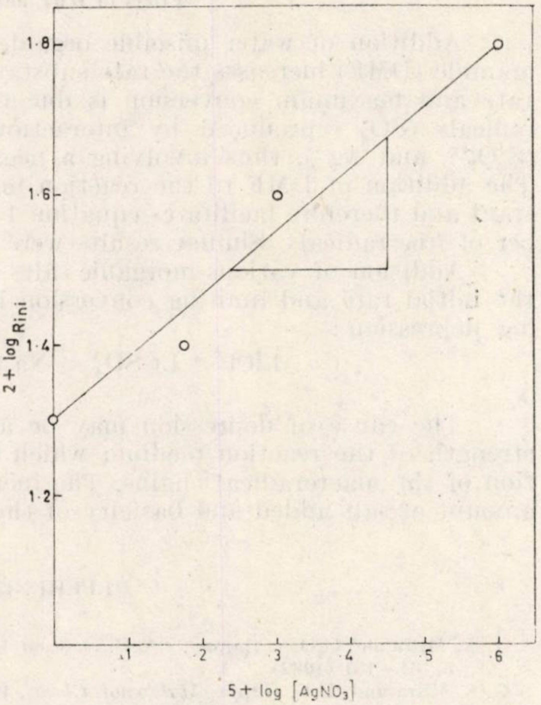

Fig. 3. — Double logarithmic plot of the initial rate of polymerization *vs.* the initial concentration of $AgNO_3$.

Temperature dependence

On increasing the temperature of reaction medium from 29° to 45°C, the formation of free radicals is facilitated and the initial rate and maximum conversion increase. The overall energy of activation has been calculated to be 15.7 kcal/deg. from Arrhenius plot (Fig. 4) which is in agreement with the values obtained by others.[3]

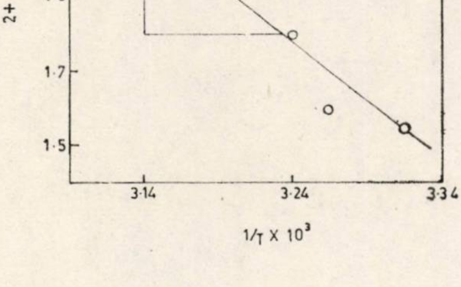

Fig. 4. — Arrhenius plot of the initial rate of polymerization *vs.* reciprocal of absolute temperature (*T*) of reaction medium.

Effect of DMF and salts

Addition of water miscible organic solvent, such as dimethyl formamide (DMF) increases the rate substantially. The observed increase in rate and maximum conversion is due to the increased number of free radicals ($SO_4^{\bullet -}$) produced by interaction of oppositely charged species ($S_2O_8^{-2}$ and Ag^+), thus involving a negative dielectric constant effect.[9] The addition of DMF to the reaction medium lowers the dielectric constant and therefore facilitates equation 1 giving rise to an increased number of free radicals. Similar results were also obtained by Bajpai et al.[10]

Addition of various inorganic salts to the reaction medium depress the initial rate and limiting conversion in the following order of increasing depression :

$$LiCl < Li_2SO_4 < Na_2SO_4 < K_2SO_4$$

The cause of depression may be attributed to the increased ionic strength of the reaction medium which results in a premature termination of the macroradical chains. The increase is also proportional to the amount of salt added and basicity of the salt.

REFERENCES

[1] G. S. Misra and U.D.N. Bajpao, "A Review on Redox Polymerization" *Prog. Polym. Sci.* **8**, 61–131 (1982).
[2] G. S. Misra and C. V. Gupta, *Makromol. Chem.*, **165**, 205 (1973).
[3] H. Narayan, S. M. Jagdale and N. D. Ghate, *J. Polym. Sci., Polym. Chem. Ed.*, **19**, 1225 (1981).
[4] S. Lenka and A. K. Dhal, *J. Polym. Sci., Polym. Chem. Ed.*, **19**, 2115 (1981).
[5] G. M. Khan and I. M. Khalli, *J. Chem. Soc. Pak.*, **3**, 125 (1981).
[6] U. S. Mehrotra and S. P. Mushran, *J. Indian Chem. Soc.*, **47**, 41 (1970).
[7] J. B. Friend and A. E. Alaxander, *J. Polym. Sci.*, A-**16** 1833 (1968).
[8] U.D.N. Bajpai and Anita Ahi, *J. Macromol. Sci. Chem.*, A **23**, 305 (1986).
[9] K. J. Laidler, "Chemical Kinetics", Tata McGraw Hill Pub. Comp., New Delhi, 213(1973).
[10] U.D.N. Bajpai and Anita Ahi, *Rev. Roumaine Chim.*, **29**, 605 (1984).

Revue Roumaine de Chimie, **33**, *6*, 635–637 (1988)

EXO- AND ENDOHORMONES. XIII[1]
SYNTHESIS OF Z-9-PENTACOSENE

LIDIA POP*, H. KREMPELS and F. HODOŞAN
Institute of Chemistry, 3400 Cluj-Napoca, Str. Fîntînele 30
Romania

Received August 2, 1987

The C_{25} chain of the title compound was obtained by a cross-coupling reaction of erucyl bromide with propylmagnesium bromide using Li_2CuCl_4 as catalyst.

Z-9-Pentacosene is the major component of the pheromonal blend released by *Fannya canicularis* (little house fly) females.[2] All the preparation metods described up to now in the literature[3-7] such as electrosyntheses[3,4] (using long chain acids such as oleic, palmitic or stearic-acids along with an adequate short chain acid) or alkylation of jojoba oil,[5] oleic alcohol,[6] docosenol[7] led to olefine mixtures. These contained Z-9-tricosene as major product and Z-9-pentacosene (I) only among various by-products. The separation of these long chain olefines to obtain the pure Z-9-pentacosene (I) was found to be tedious.

In order to avoid these difficulties we elaborated a new synthetic pathways as follows[8]:

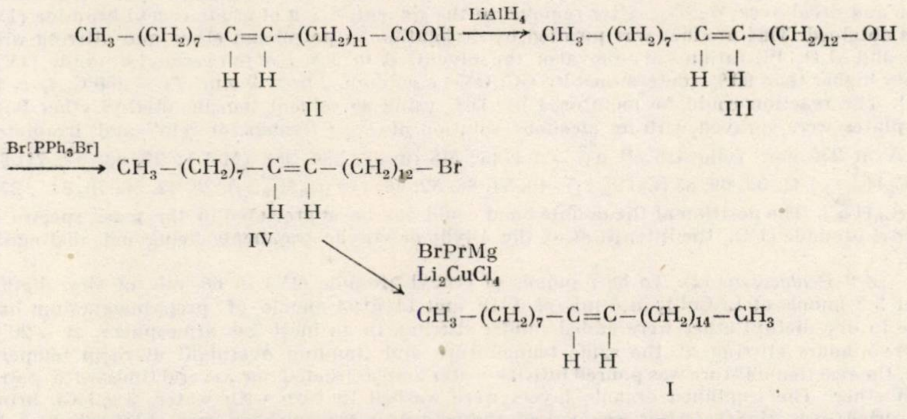

$$CH_3-(CH_2)_7-\underset{H}{C}=\underset{H}{C}-(CH_2)_{11}-COOH \xrightarrow{LiAlH_4} CH_3-(CH_2)_7-\underset{H}{C}=\underset{H}{C}-(CH_2)_{12}-OH$$

II III

$$\xrightarrow{Br[PPh_3Br]} CH_3-(CH_2)_7-\underset{H}{C}=\underset{H}{C}-(CH_2)_{12}-Br$$

IV

$$\xrightarrow[Li_2CuCl_4]{BrPrMg} CH_3-(CH_2)_7-\underset{H}{C}=\underset{H}{C}-(CH_2)_{14}-CH_3$$

I

Erucic acid (II) was obtained by alkaline hydrolysis of rapeseed oil[9] and converted into erucol (III) under the action of $LiAlH_4$.[10] The bromination of III with $[BrPPh_3]Br$ occurred quantitatively and the resulting Z-13-docosene-1-yl bromide (IV) could be utilized in the next step without purification.[11]

According to the method of Schlosser[12] and Fouquet[13] propylmagnesium bromide was coupled with erucyl bromide (IV) in the presence of Li_2CuCl_4 as catalyst.[8,13] The crude reaction product containing 70% Z-9-pentacosene (I) and unreacted erucyl bromide (IV) was purified by conversion of the latter into the water soluble pyridinium salt (overall yield 70% from erucol).

In the purified end product no E isomer could be detected by gaschromatography. The spectral data of the compounds involved in the above figured scheme were all in perfect agreement with the structures ascribed.

EXPERIMENTAL

Gas liquid chromatography was performed with a Perkin Elmer F-11 instrument. The mass spectra were recorded with a Varian MAT 311 spectrometer.

Z-13-docosen-1-ol(erucic alcohol) (*III*). To a stirred suspension of 0.1 mol of $LiAlH_4$ in 100 mL of dry diethyl ether, a solution of 0.1 mol of erucic acid (II) in 100 mL of dry diethyl ether was added dropwise maintaining the mixture at a gentle reflux. The flask was allowed to stand overnight at room temperature and 100 mL of water were added carefully. The aqueous mixture was acidulated with 25% H_2SO_4 and extracted for several times with diethyl ether. The combined organic layers were washed with water and dried over $MgSO_4$. After removal of the solvent, 30—32 g of erucic alcohol (III) were obtained in form of plates melting at 30°C; purity higher than 95% (determined by GC, OV-17 column, 2 m × 2 mm, Ar 10 mL/min., $T_i = 250°C$, $t_r = 13.67$ min). The reaction could be monitored by IR spectrometry observing the disappearance of the $C = O$ vibration at 1710 cm^{-1}; IR (KCl): 3600 (νO-H), 1060 (νC-OH), 3015 sh. (ν = C-H *cis*), 760 cm^{-1} (δ = C-H *cis*).

Z-13-docosene-1-yl-bromide (*erucyl bromide*) (*IV*). The bromination reagent, bromotriphenylphosphonium bromide $Br[Ph_3PBr]$, was prepared introducing a solution of 30 mmols of bromine in 20 mL of dry benzene within 30 min., into a stirred solution of 30 mmols of triphenylphosphine in 70 mL of benzene, at room temperature. Then 25 mmols of erucic alcohol (III) in 15 mL of dry benzene was added dropwise and the reaction mixture stirred for 3 hours at room temperature. After filtration the organic layer was washed in turn with water, brine and dried over $MgSO_4$. After removal of the solvent, 8.7 g of crude erucyl bromide (IV) were obtained. This product was purified by dissolution in petroleum ether and stirring with SiO_2 and Al_2O_3. Filtration and removal of the solvent led to 5.5 g of pure erucyl bromide (IV); purity higher than 90% (determined by GC, OV-17 column, 2 m × 2 mm, $T_i = 250°C$, $t_r = 14$ min]. The reaction could be monitored by TCL using as solvent benzine-diethyl ether 9 :1; the plates were sprayed with an alcoholic solution of 2% "Pynakritol gelb" and irradiated in UV at 250 nm. Yellowish oil $n_D^{20} = 1.4743$; MS (m/e): 386, 388 ($M^{+\bullet}$); 29, 43, 57, 71, 85, 99 ($C_nH_{2n+1}^+$) 41, 55, 69, 83 ($C_nH_{2n-1}^+$); 40, 54, 68, 82, 96, 110 ($C_nH_{2n-2}^{+\bullet}$), 28, 42, 56, 70, 84... 276, 288 ($C_nH_{2n}^{+\bullet}$). The position of the double bond could not be appreciated in the mass spectra of erucoyl bromide (IV), the intensities of the allylic or vinylic fragments being not distinguishable.

Z-9-Pentacosene (I). To 88.7 mmols of erucyl bromide (IV) in 60 mL of dry diethyl ether 3.5 mmols of Li_2CuCl_4 in 6 mL of THF and then 93 mmols of propylmagnesium bromide in dry diethyl ether were added, under stirring, in an inert gas atmosphere, at −20°C. After 5 hours stirring at the same temperature and standing overnight at room temperature, the reaction mixture was poured into ice-water and extracted for several times with petroleum ether. The combined organic layers were washed in turn with water, 5% HCl, brine, and dried over $MgSO_4$. After removal of the solvent a brownish oil was obtained (91.5 g). The crude product containing 15% unreacted erucyl bromide (IV) (determined by GC, OV coloumn, 2 m × 2 mm, $T_i = 250°C$, $t_r = 8{,}6$ min (I), $t_r = 14$ min (IV) was purified by heating on a water bath with 10 mL of pyridine, in order to remove the unreacted halo derivative IV. Finally, the reaction mixture was poured into water, extracted several times with petroleum ether. The combined organic layers were washed successively with water, 10% HCl, brine, and dried over $MgSO_4$. Z-9-Pentacosene (OI) of 94% purity was obtained after the removal of the solvent; yield 70%. IR (film): 760 (ν = C—H *cis*), 3100 (=C—H), 2962 (νCH_3asim.), 2872 (νCH_3sim.), 1450 (νCH_2O). MS showed a molecular peak at m/e 350 and a fragmentation pattern characteristic of monounsaturated hydrocarbons.

REFERENCES

[1] L. Daradics, I. Oprean, F. Hodoşan and N. Serban; Exo- and Endohormones, part XII, *J. Prakt. Chem.*, **329**, 457 (1987).

[2] H. J. Bestmann and O. Vostrowsky, "Chemistry of Insect Pheromones" in R. Wegle "Chemie der Pflanzenschutz und Schädlings bekämpfungsmittel", **6**, Springer Verlag, 1981.

[3] I. I. Krasawtev, *Ukrain. khim. Zhur.*, *46*, 776 (1980).

[4] O. Meresz, Ger. Offen. 2331, 657 (Cl. CO7C, A01n) (in *Chem. Abstr.*, 80, 95221m (1974).

[5] A. Shani, *J. Chem. Ecol.*, **5**,557 (1979); *Israeli*, **52**, 387 (Cl CO7 Cll/02) (1980); Chem. Abstr., **94**, 102797 (1981).

[6] C.M. Hennart and J. Favreau, Ger. Offen. 2 931 876 (Cl CO7C11/02)(1980); Chem. Abstr., **93**, 25 887c (1980).

[7] I. Richter Mangold, *Chem. Phys. Lipids*, **11** (3), 210—14 (1973).

[8] L. Pop, H. Krempels and F. Hodoşan, Rom. Patent 90 326 (1986).

[9] R. C. Noller and R. H. Talbot, "Organic Synthesis", Willers, New York, p. 258, 1943.

[10] L. F. Fieser and M. Fieser, "Reagents for the Organic Synthesis", **1**, 581—95; John Willey and Sons New York, London, Sydney, 1967.

[11] L. Iaenicke, T. Akintoli and F. J. Marner, *Liebigs Ann. Chem.*, **1973**, 1252—1262.

[12] M. Schlosser, "New Synthetic Methods", vol 2, p. 1.

[13] G. Fouquet and M. Schlosser, *Angew. Chem.*, **86**, 50 (1974).

[14] L. Pop, L. Daradics, A. Gocan, N. Serban and F. Hodosan; Rom. Patent 86380 (1983).

[15] L. Pop, I. Oprean, A. Barabas and F. Hodosan, *J. prakt. Chem.*, **328**, 867 (1986).

Revue Roumaine de Chimie, 33, *6*, 639–652 (1988)

IMINE DER AMINOAZOLE. IV[1]
KINETIK UND MECHANISMUS DER HYDROLYSE VON BENZYLIDEN-AMINOAZOLEN

HANS-HORST GLATT, MAMADOU FOULA BARRY, CAROL CSUNDERLIK,
ILSE BACALOGLU und SIMONA TIMOFEI

**Technische Hochschule „Traian Vuia", Laboratorium für organische Chemie,
str. Bocşa 6, 1900 Timişoara, Rumänien**

Eingegangen am 30. März 1987

Die Kinetik der sauren Hydrolyse von Benzyliden-aminoazolen wurde untersucht. Anhand des kinetischen Gesetzes, der Einflüsse der Art der Substituenten, der Lösungsmittelpolarität, sowie der scheinbaren Aktivierungsparameter wird gezeigt, daβ die Hydrolyse über wenigstens drei parallele Prozesse stattfindet. Diese bestehen in einem vorgeschobenen Protonierungsgleichgewicht, gefolgt vom nucleophilen Angriff eines Pufferions oder Wassermoleküls, bzw. in einer konzertierten Protonierung und einem nucleophilen Angriff über einen Vielzentrenübergangszustand.

The kinetics of the acid hydrolysis of benzylidene aminoazoles was studied. The kinetic law, the influences of the nature of substitutents, the solvent polarity, the activation parameters demonstrate that the hydrolysis takes place at least through three parallel processes, which consist in a rapid equilibrium protonation followed by the nucleophilic atack of a buffer ion or a water molecule, respectively, in a concerted protonation and a nucleophilic atack over a multicenter transition state.

Kinetische Studien der Hydrolysereaktionen von Azomethinen,[2-22] die wie bekannt zu Aminen und Aldehyden führen, sowie der Synthesereaktion von Schiffbasen,[6,23-26] ermöglichten die Aufklärung der wichtigsten Schritte des Reaktionsmechanismus dieser Prozesse. Es konnte gezeigt werden, daß die Geschwindigkeit der Hydrolyse erster Ordnung in bezug auf das Benzylidenanilin[2,4,5,16,17] ist, während der umgekehrte Prozess zweiter Ordnung ist.[6,23-26] Die relativ komplexen pH Abhängigkeiten[3,4,16] die Änderung der Gk-ten mit der Pufferkonzentration[2-7,14] bei konstanter Ionenstärke,[4,17] deuten auf das Eingreifen einer allgemeinen Säuren- und Basenkatalyse hin.[7-9,16] Diese Befunde, sowie die Hammett-Korrelationen,[4,5,10,11,17] die scheinbaren Aktivierungsparameter[11] legten den Schluß nahe, daß die Hydrolyse der Azomethine nach einem Additions-Eliminierungsmechanismus stattfindet. Als Zwischenstufe wurde ein Aminoalkohol formuliert, der polarographisch[14,15] sogar erfaßt werden konnte.

In der vorliegenden Arbeit wird die Kinetik der Hydrolyse von Benzyliden-aminoazolen und -benzazolen erstmals beschrieben.

ERGEBNISSE UND DISKUSSION

Reaktionsprodukte. Obzwar die Literaturangaben als Reaktionsprodukte der Hydrolyse von Benzylidenanilinen ausschließlich auf die entsprechenden Benzaldehyde und Amine hinweisen (Gleichung 1), konnten wir im Falle der von uns untersuchten Benzyliden-aminoazolen einen nucleophilen Angriff der Wassermoleküle an das von drei Heteroatomen umgebene Kohlenstoffatom nicht a priori ausschließen (Gleichung 2):

$$(1)\quad Ar\text{-}N{=}CH\text{-}Ar' + HOH \rightleftharpoons Ar\text{-}NH_2 + Ar'\text{-}CHO$$

(2)

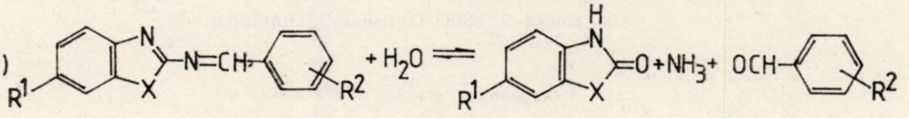

Zwecks Aufklärung der Reaktionsprodukte wurden die Dioxan-Wasser-Lösungen ($[HOH] = 11{,}11$ M/L) der Benzyliden-aminoazole ($X = NH$, $R^1 = H$, $R^2 = p\text{-}NMe_2$; $X = S$, $R^1 = OMe$, $R^2 = p\text{-}NMe_2$; $X = S$, $R^1 = OMe$, $R^2 = p\text{-}NO_2$; $X = O$, $R^1 = H$, $R^2 = p\text{-}NMe_2$) mit Salzsäure angesäuert und zwei Stunden bei 55 — 60° gehalten. Nach dem Aufarbeiten des Reaktionsgemisches konnten in allen Fällen der entsprehende Benzaldehyd und das entsprechende Aminoazol-Chlorhydrat isoliert und durch IR-spektroskopischen Vergleich mit authentischem Material identifiziert werden.

Durch Aufzeichnen von Zeit zu Zeit des ^1H NMR-Spektrums des aus *p*-Dimethylaminobenzyliden-2-aminobenzimidazol und DMSO-d_6-CF_3COOH ($[CF_3COOH] = 0{,}4$ M/L; $[HOH] = 1 - 2\ \%$) gebildeten Reaktionsgemisches bei 25°, konnte eine kontinuierliche Änderung der Spektren von jenem des heterocyclischen Imins (zum Zeitpunkt Null, beim Einführen der Trifluoressigsäure bis zu jenem eines äquimolaren Gemisches von *p*-Dimethylaminobenzaldehyd und protoniertem 2-Aminobenzimidazol (nach cca 50 — 60 Min.) festgestellt werden. Alle Zwischenspektren deuten auf das Vorhandensein ausschließlich des Imins, des Aldehyds und des Amins hin, ohne daß Banden eines Zwischenproduktes oder anderer Hydrolyseprodukte identifiziert werden konnten.

Kinetische Messungen. Bestimmung der Gk-ten. Interpretation. Unsere präparativen Versuche[27,28] hatten gezeigt, daß in den UV-Spektren der Benzyliden-aminoazole eine Absorptionsbande über 300 nm, deren molarer Extinktionskoeffizient im 15000 — 40000 1/M. cm-Bereich liegt, erscheint. Die Hydrolyseprodukte dieser Imine jedoch weisen um 50—70 nm hypsochrom verschobene UV-Absorptionen auf. Die entsprechenden molaren Extinktionskoeffizienten sind kleiner (10000—14000 für die Benzaldehyde und bzw 5000—8000 fürdie Aminoazole). Unter diesen Bedingungen, ließ sich der zeitliche Verlauf der Hydrolyse heterocyclischer Imine anhand der Extinktionsänderung ihrer Absorptionsbande verfolgen. Aus der Extinktion-Zeitabhängigkeit wurden mit einem einfachen monomolekularen Rechenmodell Gk-ten erster Ordnung errechnet.

Da unsere Vorversuche zeigten, daß die Hydrolysegeschwindigkeit stark vom pH abhängt, wurden die kinetischen Versuche bei pH-Werten von 4,5 — 5,0 in der Gegenwart eines Puffers (saures Kaliumphthalat/HCl) ausgeführt. Die für die Hydrolyse des *p*-Dimethyl-aminobenzyliden-2-amino-5(6)-nitrobenzimidazols bestimmten Gk-ten erster Ordnung sind beispielsweise in Tabelle 1 eingetragen. Aus diesen Daten ist es leicht ersichtlich, daß die Gk-ten sowohl von der Pufferkonzentration, als auch vom pH-Wert des Reaktionsmediums beeinflußt werden, und somit erweist sich diese Hydrolyse als eine typische allgemeine Säurenkatalyse. Die Abhängigkeit der Gk-ten von der Pufferkonzentration ist linear und von folgenden Gleichungen :

Tabelle 1

Gk-ten der Hydrolyse des *p*-Dimethylaminobenzyliden-2-amino-5(6)-nitrobenzimidazols in Dioxan-Wasser ([HOH] = 11,11 M/L) bei 50° bei verschiedenen pH-Werten und Phthalatkonzentrationen

pH	[Puffer] (M/L)	$k_{exp} \cdot 10^4$ (s^{-1})	$k_2^0 \cdot 10^2$ (1/M·s)	$k_1^0 \cdot 10^4$ (s^{-1})	k_3 ($1^2/M^2$ s)	k_2^P (1/M·s)	k_2^H (1/M·s)
5,00	0,01	4,172	1,287	3,002	272,6	0,01023	14,28
	0,02	5,180					
	0,03	6,746					
4,75	0,01	5,620	1,520	4,311			
	0,02	7,770					
	0,03	8,659					
4,50	0,01	7,880	1,880	6,123			
	0,02	10,13					
	0,03	11,64					

$$pH = 5{,}00\,;\; k_{exp} = 1{,}287 \cdot 10^{-2} \cdot [\text{Puffer}] + 3{,}002 \cdot 10^{-4} \quad (r = 0{,}989)$$

$$pH = 4{,}75\,;\; k_{exp} = 1{,}520 \cdot 10^{-2} \cdot [\text{Puffer}] + 4{,}311 \cdot 10^{-4} \quad (r = 0{,}972)$$

$$pH = 4{,}50\,;\; k_{exp} = 1{,}880 \cdot 10^{-2} \cdot [\text{Puffer}] + 6{,}123 \cdot 10^{-4} \quad (r = 0{,}994)$$

Sowohl die Neigung (k_2^0) als auch der Ordinatenschnitt (k_1^0) dieser Geraden hängt linear von der Hydroniumionenkonzentration ab :

$$k_2^0 = 2{,}726 \cdot 10^2 \cdot [H_3O^+] + 1{,}023 \cdot 10^{-2} \quad (r = 0{,}999)$$

$$k_1^0 = 14{,}28 \cdot [H_3O^+] + 1{,}65\ 10^{-2} \quad (r = 0{,}998)$$

Der Koordinatenschnitt der letzteren Gleichung ist relativ klein. Da sein Wert nicht mehr als 8—10% der Gk-te erster Ordnung (k_{exp}) ausmacht, kann er vernachlässigt werden.

Wie aus dem obigen Beispiel folgt, ist der Ausdruck des kinetischen Gesetzes dieser Hydrolyse eine Funktion der Puffer-sowie der Hydroniumionenkonzentration :

$$(3) \qquad k_{\text{exp}} = k_3 \cdot [\text{Puffer}] \cdot [\text{H}_3\text{O}^+] + k_2^{\text{P}} \cdot [\text{Puffer}] + k_2^{\text{H}}[\text{H}_3\text{O}^+]$$

Offensichtlich findet die Hydrolyse der Benzyliden-aminoazole durch wenigstens drei parallele Reaktionen statt, die jeweils durch die Gk-ten k_3, k_2^{P} und k_2^{H} charakterisiert werden können. Da die Anzahl der experimentellen Gk-ten pseudoerster Ordnung sehr groß ist, werden im Folgenden nur die Gk-ten dieser drei Reaktionen tabelliert.

In Tabelle 2 sind die für die Hydrolyse von verschieden substituierten Benzyliden-aminoazolen bei 50° in Dioxan-Wasser ([HOH] = 11,11 M/L) bestimmten Gk-ten zweiter und dritter Ordnung enthalten. Aus diesen Daten ist es leicht ersichtlich, daß die Geschwindigkeit der drei-

Tabelle 2

Gk-ten zweiter und dritter Ordnung der Hydrolysereaktion von verschiedenen heterocyclischen Iminen, bei 50° in Dioxan-Wasser ([HOH] = 11,11 M/L)

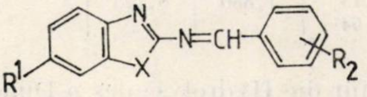

Nr.	X	R^1	R^2	$k_3 \cdot 10^{-3}$ ($1^2/M^2s$)	$k_2^{\text{P}} \cdot 10^2$ ($1/M \cdot s$)	$k_2^{\text{H}} \cdot 10^{-1}$ ($1/M \cdot s$)
1	NH	H	p-NMe$_2$	0,9268	2,125	2,679
2	NH	H	p-OMe	3,108	3,077	6,262
3	NH	H	p-Cl	3,861	2,251	2,786
4	NH	H	m-NO$_2$	5,590	4,967	1,608
5	NH	H	p-NO$_2$	7,649		1,528
6	NH	Me	p-NMe$_2$	1,103	0,5900	0,8877
7	NH	Cl	p-NMe$_2$	0,6167	0,9560	1,944
8	NH	NO$_2$	p-NMe$_2$	0,2726	1,023	1,428
9	O	H	p-NMe$_2$	0,3887	0,9300	0,7490
10	S	OMe	p-NMe$_2$	0,4254	0,6440	1,267
11	S	OMe	p-OMe	1,660	1,228	3,235
12	S	OMe	p-Cl	1,041	0,443	1,974
13	S	OMe	m-NO$_2$	0,4028	0,469	0,647
14	S	OMe	p-NO$_2$	0,6581	0,123	0.911

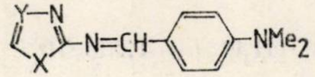

Nr.	X	Y	$k_3 \cdot 10^{-3}$ ($1^2/M^2s$)	$k_2^{\text{P}} \cdot 10^4$ ($1/M \cdot s$)	$k_2^{\text{H}} \cdot 10^{-1}$ ($1/M \cdot s$)
15	NH	N	3,574	3,390	2,723
16	S	CH	1,025	6,980	0,704

parallelen Hydrolysereaktionen in bedeutendem Maße von der Art der Substituenten am Benzylidenkern und von der Art des heterocyclischen Systems und seiner Substituenten beeinflußt wird.

Die Hammett-Darstellung der für den sowohl von Hydronium-ionen als auch vom Puffer katalysierten Hydrolyseprozess der im Benzylidenkern und bzw. im Benzimidazolkern substituierten Imine, bestimmten Gk-ten, sind linear und von folgenden Gleichungen:

— Substituenten am Benzylidenkern ($X = NH$, $R^1 = H$):

(4) $$\lg k_3 = 0{,}51 \cdot \sigma + 3{,}46 \quad (\mathit{1} - \mathit{5};\ \text{Tab. } 2)$$

— Substituenten am Benzimidazolkern ($X = NH$, $R^2 = p\text{-}NMe_2$):

(5) $$\lg k_3 = -\,0{,}65 \cdot \sigma + 2{,}95 \quad (\mathit{1},\ \mathit{6} - \mathit{8};\ \text{Tab. } 2)$$

Das verschiedene Zeichen des ρ-Parameters aus den obigen Gleichungen deutet auf das Vorhandensein von zwei aufeinanderfolgenden Reaktionen hin, in welchen der Einfluß der Substituenten entgegengesetzt wirkt. Da es sich in diesem Fall um einen von Hydroniumionen und Pufferionen katalysierten Prozess handelt, kann man voraussetzen daß der erste Schritt im raschen Protonieren des heterocyclischen Imins in einem vorgeschobenen Gleichgewicht besteht und das zur Bildung eines durch Mesomerie stabilisierten Guanidiniumkations führt:

(6)

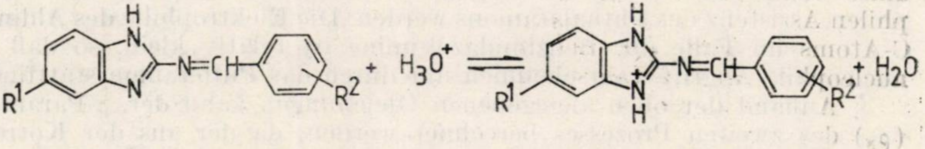

In diesem ersten Schritt spielt das Imin die Rolle des Nucleophils. Der basische Charakter der Benzyliden-aminoazole wurde schon früher[1] anhand folgender Korrelierungen bewiesen:

— Substituenten am Benzylidenkern ($X = NH$, $R^1 = H$):

(7) $$pK_a = -\,0{,}78 \cdot \sigma_{R^2} + 5{,}99$$

— Substituenten am Benzimidazolkern ($X = NH$, $R^2 = p\text{-}NMe_2$):

(8) $$pK_a = -\,0{,}71 \cdot \sigma_{R^1} + 6{,}57$$

Im zweiten Schritt muß dem Imin die Rolle des Elektrophils zukommen, da nur so ein positiver Wert des ρ-Parameters (0,51 Gleichung 4) verständlich wird. In diesem Schritt kann der langsame nucleophile Angriff entweder des Phthalatanions oder eines mit einem solchen Anion assozierten Wassermoleküls stattfinden :

(9)

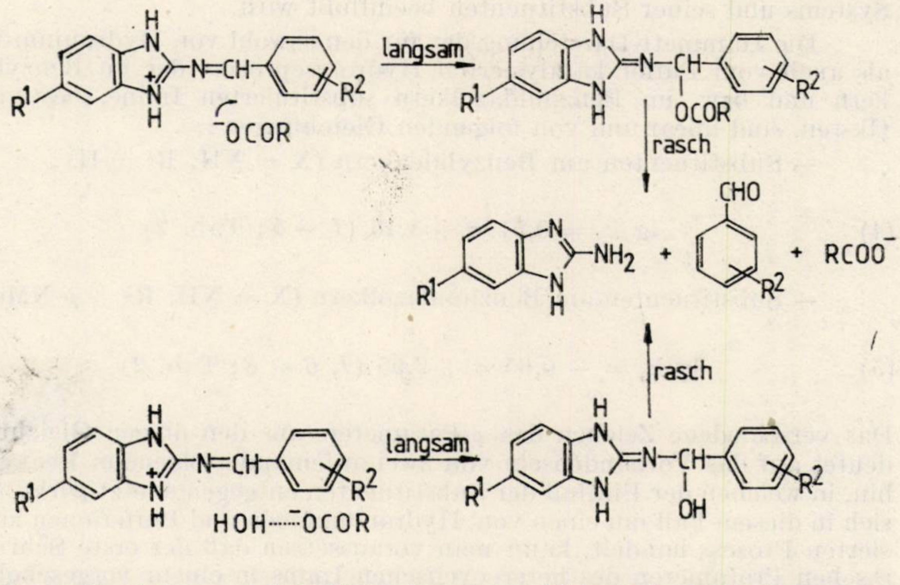

(in diesen Reaktionen ist $RCOO^-$ das saure Phthalatanion). Zwar kann zwischen diesen zwei Varianten kinetisch nicht unterschieden werden, doch ist es offensichtlich, daß je elektrophiler das Aldimin-C-Atom ist, umso bedeutender kann der Angriff des Wassermoleküls in der nucleophilen Assistenz des Phthalatanions werden. Die Elektrophilie des Aldimin-C-Atoms im Falle der Benzimidazol-imine ist relativ klein, so daß der nucleophile Angriff wahrscheinlich nur durch das Pufferanion stattfindet.

Anhand der oben angegebenen Gleichungen kann der ρ-Parameter (ρ_N) des zweiten Prozesses berechnet werden, da der aus der Korrelierung der Gk-ten erhaltene ρ-Parameter (Gleichung 4, 5) die Summe des Parameters des pK_a -Korrelierung und jenes des zweiten nucleophilen Prozesses darstellt :

— Substituenten am Benzylidenkern, $\rho_N = 1{,}39$;

— Substituenten am Benzimidazolkern, $\rho_N = 0{,}06$.

So wie es zum Erwartern war, haben die Substituenten am Benzylidenkern einen bedeuteren Einfluß auf die Geschwindigkeit des zweiten Schrittes als jene am Benzimidazolkern. Im letzteren Fall, beeinflussen die Substituenten den Prozess nur durch die von ihnen bewirkte Änderung der Basizität des Substrats.

Zu den gleichen Schlüssen führen auch die Bronsted-Korrelationen :

— Substituenten am Benzylidenkern ($X = NH$, $R^1 = H$) :

(10) $$\lg k_3 = -\,0{,}69 \cdot pK_a + 7{,}56 \qquad (1\text{—}5\,;\ \text{Tab. } 2)$$

— Substituenten am Benzimidazolkern ($X = NH$, $R^2 = p\text{-}NMe_2$) :

(11) $$\lg k_3 = 0{,}85 \cdot pK_a - 2{,}67 \qquad (1,\ 6\text{—}8\,;\ \text{Tab. } 2).$$

In Falle der Hydrolyse der am Benzylidenkern substituierten Benzyliden-2-amino-6-methoxybenzothiazole wurden folgende Hammett-Korrelierungen festgelegt ($X=S$, $R^1 = OMe$):
— elektronenspendende Substituenten:

(12) $\lg k_3 = 0{,}94 \cdot \sigma_{R^2} + 3{,}74$ (*10, 11*; Tab. 2)

— elektronenanziehende Substituenten:

(13) $\lg k_3 = -0{,}50 \cdot \sigma_{R^2} + 3{,}00$ (*12–14*; Tab. 2)

Die pK_a — Substituentenkonstanten Korrelierung ergab für diese Verbindungen folgende Gleichung[1]:

(14) $$pK = -0{,}79 \cdot \sigma + 3{,}34.$$

Aus den Gleichungen 12, 13, 14 folgt:
— für elektronenspendende Substituenten $\rho_N = 1{,}73$
— für elektronenanziehende Substituenten $\rho_N = 0{,}29$.
Es ist also auch in diesem Falle von einem Prozess die Rede, in welchem dem Imin die Rolle des Elektrophils zukommt, wobei jedoch der Einfluß der Substituenten am Benzylidenkern weniger wichtig ist. Da die Hydrolyse auch im Falle des *p*-Nitrobenzyliden-2-amino-6-methoxybenzothiazols zum entsprechenden Amin und Benzaldehyd führt, wie die Hydrolyse des *p*-Dimethylaminobenzyliden-2-amino-6-methoxybenzothiazols, sind wir gezwungen anzunehmen, daß sich im Falle der Hydrolyse der Imine des Methoxybenzothiazols beim Übergang von elektronenspendenden zu elektronenanziehenden Substituenten am Benzylidenkern der Reaktionsmechanismus ändert. Es ist offensichtlich, daß der elektrophile Charakter des Aldimin-C-Atoms im Falle der Thiazole mit elektronenanziehenden Substituenten im Benzylidenkern bedeutender sein muß als im Falle der entsprechenden Imidazolderivate. Es kann so angenommen werden, daß die Mechanismusänderung im nucleophilen Angriff des Wassers in der Assistenz des Carboxylations besteht, zum Unterschied von der vorhergehenden Situation als der Mechanismus in der nucleophilen Katalyse des Carboxylations bestand.

Die Korrelierung der im Falle der *p*-Dimethylaminobenzyliden-2--aminobenzazole vermessenen Hydrolyse Gk-ten mit den entsprechenden Basizitätskonstanten, führt zu folgender Gleichung:

(15) $\lg k_3 = 0{,}12 \cdot pK_a + 2{,}16$ (*1, 9, 10*; Tab. 2)

Dies beweist erneut, daß die mit der *p*-NMe_2-Gruppe im Benzylidenkern substituierten Imine der Benzazole nach dem gleichen Mechanismus hydrolysieren.

Die Reaktivität des Thiazol- (*16*, Tab. 2) und Triazolderivates (*15*, Tab.2) ist bedeutend größer als es anhand ihrer Basizität[1] zum Erwarten wäre. Da auch in diesen Fällen das kinetische Gesetzt das selbe ist wie zuvor, erscheint es uns glaubhaft diese Reaktivität durch sterische Effekte zu erklären.

Ebenfalls aus Tabelle 2 ist es zu Entnehmen, daß der ausschließlich im Eingreifen des Pufferions bestehende Prozess (durch die Gk-ten k_2^P charakterisiert), mit steigender Geschwindigkeit in Falle der Benzimidazole mit elektronenanziehenden Substituenten, bzw. mit fallender Geschwindigkeit im Falle der Benzothiazole mit der selben Art von Substituenten stattfindet. Diese entgegengesetzte Änderung der Hydrolysegeschwindigkeit kann im Sinne der schon angegebenen Mechanismen verstanden werden, wenn man annimmt, daß dem Pufferion weiterhin die Rolle des Nucleophils zukommt, während das Wassermolekül als Elektrophil fungiert. In diesem Falle findet der Protonenübergang von einem Wassermolekül zum Imin mehr oder weniger gleichzeitig mit dem nucleophilen Angriff des Carboxylations statt :

(16)

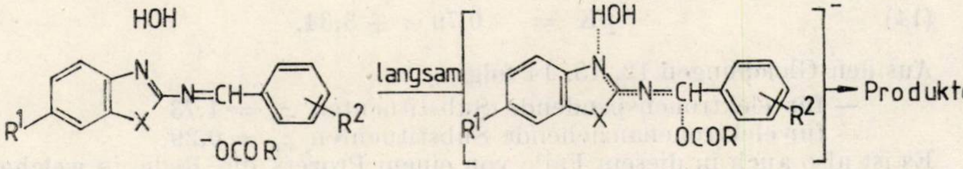

So eine Reaktion kann vorwiegend elektrophil (Benzimidazole) oder nucleophil (Benzothiazole) stattfinden, wobei dies von der relativen Geschwindigkeit der beiden Prozesse abhängt.

Die Hammett-Darstellungen der Gk-ten zweiter Ordnung, die den ausschließlich durch Hydroniumionen katalysierten Prozess charakterisiren (k_2^H), führen zu folgenden Gleichungen :

— im Benzylidenkern substituierte Benzimidazole ($X = NH$, $R^1 = H$) :

(17) $\lg k_2^H = -0{,}58\,\sigma + 1{,}62$, woraus $\rho_N = 0{,}21$; (*2–5* ; Tab. 2)

— Substituenten im Benzimidazolkern ($X = NH$, $R^2 = p\text{-}NMe_2$) :

(18) $\lg k_2^H = -0{,}40\,\sigma + 1{,}41$; $\rho_N = 0{,}19$; (*6–8* ; Tab. 2)

— im Benzylidenkern substituierte Benzothiazole ($X = S$, $R^1 = OMe$) :

(19) $\lg k_2^H = -0{,}63\,\sigma + 1{,}37$; $\rho_N = 0{,}19$; (*11–14* ; Tab. 2)

In allen drei untersuchten Fällen ist der ρ-Parameter negativ. Dieser Befund ist mit einem Mechanismus im Einklang, der aus einer raschen Protonierung gefolgt vom langsamen nucleophilen Angriff eines Wassermoleküls besteht :

(20)

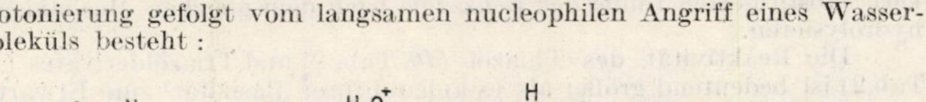

Die ρ_N-Werte sind von derselben Größenordnung wie jene im Falle des nucleophilen Angriffs des sauren Phthalations und sind mit dem vorgeschlagenen Reaktionsmechanismus in gutem Einklang. Es ist uns unverständlich weshalb die Dimethylaminogruppe und bzw die Methoxygruppe die Hydrolyse verzögert und nicht beschleunigt. Eine Mechanismusänderung ist nichtauszuschließen, kann jedoch anhand unserer wenigen Daten auch nicht bewiesen werden.

Tabelle 3

Gk-ten zweiter und dritter Ordnung der Hydrolyse einiger *p*-Dimethylamino benzyliden-2-aminobenzazole, bei 50° in Dioxan-Wasser verschiedener Konzentration

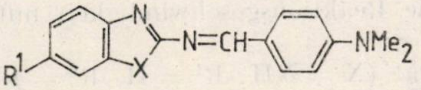

X	R¹	[HOH] (M/L)	E_T	$k_3 \cdot 10^{-2}$ ($1^2/M^2s$)	$k_2^P \cdot 10^2$ ($1/M \cdot s$)	$k_2^H \cdot 10^{-1}$ ($1/M \cdot s$)
NH	H	5,55	46,7	9,319[a]	1,197	1,651
		11,11	49,0	9,268	2,125	2,679
		22,22	52,3	8,943	3,411	6,912
O	H	5,55	46,7	0,5649	0,2410	0,348
		11,11	49,0	3,887	0,9300	0.749
		22,22	52,3	9,945	2,247	—
S	OMe	5,55	46,7	2,874	0,316	—
		11,11	49,0	4,254	0,644	1,267
		22,22	52,3	16,93	1,567	5.473

[a] der Mittelwert der drei Konstanten betragt 917.7.

In Tabelle 3 sind die bei verschiedenen Wasserkonzentrationen in Dioxan, bei 50 ° bestimmten GK-ten zweiter und dritter Ordnung der Hydrolyse einiger *p*-Dimethylaminobenzyliden-aminoazole enthalten.

Im Falle des sowohl von den Hydroniumionen als auch den Pufferionen katalysierten Prozesses (k_3) ist die Geschwindigkeit der Hydrolyse des Imidazolderivates unabhängig von der Wasserkonzentration während jene der Hydrolyse des Thiazol- und bzw Oxazolderivates mit steigender Wasserkonzentration anwächst :

— *p*-Dimethylaminobenzyliden-2-aminobenzoxazol ($X = O$, $R^1 = H$, $R^2 = p{-}NMe_2$) :

(21)
$$\lg k_3 = 2{,}07 \cdot \lg\ [HOH] + 0{,}28$$
$$\lg k_3 = 0{,}22 \cdot E_T - 8{,}19$$

— *p*-Dimethylaminobenzyliden-2-amino-6-methoxybenzothiazol ($X = S$, $R^1 = OMe$, $R^2 = p\text{-}NMe_2$) :

(22)
$$\lg k_3 = 1{,}28 \cdot \lg[HOH] + 1{,}43$$
$$\lg k_3 = 0{,}14 \cdot E_T - 4{,}16$$

Dieser Hydrolyseprozess besteht aus zwei nacheinanderfolgenden Schritten, von welchen der erste eine Protonierung ist und demzufolge von dem Anstieg der Lösungsmittelpolarität begünstigt werden muß, und der zweite als Reaktion zweier Ionen von dieser begünstigt wird. Im Falle des Imidazolderivates, dessen Basizität höher als der beiden anderen Derivate ist, läßt sich eine Kompensation dieser Effekte bemerken. Im Falle des Thiaz- und Oxazolderivates, die weniger basisch sind, ist der Lösungsmitteleinfluß auf den Protonierungsschritt ausschlaggebend.

Im Falle des ausschließlich von den Pufferionen katalysierten Prozesses (k_2^P) steigt die Reaktionsgeschwindigkeit mit der Lösungsmittelpolarität leicht an :

— Benzimidazolderivat ($X = NH$, $R^1 = H$, $R^2 = p\text{-}NMe_2$) :

$$\lg k_2^P = 0{,}75 \lg[HOH] - 2{,}48 \qquad (23)$$

$$\lg k_2^P = 0{,}08\, E_T - 5{,}63$$

— Benzothiazolderivat ($X = S$, $R^1 = OMe$, $R^2 = p\text{-}NMe_2$) :

$$\lg k_2^P = 1{,}15 \lg[HOH] - 3{,}37 \qquad (24)$$

$$\lg k_2^P = 0{,}12\, E_T - 8{,}27$$

— Benzoxazolderivat ($X = O$, $R^1 = H$, $R^2 = p\text{-}NMe_2$) :

$$\lg k_2^P = 1{,}61 \lg[HOH] - 3{,}78 \qquad (25)$$

$$\lg k_2^P = 0{,}17\, E_T - 10{,}45$$

Aus diesen Abhängigkeiten folgt, daß der Übergangszustand polarer als der Ausgangszustand ist. Wenn man jedoch den anhand der elektronischen Effekte bewiesenen Vielzentrenübergangszustand (Gleichung 16) akzeptiert, so ist man gezwungen anzunehmen, daß die Protonenübertragung und der nucleophile Angriff des Phthalations nicht streng gleichzeitig stattfinden, denn im Falle eines streng gleichzeitigen Angriffs sollte die erhöhte Lösungsmittelpolarität diese Reaktion beungünstigen. Es scheint so daß die Protonenübertragung und Kationenbildung etwas rascher verläuft als der Angriff des Anions. Eigentlich, so wie es aus den Literaturdaten hervorgeht,[10] findet selbst im basischen Medium vorerst eine Protonierung der Benzylidenaniline durch ein Wassermolekül statt, und danach der nucleophile Angriff des Hydroxydions.

Der ausschließlich durch Hydroniumionen katalysierte Prozess (k_2), der in einem raschen Protonierungsgleichgewicht, gefolgt vom nucleophilen Angriff eines Wassermoleküls besteht, wird in allen untersuchten Fällen von der steigenden Lösungsmittelpolarität begünstigt, so wie es aus folgenden Korrelationen hervorgeht :

— Benzimidazolderivat ($X = NH$, $R^1 = H$, $R^2 = p\text{-}NMe_2$) :

$$\lg k_2^H = 1{,}03 \lg[HOH] + 0{,}96 \qquad (26)$$

$$\lg k_2^H = 0{,}11\, E_T - 4{,}03$$

— Benzothiazolderivat ($X = S$, $R^1 = OMe$, $R^2 = p\text{-}NMe_2$):

$$\text{(27)} \qquad \lg k_2^{\mathrm{H}} = 2{,}11 \lg[\mathrm{HOH}] - 1{,}10$$

$$\lg k_2^{\mathrm{H}} = 0{,}19\ E_T - 8{,}33$$

— Benzoxazolderivat ($X = O$, $R^1 = H$, $R^2 = p\text{-}NMe_2$):

$$\text{(28)} \qquad \lg k_2^{\mathrm{H}} = 1{,}10 \lg[\mathrm{HOH}] - 0{,}28$$

$$\lg k_2^{\mathrm{H}} = 0{,}14\ E_T - 6{,}22$$

Der Anstieg der Lösungsmittelpolarität begünstigt zweifelsohne die Protonierung des heterocyclischen Systems, das ja eine relativ schwache Base[1] ist.

In Tabelle 4 sind die bei verschiedenen Temperaturen in Dioxan-Wasser ($[\mathrm{HOH}]) = 11{,}11$ M/L) bestimmten Gk-ten zweiter und dritter Ordnung, sowie die scheinbaren Aktivierungsparameter, für die Hydrolyse der *p*-Dimethylaminobenzyliden-2-aminobenzazole enthalten

Tabelle 4

Gk-ten zweiter und dritter Ordnung, sowie scheinbare Aktivierungsparameter der Hydrolyse von *p*-Dimethylaminobenzyliden-2-aminobenzazolen in Dioxan-Wasser ([HOH] = 11,11 M/L).

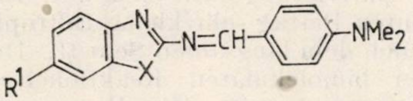

X	R¹	T (°C)	$k_3 \cdot 10^{-2}$ (l^2/M^2s)	$k_2^{\mathrm{P}} \cdot 10^3$ (1/M·s)	k_2^{H} (1/M·s)
NH	H	30	2,660	6,367	8,360
		40	6,103	8,331	16,87
		50	9,268	21,25	26,79
		$\Delta H^{\#}$ (kJ/M)	48,1	46,0	44,8
		$\Delta S^{\#}$ (J/M·K)	−29,7	−127,2	−70,3
O	*H*	30	1,559	1,269	1,585
		40	1,996	1,693	3,248
		50	3,887	9,304	7,492
		$\Delta H^{\#}$ (kJ/M)	34,4	77,7	60,9
		$\Delta S^{\#}$ (J/M·K)	−81,5	−36,9	−32,9
S	OMe	30	2,550	1,284	3,234
		40	3,291	2,600	10,36
		50	4,254	6,437	13,14
		$\Delta H^{\#}$ (kJ/M)	18,3	62,8	54,8
		$\Delta S^{\#}$ (J/M·K)	−130,2	−84,5	−44,4

Die Aktivierungsparameter des sowohl von Hydroniumionen als auch von Pufferionen katalysierten Prozesses (k_3) stellen Summen der dem Protonierungsgleichgewicht und dem nucleophilen Angriff entsprechenden Parameter dar. Die Protonierungsentropie ist im absoluten Betrag bekanntlich sehr klein, praktisch Null. Aus diesem Grund entspricht der experimentelle Wert der Entropie des langsamen Schrittes. Die Werte von −80 bis −130 J/M.K sind für einen bimolekularen Prozess charakteristisch. Der etwas größere Betrag im Falle des Imidazolderivates (−30 J/M.K) liegt im Grenzgebiet der bi- und monomolekularen Reaktionen. Wir können aber in diesem Falle einen größeren Fehler in der Bestimmung dieses Parameters nicht ausschließen. Die relativ kleine scheibare Aktivierungsenthalpie entspricht den bimolekularen Prozessen, und kommt durch teilweise Kompensierung der Aktivierungsenthalpie des langsamen Schrittes durch die relativ hohe, negative Enthalpie des Protonierungsschrittes zustande.

Dem exklusiv durch die Pufferionen katalysierten Prozess (k_2^{P}) entsprechen sehr negative Werte der scheinbaren Aktivierungsentropie, was mit einem mehr oder weniger konzertierten Übergangszustand in gutem Einklang ist. Die Aktivierungsenthalpie ist im allgemeinen größer als jene im doppelt katalysierten Prozes, was zum Erwarten ist, wenn man bedenkt, daß obzwar in diesem Fall der Protonenübergang dem nucleophilen Angriff vorangeht, doch im Augenblick dieses Angriffs noch nicht gänzlich stattgefunden hat.

Der ausschließlich durch Hydoniumionen katalysierte Prozess (k_2^{H}) weist etwas kleinere Aktivierungsentropien auf. Da der Protonierungsprozess eine im absoluten Betrag sehr kleine Entropie hat, entspricht der gemessene Wert gänzlich dem langsamen Schritt. Der Wert von −30 bis −70 J/M.K ist den bimolekularen Reaktionen charakteristisch, der zweifelsohne im langsamen Angriff eines Wassermoleküls an das durch Protonierung gebildete Kation besteht. Die Aktivierungsenthalpien entsprechen im allgemeinen mit jenen von Hydrolysen in saurer Katalyse die bekannlich[11] relativ kleine Werte aufweisen.

Die Hydrolyse der Benzyliden-aminoazole ist also ein Prozess, in dem die Protonierung des heterocyclischen Systems wesentlich ist. Man kann behapten, daß der nucleophile Angriff ohne eine vorangehende oder mit diesem Angriff fast gleichzeitige Protonierung nicht stattfinden kann. Aus diesem Grund erscheint in saurem Medium eine bedeutende Katalyse durch Hydroniumionen sowie durch Wasser. Die sich im System befindendden Anione, sowie die Wassermoleküle stellen nucleophile Agentien dar, mit welchen im langsamen Schritt die Hydrolyse beginnt. Die Carboxylatione spielen die Rolle der nucleophilen Katalysatoren. Unter diesen Bedingungen, findet die Hydrolyse der Benzyliden-aminoazole höchstwahrscheinlich durch mehrere parallele Reaktionen statt, die in der Protonierung des Substrats gefolgt vom nucleophilen Angriff des Carboxylations oder eines Wassermoleküls, bzw in einem konzertierten Protonenübergang und nucleophilen Angriff des Carboxylations bestehen. Der Prozess, der in der Protonenübertragung von einem Wass ermolekül zum Imin und dem langsamen nucleophilen Angriff eines anderen Wassermoleküls besteht, findet zu langsam statt, um in unseren experimentellen Bedingungen verfolgt werden zu können.

BESCHREIBUNG DER VERSUCHE

Die IR-spektroskopischen Messungen wurden mit einem SPECORD IR 75 (Carl Zeiss Jena) ausgeführt. Die ^{1}H-NMR-Spektren wurden mit einem TESLA BS 487 C (80 MHz) aufgezeichnet. Die UV-spektroskopischen Untersuchungen wurden mit einen CARY 17 D (Varian) unternommen. Substanzen, Lösungsmittel. Die heterocyclischen Imine wurden nach einer schon früher beschriebenen Methode hergestellt.[27,28] Das saure Kaliumphthalat (Reactivul) war von p.a. Reinheitsgrad und wurde als solches verwendet. Das Dioxan wurde aus Diethylenglykol hergestellt, mit NaOH gereinigt, 10 Std über Na getrocknet und anschließend abdestilliert.

Isolierung der Reaktionsprodukte. Es werden 1 g *p*-Dimethylaminobenzyliden-2-aminobenzazol in 50 mL Dioxan-Wasser ([HOH] = 11,11 M/L) gelöst, mit 0,5 mL konz. HCl behandelt und anschließend 2 Std bei 60° geschüttelt. Dannach wird das Reaktionsgemisch durch Vakuumverdampfen auf 5—7 mL eingeengt. Beim Erkalten fällt ein kristalliner Körper aus, der sich durch IR-spektroskopischen Vergleich mit authentischem Material als *p*-Dimethylaminobenzaldehyd erweist. Das nach dem Entfernen des Aldehyds verbliebene Filtrat wird mit dem gleichen Volumen Wasser behandelt, wobei ein zweites kristallines Produkt ausfällt, das sich ebenfalls IR-spektroskopisch durch Vergleichen mit authentischen Proben als das entsprechende 2-Aminobenzazolchlorhydrat erweist. Solche Versuche wurden für *p*-Dimethyeaminobenzyliden-2-aminobenzimidazol, *p*-Dimethylaminobenzyliden 2-aminobenzoxazol, *p*-Dimethylaminobenzyliden-2-amino-6-methoxybenzothiazol und *p*-Nitrobenzyliden-2-amino-6-methoxybenzothiazol durchgeführt.

Verfolgen der Hydrolysereaktion.

a) *durch ^{1}H-NMR-Spektroskopie*: Eine 5%-ige Lösung von *p*-Dimethyl-aminobenzyliden-2-aminobenzimidazol in DMSO-d_6 wurde zum Zeitpunkt Null mit CF_3COOH ($[CF_3COOH] \sim$ $\sim 0{,}4$ M/L im Reaktionsgemisch) angesäuert. Von Zeit zu Zeit wurde das NMR-Spektrum des Reaktionsgemisches aufgezeichnet, wobei als inneres Standard HMDS (Hexamethylidisiloxan) verwendet wurde.

b) *durch UV-Spektroskopie*: 10μl einer Benzyliden-aminoazol-Lösung in wasserfreiem Dioxan ($[\text{Imin}] = 3 \cdot 10^{-3}$ bis 10^{-2} M/L) wurden zum Zeitpunkt Null der Hydrolysereaktion in 2,5 mL einer Biphthalatpuffer-Lösung ([Puffer] = 0,01 bis 0,03 M/L) von bekanntem pH (4,5 bis 5,0) in Dioxan-Wasser ([HOH] = 5,5 bis 22,2 M/L) eingeführt. Das UV-Spektrum dieses Gemisches wurde von Zeit zu Zeit im 250—450 nm Bereich aufgenommen. Aus der Extinktion-Zeit Abhängigkeit wurden anhand eines einfachen Rechenmodells erster Ordnung,

$$k_{\mathbf{exp}} \cdot t = \ln(E_0 - E_i)/(E_t - E_i)$$

(wobei E_0, E_i, E_t die Extinktionen am Anfang, am Ende und bzw zum Zeitpunkt t der Reaktion sind) mit Hilfe eines für einen Minirechner Texas Instruments Ti 55 geschriebenen Programms, die Gk-ten erster Ordnung berechnet, wobei die Methode der kleinsten Quadrate verwendet wurde. Die Korrelationskoeffizienten waren in allen Fällen über 0,99. Das Modell erster Ordnung entsprach in allen Fällen für Umsetzungen von bis 75—90%. Die scheinbaren Aktivierungsparameter wurden anhand der wohlbekannten Gleichungen aus der Theorie des aktivierten Komplexes berechnet.

LITERATURÜBERSICHT

[1] III-te Mitt.: R. Bacaloglu, H. H. Glatt, M. F. Barry und C. Csunderlik, *Rev. Roumaine Chim.*, **31**, 283 (1986).
[2] R. L. Reeves, *J. Amer. Chem. Soc.*, **84**, 3332 (1962).
[3] R. L. Reeves und W. F. Smith, *J. Amer. Chem. Soc.*, **85**, 724 (1963).
[4] I. R. Bellobono und F. G. Favini, *Tetrahedron*, **25**, 57 (1969).
[5] R. L. Reeves, *J. Org. Chem.*, **30**, 3129 (1965).
[6] W. P. Jencks, *Progr. Phys. Org. Chem.*, **2**, 63 (1964).
[7] E. H. Cordes und W. P. Jencks, *J. Amer. Chem. Soc.*, **84**, 826 (1962).
[8] E. H. Cordes und W. P. Jencks, *J. Amer. Chem. Soc.*, **85**, 2843 (1963).
[9] K. Koehler, W. Sandstrom und E. H. Cordes, *J. Amer. Chem. Soc.*, **86**, 2413 (1964).
[10] W. Bruyneel, J. J. Charette und E. de Hoffmann, *J. Amer. Chem. Soc.*, **88**, 3808 (1966).
[11] R. K. Chaturvedi und E. H. Cordes, *J. Amer. Chem. Soc.*, **89**, 230 (1967).

[12] M. Masui, H. Ohmori, C. Veda, und M. Yamandu, *J. Chem. Soc., Perkin Trans. II* **1974**, 1448.

[13] H. Ohmori, C. Veda und M. Masui, *J. Chem. Soc., Perkin Trans. II* **1979**, 720.

[14] L. Holleck und B. Kastening, *Z. Elektrochem.*, **60**, 127 (1956).

[15] B. Kastening, L. Holleck und G. A. Melkonian, *Z. Elektrochem.*, **60**, 130 (1956).

[16] A. V. Willi und R. E. Robertson, *Canad. J. Chem.*, **31**, 361 (1953).

[17] A. V. Willi und J. F. Siman, *Ckad. J. Chem.*, **46**, 1549 (1969).

[18] A. V. Willi, *Helv. Chim. Acta*, **39**, 1193 (1956).

[19] O. Bloch-Chaudé, *C. R. Acad. Sci. Paris*, **239**, 804 (1954).

[20] M. T. A. Behme und E. H. Cordes, *J. Amer. Chem. Soc.*, **87**, 260 (1965).

[21] L. Do Amaral, W. A. Sandstrom und E. H. Cordes, *J. Amer. Chem. Soc.*, **88**, 2225 (1965).

[22] H. H. Jaffé, *Chem. Rev.*, **53**, 208 (1953).

[23] E. H. Cordes und W. T. Jencks, *J. Amer. Chem. Soc.*, **84**, 832 (1962).

[24] R. L. Hill und T. I. Crowell, *J. Amer. Chem. Soc.*, **78**, 2284 (1956).

[25] G. M. Stanerre, C. J. Hansrote und T. I. Crowell, *J. Amer. Chem. Soc.*, **80**, 1254 (1958).

[26] L. V. Kononenko, V. I. Dmitrieva und V. D. Bezuli, *Zhur. Org. Khim.*, **38**, 223 (1969).

[27] H. H. Glatt, M. F. Barry, C. Csunderlik, R. Bacaloglu, M. Medeleanu und M. Lantos, *Rev. Roumaine Chim.*, **30**, 125 (1985).

[28] H. H. Glatt, M. F. Barry, C. Csunderlik, R. Bacaloglu, M. Botoacă, S. Savu-Botoacă und D. Fechete, *Rev. Roumaine Chim.*, **31**, 273 (1986).

Revue Roumaine de Chimie, **33**, *6*, 653–656 (1988)

CONDENSATION OF *o*-AND *p*-PHENYLENEDIAMINE WITH SOME SUBSTITUTED 2-THIAZOLIN-5-ONES

H. M. HASSAN and O.M.O. HABIB
Chemistry Department, Faculty of Science, Mansoura University,
Egypt

Received March 2, 1987

4-Arylmethylene-1(2′-aminophenyl)-2-phenyl-2-imidazolin-5-ones IIa-c were prepared by fusion of 4-arylmethylene-2-phenyl-2-thiazolin-5-ones Ia-c with *o*-phenylenediamine in the presence of fused sodium acetate. Reaction of Ia-c with *o*-phenylenediamine in ethanol gave 2-amino-phenylcarboxamides of α-phenylthioamido-β-arylacrylic acids IIIa-c. Condensation of Ia-c with *o*-phenylenediamine in acetic acid containing sodium acetate yielded α-phenylthioamido-β-aryl-vinyl-benzimidazoles IVa-c. The same products were also obtained by cyclisation of compounds IIIa-c on refluxing with acetic acid and fused sodium acetate. Reaction of Ia-c with *p*-phenylenediamine in acetic acid and sodium acetate afforded the bis-imidazolone derivatives Va-c. A possible reaction mechanism is discussed.

It has been reported in literature that the reactions of 4-aryl-methylene-2-aryl-2-thiazolin-5-ones with primary aromatic amines generally leads to opening of the thiazolone ring at C_5 to give the arylcarboxamides of α-arylthioamido-β-arylacrylic acids.[1–4]

In continuation of our previous studies,[5,6] we report here the interaction of some 4-arylmethylene-2-phenyl-2-thiazolin-5-ones Ia-c with *o*- and *p*-phenylenediamines. Thus, fusion of Ia-c with *o*-phenylenediamine in the presence of freshly fused sodium acetate afforded the corresponding 4-arylmethylene-1(2′-aminophenyl)-2-phenyl-2-imidazolin-5-one IIa-c

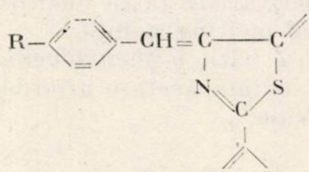

Ia-c

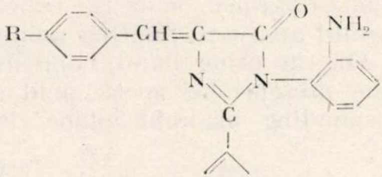

IIa-c

a ; R = H
b ; R = OCH_3
c ; R = NO_2

These products were characterised by elemental analyses and IR spectra showing absorption bands at 1720, 1640 and 3300 cm^{-1} assignable to the CONR, C=N and NH groups, respectively. They were also identified by mixed melting points with authentic samples prepared previously by the reaction of 4-arylmethylene-2-phenyl-2-oxazolin-5-ones with *o*-phenylenediamine.[5]

On the other hand, treatment of Ia-c with *o*-phenylenediamine in ethanol gave the 2-aminophenylcarboxamides of α-phenylthioamido-β-arylacrylic acids IIIa-c. The structures of these products were inferred from analytical results and IR measurements which showed stretching frequencies at 1640, 3300, 1340 and 3200 cm^{-1} characteristic for the $-C=N-$, NH, C=S and OH groups, respectively.

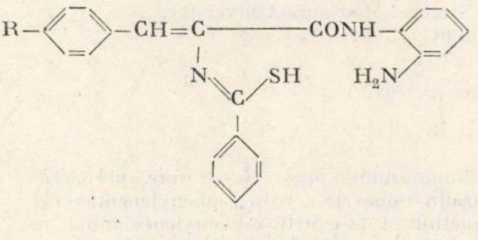
IIIa-c
a; R = H
b; R=OCH_3
c; R = NO_2

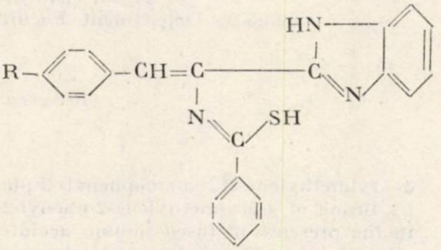
IVa-c
a; R = H
b; R = OCH_3
c; R = NO_2

Treatment of Ia-c with *o*-phenylenediamine in the presence of acetic acid and fused sodium acetate afforded α-phenylthioamido-β-aryl-vinylbenzimidazole IVa-c. These products were characterised by analytical data and IR. spectra which showed absorption bands at 1635, 1340 and 3300 cm^{-2} attributable to the $-C=N-$, $-C=S$ and NH groups, respectively.

It seems that this interaction leads to ring opening at C_2 to give 2-aminophenylcarboxamides of α-phenylthioamido-β-arylacrylic acids IIIa-c which only appear as intermediates and recyclise to the corresponding benzimidazole derivatives IVa-c under the influence of acetic acid and sodium acetate.

In order to verify this mechanism, the compounds with open structure IIIa-c were treated with acetic acid and fused sodium acetate, the products obtained being the benzimidazole derivatives IVa-c identified by elemental analyses, melting points and mixed melting points.

On the other hand, condensation of Ia-c with *p*-phenylenediamine in the presence of acetic acid and fused sodium acetate afforded the corresponding bis-imidazolone derivatives Va-c.

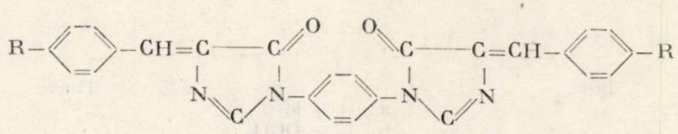
Va-c
a; R = H
b; R = OCH_3
c; R = NO_2

EXPERIMENTAL

All melting points are uncorrected. Analytical data were determined by the Microanalytical Unit, Faculty of Science, Mansoura University. IR spectra were recorded on a SP-1200 Pye-Unicam Spectrophotometer.

4-Arylmethylene-1(2′-aminophenyl)-2-phenyl-2-imidazolin-5-ones IIa-c

A mixture of 4-arylmethylene-2-phenyl-2-thiazolin-5-ones Ia-c (3 mmoles in each case), *o*-phenylenediamine (3 mmoles; 0.32 g) and freshly fused sodium acetate (0.2 g) was fused for four hours at 140°C. The reaction mixture was cooled, washed with ethanol and filtered. The obtained solid products were recrystallised from acetic acid to give 1(2′-aminophenyl)-4--arylmethylene-2-phenyl-2-imidazolin-5-one derivatives IIa-c (cf. Table 1).

Table 1

4-Arylmethylene-1(2′-aminophenyl)-2-phenyl-2-imidazolin-5-ones

Compound	M.p. °C	Yield %	Formula	Analysis % C	H	Found / Calcd.
IIa	184	76	$C_{22}H_{17}N_3O$	77.86 77.87	5.00 5.01	
IIb	199	72	$C_{23}H_{19}N_3O_2$	74.60 74.80	5.15 5.15	
IIc	165	89	$C_{22}H_{16}N_4O_3$	68.75 68.75	4.18 4.16	

p-Aminophenylcarboxamides of α-phenylthioamido-β-arylacrylic acid derivatives IIIa-c

A mixture of 4-arylmethylene-2-phenyl-2-thiazolin-5-ones Ia-c (3 mmoles in each case) and *o*-phenylenediamine (3 mmoles; 0.32 g) in ethanol (25 mL) was refluxed for two hours. The reaction mixture was cooled, and the precipitate was filtered and crystallised from ethanol to give 2-aminophenylcarboxamides of α-phenytlhioamide-β-arylacrylic acids IIIa-c (cf. Table 2).

Table 2

2-Aminophenylcarboxamides of α-phenylthioamido-β-aryl-acrylic acids IIIa-c

Compound	M.p. °C	Yield %	Formula	Analysis % C	H	Found / Calcd.
IIIa	176	85	$C_{22}H_{19}N_3OS$	70.55 70.70	4.84 5.10	
IIIb	184	65	$C_{23}H_{21}N_3O_2S$	68.23 68.41	5.15 5.20	
IIIc	199	82	$C_{22}H_{18}N_4O_3S$	62.87 63.09	4.36 4.46	

Preparation of (α-phenylthioamido-β-aryl)-vinylbenzimidazoles IVa-c

A. Reaction of Ia-c with o-phenylenediamine in acetic acid

A mixture of 4-arylmethylene-2-phenyl-2-thiazolin-5-ones Ia-c (3 mmoles in each case) and *o*-phenylenediamine (3 mmoles) in acetic acid (20 mL) containing freshly fused sodium acetate (0.2 g) was refluxed for three hours. The reaction mixture was cooled and the obtained solid was filtered and crystallised from ethanol to give the benzimidazole derivatives IVa-c (cf. Table 3).

Table 3

(α-Phenylthioamido-β-aryl)vinylbenzimidazoles IVa-c

Compound	M.p. °C	Yield %	Formula	Analysis % C	H	Found / Calcd.
IVa	209	74	$C_{22}H_{17}N_3S$	74.17 74.28	4.75 4.78	
IVb	255	69	$C_{23}H_{19}N_3OS$	71.48 71.61	4.90 4.91	
IVc	284	86	$C_{22}H_{16}N_4O_2S$	65.82 65.95	3.74 3.99	

B. Cyclisation of compounds IIIa-c

Compounds IIIa-c (1.0 g in each case) were refluxed in acetic acid (25 mL) and freshly fused sodium acetate (0.2 g) for two hours. The reaction mixture was cooled and the formed solid was filtered and crystallised from ethanol to give the benzimidazole derivatives IVa-c identified by elemental analyses, melting and mixed melting points.

Preparation of the bis-imidazolone derivatives Va-c

A mixture of 4-arylmethylene-2-phenyl-2-thiazolin-5-ones Ia-c (4 mmoles in each case), *p*-phenylenediamine (2 mmoles), acetic acid (50 mL) and freshly fused sodium acetate (0.2 g) was refluxed for two hours. The reaction mixture was cooled and the collected precipitate was crystallised from acetic acid to give yellow crystals of Va-c (cf. Table 4).

Table 4

Bis-imidazolone derivatives **Va-b**

Compound	M.p. °C	Yield %	Formla	Analysis % C	H	Found / Calcd.
Va	178	55	$C_{38}H_{26}N_4O_2$	80.00 79.98	4.36 4.59	
Vb	229	72	$C_{40}H_{30}N_4O_4$	75.96 76.17	4.58 4.79	
Vc	196	68	$C_{38}H_{24}N_6O_6$	69.56 69.09	3.74 3.66	

REFERENCES

[1] P. C. Rath, P. B. Tripathy and M. K. Rout, *J. Indian Chem. Soc.*, **41**, 107 (1964).
[2] R. Filler and S. Rao, *J. Org., Chem.*, **27**, 1330 (1962).
[3] E. B. Knott. *US Patent* 2, 743, 273 (1956).
[4] T. B. Johnson and B. H. Nicolet, *J. Amer. Chem. Soc.*, **34**, 1048 (1912).
[5] H. M. Hassan, M. S. El-Housseni and O.M.O. Habib, *J. Prakt. Chem.*, **325** (**4**), 685 (1983).
[6] A. M. Khalil, I. I. Abd El-Gawad and H. M. Hassan, *Aust. J. Chem.*, **29**, 162 (1976).

Revue Roumaine de Chimie, **33**, 6, 657–667 (1988)

SYNTHESIS AND REACTIONS OF SOME NEW 5-ARYLIDENE-1-ARYL-3-OXO-2-INDANE CARBOXANILIDE DERIVATIVES

O.M.O. HABIB, I. I. ABD EL-GAWAD and D. S. BADAWY
Chemistry Department, Faculty of Science, Mansoura University

Received March 2, 1987

2,5-Diarylidenecyclopentanones have been condensed with acetoacetanilides to give 1,2,3-trihydro-1-aryl-5-arylidene-3-oxo-2-indane carboxanilides IIa-h. Reactions of IIa-h with hydrazine hydrate, phenylhydrazine, urea, thiourea, hydroxylamine hydrochloride, semicarbazide, polyphosphoric acid, benzenediazonium chloride and Mannich bases were studied. Treatment of the pyrazolone derivatives IIIa-d with chloroazetyl chloride, benzenesulphonyl chloride, Mannich bases and benzenediazonium chloride were also investigated.

There is a great deal of interest in the synthesis of compounds containing pyrazolone moiety because of their use as analgesic and antipyretic agents.[1–3] In continuation of our previous work in this area[4–6], we study here the use of some 5-arylidene-3-oxo-2-indane carboxanilides for the synthesis of some new pyrazolones and other related derivatives.

Thus, cyclopentanone was treated with aromatic aldehydes in the presence of potassium methoxide to give the corresponding 2,5-diarylidenes Ia-d. Condensation of Ia-d with acetoacetanilides in the presence of potassium methoxide afforded 1,2,3-trihydro-1-aryl-5-arylidene-3-oxo-2-indane carboxanilides IIa-h.

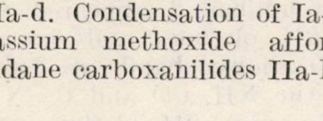

I

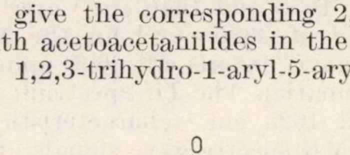

II

a, Ar = C_6H_5
b, Ar = $C_6H_4-OCH_3-p$
c, Ar = C_6H_4-Cl-p
d, Ar = $C_6H_4-N(CH_3)_2-p$

a, Ar = C_6H_5 Ar' = C_6H_5
b, Ar = C_6H_5 Ar' = C_6H_4-Cl-p
c, Ar = $C_6H_4-OCH_3-p$; Ar' = C_6H_5
d, Ar = $C_6H_4-OCH_3-p$; Ar' = C_6H_4-Cl-p
e, Ar = C_6H_4-Cl-p Ar' = C_6H_5
f, Ar = C_6H_4-Cl-p; Ar' = C_6H_4-Cl-p
g, Ar = $C_6H_4N(CH_3)_2-p$; Ar' = C_6H_5
h, Ar = $C_6H_4N(CH_3)_2-p$; Ar' = C_6H_4-Cl-p

The structures of IIa-n were established by elemental analysis and IR spectra which showed stretching frequencies at 3400–3300, 1670 and 1650 cm^{-1} characteristic for the NH, CO and CONH groups, respectively.

Treatment of IIa-h with hydrazine hydrate afforded the corresponding 1,2,3-trihydro-1-aryl-5-arylidene indane [3,2-c] pyrazol-3-ones IIIa-d. The IR spectrum of IIIa showed absorption bands at 3380, 1690 and 1640 cm^{-1} assignable to NH, CO and C=N groups, respectively. ^{1}H-NMR spectra revealed signals at δ6.7 ppm (s, 2H, olefinic), δ4.8 ppm (s, 1H, NH) and δ7.1 ppm (m, 10H, aromatic).

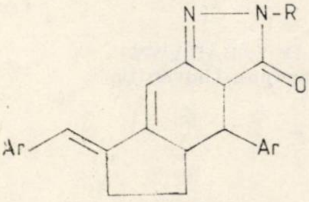

III

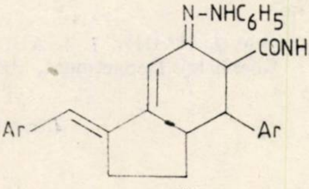

IV

a, Ar = C_6H_5 ; R = H
b, Ar = $C_6H_4.OCH_3-p$; R = H
c, Ar = $C_6H_4.Cl-p$; R = H
d, Ar = $C_6H_4N(CH_3)_2-p$; ; R = H
e, Ar = C_6H_4 ; R = C_6H_5
f, Ar = $C_6H_4.OCH_3-p$; R = C_6H_5
g, Ar = $C_6H_4.C-p$; R = C_6H_5
h, Ar = $C_6H_4N(CH_3)_2-p$; R = C_6H_5

a, Ar = C_6H_5 ; Ar′ = C_6H_5
b, Ar = C_6H_5 . ; Ar′ = C_6H_4Cl-p
c, Ar = $C_6H_4-OCH_3-p$; Ar′ = C_6H_5
d, Ar = $C_6H_4-OCH_3-p$; Ar′ = C_6H_4Cl-p
e, Ar = C_6H_4-Cl-p ; Ar′ = C_6H_5
f, Ar = C_6H_4-Cl-p ; Ar′ = C_6H_4Cl-p
g, Ar = $C_6H_4N(CH_3)_2-p$; Ar′ = C_6H_5
h, Ar = $C_6H_4N(CH_3)_2-p$; Ar′ = C_6H_4Cl-p

On the other hand, reaction of IIa-h with phenylhydrazine in acetic acid gave N-phenylpyrazol-3-ones IIIe-h. When this reaction was carried out in ethanol, the products were the corresponding phenylhydrazones IVa-h which cyclised under the effect of acetic acid into the corresponding pyrazolones IIIe-h. The IR spectrum of IIIg revealed bands at 1670 and 1640 cm^{-1} attributable to the CO and C=N groups. The band at 3380 cm^{-1} for the NH group had disappeared. ^{1}H-NMR spectra gave signals at δ6.6 ppm (s, 2H, olefinic), and 6.9 ppm (m, 18H, aromatic). The IR spectrum of IVc showed bands at 3400–3360, 1690 and 1625 cm^{-1} characteristic for the NH, CO and C=N groups. Its ^{1}H-NMR spectra gave signals at δ6.7 ppm (s, 2H, olefinic), δ3.6 ppm (m, 6H, OCH_3) and δ7.6 ppm (m, 18H, aromatic).

Treatment of IIb with semicarbazide in sodium acetate afforded the corresponding semicarbazone V which on boiling with aqueous sodium hydroxide cyclised into the N-amidopyrazolone VI. The IR spectrum of V gave bands at 3400–3300, 1640, 1670 and 1625 cm^{-1} characteristic for the NH, $CONH_2$, CON– and C=N groups, respectively.

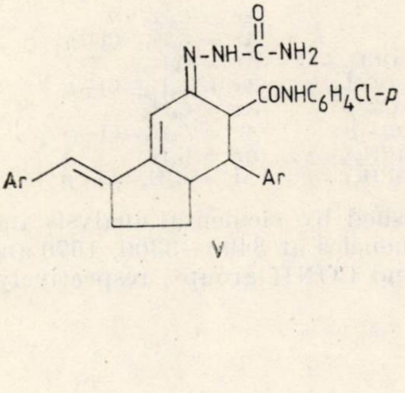

V

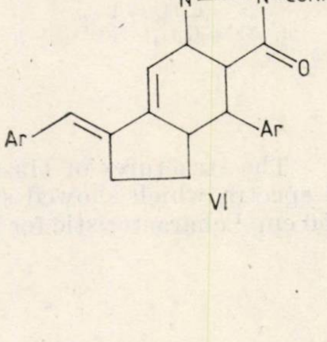

VI

Condensation of IIa,b with urea and thiourea in alcoholic potassium hydroxide afforded the corresponding 1,2,3-trihydro-1-aryl-5-arylidene-indane [3,2-c] pyrimidine-3-aryl-2,4-diones VIIa, b and 1,2,3-trihydro-1-aryl-5-arylidene indane[3,2-c] pyrimidine-3-aryl-2-thione-4-ones VIIc, d respectively.

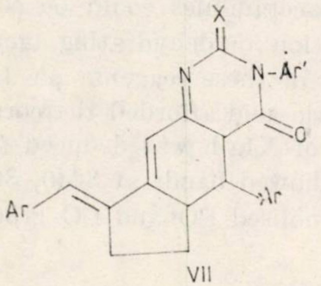

VII

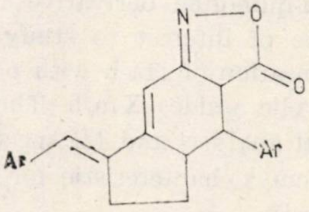

VIII

a, Ar = C_6H_5 ; Ar' = C_6H_5 ; X = O
b, Ar = C_6H_5 ; Ar' = C_6H_4Cl-p ; X = O
c, Ar = C_6H_5 ; Ar' = C_6H_5 ; X = S
d, Ar = C_6H_5 ; Ar' = C_6H_4Cl-p ; X = S

a, Ar = C_6H_5
b, Ar = $C_6H_5-OCH_3$-*p*

The IR spectrum of VIIa showed absorption bands at 1700 and 1680 cm^{-1} characteristic for the two CO groups. The IR spectrum of VIIc revealed bands at 1690 and 1270 cm^{-1} assignable to the CO and C=S groups, respectively.

Treatment of IIa, c with hydroxylamine hydrochloride in the presence of few drops of pyridine gave the corresponding isoxazolone derivatives VIIIa,b. The IR spectrum of VIIIb revealed bands at 1670 and 1625 cm^{-1} attributable to the CO and C=N groups, respectively. ^{1}H-NMR spectrum showed signals at δ6.4 ppm (m, 2H, olefinic) and δ7.1 ppm (m, 10H, aromatic).

The behaviour of α-ketoanilides towards Mannich reaction was investigated. Thus, treatment of IIa with formaldehyde and piperidine in the presence of hydrochloric acid afforded the piperidinomethyl derivative IX as hydrochloride salt. The structure of IX was established on the basis of elemental analysis and IR spectrum showing absorption bands at 3390, 1690 and 1650 cm^{-1} assignable to the NH, and 2CO groups, respectively.

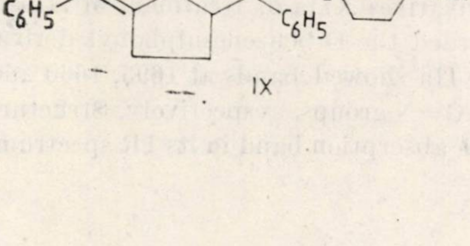

IX

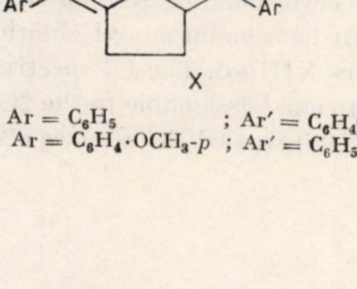

X

a. Ar = C_6H_5 ; Ar' = C_6H_4Cl-p
b, Ar = $C_6H_4 \cdot OCH_3$-*p* ; Ar' = C_6H_5

Coupling of IIb,c with benzenediazonium chloride has resulted into the reaction through the active methylene group to yield 1,2,3-trihydro-1-aryl-5-arylidene-3-oxo-phenylazo-2-indane carboxanilides Xa, b. The IR spectrum of Xa showed bands at 3380, 3060, 1600, and 1700–1680 cm^{-1} attributable to the NH, N=N and 2CO groups, respectively.

Since it is well known that acetoacetanilides could be converted into 2-quinoline derivatives by the action of dehydrating agents,[7,8] it became of interest to study the effect of these reagents on II. Thus, condensation of IIa-h with polyphosphoric acid afforded the corresponding cyclic amides XIa-h. The structure of XIa-h was deduced from elemental analysis and IR spectra which showed bands at 3440, 3090, and 1690 cm^{-1} characteristic for the NH, enolised CO and CO groups, respectively.

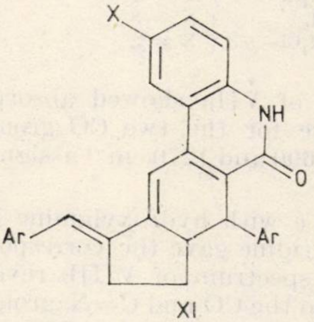

XI

a, $Ar = C_6H_5$; $X = H$
b, $Ar = C_6H_5$; $X = Cl$
c, $Ar = C_6H_4-OCH_3-p$; $X = H$
d, $Ar = C_6H_4-OCH_3-p$; $X = Cl$
e, $Ar = C_6H_4Cl-p$; $X = H$
f, $Ar = C_6H_4Cl-p$; $X = Cl$
g, $Ar = C_6H_4N(CH_3)_2-p$; $X = H$
h, $Ar = C_6H_4N(CH_3)_2-p$; $X = Cl$

On the other hand, the reaction of 1,2,3-trihydro-1-aryl-5-arylidene indane [3,2-c] pyrazol-3-ones IIIa-d with a variety of reagents has been studied in order to show the behaviour of the pyrazolinone ring.

Although the reaction of IIIa-d with chloroacetyl chloride gave the corresponding N-chloroacetyl derivatives XIIa-d, treatment of IIIa-d. with benzenesulphonyl chloride afforded the O-benzenesulphonyl derivatives XIIIa-d. The IR spectrum of XIIa showed bands at 1695, 1660 and 1610 cm^{-1} assignable to the 2CO and C=N groups, respectively. Structure XIIIa revealed the absence of the CO absorption band in its IR spectrum

Similar results for other pyrazolinone derivatives were previously reported.[5,9,10]

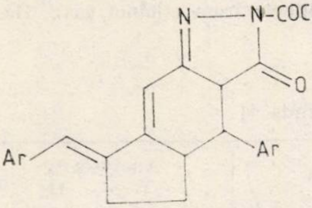

XII

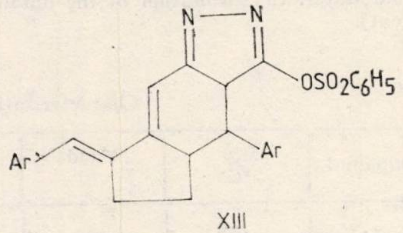

XIII

a, Ar = C_2H
b, Ar = C_2H_4—OCH_3—*p*
c, Ar = C_2H_4 l—*p*
d, Ar = $C_2H_4N(CH_3)_2$—*p*

Aminomethylation of IIIa,b was achieved using piperidine and formaldehyde in the presence of hydrochloric acid and gave the corresponding N-piperidinomethyl derivatives XIVa,b as hydrochloride salts. The IR spectrum of XIVa showed bands at 1625 and 1690 cm^{-1} attributable to the C=N and CO groups, respectively.

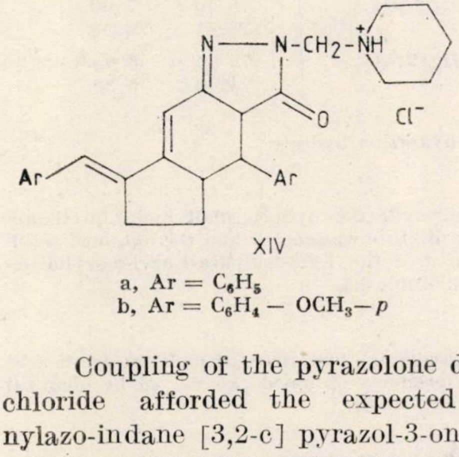

XIV

a, Ar = C_6H_5
b, Ar = C_6H_4 — OCH_3—*p*

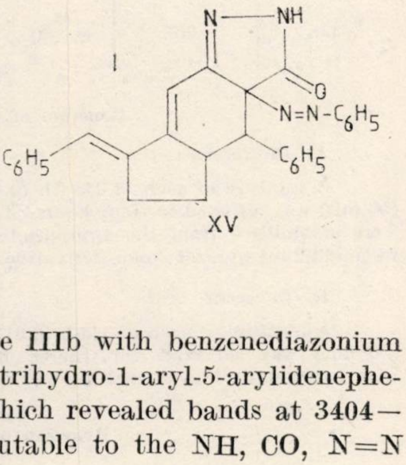

XV

Coupling of the pyrazolone derivative IIIb with benzenediazonium chloride afforded the expected 1,2,3-trihydro-1-aryl-5-arylidenephenylazo-indane [3,2-c] pyrazol-3-one XV which revealed bands at 3404—3060, 1690, 1600 and 1640 cm^{-1} attributable to the NH, CO, N=N and C=N groups, respectively.

EXPERIMENTAL

Melting points are uncorrected. Analytical data were determined by the Microanalytical Unit, Faculty of Science, Mansoura University, Egypt. Infrared spectra were recorded on a Pye-Unicam SP-1100 spectrophotometer. ^1H-NMR spectra were obtained at 60 MHz in deuteriochloroform with TMS as an internal standard.

Synthesis of 1,2,3-trihydro-1-aryl-5-arylidene-3-oxo-2-indane carboxanilides IIa-h

Acetoacetanilide or its *p*-chloroderivative (0.01 mole in each case) was added to the arylidene derivatives (0.01 mole in each case) in potassium methoxide (0.02 mole). The reaction mixture was refluxed for twelve hours, cooled to room temperature, and poured onto ice-cold water. Crystallisation of the obtained solid products from ethanol gave IIa-g (cf. Table 1).

Table 1

Characterization of compounds II

Compound	M.p. °C	Yield %	Formula	Analysis % C	H
				Found Calcd.	
IIa	183	80	$C_{29}H_{25}NO_2$	83.50 83.05	5.70 5.96
IIb	199	80	$C_{29}H_{24}ClNO_2$	76.50 76.73	5.00 5.29
IIc	195	70	$C_{31}H_{29}NO_4$	77.50 77.66	5.90 6.05
IId	188	80	$C_{31}H_{28}ClNO_4$	72.10 72.44	5.70 5.45
IIe	245	80	$C_{29}H_{23}Cl_2NO_2$	71.40 71.31	4.80 4.71
IIf	206	70	$C_{29}H_{22}Cl_3NO_2$	66.30 66.60	4.50 4.21
IIg	248	50	$C_{33}H_{35}N_3O_2$	78.10 78.41	7.00 6.93
IIh	203	60	$C_{33}H_{34}ClN_3O_2$	73.50 73.40	6.30 6.30

Reaction of IIa-h with hydrazine hydrate

A. *In ethanol*:

A mixture of each of IIa–h (0.01 mole) and hydrazine hydrate (0.01 mole) in ethano (50 mL) was refluxed for four hours. The reaction mixture was cooled and the obtained solid were crystallised from the appropriate solvent to give the 1,2,3-trihydro-1-aryl-5-arylidene indane[3,2-c)]-pyrazol-3-one derivatives IIIa-d (cf. Table 2).

B. *In acetic acid*:

A mixture of each of IIa-h (0.01 mole) and hydrazine hydrate (0.01 mole) in acetic acid (50 mL) was refluxed for theree hours. The products obtained proved to be identical with compounds IIIa-d (melting and mixed melting points).

Reaction of IIa-h with phenylhydrazine

A. *In ethanol*:

The same general procedure described for the reaction of IIa-b with hydrazine hydrate Recrystallisation of the resulting products from the proper solvents gave the corresponding phenylhydrazones IVa-h (cf. Table 3).

B. *In acetic acid*:

The same general procedure described for the reaction of IIa-h with hydrazine hydrate. Recrystallisation from the suitable solvents afforded 1,2,3-trihydro-1-aryl-5-arylidene-indane [3,2-c]-N-phenylpyrazol-3-ones IIIe-h (cf. Table 2).

Table 2

Characterization of compounds III

Compound	M.p.°C (solvent)	Yield %	Formula	Analysis % C	H	Found / Calcd.
IIIa	258 ($CHCl_3-EtOH$)	80	$C_{23}H_{20}N_2O$	80.80 81.17	5.60 5.88	
IIIb	265 (C_6H_6-EtOH)	80	$C_{25}H_{24}N_2O_3$	74.80 75.00	5.70 6.00	
IIIc	269 (AcOH)	80	$C_{23}H_{18}Cl_2N_2O$	67.50 67.48	4.10 4.40	
IIId	220 (EtOH)	80	$C_{27}H_{30}N_4O$	76.20 76.05	7.31 7.04	
IIIe	215 (EtOH)	80	$C_{29}H_{24}N_2O$	83.50 83.65	5.80 5.76	
IIIf	165 (AcOH)	80	$C_{31}H_{28}N_2O_3$	78.40 78.15	6.10 5.88	
IIIg	178 (AcOH)	75	$C_{29}H_{22}Cl_2N_2O$	71.90 71.75	4.50 4.54	
IIIh	235 (EtOH)	65	$C_{33}H_{34}N_4O$	79.10 78.88	6.60 6.77	

Table 3

Characterization of compounds IV

Compound	M.p. °C (solvent)	Yield %	Formula	Analysis % C	H	Found / Calcd.
IVa	135 (EtOH)	70	$C_{35}H_{31}N_3O$	81.99 82.51	5.90 6.09	
IVb	238 (EtOH)	60	$C_{35}H_{30}ClN_3O$	76.90 77.27	5.20 5.51	
IVc	119 (EtOH)	70	$C_{37}H_{35}N_3O_3$	78.40 78.03	6.21 6.15	
IVd	202 (EtOH)	70	$C_{37}H_{34}ClN_3O_3$	73.30 73.57	5.50 5.63	
IVe	228 ($EtOH-C_6H_6$)	60	$C_{35}H_{29}Cl_2N_3O$	72.20 72.66	5.10 5.20	
IVf	221 ($EtOH-C_6H_6$)	65	$C_{35}H_{28}Cl_3N_3O$	69.00 68.57	4.90 4.57	
IVg	131 (EtOH)	60	$C_{39}H_{41}N_5O$	78.40 78.65	6.70 6.89	
IVh	161 (EtOH)	70	$C_{39}H_{40}ClN_5O$	74.17 74.34	6.40 6.35	

Conversion of IVa-h into pyrazolones IIIe-h

Compounds IVa–h were heated under reflux in acetic acid in the presence of sodium acetate. A rapid change in colour was immediately observed and the obtained solids proved to be identical with compounds IIIe–h (melting and mixed melting points).

Reaction of IIb with semicarbazide hydrochloride

Compound IIb (0.01 mole) in ethanol (70 mL) was mixed with a solution of semicarbazide hydrochloride (0.01 mole) and sodium acetate (1.0 g) in water (10 mL). The reaction mixture was refluxed for three hours and the separated solid product was filtered and crystallised from ethanol to give the semicarbazone derivative V, m.p. 237°C, yield 65%.
Analysis : $C_{30}H_{27}ClN_4O_2$ Found : %C 70.50; %H 5.11 Calcd. : %C 70.52; %H 5.29.

Reaction of V with sodium hydroxide

A solution of V (0.5 g) in sodium hydroxide (1 N; 25 mL) was refluxed for three hours, cooled and acidified. The precipitate was filtered off and crystallised from ethanol to give the N-amidopyrazolone derivative VI, m.p. 175°C, yield 80%
Analysis : $C_{24}H_{21}N_3O_2$ Found : %C 75.00; %H 5.20 Calcd. : %C 75.19; %H 5.48.

Reaction of IIa,b with urea or thiourea

A mixture of each of IIa, b (0.01 mole), urea or thiourea (0.01 mole), potassium hydroxide (1.0 g), ethanol (50 mL) and water (1.0 mL) was refluxed for three hours. The reaction mixture was cooled and the formed precipitate was filtered off, dried and crystallised from ethanol to give the corresponding pyrimidine derivatives VIIa–d (cf. Table 4).

Table 4

Characterization of compounds VII

Compound	M.p. °C	Yield %	Formula	Analysis % C	H	Found / Calcd.
VIIa	above 260	80	$C_{30}H_{24}N_2O_2$	81.30 81.08	5.20 5.40	
VIIb	205	80	$C_{30}H_{23}ClN_2O_2$	75.10 75.32	4.90 4.80	
VIIc	197	80	$C_{30}H_{24}N_2OS$	78.00 78.26	4.90 5.21	
VIId	208	80	$C_{30}H_{23}ClN_2OS$	72.60 72.80	4.50 4.65	

Reaction of IIa,c with hydroxylamine hydrochloride

A solution of each of IIa,c (0.01 mole), hydroxylamine hydrochloride (0.01 mole) and ethanol (25 mL) was refluxed for three hours. The solid products obtained after evaporating most of the solvent were crystallised from ethanol to give 1,2,3-trihydro-1-aryl-5-aryl-idene-indane 3,2-c isoxazol-3-ones VIIIa,b, respectively (cf. Table 5).

Table 5

Characterization of compounds VIII

Compound	M.p. °C	Yield %	Formula	Analysis % C	H	Found / Calcd.
VIIIa	226	70	$C_{23}H_{19}NO_2$	80.60 80.93	5.60 5.57	
VIIIb	235	70	$C_{25}H_{23}NO_4$	74.90 74.81	5.70 5.73	

Mannich reaction of IIb

To a mixture of IIb (0.01 mole) and piperidine (0.01 mole) in methanol (50 mL), aqueous formaldehyde (35%, 2.5 mL) and hydrochloric acid (0.5 mL) were added. The reaction mixture was refluxed for eight hours, kept overnight at room temperature and the solid product obtained on dilution with water was crystallised from ethanol to give 1,2,3-trihydro-1-phenyl-5-benzylidene-3-oxo-2-piperidinomethyl-2-indene carboxanilide IX, m.p. 92°C, yield 70%. Analysis : $C_{35}H_{36}Cl_2N_2O_2$ Found : %C 72.00 ; %H 6.42 Calcd. : %C 71.55 ; %H 6.13.

Reaction of IIb,c with benzenediazonium chloride

To a cold solution of each of IIb,c (0.01 mole) in ethanolic sodium hydroxide (10% 40 mL), benzenediazonium chloride was added. Crystallisation of the resulting solids from ethanol gave the corresponding phenylazo derivatives Xa,b (cf. Table 6).

Table 6

Characterization of compounds X

Compound	M.p. °C	Yield %	Formula	Analysis % C	H	Found / Calcd.
Xa	101	70	$C_{35}H_{28}ClN_3O_2$	75.20 75.33	5.30 5.02	
Xb	85	70	$C_{37}H_{33}N_3O_4$	76.00 76.15	5.50 5.66	

Reaction of IIa-h with polyphosphoric acid

Polyphosphoric acid (20 mL) was heated with each of IIa-h (1 g) for two hours at 140–150°C. The reaction mixture was cooled and poured onto ice-cold water. The solid products were filtered off and crystallised from ethanol to give the corresponding cyclic amide derivatives XIa-h (cf. Table 7).

Table 7

Characterization of compounds XI

Compound	M.p. °C	Yield %	Formula	Analysis % C	H	Found / Calcd.
XIa	104	60	$C_{29}H_{23}NO$	86.40 86.78	5.40 5.73	
XIb	98	60	$C_{29}H_{22}ClNO$	80.00 79.90	5.08 5.05	
XIc	66	60	$C_{31}H_{27}NO_3$	80.20 80.69	5.65 5.85	
XId	79	60	$C_{31}H_{26}ClNO_3$	74.80 75.07	5.50 5.24	
XIe	94	60	$C_{29}H_{21}Cl_2NO$	74.50 74.04	4.60 4.47	
XIf	82	60	$C_{29}H_{20}Cl_3NO$	68.70 68.97	3.70 3.96	
XIg	202	60	$C_{33}H_{33}N_3O$	80.80 81.30	6.50 6.77	
XIh	161	60	$C_{33}H_{32}ClN_3O$	75.70 75.93	5.90 6.13	

Reaction of IIIa-d with chloroacetyl chloride

To a solution of chloroacetyl chloride (0.03 mole) in dry benzene (15 mL), each of IIIa-d (0.01 mole) was added. The reaction mixture was refluxed for two hours on a steam bath and left to stand at room temperature overnight. The precipitates were filtered off and recrystallised from the suitable solvents to give the corresponding N-chloroacetyl derivatives XIIa-d (cf. Table 8).

Table 8

Characterization of compounds XII

Compound	M.p. °C	Yield %	Formula	Analysis % C	H	Found / Calcd.
XIIa	125	80	$C_{25}H_{21}ClN_2O_2$	72.30 72.02	5.20 5.04	
XIIb	122	80	$C_{27}H_{25}ClN_2O_4$	67.70 67.99	5.40 5.25	
XIIc	152	80	$C_{25}H_{19}Cl_3N_2O_2$	61.90 61.79	4.10 3.91	
XIId	121	80	$C_{29}H_{31}ClN_4O_2$	69.30 69.25	6.40 6.16	

Reaction of IIIa-d with benzenesulphonyl chloride

To a solution of each of IIIa–b (0.01 mole) in pyridine (15 mL), benzenesulphonyl chloride (0.012 mole) was added. The reaction mixture was refluxed for two hours on a steam bath, then cooled to room temperature and poured onto ice-cold water. The brown solid that precipitated was filtered and crystallised from ethanol to give the corresponding O-benzenesulphonyl derivatives XIIIa-d (cf. Table 9).

Table 9

Characterization of compounds XIII

Compound	M.p. °C	Yield %	Formula	Analysis % C	H	Found / Calcd.
XIIIa	110	70	$C_{29}H_{24}N_2O_3S$	72.70 72.50	4.90 5.00	
XIIIb	120	70	$C_{31}H_{28}N_2O_5S$	69.00 68.89	4.90 5.18	
XIIIc	134	70	$C_{29}H_{22}Cl_2N_2O_3S$	62.80 63.39	4.30 4.01	
XIIId	145	70	$C_{33}H_{34}N_4O_3S$	69.70 69.96	5.90 6.00	

Mannich reaction of IIIa,b

To a methanolic solution of each of IIIa,b (0.01 mole) and piperidine (0.02 mole) in methanol (50 mL), aqueous formaldehyde (35%, 2.5 mL) and hydrochloric acid (0.5 mL) were added. The reaction mixture was refluxed for twenty four hours, left to stand at room temperature for two days. The precipitated solids were filtered off and recrystallised from methanol to give the corresponding N-piperinomethyl derivatives IVXa,b (cf. Table 10).

Table 10

Characterization of compounds XIV

Compound	M.p. °C	Yield %	Formula	Analysis % C	H	Found Calcd.
XIVa	185	80	$C_{29}H_{32}ClN_3O$	73.30 73.49	6.45 6.76	
XIVb	108	70	$C_{31}H_{36}ClN_3O_3$	69.62 69.72	6.50 6.74	

Reaction of IIIb with benzenediazonium chloride

To a cold solution of IIIb (0.01 mole) in ethanolic sodium hydroxide (10%, 40 mL), benzenediazonium chloride was added. The obtained solid was filtered off and crystallised from ethanol to give the phenylazo derivative XV, m.p. 162°C, yield 65%.
Analysis : $C_{31}H_{28}N_4O_3$; Found : %C 73.50; %H 5.40; Calcd. : %C 73.80; %H 5.55.

REFERENCES

[1] D. A. Peak, P. A. Robinson and I. Walker, *J. Chem. Soc.*, **1936**, 752.

[2] R. Jacquire, C. Patrus, F. Petrus and J. Verducci, *Bull. Soc. Chim. France*, 3003 (1967).

[3] E. M. Kandeel, A. M. Khalil and Y. M. Eldesoky, *Bull. of the Faculty of Science*, Mansoura University, 89 (1982).

[4] I. I. Abd El-Gawad, A. M. Khalil, O.M.O. Habib and H.A. Etman, *Rev. Roumaine Chim.*, **30**, 499 (1985).

[5] O.M.O. Habib, I. I. Abd EL-Gawad, E. M. Kandeel and D. S. Badawy, *Rev. Roumaine Chim.* in press.

[6] O.M.O. Habib, I. I. Abd El-Gawad, A. M. Khalil and H. A. Etman, *Polish J. Chem.*, in press.

[7] A. Albert, A. J. Brown and H. Duewell, *J. Chem. Soc.*, **1948**, 1284.

[8]. R. Huisgen, *Liebigs Annal. Chem.*, **559**, 101 (1948).

[9] G. A. Galoyan, S. G. Agbalyan and G. T. Esayan, *Arm. Khim.*, **22**, 430 (1969); *Chem. Abstr.* **71**, 70535 (1969).

[10] A. H. Harhash, F. A. Amer and M. A. Metwally, *Bull. of the Faculty of Science*, Mansoura University, 223 (1977).

Revue Roumaine de Chimie, 33, 6, 669–670 (1988)

COMPTES RENDUS

J. HOLLO (editor), "Fat. Science, 1983" Proceedings of the 16th International Society for Fat Research (ISF) Congress, Akademiai Kiado, Budapest, 1985, 2 volumes, Hard cover, 1150 pp., ISBN 963 05 4080 0 (Series)

The "Proceedings of the 16th ISF Congress" from Budapest, Hungary took place on 4–7 October 1983. The proceedings were published in 1985 in the two-volume book "Fat Science 1983" by Elsevier Publishers as volume 11 in the series "Development in Food Sciences".

The Congress was at its second edition in Hungary and it was organized by the Hungarian Scientific Society for Food Industry under the auspices of the Complex Committee of Food Sciences of Hungarian Academy of Sciences, and the Ministry of Agriculture and Food.

The Congress attracted numerous specialists from over 29 countries.

The Congress was a sum of three conferences about "Trends of development in the food industry and, within this, in the vegetable fat production" by I. Kovacs, "The technology of margarine. A tailor-made basic food" by K. F. Gander, "The importance of lipid research in medicine : requirements, utilization of results" by Gy. Biro and L. Romics (in the "Opening Session") and 100 scientific papers in 9 sections : Chemistry and Analysis : Raw Materials and Oilseed Proteins ; Nutrition, Biological Effects, Metabolism ; Processings ; Shortenings, Margarine, Edible Fats ; Soaps, Detergents, Cosmetics, Other Products ; Autoxidation ; Rapeseed Oil and Protein ; Effect of Heating on Fats.

Two other special symposia were held on : "The Role of HDL in the Pathogenesis of Arteriosclerosis" ; "Control of Hyperlipoproteinaemias, Prevention, Diet and Drug Therapy".

The opening speach was delivered by J. Hollo, Member of the Hungarian Academy of Sciences, Central Institute for Chemistry, and Chief Editor of these two volumes.

The associate editors were : M. Keltai from the National Institute of Cardiology of Budapest, M. Jeranek from the Research Institute from Vegetable Oil and Detergent Industry and D. Torley from the Department of Biochemistry and Food Technology, Technical University of Budapest.

In the "Chemistry and Analysis" section the issues dealt mainly with the determination of structure and composition of acids, proteins and lipids from food, oils, cheese etc., by means of chromatography or spectrophotometry.

The authors from this section presented technico-economical information about means of ensuring raw materials in different countries such as Hungary, India, etc. and the new technical processes for obtaining oil and proteins production as well as the physico-chemical characteristics of the latter.

Important theoretical and practical aspects were presented within the "Nutrition, Biological Aspects of Effects, Metabolism" section : an example is a study of the actual situation in the fats and edible oils industry. There were also communicated data about the analysis of lipids, biomass, determination of molecular composition of lipopeptidophosphoglycans, about bioorganic synthesis of glyceride standard, etc.

In the section "Processing" there were communicated issues about proteins and emulsifiers, biological waste-water treatment in vegetable oil industry.

Papers about margarine, palm oil, stability of fats taste and fat products were communicated in the section "Shortenings, Margarine, Edible Fats".

New types of polyfunctional detergents and problems about reutilisation of fats from various sources in cosmetic indusry, in pharmaceutical industry, were the subjects of the communications in the section : "Soaps, Detergents, Cosmetics, Other Products".

Problems about polyunsaturated lipids oxidation, sitosterol oxidation, oils oxidation and factors which influence the oxidation were presented in the "Autooxidation" section.

The works of "Rapeseed Oil and Protein" section dealt with sulphur compounds distribution in rapeseed oil, corrosion by rapeseed oil processing, influence of the kind of catalysts ; influence of nickel and inhibitors on the properties of rapeseed oils.

The results of the research work concerning the decay-processes and stability of the heat-induced deterioration through distillation of fat during seed-roasting were presented in the section "Effect of Heating on Fats".

Themes of great importance were communicated with the "Special Symposium" Section I and II referring to the effects of fats and lipids and their compounds from alimentary diet on the healthy and sick human, and animal organisms (chronic diabetes, ischaemic diseases, perovascular diseases, renal diseases, liver and biliary diseases, arterosclerosis ; in metabolism etc.) and in their prevention, diet and drug therapy.

Angela Lupu
Polytechnic Institute, Bucharest

KIRSTEN POLLMER, HANS-HEINZ EMONS, "Ein Beitrag zur Koordinations-Chemie konzentrierter Elektrolytlössungen" ("A contribution to the coordination chemistry of concentrated solutions of electrolytes"), Akademie Verlag, Berlin, 1986, 107 p.

This little book, published in the series "Abhandlungen der Sächsischen Akademie der Wissenschaften zu Leipzig. Matematisch-naturwissenschaftliche Klasse", deals with an important problem, and reviews the literature as well the author's experience, related to the solvent-solute interactions, interpreted in terms of coordination chemistry.

In the Introduction (Chapter 1, pp. 5—12) the authors outline the problem in general terms and present a short history of the concepts in this field.

Chapter 2 (pp. 12—28) introduces the coordination chemistry concepts applied to electrolyte solutions and the physical methods used for their investigation. Thus, this chapter deals with the coordinating properties of solvents, structure determinations in concentrated electrolyte solutions, investigated with the aid of nuclear magnetic resonance, Raman and infrared spectroscopy, X-ray diffraction methods. The solvation of Al^{3+}, Mg^{2+}, Li^{+} and Cl^{-} ions is discussed in detail.

Chapter 3 (pp. 29—30) presents the methods used in their own experimental investigations of aqueous or nonaqueous solutions containing the ions mentioned above.

Chapter 4 (pp. 31—94) is a comprehensive and detailed discussion of the authors' results on the solvation of LiCl, $MgCl_2$ and $AlCl_3$ in solvent mixtures, with a broad range of physical methods.

A large number of solubility isotherms for various systems containing one of the three salts cited, water and miscible organic component (glycerine, ethylene glycole, methanol, ethanol, propanol, acetic acid, dioxane, DMF, DMSO etc.) are illustrated. Solid solvates were isolated and investigated with the aid of crystallographic methods. Density, viscosity, IR-Raman spectral data, ^{27}Al NMR spectra, are all discussed in some detail.

The conclusions are summarised in Chapter 5 (pp. 94—98). This detailed investigation throws more light upon the nature of the solvated species formed in the aqueous solutions of various salts and provides experimental proof that the solvates formed are actually complexes of the cation with coordinated solvent molecules.

A list of literature references, containing 281 quotations, concludes the work.

This booklet is a somewhat unusual publication, since it is more detailed than just a review, much larger than a common research paper and deals with a narower subject than the title would imply. It looks like a Ph. D. thesis, but it has two authors and contains the results of a larger group of investigators.

The book can be of interest for both the coordination and the physical chemist, and provides much useful information for the specialised reader.

Ionel Haiduc
Cluj-Napoca University
Faculty of Chemistry

ORSZÁGOS MŰSZAKI INFORMÁCIÓS KÖZPONT ÉS KÖNYVTÁR 1883

NOTE POUR LES AUTEURS

La Revue Roumaine de Chimie publie des articles en anglais, français, russe, allemand ou espagnol. Les auteurs sont priés d'envoyer des articles et des comptes rendus inédits.

Les manuscrits seront dactylographiés à double interligne. La bibliographie, les tableaux et la légende des figures seront placés après le texte.

Si l'article fait partie d'une série numérotée, la partie précédente sera donnée comme première référence.

Chaque article sera précédé d'un résumé comprenant quinze lignes au maximum.

Les références bibliographiques dans le texte seront faites par des exposants sans parenthèses et paraîtront à la fin de l'ouvrage.

Les publications prériodiques mentionnées dans la bibliographie seront présentées suivant les prescriptions internationales : le nom de l'auteur précédé de l'initiale du prénom, le titre du périodique abrégé conformément à Chemical Abstracts et souligné par une ligne, le numéro du tome indiqué par des chiffres arabes et souligné par deux lignes, suivi de la première page de l'article : à la fin, l'année de la parution sera placée entre parenthèses. Le numéro de la revue ne sera pas indiqué si les pages du volume sont numérotées consécutivement.

Les textes des livres ou traités inclueront : le nom des auteurs, précédés de l'initiale du prénom, le titre du livre entre guillemets et sans être souligné, le numéro du tome précédé par l'abréviation « vol. » (ou « Bd. »), le numéro de l'édition, les éditions (the publisher), la localité de la parution du livre, l'année de la parution et la page de la référence précédée(s) par l'abréviation « p » (ou « S »).

Les brevets seront indiqués comme suit : l'auteur ou la firme, le pays et le numéro du brevet, la date de la revue (*Chem. Abstr.*). Par. ex. : M. Jones (to Union Carbide Co.). Brit. Pat. 610 238, 2 Sept. 1959 : cf. *Chem. Abstr.*, **54**, 12808 (1960).

Si la référence n'a pas été lue en original, on indiquera aussi la revue de références consultée.

Les diagrammes seront tracés à l'encre de Chine sur papier calque. Les tableaux et es figures (en nombre strictement nécessaire), ainsi que les courbes dans des figures seront numérotés par des chiffres arabes. Leur explication sera donnée dans la légende des figures. Prière de ne pas inscrire les mêmes données dans les tableaux et les figures. Chaque tableau aura un titre. On indiquera dans le texte la place approximative des tableaux et des figures. Les formules chimiques seront incluses dans le text ; en outre, elles seront transcrites sur papier calque à l'encre de Chine.

Les auteurs sont priés d'indiquer les caractêres italiques (en soulignant les lettres au crayon), ainsi que tout autre caractère spécial : les préfixes, *ortho*, *meta*, *para*, *cis*, *trans*, etc. seront soulignés pour indiquer leurs caractères italiques, et ne seront jamais écrits avec des majuscules.

Aucune correction à la main ne sera admise sur le manuscrit. Les corrections seront frappées à la machine. Les lettres grecques ou d'autres symboles spéciaux seront insérés à la main à l'encre clairement.

Le manuscrit sera signé par l'auteur.

Le titre courant aura 50 lettres au maximum.

L'entière responsabilité du contenu des articles appartient aux auteurs.

Sur demande on peut obtenir une note plus complète.

PRINTED IN ROMANIA

1988 AUG 0 8

TRAVAUX PARUS AUX ÉDITIONS DE L'ACADÉMIE DE LA RÉPUBLIQUE SOCIALISTE DE ROUMANIE

ELENA CEAUŞESCU, **Răşini de hidrocarburi**, vol. 1, 1988, 344 p.
ELENA CEAUŞESCU, **Progrese în chimia şi tehnologia polimerilor**, 1986, 446 p.
ELENA CEAUŞESCU, **Forschungen im Bereich der Chimie und Technologie der Polymere**, 1986, 444 p.
ELENA CEAUŞESCU, **Cercetări în chimia şi tehnologia polimerilor**, 1983, 520 p.
ELENA CEAUŞESCU, **Noi cercetări în domeniul compuşilor macromoleculari**, 1981, 536 p.
ELENA CEAUŞESCU, **Polimerizarea stereospecifică a izoprenului**, 1979, 307 p.
ELENA CEAUŞESCU, **Research work on synthesis and characterization of macromolecular compounds. Contributions**, 1974, 251 p.
I G. MURGULESCU, **Introducere în chimia fizică, Vol. I. 1. Atomi, molecule, legătură chimică**, 1976, 560 p.
I. G. MURGULESCU, V. EM. SAHINI, **Introducere în chimia fizică, Vol. I. 2. Structura şi proprietăţile moleculelor**, 1979, 604 p.
I. G. MURGULESCU, E. SEGAL, **Introducere în chimia fizică, Vol. II. 1. Teoria molecular-cinetică a materiei**, 1979, 1036 p.
I. G. MURGULESCU, TATIANA ONCESCU, E. SEGAL, **Introducere în chimia fizică, Vol.II. 2. Cinetică chimică şi cataliză**, 1981, 1024 p.
I. G. MURGULESCU, J. PĂUN, **Introducere în chimia fizică, Vol. I. 3. Nucleul atomic, reacţii nucleare, particule elementare**, 1982, 606 p.
I. G. MURGULESCU, RODICA VÎLCU, **Introducerea în chimia fizică. Vol. III. Termodinamica chimică**, 1982, 624 p.
I. G. MURGULESCU, O. M. RADOVICI, **Introducere în chimia fizică. Vol. IV. Electrochimia**, 1986, 410 p.
CRISTOFOR I. SIMIONESCU, VALERIA GORDUZA, **Implicaţii bioenergetice ale coloranţilor**, 1988, 208 p.
R. VÎLCU, M. LECA, **Termodinamica polimerilor prin cromatografie de gaze**, 1987, 238 p.
I. ZUGRĂVESCU, M. PETROVANU, **Cicloadiţii 3+2 dipolare**, 1987, 446 p.
RAUL MIHAIL, ION GROZEANU, **Estimarea secvenţială aplicată sistemelor chimice**, 1986, 406 p.
M. BREZEANU, I. PATRON, M. ANDRUH, **Combinaţii complexe polinucleare şi aplicaţiile lor**, 1986, 244 p.
A. T. BALABAN et. al., **Labelled Compounds and Radiopharmaceuticals Applied in Nuclear Medicine**, coédition avec John Wiley and Sons, 1986, 742 p.
D. PURDELA, **Nomenclatura chimiei organice — IUPAC**, 1986, 451 p.
PETRU BUDRUGEAC, **Probleme de chimie**, 1986, 280 p.
T. ONCESCU, S. G. IONESCU, **Conversie fotochimică şi stocare de energie**, 1985, 272 p.
V. DRĂGUŢAN, A. T. BALABAN, M. DIMONIE, **Olefin Metathesis and Ring-Opening Polymerization of Cyclo-Olefins**, coédition avec John Wiley and Sons, 1985, 544 p.
C. LITEANU, I. RÎCĂ, **Optimizarea proceselor analitice**, 1985, 360 p.
N. PERESCU, **Chimia extracţiei cu solvenţi şi aplicaţii**, 1985, 212 p.
V. E. SAHINI, M. HILLEBRAND, **Chimie cuantică în exemple şi aplicaţii**, 1984, 378 p.
GH. MARCU, **Chimia compuşilor coordonativi**, 1984, 415 p.
E. CORDOS, C. MANOLIU, **Spectrometria de absorbţie şi florescenţa atomică**, 1984, 178 p.
C. BODEA, **Tratat de biochimie vegetală, p. II, t. V**, 1984, 438 p.
N. ASANDEI, A. GRIGORIU, **Chimia şi structura fibrelor**, 1983, 395 p.
N. IONESCU, M. CALDARARU, **Oxidarea catalitică a olefinelor inferioare**, 1983, 178 p.
C. I. SIMIONESCU, F. DANES, **Originea vieţii**, 1983, 110 p.
C. BODEA, **Tratat de biochimie vegetală, p. II, t. IV**, 1982, 408 p.
CR. SIMIONESCU, VALERIA GORDUZA, **Polimeri biocompatibili şi biologic activi**, 1980, 479 p.
M. FLORESCU, **Metode ştiinţifice în dezvoltarea industriei chimice moderne**, 1979, 495 p.
C. GH. MACAROVICI, **Analiza chimică cantitativă anorganică**, 1979, 457 p.

ISSN 0035-3930

I. P. INFORMAŢIA c. 2182

43 426

Lei 40

F 1103

ACADÉMIE DE LA RÉPUBLIQUE SOCIALISTE DE ROUMANIE

REVUE ROUMAINE DE CHIMIE

66

TOME 33
N° 7
Juillet 1988

Rev. Roumaine Chim.

RRCHAX, 33, 7, p. 671–772 (1988), Bucarest

EDITURA ACADEMIEI REPUBLICII SOCIALISTE ROMÂNIA

ACADÉMIE DE LA RÉPUBLIQUE SOCIALISTE DE ROUMANIE

COMITÉ DE RÉDACTION

Rédacteur en chef:

I. G. MURGULESCU, membre de l'Académie de la République Socialiste de Roumanie

Rédacteurs en chef adjoints:

A. T. BALABAN et V. EM. SAHINI, membres correspondants de l'Académie de la République Socialiste de Roumanie

Collège de rédaction:

EM. BRATU, ELENA CEAUŞESCU, ECATERINA CIORĂNESCU-NENITZESCU, CR. SIMIONESCU, membres de l'Académie de la République Socialiste de Roumanie; P. SPACU, membre correspondant de l'Académie de la République Socialiste de Roumanie; M. BANCIU, M. D. GHEORGHIU, I. HAIDUC, D. I. MARCHIDAN, G. NIAC et D. SĂNDULESCU

La Revue Roumaine de Chimie paraît 10 fois par an. Toute commande de l'étranger sera adressée à ROMPRESFILATELIA — sectorul Export-Import Presă, P. O. Box 12—201, télex 10376 prsfi r 78 104 Bucarest, Calea Griviței nr. 64—66, București, Roumanie

Les manuscrits, les livres et les revues proposés en échange, ainsi que toute correspondance seront envoyés à la rédaction :

REVUE ROUMAINE DE CHIMIE
125, Calea Victoriei, 79717 Bucarest, Roumanie, téléphone 50 76 80

EDITURA ACADEMIEI REPUBLICII SOCIALISTE ROMÂNIA
125, Calea Victoriei, 79717 Bucarest, Roumanie, téléphone 50 76 80

REVUE ROUMAINE DE CHIMIE

Tome 33, N° 7 **Juillet 1988**

MARIUS ANDRUH, G. FILOTI and MARIA BREZEANU, On the electronic structure of bis(isothiocyanato)tetrakis(4-benzoyl-pyridine)iron(II) . . . 673–676

O. RADU and CONSTANŢA GHEORGHIU, As (III)–HCl–H_2O system. Part II. Solid-liquid state . . . 677–683

J. EPPERLEIN and B. BLAU, The UV-VIS-spectral behaviour of arylazo compounds. II. The UV-VIS absorption spectra of 4-amino-substituted azobenzenes . . . 685–691

H. M. ABU EL-NADER and M. R. MOSTAFA, Kinetics and mechanism of acid hydrolysis of propionamide in methanol-water mixtures . . . 693–698

ALEXANDRU T. BALABAN, Chemical graphs. Part 49. Open problems in the area of condensed polycyclic benzenoids: topological stereoisomers of coronoids and congeners . . . 699–707

OVIDIU IVANCIUC, Chemical graph polynomials. 1. The polynomial description of generalized chemical graphs . . . 709–717

CORNELIA UNCUŢA, MIRCEA D. GHEORGHIU, FILIP CHIRALEU, MARIETA PLĂVEŢI, MIHAI ELIAN and ALEXANDRU T. BALABAN, Reaction of pyrylium salts with nucleophiles. XXI. Unexpected formation of 6,6-dimethyl-5-isopropyl-2,4-cyclohexadienylidene-1-imines from primary amines and 2,6-diisopropyl-pyrylium salts . . . 719–727

HORIA PETRIDE and DAN RĂILEANU, Mesoionic oxazolones. II. Unstable non-acylated compounds . . . 729–739

O. H. HISHMAT, A. H. ABD EL RAHMAN, H. I. EL-DIWANI and SH. M. ABU-BAKR, Synthesis of substituted furobenzopyrones . . . 741–745

ILSE BACALOGLU, HANS-HORST GLATT and MAMADOU FOULA BARRY, Aminoazoleimines. 5. Molecular orbital calculations in benzylidene-aminoazole series by the Mosp method (in German) . . . 747–751

MIRCEA D. GHEORGHIU and EMILIA OLTEANU, The stereochemistry of Olah's reduction of bicyclo[2.2.1]heptene derivatives. A proof for a concerted reaction mechanism? . . . 753–754

A. M. FAHMY, KH. M. HASSAN, A. A. KHALAF and R. A. AHMED, Synthesis of some new β-lactams, 4-thiazolidinones and pyrazolines . . . 755–761

VALERIU V. JINESCU, A fundamental property of matter. Part I . . . 763–772

Rev. Roumaine Chim. **33**, 7, 671–772 (1988), Bucarest

Revue Roumaine de Chimie, **33**, 7, 673–676 (1988)

ON THE ELECTRONIC STRUCTURE OF BIS(ISOTHIOCYANATO)TETRAKIS(4-BENZOYL-PYRIDINE)IRON(II)

MARIUS ANDRUH [a], G. FILOTI [b] and MARIA BREZEANU [a]

[a] **Laboratory of Inorganic Chemistry, Faculty of Chemical Technology, Polytechnic Institute, str. Dumbrava Roşie no. 23, Bucharest, Romania**

[b] **Institute of Physics and Material Technology, I. C. Fiz., Postal Box 07, Măgurele, Romania**

Received November 14, 1987

The electronic structure of a new iron(II) coordination compound, $[Fe(4Bz-Py)_4(NCS)_2]$, where 4Bz–Py stands for 4-benzoyl-pyridine, is discussed. According to the electronic absorption spectrum, magnetic measurements and Mössbauer data, a *trans*-octahedral configuration (D_{4h} symmetry) with a ^5E_g ground state of the iron(II) ion is assigned.

1. INTRODUCTION

Eighty years ago, Grossmann and Hünseler [1] reported the synthesis of the yellow compound $[Fe(Pyridine)_4(NCS)_2]$; in 1914, Professor G. Spacu[2] prepared a violet form with the same stoichiometry. The history of these two compounds is very interesting: for more than 50 years they were considered to be *cis* and *trans* isomers, and have been the subject of controversy in many papers.[3–7] By means of Mössbauer spectroscopy and X-ray crystallographic data[6–8] it was finally concluded that the yellow form has indeed a *trans* configuration but the violet modification is, in fact, the yellow form with a small amount of some iron (III) derivative; the intense colour of that latter modification is due to a ligand→iron(III) charge transfer transition.

This phenomenon, i.e. the existence of two differently coloured forms for the same stoichiometry, was found to be general for other coordination compounds of the type $[FeL_4(NCS)_2]$,where L represents pyridine or its substituted derivatives.[9–11]

In recent years, many papers dealt with experimental and theoretical studies of the $[FeL_4(NCS)_2]$ – type complexes, with special emphasis on their electronic structures.[12–14] In preceding papers we reported on the synthesis, spectral and magnetic properties of several nickel (II) and cobalt(II) coordination compounds with 4-benzoyl-pyridine(4Bz-Py);[15–16] two other papers dealt with the non-isothermal decomposition kinetics of the nickel(II), cobalt(II) and iron(II) complexes with this organic ligand.

This paper is concerned with the electronic structure of bis(isothiocyanato) tetrakis-(4-benzoyl-pyridine)iron (II) complex.

2. EXPERIMENTAL

Bis(isothiocyanato)tetrakis(4-benzoyl-pyridine) iron(II) was obtained as follows: a solution of 4-benzoyl-pyridine (0.73 g) in 15 mL ethanol was mixed with a solution of iron(II) sulphate hepta-hydrate (0.28 g in 15 mL water) and then 15 mL hot solution containing 0.5 g KSCN in water was added. The red-violet precipitate was filtered off, washed with ethanol and dried *in vacuo* over P_2O_5. Analytical data: found: 67.0%C; 4.3% H; 10.1% N; 7.0%S; calc: 66.4 % C; 4.0 %H; 9.3 % N; 7.1 % S.

The compound is soluble in hot methanol or acetone, giving yellow solutions; from these solutions, by cooling, we get only red-violet crystals. Using solvents such as chloroform, DMF or diethyl ether we get red-violet solutions. By carrying the synthesis in the presence of a small amount of ascorbic acid, only the red-violet form precipitates.

The electronic absorption spectrum of $[Fe(4Bz\text{-}Py)_4(NCS)_2]$ was recorded both in methanolic solution (for the yellow form) and by the diffuse reflectance technique (for the red-violet form) within the range 28,000—50,000 cm^{-1}. The spectrum of the free ligand was recorded in methanolic solution.

3. RESULTS AND DISCUSSION

The shoulder and the band occurring at ~220 nm and 258 nm in the solution spectrum of bis(isothiocyanato)tetrakis(4-benzoyl-pyridyne) iron(II) were assigned to the organic ligand (Fig. 1). Assuming that the band shape at 258 nm is gaussian, one may calculate the oscillator strength, using the formula:

$$f = 4 \cdot 6 \cdot 10^{-9} \varepsilon_{\max} \sigma,$$

where $\varepsilon_{\max}$ is the molar extinction coefficient at the band maximum and σ is the half-bandwidth (in cm^{-1}). The calculated value of the oscillator strength ($f = 1.11$) for this band suggests an allowed $\pi \rightarrow \pi^*$ — type transition.

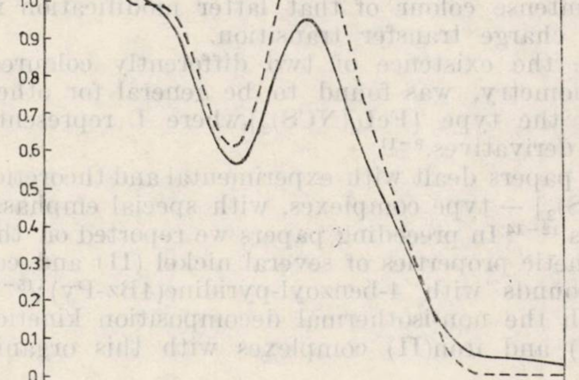

Fig. 1. — Absorption spectra of the complex (———) and of the free ligand (— — — —) in the range 28000—50000 cm^{-1} in methanol.

The diffuse reflectance spectrum of the complex is represented in figure 2. The intense (red-violet) colour of our compound is due to the band occurring at 535 nm (18,690 cm^{-1}); this band disappears in the spectrum of the yellow solution and is assigned to a ligand→iron(III) charge transfer.[8]

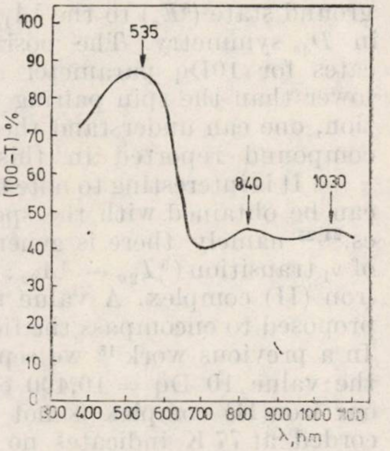

Fig. 2. — The reflectance spectrum of the complex $[Fe(4Bz-Py)_4(NCS)_2]$.

It is well known that compounds of the type $[Fe(II)A_4X_2]$ (where A stands for an organic ligand and X for halides or pseudohalides) with a ground state $^5T_{2(g)}$ have a $d-d$ spin allowed transition $^5E_{(g)} \rightarrow {}^5T_{2(g)}$ in the near infrared, split into two components.[19-21] This splitting was reported as being due to a dynamic Jahn-Teller effect or to the inequivalency between ligands or, of course, to both mentioned effects.[21]

The value of the magnetic moment ($\mu = 5.27$ BM) as well as the Mössbauer spectra (see below) suggest a splitting of the ground state into two levels (D_{4h} symmetry):

$$^5T_{2g} \rightarrow {}^5E_g + {}^5B_{2g}$$

(the value of $\mu = 5.66$ BM corresponds to a $^5T_{2g}$ ground term in a pure octahedral symmetry[9]).

Mössbauer spectra consisted of quadrupole-split doublets, as expected for distorted octahedral high-spin iron (II) complexes. Mössbauer data are given in Table 1 (we present also by comparison the Mössbauer parameters for $[FePy_4(NCS)_2]$). The room temperature isomer shifts, δ, are almost identical for the two complexes since δ depends on the value of the s-electrons wave-function only at the nucleus and one does not expect it to reflect changes of the organic ligand.[22] The magnitude of quadrupole splitting, ΔE, may be used to deduce the orbital degeneracy of the iron (II) ground state.[14] Since an orbitally degenerate ^5E_g state can produce a quadrupole splitting of the most 2 mm · s^{-1}, we conclude that the present results (Table 1) are consistent with a ^5E_g ground state, corresponding to the d_{xy}, d_{yz} doublet lying lowest. At the same time, this result suggests either an axially elongated octhaedral structure for the two coordination compounds or an in-plane field strength stronger than the axial one (in agreement with the position of ligands: NCS^-, pyridine, and 4-benzoyl-pyridine, in the spectrochemical series[16,23]).

Table 1

Mössbauer parameters and magnetic moments

Compound	T, K	δ, mm · s^{-1}	ΔE_Q, mm · $^{-1}$	μ, BM	Ref.
$[FePy_4(NCS)_2]$	291	1.21	1.54	5.47	22
$[Fe(4Bz-Py)_4(NCS)_2]$	291	1.25	1.95	5.27	this work

The solid state electronic absoption spectrum recorded at room temperature for bis(isothiocyanato)tetrakis(4-benzoyl-pyridine)iron(II) is typical for high-spin iron(II) complexes in a tetragonally distorted octahedral environment (Fig. 2). The two absorptions in the near infrared region (9,700 cm^{-1}; 11,900 cm^{-1}) are assigned to electron transitions from the ground state (^5E_g) to the $^5A_{1g}$ and $^5B_{1g}$ levels derived from ^5E_g upper state in D_{4h} symmetry. The position of these two absorption maxima indicates for 10Dq parameter a value in the range 10,000−11,000 cm^{-1}, lower than the spin pairing energy value.[19,20] According to this observation, one can understand the paramagnetic behaviour of the coordination compound reported in this paper.

It is interesting to note that quantitative data relating to field strength can be obtained with the spectra of the corresponding nickel (II) complexes,[24,25] namely there is generally a good correlation between the position of ν_1 transition ($^3T_{2g} \leftarrow {}^3A_{2g}$; 10 Dq) and the spin state of the corresponding iron (II) complex. A value for ν_1 in the range 10,400−12,750 cm^{-1} was proposed to encompass the field strength at the spin crossover for iron(II). In a previous work [15] we reported for the complex $[\mathrm{Ni(4Bz-Py)_4(NCS)_2}]$ the value 10 Dq = 10,400 cm^{-1} which suggests that a spin crossover in our iron(II) complex is not likely. Indeed, the Mössbauer spectrum recorded at 77 K indicates no lowering in the δ and ΔE_Q values ($\delta = 1.33\ \mathrm{mm \cdot s^{-1}}$; $\Delta E_Q = 2.44\ \mathrm{mm \cdot s^{-1}}$) proving the existence at that temperature of only a quintet ground state.

REFERENCES

[1] H. Grossmann and F. Hünseler, *Z. anorg. allg. Chem.*, **46**, 370 (1905).

[2] G. Spacu, *Anal. Şti., Univ. Iaşi*, **8**, 175 (1914); **9**, 347 (1915).

[3] O. Binder and P. Spacu, *Compt. rend.*, **200**, 1405 (1935).

[4] P. Spacu, M. Teodorescu and C. Lepădatu, *Rev. Roumaine Chim.*, **9**, 39 (1964).

[5] P. Spacu and C. Lepădatu, *Ann. Chim.*, **54**, 275 (1964).

[6] C. D. Burbridge, M. J. Cleare and D. M. L. Goodgame, *J. Chem. Soc. (A)*, **1966**, 1698.

[7] N. E. Erickson and N. Sutin, *Inorg. Chem.*, **5**, 1834 (1966).

[8] I. Søtofte and S. E. Rasmussen, *Acta Chem. Scand.*, **21**, 2028 (1967).

[9] C. D. Burbridge, D. M. L. Goodgame and M. Goodgame, *J. Chem. Soc. (A)*, **1967**, 349.

[10] C. D. Burbridge and D. M. L. Goodgame, *Inorg. Chim. Acta*, **4**, 231 (1970).

[11] D. M. L. Goodgame, M. Goodgame, M. A. Hitchman and M. J. Weeks, *Inorg. Chem.*, **5**, 635 (1966).

[12] K. Burger, G. Liptay, L. Korecz, I. Kirally and E. Papp-Molnar, *Magyar Kém. Folyóirat*, **77**, 90 (1971).

[13] M. Gerloch and R. F. McMeeking, *J. Chem. Soc., Dalton*, **1975**, 2452.

[14] J. S. Haynes, S. J. Retting, J. R. Sams, R. C. Thompson and J. Trotter, *Canad. J. Chem.*, **64**, 429(1986).

[15] M. Brezeanu, M. Andruh and N. Stănică, *Acta Chim. Hung.*, **124**, 391 (1987)

[16] M. Andruh, C. I. Lepădatu and M. Brezeanu, *Inorg. Chim. Acta*, **131**, 158 (1987).

[17] M. Andruh, E. Urbanovici, M. Brezeanu and E. Segal, *Thermochim. Acta*, **95**, 257 (1985).

[18] E. Urbanovici, E. Segal, M. Andruh and M. Brezeanu, *Thermochim. Acta*, **118**, 309(1987).

[19] K. Madeja and E. König, *J. Inorg. Nucl. Chem.*, **25**, 377 (1963).

[20] P. Spacu and C. I. Lepădatu, *J. Amer. Chem. Soc.*, **88**, 3221 (1966).

[21] P. Spacu, M. Teodorescu and C. I. Lepădatu, *Z. Phys. Chem. (Frankfurt)*, **88**, 285(1974).

[22] J. F. Duncan, R. M. Golding and K. F. Mok, *J. Inorg. Nucl. Chem.*, **28**, 1114 (1966).

[23] M. Andruh, C. I. Lepădatu and M. Brezeanu, *Rev. Roumaine Chim.*, **32**, 1033 (1987).

[24] M. A. Robinson, J. D. Curry and D. H. Busch, *Inorg. Chem.*, **2**, 1178 (1963).

[25] K. H. Sugyarto and H. A. Goodwin, *Austral. J. Chem.*, **40**, 775 (1987).

Revue Roumaine de Chimie, **33**, 7, 677–683 (1988)

As(III)—HCl—H_2O SYSTEM. PART II[1]

SOLID-LIQUID STATE

O. RADU [a] and CONSTANȚA GHEORGHIU [b,*]

[a] Central Institute of Chemistry, Institute for Research and Production of Semiconductors, Sos. Gării Cățelu No. 5, Sector 3, Bucharest, Romania

[b,*] Polytechnic Institute of Bucharest, Dept. of Chemical Technology, Bucharest, Romania

Received February 22, 1987

The solid -liquid state of arsenic trioxide in aqueous solution of hydrocloric acid was studied. Assuming the interphase equilibrium to be exclusively chemical, a method was devised for determining the solubility by detecting the transition from two phases to homogeneous through the limits of solubility of homogeneous phase ; the influence of physical factors that may perturb the chemical equilibrium is not considered. Thus, the standard values of molar solubility of arsenic trioxide are determined for any concentration of HCl and the standard condition of interphase equilibrium is established ; the temperature dependence of this condition is also found with a fair accurarcy. The practical implications of the results are emphasized.

In the frist part of this series [1] the possibilities of characterizing and determining the equilibrium states through relations between the initial state (the parameters of formation interaction whose values are known) and final state (the parameters of equilibrium state were studied ; these relations are underlined by the strictly chemical nature of interphase equilibria.

1. CHARACTERIZATION OF STANDARD STATE

The solid-liquid interphase equilibrium is governed by the following succession of chemical equilibrium :

$$0.5\,As_2O_3 \overset{1.5\,H_2O}{\rightleftarrows} As(OH)_3 \underset{H_2O}{\overset{HCl}{\rightleftarrows}} As(OH)_2Cl \underset{H_2O}{\overset{HCl}{\rightleftarrows}} As(OH)Cl_2 \underset{H_2O}{\overset{HCl}{\rightleftarrows}} AsCl_3$$

Solid phase liquid phase (solution)

The initial state corresponding to $As_2O_3 + HCl + H_2O$ is univocally determined by parameters C_{HCl}, R and V_{HCl}.

---

* Deceased

The restrictions which affect the number of components (C) and of variables (V) are imposed by the range of stability of As_2O_3 determined by C_{HCl} (1):

C_{HCl}	C	V
>7.5	7	5
<7.5	6	4

The phase law for the isothermal system considered here ($F = C - V$) applies with the restrictions above.

The equilibrium condition is established on the basis of determinations of solubility of arsenic trioxide in hydrochloric acid throughout the whole range of values C_{HCl}, the data available being restricted to $C_{HCl} \leqslant 5$.[2]

1.1. DETERMINATION OF STANDARD SOLUBILITY

The principle of the method consists of evidencing several final states generated by one single initial state. The multiplicity of apparently final states depends on the history of the system and should be related to various physical factors characteristic for crystallization (suprasaturation, subcooling, spontaneous or wall nucleation, etc.).

The phenomenon takes place only at high concentrations, $C_{HCl} > 5$

The action of physical factors which perturb the chemical equilibrium, responsible for the multiplicity of final metastable states, ceases at two-phase-single phase separation so that the transition may be adequately characterized by the value of R which determines it. The parameter of characterization is supplied by the limit of stability of the homogeneous phase *i.e.* the lowest R value that ensures the stability of the homogeneous state at constant C_{HCl} and T. The experimental determination of a set of $C_{HCl} - R_{lim}$ values allows one to calculate the solubility of arsenic (that is As_2O_3) by means of the relations between the states.[1]

1.2. EXPERIMENTAL

Arsenic trioxide is dissolved in warm hydrochloric acid under pressure or in boiling refluent hydrochloric acid, as described elsewhere.[1] To determine a set of $C_{HCl} - R_{lim}$ values one selects an R value which places the system in the two-phase domain at given concentration of the acid. Minute successive increases of R are effected by small controlled additions of acid (from microburette) corresponding to values of 0.075—0.050 followed by dissolutions and thermostattings for two hours until the smallest R value is obtained which ensures that the system remains homogeneous after equilibration. This is the state of $R = R_{lim}$. It is worth to note that while repeating the operations of dissolution, cooling and thermostating, the tendency of state multiplication decreases and vanishes.

Fig. II.1 shows the value of stability limit of standard homogeneous phase while in Fig. II.2 are plotted the calculated values of standard stability versus C_{HCl} (curve 1); the values obtained by other authors[2] in the range $C_{HCl} \leqslant 5$ are given for comparison (curve 2).

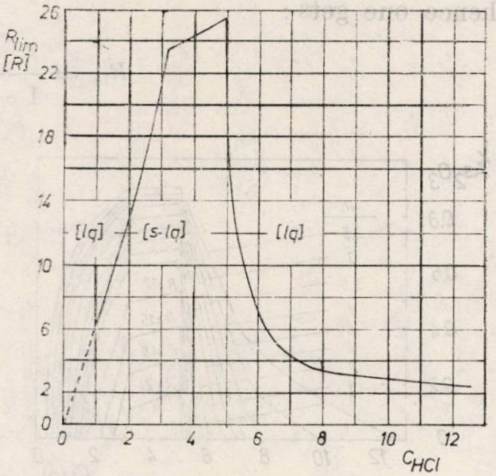

Fig. II.1. — The solid-liquid standard diagram.

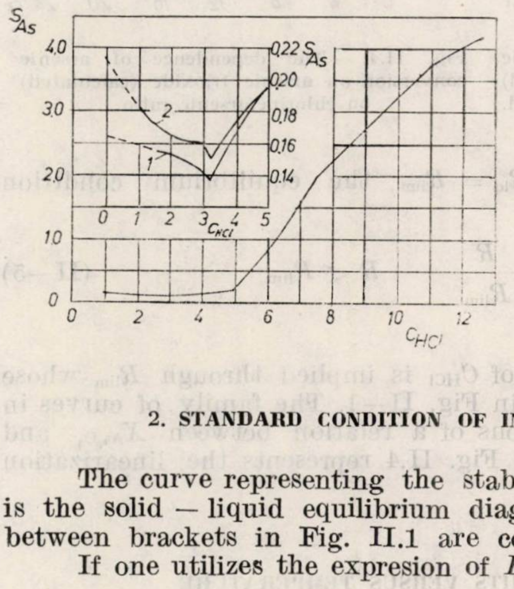

Fig. II.2. — The solubility of arsenic (gram atoms per liter) as a function of molar concentration of hydrochloric acid 1. Experimental 2. Garett et al's values. [2]

2. STANDARD CONDITION OF INTERPHASE EQUILIBRIUM

The curve representing the stability limit of homogeneous phase is the solid — liquid equilibrium diagram provided that the symbols between brackets in Fig. II.1 are considered.

If one utilizes the expresion of R in liquid phase:

$$R_{1q} = \frac{n_{Cl}}{n_{As(1q)}} \qquad (II-1)$$

and the degree of conversion of arsenic into solid arsenic trioxide:

$$X_{As_2O_3} = \frac{n_{As(s)}}{n_{As}} \qquad (II-2)$$

a relation between them is established:

$$\frac{R}{R^{lq}} = \frac{n_{As(lq)}}{n_{As}} = 1 - \frac{n_{As(s)}}{n_{As}} = 1 - X_{As_2O_3} \qquad (II-3)$$

hence one gets :

$$R_{lq} = \frac{R}{1 - X_{As_2O_3}} \qquad (II-4)$$

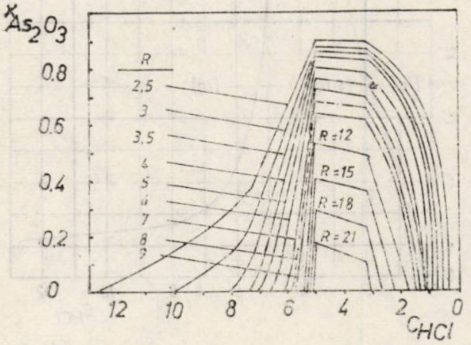

Fig. II.3. — The dependence of arsenic conversion on arsenic trioxide (calculated) on molar concentration of hydrochloric acid.

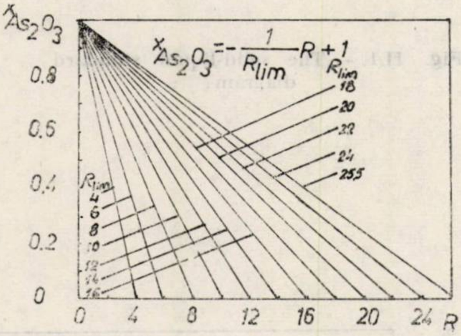

Fig. II.4. — The dependence of arsenic conversion on arsenic trioxide (calculated) on chlorine/arsenic ratio.

Because at equilibration $R_{lq} = R_{lim}$ the equilibrium condition becomes :

$$X_{As_2O_3} = 1 - \frac{R}{R_{lim}} \qquad R < R_{lim} \qquad (II-5)$$

wherein the formulation in terms of C_{HCl} is implied through R_{lim} whose values are taken from the curve in Fig. II—1. The family of curves in Fig. II.3 represents the explanations of a relation between $X_{As_2O_3}$ and C_{HCl} and the bunch of curves in Fig. II.4 represents the linearization of $X_{As_2O_3}$ with R.

3. THE SOLUBILITY LIMITS VERSUS TEMPERATURE

Temperaturea above 25° imply the vapour phase as well. Its component in conditions of closed system under pressure may not be evaluated. If one disregards the vapour phase the values of R_{lim} determined are affected by systematic errors ; these errors may be diminished by reducing to a minimum the volume available for vapours. The successive dissolutions and thermostattings at temperature are carried out in silica vessels with thick walls in which the free volume is very small. Utilization of silica allows one to see inside the vessel but brings about the danger of explosion during thermostatting. Determinations at boiling temperature were carried out in open system under reflux.

The stability limits thus obtained are plotted in Fig. II.5 and should be appreciated within the limits of accuracy and precission mentioned above. Because not relation between states of standard conditions were available, the values of $R_{\rm lim}$ may not be converted into concentration terms.

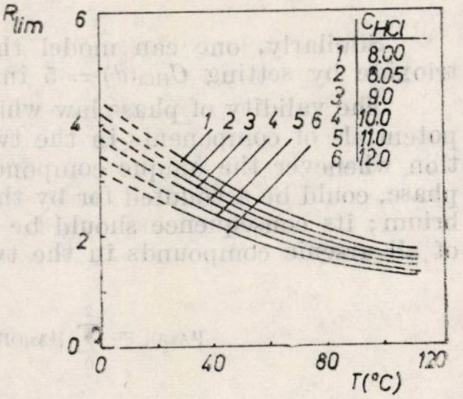

Fig. II.5.— The temperature dependence of the stability limit of homogeneous phase.

4. DISCUSSION

The interphase equilibrium should be regarded as of purely chemical nature. Therefore the equilibrium condition could be evidenced only by removing the system from under the influence of the multitude of physical factors that may perturb the chemical equilibrium at random and produce metastable states that are apprently equilibrated. The action of these factors is cancelled in solid-liquid-homogeneous transition universally characterized by the values of atomic ratio $n_{\rm Cl}/n_{\rm As}$ and concentration $C_{\rm HCl}$. The isosistic method of determination by means of this ratio — which at transition is considered the stability limit of homogeneous phase—removes the effects of physical factors upon the system, even before transition, through reiteration of identical operations. The complete set of $R_{\rm lim}$ — $C_{\rm HC}$ pairs states by itself the equilibrium condition.

The standard relations between states [1] serve to conversion in terms of standard concentration. The values of solubilities thus calculated agree to those determined by other authors [2] in a narrow concentration range ($C_{\rm HCl} < 5$) where the action of physical factors is unimportant. In this range the solubility is lower than in water probably due to the stability domain of arsenous acid whose degree of dissociation decreases with the increase of hydrogen ion concentration. For $C_{\rm HCl} > 5$ the solubility rises sharply probably in relation with formation of hydroxychlorides and then of arsenic trichloride. At $C_{\rm HCl} = 7.5$ an inflexion is present in the solubility curve which points to and confirms the formation of arsenic trichloride,[1] as a consequence of the volume variation which accompanies it.

The knoweldge of the nature and condition of equilibrium allows the obtaining of two-phase system at unperturbed chemical equilibrium.

This is possible only starting up with homogeneous phase through hydrolytic precipitation provided that in initial state the condition $C_{\rm HCl} > 5$ and $R < 25.5$ is fulfilled. One selects a value of the degree of conversion, calculates the corresponding $R_{\rm lim}$ by eqn. (II.5) and reads the $C_{\rm HCl}$ value on the equilibrium diagram. This is the dilution concentration ($C_{\rm HCl}$ (d)).

The volume of dilution water is gvien by the equation :

$$V_{H_2O(d)} = V_{HCl}\left(\frac{C_{HCl}}{C_{HCl(d)}} - 1\right)$$

Similarly, one can model the hydrolytic precipitation of arsenic trioxide by setting $C_{HCl}(d) = 5$ in the equation above.

The validity of phase law which postulates the equality of chemical potentials of components in the two phases at partial chemical dissolution whenever the unique component in solid phase is absent in liquid phase, could be accounted for by the chemical nature of interphase equilibrium; its consequence should be the equalizing of chemical potentials of all arsenic compounds in the two phases :

$$\mu_{As_2O_3} = \sum_{0}^{2} \mu_{As(OH)_{3-z}Cl_z} \qquad C_{HCl} < 7.5$$

$$\mu_{As_2O_3} = \sum_{0}^{3} \mu_{As(OH)_{3-z}Cl_z} \qquad C_{HCl} > 7.5$$

The system As(III)—HCl—H_2O in solid—liquid phase is involved in processes of interest for obtaining ultrapure arsenic. The modelling of chemical equilibrium of this state allows the control and optimization of these processes. The modelling of homogeneous state (1) holds true for all liquid phases of two-phase states.

LIST OF SYMBOLS

The parameters of initial state $As_2O_3 + HCl + H_2O$

R = n_{Cl}/n_{As}
n_{Cl} = number of gram atoms of chlorine
n_{As} = same for arsenic
V_{HCl} = the volume of HCl solution (liters)
C_{HCl} = the concentration of HCl (mol/liter)

The parameters of final solid-liquid phase

R_{lim} = the limit solubility of homogeneous phase (the ratio n_{Cl}/n_{As} at homogeneous — solid — liquid transition)
S_{As} = solubility of As in HCl (gram atom/liter)
$n_{As_{(lq)}}$ = the number of upon atoms of arsenic in liquid phase
$n_{As(s)}$ = the same in solid phase
R_{lq} = n_{Cl}/n_{As} in liquid phase
$X_{As_2O_3}$ = $n_{As(s)}/n_{As}$ = the degree of conversion of arsenic to As_2O_3

The parametrs of liquid phase

See part one of this paper [1]

REFERENCES

[1] O. Radu and C. Gheorghiu, *Rev. Roumaine Chim.*, **33**, 585 (1988).

[2] A. B. Garett, O. Holmes and A. Laube, *J. Amer. Chem. Soc.*, **62**, 2024 (1940).

Revue Roumaine de Chimie, **33**, 7, 685—691 (1988)

THE UV-VIS-SPECTRAL BEHAVIOUR OF ARYLAZO COMPOUNDS. II[1]

THE UV-VIS ABSORPTION SPECTRA OF 4-AMINO-SUBSTITUTED AZOBENZENES

J. EPPERLEIN and B. BLAU
Chemistry and Material Sciences Department, Technical University Karl-Marx-Stadt, DDR-9010 Karl-Marx-Stadt, DDR

Received January 20, 1988

Increasing concern in structure-properties-relationships together with the requirements of diminishing research costs have created a need for improved quantitative instruments to predict molecular and other properties of compounds. Prominent among these requirements is for instance the description and prediction of structure-colour-relationships in dye chemistry. In this paper, based on our foregoing publication in this journal, [1] will be given a survey on the spectral behaviour, especially the situation of the absorption maximum λ_{max}, of 4-amino-substituted azobenzenes.

THE MODEL APPROACH

Amino groups are the most convenient and widespread used donator substituents in the dye chemistry of azobenzenes. Unsymmetrically substituted azobenzenes may be considered like charge-transfer-chromogenes (cf. [1-4]). A useful segmentation is given by scheme 1.

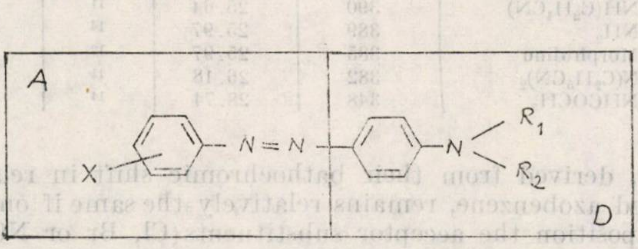

A denotes the acceptor part, **D** the donor part of the molecule. The situation of the colour-giving longest wavelength VIS-absorption band is strongly influenced by the donor strength of the R_1R_2N-group. In table 1 are listed experimental start values of azobenzenes with 36 often used amino substituents (all measurements in ethanol). The rank order of amino

Table 1

Absorption maxima of some 4-amino-substituted azobenzenes

No.	Amino-substituent	λ_{max}^{exp} in nm	$\tilde{\nu}$ in 10^3 cm^{-1}	Ref.	Increment ε_i
1	Julolidino	442	22.62	5	8.83
2	Lilolidino	425	23.53	6	7.92
3	N-Ethyl-tetrahydroquinolino	424	23.58	5	7.87
4	$N(n-C_4H_9)_2$	422	23.70	22	7.75
5	$N(n-C_3H_7)_2$	420	23.81	22	7.64
6	N-Methyl-tetrahydroquinolino	419	23.87	5	7.58
7	Tetrahydroquinolino	418	23.92	5	7.53
8	Pyrrolidino	416	24.04	12	7.41
9	$N(C_2H_5)_2$	415	24.10	7	7.35
10	$NH(i-C_3H_7)$	415	24.10	22	7.35
11	$N(C_6H_5)_2$	413	24.21	8	7.24
12	$NH(C_6H_5)$	412	24.27	8	7.18
13	$N(C_2H_5)CH_3$	411	24.33	7	7.12
14	$NH(n-C_4H_9)$	411	24.33	22	7.12
15	N-β-Cyanoethyl-tetrahydroquinolino	410	24.39	9	7.06
16	$NH(n\text{-}C_3H_7)$	410	24.39	22	7.06
17	$N(C_2H_5)C_2H_4OH$	410	24.39	4	7.06
18	$N(CH_3)_2$	407	24.57	10	6.88
19	$N(C_2H_4OH)_2$	407	24.57	11	6.88
20	$N(CH_3)CH_2C_6H_5$	406	24.63	1	6.82
21	$N(C_2H_5)C_2H_4Cl$	405	24.69	12	6.76
22	$N(CH_2C_6H_5)_2$	404	24.75	8	6.70
23	NHC_2H_5	403	24.81	22	6.64
24	$NHCH_3$	402	24.88	7	6.57
25	Piperidino	402	24.88	12	6.57
26	$NH(CH_2C_6H_5)$	400	25.00	8	6.45
27	$N(C_2H_5)C_2H_4CN$	399	25.06	11	6.39
28	$NH(C_2H_4OH)$	398	25.13	11	6.32
29	$N(C_2H_4Cl)_2$	397	25.19	13	6.26
30	$N(C_2H_4OH)C_2H_4CN$	397	25.19	11	6.26
31	$N(CH_3)C_2H_4CN$	396	25.25	11	6.20
32	$NH(C_2H_4CN)$	390	25.64	11	5.81
33	NH_2	389	25.97	14	5.75
34	Morpholino	385	25.97	12	5.48
35	$N(C_2H_5CN)_2$	382	26.18	11	5.27
36	$NHCOCH_3$	348	28.74	14	2.71

substituents, derived from their bathochromic shift in relation to the unsubstituted azobenzene, remains relatively the same if one introduces into the 4′-position the acceptor substituents (Cl, Br or NO_2 – Fig. 1). In table 2 are summarized some experimental data and the results of two approximation formulae for the bathochromic shifts.[1]

$$\Delta\tilde{\nu}_{AD} = \tilde{\nu}_0 - \tilde{\nu}_{AD} \approx \varepsilon_D + 2.27\,\varepsilon_A \tag{1}$$

$$\Delta\tilde{\nu}_{AD} = \tilde{\nu}_0 - \tilde{\nu}_{AD} \approx \varepsilon_D + 1.9 \cdot 10^{-4}\varepsilon_A \cdot \varepsilon_D \tag{2}$$

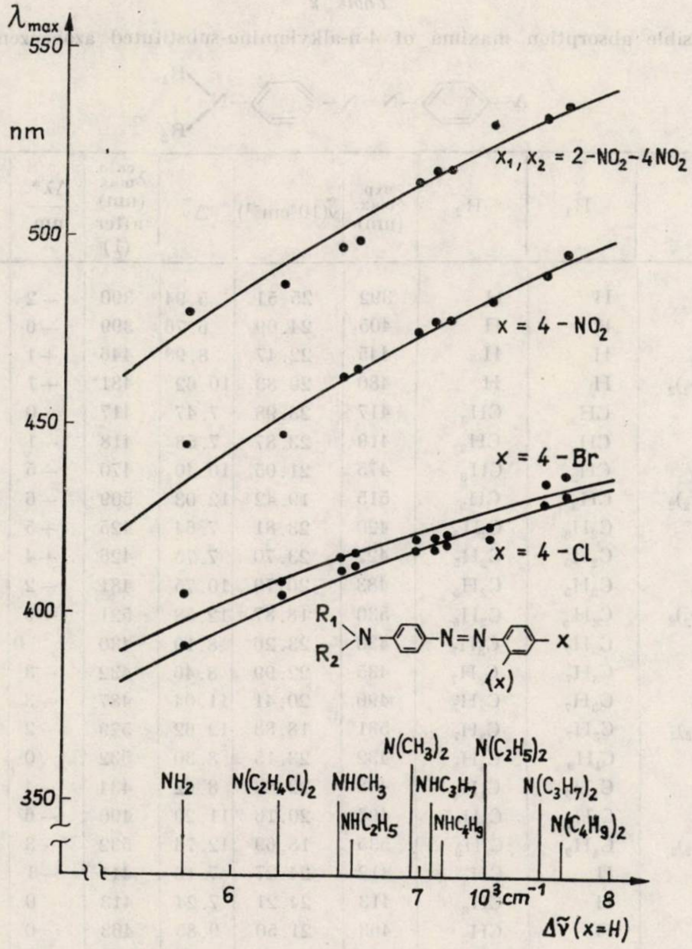

Fig. 1. — Absorption maxima λ_{max} of acceptor-substituted aminoazobenzenes in relation to the bathochromic shifts $\Delta\tilde{\nu}$ of the unsubstituted aminoazobenzenes.

THE BATHOCHROMIC POWER OF NR_1R_2-SUBSTITUENTS

The diethylamino group acts as a stronger donor than the dimethylamino group, the di-n-propylamino group is a less strong donor than the di-n-butylamino group. In respect of a systematic molecule design the question occurs in which manner the chain length of the n-alkyl-substituents influences donor strength and bathochromic shift. Our experimental results, which are given in table 2, lead to a dependence approximately like

$$\Delta\tilde{\nu} = \Delta\tilde{\nu}_\infty - ab^{-x} \quad x = 0, 1, 2 \ldots$$

Table 2

Visible absorption maxima of 4-n-alkylamino-substituted azobenzenes

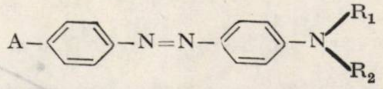

No.	A	R_1	R_2	$\lambda^{exp.}_{max.}$ (nm)	$\tilde{\nu}(10^3 cm^{-1})$	$\Delta\tilde{\nu}$	$\lambda^{calc.}_{max}$ (nm) after (1)	$\Delta\lambda^*$ nm	$\lambda^{calc.}_{max}$ (nm) after (2)	$\Delta\lambda^*$ nm
1	Cl	H	H	392	25.51	5.94	390	−2	396	+ 4
2	Br	H	H	405	24.69	6.76	399	−6	398	− 7
3	NO_2	H	H	445	22.47	8.98	446	+1	441	− 4
4	$2,4(NO_2)_2$	H	H	480	20.83	10.62	481	+1	472	− 8
5	Cl	CH_3	CH_3	417	23.98	7.47	417	0	416	− 1
6	Br	CH_3	CH_3	419	23.87	7.58	418	−1	418	− 1
7	NO_2	CH_3	CH_3	475	21.05	10.40	470	−5	471	− 4
8	$2,4(NO_2)_2$	CH_3	CH_3	515	19.42	12.03	509	−6	511	− 4
9	Cl	C_2H_5	C_2H_5	420	23.81	7.64	425	+5	425	+ 5
10	Br	C_2H_5	C_2H_5	422	23.70	7.75	426	+4	426	+ 4
11	NO_2	C_2H_5	C_2H_5	483	20.70	10.75	481	−2	485	+ 2
12	$2,4(NO_2)_2$	C_2H_5	C_2H_5	530	18.87	12.58	521	−9	529	− 1
13	Cl	C_3H_7	C_3H_7	430	23.26	8.19	430	0	431	+ 1
14	Br	C_3H_7	C_3H_7	435	22.99	8.46	432	−3	432	− 3
15	NO_2	C_3H_7	C_3H_7	490	20.41	11.04	487	−3	494	+ 4
16	$2,4(NO_2)_2$	C_3H_7	C_3H_7	531	18.83	12.62	529	−2	540	+ 9
17	Cl	C_4H_9	C_4H_9	432	23.15	8.30	532	0	433	+ 1
18	Br	C_4H_9	C_4H_9	438	22.83	8.62	434	−4	435	− 3
19	NO_2	C_4H_9	C_4H_9	496	20.16	11.29	490	−6	497	+ 1
20	$2,4(NO_2)_2$	C_4H_9	C_4H_9	535	18.69	12.76	532	−3	545	+10
21	Cl	H	CH_3	412	24.27	7.18	411	−1	411	− 1
22	Br	H	CH_3	413	24.21	7.24	413	0	412	− 1
23	NO_2	H	CH_3	463	21.50	9.85	463	0	463	0
24	$2,4(NO_2)_2$	H	CH_3	497	20.12	1.33	501	+4	499	+ 2
25	Cl	H	C_2H_5	413	24.21	7.24	412	−1	412	− 1
26	Br	H	C_2H_5	414	24.15	7.303	414	0	414	0
27	NO_2	H	C_2H_5	465	21.50	9.95	465	0	464	−1
28	$24,(NO_2)_2$	H	C_2H_5	499	20.04	11.41	502	+3	502	+ 3
29	Cl	H	C_3H_7	417	23.98	7.47	419	+2	420	+ 3
30	Br	H	C_3H_7	418	23.92	7.53	421	−3	421	+ 3
31	NO_2	H	C_3H_7	478	20.92	10.53	474	−4	476	− 2
32	$2,4(NO_2)_2$	H	C_3H_7	518	19.31	12.14	513	−5	517	− 1
33	Cl	H	C_4H_9	418	23.92	7.53	420	+2	421	+ 3
34	Br	H	C_4H_9	419	23.87	7.58	422	+3	422	+ 3
35	NO_2	H	C_4H_9	478	20.92	10.53	475	−3	478	0
36	$2,4(NO_2)_2$	H	C_4H_9	518	19.31	12.14	515	−3	520	+ 2

* $\Delta\lambda = \lambda^{calc.}_{max} - \lambda^{exp.}_{max}$

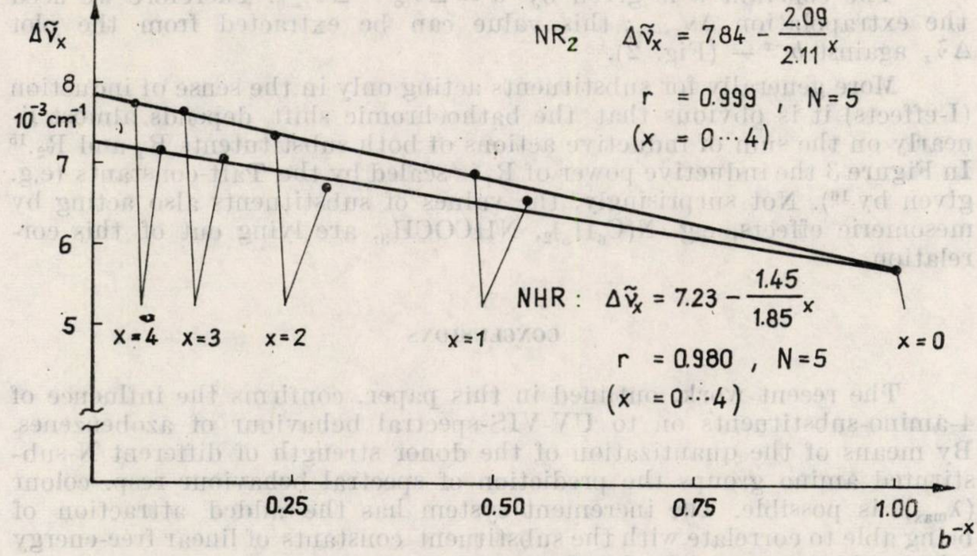

Fig. 2. — Correlations between bathochromic shifts $\Delta\tilde{\nu}$ from NR_1R_2-substituted azobenzenes and the chain length of the n-alkyl-substituents.

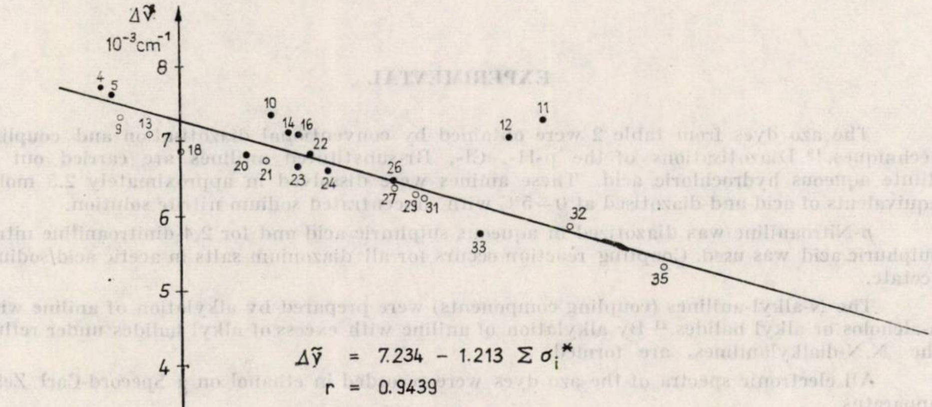

Fig. 3. — The bathochromic siffts $\Delta\tilde{\nu}$ of substituted aminoazobenzenes dependent on the substituent — specific Taft-constants σ_i^*.

The constant a is given by $a = \Delta\tilde{\nu}_{\infty} - \Delta\tilde{\nu}_{x=0}$. Therefore we need the extrapolation $\Delta\nu_{x=\infty}$; this value can be extracted from the plot $\Delta\tilde{\nu}_x$ against b^{-x} — (Fig. 2).

More generally for substituents acting only in the sense of induction (I-effects) it is obvious that the bathochromic shift depends almost linearly on the sum of inductive actions of both substitutents R_1 and R_2.[15] In Figure 3 the inductive power of R_1 is scaled by the Taft-constants (e.g. given by [16]). Not surprisingly, the values of substituents also acting by mesomeric effects, e.g. $N(C_6H_5)_2$, $NHCOCH_3$, are lying out of this correlation.

CONCLUSIONS

The recent work, outlined in this paper, confirms the influence of 4-amino-substituents on to UV-VIS-spectral behaviour of azobenzenes. By means of the quantization of the donor strength of different N-substituted amino groups the prediction of spectral behaviour resp. colour (λ_{max}) is possible. The increment system has the added attraction of being able to correlate with the substituent constants of linear free-energy relationships, e.g. with the Hammett-constants.

The bathochromic shift connected with the increasing chain length of n-alkyl groups is mainly due to induction effects.

EXPERIMENTAL

The azo dyes from table 2 were obtained by conventional diazotisation and coupling techniques.[19] Diazotisations of the p-H-, Cl-, Br-substituted anilines are carried out in dilute aqueous hydrochloric acid. These amines were dissolved in approximately 2.5 molar equivalents of acid and diazotised at 0—5°C with concentrated sodium nitrite solution.

p-Nitroaniline was diazotized in aqueous sulphuric acid and for 2,4-dinitroaniline nitrosulphuric acid was used. Coupling reaction occurs for all diazonium salts in acetic acid/sodium acetate.

The N-alkyl-anilines (coupling components) were prepared by alkylation of aniline with n-alcholos or alkyl halides.[21] By alkylation of aniline with excess of alkyl halides under reflux the N,N-dialkylanilines, are formed.

All electronic spectra of the azo dyes were recorded in ethanol on a Specord-Carl Zeiss apparatus.

REFERENCES

[1] J. Epperlein and B. Blau, *Rev. Roumaine Chim.*, **33**, 473 (1988).

[2] J. Griffiths, "Colour and Constitution of Organic Molecules", London, Academic Press, 1976, p. 140.

[3] J. Fabian, *Chimia*, **32**, 325 (1978).

[4] H. Mustroph and J. Epperlein, *J. prakt. Chem.*, **323**, 755 (1981).

[5] R. W. Catellino and G. Hallas, *J. Chem. Soc.*, **B**, 793 (1971).

[6] G Hallas, W. L. Ho and R. Todd, *J. Soc. Dyers Colour*,. **90**, 121 (1974).

[7] E. Sawicki, *J. Org. Chem.*, **22**, 915 (1957).

[8] J. Epperlein and E. Blau, *Z. Chem.*, **27**, 175 (1987).

[9] M. Saddatjou, Dissertation, University of Leeds 1977.

[10] L. M. Yagupolškij and L. Z. Gandel'sman, *Zh. obshch. Khim.*, **35**, 1252 (1965).
[11] I. Bridgeman and A. T. Peters, *J. Soc. Dyers Colourists*, **86**, 519 (1970).
[12] H. Mustroph, Z. *Chem.*, **22**, 450 (1982).
[13] W. Ross and G. Warwick, *J. Chem. Soc.*, **1956**, 1719.
[14] A. Pongratz, G. Markgraf and E. Maier-Pitsch, *Ber. Dtsch. Chem. Ges.*, **71**, 1287 (1938).
[15] R. W. Taft in "Steric Effects in Organic Chemistry", New York, Wiley 1956, p. 556.
[16] Spravočnik chimika (III), Moskva, Khimiya 1964, p. 185.
[17] V. A. Palm, in : "Grundlagen der quantitativen Theorie organischer Reaktionen", Berlin, Akademie-Verlag, 1971, p. 86.
[18] C. R. Kramer, *Z. phys. Chem.*, **267**, 2, 277 (1986).
[19] H. E. Fierz-David and L. Blangey, "Grundlegende Operationen der Farbenchemie", Wien, Springer-Verlag, 1943, p. 220.
[20] P. F. Gordon and P. Gregory, "Organic Chemistry in Colour", Berlin Springer-Verlag, 1983.
[21] R. Mayer, *J. prakt. Chem.*, **328**, 497 (1986).
[22] Our recent results.

Revue Roumaine de Chimie, **33**, 7, 693–698 (1988)

KINETICS AND MECHANISM OF ACID HYDROLYSIS OF PROPIONAMIDE IN METHANOL-WATER MIXTURES

H. M. ABU EL-NADER[a] * and M. R. MOSTAFA[b]
[a] Chemistry Department, Faculty of Science, Mansoura University
[b] Dumitta, Chemistry Department, Faculty of Science, Egypt

Received March 21, 1987

Acid hydrolysis of propionamide in aqueous hydrochloric acid solutions containing up to 80 wt. % methanol was investigated in the temperature range 20°–60°C. The reaction rate decreased with the increase of the methanol content. The isocomposition and isodielectric energies of activation were calculated and discussed in terms of solvation effects. The influence of dielectric constant on the reaction rate was discussed. The thermodynamic parameters of the activated complex were calculated and supported by the proposed mechanism.

INTRODUCTION

The effect of media on the rate constant of the reaction involving the hydrolysis of amides in aqueous organic solvents was attributed to many different factors. Acidic and basic amide hydrolysis has been studied in aqueous-organic solvents.[1–3]

A general equation for the variation of specific rate constant with dielectric constant has been recently proposed. In the present investigation, the acid hydrolysis of propionamide has been studied in water containing up to 80% methanol, at temperature range 20–60°C in order to clarify specific solvent effect on the reaction rate and mechanism.

EXPERIMENTAL

Pure propionamide, methanol and hydrochloric acid of "B.D.H." grade were used. Deionized and boiled water was used throughout. The general experimental procedure was described earlier.[2] The initial cnoncentrations of both amide and hydrochloric acid were always 0.1 M. The temperature was held constant within +0.05°C. The rate of hydrolysis was measured in the temperature range 20–60°C. The solvent compositions were accurate to +0.02 wt%. All solutions were freshly prepared before taking measurements. Rate constants were generally reproducible within +1% and represented mean values of three independent determinations.

RESULTS AND DISCUSSION

The rate of acid hydrolysis of propionamide in water + methanol media, follows an overall second-order kinetics, as shown in Fig. 1. The velocity constants, k_2(liter mol^{-1} s^{-1}) have been calculated in the various

---

* Author for correspondence.

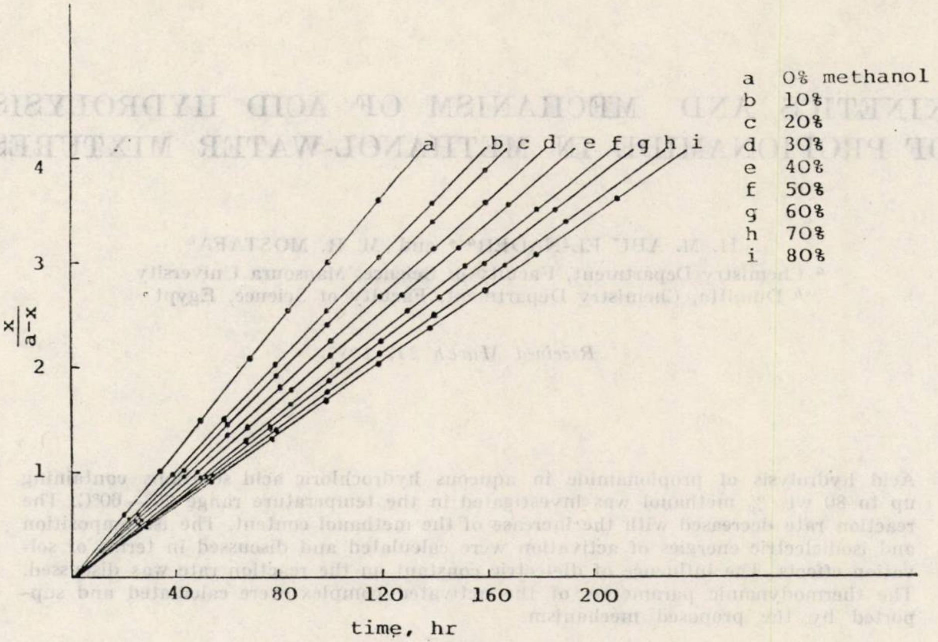

Fig. 1. — Second-order plots at 30°C.

solvents at the indicated temperatures and are given in Table 1. One observed that the reaction was inhibited by increasing the concentration of methanol. A similar observation was recorded during hydrolysis of propionamide in 1-propanol solvent.[4] The isocomposition (E_c) and isodielectric (E_d) energies of activation were calculated from plots of $\log k_c$ and $\log k_d$ against $1/T$, respectively, and their values are given in Tables 1 and 2. It can be readily seen that the velocity constant decreases while

Table 1

Velocity constants (liter $mol^{-1}s^{-1}$) and activation energy E_c, (Joule $\cdot mol^{-1}$) in methanol-water mixtures

Methanol wt %	$10^5\ k_2$					
	20°	30°	40°	50°	60°	E_c
0	0.6899	1.9498	5.2481	14.7891	35.4530	81250
10	0.6129	1.7783	5.0119	13.1825	33.8844	81391
20	0.5988	1.6788	4.8709	12.7350	33.1131	83184
30	0.5359	1.5849	4.5709	12.3026	32.7340	84636
40	0.5012	1.4790	4.3652	11.7489	31.6227	85414
50	0.4786	1.4125	4.1687	11.0919	30.9029	86100
60	0.4315	1.3032	3.9811	11.0462	30.5492	87761
70	0.4266	1.2522	3.8905	10.7151	28.8403	88233
80	0.3981	1.2003	3.8019	10.4051	28.6538	89037

the energy of activation increases with progressive alcohol addition. The increase in the activation energies with increase in alcohol content indicates the solvation of the activated complex to a lesser extent than the reactants.

Table 2

Interpolated values of k_2 at constant D, k_d, and isodielectric activation energy, E_d, (Joule mol^{-1})

D	$6 + \log k_d$					E_d
	20°	30°	40°	50°	60°	
20	0.4521	0.94444	1.5035	1.9442	2.4041	93423
40	0.5802	1.0601	1.5822	2.0283	2.4711	89176
60	0.7033	1.2023	1.6714	2.1055	2.5362	84930
80	0.8222	1.3223	1.7523	2.1914	2.6035	83987

The influence of dielectric constant on the rate of hydrolysis can be visualised by application of the Laidler-Landskroener equation[5] and Amis equation[6] where straight lines were obtained from the plots of log k_2 versus $1/D$. However, plot of log k_2 against D(Fig. 2) gave good straight lines according to Elsemong's equation.[7] The values of D were obtained by interpolatation from Akerlof's data.[8]

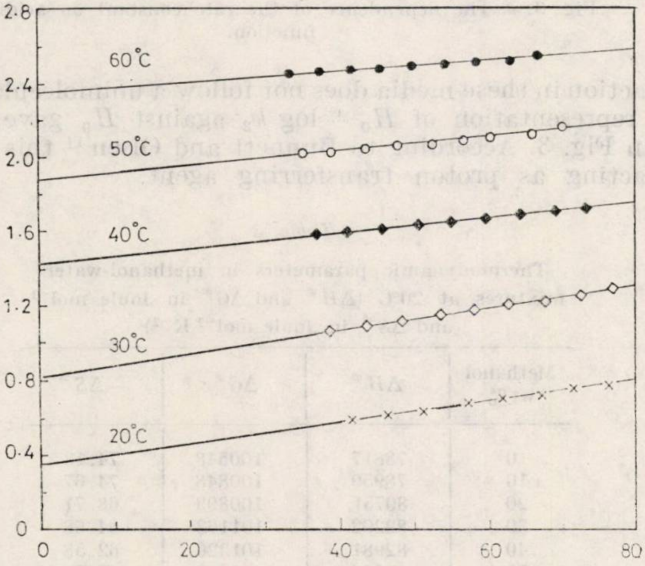

Fig. 2. — Influence of dielectric constant on reaction rate.

The increase in rate constant with increase in dielectric constant can be ascribed to the formation of activated complex more polar than the reactants, so that its formation is encouraged by media of high dielectric constant.

The dependence of the reaction rate on acidity function was discussed according to the Zucker-Hammett treatment,[9] The acidity function to HCl in methanol-water mixtures was obtained by interpolation from the data obtained by Tourky et al.[10] If the Zucker-Hammett ideas are generally applicable, then correlation of log k_2 with H_0 would provide a clear criterion of hydrolysis mechanism. However, it was indicated that the reaction in these media does not follow a unimolecular mechanism. Graphical representation of $H_0 + \log k_2$ against H_0 gave straight line as shown in Fig. 3. According to Bunnett and Olsen [11] this indicates that water is acting as proton transferring agent.

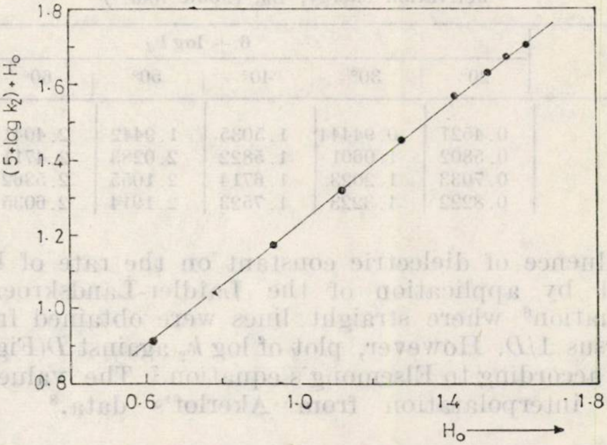

Fig. 3. — The dependence of the rate constant on acidity function.

Table 3

Thermodynamic parameters in methanol-water mixtures at 20°C ($\Delta H^{\neq}$ and $\Delta G^{\neq}$ in Joule mol^{-1} and $\Delta S^{\neq}$ in Joule mol^{-1} K^{-1})

Methanol wt %	$\Delta H^{\neq}$	$\Delta G^{\neq}$	$-\Delta S^{\neq}$
0	78817	100548	74.13
10	78959	100848	74.67
20	80751	100893	68.71
30	82202	101163	64.68
40	82981	101326	62.58
50	83666	101438	60.62
60	85328	101690	55.81
70	85800	101718	54.30
80	86640	101892	52.03

The thermodynamic properties of the activated complex are usually taken as a measure of the solvation effects. Such properties have been calculated and given in Table 3. One noticed that the valuse of $\Delta G^{\neq}$,

$\Delta H^{\neq}$ and $\Delta S^{\neq}$ increased with methanol addition. The increase in $\Delta G^{\neq}$ is an indication of the solvation of the reacting species. The nonlinear behaviour of $\Delta S^{\neq}$ with the percentage of methanol content is a criterion of specific solvation in the sense of Hudson and Saville.[12]

Solvent Effect on Reaction Mechanism

In the light of the above considerations, mechanism for the acid hydrolysis of propionamide should account satisfactorily for the role and the effect of the solvent on the reaction rate. The reaction has been studied in a wider temperature range (20—60°C). It was noticed that the hydrolysis obeyed Arrhenius equation indicating that successive addition of the alcohol alters the rate without influencing the mechanism and so the mechanism is the same for the different solvent compositions. Our kinetic data fit the proposed bimolecular mechanism [2]

$$R-CONH_2 + SH^+ \underset{k_{-1}}{\overset{k_1}{\rightleftharpoons}} T^+ + S \qquad \text{(i)}$$

(fast pre-equilibrium)

$$T^+ + HO_2 \xrightarrow[\text{Slow}]{k_2} \text{Products} \qquad \text{(ii)}$$

where S is a solvent molecule and T^+ stands for the solvated transition state in which the solvation is maintained through H-bonding. Kinetic evidence for fast protonation pre-equilibrium in acid hydrolysis of amides has been recently reported.[13]

The possible transition state (and intermediate which directly follows it) can be represented by structures (I) and II().[14]

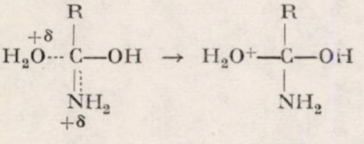

$$\overset{+\delta}{H_2O}\cdots\underset{\underset{+\delta}{NH_2}}{\overset{R}{C}}-OH \rightarrow H_2O^+-\underset{NH_2}{\overset{R}{C}}-OH$$

(I) (II)

The transition state, due to greater charge localization and a considerable degree of oxonium ion character, should be characterized by strong requirements for hydrogen-bonding type of solvation. Consequently, addition of methanol would tend to increase the stability of this transition state, i.e. to decrease the reaction rate. The values of activation parameters together with high negative value to $\Delta S^{\neq}$ supported the proposed mechanism.

REFERENCES

[1] M. M. Elsemongy, M. S. Abu Elamayem and M. N. H. Moussa, *Z. Physik. Chem. Neue Folge*, **94**, 69 (1975); **95**, 215 (1975).

[2] M. M. Elsemongy and H. M. Abu El-Nader, *J. Indian Chem. Soc.*, **54**, 1055 (1977); **55**, 60 (1978).

[3] I. M. Sidahamed, S. M. Salem and F.M. Adbel Halim, *Rev. Roum. Chim.*, **26**, 37 (1981).
[4] M. M. Elsemongy, M. F. Amira and A. M. Ahmed, *Indian J. Chem.*, **19A**, 658 (1980).
[5] K. J. Laidler and P. A. Landskroener, *Trans. Faraday Soc.*, **52**, 200 (1956).
[6] E. S. Amis, *J. Chem. Educ.*, **30**, 351 (1953).
[7] M. M. Elsemongy, *Z. Physik. Chem. Neue Folge*, **84**, 294 (1973).
[8] G. Akerlof, *J. Amer. Chem. Soc.*, **54**, 4125 (1932).
[9] C. A. Bunton, T. A. Lewis and D. R. Llewellyin, *Chem. and Ind.*, **1954**, 1154.
[10] C. H. Rochester, "Acidity functions", Academic Press, London and New York (1970).
[11] A. R. Tourky, A. A. Abdel-Hamid and I. Z. Slim, *Z. Phys. Chem. (Leipzig)*, **250**, 49 and 61 (1972).
[12] R. F. Hudson and B. J. Saville, *J. Chem. Soc.*, **34**, 4114 (1955).
[13] S. Mittal, K. S. Gupta and Y. K. Gupta, *Indian J. Chem.*, **15A**, 827 (1977).
[14] T. A. Modro, K. Yates and F. Beaufays, *Cand. J. Chem.*, **55**, 3050 (1977).

Revue Roumaine de Chimie, **33**, 7, 699—707 (1988)

CHEMICAL GRAPHS. PART 49.[1]

OPEN PROBLEMS IN THE AREA OF CONDENSED POLYCYCLIC BENZENOIDS: TOPOLOGICAL STEREOISOMERS OF CORONOIDS AND CONGENERS

ALEXANDRU T. BALABAN

Polytechnic Institute, Organic Chemistry Department,
Spl. Independenței 313, 76206 Bucharest

Received December 1, 1987

On the basis of long quasi-linear strips of condensed benzenoids (acenes which become less stable when longer, and zig-zag strips which conserve their stability even for long strips), various possibilities for topological stereoisomerism are discussed: enantiomeric and diastereomeric coronoids; cycloacenes and their zig-zag congeners, as well as the corresponding Möbius counterparts: knots; catenanes or rotaxanes involving coronoids, cycloacenes and zig-zag congeners.

1. INTRODUCTION: THE STABILITY OF ACENES *VERSUS* THAT OF HELICENES AND THEIR ISOARITHMIC SYSTEMS

Theoretical chemistry uses both numerical calculations and qualitative methods for making predictions of unknown facts and rationalizations of known data. Among the qualitative methods, those employing graph theory afford an insight into properties depending on molecular topology. The present paper will discuss topological aspects of polycyclic condensed benzenoids. These compounds are classified into catafusenes (whose dualist graphs are acyclic), perifusenes (whose dualist graphs have 3-membered rings and no larger rings), and coronoids (whose dualist graphs have larger rings than 3-membered rings); [2–4] we recall that the vertices of dualist graphs are the centres of benzenoid rings, whereas edges of these graphs connect vertices corresponding to condensed rings, i.e. to benzenoid rings sharing carbon atoms.[3,4] Unlike usual graphs, in dualist graphs * (DG) the bond angles do matter; annelations can be straight (acene-like) or kinked (phenanthrene-like). The latter type of annelation leads to increased stability; this is shown by experiment on comparing (for non-branched catafusenes with progressively larger number of rings) the decreasing stability of acenes with the practically constant stability of the zig-zag catafusenes (e.g. the isomeric pairs : tetracene-chrysene, pentacene-picene, hexacene-fulminene), or the slightly decreasing stability of helicenes (the geometrical non-planarity of helicenes also plays a destabilizing role). When the number of benzenoid rings are equal, helicenes and zig-zag nonbranched catafusenes are not only isomeric but are also isoarithmic,[5] i.e. they have equal numbers of Kekulé structures.

---

* Readers unfamiliar with dualist graphs will find examples in formulas **34**—**38** at the end of this paper.

Graph-theoretical methods allow rapid calculations of the number of Kekulé structures, explaining for instance the above stability difference : acenes with N benzenoid rings have $N + 1$ Kekulé structures, whereas isomeric zig-zag catafusenes or helicenes have much larger numbers of Kekulé structures forming the Fibonacci sequence (Table 1) where each term is the sum of the two preceding terms.[6]

Table 1

Numbers K of Kekulé structures for [N]acenes, and [N]helicenes or the isoarithmic zig-zag catafusenes

N	1	2	3	4	5	6	7	8
K for [N]acenes	2	3	4	5	5	7	8	9
K for [N]helicenes	2	3	5	8	13	25	38	63

Not only the number of Kekulé structures but also the "conjugated circuits method" [7–10] indicates the lower stability of [N]acenes than of their isomeric [N]helicenes; one can easily obtain general formulas for the numbers of conjugated circuits, hence resonance energies, for these two cases.[9]

These data explain why hexacene is so reactive and no [N]acene with $N > 6$ is known,[11] whereas [N]helicenes are known for $[N] < 15$,[12,13] and the stability of such systems is much higher than that of the isomeric acenes.[14]

It should be stressed that the particular topological feature of the condensed benzenoids under discussion is that they form planar strips which require little strain energy to become bent as in helicenes. We shall concentrate on linear acenic strips which are unstable when they are longer, and zig-zag strips which conserve their stability even when they are quite long.

2. TOPOLOGICAL STEREOISOMERS OF "FIGURE-EIGHT CORONOIDS" AND CONGENERIC SYSTEMS

In an earlier paper,[4] and in a recent book,[15a] mention was made that coronoids may exist in topologically distinct isomeric forms. Examples are the chiral systems **1** and **2**, and the achiral system **3**. For **1** we present both the usual hydrogen-depleted formula (constitutional or molecular graph) where for simplicity we have omitted the C=C double bonds, and the dualist graphs of the two enantiomeric forms. Most subsequent formulas will present only the dualist graphs of polyhexes. Compounds **1** and **2** give rise to two pairs of topological enantiomers, and **3** is a topological diastereoisomer of **2**. The pair of topological enantiomers of **2** and the achiral system **3** form a triplet of topological stereoisomers.

In systems **1**—**3** there are strings of five linearly condensed benzenoid rings which should decrease the stability; a higher stability ought to be associated with systems **4**—**6** whose dualist graphs were also mentioned in another earlier paper;[16] this higher stability should be due to the fact that there is no chain of ⩾3 linearly condensed hexagons. Should the steric strain associated with the geometrically non-planar molecule **4** be too high, one may imagine related, less congested isomeric systems such as **7** and **8**, or the larger coronoid **9**; analogously one can increase the size of the coronoids **5**—**6**. We call all such systems "figure-eight coronoids" and congeners.

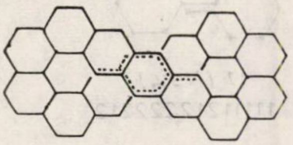

1 (N=14)

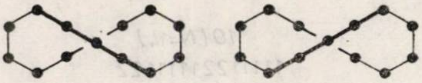

DG's of the two enantiomers *1*

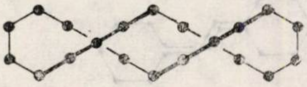

2 (N=22)

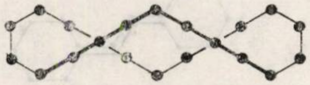

3 (N=22)

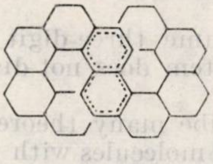

4 (N=12)

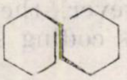

DG of *4*

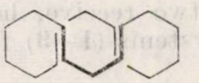

5 (N=18)

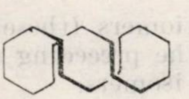

6 (N=18)

A different type of dualist graphs giving rise to analogous topological isomerism is illustrated by the achiral **10** and the chiral **11**, which are both isomeric with **1**; similarly, in order to reduce the steric strain one may imagine an achiral (**12**) and a chiral system (**13**) which are both isomeric with **5** and **6**. The achiral systems **10** and **12** constitute topological diastereoisomers of the two pairs of topological enantiomers represented by **11** and **13**, respectively.

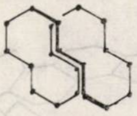

7 (N=20)

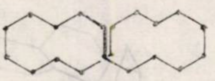

8 (N=20)

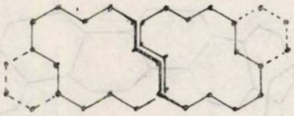

9 (N=28, 30 or 32)

The topological stereoisomerism discussed in the preceding paragraphs and illustrated with examples **1**—**13** is a new type of isomerism; for **10**—**13** the coding system imagined earlier [3,4,17] and written under each of these formulas differentiates the achiral isomer from the two enantiomers (these two receive, however, the same three-digit code). For the preceding systems (**1**—**9**) this coding system does not discriminate isomers.

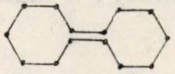

10 (N=14)
11111221111122

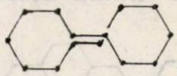

11 (N=14)
11111212222212

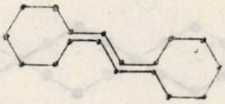

12 (N=18)
111112122111112122

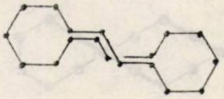

13 (N=18)
111112121222221122

Schill's book [18] and Walba's review [19] describe many theoretically anticipated and a few experimentally synthesized molecules with interesting topological features: catenanes, rotaxanes, knots, Möbius molecules, topologically non-planar molecules. The terminology used here (topological stereoisomers, enantiomers and diastereomers) was proposed by Walba.[19]

In an earlier paper on challenging problems involving benzenoid polycyclics and related systems,[20] we mentioned polyaza-kekulenes as well as polyradicals with peri-condensation. In another paper entitled "Is aromaticity outmoded?"[21] we mentioned as challenging synthetic goals catenanes and rotaxanes with aromatic or antiaromatic rings, cyclocarbyne which should be an elemental carbon molecule with *sp*-hybridized atoms, as well as cycloacenes, their Möbius counterparts, and analogs possessing only zig-zag annelation instead of linearly condensed benzenoid rings. We indicate in formulas **14** and **15** a normal and a Möbius

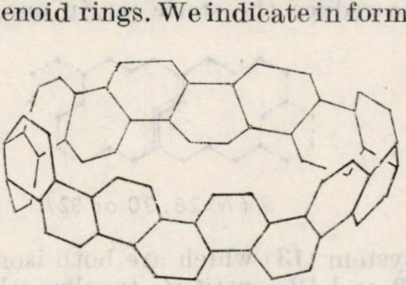

14 (N=16)

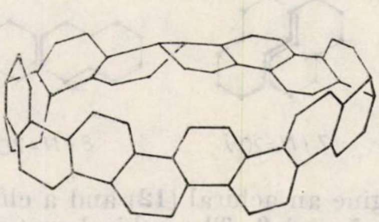

15 (N=15)

type molecule, respectively, having no fragment with ⩾ 3 linearly condensed benzenoid rings; it should be observed that the former molecule has an even number of 6-membered rings whereas the latter molecule has an odd number of such rings.

A related, simpler problem is to calculate the size of a tolerably strained cyclo-*para*-phenylene and then to obtain it; it is known that acyclic poly-*para*-phenylene chains yield valuable heat-resistant polymers.

Till now, no molecules such as **1**—**15** or congeneric systems have been prepared; they constitute interesting synthetic goals.

3. KNOTS

In Walba's review,[19] many theoretical data on knots are described together with experimental evidence for the occurrence of molecular knots in DNA strands. However, till now no discussion on knots involving coronoids can be found in the literature.

The two topological enantiomeric knots **16** and **17** can give rise to the corresponding knotted enantiomeric pairs of coronoids **18** and **19**, **20** and **21**, **22** and **23**; one should note that the last two pairs are constitutionally isomeric to one another. On the other hand, **24** is a twisted ring which is topologically diastereomeric with both **16** and **17**. From

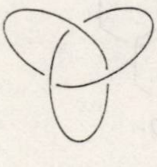

16

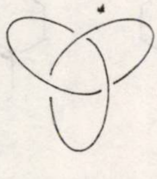

17

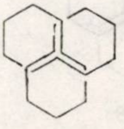

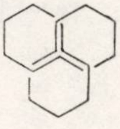

N = 18

18

19

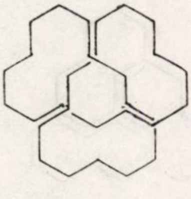

20

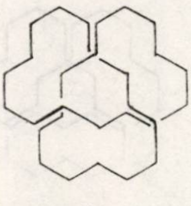

21

N = 30

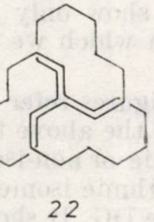

22

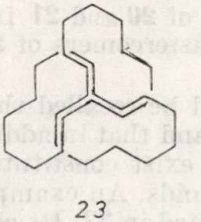

23

such twisted rings one may derive three pairs of topological enantiomers which are all topologically diastereomeric with the knots **18** and **19**; these three pairs are **25** and **26**, **27** and **28**, **29** and **30**. The total is $2^3 = 8$ topological stereoisomers, corresponding to the crossing points of the

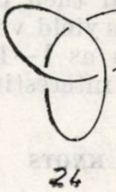

24

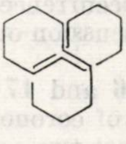

25

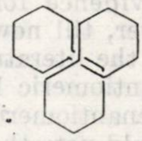

26

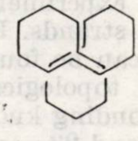

27

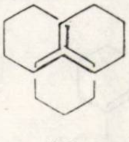

28

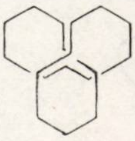

29

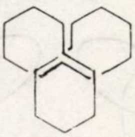

30

Code for *18,19, 25-30*: 111112111112111112

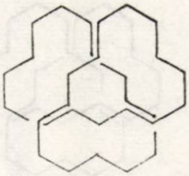

31

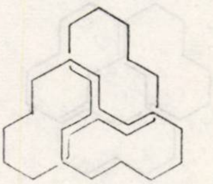

32

trefoil knots **16**, **17** or of **24**. Analogously there will be six topological diastereomers of **20** and **21** from which we show only one (**31**), and six topological diastereomers of **22** and **23** from which we display only one (**32**).

It should be recalled that the above figures refer to dualist graphs of coronoids, and that in addition to each of the above topological stereoisomers there exist constitutional isoarithmic or non-isoarithmic isomers of these coronoids. An example of an isoarithmic isomer of **18**, **19**, **25**—**30** is presented in **33**. Its code is below the DG. It should also be noted that the three-digit notation discriminates such isomers from the previous ones; however, this notation does not distinguish between **18**, **19**, **25–30**. The coding of these topological stereoisomers represents an open problem.

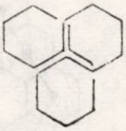

33

1111121111122222

4. CATENANES OF CORONOID SYSTEMS

Kekulene (**34**) is a known coronoid system, prepared and studied by Staab and coworkers.[22] Its inner "hole" is too small to allow a polymethylene chain to move freely into it, but larger coronoids (**35–38**) might be better suited for this purpose. The synthesis of catenanes by threading gives very low yields. However, one may imagine intramolecular threading approaches (directed catenane syntheses) by analogy with the Schill – Lüttringhaus approach; the yields in such directed syntheses are much higher.

The coronoids with longer portions of linearly condensed rings such as **35** are expected to be less stable than **34** or **37**, whilst those with no portion of $\geqslant 3$ linearly condensed rings (**36** or **38**) are the most stable. It is, however, apparent from the formulas that there is stronger repulsion between hydrogen atoms in the latter cases than in the preceding ones*. The threaded polymethylene chain, in a directed synthesis patterned after the Schill-Lüttringhaus pathway, has to rely on an "inner" dialkylamino group whose alkyl endgroups then undergo intramolecular cyclization, cf. **37** and **38**.

Finally, one may imagine bis-coronoid catenanes wherein both chains of the catenane would be coronoid systems. In such cases the size of the coronoid should be appreciably larger.

Alternative approaches to such systems may be based upon "choker annulenes" such as **39** which were depicted for the first time in a recently published book.[15b] The obvious analogues are "choker coronoids" such as **40**.

If the "inner" aromatic system which in **39** and **40** is *para*-bonded is expanded by annelation to another coronoid (one may conceive also *meta*-bonded inner strips), and if the inter-strip bonds, with proper functionalization, become broken, one should obtain a bis-coronoid catenane.

All the preceding discussion of catenanes involved simple coronoids. One can extend the same concepts to catenanes based upon cycloacenes or rather on their zig-zag counterparts such as **38**.

---

* In formulas **34** – **36** open circles denote inner hydrogens.

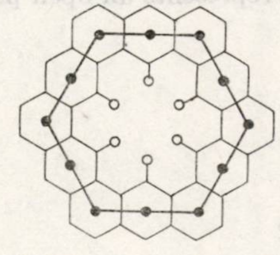

34 (*N*=12)

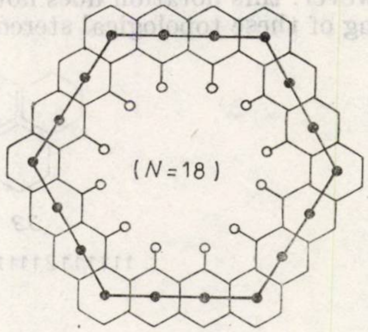

35

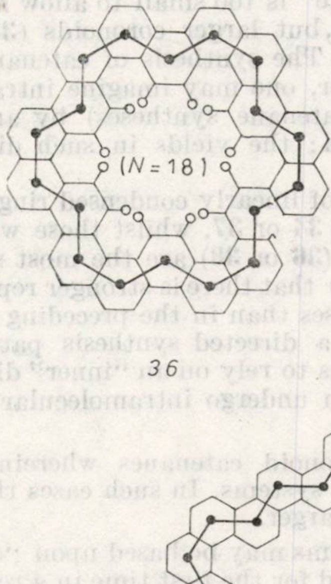

36

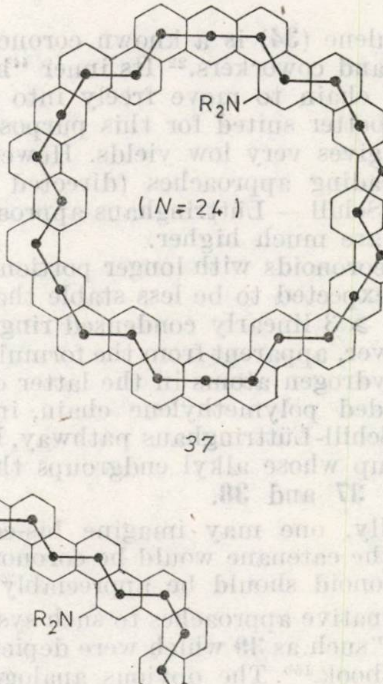

37

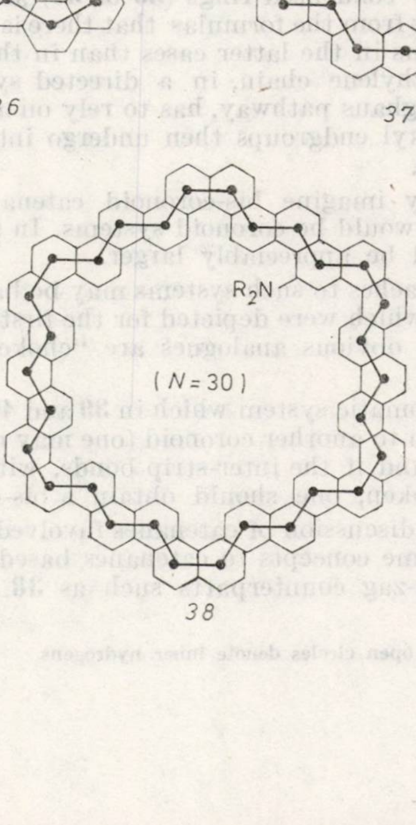

38

Finally one may apply these concepts to obtaining rotaxanes whose cyclic structure is a coronoid or a cycloacene or rather its zig-zag counterpart, e.g. **38**.

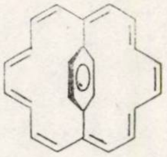

39

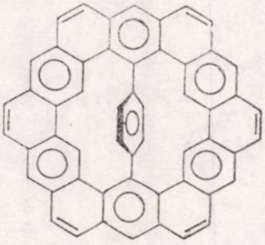

40

REFERENCES

[1] Previous part, A. T. Balaban, *Math. Chem.*, **21**, 115 (1986).

[2] A. T. Balaban, J. Brunvoll, J. Cioslowski, B. N. Cyvin, S. J. Cyvin, I. Gutman, He Wenchen, He Wenjie, J. V. Knop, M. Kovacević, W. R. Müller, K. Szymanski, R. Tosić and N. Trinajstić, *Z. Naturforsch.* **42a**, 863 (1987).

[3] A. T. Balaban and F. Harary, *Tetrahedron*. **24**, 2505 (1969).

[4] A. T. Balaban, *Tetrahedron*, **25**, 2949 (1986).

[5] A. T. Balaban and I. Tomescu, *Math. Chem.*, **14**, 155 (1983).

[6] A. T. Balaban and I. Tomescu, *Croatica Chem. Acta*, **54**, 391 (1984) ; *Math. Chem.*, **17**, 91 (1985) ; A. T. Balaban, *J. Mol. Struct. Theochem.*, **120**, 117 (1985) and further references therein ; S.T. Cyvin and I. Gutman, "Kekulé Structures in Benzenoid Hydrocarbons", Lecture Notes in Chemistry No. 46, Springer, Berlin, 1988.

[7] M. Randić, *J. Am. Chem. Soc.*, **99**, 444 (1977) ; *Tetrahedron*, **33**, 1905 (1977) ; *Pure Appl. Chem.*, **52**, 1587 (1980) ; M. Randić, B. M. Gimarc and N. Trinajstić, *Croat. Chem. Acta*, **59**, 345 (1986).

[8] J. A. N. F. Gomes, *Croat. Chem. Acta*, **59**, 333 (1980) ; *Theor. Chim. Acta*, **53**, 561 (1980).

[9] N. Trinajstić, "Chemical Graph Theory", vol. 2, chapter 3, Boca Raton, Florida, 1983.

[10] A. T. Balaban and I. Tomescu, *Math. Chem.*, **17**, 91 (1985).

[11] M. Satchell et al., *J. Chem. Soc (C)*, 468 (1971).

[12] R. H. Martin et al., *Angew. Chem. Int. Ed. Engl.*, **11**, 296 (1972) ; *Tetrahedron*, **31**, 2135 (1975).

[13] S. Obenland et al. *J. Am. Chem. Soc.*, **97**, 6633 (1975).

[14] E. Clar, "The Aromatic Sextet", Wiley-Interscience, London, 1972 ;"Polycyclic Hydrocarbons", Academic Press, London, 1964 ; J. R. Dias, "Handbook of Polycyclic Hydrocarbons. Part A. Benzenoid Hydrocarbons", Elsevier, Amsterdam, 1987.

[15] A. T. Balaban, M. Banciu and V. Ciorba, "Annulenes, Benzo-, Hetero-, Homo-Derivatives and Their Valence Isomers", CRC Press, Boca Raton, Florida, 1987 : a) vol. 1, p. 23 ; b) vol. 2, p. 70.

[16] A. T. Balaban, *Tetrahedron*, **27**, 6115 (1971).

[17] A. .T. Balaban, *Math. Chem.*, **2**, 51 (1976).

[18] G. Schill, "Catenanes, Rotaxanes and Knots", Academic Press, New York, 1971.

[19] D. M. Walba, *Tetrahedron*, **41**, 3161 (1985) ; see also D. M. Walba, in "Chemical Applications of Topology and Graph Theory" (Edited by R. B. King), p. 17, Elsevier, Amsterdam, 1983.

[20] A. T. Balaban, *Pure Appl. Chem.*, **54**, 1075 (1982).

[21] A. T. Balaban, *Pure Appl. Chem.*, **52**, 1409 (1980).

[22] F. Diederich and H. A. Staab, *Angew. Chem.*, **90**, 383 (1978) ; C. Krieger, F. Diederich, D. Schneitzer and H. A. Staab, *ibid.*, **91**, 733 (1979).

Revue Roumaine de Chimie, **33**, 7, 709–717 (1988)

CHEMICAL GRAPH POLYNOMIALS. 1

THE POLYNOMIAL DESCRIPTION OF GENERALIZED CHEMICAL GRAPHS

OVIDIU IVANCIUC *
Polytechnic Institute "Traian Vuia", Faculty of Chemical
Technology, Timişoara, Romania

Received May 16, 1987

An alternative formulation of the Sachs formula which relates the structure of a generalized graph and its μ, and acyclic ploynomials is given. Some recurrence rèlations for the generalized μ, characteristic and acyclic polynomials are presented.

1. INTRODUCTION

The graph theoretical polynomials[1] play a significant role in the area of topological chemistry, with applications to diverse areas such as the topological resonance theory (TRE)[2,3] and the topological effect on molecular orbitals (TEMO).[4] The most used graph theoretical polynomials are the characteristic, the acyclic (matching) and the μ-polynomial. We will present a slightly different formulation of the Sachs formula applied to generalized graphs. Some expressions for the generalized μ, characteristic and acyclic polynomials are obtained.

2. NOTATION AND TERMINOLOGY

We shall use the standard graph notation and terminology. G will denote a graph with n vertices: $v_1, v_2, \ldots, v_n$, m edges and r cycles: $C_1, C_2, \ldots, C_r$. We denote by t_i the weight associated to the cycle C_i. The edge connecting the vertices v_i and v_j is denoted by e_{ij}. The subgraph $G-v_i$ is obtained from the graph G by deletion of the vertex v_i. The subgraph $G-e_{ij}$ is obtained from the graph G by deletion of the edge e_{ij}. The subgraph $G-C_i$ is obtained from the graph G by deleting all the vertices of the cycle C_i. Two cycles, C_i and C_j, are disjoint if they have no vertex in common. We will denote by g_i the degree (the number of neighbours) of the vertex v_i.

---

* Correspondence address: strada N. Grigorescu, 18/2, 2750 Hunedoara, Romania

The characteristic polynomial of the graph G may be expressed as follows

$$\mathrm{Ch}(G, x) = \det|x\mathbf{I} - \mathbf{A}| = \sum_{n=0}^{N} a_n x^{N-n} \tag{1}$$

where $\mathbf{I}$ is the unit matrix and $\mathbf{A}$ is the adjacency matrix of the graph G.[5]

The coefficients a_n of the characteristic polynomial $\mathrm{Ch}(G, x)$ may be computed without using the unpractical procedure of the expansion of the determinant but from the topology of the molecular graph. Such a procedure was given by Sachs[6] in the following expression:

$$a_n = \sum_{s \in S_n} (-1)^{c(s)} 2^{r(s)} \tag{2}$$

where s is a Sachs graph, S_n is the set of all Sachs graphs with n vertices, $c(s)$ is the total number of components in s, and $r(s)$ is the number of cycles in s. The components of a Sachs graph are combinations of isolated bonds (K_2) and cycles (C_m). Recently the Sachs formula was extended to vertex-weighted graphs[7,8] and to vertex- and edge-weighted graphs[9,10], that is to say to those graphs which may be used to represent heteroconjugated molecules.

Hosoya defined[11] the acyclic (matching) polynomial as:

$$\mathrm{Ac}(G, x) = \sum_{k=0}^{N} (-1)^k P(G, k) x^{N-2k} \tag{3}$$

where $P(G, k)$ is the number of ways of choosing k disjoint edges from G.

From the two definitions one could hardly anticipate any connection between $\mathrm{Ch}(G, x)$ and $\mathrm{Ac}(G, x)$. This connection is done by the μ-polynomial, $\mu\,(G, t, x)$, which continuously transforms $\mathrm{Ac}(G, x)$ into $\mathrm{Ch}(G, x)$ when the parameter t changes from zero to unity. Gutman and Polansky defined[12] the μ-polynominal as

$$\mu(G, t, x) = \sum_{n=0}^{N} \sum_{s \in S_n} (-1)^{c(s)} 2^{r(s)} x^{N-n} T(s) \tag{4}$$

where $T(s)$ is the product of the individual weights of the $r(s)$ cycles of the Sachs graphs s.

3. THE GENERALIZED GRAPH AND POLYNOMIALS

The generalized (vertex- and edge-weighted)[10] graph G_g is a graph which has the loop l_i, located at the vertex v_i, weighted with the quantity a_i and the edge e_{ij} weighted with the quantity b_{ij}. We define the generalized set of Sachs graphs as the set formed by loops L, isolated bonds

K_2, and cycles C_m. The contribution of a loop is equal to

$$p(l_i) = a_i \tag{5}$$

that of an weighted edge is equal to

$$p(e_{ij}) = b_{ij}^2 \tag{6}$$

that of an weighted cycle is equal to

$$p(c_i) = \prod b_{ij} \tag{7}$$

where the multiplication goes over all edges in the cycle, and finally, the contribution of a Sachs graph, $p(s)$, is obtained by the multiplication of the contributions of the components of the Sachs graph :

$$p(s) = \prod_{i=1}^{c(s)} p_i \tag{8}$$

Thus, the generalized μ-polynominal is defined as

$$\mu(G_g(t, x)) = \sum_{n=0}^{N} \sum_{s \in S_n} (-1)^{c(s)} 2^{r(s)} p(s) T(s) \tag{9}$$

From the above formula it follows that the generalized characteristic polynomial is given by

$$\mathrm{Ch}(G_g(x)) = \sum_{n=0}^{N} \sum_{s \in S_n} (-1)^{c(s)} 2^{r(s)} p(s) \tag{10}$$

and the generalized acyclic polynomial has the following expresion

$$\mathrm{Ac}(G_g(x)) = \sum_{n=0}^{N} \sum_{s \in S_n} (-1)^{c(s)} p(s) \tag{11}$$

4. RECURRENCE RELATIONS

If the generalized graph G_g is obtained from the graph G by setting the weight of the vertex v_i equal to a and the weight of the edge e_{ij}, $j = \overline{1, g_i}$ equal to b_{ij}, the following equalities take place :

Proposition 1.

$$\mu(G_g) = \mu(G) - a\mu(G - v_i) -$$

$$- \sum^{g_i} (b_{ij}^2 - 1)\mu(G - v_i - v_j) - 2\sum^{j} (p(C_j) - 1) t_j \mu(G - C_j) \tag{12}$$

$$\mathrm{Ch}(G_g) = \mathrm{Ch}(G) - a\mathrm{Ch}(G - v_i) - \tag{13}$$
$$- \sum^{g_i}(b_{ij}^2 - 1)\,\mathrm{Ch}(G - v_i - v_j) - 2\sum^{f}(p(C_j - 1)(\,\mathrm{Ch}(G - C_j)$$

$$\mathrm{Ac}(G_g) = \mathrm{Ac}(G) - a\mathrm{Ac}(G - v_i) - \sum^{g_i}(b_{ij}^2 - 1)\,\mathrm{Ac}(G - v_i - v_j) \tag{14}$$

The second summation in (12) and (13) goes overall f cycles in G which contain vertex v_i.

From the previously known recurrence relations for $\mu(G)$,[12] $\mathrm{Ch}(G)$ [13] and $\mathrm{Ac}(G)$ [11,14]:

$$\mu(G) = \mu(G - e_{ij}) - \mu(G - v_i - v_j) - 2\sum t_j\mu(G - C_j) \tag{15}$$

$$\mathrm{Ch}(G) = \mathrm{Ch}(G - e_{ij}) - \mathrm{Ch}(G - v_i - v_j) - 2\sum \mathrm{Ch}(G - C_j) \tag{16}$$

$$\mathrm{Ac}(G) = \mathrm{Ac}(G - e_{ij}) - \mathrm{Ac}(G - v_i - v_j) \tag{17}$$

we obtain

Proposition 2.

$$\mu(G_g) = \mu\left(G - \sum_{j=1}^{g_i} e_{ij}\right) - a\mu(G - v_i) - \tag{18}$$
$$- \sum_{j=1}^{g_i} b_{ij}^2\mu(G - v_i - v_j) - 2\sum_{j=1}^{f} p(C_j)t_j\mu(G - C_j)$$

$$\mathrm{Ch}(G_g) = \mathrm{Ch}\left(G - \sum_{j=1}^{g_i} e_{ij}\right) - a\,\mathrm{Ch}(G - v_i) - \tag{19}$$
$$- \sum_{j=1}^{g_i} b_{ij}^2\,\mathrm{Ch}(G - v_i - v_j) - 2\sum_{j=1}^{f} p(C_j)\,\mathrm{Ch}(G - C_j)$$

$$\mathrm{Ac}(G_g) = \mathrm{Ac}\left(G - \sum_{j=1}^{g_i} e_{ij}\right) - a\,\mathrm{Ac}(G - v_i) - \sum_{j=1}^{g_i} b_{ij}^2\,\mathrm{Ac}(G - v_i - v_j) \tag{20}$$

The second summation in (18) and (19) goes over all f cycles in G which contain vertex v_i.

Proposition 3.

If every edge e_{ij}, $j = \overline{1, g_i}$, is a bridge then:

$$\mu(G_g) = \mu\left(G - \sum_{j=1}^{g_i} e_{ij}\right) - a\mu(G - v_i) - \sum_{j=1}^{g_i} b_{ij}^2\mu(G - v_i - v_j) \tag{21}$$

$$\mathrm{Ch}(G_g) = \mathrm{Ch}\left(G - \sum_{j=1}^{g_i} e_{ij}\right) - a\,\mathrm{Ch}(G - v_i) - \sum_{j=1}^{g_i} b_{ij}^2\,\mathrm{Ch}(G - v_i - v_j) \tag{22}$$

$$\mathrm{Ac}(G_g) = \mathrm{Ac}\left(G_g - \sum_{j=1}^{g_i} e_{ij}\right) - a\,\mathrm{Ac}(G - v_i) - \sum_{j=1}^{g_i} b_{ij}^2\,\mathrm{Ac}(G - v_i - v_j) \tag{23}$$

The expansion of the μ-polynomial is given in (24) in terms of the μ-polynomials of its subgraphs, corresponding to the decomposition of the graph G and its vertex v_i [15]

$$\mu(G) = x\mu(G - v_i) - \sum_{j=1}^{g_i} \mu(G - v_i - v_j) - 2\sum_{j=1}^{f} t_j\mu(G - C_j) \qquad (24)$$

where the second summation goes over all f cycles which contain vertex v_i. For the generalized graph G_g we obtain

Proposition 4.

$$\mu(G_g) = (x - a)\mu(G - v_i) - \sum_{j=1}^{g_i} b_{ij}^2\mu(G - v_i - v_j) - 2\sum_{j=1}^{f} p(C_j)t_j\mu(G - C_j) \qquad (25)$$

$$\mathrm{Ch}(G_g) = (x - a)\,\mathrm{Ch}(G - v_i) - \sum_{j=1}^{g_i} b_{ij}^2\mathrm{Ch}(G - v_i - v_j) - 2\sum_{j=1}^{f} p(C_j)\mathrm{Ch}(G - C_j) \qquad (26)$$

$$\mathrm{Ac}(G_g) = (x - a)\,\mathrm{Ac}(G - v_i) - \sum_{j=1}^{g_i} b_{ij}^2\,\mathrm{Ac}(G - v_i - v_j) \qquad (27)$$

where the second summation in (25) and (26) goes over all f cycles which contain vertex v_i.

In the following propositions, previously established [12] equalities will be presented for the case of the generalized graph G_g.

Proposition 5.

$$\begin{aligned}\mu(\mathrm{G}_g) = \mathrm{Ac}(G_g) &- 2\sum p(C_i)t_i\,\mathrm{Ac}(G_g - C_i) + \\ &+ 4\sum p(C_i)p(C_j)t_it_j\,\mathrm{Ac}(G_g - C_i - C_j) - \\ &- 8\sum p(C_i)p(C_j)p(C_k)t_it_jt_k\,\mathrm{Ac}(G_g - C_i - C_j - C_k) + \ldots\end{aligned} \qquad (28)$$

In (28) summation goes over all single, pairs, triplets, etc. of mutually disjoint cycles in G_g. The term corresponding to the summation over s mutually disjoint cycles in G_g is:

$$(-1)^s2^s\sum\left(\prod_1^s p(C_j)\prod_1^s t_j\,\mathrm{Ac}(G_g - C_1 - C_2 - \ldots - C_s)\right)$$

The inversion of this identity yields

Proposition 6.

$$\begin{aligned}\mathrm{Ac}(G_g) = \mu(G_g) &+ 2\sum p(C_i)t_i\mu(G_g - C_i) + \\ &+ 4\sum p(C_i)p(C_j)\,t_it_j\mu(G_g - C_i - C_j) + \\ &+ 8\sum p(C_i)p(C_j)p(C_k)t_it_jt_k\mu(G_g - C_i - C_j - C_k) + \ldots\end{aligned} \qquad (29)$$

In (29) summation goes over all single, pairs, triplets, etc. of mutually disjoint cycles in G_g. The term corresponding to the summation over s mutually disjoint cycles in G_g is :

$$2^s \sum \left(\prod_1^s p(C_j) \prod_1^s t_j \mu(G_g - C_1 - C_2 - \ldots - C_s) \right)$$

We express the μ-polynomial in terms of the characteristic polynomial, thus obtaining

Proposition 7.

$$\begin{aligned} \mu(G_g) = \mathrm{Ch}(G_g) + 2 \sum p(C_i)(1 - t_i)\, \mathrm{Ch}(G_g - C_i) + \\ + 4 \sum p(C_i) p(C_j)(1 - t_i)(1 - t_j)\, \mathrm{Ch}(G_g - C_i - C_j) + \qquad (30) \\ + 8 \sum p(C_i) p(C_j) p(C_k)(1 - t_i)(1 - t_j)(1 - t_k)\, \mathrm{Ch}(G_g - C_i - C_j - C_k) + \ldots \end{aligned}$$

In (30) summation goes over all single, pairs, triplets, etc. of mutually disjoint cycles in G_g. The term corresponding to the summation over s mutually disjoint cycles in G_g is :

$$2^s \sum \left(\prod_1^s p(C_j) \prod_1^s (1 - t_j)\, \mathrm{Ch}(G_g - C_1 - C_2 - \ldots - C_s) \right)$$

The identity (30) can be inverted leading to

Proposition 8.

$$\begin{aligned} \mathrm{Ch}(G_g) = \mu(G_g) - 2 \sum p(C_i)(1 - t_i)\, \mu(G_g - C_i) \\ + 4 \sum p(C_i) p(C_j)(1 - t_i)(1 - t_j)\, \mu(G_g - C_i - C_j) \qquad (31) \\ - 8 \sum p(C_i)\, p(C_j) p(C_k)(1 - t_i)(1 - t_j)(1 - t_k)\, \mu(G_g - C_i - C_j - C_k) + \ldots \end{aligned}$$

In (31) summation goes over all single, pairs, triplets, etc. of mutually disjoint cycles in G_g. The term corresponding to the summation over s mutually disjoint cycles in G_g is :

$$(-1)^s 2^s \sum \left(\prod_1^s p(C_j) \prod_1^s (1 - t_j)\, \mu(G_g - C_1 - C_2 - \ldots - C_s) \right)$$

Proposition 9.

For $T = 1$ we obtain from (28)

$$\begin{aligned} \mathrm{Ch}(G_g) = \mathrm{Ac}(G_g) - 2 \sum p(C_i)\, \mathrm{Ac}(G_g - C_i) + \\ + 4 \sum p(C_i) p(C_j)\, \mathrm{Ac}(G_g - C_i - C_j) - \qquad (32) \\ - 8 \sum p(C_i) p(C_j) p(C_k)\, \mathrm{Ac}(G_g - C_i - C_j - C_k) + \ldots \end{aligned}$$

The term corresponding to the summation over s mutually disjoint cycles in G_g is

$$(-1)^s 2^s \sum \left(\prod_1^s p(C_j)\, \mathrm{Ac}(G_g - C_1 - C_2 - \ldots - C_s) \right)$$

Proposition 10.
For $T = 0$ we obtain from (29)

$$\begin{aligned} \mathrm{Ac}(G_g) = {} & \mathrm{Ch}(G_g) + 2 \sum p(C_i)\, \mathrm{Ch}(G_g - C_i) + \\ & + 4 \sum p(C_i) p(C_j)\, \mathrm{Ch}(G_g - C_i - C_j) + \\ & + 8 \sum p(C_i) p(C_j) p(C_k)\, \mathrm{Ch}(G_g - C_i - C_j - C_k) + \ldots \end{aligned} \tag{33}$$

The term corresponding to the summation over s mutually disjoint cycles in G_g is

$$2^s \sum \left(\prod_1^s p(C_j)\, \mathrm{Ch}(G_g - C_1 - C_2 - \ldots - C_s) \right)$$

Proposition 11.
If the graph G_g possesses a single cycle C, then

$$\begin{aligned} \mu(G_g) &= \mathrm{Ac}(G_g) - 2p(C)t\, \mathrm{Ac}(G_g - C) \\ \mu(G_g) &= \mathrm{Ch}(G_g) - 2p(C)(1 - t)\, \mathrm{Ch}(G_g - C) \\ \mu(G_g) &= (1 - t)\, \mathrm{Ac}(G_g) + t\, \mathrm{Ch}(G_g) \end{aligned} \tag{34}$$

$$\begin{aligned} \mathrm{Ch}(G_g) &= \mu(G_g) - 2p(C)(1 - t)\mu(G_g - C) \\ \mathrm{Ch}(G_g) &= \mathrm{Ac}(G_g) - 2p(C)\, \mathrm{Ac}(G_g - C) \\ \mathrm{Ch}(G_g) &= \mathrm{Ac}(G_g)(t - 1)/t + \mu(G_g)/t \end{aligned} \tag{35}$$

$$\begin{aligned} \mathrm{Ac}(G_g) &= \mu(G_g) + 2p(C)t\mu(G_g - C) \\ \mathrm{Ac}(G_g) &= \mathrm{Ch}(G_g) + 2p(C)\, \mathrm{Ch}(G_g - C) \\ \mathrm{Ac}(G_g) &= \mathrm{Ch}(G_g)t/(t - 1) + \mu(G_g)/(1 - t) \end{aligned} \tag{36}$$

If the graph G_g possesses s undisjoint cycles,

$$\begin{aligned} \mu(G_g) &= \mathrm{Ac}(G_g) - 2 \sum_1^s p(C_i) t_i\, \mathrm{Ac}(G_g - C_i) \\ \mu(G_g) &= \mathrm{Ch}(G_g) + 2 \sum_1^s p(C_i)(1 - t_i)\, \mathrm{Ch}(G_g - C_i) \end{aligned} \tag{37}$$

$$\mathrm{Ac}(G_g) = \mu(G_g) + 2 \sum_{1}^{s} p(C_i) t_i \, \mu(G_g - C_i)$$

$$\mathrm{Ac}(G_g) = \mathrm{Ch}(G_g) + 2 \sum_{1}^{s} p(C_i) \, \mathrm{Ch}(G_g - C_i) \tag{38}$$

$$\mathrm{Ch}(G_g) = \mu\gamma(G_g) - 2 \sum_{1}^{s} p(C_i)(1 - t_i) \mu(G_g - C_i)$$

$$\mathrm{Ch}(G_g) = \mathrm{Ac}(G_g) - 2 \sum_{1}^{s} p(C_i) \, \mathrm{Ac}(G_g - C_i) \tag{39}$$

The following recurrence relation for the μ-polynomial was given in [12]:

$$\mu(G \cdot H) = \mu(G)\mu(H - v_2) + \mu(G - v_1)\mu(H) - x\mu(G - v_1)\mu(H - v_2) \tag{40}$$

where v_1 and v_2 are vertices of the graphs G and H, respectively, and $G \cdot H$ represents the graph obtained by identifying v_1 with v_2.

Let the weight of the vertex v_i obtained by identifying v_1 with v_2 be a and the weight of the incident edges e_{ij}, $j = \overline{1, g_i}$ be b_{ij}. We obtain the following

Proposition 12.

$$\begin{aligned}
\mu(G_g \cdot H_g) &= \mu(G_g)\mu(H_g - v_2) + \\
&+ \mu(G_g - v_1)\mu(H_g) - (x + a)\mu(G_g - v_1)\mu(H_g - v_2) - \\
&- \sum_{1}^{g_1} (b_{1j}^2 - 1)\mu(G_g - v_1 - v_j)\mu(H_g - v_2) - \\
&- \sum_{1}^{g_2} (b_{2j}^2 - 1)\mu(G_g - v_1)\mu(H_g - v_2 - v_j) - \\
&- \sum (p(C_j) - 1) t_j \mu(G_g - C_j)\mu(H_g) - \sum (p(C_j) - 1) t_j \mu(G_g)\mu(H_g - C_j)
\end{aligned} \tag{41}$$

$$\begin{aligned}
\mathrm{Ch}(G_g \cdot H_g) &= \mathrm{Ch}(G_g)\,\mathrm{Ch}(H_g - v_2) + \\
&+ \mathrm{Ch}(G_g - v_1)\,\mathrm{Ch}(H_g) - (x + a)\,\mathrm{Ch}(G_g - v_1)\,\mathrm{Ch}(H_g - v_2) - \\
&- \sum_{1}^{g_1} (b_{1j}^2 - 1)\,\mathrm{Ch}(G_g - v_1 - v_j)\,\mathrm{Ch}(H_g - v_2) - \\
&- \sum_{1}^{g_2} (b_{2j}^2 - 1)\,\mathrm{Ch}(G_g - v_1)\,\mathrm{Ch}(H_g - v_2 - v_j) - \\
&- \sum (p(C_j) - 1)\,\mathrm{Ch}(G_g - C_j)\,\mathrm{Ch}(H_g) - \sum (p(C_j) - 1)\,\mathrm{Ch}(G_g)\mathrm{Ch}(H_g - C_j)
\end{aligned} \tag{42}$$

$$\begin{aligned}\mathrm{Ac}(G_g \cdot H_g) &= \mathrm{Ac}(G_g)\,\mathrm{Ac}(H_g - v_2) + \\ &+ \mathrm{Ac}(G_g - v_1)\,\mathrm{Ac}(H_g) - (x + a)\,\mathrm{Ac}(G_g - v_1)\,\mathrm{Ac}(H_g - v_2) - \\ &- \sum_{1}^{g_1} (b_{1j}^2 - 1)\,\mathrm{Ac}(G_g - v_1 - v_j)\,\mathrm{Ac}(H_g - v_2) - \\ &- \sum_{1}^{g_2} (b_{2j}^2 - 1)\,\mathrm{Ac}(G_g - v_1)\,\mathrm{Ac}(H_g - v_2 - v_j)\end{aligned}$$

The third and fourth summation in (41) and (42) goes over all cycles in G_g which contain vertex v_1, and over all cycles in H_g which contain vertex v_2, respectively.

5. CONCLUSIONS

Several combinatorial relations between μ, characteristic and acyclic polynomials were extended to generalized graphs. The method exposed is in principle applicable to the description of heteroconjugated molecules in the framework of the HMO theory.

REFERENCES

[1] J. V. Knop and N. Triajstić, *Int. J. Quantum Chem.* : *Quantum Chem. Symp.*, **14**, 503 (1980).
[2] I. Gutman, M. Milun and N. Trinajstić, *J. Amer. Chem. Soc.*, **99**, 1692 (1977).
[3] J. Aihara, *J. Amer. Chem. Soc.*, **98**, 275 (1976).
[4] O. E. Polansky and M. Zander, *J. Mol. Struct.*, **84**, 361 (1982).
[5] D. H. Rouvray, in "Chemical Application of Graph Theory", A. T. Balaban, Ed. Academic, London, 1976, p. 175.
[6] H. Sachs, *Publ. Math. Debrecen*, **1**, 119 (1963).
[7] R. B. Mallion, N. Trinajstić and A. J. Schwenk, *Z. Naturforsch.*, **29**a, 1481 (1974).
[8] R. B. Mallion, A. J. Schwenk and N. Trinajstić, *Croat. Chem. Acta*, **46**, 171 (1974).
[9] A. Graovac, O. E. Polansky, N. Trinajstić and N. Tyutyulkov, *Z. Naturforsch.*, **30a**, 1696 (1975).
[10] N. Trinajstić, "Chemical Graph Theory", vol. I, CRC Press, Boca Raton, 1983, p. 56.
[11] H. Hosoya, *Bull. Chem. Soc. Japan*, **44**, 2332 (1971).
[12] I. Gutman and O. E. Polansky, *Theoret. Chim. Acta (Berl.)*, **60**, 203 (1981).
[13] D. Cvetcović, M. Doob and H. Hachs, "Spectra of Graphs — Theory and Application", Academic Press, New York, 1980.
[14] I. Gutman and H. Hosoya, *Theoret. Chim. Acta (Berl.)*, **48**, 279 (1978).
[15] O. E. Polansky, *Match*, **18**, 71 (1985).

Revue Roumaine de Chimie, **33**, 7, 719–727 (1988)

REACTION OF PYRYLIUM SALTS WITH NUCLEOPHILES. XXI.[1]

UNEXPECTED FORMATION OF 6,6-DIMETHYL-5-ISOPROPYL-2,4-CYCLOHEXADIENYLIDENE-1-IMINES FROM PRIMARY AMINES AND 2,6-DIISOPROPYLPYRYLIUM SALTS

CORNELIA UNCUȚA,[a] MIRCEA D. GHEORGHIU,[b] FILIP CHIRALEU,[a]
MARIETA PLĂVEȚI,[a] MIHAI ELIAN[a] and ALEXANDRU T. BALABAN [*,b]
[a] Centre of Organic Chemistry, Bucharest
[b] Polytechnical Institute, Chair of Organic Chemistry, Splaiul Independenței 313,
76206 Bucharest, Romania

Received January 10, 1988

2,6-Diisopropyl-4-neopentylpyrylium perchlorate (1A) afforded with isopropylamine in about 75% yield N,5-diisopropyl-6,6-dimethyl-3-neopentyl-2,4-cyclohexadienylidene-1-imine (4Aa) and in about 20% yield 1,2,6-triisopropyl-4-neopentylpyridinium perchlorate (2Aa). With ethylamine the yield is 3–5% in the analogous imine 4Ab, along with a 95% yield in the corresponding N-ethylpyridinium salt 2Ab. If the 4-neopentyl group in 1A is replaced by a 4-methyl group (1B) or by a 4-phenyl group (1C) the behaviour with isopropylamine is similar. Structures were determined by IR, ^{1}H-NMR, ^{13}C-NMR spectroscopy and with the aid of lanthanide shift reagents. Imines 4 yield crystalline perchlorates 3, which can be hydrolyzed to the corresponding cyclohexadienones 5.

INTRODUCTION

Most nucleophiles react with pyrylium salts by attachment to the 2 (or 6) position; the resulting 2H-pyran may valence-isomerize to an acyclic 2,4-pentadien-1-one which in some cases can recyclize forming 5-, 6, or 7-membered carbocyclic or heterocyclic rings.[2] The recyclization involves formation of a new bond either with an atom of the nucleophile, or with an atom in benzylic position of a side-chain in the pyrylium salt. Thus, alkali hydroxides convert 2,4,6-trimethylpyrylium salts into the pseudobase; this compound valence-tautomerizes to 4-metyhl-3-hepten-2,6-dione which recyclizes on heating, forming 3,5-xylenol;[3–5] pseudobase formation and pyrylium ring reclosure explain the isotopic exchange between $H_2{}^{18}O$ and pyrylium salts.[6]

Primary amines convert pyrylium salts mainly into pyridinium salts.[2–4] With aromatic substituents on the ring, taking into account that the polyarylpyridines are good leaving groups, this reaction of primary amines can lead to the replacement of the amino group by a large variety of nucleophiles.[7] However, when the NH_2 group is attached to a secondary or tertiary carbon atom, and when in position 2 and/or 6 there exist methyl or methylene groups, recyclization to a benzene derivative competes with pyridinium salt formation;[8–10] the two products can be easily separated by extraction after alkalinization since the substituted aniline is soluble in non-polar media.

It has been widely assumed that the ready conversion of pyrylium salts into pyridines, pyridinium salts, phenols or aniline derivatives had as driving force the transformation of the pyrylium ring with low aromaticity into a carbocyclic or heterocyclic system with higher aromatic delocalization. We show in the present report that in certain cases the recyclization leads to a non-aromatic 2,4-cyclohexadien-1-imine which cannot tautomerize to an aromatic system because it is 6,6-disubstituted with two geminal methyl groups.

RESULTS

We have been interested in preparing pyridines and pyridinium salts substituted with isopropyl groups for measuring intramolecular rotation barriers by dynamic NMR spectroscopy,[11] and molecular conformation by using lanthanide shift reagents.[12] Isopropyl groups behave like "Janus-type" substituents with a *t*-butyl-like and an ethyl-like face.[13] Although polyisopropylbenzene derivatives are known[14] and hexaisopropylbenzene has recently been prepared,[15] polyisopropylpyridinium salts are little known.

The present report originates from studying the reaction between isopropylamine and 2,6-diisopropyl-substituted pyrylium salts. We shall discuss three such salts, namely with a neopentyl group in position 4 (**1A**), a methyl (**1B**) or a phenyl group (**1C**) in the same position. Unless otherwise stated, the former salt (**1A**) will be assumed. Under conditions usually employed for the conversion of pyrylium salts into pyridinium derivatives (heating them with an excess of amine in ethanol or isopropanol at reflux temperature) the pyridinium salt with three contiguous isopropyl groups (**2Aa**) was formed only in about 20% yield and the main product (75% yield) was the salt **3Aa** of a 6,6-dimethyl-5-isopropyl-2,4-cyclohexadienylidene-1-imine. Ethylamine also gives rise to two analogous products but the relative yields are reversed (3–5% in cyclohexadienylidene-iminium salt **3Ab** and 90–95% in N-ethylpyridinium salt **2Ab**).

The separation of the pyridinium and iminium salts **2** and **3**, respectively, is easily performed by neutralizing the reaction mixture with aqueous ammonia, extracting the imine **4** in ethyl ether, and distilling the product in vacuum after removing the solvent. The pyridinium salt **2** does not react with ammonia and is not extracted by ethyl ether. The stability of the neopentyl-substituted imines **4A** is higher than that of the methyl-substituted imines 4B which darken rapidly on standing. However, iminium perchlorates **3** can be conserved indefinitely. The free bases **4** regenerate the salts **3** on treatment with perchloric acid.

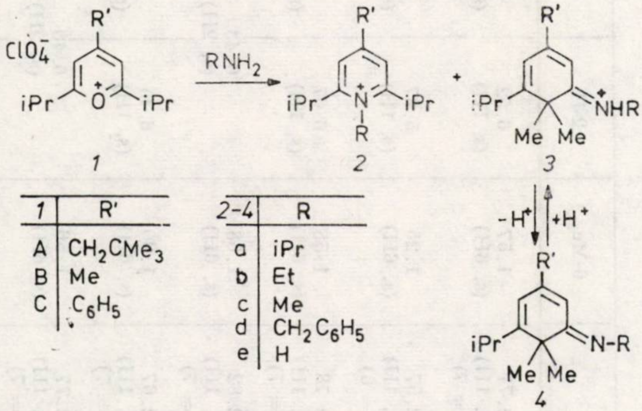

1	R'
A	CH_2CMe_3
B	Me
C	C_6H_5

2-4	R
a	iPr
b	Et
c	Me
d	$CH_2C_6H_5$
e	H

Under the same experimental conditions, methylamine and benzylamine formed only the N-methylpyridinium salt **2Ac** and the N-benzylpyridinium salt **2Ad**, respectively, whereas *t*-butylamine gave no reaction.

This unexpected formation of N-ethyl- (or N-isopropyl) -6,6-dimethyl-5-isopropyl-2,4-cyclohexadienylidene-1-iminium perchlorate with a 3-R'-substituent **3b** (or **3a**) from pyrylium salts **1** and ethylamine (or isopropylamine) is unprecedented in the chemistry of pyrylium salts.

STRUCTURE PROOF FOR 3 AND 4

Structure proofs for products **3** and **4** are based on IR, ^{1}H-NMR, and ^{13}C-NMR spectra. Both the free bases **4** and their perchlorates **3** are soluble in chloroform (of course, imines **4** are also soluble in many other non-polar solvents such as carbon tetrachloride).

In the infrared absorption spectra, a doublet of equal intensity at 1360 + 1375 cm^{-1} for **4** (CCl_4), and 1370 + 1392 cm^{-1} for **3** ($CHCl_3$) indicates the presence of a *gem*-dimethyl group. The $C = N$ and $C{=}C$ bond stretching gives rise to bands at 1695 w, 1650 m and 1585 m (for **4**, CCl_4), or 1630 m and 1580 s cm^{-1} (for **3**, $CHCl_3$); the latter perchlorate also has an NH stretching band at 3240 cm^{-1} ($CHCl_3$).

The ^{1}H-NMR assignments are presented in Table 1 and the ^{13}C-NMR data in Fig. 1, in agreement with off-resonance multiplicities.

^{1}H-NMR Spectra of the imine **4Aa** were recorded in the presence of a lanthanide shift reagent (LSR), namely Eu(fod)$_3$, in $CDCl_3$; the induced shifts values were measured in the range of molar ratios (LSR/substrate) between 0.0 and 0.5, and linear variations of the above values vs. the molar ratios were obtained. The molar induced shifts (MIS, ppm) are displayed in Fig. 2, and substantiate both the assignments presented in Table 1 and the idea that the site of complexation is the nitrogen atom.

Table 1

Chemical shifts (δ, $CDCl_3$, ppm from TMS internal standard) in the ^1H-NMR spectra of the iminium perchlorates **3** and the corresponding imines **4**.[a,b]

R′	CH_2CMe_3	Me	Ph
3	**A**	**B**	**C**

R	iPr	Et
3	**a**	**b**

Comp.	R		3-R′		5-CHMe$_2$		6-Me$_2$	2-H	4-H
3Aa	1.50 (d, 6H) ($J = 6.5$)	4.38 (sp, 1H) ($J = 6.5$)	2.58 (s, 2H)	1.05 (s, 9H)	1.22 (d, 6H) ($J = 7$)	2.77 (sp, 1H) ($J = 7$)	1.57 (s, 6H)	6.52 (s, 1H)	6.39 (s, 1H)
4Aa	1.12 (d, 6H) ($J = 6$)	3.85 (sp, 1H) ($J = 6$)	2.08 (s, 2H)	0.98 (s, 9H)	1.12 (d, 6H) ($J = 6$)	2.57 (sp, 1H) ($J = 6$)	1.25 (s, 6H)	5.97 (s, 1H)	5.75 (s, 1H)
3Ba	1.50 (d, 6H) ($J = 7$)	4.40 (sp, 1H) ($J = 7$)	2.43 (s, 3H)		1.22 (d, 6H) ($J = 7$)	2.78 (sp, 1H) ($J = 7$)	1.58 (s, 6H)	6.67 (s, 1H)	6.43 (s, 1H)
3Ca	1.56 (d, 6H) ($J = 7$)	4.53 (sp, 1H) ($J = 7$)	7.17 (m, 5H)		1.30 (d, 6H) ($J = 7$)	2.82 (sp, 1H) ($J = 7$)	1.68 (s, 6H)	6.43 (s, 2H)	
4Ca[c]	1.19 (d, 6H) ($J = 7$)	3.97 (sp, 1H) ($J = 7$)	7.42 (m, 5H)		1.14 (d, 6H) ($J = 7$)	2.67 (sp, 1H) ($J = 7$)	1.30 (s, 6H)	6.45 (s, 1H)	6.25 (s, 1H)
3Ab	1.43 (t, 3H) ($J = 7$)	3.92 (q, 2H) ($J = 7$)	2.54 (s, 2H)	1.03 (s, 9H)	1.22 (d, 6H) ($J = 7$)	2.77 (sp, 1H) ($J = 7$)	1.56 (s, 6H)	6.40 (s, 2H)	
4Ab	1.18 (t, 3H) ($J = 7$)	3.55 (q, 2H) ($J = 7$)	2.14 (s, 2H)	0.95 (s, 9H)	1.12 (d, 6H) ($J = 7$)	2.62 (sp, 1H) ($J = 7$)	1.26 (s, 6H)	6.01 (s, 1H)	5.82 (s, 1H)

[a] Abbreviations: sp stands for septet, m for multiplet and q for quartet;
[b] Coupling constants J are indicated in Hz; [c] solvent CCl_4

The iminium perchlorates 3 are hydrolysed on refluxing for several hours in 10% aqueous sodium acetate. The hydrolysis product of 3Aa is 6,6-dimethyl-5-isopropyl-3-neopentyl-2,4-cyclohexadien-1-one (5A) as shown by its elemental analysis, its strong C=O stretching band at

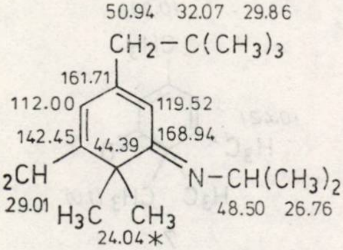
50.94 32.07 29.86
$CH_2-C(CH_3)_3$
161.71
112.00
119.52
142.45
168.94
44.39
$(CH_3)_2CH$
$N-CH(CH_3)_2$
24.64* 29.01
H_3C CH_3
48.50 26.76
24.04*

Fig. 1. — ^{13}C-NMR Chemical shifts of **4Aa** in $CDCl_3$. Asterisks indicate possible interchange.

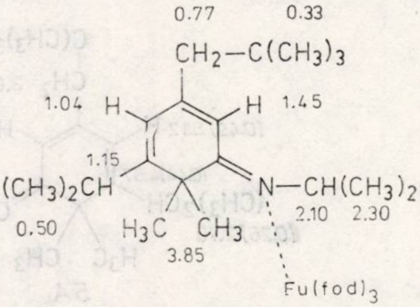
0.77 0.33
$CH_2-C(CH_3)_3$
1.04 H
H 1.45
1.15
$(CH_3)_2CH$
$N-CH(CH_3)_2$
2.10 2.30
0.50
H_3C CH_3
3.85
$Eu(fod)_3$

Fig. 2. — ^{1}H-NMR Molar induced shifts of **4Aa** by $Eu(fod)_3$ in $CDCl_3$.

1650 cm^{-1} and its ^{1}H- and ^{13}C-NMR spectra (see experimental part). It formed a crystalline red 2,4-dinitrophenylhydrazone whose analysis and ^{1}H-NMR spectrum agreed with the proposed structure for 5A.

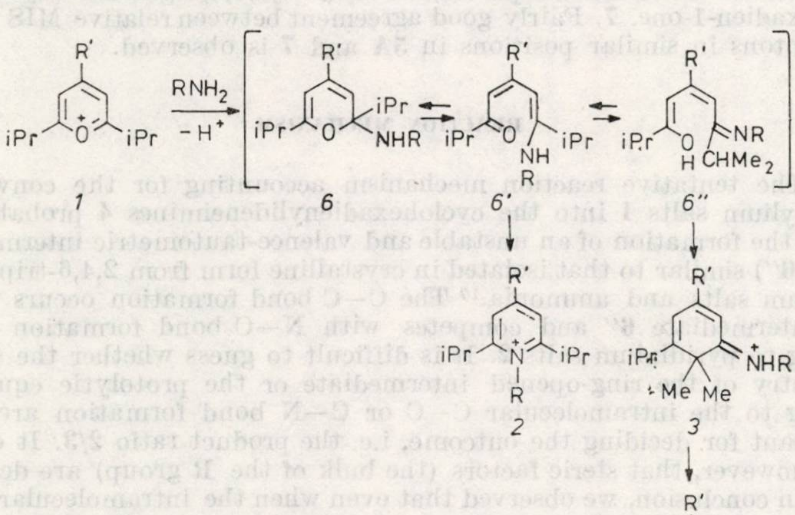
R'
iPr
O
iPr
RNH_2
$-H^+$
NHR
NH
R
NR
H CHMe$_2$
Me Me
1
6
6'
6''
2
3
5

Supplemental structure proof for 5A was obtained by recording the ^{1}H-NMR spectra in the presence of $Eu(fod)_3$ in $CDCl_3$. Linear variation of the induced shifts vs. molar ratios LSR/ketone was obtained for

molar ratio values between 0.0 and 0.5. The molar induced shifts (MIS, ppm) of **5A** along with relative MIS values (in brackets) obtained by intramolecular comparison with the 6,6-dimethyl protons are presented in Fig. 3. The figures are indicative for strong complexation of the ketone by the lanthanide, with the carbonylic oxygen as complexation site, as

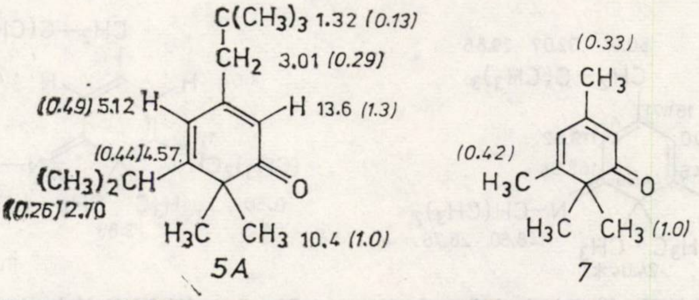

Fig. 3. — ^{1}H-NMR Molar induced shifts of **5A** by Eu(fod)$_3$ in CDCl$_3$; in brackets (*italics*), relative molar induced shift values of **5A** in CDCl$_3$ and of **7** in CH$_2$Cl$_2$, with the same LSR.

expected. For comparison, in Fig. 3 are also indicated the relative MIS values obtained by Koptyug et al.[16] using the same LSR in methylene chloride for a related compound, namely 3,4,5,6,6-pentamethyl-2,4-cyclohexadien-1-one, **7**. Fairly good agreement between relative MIS values for protons in similar positions in **5A** and **7** is observed.

REACTION MECHANISM

The tentative reaction mechanism accounting for the conversion of pyrylium salts **1** into the cyclohexadienylideneimines **4** probably involves the formation of an unstable and valence-tautometric intermediate (**6**, **6′**, **6″**) similar to that isolated in crystalline form from 2,4,6-triphenylpyrylium salts and ammonia.[17] The C—C bond formation occurs within this intermediate **6″** and competes with N—C bond formation *via* **6′** leading to pyridinium salts **2**. It is difficult to guess whether the stereochemistry of the ring-opened intermediate or the protolytic equilibria leading to the intramolecular C—C or C—N bond formation are more important for deciding the outcome, i.e. the product ratio **2**/**3**. It can be seen, however, that steric factors (the bulk of the R group) are decisive.

In conclusion, we observed that even when the intramolecular cyclization products **3** or **4** cannot have aromatic character, they may still be formed in higher yield than the aromatic pyridinium salts **2** whenever steric overcrowding in the latter compounds becomes significant.

EXPERIMENTAL PART

Instrumentation

^{1}H-NMR Spectra were recorded on Varian EM-360 L and Varian A-60A instruments, ^{13}C-NMR spectra on a Varian FT-80A instrument and IR spectra on Carl Zeiss-Jena UR 10 instrument. Melting points were determined in open capillary tubes.

Pyrylium salts 1 and its reaction with primary amines

2,6-Diisopropyl-4-neopentylpyrylium perchlorate (**1A**) was prepared by diacylation of diisobutene with isobutyric anhydride in the presence of either anhydrous zinc chloride [18] or perchloric acid [19] as catalysts.

Anhydrous zinc chloride (0.8 moles) was added with stirring and external cooling by ice-water to isobutyric anhydride (1 mole), then diisobutene (technical grade, 0.8 moles) was added dropwise over twenty minutes. Stirring was continued at room temperature for three hours, then the reaction mixture was left overnight. On addition of ethyl ether (400 mL),the pyrylium chlorozincate separated as an oil. The reaction mixture was transferred to a separatory funnel, the lower oily layer was carefully separated and the upper ethereal layer was discarded. On addition of aqueous perchloric acid to the chlorozincate, the corresponding perchlorate separated as an oil which crystallized on standing. The crude product was recrystallized from isopropanol; colourless crystals (m.p. 117°) were obtained, in 24—26% yield based on the alkene.

In an alternative procedure, 70—72% perchloric acid (0.5 moles) was added dropwise under stirring to a mixture of diisobutene (technical grade, 1 mole) and isobutyric anhydride (2.5 moles). The temperature rose rapidly after the addition of the first 2—3 mL of the acid and the reaction mixture changed colour to yellow and then to dark-brown. The temperature in the reaction mixture was kept between 70—80° by adjusting the rate at which the acid was added (and external cooling, if necessary). Stirring was continued for an additional hour, then ethyl ether was added (250—300 mL) for precipitating the pyrylium perchlorate. The crude precipitate was filtered off and washed with ethyl ether on the Buchner funnel. Recrystallization from isopropanol gave colourless crystals (m.p. 117°) in 35—38% yield based on perchloric acid. Analysis : found : C, 57.32; H, 8.26; Cl, 10.82; $C_{16}H_{27}ClO_5$ requires C, 57.39; H, 8.13; Cl 10.59%.

^{1}H-NMR (CDCl$_3$), δ(ppm) values from TMS internal standard : 1.05 (s, 9H, 4-CH$_2$C**Me**$_3$), 1.47 (d, 12H, $J = 7$ Hz, 2,6-CH**Me**$_2$), 2.93 (s, 2H, 4-C**H**$_2$CMe$_3$), 3.55 (septet, 2H, $J = 7$ Hz, 2,6-C**H**Me$_2$), 7.75 (s, 2H, 3,5-H$_2$).

2,6-Diisopropyl-4-neopentylpyridinium perchlorate **2Ae** was prepared from the pyrylium salt **1A** *via* the corresponding pyridine. Recrystallization from 1% aqueous perchloric acid gave colourless needles, m.p. 129°. Analysis : found : N, 4.17; $C_{16}H_{28}NClO_4$ requires N 4.20%.

^{1}H-NMR (CDCl$_3$): 1.00 (s, 9H, 4-CH$_2$**Me**$_3$), 1.46 (d, 12H, $J = 7$ Hz, 2,6-CH**Me**$_2$), 2.82 (s, 2H, 4-C**H**$_2$ CMe$_3$), 3.59 (septet, 2H, $J = 7$Hz, 2,6-C**H**Me$_2$), 7.43 (s, 2H, 3,5-H$_2$).

2,6-Diisopropyl-4-methylpyrylium perchlorate **1B** (m.p. 175—176°C) [20] and *2,6-diisopropyl-4-phenylpyrylium perchlorate* **1C** (m.p. 210—211°C)[21] were prepared by diacylation of *t*-butanol and α-methylstyrene, respectively, with isobutyric anhydride using perchloric acid as catalyst, according to the procedure described above for **1A**.

Formation of N,5-diisopropyl-6,6-dimethyl-3-neopentyl-2,4-cyclohexadienylidene-1-imine (**4Aa**) *and of its perchlorate* (**3Aa**). A mixture of one mole pyrylium salt **1A** and three moles isopropylamine was heated at reflux temperature in ethanol or isopropanol for two hrs., then the solvent was evaporated under reduced pressure on a warm water bath. Dilute aqueous ammonia was added, and the liberated imine **4Aa** was extracted from the suspension into ethyl ether. The aqueous suspension was filtered off leaving the pyridinium perchlorate **2Aa** which was purified by recrystallization from isopropanol or from ethanol-ethyl ether. The ethereal extract was evaporated and the imine **4Aa** was distilled under reduced pressure, b.p. 120—123°C/1 Torr. On treatment with dilute perchloric acid, the imine was converted into its perchlorate **3Aa**, m.p. 184—185° (from glacial acetic acid/ether). Analysis : found : C, 60.94; H, 9.34; N, 3.66; Cl, 9.62; $C_{19}H_{34}NClO_4$ requires C, 60.70; H, 9.12; N, 3.73; Cl, 9.34%.

The ^{1}H-NMR spectra are presented in Table 1, the ^{13}C-NMR chemical shifts are indicated on Fig. 1, and the ^{1}H-NMR molar induced shifts are shown on Fig. 2.

1,2,6-Triisopropyl-4-neopentylpyridinium perchlorate **2Aa**, m.p. 162—163° (from isopropanol). Analysis : found : C, 60.41; H, 9.33; Cl, 9.18; N, 3,99; $C_{19}H_{34}NClO_4$ requires C, 60.70; H, 9.12; Cl, 9.43; N, 3.73%.

^{1}H-NMR (CDCl$_3$): 1.00 (s, 9H, 4-CH$_2$-C**Me**$_3$), 1.49 (d, 12H, $J = 7$ Hz, 2,6-CH**Me**$_2$), 1.85 (d, 6H, $J = 7$Hz, 1-CH**Me**$_2$), 2.79 (s, 2H, 4-C**H**$_2$CMe$_3$), 3.78 (unresolved multiplet, 2H, 2,6-C**H**Me$_2$), 5.68 (septet, 1H, $J = 7$ Hz, 1-C**H**Me$_2$), 7.52 (s, 2H, 3,5-H$_2$).

Reaction of pyrylium salts **1B** *and* **1C** *with isopropylamine.* Under similar conditions to those described above, starting from 2,6-diisopropyl-4-methylpyrylium perchlorate **1B** (or 2,6-diisopropyl-4-phenylpyrylium perchlorate **1C**), two salts were again obtained, namely iminium perchlorate **3Ba** (or **3Ca**) and pyridinium perchlorate **2Ba** (or **2Ca**), in molar ratios similar to that indicated for pyrylium salt **1A**.

N,5-Diisopropyl-3,6,6-trimethyl-2,4-cyclohexadienylidene-1-iminium perchlorate **3Ba**, m.p. 158° (from 0.5% aqueous perchloric acid). Analysis: found: C, 56.45; H, 8.42; Cl. 11.48; N, 4.24; $C_{15}H_{26}NClO_4$ requires C, 56.33; H, 8.19; Cl, 11.08; N. 4.38%.

^{1}H-NMR Chemical shifts are shown in Table 1. The corresponding imine **4Ba** darkened rapidly on standing and decomposed during distillation.

1,2,6-Triisopropyl-4-methylpyridinium perchlorate **2Ba**, m.p. 211—212° (decomp.) (from isopropanol/ethyl ether). Analysis: found: C, 56.52; H, 8.47; Cl, 10.69; N, 4.68; $Cl_{15}H_{26}NClO_4$ requires C, 56.33; H, 8.19; Cl, 11.08; N, 4.38%.

^{1}H-NMR ($CDCl_3$): 1.50 (d, 12H, $J = 7$ Hz, 2,6-CH**Me**$_2$), 1.85 (d, 6H, $J = 7$ Hz, 1-CH**Me**$_2$), 2.68 (s, 3H, 4-Me), 3.77 (broad unresolved signal, 2H, 2,6-C**H**Me$_2$), 5 68 (septet, 1H, $J = 7$ Hz, 1-C**H**Me$_2$), 7.71 (s, 2H, 3,5-H$_2$).

N,5-Diisopropyl-6,6-dimethyl-3-phenyl-2,4-cyclohexadienylidene-1-iminium perchlorate **3Ca**, m.p. 200—201° (from glacial acetic acid/ether). Analysis: found: C, 62.52; H, 7.66; Cl, 8.89; N, 3.93; $C_{20}H_{28}NClO_4$ requires C, 62.90; H, 7.39; Cl, [illegible]; N, 3.66%. ^{1}H-NMR Chemical shifts are presented in Table 1.

1,2,6-Triisopropyl-4-phenylpyridinium perchlorate **2Ca**, m.p. 219° (decomp.) (from isopropanol). Analysis: found: C, 62.71; H, 7.52; Cl, [illegible].54; N, 3.71; $C_{20}H_{28}NClO_4$ requires C, 62.90; H, 7.39; Cl, 9.28; N, 3.66%.

^{1}H-NMR ($CDCl_3$ + TFA): 1.54 (d, 12H, $J = 7$ Hz, 2,6-CH**Me**$_2$), 1.85 (d, 6H, $J =$ $= 7$ Hz, 1-CH**Me**$_2$), 3.78 (broad unresolved signal, 2H, 2,6-C**H**Me$_2$), 5. 60 (septet, 1H, $J = 7$ Hz, 1-C**H**Me$_2$), 7.67 (multiplet, 5H, 4-C_6H_5), 7.88 (s, 2H, 3,5-H$_2$).

Reaction of pyrylium salt **1A** *with ethylamine* performed under similar conditions with those described for isopropylamine gave the following two salts:

N-Ethyl-5-isopropyl-6,6-dimethyl-3-neopentyl-2,4-cyclohexadienylidene-1-iminium perchlorate **3Ab**; ^{1}H-NMR chemical shifts are presented in Table 1.

1-Ethyl-2,6-diisopropyl-4-neopentylpyridinium perchlorate **2Ab**, m.p. 122—123° (from isopropanol). Analysis: found: C, 59.52; H, 9.01; Cl, 9.41; N, 3.97; $C_{18}H_{32}NClO_4$ requires C, 59,74; H, 8.91; Cl, 9.80; N, 3.87

^{1}H-NMR ($CDCl_3$): 1.00 (s, 9H, 4-CH$_2$C**Me**$_3$), 1.51 (d, 12H, $J = 6.5$ Hz, 2,6-CH**Me**$_2$), 1.62 (t, 3H, $J = 7$ Hz, 1-CH$_2$C**H**$_3$), 2.81 (s, 2H, 4-C**H**$_2$CMe$_3$), 3.60 (septet, 2H, $J = 6.5$ Hz, 2,6-C**H**Me$_2$), 4.70 (quartet, 2H, $J = 7$ Hz, 1-C**H**$_2$CH$_3$), 7.54 (s, 2H, 3,5-H$_2$)

Reaction of pyrilium salt **1A** *with methylamine* gave as sole reaction product in 96.3% yield, *2,6-diisopropyl-1-methyl-4-neopentylpyridinium perchlorate* **2Ac**, m.p. 140° (from isopropanol). Analysis: found: C, 58.76; H, 8.81; Cl, 10.53; N, 4.27; $C_{17}H_{30}NClO_4$ requires C, 58.69; H, 8.69; Cl, 10.19; N, 4.03%.

^{1}H-NMR ($CDCl_3$): 0.98 (s, 9H, 4-CH$_2$C**Me**$_3$), 1.44 (d, 12H, $J = 7$ Hz, 2,6-CH**Me**$_2$), 2.75 (s, 2H, 4-C**H**$_2$CMe$_3$), 3.64 (septet, 2H, $J = 7$ Hz, 2,6-C**H**Me$_2$), 4.28 (s, 3H, 1-Me), 7.45 (s, 2H, 3,5-H$_2$).

Reaction of pyrylium salt **1A** *with benzylamine* gave in quantitative yield *1-benzyl-2,6-diisopropyl-4-neopentylpyridinium perchlorate* **2Ad**, m.p. 183—184° (from isopropanol). Analysis: found: N, 3.59; $C_{23}H_{34}NClO_4$ requires N, 3.30%.

^{1}H-NMR ($CDCl_3$): 1.02 (s, 9H, 4-CH$_2$C**Me**$_3$), 1.37 (d, 12H, $J = 7$ Hz, 2,6-CH**Me**$_2$), 2.89 (s, 2H, 4-C**H**$_2$CMe$_2$), 3.40 (septet, 2H, $J = 7$ Hz, 2,6-C**H**Me$_2$), 6.04 (s, 2H, 1-C**H**$_2$C$_6$H$_5$), 6.92—7.50 (multiplet, 5H, 1-CH$_2$C$_6$**H**$_5$), 7.65 (s, 2H, 3,5-H$_2$).

Attempted reaction of pyrylium salt **1A** *with t-butylamine*: the mixture of pyrylium salt **1A** and t-butylamine was heated in isopropanol for 2—3 hrs, then the solvent was distilled off, leaving an oily residue. On heating part of the residue with aqueous perchloric acid, a crystalline product was obtained which, according to its melting point and ^{1}H-NMR spectrum, was the starting pyrylium salt **1A**. Treatment of the remaining oily residue with aqueous ammonia led exclusively to 2,6-diisopropyl-4-neopentylpyridine, proving that the starting material was recovered unchanged.

Hydrolysis of N,5-diisopropyl-6,6-dimethyl-3-neopentyl-2,4-cyclohexydienylidene-1-iminium perchlorate **3Aa** *to 5-isopropyl-6,6-dimethyl-3-neopentyl-2,4-cyclohexadien-1-one* **5A**; iminium perchlorate **3Aa** was hydrolyzed by refluxation in 10% aqueous sodium acetate for 3—4 hrs; the hydrolysis product (ketone **5A**) was extracted with ethyl ether and, after removing the solvent, was distilled under vacuum (b.p. 127—130°/1 Torr; m.p. ~ 40°).

IR ($CHCl_3$)$\nu_{CO} = 1650$ cm^{-1}.

^{1}H-NMR ($CDCl_3$): 0.97 (s, 9H, 3-CH$_2$C**Me**$_3$), 1.13 (d, 6H, $J = 7$ Hz, 5-CH**Me**$_2$), 1.23 (s, 6H, 6-**Me**$_2$), 2.18 (s, 2H, 3-C**H**$_2$CMe$_3$), 2.53 (septet, 1H, $J = 7$ Hz, 5-C**H**Me$_2$), 5.72 (s, 1H, 4-H), 5.95 (s, 1H, 2-H).

^{13}C-NMR ($CDCl_3$): 23.97* (6.6-Me$_2$), 24.39* (5-CH**Me**$_2$), 29.18 (5-**C**HMe$_2$), 29.87 (3-CH$_2$C**Me**$_3$), 32.31 (3-CH$_2$**C**Me$_3$), 49.30 (6-**C**Me$_2$), 50.83 (3-**C**H$_2$CMe$_3$), 120.13 (4-C), 122.14 (2-C), 155.56 (3-C), 166.03 (5-C), 205.46 (1-C); asterisks indicate possible interchange. Assignmente of the signals belonging to the carbon atoms in the conjugated unsaturated fragment of ths ring are based on data for analogous 2,4-cyclohexadien-1-ones.[22]

For elemental analysis, the *2,4-dinitrophenylhydrazone of ketone* **5A** was prepared, m.p. 147–148° (from ethanol). Analysis: found: C, 63.51; H, 7.53; N, 13.28; $C_{22}H_{30}N_4O_4$ requires C, 63.75; H, 7.30; N, 13.52%.

^{1}H-NMR ($CDCl_3$): 1,00 (s, 9H, $3\text{-}CH_2\mathbf{CMe}_3$), 1.14 (d, 6H, $J = 7$ Hz, $5\text{-}CH\mathbf{Me}_2$), 1.40 (s, 6H, $6\text{-}Me_2$), 2.30 (s, 2H, $3\text{-}\mathbf{CH}_2CMe_3$), 2.70 (septet, 1H, $J = 7$ Hz, $5\text{-}C\mathbf{H}Me_2$), 5.90 (s, 1H, 4-H), 6.05 (s, 1H, 2-H), 8.03 (d, 1H, $J = 10$Hz, 6′-H), 8.35 (dd, 1H, $J_{5',6'} = 10$ Hz, $J_{5',3'} = 2$ Hz, 5′-H), 9.18 (d, 1H, $J = 2$ Hz, 3′-H).

REFERENCES

[1] Previous part, A.T. Balaban and Choi Il, *Rev. Roum. Chim.*, **33**, 377 (1988).

[2] Reviews: A. T. Balaban, A. Dinculescu, G. N. Dorofeenko, G. W. Fischer, A. V. Koblik, V. V. Mezheritskii and W. Schroth, "Pyrylium Salts. Syntheses, Reactions, and Physical Properties", Adv. Heterocyclic Chem., Suppl. Vol. 2, Academic Press, New York, 1982; A.T. Balaban in "New Trends in Heterocyclic Chemistry", ed. R.B. Mitra et al., Studies in Organic Chemistry, vol. 3, Elsevier, Amsterdam, 1979, p. 79; A.T. Balaban, in "Organic Synthesis: Modern Trends", ed. O. Chizhov, Proc. 6th IUPAC Symposium on Organic Synthesis (Moscow, 1986), Blackwell Sci. Publ., Oxford, p. 263, 1987; K. Dimroth and K.H. Wolf, in "Newer Methods of Preparative Organic Chemistry", ed. W. Foerst, vol. 3, p. 357, Academic Press, New York 1964.

[3] A. Baeyer and J. Piccard, *Liebigs Ann. Chem.*, **407**, 332 (1914).

[4] A. T. Balaban and C. D. Nenitzescu, *Liebigs Ann. Chem.*, **625**, 74 (1959); *J. Chem. Soc.*, 3553 (1961).

[5] H. G. Rajoharison, H. Soltani, M. Arnaud, C. Roussel and J. Metzger, *Synth. Commun.*, **10**, 195 (1980).

[6] E. Gârd, A. Runge, A. Barabas and A. T. Balaban, *J. Labelled Comp.*, **3**, 151 (1967); J. M. Risley, R. L. Van Etten. C. Uncuţa and A. T. Balaban, *J. Amer. Chem. Soc.*, **106**, 7836 (1984).

[7] A. R. Katritzky, *Tetrahedron*, **36**, 679 (1980); A. R. Katritzky and C. M. Marson, *Angew. Chem. Int. Ed. Engl.*, **23**, 420 (1984); A. R. Katritzky and G. Musumarra, *Chem. Soc. Revs.*, **13**, 47 (1984).

[8] C. Toma and A.T. Balaban, *Tetrahedron*, Suppl. **7**, 9 (1966).

[9] C. Uncuţa, M. D. Gheorghiu and A. T. Balaban, *Tetrah. Lett.*, **28**, 3143 (1987).

[10] H. G. Rajoharison and C. Roussel, *Nouveau J. Chim.*, **9**, 681 (1985); *Bull. Soc. Chim., France*, 307 (1986).

[11] C. Roussel, A. T. Balaban, U. Berg, M. Chanon, R. Gallo, G. Klatte, J. A. Memiaghe, J. Metzger, D. Oniciu and J. Pierrot-Sanders, *Tetrahedron*, **39**, 4209 (1983).

[12] C. Uncuţa, T. S. Balaban, M. D. Gheorghiu, L. Stănescu, A. Petride and A. T. Balaban, *Tetrahedron Lett.*, **26**, 4673 (1985).

[13] U. Berg and C. Roussel, *J. Amer. Chem. Soc.*, **102**, 7848 (1980).

[14] E. M. Arnett and J. M. Bollinger, *J. Amer. Chem. Soc.*, **86**, 4729 (1964).

[15] J. Siegel, A. Gutierrez, W. B. Schweizer, O. Ermer and K. Mislow, *J. Amer. Chem. Soc.*, **108**, 1569 (1986).

[16] V. A. Koptyug, O. Yu. Rogozhnikova and A. N. Detzina, *Zh. Org. Khim.*, **17**, 1 (1981).

[17] A. T. Balaban and C. Toma, *Tetrahedron*, Suppl. 6, 1 (1966).

[18] A. T. Balaban, A. Ghenea and C. D. Nenitzescu, *Izv. Akad. Nauk SSSR, Otd. Khim. Nauk*, **1981**, 1102; A. T. Balaban, G. R. Bedford and A. R. Katritzky, *J. Chem. Soc.*, **1964**, 1646.

[19] A. T. Balaban and A. Bota, *Org. Prep. Proced. Int.*, **14**, 31 (1982).

[20] A. T. Balaban and C. D. Nenitzescu, *Liebigs Ann. Chem.*, **625**, 79 (1959).

[21] The 2,6-diisopropyl-4-phenylpyrylium sulfoacetate was prepared from isobutyric anhydride, α-methylstyrene and sulfoacetic acid; this salt was then converted into the corresponding perchlorate. We thank for this compound dipl.-chem.-eng. Teodor-Silviu Balaban; details will be published separately.

[22] R. Hollenstein and W. von Philipsborn, *Helv. Chim. Acta*, **55**, 2030 (1972); G. Quinkert, G. Dürner, E. Kleiner, F. Adam, G. Haupt and D. Leibfritz, *Chem. Ber.*, **113**, 2227 (1980).

Revue Roumaine de Chimie, **33**, 7, 729–739 (1988)

MESOIONIC OXAZOLONES. II[1]

UNSTABLE NON-ACYLATED COMPOUNDS

HORIA PETRIDE and DAN RĂILEANU*

Centre of Organic Chemistry — ICECHIM, Spl. Independenţei 202B, 78100 Bucharest 15, Romania

Received September 21, 1987

New oxazolo[3,2-a]pyridinium-2-olates 6b–d were generated from the corresponding perchlorates 5b–5d and characterized by their ^{1}H–NMR, IR and UV spectra. The competition between acetylation and self-acylation of these compounds has been described. Hydrolysis, ethanolysis and aminolysis of these unstable mesoionic oxazolones were studied.

Mesoionic oxazolones ("münchnones") unsubstituted in the 4-position (general formula **1**, $R''=H$) could not yet be isolated. Unlike other mesoionic compounds,[2–5] e.g. sydnone **2**, the attempts to obtain such

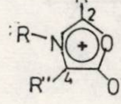

1

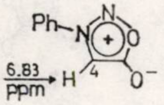
Ph–N
N
+
O
6.83 ppm
H
4
O⁻

2

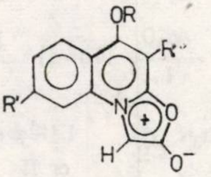

3

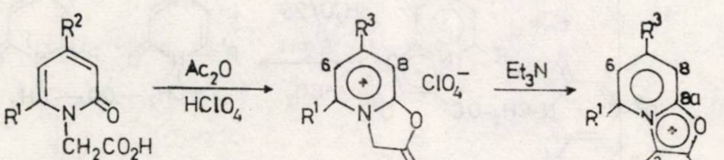
R²
R¹
N
O
CH₂CO₂H
Ac₂O
HClO₄
R³
6
8
+
R¹
N
O
O
ClO₄⁻
Et₃N
R³
6
8
8a
R¹
N
+
O
H
3
O⁻

4a–d 5a–d 6a–d

4–9	R^1	R^2	R^3
a	H	H	H
b	H	Me	Me
c	Me	H	H
d	Me	OH	OAc

monocyclic derivatives **1** (R,R'=alkyl, aryl; R''=H) led invariably to acylated compounds **1** (R''=acyl) due to the high reactivity of this mesoionic system towards electrophilic reagents.[6-9] A greater stability was observed in the case of the münchnones with fused rings **1** (R + R' = = unsaturated cycle). Thus, the pyridinium compound **6a**, while too unstable to be isolated, showed a half-life time of 30 minutes at 25°C in decimolar CH_2Cl_2 solution.[10] This made possible the recording of its IR and UV absorption spectra,[10,11] but no NMR spectral data are still available. It is worth mentioning that the quinolinium analogs **3** (R=Ac, Bz, Ts; R'=H, OH, OCH_2Ph; R''=H, Me) proved to be up to the present the sole members of the whole series of sufficient stability to be kept in crystalline state for longer periods of time.[1] Taking into account the above facts a further study of new mesoionic oxazolopyridines **6b**–**d** and their properties, especially NMR features, seemed of interest to us.

Generation of 6b–d and transformation products

Two methods were taken into consideration for the generation of **6b**–**d**: cyclization of the acylaminoacids **4b**–**d** with acetic anhydride (method I)[11,12] and the deprotonation with triethylamine of the corresponding 2,3-dihydrooxazolo [3,2-a] pyridinium perchlorates **5b**–**d** (method II).[10,11] The structure of the reaction products was influenced by the position of substituent in the pyridine nucleus.

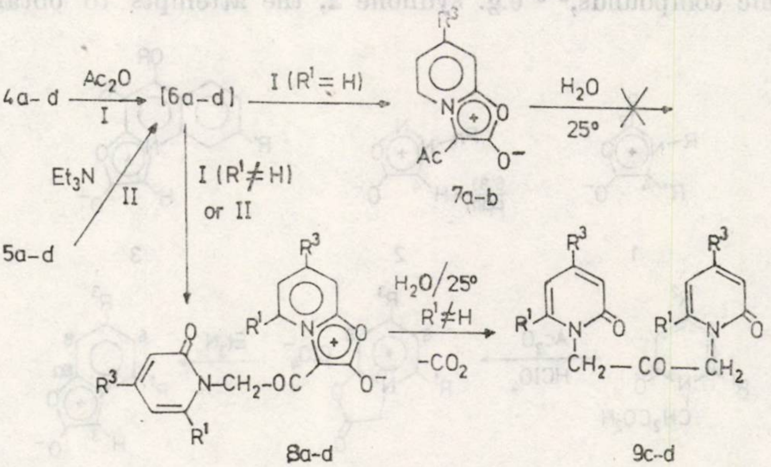

As it was to be expected by taking into account the known[12] transformation **4a** → **7a**, treatment of the acid **4b** with acetic anhydride gave the acetylated derivative **7b**. Unexpectedly, under the same conditions the acids **4c**–**d** led to the "dimeric" ketones **9c**–**d**, the decarboxylating hydrolysis products of the self-acylated münchnones **8c**–**d**. The different behaviour of **6a**–**b** and **6c**–**d** implies that the latter ones are more powerful acylating agents towards themselves than the acetic anhydride. A similar competition between acetylation and self-acylation has already been described, [8,13] but its origin is still obscure. It should be mentioned also that **9c–d** correspond to the normal products of a Dakin-West reaction.[14] In view of the above facts the cyclodehydration of **4a–d** with acetic anhydride to obtain **6a–d** proved to be unsuitable.

By the method II clear solutions of the desired compounds **6b–d** were obtained, but they had to be used instantly since a reaction of self-acylation readily takes place. Unlike the known [11] formation of the self-acylated derivative **8a** from **6a**, the 5-methyl-substituted **6c–d** afforded directly the "dimeric" ketones **9c–d**. Thus, the same reaction products were obtained by the two methods starting from **4c–d** and **5c–d**, respectively. As in the case of the method I, the attempts to isolate the intermediates **8c–d** failed. Therefore the conclusion can be drawn of a much greater stability towards water of **7a–b** and **8a** as compared to **8c–d**. A possible explanation of this dichotomy lies in the different conformation of the two series of compounds, namely the dihedral angle between the acyl rest and the planar oxazolopyridinium moiety. A discussion on this subject will be given in a following paper.[15] Although it was not possible to isolate the münchnones **6a–d** as such, their freshly prepared solutions offered the possibility of spectral characterization.

NMR-spectral properties

The ^{1}H-NMR spectra of the *in situ* generated mesoionic compounds **6a–d** from the perchlorates **5a–d** exhibit rapidly vanishing signals owing to their instability. For **6a–b** poorly resolved spectra were obtained which are only indicative for their existence, the life-time of **6a–b** being too small to allow unequivocal signal assignment. On the contrary, for the analogous compounds **6c–d** full interpretable spectra could be obatined (Table 1). To our knowledge these are the first reported NMR data for the unstable compounds of general type 1, unsubstituted in the 4-position (R''=H). Taking into account a possible incidental contamination with water, a preliminary examination might ascribe the initially obtained spectra to the self-acylated derivatives **8c–d** formed instantaneously from **6c–d**, the subsequent transfromations corresponding therefore to the hydrolysis of **8c–d** to **9c–d**. This possibility could be

Table 1

^{1}H–NMR data for **6c–d**

Compound	Solvent[(b)]	Chemical shifts[(a)]			
		H_3	H_7	H_6 and H_8	5–Me
6c	$CDCl_3$	6.05(s)	7.60(dd) (J = 7; 9 Hz)	7.20–7.25(m)	2.63(s)
6d	CD_2Cl_2	5.95(s)	2.32(s)[(c)]	6.95–7.15(m)	2.52(s)

(*a*) in ppm from internal TMS, δ scale;
(*b*) solution 0.5 M **6c–d** and 1.3 M Et_3N;
(*c*) Me signal of OAc group.

ruled out by making a comparison with the ^{1}H-NMR spectra of related acylated mesoionic oxazolones obtained by us in a different way.[15] We assume that the smaller self-acylation rate of **6c – d** relative to **6a – b** is due to a greater steric requirement for the electrophilic attack at C_3 atom caused by the 5-methyl substituent.

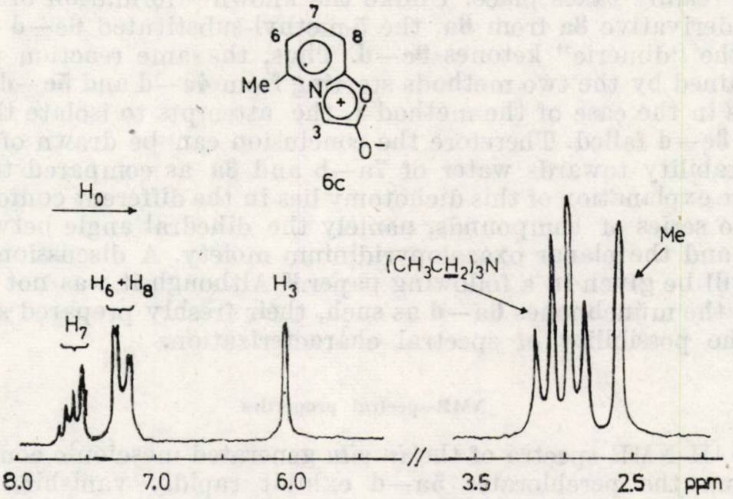

Fig. 1. — ^{1}H – NMR spectrum of **6c** generated in $CDCl_3$ from **5c** and Et_3N.

As a matter of fact, on dissolving **5c** in an $Et_3N/CDCl_3$ mixture, the first registered ^{1}H – NMR spectrum corresponds to the assumed structure, namely to **6c** (Fig. 1). As compared to the "true" pyridinium compound **10** (in DMSO – d_6)[16] which contains a full formally positive charge, the proton H_7 in **6c** is shielded by about 0.9 ppm. Most of this upfield shift can be explained by a smaller positive charge extended on the pyridinium nucleus as a result of the negative charge developed on the oxazolic region of the molecule. It results that the environment of H_7 in **6c** is quite similar to that of the γ-proton in the ylide **11** (in $CDCl_3$).[17] The shielding effect of the "acyloxy" group at the **8a**-position of **6c** offers no possibility of a comparison with **10** or **11** of the chemical shifts of H_6 and H_8. In exchange, that could be done between the chemical shifts of H_6 and H_8 in **6d** (Table 1) and those of the perchlorate **5d** which possesses a formally full positive charge on the pyridinium carbon atoms and a similar skeleton with **6d**. Again, an upfield shift of ca. 0.5 ppm can be observed on passing from **5d** to **6d**.

The chemical shift of H_3, displayed at 6.05 and 5.95 ppm for **6c** and **6d** respectively is the most characteristic feature of the NMR spectrum. The upfield shift is more than 1 ppm as compared to the quinolinium analogs **3**[1] and therefore it can be assumed that, comparatively, the canonical structure **6B** has a much greater contribution to the resonance hybrid **6A – C** than it was to be expected at a first sight. At the same time the great difference in stability between münchnones **6** and those of type **3** as well the relative resistance to acylation of the latter ones can now be readily explained, although their origin is still not well understood.

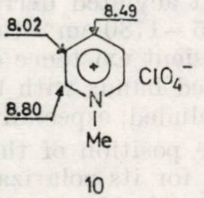

10

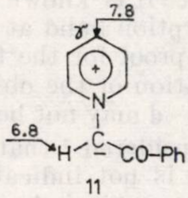

11

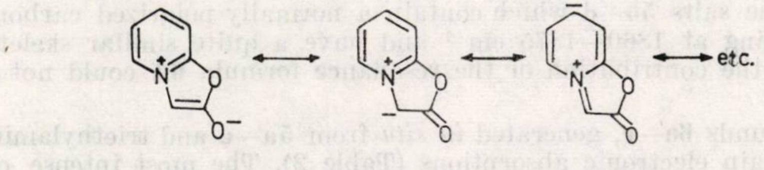

6A 6B 6C

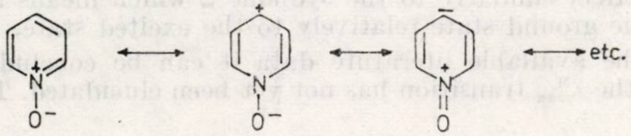

12A 12B 12C

In the same way can be explained the difference of about 0.8 ppm between the corresponding protons of sydnone **2** (in $CDCl_3$)[18] and the müchnones **6c–d**. On the other hand the ylide **11**, a compound similar to the canonical structure **6B**, exhibits a 0.8 ppm downfield shifted ylidic proton relatively to H_3 in **6c–d**. This discrepancy may be attributed among other factors, to the fused annelated structure of the carbonyloxy group in **6** as compared to the benzoyl group in **11**. In other words, from this point of view a mesoionic oxazolone like **6** may be considered as a particular case of a pyridinium ylide having a carbonyloxy group at its ylidic carbon, this group being attached simultaneously to the pyridinium cycle through an oxygen atom. From the above observations the conclusion can be drawn that canonical structures of type **6B** have a contribution increasing in the order $3 < 2 < 6$ to the respective resonance hybrids.

On the other hand the chemical shift of H_3 in **6c–d** seems too upfield located to be considered as a part of an aromatic system. Since ^1H–NMR chemical shifts are usually accepted as a qualitative estimation of aromaticity[19–21] our results strongly suggest that the studied münchnones are not aromatic, in accordance with the theoretical studies made on mesoionic compounds.[22–25]

IR and UV spectra

In the IR carbonyl region, the compounds **6b**–**d** exhibit several bands in the range 1700–1750 cm^{-1} (Table 2). Their intensity gradually decreases as new bands are arising, similarly to what has been already described for **6a**.[10] Since it is known that acylated derivatives of **6b**–**d** exhibit [15] a strong absorption band at 1765–1780 cm^{-1} this may be considered as an additional proof for the transient existence of **6b**–**d**. Nevertheless some contamination of the observed bands with those of the self-acylated derivatives **8b**–**d** may not be excluded, especially for **6b**.

It is generally considered [3] that the position of the oxazolone carbonyl bond absorption is not indicative for its polarization degree, i.e. the contribution of the canonical structure **6A**. However, taking into consideration the salts **5b**–**d** which contain a normally polarized carbonyl bond absorbing at 1860–1875 cm^{-1} and have a quite similar skeleton with **6b**–**d**, the contribution of the resonance formula **6A** could not be neglected.

Compounds **6a**–**c**, generated *in situ* from **5a**–**c** and triethylamine, show two main electronic absorptions (Table 2). The most intense one occurring at a longer wavelength (noted λ^{M}_{max}) exhibits a negatively solvatochromic effect similarly to the sydnone **2** which means an increased polarity of the ground state relatively to the excited state.

From the available literature data it can be concluded that the character of the λ^{M}_{max} transition has not yet been elucidated. Thus, for the

Table 2

IR and UV spectral data for **6a**–**d**

Compound	$\nu_{CO}(cm^{-1})^{a,b}$	$\lambda_{max}(nm)\ (\log_{10}\varepsilon)^{a,f}$		
		CH_2Cl_2	MeCN : EtOH (1 : 1 ; v/v)[g]	MeCN : H_2O (1 : 1 ; v/v)[g]
6a	1708 ; 1740[c]	320[d] ; 361[h]	349[i]	
6b	1700 ; 1726 ; 1754[d]	317[d] ; 360(4.28)		258[d] ; 326[i]
6c	1700[d] ; 1729 ; 1747	310[d] ; 353(4.29)	341.5[i]	255[d] ; 330.5[i]
6d	1708 ; 1735 ; 1770[e]			

[a] all solutions contain 1.1 molar equivalents of Et_3N ; [b] solutions ca. 0.1M in CH_2Cl_2 ; all bands are intense, except otherwise indicated ; [c] data from ref. [10] ; [d] shoulder ; [e] assigned to the acetyloxy carbonyl bond, by analogy with **5d** ; [f] solutions 10^{-4} M ; [g] contains 1 % CH_2Cl_2 ; [h] data from ref. [11] ; [i] no precise log ε values could be given because of reactions with nucleophiles ; for the λ^{M}_{max} band a value $\log\varepsilon > 4.1$ may be advanced (see exp. part)

sydnone **2** a $n \rightarrow \pi^*$ character was claimed, [26] while a $\pi \rightarrow \pi^*$ transition was suggested for the monocyclic münchnones **1** (R=Me ; R′, R″ = aryl). [27] The MO calculations of Sauer and Jung [28,29] established for the λ^{M}_{max} transition of **2** and its 3-methyl analog a $\pi \rightarrow \pi^*$ transition with an intramolecular charge transfer character. It is worth mentioning that pyridine oxide **12** displays a similar negative solvatochromic effect for which it was assumed [30] that the excited state may be best represented by the canonical structure **12C**, its contribution to the ground state being only ca. 33%. This might suggest that also in our case the contribution of the resonance formula **6C** is larger in the excited than in the ground state. Therefore it might be inferred that the λ_{max}^{M} absorption of **6a**—**c** corresponds mainly to a $\pi \rightarrow \pi^*$ transition with an intramolecular charge transfer character (from the oxazole to the pyridinium ring).

Reactivity towards nucleophiles

The hydrolysis and alcoholysis of the unstable münchnones of the general type **1** (R″=H) have not been described yet. The reaction of **6a** with primary amines, e.g. aniline, is known [11] to give amides of the acid **4a**. Alcoholysis and acid hydrolysis of the stable monocyclic compound **14** are also known, [27] but no kinetic measurements have been performed. We were able to study the hydrolysis, ethanolysis and aminolysis of the unstable fused rings münchnones **6** in dilute solutions and with a large excess of nucleophile to minimize the self-acylation reaction. The compounds **6b**—**c** were easily hydrolysed in the absence of added acid to the corresponding acids **4b**—**c**. On ethanolysis, **6c** gave the ester **13**. Analogously the anilide **15** was obtained from **6d** and aniline.

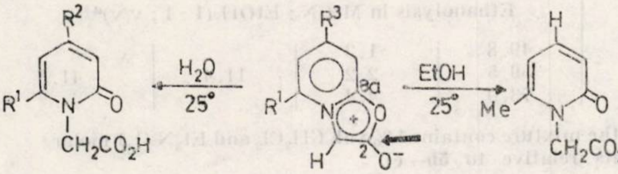

4b-c 6b-c||6c 13

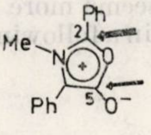

14

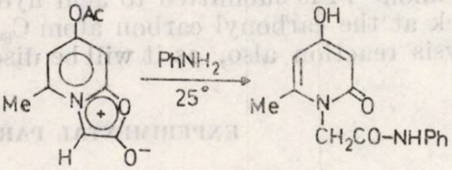

6d 15

Kinetic measurements were performed for the hydrolysis and ethanolysis reactions, the respective rate constants and activation parameter being presented in Table 3. The hydrolysis occurs within experimental errors almost identically for the two compounds **6b**—**c**. The kinetical data were obtained in order to be compared with those of their 3-acylated derivatives. [15]

Concerning the mechanism, the two possible paths are the nucleophilic attack at C_2 and/or C_{8a} atoms. The formation of a single ethanolysis product from **6c**, namely the ester **13**, indicates a regioselective attack at C_2 atom, in accordance with other literature data. [27,31] At a first sight, a similar choice cannot be made for the hydrolysis reaction considering the nature of the reaction products only, because both paths lead to the same compound. As a matter of fact, it is known[32] that nucleophilic attacks at C_2 prevails (70%) over that at C_5 when the selectively ^{18}O—labelled münchnone **14** is submitted to acid hydrolysis. However, a nucleophylic attack at the carbonyl carbon atom C_{8a} of **6** seems more likely for the hydrolysis reaction also, as it will be discussed in a following paper.[15]

Table 3

Kinetic data for hydrolysis and ethanolysis

Compound	Temp. °C	$k \cdot 10^4$ s^{-1}	ΔH^* kcal $\cdot M^{-1}$	ΔS^* cal $\cdot M^{-1} \cdot s^{-1}$
	Hydrolysis in MeCN : H_2O (1 : 1 ; v/v)[a]			
6b	35.4	2.06	17.4	−18.9
	46.5	6.2		
6c	35.4	2.08	17.4	−18.9
	46.5	6·2		
	56.5	13.7		
	Ethanolysis in MeCN : EtOH (1 : 1 ; v/v)[a]			
6c	49.8	1.3	11.4	−41.3
	59.5	2.2		
	73.0	4.4		

[a] the mixture contains 1 % vol. CH_2Cl_2 and Et_3N (1.1 molar equivalents relative to **5b—c**).

EXPERIMENTAL PART

Melting points are uncorrected. ^1H—NMR spectra were recorded on a Varian A—60A apparatus, IR spectra with a double beam UR—20 Carl Zeiss spectrophotometer and UV spectra with a a Specord UV—VIS Carl Zeiss Jena double beam spectrometer. NMR chemical shifts and coupling constants J, as well IR absorption maxima are expressed in ppm (δ scale, internal TMS), Hz and cm^{-1}, respectively.

The compounds **4a**, **4c**, **4d** and **7a** were prepared according to literature.[11,12,33,34]

4-Methyl-2-oxo-1(2H)pyridineacetic acid (**4b**) was synthesized analogously with **4c**[33] in 74% yield. M.p. 255—257°C (dec., from ethanol). $C_8H_9NO_3$ requires C, 57.48 ; H, 5.43 ; N, 8.38%. Found C, 57.20 ; H, 5.61 ; N, 8.53%.

IR (KBr) : 1642 (pyridone) ; 1721 (CO_2H) ; 2500—3000 (large, OH).

NMR (DMSO—d_6) : 2.15 (3H, s, Me), 4.56 (2H, s, CH_2), 6.09(1H, d, J = 7, H_5), 6.23 (1H, br. s, H_3), 7.52(1H, d, J = 7, H_6).

Preparation of perchlorates 5b—d

The method described by Boyd and Wright[11] for **5a** was used. Their sensitivity to moisture prevented the elemental analysis and determination of m.ps. The salts **5b—d** were purified by repeated washing with acetic anhydride followed by anhydrous ether and could be stored for a few days in a vacuum desiccator.

2,3-Dihydro-7-methyl-2-oxo-oxazolo[3,2—a]*pyridinium perchlorate* (**5b**) : 79% yield. **IR** (KBr) : 1652 (ring), 1869 (carbonyl).

2,3-Dihydro-5-methyl-2-oxo-oxazolo[3,2-a]*pyridinium perchlorate* (**5c**) : 89% yield. IR(KBr) 1651(ring), 1860(carbonyl).

7-Acetyloxy-2,3-dihydro-5-methyl-2-oxo-oxazolo[3,2-a]*pyridinium perchlorate* (**5d**) : 75% yield. IR(KBr) : 1650(ring), 1785(OAc), 1876(carbonyl).

NMR(CD_3CN) : 2.42(3H,s,OAc), 2.72(3H,s,5—Me), 5,35(2H,s, CH_2), 7.58 (2H, m, H_6 and H_8).

Generation of 6b—d and transformation products

Mesoionic compounds **6b—d** were generated *in situ* from Et_3N and **5b—d** in the appropriate solvent according to the method described [11] for the analogous transformation of **5a** in **6a**. Their spectral properties (Tables 1 and 2) were determined using fresh solutions.

3-Acetyl-7-methyl-oxazolo[3,2-a]*pyridinium-2-olate* (**7b**). The method described by Lawson and Miles[12] for **7a** was used as well as the following procedures : a suspension of **4a** (1 mmole) in acetic anhydride (1 mL) was heated at 80°C for 35—40 min. and occasionally stirred. On cooling, the clear solution deposited **7b**, which was separated by filtration, washed with water and recrystallized from benzene or toluene to give white crystals with m.p. 224—227°C in 57% yield. Alternatively, the same reaction mixture was diluted with water and extracted with 3 × 10 mL of CH_2Cl_2. The collected organic layers were dried and the solvent removed (84% yield).

$C_{10}H_9NO_3$requires C, 62.82 ; H, 4.74 ; N, 7.33%. Found C, 62.55 ; H, 4.81 ; N, 7.31%.

IR (KBr) : 1598(ring + acetyl), 1762 (carbonyl) ; (CH_2Cl_2) : 1607, 1768.

NMR ($CDCl_3$) : 2.53 (3H, s Ac), 2.58 (3H, s, Me), 7.1—7.33(2H, m, H_6 and H_8), 9.75 (1H, d, J = 7, H_5).

1,1'-(2-Oxo-1,3-propanediyl)bis[6-methyl-2(1H)pyridinone] (**9c**). *Method I* (from **4c** and Ac_2O). Similarly to the preparation of **7b**, treatment of **4c** with acetic anhydride at 80°C followed by dilution with water and extraction with CH_2Cl_2 afforded white **9c** with 217—219°C as m.p. (from CCl_4) in 54% yield.

$C_{15}H_{16}N_2O_3$ requires C, 66.16% ; H, 5.92 ; N, 10.29%. Found C, 65.95 ; H, 6.14 ; N, 10.39%.

IR(KBr) : 1665(pyridone), 1734 (ketone) ; (CH_2Cl_2) : 1664, 1744.

NMR($CDCl_3$) : 2.35(6H, s, 2× Me), 5.06(4H, s, 2×CH_2), 6.14(2H, d, J=7, 2×H_5), 6.42(2H, d, J = 9, 2×H_3), 7.33(2H, dd, J = 7 and 9, 2×H_4).

Method II (from **5c**). A clear solution made from **5c** (2 mmoles) and Et_3N (2.1 mmoles) in CH_2Cl_2 (20 mL) was left overnight at room temperature. The still homogeneous solution was stirred with an equal volume of water and the organic layer was separated and dried over anh. Na_2SO_4. Evaporation of the solvent afforded **9c** in 50% yield.

1,1'-(2-Oxo-1,3-propanediyl)bis[4-acetyloxy-6-methyl-2(1H)pyridinone] (**9d**). *Method* I (from **4d** and Ac_2O). The procedure described [12] for **7a** was followed. Removal of the excess acetic anhydride *in vacuo* gave a viscous residue which crystallized by trituration with water to **9d** with m.p. 213—215°C (from ethanol) in 56% yield.

$C_{19}H_{20}N_2O_7$ requires C, 58.76 ; H, 5.19 ; N, 7.21%. Found C, 59.08 ; H, 5.48 ; N, 7.47%.

IR(KBr) : 1665(pyridone), 1763(ketone + ester) ; (CH_2Cl_2) : 1670, 1775.

NMR ($CDCl_3$) : 2.28(6H, s, 2× Me or 2× OAc), 2.37(6H, s, 2× OAc or 2× Me), 4.95 (4H, s, 2×CH_2), 6.10(2H, m, 2× H_3 or 2× H_5), 6.35(2H, m, 2× H_5 or 2× H_3).

Method II (from **5d**). Crystalline **9d** was obtained in 50% yield from **5d** and Et_3N in CH_2Cl_2 as described for **9c**.

Reaction products from 6b—d with nucleophiles

6-Methyl-2-oxo-1(2H)pyridineacetic acid (**4c**). To a cold solution of Et_3N(0.7 mmole) in CH_2Cl_2(5mL) 0.5 mmole of perchlorate **5c** was added. This clear solution was diluted quickly with 450 mL of aqueous acetonitrile (1 : 1, v/v) and the homogeneous mixture was left undisturbed for 48 hrs at room temperature. Removal of the solvents *in vacuo* gave a residue which deposited crystals on treatment with small amounts of water and ethanol. The solid collected by filtration in 55% yield proved to be identical with an authentic sample [33] of **4c**. The acid **4b** was obtained similarly from **5b** in 50% yield.

Ethyl 6-methyl-2-oxo-1(2H)pyridineacetate (**13**). To a CH_2Cl_2 solution (5 ml) containing 0.5 mmole of **6c** generated as before, 200 mL, of anhydrous ethanol were added rapidly and the homogeneous mixture was either refluxed for 9 hrs or left at room temperature for 48 hrs.

After removal of the solvents *in vacuo*, the residue was treated with water and ether. The ethec real phase, dried and evaporated, gave crystalline **13** in 51% yield, identical with an authentisample.[33]

IR (CH_2Cl_2) : 1667(pyridone,) 1746 (ester).

NMR ($CDCl_3$) : 1.28(3H, t, J = 7, CH_3-CH_2), 2.29(3H, s, 6−Me), 4.24 (2H, q, J = 7, $O-CH_2$), 4.82(2H, s, $N-CH_2$), 6.08(1H, d, J = 7, H_5), 6.46(1H, d, J = 9, H_3), 7.28(1H, dd, J = 7 and 9, H_4).

4-Hydroxy-6-methyl-2-oxo -1(2H)pyridineacetoanilide (**15**). To a freshly prepared solution of **6d** (from 1 mmole of **5d** and 1 mmole of Et_3N in 10 mL of CH_2Cl_2) 2 mmoles of aniline were added. After 2 hrs at room temperature the solvent was evaporated *in vacuo* and the residue crystallized on trituration with $CHCl_3$. M.p. 220−222°C (from ethanol). Yield 65%. $C_{14}H_{14}N_2O_3$ requires C, 65.11 ; H, 5.46 ; N, 10.85%. Found C, 64.77 ; H, 5.51 ; N, 10, 54%.

IR(KBr) : 1609, 1664 (amide I and pyridone), 2200−3000 (large, OH), 3260 (NH).

NMR(DMSO-d_6) : 2.27(3H, s, Me), 4.77 (2H, s, CH_2), 5.55(1H, m, H_3 or H_5), 5.83(1H, m, H_5 or H_3), 6.8−7.4(5H,m, Ph), 10.33(2H, br.s, NH and OH, vanishes with D_2O).

Kinetic measurements

Aqueous or ethanolic acetonitrile solutions (1 : 1, v/v) were prepared using distilled water, anhydrous ethanol and purified[35] acetonitrile. A solution was made by dissolving Et_3N (1.1 mmole) in CH_2Cl_2(10 mL). To 0.1 mL of this cold (0°C) solution 0.001 mmole of perchlorate **5b—c** was added followed by a rapid dilution to 10 mL (volumetric flask) with the water-, respectively ethanol-acetonitrile mixture. An aliquot of this solution was introduced into the thermostated cell of the UV apparatus. The reaction was monitored to 75−80% of completion by the decay of the absorption at 30 000 cm^{-1}, in the proximity of λ^{M}_{max} transition (Table 2). The pseudo-first order rate constants and the activation parameters were calculated using the least-square method. The correlation coefficient of these lines was greater than 0.998 and the final spectrum obtained was identical with that of the reaction product synthetized on preparative scale. The decimal logarithms of the molar extinction coefficients of the mesoionic oxazolones, calculated from the regression lines, were greater than 4.1 for the λ^{M}_{max} absorption.

REFERENCES

[1] Part I : E. Tighineanu, F. Chiraleu and D. Răileanu, *Tetrahedron*, **36**, 1385 (1980).
[2] F. H. C. Stewart, *Chem. Rev.*, **64**, 129 (1964).
[3] M. Ohta and H. Kato, in "Nonbenzenoid Aromatics", J. P. Snyder ed., Academic Press, New York, London, 1969, vol. I, p. 177 ff.
[4] W. D. Ollis and C. A. Ramsden, in *Adv. Heterocyclic Chem.*, A. R. Katritzky ed., Academic Press, New York, vol. 19, 1976, p. 1.
[5] C. A. Ramsden, *Compr. Org. Chem.*, **4**, 1171 (1979).
[6] G. Sing and S. Singh, *Tetrahedron Lett.*, **1964**, 3789.
[7] W. D. Burrows, *J. Org. Chem.*, **31**, 3435 (1966).
[8] C. V. Greco, R. P. Gray and V. G. Grosso, *J. Org. Chem.*, **32**, 4101 (1967).
[9] G. V. Boyd, C. G. Davies, J. D. Donaldson, J. Silver and P. H. Wright, *J. Chem. Soc. Perkin Trans. 2*, **1975**, 1280.
[10] G. V. Boyd and P. H. Wright, *J. Chem. Soc. Perkin Trans. 1*, **1972**, 914.
[11] G. V. Boyd and P. H. Wright, *J. Chem. Soc. (C)*, **1970**, 1485.
[12] A. Lawson and D. H. Miles, *J. Chem. Soc.*, **1959**, 2865.
[13] W. Friederichsen, W. D. Schröer and T. Debaerdemaeker, *Liebigs Ann. Chem.*, **1980**, 1836.
[14] S. I. Zavyalov, N. I. Aronova and N. N. Makhova, *Reakt. i Metody Issled. Organ. Soedin.*, **22**, 9 (1971).
[15] H. Petride and D. Răileanu, in preparation.
[16] A. K. Sheinkman, L. M. Kapman, L. G. Garkh, V. E. Titov, S. N. Baranov and A. N. Kost, *Dokl. Akad. Nauk SSSR*, **193**, 366 (1970).
[17] W. G. Phillips and K. W. Ratts, *J. Org. Chem.*, **35**, 3144 (1970).
[18] G. A. Olah, D. P. Kelly and N. Suciu, *J. Amer. Chem. Soc.*, **92**, 3133 (1970).
[19] P. J. Garratt, "Aromaticity", McGraw-Hill Book Co. (UK), 1971.
[20] M. J. Cook, A. R. Katritzky and P. Linda, in *Adv. Heterocyclic Chem.*, A. R. Katritzky ed., Academic Press, New York, 1974, vol. 17, p. 255.

[21] A. T. Balaban, M. D. Banciu and V. Ciorbă, "Annulenes, Benzo-, Hetero-, Homo-Derivatives and Their Valence Isomers", CRC Press, Boca Raton Fl., 1987, ch. IIC.

[22] K. Sundaran and W. P. Purcell, *Int. J. Quant. Chem.*, **2**, 145 (1968).

[23] J. E. Bloor, R. B. Gilson and F. P. Billingsley, *Theor. Chim. Acta*, **12**, 360 (1968).

[24] M. S. Barber, S. J. Broadbent, J. A. Connor, M. J. Guest, I. H. Hillier and H. J. Puxley, *J. Chem. Soc. Perkin Trans.* 2, **1972**, 1517.

[25] M. J. S. Dewar and I. J. Turchi, *J. Chem. Soc. Perkin Trans. 2*, **1976**, 548.

[26] W. A. Lees and A. Buraway, *Tetrahedron*, **19**, 419 (1963).

[27] H. O. Bayer, R. Huisgen, R. Knorr and F. C. Schaefer, *Chem. Ber.*, **103**, 2581 (1970)

[28] J. Sauer and C. Jung, *Z. Chem.*, **13**, 434 (1973).

[29] J. Sauer and C. Jung, *Z. Phys. Chem, (Leipzig)*, **255**, 412 (1974).

[30] J. J. Jaffé, *J. Amer. Chem. Soc.*, **76**, 3527 (1954).

[31] H. Alper and M. Tanaka, *J. Amer. Chem. Soc.*, **101**, 4245 (1979).

[32] R. Knorr, *Chem. Ber.*, **104**, 3633 (1971).

[33] R. Adams and A. W. Strecker, *J. Amer. Chem. Soc.*, **71**, 1186 (1949).

[34] S. Garratt and D. Shemin, *J. Org. Chem.*, **28**, 1372 (1963).

[35] I. M. Kolthoff, S. Bruckenstein and M. K. Chantooni, *J. Amer. Chem. Soc.*, **83**, 3927 (1961).

Revue Roumaine de Chimie, **33**, 7, 741–745 (1988)

SYNTHESIS OF SUBSTITUTED FUROBENZOPYRONES

O. H. HISHMAT, A. H. ABD EL RAHMAN,[a] H. I. EL-DIWANI and SH. M. ABU-BAKR
Natural Products Department, National Research Centre, Dokki-Giza,
[a]Faculty of Science, Chemistry Department, Mansoura University, Mansoura, Egypt

Received August 30, 1986

Friedel-Crafts acylation of 2,3-diphenyl-6-methoxy-benzofuran (I) using phenylacetyl chloride in carbon disulphide gave a mixture of the 5-phenylacetyl (II) and 5,7-diphenyl acetyl (III) derivatives; acylation in benzene gave (II) only. Reaction of (II) or (III) with ethyl orthoformate gave the isoflavones (IVa and IVb) respectively, while Claisen condensation of (III) using ethyl acetate gave the substituted chromone (IVc). Use of diethyl carbonate led to the formation of the coumarin derivative (V). Compound (III) affords the bis-chalcones (VIa and VIb). Compound VIb reacted with hydroxylamine hydrochloride to form the bis-oxazoline (VIIa) and with hydrazine hydrate to yield the bis-pyrazoline (VIIb).

Substituted 6-benzofuranols show marked pharmacological properties. Some 6-benzofuranol derivatives possess hypotensive, vasodilating and spasmolytic activities.[1] Moreover they also possess antibacterial properties.[2,3]

On the other hand, 1,2-diaryl ethanones are useful as antiinflammatory, analgesics, blood plateled aggregation inhibitors and thrombosis inhibitors.[4] Also, some derivatives were found to have fungicidal[5] activity.

Therefore, we have chosen to combine the heretocyclic ring of the benzofuran and the arylethanone nucleus in order to test the antimicrobial activity of the resulting compounds.

Friedel-Crafts acylation of 2,3-diphenyl-6-methoxybenzofuran (I)[6] with phenylacetyl chloride and anhydrous aluminium chloride in carbon disulfide gave a mixture of the mono-(II) and diphenylacetyl derivative (III), separated by fractional crystalisation. When the reaction was repeated in benzene only the 5-phenylacetyl derivative (II) was obtained.

The IR spectrum of II showed bands at 1640 (*o*-hydroxy ketone)[7] and 3400 cm^{-1} (OH). The ^{1}H–NMR spectrum ($CDCl_3$) revealed signals at δ 4.4 (s, 2H, CH_2), 7.2 (s, 1H, C–7), 7.9 (s, 1, H, C–4), 12.6 (s, 1H, OH) and 7.3–7.6 (m, 15 aromatic protons). Also its mass spectrum revealed M^+ at m/e 404, ions at 313 ($M^+ - CH_2C_6H_5$), at 285 ($M^+ - COCH_2C_6H_5$) and at 91 ($CH_2C_6H_5$) as base peak.

The IR spectrum of III revealed bands at 1670 (>C=O), 1640 (*o*-hydroxyketone) and at 3400 cm^{-1}(OH). The ^{1}H–NMR spectrum

($CDCl_3$) revealed signals at 4.3 (s, 2H, CH_2), 4.4 (s, 2H, CH_2), 8.1 (s, 1H, C–4), 12.8 (s, 1H, OH) and 7.3–7.6 (m, 20 aromatic protons). It also showed M^+ at m/e 522 and the base peak at m/e 431 ($M^+ - CH_2C_6H_5$).

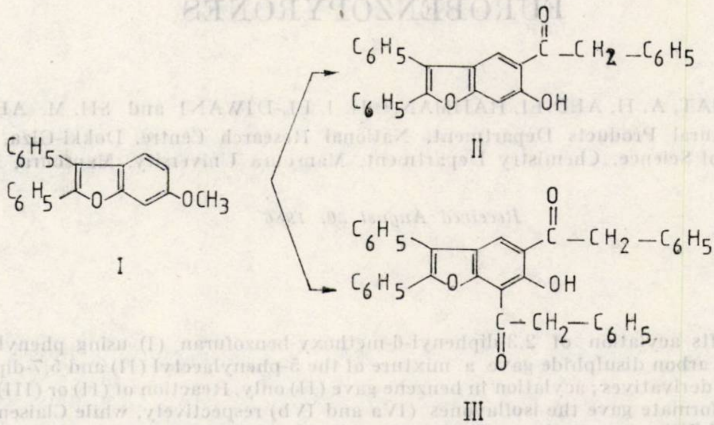

When II and III were allowed to react with ethyl orthoformate in pyridine, the isoflavones IVa and IVb were obtained, respectively.

The IR spectrum of 2,3,5-triphenyl-5H-furo[3,2-g][1]benzopyran-5-one (IVa) revealed a band at 1650 cm^{-1} (isoflavonic $>C=O^{-1}$ while 2,3,6-triphenyl-9-(phenylacetyl)-5H-furo [3,2-g] [1] benzopyran-5-one (IVb) showed bands at 1645 (isoflavonic $>C=O$) and at 1680 cm)$_2$ (phenylacetyl $>C=O$)

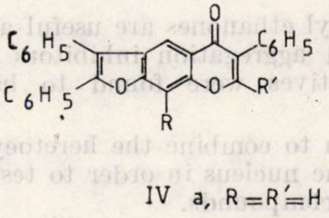

IV a, R = R′ = H

b, R = $COCH_2C_6H_5$; R′ = H

c, R = $COCH_2C_6H_5$; R′ = CH_3

On the other hand, the reaction of III with ethyl acetate in the presence of powdered sodium metal gave 2,3,6-triphenyl-7-methyl-9-(phenylacetyl)-5H-furo[3,2-g][1]benzopyran-5-one (IVc). The IR spectrum of IVc revealed bands at 1655 (chromonic $>C=O$) and at 1690 cm^{-1} (phenylacetyl $>C=O$). The ^1H–NMR spectrum ($CDCl_3$) showed bands at δ 1.15 (s, 3H, CH_3), 4.1 (s. 2H, CH_2) and 6.9–7.85 (m. 21 aromatic protons).

The reaction of III with diethylcarbonate in the presence of powdered sodium metal gave 2,3,6-triphenyl-5-hydroxy-9-(phenylacetyl 7H-furo[3,2-g] [1] benzopyran-7-one (V).

The IR spectrum of V revealed peaks at 1670 (phenylacetyl $>C=O$), 1720 (coumarin $>C=O$) and at 3400 cm^{-1} (OH).

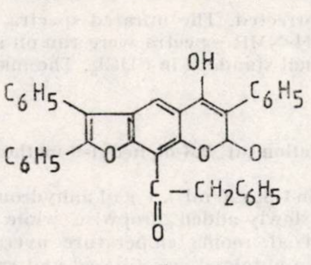

V

Condensation of the bis-compound, III with aromatic aldehydes, e.g. anisaldehyde and *p*-nitrobenzaldehyde, in the presence of sodium hydroxide affordede the bis chalcones VIa and VIb respectively. Both showed the same IR bands at 1690 (α, β-unsaturated $>C=O$) and at 3450 cm^{-1} (OH). The ^1H-NMR spectrum ($CDCl_3$) of VIa revealed signals at δ 3.75 (s, H, 2 OCH_3) and at 6.5–7.8 (m, 29 aromatic protons + 2 olefinic protons).

When the bis chalcone VIb was allowed to react with hydroxylamine hydrochloride in the presence of sodium acetate, the corresponding bis-oxazoline derivative (VIIa) was obtained having IR bands at 1625 ($>C=N$) and 3400 cm^{-1} (OH).

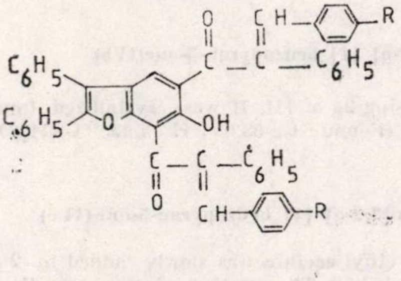

VI a, R = OCH_3
b, R = NO_2

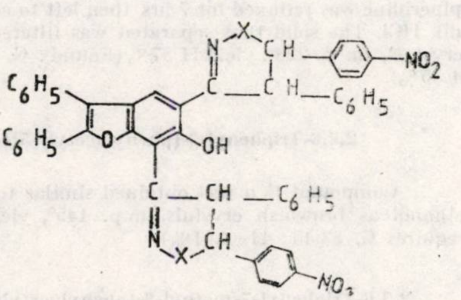

VII a, X = O
b, X = NH

When 1,1-(6-hydroxy-2,3-diphenyl-5,7-benzofurandiyl) bis [3-*p*-nitrophenyl)-2-phenyl-2-propen-1-one] (VIb) was treated with hydrazine hydrate ethanol, the bis pyrazoline VIIb was formed. Its IR spectrum revealed bands at 1630 ($>C=N$), 3340 (—NH) and at 3400 cm^{-1} (OH).

The antimicrobial activity of compounds II, III, IVa, VIb and VIIa was tested against *Staphylococcus aureus*, *Candida utilis*, *Bacillus subtilus* NRRL 543, *Escherichia coli* and *Aspergillus niger* using the disc sensitivity test. Only compound II showed moderate activity.

EXPERIMENTAL

Melting points are not corrected. The infrared spectra were recorded on a Unicam SP 2000 spectrophotometer. The ^{1}H-NMR spectra were run on a Varian EM—360 spectrometer (at 60 MHz), using TMS as internal standard in $CDCl_3$. The mass spectra were run on a Varian Mat. CH—4B spectrometer.

Friedel-Crafts acylation of 2,3-diphenyl-6-methoxy-benzofuran (I)

To a solution of I (1 g) in CS_2 (20 mL), 1 g of anhydrous aluminium chloride was added. Phenylacetyl chloride (1 g) was slowly added dropwise while stirring vigorously for 0.5 hr. The reaction mixture was left at room temperature overnight, then poured onto crushed ice and conc. HCl. The solid cake obtained was filtered and crystalized from acetone affording yellowish-orange crystals of III, m.p. 205° yield 20% (Found: C, 83.02; H, 5.10. $C_{36}H_{26}O_4$ requires C, 82.76; H, 4.98%).

The mother liquor gave a thick oil which distilled at 100°C under reduced pressure to give yellow crystals of II, m.p. 149°, yield 70% (Found: C, 82.99; H, 5.2; $C_{28}H_{20}O_3$ requires C 83.17; H, 4.95%).

The 5-phenyl acetyl derivative (II) was also obtained by dissolving 3 g of 6-methoxybenzofuran in 10 mL dry benzene and adding 1.54 g phenyl acetyl chloride and 2 g of anhydrous aluminium chloride. The reaction mixture was stirred for 10 min, left overnight, decomposed with chloroform. The solid obtained after evaporation of the solvent was crystallized from petroleum ether (b.p. 60—80°) to give yellow crystals m.p. 149°C, yield 70%.

2,3,6-Triphenyl-5H-furo[3,2-g] [1] benzopyran-5-one(IVa)

A mixture of 1.5 g II and 12 g ethyl orthoformate in 20 mL pyridine and few drops of piperidine was refluxed for 7 hrs then left to cool. The reaction mixture was decomposed with dil. HCl. The solid that separated was filtered off and crystallized from methanol as brown crystals, m. p. 228°, yield H 57% (Found: C, 83.76; 8, 4.61 $C_{29}H_{18}O_3$, requires C, 84.05; H, 4.35%).

2,3,6-Triphenyl-9-(phenylacetyl)-5H-furo[3,2-g] [1] benzopyran-5-one(IVb)

Compound IVb was obtained similar to IVa, using 2g of III. It was crystallized from ethanol as brownish crystals, m.p. 145°, yield 55% (Found: C, 83.09; H 4.42; $C_{37}H_{24}O_4$ requires C, 83.45; H, 4.51%).

2,3,6-Triphenyl-7-methyl-9-(phenylacetyl)-5H-furo[3,2-g] [1] benzopyran-5-one (IVc)

A solution of 2 g of III dissolved in 100 mL of ethyl acetate was slowly added to 2 g of freshly prepared powdered sodium metal and well shaked. The reaction mixture was then heated for 7 hrs, the solvent was removed under vacuum and the remaining cake was decomposed using dil. AcOH. The solid obtained was crystallized from ethanol as brownish crystals; m.p. 173—75°C; yield 52% (Found: C, 83.26; H, 4.9; $C_{38}H_{26}O_4$ requires: C, 83.52; H, 4.76%).

2,3,6-Triphenyl-5-hydroxy-9-(phenylacetyl)-7H-furo[3,2-g] [1] benzopyran-7-one (V)

A solution of III (2.2 g) in diethyl carbonate (50 mL) was added to powdered sodium (2.2 g) and stirred vigorously. The reaction mixture was refluxed for 2 hrs. The excess of diethyl carbonate was evaporated under vacuum and the residue extracted with ether. The aqueous layer was acidified with dil. HCl (30 mL). The solid obtained was crystallized from benzene and few drops of petroleum ether (b.p. 60—80°) as brownish crystals m.p. 161—163°, yield 60% (Around: C, 80.7; H, 4.5. $C_{31}H_{24}O_5$ requires c, 81.02; H 4.38%).

1,1-(6-hydroxy-2,3-diphenyl-5,7-benzofurandiyl) bis [3-(p-methoxyphenyl(-2-phenyl-2-propen-1-one] (VIa)]

A solution of III (1.5 g) in ethanol-chloroform mixture (50 mL) was treated with anisaldehyde (1 g) followed by 10 mL of 10% sodium hydroxide solution and refluxed for 6 hrs. The reaction mixture was acidified with dil. HCl (50 mL), filtered and crystallized from acetic acid as brownish crystals m.p. 203—204°, yield 50% (Found : C, 82.21 ; H, 5.0. $C_{52}H_{38}O_6$ requires C, 82.32 ; H, 5.0%).

1,1′-(6-hydroxy-2,3-diphenyl-5,7-benzofurandiyl) bis [3-p-nitrophenyl)-2-phenyl-2-propen-1-one] (VIb)

Similarly, as in the case of VIa, using *p*-nitrobenzaldehyde (1 g), VIb was obtained and crystallized from methanol as orange crystals, m.p. 173—175°, yield 70% (Found : C, 75.95 H, 4.0 ; N, 3.45. $C_{50}H_{32}O_8N_2$; requires C, 76.14 ; H, 4.1 ; N, 3.55%).

Bis-oxazoline derivative (VIIa)

A solution of hydroxylamine hydrochloride (1 g) and sodium acetate (2 g) in the least amount of water was added to a suspension of (VIb) (1 g) in ethanol (20 mL). The reaction mixture was refluxed for 16 hrs, cooled, filtered and washed with water. The solid formed was crystallized from acetone as brownish crystals, m.p. 173—75° (mixed m.p. with IVb 160—162°) : yield 60%. (Found : 3, 73.13 ; H, 4.0 ; N, 6.9%. $C_{50}H_{38}O_8N_6$; requires C, 73.35 ; W, 4.16 ; N, 6.85%).

Bis-pyrazoline derivative (VIIb)

The chalcone (IVb) (2 g) was dissolved in 40 mL of ethanol ; 2 mL of hydrazine hydrate were added and the reaction mixture was refluexed for 12 hrs, concentrated to about 10 mL and left to cool. The solid obtained was crystallized from methanol as yellow crystals, m.p. 195°, yield 65% (Found : C, 73.13 ; H, 4.83 ; N, 9.92. $C_{50}H_{36}O_2N_2$, requires C, 73.53 ; H, 4.41 ; N, 10.29%).

REFERENCES

[1] C. Fauran, G. Raynaud, J. Eberle and B. Pourrias (S. A. Delalande), *Ger. Offen.*, 1933, 178. (1970) ; *Chem. Abstr.*, **72**, 100486 (1970).

[2] O. H. Hishmat A. H. Abd El-Rahman, Kh. M. A. Khalil and M. I. Moawad, *J. Pharm. Sci.*, **71**, 1046 (1982).

[3] O. H. Hishmat, A. H. Abd El-Rahman, N.M.A. El-Ebrashi and H. I. El Diwani, *Indian J. Chem., sec B*, **22**, 313 (1983).

[4] Y. Hamazaki, S. Kawabata, T. Yamamoto, Y. Shiraishi, A. Ueno, K. Amemiya an d K. Saga, *US* 4, 124, 726 (1978) ; *Chem. Abstr.*, **90**, 16829 h (1979).

[5] K. Sato, H. Yamamura, T. A. Wada, I. Aoi, S. Nagai, Y. Hirota and T. Hibi, (Hokki Chemical Industry Co, Ltd) *Japan Kokai* 77—70, 019, *Chem. Abstr.*, **88**, 33181e (1978).

[6] C. Perrot and E. Cerutti, *Compt. Rend., Ser C*, **264**, 1301 (1967).

[7] L. J. Bellamy "The Infra-red Spectra of Complex Molecules", 2nd ed. Wiley, New York, 1966, p. 146.

Revue Roumaine de Chimie, 33, 7, 747–751 (1988)

IMINE DER AMINOAZOLE.5[1]

MOLEKULAR-ORBITALRECHNUNGEN IN DER REIHE DER BENZYLIDEN-AMINOAZOLE DURCH DIE MOSP-METHODE

ILSE BACALOGLU, HANS-HORST GLATT und MAMADOU FOULA BARRY

Technische Hochschule „Traian Vuia“ Timişoara, Laboratorium für
organische Chemie, str. Bocşa 6, 1900 Timişoara, Rumänien

Eingegangen am 30. März 1987

Anhand der MOSP-Rechenmethode wurden für 27 Benzyliden-aminoazole die Hückelkoeffizienten, Orbitalenergien, die effektiven $\sigma + \pi$ Gesammtladungen berechnet. Diese Größen wurden mit den chemischen Verschiebungen der Aldiminprotonen, mit der Lage der UV-Absorptionsmaxima, mit den pK -Werten sowie mit den Hydrolyse-Geschwindigkeitskonstanten korreliert.

For 27 benzylidene aminoazoles the Hückel coefficients, the MO-energies and the total $\sigma + \pi$ charges were computed by the MOSP method. The calculated values were correlated with the ^{1}H-NMR chemical shift of the aldimine protons, with the wavenumbers of the UV-spectra maxima, with the pKa values, and with the hydrolysis rate constants.

In vorangehenden Arbeiten dieser Reihe, haben wir uns mit der Synthese heterocyclischer Imine der Aminoazolreihe beschäftigt [2,3] und haben uns mit einigen Aspekten ihres chemischen Verhaltenes (Basizität,[4] Hydrolyse [1]) auseinandergesetzt, und sind dabei oft auf unerwartete Eigenheiten dieser Imine gestoßen. Zwecks besseren Verstehens des spektroskopischen und chemischen Verhaltens der Benzyliden-aminoazole haben wir quantenchemische Berechnungen ausgeführt, deren wichtigsten Ergebnisse wir in dieser Arbeit darlegen.

Die MO-Rechungen erfolgten nach der von einem von uns unlängst vorgeschlagenen MOSP (Molecular Orbitals by Specific Parametrization)-Methode,[5,6] anhand eines Rechenprogramms, das in BASIC für einen SINCLAIR ZX 81 (65 KRAM, 8 KROM) verfaßt wurde. Dabei wurden für jedes Molekül folgende Größen berechnet: die Hückelkoeffizienten, die Energien der Orbitale (in ß und eV), die π-Ladungsordnung, die effektive $\sigma + \pi$ Gesammtladung. So zum Beispiel, im Falle des p-Dimethylaminobenzyliden-2-aminobenzimid-azols, liegen die Energien der 18 MO zwischen 16 und 2,73 eV, wobei die besetzten MO zwischen 16 und 8,6 eV liegen. Die Hückelkoeffizienten weisen auf eine gewisse Lokalisierung mancher Molekülorbitale hin. So zum Beispiel ist das niedrigste Oribtal (16,39 eV) größtenteils am Imidazolring und am exocyclischen N-Atom lokalisiert. Das nächste Orbital, von 14,13 eV ist am Benzenkern und hauptsächlich am an diesen Kern gebundenen N-Atom lokalisiert, während sich das 8-te MO (9,52 eV) exclusiv an den C-Atomen des Benzenkerns befindet. Besonders wichtig ist, daβ das HOMO (8,58 eV) hauptsächlich am Imidazol-N-Atom lokalisiert ist, während sich das LUMO (6,55 eV) größtenteils am Benzyliden-C-Atom befindet, das den größten Koeffizienten aufweist. Das Benzimidazol-C-Atom, das die Aminogruppe trägt, hat einen wesentlich kleineren Koeffizienten.

Im Falle der anderen studierten Systeme wurden ähnliche Lokalisierungen der MO festgesellt Eine Tabellierung aller berechneten Koeffizienten würde ein großen Volumen von Zahlenwerten darstellen. Im Folgenden widergeben wir die Korrelierungen experimenteller Daten mit von uns errechneten Größen.

In Tabelle 1 sind einige experimentelle Daten sowie errechnete Werte für die heterocyclischen Imine zusammengefaßt.

Die chemische Verschiebung der Aldiminprotonen [2,3] lassen sich zufriedenstellend mit der Gesammtladung $(\sigma + \pi)$ am Aldimin-C-Atom korrelieren. So liegen die Benzimidazolderivate, sowie je ein Benzothiazol-(20) und bzw. Triazolderivat (27) auf folgender Geraden:

$$\delta_H = 1{,}738 . \rho_C + 9{,}045 \qquad (r = 0{,}90)$$

Die Thiazol-, Oxazol- und Triazolderivate, korrelieren nach folgender Gleichung:

$$\delta_H = 1{,}561 . \rho_C + 8{,}752 \qquad (r = 0{,}89)$$

Der Unterschied zwischen den obigen Korrelierungen kann einem Anisotropieeffekt zugeschrieben werden. Diese zufriedenstellende Korrelierung der chemischen Verschiebung mit der Gesammtladung am Aldimin-Kohlenstoffatom kann als experimenteller Beweis wenn nicht für die Ladungen dieses Atoms, so wenigstens für ihre Änderung durch Strukturmodifikationen ausgelegt werden.

Die Lage des langwelligsten Absorptionsmaximums in den UV-Spektren (als Wellenzahl in cm^{-1} ausgedrückt) ist ein Maß der Energiedifferenz zwischen HOMO und LUMO. Die entsprechende Korrelation für die untersuchten Benzyliden-aminoazole ist:

$$\tilde{\nu} = 10.789 \cdot (\varepsilon_{HOMO} - \varepsilon_{LUMO}) + 4505 \qquad (r = 0{,}841)$$

Diese Korrelierung ist zufriedenstellend, insbesondere wenn man die Verschiedenheit der heterocyclischen Imine sowie die relativ große Anzahl der Heteroatome in Betracht zieht.

Betrachtet man die Protonierung der heterocyclischen Imine als einen einfachen Donor-Akzeptor-Prozess, so ist es offensichtlich, daß die Perturbations-Energie maximal ist, wenn dem Imin die Rolle des Elektronendonators durch sein HOMO zukommt. Unter diesen Umständen müssen die pK-Werte mit den Energien der höchsten besetzten MO der Imine korrelierbar sein. Die entsprechenden Gleichungen sind:

— Benzimidazol- und Triazolderivate:

$$\mathrm{p}K_a = 36{,}271 - 3{,}474 \cdot \varepsilon_{\mathrm{HOMO}} \qquad (r = 0{,}896)$$

— Benzothiazol-, Oxazol- und Thiazolderivate:

$$\mathrm{p}K_a = 28{,}851 - 2{,}885 \cdot \varepsilon_{\mathrm{HOMO}} \qquad (r = 0{,}927)$$

Sowie es für eine sehr große Anzahl von organischen Stickstoff-Basen gezeigt wurde,[5] können diese auf insgesammt drei $\mathrm{p}K_a - \varepsilon_{\mathrm{HOMO}}$ Korrelationsgeraden liegen, je nach ihrem Solvatierungsverhalten. Im Falle der Benzyliden-aminoazole konnten also zwei dieser drei Geraden wiedergefunden werden.

Das Atom das sich effektiv protoniert, wird von der Lokalisierung des höchsten besetzten MO-s bestimmt. Es wurde bewiesen,[5] daß das Atom mit größtem Hückelkoeffizienten im HOMO protoniert wird. In allen untersuchten Benzyliden-aminoazolen ist das HOMO in größtem Maße am Azol-N-Atom lokalisiert. Unsere experimentellen Befunde[1] deuten in die selbe Richtung.

Obige Korrelierungen können also als experimentelle Bestättigung der Energien der höchsten besetzten MO-s, sowie ihrer Lokalisierung gedeutet werden.

Die Orbitalenergien der heterocyclischen Imine konnten auch mit ihren Hydrolysegeschwindigkeitskonstanten korreliert werden. So wie es in einer vorangehenden Arbeit[1] gezeigt wurde, besteht der Mechanismus der Hydrolyse von Benzyliden-aminoazolen im raschen Protonieren des Imins, gefolgt vom langsamen nucleophilen Angriff eines Puffermoleküls in den meißten Fällen, bzw. gefolgt von einem langsamen nucleophilen Angriff eines von einem Puffer molekül assistierten Wassermoleküls im Falle der Verbindungen 15, 17, 18 aus Tabelle 1.

Eine solche Reaktion kann als ein doppelter Donor-Akzeptor-Prozess verstanden werden. Die Perturbationsenergie ist maximal, wenn im ersten Donor-Akzeptor, Schritt dem Imin die Rolle des Donors (Protonieren durch das HOMO) zukommt und im zweiten jene des Akzeptors (nucleophiler Angriff durch das LUMO). Es ist so wahrscheinlich daß die vermessenen Geschwindigkeitskonstanten mit der Energie der HOMO und LUMO korrelierbar sind:

$$\lg k_3 = -26{,}686 + 4{,}272 \cdot \varepsilon_{\mathrm{HOMO}} - 1{,}090 \cdot \varepsilon_{\mathrm{LUMO}} \qquad (r = 0{,}901)$$

In diese Korrelierung reihen sich alle untersuchten Benzyliden-aminoazole, mit Ausnahme obiger drei Verbindungen ein. Im Falle der letzteren Verbindungen ist die Gleichung von der Form:

$$\lg k_3 = 57{,}588 - 13{,}171 \cdot \varepsilon_{\mathrm{HOMO}} + 9{,}087 \cdot \varepsilon_{\mathrm{LUMO}}$$

Tabelle 1

Experimentelle und berechnete Größen der Benzyliden-aminoazole

Verbindung				$\delta_H^{a)}$ (ppm)	$\lambda_{max}^{b)}$ (nm)	$pK_a^{c)}$	$k_3^{d)}$ (l^2/m^2sec)	$\rho_C^{e)}$	Orbital-energie (eV)	
									HOMO	LUMO
Nr	X	R_1	R^2	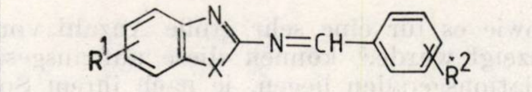						
1	NH	H	p-NMe$_2$	9,16	392	6,64	926,8	0,071	8,575	6,539
2	NH	H	p-OMe	9,30	352	—	3108,0	0,137	8,737	5,626
3	NH	H	p-Cl	9,41	355	5,82	3861	0,167	7,791	6,669
4	NH	H	m-NO$_2$	9,51	359	5,43	5590	0,238	8,841	6,912
5	NH	H	p-NO$_2$	9,51	386	5,39	7649	0,309	8,953	7,152
6	NH	5- Me	p-NMe$_2$	9,15	393	6,67	1103	0,073	8,579	6,553
7	NH	6-Me	p-NMe$_2$	9,15	393	6,67	1103	0,072	8,579	6,553
8	NH	5-Cl	p-NMe$_2$	9,10	396	6,21	617	0,075	8,597	6,567
9	NH	6-Cl	p-NMe$_2$	9,10	396	6,21	617	0,075	8,599	6,564
10	NH	5-NO$_2$	p-NMe$_2$	9,14	441	6,11	273	0,119	8,706	7,076
11	NM	6-NO$_2$	p-NMe$_2$	9,14	441	6,11	273	0,083	8,596	6,897
12	S	H	p-NMe$_2$	9,59	404	3,94	—	0,099	8,623	6,783
13	S	OMe	p-NMe$_2$	8,79	409	3,99	424	0,039	8,685	6,733
14	S	OMe	p-OMe	8,83	373	3,54	1160	0,128	8,793	6,803
15	S	OMe	p-Cl	8,98	376	3,26	1041	0,184	8,889	6,878
16	S	OMe	o-NO$_2$	9,30	390	2,46	—	0,343	9,092	7,231
17	S	OMe	m-NO$_2$	9,15	380	2,47	403	—	8,970	6,950
18	S	OMe	p-NO$_2$	—	402	2,97	658	—	9,147	7,230
19	S	OMe	o, p(NO$_2$)$_2$	—	423	1,87	—	—	9,341	7,434
20	S	OMe	o-OH	9,27	384	0,93	—	0,089	8,788	7,797
21	O	H	p-NMe$_2$	9,08	405	3,43	389	0,112	8,704	6,788
Nr	X	Y	R^2	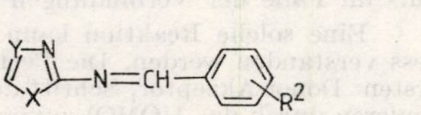						
22	S	CH	p-NMe$_2$	8,74	391	4,22	1025	0,068	8,624	6,705
23	NH	N	p-NMe$_2$	8,95	—	5,42	3574	0,084	8,751	6,509
24	NH	N	p-OMe	9,11	—	—	—	0,152	—	—
25	NH	N	p-Cl	9,20	—	—	—	0,297	—	—
26	NH	N	p-NO$_2$	9,27	—	—	—	0,342	—	—
27	NH	N	o-OH	9,35	—	—	—	0,133	—	—

a) chemische Verschiebung (TMS) des Aldiminprotens aus [2,3]

b) UV-Maxima aus [2,3]

c) pK_a aus [4]

d) Geschwindigkeitskonstanten der Hydrolyse aus [1]

e) Gesamtladung ($\sigma + \pi$) am Aldimin-C-Atom.

Werden diese drei Verbindungen mit den obigen in eine Korrelierung zusammengeschlassen, so hat dies eine bedeutende Abnahme des Korrelationskoeffizienten (0,305) zur Folge.

LITERATÜRÜBERSICHT

[1] 4-te Mitt. : H. H. Glatt, C. Csunderlik, M. F. Barry, I. Bacaloglu und S. Timofei, *Rev. Roumaine Chim.*, **33**, 637 (1988).

[2] H. H. Glatt, M. F. Barry, C. Csunderlik, R. Bacaloglu, M. Medeleanu und M. Lantoş, *Rev. Roumaine Chim.*, **30**, 125 (1985).

[3] H. H. Glatt, M. F. Barry, C. Csunderlik, R. Bacaloglu, M. Botoacă, S. Savu-Botoacă und D. Fechete, *Rev. Roumaine Chim.*, **31**, 273 (1986).

[4] R. Bacaloglu, H. H. Glatt, M. F. Barry, und C. Csunderlik, *Rev. Roumaine Chim.*, **31**, 283 (196

[5] R. Bacaloglu und I. Bacaloglu, *Bul. Ştiinţific şi Tehnic al Instit. Politeh. "Traian Vuia" (Timişoara), Ser. Chim.*, **30(44)**, 87 (1985).

[6] R. Bacaloglu und I. Bacaloglu, *Bul. Ştiinţific şi Tehnic al Instit. Politehn. "Traian Vuia" (Timişoara), Ser. Chim.*, **29(43)**, 59(1984).

Revue Roumaine de Chimie, **33**, 7, 753–754 (1988)

THE STEREOCHEMISTRY OF OLAH'S REDUCTION OF BICYCLO[2.2.1]HEPTENE DERIVATIVES. A PROOF FOR A CONCERTED REACTION MECHANISM?[1]

MIRCEA D. GHEORGHIU * and EMILIA OLTEANU
Department of Organic Chemistry, Polytechnic Institute-TCH,
76206 Bucharest 16, Romania

Received March 1, 1988

Olah's reduction (Mg$-$CH$_3$OH or CD$_3$OD/10% Pd/C) of bicyclo[2.2.1]heptene derivatives **1**–**3**, occurs on the *exo* side of the double bond, without skeletal rearrangement

The reduction of carbon-carbon double and triple bonds, in the presence of Mg/CH$_3$OH and catalytic amounts of palladium metal on carbon has become a convenient method for the reduction of nonactivated double and triple bonds.[2] To our best knowledge, no evidence for the stereochemistry of this reduction has been published.

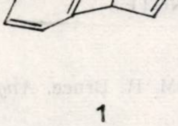

1

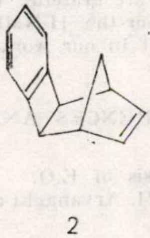

2

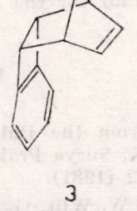

3

As substrates we have chosen bicyclo[2.2.1]heptene derivatives **1**–**3** well documented [3] for their intrinsic ability to evidence both the stereochemistry and the concerted mode of the reaction mechanism. Under typical reaction conditions, the alkenes **1**–**3** were converted (yields over 90%) in the presence of CH$_3$OH or CD$_3$OD into the saturated compounds **4a**–**6a** [4] or the deuterated norbornanes **4b**–**6b**, respectively.

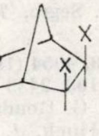

4

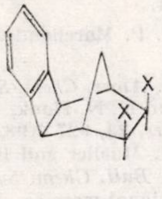

5

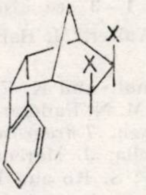

6

a: X = H
b: X = D

The reaction mode is straightforward from the stereochemistry of the products. Comparing the ^{1}H-NMR spectra of the reduced norbornane derivatives **4a**—**6a** with those of the corresponding deuterated derivatives **4b**—**6b**, one concludes that the lower field branch of the AA′BB′ system due to the ethano bridge protons of the former has virtually disappeared in the latter derivatives and has been replaced by a broad singlet. Based on literature precedence,[5] we assign the lower field signals to the *exo*-protons.

Under Olah's conditions, the reduction of the norbornene derivatives **1**—**3** occurred on the *exo*-side of the double bond, emerging thus as a process encompassed within the well-known *exo*-preferential attack.[6] ^{2}H- and ^{13}C-NMR spectra of the norbornanes **4b**—**6b** strongly suggest that during the reduction no skeletal rearrangement has occurred. In the ^{2}H-NMR spectra, only one signal was evidenced, while in the ^{13}C-NMR spectra the center of clos the triplet due to the carbon atoms bonded to deuterium was very e to the chemical shifts of the carbon atom belonging to the ethano bridge.[7] A stepwise reaction, as a result of the fact that the bicyclo[2.2.1] heptane system is prone to rearrange,[3] would very likely have led to rearranged products, in other words to deuterium scrambling. This was not the case.

The remarkable stereospecificity, and the lack of rearranged products, are our experimental evidence suggesting that Olah's reduction is a concerted reaction. Mass spectra carried out for the deuterated compounds : **4b**—**6b** have revealed that our materials were over 80% labelled.

ACKNOWLEDGEMENTS. We are grateful to Prof. Rolf Gleiter (University of Heidelberg, West Germany) for the ^{2}H-NMR and MS measurements, and to Ana Schiketanz for the interest in our work.

REFERENCES AND NOTES

[1] Taken in part from the PhD Thesis of E.O.

[2] G. A. Olah, O. K. Surya Prakash, M. Arvanaghi and M. R. Bruce. *Angew. Chem. Int. Ed. Engl.*, **20**, 92 (1981).

[3] See *inter alia* : J. W. Wilt. G. Gutman, W. J. Ronus, Jr. and A. R. Zigman, *J. Org. Chem.*, **32**, 893(1967) ; M. Avram, I. Pogany, I. G. Dinulescu, F. Chiraleu and C. D. Nenitzescu, *Rev. Roumaine Chim.*, **15**, 1207(1970) ; C. J. Adderley, J. W. Nebzydoski and M. A. Battiste, *Tetrahedron Letters*, **1971**, 3545 ; M. D. Gheorghiu, C. Drăghici and L. Pîrvulescu, *Tetrahedron*, **33**, 3296(1977) ; I. G. Dinulescu, H. L. Prasad, L. Enescu, A. Ghenciulescu and M. Avram, *Rev. Roumaine Chim.*, **24**, 833(1979).

[4] Synthesis of compounds **4a**—**6a** by Olah's procedure is described in : M. D. Gheorghiu and E. Olteanu, *J. Org. Chem.*, **52**, 5158 (1987). The deuterated compounds **4b**—**6b** were obtained in a similar manner, replacing methanol with methanol-d4. For the synthesis of norbornenes **1**—**3** see also ref. 4.

[5] J. Marshall, S. R. Walter, M. Barfield, A. P. Marchand and L. Segre, *Tetrahedron*, **32**, 537 (1976).

[6] S. Inagaki, H. Fujimoto and K. Fukui, *J. Amer. Chem. Soc.*, **98**, 4054 (1976) ; P. Caramella, N. G. Rondan, M. N. Paddon-Row and K. N. Houk, *ibid.*, **103**, 2433 (1981) ; R. Gleiter, J. Spanget-Larsen, *Tetrahedron Letters*, **23**, 927 (1982) ; N. G. Rondan, M. N. Paddon-Rou, P. Caramella, J. Mareda, P. H. Mueller and K. N. Houk, *J. Amer. Chem. Soc.*, **104**, 4974 (1982) ; S. Ito and Kakehi, *Bull. Chem. Soc. Jpn.*, **55**, 1869 (1982).

[7] The isotopic shift for C—D, carbon atom signal were *ca.* —0.47 ppm in the case of all compounds **4b**—**6b**.

Revue Roumaine de Chimie, **33**, 7, 755–761 (1988)

SYNTHESIS OF SOME NEW β-LACTAMS, 4-THIAZOLIDINONES AND PYRAZOLINES

A. M. FAHMY, KH. M. HASSAN, A. A. KHALAF and R. A. AHMED
Chemistry Department, Faculty of Science, Assiut University,
Assiut, Egypt, A.R.E.

Received June 3, 1986

N-Arylidene-*p*-aminoacetophenones (I) and/or N-arylidene-*p*-amino-1-chalcones (V) have been converted to a series of substituted β-lactams (III), 4-thiazolidinones (IV) and pyrazolines (VI, VII), respectively. Also, *p*-chloroacetamido-acetophenone (II) has been converted to a series of substituted 4-piperidino (or morpholino) acetamido chalcones (X), which undergo several cyclizations on treatment with hydrazine, phenylhydrazine or thiourea to pyrazolines (XI, XII) and pyrimidine-2-thione (XIII), respectively. The biological screening of the prepared compounds has been carried out on some strains of bacteria as well as fungi.

INTRODUCTION

Preparative methods for the β-lactam ring system have been attracting much interest with regard to the development of the analogues of β-lactam antibiotics such as pencillins, cephalosporins, nocardicins and thienamycins. [1–6] 4-Thiazolidinones have found their applications as local anaesthetics, anticonvulsant agents and as moderate tuberculostatics.[7–13] Bearing this significance in mind, this investigation has been undertaken to prepare a number of, hitherto, unreported β-lactams, 4-thiazolidinones and pyrazolines to investigate their biological activity.

RESULTS

N-arylidene-*p*-aminoacetophenone(I) has been prepared by the interaction of aromatic aldehydes and *p*-aminoacetophenone of which I_{a-d} on reaction with chloroacetyl chloride following the method of Bose *et al.*[14] failed to give expected β-lactam but resulted in hydrolytic chloroacetylation to give the corresponding *p*-(chloroacetamido-acetophenone (II). However, *o*-hydroxy-benzylideneacetophenone (I) under these conditions underwent cyclocondensation with chloroacetyl chloride giving the corresponding β-lactam (III) [IR(III) 1595 cm^{-1} (C—O of monocyclic β-lactam) and 3400 (OH) cm^{-1}]. The difference in cyclocondensation behaviour between the Schiff bases Ie and Ia-d is thought to be due to hydrogen bonding in Ie.

4-Thiazolidinones were synthesized in this investigation when mercaptoacetic acid and 4-arylidine-*p*-aminoacetophenones (Ia–e) were used. [IR (IVa-e) 1600 (CO of 4-thiazolidinones) cm^{-1}].

Pyrazolines as a class of heterocyclic compounds have many medicinal applications as anaesthetics,[15] anthelmintics,[16] and inflamation reducing agents.[17] Accordingly, the current investigation reports also on the synthesis of some new pyrazolines.

N-arylidene-*p*-amino-1-chalcones (Va-f) were prepared by the reaction of two equivalents of aromatic aldehyde with *p*-aminoacetophenone; the structure of V was confirmed by elemental and spectral analysis. Concerning the mechanism, the formation of N^1-acetylpyrazolines (VI) and N^1-phenyl-pyrazolines (VII) is believed to occur as suggested[18] before *via* 1,2- and 1,4-addition reactions.

At the same time, the hydrolysis of the azomethine group can take place through the formation of the tetrahedral carbinolamine intermediate which undergoes at least one proton transfer before breaking down to the corresponding products:

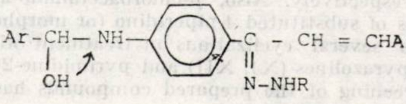

(R = H–, C_6H_5–)

The structure of compounds VI and VII was confirmed both by elemental and spectral data.

Support for the structures VI and VII comes out from the finding that all the aldehydes resulting from the hydrolysis of the imino group were detected by TLC through comparison with authentic samples.

Further confirmation of the structures was obtained through independent synthesis of the same compounds by alternative route.

N-Arylidino-N-phenylpyrazolines (VIII) were synthesised by the usual pathway using ethanol as a solvent and piperidine as a catalyst. The structures were confirmed by elemental and spectral analysis. An attempt to react compounds VIII using azomethine center to form β-lactams, thiazolidin-ones or triazines were unsuccessful, because of the bad solubility of these compounds VIII in available solvents used for these reactions.

It has been stated that the introduction of amido function in a molecule can enhance its pharmacological action. Also, piperidine and morpholine derivatives have found their wide clinical application.[19] Accordingly, the current investigation undertakes the incorporation of the later two functional groups for preparation of new amidopyrazolines. The procedure for the preparation is the reaction of piperidine and/or morpholine with compound II to form the compounds IX which react with aldehydes forming piperidino (or morpholino)4-acetoamido-1-chalcones (X_{a-d}); these chalcones (X) reacted easily with hydrazine hydrate, phenylhydrazine and thiourea giving the corresponding pyrazolines XI, XII and pyrimidine-2-thiones XIII respectively. The structures of compounds X, XI, XII, XIII were established both by elemental and spectral analysis.

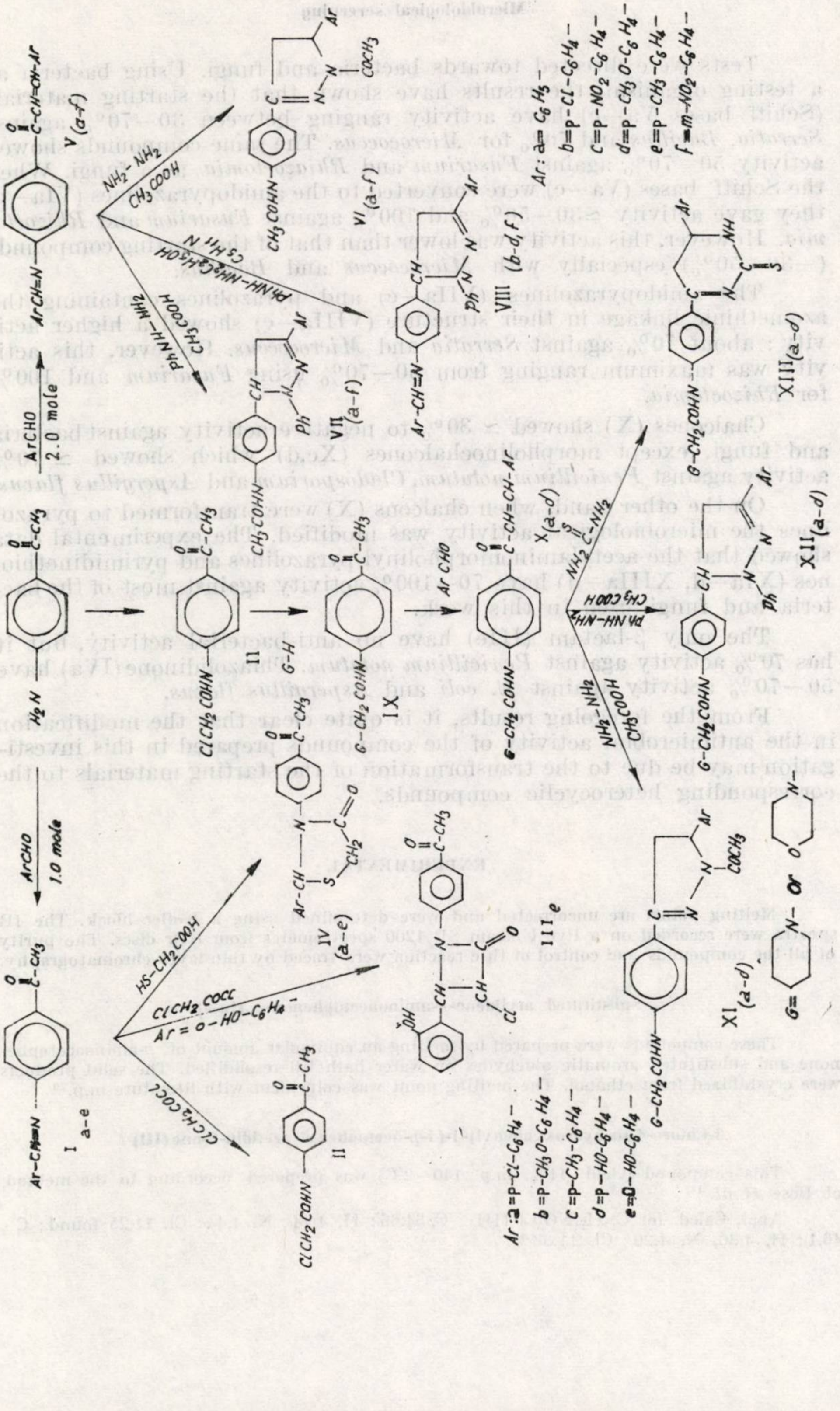
ArCHO
2.0 mole
ArCH=N
V (a-f)
NH2-NH2
CH3COOH
VI (a-f)
C5H11N
PhNH-NH2
C2H5OH
PhNH-NH2
CH3COOH
VII (a-f)
VIII (b-d, f)
XIII (a-d)
Ar: a= C6H5−
b=p-Cl-C6H4−
c=p-NO2-C6H4−
d=p-CH3O-C6H4−
e=p-CH3-C6H4−
f=m-NO2-C6H4−
H2N
ArCHO
1.0 mole
Ar-CH=N
I a-e
HS-CH2COOH
ClCH2COCl
Ar = o-HO-C6H4
ClCH2COCl
ClCH2COHN
II
IV (a-e)
III e
CH3COHN
G-H
G-CH2COHN
IX
Ar CHO
X (a-d)
NH2-NH2
CH3COOH
NH2-C-NH2 (S)
PhNH-NH
CH3COOH
XI (a-d)
XII (a-d)
G=
Or
Ar: a=p-Cl-C6H4−
b=p-CH3O-C6H4−
c=p-CH3-C6H4−
d=p-HO-C6H4−
e=O-HO-C6H4−

Microbiological screening

Tests were directed towards bacteria and fungi. Using bacteria as a testing organism, the results have shown that the starting materials (Schiff bases Va–c) have activity ranging between 30–70% against *Serratia*, *Bacillus* and 70% for *Micrococcus*. The same compounds showed activity 50–70% against *Fusarium* and *Rhiazoctomia* as a fungi. When the Schiff bases (Va–c) were converted to the amidopyrazolines (VIa–c) they gave activity ≃30–50% and 100% against *Fusarium* and *Rhizoctomia*. However, this activity was lower than that of the starting compounds (–30–50%) especially with *Micrococcus* and *Bacillus*.

The amidopyrazolines (VIIa–c) and pyrazolines containing the azomethinic linkage in their structure (VIIIa–c) showed a higher activity : about 70% against *Serratia* and *Micrococcus*. However, this activity was maximum ranging from 50–70% using *Fusarium* and 100% for *Rhizoctomia*.

Chalcones (X) showed ≃ 30% to negative activity against bacteria and fungi, except morpholinochalcones (Xc,d) which showed ≃ 70% activity against *Penicillium notatum*, *Cladosporium* and *Aspergillus flavus*.

On the other hand, when chalcons (X) were transformed to pyrazolines the microbiological activity was modified. The experimental data showed that the acetylaminomorpholinyl pyrazolines and pyrimidinethiones (XIa–d, XIIIa–d) have 70–100% activity against most of the bacteria and fungi used in this work.

The only β-lactam (IIIe) have no anti-bacterial activity, but it has 70% activity against *Penicillium notatum*. Thiazolidinone (IVa) have 50–70% activity against *E. coli* and *Aspergillus flavus*.

From the foregoing results, it is quite clear that the modification in the antimicrobial activity of the compounds prepared in this investigation may be due to the transformation of the starting materials to the corresponding heterocyclic compounds.

EXPERIMENTAL

Melting points are uncorrected and were determined using a Kofler block. The IR spectra were recorded on a Pye Unicam SP 1200 spectrometer from KBr discs. The purity of all the compounds and control of the reaction were traced by thin layer chromatography.

Substituted arylidene-*p*-aminoacetophenone (Ia-e)

These compounds were prepared by melting an equimolar amount of *p*-aminoacetophenone and substituted aromatic aldehydes on water bath till resolidified. The solid products were crystallized from ethanol. The melting point was coincident with literature m.p.[20]

3-Chloro-4-(o-hydroxyphenyl)-1-(4-*p*-acetophenyl) azetidin-2-one (III)

This compound (yield 44%, m.p. 140–2°C) was prepared according to the method of Bose *et al.* [14]

Anal. Calcd. for $C_{17}H_{14}NO_3Cl$ (III) : C, 64.66 ; H, 4.44 ; N, 4.44 ; Cl. 11.25 found ; C , 46.1 ; H, 4.30, N, 4.20 ; Cl. 11.33%.

2-Substituted aryl-3-(4-acetophenyl)thiazolidin-4-ones : (IVa-e)

These compounds were prepared according to the method of Surry *et al.* [8] The results are listed in table 1.

N-Arylidene-4-aminophenyl-1-chalcones (Va-f) [20]

These compounds were prepared by heating a mixture of *p*-aminoacetophenone (1.0 mole) and aromatic aldehydes (2.0 moles) in ethanol in the presence of 3 mL of 20 % aqueous NaOH. The product was crystallized from the proper solvent.

3-[(4-phenylacetamido)-5-substituted Aryl N^1-acetyl-] and 5-[4-phenylacetamido)-3-substituted Aryl N^1-phenyl-] pyrazolines (VIa-f), VIIa-f)

A mixtures of N-arylidine-4-aminophenyl-1-chalcone (0.003 mole) and 3 mL (0.1 mole 4 %) hydrazine hydrate or 1 mL (0,01 mole) of phenyl hydrazine in 30 mL acetic acid was refluxed for 10 hrs. The product was crystallized from proper solvent. The data are listed in table 1.

Table 1

Characterization data of 4-thiazolidinones IV(a-e), N^1-acetyl pyrazolines VI(a-f), N^1-phenylpyrazolines VIII(a-f), N-arylidene phenylpyrazolines VIII(b-d, f)*

Compd	Ar	m.p.°C	Yield %
IVa	C_6H_4Cl-*p*	154−5	66.6
IVb	$C_6H_4OCH_3$-*p*	140−2	51.5
IVc	$C_6H_4CH_3$-*p*	174−5	60.6
IVd	C_6H_4OH-*p*	148−50	55.0
IVe	C_6H_4OH-*o*	145−6	51.0
VIa	C_6H_5	255−7	48.5
VIb	C_6H_4Cl-*p*	290−2	53.3
VIc	$C_6H_4NO_2$-*p*	300−2	55.0
VId	C_6HOCH_3-*p*	220−2	45.5
VIe	$C_6H_4CH_3$-*p*	265−6	33.3
VIf	$C_6H_4NO_2$-*m*	285−6	55.0
VIIa	C_6H_5	235−6	35.1
VIIb	C_6H_4Cl-*p*	330−2	50.0
VIIc	$C_6H_4NO_2$-*p*	208−9	55.0
VIId	$C_6H_4OCH_3$-*p*	98−9	35.0
VIIe	$C_6H_4CH_3$-*p*	120−2	46.3
VIIf	$C_6H_4NO_2$-*m*	290−2	53.5
VIIIb	C_6H_4Cl-*p*	177−8	27.0
VIIIc	$C_6H_4NO_2$-*p*	16−57	33.3
VIIId	$C_6H_4OCH_3$-*p*	100−2	25.0
VIIIf	$C_6H_4NO_2$-*m*	95−6	53.3

* Satisfactory elemental analyses were obtained for all the compounds

5-(p-N-Arylidene aminophenyl)-3-substituted Aryl N^1-phenylpyrazolines VIII (b-d,f)

A mixture of N-arylidene-4-aminophenyl-1-chalcones (0.003 mole), phenylhydrazine (0.01 mole) in ethanol and two drops of piperidine was refluxed for 6 hrs. The reaction product was crystallized from the proper solvent, the data are listed in table 1.

4-Piperidino (or Morpholino) acetamido chalcones (Xa-d)

These compounds were prepared as mentioned before by using a mixture o 4-piperidino (or morpholino) acetamidoacetophenone (IX) and aromatic aldehydes. The results are listed in table 2.

Table 2

Characterization data of chalcones (Xa-d), N^1-acetyl pyrazolines (XIa-d) N^1-phenylpyrazolines (XIIa-d) and pyrimidine-2-chione (XIIIa-d)*

Comp.	Ar	G = piperidino		G = morpholino	
		m.p.°C	Yield	m.p.°C	Yield %
IX	—	105—7	94.6	93—5	96.0
Xa	C_6H_5-	170—2	44.5	158—60	40.0
Xb	C_6H_4Cl-*p*	255—6	69.0	208—9	62.0
Xc	$C_6H_4NO_2$-*p*	232—4	66.7	213—15	50.0
Xd	$C_6H_4OCH_3$-*p*	163—3	55.5	144—5	45.0
XIa	C_6H_4	105—6	30.0	190—2	30.0
XIb	C_6H_4Cl-*p*	135—6	35.0	147—8	30.0
XIc	$C_6H_4NO_2$-*p*	180—2	50.0	340—5	35.0
XId	$C_6H_4OCH_3$-*p*	110—12	37.0	95—6	33.0
XIIa	C_5H_5-	193—5	40.0	172—2	40.0
XIIb	C_6H_4Cl-*p*	195—6	45.0	120—2	55.0
XIIc	$C_6H_4NO_2$-*p*	125—6	47.0	115—6	50.0
XIId	$C_6H_4OCH_3$-*p*	80—2	42.0	140—2	45.0
XIIIa	C_6H_5-	155—7	30.0	197—200	32.0
XIIIb	C_6H_4Cl-*p*	180—2	32.0	182—3	30.0
XIIc	$C_6H_4NO_2$-*p*	255—6	35.0	210—11	35.5
XIIId	$C_6H_4OCH_3$-*p*	190—2	33.0	167—9	31.5

* Satisfactory elemental analyses were obtained for all the compounds.

3-[4′-piperidino(morpholino)acetamidophenyl]-5-substituted Aryl-N′-acetyl-and 5-[4-piperidino (morpholino) acetamidophenyl]-3-substituted Aryl-N′-phenyl-pyrazolines (XIa-d, XIIa-d)

These compounds were prepared in acetic acid as mentioned before using a mixture of compound X and hydrazine hydrate (or phenyl hydrazine). The results are listed in table 2.

4-[4′-piperidino(morpholino)acetamidophenyl]-6-substituted Aryl-1,2,5,6-tetrahydropyrimidine-2-thiones (XIIIa-d)

A mixture of 4-piperidino or (morpholino) acetamido-1-chalcones (0.002 mole), thiourea 0.3 g (0.003 mole), KOH 1.0 g, ethanol (50 mL) and water (3 mL) was refluxed for abou t 15 hrs. The reaction products were crystallized from the proper solvent. The data were represented in table 2.

REFERENCES

[1] M. S. Manhas and A. K. Bose, "Synthesis of Pencillin, Cephalosporin C., and Analogs", Marcel Dekker Inc., NY, 1969.

[2] J. C. Sheehan and E. J. Corey, *Org. React.*, **9**, 398 (1957).

[3] N. S. Isaacs, *Chem. Soc. Rev.*, **5**, 181 (1976).

[4] A. K. Mukerjee and A. K. Singh, *Tetrahedron*, **34**, 1731 (1978).

[5] T. Kamiya, M. Hashimoto, O. Nakaguchi, and T. Oka, *Tetrahedron*, **35**, 323 (1979).

[6] D. B.R. Johnson, S. M. Schmitt, F. A. Bouffar and B. G. Christensen, *J. Amer. Chem. Soc.*, **100**, 313 (1978).

[7] A. R. Surrey, *J. Amer. Chem. Soc.*, **69**, 2911 (1947).
[8] A. R. Surrey, *J. Amer. Chem. Soc.*, **71**, 3354 (1949).
[9] H D. Troutman and L. M. Long, *J. Amer. Chem. Soc.*, **70**, 3436 (1948).
[10] N. K. **Zota**, *Farmacia (Bucharest)*, **19**, 553 (1971).
[11] S. S. Parmer, O. C. Duvied, A. Chondharia and T. K. Cupta, *J. Med. Chem.*, **15**, 99 (1972).
[12] A. K. El-Shafed, Kh. M. Hassan and H. S. El-Kashef, *J. Ind. Chem.*, **54**, 60 (1977).
[13] A. E. Lipkir, K. I. Vakhreeva, P. I. Buchim D. A. Kulikvoa, and E. A. Rudzit, *Khim. Farm. Zh.*, **11**, 46 (1977),
[14] A. K. Bose, Y. H. Chiang, and M. S. Manhas, *Tetrahedron Letters*, **1972**. 4091.
[15] N. N. Valyashko and I. T. Depenshk, *J. Gen. Chem. U.S.S.R.*, **23**, 335(1953); *Chem. Abstr.* **49**, 4629h (1955).
[16] R. Libiberte. D. Compbell and F. Bruderlein, *Canad. J. Pharm. Sci.*, **2**, 37 (1967); *Chem. Abstr.*, **27**, 98059f (1967).
[17] G. Wilhelmi, *Schweiz. Med. Wochscher*, **80**, 936 (1950); *Chem. Abstr.*, **45**., 4823h (1951).
[18] G. Aziz, M.H., Nosseir, N. L. Doss and A. S. Rizk, *J. Ind. Chem.*, **14B**, 868–291 (1976).
[19] W. E. Coyne, "Medicinal Chemistry", edited by A. Burger, Wiley-Interscience, New York, 1970
[20] Scholtz and Huber, *Chem. Ber.*, **37**, 393(1904); M. Giua and E. Bagiella, *Gazz. Chim. Ital.*, **51**, II, 116–125 (1921).

Revue Roumaine de Chimie, **33**, 7, 763–772 (1988)

A FUNDAMENTAL PROPERTY CF MATTER.
PART I

VALERIU V. JINESCU
Polytechnic Institute of Bucharest, Department of Mechanics, Romania

Received February 24, 1988

The study of several phenomena in different departments of the present-day science came off as the existence of a fundamental property of matter, referred to as reluctance or generalised inertia. *A new reluctance principle is stated* to cover validity field of some well-known laws and particular principles (Newton's laws, Archimedes' law, Lenz's law, Le Chatelier's principle, homeostasis phenomena in living bodies, etc.)

1. INTRODUCTION

An earlier approach [1] on which relied a restricted phenomenological analysis furnished the idea of a basic property of resistance of matter, opposition for which the term reluctance has been proposed. In the present papers this analysis is further developed by noticing that the reluctance or resistance of matter to any external actions has the meaning of a generalized inertia.

The fundamental property characterizes material bodies which are *stable* to external actions.

A physical action upon a *stable* material body generates a phenomenon or a process of a certain nature developing with a finite speed (reaction, motion, heating speed etc...), without changing the internal structure of the material the body is made up of.

The material bodies which are *unstable* to physical ar chemical actions, instantaneously disaggregate when such an action is exerted upon them (the pehnomenon develops at an extremely high speed), release a great amount of energy and change their inside structure (be it physical, chemical or biological).

One may therefore discuss about an evolution in time over a relatively long period, following some external actions only for *stable bodies*, to be found with approximately the same structure along all the stages of their development.

The concept of *action energy*, E_a, is defined as that energy which throughout the action (of an energy field or of a body upon another field of energy or upon another material body) can be transferred to the energy field or to the material body on which the action is exerted. A generalized force P_j carries an amount of action energy, E_j, which may be partially or completely transferred to the material body, or to the energy field upon which the action is exerted.

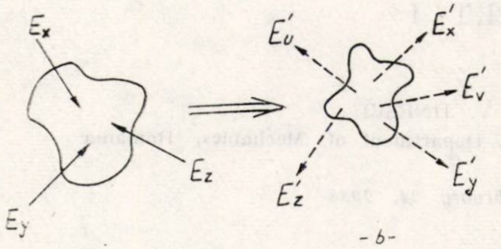

Fig. 1. — Energy action E_x, E_y and $E_z(a)$ determines the energy effect E'_x, E'_y, E'_z, E'_u and $E'_v(b)$.

The concept of *effect energy* E_e, is defined as that energy that is stored or consumed during an interaction. For example, the energy accumulated by elastic deformation, by heating, by magnetization etc., and also the energy consumed in internal or external friction.

In all interactions of material bodies and/or energy fields, it is *postulated* that *the sum of all action energy amounts equals the sum of the effect energy.*

Otherwise stated, the action energy is wholly found as the energy of the obtained effects, irrespective of the nature or form of the forces carrying energy. This postulate states the *quantitative* preservation of energy in interactions; *the forms of the energy involved as well as the amounts of the corresponding energy are generally not preserved.*[2] In other words the total energy amount is preserved in an interaction but it is the form of the energy or the ratio of energy amounts of different forms which changes. For example, if the energy amounts E_x, E_y, E_z (Fig. 1, a) of the x, y, z forms act upon a material body so that the effects obtained are the energy amounts of the same forms, E'_x, E'_y, E'_z, but of different values from the initial ones, as well as the energy amounts of forms u and v of values E_v and E'_u (Fig. 1.b), then

$$E_x + E_y + E_z = (E'_x + E'_y + E'_z) + E'_u + E'_v,$$

where, generally, $E'_u \neq E'_v$; $E'_y \neq E_y$ and $E'_z \neq E_z$

In the following chapters we refer only to *stable* materials, because only for such materials one can speak of a time development of processes or phenomena and only such materials have the reluctance or generalized inertia property.

Starting from some well known phenomena, laws and principles of contemporary science one can generally state the *principle of reluctance*. This principle refers to the transfer and change of energy. We shall further correlate the concept of reluctance with the first principle of thermodynamics, with the concept of material degradation as well as with that of reluctant force.

2. PRINCIPLE OF RELUCTANCE

By generalizing a great number of experimental facts one issues the following principle : *matter* (under any form of existence) ***is reluctant to any action modifying or tending to modify its state of energy equilibrium; if the produced disequilibrium may produce transformations of matter then matter evolves in the sense which tends to reestablish the initial state, diminishing the cause.***

This principle covers the validity fields of some wellknown principles, laws and phenomena;$^{3-8}$ Le Chatelier's principle, Newton's laws, the electromagnetic induction and self-induction pehnomena, Archimedes' law, those of heat accumulation and heat transfer, the homeostasis of living bodies etc.

3. PARTICULAR CASES WHOSE GENERALIZATION LEADS TO THE PRINCIPLE OF RELUCTANCE

3.1. Mechanical and thermomechanical phenomena

a — Body stretching generates the reciprocal attraction of the atoms or molecules making it up, whereas compressing it determines their rejection. There follows that attraction opposes expansion whereas rejection opposes compression.

The volume of a body undergoing multilateral compression under pressure p, diminishes with

$$|\Delta V(p)| = V_0 \cdot \beta_p \cdot (p - p_0)$$

where V_0 is the volume at pressure p_0 and temperature T_0 and β_p — the coefficient of isothermal compressibility.

At the same time, body temperature will increase with $\Delta T = T - T_0$, as an effect of compression. The temperatura increase leads to the volume increase with

$$\Delta V(T) = V_0 \cdot \beta_T \cdot \Delta T$$

where β_T is the coefficient of volumic thermal expansion.

The total volume variation (the volume increase is positive) following body compression is therefore

$$\Delta V = \Delta V(T) - \Delta V(p)$$

or

$$\Delta V = V_0(\beta_T \cdot \Delta T - |\beta_p \cdot \Delta p|) \tag{1}$$

Owing to the body heating, the total volume variation due to compression is much less than in isothermal compression. It follows from (eqn. 1) that the compression effect (body heating) opposes the cause compression).

If the compressed body could be entirely isolated from the environment (even from the compressing agent) and if the whole compression energy could be transformed into the thermal energy accumulated by the body, then $|\Delta V(p)| = \Delta V(T)$ and $\Delta V = 0$.

As such a thermal isolation is not practically possible, $|\Delta V(p)| > > \Delta V(T)$ and $\Delta V < 0$.

b — In *body expansion* matter will oppose to the body volume increase, through its cooling. The body cools and the phenomenon follows the inverted pattern of the preceding case.

Hence, *reluctance* damps out the evolution of physical phenomena in that the effect opposes to the cause.

c — *Fluid viscosity* is pressure dependent according to the relationship

$$\mu(p) = \mu(p_0, T_0) \cdot \exp \cdot (b_p \cdot \Delta p),$$

where $\mu(p_0, T_0)$ is the viscosity at pressure p_0 and temperature T_0; $\Delta p = = p - p_0$ and b_p — constant.

Viscosity rises with pressure increase. But the increase in viscosity is damped out because of the simultaneous temperature rise $\Delta T = T - T_0$ following compression.

The viscosity diminishes with the temperature increase, for instance, according to relationship

$$\mu(T) = \mu(T_0, p_0). \exp \left[\frac{E}{R} \left(\frac{1}{T} - \frac{1}{T_0} \right) \right]$$

where $\mu(T_0, p_0)$ is the viscosity at temperature T_0 and pressure p_0; E — — activation energy; $R = 8{,}314$ J/mol.K — the universal constant.

The temperature rise caused by compression opposes to the viscosity increase generated by compression as well.

Dependence $\mu(p) \div \mu(p_0, T_0)$ is damped out by the thermal effect with the value $\mu(T)/\mu(T_0)$, so that one may write

$$\mu(p) = \mu(p_0, T_0) \cdot \exp \left[b_p \cdot (p - p_0) - \frac{E}{R} \left(\frac{1}{T} - \frac{1}{T_0} \right) \right] \tag{2}$$

Hence, this is another case when the thermal *effect* opposes to the evolution of the phenomenon determined by compression.

d — The *law of inertia* or Newton's first law states the fact that "if interaction is absent, a body preserves its state of rest or uniform motion in a straight line with respect to any inertia system". Hence, *if there are no actions* (or interactions) the reluctance does not manifest itself and everything will remain unchanged; no effects are present either.

e — The *law of forces* or Newton's second law, expresses the equality between force, $\vec{F}$, applied to a body and its effect, $m.\vec{a}$;

$$\vec{F} = m \cdot \vec{a}, \tag{3}$$

where m is the mass of the body; $\vec{a}$ — body acceleration.

In the case of a body subject to interactions, their effect cannot be indefinitely large; the mass of the body will be reluctant to the increase of effect, $\vec{a}$.

One might say then that body mass is reluctant to a change, in its state of uniform and straight line motion or to its state of rest. Acceleration $\vec{a}$ expresses the transition intensity from one state of temporary equilibrium to another. Mass is therefore one of the forms of direct manifestation, at macroscopic level, of the property of matter reluctance or generalized inertia. Mass is correlated with the variation of the potential energy, E_p, in the gravitational field, through the relationship

$$\mathrm{d}E_p = m \cdot g \cdot \mathrm{d}h,$$

where g is the gravitational acceleration; $\mathrm{d}h$ — height variation. From the proceding relation one has

$$m = \frac{1}{g} \cdot \frac{\mathrm{d}E_p}{\mathrm{dh}} \tag{4}$$

Similarly, the expression of the thermal energy variation accumulated by a body

$$\mathrm{d}E_{th} = m \cdot c \cdot \mathrm{d}T,$$

where c is the body specific heat and $\mathrm{d}T$ — body temperature variation, yields

$$m = \frac{1}{c} \cdot \frac{\mathrm{d}E_{th}}{\mathrm{d}T} \cdot \tag{5}$$

Eqs. (4) and (5) show that mass is proportional to the action energy derivative with respect to the effect variabile (here h and T respectively).

Hence reluctance or matter reluctance to *interactions* is proportional to the action energy derivative as a function of physical variable-effect.

f — Archimedes' force. When immersing a solid body of volume V into a liquid of density ρ_l, the liquid mass $m = \rho_l \cdot V$ is reluctant to body immersion. *The reluctance* is equal to the force corresponding to the mass of the liquid displaced by the body. In the gravity field, this force is called Archimedes' force and is expressed by

$$\vec{F}_A = \rho_l \cdot \vec{g} \cdot V, \tag{6}$$

where g is the gravity acceleration. In a field of forces (other than the gravity field) characterized by acceleration $\vec{a}_f$, Arhimedes' force has the general form,

$$\vec{F}_A = \rho_l \cdot \vec{a}_f \cdot V \tag{7}$$

g. The action and reaction law, or Newton's third law, states the fact that: "when two bodies interact, the force acting upon a body is equal and of contrary sense to the force acting upon the other body". In other words, a body is reluctant to the action of the other one by reacting with the same intensity; action and reaction are equal and have contrary sense.

3.2. The electric and electromagnetic phenomena

a — Polarization of dielectrics. One knows that in a certain dielectric the intensity of the resulting electric field, $\vec{E}$, is lower than the intensity of the exterior field $\vec{E}_0$ (Fig. 2), respectively

$$\vec{E} = \vec{E}_0 + \vec{E}_p \quad \text{or} \quad |\vec{E}| = |\vec{E}_0| - |\vec{E}_p|,$$

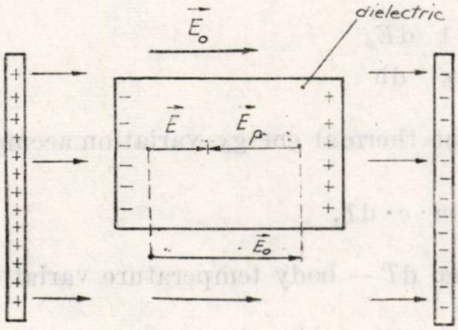

Fig. 2.—Polarization of dielectric.

where $\vec{E}_p$ is the intensity of the dielectric opposition (reluctance) to the external field.

Whether or not a dielectric is polar, the polarization charges occur so that the field they have generated and whose intensity is $\vec{E}$ opposes to the external electric field (of action) of intensity $\vec{E}_0$, which induces these charges. Hence as well, the effect (the generation of the electric field in the dielectric) opposes to the cause (the external electric field, $\vec{E}_0$).

b — Ohm's law,

$$I = \frac{U}{R} \tag{8}$$

shows that by applying a potential difference U to the ends of a conductor, the intensity I of the electric current passing through the conductor will be inversely proportional to the electric resistance R of the latter. Hence, the electric resistence, R, is reluctant (opposes) to the flow of electric current.

c — At magnetic circuits, by analogy with Ohm's law, on may write

$$\Phi = \frac{\mathcal{F}}{\mathcal{R}}$$

where Φ is the magnetic induction flux; $\mathcal{F}$ — magnetomotive force; $\mathcal{R}$— mangnetic reluctance. The magnetic reluctance opposes to the passing of the magnetic induction flux; the latter is determined by the action of the magnetomotive force on the magnetic circuit.

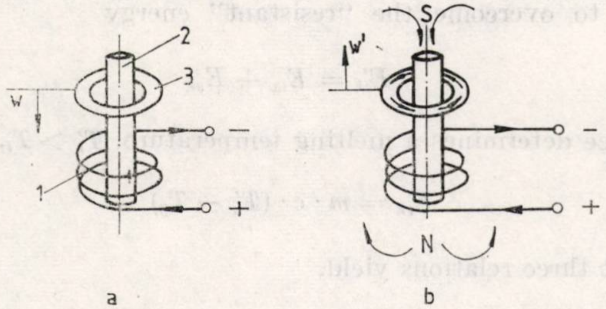

Fig. 3.—Electromagnet for demonstrating the phenomenon of electromagnetic induction.

d — The phenomenon of electromagnetic induction is another proof of the fundamental property of matter. In a d.c. supplied coil, one introduces a vertical coil, which goes out of the coil (Fig. 3, a). An iron ring, 3, with velocity $\vec{w}$ is left to drop around the metal core. One finds that after covering a certain distance the ring is pushed up with a speed $\vec{w}'$ (Fig. 3, *b*). The current flowing through the coil (inductive current) produces a magnetic field around it. A current contrary to the inductive current is induced in ring 3 during its motion in the magnetic field of the coil. As a result, the magnetic flux produced by the induced current (from ring 3) has a contrary sense to the magnetic flux—*cause*, produced by the inductive current (from coil 1). *The effect is reluctant to cause*; *matter is reluctant to the change in the equilibrium of local energy forms.*

The electromagnetic induction phenomenon is governed by *Lenz's law* "the induced tension has such a sense that, through the magnetic field it creates, the induced current will oppose to the variation of the inductive magnetic flux".

Lenz's law confirms in this way the reluctance principle.

3.3. Thermal phenomena

a — Energy accumulation. The heating of a material body leads to its temperature increase. The amount of thermal energy required to attain the melting temperature T_t, results from the relationship

$$E_{th} = m \cdot c \cdot (T_t - T_0)$$

where T_0 is the original body temperature.

Let us consider now a polymer at T_t. If during cooling from T_t to T_0 the polymer is under stress, an ordering in its macromolecules will take place. An amount of mechanical energy E_m was transferred to the polymer during cooling. This energy *is stored* by the body (it is retained) by solidifying the polymer. Therefore the *energy accumulated* inside the body has increased; the energy is reluctant to the external actions tending to cause the desorganization of macromolecules; hence reluctance has increased. When heating in order to melt the pre-stressed polymer, it is necessary to overcome the "resistant" energy

$$E'_{th} = E_{th} + E_m$$

whose presence determines a melting temperature, $T'_t > T_t$, so that

$$E'_{th} = m \cdot c \cdot (T'_t - T_0)$$

The last three relations yield,

$$T'_t = T_t + \frac{E_m}{m \cdot c} \tag{9}$$

Hence, the melting temperature – measuring the *extent of reluctance* to state changes – will increase with the increase in the energy density, E_m/m, stored by the material;

b – Thermal energy transfer. The amount of thermal energy transmitted (transferred) from body, 1, to body 2, at $T_2 < T_1$, is

$$E_{th} = k \cdot A \cdot (T_1 - T_2)$$

where A is the area of body 2 sujected to the thermal flow coming from body 1; k – the total thermal transfer coefficient.

As temperature T_2 of body under heat rises, the thermal energy flux, E_{th}/A, decreases. Hence, the *effect* (*the temperature of the heated body*) *is reluctant to the cause.* Storing thermal energy produces the continuous change in thermal equilibrium as a proof of the reluctance property.

3.4. Chemical phenomena

Le Chatelier's principle regards chemical reactions and invloves various statements;

– "if the conditions of a system, initially in equilibrium, are changed, the equilibrium will move in the direction tending to reestablish the initial conditions if such a motion is possible", or

– "when a system changes under the action of an external or internal cause, an additional change will be set off therein, tending to diminish the former";

– "when constraint is applied to a system in equilibrium, the equilibrium will move in such a way that the constraint is diminished".

In other words, a system whose equilibrium tends to be modified *is reluctant* to this modification and tends to return to its original state.

Let us consider for instance the mixture NO_2 with N_2O_4 in equilibrium at room temperature, T_0. When one molecule N_2O_4 dissociates into two NO_2 molecules,

$$N_2O_4 \rightarrow 2\ NO_2$$

an amount of heat is absorbed, $E_{th} = 63$ J/mol.

If the mixture is brought to $T_1 > T_0$, the equilibrium will change so that the original temperature T_0 can be reestablished; this means a consumption of thermal energy corresponding to the temperature difference $T_1 - T_0$. This thermal energy consumption is actually achieved by decomposing the N_2O_4 molecules, which absorb this amount of energy.

The synthesis of ammonia from nitrogen and hydrogen is exothermal. The lower the temperature, the higher the ammonia efficiency (equilibrium moves in The direction of ammonia formation). In parallel to the synthesis of each new NH_3 molecule, the mixture temperature will rise and hence the efficiency in the ammonia will decrease, together with the temperature rate increase. Hence, the effect (temperature rise) is reluctant to the cause (ammonia synthesis) thus reducing the reaction efficiency. In the industrial flow ammonia production, the ammonia is continuously discharged from the reaction zone together with the reaction heat; thus through an additional energy consumption the reaction efficiency is maintained in time.

3.5. Transport phenomena

a — Soret's effect. One introduces a fluid whose composition is known into a closed cell made up of two metallic parallel plates, 1 and 2 (Fig. 4). The cell walls adiabatically isolate it from the surrounding medium. The two plates are kept at different temperatures, $T_2 > T_1$, in order to avoid thermogravitational convection.

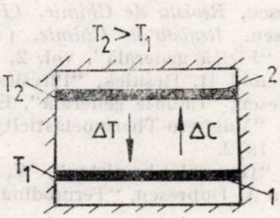

Fig 4. — Cell with adiabatic walls.

The temperature difference $\Delta T = T_2 - T_1$ determines the thermal diffusion of fluid components, Δc. The outcome of the thermal diffusion is a concentration gradient Δc whose sense is opposed to the thermal gradient.

The concentration gradient (effect) causes a diffusion flow directed towards the hottest zone thus gradually entailing the thermal diffusion (cause) up to the reciprocal compensation of the two flows.

Likewise in this case, the effect is reluctant to cause and attenuates the phenomenon evolution. Soret's effect is used for instance in separating the components of a mixture, particularly in isotopes separation.

b — Dufour's effect is the reverse of Soret's effect; some temperature gradient will appear in a gas mixture at any temperature following diffusion.

But the temperature gradient (effect) determined by the concentration gradient (cause) creates an additional gradient whose sense is opposite to the former. Thus the initial effect is gradually lessened; the effect opposes to the cause and the process tends to thermodynamic equilibrium.

c — The formal analogy of all *transport phenomena* (biological metabolism; nervous and genetic transport; information transfer; sea currents and cyclones circulation pattern; epidemics propagations; electricity transport: thermal transfer; substance transfer, etc.) is determined by the fact that each of these essentially represents *transfer of a certain kind of energy*. The present tendency to unite all transport phenomena on a common basis is determined by their formal analogy (structural resemblance of the equations which describe them). This springs from its *dependence* on the fundamental property, the reluctance, of all effects caused by interactions.

3.6. Biological phenomena

Living body homeostatis represents the tendency of all living bodies toward stabilizing the various physiological constants (body temperature, blood composition etc.) in the case of externally induced changes, toward the recovery of these constants.

The living bodies whose physiological equilibrium tends to be modified are reluctant to this change, tending to recover their original state. The homeostasis is similar to Le Chatelier's principle.

REFERENCES

[1] V. V. Jinescu, *Revista de Chimie, (București)*, **34**, 491, 1983.
[2] V. V. Jinescu, *Revista de Chimie, (București)*, **38**, 469, 1987.
[3] A. Cișman, "Fizică generală", vol. 2, Ed. Tehnică, Bucharest, 1957.
[4] D. Halliday and R. Resnick, "Physics", Wiley, New York, 1966.
[5] C. D. Nenițescu, "Chimie generală", Ed. Didactică și Pedagogică, Bucharest, 1985.
[6] H. Parkus, "Magneto-Thermoelasticity", Course held at CISM-Udine, Springer Verlag,
[7] Wien, 1972.
[8] L. Pauling, "General Chemistry", W. H. Freeman, San Francisco, 1970.
R. Vîlcu and A. Dobrescu, "Termodinamica proceselor ireversibile", Ed. Tehnică, Bucharest, 1982.

NOTE POUR LES AUTEURS

La Revue Roumaine de Chimie publie des articles en anglais, français, russe, allemand ou espagnol. Les auteurs sont priés d'envoyer des articles et des comptes rendus inédits.

Les manuscrits seront dactylographiés à double interligne. La bibliographie, les tableaux et la légende des figures seront placés après le texte.

Si l'article fait partie d'une série numérotée, la partie précédente sera donnée comme première référence.

Chaque article sera précédé d'un résumé comprenant quinze lignes au maximum.

Les références bibliographiques dans le texte seront faites par des exposants sans parenthèses et paraîtront à la fin de l'ouvrage.

Les publications périodiques mentionnées dans la bibliographie seront présentées suivant les prescriptions internationales : le nom de l'auteur précédé de l'initiale du prénom, le titre du périodique abrégé conformément à « Chemical Abstracts » et souligné par une ligne, le numéro du tome indiqué par des chiffres arabes et souligné par deux lignes, suivi de la première page de l'article : à la fin, l'année de la parution sera placée entre parenthèses. Le numéro de la revue ne sera pas indiqué si les pages du volume sont numérotées consécutivement.

Les textes des livres ou traités inclueront : le nom des auteurs, précédé de l'initiale du prénom, le titre du livre entre guillemets et sans être souligné, le numéro du tome précédé par l'abréviation « vol.» (ou « Bd »), le numéro de l'édition, les éditions (the publisher), la localité de la parution du livre, l'année de la parution et la page de la référence précédée par l'abréviation « p » (ou « S »).

Les brevets seront indiqués comme suit : l'auteur ou la firme, le pays et le numéro du brevet, la date de la revue (*Chem. Abstr.*). Par ex. : M. Jones (to Union Carbide Co.) Brit. Pat. 610 238,2 Sept. 1959 : cf. *Chem. Abstr.*, **54**, 12808 (1960).

Si la référence n'a pas été lue en original, on indiquera aussi la revue de références consultée.

Les diagrammes seront tracés à l'encre de Chine sur papier calque. Les tableaux et les figures (en nombre strictement nécessaire), ainsi que les courbes dans les figures seront numérotés par des chiffres arabes. Leur explication sera donnée dans la légende des figures. Prière de ne pas inscrire les mêmes données dans les tableaux et les figures. Chaque tableau aura un titre. On indiquera dans le texte la place approximative des tableaux et des figures. Les formules chimiques seront incluses dans le texte ; en outre, elle seront transcrites sur papier calque, à l'encre de Chine.

Les auteurs sont priés d'indiquer les caractères italiques (en soulignant les lettres au crayon), ainsi que tout autre caractère spécial : les préfixes *ortho*, *méta*, *para*, *cis*, *trans*, etc. seront soulignés pour indiquer leurs caractères italiques, et ne seront jamais écrits avec des majuscules.

Aucune correction à la main ne sera admise sur le manuscrit. Les corrections seront frappés à la machine. Les lettres grecques ou d'autres symboles spéciaux seront insérés à la main à l'encre clairement.

Le manuscrit sera signé par l'auteur.

Le titre courant aura 50 lettres au maximum.

L'entière responsabilité du contenu des articles appartient aux auteurs.

Sur demande on peut obtenir une note plus complète.

PRINTED IN ROMANIA

ORSZÁGOS MŰSZAKI INFORMÁCIÓS KÖZPONT ÉS KÖNYVTÁR 1883

TRAVAUX PARUS AUX ÉDITIONS DE L'ACADÉMIE DE LA RÉPUBLIQUE SOCIALISTE DE ROUMANIE

ELENA CEAUŞESCU, **Răşini de hidrocarburi**, vol. 1, 1988, 344 p.
ELENA CEAUŞESCU, **Progrese în chimia şi tehnologia polimerilor**, 1986, 466 p.
ELENA CEAUŞESCU, **Forschungen im Bereich der Chimie und Technologie der Polymere**, 1986, 444 p.
ELENA CEAUŞESCU, **Cercetări în chimia şi tehnologia polimerilor**, 1983, 520p.
ELENA CEAUŞESCU, **Noi cercetări în domeniul compuşilor macromoleculari**, 1981, 536 p.
ELENA CEAUŞESCU, **Polimerizarea stereospecifică a izoprenului**, 1979, 307 p.
ELENA CEAUŞESCU, **Research work on synthesis and characterization of macromolecular compounds, Contributions**, 1974, 251 p.
I. G. MURGULESCU, **Introducere în chimia fizică, Vol. I.1. Atomi, molecule, legătură chimică**, 1976, p. 560 p.
I. G. MURGULESCU, V. EM. SAHINI, **Introducere în chimia fizică, Vol. I. 2. Structura şi proprietăţile moleculelor**, 1979, 604 p.
I. G. MURGULESCU, E. SEGAL, **Introducere în chimia fizică, Vol. II.1. Teoria molecular-cinetică a materiei**, 1979, 1056 p.
I. G. MURGULESCU, TATIANA ONCESCU, E. SEGAL, **Introducere în chimia fizică, Vol. II. 2. Cinetică chimică şi cataliză**, 1981, 1024 p.
I. G. MURGULESCU, J, PĂUN, **Introducere în chimia fizică, Vol. I. 3. Nucleul atomic, reacţii nucleare, particule elementare**, 1982, 606 p.
I. G. MURGULESCU, RODICA VÎLCU, **Introducere în chimia fizică. Vol. III. Termodinamica chimică**, 1982, 624 p.
I. G. MURGULESCU, O. M. RADOVICI, **Introducere în chimia fizică, Vol. IV. Electrochimia**, 1986, 410 p.
CRISTOFOR I. SIMIONESCU, VALERIA GORDUZA, **Implicaţii bioenergetice ale coloranţilor**, 1988, 208 p.
R. VÎLCU, M. LECA, **Termodinamica polimerilor prin cromatografie de gaze**, 1987, 238 p.
I. ZUGRĂVESCU, M. PETROVANU, **Cicloadiţii 3+2 dipolare**, 1987, 446 p.
RAUL MIHAIL, ION GROZEANU, **Estimarea secvenţială aplicată sistemelor chimice**, 1986, 406 p.
M. BREZEANU, I. PATRON, M. ANDRUH, **Combinaţii complexe polinucleare şi aplicaţiile lor**, 1986, 244 p.
A. T. BALABAN et al., **Labelled Compounds and Radiopharmaceuticals Applied in Nuclear Medicine**, coédition avec John Wiley and Sons, 1986, 742 p.
D. PURDELA, **Nomenclatura chimiei organice — IUPAC**, 1088, 451 p.
PETRU BUDRUGEAC, **Probleme de chimie**, 1986, 280 p.
T. ONCESCU, S. O. IONESCU, **Conversie fotochimică şi stocare de energie**, 1985, 272 p.
V. DRĂGUŢAN, A. T. BALABAN, M. DIMONIE, **Olefin Metathesis and Ring-Opening Polymerization of Cyclo-Olefins**, coédition avec John Wiley and Sons, 1985, 544 p.
C. LITEANU, I. RICA, **Optimizarea proceselor analitice**, 1985, 360 p.
N. PERESCU, **Chimia extracţiei cu solvenţi şi aplicaţii**, 1985, 212 p.
V. E. SAHINI, M. HILLEBRAND, **Chimie cuantică în exemple şi aplicaţii**, 1984, 378 p.
GH. MARCU, **Chimia compuşilor coordinativi**, 1984, 415 p.
E. CORDOS, C. MANOLIU, **Spectrometria de absorbţie şi florescenţa atomică**, 1984, 178 p.
C. BODEA, **Tratat de biochimie vegetală**, p. II, t. V, 1984, 438 p.
N. ASANDEI, A. GRIGORIU, **Chimia şi structura fibrelor**, 1985, 395 p.
N. IONESCU, M. CĂLDĂRARU, **Oxidarea catalitică a olefinelor inferioare**, 1983, 178 p.
O. CAŞCAVAL, **Studiul polimerilor prin piroliză şi cromatografie de gaze**, 1983, 220 p.
C. I. SIMIONESCU, F. DANES, **Originea vieţii**, 1983, 110 p.
C. BODEA, **Tratat de biochimie vegetală**, p. II, t. IV, 1982, 408 p.
I. GĂLĂŢEANU, **Procese şi metode radiochimice în energetica nucleară**, 1981, 234 p.
CR. SIMIONESCU, VALERIU GORDUZA, **Polimeri biocompatibili şi biologic activi**, 1980, 479 p.
C. GH. MACAROVICI, **Analiza chimică cantitativă anorganică**, 1979, 457 p.
I. ZUGRĂVESCU, MAGDA PETROVANU, **N-ylid chemistry**, coédition avec McGraw-Hill International Book Company U.S.A., 1977, 396 p.

ISSN 0035—3930

I. P. INFORMAŢIA c. 2226

43 426

Lei 40

F 1103

66

ACADÉMIE DE LA RÉPUBLIQUE SOCIALISTE DE ROUMANIE

REVUE ROUMAINE DE CHIMIE

TOME 33
N° 8
Août 1988

Rev. Roumaine Chim.

RRCHAX, 33, 8, p. 773–850(1988), Bucarest

EDITURA ACADEMIEI REPUBLICII SOCIALISTE ROMÂNIA

ACADÉMIE DE LA RÉPUBLIQUE SOCIALISTE DE ROUMANIE

COMITÉ DE RÉDACTION

Rédacteur en chef:

I. G. MURGULESCU, membre de l'Académie de la République Socialiste de Roumanie

Rédacteur en chef adjoints:

A. T. BALABAN et V. EM. SAHINI, membres correspondants de l'Académie de la République Socialiste de Roumanie

Collège de rédaction:

EM. BRATU, ELENA CEAUŞESCU, ECATERINA CIORĂNESCU-NENITZESCU, CR. SIMIONESCU, membres de l'Académie de la République Socialiste de Roumanie; P. SPACU, membre correspondant de l'Académie de la République Socialiste de Roumanie; M. BANCIU, M. D. GHEORGHIU, I. HAIDUC, D. I. MARCHIDAN, G. NIAC et D. SĂNDULESCU

La Revue Roumaine de Chimie parait 10 fois par an. Toute commande de l'étranger sera adressée à ROMPRESFILATELIA — sectorul Export-Import Presă, P. O. Box 12—201, télex 10376 prsfi r 78104 Bucarest, Calea Griviţei nr. 64—66, Bucarest, Roumanie

Les manuscrits, les livres et les revues proposés en échange, ainsi que toute correspondance seront envoyés à la rédaction :

REVUE ROUMAINE DE CHIMIE

125, Calea Victoriei, 79717 Bucarest, Roumanie, telephone 50 76 80

EDITURA ACADEMIEI REPUBLICII SOCIALISTE ROMÂNIA
125, Calea Victoriei 79717 Bucarest, Roumanie, téléphone 50 76 80

REVUE ROUMAINE
DE
CHIMIE

ORSZÁGOS MŰSZAKI INFORMÁCIÓS KÖZPONT ÉS KÖNYVTÁR 1883

Tome 33, N° 8 **Août 1988**

S. STERNBERG, V. BRÂNZOI, LILIANA APĂTEANU and MIHAELA UNGUREANU, Polarization behaviour of the n- and p-type silicon in sulphuric acid solutions 775–780

N. BONCIOCAT, S. STERNBERG, T. VIȘAN and ADINA COTÂRȚĂ, Electrode processes with interfacial generation of the electrochemical active species. I. The kinetic model and the equation of the current density 781–787

JYOTI SHARMA, ARVIND KUMAR and B. K. PURI, Polarographic study of manganese(II)-pyridine-thiocyanate system and thermodynamic parameters 789–794

JOSETTE WEINBERG, ALEXANDRINA DONESCU and V. Em. SAHINI, β-Lactam antibiotics. II. Substituent effects on cephalosporins 795–801

IOANA ILIE, MARIA BREZEANU, LUMINIȚA PATRON and E. SEGAL, Synthesis of nickel ferrite from polynuclear coordination compounds. Part II. Study of the wet ferritization process 803–807

TINCA BURUIANĂ and ADRIAN CARACULACU, Synthesis and characterization of some 2,4′-dibenzyldiisocyanate ionic polymers. IV. Biological activity 809–814

HASSAN M. FAID-ALLAH, Dithiocarbamate series. Part II. Pyrrolidino- and indolinodithiocarbamate esters of possible antibacterial and antimicrobial activity 815–822

L. S. BOULOS, El. S. M. YAKOUT and M. M. SIDKY, Phosphonium ylides. VI. The reaction of fluorenylidenetriphenyl phosphoranes and -arsinane with quinisatins 823–826

S. EL-NAGDY, A. A. EL-KHAMRY, M. A. SHAABAN and M. M. HABASHY, Synthesis and some reactions of 2-(α-benzoylaminostyryl)-3,1(4H)-benzoxazin-4-one and 3-amino-2-(α-benzoylaminostyryl)quinazolin-4(3H)-one . . 827–832

ABDEL MOMEN A. EL-KHAMRY, S. EL-NAGDY and M. E. SHABAN, Synthesis of 2-(2′-thenyl)-3,1-(4H)-benzoxzain-4-one and its reactions with different nucleophiles 833–838

OVIDIU IVANCIUC, Topological and empirical models. I. The prediction of the Gibbs energies of formation for alkanes 839–845

COMPTES RENDUS 847–849

Rev. Roumaine Chim. 33, 8, 773–850(1988), Bucarest

Revue Roumaine de Chimie, **33**, *8*, 775–780 (1988)

POLARIZATION BEHAVIOUR OF THE n- AND p-TYPE SILICON IN SULPHURIC ACID SOLUTIONS

S. STERNBERG[a], V. BRÂNZOI[a], LILIANA APĂTEANU[b] and MIHAELA UNGUREANU[a]

[a]Polytechnic Institute of Bucharest, Dept. of Applied Physical Chemistry and Electrochemical Technology, Splaiul Independenţei 313, 76206 Bucharest, Romania
[b]Biochemical and Chemical Energetics Institute of Bucharest, Bucharest, Romania

Received May 18, 1987

The polarization behaviour of the n-type and p-type silicon electrodes in solutions of $H_2SO_4 + 0.01$ M quinhydrone was studied, comparatively with the platinum electrode in the same solutions, using the potentiostatic method. The results indicate the existence of the active-passive transition of the Si electrodes in the studied solutions and the anodic multistep oxidation of quinhydrone on the Si and Pt electrodes.

INTRODUCTION

During the last years, metallurgical industry has known a high development because of the supply of metals of high purity and of alloys with special properties. These aims were achieved by the automation and semiautomation of metallurgical processes. The modernization of the metallurgical industry could not be possible without the use of semiconductors, which lay at the basis of any automation.

Taking into account the importance of semiconductors in the automation of metallurgical processes, the present paper deals with the silicon properties in electrolytes with and without additives.

Generally the silicon/electrolyte system is much less studied and tested than the germanium/electrolyte system. This is due to the difficulties involved by the obtention of monocrystalline silicon of high purity, on the one hand, and, on the other hand, to the fact that at the contact with an aqueous electrolyte, silicon covers with an oxide layer of variable and complex composition.

At the same time, the most papers [1–11] refer to small potential or concentration ranges and the dispersion of the results is relatively high.

The present paper comparatively studies the polarization behaviour of the Pt/H_2SO_4, Pt/H_2SO_4 + quinhydrone, Si type n/H_2SO_4 + quinhydrone and Si type p/H_2SO_4 + quinhydrone systems.

EXPERIMENTAL

The polarization curves were registered by means of the potentiostatic technique. A Princeton Applied Research — Model 173 Potentiostat was used.

The scheme of the device and the operating technique were described in a previous paper.[12] The Si working electrodes were disks of 1—2 mm diameter, made from monocrystalline silicon. The disks were sealed in Pyrom glass. The electric contact at the polarization of the silicon disk was made from a copper wire immersed in hydrargyrum.

In order to prevent a Hg—Si rectifier contact, the inside of the n-type silicon disks was doped by diffusion with phosphorus from $POCl_3$ at 1255°C. In the same way, the inside of the p-type silicon disks was saturated with boron by painting with B_2O_3 and heating up to 1255°C. The reaction products formed during the thermal diffusion were removed by a special electrochemical treatment.[13]

The doped silicon slices were metallized by chemical deposition of Ni and by gold electrodeposition in aqueous solutions.

Reagents of p.a. purity were used. Experiments were carried out at a constant temperature of 20°C, in the dark. Before each determination the silicon electrode was etched in a $HNO_3 + HF$ (4 : 1) mixture, while the platinum electrode was etched in a H_2SO_4(conc) + HNO_3(conc)(1 : 1) mixture, for 2 minutes. In order to minimize the potential ohmic drop, a single compartment cell was used. The joining between the reference electrode and the compartment of the cell was realized by means of a Haber-Luggin capillary. The reference electrode was the saturated calomel electrode. Prior to experiment, the silicon electrode was maintained for 30 minutes at a potential of -1700 mV, in order to ensure a complete cleaning of the electrode surface by an intense evolution of H_2. Further, the silicon electrode was polarized from -1700 mV up to $+2500$ mV, by steps of 50 mV. For each potential step the current response was recorded.

For each electrode, more determinations were carried out, in order to obtain a good reproducibility of the results.

RESULTS AND DISCUSSION

Figure 1 shows the anodic polarization curves of 0.01 Ω cm n-type silicon in the $\rho = 1.24$ g/cm³ H_2SO_4 solution and in the $H_2SO_4 + 0.01$ M quinhydrone solution.

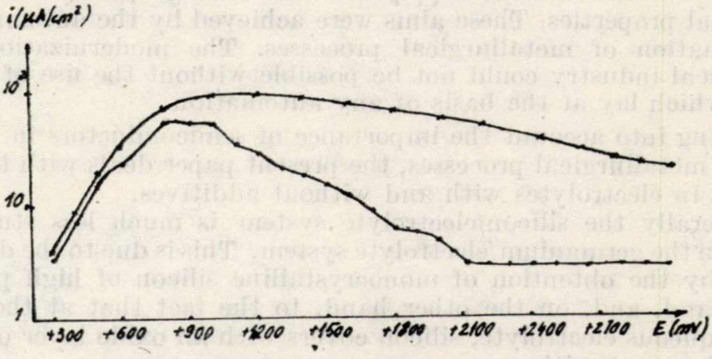

Fig. 1. — Anodic polarization curves of 0.01 Ωcm n-type silicon in : (.) H_2SO_4 ($\rho = 1.24$ g/cm³) ; (x) H_2SO_4 (1.24) + 0.01 M quinhydrone.

The analysis of the curves shows that in the case of the H_2SO_4 solution free of quinhydrone the 0.01 Ω cm n-type silicon presents a classical active-passive transition, that is : at the anodic potential sweep of the working electrode, starting from the steady-state value, the current begins to increase until the dissolution rate of the silicon equalizes the rate of the silicon oxide (a complex of oxides) formation; this is the active dissolution zone (the ascending side of the current maximum). The top of the current maximum corresponds to the equalization of the two rates. The descending side of the current maximum corresponds to the increase of the formation rate of the oxide (of the silicon dioxide, respectively) with the corresponding decrease of the current density. At the end, the silicon electrode surface is covered by a silicon dioxide layer, which passivates the electrode surface and the current density decreases to a very small value, of about 3 μA. The electrode maintains in the passive state up to very high anodic values (+ 3V) of the electrode potential. The curve 2 in figure 1 shows the anodic polarization of the 0.01Ω cm n-type silicon electrode in a solution of H_2SO_4 ($\rho = 1.24$ g/cm^3) + 0.01 M quinhydrone. In this case there is an evident difference relatively to the curve 1, that is: a larger active zone, a higher maximum of the anodic current, a retardation of the passivation process and a higher passivation current relatively to the solution free of quinhydrone.

The obtention of a much increased anodic current density must be due to the quinhydrone oxidation on the silicon-silicon dioxide system. It will be observed that the active zone (a linear zone between +300 and +500 mV, where the Tafel relation is followed) is almost identical with that obtained in the absence of quinhydrone. Starting from + 500 mV the currents obtained are higher, meaning that from this value of the potential the anodic oxidation of the quinhydrone begins, too, on the silicon electrode surface (on the silicon oxide or on silicon oxides complex, respectively). The retardation of the passivation phenomenon must be due to further oxidation of the quinhydrone adsorbed on the electrode surface or of the oxidation products of quinhydrone.

At the end, the current density decreases until the value of the passivation current is reached, simultaneously with the silicon dioxide formation, which is an insulating and protective layer on the silicon electrode surface. These results are compared with those obtained on platinum in H_2SO_4 ($\rho = 1.24$ g/cm^3) and H_2SO_4 ($\rho = 1.24$ g/cm^3) + 0.01 M quinhydrone (see figure 2).

Analysis of the two curves from figure 2 shows the following: at the anodic polarization on platinum electrodes an intense evolution of oxygen occurs starting from about + 1300 mV. A range of a very small and almost constant current could be attributed to the oxygen adsorption, accompanied by the surface oxide formation, before the oxygen evolution.

In the solutions containing quinhydrone, the limiting current is about 2 times higher than in the absence of the organic substance because of the superposition of the quinhydrone oxidation process.

On the platinum electrode there are much higher currents, about ten times higher than the maximum activation current on the 0.01 Ω cm n-type silicon and hundred times higher than the passivation currents on the 0.01 Ω cm n-type silicon electrode respectively.

Figure 3 shows the cathodic polarization curves of the 0.01 Ω cm n-type silicon in sulphuric acid solution (curve 1) and in H_2SO_4 + 0.01 M quinhydrone solution (curve 2).

At the cathodic polarization one can observe the existence of two ranges. Within the first range ($-250\,\text{mV} < E < 200\,\text{mV}$) a cathodic process takes place which is specific to the semiconductors electrodes, with small currents and a hindering is produced due to the relatively small concentration of the charge carriers. Within the second range

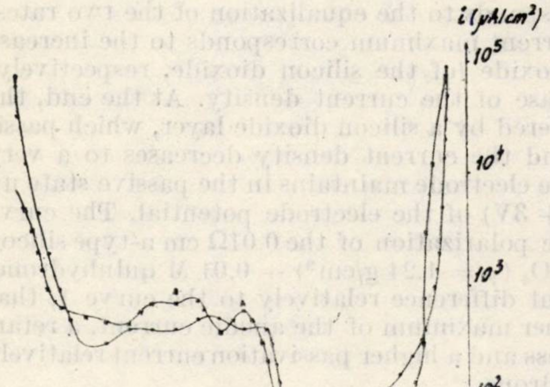

Fig. 2. — Anodic and cathodic polarization curves of the Pt electrode in : (.) H_2SO_4 ($\rho = 1.24\ g/cm^3$) ; (x) H_2SO_4 (1.24) + 0.01 M quinhydrone.

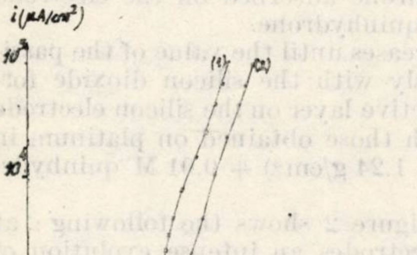

Fig. 3. — Cathodic polarization curves of 0.01 Ωcm n-type silicon in : (x) H_2SO_4 ($\rho = 1.24\ g/cm^3$) ; (.) H_2SO_4 (1.24) + 0.01 M quinhydrone.

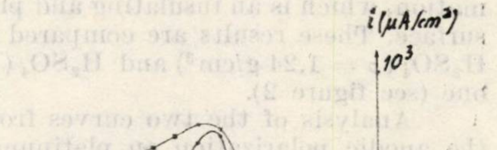

Fig. 4. — Anodic polarization curves of 0.015 Ωcm p-type silicon in : (.) H_2SO_4 ($\rho = 1.24\ g/cm^3$) ; (x) H_2SO_4 (1.24) + 0.01 M quinhydrone.

($E < -250$ mV) the cathodic current is much higher and could be compared with that obtained on platinum.

Further, the polarization behaviour of the 0.015 Ωcm n-type silicon in H_2SO_4 (1.24 g/cm^3) solution and H_2SO_4 + 0.01 quinhydrone solution was studied. Figure 4 shows the anodic polarization curves of the 0.015 Ωcm n-type silicon in H_2SO_4 and in H_2SO_4 + 0.01 M quinhydrone, respectively.

One can note the appearance of an active-passive transition, in this case as well as in the case of the 0.01 Ω cm n-type silicon, but now the active-passive transition is less well definite. The steady-state potential is more electronegative than in the case of the 0.01 Ωcm n-type silicon and the anodic currents corresponding to the maximum and the passivation currents are higher than those obtained on the n-type silicon (see Fig. 1 and Fig. 4 comparatively). At the same time one can observe that the steady-state potential on the n-type silicon is shifted towards more positive values with about 250 mV. Comparing the two anodic curves from figure 4, one can observe that in the H_2SO_4 + 0.01 M quinhydrone the current densities corresponding to the maximum and to the passive zone, respectively, are higher than in the case of the sulphuric acid free of quinhydrone solution. This could be explained in the same way as in the case of the 0.01Ω cm n-type silicon that is due to the quinhydrone oxidation on the silicon electrode (on the silicon oxide layer, respectively). The cathodic polarization curves showed in this case of 0.015 Ωcm p-type silicon in H_2SO_4 and in H_2SO_4 + 0.01 M quinhydrone solution, respectively, that the hydrogen evolution is the only process taking place on the silicon electrode.

Analysis of figure 5 shows that beside a small potential range (with a hindering characteristic of semiconductors, hence with a very small current density) there is a sudden increase of the current up to very high values, accompanied by an intense hydrogen evolution, which could be explained by the surface states formation. The current densities corresponding to the hydrogen evolution are much higher in the H_2SO_4 ($\rho = 1.24$ g/cm^3) solution than in the H_2SO_4 ($\rho = 1.24$ g/cm^3) + 0.01 M quinhydrone, at the same potential. One can suppose, in this case as well as in the case of the 0.01Ω cm n-type silicon, that in the sulphuric acid solution containing quinhydrone, the hydrogen evolution current is much smaller than in the free H_2SO_4 solution, because of the adsorption of the quinhydrone (of its reduction products respectively), on the silicon surface. In this range "surface states"

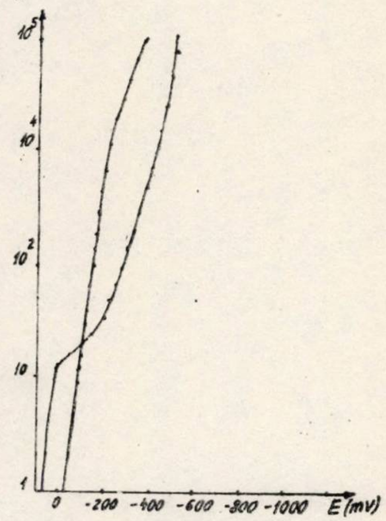

Fig. 5. — Cathodic polarization curves of 0.015 Ωcm p-type silicon in: (.) H_2SO_4 ($\rho = 1.24$ g/cm^3); (x) H_2SO_4 (1.24) + 0.01 M quinhydrone.

with a much higher number of charge carriers are probably formed, due to the hydrogen adsorption on semiconductors.

The process occurs similarly to the hydrogen evolution on metallic electrodes with Tafel slopes of about 120 mV. The quinhydrone addition produces a decrease of the cathodic current within the first range probably because of the organic substance adsorption and within the second range it produces an increase of the cathodic current because of the superposition of the quinhydrone reduction on the hydrogen evolution reaction.

REFERENCES

[1] Yu. V. Pleskov, *Doklady Akad. Nauk S.S.S.R.* **143**, 1399 (1962).

[2] Yu. V. Pleskov, *Elektrokhimiya*, **1**, 4 (1965).

[3] V. A. Tyagai, *Elektrokhimiya*, **1**, 387 (1965).

[4] A. Myamlin and V. Pleskov, "Electrochemistry of Semiconductors", Plenum Press, New York, 1967.

[5] Yu. K. Delimarskii, *Elektrokhimiya*, *9*, 10 (1973).

[6] U. Cohen, R. A. Huggins, *J. Electrochem. Soc.*, 123, 381 (1976).

[7] S.O. Izodov, V. P. Osipov, *Elektrokhimiya*, **9**, 927 (1973).

[8] S. O. Izodov, A. P. Blokhina, *Elektrokhimiya*, **9**, 1426 (1973).

[9] S. O. Izodov, A. P. Blokhina, *Elektrokhimiya*, **9**, 1138 (1973).

[10] V. A. Tyagay, E. V. Panov, Yu. K. Delimarsky, I. A. Stepanova and Yu. M. Shirsho, *Elektrokhimiya*, **14**, 1674 (1978) ; **14**, 1682 (1978).

[11] I. Lingvay and M. Scarlete, *Rev. Chim. (Bucureşti)*, **33**, 569 (1982).

[12] V. Brânzoi and S. Sternberg, *Rev. Roumaine Chim.*, **27**, 1003 (1982).

[13] S. Sternberg, M. Ungureanu, V. Brânzoi and L. Apăteanu, *Rev. Roumaine Chim.*, **30**, 105 (1985).

Revue Roumaine de Chimie, **33**, *8*, 781–787(1988)

ELECTRODE PROCESSES WITH INTERFACIAL GENERATION OF THE ELECTROCHEMICAL ACTIVE SPECIES. I

THE KINETIC MODEL AND THE EQUATION OF THE CURRENT DENSITY

N. BONCIOCAT[a], S. STERNBERG[b], T. VIŞAN[b] and ADINA COTÂRŢĂ[a]
[a]Institute of Chemical and Biochemical Energetics, Bucharest, Romania
[b]Chair of Physical Chemistry and Electrochemical Technology, Polytechnic Institute, Bucharest, Romania

Received June 8, 1987

In this paper a steady state kinetic model is proposed to describe the electrode redox reactions occurring with combined overtension of charge-transfer, and of interfacial generation of the electro-chemical active species. On its basis, a general expression of the current density has been deduced, which — because the nature of the generating processes is irrelevant for the proposed model—is applicable to all cases of pure or combined overtensions.

INTRODUCTION

Generally, the papers dealing with electrode redox reactions consider that the electrochemical active species are present in the electrolyte, and analyse the electric responses obtained when the electroactive species is converted at an electrode to the product, e.g., O + e → R, or inversely. In many cases the electron transfer reaction may be perturbed by a homogeneous chemical reaction in which the species O or R are involved. The principal aspects concerning the coupling between electrode redox reactions and homogeneous chemical reaction may be found in the literature. [1–7] There are many possible sequences by which an electron transfer reaction (E) is coupled to a chemical reaction (C), e.g., CE, EC, RCE, etc., but what is important is the fact that the species O and R are generated (positively or negatively) at some generating rates v_O, v_R, depending on the coupling sequence and on the polarization of the interface.

It is the aim of this paper to obtain a general steady-state expression of the current density that may be applied irrespective of the nature of the generating processes.

DISCUSSION

The kinetic model

Let us consider a redox reaction

$$O + e \rightleftharpoons R \qquad (1)$$

taking place at an inert metal/electrolyte interface, and let us suppose that the electrochemical active species are present only in an interfacial layer of constant thickness δ_i(Fig. 1), where they are generated by some generating processes, the nature of which is irrelevant for our model.

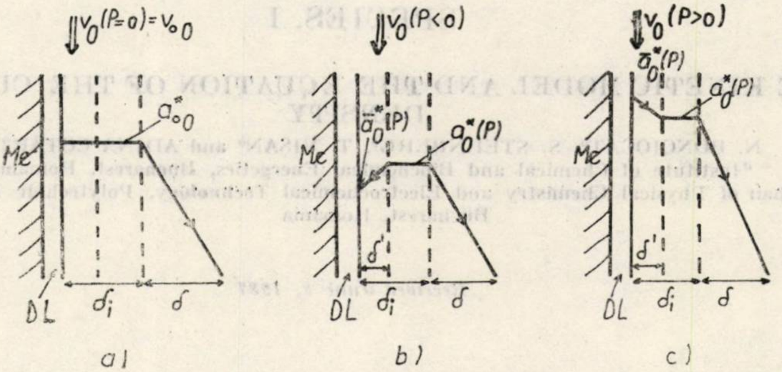

Fig. 1. — Activity profiles of the electrochemical active species O ; a. no current passes through the interface, i.e., the interface polarization P is zero ; b. $P < 0$, and therefore $i > 0$; c. $P > 0$, and therefore $i < 0$; DL-double layer ; δ, δ' — thicknesses of the diffusion layers, towards the indifferent electrolyte and the metal surface respectively ; δ_i — thickness of the interfacial layer.

What matters is the fact that the species O and R are generated at the rates $v_{\rm O}$, $v_{\rm R}$, expressing the moles per second appearing within the interfacial layer corresponding to an electrode surface of 1 cm².

The activity profiles in Fig. 1a refer to a steady state in which the moles of species O generated per second and per cm² of interfacial layer are equal to the moles disappearing per second and per cm² of interfacial layer by diffusion into the indifferent electrolyte, and consequently no current passes through the interface (i.e., the interface polarization P is equal to zero). This steady state is described by the equation :

$$v_{\rm O}(P = 0) = v_{\rm OO} = \frac{D_{\rm O} a^*_{\rm OO}}{\delta} \tag{2}$$

where D_O represents the diffusion coefficient of the species O and the other quantities have the meanings given in Fig. 1a.

The activity profiles in Fig. 1b refer to a steady state in which a net cathodic (reduction) current density ($i > 0$) passes through the interface as a consequence of a negative polarization of the interface ($P < 0$). In this case, apart from the diffusion into the indifferent electrolyte, the species O disappear also by the reduction reaction $\rm O + e \rightarrow R$ at a rate of i/F moles per second and per cm² of interfacial layer. Thus the steady states corresponding to cathodic polarizations of the interface are described by the equation :

$$v_{\mathrm{O}}(\mathrm{P}) = \frac{i(\mathrm{P})}{F} + \frac{D_{\mathrm{O}} a_{\mathrm{O}}^{*}(\mathrm{P})}{\delta} = \frac{i(\mathrm{P})}{F} + v_{\mathrm{OO}} \frac{a_{\mathrm{O}}^{*}(\mathrm{P})}{a_{\mathrm{OO}}^{*}} \tag{3}$$

Eq. (3) describes also the steady states corresponding to anodic polarizations of the interface ($\mathrm{P} > 0$). Indeed, in this case the net anodic (oxidation) current density ($i < 0$) generates species O (by the oxidation reaction $\mathrm{R} \rightarrow 0 + \mathrm{e}$) at a rate $-i/F$ moles per second and per cm² of interfacial layer.

For the current density $i(\mathrm{P})$, in the next section we shall give its "electrodic" expression, i.e., the expression obtained by analyzing the charge transfer across the energetic barrier of the interface. However, an "ionic" expression of $i(\mathrm{P})$ may also be given. To simplify the matter, et us suppose that the indifferent electrolyte is present in excess. Then, (P) may be expressed as a diffusion current by applying Fick's first law :

$$i(\mathrm{P}) = \frac{FD_{\mathrm{O}}}{\delta'} \left[a_{\mathrm{O}}^{*}(\mathrm{P}) - \bar{a}_{\mathrm{O}}^{*}(\mathrm{P})\right] \tag{4}$$

It is obvious that one may describe the above discussed steady states (i.e., for $\mathrm{P} = 0$; $\mathrm{P} < 0$; $\mathrm{P} > 0$) by equations that take into account the activity profiles of the species R (see Fig. 2). In doing this, we have to observe that now a cathodic current density will generate species R (by the reaction $\mathrm{O} + \mathrm{e} \rightarrow \mathrm{R}$) at a rate equal to $i|F$ while an anodic current density will lead to the disappearance of the species R (by the reaction

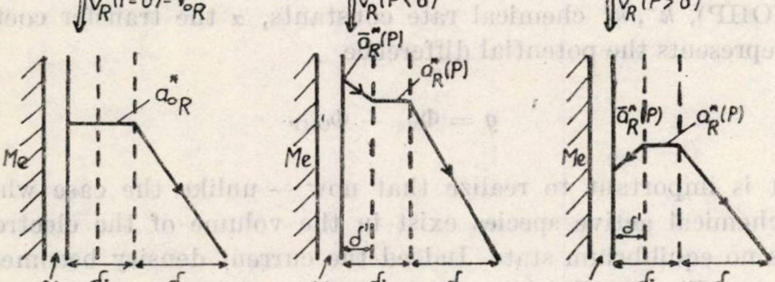

Fig. 2. — Activity profiles of the electrochemical active species R ; a. $\mathrm{P} = 0$, $i = 0$; b. $\mathrm{P} < 0$, $i > 0$; c. $\mathrm{P} > 0$, $i < 0$; DL, δ, δ', δ_i have the same meanings as in Fig. 1.

R → O + e) at a rate equal to $-i|F$. Therefore, instead of eqs. (2, 3, 4) one gets :

$$v_{\mathrm{R}}(\mathrm{P}=0)=v_{0\mathrm{R}}=\frac{D_{\mathrm{R}}a^{*}_{0\,\mathrm{R}}}{\delta} \tag{2'}$$

$$v_{\mathrm{R}}(\mathrm{P})=-\frac{i(\mathrm{P})}{\mathrm{F}}+\frac{D_{\mathrm{R}}a^{*}_{\mathrm{R}}(\mathrm{P})}{\delta}=-\frac{i(\mathrm{P})}{F}+v_{0\mathrm{R}}\frac{a^{*}_{\mathrm{R}}(\mathrm{P})}{a^{*}_{0\,\mathrm{R}}} \tag{3'}$$

$$i(\mathrm{P})=\frac{FD_{\mathrm{R}}}{\delta'}\left[\bar{a}^{*}_{\mathrm{R}}(\mathrm{P})-a^{*}_{\mathrm{R}}(\mathrm{P})\right] \tag{4'}$$

The expression of the current density

To get to the expression of the current density that takes into account the generating rates v_{O}, v_{R} of the electrochemical active species in the interfacial layer, we have to obtain first its "electrodic" expression, and then to correlate it with the equations derived in the preceding section.

The current density is given by the difference $i = i^{-} - i^{+}$, the partial cathodic (i^{-}), anodic (i^{+}) current densities having the expressions[8] :

$$i^{-}=Fk^{-}\mathrm{e}^{-\frac{F}{RT}\alpha g}\,\bar{a}^{*}_{\mathrm{O}}\,;\quad i^{+}=Fk^{+}\mathrm{e}^{-\frac{F}{RT}(1-\alpha)g}\,\bar{a}^{*}_{\mathrm{R}} \tag{5}$$

where $\bar{a}^{*}_{\mathrm{R}}$, $\bar{a}^{*}_{\mathrm{O}}$ are the corresponding activities in the outer Helmholtz plane (OHP), k^{-}, k^{+} chemical rate constants, α the transfer coefficient, and g represents the potential difference

$$g=\Phi_{\mathrm{Me}}-\Phi_{\mathrm{OHP}} \tag{5'}$$

It is important to realize that now — unlike the case where the electrochemical active species exist in the volume of the electrolyte — there is no equilibrium state. Indeed the current density becomes equal to zero (see Figs. 1a, 2a) in a steady state in which there is a permanent generation of the electrochemical active species, as well as a permanent transport of them into the volume of the indifferent electrolyte. For this reason, we shall introduce a reference steady state defined by the conditions : $i = 0$, $a^{*}_{0\mathrm{O}} = a^{*}_{0\,\mathrm{R}} = 1$. However from the kinetic point of view the fact that the reference state is an equilibrium state or a steady state has no importance. What matters is the fulfilling of the condition $i^{-} = i^{+}$(i.e., $i = 0$). Consequently the starting equations (5) will lead to current density equations that are identic to those derived in the theory of electrode redox processes [8-10]. What differs is the meaning of the quantities that refer to the used reference state. These equations express the current density either as a function of g, or as a function of the interface polarization $P = g - (g)_{i=0}$:

$$i(g) = i^{00}[\mathrm{e}^{-\alpha \frac{F}{RT}(g-g^0)} \bar{a}^*_{\mathrm{O}}(g) - \mathrm{e}^{(1-\alpha)\frac{F}{RT}(g-g^0)} \bar{a}^*_{\mathrm{R}}(g)] \tag{6}$$

respectively :

$$i(\mathrm{P}) = i^0 \left[\frac{\bar{a}^*_{\mathrm{O}}(\mathrm{P})}{a^*_{0\,\mathrm{O}}} \mathrm{e}^{-\alpha \frac{F}{RT}\mathrm{P}} - \frac{\bar{a}^*_{\mathrm{R}}(\mathrm{P})}{a^*_{0\,\mathrm{R}}} \mathrm{e}^{(1-\alpha)\frac{F}{RT}\mathrm{P}} \right] \tag{6'}$$

where :

$$i^0 = (i^-)_{i=0} = (i^+)_{i=0} \tag{7}$$

$$i^{00} = (i^-)_{i=0,\, a^*_{0\,\mathrm{O}} = a^*_{0\,R} = 1} = (i^+)_{i=0,\, a^*_{0\,\mathrm{O}} = a^*_{0\,R} = 1} \tag{7'}$$

$$g^0 = (g^-)_{i=0,\, a^*_{0\,\mathrm{O}} = a^*_{0\,\mathrm{R}} = 1} \tag{7''}$$

i^0 represents the exchange current density, while g^0, i^{00} are the electric tension respectively the exchange current density in the reference steady state.

Let us come back to eqs (2, 3, 4), respectively (2′, 3′, 4′). They give :

$$\frac{\bar{a}^*_{\mathrm{R}}(\mathrm{P})}{a^*_{0\,\mathrm{R}}} = \frac{i(\mathrm{P})\left(1 + \frac{\delta}{\delta'}\right) + F\frac{\delta}{\delta'} v_{\mathrm{R}}(\mathrm{P})}{F\frac{\delta}{\delta'} v_{0\mathrm{R}}} \tag{8}$$

$$\frac{\bar{a}^*_{\mathrm{O}}(\mathrm{P})}{a^*_{0\,\mathrm{O}}} = \frac{i(\mathrm{P})\left(1 + \frac{\delta}{\delta'}\right) - F\frac{\delta}{\delta'} v_{0}(\mathrm{P})}{-F\frac{\delta}{\delta'} v_{0\mathrm{O}}} \tag{8'}$$

Further, because $\bar{a}^*_{\mathrm{R}}(\mathrm{P}) \to 0$ for $\mathrm{P} \to \infty$, and $\bar{a}^*_{\mathrm{O}}(\mathrm{P}) \to 0$ for $\mathrm{P} \to -\infty$, it follows :

$$\left(1 + \frac{\delta}{\delta'}\right) \Big/ F\frac{\delta}{\delta'} = -v_{\mathrm{R}}(\infty)/i(\infty) = v_0(-\infty)/i(-\infty) \tag{9}$$

Using eqs. (8, 8′ and 9) one may put the expressions (6, 6′) in the final forms :

$$i(g) = \frac{i^{00}\left[\frac{v_O(g)}{v_{0O}} e^{-\alpha \frac{F}{RT}(g-g^0)} \cdot a^*_{0\,O} - \frac{v_R(g)}{v_{0R}} e^{(1-\alpha)\frac{F}{RT}(g-g^0)} \cdot a^*_{0\,R}\right]}{1 + \frac{v_O(-\infty)}{v_{0O}} \frac{i^{00}}{i(-\infty)} e^{-\alpha \frac{T}{RT}(g-g^0)} \cdot a^*_{0\,O} - \frac{v_R(\infty)}{v_{0R}} \frac{i^{00}}{i(\infty)} e^{(1-\alpha)\frac{F}{RT}(g-g^0)} \cdot a^*_{0\,R}} \tag{10}$$

$$i(\mathrm{P}) = \frac{i^0\left[\frac{v_O(\mathrm{P})}{v_{0O}} e^{-\alpha \frac{F}{RT}\mathrm{P}} - \frac{v_R(\mathrm{P})}{v_{0O}} e^{(1-\alpha)\frac{F}{RT}\mathrm{P}}\right]}{1 + \frac{v_O(-\infty)}{v_{0O}} \frac{i^0}{i(-\infty)} e^{-\alpha \frac{F}{RT}\mathrm{P}} - \frac{v_R(\infty)}{v_{0R}} \frac{i^0}{i(\infty)} e^{(1-\alpha)\frac{F}{RT}\mathrm{P}}} \tag{10′}$$

where the theoretical polarization P is equal to the experimental polarization P_{exp}, because in the presence of an indifferent electrolyte in excess, $g = \Phi_{Me} - \Phi_{OHP} = \Phi_{Me} - \Phi_{Electrolyte} = g_{exp}$.

Eqs. (10, 10′) may be particularized to give the current density corresponding to the reaction :

$$\mathrm{Me}^+ + \mathrm{e} \rightleftharpoons \mathrm{Me} \tag{1′}$$

where the species $\mathrm{Me}^+ \equiv \mathrm{O}$ is generated at a rate v, while the species $\mathrm{Me} \equiv \mathrm{R}$ s present at the interface in a practically inexhaustible quantity. It is sufficient to realize that now $i(\infty) \to -\infty$, and the ratio $v_R \,|v_{0R}$ is equal to unity, irrespective of the value of g (or P). Therefore :

$$i(g) = \frac{i^{00}\left[\frac{v(g)}{v_0} e^{-\alpha \frac{F}{RT}(g-g^0)} a^*_{0\,O} - e^{(1-\alpha)\frac{F}{RT}(g-g^0)}\right]}{1 + \frac{v(-\infty)}{v_0} \frac{i^{00}}{i(-\infty)} e^{-\alpha \frac{F}{RT}(g-g^0)} a^*_{0\,O}} \tag{11}$$

respectively :

$$i(\mathrm{P}) = \frac{i^0\left[\frac{v(P)}{v_0} e^{-\alpha \frac{F}{RT}\mathrm{P}} - e^{(1-\alpha)\frac{F}{RT}\mathrm{P}}\right]}{1 + \frac{v(-\infty)}{v_0} \frac{i^0}{i(-\infty)} e^{-\alpha \frac{F}{RT}\mathrm{P}}} \tag{11′}$$

Eq. (11′) will be used in a following paper to analyse an electrode reaction of the type (1′) where the electrochemical active species Me^+ is generated by a chemical interfacial reaction.[11]

FINAL REMARKS

Eqs. (10, 10′) give the general expression of the current density of electrode redox reactions occurring with combined overtension, of charge transfer and of interfacial generation of the electrochemical active species. Because they are valid irrespective of the nature of the generating processes, these equations have a character of generality describing all cases of pure or combined overtensions. For instance consider the case where the species O and R are present in the electrolyte at the concentrations a_O^B, a_R^B. Of course at $i = 0$, these will be also the concentrations in the interfacial layer considered by our model, i.e., $a^*_{0O} = a_O^B$; $a^*_{0R} = a_R^B$.One may interpret this situation as resulting from two diffusion processes that compensate each other, i.e., a diffusion process by which, say, the species O is brought to the interfacial layer at a rate $v_O = D_O a_O^B/\delta$, and a diffusion process by which the species O leaves the interfacial layer towards the volume of the electrolyte at a rate $D_O a^*_{0O}/\delta = v_O$. The first diffusion process is the generating process and its rate is not dependent on the polarization P applied to the interface, unlike the second one whose rate changes to $D_O a^*_O(P)/\delta$, the difference between the two rates being compensated by the current passing through the interface. Thus $v_{0O} = v_O(P) = D_O a_O^B/\delta$; $v_{0R} = v_R(P) = D_R a_R^B/\delta$ and it is easy to see that eq. (10′) particularizes in the well-known equation describing the electrode redox reactions occurring with combined overtension of charge transfer and of diffusion.

REFERENCES

[1] Z. Galus, "Fundamental of Electrochemical Analysis", E. Harwood, Ltd., Chichester, 1976.

[2] P. Delahay, "New Instrumental Methods in Electrochemistry", Wiley-Interscience, New York, 1954.

[3] I. M. Kolthoff and J. J. Lingane, "Polarography", 2nd ed., Wiley-Interscience, New York. 1952.

[4] D. D. Macdonald, "Transient Techniques in Electrochemistry", Plenum, New York, 1977,

[5] D. Pletcher, *Chem. Soc. Rev.*, **4**, 471 (1975).

[6] J. Koutecky and R. Brdička, *Coll. Czech. Chem. Comm.*, *12*, 337 (1947).

[7] A. J. Bard and L. R. Faulkner, "Electrochemical Methods", John Wiley and Sons, New York, Chichester, Brisbane, Toronto, 1980, Chap. 3.

[8] J. O'M. Bockris and A. K. N. Reddy, "Modern Electrochemistry", Vol. 2, Plenum, New York, 1970, Chap. 8.

[9] K. J. Vetter, "Electrochemical Kinetics", Academic Press, New York, 1967, Chap. 2.

[10] A. J. Bard and L. R. Faulkner, "Electrochemical Methods", John Wiley and Sons, New York, Chichester, Brisbane, Toronto, 1980, Chap. 11.

[11] S. Sternberg, N. Bonciocat, A. Cotârţă and T. Vişan, *Rev. Roumaine Chim.*, to be published.

Revue Roumaine de Chimie, 33, 8, 789—794 (1988)

POLAROGRAPHIC STUDY OF MANGANESE(II)-PYRIDINE-THIOCYANATE SYSTEM AND THERMODYNAMIC PARAMETERS

JYOTI SHARMA[a], ARVIND KUMAR[a] and B. K. PURI[b]

[a]Department of Chemistry, Delhi University, Delhi-110007, India
[b]Department of Chemistry, Indian Institute of Technology Hauz Khas, New Delhi-110016, India

Received September 20, 1986

Mn(II)-pyridine-thiocyanate system has been studied polarographically at constant pH = 7.0 and ionic strength, $\mu = 0.5$ M ($NaClO_4$) in aqueous alcohol (4 : 1) media at different temperatures. The reduction of the simple and mixed complexes is reversible and diffusion controlled. The methods of DeFord-Hume and Schaap-McMaster have been applied for the determination of composition and stability constants of simple and mixed complexes respectively. The thermodynamic parameters like ΔG, ΔH and ΔS have also been calculated.

INTRODUCTION

Potentiometric [1] pH-metric [2] and some other techniques [3-4] have been widely employed in the detailed study of mixed ligand complexes of metal ions. After the development of the Schaap and McMaster method[5] for determination of stability constants of mixed ligand complexes of metal ions, the polarographic technique has also received a considerable attention in this field. Recently, mixed ligand complexes of a few transition metals have been determined polarographically.[6] Although the polarographic behaviour of manganese in the presence of various complexing agents [7-10] has been studied, however, only a few mixed-ligand complexes of this metal have been studied by this technique.[11-12] A survey of the literature reveals that the mixed ligand complexes of manganese(II)-pyridine-thiocyanate have not been studied polarographically. In the present communication, the polarographic behaviour of Mn(II)-pyridine-thiocyanate system has been studied systematically at different temperatures and the thermodynamic parameters like ΔG, ΔH and ΔS have also been calculated.

EXPERIMENTAL

Materials

All the chemicals used were of analytical reagent grade and their solutions were prepared in conductivity water. Pyridine (py) and potassium thiocyanate (SCN) were used as ligands. Triton- X-100 (0.002%) was used as the maximum supressor. The ionic strength was maintained constant at $\mu = 0.5$ M ($NaClO_4$).

Apparatus and Procedure

Polarograms in all instances were recorded with a manual Toshniwal polarograph (CLO2) in connection with a polyflex galvanometer (Toshniwal PL 50). A saturated calomel electrode (SCE) was used as reference electrode and was connected to the polarographic cell through a potassium chloride agar-agar bridge. The dropping mercury electrode (DME) had the following characteristics, $h_{corr} = 30$ cm, $m^{2/3}t^{1/6} = 2.01\ m^{2/3}s^{-1/2}$ in 0.1 M $NaClO_4$ solution with open circuit. Oxygen was expelled by passing a slow stream of purified nitrogen gas into the test solution for 5 min. All observations were taken by using a thermostatic control o sensitivity ± 0.2°C.

RESULTS AND DISCUSSION

The stability constants of simple complexes of manganese(II) with pyridine and thiocyanate were determined separately prior to the study of mixed ligand systems. Similar conditions were maintained in both the simple and mixed systems.

Mn(II)-pyridine System

A series of polarograms were recorded with increasing concentration of pyridine (0.05—0.25 M) at constant ionic strength, $\mu = 0.5$ M $NaClO_4$ and at different temperatures 20°, 30° and 40°C. In each case, a well defined reversible diffusion controlled wave was obtained. The slopes of linear plots of $\log \frac{i}{i_d - i}$ versus $E_{d.e}$ were of the order of 30 ± 1 mV indicating the change of two electrons. The same value of 'n' was obtained by the millicoulometric studies.[13] A plot of $E_{1/2}$ versus log [py] was a smooth curve indicating the formation of successive complexes. DeFord and Hume's method [14] was applied for the determination of stability constants of successive complexes. At 20°C, Mn (II) forms four complexes with pyridine whereas at 30° and 40°C it forms only three complexes. At higher temperature, the complexes might be unstable, therefore, only three complexes are formed above 20°C. The results are summarized in Table 1.

Mn(II)-thiocyanate System

Similar studies were carried out with increasing concentration of thiocyanate (0.05—0.25 M) at constant ionic strength, $\mu = 0.5$ M $NaClO_4$ and at different temperature 20°, 30° and 40°C. In each case, a well defined, reversible with two electrons change diffusion controlled wave appeared. A plot of $E_{1/2}$versus log [SCN] was a smooth curve indicating the formation of successive complexes. DeFord and Hume's method [14] was applied for the determination of stability constants. An analysis of $F(y)$ functions reveals the formation of four successive complexes at 20°C and three successive complexes at 30° and 40°C similar to Mn(II)-py system. The results are summarized in Table 2.

Table 1

Values of $F(X)$ functions for Mn(II)-pyridine system at different temperatures Mn(II) = 0.5 mM, ionic strength, $\mu = 0.5$ ($NaClO_4$)

Temperature 0°C	[Py] M	$\Delta E_{1/2}$ V vs SCE	$\log \frac{I_S}{I_C}$	$F_0(x)$ $\times 10^{-1}$	$F_1(x)$ $\times 10^{-1}$	$F_2(x)$ $\times 10^{-1}$	$F_3(x)$ $\times 10^{-2}$	$F_4(x)$ $\times 10^{-2}$
20	0.05	0.010	0.0124	2.21	2.42	—	—	—
	0.10	0.016	0.0251	3.61	2.61	6.10	1.74	7.44
	0.15	0.022	0.0195	5.65	3.14	7.33	1.95	6.38
	0.20	0.028	0.0061	8.67	3.83	9.15	2.37	6.87
	0.25	0.032	0.0198	13.14	4.85	11.42	2.81	7.24
30	0.05	0.008	0.0299	1.97	1.90	—	—	
	0.10	0.013	0.0521	3.12	2.12	5.50	1.90	
	0.15	0.020	0.0225	4.76	2.51	7.06	2.30	
	0.20	0.025	0.0298	7.28	3.14	7.70	2.05	
	0.25	0.030	0.0321	10.74	3.89	9.16	2.22	
40	0.05	0.005	0.0198	1.53	1.06	—	—	
	0.10	0.010	0.0194	2.25	1.25	3.57	1.98	
	0.15	0.016	0.0150	3.50	1.66	5.10	2.33	
	0.20	0.021	0.0294	5.35	2.17	6.38	2.39	
	0.25	0.026	0.0301	7.86	2.74	7.37	2.31	

At 20°C $\log \beta_1 = 1.30$, $\log \beta_2 = 1.64$, $\log \beta_3 = 2.00$, $\log \beta_4 = 2.84$
At 30°C, $\log \beta_1 = 120$, $\log \beta_2 = 1.556$, $\log \beta_3 = 2.32$
At 40°C $\log \beta_1 = 0.954$, $\log \beta_2 = 1.204$, $\log \beta_3 = 2.35$

Table 2

Values of F(Y) functions of Mn(II)-thiocyanate system at different temperatures. The same conditions as in Table 1

Temperature O°C	[SCN] M	$\Delta E_{1/2}$ V vs SCE	$\log \frac{I_S}{I_C}$	$F_0(y)$ $\times 10^{-1}$	$F_1(y)$ $\times 10^{-1}$	$F_2(y)$ $\times 10^{-1}$	$F_3(y)$ $\times 10^{-2}$	$F_4(y)$ $\times 10^{-2}$
20	0.05	0.015	0.0124	3.01	4.02	4.40	—	—
	0.10	0.021	0.0251	5.26	4.26	4.61	1.41	6.10
	0.15	0.026	0.0187	8.08	4.76	6.14	1.95	7.73
	0.20	0.032	0.0061	11.79	5.39	7.97	2.38	7.90
	0.25	0.038	0.0124	17.29	6.51	10.86	3.06	9.04
30	0.05	0.0100	0.0107	2.20	2.40	—	—	
	0.10	0.0160	0.0301	3.65	2.65	6.50	2.90	
	0.15	0.0225	0.0209	5.89	3.26	8.40	3.20	
	0.20	0.0280	0.0201	8.96	3.98	9.90	3.15	
	0.25	0.0326	0.0304	13.06	4.82	11.29	3.07	
40	0.05	0.008	0.0128	1.90	1.80	—	—	
	0.10	0.014	0.0144	3.02	2.02	4.20	2.00	
	0.15	0.021	0.0120	4.76	2.50	6.00	2.66	
	0.20	0.025	0.0198	7.11	3.05	7.26	2.53	
	0.25	0.030	0.0204	10.45	3.78	8.72	2.60	

At 20°C : $\log \beta_1 = 1.57$, $\log \beta_2 = 1.50$, $\log \beta_3 = 1.903$, $\log \beta_4 = 2.88$
At 30°C : $\log \beta_1 = 1.30$, $\log \beta_2 = 1.55$, $\log \beta_3 = 2.48$
At 40°C : $\log \beta_1 = 1.204$, $\log \beta_2 = 1.34$, $\log \beta_3 = 2.38$

Mn-pyridine-thiocyanate System

The concentration of py was varied from 0.05 to 0.25 M keeping [SCN] constant at 0.2 M. The $E_{1/2}$ values were found to be more negative than those obtained in the absence of thiocyanate showing the formation of mixed complexes. The system was also repeated at another concentration of thiocyanate (0.4 M). These constant concentrations were termed as series 1 and 2 respectively. In all the cases, a well defined diffusion controlled reversible wave with the change of two electrons appeared. Therefore, the method of Schaap and McMaster [5] was applied to the determination of stability constants of the mixed complexes. The $F(x, y)$ functions (X = py, and Y = SCN) of these systems were determined. From the plots of $F(x, y)$ data versus [py], the constants A, B, C and D were obtained (Table 3). In this system, three mixed complexes were formed, $[Mn(py)SCN]^+$, $[Mn(py)(SCN)_2]$ and $[Mn(py)_2SCN]^+$ with formation constants obtained from the intercept data, $\log \beta_{11} = 1.966$, $\log \beta_{12} = 2.138$ and $\log \beta_{21} = 2.984$ at 30°C.

Table 3

Values of $F(x, y)$ as a function of Mn(II)-pyridine-thiocyanate system at 30 ± 0.1°C. The same conditions as in Table 1

[Py] M	$\Delta E_{1/2}$ V vs SCE	$\log \frac{I_S}{I_C}$	$F_0(x, y)$ $\times 10^{-1}$	$F_{10}(x, y)$ $\times 10^{-1}$	$F_{20}(x, y)$ $\times 10^{-2}$	$F_{30}(x, y)$ $\times 10^{-3}$
Series 1 [SCN] = 0.2 M (fixed)						
0.05	0.022	0.2052	8.66	5.32	—	—
0.10	0.028	0.2078	13.81	7.81	3.81	1.11
0.15	0.034	0.2175	22.37	10.91	4.60	1.26
0.20	0.040	0.2018	34.18	14.09	5.04	1.17
0.25	0.045	0.2230	52.66	18.66	5.86	1.26
Series 2 [SCN] = 0.4 (fixed)						
0.05	0.0280	0.2012	1.41	11.20	—	—
0.10	0.0325	0.2270	2.04	12.47	4.97	1.37
0.15	0.0380	0.2375	3.18	15.88	5.58	1.32
0.20	0.0440	0.2215	4.86	22.30	6.40	1.40
0.25	0.0485	0.2484	7.30	26.01	7.40	1.52

Series 1 : $\log A = 0.7781$, $\log B = 1.602$, $\log C = 2.431$, $\log D = 3.079$
Series 2 : $\log A = 0.9039$, $\log B = 1.875$, $\log C = 2.55$, $\log D = 3.146$

The results of this study at 30°C are summarized below and the numerical values shown as the log of equilibrium constants of the reactions indicated.

The tendency of thiocyanate anion to add as the second ligand to $[Mn(SCN)]^+$ and $[Mn(py)]^{2+}$ can be considered. The log K values are 0.25 and 0.76 respectively. Since, the difference is larger than the statistical factor of 2, naturally the charge neutralization will be expected. Addition of an uncharged pyridine to each of the above complexes gives rise to log K values of 0.66 and 0.35 respectively, a difference equal to that predicted by the statistical factor.

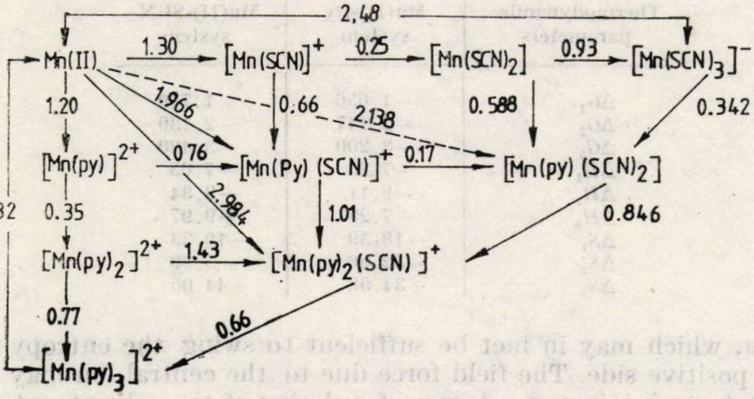

On the addition of thiocyanate anion as the third ligand to the various complexes i.e. $[Mn(SCN)_2]$, $[Mn(py)(SCN)]^+$ and $[Mn(py)_2]^{2+}$, the log K values are 0.93, 0.17 and 1.43, respectively, indicating charge neutralization.

On the other hand, the log K values for the addition of uncharged py molecule as the third ligand to $[Mn(SCN)_2]$, $[Mn(py)SCN]^+$ and $[Mn(py)_2]^{2+}$ are 0.56, 1.0 and 0.77. Here the difference is not very large, thus no charge neutralization effect would be expected

$$2[Mn(py)(SCN)]^+ \rightleftharpoons [Mn(py)_2]^{2+} + [Mn(SCN)_2]$$

The log K value for this disproportionation reaction is −0.832 indicating that the mixed complex is more stable than the simple complexes. The same is the case for the other mixed complexes.

The thermodynamic constants for the Mn(II)-py and Mn(II)-SCN complexes have been calculated using the known equations[15] and are summarized in Table 4. The values of the free energy change i.e. ΔG of the complexes give an idea of their relative stabilities. Stepwise enthalpies for the formation of mono, bis and tris-pyridine complexes of Mn are −7.21 kcal|mole, −9.11 kcal|mole and +7.28 kcal|mole; it seems that the first two ligands decrease the field splitting, in Mn(II), but the third ligand decreases the field splitting, hence $[Mn(py)_3]^{2+}$ is less stable than $[Mn(py)_2]^{2+}$. In the case of Mn(II)-thiocyanate system, $\Delta H_1 = -7.65$ kcal|mole, $\Delta H_2 = -3.34$ kcal|mole and $\Delta H_3 = +9.97$ kcal|mole, here also $[Mn(SCN)_3]^-$ is less stable than $[Mn(SCN)_2]$. The entropy change which is negative for mono and bis complexes may be due to the loss of transitional degree of freedom by ligand attached thus favouring a greater degree of order. But this may be off-set by the loss of hydration of the metal ion, which may in fact be sufficient to swing the entropy change over the positive side. The field force due to the central ion may still be sufficient to maintain some degree of ordering of the solvent outside the sphere of the ligand.

Table 4

Stepwise free energy change ΔG, enthalpy change ΔH and entropy change ΔS in kcal/mol at 30°C

Thermodynamic parameters	Mn(II)-Py system	Mn(II)-SCN system
ΔG_1	−1.656	−1.790
ΔG_2	−2.147	−2.139
ΔG_3	−3.200	−3.420
ΔH_1	−7.23	−7.65
ΔH_2	−9.11	−3.34
ΔH_3	+7.28	+9.97
ΔS_1	−18.39	−19.33
ΔS_2	−22.98	−3.99
ΔS_3	+34.58	+44.05

ACKNOWLEDGEMENTS. The sincere thanks of the authors are due to U.G.C. for providing the financial assistance to one of us (JS) and also to Dr. N. K. Kaushik for useful discussion.

REFERENCES

[1] E. G. Sare and D. V. Jahangirdar, *J. Inorg. Nuclear Chem.*, **37**, 985 (1975).

[2] S. P. Tripathi, R. C. Sharma and G. K. Chaturvedi, *J. Inst. Chem. (India)*, **52**, 211 (1980).

[3] M. Tanaka, *J. Inorg. Nuclear Chem.*, **36**, 151 (1974).

[4] H. Irving and D. N. Edigton, *J. Inorg. Nuclear Chem.*, **21**, 169 (1961).

[5] W. B. Schaap and D. L. McMaster, *J. Amer. Chem. Soc.*, **83**, 4699 (1961).

[6] D. G. Dhuley and V. G. Dongre, *Indian J. Chem.*, **20A**, 208 (1981).

[7] A. L. J. Rao and B. K. Puri, *Z. analyt. Chem.*, **254**, 362 (1971).

[8] B. K. Puri and Ashok Kumar, *Indian J. Chem.*, **22A**, 1071 (1983).

[9] B. K. Puri and Ashok Kumar, *Zhur. analit. Khim.*, **39**, 360 (1984).

[10] J. Dolezal, E. Julakova, M. Cerny and M. Kopanica, *J. Electro. Anal. Chem. Interfacial Electro. Chem.*, **52**, 261 (1974).

[11] V. F. Toropova, G. K. Budnikov and N. K. Ulabhovich, *Zhur. obshchei. Khim.*, **45**, 280 (1975).

[12] Krishna, Renu Kulshrestha and Mukhtar Singh, *J. Electro. Chem. Soc. (India)*, **33**, 271 (1984).

[13] T. Devries and J. L. Kroon, *J. Amer. Chem. Soc.*, **75**, 2484 (1953).

[14] D. N. Hume and D. D. DeFord, *J. Amer. Chem. Soc.*, **73**, 532 (1951).

[15] K. B. Yatsimirskii and V. P. Vasiler, "Instability Constants of Complex Compounds", Pergamon Press, New York, 1960.

Revue Roumaine de Chimie, **33**, 8, 795–801 (1988)

β-LACTAM ANTIBIOTICS. II*

SUBSTITUENT EFFECTS ON CEPHALOSPORINS

JOSETTE WEINBERG[a], ALEXANDRINA DONESCU[a] and V. EM. SAHINI[b]
[a] ICECHIM—Centre of Physical Chemistry, Spl. Independenţei 202, Bucharest, Romania
[b] Polytechnic Institute, Laboratory of Physical Chemistry, Blvd Republicii 13, Bucharest
Romania

A Hückel MO-study of π-electronic structure of some cephalosporin molecules is presented, corrected for the noncoplanarity of two cycles of the molecule. The cephalosporins have the advantage of a remarkable resistance against Staphylococci penicillinase and their chemical reactivity is confirmed by frontier electron indices. Correlations are established between antimicrobian properties and electronic structure of the cephalosporin molecules.

In a first variant of the Hückel calculation, this formalism was applied only to a molecular fragment according to Fig. 1.

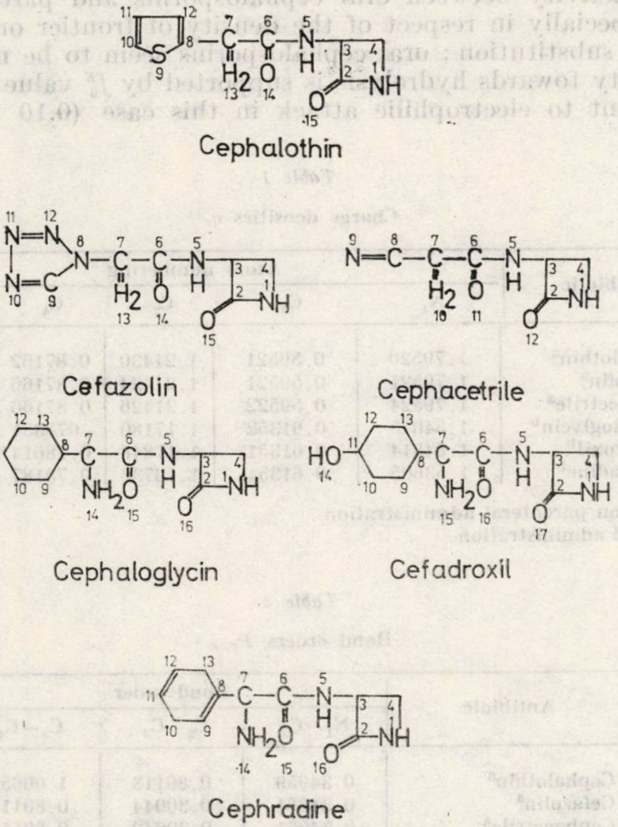

Cephalothin

Cefazolin

Cephacetrile

Cephaloglycin

Cefadroxil

Cephradine

Fig. 1 — The **notation** of molecular centers in the cephalosporin fragments.

---

* Part I: J. Weinberg and A. Donescu, *Rev. Roumaine Chim.*, **32**, 1117 (1987).

The calculated reactivity indices are listed in Tables 1—4. Then the Hückel method was applied to the whole cephalosporin molecule. Correction factors were applied for the non-coplanarity of the two rings in molecule. Eight cephalosporins were studied. Numbering of centers is according to Fig. 2. Tables 5—8 show the calculated reactivity indices.

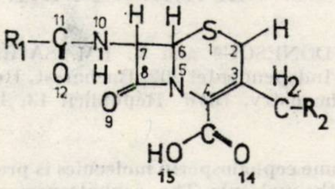

Fig. 2— The notation of molecular centers in the cephalosporins.

RESULTS AND DISCUSSION

Tables 1—4 show that the first variant yields a marked difference in C_2 atom reactivity between oral cephalosporins and parenteral cephalosporins especially in respect of the density of frontier orbitals f_2^N in a nucleophilic substitution : oral cephalosporins seem to be more efficient. Their stability towards hydrolysis is supported by f_5^E value at N_5, much more resistant to electrophilic attack in this case (0.10 against 0.28)

Table 1

Charge densities q_r

Antibiotic	Atom numbering				
	N_1	C_2	C_3	C_4	N_5
Cephalothin[a]	1.79520	0.59521	1.21430	0.87162	1.67413
Cefazolin[a]	1.79521	0.59521	1.21424	0.87166	1.67415
Cephacetrile[a]	1.79524	0.59522	1.21426	0.87166	1.67425
Cephaloglycin[b]	1.54085	0.61352	1.17180	.078351	1.57189
Cefadroxil[b]	1.54814	0.61351	1.17848	0.78614	1.57509
Cephradine[b]	1.53605	0.61351	1.16736	0.78187	1.56996

[a] Active on parenteral administration
[b] For oral administration

Table 2

Bond orders P_{r-s}

Antibiotc	Bond order		
	N_1-C_2	C_2-C_3	C_3-C_4
Cephalothin[a]	0.34959	0.80113	1.00658
Cefazolin[a]	0.34961	0.30044	0.80114
Cephacetrile[a]	0.34961	0.30042	0.80118
Cephaloglycin[b]	0.39442	0.28150	0.68469
Cefadroxil[b]	0.39461	0.28128	0.65923
Cephradine[b]	0.40096	0.28160	0.65200

(Table 3). The differences of cephradine and cefadroxil concentrations noted in serum at several time intervals after administration[1] (the former is absorbed faster but persists for a shorter time) may be assigned to the mobile order of P_{3-4} bond (Table 2), which is a little smaller compared to cefadroxil.

Table 3

Frontier orbitals densities f_r

Antibiotic	N₁			C₂			N₅		
	f_r^E	f_r^R	f_r^N	f_r^E	f_r^R	f_r^N	f_r^E	f_r^R	f_r^N
Cephalotin[a]	0.4759	0.2393	0.0027	0.0046	0.3249	0.6442	0.2812	0.1473	0.0834
Cefazolin[a]	0.4763	0.2395	0.0027	0.0046	0.3249	0.6453	0.2813	0.1473	0.0134
Cephacetrile[a]	0.4765	0.2396	0.0027	0.0046	0.3249	0.6453	0.2812	0.1373	0.0134
Cephalogycin[b]	0.5763	0.3680	0.1596	8.2×10^{-5}	0.0050	0.0100	0.1019	0.1202	0.1385
Cefadroxil[b]	0.5834	0.3681	0.1596	7.6×10^{-5}	0.0056	0.0111	0.1050	0.1202	0.1357
Cephradine[b]	0.5715	0.3678	0.1641	8.5×10^{-5}	0.69×10^{-3}	0.0093	0.1000	0.1200	0.1400

Table 4

HOMO and LUMO orbital energies

Antibiotic	HOMO (β)	LUMO (β)
Cephalothin[a]	0.19799	−0.50938
Cefazolin[a]	0.19808	−0.50938
Cephacetrile[a]	0.19819	−0.50938
Cephaloglycin[b]	0.03943	−0.24574
Cefadroxil[b]	0.03758	−0.25421
Cephradine[b]	0.04049	−0.24010

The calculations confirm the importance of amidic bond resonance i.e. as the C—N bond is less stable, the β-lactam cycle is more susceptible to the nucleophilic attack[2]; thus one may estimate the antimicrobial activity. Regarding the variation of HOMO (Table 4) one may notice that the oral cephalosporins exhibit smaller HOMO values in β-units or in other words, they are the highest in energy. This may exert an important influence on their antimicrobial activity as well as on their possibility of being rapidly and almost completely absorbed orally.

The cephalosporins are much more active against the Gram negative bacteria. Their cellular wall contains more lipids than the Gram-positive ones such that the hydrophobicity constants should exert a more important influence upon them. Thus one may affirm that between biological activity and physico-chemical parameters (pK_a, ν_{IR}, chemical shift) there is a linear relation and the deviations are due to the impossibility of ionized forms to penetrate through cell membranes.[3]

Thus cefazolin has shown an increase of activity compared to the Gram-negative bacteria.[1] The lower rate of elimination of cefazolin is mainly due to the 2-methyl-thiodiazole-thiomethyl side chain in the 3-position, which otherwise is also responsible for the higher protein binding.[1]

In the second variant of Hückel calculation the high reactivity of the cephalosporins is confirmed by the Fukui index of reactivity f_5^E (Table 7) whose value ranges within 0.1—0.3; likewise the superdelocalizability index (Table 8) confirms this behaviour.

Table 5

Coulson charge density q_r

Antibiotic	Atom numbering				
	C_3	N_5	C_8	N_{10}	C_3'
Cephalothin[a]	1.04540	1.4600	0.61540	1.6432	0.6732
Cefazolin[a]	1.03810	1.1311	0.62880	1.6277	1.0854
Cephacetrile[a]	1.03810	1.1632	0.62880	1.6278	1.0864
Cefamandole[a]	1.02570	1.5134	0.61800	1.7373	1.0853
Cephradine[b]	1.03820	1.1636	0.62740	1.5864	—
Cephaloglycin[b]	1.02310	1.6379	0.59820	1.6041	1.0412
Cefadroxil[b]	0.90078	1.4591	0.61400	1.5979	—
Cefatrizine[b]	1.07510	1.4311	0.70520	1.4454	0.7979

Table 6

Bond orders P_{r-s}

Antibiotic	The bond		
	N_5-C_8	C_6-C_7	C_{3-3}'
Cephalothin[a]	0.30460	0.68055	0.17900
Cefazolin[a]	0.39130	0.63270	0.18020
Cephacetrile[a]	0.32340	0.63278	0.17960
Cefamandole[a]	0.28510	0.73036	0.18000
Cephradine[b]	0.32459	0.61956	—
Cephaloglycin[b]	0.75860	0.86500	
Cefadroxil[b]	0.36660	0.66380	
Cefatrizine[b]	0.38896	0.54996	0.40850

Table 7

Frontier orbital densities (f^E for electrophilic, f^N for nucleophilic reactivity)

Antibiotic	$f^E_{N_5}$	$f^N_{C_8}$	$f^E_{N_{10}}$	$f^E_{C_3}$	$f^N_{C_3}$	$f^E_{C_3'}$	$f^N_{C_3'}$
Cephalothin[a]	0.1576	9.8×10^{-3}	0.2402	0.1344	8.87×10^{-4}	0.0193	0.2616
Cefazolin[a]	0.1373	1.41×10^{-2}	0.1704	0.1464	2.21×10^{-3}	1.02×10^{-2}	1.09×10^{-6}
Cephacetrile[a]	0.1373	1.41×10^{-2}	0.1703	0.1464	2.21×10^{-3}	1.03×10^{-3}	1.09×10^{-6}
Cefamandole[a]	0.3326	—	—	0.2332	—	4.25×10^{-3}	—
Cephradine[b]	0.1419	2.65×10^{-3}	0.1403	0.1441	2.61×10^{-3}	—	—
Cephaloglycin[b]	0.3213	5.21×10^{-4}	0.1202	9.44×10^{-4}	5.54×10^{-4}	0.1599	3.07×10^{-2}
Cefadroxil[b]	0.1571	6.84×10^{-4}	0.2054	0.1301	5.59×10^{-3}	—	—

Table 8

Frontier orbital energies HOMO and LUMO (β) and superdelocalizability index S_8

Antibiotic	HOMO	LUMO	S_8
Cephalothin[a]	0.25644	−0.17399	2.3998
Cefazolin[a]	0.20398	−0.29946	3.0836
Cephacetrile[a]	0.20403	−0.29945	3.0819
Cefamandole[a]	0.52609	−0.01645	—
Cephradine[b]	0.22732	−0.17926	2.7599
Cephaloglycin[b]	0.16835	−0.17031	3.35554
Cefadroxil[b]	0.27989	−0.13444	2.1537

Cephalothin, containing a thiophene-2-acetic group in the side chain, exhibits a good activity with respect to the Gram-positive and negative bacterias, which is theoretically confirmed by the value of $f^N_{C_8}$ (Table 7). That it has to be administred parenterally due to its instability in acid medium theoretically demonstrated by the high value of $f^E_{N_{10}}$ density (Table 7).

Cephaloglycin is the first cephalosporin which is sufficiently absorbed from gastro-intestinal tract to be orally administered. Its stability to hydrolysis is proved by the $f^E_{N_{10}}$ value (Table 7). As we have already shown, cefazolin has a 7-tetrazole group and a 3-thiadiazole group in the side chain; it has the same antimicrobial spectrum as cephalothin, which was also proved by the Coulson density q_{C_8} (Table 5). Cephacetrile is similar to cephalothin in its antimicrobial spectrum; however it is much more active against enterococci. This behaviour is theoretically demonstrated by the value of the superdelocalizability index S_{C_8} (Table 8) of this antibiotic.

Cephradine exhibits a minor modification compared to ampicillin because it has a 1,4-cyclohexadienyl group instead of benzene ring and has no esteric group bonded to dihydrothiazinic ring. It is eliminated unchanged, is stable in acid medium and well absorbed orally.

From the second generation of the cephalosporins,[1] cefamandole is the most active, which is confirmed by the amidic bond order $P_{N_5-O_8}$ which is energetically the weakest in all the series under study (Table 6).

In conclusion it results that the reactivity of the β-lactam ring depends on the nature of the R_1 side chain: when C_{11} is substituted by an amino group or when the methylene group is replaced by an NH group (the case of the oral cephalosporins) such derivatives may undergo an intramolecular amino attack at the β-lactam ring and the opening of the cycle is accelerated [4]; a substituent at C_3 with a more pronounced electron attracting character stabilizes to a greater extent a transition state and enhances the basic hydrolysis of the cephalosporins.

The acetoxy group plays some role in this respect.[4]

These results confirm the correlation presented in the following between calculated chemical reactivity and biological activity. Thus on the basis of calculations carried out, structure-activity correlation equations were obtained. Table 9 shows the antimicrobial activity "y" of a series of the studied cephalosporins ($y = \log 1|\mathrm{MIC}$) against Acinetobacter calcoaceticus var. Lwoffi.[5]

Table

Antimicrobial activities

Antibiotic	y	HOMO	LUMO	$f^N_{C_8}$
Cephalothin[a]	−1.8006	0.2564	−0.1740	5.81×10^{-3}
Cefazolin[a]	−2.6612	0.2039	−0.2995	1.41×10^{-2}
Cephacetrile[a]	−2.6605	0.2040	−0.2994	1.41×10^{-2}
Cephradine[b]	−1.9955	0.2273	−0.1793	2.65×10^{-3}
Cephaloglycin[b]	−2.3416	0.1683	−0.1709	5.20×10^{-4}
Cefadroxil[b]	−1.5329	0.2799	−0.1344	6.80×10^{-3}

A multilinear regression program has yielded the equations with two-six terms in the right side.

1.) $y = 0.60\ \mathrm{HOMO} + 0.418\ \mathrm{LUMO} - 0.263\,;\ r^2 = 0.99$

2.) $y = 0.68\ \mathrm{HOMO} + 0.326\ \mathrm{LUMO} - 0.104\, f_8^N - 0.253\,;\ r^2 = 0.99$

3.) $y = 0.10\, Q_{N_5} + 0.148\, Q_{C_8} - 0.139\, P_{5-8} + 0.141\, P_{6-7} + 0.486\,;$

$r^2 = 0.94$

4.) $y = 0.13\, Q_{N_5} + 0.27\, Q_{C_8} + 0.13\, Q_{N_{10}} + 0.48\, P_{6-7} - 0.249\, P_{5-8} + 0.604\,;$

$r^2 = 0.96$

5.) $y = 0.94\, P_{5-8} + 0.59\, P_{6-7} + 0.20\, Q_{N_5} + 0.27\, Q_{C_8} + 0.17\, Q_{N_{10}} -$

$- 0.33\, Q_{C_3} + 0.105\,;\ r^2 = 0.99$

The presence of the highest orbital occupied in the ground state (HOMO) and of the lowest unoccupied orbital in the same state (LUMO) in the two equations proves the important role of frontier orbitals in the reactions. The frontier orbital density on C_8 atom in a nucleophilic reaction confirm the importance of the reactivity of this atom in a nucleophilic reaction (the acylation reaction of the corresponding enzyme). The presence of bonding orbitals in the β-lactam cycle points to the importance of energy value of this cycle which is responsible for the antibiotic activity. Likewise the presence of net charge on C_8 and N_5 of the β-lactam ring supports this statement. Moreover, the net electronic charge on N_{10} and

C_3 demonstrates the influence of the affinity of these centres which is responsible for grafting of side chains to β-lactam cycle and to dihydrothiazinic cycle.

9

y and reactivity indices

P_{5-8}	P_{6-7}	Q_{N_5}	Q_{C_8}	$Q_{N_{10}}$	Q_{C_3}
0.3046	0.6806	0.5400	0.3846	0.3568	−0.0454
0.3913	0.6327	−0.1311	0.3712	0.3723	−0.0380
0.3234	0.6328	−0.1632	0.3712	0.3722	−0.0381
0.3246	0.6196	−0.1636	0.3726	0.4136	0.0383
0.7586	0.8650	0.3621	0.4020	0.3959	0.0231
0.3066	0.6638	0.5409	0.3860	0.4021	0.0992

ACKNOWLEDGEMENT. We are grateful to Professor A. T. Balaban for helpful suggestions on the manuscript.

REFERENCES

[1] L. Verbist, *Acta clin. Belg.*, *34*, 165 (1969).

[2] D. B. Boyd, *Int. J. Quant. Chem., Quant. Biology Symp.*, **4**, 161 (1977).

[3] I. Simiti and I. Schwartz, "Structură Chimică — activitate biologică", Ed. Dacia, Cluj-Napoca, 1974, pp. 102, 115—116.

[4] B. Coene, A. Schanck, J. M. Dereppe and M. Van Meerssche, *J. Med. Chem.*, **27**, 694 (1984).

[5] R. J. Fess and J. Barnishan, *Rev. Infectious Diseases*, **12**, 841 (1980).

Revue Roumaine de Chimie, **33**, *8*, 803–807 (1988)

SYNTHESIS OF NICKEL FERRITE FROM POLYNUCLEAR COORDINATION COMPOUNDS. PART II*

STUDY OF THE WET FERRITIZATION PROCESS

IOANA ILIE[a], MARIA BREZEANU[b], LUMINIŢA PATRON[c] and E. SEGAL[d]

[a]Institute of Chemical and Biochemical Energetics, ICECHIM, Splaiul Independenţei no. 202, 77208, Bucharest, Romania

[b]Chair of Inorganic Chemistry and Technology, Faculty of Chemical Technology, IPB, Dumbrava Roşie no. 23, Bucharest, Romania

[c]Center of Physical Chemistry, ICECHIM, Splaiul Independenţei no. 202, 77208, Bucharest, Romania

[d]Chair of Physical Chemistry and Electrochemical Technology, Faculty of Chemical Technology, IPB, Blvd Republicii no. 13, Bucharest, Romania

Received April 25, 1987

The wet ferritization process, which makes the object of this paper, occurs through thermal decomposition of some polynuclear coordination compounds (PCC's) directly in the reaction medium (solution). Nickel ferrite can be obtained by wet ferritization, the main reaction parameters being: the reaction medium pH value, the heating conditions and the nature of the base.

In a previous paper[1] we have shown that nickel ferrite can be obtained from solid polynuclear coordination compounds (PCC's) through thermal decomposition. This dry ferritization process requires the isolation of the parrent PCC, followed by its thermal decomposition.[2,3]

The first results concerning the kinetic and mechanism as well as the parameters of the wet ferritization belong to the Japanese researchers who obtained Fe_3O_4, $MnFe_2O_4$, $CoFe_2O_4$, $ZnFe_2O_4$ and $MgFe_2O_4$.[4–13]

This paper deals with a study concerning the synthesis of $NiFe_2O_4$ through wet ferritization. The system submitted to investigation was:

$$Fe^{II} - Ni^{II} - X - B \text{ where } X = CH_3COOH,\ HCOOH$$
$$B = NH_4OH,\ Me^{I}OH\ (Me^{I}{=}Na,K)$$

In order to establish the optimal conditions for the synthesis, the following reaction conditions were changed:

- the initial metal ratio Fe :Ni;
- the pH of the reaction medium;

---

* Part I: *Rev. Roumaine Chim.*, **32**, 1109 (1987)

- the nature of the complexing agent(X);
- the nature of the base(B);
- the influence of the heating temperature and heating time;
- the influence of air bubbling in the reaction medium.

Table 1

The various conditions of synthesis NFe_2O_4 by the wet ferritization method

Index ox. phase	Metal ratio $Fe^{III}Fe^{II}$ Ni^{II}	pH	Complex. agent	Base	*t* (°C)	Time (h)	Air Bubb	Nature of the oxide phases
1	2 : 1	7	—	NH_4OH	20	—	—	PCC
2	2 : 1	7–8	—	NH_4OH	70–90	1	—	$Fe_3O_4+NiO+PCC$
3	2 : 1	7–8	—	NH_4OH	70–90	5	—	,,
4	2 : 1	7–8	—	NH_4OH	70–90	10	—	,,
5	2 : 1	7–8	—	NH_4OH	70–90	48	—	,,
6	1 : 1	7–8	—	NH_4OH	70–90	10	—	,,
7	2 : 1	7	—	NH_4OH	20	10	+	PCC
8	2 : 1	7–8	—	NH_4OH	70–90	1	+	Fe_3O_4+NiO
9	2 : 1	7–8	—	NH_4OH	70–90	5	+	,,
10	2 : 1	9–10	—	NH_4OH	20	—	—	PCC
11	2 : 1	9–10	—	NH_4OH	70–90	1	—	$Fe_{3-x}Ni_xO_4$
12	2 : 1	9–10	—	NH_4OH	70–90	5	—	PCC
13	2 : 1	9–10	—	NH_4OH	70–90	48	—	$NiFe_2O_4$
14	2 : 1	9–10	—	NH_4OH	70–90	5–10	+	$NiFe_2O_4$
15	1 : 1	9–10	—	NH_4OH	70–90	5–10	—	$NiFe_2O_4$
16	2 : 1	12–13	—	NH_4OH	20	—	—	$Fe_{3-x}Ni_xO_4$
17	2 : 1	12–13	—	NH_4OH	70–90	1	—	,,
18	2 : 1	12–13	—	NH_4OH	70–90	5–10	—	,,
19	2 : 1	12–13	—	NH_4OH	70–90	1	+	PCC
20	2 : 1	7–8	CH_3COOH	NH_4OH	70–90	3–10	—	$Fe_3O_4+NiO+PCC$
21	1 : 1	7–8	CH_3COOH	NH_4OH	70–90	3–10	—	,,
22	2 : 1	9–10	CH_3COOH	NH_4OH	70–90	1–10	+	$NiFe_2O_4$
23	2 : 1	7–8	CH_3COOH	NHOH	70–90	1–10	+	Fe_3O_4+NiO
24	2 : 1	9–10	CH_3COOH	NH_4OH	70–90	5–10	+	$NiFe_2O_4$
25	2 : 1	9–10	HCOOH	NH_4OH	70–90	3–10	1	$Fe_3O_4+NiO+PCC$
26	1 : 1	7–10	HCOOH	NH_4OH	70–90	3–10	1	$Fe_3O_4+NiO+PCC$
27	2 :0.5 :1	7–10	HCOOH	NH_4OH	70–90	3–10	—	,,
28	2 :0.1 :1	7–10	HCOOH	NH_4OH	70–90	3–10	—	,,
29	2 :0.05 :1	7–10	HCOOH	NH_4OH	70–90	3–10	—	,,
30	4 :0.1 :1	7–10	HCOOH	NH_4OH	70–90	3–10	—	,,
31	4 :0.05 :1	7–10	HCOOH	NH_4OH	70–90	3–10	1	,,
32	2 : 1	7–8	HCOOH	NaON	70–90	1–48	—	,,
33	1 : 1	7–8	—	NaOH	70–90	1–10	—	,,
34	2 : 1	9–10	—	NaOH	70–90	1–10	+	$NiFe_2O_4$
35	2 : 1	9–10	CH_3COOH	NaOH	70–90	1–10	—	$NiFe_2O_4$
36	1 : 1	9–10	CH_3COOH	NaOH	70–90	1–10	+	$NiFe_2O_4$
37	1 : 1	9–10	CH_3COOH	NaOH	70–90	3–10	—	$Fe_{3-x}Ni_xO_4$
38	2 : 1	9–10	HCOOH	NaOH	70–90	3–10	—	,,
39	1 : 1	9–10	HCOOH	NaOH	70–90	3–10	—	,,
40	2 : 1	9–10	HCOOH	NaOH	70–90	3–10	+	$NiFe_2O_4$

The results thus obtained, listed in tables 1 and 2, allowed us to decide about the best way to obtain nickel ferrite.

Table 2

The results of chemical analysis for the oxide phases obtained by the wet ferritization method

Index ox. phase	Composition (%gr)			Fe : Ni ratios
	Fe(e/c)	Ni(e/c)	O(e/c)	
2	53.45/47.66	22.50/25.11	25.00/27.23	2.5 : 1
3	53.27	22.44	24.20	2.5 : 1
4	58.00	19.87	22.11	3 : 1
5	65.20	16.40	18.50	4 : 1
6	60.18	19.35	21.13	3.3 : 1
8	56.45	21.14	23.00	2.8 : 1
9	47.64	25.22	27.20	2 : 1
11	47.24	25.40	27.11	2 : 1
12	47.54	25.07	27.18	2 : 1
13	47.83	25.05	27.55	2 : 1
14	47.16	24.67	27.14	2 : 1
15	48.00	24.16	27.02	2 : 1
16	87.25	6.11	6.80	14.8 : 1
17	63.12	18.35	19.45	3.7 : 1
18	55.20	22.00	23.42	2.7 : 1
19	86.86	5.75	6.85	14.8 : 1
20	84.00	7.80	8.17	11 : 1
21	83.22	8.00	8.30	11 : 1
22	47.55	24.42	27.11	2 : 1
23	83.75	8.11	19.12	11 : 1
24	47.75	25.13	27.56	2 : 1
25	83.66	7.62	17.85	11 : 1
26	83.42	7.75	18.80	11 : 1
27	83.40	7.45	18.92	11 : 1
28	84.12	8.23	19.00	11 : 1
29	82.80	8.07	18.45	11 : 1
30	82.75	7.90	18.30	11 : 1
31	83.00	7.92	18.00	11 : 1
32	48.54	25.13	27.82	2 : 1
33	48.11	25.24	27.13	2 : 1
34	47.95	25.04	27.50	2 : 1
35	47.93	25.70	27.47	2 : 1
36	47.18	25.35	27.17	2 : 1
37	47.50	25.00	27.18	2 : 1
38	47.43	25.67	27.27	2 : 1
39	47.60	24.92	27.66	2 : 1
40	48.00	24.85	27.09	2 : 1

RESULTS AND DISCUSSION

1. *The influence of the initial* Fe^{II} : Ni^{II} *ratio* : By changing the atomic metal ratio Fe^{II} : Ni^{II} from 1 to 2, the mixed oxide composition did not change. Small amounts of Fe^{II} ions in the reaction medium offer the possibility to use Fe^{III} when HCOOH is used as complexing agent. In such conditions the initial ratio of the metal ions can be changed from $2Fe^{III} : 0.1Fe^{II} : 1Ni^{II}$ to $4Fe^{III} : 0.05Fe^{II} : 1Ni^{II}$.

2. *The influence of the reaction medium pH* : An important parameter for the mixed oxide nature and stability is the reaction medium pH. By changing its value between 5 and 7, some polynuclear hydroxocompounds

like $[Fe_x^{II}\ Ni_{1-x}^{II}\ Fe_2^{III}\ (OH)_8(H_2O)_2]$ were separated at room temperature. By air bubbling in the reaction medium for 10 hours, the PCC $[Fe_2^{III}Ni^{II}(OH)_{12}(H_2O)_2](NH_4)_4 \cdot 2H_2O$ was obtained. By heatingsuch PCC's at least for an hour at 70–90°C, they change into magnetic oxides, which contain Fe^{III} and Ni^{II} in various ratios, depending on the reaction medium pH and heating time. The value 2 :1 for the ratio $Fe^{III} : Ni^{II}$ was obtained only at pH values between 9 and 10. For the other pH values the ratio $Fe^{III} : Ni^{II}$ changed from 2.5 :1 to 15 :1.

3. *The influence of the nature of the complexing agents* : We did not find in the literature data concerning the use of the complexing agents in wet ferritization. Thus it was necessary a judicious preliminary choice of the complexing agents which had to react fast enough with Fe^{II} and Ni^{II} to generate the PCC's ; at the same time these PCC's should be quite instable to undergo decomposition directly in the reaction medium at low temperatures.

According to our previous results CH_3COOH and HCOOH were selected as potential ligands, due to their suitable properties (accessibility, affinity for iron and nickel ions, high volatility). With ligands, the metal ions react for values of the pH in the range 4–7 to form PCC's, probably with oxotrinuclear structure,[14, 15] which contain $Fe^{III} - Fe^{II} - Ni^{II}$. By increasing the reaction medium pH value from 7 to 8, these PCC's change into polynuclear hydroxocompounds. Through heating these compounds at temperatures in the range 70–90°C some magnetic intermediates, probably solid solutions like $Fe_3O_4 - NiFe_2O_4$, were obtained. This result explains why the ratio $Fe^{III} : Ni^{II}$ varies to such an extent.

If complexing agents are not used, the wet ferritization occurs through hydroxopolynuclear species like $[Fe_x^{II}\ Ni_{1-x}^{II}Fe_2^{III}(OH)_8(H_2O)_2]$ $0 < x < 1$, $[Fe_2^{III}Ni(OH)_8(H_2O)_2]$ and $[Fe_2^{III}Ni(OH)_{12}(H_2O)_2](NH_4)_4 \cdot 2H_2O$ which can be separated.

Taking into account these results one can conclude that wet ferritization occurs through a solid state reaction between oxide species with reactivities depending on the reaction conditions.

4. *The influence of the nature of the base* : The role of the bases is to favour the hydroxospecies formation ; by heating these PCC's and increasing the pH value from 7 to 10 they undergo decomposition into magnetic oxide phases. In the case of $NiFe_2O_4$, due to the loss of nickel by formation of the $[Ni(NH_3)_6]^{2+}$ soluble ion, the sodium and kalium hydroxides are more suitable than ammonium hydroxide.

5. *The influence of heating temperatures and heating time* : The wet ferritization generally occurs for temperatures in the range 20–90°C and variable heating periods.

The nickel ferrite can be obtained by heating the reaction system for minimum one hour in the temperature range 70–90°C, as previously shown for an optimum pH value and using alkali metals hydroxides as bases.

By increasing the heating period from one to 48 hours the nickel content of the oxide phases changes, depending on the reaction medium pH values ; thus pH values in the range 7–8, using ammonium hydroxide as base, tend to stabilise ferrites with lower nickel content, at limit Fe_3O_4. At pH >10 as previously shown one records nickel loss through solubilisation under $[Ni(NH_3)_6]^{2+}$ ion form.

With alkali metal hydroxides as bases, heating period does not influence the composition of the mixed oxides, but their crystallinities are improved.

6. *The influence of air bubbling*: Generally the air bubbling accelerates the oxidation $Fe^{II} \rightarrow Fe^{III}$ and the substitution of Fe^{II} ions by Ni^{II} ions.

REFERENCES

[1] I. Ilie, M. Brezeanu and E. Segal, *Thermochim. Acta*, *94*, 393 (1985).
[2] I. Ilie, Doctoral Dissertation, Polytechnic Institute of Bucharest, Inorganic Chemistry Dept., Bucharest, June 1985.
[3] I. Ilie, M. Brezeanu, L. Patron, E. Segal and G. Filoti, *J. Mater. Sci .Lett.*, **6**, 932(1987).
[4] T. Takada and M. Kyiama, *Proc. Int. Conf. Ferrites* (1970).
[5] M. Kyiama, *Bull. Chem. Soc. Japan*, **47**, 1646 (1974).
[6] M. Kyiama, *Bull. Chem. Soc. Japan*, **51**, 134 (1978).
[7] K. Kaneko, *Bull. Chem. Soc. Japan*, **52**, 747 (1979).
[8] J. Sakurai, *J. Phys. Soc. Japan*, **23**, 1426 (1967).
[9] K. Kaneko, *Bull. Chem. Soc. Japan.*, **52**, 1080 (1979).
[10] K. Katsura, *Bull. Chem. Soc. Japan*, **52**, 96 (1979).
[11] Y. Tamaura, *Water. Res.*, **13**, 21 (1979).
[12] Y. Tamaura and T. Katsura, *Bull. Chem, Soc. Japan*, **54**(1), 135 (1981).
[13] Y. Tamaura and T. Katsura, *Inorg. Nucl. Chem.*, **43**(4), 671 (1981).
[14] I. Ilie, M. Brezeanu and L. Patron, *Rev. Roumaine Chim.*, **32**, 1109 (1987).
[15] I. Ilie and M. Brezeanu, *Rev. Roumaine Chim.*, in press.

Revue Roumaine de Chimie, **33**, *8*, 809–814 (1988)

SYNTHESIS AND CHARACTERIZATION OF SOME 2,4'-DIBENZYLDIISOCYANATE IONIC POLYMERS. IV*

BIOLOGICAL ACTIVITY

TINCA BURUIANĂ and ADRIAN CARACULACU
Institute of Macromolecular Chemistry "P. Poni"
Aleea Gr. Ghica Vodă No. 41-A
6600-Jassy, Romania

Received May 30, 1987

The antimicrobial activity of 2,4'-dibenzyldiisocyanate ionic polymers obtained by Menschutkin reaction as well as of low molecular weight model compounds was studied. In some cases it was found that polymers inhibited the growth of a bacterial culture.

It is known that the presence of ammonium quaternary structures in some low molecular weight compounds [1] as well as in "polyelectrolyte" type macromolecular compounds [2] confer them an important biological activity.

Rembaum[2] found that the aliphatic polymers with a molecular weight between 10,000 and 40,000 resulting from polycondensation of tertiary diamines with dihalides inhibited the growth of Gram-positive and Gram-negative bacteria *S. Aureus* and *E. Coli*.

The ionenes with urethane groups which have been synthesized from a tertiary triamine (based on ricin oil and 2,4-toluylene diisocyanate, modified by reaction with alcohols containing dimethylamino end groups) and dihalides are interesting for the biomedical field. These polymers react with negatively charged biological polyelectrolytes (e.g. heparin) yielding thromboresistant materials.[3]

Due to the pharmacological properties induced by ammonium quaternary groups we have studied the antimicrobial behaviour of some cationic polyurethanes with low concentration of positive electrical charges on the quaternary nitrogen atoms, as well as of model compounds.

RESULTS AND DISCUSSION

The previous papers [4,5] presented the synthesis and characterization of some cationic polyurethanes obtained from 2,4'-dibenzyldiisocyanate by the Menschutkin reaction.

---

* Part III, *Materiale Plastice*, **24**, 143 (1987)

Ionene-chloride and ionene-bromide were obtained when a macromolecular diamine (based on poly(tetramethylene oxide)) reacted first with dihalides and then the polyetherurethanedihalide was quaternized with 1,8-diazabicyclooctane and N,N′-dimethylpiperazine.

The structures of the ionenes were shown below :

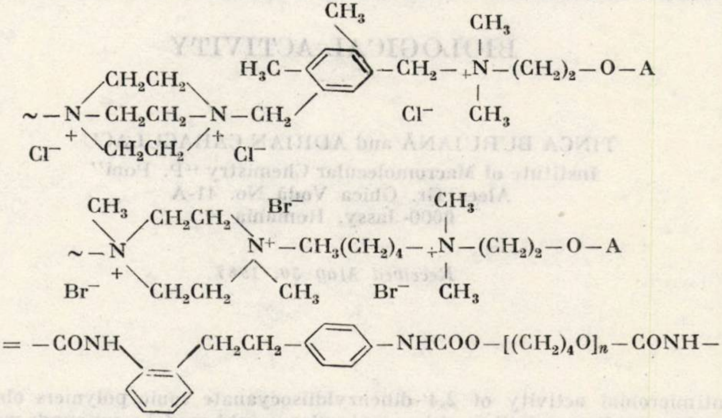

With a view to obtaining some informations regarding the antimicrobial behaviour of ammonium quaternary structures from a polyurethane backbone, cationic polyurethanes were used having different concentrations of positive electrical charges (Table 1).

Table 1

Structural characteristics of cationic polyurethanes

Cationic polyurethane	Poly(tetramethylene oxide) (MW)	Ionic halogene content (meq/100 g)
		202.25
PI_1(I)	650	156.06
PI_2(II)	1000	117.75
PI_3(III)	2000	204.12
PP_1(IV)	650	151.50
PP_2(V)	1000	116.00
PP_3(VI)	2000	

PI — ionene chloride
PP — ionene bromide

The antimicrobial activity of polymers was studied versus Gram-negative and Gram-positive bacteria of type *E.Coli*, *S.Aureus*, *Proteus* and *Proteus* with *E.Coli*, using different concentrations of polymer in ethanol : water (80 :20 v.).

The sensitivity of bacteria against synthesized polymers was tested in vitro. They were put in standardized conditions of cultivation (cultivation medium, inoculation, incubation time) in the presence of determined quantity of polymers.

Table 2 shows the biological activity of polymers *versus* bacteria mentioned above. It is noticed that concentrations of about 800 ppm inhibited in some cases the growth of bacteria.

Table 2

Antimicrobial activity of cationic polyurethanes

Cationic polyurethane	Concentration (ppm)	*E.Coli*	*S.Aureus*	*Proteus* R_i^*(mm)	*Proteus* + *E.Coli*
PI_1(I)	800	0	0	0	0
PI_2(II)	800	5	13	5	7
PI_3(III)	800	7	9	8	8
PP_1(IV)	800	0	0	0	0
PP_2(V)	800	5	8	10	8
PP_3(VI)	800	5	8	9	7
Sulphofurazole	1000	6	6	6	7

R_i* — radius of inhibition zone

One can remark from this table that *E. Coli* has a moderate sensitivity for the polymers (II, III, V, VI) and on the other hand ***Proteus***, ***S.Aureus***, ***Proteus*** with ***E.Coli*** are more sensitive versus the same polymers. The activity of cationic polyurethanes against the last bacteria was comparable with that of Sulphofurazole, at a concentration of 1000 ppm.

Surprising is the behaviour of polymers PI_1(I) and PP_1(IV) containing a higher concentration of positive electrical charges on the macromolecular chain. These polymers do not inhibit the growth of bacteria used for testing. A preliminary conclusion can be that the activity of polymers versus bacteria may be influenced by the distance between the positive electrical charges.

The testing in vitro with decreasing of polymer concentration was used also to find the minimum concentration of polymer able to inhibit the growth of bacteria.

Thus it was observed the maintenance of relation bacterium-active substance by diminishing the polymer concentration to 400 ppm. At 200 ppm the activity is null versus some bacteria, only *A.Aureus* being sensitive.

The activity of polymers II, III, V and VI versus *A.Aureus* bacteria is given at two concentrations (400 and 200 ppm) in Fig. 1 and Fig. 2.

It may be appreciated that the sensitivity of tested bacteria at low concentrations of cationic polyurethanes is comparable with that shown when some drugs were used (Negram, Nitrophurantoine).

The study on the antimicrobial activity of cationic polyurethanes was carried out comparatively with micro and macromolecular model compounds. At macromolecular model an unionic polyurethane was synthesized, from poly(tetramethylene oxide) ($M = 2000$), 2,4'-dibenzyldiisocyanate and N,N'-bis(β-hydroxyethyl) piperazine (1 : 2 : 1), (VII). The products VIII—XI from Table 4 were used as micromolecular models.

Table 3

Antimicrobial activity of cationic polyurethanes at low concentrations

Cationic polyurethane	Concentration (ppm)	*E.Coli*	*S.Aureus*	*Proteus* R_i(mm)	*Proteus* + *E.Coli*
PI_2(II)	400	5	11	5	—
PI_2	200	0	4	5	0
PI_3(III)	400	8	12	—	—
PI_3	200	7	5	0	0
PP_3(VI)	400	10	10	—	—
PP_3	200	6	2	0	4
Negram	300	8	9	8	—
Nitrophurantoine	300	8	7	7	—

R_i — radius of inhibtion zone

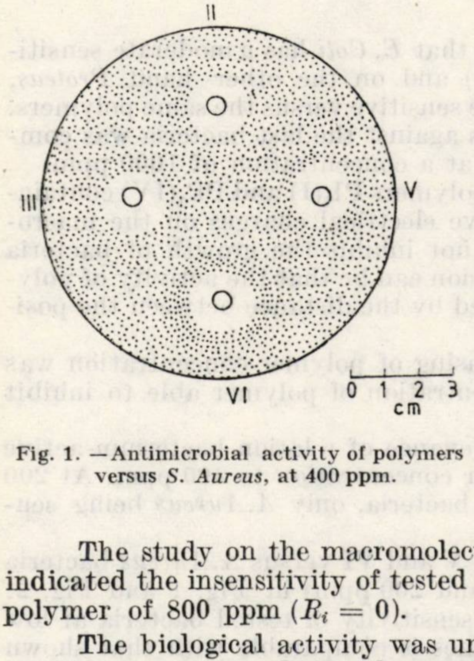

Fig. 1. — Antimicrobial activity of polymers versus *S. Aureus*, at 400 ppm.

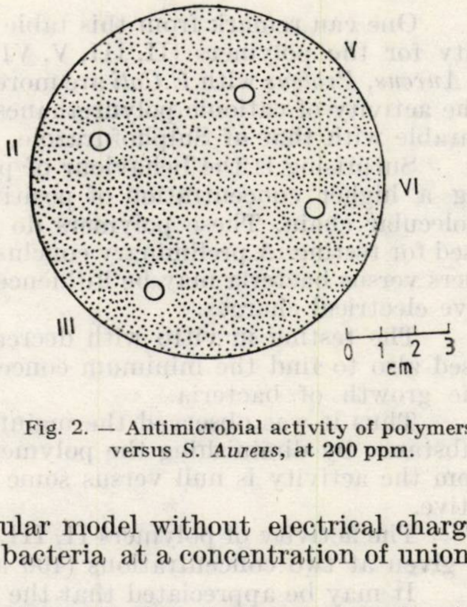

Fig. 2. — Antimicrobial activity of polymers versus *S. Aureus*, at 200 ppm.

The study on the macromolecular model without electrical charges indicated the insensitivity of tested bacteria at a concentration of unionic polymer of 800 ppm ($R_i = 0$).

The biological activity was unchanged when ionic micro molecular structures were used for that unionic macromolecule. Although high concentrations of the low molecular weight model structures were used, sensitivity of the bacteria versus tested solutions was negligible ($R_i = 0 - 2$ mm).

In conclusion, the biological activity is not due only to the presence of ionic groups in the macromolecular chain, being conditioned by a certain distribution of these groups on the chain.

Table 4

Antimicrobial activity of micro and macromolecular model compounds at 800 ppm

Compounds	*E.Coli*	*S.Aureus*	*Proteus* R_i(mm)	*Proteus* + *E. Coli*
VII. 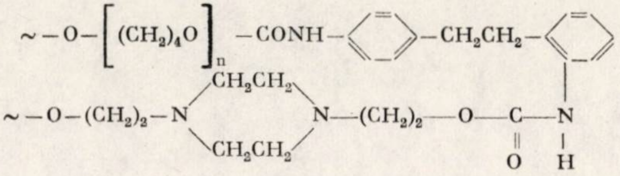	0	0	0	0
VIII. 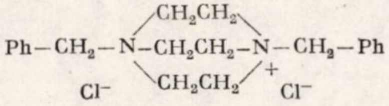	0	1	0	0
IX. 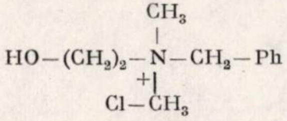 $HO-(CH_2)_2-\overset{CH_3}{\underset{Cl-CH_3}{\overset{+}{N}}}-CH_2-Ph$	1	2	0	1
X. 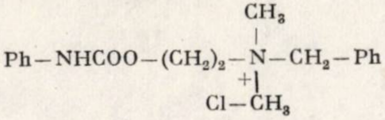 $Ph-NHCOO-(CH_2)_2-\overset{CH_3}{\underset{Cl-CH_3}{\overset{+}{N}}}-CH_2-Ph$	0	1		0
XI. 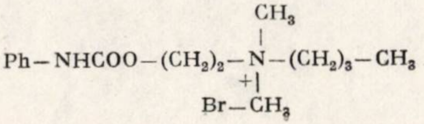 $Ph-NHCOO-(CH_2)_2-\overset{CH_3}{\underset{Br-CH_3}{\overset{+}{N}}}-(CH_2)_3-CH_3$	1	0	1	0

EXPERIMENTAL PART

Gram-positive and Gram-negative bacteria (obtained from a hospital) were used to study the antimicrobial activity of cationic polyurethanes.

Pellets with different polymer concentrations was placed on surface of a nutrient agar (Mueller — Hinton type) uniformly seeded with testing germs.

A porous inert support obtained from filter paper with $d = 6$ mm was utilized as pellet. 0.01 mL from each solution was put on this inert support.

The zones of inhibition were measured after 18—24 hours of incubation at 37°C. It was considered that the surface of inhibition zones was directy proportional to the sensitivity of bacterium against solution of polymer from the pellet.

REFERENCES

[1] S. Thesleff and D. M. J. Quastel, *Ann. Rev. Pharmacol.*, **5**, 263 (1965).
[2] A. Rembaum, *Applied Polymer Symposium*, **22**, 299 (1973).
[3] A. Rembaum, S. P. S. Yen, R. F. Landel and M. Schmir, "Biomedical Polymers", M. Dekker (Eds.), New York, p. 221, 1971.
[4] T. Buruiană, I. Beştiuc, V. Popescu and A. Caraculacu, *Die Angew. Makromolek. Chem.*, **134**, 165 (1985).
[5] T. Buruiană, I. Beştiuc and A. Caraculacu, The 12-th Session of Communications, 1986, Rm. Vîlcea, Romania

Revue Roumaine de Chimie, **33**, *8*, 815–822 (1988)

DITHIOCARBAMATE SERIES. PART II[1]

PYRROLIDINO- AND INDOLINODITHIOCARBAMATE ESTERS OF POSSIBLE ANTIBACTERIAL AND ANTIMICROBIAL ACTIVITY

HASSAN M. FAID-ALLAH

Department of Chemistry, Faculty of Science, Alexandria University, Alexandria, Egypt

Received March 22, 1987

Pyrrolidino- and Indolinodithiocarbamate esters 3 were prepared from the reaction of the sodium salts 2 with different halides. Oxidative condensation of 2 with amines yielded the thiocarbamyl sulfenamides 4. With diiodomethane 2 afforded the bis-dithiocarbamate esters 5. Mixed dithiocarbamate esters 6 were also prepared. Structures were confirmed by spectral data.

1. INTRODUCTION

Several dithiocarbamates have been used for treatment of skin diseases.[2] Other dithiocarbamates have tuberculostatic activity.[3] Ethyl pyrrolidinyldithiocarbamate proved to be effective as microbicidal substance.[4] In this report a number of dithiocarbamates of pyrrolidine and indoline were synthesized hoping that they might have antibacterial and antimicrobial value.

2. SYNTHESIS OF THE COMPOUNDS

Reaction of pyrrolidine and indoline with carbondisulfide and sodium hydroxide yielded the corresponding sodium dithiocarbamates **2a**[5] and **2b**,[6] which are stable at room temperature for several weeks. The IR spectra of these salts exhibited a thiocarbonyl absorption at 995–1010 cm^{-1} as well as a C–N band at 1260–1265 cm^{-1}. Their ^{13}C-NMR showed the expected number of peaks for these compounds as well as a CS signal at δ 212.6–214.0 ppm. However, although there are few examples on the dithiocarbamate esters of pyrrolidine in literature, [5] there appears to be no previous record on the dithiocarbamate esters of indoline. For these reasons we prepared a series of dithiocarbamate esters of pyrrolidine **3a** and indoline **3b** and studied their NMR (^{1}H and ^{13}C) spectra which are recorded in Table 2. The IR spectra of **3a** and **3b** showed two bands at 990–1005 cm^{-1} and 1250–1265 cm^{-1} for the CS and C–N absorptions respectively.

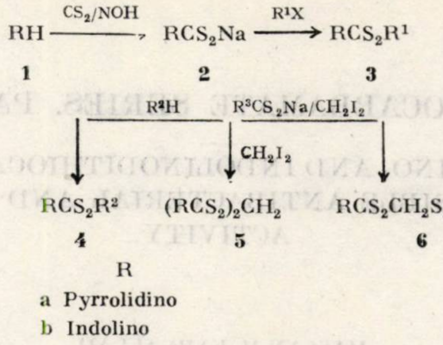

Scheme A

Oxidative condensation of the sodium salts **2a** and **2b** with primary and secondary amines afforded the thiocarbamyl sulfenamide derivatives **4**. The structures of these compounds were confirmed by their spectral data (^{1}H— and ^{13}C-NMR) (Table 3). On the other hand, reaction of 2 moles of the sodium salts **2a** or **2b** with one mole of diiodomethane afforded the bis-dithiocarbamate esters **5**. The IR spectra of the esters **5** exhibited a thiocarbonyl absorption at 995—1008 cm^{-1} and a C—N absorption at 1260—1265 cm^{-1}. Their ^{13}C and ^{1}H-NMR spectra were recorded in Table 2.

Furthermore, we prepared a new type of esters **6** from the reaction of a mixture of two different sodium dithiocarbamates with diiodomethane. Examination of the crude reaction products by T.L.C and ^{13}C-NMR showed the presence of very small amounts of the unmixed bis-dithiocarbamate esters **5** (R = piperidino, morpholino and 4-ethoxycarbonylpiperazino [1]). However, the mixed esters **6a** and **6b** were purified by repeated crystallization from methanol. The IR spectra of the esters **6** showed a thiocarbonyl absorption at 992—1006 cm^{-1} as well as a C—N band at 1250—1260 cm^{-1}. Their structures were further confirmed using NMR spectral data (Table 4).

3. EXPERIMENTAL

^{1}H—NMR spectra were recorded on a Varian EM 360L spectrometer using tetramethylsilane as internal standard. ^{13}C—NMR spectra were recorded on Jeol JHM-FX100 NMR spectrometer. IR spectra were obtained using sodium chloride plates on a Perkin-Elmer 297 spectrometer as solutions in bromoform. Melting points were measured on a Kofler hot stage apparatus and are uncorrected. The following compounds were prepared according to the literature methods : 2(R = piperidino) m.p. > 300° (Lit.[7], not recorded) ; 2(R = morpholino), m.p. > 300° (Lit.[8], not recorded) ; and 2(R = 4-ethoxycarbonylpiperazino), m.p. > 300 (Lit.[1] > 300).

3.1. Sodium dithiocarbamates (2)

Carbondisulfide (0.01 mole) was added slowly with vigorous stirring to a mixture of amine (0.01 mole) and aqueous sodium hydroxide (40%, 0.01 mole), the temperature being maintained below 10°C during this addition. The precipitated sodium salts were filtered off, washed with ether and dried.

2a : 90% yield, m.p. > 300 [Lit.[2], m.p. not recorded]. IR (cm^{-1}) : 998 (CS) ; 1260 (C—N) ; ^{1}H—NMR (δ, TMS, D_2O) : 4.0(2H, H—α, *t*, *J* = 3), 3.7(2H, H—α, *t*, *J* = 3) ; 2.1 (4*H*, H—β, m). ^{13}C—NMR (δ, Dioxane, D_2O) : 213.5 (CS) ; 54.7, 50.2 (C—2) ; 25.8, 24.3 (C—3).

Table 1

Dithiocarbamate and bis-dithiocarbamate esters (**3** and **5**)

Compound	R^1	Yield [%]	M.P. [°C]or B.P. [°C]/torr	Solvent/crystal form	Formula	Calcd. %			Found %		
						C	H	N	C	H	N
3a/1	CH_3	87	94[a]	Methanol/needles							
3a/2	C_2H_5	95	88–92/0.01[b]								
3a/3[c]	$CH_2{=}CHCH_2$	78		Chloroform methanol/oil	$C_8H_{13}NS_2$	51.3	6.9	7.5	51.0	6.8	7.3
3a/4	$CH{\equiv}C-CH_2$	80	58	Methanol/needles	$C_8H_{11}NS_2$	51.9	5.9	7.6	51.8	5.8	7.6
3a/5	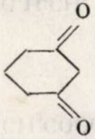	72	142	Ethanol/prisms	$C_{11}H_{15}NO_2S_2$	51.4	5.8	5.4	51.2	5.7	5.3
3a/6	$(C_6H_5)_3C$	78	152	Benzene/prisms	$C_{24}H_{23}NS_2$	74.0	5.9	3.6	73.9	5.7	3.5
3a/7[c]	$CH_2COOC_2H_5$	79		Chloroform-methanol/oil	$C_9H_{15}NO_2S_2$	46.4	6.4	6.0	46.1	6.2	6.2
3a/8	$C_6H_5CH_2$	85	36	Methanol/needles	$C_{12}H_{15}NS_2$	60.8	6.3	5.9	60.6	6.2	6.0
3a/9	p-$NO_2C_6H_4CH_2$	86	90	Methanol/needles	$C_{12}H_{14}N_2O_2S_2$	51.1	5.0	9.9	51.2	5.1	9.8
3a/10	$C_6H_5CH_2CH_2$	85	29	Methanol/needles	$C_{13}H_{17}NS_2$	62.2	6.8	5.6	62.0	6.6	5.5
3a/11	$C_6H_5COCH_2$	89	136	Ethanol/needles	$C_{13}H_{15}NOS_2$	58.9	5.7	5.3	58.7	5.4	5.3
3a/12	$p-CH_3OC_6H_4COCH_2$	88	102	Methanol/needles	$C_{14}H_{17}NO_2S_2$	57.0	5.8	4.7	57.1	5.8	4.6
3a/13	$C_6H_5SO_2$	58	122	Methanol-benzene/needles	$C_{11}H_{13}NO_2S_3$	46.0	4.5	4.9	45.9	4.3	4.7
3b/1	CH_3	86	84	Methanol/needles	$C_{10}H_{11}NS_2$	57.4	5.3	6.7	57.3	5.2	6.6
3b/2	C_2H_5	85	70	Ethanol/prisms	$C_{11}H_{13}NS_2$	59.2	5.8	6.3	59.1	5.7	6.2
3b/3	$CH_2{=}CH-CH_2$	80	67	Methanol/needles	$C_{12}H_{13}NS_2$	61.3	5.5	6.0	61.0	5.2	6.1
3b/4	$CH{\equiv}C-CH_2$	78	87	Methanol/needles	$C_{12}H_{11}NS_2$	61.8	4.7	6.0	61.7	4.5	5.9
3b/5	$CH_2COOC_2H_5$	82	55	Methanol/needles	$C_{13}H_{15}NO_2S_2$	55.5	5.3	5.0	55.2	5.1	4.9
3*b*/6	$CH_2COCOOC_2H_5$	72	102	Methanol/needles	$C_{14}H_{15}NO_3S_2$	54.4	4.9	4.5	54.6	5.0	4.6
3b/7	$C_6H_5CH_2CH_2$	79	185	Benzene/prisms	$C_{17}H_{17}NS_2$	68.2	5.7	4.7	68.1	5.6	4.6
3b/8	$C_6H_5COCH_2$	88	120	Ethanol/needles	$C_{17}H_{15}NOS_2$	65.2	4.8	4.5	65.2	4.7	4.3
3b/9	$p-CH_3OC_6H_4COCH_2$	86	133	Ethanol/plates	$C_{18}H_{17}NO_2S_2$	63.0	5.0	4.1	63.0	5.1	4.3
3b/10	CH_3SO_2	52	184	Benzene/prisms	$C_{10}H_{11}NO_2S_3$	44.0	4.0	5.1	43.8	3.9	5.2
3b/11	$C_6H_5SO_2$	62	164	Benzene/prisms	$C_{15}H_{13}NO_2S_3$	53.7	3.9	4.2	53.6	4.0	4.0
3b/12	p-$CH_3C_6H_4SO_2$	68	170	Benzene/prisms	$C_{16}H_{15}NO_2S_3$	55.0	4.3	4.0	55.2	4.3	4.1
5a		92	225	Methanol-benzene/needles	$C_{11}H_{18}N_2S_4$	43.1	5.9	9.2	43.2	6.0	9.2
5b		88	194	Methanol/needles	$C_{19}H_{18}N_2S_4$	56.7	4.5	7.0	56.5	4.3	6.8

a Lit.[9], 90°

b Lit.[4], $b_{0.01}$ 87–90°

c Purified by column chromatography on silica gel ($CHCl_3$/methanol 20 : 1)

Table 2

NMR [a]Spectral data of dithiocarbamate and bis-dithiocarbamate esters (**3** and **5**)

Compound	R^1	$^{13}C-NMR$ Pyrrolidino or C–2	Indolino *C* C–3	CS	Others	^1H-NMR Pyrrolidino or H–α (t, J=3)	Indolino[b] *H* H–β (4H, m)	Others
3a/1	CH_3	54.7, 50.2	25.8, 24.1	193.4	19.1(CH_3)	4.0(2H), 3.7(2H)	2.0	2.7(CH_3, s)
3a/2	C_2H_5	53.9, 49.7	25.3, 23.5	191.6	29.8(CH_2) ; 13.4 (CH_3)	3.9(2H), 3.7(2H)	2.0	3.3(2H, CH_2, q, J=4) ; 1.3 (3H, CH_3, t, J=4)
3a/3	$CH_2=CHCH_2$	53.7, 49.5	25.2, 23.3	191.5	132.0(CH=) ; 118.5(CH_2=) ; 39.2(CH_2)	3.9(2H), 3.6(2H)	2.1	5.5(3H, m, CH+CH_2=), 4.0 (2H, CH_2, d, J=4)
3a/4	$CH\equiv C-CH_2$	54.9, 50.2	25.8, 23.9	189.9	77.8(C≡) ; 71.1 (C*H*) ; 23.9(CH_2)	4.0(2H), 3.7(2H)	2.0	4.1(2H, CH_2, d, J=1) ; 2.3(CH t, J=1)
3a/7	$CH_2COOC_2H_5$	54.4, 49.7	25.2, 23.4	189.5	167.5(CO) ; 60.6 (CH_2O) ; 37.6 (CH_2CO) ; 13.3 (CH_3)	3.8[c]	2.1	4.3(2H, CH_2, q, J=4) ; 4.2 (2H, CH_2, s) ; 1.3(3H, CH_3, t, J=4)
3a/8	$C_6H_5CH_2$	54.1, 49.6	25.1, 23.2	190.7	135.9, 128.3, 127.5, 126.4 (Ph) ; 40.2(CH_2)	3.7(2H), 3.3(2H)	1.6	7.2(5H, Ph, s) 4.4(2H, CH_2, s)
3a/9	*p*-$NO_2C_6H_5CH_2$	55.2, 50.4	25.8, 23.9	190.5	143.5, 139.8, 127.6, 126.3 (Ph), 39.4(CH_2)	3.9(2H), 3.7(2H)	1.9	8.3(2H, d, J=4), 7.7(2H, d, J=4) ; 4.8(2H, CH_2, s)
3a/10	$C_6H_5CH_2CH_2$	54.3, 49.6	25.2, 23.3	190.4	137.0, 128.4, 127.6, 126.4 (Ph) ; 51.7 (CH_2N) 34.7(CH_2)	*d*	1.9	7.3(5H, Ph, s) ; 3.5(m, 4H) ; 3.1 (m, 4H)

3a/13	$C_6H_5SO_2$	55.2, 50.6	25.9, 24.1	190.7	138.8, 133.2, 128.5, 128.4(Ph)	3.8^c	1.9	8.2(2H, m) ; 7.7 (3H, m)
3b/1	CH_3	54.3 143.8, 134.2, 126.4 124.6, 118.1(Ph)	27.1	193.0	19.3(CH_3)	4.5	3.1	1.7(3H, CH_3, s)
3b/2	C_2H_5	54.3 143.5, 134.4, 126.6, 125.6 118.5(Ph)	27.2	192.6	30.6(CH_2) ; 13.3 (CH_3)	4.5	3.2	3.4(2H, CH_2, q, J=4) ; 1.3(3H, CH_5, t, J=4)
3b/3	$CH_2CH=CH_2$	54.4 143.6, 134.3 126.4, 125.0, 124.9, 118.3 (Ph)	27.1	191.1	131.9(CH=) ; 118.5(CH_2=) ; 39.2(CH_2)	4.3	3.1	5.5(3H, m) ; 4.0 (CH_2, d, J=4)
3b/4	$CH\equiv C-CH_2$	54.5 143.5, 134.3, 126.6, 125.4, 125.0 118.3 (Ph)	27.3	189.3	78.1(C≡) ; 71.6 (CH) ;25.0(CH_2)	4.3	3.2	4.1(CH_2, d, J=1) ; 2.2(CH, t, J=1)
3b/5	$CH_2COOC_2H_5$	54.5 143.6, 134.3, 126.4, 125.3, 124.9, 118.2 (Ph)	27.2	189.6	168.0(CO) ; 61.5 (CH_2O) ; 38.0 (CH_2CO) ; 13.9 (CH_3)	4.4	3.2	4.3(2H, CH_2, q, J=4) ;4.2(2H, CH_2, s) ;1.3(3H, CH_3, t, J=4)
3b/6	$CH_2COCOOC_2H_5$	55.1 143.4, 134.6, 126.7, 125.6, 125.1, 118.2 (Ph)	27.3	190.0	175.7(CO) ;166.4 (CO);62.5(CH_2O) 41.3(CH_2CO), 13.9$(CH)_3$	4.5	3.3	4.4(2H, CH_2, q, J=4) ;4.3(2H, CH_2,s) ; 1.4(3H, CH_3, t, J=4)
3b/11	$C_6H_5SO_2$	55.3 144.0, 134.8, 126.8, 125.9, 125.2, 118.4 (Ph)	27.6	191.2	139.9, 133.8, 128.6, 128.4(Ph)	4.5	3.3	8.2(2H, m), 7.6 (3H, m)
5a		54.6, 50.3	25.7, 24.2	193.4	44.8(CH_2)	3.9(4H), 3.7(4H)	2.1^e	5.5(2H, CH_2, s)
5b		54.3 143.5, 134.2, 126.3, 125.2, 124.8, 118.3 (Ph)	27.1	191.2	43.9(CH_2)	4.5(4H)	3.1(4H)	5.4(2H, CH_2, s)

a δ in ppm, solutions in $CDCl_3$, J = coupling constant in Hz.

b H-α and H-β of indoline appeared as 2H, t, J = 4 ; its Ph appeared at δ 9.0–9.1 (1H, d_{broad}), 7.2–7.3(3H, m)

c m, 4H.

d overlap with CH_2

e 8H

Table

Thiocarbamyl sulfenamide

Compound	R^2	Yield [%]	M.P. [°C]	Formula	Analysis calcd/found			$^{13}C-NMR[\delta]^a$ Pyrrolidino or C-2
					C	H	N	
4a/1	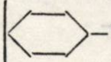	78	65	$C_{11}H_{20}N_2S_2$	54.1 53.8	8.2 8.1	11.5 11.4	54.3, 48.3
4a/2	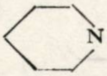	80	94	$C_{10}H_{18}N_2S_2$	52.2 52.1	7.8 7.6	12.2 12.0	54.5, 48.0
4a/3	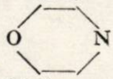	82	85	$C_9H_{16}N_2OS_2$	46.6 46.5	6.9 7.0	12.1 12.0	53.3, 48.1
4b/1	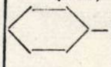	83	162	$C_{15}H_{20}N_2S_2$	61.6 61.4	6.8 6.7	9.6 9.5	55.3 143.1, 134.4, 127.0, 125.7, 125.1, 118.8(Ph)

a δ in ppm, solutions in $CDCl_3$, J = coupling constant in Hz,
b Overlap with piperidine
c Overlap with morpholine
d $J = 4$.
e $t, J = 4$.

Table

Mixed

Compound	R^3	Yield [%]	M.P. [°C]	Formula	Analysis % calcd/found			$^{13}C-NMR[\delta]$	
					C	H	H	Pyrrolidinoor C−2	Indolino *C* C−3
6a/1	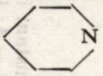	75	175	$C_{12}H_{20}N_2S_4$	45.0 45.1	6.3 6.2	8.8 8.7	55.0, 50.4	25.9, 23.9
6a/2	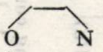	72	208	$C_{11}H_{18}N_2OS_4$	41.0 40.9	5.6 5.5	8.7 8.6	55.2, 50.6	26.0, 24.2
6a/3	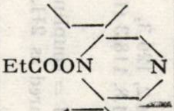	76	160	$C_{14}H_{23}N_3O_2S_4$	42.7 42.6	5.9 6.0	10.7 10.5	55.1, 50.5	25.9, 24.1
6b/1	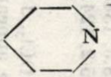	72	160	$C_{16}H_{20}N_2S_4$	52.5 52.0	5.4 5.3	7.6 7.5	55.2 143.2, 134.3, 126.6, 125.6, 125.2, 118.6 (Ph)	27.6
6b/2	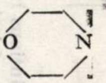	71	176	$C_{15}H_{18}N_2OS_4$	48.6 48.5	4.9 5.1	7.6 7.4	55.3 143.1, 134.4, 126.7,125.7, 125.1, 118.8 (Ph)	27.5
6b/3	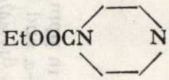	73	173	$C_{18}H_{23}N_3O_2S_4$	49.0 48.9	5.2 5.1	9.5 9.5	50.4 143.0, 134.4, 126.9, 125.6, 125.1, 118.7 (Ph)	274
6b/4	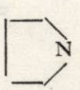	62	170	$C_{15}H_{18}N_2S_4$	50.8 50.5	5.1 5.1	79 81		

[a] in ppm, solutions in $CDCl_3$, J=coupling constant in Hz

3

derivatives **(4)**

Indolino *C* C-3	CS	Others	$^1H-NMR[\delta]^a$		Others
			Pyrrolidino or H−α (t, J=3)	Indolino H H−β (4H, m)	
25.6, 23.3	198.5	57.9, 32.5, 24.0 (cyclohexyl *c*)	4.0(2H), 3.7(2H)	2.1	2.8(1 H, m), 1.6(10H, m) (cyclohexyl).
25.9,22.9	199.0	52.8(C-2 pip.); 26.8(C-4 pip.); 22.5(C-3 pip.)	*b*	2.1	3.9(8H, m); 1.8(6H, m) (piperidine)
25.9, 22.9	197.6	67.3(C-3 morph.) 53.1(C-2 morph.)	*c*	2.0	3.7(12.H, m, morph.)
2.75	197.7	57.8, 33.0, 24.2 (cyclohexyl *c*)	4.4(2H)^d 9.1(1H), 7.2(3H, m)(Ph)	3.1(2H)^e	2.7(1H, m); 1.7 (10H, m) (cyclohexyl)

4

esters **(6)**

CS	Others	$^1H-NMR[\delta]^3$
194.2	52.2(C-2pip.); 44.7(CH_2) 29.5(C-4pip.);24.1 (C-3pip.)	5.5(2H, CH_2, s); 4.0(8H,H-α of pyrrol+H-2 of pip.m) 2.0(4H, H-β of pyrrol, m); 1.8(6H,H-β+H-γ of pip., m)
193.4	66.1(C-3morph.);51.1(C-2) morph.); 44.8(CH_2)	5.4(2H, CH_2, s); 4.1(6H, 2H-α of pyrrol+H-3 of morph., m); 3.8(6H, 2H-α of pyrrol+H-2 of morph., m); 2.0(4H, H-β of pyrrol.)
196.1	155.0(CO); 61.7(CH_2O); 50.1 (C-3pipra); 44.8(CH_2); 42.7 (C-2 pipra); 14.5(CH_3)	5.4(2H, CH_2, s); 4.1(10H, CH_2O+H-α of pyrrol.+H-2 of pipra., m); 3.6(4H, H-2 of pipra., m); 1.9(4H, H-β of pyrrol; m); 1.2(3H, CH_3, *t*, J=4)
196.4	52.3(C-2pip.); 44.8(CH_2); 25.6(C-4pip.); 24.0(C-3 pip.)	9.0(1H, d broad,); 7.3(3H, m); 5.5(2H, CH_2, s); 4.5(2H, H-2 of indoline, *t*, *J*=4); 4.0(4H, H-α of pip., m); 1.8(6H, H-β and H-γ of pip., m); 3.2(2H, H-3 of indoline, *t*, *J*=4).
197.7	66.2(C-3morph.); 51.1 (C-2 morph.); 43.9(CH_2)	9.1(1H, d broad); 7.3(3H, m); 5.4(2H, CH_2, s), 4.5(2H, H-2 of indoline, *t*, *J*=4; 4.1(4H, H-3 of morph., m); 3.8(4H, H-2 of morph., m); 3.1(2H, H-3 of indoline, *t*, *J*=4)
196.3	155.2(CO); 61.8(CH_2O); 50.1 (C-3pipra.); 44.8 (CH_2); 42.8 (C-2 pipra); 14.0(CH_3)	9.0(1H, d broad); 7.2(3H, m); 5.5(2H, CH_2, s); 4.4(2H, H-2 of indoline, *t*, *J*=4); 4.2(6H, CH_2O+ H-3 of pipra, *m*); 3.6 (4H, H-2 of pipra, m); 3.2(2H, H-3 or indoline, *t*, *J*=4); 1.3(3H, CH_3, *t*, *J*=4).
		9.2 (1H, d broad); 7.2 (3H, m); 5.5(2H, CH_2,s); 4.5 (2H, H−2 of indoline, t, J = 4); 3.9 (2H H-α of pyrrol., *t*, *J*=3); 3.6(2H, H-α of pyrrol., *t*, *J*=3); 3.2(2H, H-3 of indoline, *t*,*J*=4); 2.0(4H, H-β of pyrrol., m)

2b : 92% yield, m.p. > 300 [Lit.[6], m.p. 240°]. IR (cm^{-1}) : 995 (CS) ; 1265 (C—N). ^1H—NMR (δ, TMS, D_2O) : 4.5 (2H, H—α, *t*, *J* = 4) ; 3.1 (2H, H—β, *t*, *J* = 4) ; 9.1 (1H, d, broad), 7.2 (3H, m) (Ph). ^{13}C—NMR (δ, Dioxane ; D_2O) 212.1 (CS), 54.4 (C—2) ; 27.3 (C—3) ; 143.7, 134.2, 126.4, 124.5, 118.1 (Ph).

$C_9H_8NNaS_2 \cdot 2H_2O$ (253) Calcd : C 42.7 H 4.7 N 5.5 Found : C 42.4 H 4.8 N 5.4

3.2. Dithiocarbamate esters (3) (Tables 1 and 2)

An aqueous solution of the appropriate sodium salt **2** (0.01 mole) was stirred at room temperature with the corresponding halide (0.012 moles) for 24 h. The products which separated out were recrystallised from the appropriate solvents.

3.3. Thiocarbamayl sulfenamide derivatives (4) (Table 3)

A stirred solution of the sodium salt **2a** or **2b** (0.02 mole) the appropriate amine (0.2 mole) and aqueous sodium hydroxide (0.08 mole, 25%) in 20 mL water, treated with 60 mL aqueous solution of 10.2 parts by weight iodine and 10.2 parts by weight KI over a 2h period at 25—30°C, stirred 0.5 h, filtered, and the solids washed with water until the washings were neutral to litmus, dried at room temperature and recrystallised from ethanol in needles.

3.4. Bis-dithiocarbamate esters (5) (Tables 1 and 2)

An aqueous solution of the appropriate sodium salt **2** (0.02 mole) was stirred with diiodomethane (0.012 nole) for 24 h at room temperature. The solids which separated out were filtered, washed with water and recrystallised from methanol in needles.

3.5. Mixed esters (6) (Table 4)

Aqueous solutions of the two different sodium dithiocarbamates (0.01 mole of each) were stirred together for 1 h. Diiodomethane (0.01 mole) was then added slowly over a period of 1 h ; and the stirring continued for 48 h. The products which separated out were recrystallised for three times from methanol in needles.

REFERENCES

[1] Part I : Hassan M. Faidallah, sent for the Hungarian Academy of Science.

[2] CIBA Ltd., Swiss pat. 253, 354 (1948) (*Chem. Abstr.*, **44**, 657 (1950)).

[3] C. H. Budeanu, E. Budeanu and A. Toma, *Anal. Sti. Univ. "Al. I. Cuza" Iași*, Sect. I (Mat., fiz., Chim.), N.S., **1**, 345 (1955) (*Chem. Abstr.* **51**, 1075 (1952)).

[4] A. Rieche, G. Hilgetag, D. Martin and I. Kreyzi, *Arch. Pharm.*, **296**, 310 (1963).

[5] K. Matsushima, A. Kudamatsu and M. Miyamoto, *Noyaku Seisan Gijut-Su*, **14**, 1 (1966) (Japan) (*Chem. Abstr.*, **67**, 43534 (1967)).

[6] R. D. Bereman and D. Nalewajek, *Inorg. Chem.*, **17**, 1085 (1978).

[7] G. Marcotrigiano, G. C. Pellacani and C. Preti, *J. Inorg. Nuclear Chem.*, **36**, 3709 (1974).

[8] M. Ahmed and R. J. Magee, *Analyt. Chim. Acta*, **75**, 431 (1975).

[9] W. Reppe, et al., *Liebigs Ann. Chem.*, **596**, 80 (1955). (*Chem. Abstr.* **50**, 16782 (1956)).

Revue Roumaine de Chimie, **33**, *8*, 823–826(1988)

PHOSPHONIUM YLIDES. VI

THE REACTION OF FLUORENYLIDENETRIPHENYLPHOSPHORANES AND -ARSINANE WITH QUINISATINS

L. S. BOULOS, EL. S. M. YAKOUT and M. M. SIDKY
National Research Centre, Dokki-Cairo, Egypt

Received March 28, 1987

Fluorenylidenetriphenylphosphorane (Ia), 2,7-dibromofluorenylidenetriphenylphosphorane (Ib), and fluorenylidenetriphenylarsinane (Ic) react with quinisatin (IIa) and its N-methyl analogue (IIb) to give the corresponding ethylenes (IIIa-b). Structural assignments of the products obtained are based on analytical, chemical and spectroscopic results.

INTRODUCTION

In the previous publications we examined the action of phosphonium ylides on carbonyl functions.[1-5] The present work is an extension on the behaviour of stable ylides (I) towards certain tricarbonyl compounds namely quinisatins (II). It could be mentioned that the sole work available, due to Schönberg,[6] stated that the reaction of fluorenylidenetriphenylphosphoranes (I) with quinisatine (IIa) gave products that could not be isolated in a pure form and thus no analytical data or sharp melting points are reported.

RESULTS AND DISCUSSION

We have found that phosphorane (Ia) reacts with quinisatin (IIa), in boiling benzene, to give a coloured crystalline compound formulated as

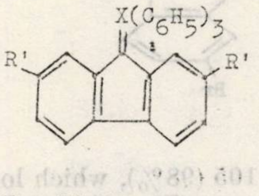

Ia, R' = H; X = P
b, R' = Br; X = P
c, R' = H ; X = As

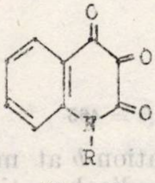

IIa, R = H
b, R = CH$_3$

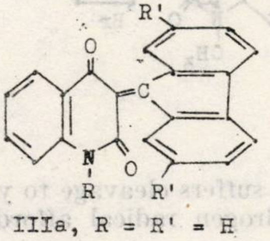

IIIa, R = R' = H
b, R = H; R' = Br
c, R = CH$_3$; R' = H
d, R = CH$_3$; R' = Br

3-(9*H* -fluoren-9-ylidene)-2,4-(1*H*, 3*H*)-quinolinedione (IIIa) based on the following evidences : (i) Compound (IIIa) gave a single tlc spot and correct elemental analysis. (ii) The IR spectrum of compound (IIIa) (in KBr) showed bands at 3200 cm^{-1} (NH), 1655 cm^{-1} (C=0, amide),[7] 1690 cm^{-1} (C=O, aryl) and 1605 cm^{-1} (C=C, aromatic). Distinctly, the absorption band at 1720 cm^{-1} assigned to the carbonyl group at position 3 in the parent compound (IIa) disappeared in the spectrum of (IIIa); (iii) The mass spectrum of (IIIa) revealed successive loss of two CO molecules from the parent ion M^+($m/Z = 323$) base peak (100%) to give cation at $m/Z = 267$ (48%).

Similar treatment of quinisatin (IIa) with phosphorane (Ib) afforded 3-(2,7-dibromo-9*H*-fluoren-9-ylidene)-2,4 (1*H*, 3*H*)-quinolinedione (IIIb) in 95% yield. Structure (IIIb) was inferred from correct analytical values, tlc (one spot) and IR spectrum which lacks the absorption band at 1720 cm^{-1}, characteristic for the carbonyl group at position 3. The mass spectrum of the brominated derivative (IIIb), besides the consecutive loss of the two CO molecules, revealed the expulsion of a bromine radical from the molecular ion M^+($m/Z = 479/481/483$ in 85%) to give $m/Z = 400/402$ in 25%) followed by ejection of another $Br^\cdot$ to give $m/Z = 321$ (in 92%).

In the same way, N-methyl quinisatin (IIb) undergoes the normal Witting reaction with FTP (Ia) and its 2,7-dibromo-analogue (Ib), in dry toluene, to give 3-(9*H*-fluoren-9-ylidene)-1-methyl-2,4-(1*H*, 3*H*)-quinolinedione (IIIc) and 3-(2,7-dibromo-9*H*-fluoren-9-ylidene)-1-methyl-2,4 (1*H*, 3*H*)-quinolinedione (IIId) in 85 and 87% yield, respectively. Their identity was established from sharp melting points, correct analytical values, tlc, and infrared spectroscopic analyses (cf. Experimental). The mass spectrum of (IIId), taken as an example, showed the molecular ion at $m/Z = 493$ (M^+, 5%). Loss of CO molecule from the parent ion peak produces the radical *a* at $m/Z = 465$.

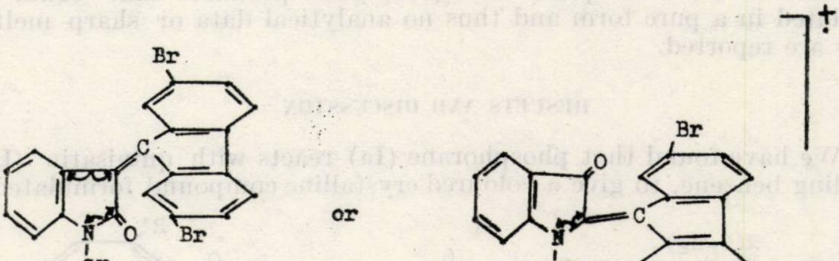

a, m/z = 465

Ion *a* suffers cleavage to yield cation *b* at $m/Z = 105$ (98%), which loses a hydrogen radical affording radical cation *c* at $m/Z = 104$ (100%).

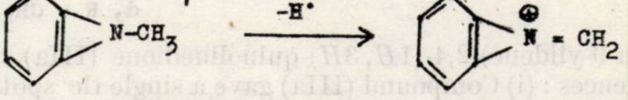

b, m/z = 105 (98%) *c*, m/z = 104 (100%)

Similarly, fluorenylidenetriphenylarsinane (Ic) reacts with quinisatin (IIa) and its N-methyl analogue (IIb), in dry benzene, to give the corresponding ethylenes (IIIa) and (IIIc) in 80 and 85% yield, respectively.

In all the above reactions triphenylphosphine oxide or triphenylarsine oxide were isolated from the filtrate in quantitative yield and identified.

The findings of the present investigation are considered to be an additional application for the Witting olefin synthesis.

EXPERIMENTAL

All mp's were uncorrected. The benzene (thiophene-free) used was dried (Na). The analyses were carried out in the Microanalytical lab., National Research Centre (Cairo). Infrared spectra were measured on a Perkin-Elmer Infracord Model 137 spectrophotometer using KBr Wafer technique. The mass spectra were recorded at 70 eV on a Varian MAT 711 Spectrophotometer.

The compounds obtained in this work are nominated in accordance with the current *Chem. Abstr.* index names.

Reaction of fluorenylidenetriphenylphosphorane (Ia) with quinisatin (IIa)

Fluorenylidenetriphenylphosphorane (Ia)[8] (0.42 g, 0.001 mol) was added to a suspension of quinisatin (IIa)[9] (0.001 mol) in benzene (25 mL) and the reaction mixture was refluxed for 12 hrs. After filtration, the solid product thus obtained was crystallized twice from THF/benzene to give (IIIa) as brown crystals m.p. 325° (90% yield).

Found C 81.3 ; H 4.1 ; N 4.32 ;

Calcd for $C_{22}H_{13}O_2N$: C 81.73 ; H 4.03 ; N 4.33.

Reaction of 2,7-dibromofluorenylidenetriphenylphosphorane (Ib) with quinisatin (IIa)

A mixture of (Ib)[10] (0.58 g, 0.001 mol) and quinisatin (IIa) (0.001 mol) in benzene (25 mL) was boiled under refux for 9 hrs. After cooling, the precipitated material was collected (87%), crystallized from chloroform to give (IIIb) as colored crystals m.p. 335°

Found C 54.73 ; H 2.18 ; N 2.83 ; Br 33.3 ;

Calcd for $C_{22}H_{11}O_2NBr_2$: C 54.89 ; H 2.29 ; N 2.91 ; Br 33.26%.

Reaction of fluorenylidenetriphenylphosporane (Ia) with N-methyl quinisatin (IIb)

A mixture of phosphorane (Ia)(0.42 g, 0.001 mol) and compound (IIb)[11] (0.18 g, 0.001 mol) in toluene (25mL) was boiled under refux for 12 hrs. After cooling, the substance that separated was collected (90%) and crystallized from chloroform to give (IIIc) as brown crystals m.p. 260°

Found C 81.8 ; H 4.51 ; N 4.23 ;

Calcd for $C_{23}H_{15}O_2N$: C 81.90 ; H 4.45 ; N 4.15%.

Reaction of 2,7-dibromofluorenylidenetriphenylphosphorane (Ib) with N methyl quinisatin (IIb)

Compound (Ib) (0.58g, 0.001 mol) was added to a suspension of N-methyl quinisatin (IIb) (0.18g, 0.001 mol) in toluene and the reaction mixture was refluxed for 12 hrs. After cooling, the solid product thus formed was gathered (90%) and crystallized from chloroform to give (IIId) as yellow crystals m.p. 270

Found C 53.73 ; H 2.7 ; N 2.75 ; Br 32.05 ;

Calcd for $C_{23}H_{13}O_2NBr_2$C : 55.76 ; H 2.63 ; N 2.83 ; Br 32.32.

Similarly, the reaction of ylide (Ic)[12] with triones (IIa) and (IIb) afforded the corresponding ethylenes (IIIa) and (IIIc) in 80 and 85% yield, respectively (mixed m.p. and comparative IR spectra).

In all the above reactions triphenylphosphine oxide or triphenylarsine oxide were isolated from the filtrate in quantitative yield and identified (m.p., mixed m.p. and comparative IR spectra).[13],[14]

REFERENCES

[1] M. M. Sidky and L. S. Boulos, *Phosphorus and Sulfur*, **4**, 299 (1978).

[2] M. M. Sidky, M. R. Mahran and L. S. Boulos, *Phosphorus and Sulfur*, **8**, 365 (1980).

[3] M. M. Sidky and L. S. Boulos, *Phosphorus and Sulfur*, **19** (1), 27 (1984).

[4] L. S. Boulos and M. M. Sidky, *Egypt. J. Chem.*, **26** (6), 547 (1983).

[5] M. M. Sidky, L. S. Boulos and E. M. Yakot, *Zeitschrift für Naturforsch.*, **40**, 50 (1985).

[6] A. Schönberg, E. Singer and A. Schulz-Pannier, *Chem. Ber.*, **106**, 2663 (1973).

[7] L. J. Bellamy, "The Infra-red Spectra of Complex Molecules", John Wiley and Sons, Inc. New York, N.Y. 244 (1964).

[8] L. A. Pinck and G. E. Hilbert, *J. Amer. Chem. Soc.*, **69**, 723 (1947).

[9] Th. Kappe, E. Lender and E. Ziegler, *Monatsh. Chem.*, **99**, 2157 (1968).

[10] A. Schönberg, K. H. Brosowski, and E. Singer, *Chem. Ber.*, **95**, 2144 (1962).

[11] H. Wittmann, *Monatsh.*, **96**, 523 (1965).

[12] M. P. Pascal, *Bull. Soc. Chim.*, **33**, 171 (1923).

[13] A. Michaelis and K. Gleichman, *Chem. Ber.*, **15**, 801 (1882).

[14] L. Coste and A. Michaelis, *Liebigs Annal. Chem.*, **201**, 243 (1880).

Revue Roumaine de Chimie, **33**, 8, 827–832(1988)

SYNTHESIS AND SOME REACTIONS OF 2-(α-BENZOYLAMINOSTYRYL)-3,1(4H)-BENZOXAZIN-4-ONE AND 3-AMINO-2-(α-BENZOYLAMINOSTYRYL-QUINAZOLIN-4(3H)-ONE

S. EL-NAGDY, A. A. EL-KHAMRY, M. A. SHAABAN and M. M. HABASHY
Chemistry Department, Faculty of Science, Ain Shams University
Abbassia, Cairo, Egypt

Received April 27, 1987

2-(α-Benzoylaminostyryl)-3,1(4H)-benzoxazin-4-one (I), could be synthesised from the reaction of anthranilic acid with 4-benzylidene-2-phenyloxazol-5-one. Compound (I) underwent ring opening on its treatment with hydrazines as well as different amines, affording (II)a-f and (III). Compound (I) reacted with hydrazoic acid to give the tetrazole derivative (IV), beside the benzimidazole derivative (V). Upon fusion of (I) with ammonium acetate 2-(α-benzoylaminostyryl)-4(3H)-quinazolin-4-one (VI) was obtained. 3-Amino-2-(α-benzoylaminostyryl)-4(3H)-quinazolin-4-one (VII) which was formed via refluxing of (I) with hydrazine hydrate in n-butanol solution, could be easily transformed into the following : i) 3-(diacetylamino)-2-(α-benzoylaminostyryl)-4(3H)-quinazolin-4-one (VIII) by the action of acetic anhydride, ii) The corresponding Schiff's bases (IX) through its condensation with some aromatic aldehydes ; iii) 3-(Ethoxycarbonyl methylamino-)-2-(α-benzoylaminostyryl)-4(3H)-quinazolin-4-one (X), via its reaction with ethyl bromoacetate and iv) 3-(Aceto-acetamido)-2-(α-benzoylaminostyryl)-4(3H)-quinazolin-4-one (XI) on its reaction with ethyl acetoacetate. On the other hand (I) reacted with ethyl acetoacetate as a carbon nucleophile affording 2-(α-aminostyryl)-3.4-dihydro-quinolin-4-one (XII), which was transformed into its hydrazone (XIII).

The present investigation is a continuation of our comparative studies [1] on some new synthesized benzoxazinone and quinazolinone derivatives bearing a bulky moiety in position-2 with specific polar effect, with the aim of finding out a role for such groups on the stability of the benzoxazine nucleous towards different nucleophiles.

The biological activity of related compounds to those in question made them worthy to be synthesized.

2-(α-Benzoylaminostyryl)-3,1(4H)-benzoxazin-4-one (I) has been prepared in fairly good yield on the reaction of 4-benzylidene-2-phenyl-oxazol-5-one with anthranilic acid pyridine solution. The IR spectrum of (I) showed νNH at 3250–3050 cm^{-1}, νCO of lactones at 1755 cm^{-1}, νCO of amides at 1650 cm^{-1}, beside ν$C=N$ at 1600 cm^{-1} (IR and analytical data Table 1).

It was previously stated [2] that primary amines react with 2-substituted-3,1-benzoxazin-4(H)-one in the presence of anhyd. zinc chloride to give 2,3-disubstituted-4-quinazolones. In the present study, aminolysis of (I) with hydrazine hydrate or phenylhydrazine or primary amines such as propylamine, benzylamine, *p*-toluidine and|or *p*-anisidine, in

Table 1

Characterization data of all compounds prepared

Compd	M.p.°C Solvent	Mol. formula	Found(%) Calc.			IR(cm^{-1})		
			C	H	N	NH,OH	CO	C=N
I	199–200 AcOH	$C_{23}H_{16}N_2O_3$	74.20 75.00	4.19 4.34	6.96 7.6	3250–3050	1755, 1650	1600
IIa	220–21 EtOH	$C_{23}H_{20}N_4O_3$	69.21 69.00	4.87 5.00	13.65 14.00	3300–3200	1690–1670, 1640	—
b	236–37 EtOH	$C_{29}H_{24}N_4O_3$	73.75 73.11	5.13 5.04	12.27 11.76	3400–3200	1670–1640	—
c	238–39 AcOH	$C_{26}H_{25}N_3O_3$	74.02 73.06	5.36 5.85	9.64 9.84	3400–3200	1660	—
d	235–36 EtOH	$C_{30}H_{25}N_3O_3$	76.02 75.79	5.13 5.26	9.21 8.84	3300–3200	1650	—
e	238–9 EtOH	$C_{30}H_{25}N_3O_3$	76.13 75.79	5.24 5.26	9.11 8.84	3400–3200	1660–1650	—
f	230–31 EtOH	$C_{30}H_{25}N_3O_4$	73.10 73.32	5.13 5.10	9.18 8.55	3350–3200	1660–1650	—
IIIa	191–92 EtOH	$C_{28}H_{27}N_3O_3$	74.73 74.17	6.18 5.96	10.30 9.27	3400–3100	1660–1630	—
IV	187–88 EtOH	$C_{23}H_{17}N_5O_3$	67.00 67.15	4.35 4.14	18.07 17.03	broad	1700–1650	1595
V	236–37 AcOH	$C_{23}H_{17}N_3O_3$	72.32 72.06	4.67 4.44	11.50 10.96	3300–3200	1760–1660	—
VI	246–47 EtOH	$C_{23}H_{17}N_3O_2$	74.98 75.20	6.51 4.63	11.23 11.44	3450–3300 63200	1660, 1630	1600
VII	187–88 EtOH	$C_{23}H_{18}N_4O_2$	73.15 72.25	5.10 4.71	15.30 14.65	3400–3300	1660–1630	1605
VIII	161–2 AcOH	$C_{27}H_{22}N_4O_4$	69.83 69.52	4.70 4.72	11.96 12.02	3350–3150	1770, 1750 1660	1610
IXa	155–56 EtOH	$C_{30}H_{21}FN_4O_2$	74.13 73.77	4.00 4.30	11.56 11.47	3400–3200	1670	1600
b	239–40 EtOH	$C_{30}H_{21}ClN_4O_2$	71.76 71.36	4.33 4.16	10.86 11.10	3350–3150	1640	1610
c	259–60 EtOH	$C_{32}H_{77}N_5O_2$	74.28 74.85	5.10 5.26	14.45 13.64	3250–3100	1660	1590
d	215–16 EtOH	$C_{30}H_{21}N_5O_4$	70.60 69.90	4.17 4.07	14.50 13.59	3300–3200	1680–1640	1595
X	197–98 AcOH	$C_{27}H_{24}N_4O_4$	69.67 69.23	5.45 5.12	12.43 11.96	3400–3250	1720, 1680 1640	1600
XI	211–212 EtOH	$C_{27}H_{22}N_4O_4$	70.10 69.52	5.32 4.72	11.97 12.01	3300–3200	1705, 1660 1640	1600
XII	220–21	$C_{17}H_{14}N_2O$	77.32	5.42	9.85	3550–3300 3200 broad	1650	1610
XIII	245–6 EtOH	$C_{17}H_{16}N_4$	74.30 73.90	6.21 5.79	21.18 20.30	3550–3300 3100–3000 broad		1590

boiling ethanol gave the corresponding N-(α-benzoylaminostyryl)anthranilic acid anilides (II) *a-f* respectively. Similarly, the secondary amine piperidine reacted with (I) to give N-(α-benzoylaminostyryl)anthranilic acid piperidide (III). The structure of either (II) or (III) was established since their IR spectrum displayed suitable values for νNH as well as νCO of amides beside their correct analytical data (Table 1).

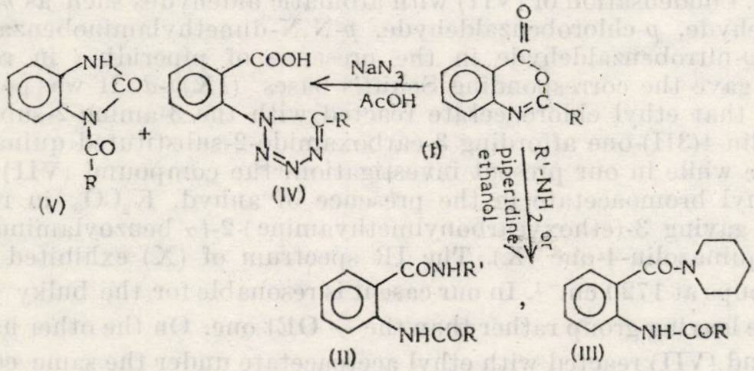

(II)	a	b	c	d	e	f
R	H_2N-NH-	C_6H_5-NH-	$CH_3-(CH_2)_2-NH-$	$C_6H_5-CH_2-NH-$	$p-C_6H_4CH_3-NH-$	$p-OCH_3C_6H_4-NH-$

R α-(benzoylaminostyryl)- = $-\underset{\displaystyle NH-COC_6H_5}{C}=CH-C_6H_5$

Reaction of compound (I) with hydrazoic acid [3] (sodium azide in acetic acid) gave a mixture of the tetrazole derivative (IV) and the benzimidazole derivative (V), which might be formed through ring opening either at position 2,3- to give the tetrazole derivative (IV) or at position 3,4- to give the benzimidazole derivative (V). The IR spectra of (IV) showed a broad band around 3μ for νOH of the carboxylic group and also the carbonyl stretching frequency at 1700 cm⁻¹. On the other hand, the IR spectrum of (V) exhibited νNH at 3300–3200 cm⁻¹ and the carbonyl stretching at 1760, 1660 cm⁻¹.

The benzoxazinone under investigation (I) underwent ring closure on fusion with ammonium acetate affording 2-(α-benzoylaminostyryl)-4(3H)-quinazolin-4-one (VI), which exists in the lactam ⇆ lactim tautomeric equilibrium (IR and analytical data; Table 1).

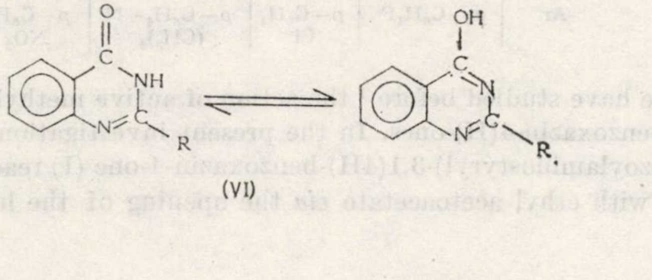

(VI)

Hydrazinolysis of (I) with hydrazine hydrate in refluxing *n*-butanol gave 3-amino-2-(α-benzoylaminostyryl)quinazolin-4(3H)-one (VII). Acetylation of (VII) with acetic anhydride afforded 3-diacetylamino-2-(α-benzoylaminostyryl)quinazolin-4(3H)-one (VIII), whose structure has been confirmed from its IR spectrum which displayed $\nu N(COCH_3)_2^4$ at 1770, 1750 cm^{-1} beside the νCO of amide at 1660 cm^{-1} (IR and analytical data Table 1). Condensation of (VII) with aromatic aldehydes such as *m*-flourobenzaldehyde, *p*-chlorobenzaldehyde, *p*-N,N-dimethylaminobenzaldehyde and/or *p*-nitrobenzaldehyde in the presence of piperidine in refluxing ethanol gave the corresponding Schiff's bases (IX)*a-d*. It was perviously stated [1] that ethyl chloroacetate reacted with the 3-amino-2-substituted quinazolin-4(3H)-one affording 3-carboxamido-2-substituted quinazolin-4-(3H)-one while in our present investigation, the compound (VII) reacted with ethyl bromoacetate in the presence of anhyd. K_2CO_3 in refluxing acetone gaving 3-(ethoxycarbonylmethyamine)-2-(α-benzoylaminostyryl)-4-(3H)-quinazolin-4-one (X). The IR spectrum of (X) exhibited νCO of ester groups at 1720 cm^{-1}. In our case it is resonable for the bulky Br-atom to be the leaving group rather than the — OEt one. On the other hand, the compound (VII) reacted with ethyl acetoacetate under the same condition to give the 3-acetoacetamido-2-(α-benzoylaminostyryl)-quinazolin-4(3H)-one (XI).

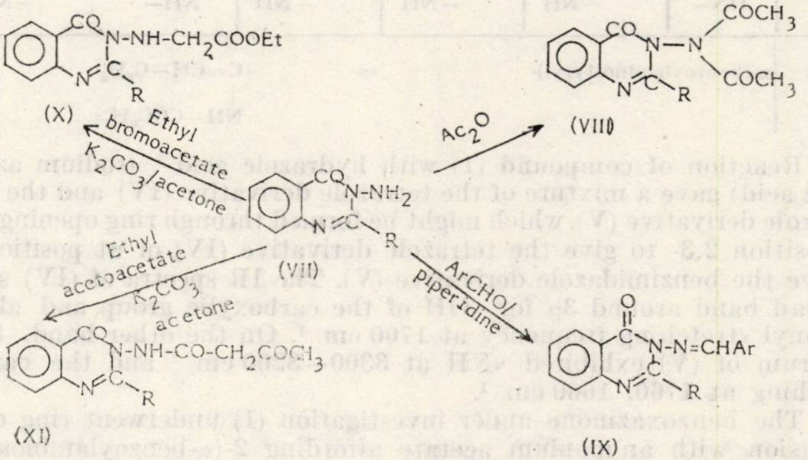

(IX)	a	b	c	d
Ar	$m-C_6H_4F$	$p-C_6H_4$ Cl	$p-C_6H_4-N$ $(CH_3)_2$	$p-C_6H_4$ NO_2

We have studied before [1] the action of active methylene compounds on 3,1-benzoxazin-4(H)-ones. In the present investigation we found that 2-(α-benzoylaminostyryl)-3,1(4H)-benzoxazin-4-one (I) reacted in a similar manner with ethyl acetoacetate *via* the opening of the heterocyclic ring in (I) by the carbanion drived from the active methylene compound affording 3-(α-aminostyryl)-3,4-dihydro-quinolin-4-one (XII), which was transformed into the corresponding hydrazone (XIII) on refluxing with hydrazine hydrate. The IR spectrum of (XII) displayed νCO at 1650 [4] cm^{-1} which disappeared completely in the IR spectrum of (XIII) (IR and analytical data Table 1).

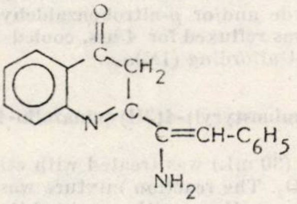
(XII)

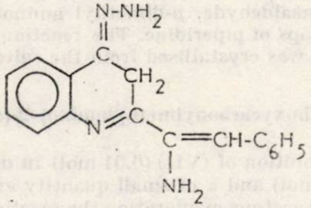
(XIII)

EXPERIMENTAL

IR spectra were recorded in KBr on a Beckman infrared spectrophotometer (cm^{-1}). All melting points are uncorrected. The characterization data of all the compounds prepared are given in Table 1.

2 (α-Benzoylaminostyryl)-3,1(4H)-benzoxazin-4-one (I)

A solution of anthranilic acid (0.01 mol) in pyridine (30 mL) was added to 4-benzylidene-2-phenyloxazol-5-one (0.02 mol). The solution was shaken for 30 min., left aside at room temperature for further 30 min. with occasional shaking, stirred in cold water, and the solid separated filtered off, washed with water and crystallized from a proper solvent to give (I).

N-(α-Benzoylaminostyryl)anthranilic acid anilides (II)a-h

A solution of (I) (0.01 mol) and the amine under investigation (0.01 mol) in ethanol was heated under reflux for 5 hr. The product that separated on cooling crystallised from a suitable solvent to give (II)a-h, using piperidine (0.01 mol) N-(*α-benzoylamino)-anthranilic acid piperidid* (III).

1-(2-Phenylcarboxy)-5-(α-benzoylaminostyryl)-tetrazole (IV) and N-(α-benzoylaminostyryl)benzimidazolone (V)

A mixture of (I) (0.01 mol) in glacial acetic acid (5 mL) was treated with a solution of sodium azide (0.015 mol) in the least amount of water, the mixture heated on a boiling water-bath for 4 hr, cooled and the solid separated filtered off to give IV. The filtrate was diluted with water to give (V)

2-(α-Benzoylaminostyryl)-4(3H)quinazolin-4-one (VI)

A mixture of (I) (0.01 mol) and ammonium acetate (0.02 mol) was found slightly over 200°C. The temperature of the mixture was kept up for 3 hr. The resultant product was washed with water and crystallised from the proper solvent to give (VI).

3-Amino-2-(α-benzoylaminostyryl)quinazolin-4(3H)-one (VII)

A solution of (I) (0.01 mol) and hydrazine-hydrate (0.01 mol) in *n*-butanol (50 mL) was heated under reflux for 3 hr, cooled and the separated solid was crystallised from the proper solvent to give (VII).

3-Diacetylamino-2-(α-benzoylamino-tyryl) quinazolin-(3H)-one (VIII)

Compound (VII) (0.01 mol) was refluxed with an excess of acetic anhydride for 4 hrs, and the reaction mixture left to evaporate slowly in a porcelain dish, producing (VIII).

The Schiff bases (IX) a-c

A solution of VII (0.01 mol) in ethanol (30 mL) was treated with *m*-fluorobenzaldehyde, *p*-chlorobenzaldehyde, *p*-dimethyl aminobenzaldehyde and/or *p*-nitrobenzaldehyde (0.01 mol) and few drops of piperidine. The reaction mixture was refluxed for 4 hrs, cooled and the separated solid was crystallised from the suitable solvent affording (IX)*a-c*.

3-(Ethoxycarbonylmethylamino)-2-(α-benzoylaminostyryl)-4(3H) quinazolin-4-one (X)

A solution of (VII) (0.01 mol) in dry acetone (30 mL) was treated with ethyl bromoacetate (0.01 mol) and a of small quantity anhyd. K_2CO_3. The reaction mixture was refluxed for 8 hrs. After acetone evaporation the reaction mixture was stirred with waterand the solid formed was filtered off to give (X). When ethyl acetoacetate was used under the same condition, the 3-*Acetoacetamido*-2-(α-*benzoylaminostyryl*)-*quinazolin*-4(3H)-*one* (XI) was obtained.

2-(α-Aminostyryl)-3,4-dihydroquinolin-4-one (XII)

A mixture of (I) (0.01 mol) and ethyl acetoacetate (0.03 mol) in dry pyridine(50 mL) was heated under reflux for 24 hrs, poured onto ice-cold HCl, and the precipitated product was filtered and crystallised from the suitable solvent.

2-(α-Aminostyryl)-3,4-dihydroquinolin-4-hydrazone (XIII)

A mixture of (XII) (0.01 mol) and hydrazine hydrate (0.02 mol) in absolute ethanol (50 mL) was refluxed for 6 hrs, poured into ice-cold HCl, and the produced solid was filtered off and crystallised from the proper solvent to give (XIII).

REFERENCES

[1] M. M. Mohamed, Abdel Momen A. El-Khamry, S. El-Nagdy and S. W. Shoshaa, *Indian J. Chem.*, **25 B**, 211 (1986).

[2] D. T. Tentmayer and E. C. Wanger, *J. Org. Chem.*, **14**, 967 (1949).

[3] M. F. Ismail, N. A. Shams and M. I. Naguib, *Indian J. Chem.*, **20 B**, 394 (1981).

[4] L. J. Bellamy, "The IR Spectra of Complex Molecules" John Wiley, New York, (1957), second edition p. 221.

Revue Roumaine de Chimie, **33**, *8*, 833–838(1988)

SYNTHESIS OF 2-(2′-THENYL)-3,1-(4H)-BENZOXAZIN-4-ONE AND ITS REACTIONS WITH DIFFERENT NUCLEOPHILES

ABDEL MOMEN A. EL-KHAMRY, S. EL-NAGDY and M. E. SHABAN
Chemistry Department, Faculty of Science, Ain Shams University,
Abbassia, Cairo, Egypt

Received April 27, 1987

2-(2′-Thenyl)-3,1-(4H)-benzoxazin-4-one (II) has been synthesized from the hitherto unknown N-(2-thenyl) anthranilic acid (I). Compound (II) reacted with primary amines, amino acids, and hydrazines *via* the heterocyclic ring opening to give (III) and also, with secondary amines to give (IV). On the other hand, (II) reacted with two mols of hydrazine hydrate in boiling butanol to give (VI). 5-Hydroxyquinazolinone derivative (VIII) has been synthesized, while 2-(2′-thenyl)-4-(3H)-quinazolin-4-one cannot be prepared through the action of formamide either on (I) or (II), instead, N-(2-thenoyl)anthranilamide (VII) was isolated. Compound (II) reacted also with hydrazoic acid to give the tetrazole derivative (IX). The reaction of (II) with some carbon nucleophiles has been also studied.

Our present investigation has been carried out in order to find out a role for the heterocyclic 2-moiety, on the stability and the reaction progress in some different reactions of the benzoxazin-4-one derivative (II).

2-Thenoyl chloride reacted with anthranilic acid in equimolecular amounts, in the presence of a catalytic amount of pyridine to give N-(2-thenoyl) anthranilic acid (I) in fairly good yield. It dissolves in sodium carbonate solution. Its IR spectrum showed νCO of carboxylic group at 1710 cm^{-1}, νCO of amides at 1670 cm^{-1}, beside, a broad absorption at 3300 cm^{-1} (3μ region)(Table 1).

On treatment of (I) with acetic anhydride,[1] 2-(2′-thenyl)-3,1-(4H)-benzoxazin-4-one (II) was obtained. Its IR spectrum exhibited strong absorption at 1750 cm^{-1} and 1590 cm^{-1} beside the lack of absorptions in the 3μ region (Table 1).

2-(2′-Thenyl)-3;1-(4H)-benzoxazin-4-one (II) was refluxed with ethanolic solution of primary amines, amino acids, and hydrazines (Scheme 1) to cause ring opening producing (III)a–i. Similarly, (II) reacted with secondary amines, namely piperidine or morpholine to give (IV) a and b. The IR spectrum of either (III) or (IV) showed strong νCO of amides (Table 1), in addition to νNH; also, for (IIIg) a very broad band around the 3μ region was observed. For (IIIe and f) νCO of carboxylic group was recorded at 1710 cm^{-1}. Compound (IIIh) was easily transformed into the

Table 1

Characterization of compounds I–XI

Compound	M.p. °C	Molecular formula	Analysis, % Required/Found				IR cm^{-1}			
Yield %	Solvent		C	H	N	S	NH, OH	CO		C=N
(I) 95 %	210–12 Benzene	$C_{12}H_9NO_3S$	58.29 59.13	3.64 3.38	5.67 5.96	12.95 —	Broad	1710	1670	
(II) 90 %	125–7 Benzene	$C_{12}H_7NO_2S$	62.82 62.71	3.05 3.32	6.11 6.43	13.97 —		1750		1590
(III) a 80 %	118–20 Light pet. 60–80°	$C_{18}H_{20}N_2O_2S$	65.85 66.31	6.09 5.90	8.53 8.88	9.57 —	3300 3190	1670	1640	
b 85 %	156–8 Light pet. 60–80°	$C_{19}H_{16}N_2O_2S$	67.85 68.49	4.76 5.15	8.33 7.77	9.52 —	3320 3150	1680	1640	
c 70 %	210–12 Light pet. 60–80°	$C_{18}H_{14}N_2O_2S$	67.08 66.93	4.35 4.17	8.69 9.49	9.94	3360 3200	1680	1640	
d 70 %	205–6 Benzene	$C_{19}H_{16}N_2O_3S$	64.77 65.10	4.54 4.47	7.95 7.67	9.09	3400 3100	1685	1675	
e 40 %	230–33 Bezene/ EtOH	$C_{19}H_{14}N_2O_4S$	62.29 63.10	3.82 4.32	7.65 6.90	8.74	Broad	1700	1660	
f 50 %	200–3 Glacial acetic acid	$C_{19}H_{14}N_2O_4S$	62.29 62.67	3.82 4.13	7.65 6.98	8.74	Broad	1710	1650	
(III) g 60 %	220–22 Acetic acid	$C_{12}N_{10}N_2O_3S$	54.96 55.50	3.81 3.70	11.47 10.90	13.11	Broad 3100 2600	1670	1640	
h 90 %	198–200 Methanol	$C_{12}H_{11}N_3O_2S$	55.17 55.19	4.21 4.54	16.09 16.52	12.26 —	3290 3200 3040	1670	1620	
i 60 %	193–95 Glacial acetic acid	$C_{18}H_{15}N_3O_2S$	64.09 65.10	4.45 4.47	7.95 7.65	9.09 —	3250 –	1660	1640	
(IV) a 70 %	201–3 Light pet. 60–80°	$C_{17}H_{18}N_2O_2S$	64.97 65.30	5.73 5.67	8.92 9.34	10.19	3210 3090	1680	1660	
b 60 %	190–92 Benzene	$C_{16}H_{16}N_2O_3S$	60.75 60.66	5.06 5.36	8.86 9.41	10.12	3400 3100	1655	—	
(V) a 70 %	185–87 Methanol	$C_{19}H_{15}N_3O_2S$	65.32 65.76	4.29 4.24	12.03 12.79	9.16	3300 3180	1660	1630	1590
b 80 %	247–50 Methanol	$C_{20}H_{17}N_3O_3S$	63.32 64.06	4.84 4.36	11.08 11.07	8.44	3360 3100	1665	1640	1600
c 70 %	202–204 Benzene	$C_{19}H_{14}ClN_3O_2S$	59.45 59.21	3.65 4.40	10.95 10.92	8.34	3300 3100	1660	1620	1580
(VI) 65 %	176–78 n-Butanol	$C_{19}H_{13}N_5OS$	52.36 52.19	4.72 4.52	25.45 24.87	11.63	3310 3150 Sharp	1650	1610	1580
(VII) 75 %	280–83 Methanol	$C_{12}H_{10}N_2O_2S$	58.53 59.10	4.06 4.20	11.38	13.00	3500 3200 3100	1660	1600	—
(VIII) 75 %	139–142 Light pet. 60–80°	$C_{12}H_8N_2O_2S$	59.01 59.30	3.27 3.30	11.47	13.11	3500 3000 3400 2900 *Broad*	1680	1640	1585
(IX) 55 %	203–205 Glacial acetic acid	$C_{12}H_8O_2N_4S$	52.94 52.90	2.92 3.20	20.58 21.81	11.76	Broad absorption	1700	—	1590
(X) 70 %	238–40 n-Butanol	$C_{16}H_{15}NO_4S$	60.56 60.10	4.73 4.90	4.41	10.09	3300 3100	1730	1660	—
(XI) 50 %	168–170 Benzene	$C_{16}H_{13}NO_3S$	64.21 64.80	4.34 4.56	4.68	10.70	— —	1740	1680	1600

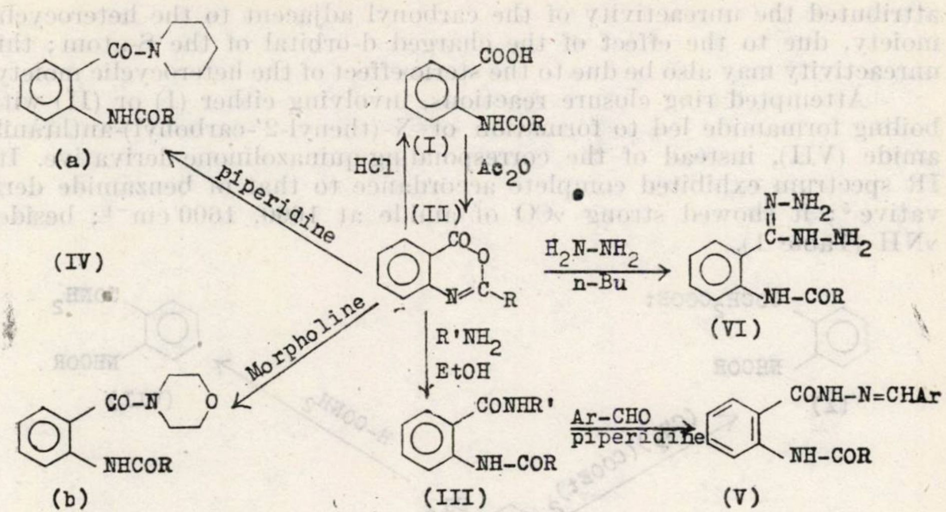
CO-N
NHCOR
(a)
COOH
NHCOR
(I)
HCl
Ac2O
piperidine
(II)
CO
O
N=C-R
(IV)
H2N-NH2
n-Bu
N-NH2
C-NH-NH2
NH-COR
(VI)
Morpholine
R'NH2
EtOH
CO-N
O
NHCOR
(b)
CONHR'
NH-COR
(III)
Ar-CHO
piperidine
CONH-N=CHAr
NH-COR
(V)

	a	b	c
Ar	C_6H_5-	$p-C_6H_4$ OCH_3	$p-C_6H_4$ Cl

(III)	a	b	c	d	e	f	g	h	i
R′	$C_6H_{11}-$	$C_6H_5CH_2$	C_6H_5-	$p-C_6H_4-$ OCH_3	$o-C_6H_4$ $COOH$	$p-C_6H_4-$ $COOH$	OH	H_2N-	$-NH$ C_6H_5
R					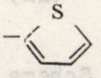				

corresponding Shiff bases (Va-c) through its reaction with aromatic aldehydes, in the presence of catalytic amount of pyridine. The ^{1}H-NMR spectrum [2] of (Vb) showed from low to high field signals of: azomethine δ 8.4—8.7 (distorted), aromatic δ 7.6—8.00 (multiplet), thenyl δ 7.0—7.4 (multiplet), and methoxyl δ 4.00 (singlet) protons, with the integrated proton ratios 1 :8 :3 :3 respectively.

It has been observed that the molarity of amines and the reaction time [3] are not the sole factors influencing the cyclisation of the anilides derivatives (III) to the corresponding 3-substituted quinazolin-4-one derivatives. The reaction temperature and the presence of a suitable dehydrating agent such as anhydrous $ZnCl_2$ or acetic anhydride must be also taken in consideration.

The above observation was stated since, on treatment of (II) with excess hydrazine hydrate in boiling *n*-butanol, (VI) was obtained *via* the consuming of two mols of hydrazine hydrate. The IR spectra of (VI) exhibited νVO of amides at 1660 cm^{-1}, beside νNH_2 (Table 1). The author attributed the unreactivity of the carbonyl adjacent to the heterocyclic moiety, due to the effect of the charged d-orbital of the S-atom; this unreactivity may also be due to the steric effect of the heterocyclic moiety.

Attempted ring closure reactions, involving either (I) or (II) with boiling formamide led to formation of N-(thenyl-2′-carbonyl)-anthranilamide (VII), instead of the corresponding quinazolinone derivative. Its IR spectrum exhibited complete accordance to that of benzamide derivative[5]; it showed strong νCO of amide at 1660, 1600 cm^{-1}; beside, νNH (Table 1).

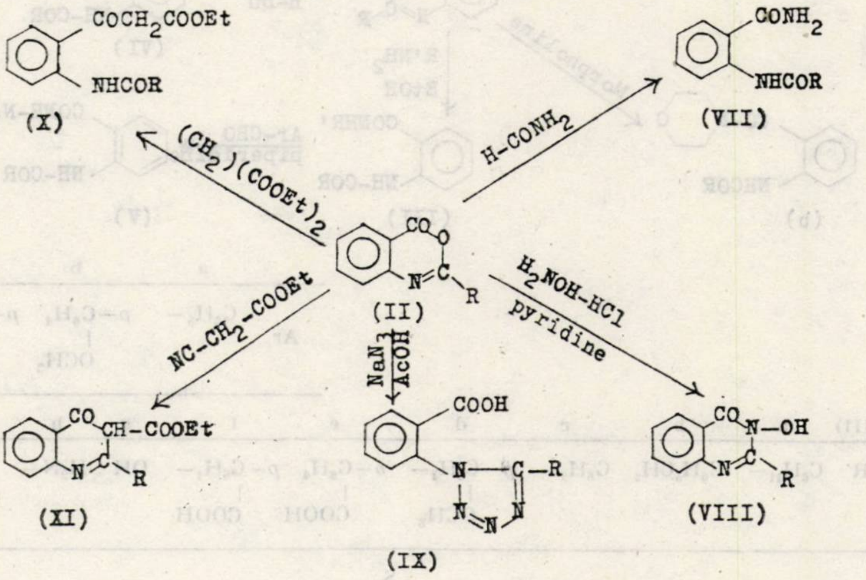

Scheme 2

On the other hand, hydroxylamine hydrochloride reacted with (II) in boiling ethanol, containing pyridine, to give 3-hydroxy-2-(2′-thenyl)-4(3H)-quinazolinone (VIII) which showed compatible IR spectral data (Table 1).

Reaction of (II) with hydrazoic acid (sodium azide in acetic acid) gave the tetrazole derivative (IX) as a sole product. Its IR spectrum showed absorption for νOH of carboxylic group and also the carbonyl stretching frequency at 1700 cm^{-1} (Table 1).

Also, the behaviour of (II) towards active methylene compounds was studied, where it reacted with diethylmalonate to result into ring opening to give the acetic ester derivative (X). Its IR spectrum showed well defined absorption bands at 1730 cm^{-1} assigned to νCO of ester, at 1660 cm^{-1} due to νCONH and at 3300 cm^{-1} due to νNH. On the other hand (II) reacted with ethyl cyanoacetate in the same manner, but with subsequent cyclisation to give 2-(2′-thenyl)-3-ethoxycarbonyl-3,4-dihydroquinolin-4-one (XI) which showed compatible IR spectral data (Table 1).

EXPERIMENTAL

All melting points are uncorrected. Infrared spectra were measured on a Pye Unicam SP 200 G as KBr wafer technique. ^{1}H—NMR spectrum was taken on a Varian EM360 instrument operating at 60 MHZ in dimethylsulphoxide solution.

Formation of N-(2-thenoyl)anthranilic acid (I)

To a solution of anthranilic acid (0.01 mol) in pyridine (50 mL), 2-thiophenoyl chloride (0.01 mol) was added dropwise with stirring and gentle warming for one hour. The reaction mixture was then stirred in cold water containing a little amount of diluted hydrochloric acid. The solid separated was filtered off and crystallised from the proper solvent to give N-(2-thiophenoyl)anthranilic acid (I).

Formation of 2-(2′-thenyl)-3,1-(4H)-benzoxazin-4-one (II)

A mixture of (I) (0.01 mol) and acetic anhydride (30 mL) was refluxed for one hour. The solution was then left to evaporate slowly in a porcelain dish. The separated colourless solid was crystallised from a suitable solvent to give 2-(2′-thiophenyl)-3,1-(4H)-benzoxazin-4-one. When a suspension of (II) (0.01 mol) in 100 mL of water, acidified with hydrochloric acid was refluxed for 30 minutes N-thiophenoyl anthranilic acid (I) was regenerated again

Action of amines on (II) : Formation of (2-thenoyl)anthranilides (III) a-i

A solution of (II) (0.01 mol) in 30 mL of ethanol was refluxed for 2 hours with (0.01mol) of amines, namely cyclohexylamine, benzylamine, aniline, *p*-anisidine, anthranilic acid, *p*-aminobenzoic, hydroxylamine hydrochloride, hydrazine hydrate or phenylhydrazine. The solid that separated after cooling and alcohol evaporation was crystallized from proper solvent to give (III a-i).

Action of piperidine or morpholine on (II) : Formation of N-(2-thenoyl)-anthranilic acid piperidide and N-(2-thenoyl)-anthranilic acid morpholide (IVa and b)

A solution of (II) (0.01 mol) and piperidine or morpholine (0.01 mol) in 30 m ethanol was heated under reflux for 3 hours. The product separated on cooling was washed with diluted hydrochloric acid and crystallized from suitable solvent to give (IV) a or b.

Condensation of (IIIh with aromatic aldehydes : Formation of 2-(carbonyl-N′-hydrazinoarylmethylene)-N-(thenyl-2′-carbonyl)-aniline (The Schiff bases Va-c)

A solution of (IIIh) (0.01 mol) and the aromatic aldehydes, namely, benzaldehyde, p-methoxybenzaldehyde, and/or *p*-chlorobenzaldehyde in 50 mL ethanol with few drops of piperidine as a general base was heated under reflux for four hours. The solid that separated on cooling was crystallised from a suitable solvent to give (V).

Action of hydrazine hydrate on (II) in n-butanol : Formation of 2-(N-thenoylamino)-hydrazinobenzaldehyde hydrazone (VI)

A solution of (II) (0.01 mol) and hydrazine hydrate (0.05 mol) in 50 mL *n*-butanol was heated under reflux for 12 hours. The solid isolated after evaporation of alcohol and cooling was crystallized from a suitable solvent to give 2-(N-thiophenamide)-hydrazinobenzaldehyde hydrazone (VI).

Action of formamide on either (I) or (II) : Formation of N-(2-thenoyl)-anthranilamide (VII)

A mixture of (II) (0.01 mol) and formamide (0.015 mol) was heated at 196°C for 12 hours. The solid product was washed with water and then crystallized from the proper solvent to give N-(thiophene-2-carbonyl-anthranilamide (VII).

Action of hydroxylamine hydrochloride on (II) in the presence of pyridine: Formation of 3-hydroxy-quinazolin-4-one derivative (VIII)

A solution of (II) (0.01 mol) and hydroxylamine hydrochloride (0.015 mol) in 50 mL ethanol containing few drops of pyridine was heated under reflux for 3 hours. The formed solid was crystallized from the proper solvent to give 3-hydroxy-quinazolin-4-one derivative (VIII).

Action of sodium azide and glacial acetic acid on (II): Formation of 1-(2′-carboxyphenyl)-5-(2′-thenyl)-tetrazole (IX)

A mixture of (II) (0.01 mol) in glacial acetic acid (5 mL) was treated with a solution of sodium azide (0.015 mol) in the least amount of water, the mixture heated on a boiling water-bath for 4 hours, the solid formed after dilution with water was filtered and crystallized from the suitable solvent to give the tetrazole derivative (IX) as colourless crystals.

Condensation of (II) with diethyl malonate: Formation of ethyl-0-(2-thenoylamino)-benzoylacetate (X)

A mixture of (II) (0.01 mol) and diethyl malonate (0.03 mol) in dry pyridine 50 mL was heated under reflux for 12 hours. The reaction mixture was poured onto ice/cold HCl, and the precipitated product was filtered off, and crystallised from a suitable solvent to give (X) as colourless crystals.

Condensation of (II) with ethyl cyanoacetate: Formation of 2-(2′-thenyl)-3-ethoxycarbonyl-3,4-dihydro-quinoline-4-one (IX)

A mixture of (II) (0.01 mol) and ethyl cyanoacetate (0.03 mol) in dry pyridine 50 mL was heated under reflux for 12 hours. The reaction mixture was poured into ice/cold HCl, and the precipitated product was filtered off, and crystallised from a suitable solvent to give 2-(2′-thiophenyl)-3-ethoxycarbonyl-3,4-dihydroquinoline-4-one (XI).

REFERENCES

[1] D. T. Zentmayer and E. C. Wagner, *J. Org. Chem.*, **14**, 967 (1949).

[2] R. M. Silverstein and G. C. Bassler, "Spectrometric Identification of Organic Compounds", New York — London Sydney, 1968.

[3] M. F. Ismail, N. A. Shams and M. I. Naguib, *Indian J. Chem.*, **20***B*, 394 (1981).

[4] Sammour, A. F. M. Fahmy and M. Mahmoud, *Indian J. Chem.*, **11**, 222 (1973).

[5] L. J. Bellamy, "The Infrared Spectra of Complex Molecules", John Wiley, New York, Second edition, 1958.

Revue Roumaine de Chimie, **33**, *8*, 839 – 845(1988)

TOPOLOGICAL AND EMPIRICAL MODELS. I

THE PREDICTION OF THE GIBBS ENERGIES OF FORMATION FOR ALKANES

OVIDIU IVANCIUC
Polytechnic Institute "Traian Vuia", Faculty of Chemical Technology,
Timişoara, Romania

Received May 16, 1987

The prediction ability for the standard Gibbs energies of formation for alkanes by using topological and empirical models is tested. A number of forty topological indices were used in correlations. Best results are obtained with equations using as parameters $^1\chi$, $^2\chi$, $^3\chi_P$, $^4\chi_P$, $^4\chi_{PC}$, $^5\chi_C$, $^5\chi_P$, W, I_{orb}, MCI, DRGI and RGI. Through the equations obtained the standard Gibbs energies of formation for alkanes are demonstrated to bear a strong relationship to topological characteristics.

1. INTRODUCTION

Accurate data about the fundamental physical and chemical properties of organic compounds are strongly needed to design and operate a large variety of technological installations. An answer to this inquiry is the existence of large compilations containing information on various physical and chemical properties of chemical compounds, under various conditions,[1] but they are of no great use when one searches for the properties of a new compound or a compound whose properties are not determined. For example, the number of alkane constitutional isomers increases very rapidly with the number of carbon atoms.[2] We cannot expect that the thermodynamic properties of so many chemical species can be determined in the laboratory. So it is practical to obtain relationships between the structure of chemical compounds and their thermodynamic properties in order to compute the unknown thermodynamic properties of isomers with higher number of carbon atoms. To solve this situation, physico-chemical properties were established, beginning with the work done by Kopp.[3] Usually, they are group additivity methods, ranging from those that consider as parameters the type of the chemical bonds to the more complex additivity functions of Smolenskii [4] and Tatevskii. [5]

Another method used in establishing correlations between structure and physico-chemical properties is to express the bonding topology of the molecular graph by a mathematical expression, which may be a matrix, a polynomial or a numerical index. Numerical indices developed in this way are called topological indices (TI).[6]

---

* Correspondence address : strada N. Grigorescu, 18/2, 2750 Hunedoara, Romania

The aim of the present paper is to establish equations for the prediction of the Gibbs free energy of formation (gas) of alkane using topological indices, and to make a comparison with the results obtained using various empirical additive schemes.

2. TOPOLOGICAL INDICES, ADDITIVE SCHEMES AND DATA USED

In the following, only the notation will be indicated for the forty topological indices used in correlations:

—The connectivity indices [7-10] ${}^{0}\chi$, ${}^{1}\chi$, ${}^{3}\chi_{P}$, ${}^{3}\chi_{C}$, ${}^{4}\chi_{P}$, ${}^{4}\chi_{C}$, ${}^{4}\chi_{PC}$, ${}^{5}\chi_{P}$, ${}^{5}\chi_{C}$, ${}^{5}\chi_{PC}$, ${}^{6}\chi_{P}$, ${}^{6}\chi_{C}$, ${}^{6}\chi_{PC}$
— The centric and quadratic indices [11] B, C, C′, Q, Q′
    B — the centric index
    C — the normalized centric index
    C′ — the binormalized centric index
    Q — the normalized quadratic index
    Q′ — the binormalized quadratic index
— The Gordon-Scantlebury index [12] N_2
— The Zagreb group index [13] M_1
— The Wiener index [14,15] W
— The Hosoya index [16] Z
— The Lovasz and Pelikan index [17] X_1
— Information indices on the graph distances [18] I_D^e, I_D^w, $\bar{I}_D^e$, $\bar{I}_D^w$
    I_D^e — the information content on the distribution of distances
    $\bar{I}_D^e$ — the mean information content on the distribution of distances
    I_D^w — the information content on realized distances
    $\bar{I}_D^w$ — the mean information content on realized distances
— Informational indices on the polynomial coefficients [18] I_{PC}, $\bar{I}_{PC}$:
I_{PC} — the information content on polynomial coefficients
$\bar{I}_{PC}$ — the mean information content on polynomial coefficients
— The graph orbits information index [19,20] $\bar{I}_{orb}$
— The chromatic information index [21] $\bar{I}_{chr}$
— Information analogous with the Randic index [22] $\bar{I}_{\chi}$
— The electropy index [23] ε
— Topological indices based on the generalized graph centre concept [24] RCI, DRCI, MCI, RGI, DRGI
— The informational centric index [24] $\bar{I}_C$

Also used in correlations was the number N of carbon atoms.

The source of data for the standard Gibbs energy of formation for alkane at 298 K was the Scott table.[1] Data on 37 isomers of alkanes between butane and octane were used in correlations.

An efficient way of equilibrium calculations for the ideal gases can be carried using standard thermodynamic properties of isomer groups, determined for alkanes in [25]. We have used their results concerning standard Gibbs energy of formation for alkane isomer groups in order to compare with the predictive ability of Ti's. With the same intention, we have used the following empirical additive schemes: the method of Tatevskii,[5] with nine parameters, the scheme of Seyfer and Smolenskii,[26] with twenty parameters, the method of van Krevelen,[27] with eight parameters and the method of Thisch [28,29] with ten parameters.

The statistical parameters for estimating the accuracy of correlations are the correlation coefficient R, the standard deviation s and the Fisher statistics F.

3. CORRELATIONAL ABILITY OF THE TOPOLOGICAL INDICES

Table 1 lists the regression coefficients as well as the statistical parameters obtained with equation

$$\Delta G^0_{f,\,298} = A_0 + A_1 P \tag{1}$$

where the property P represents the standard Gibbs energy of formation calculated with an additive scheme. However, we have to note that the additive schemes are intended to give a direct estimation of the physicochemical property under consideration, not through the agency of a correlation equation. We used this way in order to get a set of statistical parameters to compare with those obtained through equations (3), (5), (7) and (9). A good additive scheme should have A_0 close to 0 and A_1 close to 1. The method of Tatevskii satisfies these requirements, being the best one among the additive schemes used in this study:

Table 1

Regression coefficients and statistical parameters for equations of type (1)

Method	A_0	A_1	R	s	F
Tatevskii	0.478	1.01	0.987	1.87	1370.1
van Krevelen	2.19	1.05	0.968	2.97	523.8
isomer groups	7.82	1.24	0.953	3.60	345.9
Seyfer	−0.339	0.774	0.946	3.86	295.6
Thisch	3.98	1.17	0.880	5.63	120.5

$$\Delta G^0_{f,\,298} = 0.478\ (0.711) + 1.01(0.06)G \tag{2}$$

where G represents the standard Gibbs energy of formation computed with the method of Tatevskii and in parenthesis there are the 95% confidence intervals of the coefficients.

Table 2 gives the best seven equations of type

$$\Delta G^0_{f,\,298} = A_0 + A_1 TI \tag{3}$$

Table 2

Regression coefficients and statistical parameters for the best equations of type (3)

TI	A_0	A_1	R	s	F
N	−58.0	9.186	0.952	3.63	339.7
$\bar{I}_D^W$	−68.4	17.87	0.941	4.01	271.1
${}^0\chi$	−60.9	11.54	0.937	4.15	251.2
${}^1\chi$	−53.7	18.82	0.932	4.29	232.0
ε	−35.6	0.235	0.924	4.53	204.6
I_D^W	−15.9	0.098	0.908	4.98	163.7
W	−19.5	0.503	0.903	5.09	154.7

The best set of statistical parameters is obtained by the use of the carbon number N, but it is not a satisfactory equation :

$$\Delta G^0_{f,\ 298} = -58.0(7.25) + 9.19(1.01)N \tag{4}$$

In order to obtain better estimations, the set of 820 biparametric equations of type (5) was computed and the best ten equations are presented in table 3.

$$\Delta G^0_{f,\ 298} = A_0 + A_1 TI1 + A_2 TI2 \tag{5}$$

Table 3

Regression coefficients and statistical parameters for the best ten equations of type (5)

TI1	TI2	A_0	A_1	A_2	R	s	F
${}^1\chi$	${}^4\chi_{PC}$	−52.27	7.27	3.79	0.981	2.35	431.3
N	${}^3\chi_P$	−49.03	6.55	6.61	0.976	2.64	336.3
${}^3\chi_P$	I_D^W	−21.09	9.36	0.062	0.975	2.66	332.4
${}^2\chi$	M_1	−33.79	15.96	3.23	0.975	2.66	331.4
${}^3\chi_P$	W	−23.47	9.54	0.315	0.975	2.67	329.1
${}^1\chi$	${}^5\chi_C$	−53.93	18.49	7.94	0.973	2.77	304.6
${}^3\chi_C$	M_1	−40.91	−9.41	2.10	0.973	2.77	303.3
${}^1\chi$	$\bar{I}_C$	−51.04	24.46	−13.97	0.973	2.78	301.0
${}^1\chi$	RGI	−54.40	15.40	0.595	0.971	2.86	284.5
${}^1\chi$	${}^3\chi_P$	−44.88	12.51	7.89	0.971	2.90	277.2

Thus, even at this level of biparametric equation the topological method appears to give a reasonable basis for describing the effects of molecular structure on the standard Gibbs energy of formation. The best biparametric equation is obtained with two connectivity indices :

$$\Delta G^0_{f,298} = -52.34(13.48) + 17.27(2.39)^1\chi + 3.79(0.53)^4\chi_{PC} \qquad (6)$$

To test further the usefulness and validity of the topological model, the set of 10,660 three parameters correlation equations of type (7) was computed and the best ten of them were selected and presented in table 4.

$$\Delta G^0_{f,298} = A_0 + A_1TI1 + A_2TI2 + A_3TI3 \qquad (7)$$

Table 4

Regression coefficients and statistical parameters for the best ten equations of type (7)

TI1	TI2	TI3	A_0	A_1	A_2	A_3	R	s	F
$^2\chi$	M_1	MCI	−28.97	−14.00	2.497	0.036	0.989	1.83	479.9
$^1\chi$	$^3\chi_P$	MCI	−38.61	8.69	6.21	0.033	0.988	1.91	441.0
$^1\chi$	$^4\chi_{PC}$	$\overline{I}_{orb}$	−54.24	19.73	3.45	−2.88	0.988	1.92	435.3
$^3\chi_P$	$^4\chi_P$	MCI	−22.36	9.46	8.39	0.042	0.988	1.92	433.7
$^1\chi$	$^5\chi_C$	$^5\chi_{PC}$	−50.08	16.57	5.95	3.89	0.987	1.99	400.4
$^1\chi$	$^5\chi_P$	$^5\chi_C$	−59.36	20.82	−11.72	6.26	0.986	2.03	389.7
$^3\chi_P$	W	MCI	−23.49	7.94	0.223	0.028	0.985	2.08	369.4
$^0\chi$	$^2\chi$	RGI	−61.83	14.33	−11.15	0.784	0.985	2.08	368.9
$^1\chi$	$^4\chi_{PC}$	MCI	−47.71	14.49	2.94	0.020	0.985	2.09	366.0
$^1\chi$	$^4\chi_P$	$^4\chi_{PC}$	−45.39	13.72	6.06	4.76	0.985	2.09	363.7

Comparing the two important statistical parameters, correlation coefficient and standard deviation, of equation (2) with those of equation (8), we conclude that the topological model has a greater predictive ability.

$$\Delta G^0_{f,298} = -28.97(7.28) - 14.2(2.22)^2\chi + 2.497(0.396)M_1 + 0.036(0.006)MCI \qquad (8)$$

Taking into account the great number of equations with four parameters which can be formed by combinations of 41 parameters, we computed only a limited set of equations of type (9) from which a selection is presented in table 5. Of course, due to the limited search, they are not the best equations of type (9).

$$\Delta G^0_{f,298} = A_0 + A_1TI1 + A_2TI2 + A_3TI3 + A_4TI4 \qquad (9)$$

Use of two connectivity indices, the Zagreb group index M_1, and a topological index based on the generalized graph centre concept, MCI, provides the basis for an excellent correlation :

$$\Delta G^0_{f,298} = -28.90(7.64) - 13.11(2.58)^2\chi + 1.76(0.35)^4\chi_P + $$

$$+2.37(0.47)M_1 + 0.034(0.007)MCI \qquad (10$$

Table 5

Regression coefficients and statistical parameters for a selection of equations of type (9)

TI1	TI2	TI3	TI4	A_0	A_1	A_2	A_3	A_4	R	s	F
$^2\chi$	$^4\chi_P$	M_1	MCI	−28.90	−13.11	1.76	2.37	0.034	0.990	1.78	380.5
$^1\chi$	$^3\chi_P$	$^5\chi_C$	$^5\chi_{PC}$	−47.48	14.65	2.99	4.68	3.10	0.990	1.79	376.4
$^1\chi$	$^3\chi_P$	$^4\chi_{PC}$	I_{orb}	−51.41	17.97	3.04	2.36	−3.16	0.989	1.81	369.5
$^1\chi$	$^4\chi_P$	$^4\chi_{PC}$	MCI	−42.18	11.71	5.32	3.89	0.018	0.989	1.87	344.2
$^1\chi$	$^3\chi_P$	$^4\chi_{PC}$	MCI	−41.64	10.58	4.14	1.09	0.028	0.989	1.88	342.6
$^1\chi$	$^3\chi_P$	I_D^e	MCI	−41.89	10.59	5.84	−0.054	0.034	0.988	1.93	323.2
$^1\chi$	$^3\chi_P$	W	MCI	−37.46	8.02	6.33	0.019	0.033	0.988	1.94	321.2
$^3\chi_P$	W	I_D^W	MCI	−25.24	7.98	0.447	−0.045	0.030	0.986	2.09	274.9

Statistical evaluation of the computed equations concerning the estimation of standard Gibbs energies of formation for alkanes indicates that the topological models give best correlations and are using fewer parameters than the additive schemes.

Best results are obtained with equations which contain as parameters combinations of the following topological indices : the connectivity indices $^1\chi$, $^2\chi$, $^3\chi_P$, $^4\chi_P$, $^4\chi_{PC}$, $^6\chi_C$, $^6\chi_{PC}$, the Wiener index W, the graph orbits information index $\bar{I}_{orb}$, and the topological indices based on the generalized graph centre concept MCI, DRGI and RGI.

Through the equations obtained, the standard Gibbs energies of formation of alkanes is demonstrated to bear a strong relationship to topological characteristics.

REFERENCES

[1] D. W. Scott, "Chemical Thermodynamic Properties of Hydrocarbons and Related Substances : Properties of the Alkane Hydrocarbons, C_1 through C_{10} in the Ideal Gas State from 0 to 1500 K", U. S. Department of the Interior, Bureau of Mines Bulletin 666, 1974.

[2] J. V. Knop, W. R. Muller, K. Szymanski and N. Trinajstić, "Computer Generation of Certain Classes of Molecules", Kemija i Industrii, Zagreb 1985, p. 38.

[3] H. Kopp, *Ann. Chem.*, **41**, 79, 169 (1842).

[4] E. A. Smolenskii, *Zhur. Fiz. Khim.*, **38**, 1288 (1964).

[5] V. M. Tatevskii, "Metody rascheta fiziko-khimicheskikh svoystv uglevodorodov", Toptekhizd., Moscou, 1960.

[6] A. T. Balaban, I. Motoc, D. Bonchev and O. Mekenyan, *Top. Curr. Chem.*, **114**, 21 (1983), Eds. M. Charton and I. Motoc, Springer, Berlin.

[7] M. Randic, *J. Amer. Chem. Soc.*, **97**, 6609 (1975).

[8] L. B. Kier, L. H. Hall, W. J. Murray and M. Randić, *J. Pharm. Sci.*, **64**, 1971 (1975).

[9] L. B. Kier, L. H. Hall, W. J. Murray and M. Randić, *J. Pharm. Sci.*, **65**, 1226 (1976).

[10] L. B. Kier and L. H. Hall, "Molecular Connectivity in Chemistry and Drug Research", Academic, New York, 1976.

[11] A. T. Balaban, *Theor. Chim. Acta*, **53**, 355 (1979).

[12] M. Gordon and G. R. Scantlebury, *Trans. Faraday Soc.*, **60**, 605 (1964).

[13] I. Gutman and N. Trinajstić, *Chem. Phys. Lett.*, **17**, 535 (1972).

[14] H. Wiener, *J. Amer. Chem. Soc.*, **69**, 17, 2636 (1947).

[15] H. Wiener, *J. Chem. Phys.*, **15**, 766 (1947).

[16] H. Hosoya, *Bull. Chem. Soc. Japan*, **44**, 2332 (1971).

[17] L. Lovasz and J. Pelikan, *Period. Math. Hung.*, **3**, 175 (1973).
[18] D. Bonchev and N. Trinajstić, *J. Chem. Phys.*, **67**, 4517 (1977).
[19] N. Rashevsky, *Bull. Math. Biophys.*, **30**, 229 (1955).
[20] E. Trucco, *Bull. Math. Biophys.*, **18**, 129 (1956).
[21] A. Mowshowits, *Bull. Math. Biophys.*, **30**, 175, 225, 387, 533 (1968).
[22] S. H. Bertz, *J. Amer. Chem. Soc.*, **103**, 3599 (1981).
[23] W. T. Yee, K. Sakamoto and Y. J. L'Haya, *Rept. Univ. Electro-commun.*, **27**, 53 (1976).
[24] D. Bonchev, A. T. Balaban and U. Mekenyan, *J. Chem. Inf. Comput. Sci.*, **20**, 106 (1980).
[25] R. A. Alberty and C. A. Gehrig, *J. Phys. Chem. Ref. Data*, **13**, 1173 (1984).
[27] A. L. Seyfer and E. A. Smolenskii, *Zhur. Fiz. Khim.*, **38**, 2230 (1964).
[26] D. van Krevelen and H. Chermin, *Chem. Eng. Sci.*, **1**, 238 (1952).
[28] T. P. Thisch and T. K. Trong, *Canad. J. Chem. Eng.*, **54**, 344 (1976).
[29] T. P. Thisch, I. L. Duran and R. S. Remalho, *Ind. Eng. Chem.-Proc., Res. Dev.*, **10**, 576 (1971).

Revue Roumaine de Chimie, **33**, *9*, 847–848(1988)

COMPTES RENDUS

"Electronegativity" (K.D. Sem and C.E. Jørgensen, eds.), Structure and Bonding, No. 66, Springer-Verlag, Berlin, Hard cover, 188 pp, 138 DM, ISBN 3–540–17740–X.

The volume includes seven articles by well-known chemists who explore present-day theories and applications of the old electronegativity concept introduced by Pauling in 1932. As emphasized in the Editor's note, electronegativity which is perhaps the most popular intuitive concept in chemistry can now be treated as a quantum chemical parameter.

J. Mullay's chapter (Estimation of atomic and group electronegativities) reviews the classical and modern scales in critical fashion, indicating how widespread the scales have been used. While some of the scales are dimensionless (Sanderson's), most other ones have various units. Since Pauling's time, it was recognized that for one and the same element different orbitals or charges lead to different electronegativity values.

L.J. Bartolotti's chapter (Absolute electronegativities as determined from the Kohn-Sham theory) bridges the gap for putting electronegativity in the framework of quantum mechanics on the basis of density functional theory. The Kohn-Sham Lagrange multipliers are used and electronegativities are calculated as the chemical potential with inverted sign, and the chemical potential is in turn the derivative of the energy versus the number of electrons involved in ionization at constant external potential. In neutral atoms one obtains thus the Mulliken electronegativity formula.

J. A. Alonso and L. C. Balbás use simple density functional theory for quantitative computations of electronegativities of atoms and ions. By using improved electron density functionals (Weizsäcker type models) good agreement between theory and experiment is obtained for various atoms, and for small metallic particles as heterogeneous catalyst models.

J. L. Gazquez, A. Vela and M. Galván present a unified approach for the description of electronegativity (χ), Fukui functions and absolute hardness (η). Density functional theory allows to define hardness as half of the second derivative of energy with respect to the number of electrons involved in ionization at constant external potential. On applying the method of finite differences one obtains that in approximative form, with $I = E(Z - 1) - E(Z)$ and $A = E(Z) - E(Z + 1)$ being the ionization potential and electron affinity, respectively, then $2\chi \simeq I + A$, and $2\eta \simeq I - A$. Also, the derivative of the charge density is known as the frontier or Fukui function (different for electrophilic, nucleophilic or radicalic reactions), and this leads to a unified criterion for chemical reactivity. Kohn and Sham's method is again used.

K. D. Sen, M. C. Bohm and P. C. Schmidt's chapter (Electronegativity of atoms and molecular fragments) uses the approximate local density approach for calculating electronegativity and hardness values for atoms and molecules such as simple organic fragments or organolithium compounds assuming various geometries.

W. J. Moxtier (Electronegativity equalization and its applications) applies Sanderson's postulate on the equalization of electronegativities when two or more different atoms combine to form a molecule.

The final chapter by D. Bergman and J. Hinze is entitled "Electronegativity and charge distribution". This is the longest chapter and it presents detailed tables on electronegativities and parameters for elements in various valence states and for groups of atoms.

Three correlations with molecular properties are presented: with bond length, with NMR chemical shifts, and with proton affinities. The NMR data involve $^{13}C-NMR$ chemical shift differences between methyl and methylene carbon atoms bonded to various residues (54 compounds): the correlation ($r = 0.861$) is, however, fallacious according to the present reviewer and is exclusively due to the overwhelming influence of two groups of compounds, namely 19 having Et–O bonds and $\Delta\delta = 20$ to 60 ppm, and 22 having Et–C bonds and $\Delta\delta = 2 - 15$ ppm. Moreover, one compound $(EtO)_2SO_2$ is shown twice with two different numerical data.

All chapters provide a wealth of bibliographic references and are written by scientists actively contributing to the respective research area. The book is recommended to all chemists wishing to learn more up-to-date information on electronegativity than provided in current textbooks or in reviews such as that of H. Chermette and R. Lissilour (L'Actualité Chimique, April 1985, p. 59).

A. T. Balaban
Polytechnic Institute, Bucharest

B. K. Teo, "EXAFS: Basic Principles and Data Analysis" (Inorganic Chemistry Concepts vol. 9), Springer-Verlag, Berlin, 1986, 349 pp, hard cover, DM 188, ISBN 3–540–15833–2

The 9th volume in the series "Inorganic Chemistry Concepts" is concerned with a recent method, which has already become a powerful tool for structural analysis of chemical and biological systems: Extended X-ray Absorption Fine Structure (EXAFS) Spectroscopy. It is the merit of the editors to publish monographs included in these series, devoted to new experimental techniques or to some up-to-day information derived from "classical" techniques, such as magnetic measurements, Mössbauer spectroscopy, hot-atom chemistry etc.

Although the phenomenon of Extended X-ray Absorption Fine Structure has been known for a long time, only recent developments, initiated in early 1970s, have led to the recognition of the structural content of this technique, especially for structural analysis of chemical and biological systems, where conventional diffraction methods are not applicable. The utilization of synchrotron radiation-sources in EXAFS since 1975 greatly improved the acquisition and the quality of the EXAFS data. The phenomenon EXAFS refers to the oscillatory variation of the X-ray absorption as a function of photon energy beyond the absorption edge. The absorption can be determined from the measurement of the attenuation of X-rays upon their passage through a material.

The book contains eight chapters; the first one ("X-Rays and Electrons") provides the background of the generation of X-rays and their interaction with electrons in atoms and molecules. In the second chapter, the EXAFS spectroscopy is qualitatively described and Chapter 3 presents the main variables and functions; the EXAFS parameters as well as their effects and correlations are qualitatively and graphically discussed. Chapter 4 gives the background to the theory of EXAFS. It is extended to problems in the real world, emphasizing in Chapter 5 the physical significance of phase and amplitude problems, disorder effects and multiple scattering.

A discussion of the advantages of various approaches to data analysis in practice is given in Chapter 6; there are basically two major approaches to EXAFS data analysis: the Fourier transform and the curve fitting techniques. A compromise of these two methods is Fourier filtering followed by curve fitting, which is the most commonly used technique; other methods are described in some detail. A further improvement is theoretical amplitude and phase functions, to which the accuracy of EXAFS results is intimately related (Chapter 7). The last chapter is devoted to a description of multiple scattering and bond angle determination. The usefulness and the accuracy of this method are demonstrated by the author for three compounds: $Na_2Fe(CO)_4$, $K_2Pt(C_2O)_2$ and $K_2Pt(SO)_4.(H_2O)_2$, by comparison with classical X-ray crystallographic data. Extension of the application of the angle determination technique to a wide variety of systems is obvious: stereochemical information beyond the first coordination shell of inorganic and biological systems, ligation of simple molecules to biological molecules in solution etc.

The book includes seven very useful appendices providing data and functions for the understanding of EXAFS spectroscopy and interpretation of results. The literature coverage is up-to-date counting 1276 references.

The book "EXAFS: Basic Principles and Data Analysis" is very useful for scientists who are already working in the field of EXAFS spectroscopy as well as for researchers working in the fields of physics, chemistry, biology and material science.

Marius Andruh
Polytechnic Institute, Bucharest

P. Pyykkö, "Relativistic theory of atoms and molecules" (Lecture Notes in Chemistry, No. 41, Springer-Verlag, Berlin, Heidelberg, 1986).

The volume with this title represents, in the scientific literature, the first wide and systematic bibliographical evidence concerning the application of the relativistic theory to the field of structure of atoms and molecules. A major event in this study, the book of Professor Pekka Pyykkö from the University of Helsinki (started in co-operation with Dr. Paul Deselaux) comprises 3119 systematically ordered complete bibliographical references, covering the first seventy years (1916—1985) of the history of this important chapter of physics and physical chemistry.

The abundant bibliographical material is divided into eight chapters, corresponding to the following themes:

- One-particle problems
- Quantum electrodynamical effects
- Multielectron atoms: methods
- Multielectron atoms: results
- Symmetry
- Molecular calculations
- Solid-state theory
- Relativistic effects and heavy-element chemistry.

The volume also includes an introduction concerning the monographs and other general references, some coments on notation and terminology as well as a list of acronyms and symbols. The major and significant part of the volume is formed by the wide, well-ordered bibliography.

Written carefully and accurately, the present volume is a remarkable guide book for all those interested in the respective field.

V.E. Sahini
Polytechnic Institute, Bucharest

NOTE POUR LES AUTEURS

La Revue Roumaine de Chimie publie des articles en anglais, français, russe, allemand ou espagnol. Les auteurs sont priés d'envoyer des articles et des comptes rendus inédits.

Les manuscrits seront dactylographés à double interligne. La bibliographie, les tableaux et la légende des figures seront placés après le texte.

Si l'article fait partie d'une série numérotée, la partie précédente sera donnée comme première référence.

Chaque article sera précédé d'un résumé comprenant quinze lignes au maximum.

Les références bibliographiques dans le texte seront faites par des exposants sans parenthèses et paraîtront à la fin de l'ouvrage.

Les publications périodiques mentionnées dans la bibliographie seront présentées suivant les prescriptions internationales : le nom de l'auteur précédé de l'initiale du prénom, le titre du périodique abrégé conformément à « Chemical Abstracts » et souligné par une ligne, le numéro du tome indiqué par des chiffres arabes et souligné par deux lignes, suivi de la première page de l'article : à la fin, l'année de la parution sera placée entre parenthèses. Le numéro de la revue ne sera pas indiqué si les pages du volume sont numérotées consécutivement.

Les textes des livres ou traités inclueront : le nom des auteurs, précédé de l'initiale du prénom, le titre du livre entre guillements et sans être souligné, le numéro du tome précédé par l'abréviation « vol. » (ou « Bd »), le numéro de l'édition, les éditions (the publisher), la localité de la parution du livre, l'année de la parution et la page de la référence précédée par l'abréviation « p » (ou « S »).

Les brevets seront indiqués comme suit : l'auteur ou la firme, le pays et le numéro du brevet, la date de la revue (*Chem. Abstr.*). Par ex. : M. Jones (to Union Carbide Co.) Brit. Pat. 610 238,2 Sept. 1959 : cf. *Chem. Abstr.*, **54**, 12808 (1960).

Si la référence n'a pas été lue en original, on indiquera aussi la revue de références consultée.

Les diagrammes seront tracés à l'encre de Chine sur papier calque. Les tableaux et les figures (en nombre strictement nécessaire), ainsi que les courbes dans les figures seront numérotés par des chiffres arabes. Leur explication sera donnée dans la légende des figures. Prière de ne pas inscrire les mêmes données dans les tableaux et les figures. Chaque tableau aura un titre. On indiquera dans le texte la place approximative des tableaux et des figures. Les formules chimiques seront incluses dans le texte ; en outre, elle seront transcrites sur papier calque, à l'encre de Chine.

Les auteurs sont priés d'indiquer les caractères italiques (en soulignant les lettres au crayon), ainsi que tout autre caractère spécial : les préfixes *ortho*, *méta*, *para*, *cis*, *trans*, etc. seront soulignés pour indiquer leurs caractères italiques, et ne seront jamais écrits avec des majuscules.

Aucune correction à la main ne sera admise sur le manuscrit. Les corrections seront frappées à la machine. Les lettres grecques ou d'autre symboles spéciaux seront insérés à la main à l'encre clairement.

Le manuscrit sera signé par l'auteur.

Le titre courant aura 50 lettres au maximum.

L'entière responsabilité du contenu des articles appartient aux auteurs.

Sur demande on peut obtenir une note plus complète.

PRINTED IN ROMANIA

PETROLEUM AND GAS INSTITUTE
(INSTITUTUL DE PETROL ȘI GAZE)

B-dul București No. 39
Ploiești
ROMANIA

Founded in 1948, the Petroleum and Gas Institute furthering the tradition of the Romanian education and training in petroleum, brings its direct contribution to the development and modernisation of the petroleum and gas industry in Romania and to the Romanian science and technology in this field, both by providing specialists with a high professional training and by the research work carried out by the teaching staff.

The Institute is thus one of the most important higher technical education units in this field throughout the world.

The Institute has two faculties :

The Faculty of Petroleum and Gas Drilling and Production

The Faculty of Petroleum Equipment and Petrochemical Engineering with the following departments :

- **Engineering for Petroleum and Petrochemical Equipments**
- **Petroleum Refinary and Petrochemical Engineering**

Petroleum and Gas Institute awards the degrees master and doctor of Engineering Science.

The Institute organizes and provides the following post graduate university and specialization courses : petroleum reservoir engineering ; petroleum production and transport ; equipment for refineries and petrochemical plants ; equipment for drilling and production ; engineering of petroleum and petrochemical processes.

The Institute grants technical assistance to industrial units, research centers and higher education institutes.

Nouveaux produits de l'entreprise de détergents DERO PLOIEŞTI

PLASTIFIANT CN

Utilisé à la réception de fabrication des tapis roulants à insertion métallique pour augmenter l'adhérence du caoutchouc au fil de fer.

ACCELERATOR 6 %

Utilisé comme accélérateur pour endurcir les lacs polyestériques non saturés.

LUBREFIANT C. 175

Utilisé à la tréfilation des fils d'acier dur laitonnés, nécessaires à la fabrication de la corde métallique.

DEROPOR T6

Utilisé à la préparation des bétons légers et thermo-isolants pour les constructions, en leur conférant un poids réduit et une grande résistance thermique.

Liquides pénétrants d'usage nucléaire

On les livre par lots de trois produits:

- *pénétrant Deropen N1*
- *dégraissant Derogres N1*
- *développant Derodev N1*

ORSZÁGOS MŰSZAKI INFORMÁCIÓS KÖZPONT ÉS KÖNYVTÁR 1883 H

[illegible]

TRAVAUX PARUS AUX ÉDITIONS DE L'ACADÉMIE DE LA RÉPUBLIQUE SOCIALISTE DE ROUMANIE

ELENA CEAUŞESCU, **Răşini de hidrocarburi, vol. 1**, 1988, 344 p.
ELENA CEAUŞESCU, **Progrese în chimia şi tehnologia polimerilor**, 1986, 446 p.
ELENA CEAUŞESCU, **Forschungen im Bereich der Chemie und Technologie der Polymere**, 1986, 444 p.
ELENA CEAUŞESCU, **Cercetări în chimia şi tehnologia polimerilor**, 1983, 520 p.
ELENA CEAUŞESCU, **Noi cercetări în domeniul compuşilor macromoleculari**, 1981, 536 p.
ELENA CEAUŞESCU, **Polimerizarea stereospecifică a izoprenului**, 1979, 307 p.
ELENA CEAUŞESCU, **Research work on synthesis and characterization of macromolecular compounds. Contributions**, 1974, 251 p.
I. G. MURGULESCU, **Introducere în chimia fizică, Vol. I. 1. Atomi, molecule, legătură chimică**, 1976, 560.
I. G. MURGULESCU, V. EM. SAHINI, **Introducere în chimia fizică, Vol. I. 2. Structura şi proprietăţile moleculelor**, 1979, 604 p.
I. G. MURGULESCU, E. SEGAL, **Introducere în chimia fizică, Vol. II. 1. Teoria molecular-cinetică a materiei**, 1979, 1036 p.
I. G. MURGULESCU, TATIANA ONCESCU, E. SEGAL, **Introducere în chimia fizică. Vol. II. 2. Cinematică chimică şi cataliză**, 1981, 1024 p.
I. G. MURGULESCU, J. PĂUN, **Introducere în chimia fizică, Vol. I. 3, Nucleul atomic, reacţii nucleare, particule elementare**, 1982, 606 p.
I. G. MURGULESCU, RODICA VÎLCU, **Introducerea în chimia fizică, Vol. III. Termodinamica chimică**, 1982, 624 p.
I. G. MURGULESCU, O. M. RADOVICI, **Introducere în chimia fizică, vol. IV, Electrochimia**, 1986, 410 p.
CRISTOFOR I. SIMIONESCU, VALERIA GORDUZA, **Implicaţii bioenergetice ale coloranţilor**, 1988, 208 p.
R. VÎLCU, M. LECA, **Termodinamica polimerilor prin cromatografie de gaze**, 1987, 238 p.
I. ZUGRĂVESCU, M. PETROVANU, **Cicloadiţii 3+2-dipolare**, 1987, 446 p.
RAUL MIHAIL, ION GROZEANU, **Estimarea secvenţială aplicată sistemelor chimice**, 1986, 406 p.
M. BREZEANU, L. PATRON, M. ANDRUH, **Combinaţii complexe polinucleare şi aplicaţiile lor**, 1986, 244 p.
A. T. BALABAN et al., **Labelled compounds and radiopharmaceuticals applied in nuclear medicine**, coédition avec John Wiley and Sons, 1986, 742 p.
D. PURDELA, **Nomenclatura chimiei organice — IUPAC**, 1986, 454 p.
PETRU BUDRUGEAC, **Probleme de chimie**, 1986, 280 p.
T. ONCESCU, S. G. IONESCU, **Conversie fotochimică şi stocare de energie**, 1985, 272 p.
V. DRĂGUŢAN, A. T. BALABAN, M. DIMONIE, **Olefin Metathesis and Ring-Opening Polymerization of Cyclo-Olefins**, coédition avec John Wiley and Sons, 1985, 544 p.
C. LITEANU, I. RICA, **Optimizarea proceselor analitice**, 1985, 360 p.
N. PERESCU, **Chimia extracţiei cu solvenţi şi aplicaţii**, 1985, 212 p.
V. E. SAHINI, M. HILLEBRAND, **Chimie cuantică în exemple şi aplicaţii**, 1984, 378 p.
GH. MARCU, **Chimia compuşilor coordinativi**, 1984, 415 p.
E. CORDOŞ, C. MANOLIU, **Spectrometria de absorbţie şi fluorescenţă atomică**, 1984, 178 p.
C. BODEA, **Tratat de biochimie vegetală, p. II, t. 5**, 1984, 438 p.
N. ASANDEI, A. GRIGORIU, **Chimia şi structura fibrelor**, 1983, 395 p.
N. IONESCU, M. CĂLDĂRARU, **Oxidarea catalitică a olefinelor inferioare**, 1983, 178 p.
C. CAŞCAVAL, **Studiul polimerilor prin piroliză şi cromatografie de gaze**, 1983, 220 p.
C. I. SIMIONESCU, F. DANES, **Originea vieţii**, 1983, 110 p.
C. BODEA, **Tratat de biochimie vegetală, p. II. t. IV**, 1982, 480 p.
I. GĂLĂŢEANU, **Procese şi metode radiochimice în energetica nucleară**, 1981, 234 p.
CR. SIMIONESCU, VALERIA GORDUZA, **Polimeri biocompatibili şi biologic activi**, 1980, 479 p.
M. FLORESCU, **Metode ştiinţifice în dezvoltarea industriei chimice moderne**, 1979, 256 p.
C. GH. MACAROVICI, **Analiza chimică cantitativă anorganică**, 1979, 457 p.
I. ZUGRĂVESCU, MAGDA PETROVANU, **N-ylid chemistry**, coédition avec McGraw-Hill International Book Company U.S.A., 1977, 386 p.

ISSN 0035—3930

I. P. Informaţia c. 2278

43 426

Lei 40

F 1103 04 ~~66~~

ACADÉMIE DE LA RÉPUBLIQUE SOCIALISTE DE ROUMANIE

REVUE ROUMAINE DE CHIMIE

TOME 33
N°s 9–10
Septembre—Octobre 1988

Rev. Roumaine Chim. RRCHAX, 33, *9–10*, p. 849–944 (1988), Bucarest
EDITURA ACADEMIEI REPUBLICII SOCIALISTE ROMÂNIA

ACADÉMIE DE LA RÉPUBLIQUE SOCIALISTE DE ROUMANIE

COMITÉ DE RÉDACTION

Rédacteur en chef:

I. G. MURGULESCU, membre de l'Académie de la République Socialiste de Roumanie

Rédacteurs en chef adjoints:

A.T. BALABAN et V.EM. SAHINI, membres correspondants de l'Académie de la République Socialiste de Roumanie

Collège de rédaction:

EM. BRATU, ELENA CEAUŞESCU, ECATERINA CIORĂNESCU-NENITZESCU, CR. SIMIONESCU, membres de l'Académie de la République Socialiste de Roumanie ; P. SPACU, membre correspondant de l'Académie de la République Socialiste de Roumanie ; M. BANCIU, M. D. GHEORGHIU, I. HAIDUC, D. I. MARCHIDAN, G. NIAC et D. SĂNDULESCU

La Revue Roumaine de Chimie paraît 10 fois par an. Toute commande de l'étranger sera adressée à ROMPRESFILATELIA — sectorul Export-Import Presă, P. O. Box 12—201, télex 10376, prsfi r 78 104 Bucarest, Calea Griviţei nr. 64—66, Roumanie

Les manuscrits, les livres et les revues proposés en échange, ainsi que toute correspondance seront envoyés à la rédaction

REVUE ROUMAINE DE CHIMIE
125, Calea Victoriei, 79717 Bucarest, Roumanie, téléphone 50 76 80

EDITURA ACADEMIEI REPUBLICII SOCIALISTE ROMÂNIA
125, Calea Victoriei, 79717 Bucarest, Roumanie, téléphone 50 76 80

REVUE ROUMAINE DE CHIMIE

Tome 33, N°s 9—10 **Septembre—Octobre, 1988**

IOAN SILAGHI-DUMITRESCU and IONEL HAIDUC, Electronic structure and bonding in diamidoboron cations. A molecular orbital study of $[H_2NBNH_2)^+$ . . . . 851—856

M. P. ALVAREZ MACHO, A kinetic and mechanistic study of reduction of Cr(VI) by acetone in sulfuric acid medium (in Spanish) . . . . 857—863

M. F. ABDEL MEGEED, M. GABER, R. M. ISSA and H. A. IBRAHIM, Mass spectral fragmentation pattern studies of tartaric acid hydrazide and some of its arylidene derivatives . . . . 865—874

M. M. ABDEL BADEI and M. F. EL-SHAHAT, Oxidative microdetermination of some inorganic sulphur compounds by indirect spectrophotometric method using ferricyanide-thymolphthalein reagent and osmium tetroxide as a catalyst . . . . 875—879

JAN OGONOWSKI, The influence of activators on activity of PbO/MgO catalyst in the reaction of oxidative dehydrodimerization of toluene . . . . 881—884

IOANA ILIE, MARIA BREZEANU, LUMINIȚA PATRON, E. SEGAL and G. FILOTI, Synthesis of nickel ferrite from polynuclear coordination compounds. Part III. Structural data of $NiFe_2O_4$ obtained by the wet ferritization method . . . . 885—891

M. BANCIU, ANCA BANCIU, M. ELIAN, C. DRĂGHICI, N. PALIBRODA and ECATERINA CIORĂNESCU, Synthesis of bis (9,10-phenanthro) [*a*, *e*]cycloocta-1,5-diene by sulphone pyrolysis . . . . 893—901

F. IORDACHE, MARIANA DĂNILĂ, ANA SCHIKETANZ, M. GHEORGHIU and F. BADEA, The reaction of cyclohexa-3,5-diene-1,2-dicarboxylic acid derivatives with *para*-benzoquinone and azo compounds. I . . . . 903—910

ALEXANDRU CAȘCAVAL and ȘTEFAN CILIANU BIBIAN, 2-Hydroxyketones. XX. New *Mannich-Werner* bases of 7-hydroxy-4-methyl-6- and 8-propionylcoumarin . . . . 911—916

R. AGARWAL and P. BEHADUR, Synthesis of 2-alkyl-7-benzo-coumaranones 917—919

A. CĂLUȘARU, Mathematical foundation of chemical transformations on the basis of REDOX and COLHOM processes . . . . 921—935

VICTOR DAVID, An informational representation of the spectral analytical systems as communication systems with data decoding . . . . 937—942

BOOK REVIEWS 943

Rev. Roumaine Chim. 33, *9—10*, 849—944 (1988), Bucarest

Revue Roumaine de Chimie, 33, *9–10*, 851–856 (1988)

ELECTRONIC STRUCTURE AND BONDING IN DIAMIDOBORON CATIONS. A MOLECULAR ORBITAL STUDY OF $[H_2NBNH_2]^+$

IOAN SILAGHI-DUMITRESCU and IONEL HAIDUC *
Chemistry Department, Babeș-Bolyai University, R-3400 Cluj-Napoca, Romania

Received November 14, 1987

A molecular orbital treatment of the bonding in diamidoboron cations $[R_2NBNR_2]^+$ has been undertaken. The calculations show the preference of these systems for D_{2d} allene type conformation, due to a more efficient π bonding than in the case of D_{2h} planar conformation. The CNDO/2 BN bond order (1.63) is in good agreement with the available infrared data.

INTRODUCTION

The existence of dicoordinated boron cations was suggested in the early seventies.[1,2] A diphenylboron cation, Ph_2B^+, was postulated even earlier, as the reaction product of diphenylboron chloride and aluminium chloride,[3,4] but the Pariser–Parr–Pople calculations reported by Armstrong and Perkins[5] showed that such a cation should add a donor solvent and become tricoordinate. Recent reports, however, firmly established the existence of $[(iPr)_2NBN(iPr)_2{}^+]$[6], $[tmpBNR_2]^+$ (tmp = 2, 2, 6, 6 tetramethylpiperidino),[7] and, in addition an X-ray structure determination of the later (R = Me) unequivocally demonstrated its allene type skeleton.

Cations such as $[R_2NBNR_2]^+$ arouse some interesting questions about the bonding realized by the central, coordinately unsaturated boron atom. A point to discuss arises from the cannonical formulas which can be written:

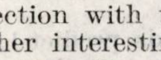
1

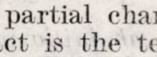
2

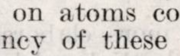
3

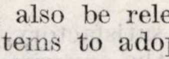
4

i.e. to what extent the BN bond is a classical single or double bond. In connection with this, partial charges on atoms could also be relevant. Another interesting fact is the tendency of these systems to adopt an allene type D_{2d} conformation against the planar one of D_{2h} symmetry.

---

* Author to whom all correspondence should be addressed

In order to throw some light on these problems we performed molecular orbital calculations on the model $[H_2NBNH_2]^+$ cation.

CALCULATIONS

The molecular orbital calculations have been carried out with, frequently used, approximations – Extended Hückel [8] and CNDO/2.[9] The Slater type orbitals with standard parameters were used. For hydrogen 1s orbitals the 1.2 value of exponent was taken instead of 1.0 expected from the Slater rules. The coordinate reference system use in this work is given in Figure 1.

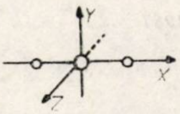

Fig. 1. – The reference coordinate system used throughout this paper. For D_{2h} symmetry the hydrogen atoms lie in the xz plane. For D_{2d}, two are in the yz and two in the xz planes respectively.

Only the heavy atom positions are shown, the coordinates of hydrogen atoms depend on the particular symmetry adopted for calculations. Planar D_{2h}, allene type D_{2d}, and also C_{2h} nonplanar models have been taken into consideration. For D_{2h} and D_{2d} symmetry, BN bond length, and (HBN, BNH) dihedral angles were varied until the minimum of the total energy was reached. NH bond lengths and HNH bond angles were kept fixed during the search for minimum.

The CNDO/2 calculations were done by a modified version of the PARAMOL 2 program.[10] For the Extended Hückel treatment we designed a super-Basic program for a SINCLAIR QL microcomputer. A typical run, without compilation takes about 15 minutes for a 16 orbital system.

RESULTS AND DISCUSSION

The energies of D_{2h} and D_{2d} conformers, at various BN bond lengths are listed in Table 1. Hence the equilibrium BN bond length is 1.141 Å for the planar cation, and 1.38 Å for the allene type conformer. This value is quite satisfactory, as more elaborated, *ab initio* methods predict 1.33 Å, while the experimental BN bond length from X-ray structure determinations lies between 1.42 Å and 1.33 Å (from $[Me_2NB(tmp)]^{+7}$ and (benzyl-t-butylamino) borinium cation [11] respectively). Note that the D_{2d} conform-

Table 1

The energies of $[H_2NBNH_2]^+$ D_{2h} and D_{2d} conformers at various BN bond lengths (a.u.)

R_{BN} (Å)	D_{2h}	D_{2d}
1.44	−29.6900	−29.7046
1.42	−29.6969	−29.7123
1.40	−29.7001	−29.7162
1.38	−29.7012	−29.7184
1.36	−29.6982	−29.7161
1.34	−29.6898	−29.7086

er appears to be favorized by about 11 kcal/mole. The *ab initio* calculation of Nöth et al. [7] also predicts the preference of this system for the allenic structure D_{2d}; their energy difference is, however, higher — 18 kcal/mole.

Other geometries inspected include those belonging to C_{2h} point group, derived from the planar D_{2h} by twisting the hydrogen atoms of the amino groups out of the xz plane (two hydrogens above and the other two, under this plane) — Figure 2.

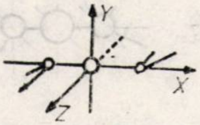

Fig. 2. — The C_{2h} model investigated.

Both CNDO/2 and Extended Hückel methods give higher total energies than for the parent planar cation, suggesting that pyramidal nitrogen is less favorable in this system than the planar one; subsequently only the D_{2h} and D_{2d} conformers will be referred.

To check whether the lower energy of D_{2d} conformer is due to some interactions between nonbonded atoms or is a consequence of interactions between chemically bonded (directly bonded) atoms, we inspected the E_{AB} components of total energy (for the expansion of the total energy in terms of monoatomic and biatomic components, see ref. 12). These values are given in Table 2.

Table 2

E_{AB} components of total energy of $[H_2NBNH_2]^+$ (values for D_{2d} are above the main diagonal) (a.u.)

D_{2d} D_{2h}	B_1	N_2	N_3	H_4	H_5	H_6	H_7
B_1		−1.4198	−1.4198	0.0045	0.0045	0.0045	0.0045
N_2	−1.3974		0.0128	−0.7317	−0.7317	−0.0090	−0.0090
N_3	−1.3974	0.0125		−0.0090	−0.0090	−0.7317	−0.7317
H_4	0.0018	−0.7286	−0.0103		0.0025	0.0076	0.0076
H_5	0.0018	−0.7286	−0.0103	0.0219		0.0076	0.0076
H_6	0.0018	−0.0103	−0.7286	0.0086	0.0086		0.0025
H_7	0.0018	−0.0103	−0.7286	0.0086	0.0086	0.0219	

At the first sight, the interactions between nonbonded atoms seem to favor the planar D_{2h} structure ($E_{B\cdots H}$ is repulsive, 0.0045 au for D_{2d} and only 0.0018 au for D_{2h} : $E_{N\cdots H} = -0.0090$ au for D_{2d} and -0.0103 au for D_{2h}, giving a net attractive result, greater for D_{2h}) but chemically bonded atoms generously overcome this difference (see for example $E_{B-N} = -1.4198$ au for D_{2d} versus -1.3974 au for D_{2h}). Hence the difference in the energies of the conformers stems in the electronic effects accompanying the formation of BN bonds and not in the through-space interactions between chemically non-bonded atoms. In other words, in the D_{2d} conformer, the available orbitals and electrons are used in a more economical way, so that stronger bonds are realized. How the atomic orbitals combine to give this effect can be inferred from the composition and energy of the molecular orbitals.

The molecular orbitals of $[H_2NBNH_2]^+$

The approximate shape of molecular orbitals of $[H_2NBNH_2]^+$ are sketched in Figure 3. Since the qualitative features of these orbitals provide enough information, no attempts have been made to scale these pictures.

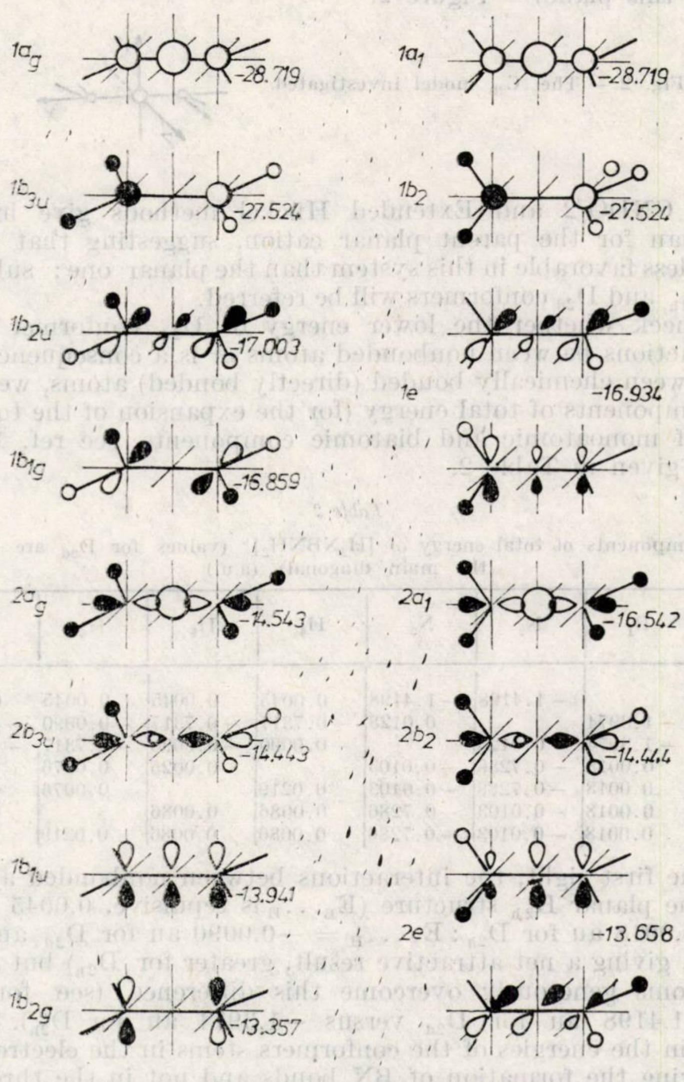
D_{2h}
D_{2d}
$1a_g$
-28.719
$1a_1$
-28.719
$1b_{3u}$
-27.524
$1b_2$
-27.524
$1b_{2u}$
-17.003
$1e$
-16.934
$1b_{1g}$
-16.859
$2a_g$
-14.543
$2a_1$
-16.542
$2b_{3u}$
-14.443
$2b_2$
-14.444
$1b_{1u}$
-13.941
$2e$
-13.658
$1b_{2g}$
-13.357

Fig. 3. — Approximate shape of occupied molecular orbitals. Energ levels from extended Hückel calculations of the two conformers are given for comparison.

As expected, the lowest m.o.'s are composed mainly from the in-phase combinations of *s* orbitals, and describe the σBN and σNH bonds respectively ($1a_g$, $1b_{3u}$ for D_{2h} and $1a_1$, $1b_2$ for D_{2d}). Although the next two m.o.'s have different shapes for the two conformers ($1b_{2u}$, $1b_{1g}$ of D_{2h} and the degenerate pair 1e of D_{2d}), all of them essentially describe σNH bonds coming from nitrogen 2p and hydrogen 1s orbital interactions. The following molecular orbitals of D_{2d} ($2a_g$ and $2b_{3u}$) are extended over the whole skeleton, they belong to the σ framework of molecule. The corresponding $2a_1$ and $2b_2$ of D_{2d} conformer parallel in shape and energy $2a_g$ and $2b_{3u}$ of D_{2h} respectively. So far no sensible difference between D_{2d} and D_{2h} conformers can be noticed.

The highest occupied m.o.'s of D_{2d} are of π type, they have very small contributions from the hydrogen 1s orbitals; this 2e set is quite well localized at the level of the two BN bonds. Taking now a look at the D_{2h} orbitals we remark that only $1b_{1g}$ is bonding while the next (and last) occupied mo ($1b_{2g}$) is nonbonding. As all σ mo's have almost the same energies in the two conformers, the $D_{2d} - D_{2h}$ energy difference is due to different ways of realizing the π bonding. In the first case (D_{2d}) we can talk about two π bonds but in the planar (D2h) conformer only one π bonding molecular orbital is delocalized over three centers. Thus a stronger π bonding system is achieved in the allene type D_{2d} conformer. This result is in agreement with the conclusions of Burdett and Albright[13] based on the angular overlap model which predicts that sharing the central atom orbital (2p of boron in our case) is not favored if the M−L bonding partner is occupied.

Orbital population and bond orders

The CNDO/2 wave functions at the optimum energy give the orbital populations shown in Table 3.

Table 3

Orbital populations in $[H_2NBNH_2]^+$

	D_{2d}	$s + p_x$	$p_y + p_z$	D_{2h}	$s + p_x$	$p_y + p_z$
B						
2s	0.857	1.593		0.875	1.626	
$2p_x$	0.736			0.751		
$2p_y$	0.483		0.966	0.365		0.930
$2p_z$	0.483			0.565		
charge	0.441			0.444		
N						
2s	1.187	2.457		1.180	2.435	
$2p_x$	1.270			1.285		
$2p_y$	1.113		2.740	1.094		2.811
$2p_z$	1.627			1.717		
charge	−0.196			−0.250		
H						
1s	0.761			0.752		

It is noteworthy that the boron $2p_y$ and $2p_z$ orbitals, initially empty, have appreciable population which denotes a remarkable π bonding by donation from nitrogen 2p orbitals. However, the nitrogen atoms do not reach positive charge, since the σBN bonds have oposite polarity. In this respect the resonances 1—4 are not complete, as they imply only π electron delocalization and the charges assigned to atoms are not real charges. To be more explicit, a multiple BN bond does not imply necessarily a (real) positive charge on nitrogen or otherwise, a (formal) negative charge on nitrogen does not mean that only a single BN bond is formed.

As a measure of bond multiplicity we use here the Wiberg bond index.[14] Its value of 1.63 for the BN bond is indeed indicatory for a quite strong π bond. This magnitude of the BN bond order is supported by an estimation of the BN force constant calculated by using Siebert's formula[15] and of the BN bond vibration frequency. A force constant of 7.85 mdyne/Å leads to $\nu_{BN} = 1869$ cm^{-1}, in good agreement with the frequencies of boron-nitrogen bonds (1830—1900 cm^{-1}) compiled in reference.[16]

REFERENCES

1. H. Nöth, *Progr. Boron Chem.*, **3**, 211 (1970).
2. R. Schnell, Ph. D. Thesis, Univ. of Marburg, 1969.
3. J. M. Davidson and C. M. French, *J. Chem. Soc.*, **114** (1958) ; 3364 (1962).
4. R. B. Moodie, B. Ellut and T. M. Connor, *Chem. Ind.* (London), 767 (1966).
5. D. R. Armstrong and P. G. Perkins, *J. Chem. Soc.* A, 1026 (1966).
6. J. Higashi, A. D. Eastman and R. W. Parry, *Inorg. Chem.*, **21**, 716 (1982).
7. H. Nöth, R. Staudigl and H. W. Wagner, *Inorg. Chem.*, **21**, 706 (1982).
8. R. Hoffman, *J. Chem. Phys.*, **39**, 1397 (1963).
9. J. A. Pople and G. A. Segal, J. Chem. Phys., **43**, S129, S136 (1965).
10. D. A. Zhogolev and V. B. Volkov, "Methods, Algorithms and Programs for Quantochemical Calculations of Molecules" (in Russian), Kiev, Naukova Dumka, 1976.
11. Quoted in ref. 16.
12. F. K. Fischer and H. Kolmar, *Theor. Chim. Acta*, **13**, 213 (1969).
13. J. K. Burdett and T. A. Albright, *Inorg. Chem.*, **18**, 2112 (1979).
14. K. B. Wiberg, *Tetrahedron*, **24** 1083 (1968).
15. H. Siebert, *Z. anorg. allg. chem.*, **273**, 170 (1953) ; **274**, 24, 34 (1953).
16. P. Kolle and H. Nöth, *Chem. Rev.*, **85**, 411 (1985).

Revue Roumaine de Chimie, **33**, *9–10*, 857–863 (1988)

ESTUDIO CINÉTICO DE LA REDUCCIÓN DEL Cr(VI) POR ACETONA EN MEDIO DE ÁCIDO SULFÚRICO

M. P. ALVAREZ MACHO

Departamento de Química Física, Facultad de Ciencias, Universidad 47005 Valladolid, España

Recibido: el 25 de Mayo de 1987

Se ha realizado un estudio cinético de la reducción de Cr(VI) por acetona. La reacción procede en dos etapas, la primera produciendo Cromo (V) y la segunda Cr(IV). Ambas etapas son de primer orden en acetona, mientras que el oxidante cambia el orden de uno a cero. La variación de la velocidad de reacción con la concentración de ácido ha sido analizada en términos de la función de acidez de exceso (función X). Se propone un possible mecanismo.

The kinetics of the reduction of Cr(VI) by acetone has been studied. The reaction proceeds in two stages, the first giving chromium (V) and the second giving chromium (IV). Both stages are first order in acetone, a change from first- to zero-order dependence in the oxidant. The variation in reaction rate with varying acid concentration is treated in terms of the "excess acidity" of the medium (X-function). A possible mechanisms is discussed.

INTRODUCCIÓN

La reacción de oxidación de cetonas por Cr(VI) en medio ácido ha sido estudiada por Littler[1] y Roček[2] quienes siguen la evolución de la reacción haciendo uso de técnicas espectrofotométricas, empleando el método de las velocidades iniciales de Van't Hoff[3] para el análisis de los datos cinéticos. Ambos investigadores se han centrado preferentemente en la oxidación de la ciclohexanona y derivados, y proponen un mecanismo en el que la reacción tiene lugar a través del enol, pero en el orden de reacción respecto de la especie oxidante no se ponen de acuerdo.

Por otra parte, en una investigación precedente[4] realizada en este Departamento, se encontró que valencias intermedias del cromo influyen en las etapas determinantes en los procesos de oxidación crómica de compuestos orgánicos.

En el presente trabajo se ha realizado un estudio cinético de la reacción de propanona con dicromato potásico en medio de ácido sulfúrico. Se analiza el papel de las valencias intermedias del cromo en el mecanismo de reacción propeuesto, y se interpretan los resultados experimentales a través de etapas monoelectrónicas.

PARTE EXPERIMENTAL

El estudio cinético se ha realizado mediante un método dinámico, tomando como especie química de control et Cr (VI), cuya concentración en cada instante se determinaba midiendo la correspondiente absorción a 350 nm en un espectrofotómetro Perkin Elmer modelo Coleman 55, provisto de una microcubeta termostatada mediante un flujo de agua procedente de un termostato Heto que garantiza la constancia de la temperatura de ±0.05°C.

En todos los experimentos la mezcla de reacción ha sido obtenida como se indica: Se preparaba una disolución de dicromato potásico utilizando como disolvente una disolución acuosa de ácido sulfúrico y se anadía un volumen determinado de acetona, de tal forma que al final la la mezcla reaccionante fuese de las concentraciones adecuadas.

Los reactivos empleados: acetona y dicromato potásico fueron, Merk, el ácido sulfúrico de Panreac y se utilizó agua bidestilada para la preparación de las disoluciones.

ECUACIÓN DE VELOCIDAD

Dadas las condiciones experimentales, se ha trabajado en exceso de las concentraciones de todos los reactivos frente a la concentración de Cr(VI), siendo ésta, la única concentración que varia de forme apreciable durante el proceso de reacción. Además, se han analizado los datos cinéticos mediante el método diferencial de Letort[3] encontrándose que el orden cinético respecto del tiempo para la especie Cr(VI) estaba comprendido entre $0{,}48 < n_t < 0{,}80$ y que disminuia a medida que aumentaba la acidez del medio. De esto se ha deducido que alguno de los productos intermedios de la reacción intervienen en las etapas determinantes del mecanismo.

Una vez orientados sobre el cambio de orden parcial de la especie cinéticamente activa Cr (VI), el paso siguiente ha sidom proponer un esquema de reacción en el que intervienen especies intermedias de Cr y deducir la ecuación de velocidad[4,5]; por último, comprobar si los valores experimentales de concentración de Cr (VI)—tiempo cumplen la ecuación integrada de velocidad.

Esquema del mecanismo

$$\mathrm{Cr\ (VI)} + \mathrm{S} \xrightarrow{K_1} \mathrm{X} \longrightarrow \cdots \longrightarrow \mathrm{Cr\ (V)} + \mathrm{Radicales}$$

$$\mathrm{Cr\ (V)} + \mathrm{S} \xrightarrow{k_2} \mathrm{Y} \longrightarrow \cdots \longrightarrow \mathrm{Cr\ (IV)} + \mathrm{Radicales}$$

$$\mathrm{Cr\ (VI)} + \mathrm{Cr\ (VI)} \longrightarrow 2\ \mathrm{Cr(VI)}$$

siendo X e Y compuestos intermedios de Cr (V) y Cr (IV) respectivamente y S la especie reductora. Formulando la ecuación segun la expresión

$$-\frac{\mathrm{d}[\mathrm{Cr\ (VI)}]}{\mathrm{d}t} = k_1\,[\mathrm{S}][\mathrm{Cr\ (VI)}] + k_2[\mathrm{S}]\,[\mathrm{Cr(V)}] \qquad (1)$$

si designamos por c y c_0 las concentraciones de Cr(VI) a un tiempo t y en el instante inicial respectivamente. Y considerando que $|\mathrm{S}| \gg c_0$ la ecuación anterior toma la forma

$$-\frac{\mathrm{d}c}{\mathrm{d}t} = k_1\,[\mathrm{S}]\,c + k_2\,[\mathrm{S}]\,(c_0 - c) \qquad (2)$$

agrupando variables

$$\frac{\mathrm{d}c}{k_1c + k_2(c_o - c)} = [\mathrm{S}]\,\mathrm{d}t \tag{3}$$

integrando entre $t = 0$ y $t = t$ se obtiene

$$\mathrm{Ln}\,\frac{(k_1 - k_2)\,c + k_2c_o}{k_1c_o} = (k_2 - k_1)[\mathrm{S}]t \tag{4}$$

Las constantes de velocidad k_1 y k_2 de los procesos monoelectrónicos de formación de complejos de Cr(V) y Cr (IV) respectivamente, se han determinado ajustando por el método de mínimos cuadrados las correlaciones lineales obtenidas al representar $\mathrm{Ln}\,\frac{(k_1 - k_2)\,c + k_2c_o}{k_1c}$ frente a t mediante un método iterativo de cálculo.

RESULTADOS

Se comprobó en todos los casos el cumplimiento de la ecuación (4) iendo por tanto el orden respecto de la especie Cr(VI), de uno y cero en, la primera y segunda etapas determinantes de la reacción estudiada.

Para determinar el orden cinético respecto del reductor en ambas etapas de reacción, se realizaron una serie de experimentos cinéticos en los que se hacía variar la concentración de acetona (cinco concentraciones diferentes comprendidas entre 0,68 M y 1,20 M), manteniendo constante la concentración inicial de dicromato potásico y la acidez del medio. Esto mismo se realizó a distintas concentraciones de ácido sulfúrico, encontrándose que ambas etapas determinantes son de primer orden respecto de la especie reductora. En la Tabla 1, se recogen los valores medios de las constantes de velocidad k_1 y k_2 a distintas acideces del medio.

Tabla 1

Dependencia de las constantes de velocidad k_1 y k_2 con la acidez del medio

$[K_2Cr_2O_7] = 6.0 . 10^{-4}$ mol dm^{-3} y temperatura 25°C		
$[H_2SO_4]$/mol dm^{-3}	$k_1 \cdot 10^2$/dm^{3}mol^{-1}min^{-1}	$k_2 \cdot 10^2$/dm^{3}mol^{-1}min^{-1}
6,0	$1,3 \pm 0,2$	$0,07 \pm 0,03$
6,5	$1,8 \pm 0,4$	$0,10 \pm 0,02$
7,0	$2,1 \pm 0,2$	$0,22 \pm 0,02$
7,5	$2,9 \pm 0,3$	$0,29 \pm 0,04$
8,0	$3,7 \pm 0,6$	$0,49 \pm 0,05$
8,5	$4,8 \pm 0,2$	$0,80 \pm 0,06$
9,0	$7,2 \pm 0,5$	$1,34 \pm 0,04$

Para analizar la influencia de la acidez del medio, se aplicó el método de Cox y Yates,[6] que nos permiten relacionar la variación de la velocidad de la reacción con la concentración de ácido sulfúrico en términos de función de acidez de exceso (función X) y, a partir de los parametros $m^{\neq}$, deducir el mecanismo de reacción. En la Tabla 2 se resumen los resultados de la aplicación de este criterio, como los valores de los parámetros $m^{\neq}$

Tabla 2

Resultados de la aplicación del método de Cox-Yates

representación	pendiente	$m^{\neq}$	r_{xy}
$\log k_1 - \log c_{H^+}$ vs X	0,64	0,53	0,998
$\log k_2 - \log c_{H^+}$ vs X	1,08	0,90	0,993

r_{xy} coeficiente de correlación lineal

obtenidos para ambas etapas determinantes están comprendidos entre $0{,}5 < m^{\neq} \leqslant 1{,}0$, se deduce que ambas etapas corresponden a la farmación de los compuestos intermedios de Cr (V) y de Cr (IV).

Los resultados indicatos en la Tabla 3 ponen de manifiesto la influencia de la temperatura **sobre las constantes de velocidad de segundo orden obtenidas a partir de la ecuación,[4] encontrándose un satisfactorio cumplimiento de la ecuación de Arrhenius y siendo la energía de activación para ambas etapas cinéticas muy parecida.**

Tabla 3

Influencia de la temperatura sobre la velocidad de reacción

$[K_2Cr_2O_7] = 6{,}0 \cdot 10^{-4}$ mol dm^{-3} y $[H_2SO_4] =$
$= 7{,}0$ mol dm^{-3}

T/°C	$10^2 k_1$/dm^{3}mol^{-1} min^{-1}	$10^2 k_2$/dm^{3}mol^{-1} min^{-1}
25,0	2,1	0,22
27,5	2,7	0,28
30,0	3,3	0,34
32,5	4,0	0,43
35,0	4,8	0,51

$Ea_1 = 61$ kJ mol^{-1} ($r_{xy} = 0{,}998$) $Ea_2 = 66$ kJ mol^{-1}
($r_{xy} = 0{,}997$)

Por otra parte, a la mezcla reaccionante se añadió la especie Cl_2Hg, observándose que durante la misma aparecía un precipitado de Cl_2Hg_2, que parece indicar la formación de radicales libres en el transcurso de la reacción.[7, 8]

Por último, se encontró al hacer un registro continuo de los productos de reacción que presentaban una banda centrada aproximadamente a 590 nm, que coincide practicamente con la que presenta el Cr(III) en medio de ácido sulfúrico $-H_2O$.[9,10]

DISCUSIÓN

En las reacciones de reducción de Cr(VI) por acetona sa han tenido en consideración, además de los resultados experimentales obtenidos en la presente investigación, las informaciones encontradas en bibliografía relativas a este tipo de reacciónes :

1. — Estudios realizados anteriormente [11,12] en disoluciones de dicromato potásico en medio agua-ácido sulfúrico, permiten establecer preferentemente a $HOCrO_2-OSO_3H$ como la especie de Cr (VI) presente en las condiciones experimentales de la actual investigación.

2. — Se han tenido en cuenta los estudios cinéticos realizados sobre la tautomería cetoenólica [13,16]. Como se puede observar, el medio interviene en el mecanismo de reacción, proponiendose en medio ácido el siguiente :

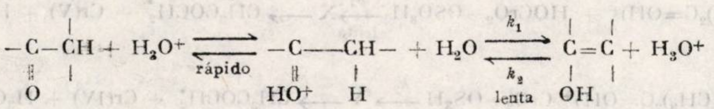

$$-\underset{\underset{O}{\|}}{C}-\underset{|}{\overset{|}{C}H} + H_3O^+ \underset{\text{rápido}}{\rightleftharpoons} -\underset{\underset{HO^+}{\|}}{C}-\underset{\underset{H}{|}}{CH}- + H_2O \underset{\underset{\text{lenta}}{k_2}}{\overset{k_1}{\rightleftharpoons}} \underset{\underset{OH}{|}}{\overset{|}{C}}=\underset{|}{\overset{|}{C}} + H_3O^+$$

En el caso concreto de la acetona [17,18] el equilibrio cetoenólico se encuentra poco desplazado hacia la forma enólica, siendo su constante de equilibrio $K = 6{,}0 \cdot 10^{-9}$.

3. — Littler [1] y Roček [2] proponen como etapa determinante en las oxiciones crómicas de cetonas en medio ácido, la formación de complejos de entre el Cr(VI) y la forma anólica de la cetona.

Por otra parte, en nuestras condiciones experimentales la concentración de la forma enólica : de la propanona, es aproximadamente del mismo orden que la concentración de la especie oxidante Cr (VI). Teniendo en consideración, que todos nuestros experimentos cumplen la ecuación[4] que ha sido deducida para aquellos casos en los cuales la concentración de la especie reductora está en exceso respecto de la especie cinéticamente activa Cr(VI), parece poco probable que sea la forma enólica de la propanona la especie reductora en ambas etapas determinantes observadas.

4. — Sin embargo, estudios espectrofotométricos sobre la interacción entre la acetona y disoluciones de ácido sulfúrico-agua [19] indican la formación del catión acetonium, $((CH\ )\ C = OH)^+$, que ha sido predicho en los estudios cinéticos de la tautomería cetoenólica , [13,16] habiendo estudiado Hammett y Col. [20,21] sus propiedades básicas. Además, en nuestras condiciones experimentales, prácticamente la acetona está en forma de catión acetonium.

5. — En la oxidación de las cetonas por ácido crómico, [22] se rompe la cadena carbonada a una u otro lado del grupa carbonilo, dando ácidos carboxílicos con menor número de átomos de carbono que la cetona del punto de partida. Esta degradación oxidativa de las cetonas tiene interés para determinar la estructura de la cetona de procedencia. La propanona se oxida dando ácido acético y anhídrido carbónico. Esto se ha confirmado realizando un estudio de la estequiometría de la reacción mediante un procedimiento espectrofotométrico [23] encontrándose que la relación

acetona, dicromato es de 3/4 que corresponde a la ecuación estequiométrica siguiente :

$$3CH_3COCH_3 + 4K_2Cr_2O_7 + 16H_2SO_4 \longrightarrow$$

$$\longrightarrow 3CH_3COOH + 3CO_2 + 4\,K_2SO_4 + 4Cr_2(SO_4)_3 + 19H_2O$$

En el estudio del mecanismo de reducción del Cr(VI) por acetona se ha considerado, el hecho de que cada paso en la reacción es monoelectrónico aunque la transferencia neta en la reducción del Cr(VI) sea de tres electrones ; es evidente que los estados de valencias intermedias del cromo en el proceso son importantes.

Así, podemos esquematizar que la reacción transcurre a través de dos etapas determinantes como :

$$((CH_3)_2C{=}OH)^+ + HOCrO_2{-}OSO_3H \xrightarrow[\text{lenta}]{k_1} X \longrightarrow CH_3COCH_2^{\bullet} + Cr(V) + H_3O^+$$

$$((CH_3)_2C{=}OH)^+ \; CrO_2{-}OS_3H \xrightarrow[\text{lenta}]{k_2} Y \longrightarrow CH_3COCH_2^{\bullet} + Cr(IV) + H_3O^+$$

En la primera etapa determinante monoelectronica se forma un complejo de Cr(V), X, entre la especie oxidante Cr(VI) y el catión acetonium

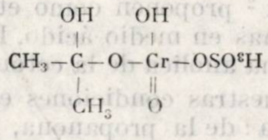

$$CH_3{-}\overset{\displaystyle OH}{\underset{\displaystyle CH_3}{C}}{-}O{-}\overset{\displaystyle OH}{\underset{\displaystyle \| \atop O}{Cr}}{-}OSO^{3}H$$

(X)

la ruptura de este compuesto intermedio Cr(V) mediante etapas cinéticas rápidas da lugar a radicales $CH_3COCH_2^{\bullet}$, Cr (V) y H_3O^+. En la segunda, etapa determinante, también se forma un complejo de Cr (VI), Y, (formado entre el catión acetonium y O_2Cr-OSO_3H) de estructura muy semejante a X, cuya ruptura da lugar a radicales $CH_3COCH_2^{\bullet}$, Cr(IV) y H_3O^+. Finalmente deben existir una serie de etapas cinéticas rápidas de oxidación-redución que den lugar a los productos finales de la reacción global de reducción del Cr (VI) por propanona como son Cr(III), ácido acético y anhídrido carbónico.

AGRADECIMIENTO. Quiero agradecer al Dr. D. Luis Ferrari sus amables consejos y utiles comentarios, así como la colaboración prestada en la discusión y redacción final de este trabajo.

BIBLIOGRAFÍA

[1] J. S. Littler y col., *J. Chem. Soc.*, 822—832 (1972).

[2] J. Roček y col., *J. Am. Chem. Soc.*, **88**, 4749 (1966) y **89**, 6691 (1967).

[3] K. J. Laider, „Cinética de reacciones", capitulo 1, Alhambra, Madrid (1971).

[4] M. P. Alvarez Macho y O. Diez Higuera, *An. Quím*, **82**, 231 (1986).

[5] J. M. Espenson, „Chemical Kinetics and Reaction Mechanism”, capitulo 2, Mc Graw-Hill, Nueva York (1981).

[6] R. A. Cox y K. Yates, *J. Am. Chem. Soc.*, **100**, 3861, (1978) ; *Canada, J. Chem.*, **57, 2944** (1979) ; **59**, 2853, (1981) ; **60**, 3061, (1982) ; **62**, 1613 (1984)

[7] F. Hasan y J. Roček, *J. Am. Chem. Soc.*, **87**, 1444 (1975).

[8] K. G. Strinivasan y J. Rocek, *J. Am. Chem. Soc.*, **100**, 2789 (1978).

[9] N. Fogel, KJ. M. Tai y J. Yarborough, *J. Am. Chem. Soc.*, **84**, 1145 (1962).

[10] J. E. Finholt y J. N. Deming, *Inorf. Chem.*, **6**, 153 (1967).

[11] G. P. Haight, D. C. Richardson y N. H. Coburn, *Inorg. Chem.*, **3**, 1777 (1964).

[12] D. G. Lee y R. Stewart, *J. Am. Chem. Soc.*, **86**, 2051 (1964).

[13] F. A. Long y R. Bakule, *J. Am. Chem. Soc.*, **85**, 2312 (1963).

[14] G. E. Lienhard y T. Wang, *J. Am. Chem. Soc.*, **91**, 1146 (1969).

[15] J. E. Dubois, M. El-Alaoui y J. Toullec, *J. Am. Chem. Soc.*, **103**, 5393 (1981).

[16] Y. Chiang, A. J. Kresge y J. Wirz, *J. Am. Chem. Soc.*, **106**, 6392 (1986).

[17] P. Guthrie, J. Cossar y A. Klym, *J. Am. Chem. Soc.*, **104**, 895 (1982).

[18] Y. Chiang, A. J. Kresge y Y. Tang, *J. Am. Chem. Soc.*, **196**, 460 (1984).

[19] S. Nagakura, A. Minegishi y K. Stanfield, *J. Am. Chem., Soc.*, **79**, 1033 (1957).

[20] L. P. Hammett, Physical Organic Chemistry'' 2 Ed. McGraw-Hill, Nueva York (1970).

[21] L. P. Hammett y col., *J. Am. Chem. Soc.*, **58**, 2103 (1935) ; **60**, 685 (1938) y **61**, 2785 (1939).

[22] N. L. Allinger y col., „Quimica Orgánica”, pag. 717, Reverté, Barcelona (1980).

[23] S. Senent, F. Mata y J. M. Leal, An. Quim, **72**, 327 (1976).

Revue Roumaine de Chimie, 33, *9–10*, 865–874 (1988)

MASS SPECTRAL FRAGMENTATION PATTERN STUDIES OF TARTARIC ACID HYDRAZIDE AND SOME OF ITS ARYLIDENE DERIVATIVES

M. F. ABDEL MEGEED, M. GABER, R. M. ISSA and H. A. IBRAHIM
Chemistry Department, Faculty of Science, Tanta University, Tanta, Egypt

Received May 16, 1987

The mass spectral fragmentation patterns of tartaric hydrazide and its arylidene derivatives are established and discussed in terms of their molecular structure. Mechanisms leading to the important different fragment ions are suggested and identified. The predominant γ-hydrogen transfer of Retero Diels-Alder like mechanism is as well considered. The linear plots of the relative abundance (RA%) of the fragments ions $ArCH{=}N^+$, $Ar{-}C{\equiv}N^+$, $Ar{-}CH{=}N{-}\overset{+}{N}H$ and $Ar{-}CH{=}N{-}NH_2^+$ as functions of σ_x or $\sigma^*_{\varphi_x}$ are explored.

INTRODUCTION

The present study deals with the mass spectral fragmentation of tartaric hydrazide and some of its arylidene derivatives, an extension of our interest to study the chemistry of hydrazides and their arylidene derivatives, namely their different types of spectra,[1,6] their tendency for complexation [7,9] and their polarographic behaviour.[10,11] The availability of these hydrazides and their arylidene derivatives prompted us to study the mode of fragmentation in order to establish the mechanisms leading to different fragment ions.

EXPERIMENTAL

Tartaric hydrazide was prepared by the action of hydrazine hydrate on diethyl tartarate while their arylidene derivatives were obtained by the condensation of hydrazide with the corresponding aldehyde in basic medium. The mass spectra were recorded with a JOEL. JMS-BS-300 spectrometer, at 70 eV and 100 MA energy, using a direct insertion probe at temperature 90–110°C.

RESULTS AND DISCUSSION

The mass spectral fragmentation pattern of the tartaric acid hydrazide can be represented by Scheme 1. The low relative abundance of the molecular ion peak at m/z 178 (1.3%) indicates its low stability under prevailing electron impact conditions. The fragmentation mode is characterized by the symmetrical cleavage of the molecular ion to give the fragment ion at m/z 89 (30.39%). It is noteworthy to mention that the frag-

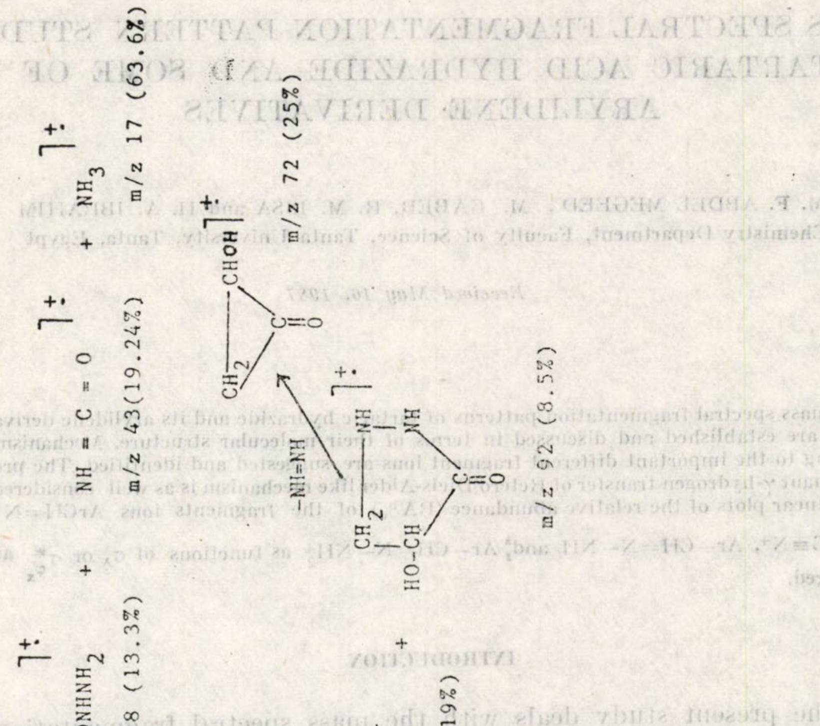
Route A
Route B
m/z 118 (13.3%)
m/z 43(19.24%)
m/z 17 (63.6%)
m/z 30 (36.5%)
m/z 18(19%)
m/z 92 (8.5%)
m/z 72 (25%)

Scheme (1)

ment ion at m/z 118 (13.31%) can be formed by γ-hydrogen transfer accomplished by complex fission of both N—N and CO—CH bonds (route

A in Scheme 1). This process can also be made use of to interpret the formation of the fragment ion at m/z 43 (19.24%). The same process is also observed (route B, Scheme 1) leading to the fragment ions at m/z 30 (36.5%), m/z 18 (19%) and m/z 92 (8.5%). The fragment ion at m/z 92 readily loses $NH{=}NH$ to give fragment ion at m/z 72 (25%). A general fragmentation pattern of tartaric acid hydrazide is also represented in Scheme 2.

The high relative abundance fragment ion at m/z 119 (60.54%) can be formed by simple fission of the $CH-CO$ bond of the molecular ion. This process can be supported by the presence of the fragment ion $CH_3N_2O^+$ at m/z 59 (49.49%). It can also be suggested that the latter ion is formed by simple cleavage of both $CO-CH$ followed by loss of a hydrogen atom to give the fragment ion $C_2H_3O_2{}^+$, while fragment ion at m/z 59 (35.23%) can be produced by a γ-hydrogen transfer mechanism (Scheme 2).

The arylidene derivatives under investigation have the general formula

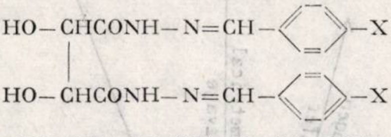

where X = H(I), Cl (II), NO_2 (III), CH_3 (IV), Br (V), OCH_3 (VI), and $N(CH_3)_2$ (VII)

Generally, the mass spectra of the compounds show their molecular ion peak at $M^+ + 2$ due to the diprotonation of the azomethine nitrogen atoms except in the case of compound (VII) that shows its molecular ion at m/z 440 (46.49%). The protonated and diprotonated molecular ions are characterised by their relatively low intensities which indicate their low stability under electron impact. The fragmentation mode of such compounds can be summarized as predominating γ-hydrogen transfer of Retero Diels-Alder process. This process can be represented as $NH-N$ bond or $NH-C{=}0$ bond rupture leading to fragment ions shown in Schemes (3) and (4). Firstly scheme (3) is characterized by two pathways A and B. Pathway A involves simple cleavage of $N-NH$ bond to form the fragment ion $ArCH{=}N^+$ (a) and fragment ion $M^{+\bullet}-ArCH{\equiv}N$ (b). Pathway B also includes a complex fission of Retero Diels-Alder process to give the fragment ions $Ar-C{\equiv}N^+$ and$M^{+\bullet}-ArC{\equiv}N$ (d). A simple $CO-NH$ rupture is also observed in Scheme (4). Pathway A gives the fragment ion $ArCH{=}N-\overset{+}{N}H$ (e) and fragment ion $M^{+\bullet}-ArCH{=}N-NH$(f). Retero Diels-Alder process is also considered in pathway B to give the fragment ions $ArCH_2N{=}NH$ (g), and $M^{+\bullet}-ArCH_2N = NH$(h). Consequently the daughter ion (h) expulses formyl and carbonyl groups successively to give the fragment ion (i). The fragment ion (i) can be formed from symmetrical cleavage of the parent ion. This fragment ion can eliminate CH_2O and CO to give fragment ions (j) and (e) respectively. The fragment ion (j) can be formed through simple $CO-CHOH$ bond cleavage.

It is worthy to mention that two major γ-hydrogen transfer mechanisms are observed as shown in schemes (5) and (6). Scheme (5) is charac-

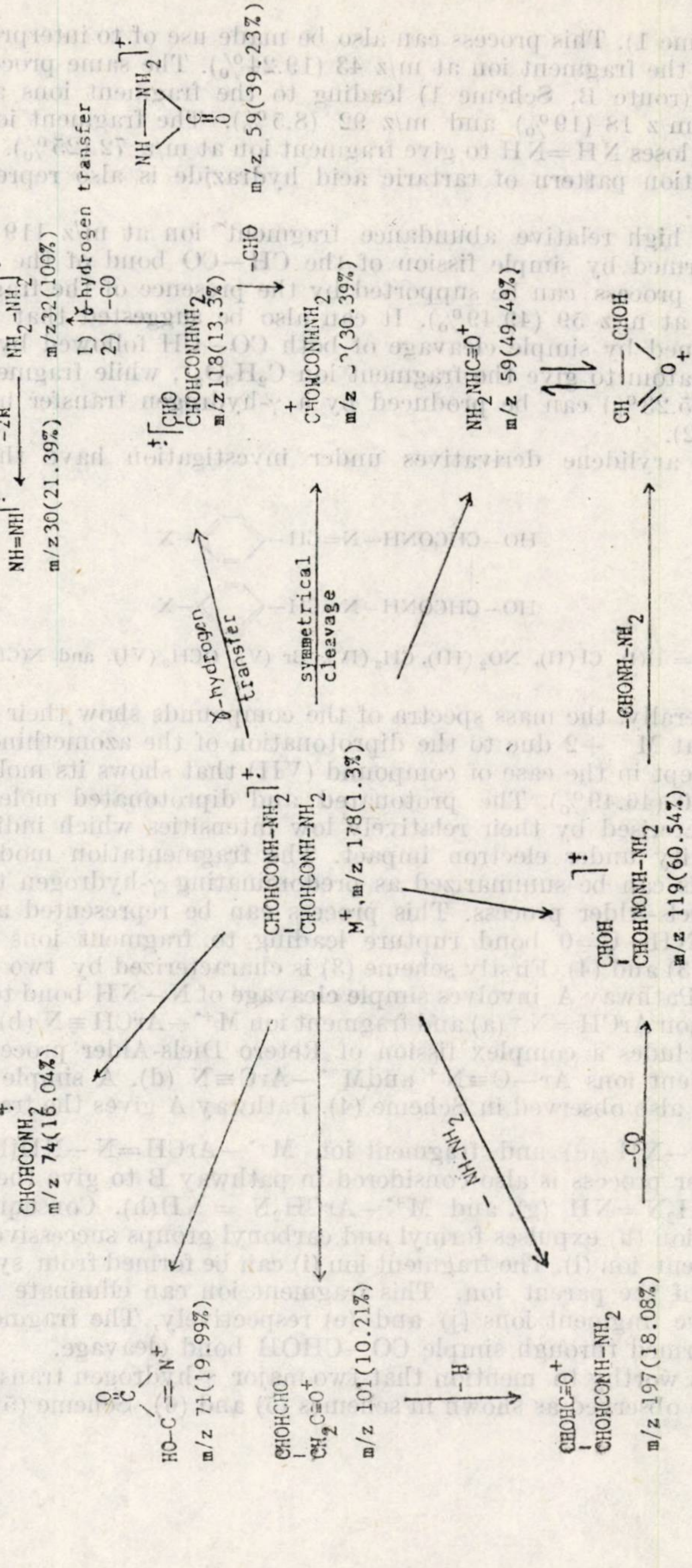
NH=NH]+.
m/z 30(21.39%)
-2H
CHO CHOHCONHNH2 m/z 118(13.37%)
NH2NH2]+. m/z 32(100%)
γ-hydrogen transfer
-CO
-CHO
NH—NH2 C=O m/z 59(39.23%)
CHOHCONHNH2 m/z 90(30.39%)
NH2NHC=O+ m/z 59(49.49%)
CH—CHOH O+
γ-hydrogen transfer
symmetrical cleavage
CHOHCONH-NH2 CHOHCONH-NH2]+. M+ m/z 178(1.3%)
-CHONH-NH2
CHOH CHOHNOH-NH2]+. m/z 119(60.54%)
CHOHCONH2 m/z 74(16.04%)
-NH-NH2
HO-C≡N+ m/z 71(19.99%)
CHOHCHO CH2C=O+ m/z 101(10.21%)
-H
-CO
CHOHC=O+ CHOHCONH-NH2 m/z 197(18.08%)

Scheme (2)

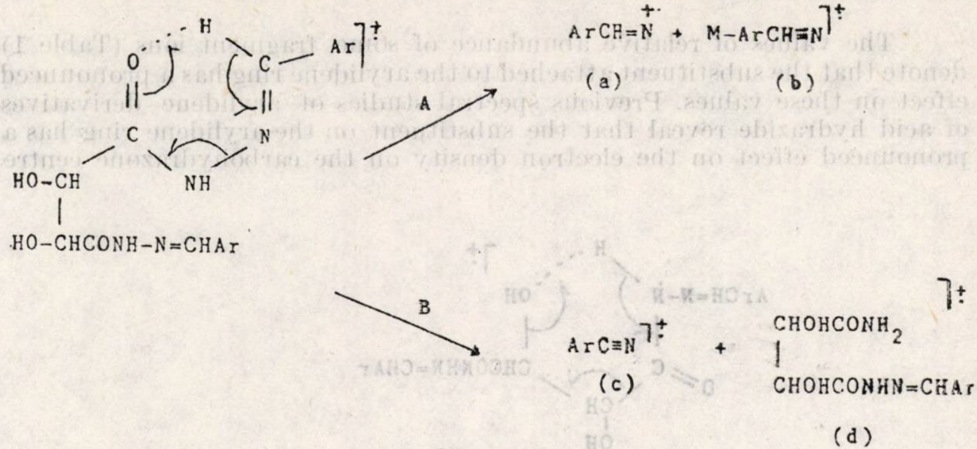

A
B
ArCH=N
M-ArCH≡N
(a)
(b)
ArC≡N
(c)
CHOHCONH2
CHOHCONHN=CHAr
(d)
HO-CH
HO-CHCONH-N=CHAr

Scheme (3)

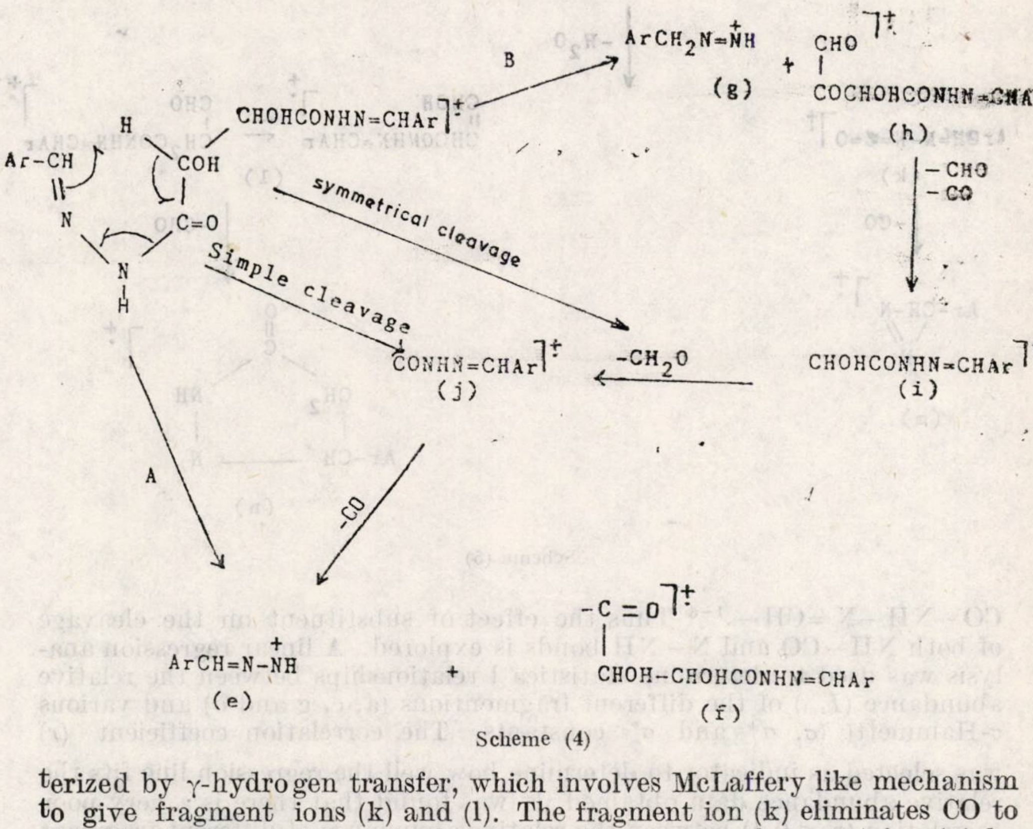

ArCH2N=NH
CHO
COCHOHCONHN=CHAr
(g)
(h)
-CHO
-CO
CHOHCONHN=CHAr
symmetrical cleavage
Simple cleavage
CONHN=CHAr
(j)
-CH2O
CHOHCONHN=CHAr
(i)
A
B
-CO
ArCH=N-NH
(e)
-C=O
CHOH-CHOHCONHN=CHAr
(f)

Scheme (4)

terized by γ-hydrogen transfer, which involves McLaffery like mechanism to give fragment ions (k) and (l). The fragment ion (k) eliminates CO to give the fragment ion (m) whereas ion (l) can give fragment ion (n) by CHO expulsion. The same phenomenon is observed in Scheme (6). Complex bond fission accomplished by γ-hydrogen transfer mechanism can be also observed to give fragment ions (o) and (p) with expulsion of glyoxal molecule. The fragment ion (o) loses hydrogen radical to give fragment ion (e). On the other hand fragment ion (p) gives fragment ion (e) by elimination of CHO and CO successively through the formation of fragment ion (j).

The values of relative abundance of some fragment ions (Table 1) denote that the substituent attached to the arylidene ring has a pronounced effect on these values. Previous spectral studies of arylidene derivatives of acid hydrazide reveal that the substituent on the arylidene ring has a pronounced effect on the electron density on the carbohydrazone centre

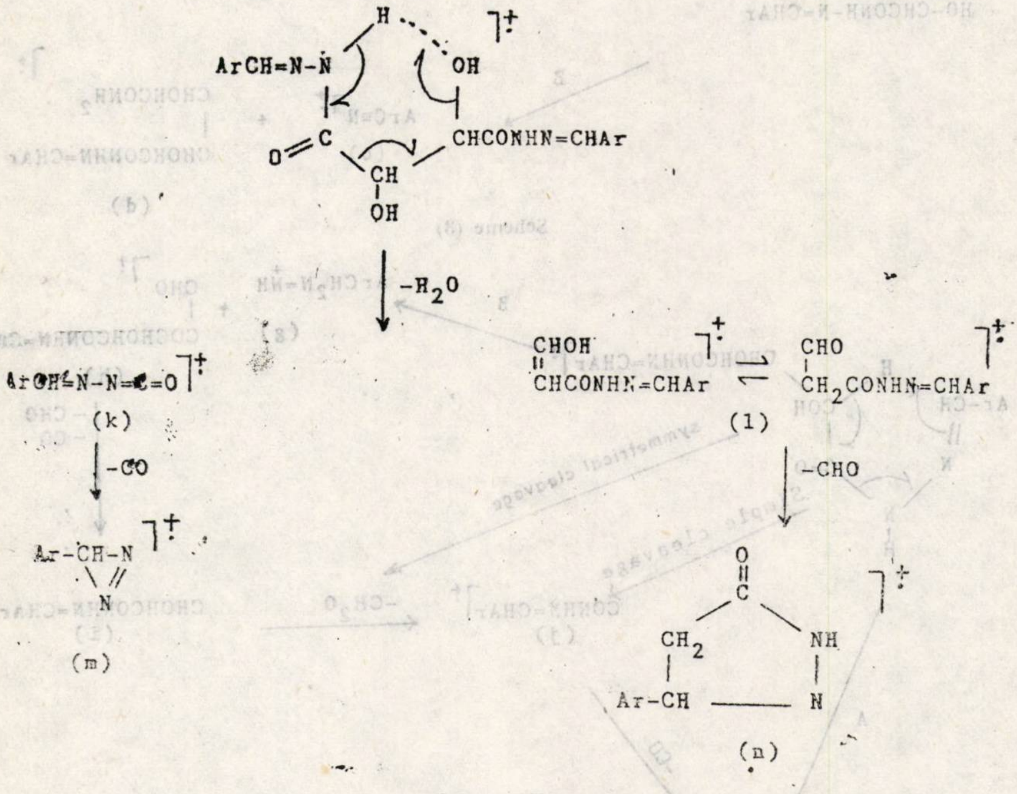

Scheme (5)

CO—NH—N=CH—.[1-6] Thus the effect of substituent on the cleavage of both NH—CO and N—NH bonds is explored. A linear regression analysis was used to determine statistical relationships between the relative abundance (I_{rel}) of the different fragmentions (a, c, g and o) and various σ-Hammett((σ, σ^+ and $\sigma^*_{\varphi_x}$ constants. The correlation coefficient (r) was selected as indicator to determine how well the regression line fits the relative abundance data obtained. It was found that there is a very poor correlation ($r < 0.4$) between the relative abundance of different fragment ions and normal σ-Hammett constant. A reasonable correlation was found between the relative aundance of different fragment ions and (σ^+ and $\sigma^*_{\varphi_x}$) Hammett constants. The correlation is satisfactory between σ^+ or $\sigma^*_{\varphi_x}$ and the relative abundance (I_{rel}) of the fragment ions (g)* and (c) for compounds which carry an electron acceptor group on the arylidene ring. The relations holding can be given as follows :

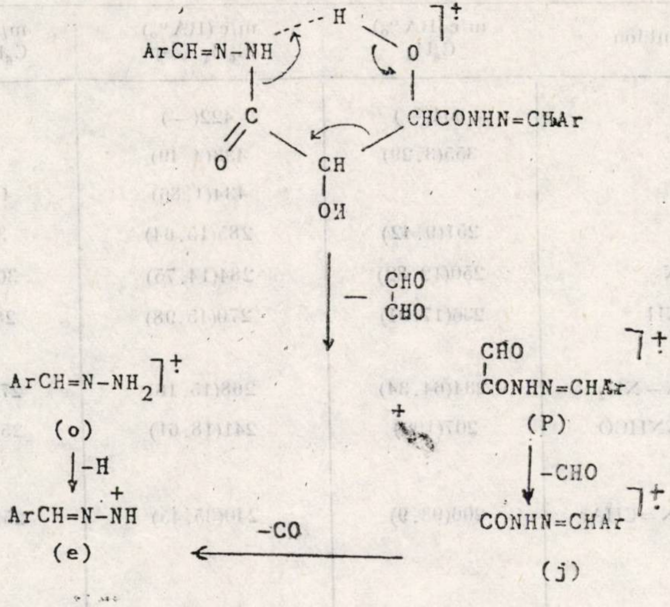
ArCH=N-NH
H
O
C
O
CH
OH
CHCONHN=CHAr
– CHO CHO
ArCH=N-NH2
(o)
-H
ArCH=N-NH
(e)
-CO
CHO CONHN=CHAr
(P)
-CHO
CONHN=CHAr
(j)

Scheme (6)

(i) For fragment ion (g).

$$I_{\mathrm{rel}_{(x)}} = -21.233\,\sigma_x^{+} + 30.1449 \quad (r = 0.487)$$

$$I_{\mathrm{rel}_{(x)}} = -18.4224\,\sigma^{*}_{\varphi_x} + 40.992 \quad (r = 0.6)$$

(ii) For fragment (*c*)

$$I_{\mathrm{rel}_{(x)}} = 11.7212\,\sigma_x^{+} + 16.03 \quad (r = 0.906)$$

$$I_{\mathrm{rel}_{(x)}} = 10.104\,\sigma^{*}_{\varphi_x} + 10.1045 \quad (r = 0.903)$$

The analysis indicates also that the correlation fragment (p) between I_{rel} and σ or $\sigma^{*}_{\varphi_x}$ is reasonable for compounds with electron donating groups with correlation coefficients ($r = 0.606$) and ($r = 0.81$) for σ^{+} and $\sigma^{*}_{\varphi_x}$ regressions respectively. The existence of such correlations with σ^{+}

Table

Mass spectral data of tartaric acid hydrazide

Fragment ion	m/e (RA %) C_6H_5	m/e (RA %) $C_6H_4 \cdot Cl$-p	m/e (RA %) $C_6H_4 \cdot NO_2$-p
M^+	354(−)	422(−)	444(−)
$M^+ + n$	355(3.29)	433(4.49)	
$M^+ + 2$		434(1.86)	446(4.21)
$M^+ - ArC \equiv M$	251(9.42)	285(15.64)	306(100)
$M^+ - ArCH = N$	250(12.82)	284(14.75)	305(15.34)
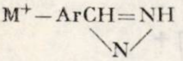	236(17.01)	270(15.98)	281(12.93)
$M^+ - ArCH = N - NH_2$	234(64.34)	268(15.18)	279(12.23)
$M^+ - ArCH = NNHCO$	207(100)	241(18.61)	252(46.77)
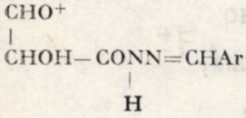 $\begin{array}{l} CHO^+ \\ \vert \\ CHOH-CONN=CHAr \\ \qquad\qquad \vert \\ \qquad\qquad H \end{array}$	206(93.9)	240(35.45)	251(75.10)
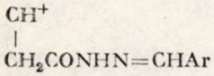 $\begin{array}{l} CH^+ \\ \vert \\ CH_2CONHN=CHAr \end{array}$	190(43.08)	224(29.90)	235(12.34)
$\overset{+}{C}HOHNHN = CH - Ar$	177(93.88)	221(23.92)	222(10.14)
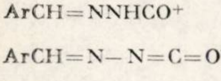 $\begin{array}{l} CHO^+ \\ \vert \\ CO-NHN=CHAr \end{array}$	176(37.70)	210(12.30)	221(10.14)
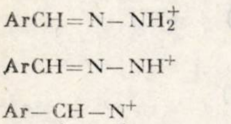	162(14.40)	196(16.32)	207(17.67)
$ArCH = NNHCO^+$	147(15.82)	181(31.32)	192(29.63)
$ArCH = N - N = C = O^+$	146(10.81)	180(13.15)	191(29.94)
$ArCH = N - NH_2^+$	120(25.21)	154(100)	165(32.60)
$ArCH = N - NH^+$	119(17.37)	153(31.34)	164(10.58)
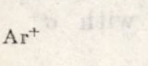	118(10.39)	152(16.26)	163(10.93)
$ArCH \equiv N^+$	104(36.10)	138(45.83)	149(34.41)
$ArC \equiv N^+$	103(18.53)	137(16.22)	148(25.82)
Ar^+	77(44.23)	111(22.47)	122(12.15)

I

and some of its arylidene derivatives

m/e (RA %) $C_6H_4-N(CH_3)_2$	m/e (RA%) $C_6H_4OCH_3$-p	m/e (RA %) C_6H_4Br-p	m/e (RA %) $C_6H_4 \cdot CH_3$-p
440(46.49)	414(−)	510(−)	382(−)
441(9.26)		511(6.51)	
422(6.17)	416(3.52)	512(8.90)	384(5.25)
294(100)	281(10.33)	329(29.2)	265(13.32)
293(19.88)	280(11.49)	328(10.69)	264(12.84)
279(24.37)	266(16.10)	314(37.15)	250(13.88)
277(16.40)	264(24.75)	312(28.92)	248(18.33)
250(22.04)	237(14.06)	285(47.60)	221(17.39)
249(19.45)	236(18.80)	284(19.73)	220(10.50)
233(14.23)	220(21.62)	268(42.25)	204(33.83)
220(18.28)	207(12.53)	255(24.38)	191(22.56)
219(33.87)	207(25.03)	254(29.67)	190(33.38)
205(12.40)	192(10.03)	240(10.18)	176(17.66)
190(11.54)	177(13.16)	225(66.16)	161(14.78)
189(11.54)	176(12.20)	224(12.09)	160(16.09)
163(68.06)	150(100)	198(100)	134(21.07)
162(11.80)	149(12.53)	197(38.91)	133(29.15)
161(15.05)	148(26.39)	196(38.91)	132(20.16)
147(68.63)	134(51.32)	182(30.13)	118(100)
146(19.19)	133(10.99)	181(51.92)	117(34.12)
120(78.24)	107(25.53)	155(31.64)	91(68.80)

and $\sigma^{*}_{\phi_x}$ indicates that there is an interaction between the arylidene ring and the positive charge of the fragment ion. Moreover it indicates that the stability of the considered fragment ions can be correlated with the electron density on the $-CO-NH-N=CH-$ centre according to the linear free energy relationship.

REFERENCES

[1] H. Y. F. El-Baradie, M. Gaber and Y. M. Issa, *Egypt J. Chem.* (in press), 1984.

[2] M. M. El Kersh, M. Gaber, A. M. Habib and K. Y. F. El-Baradie, *Egypt J. Chem.* (in press), 1985.

[3] R. M. Issa, M. A. Kjattab, H. Y. F. El-Baradie and J. Y. Maghrabi, *Indian J. Chem.*, **18A**, 144 (1979).

[4] M. A. Khattab, R. M. Issa, J. I. Maghrabi and H. Y. F. El-Baradie, *Egypt J. Chem.*, **23**, 13 (1980).

[5] M. A. Khattab, M. F. Andel-Mageed, H Y. F. El-Baradie and R. M. Issa, *Proc. Pakist. Aka d Sci.*, **18**, 1 (1981).

[6] H. Y. F. El-Baradie, M. A. Khattab, R. M. Issa and J. Y. Maghrabi, *J. Chem. Tech. Biotechnol.*, **33A**, 123 (1983).

[7] R. M. Issa, *et al.*, *Z. anorg. Chem.*, **354**, 90 (1967) ; **354**, 98 (19767).

[8] I. M. Issa, R. M. Issa, M. M. Ghoneim and Y. M. Temerk, *Egypt J. Chem.*, **17**, 97 (1974).

[9] I. M. Issa, R. M. Issa, Y. M. Temerk and M. M. Ghoneim. *Egypt J. Chem.*, **18**, 1 (1975).

[10] M. M. Ghoneim, R. M. Issa, M. Gaber, E. Mabrouk and E. S. El-Halag. Spring meeting. The American Electrochemical Society. Boston, Massachusetts, May 4—9 pp. 9840—841 (1986).

[11] R. M. Issa, M. M. Ghoneim, E. Mabrouk and Y. I. Moharam, *Ibid.*, May 4—9 p. 842 (1986).

Revue Roumaine de Chimie, 33, *9–10*, 875–879 (1988)

OXIDATIVE MICRODETERMINATION OF SOME INORGANIC SULPHUR COMPOUNDS BY INDIRECT SPECTROPHOTOMETRIC METHOD USING FERRICYANIDE-THYMOLPHTHALEIN REAGENT AND OSMIUM TETROXIDE AS A CATALYST

M. M. ABDEL BADEI * and M. F. EL-SHAHAT
Chemistry Department, Faculty of Science, Ain Shams University, Abbasia, Cairo, Egypt

Received May 16, 1987

Microdeterminations of thiosulphate, thiocyanate, sulphite, metabisulphite and dithionite have been developed. Alkaline potassium hexacyanoferrate(III) was added in excess to the sample solution under investigation in the presence of osmium tetroxide as a catalyst. The excess of hexacyanoferrate(III) was measured spectrophotometrically by thymolphthalein at 592 nm. The method was found to be suitable for the determination of a mixture of the sulphur compounds after separation by thin layer chromatography. The method is simple, reproducible and with an average error ±0.2 %.

INTRODUCTION

The salts of dithionites, sulphites and thiosulphates are probably better known than others of polythionic acids. They are much stronger reductants and form insoluble salts with many metal ions. They readily undergo decomposition with dilute mineral acids but are more stable in alkaline solution.

As they are oxidimetric in nature, titrimetric[1,2] techniques are used for their determination. However thiocyanate could be oxidised completely to sulphate and cyanate by alkaline ferricyanide in the presence of catalyst [3] and the reaction was followed titrimetrically

$$SCN^- + 8\,Fe(CN)_6^{3-} + 10\,OH^- \rightarrow SO_4^{2-} + CNO + 8\,Fe(CN)_6^{4-} + 5\,H_2O$$

The same procedure was applied to the determination of dithionite in mildly acidic or middly alkaline medium[4]

$$S_2O_4^{2-} + 2\,Fe(CN)_6^{3-} + 4\,OH^- \rightarrow 2\,SO_3^{2-} + 2\,Fe(CN)_6^{4-} + 2H_2O$$

---

* Correspondence address : Chemistry Department, Faculty of Science, Benha University, Benha, Qalubia, Egypt.

Dithionite was also determined titrimetrically through the oxidation with ferricyanide under argon atmosphere in the presence of ferrous dimethylglyoximate as an indicator.[5]

Thiosulphate can be oxidised to sulphate with ferricyanide in the presence of osmium tetroxide as catalyst[6] where the end point may be detected amperometrically or potentiometrically

$$S_2O_3^{2-} + 10\,OH^- + 8\,Fe(CN)_6^{3-} \rightarrow 2\,SO_4^{2-} + 8\,Fe(CN)_6^{4-} + 5\,H_2O$$

Potassium hexacyanoferrate(III) belongs to the class of oxidising agents in which the oxidising species is a complex abstracting ion[7]

$$Fe(CN)_6^{3-} + e \rightleftharpoons Fe(CN)_6^{4-}$$

The oxidising capacity of ferricyanide is practically superior in alkaline to acidic medium. Alkaline solution of hexacyanoferrate(III) is stable even at elevated temperature.

Referring to our previous articles[8] in using thymolphthalin (reduced form of thymolphthalein) as an analytical reagent for the determination of ferricyanide spectrophotometrically the present work deals with the determination of thiosulphate, thiocyanate, sulphite and their mixtures after separation by thin layer chromatography[9,10] and also for the determination of metabisulphite and dithionite.

EXPERIMENTAL

Materials

1. *Thymolphthalein reagent*

A mixture of 0.4 g of thymolphthalein (Merck), 4.0 g of sodium hydroxide pellets (Merck) 4.0 g zinc powder (pure grade Baker) and 20 mL bidistilled water in 50 mL round bottom flask washeated for 2hr under reflux followed by cooling and filtering through a hardened filter paper. Dilution of the filtrate to 100 mL with oxygen free fidistilled water (it is obtained by boiling bidistilled water for 5 min and stored in a closed bottle) was carried. The resulting solution was stocked in a dark bottle containing a few granules of zinc (pure B.D.H.). Before use, 10 mL of the stock solution were diluted to 100 mL to obtain 9.29×10^{-4} M as calculated.

2. *Potassium ferricyanide*

0.1554 of $K_3[Fe(CN)_6]$ (Merck A. R.) was dissolved in bidistilled water to obtain $4.27 \times \times 10^{-4}$ M. It was standardised iodometrically against sodium thiosulphate.[11]

The stock aqueous potassium ferricyanide solution was protected from light to remain stable for a long period.

3. *Osmic acid*

One g of osmic tetroxide was dissolved in 400 mL of 0.1 N sulphuric acid.

4. *Sodium hydroxide 4—5 N*

5. *Aqueous standard solution*

20 μg per mL (sodium thiosulphate, potassium thiocyanate, sodium sulphite, sodium metabisulphite and sodium hydrosulphite (sodium dithionite) were freshly prepared from an appropriate weight to obtain 1000 μg per mL solution (stock solution). All chemicals used were of analytical grades.

General procedure

Into a 25 mL standard flask, an appropriate volume of the determinant (Note 1) was placed, the pH was raised to 12—13 by addition of 3 drops of 4—5 N sodium hydroxide. 3.5 mL potassium hexacyanoferrate (III) (0.472 mM) were then added and finally 2 drops of osmic acid. The mixture was digested by warming to 50—60°C for 10 min. and cooled to room temperature. To the latter solution, 4mL of thymolphthalein reagent (0.929 mM) were added, and diluted to the mark with bidistilled water. The solution was allowed to stand for 15 min and the absorbance was measured at 592 nm. From the recorded measurements the corresponding equivalent absorbance could be calculted by difference.

Note (1) :

The final concentrations of the sulphur compounds to be analysed by this method per mL are : 2.5—10 μg sodium thiosulphate. 2.4—4.8 μg pot. thiocyanate, 4.0—20 μg sodium sulphite, 4.0—20.0 μg sod.metabisulphite, 3.6—18.12 μg sod. hydrosulphite (dithionite).

RESULTS AND DISCUSSION

The oxidising capacity and stability of ferricyanide is superior in alkaline to acidic media in the presence of a catalyst and/or at elevated temperature.[7]

In order to optimize the reaction conditions the following factors were studied :

Effect of catalyst

The reaction was studied in the presence and absence of the catalyst by using the same above procedure. The obtained data are illustrated in table 1.

Table 1

Microdetermination of sulphur compounds

Sulphur compound	Limits of identification without catalyst	Recovery (%)	Limits of identification with catalyst	Recovery (%)
$Na_2S_2O_3$	0.6325—2.5301 mg/mL	78.1	2.548—10.19 μg/mL	99.8
Na_2SO_3	50.4—201.6 μg/mL	68.3	4.0—20.0 μg/mL	99.89
$Na_2S_2O_4$	7.68—30.7 μg/mL	78.4	3.62—18.12 μg/mL	99.78
CNS^-	ammonium 0.304—1.217 mg/mL	78.6	potassium 2.4—4.8 μg/mL	99.9

Comparing the above limits of determination in table (1), it is clear that the results obtained in the presence of a catalyst are more reliable, sensitive and accurate.

The effect of osmium tetroxide was explained by Deshmukh and Bapat.[12] The octavalent osmimum forms a precompound with alkali, which behaves as a strong oxidant. However the reductant so far cited for its reduction to hexavalent osmate could be reoxidised to the preosmate by the akaline ferricyanide.

Effect of pH

Solymosi[13,14] found that dithionite could be oxidised to sulphate with ferricyanide in strongly alkaline medium in the presence of osmium tetroxide. The end point can be indicated poteniometrically.

It was found that the intensity and stability of developed color decreases with increasing the final sodium hydroxide concentration.[8] The optimum alkalinity ranged between 12 and 13. This range of alkalinity was selected to overcome the action of acidity of osmic acid and prevent the limited recovery of the reaction ; also above this range a slight decomposition of ferricyanide occurs during digestion as confirmed by blank experiment.

Effect of temperature

A maximum oxidation capacity was achieved for the tested sulphur compounds at 50—60°C. A very slow reaction takes place at 25°C even at higher pH and in the presence of a caltalyst. It was concluded that a quantitative reaction was achieved at 50—60°C.

Effect of time

It was found that 10 minutes were required for a maximum oxidation capacity to the tested sulphur compounds.

The method could be applied to a mixture of sodium thiosulphate, potassium, thiocyanate and sodium sulphite after their separation by a suitable chromatographic technique (paper chromatography)[9] using ethyl acetate, pyridine, ammonia and water in the ratio of (15 :5 :1 :4) as eluent. Also a mixture of sulphite and thiosulphate was separated by thin layer chromatography[10] using cellulose coated plates and n-propanol, 1 M ammonia, acetone as eluent in the ratio of (30 : 20 : 2 v/v).

The location of the sulphur compound was ascertained by staining the pilot chromatogram. After excision of the zones, the sulphur compound was eluted from paper by water : it could be removed from the layer by scraping and extracted with water.

The eluate was then filtered and the sulphur compound extracted with water. The sulphur compound was determined in the filtrate by the proposed method.

Table 2 illustrates the data obtained for the recovery of thiocompounds by chromatographic techniques.

Interferences

The following foreign ions interfere with the thymolphthalein-ferricyanide reagent and must be absent or removed from the test solution : MnO_4^-, IO_4^-, Au^{3+}, H_2O_2, hydrazide sulphate, hydroxylamine hydrochloride, phenyl-hydrazine hydrochloride, hydroquinone and semicarbazide hydrochloride.

Table 2

Recovery of sulphur compound by chromatographic techniques

Sulphur compounds	Paper chromatography *				Thin layer chromatog.**			
	Amounts		R_f	reco-very	Amounts		R_f	reco-very
	Appli-ed (μg)	Found (μg)		%	appli-ed (μg)	found (μg)		%
$Na_2S_2O_3$	3.0	2.98	0.09	99.6	4.0	3.98	0.51	99.5
Na_2SO_3	5.0	4.99	0.20	99.8	6.0	5.98	0.7	99.7
KCNS	3.0	2.99	0.66	99.7	—	—	—	—

* the solvent system used was ethyl acetate, pyridine, ammonia, water with the ratio (15 : 5 : 1 : 4);

** the solvent system used was n-propanol, 1M ammonia, acetone with the ratio (30 : 20 : 3 v/v).

REFERENCES

[1] J. P. Mehling, *Chemist-Analyst*, **44**, 87 (1955).
[2] D. T. Jackson and J. L. Parson, *Ind. Eng. Chem. Analyst*, **9**, 14 (1987).
[3] B. Suseela, *Z. analyt. Chem.*, **145**, 175 (1955).
[4] G. Charlot, *Bull. Soc. Chim. France*, **6**, 977 (1939).
[5] W. Wawrzyczek and Rychick, *Z. Anal. Chem.*, **202**, 21 (1964).
[6] F. Solymosi and A. Varga, *Acta Chim. Acad. Sci. Hung.*, **20**, 295 (1969).
[7] B. R. Sant and S. B. Sant, *Talanta*, **3**, 261 (1960) .
[8] M. F. El-Sjhahat, A. B. El-Sayed, M. M. Abdel Badei and A. I. Amer, *J. Chin. Chem. Soc.* **32**, 307 (1985).
[9] I. I. M. El-Beih and G. G. Gabra, *Chemist-Analyst.*, **52**, 36 (1963).
[10] A. C. Handa and K. N. Johri, *Talanta*, **20**, 219 (1973).
[11] J. Bassat, R C Denny, G. H. Jeffery, J. Mendham; „Vogel's Textbook of Quantitative Inorganic Analysis", 4th ed. p 385 (1978).
[12] G. S. Deshmukj and M. G. Bapat, *Z. analyt. Chim.*, **156**, 105 (1957) .
[13] F. Solymosi and A. Varga, *Anal. Chim. Acta*, **17**, 608 (1957).
[14] F. Solymosi and A. Varga, *Magyar Kém. Folyóirat*, **65**, 52 (1959).

Revue Roumaine de Chimie, **33**, *9–10*, 881–884 (1988)

THE INFLUENCE OF ACTIVATORS ON ACTIVITY OF PbO/MgO CATALYST IN THE REACTION OF OXIDATIVE DEHYDRODIMERIZATION OF TOLUENE

JAN OGONOWSKI

Institute of Organic Chemistry and Technology, Polytechnical University, Kraków, Poland

Received September 16, 1987

The activity of PbO catalyst activated by cations characterized by different q_k/r_k ratios was studied. The above ratio has been connected with the activity of the catalyst. An increase of q_k/er_k ratio causes the decrease of stilbene concentration in the reaction products from 13.39 % (for bismuth, $q_k/r_k = 2.50$) to 7.62 % (for molybdenum, $q_k/r_k = 9.70$).

INTRODUCTION

The reaction of allylic oxidation of hydrocarbons occurs according to the Mars and Van Krevelen mechanism of oxidation-reduction.[2]

The π and π allylic complexes formed at the catalyst surface lead, in dependency on the active centre nature, to the formation of the structure of cation or allylic radical type.[2] In the first case it results in the products of oxidative attack of the nucleophilic network oxygen O^{2-} of the catalyst on the positive carbon atom while in the second one it leads to the formation of the dehydrocondensation products. In both cases it reduces the cation of a catalyst.

The metal oxides are catalysts of the oxidative dehydrodimerization reaction of toluene to stilbene.[3]

The activity of oxide catalyst depends on oxidation rate of the cation. In the case of leaden catalyst the most advantageous results have been obtained using PbO.[4]

Mn_2O_3 turned out to be the most suitable as far as the manganium oxides are concerned.[5]

The purpose of the present paper was to investigate the influence of the chosen activators on the activity of PbO catalyst.

EXPERIMENTAL

The applied catalysts were obtained by suspending the required amounts of lead nitrate magnesium oxide and activators in distilled water.

Pellets were formed from the obtained suspension. All the obtained pellets were dried and activated in an electric oven at 673 K for 4 hrs and for 2 hrs at 773 K afterwards.

The PbO contents in the catalyst was 20% by weight.

The content of activator was $3.83 \cdot 10^{-2}$ gram-ion per Pb gram-ion.

Investigations were carried out using the flowing reactor. The detailed description of the apparatus and the methods of test were described in a previous paper. [3]

The experimental conditions were the following:
- the catalyst apparent volume — 20 cm^3
- the catalyst load — $2.3 \cdot 10^{-4}$ cm^3/s
- flow intensity — $4.21 \cdot 10^{-1}$ cm^3/s

All the products were analysed by means of programmed temperature gas chromatograph (Chrom 4 Laboratorni Pristroje, Praha, SRC), temperature range 363—513 K, helium as the carrier gas, column (1 m length) filled up with Apiezon L 10% on Chromosorb G.

RESULTS AND DISCUSSION

The oxidative dehydrodimerization of toluene to stilbene proceedes as presented below:

$$2\,C_6H_5-CH_3 \xrightarrow{\text{catalyst}} C_6H_5-CH=CH-C_6H_5 + H_2O$$

In the above reaction, network oxygen of the contact oxides is the oxidative agent. The activity of lead contact, determined by the concentration of stilbene in the reaction products depends on the kind of the used activator. The character of the activator cation was determined by the ratio of the charge to the respective radius (q_k/r_k). The q_k/r_k varied in the range from 2.50 to 9.70 (unit of charge per Å).

It is seen from the data presented in table 1 that an increase of q_k/r_k ratio leads to a decrease of the contact activity.

Table 1

The influence of activators on the activity of PbO catalyst in the reaction of oxidative dehydrodimerization of toluene to stilbene.

Activator	Composition of reaction products % by weight		S [benzene]/[stilbene] %	a_k/r_k
	Benzene	Stilbene		
Bi	3.63	13.39	27.10	2.5
La	1.63	11.74	13.88	2.6
Ce	5.59	12.64	44.22	2.7
Co	2.62	11.24	23.30	2.7
Cu	3.45	11.72	29.43	2.8
Y	1.85	12.16	15.21	3.2
Cr	3.27	10.11	32.24	4.3
Ti	3.19	9.91	32.18	5.9
Se	2.59	9.52	27.20	8.0
V	2.82	9.19	30.68	8.4
W	1.71	9.17	18.64	8.8
Mo	3.92	7.62	51.44	9.7

Concentration of stilbene in the postreaction mixture changed at the range of 7.62—13.59%. The maximum yield of stilbene was obtained using the catalyst activated by bismuth (13.39%) while the lowest one when the contact activated by molybdenum (7.62%) was applied.

Benzene was the byproduct of the reaction. Its yield however depended in some cases on the changes of q_k/r_k ratio of the activator while in other cases the achieved values were much lower than it was expected from the respective q_k/r_k values. The above is clearly seen in the case of lanthanum as well as yttrium.

Coefficient "*S*" has been defined as a measure of selectivity : its changes in relation to the kind of the activator are presented in table 1. In the case of lanthanum or yttrium the respective coefficient *S* achieves the lowest values. In those cases the oxidative dehydrodimerization carried out on PbO contact is characterized by the highest selectivity.

In the case of molybdenum or cerium used as activator the marked amounts of benzene are produced. The respective coefficients *S* are 51.44 and 44.22%. These activators make the selectivity of PbO contact poor.

It is seen from the presented data that the activators indicating high activity towards stilbene formation are in some cases of low activity so far as the formation of benzene is concerned. It may be evidenced that the subsequent stages of the process occur at different active centers of the catalyst.

The dependence of the activity of PbO catalyst (measured by the total concentration of benzene and stilbene in the reaction products) on the c_k/r_k ratio of activator is presented in Fig. 1.

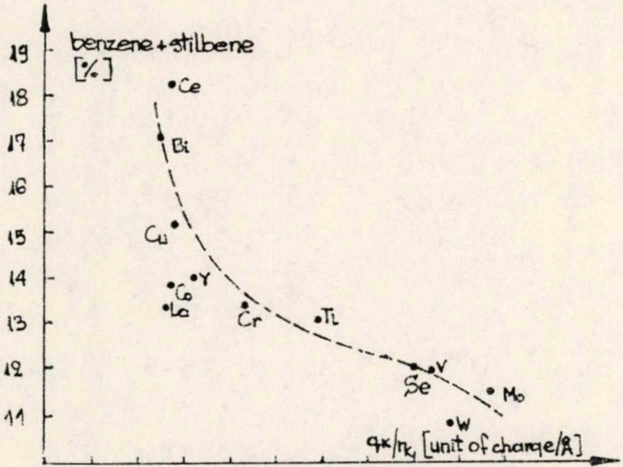

Fig. 1. — The influence of q_k/r_k ratio of the activator on the yield of benzene and stilbene in postreaction mixture.

In the case of tungsten and lanthanum activators the activities of the tested contact were poor whereas in the case of cerium the PbO contact indicated the highest activity.

CONCLUSION

The activity of PbO contact depends on the q_k/r_k ratio of the activator. The yield of stilbene decreases with an increase of the q_k/r_k ratio. It was found that application of activators having strongly concentrated large charge is disadvantageous in the discussed process.

REFERENCES

[1] P. Mars and D. W. van Krevelen, *Chem. Eng., Sci. Sp. Suppl.*, **3**, 41 (1954).

[2] J. Haber, *Kinet. Katal.*, **28**, 74 (1987).

[3] J. Ogonowski, F. Gajewski and B. Dusza, *Przemysl. Chem.*, **62**, 156 (1983).

[4] J. Ogonowski, *Chem. Stos.*, **28**, 427 (1984).

[5] J. Ogonowski, *Chem. Stos.*, **30**, 553 (1986).

Revue Roumaine de Chimie, **33**, *9–10*, 885–891 (1988)

SYNTHESIS OF NICKEL FERRITE FROM POLYNUCLEAR COORDINATION COMPOUNDS. PART III

STRUCTURAL DATA OF $NiFe_2O_4$ OBTAINED BY THE WET FERRITIZATION METHOD

IOANA ILIE [a], MARIA BREZEANU [b], LUMINIŢA PATRON [c], E. SEGAL [d] and G. FILOTI [e]

[a] Institute of Chemical and Biochemical Energetics, ICECHIM, Str. Splaiul Independenţei no. 202, Bucharest, 77208, Romania

[b] Polytechnic Institute Bucharest, Faculty of Chemical Technology, Laboratory of Inorganic and Technological Chemistry, Str. Dumbrava Roşie no. 23, Bucharest, Romania

[c] Center of Physical Chemistry, ICECHIM, Str. Splaiul Independenţei no. 202, Bucharest, 77208, Romania

[d] Polytechnic Institute Bucharest, Faculty of Chemical Technology, Laboratory of Physical Chemistry and Electrochemical Technology, Blvd. Republicii no. 13, Bucharest, Romania

[e] Institute of Physics and Materials Technology, I. C. Fiz., Post Box 07, Măgurele, Romania

Received November 21, 1987

The authors present some results concerning the structural characterization of nickel ferrite obtained by the wet ferritiziation method.

In this paper the results of structural investigation of nickel ferrite obtained by the wet ferritization method are presented and discussed. Various mixed oxides obtained previously [1] were analysed. In order to obtain informations on the thermal stability of the mixed oxides, the structural investigation was extended to some thermally treated samples. The experimental procedures applied to get the structural data were : X-ray diffraction, Mössbauer spectra, magnetic measurements and IR spectra.

EXPERIMENTAL

The X-ray diffraction patterns were recorded with a Philips P 1140 diffractometer using chromium K_α radiation.

To obtain the Mössbauer spectra an IFTM Mössbauer spectrometer with Co^{57} source was used.

The magnetic measurements were performed by the Faraday method.

The hysteresis curves were obtained by using an installation described elsewhere.[5]

A specord IR Carl Zeiss-Jena spectrometer was used to record the IR spectra.

RESULTS AND DISCUSSION

The notations of the samples are similar to those mentioned in a previous paper.[1] For the samples calcined in air the temperature of thermal treatment is also indicated.

X-Ray diffraction

From the X-ray diffraction data, listed in Table 1, the following general trends are obvious :

— The oxide phases obtained in the pH range 7—8, (2—6, 20, 21, 23, 25—33) exhibit the diffraction patterns of a spinel structure which, within the limits of experimental errors, can be assigned to $NiFe_2O_4$, Fe_3O_4, γ-Fe_2O_3 and cubic NiO. At the values of 2θ in the range 4—25° the diffractograms exhibit diffraction lines corresponding to an untransformed coordination compound;

— The air bubbling in the reaction system (samples 8, 9, 22, 24, 34, 36—40) favours the decomposition of the polynuclear precursors and the stabilisation of a well formed spinel structure;

— The samples prepared in the pH range 9—10, (11—19, 34—40) exhibit the spinel diffraction lines, independently of the complexing agent, nature, of the base and heating period;

— All the oxide phases calcined in air at 400°C show a well crystallised spinel structure without impurities;

— For the same thermal treatment in the temperature range 600—800°C (1 hour) two phases, a spinel one and α-Fe_2O_3, were evidenced; the concentration and crystallinity of hematite increase in the following order :

$$2-600 < 33-600 < 20-600 < 23-600;$$

— The samples heated at 1000°C exhibit a lower concentration of hematite with respect to the previous ones; sample 33—1000 does not contain hematite at all. This result is similar to the previously mentioned one for $NiFe_2O_4$ obtained by the dry ferritization.[2]

Mössbauer spectroscopy

The Mössbauer data given in Table 2 show that the structures of the oxide phases differ significantly, as a function of the wet ferritization conditions.

In the samples prepared in the pH range 7—8 two phases, Fe_3O_4 and 11—13.5% paramagnetic phase were put in evidence; the paramagnetic phase can be assigned to the initial untransformed polynuclear coordination compound. This statement is confirmed by the fact that paramagnetic phase concentration is the largest for the oxides obtained in the presence of the complexing agents (20, 21, 25—31) and practically vanishes for those obtained by air bubbling (sample 23).

Table 1

The X-ray diffraction data for the oxide phases obtained by the wet ferritization method.

Index of the sample	d(Å)	$d(ASTM)_{NiFe_2O_4}$
2–6	2.94 2.51 2.40 2.08 8.76 10.07	2.9485 2.513 2.408 2.085 CP CP
8–9	2.94 2.51 2.40 2.08	
20, 21, 25–31	2.94 2.51 2.39 2.08 8.76 10.07	CP CP
22, 23, 24	2.92 2.50 2.40 2.71	
11–19	2.92 2.50 2.40 2.71	
32, 33	2.94 2.63 2.52 2.41 2.09 8.76 10.07	α-Fe_2O_3 CP CP
35, 37–39	2.92 2.50 2.71	
36, 40	2.94 2.51 2.09	
34	2.94 2.50 2.39 2.08 2.70 1.60	

Index of the sample	d(Å)	$d(ASTM)_{NiFe_2O_4}$
2–400	2.94 2.50	
2–600	2.95 2.69 2.51	α-Fe_2O_3
2–800	2.92 2.69 2.50	α-Fe_2O_3
2–1000	2.92 2.69 2.51 2.41	α-Fe_2O_3
20–400	2.94 2.50	
20–600	2.95 2.69 2.51 2.40	α-Fe_2O_3
20–800	2.95 2.69 2.51 2.40	α-Fe_2O_3
20–1000	2.95 2.69	α-Fe_2O_3
32–400	2.92 2.51 2.39	
32–600	2.69 2.92 2.40	α-Fe_2O_3
32–800	2.92 2.69 2.51 2.40 2.08	α-Fe_2O_3

Table 1 (continued)

Index of the sample	d(Å)	$d(ASTM)_{NiFe_2O_4}$	Index of the sample	d(Å)	$d(ASTM)_{NiFe_2O_4}$
			33–1000	2.95	
				2.52	
23–4000	2.92		23–800	2.95	α-Fe_2O_3
	2.50			2.94	
	2.39			2.69	
	2.08			2.51	
	1.70			2.40	
	1.60			2.21	
23–600	2.95	α-Fe_2O_3	23–1000	2.95	α-Fe_2O_3
	2.50			2.50	
	2.69			2.69	
	2.40			2.51	
	2.08			2.40	
				2.08	

CP = untransformed polynuclear coordination compound

Table 2

The Mössbauer data for the oxide phases obtained by the wet ferritization process

Index of the sample	Subsp.	H(Koe)	ΔQ(mm/s)	δ (mm/s)	Γ(mm/s)	Rel. areas (%)	Oxide phases
2	1	483.3	−0.06	0.45	0.61	0.6240	Fe_3O_4+NiO
	2	449.2	−0.20	0.75	0.91	0.2646	
	3	0.0	0.60	0.50	0.45	0.113	+CP
2–400	1	503.1	−0.02	0.54	0.46	0.0060	$\gamma-Fe_2O_3-$
	2	491.7	−0.04	0.44	0.69	0.0090	$NiFe_2O_4$ +
	3	407.8	−0.56	0.51	1.22	0.0020	+FP′
	4	0.0	0.76	0.49	0.54	0.0130	
2–600	1	514.7	−0.16	0.53	0.40	0.6380	$NiFe_2O_4$+
	2	483.1	−0.02	0.39	0.60	0.3620	$\alpha-Fe_2O_3$
2–800	1	615.1	−0.14	0.51	0.43	0.5959	$NiFe_2O_4$+
	2	486.1	−0.04	0.42	0.50	0.4041	$\alpha-Fe_2O_3$
2–1000	1	520.0	0.00	0.51	0.41	0.4112	$NiFe_2O_4$
	2	490.0	0.00	0.41	0.55	0.5888	$\alpha-Fe_2O_3$
32	1	485.4	−0.04	0.48	0.56	0.5962	Fe_3O_4+NiO
	2	456.0	−0.02	0.79	0.72	0.2829	+CP
	3	0.0	0.54	0.52	0.36	0.1209	
23	1	485.7	0.00	0.45	0.49	0.5746	$Fe_3O_4-\gamma$
	2	456.1	0.00	0.82	0.67	0.4254	Fe_2O_3+NiO
20–1000	1	518.3	−0.10	0.52	0.42	0.4574	$NiFe_2O_4$+
	2	490.9	−0.04	0.42	0.59	0.5426	$\alpha-Fe_2O_3$

CP = paramagnetic untransformed coordination compound; FP′ = superparamagnetic phase

The $Fe^{3+}(B)$ position from Fe_3O_4 is significantly influenced by Ni^{2+} ions whose unhomogeneous distribution preserves the Fe_3O_4 structure. Thus, these oxide phases can be considered as solid disordered solutions, $Fe_{3-x}Ni_xO_4$, with small amounts of paramagnetic phases (polynuclear precursors).

By increasing the pH from 7—8 to 9—10 and the heating period (at 400°C) from 1 to 5—10 hours, the solid solutions $Fe_{3-x}Ni_xO_4$ change into $(Fe^{3+}_x Ni^{2+}_{1-x})$ $[(Fe^{3+}, Fe^{2+})_{2-x}Ni^{2+}_x]O_4$ and the paramagnetic precursor disappears.

After 30—48 hours of heating and by air bubbling, the spinel structure corresponds to pure $NiFe_2O_4$ with various inversion degrees.

The oxides calcined at 400°C convert to solid solutions γ-Fe_2O_3—$NiFe_2O_4$ and a paramagnetic surface oxide phase providing superparamagnetic interactions. The solid solutions resulted from the partial oxidation of Fe_3O_4 to γ-Fe_2O_3 and from the uncontrolled competition of Ni^{2+} with cationic vacancies.

By increasing the temperature from 400 to 600, 800 and 1000 C°, the formation of $NiFe_2O_4$ is favoured, but mixed with α-Fe_2O_3.

As seen from Figure 1, the Fe^{3+} (B) content increases with temperature from 36% (at 400°C) to 59% (at 1000°C).

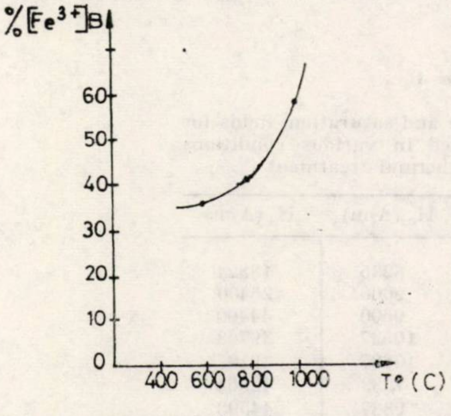

Fig. 1. — Plot of Fe^{3+} (B) versus temperature (°C).

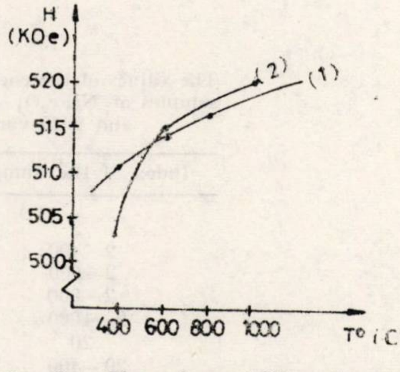

Fig. 2. — Plot of crystallite sizes in units of hyperfine field (KOe) versus temperature (°C).

The crystallite sizes and inversion degree also increase with temperature, as seen in Figure 2.

Magnetic measurements

The saturation magnetic susceptibility values for various samples of $NiFe_2O_4$ are in the range 40—45 Gs. cm^3/g, in good agreement with those reported in the literature.[3]

The hysteresis curves and their change for various thermal treatments are given in Figure 3.

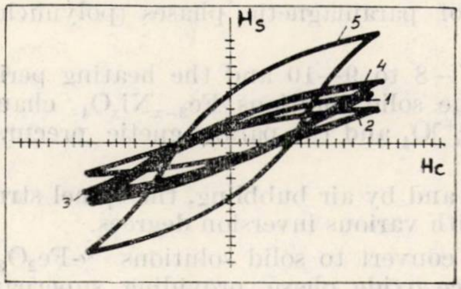

Fig. 3. — The hysteresis curves as a function of thermal treatment : 1. sample — 2— (70—90°C); 2. sample — 2 —400°C ; 3. sample —2—600°C ; 4. sample —2— 800°C ; 5. sample —2—1000°C.

From the saturation hysteresis curves the values of the coercitive and saturation field, listed in Table 3, were calculated.

IR Spectra

The IR spectra exhibit a strong absorption in the range 560—600 cm^{-1} which can be assigned to the M—O vibration.[4] The bands from 1000 and 1600 cm^{-1} associated with the large band at 3200—3500 cm^{-1} prove the presence of OH groups from water and untransformed polynuclear hydroxyprecursor mixed with $NiFe_2O_4$.

Table 3

The values of the coercitive and saturation fields for samples of $NiFe_2O_4$ obtained in various conditions and with various thermal treatment

Index of the sample	H_c (A/m)	H_s (A/m)
2	8235	18824
2—400	9600	26400
2—600	9600	44400
2—800	10527	39763
2—1000	10687	39187
20	7333	42864
20—400	9387	44593
20—600	10959	36798
20—800	10831	44005
20—1000	8504	34020
32	7933	39672
32—400	9387	22531
32—600	10200	42600
32—800	9917	42577
32—1000	9000	43200
23	10594	41195
23—400	10800	35400
23—600	2000	2800
23—800	4178	10288
23—1000	11286	30469
34	9512	44587
36—40	7200	31800
8—9	8234	43398

CONCLUSIONS

The $NiFe_2O_4$ samples obtained by the wet ferritization process have different oxide compositions as a function of reaction parameters and thermal treatment. The structural data presented in this paper suggest the following mechanism of ferritization :

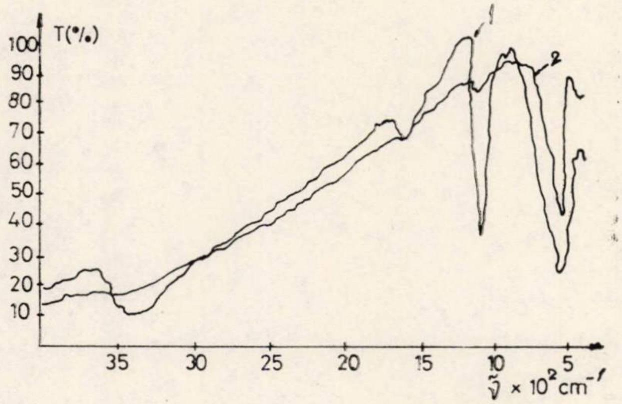

Fig. 4. — IR Spectra of $NiFe_2O_4$ as a function of heating period : 1. after 1—5 hours of heating at 70—90°C ; 2. after 10—48 hours of heating at 70—90°C.

$$\begin{tikzcd}
& {[Fe_x^{2+}Ni_{1-x}^{2+}Fe_2^{3+}(OH)_8(H_2O)_2]} \arrow[d, "pH = 7-8"] & \\
& Fe_3O_4 + NiO + FP \text{ or } Fe_{3-x}Ni_xO_4 \arrow[d, "{pH = 9-10,\ 70-90^\circ C}"] & \\
& (Fe_x^{3+}Ni_{1-x}^{2+})[(Fe^{3+}, Fe^{2+})_{2-x}Ni_x^{2+}]O_4 \arrow[dl, "400^\circ C"'] \arrow[d] \arrow[dr, "600-1000^\circ C"] & \\
\gamma\text{-}Fe_2O_3-NiFe_2O_4 + FP' & NiFe_2O_4 & NiFe_2O_4 + \alpha\text{-}Fe_2O_3
\end{tikzcd}$$

The role of polynuclear coordination compounds as intermediates and the $NiFe_2O_4$ generation on a Fe_3O_4 structure initially formed are the main assumptions of the proposed mechanism which agrees well with the structural data.

REFERENCES

[1] Ioana Ilie, Maria Brezeanu, Luminiţa Patron and E. Segal, *Rev. Roumaine Chim.*, **32**, 1109(1987)

[2] Ioana Ilie, Maria Brezeanu, Luminiţa Patron and E. Segal, *Rev. Roumaine Chim.*, in press.

[3] S. Cedighean, "Ferite", Ed. Tehnică, Bucharest, 38, 1966.

[4] C. G. Macarovici, D. Macarovici, "Chimia oxizilor dubli și utilizările lor", Ed. Academiei, Bucharest, p. 127, 1975.

[5] Coletta de Sabata, A. Policec and Ec. Rusu, *Silicates Industriels*, **XXXVI** (5), 139 **(1972)**.

Revue Roumaine de Chimie, 33, 9–10, 893–901 (1988)

SYNTHESIS OF BIS(9,10-PHENANTHRO)[*a*, *e*]CYCLOOCTA-1,5-DIENE BY SULPHONE PYROLYSIS

M. BANCIU [a], ANCA BANCIU [b], M. ELIAN [b], C. DRĂGHICI [b], N. PALIBRODA [c]
and ECATERINA CIORĂNESCU [a,b]

[a] Organic Chemistry Department, The Polytechnic, TCH, Spl. Independenței 313, 76206 Bucharest, Romania
[b] Centre of Organic Chemistry — ICECHIM, Spl. Independenței 202B, 78100 Bucharest, Romania
[c] Institute of Molecular and Isotopic Technology, Cluj-Napoca, Romania

Received March 10, 1988

Contrary to various claims in the literature bis(9,10-phenanthro)-cycloocta-1,5-diene **(3)** was not definitely obtained until now. Gas-phase pyrolysis of 10,21-dithia-9,10,11,20,21,22-hexahydro-diphenanthro[*a*, *f*]cyclodecene-S,S,S′,S′-tetroxide **(12)** afforded at 500°C and 0.1 Torr the title compound **3** along with 9,10-dimethylphenanthrene and phenanthro[9, 10c]thiophene. Attempted purification of **3** by vacuum sublimation conducted to partial decomposition with probable formation of tetrabenzo[*a*, *c*, *h*, *j*]anthracene **(10)**.

INTRODUCTION

Some years ago we described [1] the synthesis of cyclic hydrocarbons **1** and **2** using as key-step the pyrolysis of corresponding disulphones. The hydrocarbon **1** with a twelve-membered central ring comprises two biphenyl moieties, whereas **2** with a ten-membered central ring includes a biphenyl- and a phenanthrene-moiety. A related compound **3**, with an eight-membered central ring, and two phenanthrene moieties should complete this series of cyclic hydrocarbons isomeric with the known *para*-cyclophanes **4**, **5** and **6** synthesized by Staab and Haenel.[2]

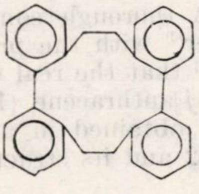
1

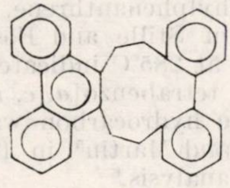
2

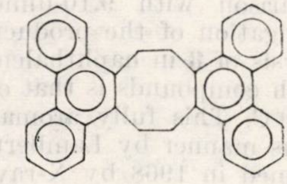
3

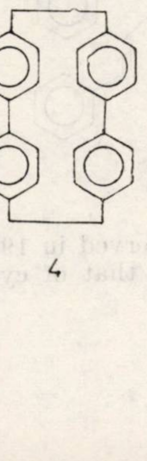
4

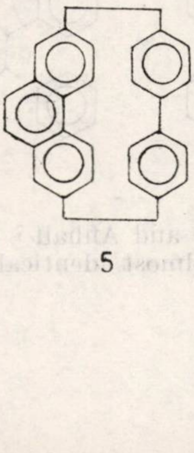
5

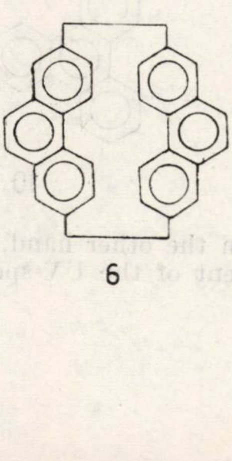
6

Due to its structural features, phenanthrenophane **6** can exist in two isomeric forms (*syn* and *anti*), and actually a 1 : 5 mixture of these isomers resulted in the synthesis.[2] Such an isomerism cannot occur for bis(9,10-phenanthro)[*a*, *e*]cycloocta-1,5-diene (**3**).

Screening of the literature data concerning **3** reveals some interesting observations. In 1963 Stille and Foster[3] obtained, in three different pyrolytic reactions – involving 9,10-phenanthro-quinodimethane – a compound with m.p. 438–440°C, for which they ascribed the structure of bis(9,10-phenanthro)cycloocta-1,5-diene (**3**). The reactions performed by Stille and Foster were[3] : (a) pyrolysis of acetate **7** at 500°C in a tube filled with Pyrex helices, (b) pyrolysis of the Diels-Alder dimer **8** of 9,10-phenanthroquinodimethane in diethylphthalate at 275°C and (c) pyrolysis of monosulphone **9** in diethylphthalate at reflux. The structural identity for the pyrolysis products obtained in the all three mentioned reactions was ascribed [3] by comparing their melting points, IR- and UV-spectra.

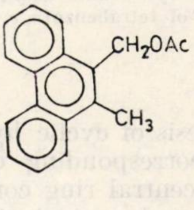

7

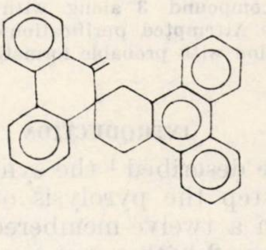

8

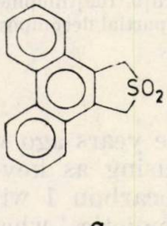

9

In 1972 Anhalt and White [4] arose doubt concerning the structure of the product of Stille and Foster [3] due to the very large bathochromic shift (38 nm) observed in the UV spectrum of the above compound in comparison with 9,10-dimethylphenanthrene. A thorough comparative investigation of the product of Stille and Foster [3] with the product of pyrolysis of **8** in naphthalene at 285°C indicated [4] that the real structure of both compounds is that of tetrabenzo[*a*, *c*, *h*, *j*]anthracene (**10**), m.p. 428–9°C. This fully aromatic hydrocarbon was obtained in an unambiguous manner by Lambert and Martin[5] in 1952 and its structure was confirmed in 1968 by X-ray analysis.[6]

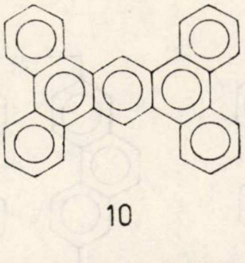

10

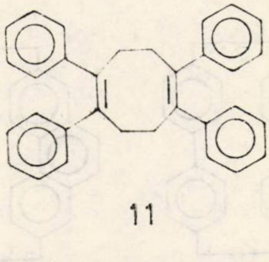

11

On the other hand, White and Anhalt [7] observed in 1965 "the development of the UV-spectra almost identical to that of cyclopentanophenanthrene and of correct intensity on UV-irradiation of incompletely degassed solutions of tetraphenylcyclooctadiene **11**"; the authors noted further : "this photochemical conversion of *cis*-stilbenes into phenanthrenes is apparently a very general reaction" [7]. Some years later the same authors [4] stated more explicitely : "we noted[7] that irradiation of **11** in the presence of oxygen led to the *apparent* formation of bis(9,10-phenanthro)cycloocta-1,5-diene (**3**) with a UV-spectrum consistent with the presence of two isolated phenanthrene chromophores".

On the basis of all above data it seems that *compound* **3** *was not definitely obtained as a pure substance until now*. Therefore, we decided to investigate the possibility of synthesis of **3** analogously to **1** and **2**, i.e. *via* gas-phase pyrolysis of the corresponding disulphone **12**. The synthesis of the disulphone **12** was described by us in a preliminary paper.[8]

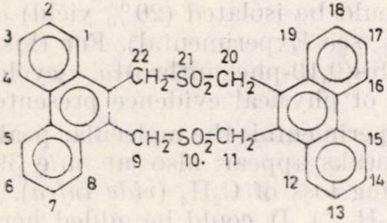

12

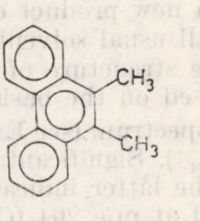

13

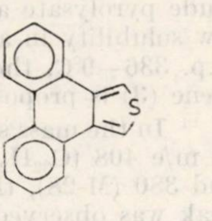

14

Pyrolysis of **12** at 500°C using a vacuum of 0.5 ÷ 2 Torr afforded[8] a mixture of 9,10-dimethylphenanthrene(**13**) and phenanthro[9,10c]-thiophene(**14**) instead of the expected **3**. The structure of these reaction products as well as control experiments indicated that in the conditions used, the disulphone **12** – due to its high melting point (370–372°C) – was not evaporated but reacted practically in condensed phase (melt). In order to test further the possibility of obtaining **3**, a higher vacuum seemed necessary.

In the present paper we describe the synthesis of **3** by gas-phase high-vacuum pyrolysis of disulphone **12**.

RESULTS

The disulphone **12** was obtained, as described in our previous paper,[8] by coupling 9,10-bis(bromomethyl)phenanthrene (**15**) with 9,10-bis (mercaptomethyl) phenanthrene (**16**) followed by oxidation of the resulted disulphide **17** (Scheme 1).

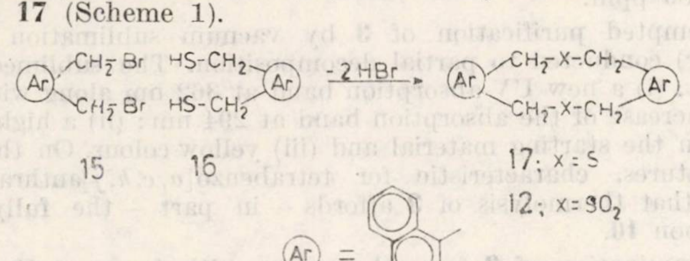

(Scheme 1)

Preliminary control experiments indicated that the optimal temperature range for the pyrolysis of **12** was 500—525°C; above 525°C extensive carbonisation was observed and no definite product could be isolated.

Pyrolyses of disulphone **12** were thus performed at 500°C in the slightly modified apparatus (see Experimental) used for syntheses of **1** and **2**[1] and using as vacuum source a diffusion pump. The initial vacuum in the pyrolysis oven was 10^{-4} Torr. However, as the pyrolysis proceeded, the fast evolution of gaseous SO_2 dramatically increased the pressure. A reasonable compromise was reached by diminishing the samples of **12** to about 80 mg per run, when the residual pressure remained 0.1 Torr or less.

Two products of pyrolysis, the known 9,10-dimethylphenanthrene (**13**) and phenanthro[9, 10c] thiophene(**14**) were easily separated and characterized as described in our previous paper.[8] In addition, from the crude pyrolysate a new product could be isolated (20% yield) due to its low solubility in all usual solvents (see Experimental). For this product, m.p. 336—9°C, the strcucture of bis(9,10-phenanthro)[*a*, *e*]cycloocta-1,5-diene (**3**) is proposed on the basis of physical evidence presented below.

In the mass spectrum (see Experimental) the molecular peak appears at m/e 408 ($C_{32}H_{24}^+$). Significant peaks appear also at m/e 393 (M-15) and 380 (M-28), the latter indicating loss of C_2H_4 (*vide infra*). The base peak was observed at m/e 204 ($C_{16}H_{12}^+$). It could be added here that in the mass spectrum of phenanthrenophane **6** (isomeric with **3**) the base peak was found also at m/e 204.[2] Nevertheless, a prominent ion at m/e 204 ($C_{16}H_{12}^+$) was considered by Anhalt and White[4] to be essential for a compound which should possess structure **3**.

The UV-spectrum (data in CH_2Cl_2 are presented in the Experimental part) compares favourably with those of 9,10-dimethylphenanthrene (Fig. 1) and 9,10-cyclopentanophenanthrene.[9] On the other hand, it differs markedly — mainly in extinction values — from the spectrum of tetrabenzoanthracene **10** which presents the following data,[2] λ_{max} (lgε) : 259 (4.63); 269 (4.70) : 294 (4.98); 304 sh (4.85); 333 (4.58); 362 (3.39); 3.71 (2.87) and 382 nm (3.33).

The ^{1}H-NMR spectrum could not be run in usual solvents due to the very poor solubility: even in $AsCl_3$, d_6-dimethylsulphoxide, conc. sulphuric acid, or PBr_3, a useful concentration cannot be reached. However in d_5-pyridine at 112°C a singlet due to CH_2 groups was recorded at $\delta = 3.89$ ppm.

Attempted purification of **3** by vacuum sublimation (300°C at 10^{-3} Torr) conducted to partial decomposition. The sublimed material presented: (i) a new UV-absorption band at 362 nm along with a considerable increase of the absorption band at 294 nm; (ii) a higher melting point than the starting material and (iii) yellow colour. On the basis of these features, characteristic for tetrabenzo[*a*, *c*, *h*, *j*]anthracene (**10**), it seems that thermolysis of **3** affords — in part — the fully aromatic hydrocarbon **10**.

Contamination of **3** from the outset with *traces* of **10** cannot be ruled out (both compounds possess very similar spectral data: IR; UV—λ values; some peaks in MS) — but the extensive decomposition of **3** during sublimation was undoubtfully observed.

DISCUSSION

On the basis of previous [8] as well as present results, the mechanism of pyrolysis of disulphone **12** could be rationalized as follows (Scheme 2).

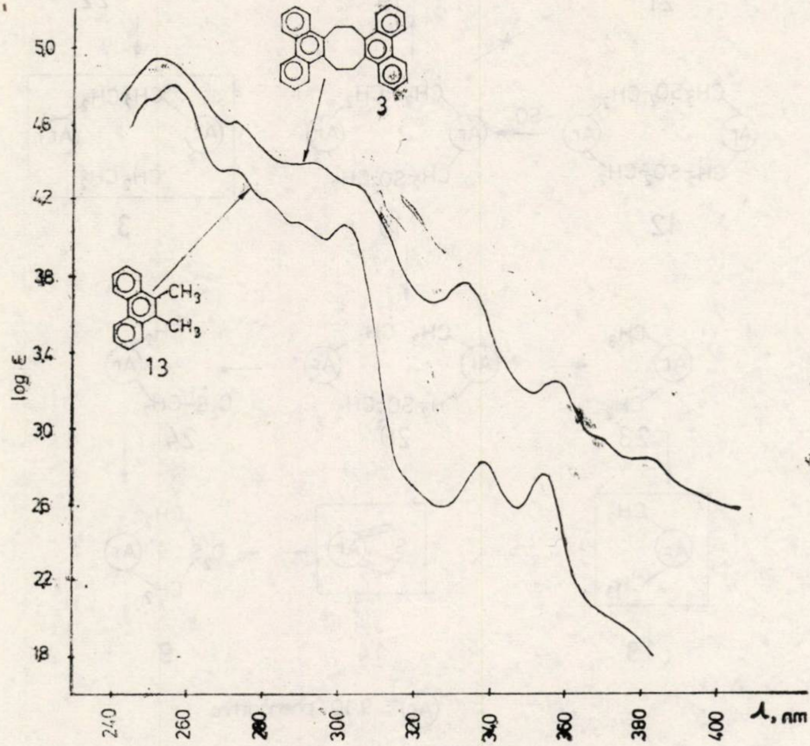

Fig. 1. — UV spectra of bis(9,10-phenanthro)[*a*, *e*]cycloocta-1,5-diene(**3**) and 9,10-dimethylphenanthrene (**13**) in CH_2Cl_2.

The usual pyrolytic reaction of disulphones is known to be the sequential extrusion of two SO_2 groups by radicalic mechanism.[2] By such a sequence, diradical **18** may appear from **12**; intramolecular bonding of the two radicalic centres may afford **19**. As in other cases[2] this monosulphone could not be isolated in reaction conditions, but reacts further in the same way, in gas phase, affording **3** *via* a new diradicalic species **22**. Another imaginable route from **18** to **3**, via **21**, could be ruled out — due to the lack of symmetric products in pyrolyses of unsymmetric disulphones (as was demonstrated e.g. in the previously described synthesis of **2**[1]). Formation of **13** and **14** by steps involving hydrogen abstraction — as described[8] — (see also scheme 2) — points out that even in the reaction conditions used in the present work ($10^{-4} \div 10^{-1}$ Torr; 500°C) the disulphone **12** reacts partly in condensed phase.

The failure of the attempted purification of **3** by vacuum sublimation seems to be due to easy thermolysis of this compound conducting to **10**. The following mechanism is suggested for this transformation(Scheme 3).

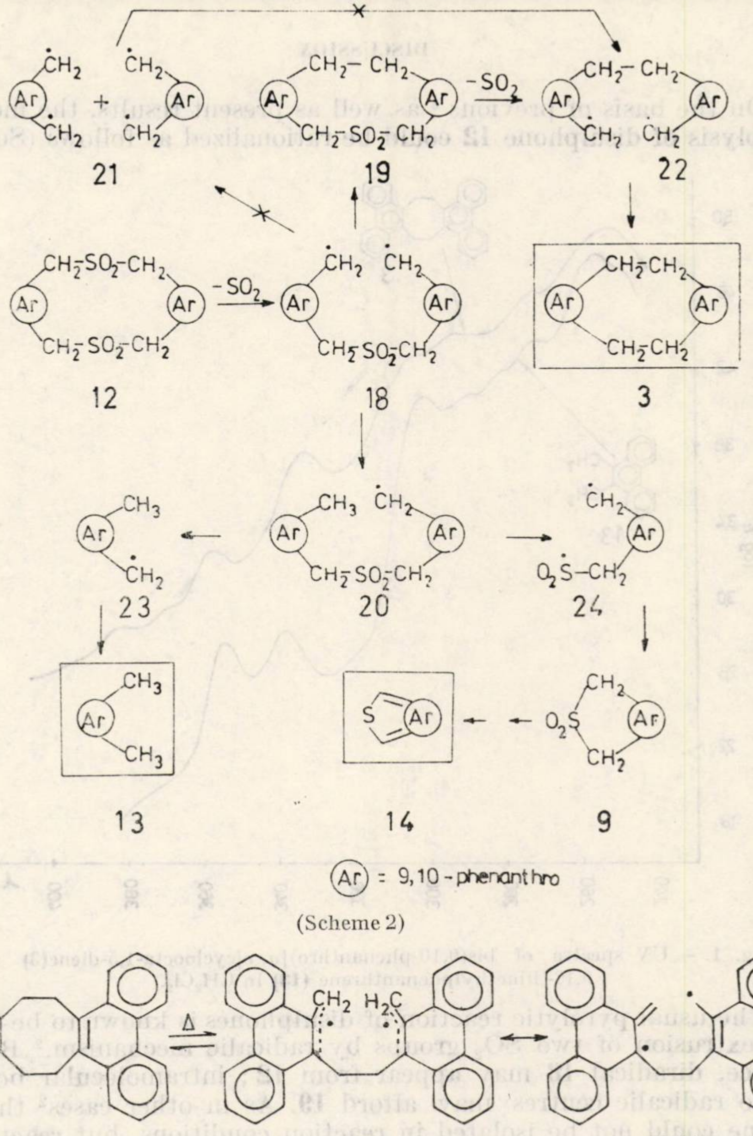
21
19
22
12
18
3
23
20
24
13
14
9
-SO2
Ar = 9,10-phenanthro

(Scheme 2)

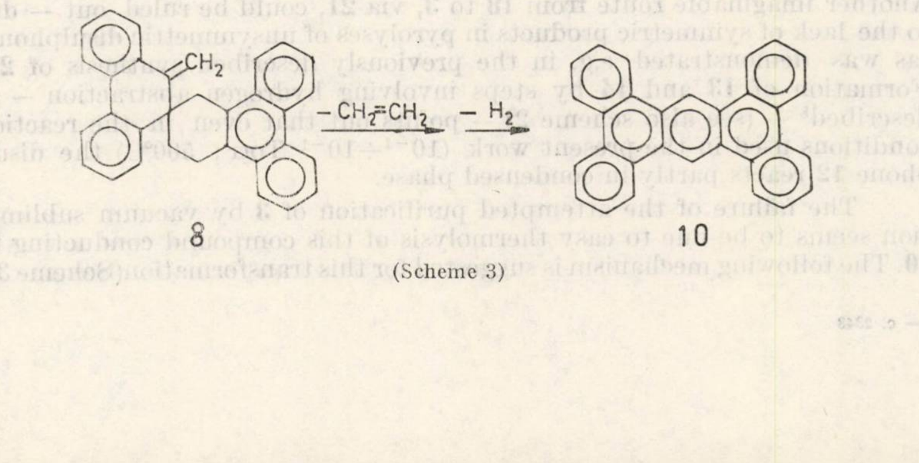
3
25a
25b
8
10
Δ
−CH2=CH2
−H2

(Scheme 3)

Equilibration of cyclooctadiene, octadienyl-diradical and vinylcyclohexene was convincingly proved for non-benzoannelated species.[10] Analogously, **8** could appear thermally from **3**. Further thermal conversion of **8** into **10** with loss of ethene and hydrogen, was demonstrated undoubtfully by Anhalt and White[4] (who proposed either a concerted or a two-step mechanism for this transformation).

The mechanism from scheme 3 could explain the appearance of (M-28) peak in the mass spectrum of **3** (the same peak, namely at m/e 380, appears in the mass spectrum of **8**[4]).

The thermal conversion of **3** into **10** could also explain the above mentioned results of Stille and Foster[3] who purified their (possibly) obtained hydrocarbon **3** either by vacuum sublimation or by recrystallization from diethylphthalate (b.p. 299°C) or from α-chloronaphthalene (b.p. 263°C). In this case attempted purification leads to the disappearance of the product.

In conclusion this work demonstrated the formation of bis-(9,10-phenanthro)[*a*, *e*]cycloocta-1,5-diene (**3**) by high-vacuum gas-phase pyrolysis of the corresponding disulphone **12**, as well as the thermal decomposition of **3** affording probably tetrabenzo[*a*, *c*, *h*, *j*] anthracene (**10**). At the same time the present results complet the series **1**, **2**, **3** of related cyclic hydrocarbons obtained directly by pyrolysis of disulphones.

EXPERIMENTAL

Melting points are uncorrected. IR spectra were recorded with a UR 20-Zeiss Jena double beam spectrophotometer, UV spectra with a SPECORD UV-VIS spectrophotometer, ^{1}H-NMR spectra with a VARIAN A 60A spectrometer (TMS — as internal standard) and the mas spectrum (at 185°) with a VARIAN MAT-SM$_1$ apparatus with direct inlet.

10,21-Dithia-9,10,11,20,21,22-hexahydrodiphenanthro[*a*, *f*]cyclodecene-S,S,S′S′-tetroxide (12)

The disulphone **12**, m.p. 370—372°C, was obtained as described previously[8] by H_2O_2-oxidation of disulphide **17**, resulted from reaction between 9,10-bis(mercaptomethyl)phenanthrene (**16**) and 9,10-bis(bromomethyl)phenanthrene (**15**).[8,11]

Pyrolysis of disulphone 12

Pyrolysis of disulphone **12** was performed in the slightly modified apparatus (Fig. 2) described by us previously[1]. The pyrolysis reactor — a quartz tube of 80 cm length and 1.8 cm diameter — was fitted with a mobile exterior cylindrical electrical oven, a thermocouple and devices for measuring the inert gas flow-rate and vacuum as well as with a cooled receiver vessel. The vacuum source was a diffusion pump affording — at the beginning of the reaction — a vacuum of 10^{-4} Torr. The pyrolysis sample (80 mg **12** per run) was introduced in a small quartz tube having its both ends fitted with glass wool. Concomitantly to diminution of pressure a small stream of pure argon was passed for ten minutes through the apparatus, then stopped allowing the vacuum to reach 10^{-4} Torr. The electrical oven, situated at the beginning in the central zone of the pyrolysis tube (figured with dotted line in fig. 2) was heated at 500—525°C. In this moment the electrical oven was translated rapidly in order to encircle the sample zone (position marked with full line in Fig. 2). In about 2—3 minutes the pyrolysis zone reached 500°C (temperature measured by means of the thermocouple) and the pressure begins to increase up to 0.1 Torr (or less) when the sample of **12** is about 80 mg. The reaction needed about 10—15 minutes for completion : during this time four distinct zones of products were formed in the pyrolysis tube (noted I—IV in Fig. 2) and practically no product was collected in the cooled receiver.

The pyrolysis products from zones I—IV were collected individually by dissolving in chloroform (and scratching). In the sample tube about 6 mg of black residue remained at each run. The above procedure was repeated for eight similar runs. The same distribution of zones I—IV being always observed, the products from the corresponding zones were collected together. The separation and identification of reaction products was performed as follows (starting material 8 × 80 mg = 0.64 g **12**).

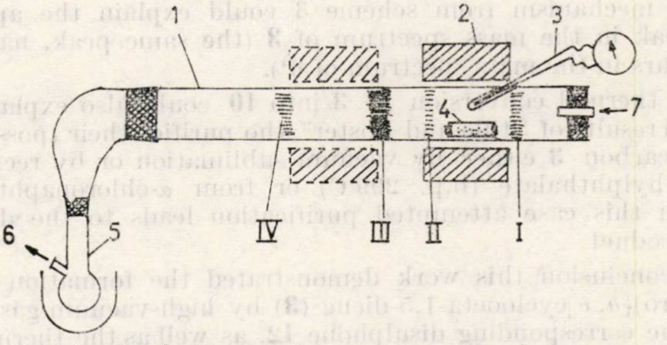

Fig. 2 — Pyrolysis apparatus. 1. — pyrolysis quartz tube; 2—electrical oven; 3—thermocouple; 4—pyrolysis sample tube; 5— receiver; 6 — to vacuum pump; 7 — inert gas inlet; I, II, III, IV — zones of pyrolysis products.

A) Zone IV — affords 70 mg (about 14% yield) yellow crystals, which on ^{1}H-NMR analysis proved to consist from a mixture of 9,10-dimethylphenanthrene(**13**) and phenanthro[9, 10c]thiophene (**14**) in about 1 : 1 ratio. This mixture was chromatographed on a small neutral alumina column with petroleum ether (b.p. 30—50°C) as eluent (in the manner described previously [8]); the compounds **13** (m.p. 142—144°C; lit.[13] m.p. 145°C) and **14** (m.p. 167°; lit.[12] m.p. 168—169°C) were separated and identified after their characteristic spectral data.[8,12,13]

B) The products from zone III (245 mg) and zone I (75 mg) proved — by IR, ^{1}H-NMR spectra — to be identical in composition and therefore they were combined affording 320 mg (about 65% yield) of an orange-brown solid. Addition of 4—5 mL chloroform conducted to separation of pale gray crystals which were filtered, washed with 2 mL chloroform affording *bis(9,10-phenanthro)*[a, e]*cycloocta-1,5-diene* (**3**) (90 mg; 18.5% yield), m.p. 336—9°C. From the chloroform filtrate small additional quantities of **3** (about 12 mg, 2.5% yield), m.p. 330—338°C precipitate on partial evaporation.

IR spectrum (KBr : cm^{-1}) : 721s, 759s, 850w, 874w, 943w, 974w, 1046w, 1154 w, 1206w; 1236 w, 1423w, 1441w, 1495w, 1579w, 1604w, 2924w, 2974w and 3063 w.

Mass spectrum (70 eV) m/e (relative intensity) : 410 (4); 409 (18); 408 (55, molecular peak); 394 (7); 393 (19); 382 (2); 381 (14) : 380 (46); 379 (22); 378 (41); 377 (5); 376 (7); 375 (1.5); 374 (3.5); 234 (5); 229 (11); 217 (4) : 216 (9); (215 (8); 206 (3.5); 205 (23); 204 (100, base peak) : 203 (82); 202 (44); 191 (7); 190 (10); 189 (21); 188 (5); 187 (4); 176 (4) and 165 (9).

UV spectrum (CH_2Cl_2); $\lambda_{max,nm}$(lg ε) : 254 (4.93); 273 (4.60); 294 (4.39); 307 (4.25); 332.5 (3.78); 357 (3.25) : 372 (2.88) and 382 (2.87) (see also Fig. 1).

^{1}H-NMR spectrum (d_5-pyridine, at 112°C, δppm); 3.89 (s, CH_2) along with a complex signal of aromatic protons from **3** and non-deuterated pyridine.

Total evaporation of the latter filtrate affords about 200 mg of a brown solid; the ^{1}H-NMR spectrum of this material indicates again the presence of **13** and **14**, possibly along with other component(s) which were not further investigated.

C) Zone II from the pyrolysis tube affords about 20 mg of a black solid which indicates in ^{1}H-NMR spectrum no aromatic proton signal; this product was also not further investigated.

Thermolysis of bis(9,10)-phenanthro[*a*, *e*]cycloocta-1,5-diene (3)

A sample of **3** (30 mg) was introduced in a vaccuum sublimation apparatus provided with a heating bath (Wood alloy). The sublimation was performed at 10^{-3} Torr by heating the app aratus from 175°C to 300°C during 45 min. The sublimated product, yellowish crystals (about 20 mg) indicated an UV spectrum resemblant with that of **3** but with an increased maximum at 294 nm and with a new band of small extinction coefficient at 362 nm.

About 5 mg of black porous solid remained in the sublimation apparatus.

The above mentioned sublimated product was sublimated again at $10^{-3}-10^{-4}$ Torr and 240°–300°C during 20 min; the new product, about 10 mg of yellow solid, began to melt at 330° and was not completely melted at 365°. In the UV spectrum the bands from 362 and 294 nm indicated a new increase in comparison with the product of the first sublimation.

ACKNOWLEDGEMENTS: We express our thanks to Professor Iuliu Pogany and Drs. Anca Voicu and Filip Chiraleu for helpful discussions and technical help.

REFERENCES

[1] M. Banciu, I. Pogany, D. Mosora, P. Rusu, R. Stănciulescu and M. Dezsö, *Rev. Roumaine Chim.*, **30**, 703 (1985).

[2] H. A. Staab and M. Haenel, *Chem. Ber.*, **106**, 2190 (1973).

[3] J. K. Stille and R. T. Foster, *J. Org. Chem.*, **28**, 2708 (1963).

[4] J. P. Anhalt and E. H. White, *Tetrahedron*, **28**, 2921 (1972).

[5] P. Lambert and R. H. Martin, *Bull. Soc. Chim. Belges*, **61**, 124 (1952).

[6] J. van Thuyjl and C. Romers, *Req Trav. Chim. Pays-Bas*, **87**, 5 (1968).

[7] E. H. White and J. P. Anhalt, *Tetrahedrnon Letters*, **1965**, 3937.

[8] M. Banciu, A. Banciu, M. Elian, C. Drăghici and E. Cioranescu, *Rev. Roumaine Chim.*, **32**, 961 (1987).

[9] A. Butenandt, H. Dannenberg and Aziz-Ur Rahman, *Chem. Ber.*, **88**, 1395 (1955).

[10] F. Badea, „Reaction Mechanisms in Organic Chemistry'', Abacus Press, Tunbridge Wells, Kent, 1977, p. 650 : G. S. Hammond and C. D. de Boer, *J. Amer. Chem. Soc.*, **86**, 899 (1964) ; D. J. Trecker and J. P. Henry, *J. Amer. Chem. Soc.*, **86**, 902 (1964) ; R. Srinivasan and A. A. Levi, *J. Amer. Chem. Soc.*, **86**, 3756 (1964) ; S. W. Benson, *J. Chem. Phys.*, **46**, 4920 (1967).

[11] T. Zincke and W. Tropp, *Liebigs Annal. Chem.*, **362**, 242 (1908).

[12] J. E. Shields, D. E. Remy and J. Bornstein, *J. Org. Chem.*, **40**, 477 (1975).

[13] S. Hauptmann, *Chem. Ber.*, **93**, 2604 (1960).

rature from 155°C to 300°C during 40 min. The sublimated product, yellowish crystals (about 20 mg) indicated an UV spectrum resembling with that of 3 but with an increased maximum at 304 nm and with a new band of small extinction coefficient at 362 nm.

About 5 mg of black porous solid remained in the sublimation apparatus.

The above mentioned sublimated product was sublimated again at 10^{-2}–10^{-3} Torr and 240–300°C during 20 min; the new product, about 10 mg of yellow solid, began to melt at 290° and was not completely melted at 300°. In the UV spectrum the bands from 302 and 294 nm indicated a new increase in comparison with the product of the first sublimation.

ACKNOWLEDGEMENTS. We express our thanks to Professor Iulia Pogany and Mrs. Anca Voicu and Filip Chiraleu for helpful discussions and technical help.

REFERENCES

[1] M. Banciu, L. Pogany, [illegible] P. Rosu, P. Stănculescu and M. Elian, *Rev. Roumaine Chim.*, **30**, 708 (1985).
[2] H. A. Staab and M. Haenel, *Chem. Ber.*, **106**, 2190 (1973).
[3] J. K. Stille and D. T. Foster, *J. Org. Chem.*, **28**, 2708 (1963).
[4] J. P. Anhalt and E. H. White, *Tetrahedron*, **28**, 2421 (1972).
[5] P. Lambert and R. H. Martin, *Bull. Soc. Chim. Belges*, **61**, 124 (1952).
[6] L. van Tuyll and C. Romers, *Rec. Trav. Chim. Pays-Bas*, **87**, 5 (1968).
[7] E. H. White and J. P. Anhalt, *Tetrahedron Letters*, 1965, 3937.
[8] M. Banciu, A. Banciu, M. Elian, C. Drăghici and E. Cioranescu, *Rev. Roumaine Chim.*, **32**, 981 (1987).
[9] A. Butenandt, H. Dannenberg and Ada v. Dresler, *Chem. Ber.*, **88**, 1295 (1955).
[10] [illegible], "Reaction Mechanisms in Organic Chemistry", Abacus Press, Tunbridge Wells, Kent, 1975, p. 850; T. S. Hammond and C. D. de Boer, *J. Amer. Chem. Soc.*, **86**, 899 (1964); D. J. Trecker and J. P. Henry, *J. Amer. Chem. Soc.*, **86**, 902 (1964); R. Srinivasan and A. A. Levi, *J. Amer. Chem. Soc.*, **86**, 3756 (1964); S. W. Benson, *J. Chem. Phys.*, **46**, 4920 (1967).
[11] T. Zincke and W. Tropp, *Liebigs Annal. Chem.*, **362**, 242 (1908).
[12] J. P. Shields, D. R. Berry and R. Bornstein, *J. Org. Chem.*, **40**, [illegible] (1975).
[13] S. Hünig [illegible], *Chem. Ber.*, **93**, 2804 (1960).

Revue Roumaine de Chimie, **33**, *9–10*, 903–910 (1988)

THE REACTION OF CYCLOHEXA-3,5-DIENE-1,2-DICARBOXYLIC ACID DERIVATIVES WITH *PARA*-BENZOQUINONE AND AZO COMPOUNDS. I

F. IORDACHE,[a] MARIANA DĂNILĂ,[b] ANA SCHIKETANZ,[a] M. GHEORGHIU[a]
and F. BADEA[a]

[a] Laboratory of Organic Chemistry, Polytechnic Institute — T.C.O. 77208 Bucharest, Splaiul Independenţei 313, Romania

[b] Institute of Research of Pesticides — ICECHIM — Bucharest, Splaiul Independenţei 202, Romania

Received March 28, 1988

The reactions of cyclohexa-3,5-diene-1,2-dicarboxylic acid derivatives (ester and anhydride) with *p*-bentoquinone, ethyl azodicarboxylate and 4-N-phenyl-1,2,4 triazoline-3,5-dione (**6**) are described. The configurations of the newly obtained compounds were determined by ^{1}H-NMR, IR, and mass spectrometry; their reactions were also studied.

INTRODUCTION

Although the Diels-Alder reaction of cyclohexa-3,5-diene with *p*-benzoquinone was described,[1] the adducts of *p*-benzoquinone with *cis* and *trans* methyl esters (**2** and **3**, respectively) of cyclohexa-3,5-diene-1,2-dicarboxylic acid (**1**) are unknown in the literature.

In the present paper we report the preparation of the diene adduct of *p*-benzoquinone with the *trans* ester **3**.

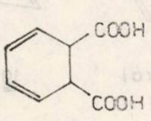

1

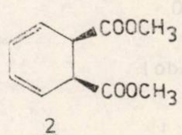

2

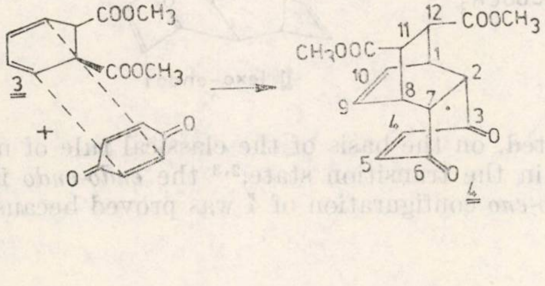

Our attempt to obtain (4+2) cycloaddition adduct from *p*-benzoquinone and dihydrophthalic anhydride or *cis* methyl-ester of cyclohexa-3,5-diene-1,2-dicarboxylic acid (**2**) has failed. In both cases, from the reaction mixture, quinhydrone and phthalic anhydride or ester was isolated.

We also report in the present paper the preparation of the new adduct of dihydrophthalic anhydride (**4**) with 4-N-phenyl-1,2,4-triazoline-3,5-dione (**6**, PTAD) generated *in situ* by oxidation of the 4-phenylurazole (**8**) with t-butyl hypochlorite in anhydrous acetone at temperatures −5...0°. An adduct **7**, which was obtained as a white solid product (m.p. 236°), was isolated.

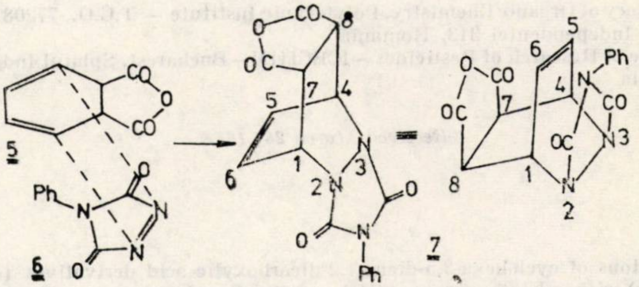

RESULTS

There are four possible stereoisomers with the carbomethoxy groups in *trans* position for the adduct of *p*-benzoquinone with the *trans* ester **3** (**4**, **9**,—**11**).

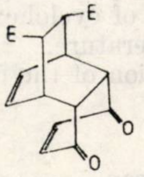

4 (endo-endo)

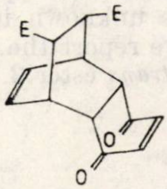

9 (endo-exo)

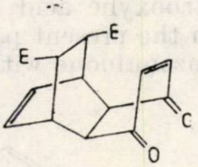

10 (exo-exo)

E = −COOCH$_3$

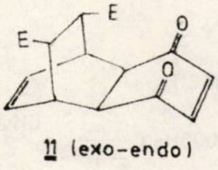

11 (exo-endo)

As expected, on the basis of the classical rule of maximum overlap of π-electrons in the transition state,[2,3] the *endo-endo* isomer **4** was isolated. The *endo-eno* configuration of **4** was proved because on irradiating it with a medium pressure mercury UV lamp, for four hours in anhydrous acetone, a cage compound **12**, m.p. 160 was obtained (we suppose that no other isomerisation took place).

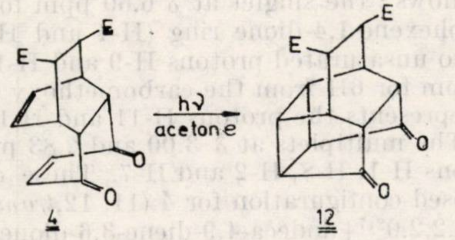
E
E
E
hν
acetone
O
O
O
4
12

The structure of **4** was also proved by its oxidation with potassium permanganate. The oxidation of **4** can follow two reaction pathways: an attack to the C-9—C-10 double bond, which would yield the acid-ester **16**, or an attack to the C-4—C-5 double bond, which would yield tetracarboxylic acid (±) —**14** (Scheme 1.)

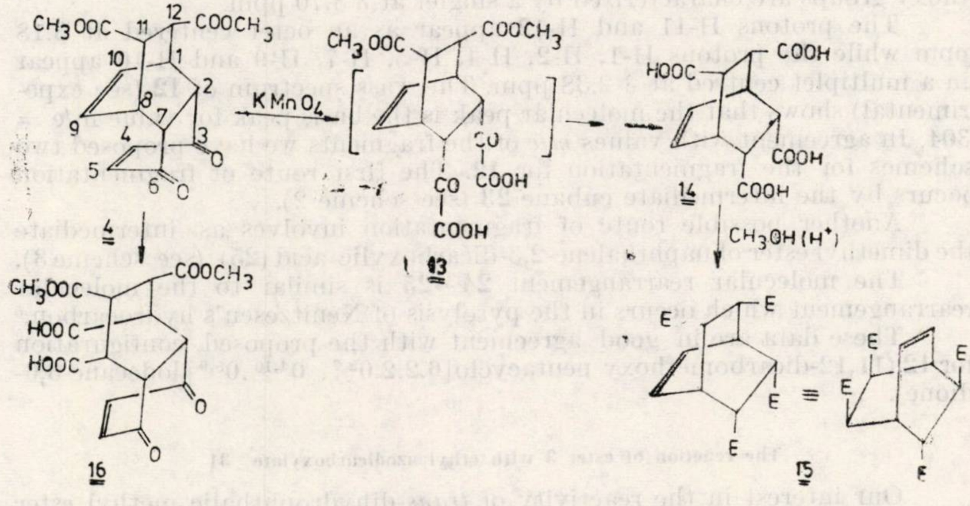
CH3OOC
11
12
COOCH3
10
1
2
8
9
4
3
5
6
O
O
KMnO4
CH3OOC
COOCH3
CO
CO
COOH
COOH
13
COOH
HOOC
COOH
COOH
14
CH3OH (H+)
4
CH3OOC
COOCH3
HOOC
HOOC
O
O
16
E
E
E
E
E
E
E
E
15

Scheme 1

As expected, considering that C-4—C-5 double bond is activated by vicinity of the carboxyl groups from C-3 and C-6 positions, acid (±) —**14** was obtained.

The acid ±**14** was transformed by esterification with methanol in the presence of catalytic traces of sulphuric acid, into the ester (±)—**15**, caracterized by IR, ^{1}H-NMR spectra which conformed the known configuration, described in the previous paper.[4] (See experimental).

Configuration of esters 4 and 13

In order to establish the configuration of these compounds we used the IR, ^{1}H-NMR and mass spectra.

The IR spectrum (KBr) of **4** presents two characteristic bands at 1730 cm^{-1} (carboxyl groups) and at 1680 cm^{-1} (double bonds).

The ^{1}H—NMR spectrum of **4**, recorded in $CDCl_3$ presents seven signals (δ, ppm) : 2.83, 3.00, 3.20, 3.60, 3.78, 6.20 and 6.60 attributed without difficulty as follows : the singlet at δ 6.60 ppm for two unsaturated protons of the cyclohexene-1,4-dione ring (H-4 and H-5), the multiplet at δ 6.20 ppm for two unsaturated protons H-9 and H-10 and the singlets at δ 3.78 and 3.60 ppm for 6H from the carbomethoxy groups. The signal at δ 3.20 ppm (2H) represents the protons H-11 and H-12 adjacent to carbomethoxy groups. The multiplets at δ 3.00 and 2.83 ppm (4H) represent the bridgehead protons H-1, H-8, H-2 and H-7. These data are in agreement with the proposed configuration for **4** (11, 12,*trans*-dicarbomethoxy-*endo-endo*-tricyclo [6.2.2.0^{2,7}] dodeca-4,9-diene-3,6-dione).

The IR spectrum of the cage compound **12** presents a vibrational band at 1720 cm^{-1} assigned to the carbonyl groups from the ester and does not exhibits a stretching vibration for the double bond.

The ^{1}H-NMR spectrum of **12** recorded in hexadeuteroacetone shows the disappearance of the signals at δ 6.20 and 6.50 ppm due to the unsaturated protons from the adduct **4**. The methyl groups from both carbomethoxy groups are characterized by a singlet at δ 3.70 ppm.

The protons H-11 and H-12 appear as an octet centered at 3.18 ppm while the protons H-1, H-2, H-4, H-5, H-7, H-9 and H-10 appear in a multiplet centred at δ 2.38 ppm. The wass spectrum of **12** (see experimental) shows that the molecular peak is the basis peak for value m/e = 304. In agreement with values *m/e* of the fragments we have proposed two schemes for the fragmentation for **12**. The first route of fragmentation occurs by the intermediate cubane **23** (see scheme 2).

Another possible route of fragmentation involves as intermediate the dimethyl ester of naphthalene-2,3-dicarboxylic acid (**25**) (see scheme 3).

The molecular rearrangement **24**→**25** is similar to the molecular rearrangement which occurs in the pyrolysis of Nenitzescu's hydrocarbon.[5]

These data are in good agreement with the proposed configuration for **12** (11,12-dicarbomethoxy-pentacyclo[6.2.2.0^{2,7}. 0^{4,10}.0^{5,9}]dodecane-3,6-dione).

The reaction of ester 3 with ethyl azodicarboxylate 31

Our interest in the reactivity of *trans*-dihydrophthalic methyl ester **3** in Diels-Alder reactions led us to the new diene adduct **32**, formed in the reaction with azodicarboxylic ethyl ester **31**.

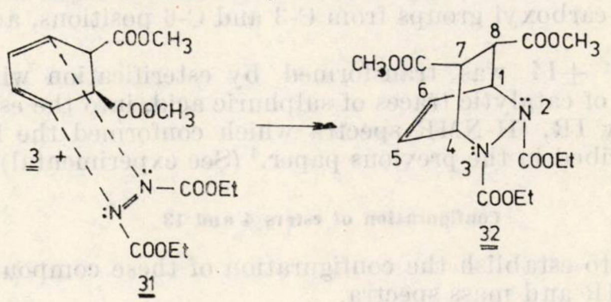

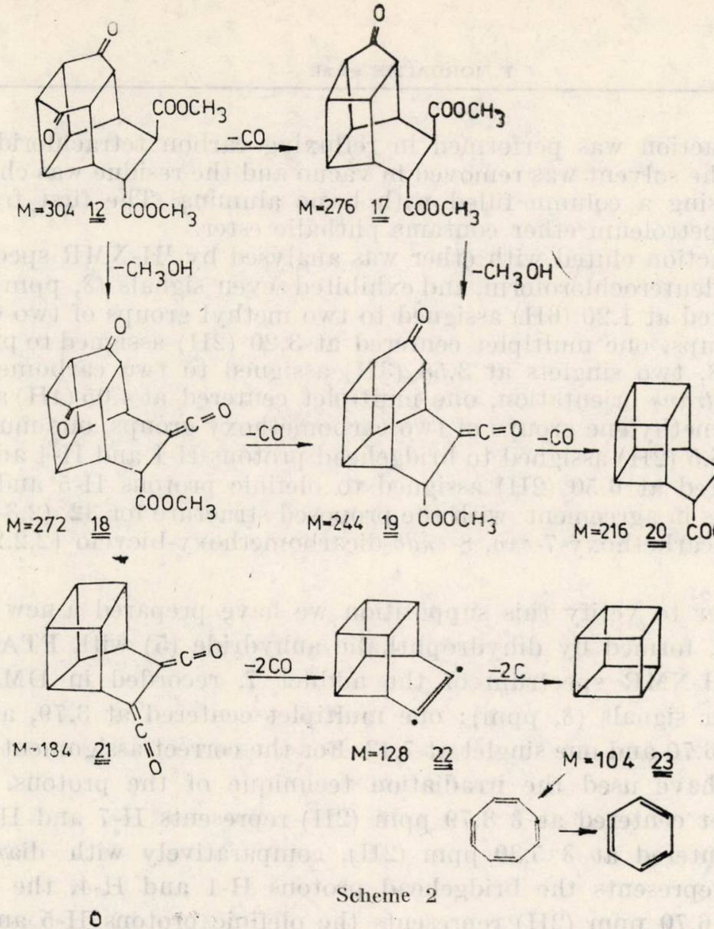
COOCH$_3$
M=304 12 COOCH$_3$
−CO
M=276 17 COOCH$_3$
−CH$_3$OH
−CH$_3$OH
C=O
COOCH$_3$
M=272 18
−CO
M=244 19 COOCH$_3$
−CO
M=216 20 COOCH$_3$
M=184 21
−2CO
M=128 22
−2C
M=104 23

Scheme 2

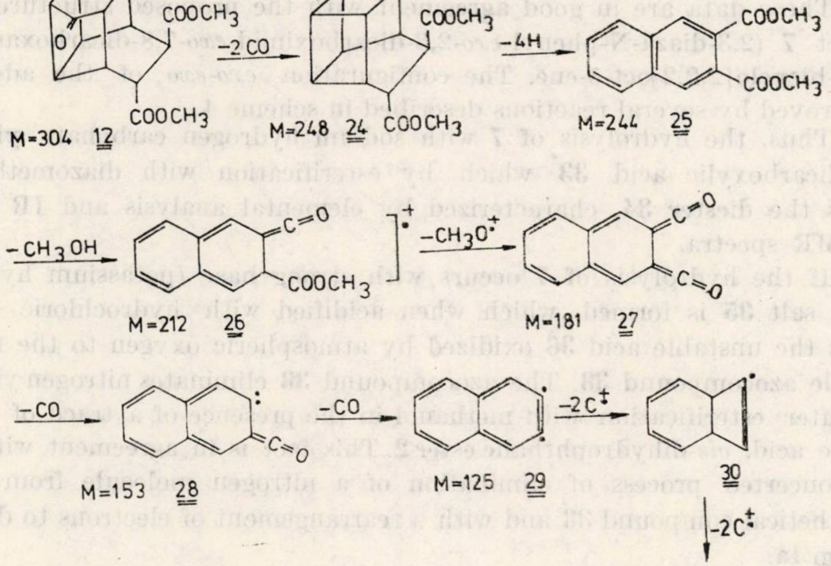
COOCH$_3$
M=304 12 COOCH$_3$
−2 CO
M=248 24 COOCH$_3$
−4H
M=244 25 COOCH$_3$
−CH$_3$OH
M=212 26 COOCH$_3$
$-CH_3O^{+}$
M=181 27
−CO
M=153 28
−CO
M=125 29
$-2C^{+}$
30
$-2C^{+}$

Scheme 3

The reaction was performed in refluxing carbon tetrachloride, for two hours. The solvent was removed in vacuo and the residue was chromatographed using a column filled with basic alumina. The first fraction eluted with petroleum ether contains phthalic ester.

The fraction eluted with ether was analysed by ^{1}H-NMR spectrum, recorded in deuterochloroform, and exhibited seven signals (δ, ppm); one triplet centered at 1.20 (6H) assigned to two methyl groups of two carbomethoxy groups, one multiplet centered at 3.20 (2H) assigned to protons H-7 and H-8, two singlets at 3.58 (3H) assigned to two carbomethoxy groups with *trans* orientation, one multiplet centered at 4.05 (4H) assigned for two methylene groups of two carbomethoxy groups, one multiplet centered at 5.5 (2H) assigned to bridgehead protons H-1 and H-4 and one triplet centered at 6.50 (2H) assigned to olefinic protons H-5 and H-6. These data as in agreement with the proposed structure for **32** (2,3-diazo-N,N-2-*exo*-dicarbethoxy-7-*exo*, 8-*endo*-dicarbomethoxy-bicyclo [2.2.2] oct--5-ene.

In order to verify this supposition we have prepared a new diazacompound **7**, formed by dihydrophthalic anhydride (**5**) with PTAD (**6**).

The ^{1}H-NMR spectrum of the adduct **7**, recorded in DMSO-d_6, presents four signals (δ, ppm); one multiplet centered at 3.79, another centered at 6.70 and one singlet at 7.43. For the correct assignment of the signals we have used the irradiation technique of the protons. Thus, the multiplet centered at δ 3.79 ppm (2H) represents H-7 and H-8 the multiplet centered at δ 5.30 ppm (2H), comparatively with diazocompound **32**, represents the bridgehead protons H-1 and H-4, the triplet centered at 6.70 ppm (2H) represents the olefinic protons H-5 and H-6 and the singlett at 7.43 (5H) represents the aromatic protons.

These data are in good agreement with the proposed structure for adduct **7** (2,3-diaza-N-phenyl-*exo*-2,3-dicarboximid-*exo*-7,8-dicarboxanhydride-bicyclo[2.2.2]oct-5-ene. The configuration *exo-exo* of the adduct **7** is proved by several reactions described in scheme 4.

Thus, the hydrolysis of **7** with sodium hydrogen carbonate yields the dicarboxylic acid **33** which by esterification with diazomethane yields the diester **34**, characterized by elemental analysis and IR and ^{1}H-NMR spectra.

If the hydrolysis of **7** occurs with strong base (potassium hydroxide), salt **35** is formed, which when acidified with hydrochloric acid yields the unstable acid **36** oxidized by atmospheric oxygen to the nonisolable azocompound **38**. The azocompound **38** eliminates nitrogen yielding after esterification with methanol in the presence of a trace of sulphuric acid, *cis*-dihydrophthalic ester **2**. This fact is in agreement with a non-concerted process of elimination of a nitrogen molecule from the hypothetical compound **38** and with a rearrangement of electrons to diene system **1a**.

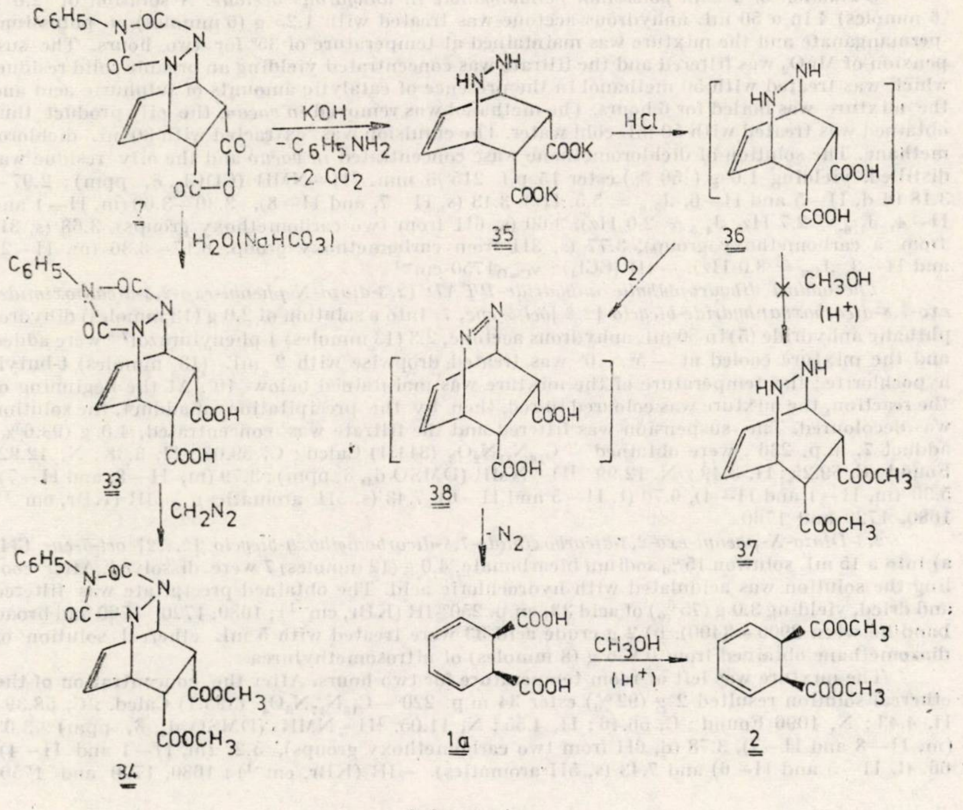
C6H5
N-OC
N
OC-N
CO
OC-O
7
KOH
-C6H5NH2
2 CO2
H2O(NaHCO3)
HN
NH
COOK
COOK
35
HCl
HN
NH
COOH
COOH
36
O2
CH3OH
(H+)
C6H5
N-OC
N
OC-N
COOH
COOH
33
N
N
COOH
COOH
38
HN
NH
COOCH3
COOCH3
37
CH2N2
-N2
C6H5
N-OC
N
OC-N
COOCH3
COOCH3
34
COOH
COOH
1a
CH3OH
(H+)
COOCH3
COOCH3
2

Scheme 4

EXPERIMENTAL

The adduct of trans-dihydrophthalic ester with p-benzoquinone (11, 12-dicarbomethoxytricyclo [6.2.2.$0^{2,7}$] dodeca-4,9-diene-3,6-dione (4))

A mixture of 2.0 g (28 mmoles) p-benzoquinone, 6.0 g (30 mmoles) ester *trans*-dihydrophthalic (3) and 50 mL carbon tetrachloride was heated at reflux for two hours.

After the solvent was removed *in vacuo*, the oily residue was treated with 50 mL methanol, the separated solid was filtered, yielding, 6.0 g (70%) 4, m.p. 134° (from methanol). $C_{16}H_{16}O_6$ (304.1) Calcd.; C, 63.15; H, 65.26. Found: C, 62.77; H, 5.44 ^{2}H—NMR ($CDCl_3$, δ, ppm): 2.83 and 3.00 (m, H—1, H—8, H—2, and H—7) 3.2 (m. H—11 and H—12). 3.6 and 3.78 (s, 6H from two carbomethoxy groups), 7.2 (sextet, H—9 and H—10) and 6.6 (s, H—4, and H—5). IR (KBr, cm^{-1}): $\nu_{C=C}$ 1680: $\nu_{C=0}$ 1730.

11,12-Dicarbomethoxy-pentacyclo [6. 2.2.$0.^{3,7}.0^{4,10}.0^{5,9}$] dodeca-3,6-dione (12)

A solution of 2.0 g (16 mmoles) 4 in 75 mL anhydrous acetone was irradiated with UV by a medium pressure mercury lamp, for four hours. After the solvent removed *in vacuo*, the organic product was left in exicator for 24 hours; 1 9 (95%) of cage adduct 12, m.p. 160° were obtained. $C_{16}H_{16}O_6$ (304.1) MS, m/e, u.a.m. (relative abundance %); 304 (100, PM), 276 (311) 248 (44), 244 (387), 212 (151), 184 (321), 181 (4), 153 (5), 125 (15), 104 (191), 102 (86), 78 (386). H—NMR ($D_3C—CO—CD_3$, δ, ppm); 2 .32 (m, H—1, H—2, H—4, H—5, H—7, H—9 and H—10) 3.18 (octet, H—11 and H—12). 3.70 (6 H from two carbomethoxy groups). —IR (KBr, cm^{-1}); ν_{CO} 1730 cm^{-1}.

Oxidation of **4** *with potassium permanganate in anhydrous acetone*. A solution of 2.0 g (6 mmoles) **4** in a 50 mL anhydrous acetone was treated with 1.25 g (6 mmoles) of potassium permanganate and the mixture was maintained at temperature of 35° for two hours. The suspension of MnO_2 was filtered and the filtrate was concentrated yielding an organic solid residue, which was treated with 50 methanol in the presence of catalytic amounts of sulphuric acid and the mixture was boiled for 6 hours. The methanol was removed *in vacuo*, the oily product thus obtained was treated with 50 mL cold water. The emulsion was extracted with 30 mL dichloromethane. The solution of dichloromethane wasc concentrated *in vacuo* and the oily residue was distilled, yielding 1.0 g (50 %) ester **15** p.f. 215°/3 mm. ^1H-NMR ($CDCl_3$, δ, ppm); 2.97—3.18 (d d, H—5 and H—6, $J_{5.6} = 5.5.$ Hz). 3.13 (s, H—7, and H—8), 3.30—3.60 (m, H—1 and H—4, $J_{1.6} = 2.7$ Hz, $J_{4.5} = 2.0$ Hz), 3.60 (s, 6H from two carbomethoxy groups), 3.68 (s, 3H from a carbomethoxy group), 3.77 (s, 3H from carbomethoxy group, 6.17—6.36 (m, H—2, and H—3, $J_{2,3} = 8.0$ Hz). — IR (CCl_4) : $\nu_{C=O}$1750 cm^{-1}

The adduct dihydrophthalic anhydride-PTAD (2,3-diazo-N-phenyl-exo-2,3-dicarboximide-exo-7,8-dicarboxyanhydride-bicyclo-[2.2.]oct-5-ene, 7. Into a solution of 2.0 g (13 mmoles) dihydrophthalic anhydride (**5**) in 50 mL anhydrous acetone, 2.3 (13 mmoles) 4-phenylurazol[7,6] were added and the mixture cooled at —5°. . .0° was treated dropwise with 2 mL (13 mmoles) t-butylhypochlorite; the temperature of the mixture was maintained below 10°. At the beginning of the reaction, the mixture was coloured in red, then by the precipitation of adduct, the solution was decoloured. The suspension was filtered and the filtrate was concentrated, 4.0 g (93.6 %) adduct **7**, m.p. 236°, were obtained — $C_{16}N_{11}N_2O_3$ (311,1) Calcd : C, 59.08 ; H, 3.38 ; N, 12.92. Found : C, 59.25 ; H, 3.49 ; N. 12.99 ^1H-NMR (DMSO d_4, δ, ppm) ; 3.79 (m, H—8, and H—7), 5.30 (m, H—1 and H—4), 6.70 (t. H—5 and H—6), 7.43 (s, 5H aromatics). — IR (KBr, cm^{-1} : 1680, 1720 and 1760.

2,3-Diazo-N-phenyl-exo-2,3-dicarboximide-7,8-dicarbomethoxy-bicyclo [2.2.2] oct-5-ene (**34**) a) Into a 15 mL solution 15 % sodium bicarbonate, 4.0 g (12 mmoles) **7** were dissolved. After cooling the solution was acidulated with hydrochloric acid. The obtained precipitate was filtered and dried, yielding 3.0 g (75 %) of acid **33**, m.p. 250°-IR (KBr, cm^{-1}) ; 1680, 1720, 1760 and broad band between 2900—3400). b) 2 g crude acid **33** were treated with 5 mL ethereal solution of diazomethane obtained from 0.856 g (8 mmoles) of nitrosomethylurea.

The mixture was left at room temperature for two hours. After the concentration of the ethereal solution resulted 2 g (92 %) ester **34** m.p. 220°—$C_{18}N_{17}N_3O_4$ (393.1) Calcd. : C, 58.39 ; H, 4.43 ; N, 1096 Found : C, 56.46 ; H, 4.55 ; N, 11.05. ^1H-NMR (DMSO d_4, δ, ppm) : 3.03 (m, H—8 and H—7), 3.78 (d, 6H from two carbomethoxy groups), 5.2 (m, H—1 and H—4), 66. (t, H—5 and H—6) and 7.43 (s, 5H aromatics). — IR (KBr, cm^{-1}) : 1680, 1720 and 1750.

Hydrolysis of **7** *with strong base (KOH)*

2.0 g (6 mmoles) of **7** were treated with 5 mL solution 10 % of potassium hydroxide and refluxed until the mixture was dissolved. Afterwards the watery solution was extracted with 10 mL benzene, and was treated with hydrochloric acid until neutral. The precipitated salt was filtered and the filtrate was evaporated to dry in vacuum.

The residue (which contained an acid component, as shown by the IR spectrum) was treated with an excess of methanol in the presence of catalytic traces of sulphuric acid and the mixture was boiled for 6 hours. Afterwards the methanol was removed in vacuo, an oily product was obtained, which was treated with 50 mL cold water. The emulsion was extracted with 30 mL dichloromethane. The solution of dichloro-methane was concentrated in vacuo and the oily residue was distilled, yielding 1.0 g (85 %) of *cis*-dihydrophthalic ester (**2**), characterized by the ^1H-NMR spectrum. The benzene solution was treated by bubbling with gaseous hydrochloric acid and aniline salt was precipitated.

REFERENCES

[1] O. Diels and K. Alder, *Ber. dtsch. chem. Ges.*, **62**, 2364 (1929).

[2] K. Alder and G. Stein, *Liebigs Ann. Chem.*, **504**, 222 (1933).

[3] K. Alder and G. Stein, *Angew. Chem.*, **50**, 514 (1937).

[4] F. Iordache, F. Chiraleu and M. Avram, *Rev. Roumaine Chim.*, **20**, 233 (1975).

[5] C. D. Nenitescu, M. vrAvram, I. I. Pogany, Ch. D. Mateescu and M. Fărcaşiu, *Stud. Cercet. Chim. R.P.R.*, **11**, 7 (1963).

[6] R. C. Cookson, S. S. Gupta, I. D.R., Stevans and G. T. Watts, *Org. Synth.*, **51**, 121 (1971).

[7] J. Thiele and O. Stange, *Liebings Ann. Chem.*, **283**, 45 (1894).

Revue Roumaine de Chimie, 33, *9–10*, 911–916 (1988)

2-HYDROXYKETONES. XX[1]

NEW *MANNICH-WERNER* BASES OF 7-HYDROXY-4-METHYL-6- AND 8-PROPIONYLCOUMARIN

ALEXANDRU CAŞCAVAL[a] and ŞTEFAN CILIANU BIBIAN[b]

[a] Department of Organic and Macromolecular Chemistry, Polytechnic Institute of Iaşi, Calea 23 August 22, R-6600 Iaşi, Romania

[b] Central Research Institute of Pharmaceutical Chemistry, Şoseaua Vitan 112, Bucharest, Romania

Received November 20, 1987

4,6-Dimethyl-6-diethylamino(or piperidino)methyl-2H, 5H-6,7-dihydrobenzo [1,2b : 4,5b']dipyran-2,5-dione **8a,b** and 4,9-dimethyl-9-diethylamino or (piperidino)methyl-2H, 10H-8,9-dihydrobenzo[1. 2b : 3,4 b']dipyran-2,10-dione **10 a,b** are synthesized by the *Mannich-Werner* reaction of selected ethyl *ortho*-hydroxycoumarin ketones **5, 6**. The corresponding hydrochlorides **12 a, b** were evaluated for their hypotensive activity.

Linear as well as angular pyranocoumarins are two classes of photobiological agents on which the major part of the photochemical and photobiological studies have been so far performed.[2] D. N. Robertson and K. P. Link [3] initiated the use of various hydroxycoumarins as reactive heteroaromatic nucleus in the *Mannich* reaction; later, R. B. Desai [4] described the behaviour of 7-hydroxy-4-methylcoumarin and stated that, like other usual electrophylic aromatic substitutions, the *Mannich* reaction leads exclusively to 8-alkylaminomethylderivatives. D. Molho and E. Boschetti [5] reported interesting properties of a series of Mannich bases of 7-hydroxy-4-methylcoumarin (methylumbelliferone) as stimulating agent of central nervous system. A. K. Rao and others [6] have more recently reported remarkable antimicrobial and antifungal activity for 7-hydroxy-8-morpholinomethyl-4-phenylcoumarin.

Although a considerable effort was made for condensation of alkyl *ortho*-hydroxyphenyl ketones with formaldehyde and ammonia[7] or amines,[8–10] there appears to exist only a single publication [13] dealing with the use of an *ortho*-hydroxy-acetylcoumarin in this well-known reaction.

Our interest in the synthesis of various oxygen-containing heterocycles with marked physiological activity by using differently substituted alkyl *ortho*-hydroxyphenyl ketones [14–15] led us to undertaking an intensive study upon coumarin derivatives having in mind the following arguments: the coumarin moiety is contained in a variety or highly physiologically active compounds both natural (like VISNADIN **1**,[16] a known coronary vasodilator and angioprotective agent, or MESHUAGIN **2** – a new plant antibiotic from Meshua Ferre Linn[17]) and synthetic (like CARBOCROMEN **3** with useful coronary dilatory activity as well as antifibrilant and antiarrhythmic action [18]).

We wish here to report a very simple "one step" new *Mannich-Werner* reaction using 7-hydroxy-4-methyl-6-propionylcoumarin **5** and 7-hydroxy-4-methyl-8-propionylcoumarin **6**, easily accessible by the Fries

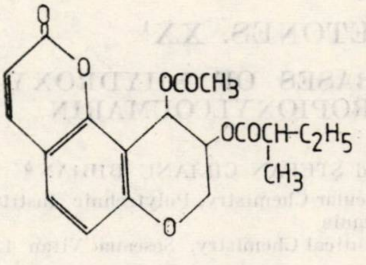
OCOCH3
OCOCH–C2H5
CH3

VISNADIN , CARDUBEN
1

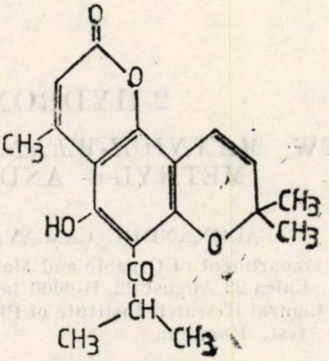
CH3
CH3
CH3
HO
CH
CH3
CH3

MESHUAGIN ,
2

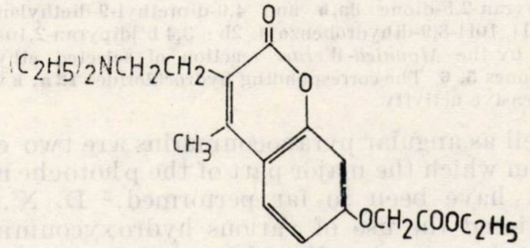
(C2H5)2NCH2CH2
CH3
OCH2COOC2H5

CARBOCROMEN R INTENSAIN
3

rearrangement of 4-methyl-7-propionyloxycoumarin 4[19], followed by a careful purification of the reaction mixture :

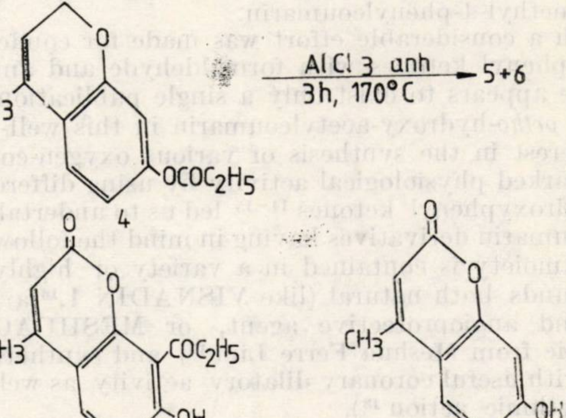
CH3
OCOC2H5
4
AlCl 3 unh
3h, 170°C
5+6
CH3
COC2H5
OH
6 (yield 70%)
CH3
OH
COC2H5
5 (yield 10%)

By refluxing a mixture of **5**, paraformaldehyde and secondary amines **7 a,b** in ethanol, we obtained in good yield the new *Mannich-Werner* bases **8a,b** as follows :

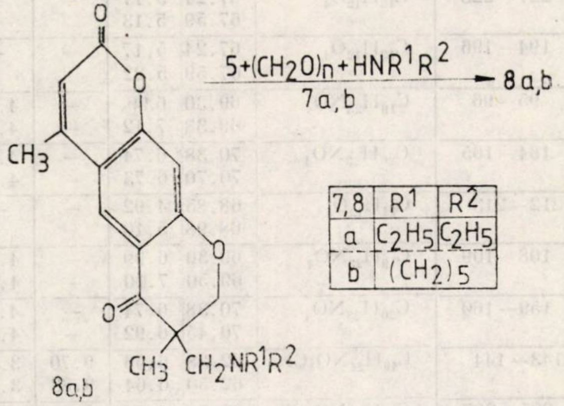
5+(CH2O)n+HNR1R2
7a,b
8a,b
CH3
CH3 CH2NR1R2
8a,b
7,8 | R1 | R2
a | C2H5 | C2H5
b | (CH2)5

In a similar reaction, **6** reacted with paraformaldehyde and secondary amines **7 a,b** to give the new *Mannich-Werner* bases **10 a,b** :

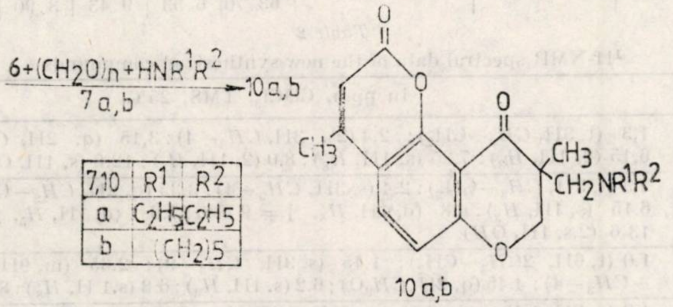
6+(CH2O)n+HNR1R2
7a,b
10a,b
CH3
CH3
CH2NR1R2
7,10 | R1 | R2
a | C2H5 | C2H5
b | (CH2)5
10a,b

We have also obtained the new compounds **10 a,b** by a normal *Mannich* reaction of 4,9-dimethyl-2H,10H-8,9-dihydrobenzo[1,2 b : 3,4b′)] dipyran-2, 10-dione **9** :

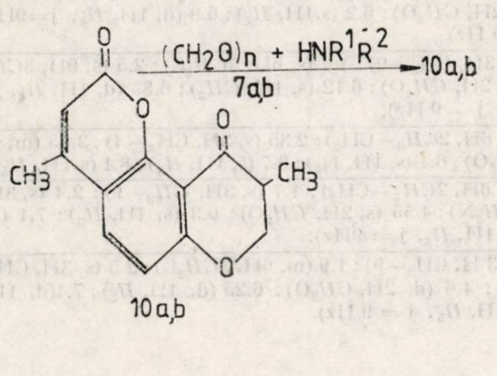
(CH2O)n + HNR1R2
7a,b
10a,b
CH3
CH3
10a,b

Table 1

New synthesized compounds

Comp.	Yield (%)	M.p. (°C)	Formula	Calcd./Found				IR ν cm⁻¹
				C%	H%	Cl%	N%	
5	10	227–228	$C_{13}H_{12}O_4$	67.24 67.59	5.17 5.13	—	—	1720, 1635
6	70	194–196	$C_{13}H_{12}O_4$	67.24 67.59	5.17 5.22	—	—	1720, 1630
8a	75	95–96	$C_{19}H_{23}NO_4$	69.30 69.38	6.99 7.12	— —	4.25 4.38	1720, 1690
8b	69	164–165	$C_{20}H_{23}NO_4$	70.38 70.70	6.74 6.73	— —	4.10 4.20	1720, 1690
9	78	212–213	$C_{14}H_{12}O_4$	68.85 68.98	4.92 5.10	—	—	1720, 1695
10a	59	108–109	$C_{19}H_{23}NO_4$	69.30 69.50	6.99 7.10	— —	4.25 4.32	1720, 1685
10b	56	159–160	$C_{20}H_{23}NO_4$	70.38 70.45	6.74 6.92	— —	4.10 4.27	1715, 1690
11a	82	143–144	$C_{19}H_{24}NO_4Cl$	62.38 62.50	6.56 6.64	9.70 9.83	3.83 3.81	1710, 1680
11b	86	205–207	$C_{20}H_{24}NO_4Cl$	63.58 63.73	6.36 6.35	9.39 9.67	3.70 4.02	1710, 1690
12a	95	194–195	$C_{19}H_{24}NO_4Cl$	62.38 62.54	6.56 6.70	9.70 9.90	3.83 3.92	1710, 1690
12b	97	209–210	$C_{20}H_{24}NO_4Cl$	63.58 63.70	6.36 6.53	9.39 9.43	3.70 3.90	1710, 1690

Table 2

¹H-NMR spectral data of the new synthesized compounds

Comp.	in ppm, $CDCl_3$, TMS, 25°C
5	1,3 (t, 3H, CH_3-CH_2); 2,4 (2s, 3H, CH_3-4); 3,15 (q, 2H, CH_2-CH_3); 6,15 (2, 1H, H_3); 7.25 (s, 1H, H_8): 8.0 (2, 1H, H_5): 12.8 (s, 1H, OH).
6	1.3 (t, 3H, CH_3-CH_2); 2.4 (s. 3H, CH_3-4); 3.35 (q, 2H, CH_2-CH_3); 6.15 (s, 1H, H_3); 6.8 (d, 1H, H_6, j = 9 Hz); 7.6 (d, 1H, H_5, j = 9 Hz); 13.6 (2,s, 1H, OH).
8a	1.0 (t, 6H, $2CH_3-CH_2$); 1.15 (s, 3H, CH_3-9); 2.65 (m, 9H $3CH_2N+$ $+CH_3-4$); 4.45 (q, 2H, CH_2O); 6.2 (s. 1H, H_3); 6.8 (s,1 H, H_8); 8.1 (s.1H,H_5)
8b	1.2 (s, 3H, CH_3-9); 2.55 (m, 9H), $3CH_2N + CH_3-4$); 4.35 (q, 2H, CH_2O); 6.15 (s, 1H, H_3); 6.8 (s, 1H, H_8); 8.12 (s, 1H, H_5).
9	1.25 (d, 3H, CH_3-CH); 2.4 (s, 3H, CH_3-4); 4.45 (m, 3H, $CH-CH_3+CH_2O$); 6.2 (s, 1H, H_3); 6.9 (d, 1H, H_6, j = 9 Hz); 7.8 (d, 1H, H_5, j = 9 Hz).
10a	1.0 (t, 6H, $2CH_3-CH_2$); 1.2 (s, 3H, CH_3-9); 2.55 (m, 9H, $3CH_2N+CH_3-4$); 4.4 (q, 2H, CH_2O); 6.2 (s,1H, H_3); 6.9 (d, 1H, H_6, j=9Hz); 7.7 (d,1H, H_5, j = 9 Hz)
10b	1.15 (s, 3H, CH_3-9); 1.4 (s, 6H, $3CH_2C$): 2.5 (s, 9H, $3CH_2N+CH_3-4$); 4.35 (q, 2H, CH_2O); 6.12 (s, 1H, CH_3); 6.85 (d, 1H, H_6, j = 9 Hz); 7.6 (d, 1H, H_5, j = 9 Hz).
11a	1.5 (m, 6H, $2CH_3-CH_2$); 2.35 (s, 3H, CH_3-4); 3.55 (m, 6H, $3CH_2N$); 4.7 (s, 2H, CH_2O); 6.1 (s, 1H, H_3); 6.7 (s, 1H, H_8); 8.1 (s,1H, H_5).
12a	1.45 (t, 6H, $2CH_3-CH_2$); 1.7 (s, 3H, CH_3-9): 2.4 (s, 3H, CH_3-4): 3.4 (q, 6H, $3CH_2N$); 4.55 (s, 2H, CH_2O); 6.3 (s, 1H, H_3); 7.1 (d, 1H, H_6, j = 9Hz); 7.9 (d, 1H, H_5, j = 9Hz).
12b	1.55 (s, 3 H, CH_3-9); 1.9 (m, 6H, $3CH_2C$); 2.5 (s, 3H, CH_3-4); 3.5 (m, 6H, $3CH_2N$); 4.6 (d, 2H, CH_2O); 6.25 (d, 1H, H_3); 7.1(d, 1H, H_6, j=9Hz); 7.9 (d,1H, H_5, j = 9 Hz).

A suspension of **8 a,b** or **10 a,b** in acetone was treated with conc. hydrochloric acid at room temperature to give in near quantitative yields the corresponding water-soluble hydrochlorides **11 a,b** or **12 a,b**. In the experimental section the synthesis of all new compounds, elemental analysis as well as spectral data (I R and NM R) which confirmed the proposed structures are given. The hydrochlorides **12 a,b** showed in a preliminary screening highly antihypertensive activity and we hope that the present clinical screening will offer a new drug, interesting from a practical point of view.

EXPERIMENTAL PART

M. P. : Uncorr., I R spectra were recorded with a Perkin Elmer 577 spectrophotometer in potassium bromide pellets and NMR spectra with a JEOL C-60 HL spectrometer.

7-Hydroxy-4-methyl-6-(or-8)-propionylcoumarin (5 and 6)

In a flask provided with an air condenser, 44.0 g of 4-methyl-7-propionyloxycoumarin **4** were mixed with 100 g of dry aluminium chloride and heated on an oil bath at 170°C for 3 hours. The reaction mixture was decomposed with 250 mL ice-water and, by repeated recrystallizations from N, N-dimethylformamide, **5** (4.4 g, m.p. 227—228°C) and **6** (30.8, m.p. 194—196°C) were obtained.

Mannich—Werner bases 8 a,b and 10 a,b—General Procedure

Compounds **5** and **6** were cyclocondensed and aminomethylated with paraformaldehyde and diethylamine or piperidine. A typical procedure is given for **10 b** : 3 g of **6**, piperidine (3 mL), paraformaldehyde (1 g) and ethanol (25 mL) were refluxed for 2 hours, then the reaction mixture was allowed to stand at room temperature for 48 hours. The precipitated solid was purified by wo crystallizations from methanol to give **10b** (3.5 g, 79% yield) with m.p. 159—160°. All bases trepared in this general way are listed in Table 1. In a similar manner reacted **9** with diethylampine **7a** and piperidine **7b** to give **10a** and **10b** respectively.

The hydrochlorides 11 a,b and 12 a,b—General Procedure

A typical procedure given below for **12 b** compound (1 g) in acetone (50 mL) is treated at room temperature with conc. hydrochloric acid (1 mL) and allowed to stand for 24 hours at room temperature. The initial clear solution became a slurry mass which was filtered, and purified by two crystallizations from acetone to give analytically pure **12b** (1 g, 95% yield, m.p. 209—210°, Table 1, 2).

ACKNOWLEDGEMENTS. We express our thanks to the "Alexander von Humboldt" Stiftung Bonn-Bad Godesberg for financial assistance and help during fellowship, 1987 for one of us (A. Caşcaval) and also to the BASF-LUDWIGSHAFEN Company (West Germany) for a gift of many useful intermediates.

REFERENCES

[1] Part, XIX, A. Caşcaval, *Synthesis*, **1985**, 428.
[2] P. Rodighiero, P. Manzini, G. Pasotrini, F. Bordin and A. Guiotto, *J. Heterocyclic Chem.*, **24**, 485 (1987).
[3] D. N. Robertson and P. K. Link, *J. Amer. Chem. Soc.*, **75**, 1883 (1953).
[4] R. B. Desai, *J. Org. Chem.*, **26**, 5251 (1961).
[5] D. Molho and E. Boschetti, Fr. 1310535 (30.11.1962) cf. *Chem. Abstr.* **58**, 12517e (1963).

[6] A. K. Rao, M. S. Raju and K. M. Raju, *J. Indian Chem. Soc.*, **58**, 1021 (1981).
[7] A. Caşcaval, Romanian Patent 89358/30.10.1985.
[8] J. A. Gautier, M. Miocque and D. Q. Quan, *Compt. rend.*, **258**, 3731 (1964).
[9] A. M. Kuliev, M. S. Guesimov, Sandarova and T. Yu. Iskenderova, *Zhur. Org. Khim.*, **8**, 1302 (1972).
[10] U. Rehse, *Arch. Pharm. (Weinheim)*, **308**, 881 (1975).
[11] W. Werner, *Arch. Pharm. (Weinheim)*, **309**, 1011 (1976).
[12] A. Caşcaval, *Synthessis*, **1983**, 589 and further references therein.
[13] D. S. Samant, K. D. Deodhar and R. A. Kuljarni, *Indian J. Chem.*, **208**, 215 (1981).
[14] A. Caşcaval, *Liebigs Ann. Chem.*, **1980**. 669.
[15] A. Caşcaval, *Synthesis*, **1984**, 277.
[16] M. Negwer, "Organischen-chemische Arzneimittel und ihre Synonyma", Akademie Verlag, Berlin, 11978.
[17] P. Bhattacharrya, D. Chatterjee, A. Charkrabarti and D. P. Chakrabarty, *Indian J. Chem.*- **17B**, 111 (1979).
[18] A. Russel and J. R. Frye, *Org. Synth. Coll., Vol.* 3, 281 (1960).

Revue Roumaine de Chimie, **33**, *9–10*, 917–919 (1988)

SYNTHESIS OF 2-ALKYL-7-BENZO-COUMARANONES

R. AGARWAL * and P. BEHADUR

Department of Chemistry, South Gujarat University, Surat—395 007, India

Received October 10, 1986

Some 2-alkyl-7-benzo-coumaranones have been sythesized by the cyclisation of ω-diazo-ω-alkyl-2-acetyl-1-hydroxy-naphthalene. They exhibit keto-enol tautomerism. Due to aromatisation of benzo-coumaranone ring, the enol form was dominating over the keto form. The percentage of enol form was determined in the mixture. The cyclisation took place by the intermediate formation of diazonium and oxonium ion.

The present paper describes the synthesis of some 2-alkyl-7-benzo-coumaranones.

Reaction of some diazoalkanes with 1-hydroxy-2-naphthoyl chloride affords ω-diazo-ω-alkyl-2-acetyl-1-alkoxy-naphthalene and ω-diazo-ω-alkyl-2-acetyl-1-hydroxy-naphthalene. The mixture of the two compounds was treated with 1% NaOH[2,3,4] solution, when ω-diazo-ω-alkyl-2-acetyl-1-hydroxy-naphthalene migrates in aqueous layer; on immediate acidification by dilute HCl, this compound underwent cyclisation,[1] through intermediate diazonium and oxinium ion formation, and gave 2-alkyl-7-benzo-coumaranones.

The mechanism of cyclisation to coumaranones can be depicted as follows:

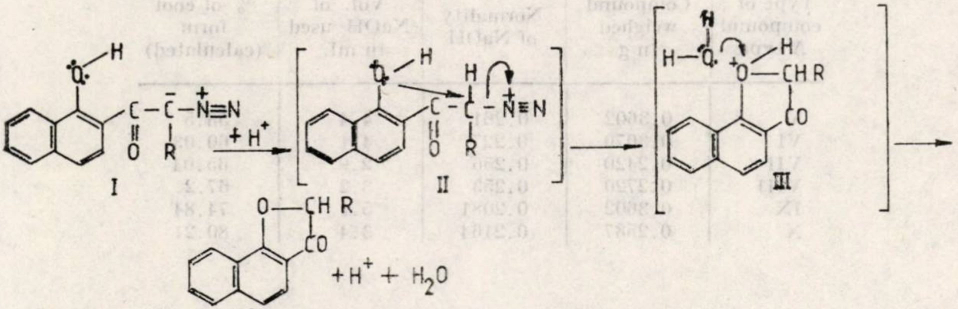

---

* Correspondence address: R. Agarwal, Chemist, Oil & Natural Gas Commission, Chemistry Section, Sabarmati, Ahmedabad-380 005 Gujarat, India.

Primarily, a proton from the acid attacks the nucleophilic methine carbon forming an intermediate diazonium ion II, which loses nitrogen forming an oxonium ion III. The latter gave with water 2-alkyl-7-benzocoumaranones IV (R—H, CH_3, C_2H_5, C_3H_7, n-C_5H_{11}, n-C_7H_{15}), simultaneously regenerating the proton.

As the reactive methylene group lies between two more electronegative groups, compounds IV show keto-enol tautomerism, thus offering an opportunity to study the enolic forms 5-alkyl-4-hydroxy(naphthalene-1′,2′,2,3-furane)-dihydride IVA (R = H, CH_3, C_2H_5, C_3H_7, n-C_6H_{11}, n-C_7H_{15}).

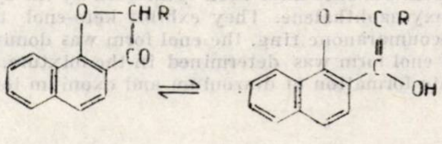

IV IVA

The percentage of enol form was estimated in the mixture by adopting the method of Siedel et al. (Table 1).

Table 1

Estimation of %-enol form

Type of compound A type	Compound weighed in g	Normality of NaOH	Vol. of NaOH used in mL	% of enol form (calculated)
V	0.3602	0.261	4.4	58.5
VI	0.3070	0.227	4.1	60.03
VII	0.2420	0.256	2.9	65.04
VIII	0.2720	0.253	3.2	67.2
IX	0.3602	0.2081	5.1	74.84
X	0.2587	0.2164	3.4	80.21

All the above synthesized 2-alkyl-7-benzo-coumaranones were red or yellow crystalline solids, characterized by elemental analysis and IR spectra[6,7,8] (Table 2).

All compounds IV gave green colouration with $FeCl_3$ solution in alcoholic medium.

Table 2

Characterization of compounds V – X

Compound*	m.p. °C	IR frequencies (cm^{-1})
V	94	$C{=}O$: 1690 ; $-CH_2-CO-$: 1440 ; $Ar-OH$: 1260 ; $-CH=$:1315.
VI	160	$C{=}O$; 1680 ; $-\underset{\substack{\vert \\ CH_3}}{CH}-CO$: 1450 ; $Ar-OH$: 1240 ; $-CH{=}1320$.
VII	74	$C{=}O$: 1678 ; $-\underset{\substack{\vert \\ C_2H_5}}{CH}-CO$: 1460 : $Ar-OH$; 1244 : $-CH=$: 1330.
VIII	110	$C{=}O$: 1676 ; -*n*-propyl : 1460 ; $Ar-OH$: 1221 ; $-CH = 1328$.
IX	56	$C{=}O$: 1678 ; $-CH_2-$in *n*-amyl : 1460 : $Ar-OH$: 1242 ; $-CH = 1328$.
X	155	$C{=}O$: 1680 : $-CH_2-$in *n*-heptyl : 1470 ; $Ar-OH$: 1248 : $-CH{=}1440$.

* The values of C and H estimation were found in accordance with the corresponding formulas.

EXPERIMENTAL

The benzo-coumaranones IV isolated and studied, are 2-alkyl-7-benzo-coumaranone(IV) ; (V), $R = H$; (VI), $R = CH_3$; (VII), $R = -C_2H_5$; (VIII) $R = -C_3H_7$; (IX), $R = C_5H_{11}$; (X) $R = -C_7H_{15}$.

REFERENCES

[1] R. P. Kapoor and S. M. Gupta, *J. Indian Chem. Soc.*, **38**, 776 (1961).

[2] Gopal Krishan and S. M. Gupta, *Agra Uni. J. Res. (Sc.)*, **21**, II, 27–30 (1972).

[3] Satish Kumar and S. M. Gupta, *Indian J. Appl. Chem.*, **29**, 83 (1966).

[4] Siedel, Thier. Uber and Dittmer, *Ber. dtsch. chem. Ges.*, **69**, 650 (1936).

[5] B. Colthup, "Introduction to Infra-red and Raman Spectroscopy", Academic Press, New York and London (1964).

[6] J. R. Dyer, "Applications of Absorption Spectroscopy of Organic Compounds", Prentice Hall of India Pvt. Ltd., New Delhi (1978).

[7] L. J. Ballamy, "The Infra-red Spectra of Complex Molecules", Methuen and Co. Ltd., London (1968).

[8] K. Nakanishi, "Infra-red Absorption Spectroscopy", Holden Day, Inc. San Francisco and Nankodo Co. Ltd., Tokyo (1962).

Revue Roumaine de Chimie, **33**, *9–10*, 921–935 (1988)

MATHEMATICAL FOUNDATION OF CHEMICAL TRANSFORMATIONS ON THE BASIS OF *REDOX* AND *COLHOM* PROCESSES

A. CĂLUŞARU
Institute of Chemical Research, Spl. Independenţei 202, 77208 Bucharest, Romania

Received March 1, 1988

Starting from two fundamental matrices, the pairs of the matrices of reaction of both the REDOX and COLHOM processes were deduced. By an addition operation the matrices of the heterolytic transformations were composed, obtaining finally 10 2×2 matrices of reaction. It is possible to find the characteristic matrix of any chemical transformation in n-atom centers of reaction, by introducing the entries of a few from these 10 matrices in the corresponding $n\times n$ matrix of reaction by an addition operation.

It is well known actually that the chemical structures have as closest mathematical correspondents the graphs, in which the vertices are the atoms and the edges the covalent bonds. The work with graphs implies rigorous mathematical operations, where always both vertices and edges must be taken into consideration. In its most common form, chemistry still ignores this close relationship between graphs and chemical structures and uses the sign of equality between educt and product species showing the conservation of the number of atomic species only. The fate of the chemical bonds, although the most salient aspect of any chemical transformation, is not expressed in the actual form of symbolism of the chemical reactions and the consequence is that in mathematical terms two distinct non equal graphs are equalised. However, when the graphs are converted into structure matrices,[1] a new element appears, which allows the mathematically correct expression of a chemical reaction : this is the so-called matrix of reaction, accounting all electrons participating in chemical transformations, by break or formation of covalent bonds and entering in or going away from the bonds as non-participating electrons. The matrix of reaction accounts therefore the regrouping of the electrons belonging to the atoms of the center of reaction.[2] Owing to the obvious conservation law of the electrons in the center of reaction, the sum of the entries of a matrix of reaction is zero. But the most salient quality of a matrix of reaction is the ability of this symbol to give a quantitative basis for a mathematical foundation of the chemical transformations. [3]

It has been found that two kinds of pairs of one-electron processes namely REDOX and COLHOM (*col*igation|*hom*olysis) are the fundamental components of any chemical reaction.[4] To the two pairs correspond four matrices, but owing to the simple interrelation of the matrices corresponding to any pair, it is easy to deduce that only two elementary matrices are factually necessary to constitute any other matrix of reaction. The problem arises to find a matrix only, including the two counterparts of the both REDOX and COLHOM pair processes. In this way the entire ensemble of the matrices of reaction can be mathematically stated.

1. PAIRS OF CHEMICAL TRANSFORMATION

A chemical transformation can never be a unitary act, having a intrinsic dual nature; the transformation in a direction implies the possibility of the reverse reaction path. The situation is obvious for the notation adopted in the case of the reversible transformations (E = educt and P = product of reaction):

$$E \rightleftharpoons P \tag{1}$$

But also in the most general case a transformation in both directions is principally possible for any chemical reaction, even for the non-reversible conditions. In this case, reaction (1) can be expressed in the form of a pair of two separated reactions:

$$E \rightarrow P \tag{2}$$

$$E \leftarrow P \tag{3}$$

As we have shown in the introductory part, a chemical reaction is rigorously described only in the form of structure and reaction matrices allowing in this way the use of the equality sign between the educt and product of reaction. Reactions (2) and (3) can be written as follows:

$$E + R = P \tag{4}$$

$$E \quad = P - R \tag{5}$$

The two directions of a reaction imply the pair of two matrices of reaction $\pm R$, which are, obviously, the roots of a matrix equation of the second degree:

$$x = \pm\sqrt{R^2} = \pm R_i \tag{6}$$

In this way a new element appears, namely the matrix R^2 generating by square root the two matrices of the pairs of reaction (4) and (5), reciprocally correlated. But relation (6) raises the significance of the meaning of multiplication operation for the matrices of reaction. The entries of such matrix are of two kinds: (1) diagonal entrise expressing the gain (+) or loss (−) of electrons and (2) off diagonal entries representing the formation (+1) or the break (−1) of a covalent bond. In both cases the multiplication with a scalar is a meaningful operation which shows how many electrons are transferred and how many bonds are transformed in a specified transformation. But the square of any element itself remains a formal operation. However, even in this case, appears the problem of selection between two possible alternatives : (1) the multiplication of the correlated matrix entries and (2) the multiplication of a line in the first matrix with the entries of the column belonging to the second matrix. The first alternative appears as the most suitable for the present case, since the entries in a matrix of reaction are not interconnected by the line| column rule.

2. GENERATING MATRICES FOR THE ELEMENTARY PROCESSES

The study of the matheamatical forms of chemical reactions allowed to conclude that only two pairs of processes are the constituents of any matrix of reaction and therefore are the basic components of all chemical transformations. These pairs are (1) *redox* (reduction|oxidation) and (2) *colhom* (coligation|homolysis) reactions.[4]

2.1. One-electron *redox* reactions

The pair of reactions corresponding to the redox couple are the electron dissociation (D_e) or oxidation and the electron association (A_e) or reduction. R_1 denotes the matrix of reaction for D_e and R_2 the same matrix for A_e processes. The interrelation between these two matrices is : $R_2 = -R_1$. As it has been shown previously [2-4] the explicit forms of these matrices are :

$$R_1 = \begin{pmatrix} -1 & 0 \\ 0 & 1 \end{pmatrix} \text{ and } R_2 = \begin{pmatrix} 1 & 0 \\ 0 & -1 \end{pmatrix} \tag{7}$$

therefore $\pm R_i$ (relation (6)).

Both R_1 and R_2 squared give the following single matrix :

$$R^2_{ro} = \begin{pmatrix} 1 & 0 \\ 0 & 1 \end{pmatrix} \tag{8}$$

This is a diagonal form and therefore its square root is in any definition of matrix multiplication, the following :

$$\pm R_{ro} = \begin{pmatrix} \pm\sqrt{1} & 0 \\ 0 & \pm\sqrt{1} \end{pmatrix} \tag{9}$$

There are four solutions of this operation :

$$R_1 = \begin{pmatrix} -1 & 0 \\ 0 & 1 \end{pmatrix};\ R_2 = \begin{pmatrix} 1 & 0 \\ 0 & -1 \end{pmatrix};\ R_1' = \begin{pmatrix} -1 & 0 \\ 0 & -1 \end{pmatrix};\ R_2' = \begin{pmatrix} 1 & 0 \\ 0 & 1 \end{pmatrix} \tag{10}$$

As a consequence of the law of electron conservation the entries of a matrix of reaction must fulfil the following conditon :

$$\sum r_{ij} = 0 \qquad (11)$$

Only R_1 and R_2 of the four solutions (10) are in agreement with the condition (11), and therefore these describe the oxidation and reduction processes shown by relations (7). The matri x (8) represents thus the generating matrix for the one-electron *redox* couple.

As an example of one-electron oxidation reaction, the following general scheme can be given :

$${}^{\bullet}A_i + A_j \rightarrow A_i + {}^{\bullet}A_j \qquad (12)$$

Here the electrical charges were neglected. In matrix form reaction (12) becomes :

$$\begin{array}{c} \begin{matrix} i & j \end{matrix} \\ \begin{pmatrix} 1 & 0 \\ 0 & 0 \end{pmatrix} \end{array} + \begin{array}{c} \begin{matrix} i & j \end{matrix} \\ \begin{pmatrix} -1 & 0 \\ 0 & 1 \end{pmatrix} \end{array} = \begin{array}{cc} \begin{matrix} i & j \end{matrix} & \\ \begin{pmatrix} 0 & 0 \\ 0 & 1 \end{pmatrix} & \begin{matrix} i \\ j \end{matrix} \end{array} \qquad (13)$$

The matrix of reaction is R_1.

The reverse or permuted reaction of the couple is a one-electron reduction :

$$A + {}^{\bullet}A \rightarrow {}^{\bullet}A + A \qquad (14)$$

or in matrix form :

$$\begin{array}{c} \begin{matrix} i & j \end{matrix} \\ \begin{pmatrix} 0 & 0 \\ 0 & 1 \end{pmatrix} \end{array} + \begin{array}{c} \begin{matrix} i & j \end{matrix} \\ \begin{pmatrix} 1 & 0 \\ 0 & -1 \end{pmatrix} \end{array} = \begin{array}{cc} \begin{matrix} i & j \end{matrix} & \\ \begin{pmatrix} 1 & 0 \\ 0 & 0 \end{pmatrix} & \begin{matrix} i \\ j \end{matrix} \end{array} \qquad (15)$$

Here the matrix of reaction is R_2.

An important property of the R_1 and R_2 matrices is their sensitivity to the permutation operation :

$$\begin{pmatrix} -1 & 0 \\ 0 & 1 \end{pmatrix} \xrightarrow{\text{lines}} \begin{pmatrix} 0 & 1 \\ -1 & 0 \end{pmatrix} \xrightarrow{\text{columns}} \begin{pmatrix} 1 & 0 \\ 0 & -1 \end{pmatrix} \qquad (16)$$

This means that reaction (12) can be transformed into (13),by a reversing or premuting operation.

2.2. *Colhom* reactions

The *colhom* (radicalic) reactions refer to the dissociation process of the covalent bonds (homolysis) (D_R) and to the association reaction of two radicalic species (coligation) (A_R). In the *colhom* pairs of processes, the two components are in reciprocal reversion relation, unlike the *redox* transformations which are correlated by both the permutation and reversion operations.

For these processes R_3 denotes the matrix of reaction for D_R and R_4 the same matrix for A_R processes. As in the previous case the interrelation between these two matrices is $R_4 = -R_3$. The explicit forms of these matrices are, as shown previously[2-4]:

$$R_3 = \begin{pmatrix} 1 & -1 \\ -1 & 1 \end{pmatrix} \quad \text{and} \quad R_4 = \begin{pmatrix} -1 & 1 \\ 1 & -1 \end{pmatrix} \tag{17}$$

In this case both diagonal and off diagonal entries are different from zero and therefore an alternative of the two possible definitions must be selected. We have already shown that the multiplication of the correlated matrix entries in the most suitable.

Thus by squaring each entry of the matrices (17) the following single matrix is obtained:

$$R_{ch}^2 = \begin{pmatrix} 1 & 1 \\ 1 & 1 \end{pmatrix} \tag{18}$$

The square root of this matrix is, according to the adopted definition, the following:

$$R_{ch} = \begin{pmatrix} \pm\sqrt{1} & \pm\sqrt{1} \\ \pm\sqrt{1} & \pm\sqrt{1} \end{pmatrix} \tag{19}$$

In addition to the conservation law expressed by (11), the symmetry rule must also be observed. According to this rule, for each off diagonal entry, the relation $e_{ij} = e_{ji}$ holds, since the $A_i{-}A_j$ bond is the same as $A_j{-}A_i$ one. In this way among the 16 matrices, resulting from (19), only two are in agreement with both the conservation law and symmetry rule, as shown by (17).

As examples of homolytic reactions, the following general schemes can be given:

$$A_i - A_j \rightarrow {}^{\bullet}A_i + {}^{\bullet}A_j \tag{20}$$

$$A_i = A_j \rightarrow {}^{\bullet}A_i - {}^{\bullet}A_j \tag{21}$$

$$A_i \equiv A_j \rightarrow {}^{\bullet}A_i = {}^{\bullet}A_j \tag{22}$$

In matrix form these reactions become :

$$\begin{array}{c} \begin{matrix} i & j \end{matrix} \\ \begin{pmatrix} 0 & 1 \\ 1 & 0 \end{pmatrix} \end{array} + \begin{array}{c} \begin{matrix} i & j \end{matrix} \\ \begin{pmatrix} 1 & -1 \\ -1 & 1 \end{pmatrix} \end{array} = \begin{array}{c} \begin{matrix} i & j \end{matrix} \\ \begin{pmatrix} 1 & 0 \\ 0 & 1 \end{pmatrix} \begin{matrix} i \\ j \end{matrix} \end{array} \tag{23}$$

$$\begin{array}{c} \begin{matrix} i & j \end{matrix} \\ \begin{pmatrix} 0 & 2 \\ 2 & 0 \end{pmatrix} \end{array} + \begin{array}{c} \begin{matrix} i & j \end{matrix} \\ \begin{pmatrix} 1 & -1 \\ -1 & 1 \end{pmatrix} \end{array} = \begin{array}{c} \begin{matrix} i & j \end{matrix} \\ \begin{pmatrix} 1 & 1 \\ 1 & 1 \end{pmatrix} \begin{matrix} i \\ j \end{matrix} \end{array} \tag{24}$$

$$\begin{array}{c} \begin{matrix} i & j \end{matrix} \\ \begin{pmatrix} 0 & 3 \\ 3 & 0 \end{pmatrix} \end{array} + \begin{array}{c} \begin{matrix} i & j \end{matrix} \\ \begin{pmatrix} 1 & -1 \\ -1 & 1 \end{pmatrix} \end{array} = \begin{array}{c} \begin{matrix} i & j \end{matrix} \\ \begin{pmatrix} 1 & 2 \\ 2 & 1 \end{pmatrix} \begin{matrix} i \\ j \end{matrix} \end{array} \tag{25}$$

The matrix of reaction in this case is R_3.

The reverse reactions of the *colhom* couple are the coligation reactions :

$${}^{\bullet}A_i + {}^{\bullet}A_j \rightarrow A_i - A_j \tag{26}$$

$${}^{\bullet}A_i - {}^{\bullet}A_j \rightarrow A_i = A_j \tag{27}$$

$${}^{\bullet}A_i = {}^{\bullet}A_j \rightarrow A_i \equiv A_j \tag{28}$$

Transposed in matrix form these reactions are as follows :

$$\begin{array}{c} \begin{matrix} i & j \end{matrix} \\ \begin{pmatrix} 1 & 0 \\ 0 & 1 \end{pmatrix} \end{array} + \begin{array}{c} \begin{matrix} i & j \end{matrix} \\ \begin{pmatrix} -1 & 1 \\ 1 & -1 \end{pmatrix} \end{array} = \begin{array}{c} \begin{matrix} i & j \end{matrix} \\ \begin{pmatrix} 0 & 1 \\ 1 & 0 \end{pmatrix} \begin{matrix} j \\ i \end{matrix} \end{array} \tag{29}$$

$$\begin{array}{c} \begin{matrix} i & j \end{matrix} \\ \begin{pmatrix} 1 & 1 \\ 1 & 1 \end{pmatrix} \end{array} + \begin{array}{c} \begin{matrix} i & j \end{matrix} \\ \begin{pmatrix} -1 & 1 \\ 1 & -1 \end{pmatrix} \end{array} = \begin{array}{c} \begin{matrix} i & j \end{matrix} \\ \begin{pmatrix} 0 & 2 \\ 2 & 0 \end{pmatrix} \begin{matrix} i \\ j \end{matrix} \end{array} \tag{30}$$

$$\begin{array}{c} \begin{matrix} i & j \end{matrix} \\ \begin{pmatrix} 1 & 2 \\ 2 & 1 \end{pmatrix} \end{array} + \begin{array}{c} \begin{matrix} i & j \end{matrix} \\ \begin{pmatrix} -1 & 1 \\ 1 & -1 \end{pmatrix} \end{array} = \begin{array}{c} \begin{matrix} i & j \end{matrix} \\ \begin{pmatrix} 0 & 3 \\ 3 & 0 \end{pmatrix} \begin{matrix} j \\ i \end{matrix} \end{array} \tag{31}$$

The matrix of reaction is therefore R_4. This matrix is not sensitive to permutation, since by change of both the lines and columns the same matrix is obtained :

$$\begin{pmatrix} -1 & 1 \\ 1 & -1 \end{pmatrix} \xrightarrow{\text{lines}} \begin{pmatrix} 1 & -1 \\ -1 & 1 \end{pmatrix} \xrightarrow{\text{columns}} \begin{pmatrix} -1 & 1 \\ 1 & -1 \end{pmatrix} \tag{32}$$

The matrices R^2_{ro} (8) and R^2_{ch} (18) are the generating matrices for *redox* and *colhom* reactions respectively. As it is shown below, these matrices are the elements to construct the matrix of any chemical transformation.

3. MATRICES FOR TWO-ELECTRON *REDOX* REACTIONS

The matrices R_1 and R_2 correspond to one-electron *redox* reactions. When two electrons are transferred, the corresponding matrices can be deduced by multiplication of R_1 and R_2 with the scalar 2. Thus the matrices for the two-electron *redox* reactions are :

$$R_5 = 2\ R_1 = \begin{array}{cc} \begin{array}{cc} i & j \end{array} & \\ \begin{pmatrix} -2 & 0 \\ 0 & 2 \end{pmatrix} & \begin{array}{c} i \\ j \end{array} \end{array} \tag{33}$$

for the oxidation reaction, and :

$$R_6 = 2\ R_2 = \begin{array}{cc} \begin{array}{cc} i & j \end{array} & \\ \begin{pmatrix} 2 & 0 \\ 0 & -2 \end{pmatrix} & \begin{array}{c} i \\ j \end{array} \end{array} \tag{34}$$

for the reduction reaction.

4. MATRICES OF REACTION FOR HETEROLYTIC TRANSFORMATIONS

The heterolytic transformations are dielectronic processes in two-atom centers of reaction. The corresponding matrices of reaction can be deduced starting from two couples of *redox* and *colhom* transformations, therefore from the two matrices previously shown, (8) and (18). On the other hand the matrices of reaction of all chemical transformations can be constructed from *redox*, *colhom* and *heterolytic* corresponding matrices. In this way one is possible to show finally that all matrices of reaction can be generated from only two unity matrices, and therefore at the basis of all chemical transformations lie only two principles.

The heterolytic processes embrace two pairs of correlated processes : (1) electrofugic dissociation and electrophilic association and (2) nucleofugic dissociation and nucleophilic association.

4.1. Electrofugic dissociation, $D_E = D_R A_e$

In a two-atom center of reaction the asymmetrical splitting of a chemical bond is a process sensitive to the permutation operation. When the break of the bond is carried out on the part of A_j atom the process is termed as electrofugic dissociation. The general schemes are :

$$A_i - \wr A_j \to \bar{A}_i^- + A_j^+ \tag{35}$$

$$A_i = \wr A_j \to \bar{A}_i^- - A_j^+ \tag{36}$$

$$A_i \equiv \wr A_j \to \bar{A}_i^- = A_j^+ \tag{37}$$

The electron pair, constituting the interatomic bond is transferred by this process to the species A_i, which reaches thus a negative charge. The species A_j loses an electron and therefore becomes positively charged.

It is interesting to observe that the matrix of reaction describing this process can be deduced by a summation of the R_3 and R_2 matrices. Thus reaction (35) for instance can be described as a stepwise reaction:

$$A_i - A_j \xrightarrow{D_R} {}^{\bullet}A_i + {}^{\bullet}A_j \xrightarrow{A_e} \bar{A}_i^- + \bar{A}_j^+ \tag{35a}$$

The first step is a *colhom* process, by a component of radicalic dissociation, D_R, while the second one is a *redox* process expressed by an electronic reductive association, A_e. The electrofugic dissociation can be therefore described as a composed process, D_RA_e:

$$R_7 = R_3 + R_2 = \underset{\mathrm{D}_R}{\begin{array}{cc} i & j \\ \left(\begin{array}{c} 1 \\ -1 \end{array}\right. & \left.\begin{array}{c} -1 \\ 1 \end{array}\right) \end{array}} + \underset{\mathrm{A}_e}{\begin{array}{cc} i & j \\ \left(\begin{array}{c} 1 \\ 0 \end{array}\right. & \left.\begin{array}{c} 0 \\ -1 \end{array}\right) \end{array}} = \underset{D_E = D_RA_e}{\begin{array}{ccc} i & j & \\ \left(\begin{array}{c} 2 \\ -1 \end{array}\right. & \left.\begin{array}{c} -1 \\ 0 \end{array}\right) & \begin{array}{c} i \\ j \end{array} \end{array}} \tag{38}$$

If one takes into account the definition of the chemical distance[5] one can see that this distance is not the same if it is deduced from the sum of the component matrices D_RA_e when it is equal to six or on the basis of the final matrix D_E when it is 4. This difference arises from the entry zero of the matrix D_E, obtained by the sum $1-1 = 0$, while for the chemical distance the sum $|1|+|1|=2$ is considered.

4.2. Electrophilic association, $A_E = D_eA_R$

The reverse reactions (35)—(37) are the general schemes of the process of electrophilic association, A_E:

$$\bar{A}_i^- + A_j^+ \rightarrow A_i - A_j \tag{39}$$

$$\bar{A}_i^- + A_j^+ \rightarrow A_i = A_j \tag{40}$$

$$\bar{A}_i^- = A_j^+ \rightarrow A_i \equiv A_j \tag{41}$$

By interaction of electrical charges the atomic species approaches and the electron pair of the $\bar{A}_i^-$ species is used to form a chemical bond with the species A_j^+. As previously shown, reaction (39) can occur stepwise in the following form:

$$\bar{A}_i^- + A_j^+ \xrightarrow{D_e} {}^{\bullet}A_i + {}^{\bullet}A_j \xrightarrow{A_R} A_i - A_j \tag{39a}$$

The first step is an oxidative dissociation, D_e (*redox* component), followed by a radicalic association, A_R (coligation, *colhom* process). The matrix of reaction for an electrophilic association process is therefore :

$$R_8 = R_1 + R_4 = \underset{D_e}{\begin{array}{c} \begin{array}{cc} i & j \end{array} \\ \begin{pmatrix} -1 & 0 \\ 0 & 1 \end{pmatrix} \end{array}} + \underset{A_R}{\begin{array}{c} \begin{array}{cc} i & j \end{array} \\ \begin{pmatrix} -1 & 1 \\ 1 & -1 \end{pmatrix} \end{array}} = \underset{A_R = D_e A_R}{\begin{array}{c} \begin{array}{cc} i & j \end{array} \\ \begin{pmatrix} -2 & 1 \\ 1 & 0 \end{pmatrix} \begin{array}{c} i \\ j \end{array} \end{array}} \tag{42}$$

In the addition operation of the matrices the order of the component processes, obviously, does not matter.

4.3. Nucleofugic dissociation, $D_N = D_R D_e$

If the interatomic bond is splitted on the side of the A_i species, then the process is termed as nucleofugic dissociation, D_N. The general schemes by which this process is described are :

$$A_i \wr - A_j \rightarrow A_i^+ + \bar{A}_j^- \tag{43}$$

$$A_i \wr = A_j \rightarrow A_i^+ - \bar{A}_j^- \tag{44}$$

$$A_i \wr \equiv A_j \rightarrow A_i^+ = \bar{A}_j^- \tag{45}$$

The electron pair of the covalent bond is now transferred to the species A_j, reaching in this way a negative charge, while the species A_i remains with a positive charge. In the form of a stepwise reaction composed of *redox* and *colhom* processes, reaction (43) can be written as follows :

$$A_i - A_j \xrightarrow{D_R} {}^{\bullet}A_i + {}^{\bullet}A_j \xrightarrow{D_e} A_i^+ + \bar{A}_j^- \tag{43a}$$

In this way the process is composed of a radicalic dissociation step, followed by an electronic dissociation reaction. The matrix of reaction is given by the sum :

$$R_9 = R_3 + R_1 =$$

$$\underset{D_R}{\begin{array}{c} \begin{array}{cc} i & j \end{array} \\ \begin{pmatrix} 1 & -1 \\ -1 & 1 \end{pmatrix} \end{array}} + \underset{D_e}{\begin{array}{c} \begin{array}{cc} i & j \end{array} \\ \begin{pmatrix} -1 & 0 \\ 0 & 1 \end{pmatrix} \end{array}} = \underset{D_N = D_R D_e}{\begin{array}{c} \begin{array}{cc} i & j \end{array} \\ \begin{pmatrix} 0 & -1 \\ -1 & 2 \end{pmatrix} \begin{array}{c} i \\ j \end{array} \end{array}} \tag{46}$$

The nucleofugic dissociation is therefore composed from two elementary processes of dissociation : radicalic dissociation and oxidative electronic dissociation.

4.4. Nucleophilic association, $A_N = A_e A_R$

The general schemes describing the nucleophilic association process are :

$$A_i^+ + \bar{A}_j^- \rightarrow A_i - A_j \tag{47}$$

$$A_i^+ - \bar{A}_j^- \rightarrow A_i = A_j \tag{48}$$

$$A_i^+ = \bar{A}_j^- \rightarrow A_i \equiv A_j \tag{49}$$

The pair of nonparticipating electrons of the $\bar{A}_j^-$ species is transferred now to form a covalent bond with the A_i^+ species and in this way the couple $A_i - A_j$ is formed. Reaction (47) can be now expressed as a stepwise process :

$$A_i^+ + \bar{A}_j^- \xrightarrow{A_e} {}^\bullet A_i + {}^\bullet A_j \xrightarrow{A_R} A_i - A_j \tag{47 a}$$

Here a reduction electronic process, A_e, is produced together with a radicalic association process, A_R. The matrix of reaction for the nucleophilic association is composed by the sum :

$$R_{10} = R_2 + R_4 =$$

$$\begin{array}{c} \begin{array}{cc} i & j \end{array} \\ \begin{pmatrix} 1 & 0 \\ 0 & -1 \end{pmatrix} \end{array} + \begin{array}{c} \begin{array}{cc} i & j \end{array} \\ \begin{pmatrix} -1 & 1 \\ 1 & -1 \end{pmatrix} \end{array} = \begin{array}{cc} \begin{array}{cc} i & j \end{array} & \\ \begin{pmatrix} 0 & 1 \\ 1 & -2 \end{pmatrix} & \begin{array}{c} i \\ j \end{array} \end{array} \tag{50}$$

A covalent bond is now formed with a nonparticipating electron pair of the A_j species.

5. FORMATION OF HIGHER ORDER MATRICES

The elementary typical matrices 2×2 in two-atom centers of reaction are submatrices of higher order ensembles determined by the number of atoms in the center of reaction. The matrix of any reaction is therefore a sum of a few matrices among the ten 2×2 ones previously described. In order to carry out this summation the entries of the corresponding 2×2 matrix must be arranged as entries in the $n \times n$ matrix of the studied reaction to occupy the site corresponding to the reactant species. In the general case the summation of the matrices of the elementary processes is noted as a squared sum :

$$R_p = R_m \boxplus R_n \tag{51}$$

Since R_m and R_n must be enlarged forms of lower order matrices, a series of rows/columns contains zero entries only. R_p is a $p \times p$ matrix since p is the number of the atoms in the center of reaction.

6. MATRICES FOR PAIRS OF PROCESSES IN THREE-ATOM CENTERS OF REACTION

One of the most often encountered processes in organic reaction is composed of the break of a covalent bond and the formation of the same type of bond with another species present in the system. This process is termed as substitution process. Two such substitution reactions are the most important : electrophilic and nucleophilic ones, each with the mono-molecular and bimolecular variant. A sequence of two one- or two-electron steps implies a three-atom center of reaction.

6.1. Monomolecular electrophilic substitution, $S_E1 = D_EA_E$

In an electrophilic substitution reaction, the first step is the splitting of a covalent bond by an electrofugic dissociation process, D_E, and the second step is the formation of a covalent bond by electrophilic association, A_E, of another atomic species.

The general scheme of reaction is the following :

$$A_i - A_j + A_k^+ \xrightarrow{D_E} \bar{A}_i^- + A_j^+ + A_k^+ \xrightarrow{A_E} A_i - A_k + A_j^+ \tag{52}$$

Examples of chemical reactions following this scheme are given in ref.[3]

The matrix of reaction corresponding to a D_E process is R_7, with entries arranged on i, j rows/columns and A_E step is R_8 with entries on i, k. The matrix of reaction for the process (52) is therefore :

$$R_{11} = R_7(i, j) \boxplus R_8(i, k) =$$

$$= \begin{array}{c} \begin{matrix} i & \;\; j & \;\; k \end{matrix} \\ \begin{pmatrix} 2 & -1 & 0 \\ -1 & 0 & 0 \\ 0 & 0 & 0 \end{pmatrix} \end{array} + \begin{array}{c} \begin{matrix} i & j & k \end{matrix} \\ \begin{pmatrix} -2 & 0 & 1 \\ 0 & 0 & 0 \\ 1 & 0 & 0 \end{pmatrix} \end{array} = \begin{array}{cc} \begin{matrix} i & \;\; j & \;\; k \end{matrix} & \\ \begin{pmatrix} 0 & -1 & 1 \\ -1 & 0 & 0 \\ 1 & 0 & 0 \end{pmatrix} & \begin{matrix} i \\ j \\ k \end{matrix} \end{array} \tag{53}$$

6.2. Bimolecular electrophilic substitution, $S_E2 = A_ED_E$

As compared to the previous mechanism, the present one represents the permutation of the succession of the same two processes. There is therefore a process A_ED_E initiated by an electrophilic association, forming a chemical bond, followed by an electrofugic dissociation splitting the other bond. The electrophilic association can be produced only if a positively charged particle can find an oposite charge or an unoccupied electron pair to the partner atom.

The general reaction scheme is :

$$\bar{A}_i - A_k + A_j^+ \xrightarrow{A_E} A_j - A_i^+ - A_k \xrightarrow{D_E} \bar{A}_i - A_j + A_k^+ \tag{54}$$

In this case the matrix R_8, A_E process, applies to i, j indices and the matrix R_7, D_E process, to i, k ones. The matrix of reaction is therefore the following :

$$R_{12} = R_8(i,j) \boxplus R_7(i,k) = \begin{array}{c} \\ \\ \\ \\ \end{array}\begin{array}{ccc|c} i & j & k & \\ 0 & 1 & -1 & i \\ 1 & 0 & 0 & j \\ -1 & 0 & 0 & k \end{array} \tag{55}$$

$$A_E D_E$$

We can see that in the R_{11} matrix the indices i, j, k can be permuted in six different forms and therefore six matrices can thus be obtained. One of these is R_{12}, corresponding to the scheme (54).

6.3. Monomolecular nucleophilic substitution, $S_N 1 = D_N A_N$

The electrophilic substitution was described by means of the matrices R_7 (mechanism D_E) and R_8 (mechanism A_N). Similarly in nucleophilic substitution, the matrices R_9 (mechanism D_N) and R_{10} (mechanism A_N) are used.

The sequence in which the first step is a nucleofugic dissociation (D_N) and the second a nucleophilic association (A_N) is expressed by the following general scheme :

$$A_i \wr - A_j \times + \bar{A}_k \rightarrow A_k - A_i + \bar{A}_j^- \tag{56}$$

The splitting of the covalent bond on the side of the species A_i is the mechanism described by the matrix R_9. The next step is the association of the species $\bar{A}_k^-$ to A_j^+. This is the mechanism of association to an unoccupied pair of the fragment A_k, whose matrix is R_{10}.

The matrix of the reaction corresponding to the mechanism $D_N A_N$ is :

$$R_{13} = R_9(i,j) \boxplus R_{10}(i,k) = \begin{array}{ccc|c} i & j & k & \\ 0 & -1 & 1 & i \\ -1 & 2 & 0 & j \\ 1 & 0 & -2 & k \end{array} \tag{57}$$

6.4. Bimolecular nucleophilic substitution, $S_N 2 = A_N D_N$

When the order of the previous steps is reversed, then the sequence $A_N D_N$ is obtained. For this case the general scheme is :

$$A_i - A_k + \bar{A}_j^- \xrightarrow{A_N} A_k - A_i^- - A_j \xrightarrow{D_N} A_i - A_j + \bar{A}_k^- \tag{58}$$

The first step is a mechanism of nucleophilic association by which an electron pair is transfered from the species $\bar{A}_j^-$ to A_i ; in this way an intermediate product is obtained. The stabilisation of the system is produced by the elimination of the species A_k by the splitting of the covalent bond with A_i.

The matrix of reaction is obtained by the sum :

$$R_{14} = R_{10}(i,\ j) \boxplus R_9(i,\ k) = \begin{array}{cc} \begin{array}{ccc} i & j & k \end{array} & \\ \begin{pmatrix} 0 & 1 & -1 \\ 1 & -2 & 0 \\ -1 & 0 & 2 \end{pmatrix} & \begin{array}{c} i \\ j \\ k \end{array} \\ A_N D_N & \end{array} \tag{59}$$

6.5. Other substitution reactions

In addition to the previously described substitution reactions, there are also two kinds of radicalic substitution : monomolecular radicalic substitution ($S_R1 = D_R A_R$) and bimolecular radicalic substitution ($S_R2 = A_R D_R$). In the same class the one-electoron and two-electron transfer mediated processes are included. But these mechanisms are not frequently encountered in practice.The reaction schemes and the corresponding matrices are described in detail in ref.[3]

7. MATRICES IN MULTI-ATOM CENTERS OF REACTION

The correlated pairs of processes in three-atom centers of reaction were already described. In addition, in the three-atom centers of reaction, two others types of processes can occur : elimination ($D_E A_N D_N$) with the matrix $R_{3,1}$ and addition ($D_N A_N A_E$) with the $R_{3,2}$ matrix reactions.

The matrices of reaction in these cases can be deduced by the simple addition of the component processes, as previously shown, therefore :

$$R_{3,1} = R_7 \boxplus R_{10} \boxplus R_9 \quad \text{and} \quad R_{3,2} = R_9 \boxplus R_{10} \boxplus R_8 \tag{60}$$

As a further example we consider the case of four-atom center of reaction, in which about 51% of the organic reactions occur. For this case the following general scheme of reaction is studied :

$$A_i - \wr A_j + A_k \wr - A_l \rightarrow A_i - A_k + A_l - A_j \tag{61}$$

In this reaction two bonds are splitted and two others are formed. An electrofugic dissociation, D_E, of the species A_i, A_j and a nucleofugic dissociation, D_N, of the species A_k, A_l are produced. Then the species A_i, A_k undergo an electrophilic and A_j, A_l a nucleophilic association. The sequence of the reaction steps is : $D_E(i, j)$ $D_N(k, l)$, $A_E(i, k)$ and $A_N(j, l)$. The $D_E A_E$ and $D_N A_N$ pairs can be therefore associated.

The matrix of reaction is given by the sum :

$$R_{4.1} = R_7 \boxplus R_8 \boxplus R_9 \boxplus R_{10} = \\ = \begin{array}{c} \\ \\ \end{array}\begin{array}{ccccc} & i & j & k & l \\ & 0 & -1 & 1 & 0 \\ & -1 & 0 & 0 & 1 \\ & 1 & 0 & 0 & -1 \\ & 0 & 1 & -1 & 0 \end{array}\begin{array}{c} \\ i \\ j \\ k \\ l \end{array} \tag{62}$$

As an example the following reaction occurs according to the mechanism $R_{4.1}$:

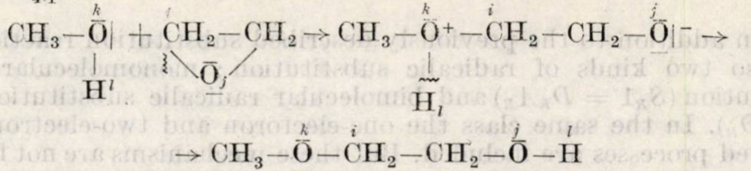

$$CH_3-\overset{k}{\bar{O}}|(-\overset{l}{H}) + \overset{i}{C}H_2-CH_2(\bar{O}_j) \to CH_3-\overset{k}{\ddot{O}^+}(-H_l)-\overset{i}{C}H_2-CH_2-\overset{j}{\bar{O}}|^- \to \\ \to CH_3-\overset{k}{\bar{O}}-\overset{i}{C}H_2-CH_2-\overset{j}{\bar{O}}-\overset{l}{H} \tag{63}$$

In general the reactions occurrding in centers of reactions with odd number of atoms are less frequent. This is why, as a further example, the reactions in six-atom center of reaction are treated. For this case the following general scheme is given :

$$A_i - \wr A_l + A_j - \wr A_n + A_k - \wr A_n \to A_i - A_n + A_j - A_l + A_k - A_m \tag{64}$$

Three covalent bonds are splitted by electrofugic dissociation and three others are formed by electrophilic association. The matrix of reaction is :

$$R_{4.1} = \begin{array}{c} \\ \\ \end{array}\begin{array}{ccccccc} i & j & k & l & m & n & \\ 0 & 0 & 0 & -1 & 0 & 1 & i \\ 0 & 0 & 0 & 1 & 0 & 1 & j \\ 0 & 0 & 0 & 0 & 1 & -1 & k \\ -1 & 1 & 0 & 0 & 0 & 0 & l \\ 0 & 0 & 1 & 0 & 0 & 0 & n \\ 1 & 1 & -1 & 0 & 0 & 0 & m \end{array} \quad D_E A_E D_E A_E D_E A_E \tag{65}$$

In this class are included the reactions of the Diels-Alder type, where compounds with double conjugated bonds form a cycle by reacting with an olephinic double bond :

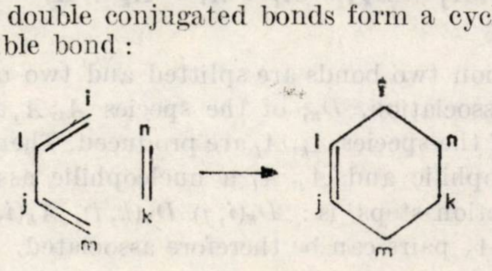

A series of well-known reactions in organic chemistry occur in six-atom centers of reactions. A series of examples can be found in ref.[2,3,6]

8. CONCLUDING REMARKS

It has been found that the use of the matrix form in expressing the chemical structures and reactions enables to establish a mathematical foundation of all chemical transformations. The basic elements, irreducible to simpler forms, allowing the modeling of any chemical reaction, are the *redox* and the *colhom* processes [4]. The matrices of reaction corresponding to these two pairs of processes can be deduced starting from two generating 2×2 unity matrices. While the *redox* matrices are sensitive both to the permutation and reversion operation the *colhom* ones can be interchanged by reversing the corresponding reaction only.

In a two-atom center of reaction the matrices of the heterolytic transformations can be deduced by addition operations using *redox* and *colhom* pairs matrices. The *redox* component introduces the sensitivity to permutation and the *colhom* component to reversion operation.

In multi-atom centers of reactions the more complex matrices of reaction can be composed of the simpler ones using always a matrix addition operation. As the number of atoms in the center of reaction increases, there are more complex variants in expressing the peculiar paths of reaction. But this variety is produced uniquely in the various possibilities to combine the elementary matrices of reaction, using the matrix addition operation only.

REFERENCES

[1] A. T. Balaban (editor), "Chemical Application of Graph Theory", Academic Press, London 1976.

[2] A. Călușaru, "Representation of Chemical Structures by Matrices and Computer Algorithms" in : "Heat and Mass Transfer", Vol. 3 (N. P. Cheremisinoff, editor), Gulf Publishers, New Jersey, 1988.

[3] A. Călușaru, *Rev. Chim. (București)*, **38**, 373 (1987) ; idem, *ibid.*, **38**, 461 (1987) ; idem, *ibid.*, **38**, **869** (1987).

[4] A. Călușaru, *Rev. Chim. (București)*, **38**, 869 (1987).

[5] A. Călușaru, and C. Volanschi, *Rev. Chim. (București)*, **35**, 598 (1984) ; idem, *Intern. Chem. Eng.*, **276**, 441 (1986).

[6] M. Kratochvil, J. Koča and V. Kvasnicka, *Chem. listy*, **78**, 1 (1984).

Revue Roumaine de Chimie, **33**, *9–10*, 937–942 (1988)

AN INFORMATIONAL REPRESENTATION OF THE SPECTRAL ANALYTICAL SYSTEMS AS COMMUNICATION SYSTEMS WITH DATA DECODING

VICTOR DAVID

Center for Protection and Hygiene of Work, Str. Pop de Băsești, no. 59, sec. 2, Bucharest
72244, Romania

Received November 21, 1987

The general information representation of the spectral analytical measuring systems takes into account the data encoding and decoding. For the decoding process a new information representation is given and the main probabilities encountered within its framework are discussed.

1. INTRODUCTION

A chemical-analytical process is one of obtaining and measuring information. Chemical information coming out from an analytical experiment is being encoded as a set of analytical signals situated into an analytical domain (spectral, potential, intensity, etc.). Then, the signal decoding takes place within the framework of the analytical process, which is very frequently fulfilled with the aid of data stored up into a data bank; their decoding is made by comparison. For qualitative analyses the decoding of signals is made by assigning them to certain chemical components using information stored in a data bank, while for quantitative analyses they are decoded using calibration curves.[1,2]

The purpose of the paper is to give a new representation from the information viewpoint for the spectral analytical systems taking into account data encoding and decoding, which can be applied to the spectral experiments with many informations, such as in mass-, emission- or IR-spectroscopy.

2. BACKGROUND

A transmission system of chemical-analytical informations is the system consisting of the sets X and Y, and a conditional probability $q(y_j|x_i)$, defined onto Y for each $x_i \in X$, which is denoted by $\{X, q(y_j)|x_i), Y\}$. The set X will be called the set of chemical components x_i, $i = \overline{1, n}$, a priori to analytical experiment, so that for each x_i will correspond an existence probability p_i, $i = \overline{1, n}$, while the set Y will be called the set of components y_i, $j = 1, m$ $(m \leqslant n)$, a posteriori to analytical experiment so that for each component y_j will correspond after the experiment an existence probability q_j, $j = 1, m$; $q(y_j \mid x_i)$ represents the probability, when carrying out the experiment, to find y_j instead of x_i. These three probabilities are bound by the relation:

$$q_j = \sum_{i=1}^{n} p_i \, q(y_j \mid x_i) \tag{1}$$

Thus, the transmission system without data encoding can be represented in the following manner[3]:

$$\{X, x_i, p_i, \quad i = \overline{1, n}\} \xrightarrow{p(y_j|x_i)} \{Y. y_j q_j, \quad j = \overline{1, m}\}$$

By data encoding, each component $x_i \in X$ will be represented by a multitude of n_i analytical signals u_α, denoted by $\{u_\alpha\}_{\alpha=1,n_i} \in U$, and called the code (spectrum) of x_i. The set U represents the set of all analytical signals u stored in the data bank, and N is their number ($\sum^{i} n_i \geqslant N$). Similarly, to each component y_j will correspond a code denoted by $\{v_\beta\}_{\beta=1,n_j} \in V$. In fact, the sets X and Y, U and V respectively, are identical, but here they were differently denoted for the formal treatment of the problem.

3. REPRESENTATION OF AN ANALYTICAL SYSTEM AS DATA ENCODING TRANSMISSION SYSTEM

Analytical measuring systems taken as data transmision systems with encoding and decoding can be represented sas follows:

$$\begin{tikzcd}
\text{SOURCE} \arrow[r] & \text{ENCODING} \arrow[r] & \text{CHANNEL} \arrow[r] & \text{DECODING} \arrow[r] \arrow[d, shift left] & \text{RECEPTION} \\
 & & & \text{DATA BANK} \arrow[u, shift left] &
\end{tikzcd}$$

The analytical sample is the source of the system and it is given by the probability field before the analytical experiment $\{X, x_i, p_i, i = \overline{1, n}\}$. By this representation each component x_i of the sample is characterized by a probability p_i to exist and consequently $(1 - p_i)$ is the probability as x_i not to exist in sample. The information entropy[5] corresponding to each component x_i, before the experiment, is given by:

$$H_i(\text{a priori}) = -p_i \log p_i - (1 - p_i) \log (1 - p_i) \tag{2}$$

(Here and henceforth log is taken in binary scale).

For n components one obtains the following relation for information entropy:

$$H(\text{sample}) = \sum_{i=1}^{n} H_i = -\sum_{i=1}^{n} p_i \log \frac{p_i}{(1 - p_i)} - \log \prod_{i=1}^{n} (1 - p_i) \tag{3}$$

If $p_i = 0$ or 1, this means we know the sample composition, and by computing in (3) we obtain H (sample) $= 0$. The maximum of the expression above becomes n bits for $p_i = 0.5$, $i = 1, 2, \ldots, n$. One can say that the establishment of the nature of the chemical components x_i and the assignment before experiment of their probabilities p_i to exist in the sample represents the analytical problem that will be partly or entirely solved with the aid of the analytical process. Before the experiment, to the set of components x_i of the sample will correspond by encoding a set of analytical signals, denoted by $U = \{u_\alpha\}$, $\alpha = \overline{1, N}$. Thus, to each signal $u_\alpha \in U$ will correspond before the experiment a probability, denoted by ρ_α. Therefore, the information entropy for the set U, before the experiment, has the following expression :

$$H(U)_{\text{a priori}} = -\sum_{\alpha=1}^{N} \rho_\alpha \log \frac{\rho_\alpha}{1-\rho_\alpha} - \log \prod_{\alpha=1}^{N} (1-\rho_\alpha) \qquad (4)$$

The value of ρ_α is situated within the interval $[0, 1]$.

The channel of the system is the analytical experiment itself, which transmits a set of analytical signals, i.e. it transmits which of the signals u_α belonging to the set U exists and which does not. Therefore, a posteriori to the analytical experiment, to each signal u_α corresponds a probability of existence, denoted by δ_α which depends upon the ratio signal/noise.[6] In fact, after experiment the set U has anoter information entropy :

$$H(U)_{\text{a posteriori}} = -\sum_{\alpha=1}^{N} \delta_\alpha \log \frac{\delta_\alpha}{1-\delta_\alpha} - \log \prod_{\alpha=1}^{N} (1-\delta_\alpha) \qquad (5)$$

The information quantity of the analyical signals will be given by the following relation :

$$\Delta H(U) = \log \prod_{\alpha=1}^{N} \frac{(1-\delta_\alpha)}{(1-\rho_\alpha)} - \sum_{\alpha=1}^{N} \left(\rho_\alpha \log \frac{\rho_\alpha}{1-\rho_\alpha} - \delta_\alpha \log \frac{\delta_\alpha}{1-\delta_\alpha} \right) \qquad (6)$$

By decoding the set $\{u_\alpha\}$ obtained by experiment, one obtains as a result the probability field, a posteriori to the analytical experiment, denoted by $\{X, x_i, q_i, i = \overline{1, n}\}$. It characterizes the final uncertainty about the sample composition or about the analytical problem. Generally, the a posteriori probability field is characterized by q_i probabilities, which tend towards their possible limits, i.e. $q_i \to 0$ or 1. The a posteriori information entropy will become :

$$H(\text{reception}) = -\sum_{i=1}^{n} q_i \log \frac{q_i}{(1-q_i)} - \log \prod_{i=1}^{n} (1-q_i) \qquad (7)$$

The information quantity of the analytical problem is given by the difference between the relations (3) and (7) :

$$\Delta H(X) = \log \prod_{i=1}^{n} \frac{(1-q_i)}{(1-p_i)} - \sum_{i=1}^{n} \left(p_i \log \frac{p_i}{1-p_i} - q_i \log \frac{q_i}{1-q_i} \right) \qquad (8)$$

Data bank will be represented by the set X^* of the stored components x_k whose number is $n^* \geqslant n$. By encoding, to X^* corresponds the set U^* of analytical signals u, whose number is $N^* \geqslant N$. Thus, the data bank can be represented informationally :

$$\{X^*, x_k, \quad k = 1,\ n^*;\ n^* \geqslant n\} \underset{\text{decoding}}{\overset{\text{encoding}}{\rightleftarrows}} \{U^*, u_\gamma, \quad \gamma = 1,\ N^*;\ N^* \geqslant N\} \tag{9}$$

4. AN INFORMATIONAL REPRESENTATION OF DECODING PROCESS

The first step of the decoding process is setting up of the set containing analytical signals obtained from experiment, denoted by U_{exp}, distinguishable from the background. Then, the decoding is individually made by intersecting the sets of signals belonging to all components i with the set of signals obtained from experiment. If : $U_{\text{exp}} \subset \{u_\alpha \in i\}_{\alpha=1,\, n_i}$, there results that the probability as i to exist is a positive number; $U_{\text{exp}} \not\subset \{u_\alpha \in i\}_{\alpha=1,\, n_i}$, then $q_i = 0$. For each signal belonging to the i–th code or spectrum corresponds a probability δ which can have a maximum value of 1. With these probabilities one can compute the a posteriori probabilities q_i, thus :

$$q_i = \delta_1 \delta_2 \ldots \delta_{n_i} = \prod_{\alpha=1}^{n_i} \delta_\alpha \tag{10}$$

n_i being (in accordance with the information theory) the length extension of the i-th component code.

The relation (10) expresses the fact that it is sufficient that a certain signal belonging to the component i be not obtained in the spectrum in order to draw the conclusion that i does not exist in the sample ($q_i = 0$). As a result of it, the rest of $(n_i - 1)$ analytical signals belongs to one or more components x of the set X, thus interfering with x_i. If at least one of the $(n_i - 1)$ signals does not belong to a certain component x from the data bank X, then this signal can be a result of an error, or it belongs to a new component $x \notin X$ which was thus discovered in the sample. Afterwards, the new component thus discovered and its code (spectrum) is introduced into the data bank, obtaining a new set X^* and its set of signals, U^*, respectively. With the above relation one can compute the a priori probabilities $p_i^!$ depending upon the probabilities ρ of the signals. We can finally say that the analytical decoding process is informationally the establishment of q_i probabilities for a component i of the analytical problem, depending upon the probabilities δ_α of the signals u_α belonging to the component. Furthermore, by the decoding process one follows several other probabilities, which will be subsequently discussed.

5. PROBABILITIES INVOLVED IN THE ANALYTICAL DECODING PROCESS

The probability for a signal u_α to belong to a certain component i can be a priori denoted by $p(u_\alpha \in i)$, and a posteriori $q(u_\alpha \in i)$. These probabilities are given by the relation :

$$p(u_\alpha \in i) = \frac{1}{\nu_\alpha}\,; \quad q(u_\alpha \in i) = \frac{1}{\mu_\alpha} \tag{11}$$

where ν_α is the number of interferences which can at most interfere in signal u_α, and μ_α is the number of existing interferences, set up by decoding.

The probability that an obtained signal u_α belongs to the component i depends upon the existence of some other signals, belonging to the component i and interferents with i, which have in their code the signal u_α[7]. One defines the probability as the signal u_α to belong to the component i conditioned by the existence of u_β, denoted by $p\,(u_\alpha \in i_\beta | u)$. The existence of the signal u_β belonging to the component i implies the increase of the probability for $u_\alpha \in i$, whereas the existence of signal u_β belonging to an interferent j implies the decrease of the probability for $u_\alpha \in i$. On the contrary, the absence of signal u_β belonging to i implies the decrease of the probability for $u_\alpha \in i$, i.e. $q(u_\alpha \in i) = 0$, whereas, u_β belonging to an interferent j implies the increase of the probability for $u_\alpha \in i$. All the cases described above are considered in the next relation :

$$q(u_\alpha \in i) = \prod_{\beta} q(u_\alpha \in i \,|\, u_\beta) \leqslant 1 \tag{12}$$

Then, the existence probability for the component i is :

$$q_i = \prod_{\alpha} q(u_\alpha \in i) = \prod_{\alpha} \prod_{\beta} q(u_\alpha \in i \,|\, u_\beta) \tag{13}$$

Another conditional probability is that for the signal u_α to belong to the component i in the case of existence of the interferent j, $q(u_\alpha \in i | j)$ which can be written :

$$q(u_\alpha \in i \,|\, j) = q(u_\alpha \in i \,|\, \{u_\beta \in j\}, \quad \beta = 1, n_j) = \prod_{\beta=1}^{n_j} q(u_\alpha \in i \,|\, u_\beta \in j) \tag{14}$$

By summing over $\alpha = \overline{1, n_i}$, one obtains q_i.

The probability as a signal u_α to belong to the components i and j at the same time, is denoted by $q\,(u_\alpha \in i, u_\alpha \in j)$ and is given by :

$$q(u_\alpha \in i, u_\alpha \in j) = q(u_\alpha \in i)\ q(u_\alpha \in j \mid u_\alpha \in i) \tag{15}$$

where $q\,(u_\alpha \in j \mid u_\alpha \in i)$ is the conditional probability for the signal u_α to belong to the component j, when u_α belongs to the component i[3].

REFERENCES

[1] K. Eckschlager and V. Stepanek, "Information Theory as Applied to Chemical Analysis", Wiley, New York, 1979.

[2] H. Kaiser, *Fresenius'Z. Anal. Chem.*, **260**, 252 (1972).

[3] S. Guiaşu and R. Teodorescu, "Matematica şi Informatica", Ed. Ştiinţifică, Bucharest, 1965, p. 112 ; 120.

[4] V. David and D. Ciomârtan, *Rev. Chim. (Bucureşti)*, **36**, 954 (1985).

[5] C. E. Shannon, *Bell. Syst. Tech. J.*, **27**, 623 (1948).

[6] C. Liteanu and I. Rică, "Optimizarea Proceselor Analitice", Ed. Academiei, Bucharest, 1985, p. 38.

[7] V. David and D. Ciomârtan, *Rev. Roumaine Chim.*, **31**, 823 (1986).

Revue Roumaine de Chimie, **33**, *9—10*, **943** (1988)

COMPTES RENDUS

G. NÁRAY-SZABÓ, P. R. SURJÁN and J. ÁNGYÁN, "Applied Quantum Chemistry", Akadémiai Kiadó, Budapest, 1987, 489 pp.

This book is based on an earlier version published in Hungarian. *Applied Quantum Chemistry* is written for theoretical and structural chemists, spectroscopists and biochemists who wish to gain insight into methods and applications of quantum chemistry. Graduate students, having some experience in quantum chemical methods, may also use the book as a general overview. Part one deals with the methods and most important concepts of quantum chemistry emphasizing the chemical aspect. Part two is devoted to the chemical bond while molecular structure (geometry, spectroscopy, electric and magnetic properties) is treated in part three. Chemical reactions are discussed in part four. Numerous tables help the reader in forming an opinion on the reliability of various quantum chemical methods while illustrative figures are included to make the text more readable. The interested reader may find 1500 references to recent and classical works for further information. This book is a joint edition published by Akadémiai Kiadó Budapest, Hungary and D. Reidel Publishing Company, Dordrecht, Holland as Vol. 1 in the series "Understanding Chemical Reactivity".

One of the main goals of the book is to show that the basic principles and equations of quantum mechanics can be applied to a vast variety of problems concerning molecular structure and chemical reactions. Since the authors discuss a very large number of examples and applications, not only quantum chemists but structural chemists, spectroscopists, theoretical organic chemists and biochemists may find the book useful as a general overview of the practical aspects of theoretical chemistry. The graduate students can use the book also with success. A more or less deductive treatment is given : starting from the numerically accurate solutions of the Schrödinger equation the authors approach gradually to more general, qualitative concepts. While such concepts can rarely be deduced exactly from the basic equations of quantum chemistry they play an outstanding role in understanding nature ; therefore the authors discussed them with special care. The authors had to reconcile the physicist's and chemist's ways of thinking, which is by no means simple. Therefore, the authors had to make some compromise, especially by avoiding more detailed analyses and making the text sometimes extremely terse. This was imperative since the extent of the book was limited, but numerous papers and books from the relevant literature are cited. These may help the interested reader to pick up more information on a specific topic. A further compromise is that part one, dealing with methods of quantum chemistry, cannot be considered as a didactic introduction — this can be found in numerous textbooks. It is rather an overview for those who have some experience in methods of quantum mechanics.

Undoubtedly, owing to the rapid progress in the field, this book will be a valuable guide and reference work for researchers interested in such aspects or having contigencies with them being of a real use to the graduate students and to the teaching staff as well.

D. Marchidan

Institute of Scientific Research, Technological Engineering, Design and Production for the Industries of Inorganic Chemistry and Non-Ferrous Metallurgy (IAMN)

The main activity of the institute consists in the elaboration of studies, research work, engineering design, general and detail design, consulting as well as small tonnage production in the following fields :

- heavy and accompanying non-ferrous metals ;
- light and rare metals ;
- primary and secondary non-ferrous metals ;
- metallic powders ;
- oxides and special inorganic salts ;
- catalysts and auxiliary products ;
- inorganic pigments ;
- ingredients for antiperspirant products

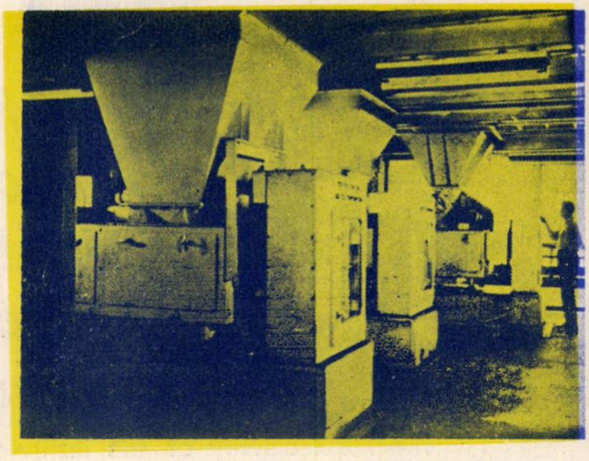

I. RESEARCH DEPARTMENT

Elaborates studies and performs research for manufacturing new products, up-dating and improvement of the technologies in the fields of inorganic chemistry and non-ferrous metallurgy. A special emphasis is laid on solving the problems generated by processing raw materials with low content of useful substances for recovery of recycled materials used in industrial fabrications, the result being increased economic efficiency with a low energy and fuel consumption. Research is performed in the following directions :

- electrolysis in molten salts and in solution ;
- solubilization at high pressures and temperatures ;
- separation of valuable elements by selective precipitation, ion exchange, liquid-liquid extraction, fractionated crystallization as well as hydrochlorinations and chlorinations in vapour phase ;
- chemical and metallurgical ore processing ;
- obtention of metals and alloys by electro-thermal and metallothermal processes (based on reduction with Mg, Al, Na etc.) ;
- use of plasma for non-ferrous raw material processing to obtain metals and metallic compounds ;
- melting of metals and alloys in induction furnaces, with electron bombardment or consumable electrodes ;
- obtention and processing of metallic powders by pulverization in air or reducing gas and by electrochemical methods ;
- sinterings in vacuum or in controlled atmosphere ;
- obtention and processing of non-ferrous metals and alloys by plastic deformation, extrusion, drawing, rolling ;
- technologies for recovery of non-ferrous metals from wastes ;
- process of separation and purification by separation in vapour phase, selective condensation, reflux condensation etc. ;
- continuous processes of gas absorption-desorption ;
- processes of crystallization and selective condensation ;
- obtention of oxides with certain structural and textural properties.

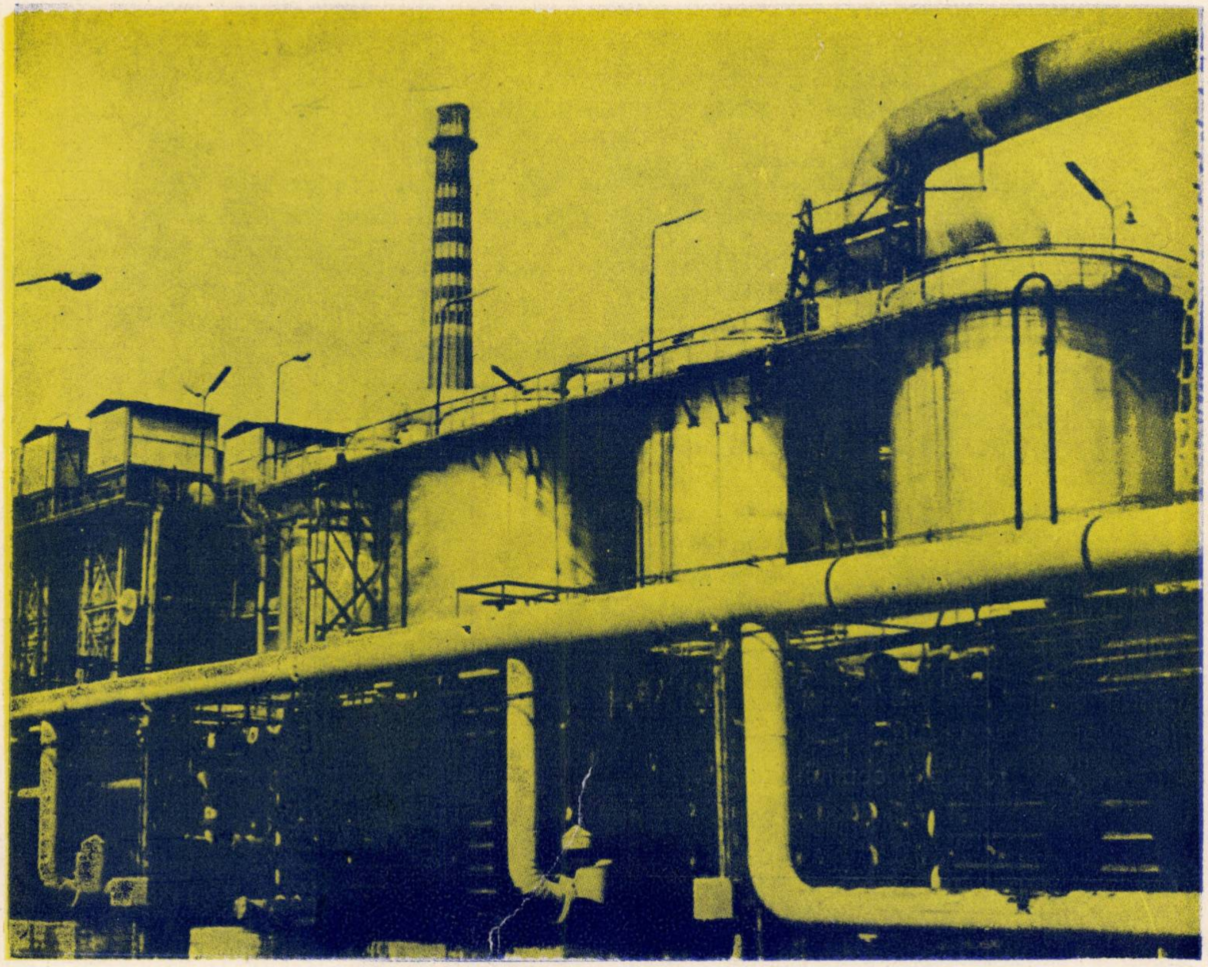

II. DESIGN DEPARTMENT

1. STUDIES :

- process documentation ;
- prognoses concerning the development of processes, branches or categories of products ;
- feasibility design and studies ;
- profile and location studies ;
- technical and economic analyses for investment promotion ;
- engineering design ;
- technology expert reports ;
- optimization of processes and installations ;
- systematizations, modernizations and improvements of existing installations.

2. PROCESS, TECHNICAL AND EXECUTION DESIGN :

- design and documentation for complete plants or industrial lines and separate units carried out in various stages : technico-economic studies, general design, execution design, etc. adapted to customers' requirements ;
- design of process equipment up to the execution stage ;
- design of auxiliary units ; transport of materials and equipment in chemical and metallurgical industries ;
- design for ventilation elements, waste water treatment, environment protection etc., adapted to the customers' requirements with observation of their specific norms ;
- design for solving protection and problems including fire protection problems ;
- technical assistance throughout all stages of plant construction, up to plant commissioning.

ORSZÁGOS MŰSZAKI INFORMÁCIÓS KÖZPONT ÉS KÖNYVTÁR 1883

**Correspondence
should be addressed to :
Director,
dipl.-chem. eng. Gheorghe Bujg
Institutul Anorganică și Metale
Neferoase (IAMN)
Bulevardul Biruinței 102
79616 Bucharest, Romania**

NOTE POUR LES AUTEURS

La Revue Roumaine de Chimie publie des articles en anglais, français, russe, allemand ou espagnol. Les auteurs sont priés d'envoyer des articles et des comptes rendus inédits.

Les manuscrits seront dactylographiés à double interligne. La bibliographie, les tableaux et la légende des figures seront placés après le texte.

Si l'article fait partie d'une série numérotée, la partie précédente sera donnée comme première référence.

Chaque article sera précédé d'un résumé comprenant quinze lignes au maximum.

Les références bibliographiques dans le texte seront faites par des exposants sans parenthèses et paraîtront à la fin de l'ouvrage.

Les publications périodiques mentionnées dans la bibliographie seront présentées suivant les prescriptions internationales : le nom de l'auteur précédé de l'initiale du prénom, le titre du périodique abrégé conformément à « Chemical Abstract » et souligné par une ligne, le numéro du tome indiqué par des chiffres arabes et souligné par deux lignes, suivi de la première page de l'article : à la fin, l'année de la parution sera placée entre parenthèses. Le numéro de la revue ne sera pas indiqué si les pages du volume sont numérotées consécutivement.

Les textes des livres ou traités incluront : le nom des auteurs, précédés de l'initiale du prénom, le titre du livre entre guillemets et sans être souligné, le numéro du tome précédé par l'abréviation « vol. » (ou « Bd. »), le numéro de l'édition, les éditions (the publisher), la localité de la parution du livre, l'année de la parution et la page de la référence précédée (s) par l'abréviation « p » (ou « S »).

Les brevets seront indiqués comme suit : l'auteur ou la firme, le pays et le numéro du brevet, la date de la revue (*Chem. Abstr.*). Par ex. : : M. Jones (to Union Carbide Co.). Brit. Pat. 610 238, 2 Sept. 1959 : cf. *Chem. Abstr.*, **54**, 12808 (1960).

Si la référence n'a pas été lue en original, on indiquera aussi la revue de références consultée.

Les diagrammes seront tracés à l'encre de Chine sur papier calque : Les tableaux et les figures (en nombre strictement nécessaire), ainsi que les courbes dans des figures seront numérotés par des chiffres arabes. Leur explication sera donnée dans la légende des figures. Prière de ne pas inscrire les mêmes données dans les tableaux et les figures. Chaque tableau aura un titre. On indiquera dans la texte le place approximative des tableaux et des figures. Les formules chimiques seront incluses dans le texte ; en outre, elles seront transcrites sur papier calque à l'encre de Chine.

Les auteurs sont priés d'indiquer les caractères italiques (en soulignant les lettres au crayon), ainsi que tout autre caractère spécial : les préfixes, *ortho*, *meta*, *para*, *cis*, *trans*, etc. seront soulignés pour indiquer leurs caractères italiques, et ne seront jamais écrits avec des majuscules.

Aucune correction à la main ne sera admise sur le manuscrit. Les corrections seront frappées à la machine. Les lettres greques ou d'autres symboles spéciaux seront insérés à la main à l'encre clairement.

Le manuscrit sera signé par l'auteur.

Le titre courant aura 50 lettres au maximum.

L'entière responsabilité du contenu des articles appartient aux auteurs.

Sur demande on peut obtenir une note plus complète.

PRINTED IN ROMANIA

1988 OKT 2 1

TRAVAUX PARUS AUX ÉDITIONS DE L'ACADÉMIE DE LA RÉPUBLIQUE SOCIALISTE DE ROUMANIE

ELENA CEAUŞESCU, **Răşini de hidrocarburi**, vol. 1, 1988, 344 p.
ELENA CEAUŞESCU, **Progrese în chimia şi tehnologia polimerilor**, 1986, 446 p.
ELENA CEAUŞESCU, **Foschungen im Bereich der Chimie und Technologie der Polymere**, 1986, 444 p.
ELENA CEAUŞESCU, **Cercetări în chimia şi tehnologia polimerilor**, 1983, 520 p.
ELENA CEAUŞESCU, **Noi cercetări în domeniul compuşilor macromoleculari**, 1981, 536 p.
ELENA CEAUŞESCU, **Polimerizarea stereospecifică a izoprenului**, 1979, 307 p.
ELENA CEAUŞESCU, **Research work on synthesis and characterization of macromolecular compounds. Contributions**, 1974, 251 p.
I. G. MURGULESCU, **Introducere în chimia fizică, Vol. I. 1. Atomi, molecule, legătură chimică**, 1976, 560 p.
I. G. MURGULESCU, V. EM. SAHINI, **Introducere în chimia fizică, Vol. I. 2. Structura şi proprietăţile moleculelor**, 1979, 604 p.
I. G. MURGULESCU, E. SEGAL, **Introducere în chimia fizică, Vol. II. 1. Teoria molecular-cinetică a materiei**, 1979, 1036 p.
I. G. MURGULESCU, TATIANA ONCESCU, E. SEGAL, **Introducere în chimia fizică, Vol. II. 2. Cinetică chimică şi cataliză**, 1981, 1024 p.
I. G. MURGULESCU, J. PĂUN, **Introducere în chimia fizică, Vol. I. 3. Nucleul atomic, reacţii nucleare, particule elementare**, 1982, 606 p.
I. G. MURGULESCU, RODICA VÎLCU, **Introducere în chimia fizică. Vol. III. Termodinamica chimică**, 1982, 624 p.
I. G. MURGULESCU, O. M. RADOVICI, **Introducere în chimia fizică. Vol. IV. Electrochimia**, 1986, 410 p.
CRISTOFOR SIMIONESCU, VALERIA GORDUZA, **Implicaţii bioenergetice ale coloranţilor**, 1988, 208 p.
R. VÎLCU, M. LECA, **Termodinamica polimerilor prin cromatografie de gaze**, 1987, 238 p.
I. ZUGRĂVESCU, M. PETROVANU, **Cicloadiţii** $3+2$ **dipolare**, 1987, 446 p.
RAUL MIHAIL, ION GROZEANU, **Estimarea secvenţială aplicată sistemelor chimice**, 1986, 406 p.
M. BREZEANU, I. PATRON, M. ANDRUH, **Combinaţii complexe polinucleare şi aplicaţiile lor**, 1986, 244 p.
A. T. BALABAN et al., **Labelled Compounds and Radiopharmaceuticals Applied in Nuclear Medicine**, coédition avec John Wiley and Sons, 1986, 742 p.
D. PURDELA, **Nomenclatura chimiei organice – IUPAC**, 1986, 451 p.
PETRU BUDRUGEAC, **Probleme de chimie**, 1986, 280 p.
T. ONCESCU, S. G. IONESCU, **Conversie fotochimică şi stocare de energie**, 1985, 272 p.
V. DRĂGUŢAN, A. T. BALABAN, M. DIMONIE, **Olefin Metathesis and Ring-Opening Polymerization of Cyclo-Olefins**, coédition avec John Wiley and Sons, 1985, 544 p.
C. LITEANU, I. RÎCĂ, **Optimizarea proceselor analitice**, 1985, 360 p.
N. PERESCU, **Chimia extracţiei cu solvenţi şi aplicaţii**, 1985, 212 p.
V. E. SAHINI, M. HILLEBRAND, **Chimia cuantică în exemple şi aplicaţii**, 1984, 378 p.
GH. MARCU, **Chimia compuşilor coordinativi**, 1984, 415 p.
E. CORDOŞ, C. MANOLIU, **Spectrometria de absorbţie şi fluorescenţă atomică**, 1984, 178 p.
C. BODEA, **Tratat de biochimie vegetală**, p. II, t. V, 1984, 438 p.
N. ASANDEI, A. GRIGORIU, **Chimia şi structura fibrelor**, 1983, 95 p.
N. IONESCU, M. CALDARARU, **Oxidarea catalitică a olefinelor inferioare**, 1983, 178 p.
C. I. SIMIONESCU, F. DANES, **Originea vieţii**, 1983, 110 p.
C. BODEA, **Tratat de biochimie vegetală, p. II, t. IV**, 1982, 408 p.
CR. SIMIONESCU, VALERIA GORDUZA, **Polimeri biocompatibili şi biologic activi**, 1980, 479 p.
M. FLORESCU, **Metode ştiinţifice în dezvoltarea industriei chimice moderne**, 1979, 495 p.
C. GH. MACAROVICI, **Analiza chimică cantitativă anorganică**, 1979, 457 p.

ISSN 0035–3930

I. P. INFORMAŢIA c. 2348

43 426

Lei 40

F 1103

04

ACADÉMIE DE LA RÉPUBLIQUE SOCIALISTE DE ROUMANIE

REVUE ROUMAINE DE CHIMIE

TOME 33

N°s 11–12

Novembre – Décembre 1988

Rev. Roumaine Chim.

RRCHAX, 33, *11–12*, p. 945–1076 (1988), Bucarest

EDITURA ACADEMIEI REPUBLICII SOCIALISTE ROMÂNIA

ACADÉMIE DE LA RÉPUBLIQUE SOCIALISTE DE ROUMANIE

COMITÉ DE RÉDACTION

Rédacteur en chef:

I. G. MURGULESCU, membre de l'Académie de la République Socialiste de Roumanie

Rédacteurs en chef adjoints:

A. T. BALABAN et V. EM. SAHINI, membres correspondants de l'Académie de la République Socialiste de Roumanie

Collège de rédaction:

EM. BRATU, ELENA CEAUȘESCU, ECATERINA CIORĂNESCU-NENITZESCU, CR. SIMIONESCU, membres de l'Académie de la République Socialiste de Roumanie ; P. SPACU, membre correspondant de l'Académie de la République Socialiste de Roumanie ; M. BANCIU, M. D. GHEORGHIU, I. HAIDUC, D. I. MARCHIDAN, G. NIAC et D. SĂNDULESCU

La Revue Roumaine de Chimie paraît 10 fois par an. Toute commande de l'étranger sera adressée à ROMPRESFILATELIA — sectorul Export-Import Presă, P. O. Box 12—201, télex 10376, prsfi r 78 104 Bucarest, Calea Griviței nr. 64—66, București, Roumanie

Les manuscrits, les livres et les revues proposés en échange, ainsi que toute correspondance seront envoyés à la rédaction

REVUE ROUMAINE DE CHIMIE

125, Calea Victoriei, 79717 Bucarest, Roumanie, téléphone 50 76 80

EDITURA ACADEMIEI REPUBLICII SOCIALISTE ROMÂNIA
125, Calea Victoriei, 79717 Bucarest, Roumanie, téléphone 50 76 80

REVUE ROUMAINE DE CHIMIE

Tome 33, Nos 11—12 **Novembre—Décembre, 1988**

ORSZÁGOS MŰSZAKI INFORMÁCIÓS KÖZPONT ÉS KÖNYVTÁR

ECATERINA JURCONI and GH. S. IONESCU, On the mechanism of some manganese (III) complex oxalates thermal decomposition . . . . 947—951

MAGDALENA PALAGHIȚĂ and DAN RĂILEANU, Nenitzescu synthesis of 5-hydroxyindoles. III. A diazaheptalenedione from 3-aminocinnamic ester . . . . 953—967

FLORICA ZALARU, AURELIA MEGHEA, D. IONESCU and FELICIA CORNEA, Some new copper(II) bromocomplex compounds with imidazole derivatives . . 969—974

HANS-HORST GLATT, CAROL CSUNDERLIK, INGRID GLATT, HORIA DULVAC und VICTORIA SCOROBETE, Syntheses of heterocycles using carbonic acid derivatives. XI. Reaction of *o*-formylarylcyanates with NH-heterocycles affording benzoxazine derivatives (in German) . . . . 975—979

MOHAMED F. ABDEL-MEGEED and A. TENIOU, Synthesis of some new 3-substituted 4(3*H*)-quinazolinone and 4(3*H*)-quinazolinethione derivatives and related fused biheterocyclic ring systems . . . . 981—986

MARIE-HÉLÈNE DARBIEU et CHRISTINE RIPOLL, Biosynthesis of the vitamin B_{12} (in French) . . . . 987—992

I. V. NICOLESCU, MARIANA UDREA, ALA NICOLESCU, I. UDREA and D. CRIȘAN, Catalytically active aluminas from precursors obtained by supersaturation of reactants. I. Synthesis of precursors and reaction mechanisms . . . . 993—1004

MARIANA UDREA, I. UDREA, ALA NICOLESCU, D. CRIȘAN and I. V. NICOLESCU, Catalytically active aluminas from precursors obtained by supersaturation of reactants. II. Textural and structural properties and their relation to the nature of precursors and the thermal treatment . . . . 1005—1011

MARIANA UDREA, I. V. NICOLESCU, ALA NICOLESCU, I. UDREA and D. CRIȘAN, Catalytically active aluminas from precursors obtained by supersaturation of reactants. III. The catalytic activity of aluminas in isomerization of cyclohexene test reaction. . . . . 1013—1019

MARIANA UDREA, I. UDREA, I. V. NICOLESCU and ALA NICOLESCU, Catalytically active aluminas from precursors obtained by supersaturation of reactants. IV. Kinetics of cyclohexene isomerization . . . . 1021—1030

MARIANA UDREA, I. V. NICOLESCU, I. UDREA and ALA NICOLESCU, Catalytically active aluminas from precursors obtained by supersaturation of reactants. V. Adsorption of cyclohexene by gas chromatography . . . . 1031—1039

VASILE PÂRVULESCU, VIORICA PÂRVULESCU, IOAN V. NICOLESCU and IOAN SĂNDULESCU, Hydrogenation of styrene on bimetallic supported catalysts $Pd-Me/\gamma-Al_2O_3$ (Me = Mn, Fe, Co, Ni and Cu). . . . . 1041—1053

BOOK REVIEWS . . . . 1055—1061

AUTHOR INDEX . . . . 1063—1071

SUBJECT INDEX . . . . 1072—1076

| Rev. Roumaine Chim. | **33**, *11—12*, 945—1076 (1988), Bucarest

Revue Roumaine de Chimie, **33**, *11–12*, 947–951 (1988)

ON THE MECHANISM OF SOME MANGANESE (III) COMPLEX OXALATES THERMAL DECOMPOSITION

ECATERINA JURCONI and GH. S. IONESCU
Department of Physical Chemistry, Polytechnic Institute of Bucharest,
Blvd Republicii 13, R-70346, Romania

Received June 8, 1987

The effect of the substrate concentration on the thermal decomposition rates of $K_3[Mn(C_2O_4)_3]$ and *trans*-$K[Mn(C_2O_4)_2(H_2O)_2]$ in aqueous solutions was studied and revealed specific features which were conveniently explained by using Noyes' model of geminate recombination. The experimental supported a mechanism including the scavenging step of $C_2O_4^{\bullet -}$ short lived intermediates by the molecules of the original complex. This is a common feature of the photoredox and thermal redox decompositions of these manganese oxalate complexes.

INTRODUCTION

Both thermal and photochemical redox decomposition of $K_3[Mn(C_2O_4)_3]$ and *trans*-$K[Mn(C_2O_4)_2(H_2O)_2]$ in nonaqueous solutions have been extensively studied in the last decade.[1–10] The spectroscopic and kinetic results outlined the fact that the $C_2O_4^{\bullet -}$ radical ion is the main short lived intermediate implied in these redox decompositions.[11–13] The dependence of the reaction quantum yields of *trans*-$K[Mn(C_2O_4)_2(H_2O)_2]$ photoredox decomposition in dimethylformamide solutions on the complex concentration[7] was the first experimental evidence of the fact that such redox decompositions, concerned scavenging steps of $C_2O_4^{\bullet -}$ short lived intermediates. These scavenging steps cannot be described in the terms of conventional rate constants but surprisingly well by using Noyes' model[14–15] of geminate recombination.[8] The photoaccelerated redox decomposition of $K_3[Mn(C_2O_4)_3]$ in potassium oxalate aqueous solutions showed striking similarities with that of *trans*-$K[Mn(C_2O_4)_2(H_2O)_2]$ in what the nonconventional kinetics of the scavenging reaction is concerned.[16] This system furnished preliminary experimental evidences that even the thermal redox reaction of $K_3[Mn(C_2O_4)_3]$ proceeds via such scavenging steps. The aim of this work was to provide valuable data supporting the hypothesis of this general feature concerning the mechanism both of photoredox and thermal redox decompositions of these manganese (III) complex oxalates.

EXPERIMENTAL

$K_3[Mn(C_2O_4)_3]$ and *trans*-$K[Mn(C_2O_4)_2(H_2O)_2]$ were synthetized from $H_2C_2O_4 \cdot 2H_2O$ and $KMnO_4$ reagent grade by using Cartedge and Ericks' method.[17]

Solutions of $K_3[Mn(C_2O_4)_3]$ ranging from 10^{-4} M up to 10^{-2}M were prepared by using 0.1 M $K_2C_2O_4$ aqueous solution as a solvent. The excess of $K_2C_2O_4$ hindered the aquation of the complex. Solutions of $K[Mn(C_2O_4)_2(H_2O)_2]$ were prepared by using distilled water of pH about 6.5.

The kinetic measurements were carried out under controlled conditions in the thermostated quartz cell of a SP 800 Pye Unicam spectrophotometer. The absorbance values were measured at constant intervals and meanwhile the monitoring light beam was shuttered in order to prevent the photoacceleration of the thermal redox reaction.

The absorbance values, A_0, A_∞, A at the beginning of the reaction, at the end of it and at the moment t were used to verify the equation of a first order kinetics:

$$\ln \frac{A_0 - A_\infty}{A - A_\infty} = k_1 t \qquad (1)$$

k_1 is the first order rate constant (s^{-1}).

We performed more than four kinetic runs for each complex concentration of the sample at constant temperature ($T = 25°$) in the concentration range 10^{-4} M — 10^{-2}M.

The statistical method we used to checkout and support our equations was that proposed by Squires [18].

RESULTS AND DISCUSSION

The thermal redox decompositions of the two manganese (III) oxalate complexes we studied obeyed fairly first order kinetics at constant initial concentrations as can easily be seen in Figures 1 and 2.

Similar plots were obtained for the whole concentration range we investigated. Typical data concerning the rate constants, evaluated at 25° and different starting concentrations are summarized in Table 1 and Table 2.

One can easily notice that the rate constants are strongly dependent on the starting concentration of the complex substrate, doubling for each one order change of the concentration.

The first explanation of these results is to consider the redox decompositions we studied obey pseudofirst order kinetics, which is in disagreement with the general mechanism adopted up to date. The preliminary results obtained for the photoaccelerated decomposition of $K_3[Mn(C_2O_4)_3]$ under similar conditions [10,16] determined us to take into account the nonconventional kinetics of the scavenging reaction between the short lived ($< 10^{-7}$ s) $C_2O_4^{\cdot -}$ intermediates and the original complex molecules. In this case the rate constant has to be proportional to the square root of the starting complex substrate concentration.

Figures 3 and 4 support this last supposition.

We have to underline the fact the statistical calculations showed a better correlation for the nonconventional kinetics, i.e. $r = 0.9970$ and respectively $r = 0.9997$ than for a conventional one : $r = 0.986$ and respectively $r = 0.984$.

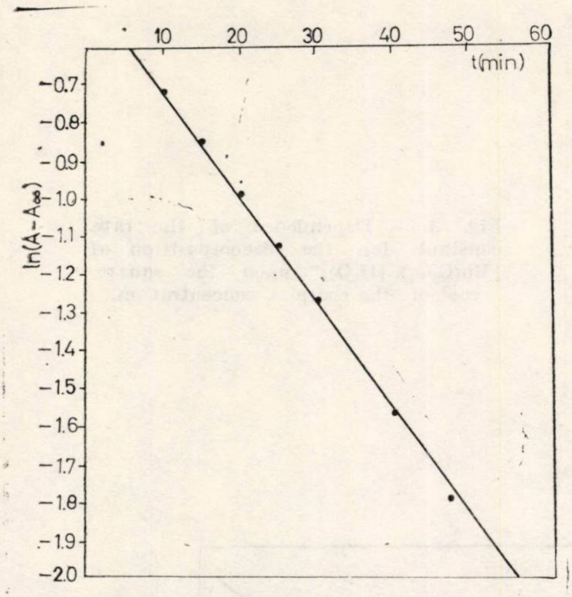

Fig. 1. — First order kinetics for the thermal redox decomposition of $[Mn(C_2O_4)_2(H_2O)_2]^-$ at conditions: $T = 25°$, $\lambda = 450$ nm; $d = 4$ cm; $c_{complex} = 2 \times 10^{-3}$M; $k = 4.2 \times 10^{-4}s^{-1}$; $r = 0.995$.

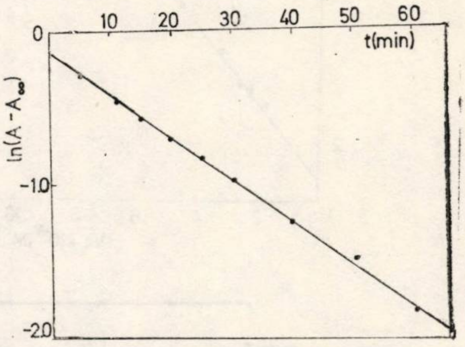

Fig. 2. — First order kinetics for the thermal redox decomposition of $[Mn(C_2O_4)_3]^{3-}$ at conditions: $T = 25°$, $\lambda = 500$ nm; $d = 4$ cm; $c_{complex} = 9 \times 10^{-4}$M; $k = 4.5 \times 10^{-4}s^{-1}$; $r = 0.996$.

The results we obtained are in good agreement with those concerning the photoredox and photoaccelerated decomposition of the complexes we studied, supporting the general feature of such reactions — the scavenging processes in what $C_2O_4^{\cdot -}$ species are implyied.

Table 1

Rate constants at 25° for the thermal redox decomposition of $[Mn(C_2O_4)_2(H_2O)_2]^-$

$c_{complex}$(M)	$k \times 10^4(s^{-1})$
0.0003	2.60
0.0005	2.86
0.0007	2.92
0.0010	3.50
0.0020	4.25
0.0030	4.70
0.0040	5.11
0.0050	5.65
0.0060	6.33
0.0070	6.50
0.0090	7.50
0.0100	7.65

Table 2

Rate constants at 25° for the thermal redox decomposition of $[Mn(C_2O_4)_3]^{3-}$

Complex (M)	$C_{K_2C_2O_4}$ (M)	$k \times 10^4(s^{-1})$
0.0003	0.03	4.03
0.0005	0.05	4.16
0.0007	0.07	4.18
0.0008	0.08	4.50
0.0009	0.09	4.35
0.0010	0.10	4.52
0.0020	0.20	4.99
0.0030	0.30	5.22
0.0040	0.40	5.84
0.0050	0.50	5.88
0.0060	0.60	6.10
0.0070	0.70	6.40
0.0080	0.80	6.62
0.0090	0.90	6.78
0.0100	1.00	7.25

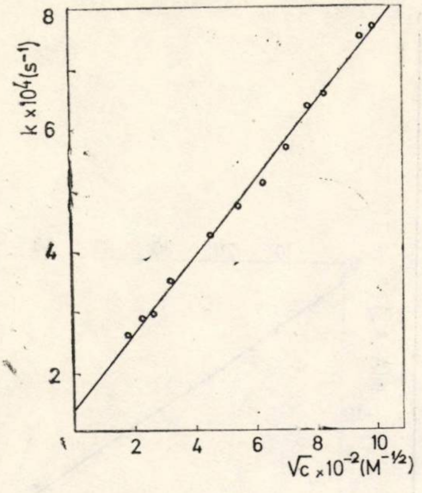

Fig. 3. — Dependence of the rate constant for the decomposition of $[Mn(C_2O_4)_2(H_2O)]^-$ upon the square root of the complex concentration.

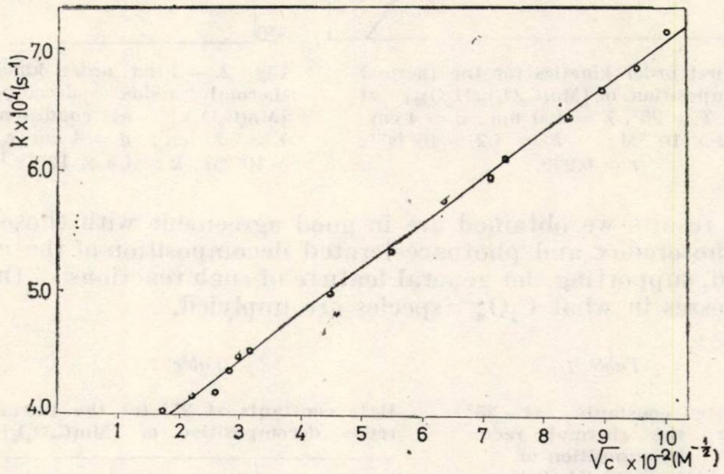

Fig. 4. — Dependence of the rate constant for the decomposition of $[Mn(C_2O_4)_3]^{3-}$ upon the square root of the complex concentration.

REFERENCES

[1] Tatiana Oncescu and Ecaterina Jurconi, *Rev. Roumaine Chim.*, **21,** 805 (1976).
[2] Tatiana Oncescu and Ecaterina Jurconi, *Rev. Roumaine Chim.*, **21,** 985 (1976).
[3] Tatiana Oncescu and Ecaterina Jurconi, *Rev. Roumaine Chim.*, **22,** 69 (1977).
[4] Tatiana Oncescu and Ecaterina Jurconi, *Rev. Roumaine Chim.*, **22,** 1971 (1977).
[5] Ecaterina Jurconi and Gh. Spinu, *Rev. Chim. București*, **36,** 925 (1985).
[6] I.G. Murgulescu, Tatiana Oncescu and S.G. Ionescu, *Rev. Roumaine Chim.*, **17,** 423(1972).
[7] Tatiana Oncescu, S. G. Ionescu and C. Andreescu, *Rev. Roumaine Chim.*, **22,** 697 (1977).
[8] Tatiana Oncescu and S.G. Ionescu, *J. Photochem*, **13,** 181 (1980).
[9] S.G. Ionescu and Tatiana Oncescu, *J. Photochem*, **20,** 299 (1982)
[10] M.A. Mansour, Dissertation, Bucharest, 1983.

[11] G.A. Shagisultanova, L.N. Neokladnova and A.L. Posnyak, *Doklady Akad. Nauk. SSSR*, **162** 1333(1965).

[12] A.L. Posnyak, G.A. Shagisultanova and L.N. Neokladnova, *Teor. Eksp. Khin.*, **4**, 567 (1968).

[13] G.D. Cooper and B.A. De Graff, *J. Phys. Chem.*, **75**, 2897 (1971).

[14] R.M. Noyes, *J. Amer. Chem. Soc.*, **77**, 2042 (1955).

[15] R.M. Noyes, *J. Amer. Chem. Soc.*, **78**, 5486 (1956).

[16] S.G. Ionescu, Tatiana Oncescu and M.A.Mansour, to be published.

[17] G.H. Cartledge and W.P. Ericks, *J.Amer. Chem. Soc.*, **58**, 2061 (1936).

[18] G.L.Squires, "Practical Physics", McGraw Hill, London, 1968, ch. 3.

Revue Roumaine de Chimie, **33**, *11—12*, 953—967 (1988)

NENITZESCU SYNTHESIS OF 5-HYDROXYINDOLES. III[1]

A DIAZAHEPTALENEDIONE FROM 3-AMINOCINNAMIC ESTER

MAGDALENA PALAGHIŢĂ* and DAN RĂILEANU**
Organic Chemistry Center ICECHIM—Bucharest 12
Spl. Independenţei 202 B, R 78100, Romania

Received October 14, 1987

The Nenitzescu reaction between 3-aminocinnamic ester and *p*-benzoquinone when carried out in an alcohol (preferably 1-butanol) as solvent led to the 2,8-diazaheptalenedione derivative **7** instead of the expected 5-hydroxyindole **6**. On reduction with Zn and acetic acid the dihydrodihydroxydiazaheptalene **14** resulted which by heating in *o*-dichlorobenzene solution afforded the diazaheptalenone **15**. The dication of **7** (**20**) was obtained in fluorosulfuric acid as well as an "enolate" of **15** (**21**). The structure determination of **7** is described and the reaction mechanism of its formation is discussed along with the occurrence of the 5-hydroxyindole by-product **8**.

The Nenitzescu reaction between *para*-benzoquinone (**1**) and 3-aminocinnamic ester (**2**) is the first case when a key intermediate, namely the hydroquinone derivative **3**, could be isolated as a main reaction product. The reaction is strongly influenced by the nature of the solvent owing to the presence of the phenyl group unlike the previously described cases which used the 3-aminocrotonic ester and its homologues. While the 5-hydroxyindole **6** could be obtained only in refluxing acetic acid, the solvents in common use as chloroform, dichloroethane, acetone or benzene gave as a main product of the reaction the enaminohydroquinone **3** and as secondary products a mixture of the disubstituted quinone **4** and hydroquinone (**5**).[2] Right from the beginning its discoverer[3] suggested that derivatives of type **3** should be key intermediates of the reaction.

We wish now to report the results obtained when the reaction between benzoquinone (**1**) and 3-aminocinnamic ester (**2**) was carried out in an alcohol (preferably butanol). Quite unexpectedly a new compound resulted which proved to be a derivative of 2,8-diazaheptalene-1,5-dione (**7**). The ester **2** was used in excess and the best yields were obtained in butanol (Chart I). The reaction mixture was refluxed when a red colour developed which disappeared after 20 min. At this moment the reaction was considered as completed and working-up of the reaction mixture afforded yellow crystals with mp 320° (dec.) after recrystallization from nitromethane, the yield being 20% of the theoretical based on quinone. The product is stable and could be sublimed at 290°/12 Torr. In the mass spectrum the molecular ion $M^+ = 484$ was obtained while the elementary analysis led to the molecular formula corresponding to the structure **7** which was assigned on the basis of the spectral analysis and chemical properties which will be further described.

---

* Part of the doctoral dissertation, Organic Chemistry Center, Bucharest.

** To whom correspondence should be addressed.

The ethereal filtrate of **7** by working-up furnished the by-product **8**, white needles with mp. 217°, whose elemental analysis and spectra showed it to be a 5-hydroxyindole with an enamino group substituent in the 4-position (yield 11%). Such compounds have already been obtained by Kuckländer starting from 3-amino- and 3-methylaminocrotonic esters.[4]

Unlike the case of 5-hydroxyindoles, the diazaheptalenedione **7** is an oxidation product, three quarters of the benzoquinone introduced into the reaction being consumed in the formation of hydroquinone. This phenomenon has already been observed in the formation of disubstituted quinone **4** as well as in the case of the secondary product **8** when two thirds and respectively half of the benzoquinone is transformed into hydroquinone (Equations A, B, C, and D).

$$\text{(A)}\ 4(\mathbf{1}) + 2(\mathbf{2}) = (\mathbf{7}) + 3(\mathbf{5})$$

$$\text{(B)}\ 3(\mathbf{1}) + 2(\mathbf{2}) = (\mathbf{4}) + 2(\mathbf{5})$$

$$\text{(C)}\ 2(\mathbf{1}) + 2(\mathbf{2}) = (\mathbf{8}) + (\mathbf{5}) + H_2O$$

$$\text{(D)}\ (\mathbf{1}) + (\mathbf{2}) = (\mathbf{6}) + H_2O$$

Structure determination of heptalenedione **7**. The ^{1}H-NMR spectrum (Fig. 1) indicates the presence of two non-equivalent carbethoxy groups, two phenyl groups and two deuterable offset protons, one of them coupled ($J = 7$ Hz) and being part of an enamine group $-NH-CH=CH-$ ($J_{1,2} = 7$ Hz; $J_{2,3} = 9.5$ Hz). From examination of the IR spectra it could be ascertained that the two deuterable protons belong to two NH groups ($\nu_{NH} = 3440$ and $3412\ cm^{-1}$ in $CHCl_3$). The ^{13}C-NMR spectrum indicates the presence of four carbonyl groups corresponding to two ester functions (163.6 and 163.0 ppm), to an unsaturated amide (168.3 ppm) and most likely to a quinoid carbonyl bearing an adjacent electronegative group (179.4 ppm).[5] Primary amides which exhibit absorption in the same region can be excluded on the basis of the IR spectrum. Therefore the presence in the molecule of 6 oxygen atoms and of two NH groups is confirmed.

Besides the four carbonyl and two phenyl groups the presence of three strongly polarized double bonds (four singlets and two doublets) and one less polarized double bond (two singlets) can be observed (Table 1)

The two doublets in Table 1 correspond to the above mentioned enamino group. The unsaturation number of the molecular formula $C_{28}H_{24}N_2O_6$ is 18 while the number of unsaturations observed amounts to 16. The difference between the two values means the existence of two supplementary cycles in the molecule. Taking into account that one carbonyl group is implied in a quinoid structure and a second one in an unsaturated amide group one might presume the existence of a seven-membered quinoid ring, namely the ring B in structure **7**. For the second ring we must accomodate the remaining two strongly polarized bonds cor-

CHART 1

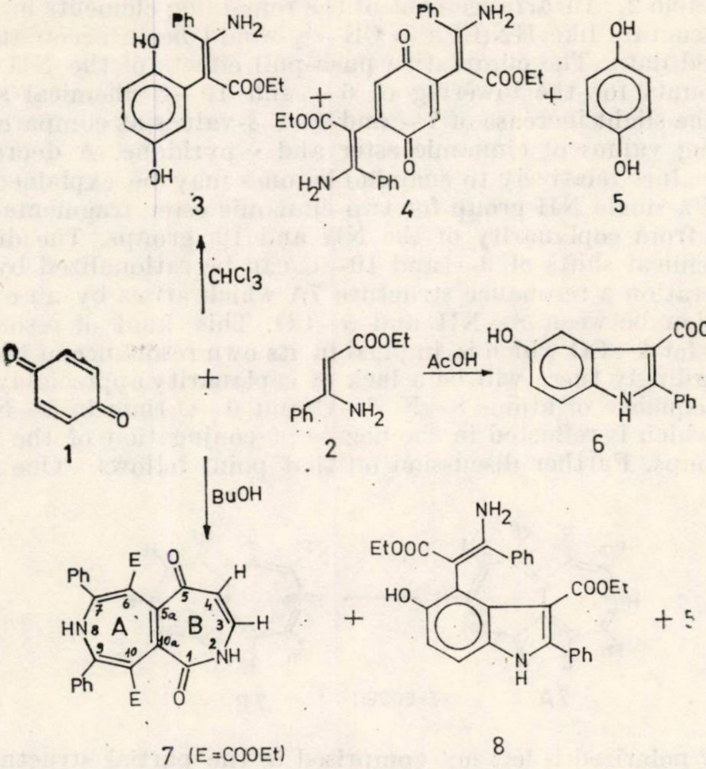
Ph
NH2
HO
COOEt
OH
3
EtOOC
O
H2N
Ph
4
5
CHCl3
AcOH
1
2
6
BuOH
E
H
HN
A
B
NH
7 (E = COOEt)
EtOOC
8
+ 5

Table 1

^{13}C-NMR chemical shifts of the nonaromatic C=C bonds in 7

Assignment	δ, ppm	Multiplicity	δ, ppm
Δ−10,9	100.8	singlets	147.3
Δ−6,7	105.3	singlets	147.9
Δ−4,3	111.3	doublets	139.1
Δ−5a, 10a	124.2	singlets	129.3

Table 2

^{13}C- NMR chemical shifts of push-pull model compounds

Model compound	Assignment	δ, ppm		Ref.
Ethyl cinnamate	Δ−3,2	118.4	144.6	(6)
γ-Pyridone	Δ−3,2	115.9	139.8	(7)
3-Amino-1-phenyl-2-propenone	Δ−2,3	110.9	157.6	(8)
3-Dimethylamino-2-cyclohexenone	Δ−2,3	98.2	165.5	(9)

responding to four singlets. Enamines, cinnamic esters and pyrridones may be taken as model substances in very good agreement as it can be seen from Table 2. An arrangement of the remaining elements in a divinylamine structure like $HN(CPh = CE-)_2$ would be in accordance with the tabulated data. The cumulative push-pull effects of the NH and Ph groups accounts for the lowering of 6— and 10—C chemical shifts as well as for the slight increase of 7— and 9—C δ-values as compared to the corresponding values of cinnamic ester and γ-pyridone. A decrease of the former values relatively to enamino ketones may be explained by the existence of a single NH group for two cinnamic ester fragments and by a deviation from coplanarity of the NH and Ph groups. The difference between chemical shifts of 6— and 10—C can be rationalized by taking into consideration a resonance structure **7A** which arises by an extension of conjugation between 8—NH and 5—CO. This kind of resonance is not possible for 1—CO which is implied in its own resonance of the amide group. Accordingly there will be a lack of coplanarity appreciably stronger in the sequence of atoms 8—N, 7—C and 6—C than in 8—N, 9—C and 10—C which is reflected in the degree of conjugation of the implied enamino groups. Further discussion on that point follows. One double-bond weakly polarized is left not comprised in the partial structures described above. This can be assigned to the junction double-bond between 5a—C and 10a—C. The weak polarization is a result of the dienamino ketone structure as represented by **7 B**. In accordance with the exposed considerations the chemical shift assignments are shown in Fig. 2. The conformation of the phenyl groups has also been taken into account, only one of the two phenyl groups being more or less coplanar to the adjacent double-bond and consequently more shielded excepting the carbon of junction. The data given by Jalander[6] in this respect were taken into consideration. Nevertheless the assignments for each of the two phenyl and carbethoxy groups are somewhat arbitrary but unessential for the structure determination.

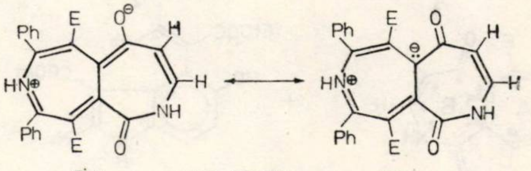

7A (E=COOEt) 7B

Mass spectrum. A preliminary examination of the mass spectrum indicates that all the peaks of major intensity correspond to fragments of a mass very close to the molecular ion. This may be considered as an additional evidence in favour of a fused cyclic system lacking chain substituents namely enamino ester groups in our case. The more significant transitions are represented by the elimination of two molecules of CO (Chart 2) to whom are corresponding the peaks m/z = 456 (base-peak) and m/z = 428 (13.5% intensity of the base-peak). The molecular ion peak, m/z 484 has an intensity of 13%. The fact is well known[10] that tropones and quinones readily eliminate CO in the mass spectrometer.

In our case the fragment ion m/z 456 corresponds to an α-pyridone (**9**). Pyridones in their turn are also characterized by elimination of CO with formation of the corresponding pyrroles.[11] From **9** will result the pyrrole **10**. The formation of a γ-pyridone in the first stage seems less probable since lactamic structures eliminate CO more difficultly than tropones and quinones.[12] Two other major peaks m/z 410 (36%) and 337 (40%) are likely to represent the radical ion **11** and the ion **12**. Two prominent ions at m/z 191 and 178 may be ascribed to fragments corresponding to iminophenanthrene (**13**) and phenanthrene, 10.5% and 11.5% of the base-peak respectively. This should be considered as evidence in favour of the existence of an iminodibenzyliden moiety in the structure of molecule **7**. The fragment ion **13** results from **10 A**, a valence tautomer of pyrrole **10**. The equilibrium between azepine and benzeneimine is known to occur.[13] A double cleavage of **10 A** accompanied by a double McLafferty rearrangement leads to **13**. A similar fragmentation pathway may explain the formation of the phenanthrene peak.

CHART 2

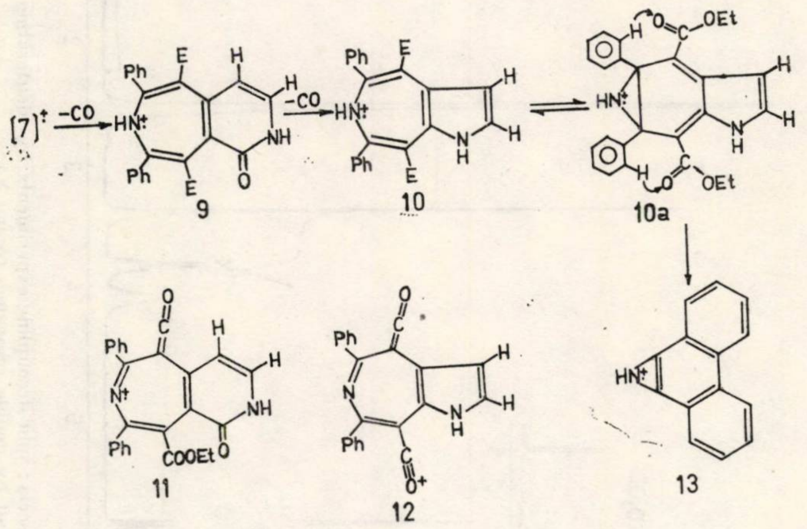

Discussion on the conformation of the diazaheptalenedione **7**. Literature data for heptalene,[14] cycloheptatriene[15] and azepine derivatives [16] indicate a boat conformation as being the most probable. It can be seen from the ^{1}H-NMR spectrum of **7** (Fig. 1) that one of the ester methylene groups is sterically hindered at 20°. The steric hindrance is no more observable at 39°. A boat or chair conformation of the cycle **A** symmetrical to a median plane passing through the 8-NH group could not explain this phenomenon. A puckered heptagon such as represented in Fig. 3 seemed to us to be suited to account for it. In the planar section of cycle **A** the phenyl group is strongly deviated from coplanarity while the ethoxycarbonyl group is sterically hindered between the adjacent phenyl

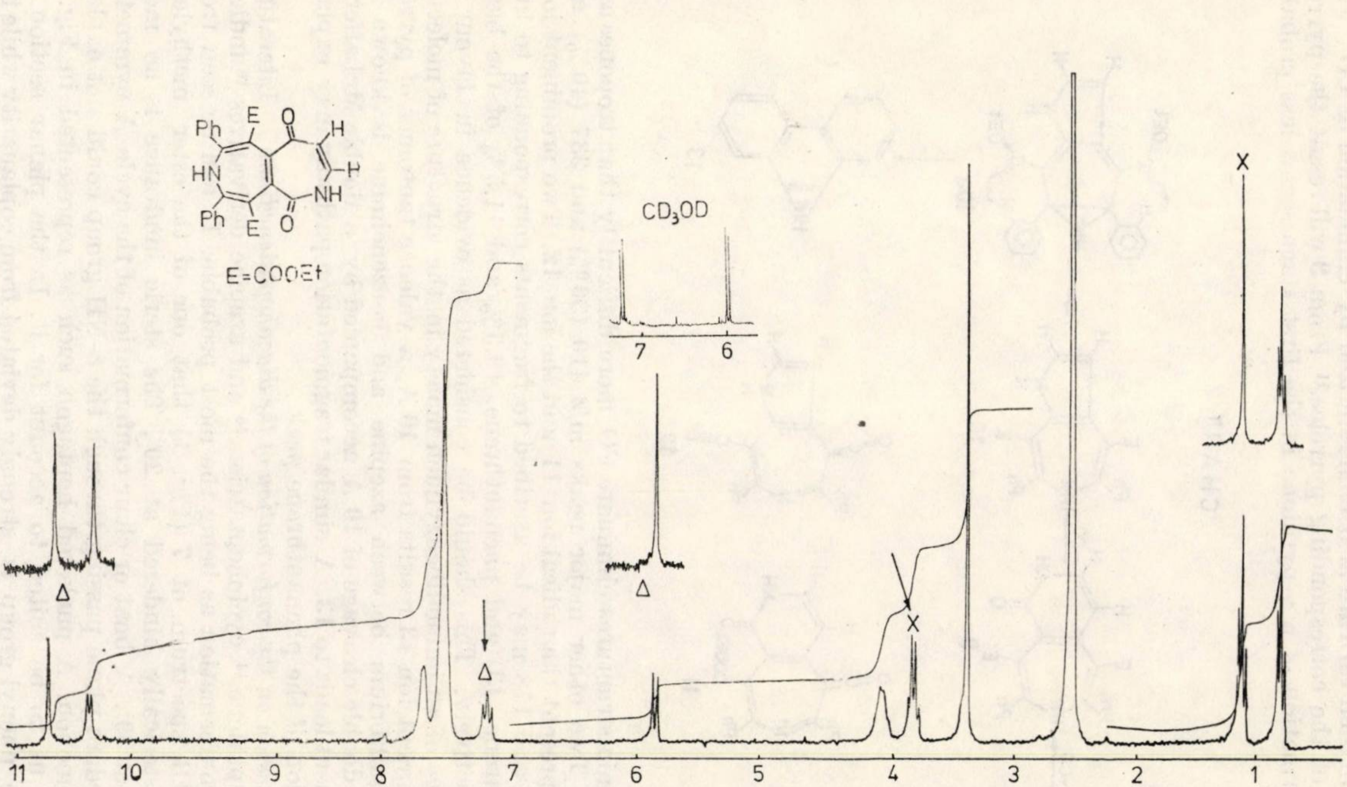

Fig. 1. — ^{1}H-NMR spectrum of **7** in DMSO$-d_6$ at 250 MHz. Inserts : spin decoupling experiments by deuteration of NH groups in CD$_3$OD (vinylic region) and by double resonance (Δ and X).

and the carbonyl group of the neighbouring cycle. The second phenyl and ethoxycarbonyl groups are grafted on the puckered section of cycle **A**. The 6-ethoxycarbonyl group is no more sterically hindered while the 7-phenyl group is at least partially conjugated to the adjacent cinnamic double bond. This could be deduced from the aromatic chemical shifts of the two phenyl groups protons. At 250 MHz (Fig. 1) only two protons are deshielded at δ 7.68 while the rest of the aromatic protons are included in a sole sharp band with traces of secondary splitting observable. As shown before the selection of the puckered cinnamic fragment has been made by examination of resonance possibilities (**7** ↔ **7A**). An extended conjugation is possible only for the region including atoms 8, 9, 10, 10a, 5a and 5, the alternative possibility being excluded by the lactamic group which does possess its own resonance. Therefore it may be inferred that 6–C and 7–C represent the puckered region. This part of the molecule will display no steric hindrance. According to this hypothesis the second ring **B** should adopt a twisted boat conformation which allows the dienaminocarbonylic extended conjugation.

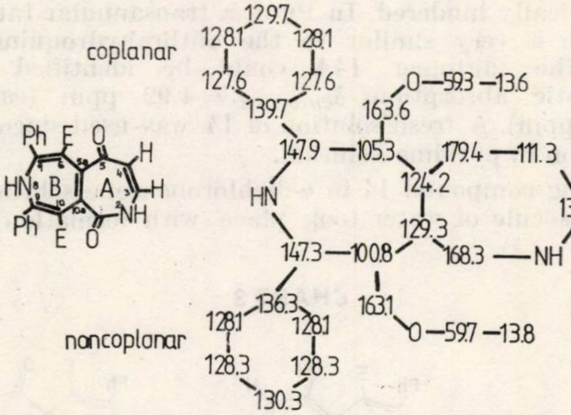
coplanar
129.7
128.1
128.1
127.6
127.6
139.7
163.6
O—59.3 —13.6
Ph
E
O
H
HN
B
A
H
NH
Ph
E
O
147.9 —105.3
179.4 —111.3
124.2
HN
139.1
129.3
147.3—100.8
168.3 —NH
136.3
163.1
128.1
128.1
O—59.7 —13.8
noncoplanar
128.3
128.3
130.3

Fig. 2. — ^{13}C-NMR chemical shift assignments for **7** (in DMSO$-d_6$).

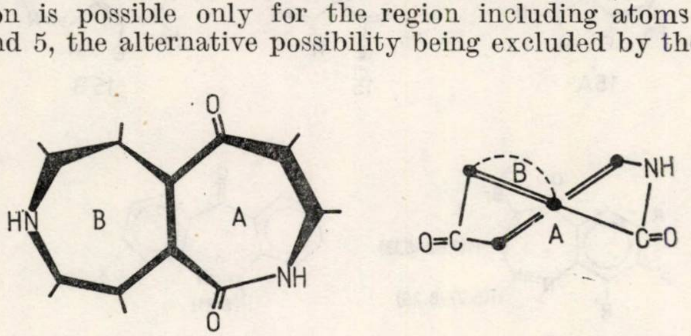
O
HN
B
A
NH
O
B
NH
O=C
A
C=O

Fig. 3. — Conformation of the diazaheptalenedione **7**.

Chemical properties. Formation of a 2,8-*diazaheptaleonne* (**15**). Diazaheptalenedione **7** could be reduced with Zn powder and acetic acid in hot dioxane solution when the corresponding dihydroderivative **14** did result (Chart 3). Its structure, a dihydrodihydroxydiazaheptalene, is in agreement with elementary analyses and the ^{1}H-NMR spectrum in DMSO-d_6. Owing to the double-bond modified arrangement the seven-membered rings become somewhat flatter and as a result both ester methylene groups are sterically hindered. In Py-d_5 a transannular tautomery can be observed which is very similar to the anthrahydroquinone-oxanthrone equilibrium. The tautomer **14A** could be identified by means of its characteristic absorption $\delta_{CH(OH)NH} = 4.92$ ppm (calculated after Shoolery 5.05 ppm). A fresh solution of **14** was used since decomposition occurs very soon in pyridine solution.

By heating compound **14** in *o*-dichlorobenzene solution the elimination of one molecule of water took place with formation of an azepino-

CHART 3

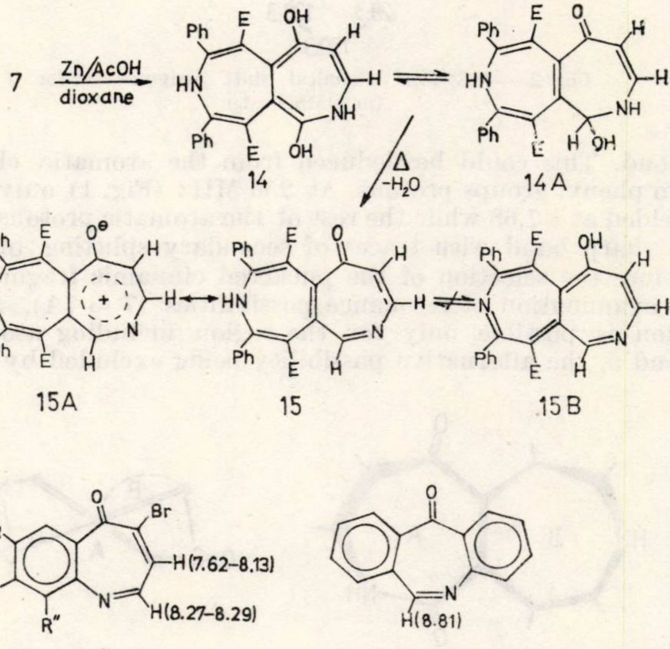
7
Zn/AcOH
dioxane
Ph
E
OH
H
HN
NH
14
14 A
Δ
-H₂O
O
O⁻
+
N
15A
15
15B

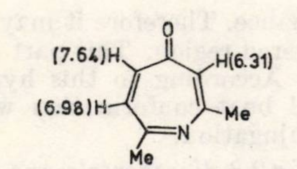
O
Br
R
R'
R''
N
H(7.62–8.13)
H(8.27–8.29)

16 (δ, ppm)

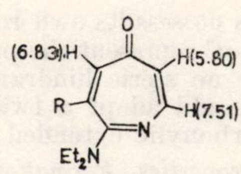

17 (δ, ppm)

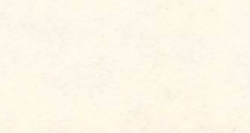
O
(7.64)H
H(6.31)
(6.98)H
Me
N
Me

18 (δ, ppm)

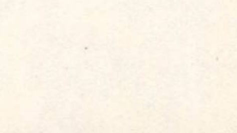
O
(6.83)H
H(5.80)
R
H(7.51)
N
Et₂N

19 (δ, ppm)

azatropone **15**, orange crystals with mp 160°. In comparison with **7** and **14** the NMR absorptions of the protons in **15** exhibit appreciably lower values, namely 8.23, 8.68, and 7.77 ppm for the protons 1, 3 and 4 respectively. At the same time a sensible decrease of the coupling constant, $J_{3,4} = 5.25$ Hz, takes place. This cannot be easily explained at the first sight. It is known from literature[17,18] that the position of ring protons in 4-azatropones remains well within the vinyl region and comparatively to the corresponding azepinediones no significant deshielding can be observed. Exceptions have been registered such as **16**[19] and **17**[17]. The authors of the latter example sustained that this could be explained alternatively either by conventional deshielding effects or by a ring current. However no coupling constants were available. Two other interesting examples are **18**[20] and **19**[21]. On the other hand both chemical shifts and coupling constant of **15** remind us of the pyridine ($J_{2,3} = 5.5$ Hz), the quinoline ($\delta_{2-H}=8.84$; $\delta_{3-H}=7.24$; $J_{2,3} = 5$ Hz) and generally the azines and their benzologues ($J_{2,3} = 4.1 - 6.0$ Hz). At the same time a comparison between the fixed double-bonds of tropone ($J_{2,3} = 12$ Hz) and the rapidly fluctuating double-bonds of tropolone ($J_{3,4} = 10.9$ Hz) does not show an appreciable decrease of the coupling constant. Taking into account the above facts the real structure of **15** should imply delocalized double-bonds as shown in **15A**. The presence of a diazaheptalene tautomer (**15B**) has not been observed on examination of the spectra. A structure of this type should be formed by enolization of **15** in alkaline medium. This will be further described.

A diazaheptalene dication (**20**). It was to be expected that by the addition of two protons to the two carbonyl groups of diazaheptalenedione **7** in strongly acidic media the formation of a dication should take place possessing the heptalene double-bond pattern. Actually while solutions of **7** in acetic or trifluoracetic acids display various shades of yellow or orange, in sulfuric acid solution the colour becomes blood-red. The UV-VIS spectrum exhibits a strong bathochromic shift accompanied by a hyperchromic effect. The long-wave maximum is shifted from 415 nm ($\log \varepsilon = 4.09$) to 566 nm ($\log \varepsilon = 4.28$). The ^{1}H-NMR spectrum of **7** in fluorosulfuric acid was measured at 250 MHz (Fig. 4). A general deshielding could be observed. The fluorosulfuric acid extracts from the ester groups the ethyl carbocation which is being transformed into ethyl fluorosulfate. Therefore the two methylene groups become isochronous as well as the two methyl groups. Their true chemical shifts can be observed in D_2SO_4 as distinct absorptions but the spectrum as a whole is much less clear. Another important feature is the lowering of the coupling constant $J_{3,4}$ from 9.5 Hz in **7** to 8.1 Hz in **20**. This can be interpreted as a lack of fixation of the double bonds as shown by the formulae **20A** and **20B**. Each of the two valence isomers displays a delocalization of the positive charges as represented by the resonance structures **20 C** and **20D** (Chart 4) and many others of the same type. The rapid fluctuation between **20 A** and **20 B** could allow a formulation of the dication on the NMR time scale as **20 E** which means delocalisation of the positive charges without aromatisation. As a matter of fact the delocalized double bonds in **15 A** led to an appreciably smaller coupling constant as it was shown before.

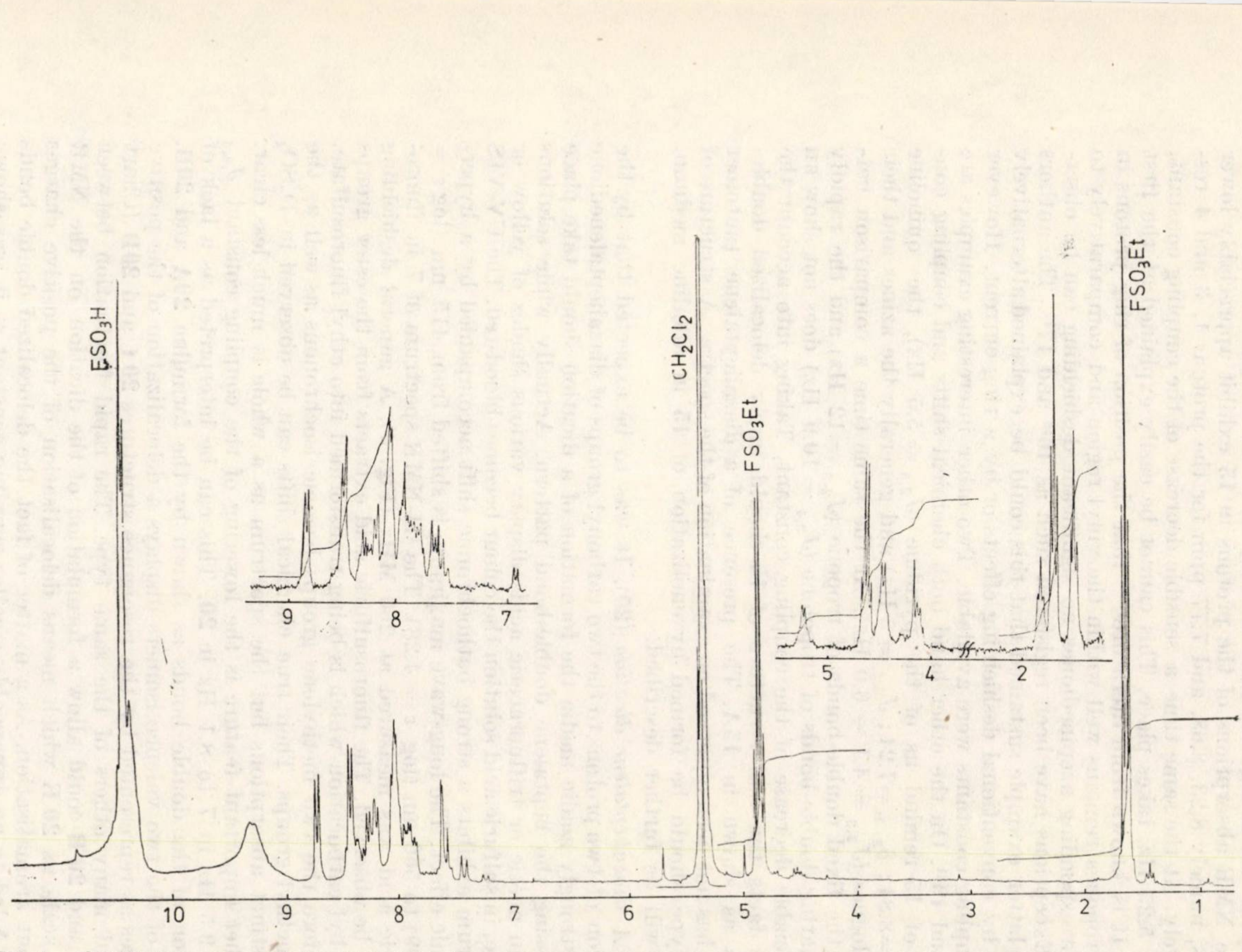

Fig. 4. — ^{1}H-NMR spectrum of **20** obtained by dissolving **7** in FSO_3H. Inserts: fragments of the same spectrum in D_2SO_4 where two distinct ethyl groups can be observed.

Discussion on a diazaheptalenolate anion (**21**). As mentioned earlier, by the enolization of the diazaheptalenone **15** in alkaline medium the formation of an enolate (**21**) was expected. A shielding of the molecule as a whole would ensue owing to the negative charge of the enolate and to the replacement of the double-bond delocalization in the azatropone nucleus by a rapid fluctuation of the double bonds such as is known to occur in heptalene. An examination of the UV-VIS spectrum of **21** showed the long-wave maximum to be shifted to 493 nm from 400 nm in **15**. This strong bathochromic effect was accompanied by a change of colour from light-orange to purple-red. Unexpectedly however the ^{1}H-NMR spectrum of the enolate **21** accounts for only small changes as compared to **15** (Table 3 – Experimental Part). A slight shielding of all the protons with one exception can be observed which is not accompanied by an increase of the coupling constant $J_{3,4}$ which remains practically unchanged. These data would suggest that no enolization takes place but instead the 8-NH group gives up a proton becoming negatively charged. The two adjacent cinnamic ester groups could account satisfactorily for the increase in acidity. This seems to exert only a slight influence on the azatropone ring, namely the distribution of the positive charge. The structure **21 A** would best represent these features. Minor contributions of resonance structures of type **21** are also implied if we take into account the fact that the bathochromic shift in the UV-VIS spectrum described above

CHART 4

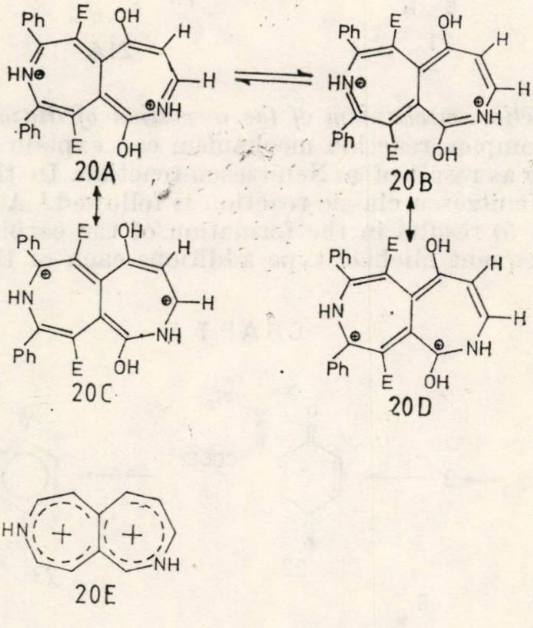

is accompanied by a hypsochromic effect which can be interpreted as a smaller probability of the corresponding transition.

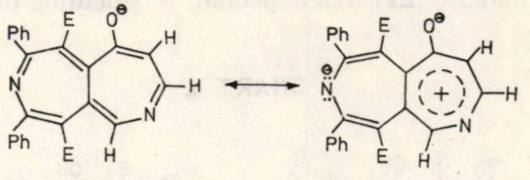
Ph
E
O⊖
H
N
H
N
Ph
E
H
Ph
E
O⊖
H
⊕N
+
H
N
Ph
E
H

21 21A

On the reaction mechanism of the formation of diazaheptalenedione **7**. Only a rather complex reaction mechanism can explain the formation of a diazaheptalene as result of a Nenitzescu reaction. In the first stage the scheme of the Nenitzescu classic reaction is followed.[1] A first sequence of reactions (Chart 5) results in the formation of the carbinolamine adduct **25** by two consequent Michael type additions each of them followed by

CHART 5

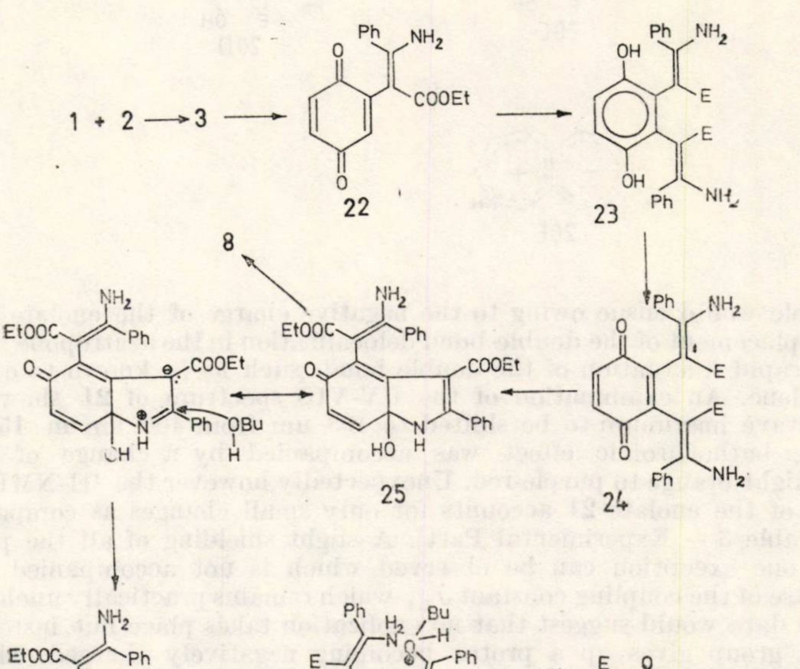
1 + 2 → 3 →
O
Ph
NH₂
COOEt
O
22
OH
Ph
NH₂
E
E
OH
Ph
NH₂
23
Ph
NH₂
O
E
E
O
Ph
NH₂
24
NH₂
EtOOC
Ph
COOEt
N
Ph
HO
H
25
8
NH₂
EtOOC
Ph
O
COOEt
N⊕
H
Ph
OBu
H
OH
NH₂
EtOOC
Ph
O
COOEt
-H₂O
Ph
N
OBu
H
HO
H
26
Ph
NH₂
Bu
O
H
Ph
E
O
E
OH
N
27
(E=COOEt)
Ph
E
O
H
H₂N⊕
N
Ph
E
OH
-H⊕
→7

the oxidation of the intermediate hydroquinone derivative (**3** and **23**) to the corresponding quinones **22** and **24** on the expense of the initial still unreacted quinone **1**. The occurrence of the *p*-disubstituted quinone **4** could not be observed althought it probably takes place also, but isolation is prevented by its instability in alcoholic solution*. Monocyclization of quinone **24** leads to the carbinolamine **25**. This type of compound has been foreseen[3] and subsequently experimentally certified[4,22] as an intermediate of the Nenitzescu reaction. At this point the specific role of the solvent does intervene. Only a small part of the carbinolamine **25** follows the established path of the Nenitzescu reaction and leads to the 4-substituted indole **8**. For the rest of **25**, its major part, a nucleophilic attack of the alcohol at 2-position makes possible the opening of the pyrroline cycle of **26** through the transfer of a hydride ion to unreacted quinone which turns into the hydroquinone anion. The result of these transformations is the formation of a nitrene intermediate **27** which undergoes a nucleophilic rearrangement 1,2 from carbon to nitrogen. A ring enlargement ensues with the formation of the azepinedione nucleus **B**. The elimination of the initial molecule of solvent by attack of the enamino nitrogen leads to a second ring-closure with formation of the azepine cycle **A**. The transfer of a proton to the previously formed hydroquinone anion gives the final heptalenedione **7**. The expansion of quinones by nitrene insertion is known especially in the case of the Schmidt reaction,[23] the reagent being hydrazoic acid in the presence of sulfuric acid.

Conclusion. No aza- and diazaheptalenes have been described in the literature up to the present. In the context of the antiaromatic chemistry[24] taking into account the lability of such compounds, the stabilizing influence of the nitrogen could open new research possibilities. Research is being continued to establish the scope of the reaction and to gain new insights on this new heterocyclic system.

EXPERIMENTAL PART

NMR spectra were recorded on Varian A 60-A and Bruker WM 250 instruments. UV-VIS spectra were determined with a Specord Carl Zeiss-Jena spectrometer and IR spectra with UR-20 Carl Zeiss-Jena and Perkin-Elmer 621 spectrometers. The mass spectrum was measured with a Varian MAT CH5 mass spectrometer.

Diethyl 1,5(2*H*,8*H*)-dioxo-7,9-diphenyl-2,8-diazaheptalene-6,10-dicarboxilate (7).

(A) *Solvent 1-butanol*. To a solution of 4 g (37 mmole) of benzoquinone in 60 mL of 1-butanol, 8.7 g (46 mmole; 8 mL) of ethyl 3-aminocinnamate (**2**) were added and the whole was refluxed for 20 min. when the red colour initially formed gradually disappeared. The solvent was removed *in vacuo* when **7** began to crystallize. The partially crystallized residue was treated with ether and left over night. After filtration and washing with ether 0.9 g of **7** were obtained, yellow crystals with mp 308° (dec.; Boetius microplate). The yield was 20% based on the quinone introduced in the reaction.

(B) *Other alcohols as solvents*. The same yield was obtained in propanol after refluxing for 45 min. In dry ethanol after refluxing for 2 hours the yield was 14% while in ethanol 96% it was lowered to 11% of impure product. After 4 hours of refluxing in methanol a yield of 12% was obtained.

When the reaction was carried out with stoichiometrical amounts of the reagents in butanol the yield fell to 10%.

---

* The UV-VIS spectrum of quinone **4** in alcoholic solution could not be registered because of its rapid alteration.

Molecular ion : $M^{+\bullet} = 484$. Found : C, 69.17 ; H, 5.12 ; N, 5.79. Calcd. for $C_{28}H_{24}N_2O_6$: C, 69.40 ; H, 5.00 ; N, 5.78. UV : λ_{max}^{EtOH} (log ε) = 410 (4.03), 268 (4.47), 224 nm (4.42) ; $\lambda_{max}^{H_2SO_4}$ (log ε) = 567 nm (4.28). IR ($CHCl_3$) : 3440 (NH), 3410 (NH), 1710 (CO ; vs ; broad with shoulders), 1620 cm^{-1} (vs ; broad with shoulder at 1640). ^1H-NMR (DMSO-d_6 ; at 60 MHz and 39° ; Fig. 1) : δ = 0.85 (t, 3H, CH_3), 1.15 (t, 3H, CH_3), 3.82 (q, 2H, OCH_2), 4.08 (q, 2H, OCH_2), 5.87 (d, 1H, 4−H), 7.20 (dd, 1H, 3-H), 7.53 (s, 10H, 2Ph), 10.25 (d, 1H, 2−NH), 10.58 (s, 1H, 8−NH) ; $J_{2,3} = 7$, $J_{3,4} = 9.5$ Hz ; (at 250 MHz and 20°) : 4.05 (broadened d, 2H, hindered OCH_2), 7.68 (broadened s, 2H, *o*-protons of one Ph), the remainder of chemical shifts unchanged) ; (FSO_3H at 250 MHz and 20°) : 7.63 − 8.48 (m, 10H, 2Ph), 8.41 (d, 1H, 4−H), 8.74 (d, 1H, 3−H), 9.31 (broadened d, 4H, 2 OH + 2NH) ; $J_{3,4} = 8.1$ Hz. ^{13}C-NMR (DMSO−d_6) : Fig. 2.

Ethyl Z-(2-amino-1-ethoxycarbonyl-2-phenylvinyl)-5-hydroxy-2-phenylindole-3-carboxylate (8). The filtrate from **7** was concentrated and a small amount of butanol was removed *in vacuo*. After cooling the residue was redissolved in ether and left to stay for several days when white crystals of **8** separated. After filtration and washing with ether 1.3 g were obtained, mp 211° (yield 15%). A small sample was recrystallized from alcohol, mp 219° (sealed capillary.).

Found : C, 71.23 ; H, 5.85 ; N, 5.86. Calcd. for $C_{28}H_{26}N_2O_5$: C, 71.47 ; H, 5.57 ; N, 5.95. UV : λ_{max}^{EtOH} (log ε) = 312 (4.04), 260 (3.91), 225 nm (4.12). IR ($CHCl_3$) : 3504 (OH), 3470 (NH), 3228 and 3165 (NH_2), 1712 (indole COOEt), 1670 cm^{-1} (enamino COOEt). ^1H-NMR (PhCN) : δ = 0.53 (t, 3H, CH_3), 0.80 (t, 3H, CH_3), 2.27 (s, 1H, OH), 3.67 (q, 2H, OCH_2), 3.98 (q, 2H, OCH_2), 8.47 (v. broadened, 2H, NH_2), 8.97 (s, 1H, NH) ; the solvent as internal standard ; (DMSO) : 6.65 (d, 1H, 6−H), 7.08 (d, 1H, 7−H), 7.03−7.70 (m, 13H, 2Ph + 7−H+ + NH_2), 8.08 (s, 1H, OH), 11.30 (s, 1H, NH) ; $J_{6,7} = 9$ Hz ; the solvent as internal standard.

Diethyl 2,8-dihydro-1,5-dihydroxy-7,9-diphenyl-2,8-diazaheptalene-6,10-dicarboxylate (14). In 120 mL of dioxane 1.5 g of **7** were dissolved by heating to the boiling point of the solvent. After complete dissolution occurred heating was interrupted and 5 min. later 7.5 mL of glacial acetic acid and 3 g of Zn powder were added with stirring. Almost immediately the yellow colour of the reaction mixture became very pale. Stirring was continued for 10 min after which time the consumed zinc was filtered and the filtrate concentrated *in vacuo* to a small volume. After cooling the concentrate was poured into 400 mL of distilled water. The separated precipitate after filtration and drying in a desiccator gave 1.2 g of impure product. By stirring it in 550 mL of ethanol for several hours and subsequent filtration and drying 0.75 g of **14** resulted, mp 200° (dec. ; in sealed capillary). Yield 50 %. A small sample was recrystallized from DMSO and after washing with acetone and ether the dried substance had a mp of 216° (dec.).

Found : C, 69.20 ; H, 5.66 ; N, 5.75. Calcd. for $C_{28}H_{26}N_2O_6$: C, 69.12 ; H, 5.38 ; N, 5.76. UV : λ_{max}^{EtOH} (log ε) = 303 (4.15 ;sh), 263 (4.38), 230 nm (4.48 ; sh) ; the UV spectrum corresponds to the carbinolamine tautomer. IR (KBr) : 3270 (OH), 3210 (NH), 3110 (NH), 1705 (CO ; broad), 1638 cm^{-1} (broad with sh at 1610). ^1H-NMR (DMSO-d_6) : δ = 0.58 (t, 3H, CH_3), 1.08 (t, 3H, CH_3), 3.64 (q-secondary splitting, 2H, OCH_2), 3.85 (q-secondary splitting, 2H, OCH_2), 5.62 (d, 1H, 4−H), 7.12 (d, 1H, 3−H), 7.50 (s, 10H, 2Ph), 10.10 (d, 1H, 2−NH), 10.57 (s, 1H, 8−NH) ; $J_{3,4} = 9.5$ Hz and $J_{2,3} = 7$ Hz ; the spectrum corresponds to the dihydroheptalenediol tautomer ; (Py−d_5) : δ = 4.93 (s, 1H, 1−H of the carbinolamine tautomer), 4.94 (d, 1H, 4−H), 6.22 (d, 1H, 3−H), 11.36 (d, 1H, 2−NH), 12.08 (s, 1H, 8−NH) ; $J_{2,3} = 7$ Hz and $J_{3,4} = 9$ Hz.

Diethyl 5(8H)-oxo-7,9-diphenyl-2,8-diazaheptalene-6,10-dicarboxylate (15). Without any further purification 0.75 g of compound **14** were introduced into 15 mL of *o*-dichlorobenzene and the suspension was heated with stirring up to 165−170° when dissolution occurred with the appearance of a strong yellow colour. The solvent was removed *in vacuo* and the residue which crystallized on cooling was redissolved in ether. By concentration of the ether solution 0.35 g of **15** were obtained, orange crystals with mp 160°, yield 48%.

Found : C, 71.51 ; H, 5.26 ; N, 5.94. Calcd. for $C_{28}H_{24}N_2O_5$: C, 71.78 ; H 5.16 ; N, 5.98. UV : λ_{max}^{EtOH} (log ε) = 403 (3.88), 268 (4.38), 207 nm (4.59) ; K^+ enolate$^-$: λ_{max}^{EtOH} (log ε) = = 496 (3.61), 302 (4.35), 248 nm (4.39). IR (CCl_4) : 3453 (NH), 1710 (CO ; broad with shouders), 1630 cm^{-1} (m ; tentatively assigned to azatropone−CO). ^1H-NMR at 60 MHz ($CDCl_3$) : δ = 1.00 (t, 3H, CH_3), 1.15 (t, 3H, CH_3), 4.14 (q, 2H, OCH_2), 4.19 (q, 2H, OCH_2), 7.50 (m, 10H, 2Ph), 7.77 (d, 1H, 4−H), 8.23 (s, 1H, 1−H), 8.68 (d, 1H, 3−H), 9.52 (s, 1H, 8−NH) ; $J_{3,4} = 5.25$ Hz.

Table 3

^{1}H-NMR chemical shifts at 250 MHz in CD_3OD

	CH_3		OCH_2		4–H(d)	1–H(s)	3–H(d)
15	1.02	1.10	4.11	4.12	7.85	8.12	8.63
K$^+$ enolate$^-$ (**21**)	0.98	1.08	4.01	4.11	8.07	7.84	8.54
			Ph(m)				
15	—		7.49	(6H)	7.57	(4 *o*-H)	
K$^+$ enolate$^-$ (**21**)	7.37	(3H)	7.49	(3H)	7.56	(4 *o*-H)	

ACKNOWLEDGEMENT. We thank Prof. Gerhardt Schröder of the Karlsruhe University for making possible and dr. H. Röttele of the same University for carrying out the ^{13}C-NMR spectrum, the ^{1}H-NMR spectra at 250 MHz and a mass spectrum. We also thank dr. M. Elian for helpful suggestions. Performance of UV-VIS and ^{1}H-NMR at 60 MHz spectra by dr. F. Chiraleu and elemental microanalyses by Miss Elvira Sliam is kindly acknowledged.

REFERENCES

[1] D. Răileanu, M. Palaghiță and C.D. Nenitzescu, *Tetrahedron*, **27**, 5031 (1971).
[2] D. Răileanu and C.D. Nenitzescu, *Rev. Roumaine Chim.*, **10**, 339 (1965).
[3] C.D. Nenitzescu, *Bul. Soc. Chim. Romania*, **11**, 37 (1929).
[4] U. Kuckländer, *Tetrahedron*, **29**, 921 (1973).
[5] E.Kleinpeter and R. Borsdorf, "^{13}C-NMR Spektroscopie in der organischen Chemie", Akademie Verlag, Berlin, 1981, pp. 115 and 125.
[6] L. Jalander, *Finn. Chem. Letters*, **1982**, 49.
[7] V. Vögele and A. von Philipsborn, *Org. Magn. Reson.*, **5**, 551 (1973); C.J. Turner and G.U.H. Cheesman, *ibid.*, **6**, 663 (1974); W.J. Still and N. Plavac, *Canad. J. Chem.*, **54**, 284 (1976).
[8] E. Kleinpeter and M. Pulst, *J. prakt. Chem.*, **322**, 575 (1980).
[9] Y.L. Chen, P.S. Mariano, G.M. Little, D.O'Brien and P.L. Huermann, *J. Org. Chem.* **46**, 4651 (1981).
[10] J.H. Beynon and A.E. Williams, *J. Appl. Spectroscopy*, **14**, 156 (1960); J.M. Wilson, M. Ohashi, H. Budzikiewicz, C. Djerassi, Sho Ito and T. Nozoe, *Tetrahedron*, **19**, 2247 (1963; G. Spitteler, "Massenspektrometrische Strukturanalyse organischer Verbindungen", Verlag Chemie, Weinheim, 1966, p. 272.
[11] G. Spiteller and M. Spiteller-Friedmann, *Monats. Chem.*, **93** 1395 (1962); G. Spiteller, *loc. cit.* ref. 10, p. 177.
[12] N. Nenner-Jehle, Dissertation, Göttingen University, 1966; G. Spiteller, *loc. cit.* ref. 10, p. 272.
[13] H. Prinzbach, H. Babsch, H. Fritz and P. Hug, *Tetrahedron Letters*, **1977**, 1355.
[14] H.J. Lindner, and B. Kitshke, *Angew. Chem.*, **88**, 123 (1976); J. Stegemann and H.J. Lindner, *Tetrahedron Letters*, **1977**, 2515; L.A. Paquette, *Israel J. Chem.*, **20**, 233 (1980).
[15] H. Günther, M. Görlitz and H. Meisenheimer, *Org. Magn. Reson.*, **6**, 388 (1974).
[16] L.A. Paquette, "Azepines, Oxepines and Thiepines", *Nonbenzenoid Aromatics*, Vol. 1 (ed. J.P. Snyder), Academic Press, New-York, 1969, p. 249.
[17] E. Moriconi and I. Maniscalco, *J. Org. Chem.*, **37**, 208 (1972).
[18] F. Pietra, *Chem. Rev.*, **73**, 293 (1973).
[19] A. Cromarty and G.R. Proctor, *J. Chem. Soc.*, *Perkin Trans. 1*, **1972**, 2012.
[20] E. Bullock, B. Gregory and A.W. Johnson, *J. Amer. Chem. Soc.*, **84**, 2260 (1962).
[21] R. Sundberg, S. Suter and M. Brenner, *J. Amer. Chem. Soc.*, **94**, 513 (1972).
[22] U. Kuckländer, *Tetrahedron*, **28**, 5251 (1972).
[23] D. Misiti, H. Moore and R. Folkers, *Tetrahedron Letters*, **1965**, 1071; R. Richards and R. Smith, *Tetrahedron Letters*, **1966**, 2361; G.R. Bedford, G. Jones and B.R. Webster, *Tetrahedron Letters*, **1966**, 2367.

Revue Roumaine de Chimie, **33**, *11–12*, 969–974 (1988)

SOME NEW COPPER(II) BROMCCOMPLEX COMPOUNDS WITH IMIDAZOLE DERIVATIVES

FLORICA ZALARU, AURELIA MEGHEA, D. IONESCU and
FELICIA CORNEA
Polytechnic Institute, Department of Chemical Technology,
Bucharest, Romania

Received September 21, 1987

The present paper reports the synthesis and characterization of several new complex compounds of Cu(II) with imidazole derivatives : 5-nitro-1H-imidazolyl-4-carboxamide (A) and N-substituted 5-nitro-1H-imidazolyl-4-carboxamide (B). The donor atoms and the possible geometries for the new complex compounds were assigned on the basis of electronic, ESR and IR spectra, correlated with the chemical composition.

Imidazole is of peculiar importance as a ligand because it makes possible for biologically active natural organic compounds – in whose molecule it occurs – to coordinate metallic ions. It is very useful to know the behaviour of imidazole and of some of its derivatives both for the explanation of the role played by the metallic ions, the way in which they interact with different organic compounds, and for their effect on the electronic distribution in ligand.

Our investigation followed the influence of the bromide anion and of the reaction medium on the coordination possibilities of imidazole derivatives of the type :

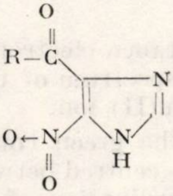

where R = $-NH_2$(A) ; $-NHCH_2COOC_2H_5$(B) in interaction with $CuBr_2$. Analysis of the interaction of the same ligands with $CuCl_2$ led to further researches.[1]

RESULTS AND DISCUSSION

Syntheses were carried out in a molar ratio $CuBr_2 : L = 1 : 1$ using the mixture ethanol : water = 10 : 1 as a reaction medium. Under these conditions, for ligands A and B, the green compounds resulted are formulated on the basis of the elemental chemical analysis : CuABr and CuBBr. The use of other molar ratios (Cu : L = 1 : 2 and 1 : 4) led to the separation of the same compounds.

Table 1

Results of the elemental chemical analysis

Molar ratio Cu : L	Ethanol-water	Compound	Cu% $\frac{F}{C}$	Br% $\frac{F}{C}$	N% $\frac{F}{C}$
1 : 1	10 : 1	CuABr (green)	$\frac{21.70}{21.33}$	$\frac{26.10}{26.26}$	$\frac{19.21}{18.66}$
		CuBBr(green)	$\frac{15.68}{16.48}$	$\frac{20.35}{20.75}$	$\frac{14.90}{14.50}$
	1 : 1	$CuA_2 \cdot 2H_2O$ (blue)	$\frac{15.11}{15.43}$	—	$\frac{30.42}{29.82}$

A = Ligand for R = $-NH_2$; B = Ligand for R = $-NHCH_2COOC_2H_5$

F = found ; C = calcd.

When the mixture ethanol : water = 1 : 1 was used as a reaction medium, a blue compound – formulated $CuA_2 \cdot 2H_2O$ – resulted only from the interaction of ligand A with $CuBr_2$. The same compound, $CuA_2 \cdot 2H_2O$, was formed by transforming compounds CuABr in the presence of water, slowly in the cold, and faster in hot solutions.

$$\underset{\text{green}}{2CuABr} \xrightarrow{+2H_2O} \underset{\text{blue}}{CuA_2 \cdot 2H_2O} + CuBr_2$$

Electronic spectra. Reflectance electronic spectra of the green compounds are different from the spectrum of the blue compound suggesting different geometries for the Cu(II) ion.

Thus, the spectrum of the green compounds CuABr and CuBBr shows a broad band with λ_{max} centred between 760 and 780 nm that can be associated with a pentacoordination of the Cu(II) ion. [2-6]

The electronic spectrum of the blue compound $CuA_2 \cdot 2H_2O$ has a shoulder at $\lambda \simeq 600$ nm and two peaks $\lambda_{max} = 660$ nm and $\lambda_{max} = 700$ nm. Such a spectrum is compatible with the hexacoordinated Cu(II) ion with a geometry of distorted tetragonal octahedron. [2-5]

ESR spectra. The green compounds do not show a detectable ESR signal, their diamagnetism being probably the result of an intense spin coupling specific to dimere structures.

For the blue compound $CuA_2 \cdot 2H_2O$, an intense ESR signal is obtained characteristic of a monomeric species of Cu(II), with a third order anisotropy for the factor $g(g_1 = 2.2214,\ g_2 = 2.1123,\ g_3 = 2.0669)$. This anisotropy is compatible with Cu(II) in a rhombic distorted geometry, elongated axially.[2,6] The ESR spectrum confirms the geometry of the distorted octahedron appreciated in the reflectance electronic spectra of this compound.

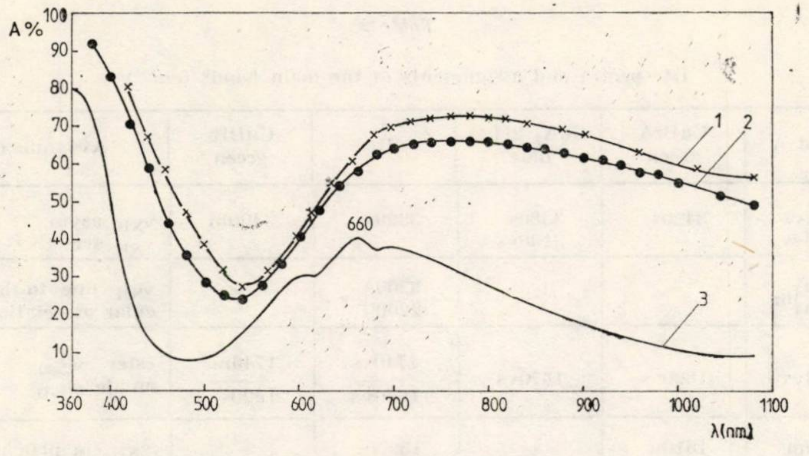

Fig. 1. — Electronic reflectance spectra : ———— $\text{CuA}_2 \cdot 2\text{H}_2\text{O}$; x—x—x—x CuABr ; — . — . — . CuBBr.

IR spectra. Comparison of the IR spectra of the green and blue compounds with the spectra of the free ligands shows the same changes, suggesting coordination by the same donor atoms. Thus, the disappearance of the ν_{NH} band, characteristic of the intermolecularly associated imidazole $(3100 - 2100\ \text{cm}^{-1})$ and the existence of only one band within the ν_{NH} range $(3500 - 3000\ \text{cm}^{-1})$ showing the presence of a

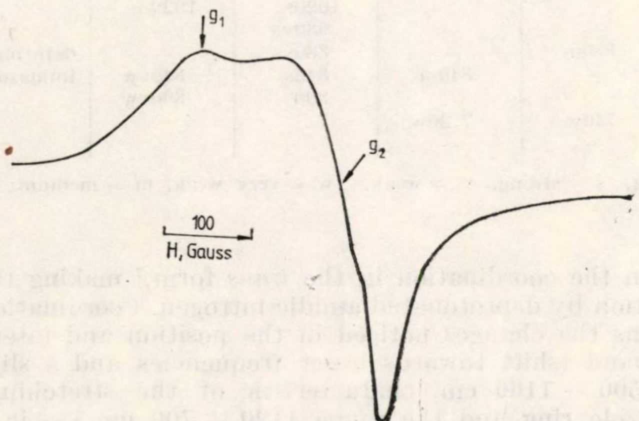

Fig. 2. — ESR spectra for $\text{CuA}_2 \cdot 2\text{H}_2\text{O}$ compound

secondary amide, are noticed. These changes could suggest that the amide group takes part in coordination by substituting a hydrogen atom.

The disappearance of the characteristic δ_{NH_2} band, in the IR spectrum of the CuBBr compound suggests that the secondary amide might participate in the coordination in the *trans* form,[7] making thus possible the coordination by deprotonated amidic nitrogen. Coordination by amide group explains the changes noticed in the position and intensity of the $\nu_{C=O}$ amide band (shift towards lower frequencies and a slight width). The range 1500 – 1100 cm, characteristic of the stretching vibration of the imidazole ring and the range 1120 – 700 cm^{-1} – in which the bands due to the deformation of the imidazole ring appear – are strongly modified.[8] These changes show the participation in coordination of the N(3) atom of the imidazole ring, as the ligands have a bidentate action.

Table 2

IR spectra and assignments of the main bands (cm^{-1})

Ligand A	CuBrA green	$CuA_2 \cdot 2H_2O$ blue	B	CuBBr green	Assignments
3420vs	3420s	3380s	3390s	3400m	ν_{NH} asym
3180vs	—	3100vs			ν_{NH} sym.
3200 2200 } br	—		3200 2200 } br	—	ν_{NH} due to the molecular associations
1700vs	1690vs	1670vs	1740vs	1740m	ester $\nu_{C=O}$
			1670vs	1620s	amide $\nu_{C=O}$
1620m	1610w	—	1590m	—	δ_{NH_2} in plan
1530vs	1535s	1500s	1530vs	1510	ν_{NO_2} asym
1480 1450 }	1500s	1450	1480 1460 } vs	1470s	
			1400		
1380vs	1400s	1380s	1380s	1380m	ν_{NO_2} sym
1340m			1340		
1310m	1300s		1302		
1280vs		1280vs	1235vs	1200m	ν imidazole cycle
1230	—	—			
1180vs	1120s	1100s	1100s	1110s	
			1020s	1020m	
980s	—	—	980vs	—	
880s	880m	—	880vs	—	deformation of the
840m	—	840m	840s	840vw	imidazole cycle
			800	800vw	
780m	740w	7.20w			
700m	—	—			

vs – very strong, s = strong, w = weak, vw = very weak, m = medium; sh = shoulder, br = broad.

Analysis of the IR spectra shows the same donor atoms : the atom of amidic nitrogen by deprotonation and the atom of imidazole nitrogen N_3, by varied geometries, as a function of the chemical composition of compounds : hexacoordinated for the blue compound $CuA_2 \cdot 2H_2O$ and possibly pentacoordinated in a square pyramid geometry for the green compounds CuABr and CuBBr (Fig. 3).

EXPERIMENTAL

$CuBr_2$ p.a. was used and ligands prepared according to indications in the literature[9]. Molar ratio Cu : L = 1 :1 in ethanol-water medium = 10 : 1 and 1 : 1. The compounds obtained were separated by filtration under vacuum, washed with small quantities of ethanol-water and dried at room temperature.

CuABr separates as a gelatinous green precipitate, which by drying at room temperature changes into a compact green mass. This compound turns blue in the presence of water and it has the same composition as the CuA_2 $2H_2O$ blue compound separated in ethanol-water medium = 1 : 1.

CuBBr. By adding the ethanolic solution to the ligand solution, separates a gelatinous green precipitate, which by drying at room temperature changes into a compact green mass.

Copper was determined gravimetrically after breakdown of the complex with H_2O_2 and concentrated H_2SO_4. Bromine was determined gravimetrically. Diffuse reflectance spectra were obtained with a VSU_2 Zeiss-Jena spectrophotometer within the 400 — 1000 nm range in dilution with MgO at a compound/Mg ratio of 1 : 2.

The IR spectra were recorded in the region 700 — 4000 cm^{-1} on a Specord 71 spectrophotometer. Samples were mounted in potassium bromide disks. ESR spectra were recorded at room temperature on polycrystalline powders, with an ART-5-IFA spectrograph. The klystron frequency was 9060 MHz and the modulation of the magnetic field was 100 kL/s ESR parameters were calculated versus Mn(II) standards.

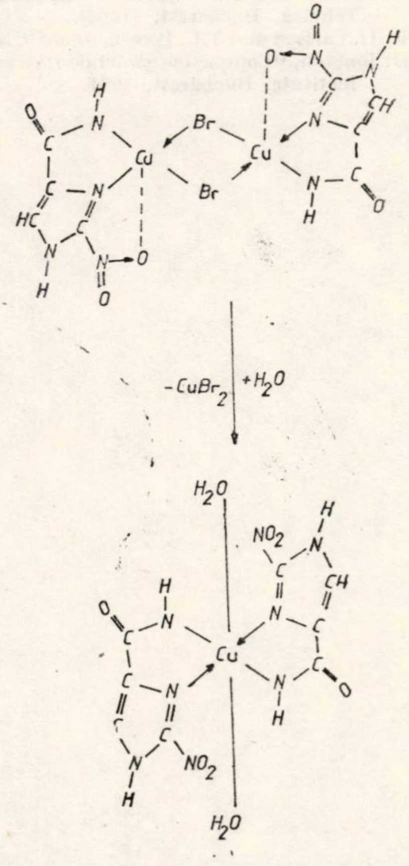

Fig. 3. — Structural formula proposed for CuABr and $CuA_2 \cdot 2H_2O$ compounds.

CONCLUSIONS

The presence of the bromide anion determined the obtention, with the same ligands, of other types of compounds than in the case of $CuCl_2$ interaction.[1]

The influence of the reaction medium on the type of compounds was evidenced.

REFERENCES

[1] A. Meghea, F. Zălaru and D. Ionescu, *Rev. Roumaine Chim.*, **30**, 297 (1985).

[2] B. J. Hathaway and D. E. Billing, *Coord. Chem. Rev.*, **5**, 143 (1970).

[3] B. J. Hathaway, *J. Chem. Soc. A*, **1972**, 1196.

[4] B. J. Hathaway, I. M. Procter, R. C. Slade and A.A.G. Tomlinson, *J. Chem. Soc. A.*, **1969**, 2219.

[5] E. D. Mc Kenzie, *J. Chem. Soc. A*, **1970**, 3095 .

[6] B. J. Hathaway, Structure and Bonding, 57, 56 (1984), Springer-Verlag, Berlin Heidelberg.

[7] M. Avram and Gh. Mateescu, "Spectropia in infraroşu. Aplicaţii in chimia organică," Ed. Tehnică, Bucharest, (1966).

[8] R. H. Carlson and T.L. Brown, *Inorg. Chem.*, **5**, 268 (1966).

D. Ionescu, "Compuşi organici de sinteză cu acţiune biologică", Doctoral Thesis, Polytechnic Institute, Bucharest, 1981.

Revue Roumaine de Chimie, **33**, *11–12*, 975–979(1988)

HETEROCYCLENSYNTHESEN MIT KOHLENSÄUREDERIVATEN. XI[1]

UMSETZUNG VON *o*-FORMILARYLCYANATEN MIT NH-HETEROCYCLEN ZU BENZOXAZINVERBINDUNGEN

HANS-HORST GLATT, CAROL CSUNDERLIK, INGRID GLATT, HORIA DULVAC
und VICTORIA SCOROBETE
Technische Hochschule „Traian Vuia“ Timişoara, Laboratorium für Organische
Chemie, str. Bocşa 6, 1900 Timişoara, S. R. Rumänien

Eingegangen am 21. November 1987

o-Formilarylcyanate lassen sich mit NH-haltigen Heterocyclen, wie z.B. Benz (ox,-imid-, thi-) azolin-2-thionen. Aminobenzimidazolen. Triazolen, Tetrazolen. Thiazolen zu den entsprechenden Benzoxazin-Derivaten umsetzen. Die erhaltenen Produkte, von denen 12 neu sind, wurden durch Schmelzpunkt, IR- aund ^{1}H-NMR-Spektroskopie und Elementaranalyse charakterisiert.

o-Formyl-arylcyanates react with NH containing heterocycles, e.g. benz (ox-, imid- thi-) azolin-2-thiones, aminobenzimidazoles, triazoles, tetrazoles, thiatriazoles forming benzoxazines. The products from which 12 are new compounds were caracterized by their melting points, IR- and ^{1}H-NMR-spectra and elemental analyses.

EINLEITUNG

Die Reaktionen der Arylcyanate mit Nucleophilen sind vielfach zur Synthese heterocyclischer Verbindungen eingesetzt worden.[2] Werden als Reaktionspartner Dinucleophile benützt, so können direkt Heterocyclen entstehen (siehe z.B. [3–7]). Werden jedoch Mononucleophile benützt, so müssen die vorerst acyclischen Additionsprodukte mit einem passenden elektrophilen Reaktionspartner cyclisiert werden.[2] Sind jedoch im Arylcyanatmolekül von vornhinein auch elektrophile Gruppen eingebaut, so können diese in die Reaktion eingreifen und zu Heterocyclen führen. Letztere anziehende synthetische Möglichkeit wurde bisher nur für die Reaktionen der Nucleophile mit aromatischen Cyansäureester mit *ortho*-ständiger Carbonsäureestergruppe ausgebeutet [2,8]. In der vorliegenden Arbeit haben wir die Reaktionen von *o*-Formilarylcyanaten mit NH-haltigen Heterocyclen untersucht.

ERGEBNISSE UND DISKUSSION

In einer vorangehenden Arbeit [9] konnten wir zeigen, dass die Behandlung von Benzoxazolin-2-thion **2a** mit *o*-Formilphenylcyanat **1A** nicht zu dem erwarteten Benzoxazolin-thion-N-imidsäureester[10] führt, sondern das 4-Hydroxy-2-[1′-(benzoxazolinyl-2′-thion)]-4H-1,3-benzoxazin **3aA** (R = H, X = 0) entsteht.

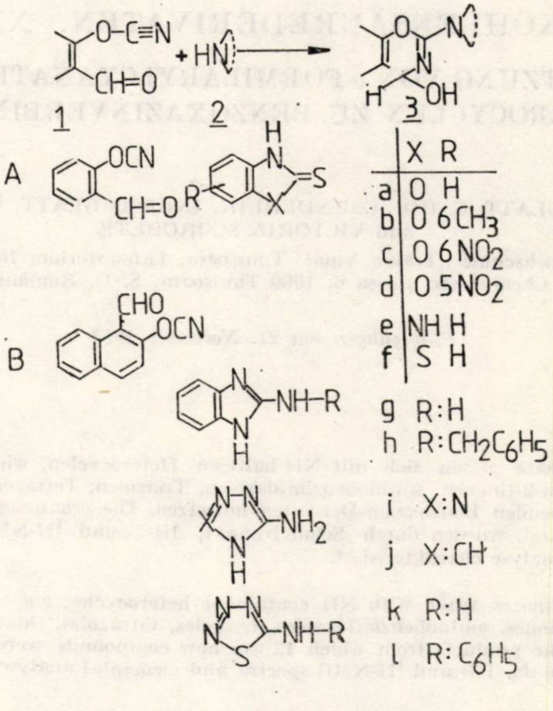

Diese Reaktion kann auch mit anderen NH-haltigen Azolen ausgeführt werden, wobei sich stets die entsprechenden Benzoxazinderivate *3* bilden. Im Versuchsteil sind die dargestellten Produkte aufgezählt, wobei **3Ab** — **3Al** und **3Ba** noch nicht beschriebene Verbindungen sind. Die Struktur der Benzoxazine **3** wurde durch Elemetaranalyse sowie IR- und ^{1}H-NMR-spektroskopisch sichergestellt.

In den IR-Spektren lassen sich die relativ breiten Banden bei 3170 — —3370 cm^{-1} der Valenzschwingung der HO-Gruppe zuordnen. Auch verschwindet die IR-Bande von 1690 cm^{-1} ($\nu_{C=O}$ aus dem Cyansäureester **1**) und in diesem Bereich erscheint eine der C=N-Gruppe zuzuschreibende Absorptionsbande im 1640 —1710 cm^{-1}-Bereich. Im Falle der Verbindung **3Af** wurde der zeitliche Ablauf der Synthese sogar IR-spektroskopisch verfolgt. Nach dem innigen Vermischen zum Zeitpunkt Null der Reaktion, von zwei Lösungen von **1A** (0.12 M/kg) und **2f** (0.12 M/kg) in Dioxan bei 40°C wurde die Extinktion-Zeit Änderung der OCN-Bande (**1A**ν_{OCN} 2250 cm^{-1}), der CHO-Bande ($\nu_{C=O}$in **1A** 1690 cm^{-1}) und der C=N-Bande ($\nu_{C=N}$ 1660 cm^{-1} in **3Af**) untersucht. Es konnte festgestellt werden, dass die Extinktionen der Absorptionsbanden ν_{OCN} und $\nu_{CH=O}$ gleichzeitig abnehmen-wobei sofort die Produktbande ($\nu_{C=N}$) erscheint. Die letztere Bande gewinnt so lange an Intensität bis im Reaktionsgemisch *o*-Formilphenylcyanat 1A vorliegt. Am Ende der Reaktion verschwinden die Banden des Cyansäureesters (ν_{OCN}, ν_{CHO}) gleichzeitig.

In den ^{1}H-NMR-Spektren lassen sich nebst den aromatischen Protonen, jene der CH-OH Gruppe des Benzoxazins **3** erkennen. So erscheint das mit dem Hydroxyl-Gruppen-Proton gekoppelte CH-Proton bei einer chemischen Verschiebung von 5.7 –5.9 ppm als Dublett, das durch Behandlung mit D_2O in ein Singulett übergeht. Das HO-Proton erscheint um 6,7 –6,8 ppm auch als Dublett, das jedoch nach der D_2O-Behandlung gänzlich verschwindet.

Diese Umsetzungen der *o*-Formilarylcyanate mit NH-haltigen Azolen weichen im allgemeinen von den bekannten Reaktionen einfacher aromatischer Cyansäureester mit solchen heterocyclischen Amin-Systemen ab.

So ist für die Reaktion des Benzimidazolin-2-thions (**2e**) mit Arylcyanaten in [11,12] angegeben, dass sich die entsprechenden 3-Aroxy-benzimidazolo[1.2-d](1.2.4) thiadiazoline bilden. Wird jedoch als Arylcyanat **1A** verwendet, so wird das in [11] als Isoharnstoff formulierte schwer isolierbare Zwischenprodukt als Benzoxazin-Derivat **3Ae** abgefangen. Diese Abweichreaktion untermauert den in [11] formulierten Mechanismus der Reaktion von Arylcyanaten mit 2**e**.

2-Thion-benzothiazolin (**2f**) reagiert laut [10] mit Arylcyanaten zu Bis-benzothiazolyl-disulfid. Wir fanden jedoch, dass auch in diesem Falle mit **1A** eine vom obigen Schema abweichende Reaktion zum Benzoxazin-Derivat **3Af** stattfindet.

Mit 2-Aminobenzimidazol **2g**, das sich bekanntlich mit Arylcyanaten am endo-cyclisch-ständigen N-Atom zu dem entsprechenden N-Imidsäureester acyliert [13–15] bildet 1A das entsprechende **3Ag**. Zu dem selben Benzoxazin-Derivat gelangt man auch durch die Umsetzung von zwei Mol 1A mit einen Mol *o*-Phenylendiamin :

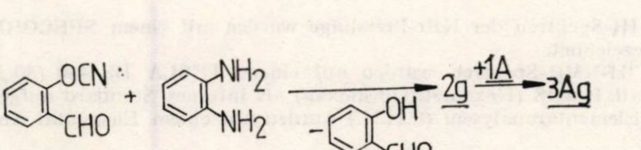

Auch andere Aminoazole (**2i**, **2j**) reagieren am endocyclischen N-Atom zu **3i** bzw. **3j** unter Beibehaltung der primären Aminogruppe.

Im Falle des 5-Amino-1.2.3.4-thiatriazols 2k, das selbst im Kalten mit Arylcyanaten unter N -Entwicklung zu den entsprechenden Thiadiazolen reagiert [16 17] entsteht mit **1A** ebenfalls unter N_2-Bildung ein 2 : 1-

Addukt, dessen Struktur anhand der spektroskopischen Befunde nur als Bis-benzoxazin-derivat **3Ak** auslegbar ist:

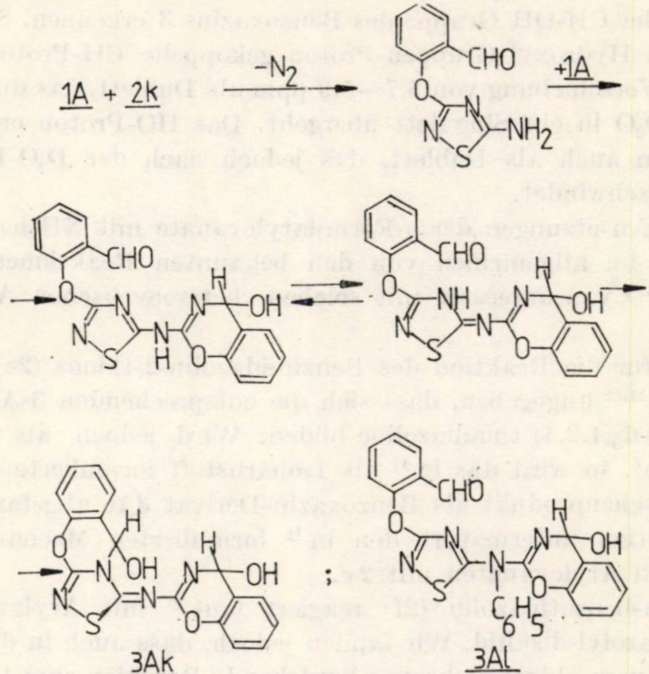

3Ak

3Al

Wird jedoch eines der Protonen der 5-Amino-Gruppe aus 2k durch eine Phenylgruppe ersetzt (in **2l** z.B.) so kann obiges Tautomerie-Gleichgewicht nicht mehr zustande kommen. Das Reaktionsprodukt, ebenfalls ein 2 : 1 – Addukt, ist das Benzoxazin-Derivat **3Al**.

BESCHREIBUNG DER VERSUCHE

Die IR-Spektren der KBr-Presslinge wurden mit einem SPECORD IR 75 (Carl Zeiss Jena) aufgezeichnet.

Die ^{1}H-NMR-Spektren wurden auf einem TESLA BS 480 (80 MHz) als DMSO-d_6 Lösungen mit HMDS (Hexamethyldisiloxan) als internes Standard aufgenommen.

Die Elementaranalysem (C.H.N.) wurden mit einem Elemental Analyser (Varian) vorgenommen.

Darstellung der Benzoxazine 3 (allgemeine Methode): 5 mMol Arylcyanat in 5 mL Dioxan werden bei −10° mit 5 mMol Azol-Lösung in 30 mL Dioxan innig vermischt, bei dieser Temperatur 1 Stunde gehalten und nachher noch 2 Studen bei Raumtemperatur nachgerührt. Nach dem Einengen des Lösungmittels wird der Rückstand aus etwa 5 mL Dioxan umkristallisiert. Nach dieser Methode wurden folgende Benzoxazin-one **3** dargestellt: [**3Aa**, aus **1A** und **2a** nach[9]

3Ba, aus **1B** und **2a** mit einer 41 %-igen Ausbeute; F 140– 3°; IR (cm^{-1}): HO 3290, C=N 1670;

3Ab aus **1A** und **2b**, mit einer 30,2 %-igen Ausbeute; F 143–4°; IR (cm^{-1}): HO 3300, C=N 1670.

3Ac aus **1A** und **2c**, mit einer 77%-igen Ausbeute; F 180–2°; IR (cm^{-1}): HO 3370, C=N 1680.

3Ad aus **1A** und **2d**, mit einer 12,2 %-igen Ausbeute; F 167-8°; IR (cm^{-1}): HO 3280, C=N 1670.

3Ae aus **1A** und **2e**, mit einer 78,6 %-igen Ausbeute; F 180—3°; IR (cm^{-1}): HO 3170, C=N 1640; ^{1}H-NMR (δ ppm): CH 5,83 **d** (6.5 Hz) (wird zum *s* mit D_2O); HO 6,68 **d** (6,5 Hz) (verschwindet mit D_2O); CH arom. 7,2 — 7,6 (9H).

3Af aus **1A** und **2f** mit einer 79 %-igen Ausbeute; F 130—1°; $C_{15}H_{10}N_2O_2S_2$ (M=314,39); ber. %C 57,30, %H 3,21, %N 8.91; gef. %C 56,86, %H 3,05, %N 8,84; IR (cm^{-1}): HO 3310 C=N 1660; ^{1}H-NMR (δ ppm): CH 5,95, **d**, 1H (mit D_2O wird es zum s): OH 6,81 **d** 1H (verschwindet mit D_2O); CH arom. 7,4 — 8,0 *m* 8H.

3Ag aus **1A** und **2g** mit 98 %-iger Ausbeute; F 224—5° (Zers.); $C_{15}H_{12}N_4O_2$ (M = 280,29); ber. %C 64,24, %H 4,32, %N 19,99; gef. %C 64.07, %H 4,35, %N 19,71; IR (cm^{-1}): HO 3230, NH_2 3380, 3250; C=N 1670.

3Ah aus **1A** und **2h** mit 68 %-iger Ausbeute; F 175—6°; IR (cm^{-1}): NH 3400, HO 3230; C=N 1680.

3Ai aus **1A** und **2i** mit 30 %-iger Ausbeute; F über 260°; IR (cm^{-1}): NH_2 3380, 3280; HO 3320; C=N 1700.

3Aj aus **1A** und **2j** mit 87,5 %-iger Ausbeute; F 190—3°; IR (cm^{-1}): NH_2 3380, 3260; HO 3130; C=N 1700.

3Ak aus **1A** und **2k** mit 45 %-iger Ausbeute; F 180—2°; $C_{17}H_{12}N_4O_4S$ (M=368,38); ber. %C 55,43, %H 3,28, %N 15,21; gef. %C 55,13, %H 3,20, %N 15,35; IR (cm^{-1}): HO 3200; C=N 1710.

3Al aus **1A** und **2l** mit 42,5 %-iger Ausbeute; F 148—50°; $C_{23}H_{16}N_4O_4S$ (M = 444,47); ber %C 62,15, %H 3,63, %N 12,61; gef. %C 61,95, %H 3,58, %N 12,49; IR (cm^{-1}): HO 3190; CHO + C=N 1690.

LITERATURÜBERSICHT

[1] X-te Mitt.: H.H. Glatt und I. Glatt. *Rev. Chim.* in Vorbereitung.

[2] D. Martin und R. Bacaloglu „*Organische Synthesen mit Cyansäureester*", Akademie-Verlag, Berlin 1980.

[3] H. H. Glatt, R. Bacaloglu, S. A. Saleh, D. Szeibert und V. Szenasi *Rev. Roumaine Chim.*, **28**, 631 (1983).

[4] H. H. Glatt R. Bacaloglu und D. Muntean, *Bul. Stiint. Tehn. Inst. Politech. „Traian Vuia" (Timişoara), Ser. Chim.*, **27**, 125 (1982).

[5] H. H. Glatt, I. Bacaloglu, T. T. Ky, C. Boeriu, R. Bacaloglu, D. Martin und H. Graubaum, *J. prakt. Chem.*, **322**, 1053 (1980).

[6] H. H. Glatt, R. Bacaloglu, C. Csunderlik, S. A. Saleh, F. Szeibert, und V. Szenasi, *Bul. Ştiint. Tehn. Inst. Politeh. „Traian Vuia" (Timişoara), Ser. Chim.*, **26**, 11 (1981).

[7] I. Bacaloglu, T. T. Ky, H. H. Glatt, C. Boeriu, R. Bacaloglu und D. Martin, *Rev. Roumaine Chim.*, **26**, 1135 (1981).

[8] E. Grigat und R. Pütter, *Chem. Ber.*, **97**, 3560 (1964).

[9] H. H. Glatt, R. Bacaloglu, C. Csunderlik und D. Muntean, *J. prakt. Chem.*, **326**, 129 (1984).

[10] D. Martin und A Wenzel, *J. prakt. Chem.*, **322**, 253 (1980).

[11] D. Martin und A. Wenzel, *J. prakt. Chem.*, **320**, 677 (1978).

[12] H. H. Glatt, K. Valenta, O. Iancu und I. Glatt, *Z. Chem.* im Druck.

[13] I. Bacaloglu, T.T. Ky, H.H. Glatt, C. Boeriu, H. Graubaum, R. Bacaloglu, D. Martin und C. Csunderlik, *Bul. Ştiint. Tehn. Inst. Politeh. „Traian Vuia" (Timişoara), Ser. Chim.*, **30**, 81 (1985).

[14] M. Augustin und K. R. Kuppe, *Tetrahedron*, **30**, 3533 (1974).

[15] D. Martin und H. Graubaum, *J. prakt. Chem.*, **321**, 315 (1979).

[16] D. Martin, H. Graubaum und S. K. Kuppe, *Tetrahedron*, im Druck.

[17] H. H. Glatt und G. Herăscu-Tölgy, *Rev. Roumaine Chim.*, im Druck.

Revue Roumaine de Chimie, **33**, *11–12*, 981–986(1988)

SYNTHESIS OF SOME NEW 3-SUBSTITUTED 4(3*H*)-QUINAZOLINONE AND 4(3*H*)-QUINAZOLINETHIONE DERIVATIVES AND RELATED FUSED BIHETEROCYCLIC RING SYSTEMS

MOHAMED F. ABDEL-MEGEED and A. TENIOU*
Chemistry Department, Faculty of Science, Tanta University, Tanta, Egypt

Received May 16, 1987

The reaction of 2-phenyl-4(3*H*)-quinazolinone, 2,-phenyl-3-amino-4(3*H*)-quinazolinone and the corresponding thiones with phenyl isocyante or phenyl isothiocyanate was investigated. The resulting urea and thiourea quinazolinone or quinazolinethione derivatives reacted with hydrazine hydrate, phenylhydrazine and urea or thiourea and led to the formation of an interesting fused biheterocyclic ring system of potential biological activities. The obtained products were identified by IR, ^{1}H-NMR and mass spectroscopy.

4(3*H*)-Quinazolinone derivatives have been reported to possess Central Nervous System (CNS) depressant,[1–4] anticonvulsant[5,6] antimalarial, [7–9] antibacterial [10,11] and antimicrobial activities.[12] Our interest is oriented to the synthesis of some new 3-substituted-4 (3*H*)-quinazolinones and their corresponding thiono analogues. On the other hand the synthesis of related fused biheterocyclic ring systems has also been investigated. The cyclocondensation of carbonyl and/or thiocarbonyl of the quinazolinone and/or quinazolinethione nucleus and carbonyl and/or thiocarbonyl of 3-position side chain gives various fused biheterocyclic ring systems, depending on the reagent and the cyclisation conditions.

The present work deals with the reaction of 2-phenyl-4(3*H*)-quinazolinone **1a**, 3-amino-2-phenyl-4(3*H*)-quinazolinone **2a** as well as their corresponding thiones **1b** and **2b** with phenyl isocyanate or phenylisothiocyanate.

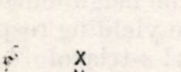

1

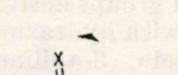

2

a ; X = O b; X = S

---

* Present address: Institut de Chimie, Universite de Constantine, Constantine, Algerie

The starting 2-phenyl-4(3*H*)-quinazolinone **1a** is obtained from the reaction of 2-phenyl-4*H*-3,1-benzoxazin-4-one[13] with formamide.[14] The corresponding thione **1b** is prepared by the reaction of **1a** with triethylamine solubilised phosphorous pentasulfide.[15] 3-Amino-2-phenyl-4(3*H*)-quinazolinone **2a** is produced from the reaction of 2-phenyl-4*H*-3,1-benzoxazin-4-one with hydrazine hydrate. The corresponding thione **2b** is formed by the reaction of 2-phenyl-4*H*-3,1-benzothiazin-4-thione with hydrazine hydrate.

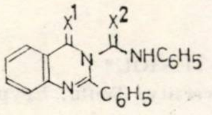

3

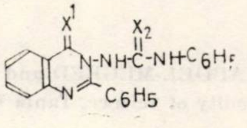

4

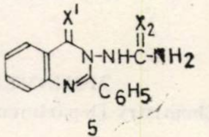

5

	X^1	X^2
a ;	O	O
b ;	O	S
c ;	S	O
d ;	S	S

3-(N′-Phenylamido)-2-phenyl-4(3*H*)-quinazolinone **3a**, 3-(N′-phenylthioamido)-2-phenyl-4(3*H*)-quinazolinone **3b**, 3-(N′-phenylamido)-2-phenyl-4(3*H*)-quinazolinethione **3c**, and 3-(N′-phenylthioamido)-2-phenyl-4(3*H*)-quinazolinethione **3d** are obtained from the reaction of **1a** and **1b** with phenylisocyanate or phenylisothiocyanate, respectively. The N-phenyl-N′-[2-phenyl-4(3*H*)-quinazolinone-3-yl] urea **4a**, N-phenyl-N′-[2-phenyl-4(3*H*)-quinazolinone-3-yl] thiourea **4b**, N-phenyl-N′-[2-phenyl-4(3*H*)-quinazolinthione-3yl]urea **4c** and N-phenyl-N′-[2-phenyl-4(3*H*)-quinazolinethione-3-yl]thiourea **4d** are obtained by the reaction of **2a** or **2b** with phenylisocyanate or phenylisothiocyanate, respectively. 2-Phenyl-3-carbamidoamino-4(3*H*)-quinazolinone **5a**, 2-phenyl-3-thiocarbamidoamino-4(3*H*)-quinazolinone **5b**, 2-phenyl-3-carbamidoamino-4(3*H*)-quinazolinethione **5c** and 2-phenyl-3-thiocarbamidoamino-4(3*H*)-quinazoline-thione **5d** are formed by the reaction of 2-phenyl-3,1-benzoxazin-4-one or 2-phenyl-3,1-benzothiazin-4-thione with semicarbazide or thiosemicarbazide, respectively.

Compounds **3a-d**, **4a-d** and **5a-d** are characterised by carbonyl and/or thiocarbonyl groups activated by the neighbouring nitrogen atoms. They react readily with hydrazine hydrate yielding respectively the cyclocondensation products, 3-anilino-5-phenyl-*s*-triazolo[4,3-*c*]quinazoline **6**, 3-anilino-6-phenyl-4H-*s*-tetrazino[1,6-c]quinazoline **7** and 3-amino-6-phenyl-4*H*-*s*-tetrazino[1,6-*c*]quinazoline **8**.

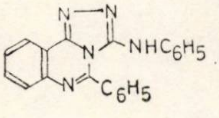

6

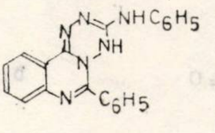

7

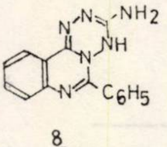

8

Similarly, the reaction of **3a-d**, **4a-d** and **5a-d** with phenylhydrazine affords the fused biheterocyclic ring systems, 2,3-dihydro-2,5-diphenyl-3-(phenylimino)-*s*-triazolo[4,3-**c**]quinazoline **9**, 3-anilino-2,6-diphenyl 2*H*-*s*-tetrazino[1,6-*c*]quinazoline **10** and 3-amino-2,6-diphenyl-2*H*-*s*-tetrazino [1,6-**c**] quinazoline **11**, respectively.

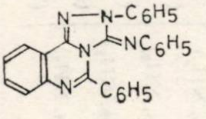
9

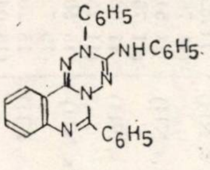
10

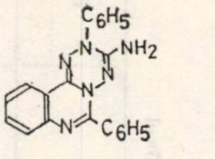
11

Fussion of **3a-d**, **4a-d** and **5a-d** with urea or thiourea at elevated temperature gives the cyclocondensation biheterocyclic-fused ring systems, 6-phenyl-4-anilino-2*H*-*s*-triazino[1,2-*c*]quinazolin-2-one **12a**, 6-phenyl-4-anilino-2*H*-*s*-triazino[1,2-*c*]quinazolin-2-thione **12b**, 4-anilino-7-phenyl[1,2,4,6]tetrazepino[1,7-*c*]quinazolin-2(5*H*)-one **13a** or 4-anilino-7-phenyl[1,2,4,6]tetrazepino[1,7-*c*]quinazolin-2(5*H*)-thione **13b** and 4-amino-7-phenyl[1,2,4,6]tetrazepino[1,7-*c*]quinazolin-2(5*H*)-one **14a** or 4-amino-7-phenyl[1,2,4,6]tetrazepino[1,7-*c*]quinazolin-2(5*H*)-thione **14b**, respect vely.

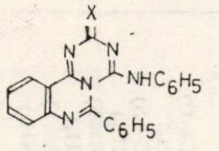
12

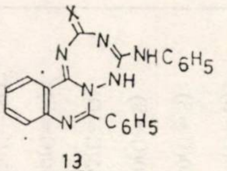
13

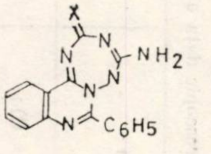
14

a ; X = O b ; X = S

The preliminary screening data of compounds **6**, **7**, **8**, **9**, **10**, **11**, **12a**, **b**, **13a**, **b** and **14a**, **b** suggested promising antibactericidal and antifungicidal activities. The biological data will be published in detail separately.

EXPERIMENTAL

All melting points are uncorrected. The IR spectra were measured with a UNICAM-1200 Spectrometer. Potassium bromide technique was used. The ^{1}H-NMR spectra were recorded with VARIAN-A-60 MHz Spectrometer using DMSO-d6 (40 mg/0.4 mL) as a solvent. The chemical shift values were expressed in δ units using tetramethylsilane as an internal standard. The mass spectra were determined with a NERMEG R10—10C Spectrometer with direct inlet source temperature 110° C and beam energy of 70 eV.

Reaction of Phenylisocyanate or Phenylisothiocyanate with compounds 1a-d and 2a-d : Formation of compounds 3a-d and 4a-d

An equimolecular mixture of phenylisocyanate or phenylisothiocyanate (0.01 mol) and the appropriate 4(3H)-quinazolinone **1a** or **2a** or 4(3H)-quinazolinethione **1b** or **2b** (0.01 mol) in dry benzene (25 mL) was refluxed for three hours. The reaction mixture was concentrated

Table 1

Physical, analytical and spectroscopic data of compounds **3a-d**, **4a-d** and **5a-d**

Compd (Yield %)	m.p. : °C	Formula $(M^+)^a$	IR spectra cm^{-1}	^1H-NMR spectra δ in ppm	Analyses[b] Found (Calc)	
					N %	S %
3a (75)	201 − 2	$C_{21}H_{15}N_3O_2$ (341)	1695(C=O) ; 1660(C=O) ; 3350(NH)	6 .7 − 8 .3(14H, s, ArH), 10 .3(1H, s,NH)	12 .10 (12 .31)	—
3b (72)	177 − 8	$C_{21}H_{15}N_3OS$ (357)	1690(C=O) ; 1240(C=S) ; 3345(NH)	6 .8 − 8 .2(14H, s, ArH) ; 10 .7(1H, s, NH)	11 .52 (11 .76)	8 .83 (8 .97)
3c (65)	182 − 3	$C_{21}H_{15}N_3OS$ (357)	1680(C=O) ; 1260(C=S) ; 3360(NH)	6 .6 − 8 .2(14H, s, ArH) ; 10 .5(1H,s,NH)	11 .54 (11 .76)	8 .78 (8 .97)
3d (68)	162 − 3	$C_{21}H_{15}N_4S_2$ (373)	1245(C=S) ; 1250(C=S) 3330(NH)	6 .8 − 8 .4(14H, s, ArH) ; 10 .8(1H, s, NH)	11 .06 (11 .25)	17 .00 (17 .17)
4a (88)	207 − 8	$C_{21}H_{16}N_4O_2$ (356)	1690(C=O) ; 1665(C=O) 3360 − 3340(NH)	6 .6 − 8 .3(14H, s, ArH) ; 10,5(1H, s, NH) 11,6(1H,s,NH)	15 .50 (15 .72)	— —
4b (80)	193 − 4	$C_{21}H_{16}N_4OS$ (372)	1690(C=O) ; 1250(C=S) ; 3360 − 3320(NH)	6 .7 − 8 .3(14H, s, ArH) ; 10 .8(1H, s, NH) 11 .8(1H,s,NH)	15 .20 (15 .04)	8 .50 (8 .61)
4c (76)	236 − 7	$C_{21}H_{16}N_4OS$ (372)	1695(C=O) ; 1245(C=SO ; 3350 − 3330(NH)	6 .6 − 8 .4(14H, s, ArH) ; 10.8(1H, s, NH) 11 .6(1H,s,NH)	15 .10 (15 .04)	8 .40 (8 .61)
4d (86)	168 − 9	$C_{15}H_{16}N_4S_2$ (388)	1240(C=S) ; 1250(C=S) ; 3350 − 3330(NH)	6 .8 − 8 .5(14H, s, ArH) ; 10 .8(1H, s, NH) 11,8(1H,s,NH)	14 .30 (14 .42)	16 .38 (16 .51)
5a (70)	298 − 9	$C_{15}H_{12}N_4O_2$ (280)	1690(C=O) ; 1645(C=O) 3460, 3380(NH, NH_2)	7 .3 − 8 .5(9H, s, ArH) ; 9 .6(2H,bs, NH_2) 11 .6(1H, s, NH)	19 .82 (19 .99)	— —
5b (78)	178 − 9	$C_{15}H_{12}N_4OS$ (296)	1690(C=O) ; 1240(C=S) 3450, 3380 (NH, NH_2)	7 .3 − 8 .4(9H, s, ArH) ; 9 .8(2H, bs, NH_2) 11,6(1H,s,NH)	18 .74 (18 .91)	10 .62 (10 .81)
5c (68)	224 − 5	$C_{15}H_{12}N_4OS$ (296)	1660(C=O) ; 1245(C=S) 3450 − 3370(NH, NH_2)	7 .3 − 8 .5(9H, s, ArH) ; 9 .6(2H, bs, NH_2) 11,7(1H,s,NH)	18 .76 (18 .91)	10 .80 (10 .81)
5d (62)	156 − 7	$C_{15}H_{12}N_4S_2$ (312)	1240(C=S) ; 1245(C=S) 3450 − 3365 (NH, NH_2)	7 .3 − 8 .5(9H, s, ArH) ; 9.8(2H, bs, NH_2) 11,8(1H,s,NH)	17 .72 (17 .94)	20 .44 (10 .52)

[a] From molecular weight determinations.

[b] Satisfactory microanalytical data (± 0.3% for C, H) were obtained for all compounds listed in this Table.

Table 2

Physical, analytical and spectroscopic data of compounds **6**–**11** and **12a-e**, **13a-e**, **14a-e**

Compd (Yield %)	m.p °C	Formula (M$^+$)^a	IR spectra cm^{-1}	^{1}HNMR spectra δ in ppm	Analyses^b Found (Calc.) N %	Analyses^b Found (Calc.) S %
6 (65)	192–3	$C_{21}H_{15}N_5$ (337)	1645(C=N); 3340(NH)	6.5–8.5(14H, m, ArH); 9.9(1H, s, NH)	20.56 (20.78)	— —
7 (58)	203–4	$C_{21}H_{16}N_6$ (352)	1635(C=N); 3330(NH)	6.6–8.4(14H, m, ArH); 10.5(1H, bs, NH) 10.8(1H,bs,NH).	23.80 (23.85)	— —
8 (68)	222–3	$C_{15}H_{12}N_6$ (276)	1640(C=N); 3345(NH)	7.3–8.4(9H, m, ArH); 9.6(2H, bs, NH_2) 10.8(1H,s,NH).	30.50 (30.42)	— —
9 (72)	216–7	$C_{27}H_{19}N_5$ (413)	1640(C=N)	6.6–8.5(19H, m, ArH)	16.82 (16.94)	— —
10 (52)	232–3	$C_{27}H_{20}N_6$ (428)	1645(C=N), 3340(NH)	6.6–8.4(19H, m, ArH); 9.8(1H, s, NH)	19.48 (19.61)	— —
11 (78)	245–6	$C_{21}H_{16}N_5$ (338)	1640(C=N), 3450–3350(NH_2)	6.6–8.5(14H, m, ArH); 9.6(2H, s, NH_2)	20.50 (20.70)	— —
12a (66)	219–20	$C_{22}H_{15}N_5O$ (365)	1660(C=O); 3340(NH)	6.6–8.4(14H, m, ArH); 9.9(1H, s, NH)	19.20 (19.17)	— —
12b (57)	230–31	$C_{22}H_{15}N_5S$ (381)	1240(C=S); 3350(NH)	6.7–8.5(14H, m, ArH); 10.0(1H, s, NH)	18.21 (18.36)	8.20 (8.41)
13a (63)	233–4	$C_{22}H_{16}N_6O$ (379)	1665(C=O); 3330(NH)	6.6–8.4(14H, m, ArH); 9.8(1H, s, NH) 10.8(1H, s, NH)	22.00 (22.15)	— —
13b (52)	226–7	$C_{22}H_{16}N_6S$ (396)	1240(C=S); 3335(NH)	6.7–8.5(14H, m, ArH); 9.9(1H, s, NH) 10.8(1H,s,NH)	21.30 (21.20)	8.00 (8.08)
14a (67)	238–9	$C_{16}H_{11}N_6O$ (303)	1665(C=O); 3450–3360(NH_2)	7.3–8.4(9H, m, ArH); 9.6(2H, s, NH_2)	27.38 (27.62)	— —
14b (58)	226–7	$C_{16}H_{11}N_6S$ (319)	1245(C=S) 3460–3360(NH_2)	7.4–8.5(9H, m, ArH); 9.8(2H, s, NH_2)	26.20 (26.23)	10.00 (10.01)

^{a} and ^{b} see footnote Table 1.

under reduced pressure. On cooling the solid mass which separated out was filtered off, washed repeatedly with dilute HCl followed by ether and recrystallised from ethanol to give compounds **4a-d** and **5a-d**, respectively. The data are recorded in (Table 1).

Reaction of semicarbazide or thiosemicarbazide with 2-phenyl-3,1-benzoxazin-4-one or 2-phenyl--3,1-benzothiazin-4-thione : Formation of compounds 5a-d

To a solution of 2-phenyl-3,1-benzoxazin-4-one or 2-phenyl-3,1-benzothiazin-4-thione (0.01 mol) in ethanol (30 mL) a mixture of semicarbazide hydrochloride or thiosemicarbazide hydrochloride (0.012 mol) and sodium acetate (0.5 g) was added. The reaction mixture was heated under reflux temperature for 5 hrs., concentrated and then cooled. The crystalline solid product was filtered off, washed repeatedly with ethanol and recrystallised from ethanol. The results obtained are reported in Table 1.

Reaction of compounds 3a-d, 4a-d or 5a-d with hydrazine hydrate or phenylhydrazine : Formation of compounds 6–8 and 9–11

A mixture of compounds **3a-d**, **4a-d** or **5a-d** (0.01 mol) and hydrazine hydrate or phenyl hydrazine (15 mL) was heated at 150–160° C in an oil bath for three hours. The reaction mixture was poured in an ice cold water (100 mL). The solid products were filtered, washed, several times with ethanol and recrystallised from ethanol to give **6**, **7** or **8** and **9**, **10** or **11** respectively. The obtained results are collected in Table 2.

Reaction of urea or thiourea with compounds 3a-d, 4a-d or 5a-d : Formation of compounds 11a,b, 12a, b and 13a, b

A mixture of urea or thiourea (0.15 mol) with the appropriate 3-substituted quinazoline or 3-substituted quinazolinethione **3a-d**, **4a-d** or **5a-d** (0.01 mol) and anhydrous $ZnCl_2$ (0.5 g) was heated in an oil bath maintained at 140–150° C for three hours. The produced caky material was cooled, washed with water and then with HCl (5 % solution) and filtered. The product was thoroughly rewashed with water to remove any traces of $ZnCl_2$ and recrystallised from ethanol to give compounds **11a-d**, **12a-d** or **13a-d**. The products are listed in Table 2.

ACKNOWLEDGEMENT: We thank Dr. Kurt L. Loening, Nomenclature Director, Chemical Abstract Service for providing the nomenclature of the fused biheterocyclic ring systems.

REFERENCES

[1] S S. Tiwari, R. K. Satsangi and R. Agarwal, *Current Sci.*, **48**, 568 (1979).
[2] D. D. Mukerji, S. R. Nautiyl and C. R. Prasad, *Indian Pharm. Sci.*, **40**, 44 (1978).
[3] S. S. Tiwari, R. K. Satsangi and S. Misra, *Indian Pharm. Sci.*, **40**, 40 (1978).
[4] J. Tani, Y. Yamada, T. Oine, T. Ochiai, R. Ishida and I. Inoue, *J. Med. Chem.*, **22**, 95 (1979).
[5] C. M. Gupta, A. P. Bhaduri and N. M. Khanna, *J. Med. Chem.*, **11**, 392 (1968).
[6] S. S. Tiwari, M. I. Husain and G. C. Srivasatva, *J. Indian Chem. Soc.*, **57**, 330 (1980).
[7] R. Lakham *Chem. Pharm. Bull.*, **17**, 2357 (1969).
[8] W. H. C. Richards, *Adv. Pharmacol. Ther. Proc. Int. Cong. Pharmacol.* 7th (1978) pub. **10**, 71 (1979), Eng. Edited by Adolphe, M Pergamon, Oxford Eng.; *Chem. Abstr.* **91**, 150905s (1979)
[9] N. Singhal, I. S. Gupta, and P. C. Bansel, *J. Indian Chem. Soc.*, **61**, 690 (1984).
[10] A. I. Eid, N. M. Aboul-Enein, S. El-Difrawy, M. Bibers and S. El-Hawary, *Eur J. Med. Chem.*, **14**, 361 (1979).
[11] L. Novacek, J. Belusa, V. Hruskova and D. Vavrinova, *Cesk. Farm.*, **27**, 173 (1978); *Chem. Abstr.* **90**, 81450e (1979).
[12] V. K. Pandey, A. K. Agawal and H. C. Lohani, *Boil. Mem.*, **8**, 74 (1983).
[13] D. I. Bain and R. K. Smally, *J. Chem. Soc.*, **1968**, 1593.
[14] V. S Patel and S. R. Patel, *J. Indian Chem. Soc.*, **42**, 53 (1965).
[15] B. Dash, E. K. Dora and C. S. Panda, *Heterocycles*, **19**, 2083 (1982).
[16] L. Pentimolli, G. Milani and F. Biavati, *Gazz. chim. Ital.*, **105**, 777 (1975).
[17] T. Okaba, E. Taniguchi and K. Maekawa, *J. Fac. Agr.*, Kyushu University, **20**, 7 (1975).

Revue Roumaine de Chimie, **33**, *11–12*, 987–992(1988)

BIOSYNTHÈSE DE LA VITAMINE B_{12}

MARIE-HÉLÈNE DARBIEU* et CHRISTINE RIPOLL
Laboratoire de Chimie de Coordination du CNRS UER des Sciences
Pharmaceutiques 35, Chemin des Maraîchers, 31400 Toulouse, France

Reçu le 16 mai 1987

La biosynthèse de la Vitamine B_{12} fait intervenir un mécanisme long compte tenu de l'extrême complexité structurale de la molécule. Le présent article souligne l'importance d'un intermédiaire clé, l'acide cobyrinique. L'obtention de ce composé qui dérive lui-même de l'uroporphyrinogène III est réalisée à partir de différentes séquences, l'une d'entre elles étant responsable de l'élimination de l'atome C_{20} à partir du macrocyclique du précurseur. Mais, cette transformation fait intervenir également un certain nombre de méthylations. Certains groupements méthyle sont fournis par la Sadenosyméthionine ou bien résultent d'un phénomène de décarboxylation de l'acide acétique. Par la suite, la formation de la Vitamine B_{12} *in vivo*, à partir de l'acide cobyrinique, nécessite la présence de différents systèmes enzymatiques. Enfin, il faut souligner que ces mécanismes ont pu être mis en évidence grâce à l'emploi de certaines techniques telles que l'étude des spectres d'absorption, la RMN et surtout l'utilisation de composés radiomarqués.

I. QUELQUES DATES IMPORTANTES DANS L'HISTOIRE DE SA DÉCOUVERTE

Les recherches, débutées par Wipple et ses collaborateurs en 1925, constituent le début des travaux sur la Vitamine B_{12}. Mais, il est intéressant de constater que si l'élan dans ce domaine a d'abord été donné par les médecins, le relais a été très vite pris par les microbiologistes et les biochimistes dont la phase d'activité spectaculaire a été l'isolement de la Vitamine B_{12} en 1948.

La deuxième période (de 1948 à 1955) a coïncidé avec le développement des méthodes de production par des techniques de fermentation. Mais, la découverte de sa structure a accru l'intérêt porté à cette molécule (figure 1). Pour les biochimistes, son importance demeure certaine car son utilisation a marqué un tournant décisif dans le traitement de l'anémie pernicieuse.

II. PRINCIPAUX ASPECTS DE SA BIOSYNTHÈSE

La Vitamine B_{12} est biosynthétisée à partir de l'acide cobyrinique. Il est donc intéressant de rechercher le métabolisme de cet acide et sa transformation en Vitamine B_{12}.

Les différentes étapes sont montrées sur la figure 2[1].

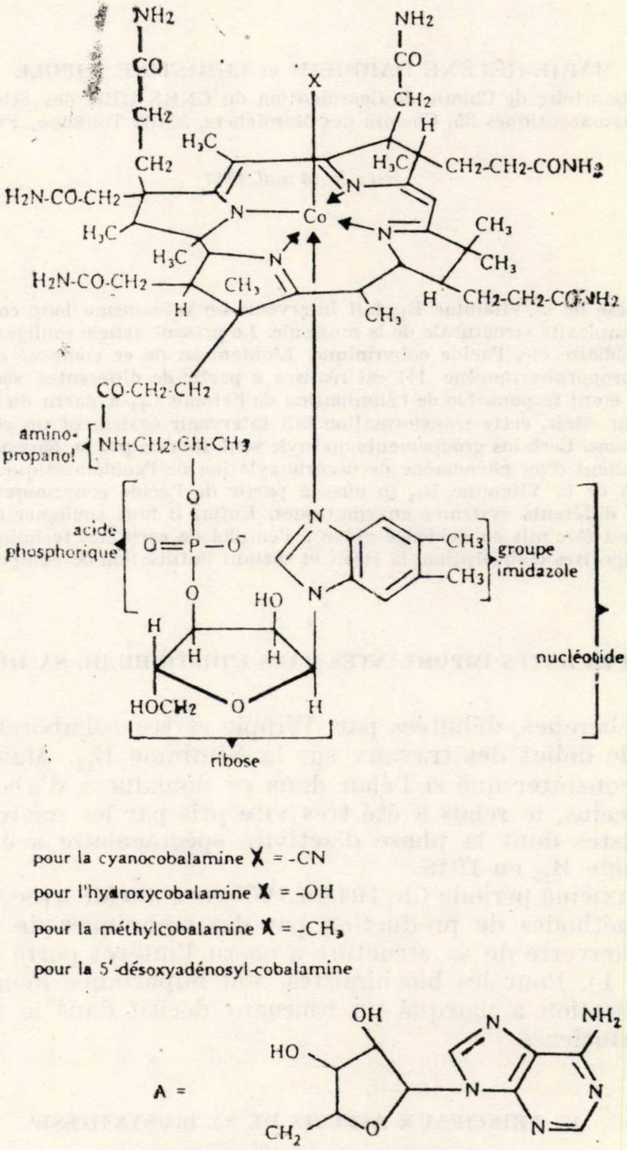
NH2
CO
CH2
CH2
H3C
CH2
H2N-CO-CH2
H3C
H3C
H2N-CO-CH2
CH3
H
NH2
CO
X
CH2
H
H3C
CH2-CH2-CONH2
N
N
Co
N
N
CH3
CH3
CH3
H
CH2-CH2-CONH2
CO-CH2-CH2
amino-propanol
NH-CH2-CH-CH3
O
acide phosphorique
O=P—O
O
CH3
CH3
groupe imidazole
N
N
HO
H
H
H
HOCH2
O
H
nucléotide
ribose
pour la cyanocobalamine X = -CN
pour l'hydroxycobalamine X = -OH
pour la méthylcobalamine X = -CH3
pour la 5'-désoxyadénosyl-cobalamine
A =
OH
HO
NH2
N
N
N
N
CH2
O

Fig. 1. — Structure de la Vitamine B_{12}.

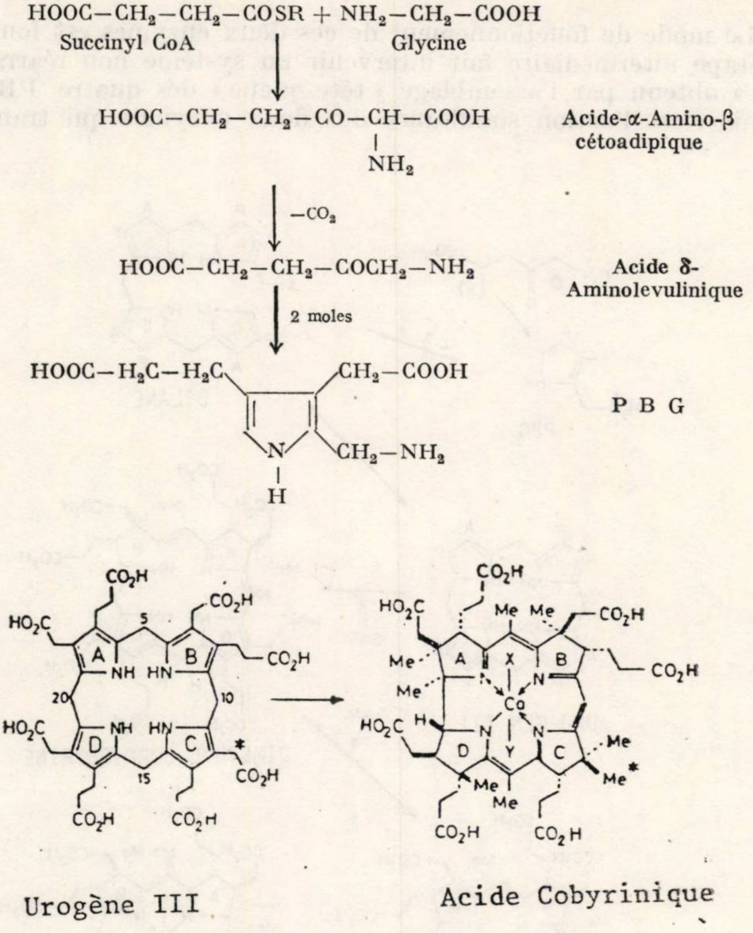
HOOC−CH₂−CH₂−COSR + NH₂−CH₂−COOH
Succinyl CoA
Glycine
HOOC−CH₂−CH₂−CO−CH−COOH
NH₂
Acide-α-Amino-β cétoadipique
−CO₂
HOOC−CH₂−CH₂−COCH₂−NH₂
Acide δ-Aminolevulinique
2 moles
HOOC−H₂C−H₂C
CH₂−COOH
N
CH₂−NH₂
H
P B G
CO₂H
HO₂C
A
B
C
D
NH
HN
5
10
15
20
Urogène III
Me
X
Y
Co
N
H
Me*
Acide Cobyrinique

Fig. 2. — Synthèse de l'acide cobyrinique.

A) Synthèse du Porphobilinogène = PGB [2]

On sait actuellement que le noyau corrine comme celui de l'hème et de la chlorophylle sont formés dans la nature à partir de l'acide δ aminolevulinique, obtenu par condensation de la glycine avec le succinyl coenzyme A. On obtient, dans un premier temps, l'acide α-amino-β-céto adipique qui par suite du départ d'une molécule de gaz carbonique conduit à l'acide δ-aminolevulinique. Par condensation de deux molecules de cet acide, il y a formation du porphobilinogène PBG.

B) Synthèse de l'Uroporphyrinogène III

L'uroporphyrinogène III est formé à partir de 4 molecules de porphobilinogène. Cette transformation se fait sous l'influence de deux enzymes, la déaminase et la cosynthétase.

Le mode de fonctionnement de ces deux enzymes est fondamental. Une étape intermédiaire fait intervenir un système non réarrangé, « un bilane » obtenu par l'assemblage « tête-queue » des quatre PBG (figure 3). Mais c'est l'action simultanée des deux enzymes qui transforme le Bilane en Urogène III. Par contre si la déaminase fonctionne seule, l'urogène III n'est pas formé et ne pourra pas être formé par l'action ultérieure de la cosynthétase.

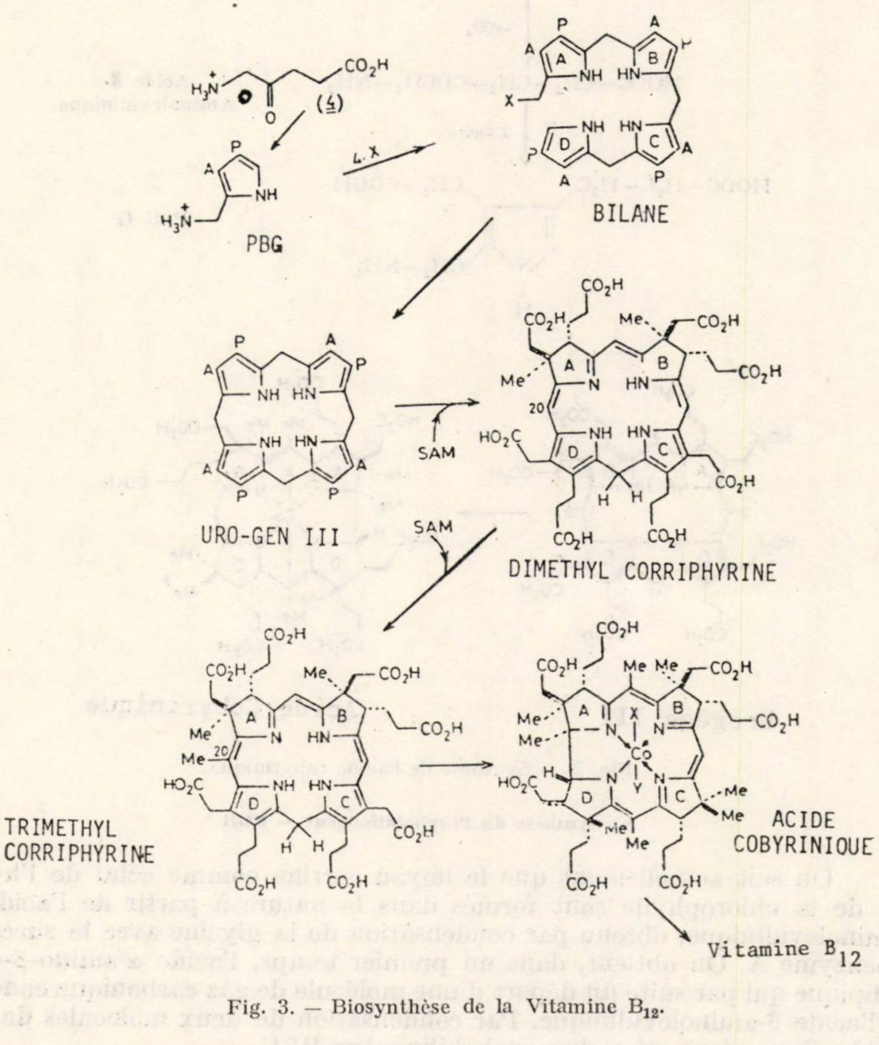
(4)
4. X
PBG
BILANE
URO-GEN III
SAM
DIMETHYL CORRIPHYRINE
SAM
TRIMETHYL CORRIPHYRINE
ACIDE COBYRINIQUE
Vitamine B12

Fig. 3. — Biosynthèse de la Vitamine B_{12}.

Il y a quatre sites de liaison sur la déaminase qui reconnaît les quatre noyaux pyrroles.

La première unité de PBG formera le cycle A avec le carbone 20.

La deuxième formera le cycle B avec le carbone 10,

la troisième, le cycle C avec le carbone 15,
la quatrième, le cycle D.

A est assemblé en premier, D en dernier. Le bilane non réarrangé peut apparaître dans le milieu sous forme d'hydroxyméthyl bilane. En présence de la cosynthétase, il y a fermeture du cycle par réarrangement intramoléculaire.

C) Synthèse de l'Acide Cobyrinique [3,4]

Pour former l'acide cobyrinique, des modifications apparaissent au niveau du cycle D qui provient du PBG par le biais de réarrangements intramoléculaires.

Les étapes du passage de l'urogène III en acide cobyrinique sont importantes. Elles comprennent diverses méthylations qui se font grâce à la S Adenosyl-Méthionine (SAM).

Pour que l'urogène III soit transformé en acide cobyrinique, huit méthylations sont nécessaires.

On sait actuellement que 7 groupements méthyle sont fournis par la S.A.M. (S-Adénosyl-Méthionine) sur les carbones 1,2,5,7,12,15,17. Le huitième méthyle résulte de la décarboxylation de l'acide acétique latéral en C_{12} sur le noyau C.

Les différentes étapes sont représentées sur la figure 3.

L'extraction du C_{20} à partir du squelette de l'urogène III a soulevé de nombreuses questions. On pense actuellement qu'il s'agit d'une conversion enzymatique qui se produit par perte de formaldéhyde[5].

D) Formation de la Vitamine B_{12}

La Vitamine B_{12} est formée ensuite *in vivo* à partir de l'Acide Cobyrinique. Les différents résidus amides et le nucléotide sont additionnés à la fin de la séquence de biosynthèse.

Les corrinoïdes contenant du Benzimidazole sont formés en milieu aérobie.

Le 5,6-Diméthylbenzimidazole est formé par les bactéries : *Bacillus mégathérium*, *Nocardia rugosa.*

L'oxygène est nécessaire à la synthèse. La base est formée à partir de la transformation de la riboflavine en diméthyl-benzimidazole. Ceci étant réalisé par une réduction de la riboflavine ou l'un de ses dérivés phosphorylés. La formation du diméthylbenzimidazole est stimulée par la nicotinamide et l'acide nicotinique.

A partir de ce précurseur, trois enzymes interviennent :

— 5,6-Diméthyl Benzimidazole Synthétase
— α-Ribazole-5'-Phosphatase Synthétase
— Trans-N-Glycosidase.

Quant aux chaînes latérales, elles résultent d'une amidification terminale.

On voit donc que la biosynthèse de la Vitamine B_{12} fait intervenir un mécanisme complexe. De nombreux blocages peuvent intervenir au cours des différentes étapes et si la vitamine B_{12} a été, dès les premiers

temps, synthétisée à partir des microorganismes, on comprend, dès lors, pourquoi la synthèse chimique a pris le relais.

BIBLIOGRAPHIE

[1] Ch. Ripoll, Thèse de Doctorat Pharmacie, nº 44, 1985.

[2] B. Zagala, *Proceedings of the 3rd European Symposium of Vit. B_{12}*, Ed. W. de Gruyter, 1979.

[3] C. Nussbanmer et M. Imfeld, *Biosynthesis of Vitamine B_{12}, Mode of incorporation of factor III into Cobyrinic acid*, Proc. Natl. Acad. Sci., USA, 78, p. 9, 1981.

[4] A. R. Battersby, *Biosynthesis of Vitamine B_{12}*, Proc. Natl. Acad. Sci., Vol. 78, nº 1, p. 13.15, 1981.

[5] L' Mombelli et C. Nussbanmer *Nature of Volatile fragment generated during formation of the corrin ring system*, Proc. Natl. Acad. Sci., USA, Vol. 78. nº 1, p. 11–12, 1981.

Revue Roumaine de Chimie, **33**, *11–12*, 993–1004(1988)

CATALYTICALLY ACTIVE ALUMINAS FROM PRECURSORS OBTAINED BY SUPERSATURATION OF REACTANTS. I

SYNTHESIS OF PRECURSORS AND REACTION MECHANISMS

I. V. NICOLESCU[a], MARIANA UDREA*, ALA NICOLESCU[b],
I. UDREA[a] and D. CRIŞAN[b]

[a] Faculty of Chemical Technology, Polizu 1, Bucharest, Romania
[b] Centre of Physical Chemistry, Spl. Independenţei 202, Bucharest, Romania

Received March 16, 1988

This contribution presents the preparation method of catalytically active aluminas from hydrated crystalline reactants of some aluminum salts (chloride, nitrate, sulphate) and acid or neutral ammonium carbonate, initially in solid state. The reactions are produced at interface by mechanical energy in supersaturation conditions i.e. by mixing. The final products resulted possess special surface properties, unstable thermodynamic states with excess free energy which appears as dispersion surface energy. The variation of pH, differential thermal gravimetry, differential thermal analysis, IR spectroscopy and X-ray diffraction were employed in characterization of reaction intermediate steps. These precursors are utilized, after subsequent thermal treatments in synthesis of some catalytically active aluminas.

INTRODUCTION

The diversity of active alumina-supported catalysts and utilization of aluminas as catalysts have imposed manufacturing of various aluminas which differ by the properties related to structure and by the physicochemistry of surface.

*** Mariana Udrea born in January 23, 1942, died on November 10, 1987 in full creative activity. She got B.S. in chemistry at the University of Bucharest and the Ph. D. in 1977. She was affiliated as senior researcher with the Centre of Physical Chemistry and the Institute of Chemical and Biochemical Energetics in Bucharest. She received the Romanian Academy Award "Gheorghe Spacu" for chemistry in 1975. Among her 65 works, patents and technical reports, issued during 23 years of research activity, a major part is concerned with basic and applied studies in heterogeneous catalysis as : the relationship between genesis, properties and catalytic activity of aluminas, metal-supported catalysts (Ni/Al_2O_3, Pd/Al_2O_3 etc.), oxidic catalysts of spinelic structure utilized in processes of carbon monoxide methanation, hydrocarbon isomerization, selective hydrogenation of acetylene from phyrolysis gases, methane reforming, carbon monoxide hydrogenation to light olefins and synthetic fuels. Mariana Udrea's conception of research and the results obtained have placed her among the outstanding specialists in heterogeneous catalysis in Romania. All those who knew her personally valued greatly her gentleness and equable temper; they will always remember the gifted scientist and kind woman.**

Our studies have aimed at developing a new method of preparing active aluminas[1] based on the reaction at interface between reactants in solid phase under the action of mechanical force, by mixing.

The system belongs to the class of topochemical reactions between a reactant (an aluminum salt — a hydrated crystal i.e. chloride, nitrate, sulphate) and an ammonium base i.e. neutral or acid carbonate, both reactants being initially in solid state. The theoretical foundation of the method may be found in the theory of supersaturation[2,3] which deals with the formation of active surfaces of solids utilized as catalyst; these surfaces possess excess free energy.

The extent of supersaturation is measured by the maximum work of the reaction:

$$\alpha A + \beta B + \gamma C + \ldots \rightarrow xX + yY + zZ + \ldots$$

and expressed as difference between the chemical potentials of the substances attending the reaction at time "i" and at equilibrium:

$$M = \sum^{a \rightarrow z} \varepsilon RT \ln [X]_i - \sum^{a \rightarrow z} \varepsilon RT \ln [X]_0$$

where:

M is the maximum work of the reaction, α, β, γ, x, y, z are the stoichiometric coefficients, A, B, C the reactants, X, Y, Z the products of reaction, ε the stoichiometric coefficient, $[X]_i$ the concentration of one component at time "i" and $[X]_0$ the equilibrium concentration of one component.

At equilibrium:

$$K = \frac{X^x Y^y Z^z \ldots}{A^\alpha B^\beta C^\gamma \ldots}$$

and it may be written:

$$M = RT \ln \frac{K}{K'}$$

where K′ is a fraction which is similar to equilibrium constant K which includes the current concentrations of the substances that participate in reactions. The maximum work and the maximum supersaturation of the system are obtained for K/K′ ratios as different from unit as possible i.e. for the K′ values farthest from equilibrium.

The reactions between the components of the system are accompanied by an endothermal effect originating in separation of a part of the crystallization water. The mechanism of reaction is specific to each hydrated crystal; to a great extent this mechanism is controlled by the position and state of water molecules.

EXPERIMENTAL

The active aluminas are obtained in two steps: in the first, the precursor is obtained and in the second it is transformed into active alumina. The precursors are prepared from compounds as hydrated crystalline chloride, nitrate or sulphate of aluminum which are mixed in a mortar or mixer with a calculated amount of neutral or acid ammonium carbonate, both reactants being in powdery state. The products are washed with distilled water until the anion is washed away and dried at 110°C for six hours. These products (HT) are denoted by HTC (from aluminum chloride); HTA (from aluminum nitrate) and HTS (from aluminum sulphate) and represent the precursors of catalytic aluminas which result from their calcination at 500, 600, 700, 800°C.

This contribution deals with the first part of the process i.e. the synthesis of HTC, HTA and HTS products. The reactions of this part are characterized by three distinct steps which are discussed separately for each system :

(a) fluidization of reaction mass ;
(b) solidification of reaction mass ;
(c) decomposition of the intermediate with evolution of carbon dioxide.

The complete method of preparation was presented elsewhere[3].

The products obtained in this first step where characterized by differential thermal and thermal-gravimetric analysis (with a SETARAM thermoanalyzer with 3.6°/min heating speed), by X-ray diffraction spectroscopy (with a TUR-M 61 apparatus equipped with HZG — 3 diffractometer which utilized CuK-α radiation filtered through nickel), by IR spectroscopy (with a UR 10 apparatus) and by elemental chemical analyses.

RESULTS AND DISCUSSION

1. The reaction of hexahydrated aluminum chloride and ammonium carbonate. The obtention of HTC product

From among the hydrated crystalline aluminum salts the chloride is special because the whole amount of water is engaged in complete coordination of the cation as octahedral water-complexes of $Al(H_2O)_6^{3+}$ type.

Because of this feature we considered that in the case of mechanical mixing of powders of aluminum chloride with acid ammonium carbonate, the fluidization at room temperature is caused by a part of the crystallization water through an internal hydrolysis reaction accelerated by the presence of acid ammonium carbonate.

The dynamics of the process and the succession of intermediate steps was monitored by the variation of pH at the medium during the reaction (Fig. 1).

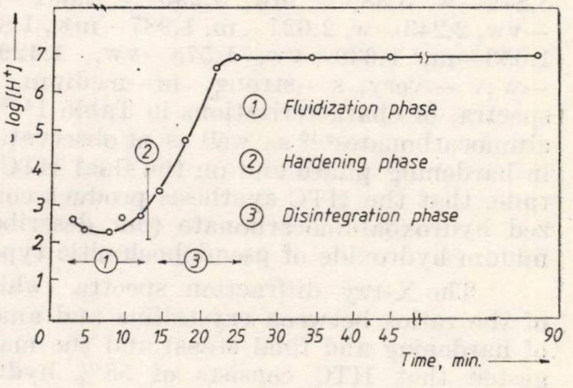

Fig. 1 — Time dependence of reaction medium pH ; HTC product.

The initial decrease of pH down to 2.2 is probably caused by formation of basic chlorides as intermediates ; they are strongly basic and dissociated in the reaction medium. It is assumed that the fluidization stage, which ends with formation of hardening phase, occurs through the following sequence of reactions :

$$AlCl_3 \cdot 6H_2O + NH_4HCO_3 \rightarrow [Al(H_2O)_5OH]Cl_2 + NH_4Cl + H_2O + CO_2 \qquad (1)$$

$$[Al(H_2O)_5OH]Cl_2 + NH_4HCO_3 \rightarrow$$

$$\rightarrow [Al(H_2O)_4(OH)_2]Cl + NH_4Cl + H_2O + CO \qquad (2)$$

In conditions of very high concentration of aluminum chloride the stable product of hydrolysis is the basic chloride of reaction (2). However, because during the reaction there is a well defined step which consists of formation of a solid product, the hardening phase, which includes all the water in the system it is assumed that a reaction follows between the resulted basic chloride and the ammonium acid carbonate with formation of an ammonium alumocarbonate by the reaction :

$$[Al(H_2O)_4(OH)_2]Cl + NH_4HCO_3 \xrightarrow{H_2O}$$

$$\rightarrow NH_4[Al(OH)_2CO_3] \cdot nH_2O + NH_4Cl + H_2O + CO_2 \qquad (3)$$

where $n = 3$.

Further addition of acid ammonium carbonate and water breaks up the solid mass causing the pH to rise to 7.0 – 7.5 which suggests that, during this final stage, the alumocarbonate hydrolizes to form pseudoboehmitic aluminum hydroxide :

$$NH_4[Al(OH)_2CO_3] \cdot nH_2O \xrightarrow{H_2O} AlOOH + (n+1)H_2O + CO_2 + NH_3 \qquad (4)$$

Examination of X-ray diffraction lines (5.784 – vs, 4.036 – m, 3.872 – w, 3.385 – mw, 3.299 – s, 2.891 – m, 2.733 – w, 2.561-sm, 2.348 – – vw, 2.243 – w, 2.027 – m, 1.987 – mw, 1.852 – vw, 1.812 – vw, 1.726 – mw, 1.653 – m, 1.630 – vw, 1.578 – vw, 1.4296 – m, 1.3462 – vw, 1.3156 – – w; v – very, s – strong, m – medium, w – weak), of IR absorption spectra, of characterizations in Table 1[4–8] and of DTA curves specific to alumocarbonates[9,10] as well as of observations in Table 2 on the products in hardening phase and on the final HTC product shows, with fair certitude, that the HTC synthesis product consists of a mixture of crystallized hydroxoalumocarbonate (not described in the literature) and aluminum hydroxide of pseudoboehmitic type.

The X-ray diffraction spectra (which have afforded calculation[11] of the ratios between crystalline and amorphous phases in the products of hardening and final steps) and the mass loss determined by TG suggested that HTC consists of 58% hydroxoalumocarbonate and 42% aluminum hydroxide (Table 2).

The experimental data confirm also the mechanism of formation of the intermediates of the reaction under study.

Table 1

IR Spectrum of HTC sample

Band position (cm^{-1})	Vibrational mode	Species
475 630	$\delta(Al^{VI}-O)$ $\gamma(OH)$	hydroxide complex
785	$\nu(Al-OH)$	boehmite
860	$\delta(OH)$	hydroxide complex
990	$\delta(Al-OH)$ $\nu_2(HO-CO_2)$	aluminum bicarbonate hydroxide complex
1070 1110	$\delta(OH)$	boehmite
1410 1460 1560	$\nu_5(CO_3^{2-})+\delta(NH_4^+)$ $\nu_3(CO_3^{2-})$	unidentate carbonate
1640	$\delta(HOH)$	gel of hydroxide, hydroxide complex
1814 2420	$\nu+\delta(HOH)$	aluminum carbonate hydroxide complex
3190 3470	$\nu(OH\ldots O)$	

Table 2

Thermogravimetric analysis of HTC sample

Temperature t °C	Mass loss %		Structural changes
	experimental	calculated*	
130 $(50<t<175)$	17.9	16.31	Loss of crystallization water
220–225 $(175<t<260)$	23.20	23.87	Loss of NH_3, CO_2, H_2O molecules and formation of hydroxide of boehmite type
302 $(260<t<500)$	9.32	8.98	Pseudoboehmite and boehmite gel decomposition

* for 58.3% hydroxoalumocarbonate in the sample

2. The reaction of nonahydrated aluminum nitrate with ammonium carbonate. The obtention of HTA product

In this reaction after mixing the solid reactants the mixture fluidizes (the reaction is rapid with strong CO_2 evolution) the medium pH becomes more acid 0.8–1 then, as in aluminum chloride, the mixture solidifies (the hardening phase appears).

The curve of pH variation during reaction advancement is shown in Fig. 2 and is similar to that obtained in hexahydrated aluminum chloride except that the pH minimum is lower ($pH < 1$).

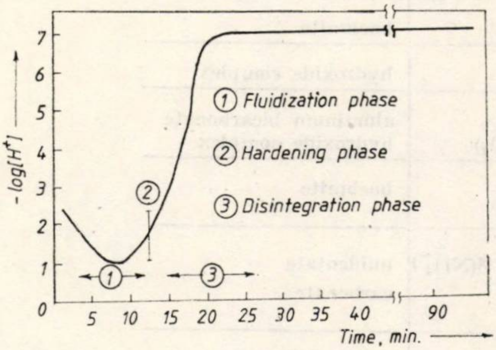

Fig. 2 — Time dependence of reaction medium pH; HTA product.

Unlike hexahydrated aluminum chloride, in this case there is an initial instantaneous fluidization induced by the elimination of the three water molecules in the hydrated crystal which are weakly bonded:

$$Al(NO_3)_3 \cdot 9H_2O \xrightarrow{-3H_2O} Al(NO_3)_3 \cdot 6H_2O \qquad (5)$$

In the presence of ammonium carbonate there is a gradual hydrolysis with formation of hydroxynitrates soluble in the medium:

$$2Al(NO_3)_3 \cdot 6H_2O + (NH_4)_2CO_3 \rightarrow$$
$$\rightarrow Al_2(NO_3)_4(OH)_2 + 2NH_4NO_3 + CO_2 + 11\,H_2O \qquad (6)$$

$$Al_2(NO_3)_4(OH)_2 + (NH_4)_2CO_3 + 2H_2O \rightarrow$$
$$\rightarrow Al_2(NO_3)_2(OH)_4 + 2NH_4NO_3 + CO_2 + H_2O \qquad (7)$$

$$Al_2(NO_3)_2(OH)_4 + (NH_4)_2CO_3 + nH_2O \rightarrow \underset{\text{(hydroxide gel)}}{Al_2(OH)_6 \cdot nH_2O} \qquad (8)$$

The presence of basic aluminum nitrates in dimer form is justified by their tendency of forming olation compounds with polymer structure of the $Al_2(OH)_y(NO_3)_z \cdot nH_2O$ type during hydrolysis.[12]

In the X-ray diffraction spectrum ot hardened product the characteristic lines of a basic oxide are noted; it was identified to be the HTA final product according to Fig. 3.

The presence of complex basic carbonate was also evidenced by IR spectra (hardened phase and HTA product) according to specifications [4–11] in Table 3.

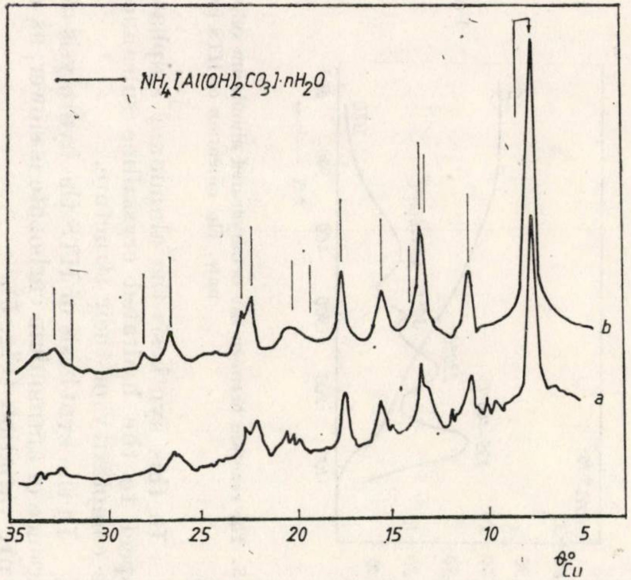

Fig. 3 — X-ray diffraction spectrum of HTA: (a) during hardening; (b) finished product.

Table 3

IR Spectrum of HTA sample

Band position (cm^{-1})	Vibration mode	Species
480—540	$\delta(Al^{VI}-O)$	
630	$\gamma(OH)$	hydroxyl
770—780	$\nu(Al-OH)$	
860	$\delta(OH)$	carbonate hydroxide complex
990—995	$\delta(OH)+\nu_2(HO-CO_2)$	bicarbonate
1110—1115	$\nu_1(CO_3^{2-})$	
1390—1400	$\nu_5(CO_3^{2-})+\delta(NH_4^+)$	
1460—1470	$\nu_3(CO_3^{2-})$	
1560	$\nu_6(CO_3^{2-})+\delta(H_2O)$	
1630—1640	$\delta(H_2O)$	gel of hydroxide
1740	ν_4	basic carbonate
1830		aluminium carbonate hydroxide complex
2420—2430		H_2O as ligand
3140—3470	$\nu(OH\ldots O)$	microcrystalline gels of hydroxides

The mass losses (recorded on TG curves in Fig. 4) which accompany the thermal effects determined by DTA allow one to distinguish between various kinds of water in the structure of hydroxoalumocarbonate and pseudoboehmitic hydroxide and to establish a correspondence between the losses determined by experiments at an approximate composition of the product ot 52.4% hydroxide and 47.4% hydroxoalumocarbonate and the theoretical losses by thermal decomposition of these components (Table 4).

The structure of intermediate and final products as well as the mechanism of the process are also confirmed satisfactorily.

Table 4

Thermogravimetric analysis of HTA sample

Temperature t °C	Mass loss %		Structural changes
	experimental	calculated*	
135–140 ($40<t<180$)	16.00	16.16	Loss of crystallization water
230 ($180<t<340$)	16.00	17.72	Loss of HO^-, NH_3, CO_2
400 ($340<t<600$)	10.5	9.91	Dehydration of boehmite (initial and formed from the complex)

* for 47.36% hydroxoalumocarbonate in the sample

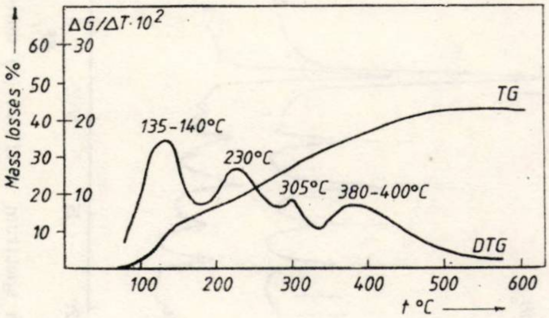

Fig. 4 — TG and DTG of HTA finished product.

3. The reaction between the octahydrated aluminum sulphate and the ammonium carbonate. The obtention of HTS product

In this synthesis the aluminum sulphate behaves differently with respect to the hydrated crystalline substances described[13] because of the complexity of their structure.

In the synthesis of HTS the hydrolysis of aluminum sulphate in the presence of ammonium carbonate is slower, as one may note in the curve of pH variation (Fig. 5).

It has been considered that in the first step a basic aluminum sulphate is formed according to the reaction :

$$3Al_2(SO_4)_3 \cdot 18H_2O + 6(NH_4)_2CO_3 \rightarrow$$

$$\rightarrow (NH_4)_2Al_6(SO_4)_4(OH)_{12}nH_2O + 5(NH_4)_2SO_4 + 6CO_2 + mH_2O \qquad (9)$$

Fig. 5 — Time dependence of reaction medium pH ; HTS product.

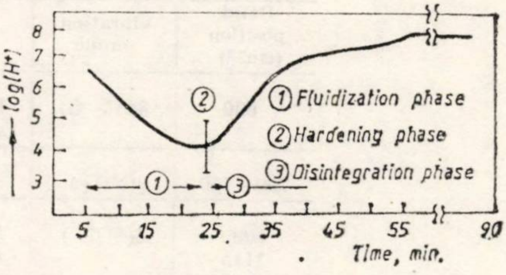

This sulphate is mentioned in literature and is the isomorphous of the mineral called alunite.[14,15]

The formation of this compound was confirmed by comparing the X-ray diffraction spectrum of the product obtained at hardening (Fig. 6) with those mentioned in the literature for compounds of similar structure.[16]

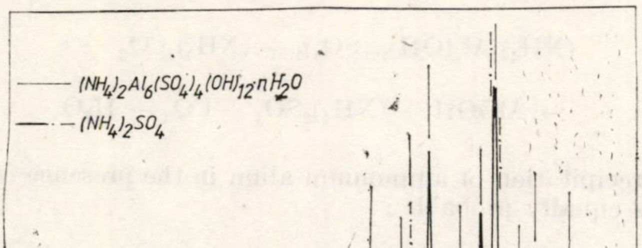

Fig. 6 — X-ray diffraction spectrum of HTS product during hardening.

The existence of basic alum in this intermediate step also results from identification in IR absorption spectrum,[11,16] according to the observations in Table 5.

On addition to the reaction mass corresponding to hardening mass, of a new amount of ammonium carbonate in excess to the stoichiometric one and of more water the process continues and a pH increase to 75.—8.0 is recorded. This alkalinity increase may trigger a reaction of decomposition of the initial basic salt initially formed, according to the reaction :

Table 5

IR Spectrum of the intermediate obtained in HTS synthesis

Band position (cm^{-1})	Vibration mode	Species
630	$\delta(Al-O)$	basic aluminum sulphate hydrate
700—750	$\gamma(NH_4^+)$	
1000 1115 1185	$\delta(SO_4^{2-})$	distorted tetrahedra of SO_4^{2-}
1420	$\delta(NH_4^+)$	NH_4^+
1640	$\delta(H_2O)$	H_2O
3500	$\nu(OH\ldots O)$	

$$(NH_4)_2Al_6(OH)_{12}(SO_4)_4 + (NH_4)_2CO_3 \rightarrow$$

$$\rightarrow \underset{\downarrow}{AlOOH} + (NH_4)_2SO_4 + CO_2 + H_2O \qquad (10)$$

The precipitation of ammonium alum in the presence of ammonium carbonate is equally probable :

$$NH_4Al(SO_4)_2 \cdot 12H_2O + (NH_4)_2CO_3 \rightarrow$$

$$\rightarrow \underset{\downarrow}{AlOOH} + 2(NH_4)_2SO_4 + CO_2 + 12H_2O + NH_3 \qquad (11)$$

The X-ray diffraction spectrum of the final synthesis product (Fig. 7) (washed to complete removal of SO_4^{2-} ion and dried at 110°C) is that of a microcrystalline hydroxide of pseudoboehmitic type without the characteristic lines of hydroxoalumocarbonate identified in previous syntheses.

Table 6

Crystallite mean-size in the HT series

Sample	$D_{(020)}$, Å
HTA	128.7
HTC	116.0
HTS	24.5

The average dimensions of crystallites were also calculated by the Scherrer equation[17] (making use of metallic aluminum as standard) to improve the characterization of HT products obtained as precursors for synthesis of catalytic aluminas (Table 6).

The dimensions of crystallites as well as their shape determine a certain type of packing of primary particles i.e. conglomerates with differently shaped and sized pores which is emphasized by the hysteresis curves obtained for the three products (Fig. 8).

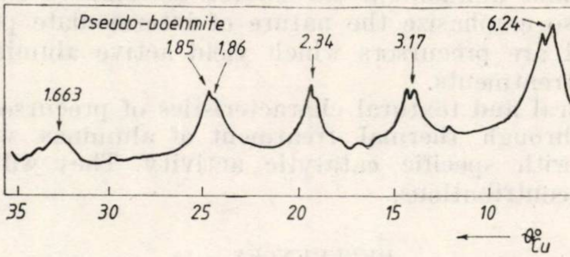

Fig. 7 — X-ray spectrum of finished HTS product.

The HTA and HTC products fit the type A hysteresis[18] characteristic of cylindrical pores while HTS shows a different hysteresis cycle, similar to type B which is encountered in porous products with amorphous character.

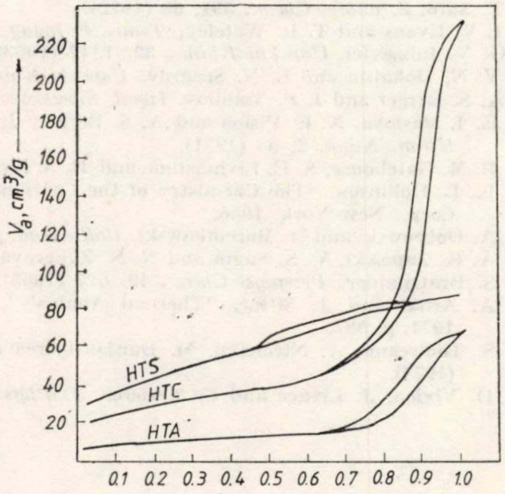

Fig. 8 — Adsorption-desorption isotherms of nitrogen at − 196°C for HTA, HTC and HTS samples.

The main textural features which distinguish the synthesized products are listed in Table 7.

Table 7

Textural properties of HT samples

Sample	d_r (gcm^{-3})	V_t pores (cm^3g^{-1})	V_{macro} ($r > 150$ Å) (cm^3g^{-1})	V_{micro} ($r < 150$ Å) (cm^3g^{-1})	S_{sp} (m^2g^{-1})
HTC	2.00	0.6566	0.5096	0.1470	41
HTA	1.97	1.066	0.9468	0.1192	117
HTS	2.32	0.4366	0.2456	0.1910	184

In conclusion it is worth to mention :

The experiments explain the steps and mechanisms of reactions occurring at solid-solid interface between hydrated crystals of some aluminum salts and ammonium carbonates determined by mechanical friction ; they also emphasize the nature of intermediate products. The products resulted are precursors which yield active aluminas following various thermal treatments.

The structural and textural characteristics of precursors determine the obtention through thermal treatment of aluminas with different properties and with specific catalytic activity. They will make the object of future contributions.

REFERENCES

M. Udrea, Doctoral Thesis, Bucharest, 1977 ; A. Nicolescu and M. Gruia, *Rev. Roumaine Chim.*, **11**, 847 (1966) ; M. Udrea and I. Udrea, *Rev. Chim Bucureşli*, **23**, 351 (1972).

[2] S. Z. Roghinski, *Zhur. priklad. Khim.* **17**, 97 (1944) ; *Acta Physico-Chimica*, **4**, 6 (1936) ; *Kinetica i Kataliz*, **8**, 1054 (1967).

[3] I. V. Nicolescu, M. Udrea, A. Nicolescu, G. Musca, I. Suciu, V. Părăuşanu, S. Blejoiu and I. Melichian, Romanian Patent, 58724, 1974.

[4] A. S. Berger, N. P. Tomilov and I. A. Vorsiuc, *Zhur. neorg. Khim.*, **16**, 81 (1971).

[5] T. Sato, *Z. anorg. Chem.*, **391**, 69 (1972).

[6] I. V. Evans and T. L. Wateley, *Trans. Faraday Soc.*, **63**, 539 (1967).

[7] G. V. Iuhnevici, *Uspekhi Khim.*, **32**, 1347 (1963).

[8] V. N. Mokatun and L. N. Scegrov, *Uspekhi Khim.*, **41**, 1937 (1972).

[9] A. S. Berger and I. P. Tomilov, *Izvest. Sibirskogo Otdel. Akad. Nauk*, **4**, 74 (1969).

[10] E. I. Maslova, N. E. Pisina and A. S. Berger, *Izvest. Sibirskogo Otdel. Akad. Nauk, SSSR, Khim. Nauk*, **2**, 33 (1971).

[11] B. M. Gatehouse, S. E. Livingstone and R. S. Nyholm, *J. Chem. Soc*,. **9**, 3137 (1958).

[12] K. L. Rollinson, "The Chemistry of the Coordination Compounds", Ed. by Reinhold Publ. Corp., New York, 1956.

[13] A. Dobrowski and R. Marcinkowski, *Bull. Acad. polon. Sci., Ser. Sci. chim.*, **21**, 515 (1973).

[14] A. K. Zapolski, V. S. Sagin and N. N. Zaharova, *Ukrain. khim. Zhur.*, **37**, 30 (1971).

[15] S. Bratznajder, *Przemysl Chem.*, **42**, 677 (1963).

[16] A. Arhar and J. Siftar, "Thermal Analysis", vol. 2, Proceedings III-rd ICTA, Davos, 1971, p. 587.

[17] S. Todireanu, A. Nicolescu, M. Dardan-Udrea and I. V. Nicolescu, *J. Catalysis*, **35**, 472 (1974).

[18] D. Vivien, J. Livace and C. Mezieres, *J. Phys. Chem.*, **67**, 199 (1970).

Revue Roumaine de Chimie, **33**, *11–12*, 1005–1011 (1988)

CATALYTICALLY ACTIVE ALUMINAS FROM PRECURSORS OBTAINED BY SUPERSATURATION OF REACTANTS. II[1]

TEXTURAL AND STRUCTURAL PROPERTIES AND THEIR RELATION TO THE NATURE OF PRECURSORS AND THE THERMAL TREATMENT

MARIANA DUREA*, I. UDREA[a], ALA NICOLESCU[b],
D. CRIȘAN[b] and I. V. NICOLESCU[a]

[a]Faculty of Chemical Technology, Polizu 1, Bucharest, Romania
[b]Centre of Physical Chemistry, Spl. Independenței 202, Bucharest, Romania

Received March 16, 1988

The reaction at interface between hydrated crystals of some aluminum salts (chloride nitrate, sulphate) and an ammonium base (neutral or acid ammonium carbonate) in conditions of supersaturation (in powdery state) and mechanical mixing yields a semifluid mass which after washing, filtering and drying yields the products denoted by HTC, HTA, HTS consisting of mixtures of hydroxoalumocarbonate and aluminum hydroxide of pseudoboehmitic type. Through thermal treatment (500–800°C) these products transform into catalytically active aluminum oxides. This contribution presents the dependence of structural and textural properties of these aluminum oxides on the genesis of precursors and the thermal treatment.

In a previous paper[1] the results of experiments aiming at developing a new method of preparing catalytically active aluminas in conditions of supersaturation are presented[2]; this method is based on the reaction at interface between the reactants in solid state under the action of mechanical force (mixing). The reactions occurring between systems of reactants consists of hydrated crystals of aluminum chloride, nitrate and sulphate and an ammonium base (neutral or acid ammonium carbonate) initially in solid state (powder) at ambient temperature.

Three types of products were obtained, denoted by HTC, HTA and HTS.

The method has two steps: during the former the precursors of aluminum oxides (HT) whose composition corresponds to various mixtures of ammonium hydroxoalumocarbonate and pseudoboehmitic hydroxides (HTC, HTA) or only hydroxide (HTS product).

The latter step of the method, which is the object of this paper, deals with transformation of precursors (HT), through thermal treatments at temperatures t within 500–800°C, into active aluminas, according to the following possible reactions:

---

* Deceased November 10, 1987

$$NH_4[Al(OH)_2CO_3]\cdot nH_2O \xrightarrow{60 < t < 180°\,C} NH_4[Al(OH)_2CO_3] \qquad (1)$$

$$NH_4[Al(OH)_2CO_3] \xrightarrow{180 < t < 340°\,C} AlOOH + NH_3 + CO_2 + H_2O \qquad (2)$$

$$2AlOOH \xrightarrow{340 < t < 550°\,C} Al_2O_3 + 2H_2O \qquad (3)$$

The dependence of textural and structural properties of aluminas resulted (according to conventional notations in Table 1) on the genesis of the precursor and the thermal treatment temperature are discussed in this contribution.

Table 1

The precursors (initial reactants, synthesis products) of obtained aluminum oxides and their conventional notation

Aluminum salt	Synthesis products	Products after thermal activation (Al_2O_3–T)*
$AlCl_3\cdot 6H_2O$	HTC	Al_2O_3 – TC_5 Al_2O_3 – TC_6 Al_2O_3 – TC_7 Al_2O_3 – TC_8
$Al(NO_3)_3\cdot 9H_2O$	HTA	Al_2O_3 – TA_5 Al_2O_3 – TA_6 Al_2O_3 – TA_7 Al_2O_3 – TA_8
$Al_2(SO_4)_3\cdot 18H_2O$	HTS	Al_2O_3 – TS_5 Al_2O_3 – TS_6 Al_2O_3 – TS_7 Al_2O_3 – TS_8

* The subscript refers to thermal activation temperature, $\times 10^{-2}$ °C.

EXPERIMENTAL

HTC, HTA and HTS precursors were thermally treated in an electric furnace with programmed temperature at 500, 600, 700 and 800°C. DTA, TG as well as the determination of structural elements by X-ray diffraction were performed as indicated in a previous contribution.[1]

The physico-structural characteristics were determined as follows: real density, d_r, by pycnometric method with water; apparent density, d_a, which characterizes the secondary particle by pycnometric method with mercury; the volumes of micro and macro-pores from the adsorption isotherms of nitrogen at –196°C and from the programs yielded by the porosimetry with mercury; the radii, R_m, corresponding to the maxima of pore radii distribution were also calculated.

The average pore radius, R_a, the total pore volume, V_t, and the porosity, θ, were calculated by the equations :

$$V_t = \frac{1}{d_a} - \frac{1}{d_r}; \quad R_m = \frac{2V_t}{S_{sp}}; \quad \theta = 1 - \frac{d_a}{d_r}$$

(where S_{sp} is the BET specific surface area)

RESULTS AND DISCUSSION

As already mentioned, the evolution of structural phases that are formed at thermal treatment of precursors (HT) was determined first.

The structural transformations occurring in the lattice of aluminum oxides are mainly caused by the degree of crystal lattice ordonation imposed by the nature and the features of the precursor.$^{3-5}$

The crystalline phases identified by X-ray diffraction are listed in Table 2.

Table 2

Crystalline phases of aluminas, determined by X-ray diffraction, for precursor nature and thermal treatment indicated

Al_2O_3	Crystalline phases	Comments
TC_5	γ (microcrystalline)	symmetrical (400) and (440) peaks*
TC_6	γ (well crystallized)	symmetrical and split (400) and (440) peaks.
TC_7	$\gamma + (\delta)$	splitting and symmetry of (400) and (440) peaks maintained.
TC_8	$\delta + (\gamma)$	peaks corresponding to δ phase become visible at $d = 1.54$ and 1.40 Å.
TA_5	η (poorly crystallized)	marked asymmetry at (400) and (440) peaks
TA_6	η	marked asymmetry at (400) and (440) peaks
TA_7	η	marked asymmetry at (400) and (440) peaks
TA_8	$\eta + (\delta)$	asymmetry of (400) and (440) peaks
TS_5	$\eta + (\gamma)$ (poorly crystalized)	asymmetry for (400) ad (440) peaks with splitting of the latter.
TS_6	$\eta + \gamma$	
TS_7	$\eta + \gamma$	
TS_8	$\eta + \gamma + (\delta)$	weak asymmetry of (400) and (440) peaks; marked tendency of splitting at (400) and evident splitting at (440)

* The (400) peak corresponds to $d = 1.97$ and (440) to $d = 1.399$ Å

The structural evolution of phases during thermal treatment within 500–800°C has shown that, depending on the nature of precursors (HTC, HTA, HTS) the oxides resulted (TC, TA, TS) exhibit various degrees of ordering, as follows :

— the maximum degree of ordering is exhibited by Al_2O_3 — TC which is illustrated by the appearance of phase δ, in appreciable amounts, together with phase γ at 800°C (Fig. 1).

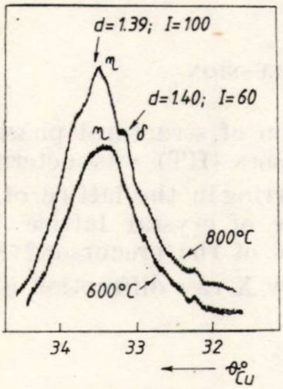

Fig. 1. — The dependence of (440) maximum of TC oxides on calcination temperature.

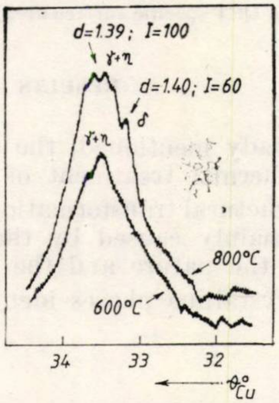

Fig. 2. — The dependence of (440) maximum of TA oxides on calcination temperature.

— in case of Al_2O_3 — TA and Al_2O_3 — TS the structural differences are less obvious, the $\eta-Al_2O_3$ phase remains predominant over the temperature range up to 800°C (Figs. 2, 3).

This observation stands true for the variation of the average crystallite dimension ; it depends on the nature of thermal treatment and the nature of the precursor. For Al_2O_3 — TC one may note in Fig. 4 a normal increase of crystallinity with temperature because of the evolution of a well crystallized phase ; in Al_2O_3 — TA and Al_2O_3 — TS whose phases are

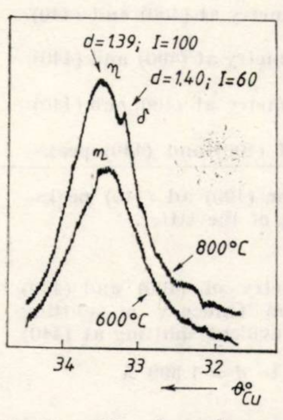

Fig. 3. — The dependence of (440) maximum of TS oxides on calcination temperature.

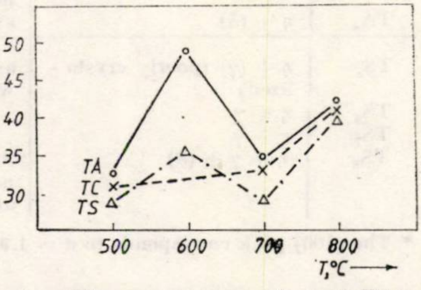

Fig. 4. — The average size of crystallites D_{440} versus the calcination temperature of aluminas.

weakly crystallized one evidences a phenomen of crystallite breaking during the re-arrangement of crystal lattice.

The main textural features are listed in Table 3. Figs. 5—7 show adsorption-desorption isotherms of nitrogen at —196°C while Figs. 8—10 show the distribution curves of pore volumes versus the radius of the three types of aluminas studied.

Table 3

Physical and textural properties of aluminum oxides in the TC, TA and TS series

Al_2O_3	d_r g/cm³	d_a g/cm³	V_t cm³/g	R_m Å	θ	S_{sp} m²/g
TC_5	3.33	0.977	0.7233	70.0	0.71	207
TC_6	3.55	1.052	0.6692	78.3	0.70	171
TC_7	3.58	1.059	0.6641	76.8	0.70	173
TC_8	3.78	1.063	0.6835	84.4	0.73	162
TA_5	3.08	0.958	0.7986	74.3	0.72	215
TA_6	3.34	1.060	0.6510	60.6	0.68	212
TA_7	3.36	1.260	0.4911	63.8	0.62	154
TA_8	3.43	1.320	0.4668	70.2	0.61	133
TS_5	3.16	1.350	0.4341	44.3	0.57	196
TS_6	3.24	1.250	0.4922	55.0	0.61	182
TS_7	3.38	1.270	0.4961	59.1	0.62	168
TS_8	3.48	1.280	0.5003	63.3	0.63	158

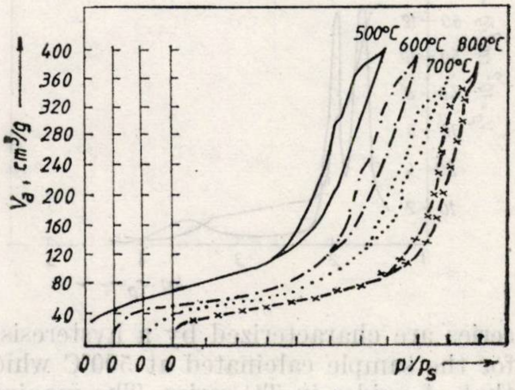

Fig. 5. — The nitrogen adsorption-desorption isotherms for aluminas in TC series.

The oxides in TC series possess a complex pore structure; the hysteresis is more intricate : a combination of the two known types, A and E characteristic of cylindrical or tubular pores of various diameters (Fig. 5). It conveys the pores distribution a peculiar feature : two maxima centred at 50 and 100 Å (Fig. 8) in the range of medium pore radii which were observed in all samples calcinated up to 800°C. The oxides in TA series are characterized by a hysteresis close to type E (Fig. 6), except for the sample calcinated at 500°C which exhibits a hysteresis similar to that of oxides in TC series. The maxima of pores distribution curves lie

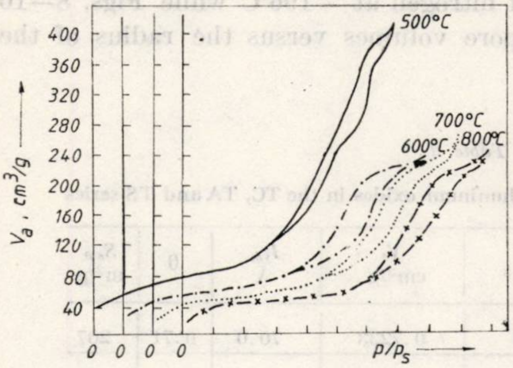

Fig. 6. — The nitrogen adsorption-desorption isotherms for aluminas in TA series.

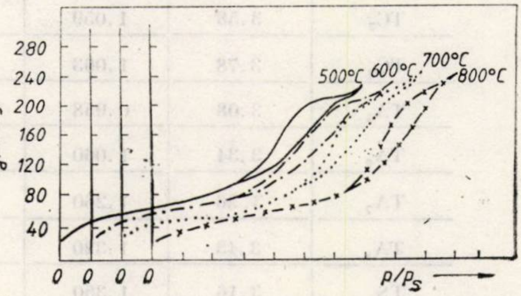

Fig. 7. — The nitrogen adsorption-desorption isotherms for aluminas in TS series.

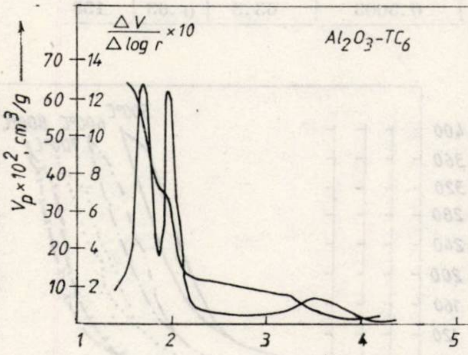

Fig. 8. — The volume pore distribution versus the radii for TC aluminas (exemplified by TC_6 alumina).

at 40 Å. In the oxide calcinated at 500°C there is one more maximum at about 87 Å (Fig. 9).

The oxides in TS series are characterized by a remarkable thermal stability with E-type hysteresis (Fig. 7) and pore radii distributions similar with each other showing maxima within the 35–45 Å range (Fig. 10).

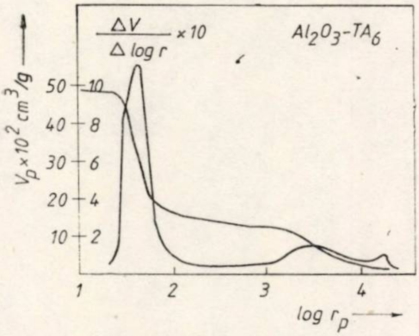

Fig. 9. — The volume pore distribution versus the radii for TA aluminas (exemplified by TA_6 alumina).

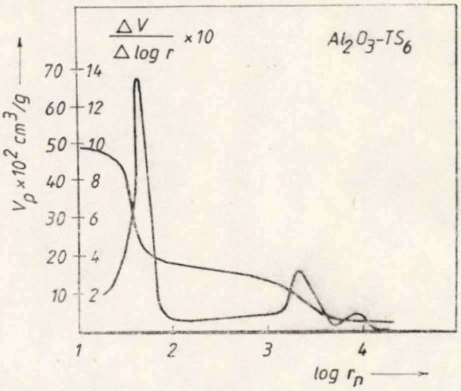

Fig. 10. — The volume pore distribution versus the radii for TS aluminas (exemplified by TS_6 alumina).

The data in Table 3 evidence one decrease of overall pore volume and specific surface with the increase of calcination temperature. For a constant thermal treatment temperature (600°C) the values of overall pore volume increase in the sequence : $Al_2O_3 - TC > Al_2O_3 - TA > Al_2O_3 - TS$.

In conclusion the structural and textural properties of aluminum oxides depend on the degree of ordination and the crystallinity of precursors at given conditions of thermal treatments.

The oxides resulted possess structures and textures which depend on the nature of the precursors and the thermal treatment applied; the surface properties of these oxides ensure the high activity of the obtained catalysts.[6–8]

REFERENCES

[1] I. V. Nicolescu, M. Udrea, A. Nicolescu, I. Udrea and D. Crișan, *Rev. Roumaine Chim.*, part I, see the previous paper.

[2] S. Z. Roghinski, *Doklady Akad. Nauk*, **27**, 453 (1940).

[3] A. Nicolescu, M. Udrea and G. Popa, *Rev. Roumaine Chim.*, **23**, 361 (1978).

[4] J. B. Peri, *J. Phys. Chem.*, **69**, 231 (1965).

[5] B. C. Lippens and J. H. de Boer, *Acta Cryst.*, **17**, 1312 (1964).

[6] I. V. Nicolescu, M. Dardan-Udrea, A. Nicolescu, G. Muscă, I. Suciu, V. Părăușanu, S. Blejoiu and I. Melichian, Romanian Patent, 58724, 20 Nov. 1974.

[7] S. Todireanu, A. Nicolescu, M. Dardan-Udrea and I.V. Nicolescu, *J. Catalysis*, **35**, 472 (1974).

[8] G. Pop, A. Mihai, I. V. Nicolescu, E. Angelescu, V. Ioniță, V. Părăușanu and M. Dardan-Udrea, Romanian Patent, 53011, 7 Aug. 1970.

at 40 Å for the oxide calcined at 1,000°C there is one more maximum at about 87 Å (Fig. 9).

The oxides in TS series are characterized by a remarkable thermal stability (with E1 type structure as (Fig. 5) and their radii distributions similar with each other showing maxima within the 35 – 45 Å range (Fig. 10).

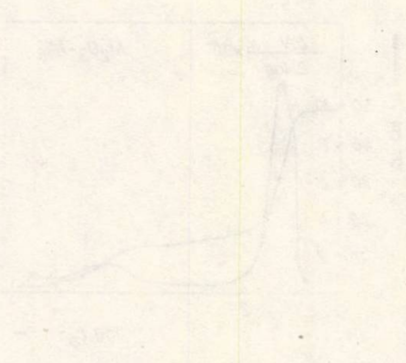

Fig. 9. — The volume pore distribution versus r for E1 alumina (prepared by TA, alumina).

Fig. 10. — The volume pore distribution versus the r for E1 aluminas (prepared by TS, alumina).

The data in Table 3 exhibit the decrease of overall pore volume and specific surface with the increase of calcination temperature. For the same thermal treatment temperature (1,000°C) the values of overall pore volume increase in the sequence: Al_2O_3 – E1 < Al_2O_3 – TA < Al_2O_3 – TS.

In conclusion the structural and textural properties of aluminium oxides depend on the degree of hydration and the crystallinity of the [illegible], as given by conditions of thermal treatments.

The oxides obtained [illegible] regard to [illegible] which depend on the nature of the precursors and the thermal treatment applied; the surface properties of these oxides ensure the high activity of the obtained catalysts[6–8].

REFERENCES

1. V. Nicolescu, M. Ionescu, A. Nicolescu, [illegible] and [illegible], Rev. Roumaine Chim., part I, see the previous paper.
2. [illegible], [illegible], 37, [illegible].
3. [illegible], [illegible] and [illegible], [illegible], 28, 301 [illegible].
4. [illegible], J. Phys. Chem., 60, [illegible].
5. B. C. Lippens and J. H. de Boer, Acta Cryst., 17, 1312 (1964).
6. [illegible], [illegible], [illegible], Romanian patent [illegible].
7. [illegible], [illegible], [illegible], 25, [illegible].
8. [illegible], Romanian Patent [illegible].

Revue Roumaine de Chimie, **33**, *11–12*, 1013–1019 (1988)

CATALYTICALLY ACTIVE ALUMINAS FROM PRECURSORS OBTAINED BY SUPERSATURATION OF REACTANTS. III[1,2]

THE CATALYTIC ACTIVITY OF ALUMINAS IN ISOMERIZATION OF CYCLOHEXENE TEST REACTION

MARIANA UDREA*, I. V. NICOLESCU[a], ALA NICOLESCU[b], I. UDREA[a]
and D. CRIŞAN[b]
[a] Faculty of Chemical Technology, Polizu 1, Bucharest, Romania
[b] Centre of Physical Chemistry, Spl. Independenţei 202, Bucharest, Romania

Received March 16, 1988

The catalytically active aluminas from precursors obtained in conditions of super saturation of reactants were calcinated at 500, 600, 700 and 800°C and tested in reactions of cyclohexene isomerization. The correlation of their activity with the physico-structural properties of samples has yielded relations which characterize the surface of aluminum oxides as a function of precursor nature and thermal treatment. For the samples that do not evidence any phase transition but only a monotonous orientation of the lattice the catalytic activity depends on the extent of the specific surface. On the other hand the formation of a new phase in the system entails a marked increase of activity, probably due either to the increase of active centres concentration at interface between phases or to prevalence of amorphous phase which increases the degree of dispersion and consequently the catalytically active surface.

The previous contributions[1,2] presented an original method of obtaining catalytically active aluminas; the influence of precursor nature upon the physico-structural properties of aluminas was evaluated.

Very often in the literature a disagreement appears between the determinations of acidity on aluminum oxide surfaces and their catalytic activity in acid-basic reactions as isomerization of hydrocarbons, dehydration of alcohols etc.[3,4] This disagreement originates in the dependence of the number of centers that participate in each reaction and their efficiency on factors related to the structural features of reactants, the accessibility of surface and, most of all, the heterogenity of surface; this heterogenity is induced by the distribution and the strength of surface sites which determine the energetics of reactant-catalyst interaction.[5–8]

In this contribution the isomerization of cyclohexene to methylcyclopentene (which is specific to estimation of concentration and strength of acid-type centers) was chosen as model reaction in characterization of active state of studied aluminas.[9]

---

* Deceased November 10, 1987.

This reaction implies two types of isomerizations, both interpreted in terms of the theory of carbonium ions[10,11]:

(1) isomerization on skeleton of cyclohexene to methylcyclopentene;

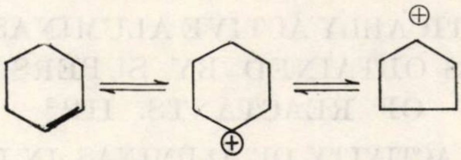

(2) migration of double band into pentanic cycle and out of it according to the scheme:

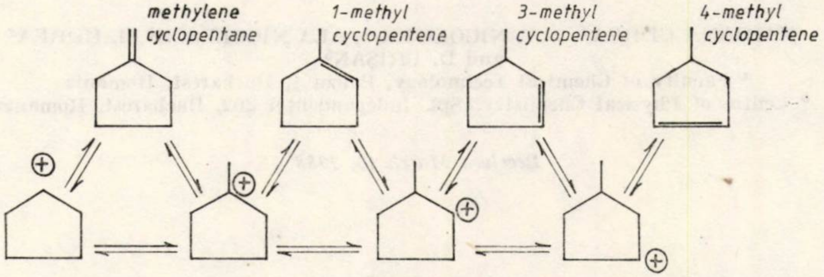

Table 1

The standard free enthalpies and energies of the steps of cyclohexene-methylcyclopentene isomerization reaction*

Reaction	ΔH_r, kcal/mol					ΔG_r, kcal/mol				
	320°	360°	400°	440°	460°	320°	360°	400°	440°	460°
cyclohexene → 1-methylcyclopentene	−0.68	−0.17	−0.85	−0.96	−1.00	−1.8	−2.0	−2.1	−2.1	−2.2
cyclohexene → 3-methylcyclopentene	+2.65	+2.67	+2.55	+2.44	+2.35	+1.1	+1.0	+0.8	+0.8	+0.8
cyclohexene → 4-methylcyclopentene	+4.17	+4.1	+3.97	+3.88	+4.03	+2.3	+2.2	+2.1	+2.0	+2.0
1-methylcyclopentene → 3-methylcyclopentene	+3.33	+3.44	+3.40	+3.40	+2.90	+3.0	+2.9	+2.9	+3.0	+2.94
1-methylcyclopentene → 4-methylcyclopentene	+4.85	+4.87	+4.82	+4.84	+4.84	+4.11	+4.2	+4.2	+4.1	+4.2
3-methylcyclopentene → 4-methylcyclopentene	+1.52	+1.43	+1.42	+1.44	+1.44	+1.21	+1.2	+1.3	+1.2	+1.2

* Thermodynamic data available in reference[13] were used in calculations.

Methylcyclopentene is very unstable such that its equilibrium concentration does not exceed 0.2 — 0.3%.[12]

The standard values of free enthalpies and energies of reaction corresponding to the sequence assumed have shown that, from thermodynamic viewpoint, the most easily achievable is the formation of 1-methylcyclopentene (Table 1); 3-methylcyclopentene is much harder to obtain from cyclohexene while 4-methylcyclopentene may result only from 3-methylcyclopentene, obviously at high temperatures.

EXPERIMENTAL

The studied alumina samples, resulted from activation of precursors obtained in conditions of supersaturation of reactants[1,2] at 500, 600, 700 and 800°C are listed in Table 2.

Table 2

The precursors (initial reactants, synthesis products) of obtained aluminum oxides and their conventional notation

Aluminum salt	Synthesis products	Products after thermal activation (Al_2O_3 — T)*
$AlCl_3 \cdot 6\ H_2O$	HTC	Al_2O_3 — TC_5 Al_2O_3 — TC_6 Al_2O_3 — TC_7 Al_2O_3 — TC_8
$Al(NO_3)_3 \cdot 9\ H_2O$	HTA	Al_2O_3 — TA_5 Al_2O_3 — TA_6 Al_2O_3 — TA_7 Al_2O_3 — TA_8
$Al_2(SO_4)_3 \cdot 18\ H_2O$	HTS	Al_2O_3 — TS_5 Al_2O_3 — TS_6 Al_2O_3 — TS_7 Al_2O_3 — TS_8

* The subscript refers to thermal activation temperature, $\times 10^{-2}$ °C.

The activity tests were carried out in a flow reactor with 12 cm^3 catalyst, under atmospheric pressure.

Before each reaction the catalyst was activated one hour in the reactor at 500°C in air stream then cooled in pure nitrogen atmosphere at reaction temperature.

The catalytic activity of samples was determined within 320 — 460° at a reactant space velocity of 1 h^{-1}.

The times required to reach the working regime and stationary state were recorded in each experiment.

The stationary state of the catalyst was checked by resuming the activity tests at a lower temperature within the studied range; the conversion values obtained in identical experimental conditions were the same with the previous results.

The structures of studied aluminas were determined by X-ray diffraction with a TUR-M 61 apparatus equipped with HZG-3 diffractometer and a VAD-53.1 recording potentiometer; Cu K-α radiation filtered with nickel was employed; the tube voltage was 30 kV while the goniometer speed was 0.5 degrees/min.

The specific surfaces were determined by BET method of nitrogen adsorption isotherms at — 196°C making use of a Carlo Erba sorptometer.

RESULTS AND DISCUSSION

The following criteria of activity evaluation were employed to classify samples according to their capacity of catalyzing the reaction of isomerization of cyclohexene : T_j — the temperature corresponding to a 50% transformation, the conversion and the selectivity.

The dependence of these parameters on the reaction temperature and the physico-structural properties of samples has afforded the establishing of certain relations which characterize the surface of aluminium oxides in terms of the origin of the sample (the nature of the precursor) and the thermal treatment applied.

The experimental results carried out within 320 — 460°C at a space velocity of 1 h^{-1} evidence the difference of catalytic behaviour between the aluminas studied.

Thus, if the criterion of activity evaluation is the temperature corresponding to a 50% transformation, (Figs. 1—3) the aluminas are arranged in a sequence of decreasing activity and increasing T_j values as follows :

$$\mathrm{TC} > \mathrm{TA} > \mathrm{TS}$$

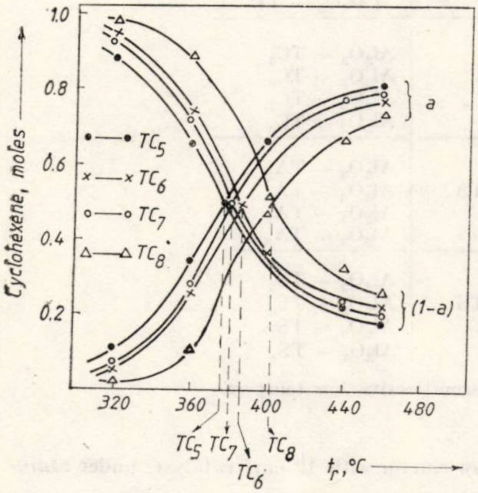

Fig. . — Temperature dependence of the number of moles of converted (a) and unconverted 1-a) cyclohexene for TC samples. T_j has the values : 377, 387, 381 and 402°C for TC_5, TC_6, TC_7, TC_8 respectively.

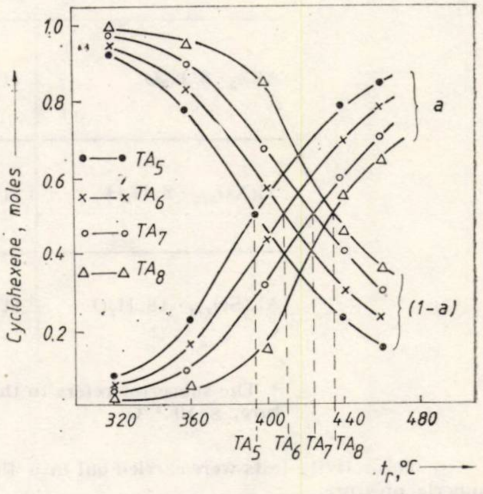

Fig. 2. — Temperature dependence of the number of moles of converted (a) and unconverted (1-a) cyclohexene for TA samples. T_j has the values 394, 410, 425 and 435 °C for TA_5, TA_6, TA_7 and TA_8 respectively.

On the other hand, taking account of the difference between the concentrations of isomers obtained at stationary state, C_{st} and at equilibrium C_{eq} (Table 3) for various temperatures, curves that illustrate a certain rate of reaching equilibrium on the surface are obtained. The more active are the aluminas, the higher is this rate, hence $\Delta(C_{e1} - C_{st})$ approaches zero.

Fig. 4 shows the $\Delta(C_{eq} - C_{st})$ curves versus temperature only for 1-methylcyclopentene, because the reactions of obtaining 3- and 4-methylcyclopentenes are parallel with that for 1-methyl-cyclopentene.

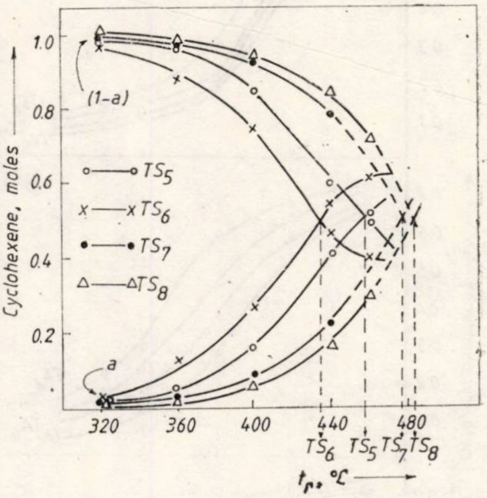

Fig. 3. — Temperature dependence of number of moles of converted (a) and unconverted (1-a) cyclohexene for TS samples. T_j has the values 457, 435, 476 and 482°C for TS_5, TS_6, TS_7 and TS_8 respectively.

Figs. 5—8 show the dependence of conversion on the temperature of alumina calcination. Thus oxides in TC series show two maxima of activity for samples activated at 500° and 700°C respectively (Fig. 5), the TS aluminas one maximum corresponding to samples at 600°C (Fig. 6) while TA aluminas exhibit a continuous decrease with calcination temperature (Fig. 7). The phenomenon illustrates the processes of crystallization and phase transitions occurring during thermal treatment.[2]

Table 3

The values of equilibrium concentration of isomers in the temperature range 320—460°C

Reaction temperature, °C	Equilibrium concentration, %		
	1-methyl-cyclo-pentene	(3 + 4)-methyl cyclo-pentene	unconverted cyclohexene
320	72.3	18.7	9.00
360	71.1	20.4	8.50
400	70.0	22.0	8.0
440	69.2	23.5	7.3
460	68.7	24.3	7.0

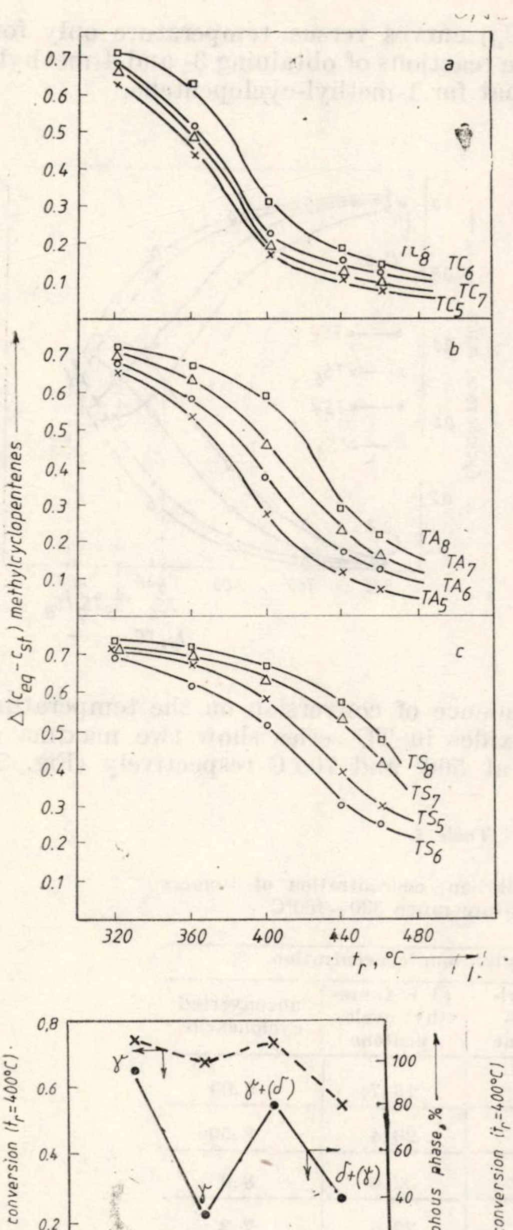

Fig. 4. – The $\Delta(C_{eq} - C_{st}) = f(T)$ curves for a) TC aluminas; b) TA aluminas; c) TS aluminas.

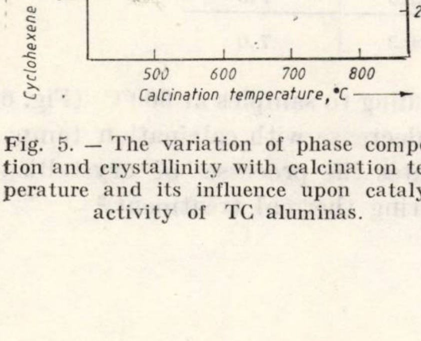

Fig. 5. – The variation of phase composition and crystallinity with calcination temperature and its influence upon catalytic activity of TC aluminas.

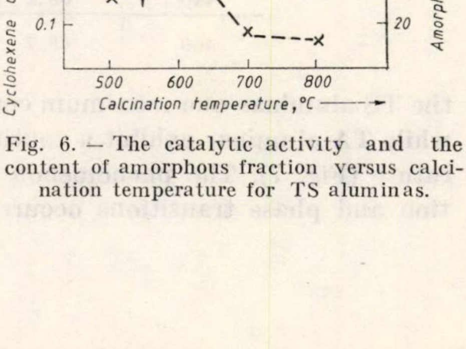

Fig. 6. – The catalytic activity and the content of amorphous fraction versus calcination temperature for TS aluminas.

Wherever no phase transition is evidenced and only a monotonous ordering of lattice occurs the decrease of catalytic activity is determined by the decrease of specific surface (the case of TA-aluminas, Fig. 7).

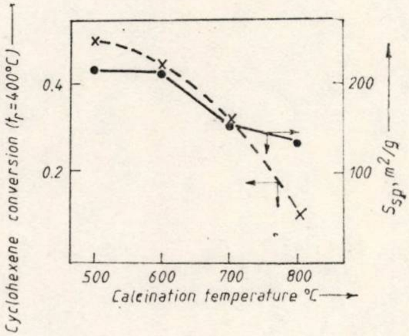

Fig. 7. — Simultaneous decrease of the activity and the specific surface with the calcination temperature for TA aluminas.

The formation of new phases in the system is accompanied by an increase of activity probably due to the increase of concentration of active centres at phase interface or to the preponderance of amorphous phase which rises the degree of dispersion and consequently the catalytically active surface area (the case of TC_7 alumina in which a new δ-Al_2O_3 phasis is formed besides γ Al_2O_3 — Fig. 5).

Thus TS_5 alumina is an anomaly. Although it possesses a very high percent of amorphous phase and is characterized, from structural viewpoint, by the coexistence of two phases, η and γ the activity of TS_5 sample is unexpectedly low (Fig. 6). This might ascribe either to the blocking of active centres with strongly adsorbed reacting molecules or to some diffusion limitations.

REFERENCES

[1] I. V. Nicolescu, M. Udrea, A. Nicolescu, I. Udrea and D. Crisan, *Rev. Roum. Chim.*, part I, see the previous papers.

[2] M. Udrea, I. Udrea, A. Nicolescu, D. Crisan and I.V. Nicolescu, *Rev. Roum. Chim.*, part II, see the previous papers.

[3] A. Ghorbel, H. V. Can and S. Y. Teichner, *J. Catal.*, **30**, 298 (1973).

[4] L. Forni, *Catal. Rev.*, **8**, 65 (1973).

[5] E. Wicke, "Mémoire de la Société Royale des Sciences de Liège", 1971, p. 211.

[6] N. Wakao and J. M. Smith, *Ind. Eng. Chem. Fundamentals*, **3**, 123 (1964).

[7] R. W. Maatman, *J. Catal.*, **19**, 64 (1970).

[8] M. I. Temkin, *Kinet. Katal.*, **13**, 555 (1972).

[9] I. V. Nicolescu, A. Nicolescu, M. Gruia, A. Terlecki-Baricevič and M. Dardan-Udrea, "Proc. Int. Congr. Catal. 4th Moscow 1968", Akad. Kiado, Budapest, 1971, vol. 2, p. 388.

[10] J. E. Germain, L. Bassery and M. Blanchard, *Bull. Soc. chim. France*, 958 (1958).

[11] L. Bassery, *Bull. Soc. chim. France*, 1077 (1969).

[12] L. Bassery, Thèse, Université de Lille, 1965.

[13] D. R. Stull, E. F. Westrum jr. and G. C. Sinke, "The Chemical Thermodynamics of Organic Compounds", John Wiley, New York, 1969.

[14] A. Wheeler, "Catalysis", 1955, vol. 2, p. 105.

Whenever no phase transition is evidenced and only a monotonous ordering of lattice occurs the decrease of catalytic activity is determined by the decrease of specific surface (the case of TA aluminas, Fig. 7).

Fig. 7. — Simultaneous decrease of the activity and the specific surface with the calcination temperature for TA aluminas.

The formation of new phases in the system is accompanied by an increase of activity, probably due to the increase of concentration of active centres at phase interface or to the preponderance of amorphous phase which rises the degree of dispersion and consequently the catalytically active surface area (the case of TC_1 alumina in which a new δ-Al_2O_3 phase is formed besides γ-Al_2O_3, Fig. 1).

Thus TS_1 alumina is an anomaly. Although it possesses a very high amount of amorphous phase and is characterized, from structural viewpoint, by the coexistence of two phases, χ and γ, the activity of TS_1 sample is unexpectedly low (Fig. 6). This might ascribe either to the blocking of active centres with strongly adsorbed reacting molecules or to some diffusion limitations.

REFERENCES

[1] I. V. Nicolescu, M. Ilieva, V. Nicolescu [illegible] and D. Gavra, Rev. Roum. Chim., part I, see the previous paper.

[2] M. Ilieva, I. Andrei, A. Vasilescu, D. [illegible] and I. V. Nicolescu, Rev. Roum. Chim., part II, see the previous paper.

[3] V. [illegible], D. [illegible] and S. [illegible], J. Catal., 23, [illegible] (1972).

[4] L. Pottel, [illegible], 8, 75 (1971).

[5] [illegible], "Mémoire de la Société Royale des Sciences de Liège", 1971, p. [illegible].

[6] [illegible] and [illegible] Smith, Adv. Catal. [illegible], 8, 123 (1956).

[7] R. W. Maatman, J. Catal., 19, 64 (1970).

[8] M. [illegible], J. Catal., 17, [illegible] (1972).

[9] I. V. Nicolescu, [illegible], M. [illegible], [illegible] and M. [illegible], Proc. Int. Congr. Catal., 4th Moscow (1968), Akad. Kiado, Budapest, 1971, vol. 2, p. [illegible].

[10] [illegible], [illegible] and M. [illegible], Bull. Soc. chim. France, [illegible].

[11] L. [illegible], Bull. Soc. chim. France, 1957 (1957).

[12] [illegible], Thesis, Université de [illegible], 1965.

[13] D. R. Stull, E. F. Westrum jr. and G. C. Sinke, "The Chemical Thermodynamics of Organic Compounds", John Wiley, New York, 1969.

[14] A. Wheeler, "Catalysis", 1955, vol. 2, p. 105.

Revue Roumaine de Chimie, **33**, *11–12*, 1021–1030 (1988)

CATALYTICALLY ACTIVE ALUMINAS FROM PRECURSORS OBTAINED BY SUPERSATURATION OF REACTANTS. IV[1–3]

KINETICS OF CYCLOHEXENE ISOMERIZATION

MARIANA UDREA*, I. UDREA,[a]
I. V. NICOLESCU[a] and ALA NICOLESCU[b]
[a]Faculty of Chemical Technology, Polizu 1, Bucharest, Romania
[b]Centre of Physical Chemistry, Spl. Independenţei 202, Bucharest, Romania

Received March 16, 1988

The kinetics of cyclohexene isomerization on catalytically active aluminas prepared from precursors obtained in conditions of supersaturation of reactants was studied. The intrinsic rate constants were determined from experimental rate constants corrected with the effectiveness factor. The correlation of catalytic activity with the apparent activation energies determined from Arrhenius curves has revealed the presence of a compensation effect for aluminas originating in different precursors. It was established that this effect may be accounted for by the modification of active centres concentration and distribution on the surface of these aluminas which is caused by the nature of the precursor and the thermal treatment applied.

In previous contributions [1–3] an original method was described for preparing catalytically active aluminas from precursors obtained in conditions of supersaturation of reactants; the physico-structural properties of aluminas and their dependence on the nature of precursors and on the thermal treatment applied were also discussed there together with the way these properties are mirrored by the catalytic activity of samples in the cyclohexene isomerization reaction.

This note deals with determination of rate constants for the aluminas employed in isomerization of cyclohexene, with establishing to what extent the diffusive limitations affect the values of these rate constants and with calculations of apparent activation energy and of pre-exponential factors.

EXPERIMENTAL

The samples of aluminas studied, resulted from activation of precursors obtained in conditions of supersaturation of reactants[1,2] at 500, 600, 700 and 800°C are listed in Table 1.

The activity tests were performed in a laboratory device equipped with dynamic regime microreactor making use of 12 cm^3 of catalyst.

---

* Deceased November 10, 1987

Before each reaction the catalyst was activated one hour in reactor at 500°C in air stream then cooled in pure nitrogen to reaction temperature.

The catalytic activity of samples was determined within 320–460°C at reactant space velocities of 0.8, 1.0, 1.2 and 1.4 h^{-1}.

Table 1

The precursors (initial reactants synthesis products) of obtained aluminum oxides and their conventional notation

Aluminum salt	Synthesis products	Products after thermal activation (Al_2O_3 – T)*
$AlCl_3 \cdot 6H_2O$	HTC	Al_2O_3 – TC_5 Al_2O_3 – TC_6 Al_2O_3 – TC_7 Al_2O_3 – TC_8
$Al(NO_3)_3 \cdot 9\,H_2O$	HTA	Al_2O_3 – TA_5 Al_2O_3 – TA_6 Al_2O_3 – TA_7 Al_2O_3 – TA_8
$Al_2(SO_4)_3 \cdot 18\,H_2O$	HTS	Al_2O_3 – TS_5 Al_2O_3 – TS_6 Al_2O_3 – TS_7 Al_2O_3 – TS_8

* The subscript refers to thermal activation temperature, $\times 10^{-2}$ °C.

The time required to reach the operating state and the stationary state was recorded in each run.

The stationary state of the catalyst was checked by resuming the activity tests at a lower reaction temperature within the range in study to see if the same values of conversion previously found are obtained in the same conditions of experiment.

The reaction products collected were analyzed by chromatography on a column with 400-polyethylene glycol as packing 4 m long at 45°C and with hydrogen as carrier gas.

RESULTS AND DISCUSSION

In catalytic heterogeneous reactions the dependence of reaction rate on the composition of reaction mixture and temperature ($p = 1$ at) may be written as follows:

$$r = k(T) \cdot f(C_i,\ C_j) \tag{1}$$

Solving function f in eqn. (1) is rather difficult and therefore it is handier to evaluate the catalytic activity from the rate constant which depends only on temperature.

The determination of rate constants is based on the following considerations:

(1) isomerization on aluminas under study within 320 – 460°C obeys a first or pseudo-first order kinetics;

(2) the reaction occurs mainly on the internal surface of pores;
(3) the temperature gradient in catalyst bed is negligible.

For the first order reaction the rate constants may be determined by the equation:

$$2.3 \log \frac{1}{1 - x/x_{eq}} = k \cdot \varphi_R \tag{2}$$

where x stands for conversion, x_{eq} for equilibrium conversion, k for the rate constant, φ_R for the contact time.

The contact time (seconds) may be calculated by the equation:

$$\varphi_R = \frac{273}{T} \cdot \frac{3600 \cdot M}{d_L \cdot 22400} \cdot \frac{V_c}{F} \cdot \frac{d_p}{d_a} \tag{3}$$

where T is temperature (°K), d_L the density of liquid cyclohexene (g/cm^3), M the number of cyclohexene moles, F the flow rate (cm^3/hour), V_c the volume of catalyst bed (cm^3), d_a the apparent density of catalyst grains (g/cm^3), d_p the density of catalyst bed (g/cm^3).

The d_p/d_a ratio which enters φ_R calculations takes account of the correction related to the compactness of catalyst grains in the reactor.

The plots of conversion versus the time of contact in the coordinates of eqn. (2) yield, in most aluminas investigated, straight lines passing through the origin as in Fig. 1 proving that the reaction order is close to one.

The only deviations from linearity were found in TS$_6$ alumina at reaction temperatures over 400°C. They are probably due either to the modification of adsorption-desorption equilibrium of the reactant and reaction products on catalyst surface or to the presence of diffusive limitations.

Thus, as temperature rises, the values of experimental rate constants calculated by eqn. (2) in terms of conversion data should come out lower because of diffusive impediments induced by the dimensions and sizes of pores. Then, the degree of accessibility of surface expressed as effectiveness factor η decreases.[4]

The effectiveness factor defined as:

$$\eta = \frac{\text{experimental reaction rate}}{\text{theoretical reaction rate in absence of diffusive limitations}} \tag{4}$$

varies from zero to one.

The one value which shows the maximum degree of surface utilization is reached only when the reaction rate is not affected by diffusion.

The $\eta < 1$ values point to a hindering of mass transfer through diffusion which is stronger for lower η values.

Determination of effectiveness factor affords correcting of the experimental rate constant, k_{exp}, so that to obtain the intrinsic rate constant,

k_v, according to the equation :

$$k_{exp} = k_v \cdot \eta \tag{5}$$

Determining the effectiveness factor comes in fact to knowing Thiele dimensionless modulus, h, which may be expressed as :

$$h = L\sqrt{\frac{k_v \cdot d_a}{D_{eff}}} \tag{6}$$

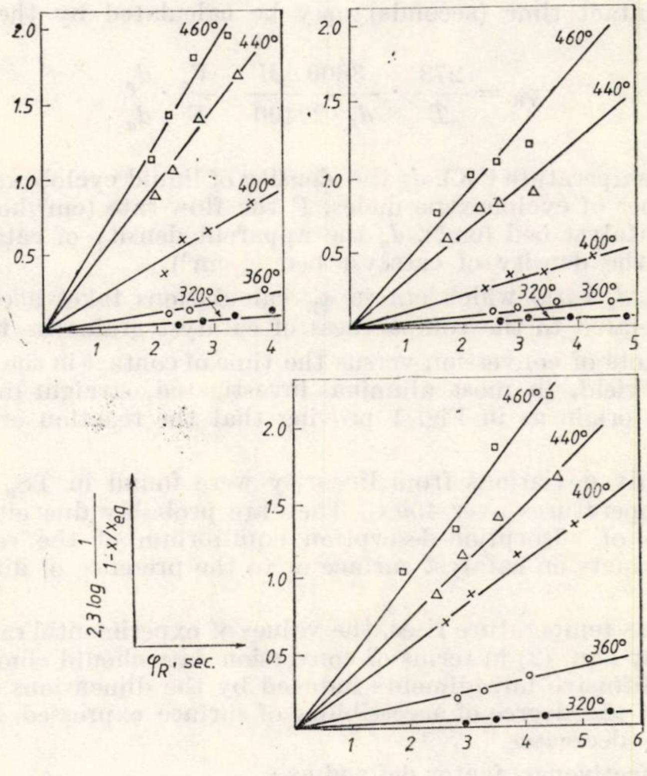

Fig. 1. — The plots of log $\frac{1}{1 - x/x_{eq}}$ versus φ_R for samples :
(a) — TA_6, (b) — TS_6, (c) — TC_6.

where L is the length of pores, k_v the intrinsic rate constant, d_a the apparent density and D_{eff} the effective diffusion coefficient, η being related to h through the equation :

$$\eta = \frac{1}{h}\left[\frac{1}{\tanh 3h} - \frac{1}{3h}\right] \tag{7}$$

In practice because the experimental rate constants k_{exp} were known, to calculate η use has been made of the experimental modulus, Φ which illustrates the competition between the chemical and diffusive process[5] through the equation :

$$\Phi = \frac{k_{exp}}{k_D} \tag{8}$$

The quantity k_D represents the diffusion constant whose value for spherical as well as cyclindrical particles is given by the equation :

$$k_D = \frac{36 D_{eff}}{a^2 \cdot d_a} \cdot d_p \tag{9}$$

where a stands for the diameter of catalyst particle.

The D_{eff} coefficient may be determined by the equation :

$$D_{eff} = \frac{D\theta}{\tau} \tag{10}$$

where θ is the porosity of the sample, τ the tortuosity which takes account of the shape and length of the pore and D the overall diffusion coefficient.

The overall diffusion coefficient includes the coefficients of ordinary molecular diffusion occurring in gas phase and in macro-pores, D_{12}, and Knudsen diffusion in micro-pores, D_K, according to the equation :

$$\frac{1}{D} = \frac{1}{D_{12}} + \frac{1}{D_K} \tag{11}$$

The diffusion coefficient D_{12} may be calculated by an equation deduced on the basis of modern kinetic theory and the Lennard-Jones expression for intermolecular forces[6] for a binary gas mixture; this equation applied to cyclohexene (CH)-methyl-cyclopentene (MCP) system may be written as follows :

$$D_{12} = \frac{0.001858 T^{3/2} (2/M)^{1/2}}{P \sigma_{12}^2 \Omega_D} \tag{12}$$

where T is the absolute temperature (°K), $M = M_{(\mathrm{CH})} = M_{(\mathrm{MCP})} = 82.41$ is the molecular weight of interdiffusing gases, P the overall pressure (at), Ω_D the collision integral as a function of KT/ε_{12}; σ_{12}, ε_{12} the force constants entering the Lennard-Jones potential function which may be calculated by the following empirical quations :

(a) for component "i" of gas mixture :

$$\frac{KT}{\varepsilon_i} = 1{,}3 \frac{T}{T_c^i}$$

where T_c^i is the critical temperature : $T_c^{(\mathrm{CH})} = 560$, $T_c^{(\mathrm{MCP})} = 517.7$, $\sigma_i = 1.18 (V_b^i)^{1/3}$, V_b^i is the molar volume at the normal boiling temperature of component "i" calculated additively from atomic volume increments: $V_b^{(CH)} = 110.8$; $V_b^{(MCP)} = 114.3$;

(b) for binary gas mixtures:

$$\frac{KT}{\varepsilon_{12}} = \frac{KT}{\sqrt{\varepsilon_1 \varepsilon_2}}; \quad \sigma_{12} = \frac{1}{2}(\sigma_1 + \sigma_2) = 5.697$$

The experimental values D_{12} for cyclohexene-methylcyclopentene system within 320–460°C range between 0.1042 and 0.1568 cm²/s.

Knudsen diffusion coefficients, D_K, were determined by an equation developed for the model of cylindrical pores:

$$D_K = 9700 \cdot r_m \sqrt{\frac{T}{M}} \tag{13}$$

where r_m is the average radius of pores (cm), M the molecular weight of diffusing substance.

The D_K values for samples under study at 320–460°C are within 0.0115–0.0245.

Once the diffusion coefficients D_{12} and D_K are known the overall diffusion coefficients (D) were calculated by eqn. (11) and the effective diffusion coefficients by eqn. (10).

In the calculations the empirical value for tortuosity $\tau = 2$ suggested by Wheeler for idealized cylindrical pore model was eliminated because, as numerous experimental data suggest, it does not always stand true. More useful was considered the direct utilization of $\frac{\theta}{\tau} = 0.12$ values resulted from Katzuzawa et al's.[7] experiments as a characteristic constant of aluminas with textural properties similar to those of aluminas we studied and independent of the nature of diffusing gases.

The values of effective diffusion coefficients for the aluminas studied range within 0.00124 (TS_5 sample) and 0.00238 (TC_6 sample).

The effective diffusion coefficients have allowed calculation of diffusion constants, k_D, by eqn. (9) and of experimental modulus Φ by eqn. (8).

η, Φ and h are related by the equation:

$$\eta = \frac{\Phi}{h^2} \text{ or else } \Phi = \eta \cdot h^2 \tag{14}$$

such that:

$$\Phi = h\left[\frac{1}{\tanh 3h} - \frac{1}{3h}\right] \tag{15}$$

Solving eqns. (14) and (15) for h yields a direct relationship between η and Φ representing a simple curve (Fig. 2) which afforded interpolation of effectiveness factor and whose validity was checked on a large number of catalysts.[5]

The results for active aluminas at 500°C are listed in Table 2.

Examination of the data in Table 2 shows that at reaction temperatures higher than 400°C the Φ values lie between 1 and 2 evidencing the existence of diffusion limitations. At temperatures below 400°C the low Φ values (high η values) suggest that in these conditions diffusion is not rate-determining.

The curves showing the temperature dependence of experimental constants in Arrhenius coordinates (Figs. 3–5) bent at 400°C.

Introducing the surface accessibility correction through eqn. (5) and plotting the intrinsic rate constants k_v versus temperature in Arrhenius coordinates one obtains the linearization of curves. The break at 400°C is observed only for aluminas in TC series (Fig. 5) probably because of carbon deposition on surface as a consequence of the higher acidity of these samples.[8]

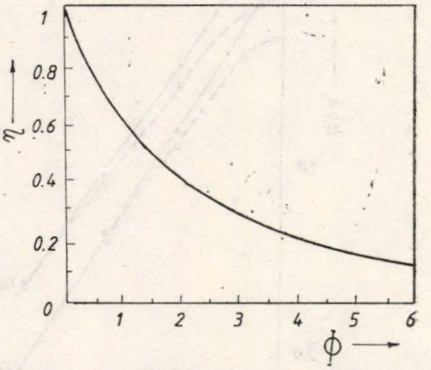

Fig. 2. — Experimental $\eta = f(\Phi)$ plot.

Table 2

Kinetic parameters for aluminas activated at 500°C

Alumina	t_r (°C)	x/x_{eq}	k_{exp} (s^{-1})	k_D (s^{-1})	Φ	η	k_v
TC_5	320	0.127	0.0367	0.348	0.105	0.96	0.0382
12 mL = 5.9 g	360	0.376	0.126	0.363	0.347	0.86	0.147
$d_a = 1.053$	400	0.728	0.422	0.374	1.128	0.768	0.549
$d_p = 0.492$	440	0.820	0.588	0.394	1.492	0.650	0.905
	460	0.874	0.631	0.404	1.563	0.503	1.254
TA_5	320	0.082	0.022	0.517	0.043	0.980	0.0224
12 mL = 5.8 g	360	0.243	0.0785	0.540	0.145	0.932	0.0842
$d_a = 0.958$	400	0.598	0.273	0.564	0.484	0.805	0.339
$d_p = 0.48$	440	0.836	0.554	0.588	0.941	0.542	1.02
	460	0.906	0.774	0.598	1.294	0.560	1.375
TS_5	320	0.023	0.0052	0.258	0.021	0.99	0.0053
12 mL = 8.45 g	360	0.038	0.0187	0.272	0.068	0.97	0.0193
$d_a = 1.35$	400	0.172	0.0493	0.282	0.175	0.92	0.0536
$d_p = 0.704$	440	0.442	0.175	0.293	0.599	0.78	0.224
	460	0.556	0.249	0.296	0.842	0.692	0.360

Arrhenius plots were employed to calculate the activation energies of the isomerization reaction and the pre-exponential factors, k_0, whose values corrected by least square method are listed in Table 3.

One may note that in a series of aluminas of the same provenience the most active samples are characterized by the lowest activation energies.

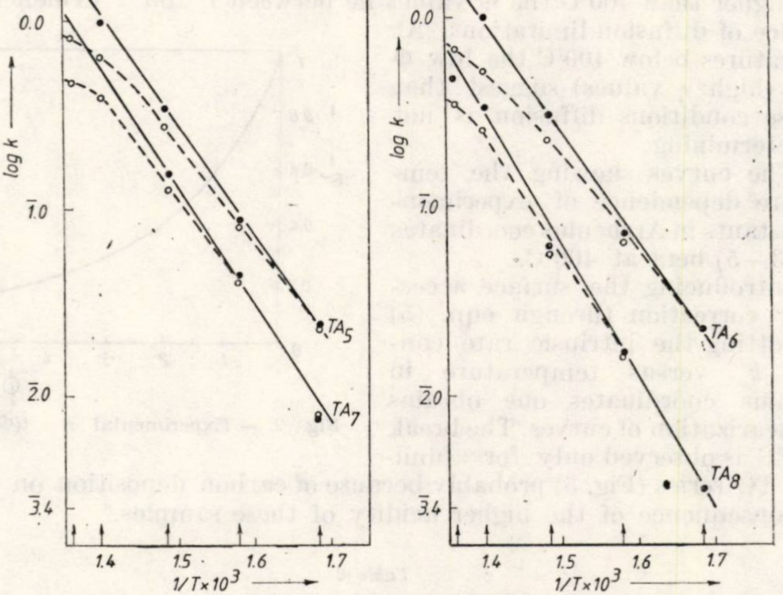

Fig. 3. — Arrhenius plots for TA series aluminas :
— — — $\log k_{exp} = f(1/T)$, ——— $\log k_v = f(1/T)$.

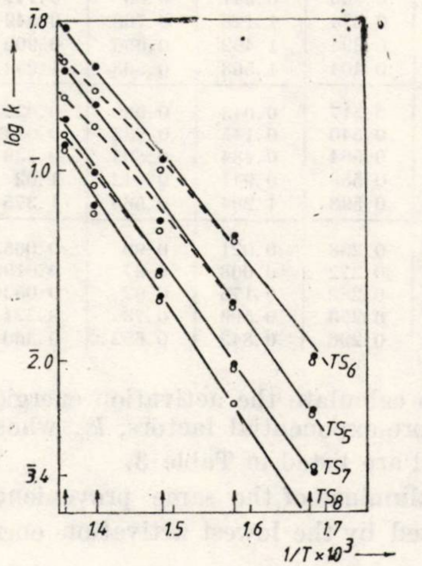

Fig. 4. — Arrhenius plots for TS series aluminas :
— — — $\log k_{exp} = f(1/T)$, ——— $\log k_v = f(1/T)$.

However a comparison of aluminas originating in different precursors thermally activated at the same temperature evidences an abnormal variation of apparent activation energy with catalytic activity, the most active sample exhibiting the highest E_a value. The phenomenon is characterized by a linear dependence of the pre-exponential factor on the apparent activation energy (Fig. 6) which illustrates the compensation effect in these aluminas.

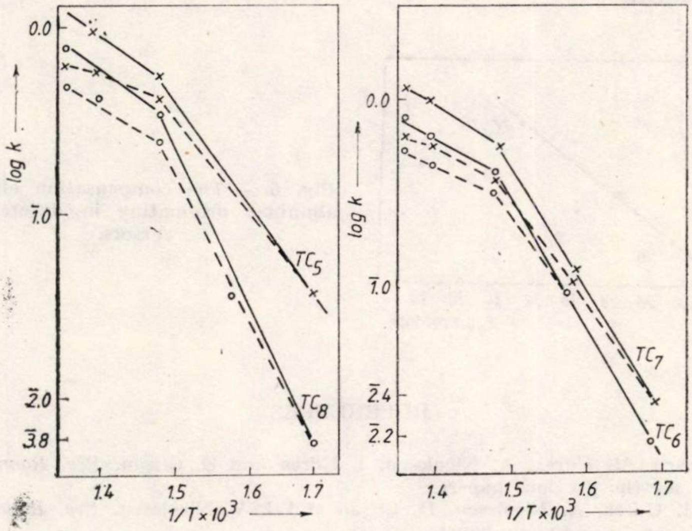

Fig. 5. — Arrhenius plots for TC series aluminas : — — — log $k_{exp} = f(1/T)$, ——— log $k_v = f(1/T)$.

Table 3

Activation energies and pre-exponential factors for cyclohexene isomerization onto studied aluminas

Alumina	E_a (kcal/mol)	log k_0
TA_5	26.75	8.22
TA_6	27.45	8.39
TA_7	28.47	8.61
TA_8	31.37	9.03
TC_5	26.01	8.92
TC_6	32.79	10.25
TC_7	30.05	9.59
TC_8	40.26	12.59
TS_5	25.49	7.13
TS_6	24.61	7.10
TS_7	25.97	7.20
TS_8	28.86	7.71

Because in heterogeneous catalysis k_0 is considered proportional to the number of active centres one may assign this effect to the modification of active centres concentration and distribution on aluminum oxide surface which, in its turn is determined by the nature of precursor and the thermal treatment.

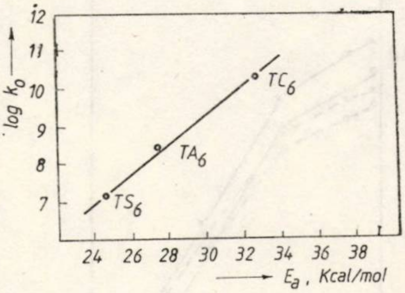

Fig. 6. — The compensation effect for aluminas originating in different precursors.

REFERENCES

[1] I. V. Nicolescu, M. Udrea, A. Nicolescu, I. Udrea and D. Crișan, *Rev. Roumaine Chim.*, part I, see the previous papers.

[2] M. Udrea, I. Udrea, A. Nicolescu, D. Crișan and I. V. Nicolescu, *Rev. Roumaine Chim.*, part II, see the previous papers.

[3] M. Udrea, I. V. Nicolescu, A. Nicolescu, I. Udrea and D. Crișan, *Rev. Roumaine Chim.*, part III, see the previous papers.

[4] C. N. Scetterfield, "Mass Transfer in Heterogeneous Catalysis", MIT Press, 1970.

[5] R. Montarnal, Thesis, Université de Paris, 1966.

[6] J. O. Hirschfelder and C. F. Curtis, "Molecular Theory of Gases and Liquids", Wiley, New York, 1954.

[7] H. Katzuzawa, J. Kobayashi and I. Higuki, *Nippon Kagaku Kaishi*, 1, 27 (1974).

[8] I. V. Nicolescu, M. Udrea, A. Nicolescu and L. Frunză, *Rev. Roumaine Phys.*, **24**, 673 (1979).

Revue Roumaine de Chimie, **33**, *11–12*, 1031–1039 (1988)

CATALYTICALLY ACTIVE ALUMINAS FROM PRECURSORS OBTAINED BY SUPERSATURATION OF REACTANTS. V[1–4]

ADSORPTION OF CYCLOHEXENE BY GAS CHROMATOGRAPHY

MARIANA UDREA*, I. V. NICOLESCU[a], I. UDREA[a]
and ALA NICOLESCU[b]
[a]Faculty of Chemical Technology, Polizu 1, Bucharest, Romania
[b]Centre of Physical Chemistry, Spl. Independenței 202, Bucharest, Romania

Received March 16, 1988

Use has been made of gas chromatography in study of cyclohexene adsorption (at low coverage) on aluminas prepared by an original method. The variation of the main thermodynamic quantities is discussed regarding the reactant-active surface interaction energetics in the pre-catalytic stage (130–170°C) and its influence upon the performance of aluminas studied in the isomerization of cyclohexene.

In previous parts [1–4] an original method for preparing catalytically active aluminas from precursors obtained in conditions of reactant supersaturation was presented; the physico-structural properties of aluminas determined by precusor nature and thermal treatment applied and the way these properties are mirrored by the catalytic activity of samples in isomerization of cyclohexene were also discussed. On the basis of variations of the main thermodynamic and kinetic quantities useful correlations were established which characterize the surface of aluminas and the energetics of reactant-catalyst interaction.

To supplement information regarding the reactant-surface interaction in this contribution a study of cyclohexene adsorption at low coverage by gas chromatography was undertaken. The chromatographic method is outstandingly profitable in characterization of heterogeneous surfaces because it evidences the most energetic centres whose affinity towards the reactant is highest.[5]

The system under study, cyclohexene-aluminum oxide, belongs to the systems with specific interactions[6] achieved through participation of π electrons of cyclohexene to the bond with surface acceptors.

The results obtained have a particular significance as they allow elucidation of the specific adsorption effect upon the elementary act of catalytic process.[7]

---

* Deceased November 10, 1987

EXPERIMENTAL

The experimental determinations were carried out on a GCHF 18.2 gas chromatograph equipped with columns 0.6 cm in diameter and 1 m long, at 130—170°C.

The aluminas studied, resulted from activation of precursors obtained in conditions of supersaturation of reactants[1,2] at 500, 600, 700 and 800°C are listed in Table 1.

Table 1

The precursors (initial reactants, synthesis products) of obtained aluminum oxides and their conventional notation

Aluminum salt	Synthesis products	Products after thermal activation (Al_2O_3—T)*
$AlCl_3 \cdot 6H_2O$	HTC	$Al_2O_3 - TC_5$
		$Al_2O_3 - TC_6$
		$Al_2O_3 - TC_7$
		$Al_2O_3 - TC_8$
$Al(NO_3)_3 \cdot 9H_2O$	HTA	$Al_2O_3 - TA_5$
		$Al_2O_3 - TA_6$
		$Al_2O_3 - TA_7$
		$Al_2O_3 - TA_8$
$Al_2(SO_4)_3 \cdot 18H_2O$	HTS	$Al_2O_3 - TS_5$
		$Al_2O_3 - TS_6$
		$Al_2O_3 - TS_7$
		$Al_2O_3 - TS_8$

*** The subscript refers to thermal activation temperature, × 10^{-2} °C.**

The alumina samples of granulation 0.16 — 0.315 mm were previously dried in an oven at 250°C. After introduction into the column they were activated at 150°C 24 hours in nitrogen stream as carrier gas.

Samples of 1 — 10 μL of p.a. grade cyclohexene were introduced with a Hamilton syringe.

RESULTS AND DISCUSSION

The calculation of adsorption isotherms according to Glueckhauf[6] starts from Wilson's[8] and Vault's[9] theory of elution process in conditions of equilibrium distribution of adsorbate between the stationary and mobile phase.

Glueckhauf's method is based on the fact that the specific retention volume corresponding to a certain amount of injected sample equals the derivative of adsorption isotherm at c_i^m concentration :

$$(V_g)_i = \frac{dc_i^s}{dc_i^m} \qquad (1)$$

The adsorbate concentration in mobile phase (c_i^m expressed as g of adsorbate/cm^3 in gas phase) is proportional to height h of the chromatographic peak obtained so that :

$$c_i^m = k \cdot h \tag{2}$$

The proportionality constant k depends on the concentration g of substance introduced in the column, and the surface area of chromatographic peak, S_v according to the equation :

$$k = \frac{g \cdot w}{F \cdot S_v} \tag{3}$$

where w stands for the recorder chart speed cm/min, F for the carrier gas flow rate cm^3/min at column temperature and pressure.

The concentration of the component in stationary state c_i^s (expressed as grams of adsorbate per gram of adsorbent in the column) is determined by graphic integration directly from the chromatogram according to Huber-Keulemans' method :[10]

$$c_i^s = \frac{S_{ads}}{S_v} \cdot \frac{g}{G} \tag{4}$$

where S_{ads} is the adsorption surface area, cm^2, G the amount of adsorbent in grams.

If the mobile phase concentration c_i^m is known one can readily calculate the partial pressure of adsorbed component p_i required to determine the adsorption isotherms $c_i^s = f(p_i)$:

$$p_i = \frac{c_i^m}{M_i} RT \tag{5}$$

where M_i is the molecular weight of adsorbate and T the column temperature, °K.

Gas chromatography also allows determination of isosteric heats q_{ist} from the adsorption isosteric curves :

$$(p_i)c_i^s = f(T) \tag{6}$$

by applying Clausius-Clapeyron equation :

$$-q_{ist} = \frac{d(\ln p_i)}{\mathrm{d}(1/T)} \tag{7}$$

The variation of standard free energy of adsorbate molecules on transfer from free state to adsorbed state is given by the equation :

$$-\Delta G = RT \ln K \tag{8}$$

where K is the equilibrium constant which in this case represents the ratio of the concentration of substance in adsorbed state and in the mobile phase of the column:

$$K = \frac{c_i^s}{c_i^m} \tag{9}$$

The differential entropy of adsorption, ΔS, is the difference between the standard molar entropy in gas phase and that in adsorbed state at a certain temperature and amount of adsorbate introduced in the column and may be determined by the equation:

$$-q_{ist} = \Delta G + T\Delta S \tag{10}$$

The adsorption isotherms obtained, expressed as g of adsorbed substance$/G_{\mathrm{Al_2O_3}} = f(p)$ are similar to those shown in Figs. 1—3 for aluminas calcinated at 500°C. They correspond as shape to Freundlich isotherm which characterizes heterogeneous surfaces with exponential energy distribution of sites involved in adsorption.

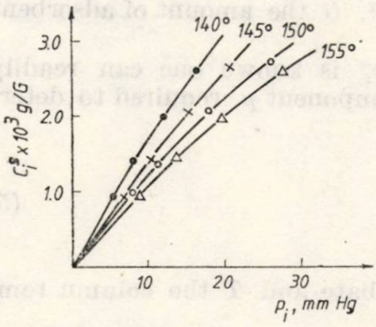

Fig. 1. — Cyclohexene adsorption isotherms for TA$_5$ sample.

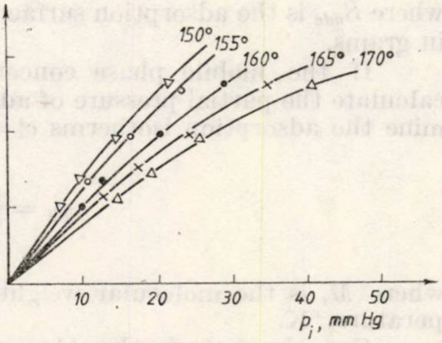

Fig. 2. — Cyclohexene adsorption isotherms for TC$_5$ sample.

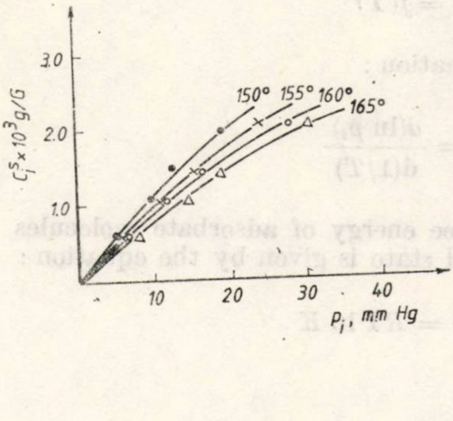

Fig. 3. — Cyclohexene adsorption isotherms for TS$_5$ sample.

Thus, one can expect a decrease of the heats of adsorption proportional to the logarithm of surface coverage :

$$q_\theta = q_0 - C \ln \theta \tag{11}$$

where C is a constant, q_θ the heat of adsorption corresponding to a coverage θ, q_0 the heat of adsorption for $\theta \to 0$.

Calculation of the isosteric heats of adsorption for various coverages of surface has required the drawing of isosteres from adsorption isotherms corresponding to a constant concentration of adsorbed substance. The slope of $\log p_i$ vs. $1/T$ lives supplies directly the isosteric heats of adsorption whose values range within 8 and 13 kcal/mole (Table 2). They decrease with the increase of adsorbed substance concentration on surface and tend to a limiting value which is the heat of condensation of the adsorbent, L^*.

Table 2

Adsorption heat of studied aluminas as a function of reactant quantity

Alumina	$c_i^s \times 10^3$ (g/$G_{\text{adsorbent}}$)				$-q_{\text{ist}}$ (kcal/mol)			
TA_5	0.91	1.4	1.95	2.6	11.79	10.55	9.52	8.64
TA_6	0.83	1.44	1.92	2.73	10.76	9.3	8.71	8.07
TA_7	1.03	1.75	2.55	3.355	8.85	7.75	7.38	6.20
TA_8	0.4	0.7	1.26	2.4	8.45	7.50	6.93	6.20
TC_5	1.1	1.43	1.9	2.60	12.00	11.28	10.6	9.65
TC_6	0.75	1.23	1.59	2.15	10.28	9.43	8.71	8.41
TC_7	0.70	1.19	1.68	2.505	11.00	9.73	9.30	8.71
TC_8	0.83	1.33	1.83	2.05	9.02	8.32	7.96	7.40
TS_5	0.57	1.05	1.44	2.07	11.99	10.17	9.2	8.28
TS_6	0.73	1.27	1.75	2.60	9.90	8.69	8.11	7.45
TS_7	0.65	1.12	1.56	2.32	10.45	9.00	8.55	7.25
TS_8	0.47	0.93	1.24	2.00	11.00	8.72	8.15	6.2

This is explained by the existence of a surface heterogenity the centres being occupied in the decreasing sequence of their interaction energy, and by the adsorbate-adsorbate interactions which turn stronger as the number of molecules adsorbed on surface increases thus diminishing the interaction of the molecule with the adsorption site.[11,12]

The decrease of adsorption heats with the surface concentration of cyclohexene is different from one alumina to the other (Figs 4–6) which may be accounted for either in terms of the different concentration of centres with a certain affinity towards the reactant or in terms of a particular distribution of centres of similar strength with respect to each other.[13,14] Thus, one asssumes that exposure is restricted to preferred planes of the lattice with a certain structure (regarding the nature, concentration and distribution of centres available to adsorption).

It is considered that when all these centres are covered and cyclohehexene is condensed on surface the concentration of adsorbed substance

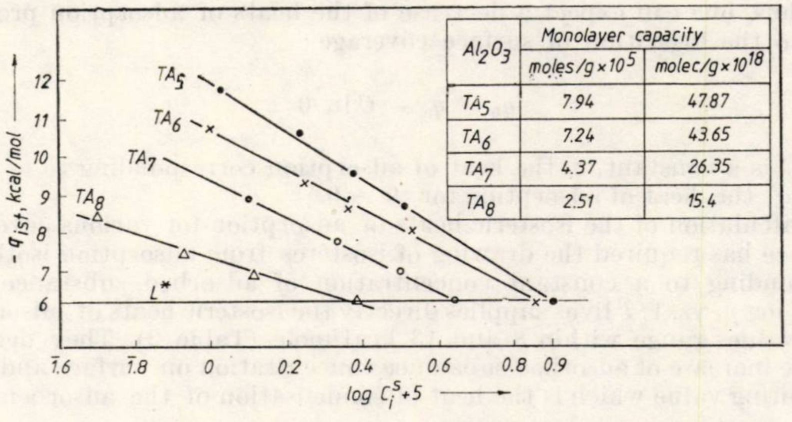

Al_2O_3	Monolayer capacity	
	moles/g × 10^5	molec/g × 10^{18}
TA_5	7.94	47.87
TA_6	7.24	43.65
TA_7	4.37	26.35
TA_8	2.51	15.4

Fig. 4. — Isosteric heat of adsorption versus the concentration of adsorbed substance for TA series.

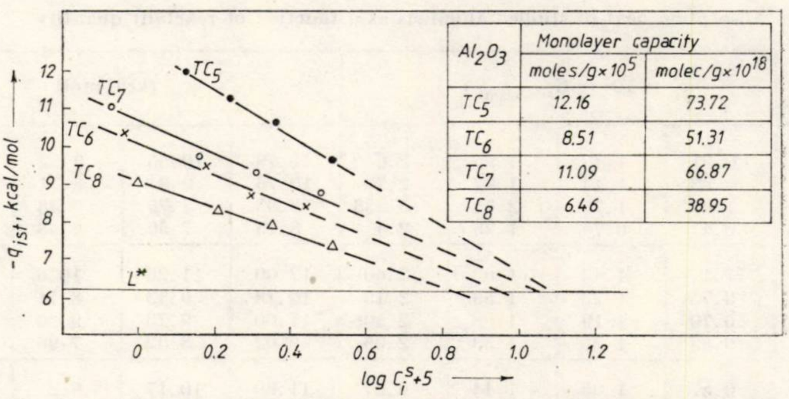

Al_2O_3	Monolayer capacity	
	moles/g × 10^5	molec/g × 10^{18}
TC_5	12.16	73.72
TC_6	8.51	51.31
TC_7	11.09	66.87
TC_8	6.46	38.95

Fig. 5. — Isosteric heat of adsorption versus the concentration of adsorbed substance for TC series.

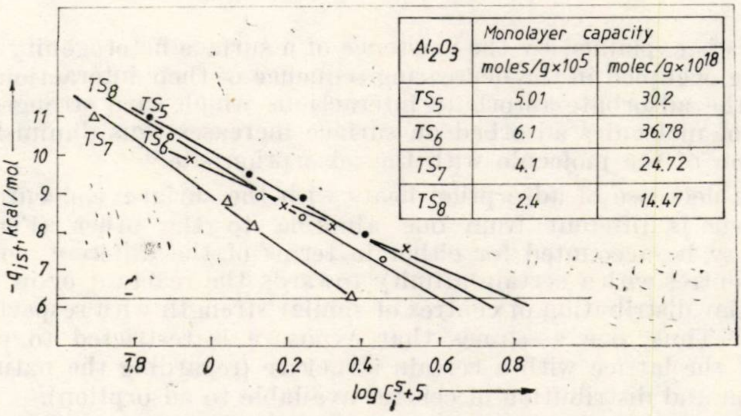

Al_2O_3	Monolayer capacity	
	moles/g × 10^5	molec/g × 10^{18}
TS_5	5.01	30.2
TS_6	6.1	36.78
TS_7	4.1	24.72
TS_8	2.4	14.47

Fig. 6. — Isosteric heat of adsorption versus the concentration of adsorbed substance for TS series.

corresponding to the heat of condensation L^*, may be assimilated with the capacity of monolayer adsorbed (C_m) reversibly on sample surfaces. We noted a parallelism between the monolayer capacity and the catalytic activity of aluminas studied (Fig. 7).

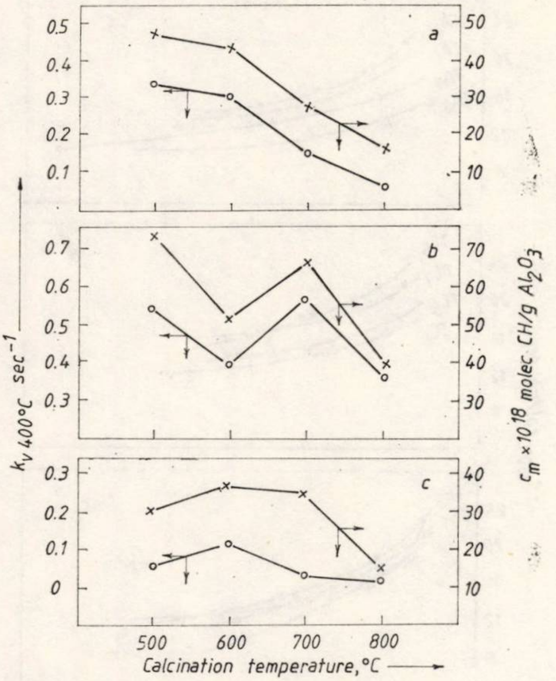

Fig. 7. — Variation of the rate constant of cyclohexene (CH) isomerization reaction at 400°C with monolayer capacity determined by chromatography in aluminas: (a) — TA, (b) — TC, (c) — TS.

Information regarding the energetics of reactant-active surface in various conditions of concentration and temperature is supplied by the variation of thermodynamic quantities — especially the differential entropy — at transition of molecules from gas to adsorbed state.

Because experiments were conducted in a relatively narrow temperature range this quantity is exemplified through its values at 150°C.

The differential entropy ΔS reflects the loss of degrees of freedom of adsorbed molecules, its highest values corresponding to the lowest surface mobility.

The decrease of its values with increasing degree of coverage of the surface (Fig. 8) points to an increase of molecular mobility.

It is worth to note that the sequence of $\Delta S_{150°C}$ values is that of catalytic activity. The only exception is the TS_6 alumina which although the most active in the series at lower surface concentrations exhibits a small entropy variation. As the surface concentration increases the entropy variation tends to exceed those corresponding to the other aluminas in TS series.

It is likely that in the conditions of cyclohexene isomerization to methylcyclopentenes studied the coverage belongs to this concentration range; TS_6 sample is on a higher interaction energy level than the other aluminas in the series.

Hence it results the importance of determinations of surface coverage to evidence the influence of catalytic activity of samples.

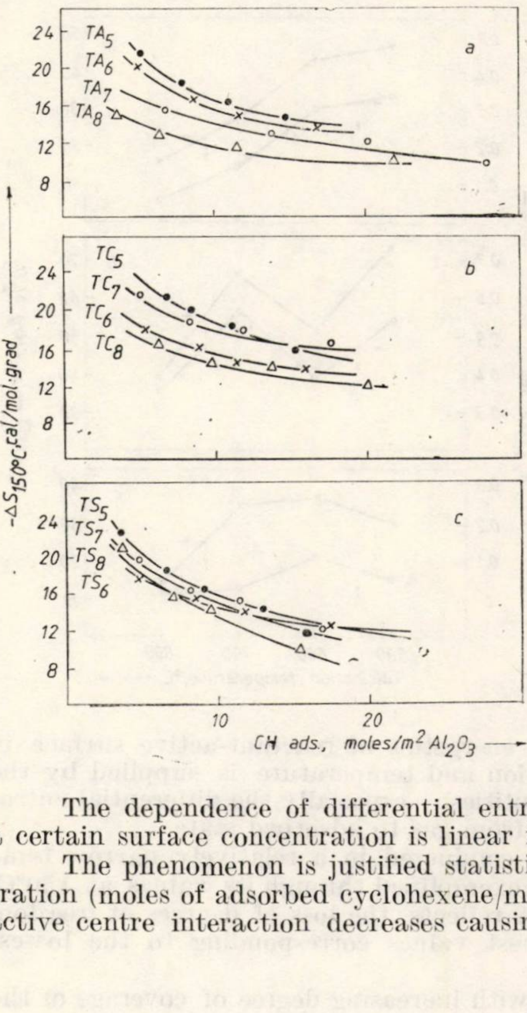

Fig. 8. — The differential entropy of adsorption versus the amount of cyclohexene adsorbed in moles/m² Al_2O_3 for the aluminas in the series: (a) — TA, (b) — TC, (c) — TS, (CH = cyclohexene).

The dependence of differential entropy on heat of adsorption for a certain surface concentration is linear in all aluminas studied (Fig. 9).

The phenomenon is justified statistically i.e. as the surface concentration (moles of adsorbed cyclohexene/m² Al_2O_3) increases the adsorbate-active centre interaction decreases causing a decrease of heats and diffe-

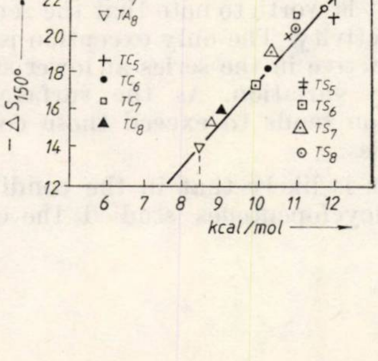

Fig. 9. — Differential entropy of adsorption versus isosteric heats of adsorption (for the same amount of injected sample — 2μL).

rential entropy of adsorption. Because, regardless of the source of aluminas, they obey this law, it is obvious that the same type of centres is involvde in the reactant-catalyst specific interaction. The different interaction energetics as well as heats of adsorption originate mainly in the frequency of these centres on alumina surface.

REFERENCES

[1] I. V. Nicolescu, M. Udrea, A. Nicolescu, I. Udrea and D. Crişan, *Rev. Roumaine Chim.*, part I, see the previous papers.

[2] M. Udrea, I. Udrea, A. Nicolescu, D. Crişan and I. V. Nicolescu, *Rev. Roumaine Chim.*, part II, see the previous papers.

[3] M. Udrea, I. V. Nicolescu, A. Nicolescu, I. Udrea and D. Crişan, *Rev. Roumaine Chim.*, part III, see the previous papers.

[4] M. Udrea, I. Udrea, I. V. Nicolescu and A. Nicolescu, *Rev. Roumaine Chim.*, part IV, see the previous papers.

[5] S. Ross, "Physical Adsorption by Homogeneous and Heterogeneous Solid Surfaces", L. J. Bonis and H. H. Hausner Ed. Fundamental Phenomena in the Material Sci., Plenum Press, New York, 1966, p. 109.

[6] A. V. Kiselev and Ia.I. Iashin, "Gazo-adsorbtionnaia Khromatographia", Moskva, 1967.

[7] I. I. Smirnova and K. V. Topcieva, *Internat. Chem. Eng.*, **14**, 687 (1974).

[8] J. N. Wilson, *J. Amer. Chem. Soc.*, **62**, 1585 (1940).

[9] D. De Vault, *J. Amer. Chem. Soc.*, **65**, 532 (1943).

[10] H. F. Huber and A.J.M. Keulemans, "Gas Chromatography", Ed. M. Van Swaay, Butterworth, London, 1962, p. 26.

[11] M. Sanesi and V. Wagner, *Z. Naturforsch.*, **23a**, 980 (1968).

[12] M. Sanesi and V. Wagner, *Z. Naturforsch.*, **25a**, 688 (1970).

[13] J. C. Giddings, *Analyt. Chem.*, **35**, 199 (1963).

[14] J. C. Giddings, *Analyt. Chem.*, **36**, 1170 (1964).

partial entropy of adsorption. Because [illegible] of the [illegible] of [illegible] one, [illegible] this [illegible] that the [illegible] of [illegible] is [illegible] in the [illegible] specific [illegible]. The different [illegible] as well as heats of adsorption originate [illegible] the frequency of these [illegible] on alumina surface.

REFERENCES

[1] [illegible] V. [illegible], [illegible] and [illegible], Recl. [illegible] Chim., part I, see the previous paper.
[2] M. [illegible], [illegible], A. [illegible], [illegible] and [illegible] V. [illegible], [illegible], part II, see the previous paper.
[3] M. [illegible], [illegible] V. [illegible], [illegible] and [illegible], [illegible], part III, see the previous papers.
[4] M. [illegible], [illegible] and A. [illegible], [illegible] Chim., part IV, see the previous paper.
[5] [illegible] by [illegible] in [illegible] Surfaces", [illegible], Fundamental Phenomena in the [illegible], [illegible], New York, 19[illegible], p. 109.
[6] [illegible] and [illegible], [illegible] Chromatographie", [illegible].
[7] [illegible] and [illegible], International [illegible], [illegible] (19[illegible]).
[8] [illegible] Wilson, [illegible] Soc., 62, [illegible] (1940).
[9] [illegible] Soc., 53, [illegible] (19[illegible]).
[10] [illegible] "Gas Chromatography", Ed. [illegible], London, 19[illegible], p. [illegible].
[11] [illegible], Nature, 2[illegible] (19[illegible]).
[12] [illegible], Nature, 2[illegible] (19[illegible]).
[13] [illegible], [illegible] Chem., 35, [illegible] (19[illegible]).
[14] [illegible] Chem., 3[illegible] (19[illegible]).

Revue Roumaine de Chimie, **33**, *11–12*, 1041–1053 (1988)

HYDROGENATION OF STYRENE ON BIMETALLIC SUPPORTED CATALYSTS Pd–Me/γ–Al_2O_3 (Me = Mn, Fe, Co, Ni and Cu)

VASILE PÂRVULESCU, VIORICA PÂRVULESCU, IOAN V. NICOLESCU and IOAN SĂNDULESCU

Polytechnic Institute of Bucharest, Department of Chemical Technology, Bucharest, Romania

Received March 19, 1988

The study of the second metal influence upon the basic catalyst Pd/γ–Al_2O_3 was made by a test reaction : styrene hydrogenation. Catalysts with variable contents of palladium but in which the concentration of the second metal was constantly maintained were prepared. The choice of the second metal was made from the first transitional series Mn, Fe, Co, Ni and Cu. The kinetics of the hydrogenation reaction as influenced by addition of the second metal to palladium was also investigated. Some correlations between catalytic activity and selectivitiy of bimetallic catalysts Pd–Me/γ–Al_2O_3 and possible interactions of the supported components and support were established.

INTRODUCTION

Researches regarding bi- and multimetallic catalyts with high dispersion were directed to the identification of some systems with higher activity and selectivity in a certain process or to the complete characterization of the state in which the supported metals are found.

Connected with the second direction, the researches obtained were concentrated upon the real interaction between the supported components and between the supported components and the support, trying to establish a link betwen them and the possible active centers in a reaction.

Owing to the fact that the form of the small particles is unknown, the relation between form and dimension is not clear. In the last researches,[1] the metal was supposed to be like small clusters, which no doubt are not spread in atomic state, but were found in overlayers.

In fact, there is not a certain case of atomic dispersion in which a single atom is to be found in zero valence state both accessible and stable.

The experimental data obtained on different bimetallic systems and in different chemical reactions were considered to be satisfactorily explained due to two models : the ensemble dimension effect and the ligand effect.[2,3]

Thus, the required configuration for different reactions asks different dimensions for the ensembles due not only to reactants but also to the products of reactions.[4]

In this paper the way in which the introduction of the second metal, which belongs to the first transitional series, indicates the activity and selectivity of a main catalyst, such as $Pd/\gamma-Al_2O_3$, was followed.

As test reaction has been chosen the styrene hydrogenation reaction. At the same time, based upon the experimental results, an estimate upon interactions which took place between the supported components and between them and the support has been tried.

EXPERIMENTAL

Catalysts as $Pd-Me/\gamma\text{-}Al_2O_3$ in which Me belongs to the first series of transitional metals : Mn, Fe, Co, Ni and Cu were prepared.

The preparation of metallic catalysts was carried out by successive impregnation using extrudates with 3.1 mm diameter and 3—4 mm length of $\gamma\text{-}Al_2O_3$ in solution of active species.

Palladium deposition was carried out by support impregnation with an acid solution of H_2PdCl_4. After step drying up to 110°C and calcination to 500°C the catalysts were brought up in H_2 flow. The introduction of the second metal was carried out by impregnation of $Pd/\gamma\text{-}Al_2O_3$ catalysts with a solution of the above-mentioned metals nitrates. After a step drying up to 80°C, the reduction in H_2 flow followed.

For Fe, Co and Ni the reduction temperature was 500°C, for Mn 700°C and 400°C for Cu.

Palladium content in bimetallic catalysts was 0.1%, 0.3% and 0.5% while the second metal content was constantly 1%.

In order to have a more detailed characterization of the catalytic act on supported bimetallic catalysts, monometallic catalyst such as $1\%Me/\gamma\text{-}Al_2O_3$ and catalysts Pd/Al_2O_3 with a palladium content of 0.1%, 0.3% and 0.5% were also prepared and tested.

The test reactions were carried out in an isotherm displacement reactor, in which 9.5 cm³ catalyst were introduced.

Styrene introduction was carried out by hydrogen vapours which took over only the quantity corresponding to styrene vapours tension in an evaporator with mantle.

The space velocities of hydrogen covered between 360 and 3140 h^{-1}. The reaction temperature was of about 60 to 88°C and the evaporator temperature was between 85° and 98°C.

The reaction products were analyzed chromatographically using a chromatograph Chromatron 18G—4.3. The peaks were identified using chromatographic standards.

RESULTS AND DISCUSSION

Activity data

Figures 1.a—d show the change of totalc onversion of styrene for two space velocities upon bimetallic catalysts $Pd\text{-}Me/\gamma-Al_2O_3$ (Me = Mn, Fe, Co, Ni and Cu) and upon monometallic catalysts $Pd/\gamma\text{-}Al_2O_3$ and $Me/\gamma-Al_2O_3$.

For all the catalysts a diminution of the total conversion with the increase of space velocity is established.

The figure shows the positive effect of 1% Ni addition to the basic catalyst $Pd/\gamma-Al_2O_3$ no matter the palladium concentration. Regarding this metal —Ni— even at small contact times, styrene conversion is maintained to high values. These values are close to the ones determined at high contact times.

Positive effect is obvious at a 0.3% Pd concentration in the Fe and Co case. The other tested metals, Mn and Cu, proved to have a negative effect upon the level of conversion in comparison with the one obtained on monometallic catalyst Pd/$\gamma-Al_2O_3$. If the conversion values determined on bimetallic catalysts Pd$-$Me/$\gamma-Al_2O_3$ are reported to those obtained on monometallic catalysts 1% Me/$\gamma-Al_2O_3$ no matter which is the metal taken in discussion, it is observed that the presence of palladium determines a significant increase.

At the same time, the figure reveals the high values of conversion obtained on catalysts with small Pd content but with a 1% nonplatinic metal content to small space velocities. It is particularly the case of Ni for which the styrene conversion is total in these conditions, but Fe and Co are also included in the same class.

The selectivity variation to ethylbenzene in styrene hydrogenation reaction appears in figures 2.a-d.

One has to notice the fact that in bimetallic catalysts 0.1% Pd$-$1% Me/$\gamma-Al_2O_3$, no matter the nature of nonplatinic metal, the styrene hydrogenation takes place selectively with only ethylbenzene formation.

For the bimetallic systems based on Mn, Fe, Co and Ni the increase of palladium content is accomplished by a decrease of selectivity to ethylbenzene. The selectivity values obtained on 0.5% Pd$-$1%Me/$\gamma-Al_2O_3$ (Me = Mn, Fe, Co and Ni) catalysts are pretty close to those obtained on monometallic catalysts 1%Me/$\gamma-Al_2O_3$ (Me = Mn, Fe ,Co and Ni) but are different from the conversion values.

Hydrogenation reaction on bimetallic catalyst Pd$-$Cu/$\gamma-Al_2O_3$ takes place selectively no matter the palladium concentration.

The same threshold of selectivity for monometallic catalyst 1%Co/$\gamma-Al_2O_3$ has also been determined.

The modification of temperature values in the investigated field 60°$-$88°C determines an increase of the conversion values with the increase of temperature.

Kinetic results

The kinetic parameters of styrene hydrogenation on bimetallic catalysts were determined considering its occurrence in an ideal type of displacement reactor.[5]

The characteristic equation of the reactor, considering stationary conditions, no axial mixture and a plane profile of velocities, is :

$$\frac{d(u_z c_A)}{d_z} = - V_A$$

where :

— u_z — the linear velocity on z direction ;

— V_A — the velocity of reaction ;

— c_A — the concentration of the reactant A.

Tables 1 and 2 give the calculated values for the styrene hydrogenation for the kinetic parameters.

The experimental data have checked up, both for the first step of reaction and for the second one, a pseudomonomolecular kinetics.

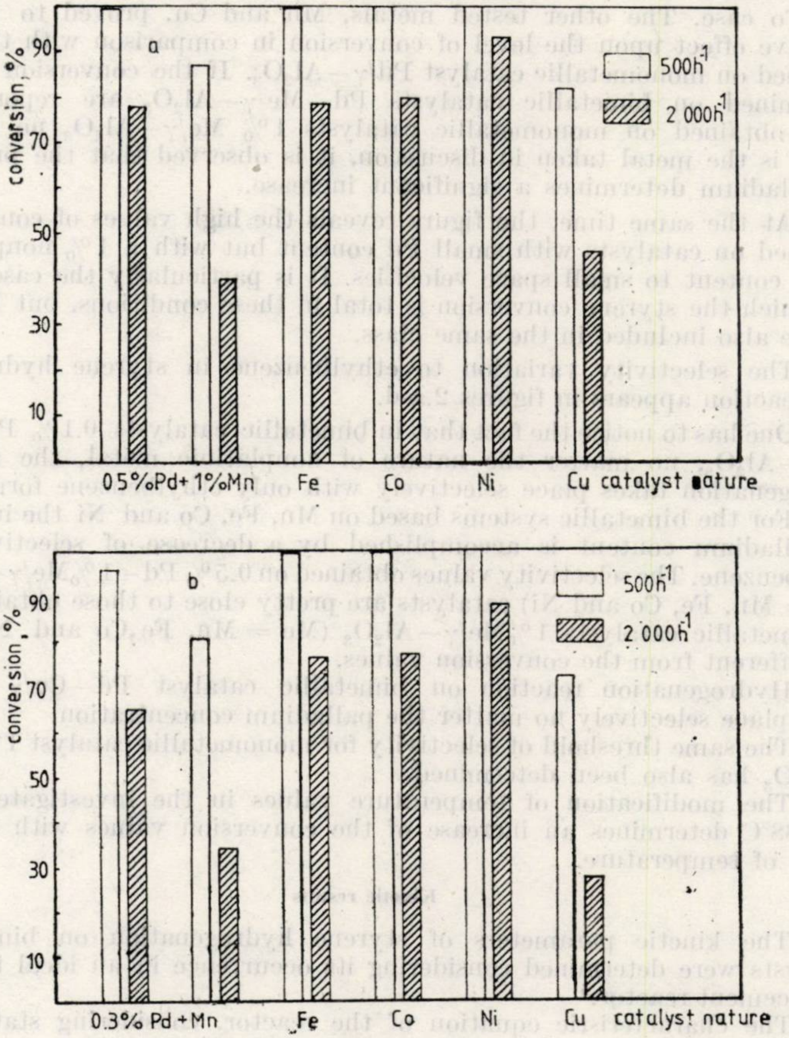

Fig. 1a, b.

Since the molar rate hydrogen/styrene is much overplus — about 10^3 — the results are not at all surprising.

It has been checked up with a pretty good accuracy that styrene hydrogenation upon bimetallic systems Pd—Mn, Pd—Fe, Pd—Co and Pd—Ni, to concntrations greater than 0.3% Pd takes place after an open sequence of consecutive reactions. On the other catalysts the hydrogenation takes place after a first order ireversible reaction.

The analysis of the activation energies of bimetallic catalysts for the first step of hydrogenation shows a curious maximum for the concentrations of 0.5%Pd in disagreement with the slightly higher activities obtained on these catalysts. These values can only be accepted admitting the

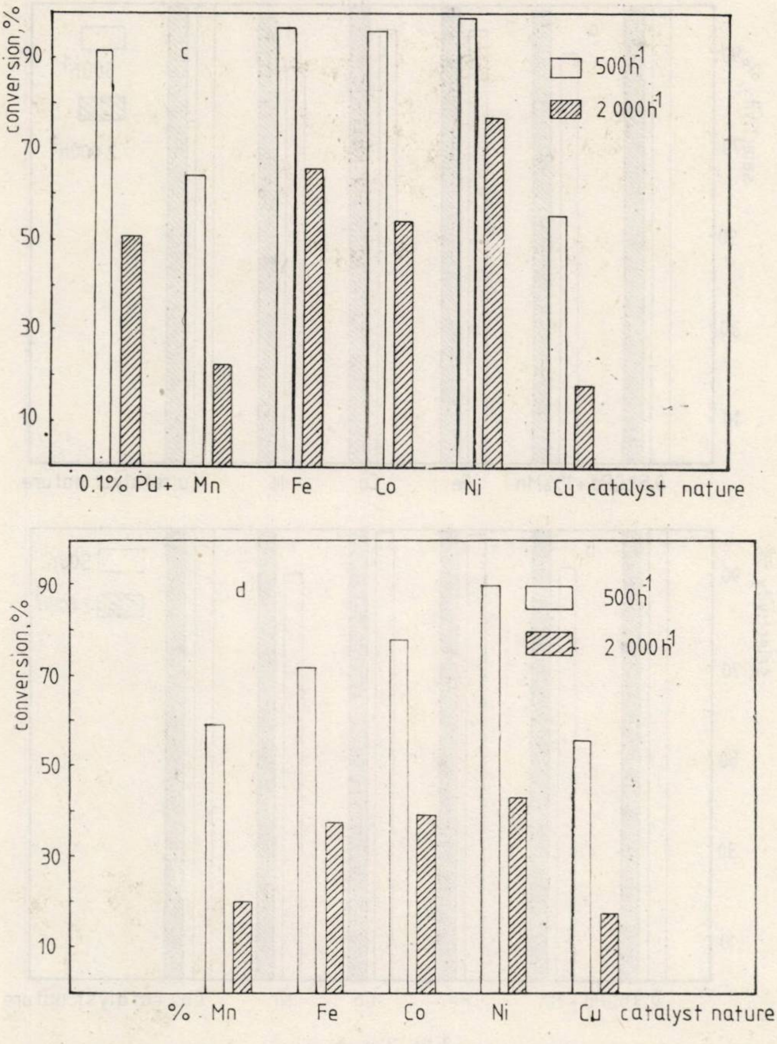

Fig. 1. — Variation of the conversion with nature of the catalyst depending on the space velocity. a — 0.5 %Pd—1 %Me/γ—Al_2O_3; b — 0.3 %Pd — 1 %Me/γ — Al_2O_3 c — 0.1 %Pd — 1 %Me/γ — Al_2O_3; d — 1 %Me/γ—Al_2O_3; temperature 70°C.

existence of a different superficial order in the case of the three concentrations of palladium.

The small values of activation energies bmaye satisfactorily associated with the reaction conditions, respectively with the rate hydrogen/styrene.

Discussion

In the previous papers,[6–8] a model both for bimetallic catalysts Pd—Me/γ-Al_2O_3 tested in conditions of chromatographic pulse and for cata-

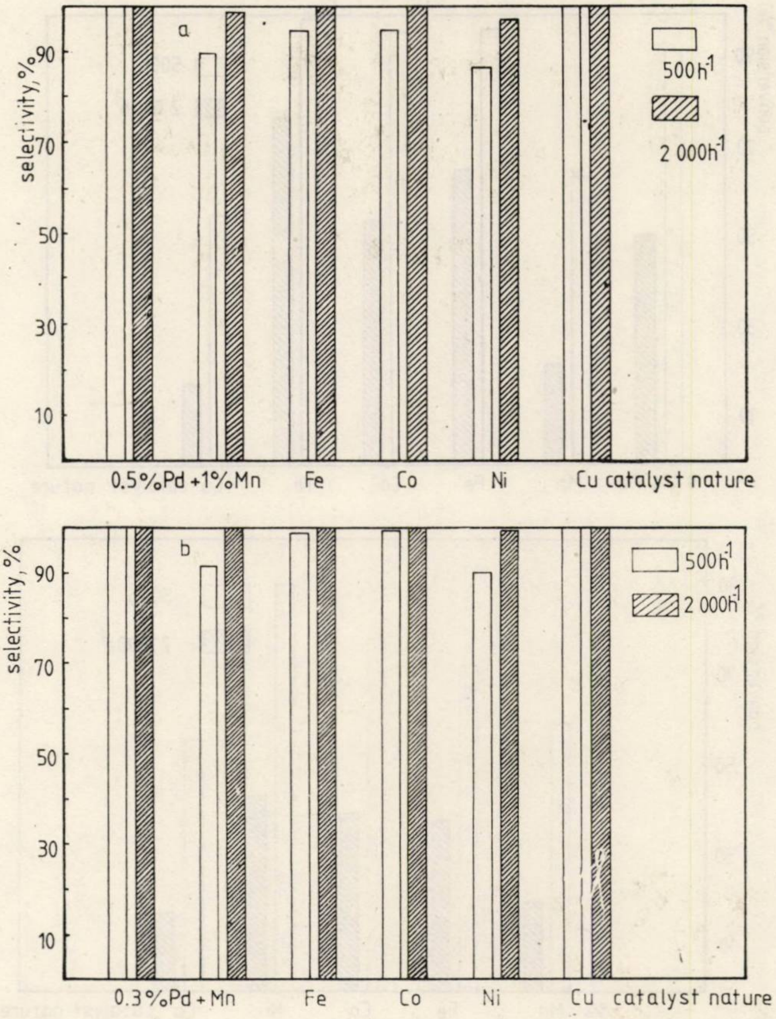

Fig. 2 a, b

lysts Pd–Fe/γ–Al_2O_3 tested in reactor with displacement has been proposed :

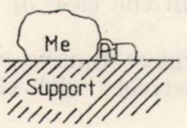
Me
Pd
Support

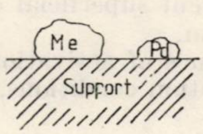
Me
Pd
Support

where Me and Pd stand for the presence of metals in all their oxidation states which are superficially found.

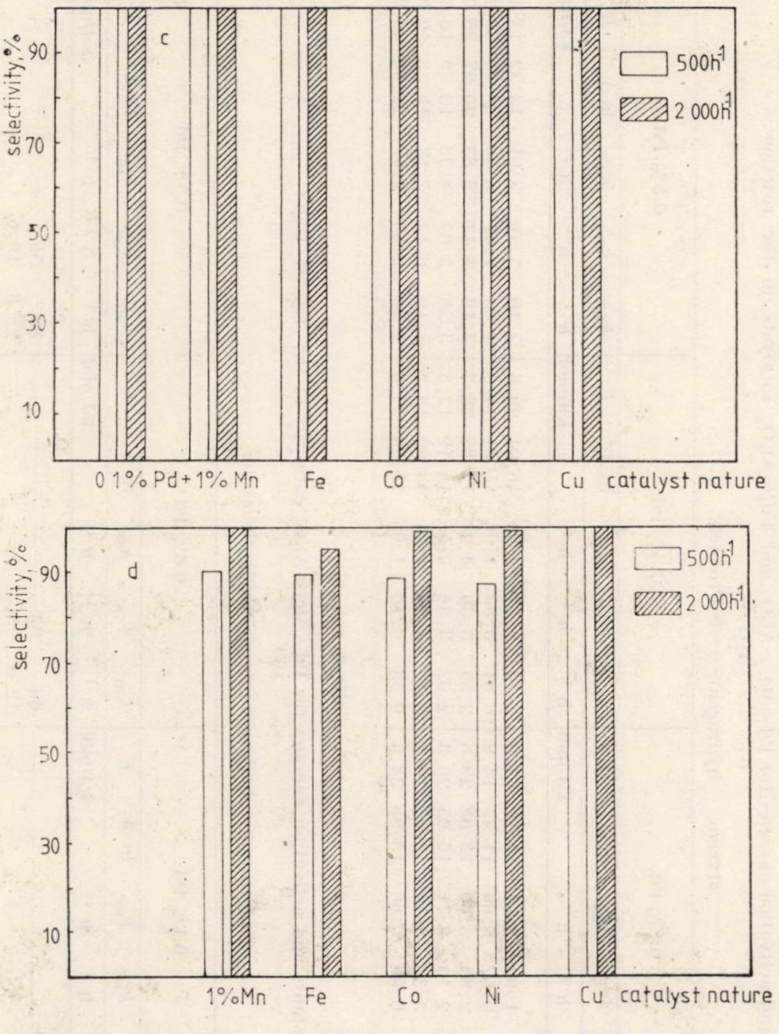

Fig. 2. — Variation of selectivity with the nature of the catalyst depending on the space velocity. *a* — 0.5%Pd — 1%Me/γ—Al_2O_3; *b* — 0.3%Pd — 1%Me/γ—Al_2O_3; *c* — 0.1%Pd — 1%Me/γ—Al_2O_3; *d* — 1%Me/γ—Al_2O_3; temperature 70°C.

Based on this model, the bicomponent particles have a supplementary free energy in comparison with the monocomponent particles because one more term is added : the interfacial energy. At the same time, due to this supplementary term, the model of bicomponent particle may become a forerunner of the segregated phase model.

The model also pointed out the decisive part of metal-support interaction and is backed by the existence of the compensation effect for almost all the tested systems. This effect has been assigned to energetical heterogeneity of surface and it is justified by the existence of the three formations.

Table 1

Values of rate constants and activation energies for Pd$-$Me/γ-Al_2O_3 and Pd/γ-Al_2O_3 catalysts in the reaction:

$$\text{styrene} + \text{hydrogen} \xrightarrow{k_1^{(1)}} \text{Products}$$

Catalyst	0.1% Pd					0.3% Pd					0.5% Pd				
$k \times 10^{-3}$	$k_{70°}$	$k_{78°}$	$k_{88°}$	ln A	E	$k_{70°}$	$k_{78°}$	$k_{88°}$	ln A	E	$k_{70°}$	$k_{78°}$	$k_{88°}$	ln A	E
	h^{-1}	h^{-1}	h^{-1}		kJ/mol	h^{-1}	h^{-1}	h^{-1}		kJ/mol	h^{-1}	h^{-1}	h^{-1}		kJ/mol
Pd/γ-$-$$Al_2O_3$	1.42	1.94	2.57	19.22	34.3	2.12	2.78	3.54	18.01	29.6	3.10	3.51	3.91	13.32	15.1
Pd$-$Mn/γ-Al_2O_3	0.51	0.57	0.66	11.45	14.9	0.84	0.89	1.08	11.81	14.5	1.03	1.61	3.08	28.98	63.2
Pd$-$Fe/γ-Al_2O_3	2.15	2.80	3.60	18.08	29.8	2.55	3.30	4.21	17.87	28.7	3.18	3.42	5.83	20.27	35.0
Pd$-$Co/γ-Al_2O_3	1.72	2.10	2.71	16.65	26.3	2.92	3.36	3.55	14 19	17.8	3.29	3.67	4.36	13.79	16.3
Pd$-$Ni/γ-Al_2O_3	2.96	3.36	3.74	13.62	16.1	3.42	4.15	4.81	14.05	16.9	5.10	6.12	7.12	15.28	19.3
Pd$-$Cu/γ-Al_2O_3	0.40	0.53	0.66	15.95	28.5	0.58	0.76	1.06	18.24	34.0	1.22	2.30	2.67	22.88	45.2

Table 2

Values of rate constants and activation energies for Pd$-$Me/γ-Al_2O_3 catalysts in the second step:

$$\text{ethylbenzene} + \text{hydrogen} \xrightarrow{k_1^{(2)}} \text{ethylcyclohexane}$$

Catalyst	0.1% Pd					0.3% Pd					0.5% Pd				
	$k_{70°}$	$k_{78°}$	$k_{88°}$	ln A	E	$k_{70°}$	$k_{78°}$	$k_{88°}$	ln A	E	$k_{70°}$	$k_{78°}$	$k_{88°}$	ln A	E
	h^{-1}	h^{-1}	h^{-1}		kJ/mol	h^{-1}	h^{-1}	h^{-1}		kJ/mol	h^{-1}	h^{-1}	h^{-1}		kJ/mol
Pd$-$Mn/γ-Al_2O_3	—	—	—	—	—	69	33	—	—	—	83	39	—	—	—
Pd$-$Fe/γ-Al_2O_3	—	—	—	—	—	12.0	5.4	—	—	—	28.8	16.6	—	—	—
Pd$-$Co/γ-Al_2O_3	—	—	—	—	—	0.67	1.72	—	—	—	27.5	18.3	—	—	—
Pd$-$Ni/γ-Al_2O_3	—	—	—	—	—	66.5	25.2	—	—	—	73.2	30.2	—	—	—

In the same papers, it was appreciated that the styrene-catalyst interaction is a Blyholden-Allen[9] one in which an electronic donation from molecular orbitals of organic molecule to unoccupied metallic orbitals (preferably "d") and a back donation from metallic orbitals to unoccupied orbitals (antiligands) has been realized. This kind of interaction is well known to those who are involved in organometallic chemistry[10] and it is backed up by the developed theories regarding the bonds in the compounds.

Thus, it is understood that the acceptor capacity of the basic element is determinant for the activity and selectivity of the metallic supported catalysts.

Palladium has a $4d^{10}$ structure and so its acceptor capacity is limited by the "s°" level. Thus, the more occupied the 3d level of the second metal, the less the difference between the standard potential of this one and of the palladium standard potential and hence the electrophilic character of bimetallic formations is lower.

Due to the "d" character of the nonplatinic metal, the interaction Pd-nonplatinic metal led on the one hand to the formation of some centers with increased electronic density and on the other hand to other centers with decreased density in comparison with monometallic catalysts. As it has been shown, by palladium or nonplatinic metal is to be understood all the states which are formed by them.

The achievement of bimetallic couples shapes this process, favoring one or another of these directions and so the activity variation is illustrated with the palladium concentration for the given system.[11]

Activity data supported by measured properties by Mössbauer spectroscopy ESR EXAFS show that the proposed model may be regarded as made from impure clusters in which the main one is the palladium cluster.[12]

Modification is to be understood by the hybridization perturbation of the partners conductive orbitals which give birth to some characteristics shaping the ligand effect during the catalytic act. These characteristics are tied by the ligands field of active ensembles resulted from the participation with a different rate to interaction of the metallic components depending on the completion of "d" level with the caracteristic electron.

The activity and selectivity data mentioned in literature sustain the existence of two effects : the ligand effect and the ensemble effect.

In agreement with the first effect, the interaction between metal and styrene is due to a coordinative interaction in which the bond metal-ligand may be realized even with a singular orbital of the metal (for the vinylic group) or less than three orbitals (for phenylic radical), the other free orbitals being available for hydrogen.

Coordinative combinations with plan-square symmetry and with coordination number four are characteristic for palladium.

Complex coordinations with the same symmetry are also formed by copper.

Combinations in which the metal is found in an octahedral symmetry with coordination number six are mostly specific for the other metals.

Due to these properties in the case of Cu and Pd, the two metals may be tied up by two coordinative valences by surface, remaining other two for the interaction with styrene molecule and hydrogen.

In the case of Mn, Fe, Co and Ni is possible that within the octahedral symmetry, even if these metals are tied up by three coordinative valences by surface, still remain other three valences for the organic molecule and hydrogen. So, it is explained the catalysts $Pd/\gamma-Al_2O_3$ and $Cu/\gamma-Al_2O_3$ selectivity of the other bimetallic systems, as well the modelling effect of palladium.

If the ligand effect is to be associated with the bimetallic catalysts selectivity the effect of ensemble dimension is to be tied to their activity expressed by conversion. This effect is checked up by the reduction grade of active species.

The study of impregnation process of catalysts has revealed the diffusion coefficient part of cation upon the impregnation profile of catalysts. So, if for manganese was calculated a diffusion coefficient with a size rate smaller than for the other cations, and therefore the geometrical effect of the presence of palladium determines the formation of sediments at the pores opening, for copper its higher value leads to a dispersion somewhat homogenous, in the impregnation space of palladium. This can be found as it was shown in an inferior activity of Pd—Mn catalysts and a superior activity of this system for the catalysts $Pd-Cu/\gamma-Al_2O_3$.

Anyway, the activity measured rates reveal the determined part which the characteristic electron has upon the bimetallic catalysts $Pd-Me/\gamma-Al_2O_3$. So, it can be appreciated the effect of electron $3d^6-3d^8$ in interaction with the "$4d^{10}$" structure of palladium.

The above-mentioned explications complete the electronic theory of metal-semiconductor contact and semiconductor-semiconductor contact.

The result of the touching phenomenon at the border of metal-semiconductor contact, the energetical zones of the support appear curved through the size of potential energy of electron in the contact center.[13]

The theoretical studies made up to now have settled with accuracy the correlation existing between the extraction work, the semiconductor character of the active phases and the position of the Fermi level. It is known that if the extraction work χ_{Me} is bigger than the one of the semiconductor, χ_S, the bands of energies will be deflected to lower levels. In the case of the sediment of semiconductor phase type "p" upon a support type "n", the Fermi level in the loading particle is settled higher than in semiconductor till its entrance in contact with the support and this case is favorable to the acceptor reactions.

The capitalization of the proposed model for organic molecule with active catalyst leads to the following explanations :

Metallic components superficially laid down are found in metallic state and in different oxidation states.[13]

Superficial oxidized form s have semiconductor characters. So, for iron resulted $(Fe_2O_3+Fe^{2+})$ with semiconductor "p" character and $(FeO+Fe^{3+})$with semiconductor "n" character ; for copper, $(CuO + Cu^{1+})$ with semiconductor "p" character and $(Cu_2O + Cu^{2+})$ with semiconductor "n" character and for Co and Ni, $(CoO + Co^{3+})$ and $(NiO + Ni^{3+})$ with semiconductor "p" character.

The correlation of the extraction work values determined by the contact potential method[14] with the character of supported formations expressed by the identification of inequalities:

$$\chi Pd > \chi Al_2O_3 \qquad \text{for Pd;}$$

$$\chi Fe > \chi(Fe_2O_3 + Fe^{2+}) \qquad \text{for Fe;}$$

$$\chi Fe < \chi Al_2O_3$$

$$\chi Cu > \chi(CuO + Cu^{1+}) \qquad \text{for Cu;}$$

$$\chi Cu > \chi(Cu_2O + Cu^{2+})$$

$$\chi Cu < \chi Al_2O_3$$

$$\chi Me < \chi(MeO + Me^{3+})$$

$$\chi Me < \chi Al_2O_3 \qquad \text{for Me = Co, Ni}$$

justifies the activity data obtained for monometallic catalysts supported in the styrene hydrogenation reaction.

In the case of bimetallic catalysts Pd—Me/γ—Al_2O_3 the existence of both isolated metallic formations and some formations in interaction involved the necessity of taking into account other structures:

$$\chi Fe,\ \chi Fe-Pd < \chi Al_2O_3$$

$$\chi Pd > \chi Al_2O_3 \qquad \text{for Fe;}$$

$$\chi Fe,\ \chi Fe-Pd > \chi(FeO + Fe^{3+})$$

$$\chi Pd > \chi(CuO + Cu^{1+})$$

$$\chi Cu < \chi Al_2O_3$$

$$\chi Cu-Pd > \chi(CuO + Cu^{1+}) \qquad \text{for Cu;}$$

$$\chi Pd < \chi(MeO + Me^{3+})$$

$$\chi Me,\ \chi Me-Pd < \chi(MeO + Me^{3+}) \qquad \text{for Me = Co, Ni}$$

$$\chi Pd > \chi Al_2O_3$$

The analysis of these structures justifies the increased activity of these catalysts and the growth of the activity with the palladium content. At the same time these elements give a full view upon the way in which styrene participates in the reaction.

CONCLUSIONS

The activity study for a number of bimetallic catalysts Pd—Me/γ—Al_2O_3 with the second metal belonging to the first transitional series Mn, Fe, Co, Ni, Cu has shown a clear dependence between them and the nature of the system achieved. The nature of the system is highly influenced by its electronic structure which determined both the physical and chemical properties resulting from this structure.

Achievement of a certain kind of bimetallic interaction also depends on the conditions in which the catalyst is prepared : rate of penetration during impregnation, migration velocity of components during thermal operations.

The realization of a certain percentage from an oxidation state (for example Cu^{2+} or Cu^{1+} for copper) may lead to the achievement of a certain superficial form like semiconductor which can be directed to another way or another rate of the spreading reaction.

From this resulted the sensibility of the catalytic process conduction so much difficult to achieve in the case of some reactions which impose different selectivities.

The sensibility of the process is first of all determined by the reduced content of active reduced metal.

Since in the case of the above-mentioned catalysts the full quantity of the reduced metal is under 1.5% and even 1%, because a good part of these metals is found in different oxidation states, a les sreduced participation of the metals has resulted through the above described inequalities of electronic theory of the metal semiconductor contact.

So, it is achieved the main difference versus the catalysts with a large content of superficially supported metal (over 5%). Due to the high rate of the reduced component these catalysts are catalysts with great structural insensibility.

Small modifications in the active component concentration, such as 0.2% Pd for this field of concentrations represent a variation of minimum 13% from the total metal content, versus at most 4% represented for more than 5% of active metal. But as the reduced metal concentration represents only one percentage from 0.2%, this gives the difficulty of the control in some superficial structures.

These properties identified by us showed a bimetallic active system in the styrene hydrogenation reaction and one can notice the influence of the characteristic electron "d^6-d^8" coupled with the "d^{10}" configuration of palladium.

REFERENCES

[1] M. Boudart, *J. Mol. Catal.*, **30**, 27 (1985).

[2] W. M. H. Sachtler, *J. Mol. Catal.*, **25**, 1, (1984).

[3] W. M. H. Sachtler, *Catal. Rev. Sci. Eng.*, **14**, 193 (1976).

[4] J. H. Sinfelt, *J. Catal.*, **29**, 308 (1973).

[5] G. F. Fromant and K. B. Bischoff, "Chemical Reactor Analysis and Design," Wiley, New York, 1979.

[6] I. Săndulescu, I. V. Nicolescu, Xu Yandong and V. Pârvulescu, *Rev. Roumaine Chim.*, **28**, 7. 669 (1983).

[7] I. V. Nicolescu, V. Pârvulescu, I. Săndulescu, E. Szabo and Al. Popa, *Rev. Roumaine Chim.*, **31**, 4, 375 (1986).

[8] V. Pârvulescu, I. V. Nicolescu and I. Săndulescu, *Rev. Roumaine Chim.*, in press.

[9] G. Blyholden and M. C. Allen, *J. Amer. Chem. Soc.*, **91**, 3158 (1969).

[10] I. Haiduc and J. J. Zuckerman, "Basic Organometallic Chemistry", Walter de Gruyter., Berlin, New York, 1985.

[11] I. Săndulescu, Xu Yandong and V. Pârvulescu, *Rev. Chim. (București)*, **34**, 4, 311 (1983).

[12] V. Pârvulescu, I. V. Nicolescu, G. Filloti, N. Grecu, and D. Macovei, *Rev. Roumaine Chim.*, in press.

[13] V. L. Vinetki, I. V. Kelman and D. V. Sokolski, *Zher. fiz. Khim.*, **7**, 1686 (1977).

[14] "Fiziko-khimicevskaia svoistra elementov", Akad. Nauk. Ukrankoi SSR, Kiev, 1965

[15] L. D. Landau and E. M. Lifsitz, "Quantum—Mechanics—Non Relativisctic Theory", 3rd. ed. Pergamon Press, Oxford, 1977.

[16] V. Pârvulescu, I. V. Nicolescu, V. Pârvulescu and I. Săndulescu, *Rev. Roumaine Chim.*, in press.

Revue Roumaine de Chimie, **33**, *11–12*, 1055–1061 (1988)

COMPTES RENDUS

Z. V. Todres, "Ion-Radicals in Organic Synthesis" (in Russian), Khimia Publishers, Moscow, 1986, 240 pp., 2.80 rbl.

During the last ten years several books dedicated to radicals in organic synthesis have appeared, as well as a book on ion-radicals. However, this is the first book to have been published about ion-radicals in organic synthesis.

The first chapter, "Structure and Reactivity of Organic Ion-Radicals" describes first anion-radicals : their spin density, fragmentation modes, interaction with protons, disproportionation and dimerization. Many examples from the recent literature emphasize the decisive role of the solvent or counterion on the course of these reactions. Similar treatments are given to cation-radicals, and to inorganic ion-radicals (superoxide $O_2^{\cdot -}$, as well as $O^{\cdot -}$, $HO^{\cdot}$, $CO_2^{\cdot -}$, $SO_4^{\cdot -}$) in their reactions with organic substrates.

In the second chapter, "Methods for Obtaining Organic Ion-Radicals", electrochemical and chemical methods are described such as Birch reduction or the reaction with $C_8H_8K_2$ for anion-radicals, and for cation-radicals oxidation of substrates by Lewis acids or by organic electron-acceptors such as quinones, aroxyls, nitroxides, hydrazyls or aminium salts. Special attention is paid to phenomena around electrodes (heterogeneous electron transfer). The survey is concluded with a discussion of solid ion-radical salts and of organic metals such as $TTF^{\cdot +}$ $TCNQ^{\cdot -}$.

Chapter 3 ("Methods for Determining the Ion-Radicalic Mechanism of Organic Reactions") is a comprehensive review of the findings during the last 15 years concerning single electron transfer reactions; these findings have changed much of the previously accepted mechanistic concepts in organic and inorganic substitution reactions. A brief enumeration of chemical methods follows : nature of reaction products ; non-conformity with Hammett's relationship ; lack of correlation with the nature of leaving groups ; isotopic effects ; other kinetic methods ; orientation of substitutions according to spin densities. Among the physical methods, one may cite : ESR spectrometry : CIDNP effects ; NMR ; UV–VIS spectrophotometry ; IR spectroscopy ; mass spectrometry ; electrochemical modelling of ion-radicalic reactions. Finally, one may use as probes for radicalic mechanisms the initiation of homolytic polymerization, the sensitivity to inhibitors, the use of spin traps such as nitrones or nitroso-compounds. Several examples are discussed : the reaction of hydroxides with phosphites and sulphides ; the Ter Meer reaction (formation of 1,1-dinitroalkanes from alkali nitrites and 1-halo-1-nitroalkanes), the homolytic nitration in gaseous or liquid phase in non-polar solvents with N_2O_4 or with tetranitromethane (although ^{1}H-NMR spectra do not evidence CIDNP, the ^{15}N-NMR spectra do).

The fourth chapter is entitled "Optimization of Ion-Radicalic Reactions". The influence of magnetic or electric fields, and of light is discussed. Also various chemical additives (e.g. alkoxides or sulphur in nucleophilic substitutions of haloarenes by thiols) or adequate solvents may strongly accelerate ion-radicalic reactions. A significant effect is exerted by counterions or by added complexing agents such as crown ethers.

Chapter 5 ("Stereochemical Aspects of Ion-Radicalic Reactions") brings additional details on such reactions. Differences in the reactivity of *ortho*-nitro-derivatives from those of *para*-substituted ones are explained by the absence of conjugation in the former compounds owing to steric effects. Stereo- and regio-selectivities are correlated. Chelate rings involving alkali metals are often formed when the radical-anions possess closely situated functional groups. Interesting valence isomerizations are observed in anion-radicals in the presence of strong steric hindrance. Conformational effects in ion-radicals of saturated rings and in dianions of annulenes are discussed. The chapter continues with reviews of E–Z-interconversions occurring via radical-ions (including ferrocenyl-ethenes), of the stereochemistry of substitutions involving chiral reagents, and of cation-radicalic pericyclic reactions.

The last chapter, "Ion-radicals in Organic Synthesis", provides examples (including recipes) of several ion-radicalic reactions with synthetic value. These reactions are classified into anion-radicalic and cation-radicalic ones.

Among the countries where ion-radicalic reactions were investigated, the most active in the past 25 years were USA, USSR, Italy and Japan.

The book is concluded with a list of 286 references up to 1985.

The author has contributed substantially to this active research field and has written earlier two reviews in *Usp. Khim.* (*Russ. Chem. Rev.*) on similar topics. He has now provided a comprehensive and excellent survey of ion-radicalic reactions which will be very useful to all organic chemists interested in mechanistic aspects and in organic synthesis.

A. T. Balaban
Polytechnic Institute, Bucharest

"Solid State Chemistry", Structure and Bonding, No. 65, Springer-Verlag, Berlin, 1987; 141 pp., hard cover, DM 116, ISBN 3-540-17581-4.

The three chapters of this volume present in-depth analyses of important chemical aspects but the volume title is a misnomer because the first two chapters cover a much wider area than suggested by the restricted field of solid state chemistry.

M. Ardon and A. Bine's first chapter (28 pages) is entitled "A new aspect of hydrolysis of metal ions; the hydrogen-oxide bridging ligand ($H_3O_2^-$)". The ligand under discussion was discovered in 1981 by X-ray diffraction studies of Mo and W cluster-ions obtained serendipitously; it involves a short and strong hydrogen bond ($\leqslant$ 2.47Å, $\geqslant$ 100 kJ/mole). When an aqueous solution of chromium bipyridyl nitrate was submitted to the method TPVT (three-phase-vapor tensiometry) by titrating in a saturated barium nitrate solution it was established that bridging by $H_3O_2^-$ occurs also in solution. Thus the mechanisms of olation reactions must take into account the existence of such species.

The most substantial chapter of the volume is J.K. Burdett's review "Some structural problems examined using the method of moments" (62 pages). As in a recent review by the same author (*Acc. Chem. Res.*, 1988, **21**, 189), a unifying topological concept is shown to encompass a wide area, systematizing many structural aspects of molecules and solids. The method of moments was used so far by solid-state physicists; lately, Roald Hoffmann makes extensive use of the energy density of states for rationalizing the solid state. Professor Burdett's approach allows to treat in a similar manner the Hückel aromaticity/antiaromaticity rule, Woodward-Hoffmann's rules, the VSEPR rules of Sidgwick, Powell, Nyholm and Gillespie, as well as a series of crystal structures. Interestingly, no symmetry considerations are necessary in the present treatment, unlike the traditional methods which rely heavily on the symmetry of frontier orbitals. Burdett's approach, although based on the simple Hückel method (hence only a first approximation) is powerful enough to be able to rationalize adequately why cyclobutadiene does, and benzene does not, undergo a Jahn-Teller distortion: why some triatomic molecules or ions are bent and other ones linear; why allene has a twisted geometry whereas its electron-deficient analog is twisted, in agreement with Schleyer's elaborate ab-initio calculations. The topological component of the moments approach via the self-returning walks is a very strong one.

The last chapter (42 pages) is entitled "Electronic structure of intermetallic B32 type Zintl phases." Such Zintl phases are intermetallic (alkali or alkaline earth metals alone or in alloys with 4th, 5th and partly 3rd group of the Periodic Table) which crystallize in typical "non-metal" crystal structures and are expected to have an ionic contribution to the chemical bond. Examples are NaTl, LiZn and LiCd. Crystal structures are described, and optical or magnetic properties are discussed. Coloured Zintl phases are found in ternary alloys $Li_2Cd_{2-x}In_x$ ($0.6 \leqslant x \leqslant 1.0$) and $Li_2Zn_{2-x}Cd_x$ ($1.2 \leqslant x \leqslant 1.6$). One can measure the Knight shifts in NMR spectra, or the magnetic susceptibilities. The role of the sizes of the atoms on the stability of the B32 Zintl phases is analyzed. The data are interpreted in terms of the density of states.

In conclusion the volume under discussion contains authoritative and up-to-date reviews written by the scientists who have been responsible for the most numerous recent developments in the respective areas.

A. T. Balaban
Polytechnic Institute, Bucharest

K. Sone and Y. Fukuda, "Inorganic Thermochromism", Inorganic Chemistry Concepts No. 10, Springer-Verlag, Berlin, 134 pp., hard cover, DM 168, ISBN 3-540-17662-4.

Professor Kozo Sone and his younger associate, Yutaka Fukuda, have studied for more than 20 years inorganic compounds, metal complexes and chelates whose colours change upon heating or cooling. Such compounds are called "thermochromic". No book existed so far on this topic; the present book aims at instructing the readers of undergraduate level on this phenomenon and its causes.

A brief introductory chapter discusses thermochromism (including irreversible thermochromism caused by chemical reactions such as the dehydration of $CuSO_4 \cdot 5H_2O$). Among other chromotropic phenomena, the book will cover piezochromism and solvatochromism, but not photo- and electrochromism which are left out on purpose because they are less well understood. Examples for thermochromism are: the $N_2O_4 \rightleftharpoons 2NO_2$ equilibrium in the gaseous phase, solvatochromic iodine solutions in various solvents presenting charge transfer complexation in n- or π-donor solvents, thermochromic iodine-amylase blue clathrate complexes in liquid phases, and thermochromic ruby or halides of mercury and silver in the solid phase.

The second chapter presents in descriptive terms thermochromic and chromotropic phenomena of cobalt (II) chloride solutions and related systems. It is well known that $[Co(H_2O]_6]Cl_2$ aqueous solutions are pale pink (octahedral coordination) while anhydrous $CoCl_2$ is blue (tetrahedral coordination which includes two molecules of solvent such as an alcohol). Concentrated aqueous solutions of cobalt (II) chloride are reversibly thermochromic; even more so are the violet solutions in methanol or in a mixed water-ethanol solvent: on heating they become blue and on cooling to 0° they become pink (the polarity of water decreases with increasing temperature). Spectrophotometric studies evidence that methanol presents the most marked solvatochromy, other primary alcohols less so, and secondary alcohols much less so. In mixed solvents, more water is needed to lead to pink four-coordinated complexes for tBuOH than for s-BuOH; for s-BuOH than for n-BuOH; and for n-BuOH than for MeOH. High pressure also causes the blue color to fade. Interestingly, if one adds excess of Cl^- to hot concentrated aqueous cobalt (II) chloride one obtains blue solutions; a similar effect is caused by adding $NaClO_4$. In the former case the cause is formation of $[CoCl_4]^{2-}$, in the latter case the activity of water decreases owing to solvation of the inert salt. Even stronger solvation occurs with $Mg(ClO_4)_2$, $Ca(ClO_4)_2$ and $Sr(ClO_4)_2$. In reversed micelles of tetraalkylammonium salts, owing to the large concentration of Cl^- anions in the aqueous phase, cobalt(II) chloride is blue. The chapter then discusses $CoCl_2$ solutions in aprotic solvents and the chromotropism of Cu(II) and Ni(II) halides in solution. Particular attention is paid to $Me_4N^+Cl^-$which, having a less hydrated cation than alkali chlorides contains, a more "naked" chloride anion, allowing the formation of blue $[NiCl_4]^-$ species in hot water.

The third chapter discusses the thermochromism of nickel(II) chelates in solution. Organic chelating agents can be designed and tailored to fit any need: tetrammine-type chelalates which afford low-spin, square-planar orange-colored nickel complexes, unlike the low -spin violet-coloured octahedral chelates or the analogous, green crystallohydrates; β-diketon kelates; mixed diamine — β-diketonate chelates; nitrato-, nitro-, nitrito-, halogeno-, pseudo-halo-geno-complexes; Schiff bases; etc. In all cases chromotropic behaviour was observed. Solvatochromic phenomena are correlated with Gutmann's donor number. Equilibria between monomeric and polymeric forms, tetrahedral or square planar complexes, and in some cases formation of five-membered chelate rings accounts for the chromotropic behaviour.

Copper(II) chelates are discussed in the next chapter. Again, octahedral, tetragonal or square-planar forms may appear (nothing is said about bond-stretch isomerism). The discussion enumerates acetylacetonates, tetrammine-type and mixed diamine-β-diketonate complexes. This time the solvatochromy is correlated with the Dimroth-Reichardt E_T solvent parameter.

Miscellaneous chromotropic phenomena in solutions of metal complexes are then discussed, such as spin crossover in Fe(II) or Fe(III) complexes, or formation of ligand radicals.

The last chapter presents thermochromism of transition metal complexes in the solid state. The discussion includes the so-called „irreversible thermochromism caused by loss of water from crystallohydrates, and the „deaquation-anation" i.e. subsequent coordination of anions. Copper (II) and nickel(II) afford reversible thermochromic compounds in the solid state. On the practical side, colour indicators of temperature changes have been proposed on the basis of inorganic thermochromic compounds; however, they do not compete successfully with the cholesteric liquid crystals.

The first book on inorganic thermochromism, written in a phenomenological descriptive style, is recommended to students and advanced students.

A. T. Balaban
Polytechnic Institute, Bucharest

H. F. Franzen, „Physical Chemistry of Inorganic Crystalline Solids", Springer, Berlin, 1986, 158 pp., DM 92, hard cover, ISBN 3-540-16580-0

The new book authored by Professor Hugo F. Franzen continues and develops the basic ideas of his preceding work, "Second-Order Phase Transitions and the Irreducible Representations of Space Groups" (Springer, 1982), which was reviewed also in our Journal.

The author gives a rigorous introduction to basic principles of symmetry, group theory and thermodynamics that apply to problems in the areas of the structure, electronic structure and synthesis of crystalline solids.

In the Introduction the author presents the conceptual framework used by solid-state chemists in their attempts to understand the interrelationships between crystal structure and physical properties of solids and the electronic interactions within the solid. Three chapters are devoted to the discussion of the three-dimensional periodicities in terms of space lattices, developed on the theory of symmetry in crystalline solids — the theory of space groups and their representations (Chapters III and VI).

Chapter IV, entitled "A Brief Sampling of Some Inorganic Structure Types", surveys the key structures and structure types in order to provide an introduction to this vast subject. A small selection of particularly simple crystal structure types important in solid state chemistry is made : NaCl, WC, CsCl, NiAs, ZnS, CaF_2, ReO_3 as well as the layered dichalcides, perovskite, $\alpha - Al_2O_3$ and rutile structure types are described together with their interrelationships. The possibility of relatively strong metal-metal interactions, comparable to those in the elemental metal, is also emphasized (two simple exemples of structures in this category are Ti_2O and Hf_2S).

Chapter V deals with the thermodynamics of the solid state, according to the importance of the former in heterogeneous equilibria. The understanding of such equilibria is made especially important by the occurrence of nonstoichiometry in solids. Thermodynamics of defects, phase diagrams, stability and instability with respect to disproportionation, together with basic concepts and assumptions are presented.

The 7th Chapter ("Second-Order Phase Transitions") treats the thermodynamic and group theoretical techniques useful in the consideration of phase transitions which occur without the coexistence of two phases (without the nucleation and the growth of a new phase). Landau's theory of the thermodynamics of second-order phase transitions without and with consideration of symmetry is discussed.

The first part of Chapter IX treats applications of Landau's theory of symmetry and phase transitions to a variety of order-disorder processes.

Chapters VIII ("Diffraction by Crystalline Solids") and X ("The Electronic Structure of Crystalline Solids") complete the book, the latter providing an elementary introduction to the principles and results of band theory which makes extensive use of symmetry and reciprocal space concepts.

The volume contains a subject index.

Research workers undergoing conventional training in inorganic chemistry as well as students in Chemistry or Physics can gain an application of many of the basic concepts of solid state physics that illuminate this subject at the boundary between chemistry and physics.

Marius Andruh
Polytechnic Institute, Bucharest

"Chromatography' 85", edited by H. Kalász and L. S. Ettre, Akadémiai Kiadó, Budapest, 1986, 695 pp. (cloth-bound).

Published in the series "Symposia Biologica Hungarica", the volume "Chromatography '85" contains scientific contributions to the 5th American-Eastern European Symposium on Chromatography, which took place in 1985, in Budapest.

The number of papers (plenary lectures and posters) presented at the meeting exceeded one hundred, from which fifty five were published in the Proceedings of them Symposium.

The scope of the scientific contributions ranges from theory to practice, both in gas and liquid chromatography, but a considerable part of them deal with biological and medical applications of liquid chromatography (a method for isolation and quantitative determination of insulin A and B, produced by cloned genes ; fast analysis of free aminoacids and peptides in biological fluids, determination of steroids, of drug metabolites or enzymes etc). Most of these complex analyses required the use of combined separation techniques of liquid chromatography, from simple column or thin-layer chromatography to high performance liquid chromatography.

Other interesting reports are presented, in the following areas :

— development of new techniques in liquid or in gas chromatography, for difficult separations (multistep gradient elution for overpressure layer chromatography, size-exclusion liquid chromatography, reversed-phase liquid chromatography, analytical capillary isotachophoresis etc).

— development of new stationary phases (composite compounds for ion-exchange chromatography, used in protein separations ; chiral stationary phases for separations of enantiomers, in both gas and liquid chromatography ; crown ethers or cyclodextrines — well known for their property to form inclusion compounds).

— non-analytical applications of chromatography (study of weak complexes formed between ions of several transition metals and amines or nitrogen containing heterocyclic compounds, by gas-liquid chromatography ; determination of critical concentration of micelle formation in surfactants by microcolumn exclusion chromatography ; determination of Henry constants and heats of adsorption of compounds with different polarities on graphitized carbon black modified with monolayers of crown ethers etc).

— development of new detection systems : a redox chemiluminescence detector, used in either gas or liquid chromatography, for nitrogen compounds analysis.

— new computer systems for evaluation of chromatograms.

The volume contains a subject index and the list of contributors to the Symposium.

The reports included in this volume contain valuable up-dated information and therefore, the book is useful for all research chemists working in the field of separation techniques.

Domnina Răzuş

"Theoretical Approaches", Structure and Bonding No. 68, Springer-Verlag, Berlin, 1987. Hard cover, 175 pp., ISBN 3—540—18058—3—

The volume contains three contributions. The first one is a very concise exposition by O.S. Mortensen of "A noncommuting generator approach to molecular symmetry" (29 pages). The conventional group representation theory is both too difficult for the average physicist or chemist to fully master, and too little informative to be really worth the effort. The author of this chapter proposes to find common eigenfunctions to sets of *non-commuting operators;* these operators are the generators of the molecular symmetry group. The theory is as simple as the usual one for point groups but, unlike the latter, has the advantage of treating systems of half-integer spin (without introducing "double groups") just as easily as integer spin systems. The character table is replaced by an eigenvalue table which allows the calculation of matrix elements through the Wigner—Eckart theorem.

Professor Mortensen lectured on this approach at the Odense University, applying the method to Raman and vibrational spectra. The source of inspiration was Golebiewski's set of *commuting operators,* which unfortunately has been ignored so far. The chapter is concluded by an appendix of eigenvalue tables.

D.M.P. Mingos and R. I. Johnston's contribution, "Theoretical models of cluster bonding" is, in the reviewer's opinion, the most substantial chapter of the book. For polyhedral boranes, carbocations and metal clusters which are electron-deficient systems, modern spectroscopic and X-ray crystallographic techniques revealed their geometry but the theoretical rationalizations and predictions have lagged behind experiment. The authors review in their 60-page chapter first the localized cluster models including Lipscomb's s-t-y-x formalism for boranes, Kettle's topological equivalent orbital method, and various electron count rules. Then the delocalized cluster bonding models are described, emphasizing Wade's and Mingos's approaches based on skeletal electron pairs. The importance of isolobal relationships proposed by M. Elian and R. Hoffmann is recognized. Platinum and gold clusters illustrate the capping and decapping (Rudolph's Debor) principles, whereas high-nuclearity clusters are analyzed by the polyhedral inclusion principle. Finally, free electron cluster bonding models are reviewed, including the tensor surface harmonic theory proposed by Stone, and extended by Fowler and Porterfield. This theory is applied to 3- and 4-connected clusters. King's graph-theoretical method performs less well. The chapter has over 180 references. In conclusion this treatment of cluster bonding is an excellent and up-to-date review and its only criticizable aspect is that no mention is made of polyhedral organic cations.

The last and most extensive chapter (80 pp) is by O. Kahn and is entitled "Magnetism of heteropolymetallic systems". Cytochrome oxidase contains magnetic metal centres Cu(II)—Fe(II) while superoxide dismutase contains Cu(II)—Zn(II), and many studies have been devoted to analogs and model compounds such as Cu(II)—Ni(II), or Cu(II)—Mn(II) which could be the first molecular ferromagnet. The theoretical level of the discussion is high.

The numerous (167) references and the various crystal structures with a variety of transition metals and a still larger variety of organic ligands provide a wealth of experimental data for the reader.

In summary, the volume presents three outstanding reviews by creative chemists on problems of high present interest for a wide audience.

Alexandru T. Balaban
Polytechnic Institute, Bucharest

H.-G. Franck and J. W. Stadelhofer, "Industrial Aromatic Chemistry — Raw Materials, Processes, Products", Springer-Verlag, Berlin 1988, 500 pp, 206 Figures, Hardcover, 128 DM, ISBN 0—387—18940—8, ISBN 3—540—18940—8

Springer-Verlag deserves to be complimented on the excellent production of Professor H.-G. Franck and Dr. J. W. Stadelhofer's translation of their 1987 book "Industrielle Aromatenchemie". The book which is self-contained, is aimed at describing the production and uses of aromatics throughout the world on the industrial level in the mid-eighties. Historically important processes and future trends of industrial production of aromatics are also discussed in the text which is divided into 16 chapters, the first being specially dedicated to historical aspects, while the last chapter summarizes the future developments.

The authors have successfully accomplished the difficult tasd of assembling the material which covers most of the technological organic chemistry courses taught to chemistry (and chemical engineering) students, namely: basic organic technology, petrochemistry, carbochemistry, pesticides, dyestuffs and to a lesser extent the courses on pharmaceuticals.

"The Nature of the Aromatic Character" is the title of the second chapter, which is also introductory; it considers the molecular and mechanistic aspects of the formation and the principal reactions of aromatics. The thirh chapter discusses extensively the basic materials for aromatic chemicals, while the fourtb chapter is devoted exclusively to the production of benzene, toluene, and xylenes, the most important aromatics. The production and uses of derivatives of benzene, toluene and xylenes are treated each in the subsequent three chapters of which the first (Chapter 5 — Production and Uses of Benzene Derivatives) is the largest chapter of the book with over one hundred pages. The subsequent chapters (6 through 14) discuss the production and uses of: polyalkylated benzenes, naphthalene, alkylnaphthalenes and other bicyclic aromatics, anthracene, additional polynuclear aromatics, carbon products from mixtures of condensed aromatics, and aromatic heterocycles, respectively. The toxicological and environmental aspects of aromatics are considered in chapter 15, which contains an alphabetically ordered table with data on maximum workplace concentratioh values for over 100 common aromatics; curiously, in this table the very toxic 2,3,7,8-tetrachloro-dibenzo-1,4-dioxin is considered only as a non-proved human carcinogen like *ortho*-toluidine or various nitro-derivatives.

The book is well illustrated with over two hundred figures comprising mostly flow diagrams for various processes, pictures of chemical plants in operation, charts and diagrams. The structural formulae (over 700) are excellently drawn and well spaced giving the book a pleasant and artistic look; however, the unshared electron pair at formulae with bases or the diazonium group look misleadingly like iodine. The tabular material (87 tables) is carefully selected and summarises for the readers' convenience the pertinent data.

The bood is concluded by an appendix which lists the formulae, melting and boiling points of about 159 compounds; the bibliography which is cited separately for each chapter and which is selective and well documented totalling almost 400 references; and a rich subject index with over 1600 entries.

Written in textbook form, the work is very readable due to the clear, ordered, concise, and methodical style which can be accomplished only after repetitive cycles consisting of teaching, examination of students, revision and updating of the text. The book can also serve as a reference text to which the index and the detailed table of contents facilitate the entry.

A minor criticism to a practically error-free type setting is that some tables (e.g. 3.24) which could have been easily fitted into one page (without disrupting the text) have been split over two non-opposite pages. Also an index to the processes discussed (or to their flowcharts) might have been useful.

The book is highly recommended to teachers and students of organic chemistry and chemical engineering, to scientists, production managers or chemical plant designers dealing with aromatic chemistry which as stated in the preface accounts for about one third of the total chemical production.

Springer-Verlag could provide a considerable service to the chemical community if it would commission a comparable volume of the same quality on industrial aliphatic chemistry.

Teodor-Silviu Balaban
Centre of Organic Chemistry
ICECHIM—Bucharest

Revue Roumaine de Chimie, **33**, *11–12*, 1063–1071 (1988)

INDEX DES AUTEURS

ABDEL BADEI M. M. and M. F. EL-SHAHAT, Oxidative microdetermination of some inorganic sulphur compounds by indirect spectrophotometric method using ferricyanide-thymolphthalein reagent and osmium tetroxide as a catalyst 875
ABDEL-FATTAH ALI HARB, voir ABED NOSRAT MUSTAFA 393
ABD EL-GAWAD I. I., voir HABIB O.M.O. 445
ABD EL-GAWAD I. I., voir HABIB O.M.O. 657
ABDEL-GHANI ALI ELAGAMEY, voir ABED NOSRAT MUSTAFA 393
ABDEL MEGEED M. F. and M. GABER, R. M. ISSA, H. A. IBRAHIM, Mass spectral fragmentation pattern studies of tartaric acid hydrazide and some of its arylidene derivatives 865
ABDEL MEGEED M. F. and A. TENICU, Synthesis of some new 3-substituted 4(3H)-quinazolinone and 4(3H)-quinazolinethione derivatives and related fused biheterocyclic ring systems 981
ABED NOSRAT MUSTAFA and ABDEL-GHANI ALI ELAGAMEY, SALAH ZAKI SOWELLIM, ABDEL-FATTAH ALI HARB, Some reactions of α, β-unsaturated acyl isothiocyanates 393
ABD EL RAHMAN A. H., voir HISHMAT O.H. 741
ABD EL-RAZAK, voir AHMED M. NOUR EL-DIN 183
ABOUL-FETOUH E. MOURAD, Charge-transfer complexes of benzanilides with π-acceptors 617
ABU-BAKR SH. M., voir HISHMAT O.H. 741
ABU EL-NADER H. M. and M. R. MOSTAFA, Kinetics and mechanism of acid hydrolysis of propionamide in methanol-water mixtures 693
AGARWAL R. and P. BEHADUR, Synthesis of 2-alkyl-7-benzo-coumaranones . . . 917
AGARWAL R. K. and GYANENDRA SINGH, Synthesis and characterization of some oxovanadium (IV) complexes of octamethyl-pyrophosphoramide and nonamethylimido-diphosphoramide 537
AGARWAL SURESH K. and D. R. TUTLANI, Synthesis and structural characterization of Cr(III) and cobalt (III) complexes with terephthalic acid hydrazide Schiff bases 533
AHMAD JAMIL and K. BRIAN ASTIN, Correlation of reduction potentials of cyanine dyes with their orbital energies 321
AHMED M. NOUR EL-DIN, ABD EL-RAZAK M. TAWIK, RAMADAN MEKAMER, Reactions of dibenzoylacetylene with N-alkyl nitrones heteroaromatic-N-oxides diazo and azoxy compounds 183
AHMED R. A., voir FAHMY A. M. 755
ALEXANDROAEI M., voir IACOMI F. 149
ALY M. M. and I.M.A. AWAD, A. M. FAHMY, Photochemical bromination of anilides by benzenehexabromide 167
ANDREI C. and I. HOGEA, V. DOBRESCU, Photodegradation and photostabilization of ethylene-vinyl acetate copolymers. II. New facts which support the scheme of photodegradation mechanism 53
ANDREI C., voir DOBRESCU V. 399
ANDREI S., voir DOBRESCU V. 399
ANDRUH M. and G. FILOTI, M .BREZEANU, On the electronic structure of bis(isothiocyanato)tetrakis(4-benzolyl-pyridine) iron (II) 673
APĂTEANU L., voir STERNBERG S. 111
APĂTEANU L., voir STERNBERG S. 775
APOSTOL M., voir CĂLUȘARU A. 25

ARAMENDIA M. A. and V. BORAU C. JÌMENEZ and J. M. MARINAS, Catalytic activity of Pt/AlPO$_4$ and related systems. I. Gas-phase hydrogenation of mono-alkylbenzenes 17
ASHOK KUMAR SAHU, voir PATI S. C. 157
ASTIN BRIAN K., voir AHMAD J. 327
AWAD I.M.A.,., voir ALY M.M. 161

BACALOGLU ILSE, voir GLATT H. H. 639
BACALOGLU ILSE and H. H. GLATT, MAMADOU POULA BARRY, Aminoazoleimines.5. Molecular orbital calculations in benzylidene-aminoazole series by the Mosp method (in German) 747
BADAWY D.S., voir HABIB O.M.O. 445
BADAWY D.S., voir HABIB O.M.O. 657
BADEA F., voir IORDACHE F. 903
BEHADUR P., voir AGARWAL R. 917
BAIULESCU G. E., voir DAVID V. 603
BAJPAI A. K., voir BAJPAI U.D.N. 629
BAJPAI U.D.N. and ALKA JAIN, A. K. BAJPAI, Silver ion catalyzed redox polymerization of acrylamide 629
BALABAN A.T., On a 3-connected carbon net (infinite tridimensional lattice of sp^2-hybridized carbon atoms) and congeneric systems 359
BALABAN A. T. and CHOI IL, Reactions of pyrylium salts with nucleophiles. XX. Synthesis of 4-(N-pyridinium)-4'-dialkylaminoazobenzene and 4-(4-dialkylaminophenylazo)-4'-(N-pyridinium)-biphenyl derivatives 377
BALABAN A. T., Chemical graphs. Part 49. Open problems in the area of condensed polycyclic benzenoids : topological stereoisomers of coronoids and congeners 690
BALABAN A. T. voir UNCUȚA C. 719
BAIDEA I., voir POP I. 283
BANCIU A.C., Electronic spectra and magnetic moments of Ni(III) complexes synthesized with ligands from the class of substituted 1-methyl-2-carbethoxy-glyoxalanil-(1)-phenyhyldrazones - (2). The square - planar isomerism of these complexes 225
BANCIU ANCA, voir BANCIU MIRCEA 893
BANCIU M. and ANCA BANCIU, M. ELIAN, C. DRĂGHICI, N. PALIBRODA, ECATERINA CIORĂNESCU, Synthesis of bis(9, 10-phenanthro)[*a*, *e*]cycloocta-1,5-diene by sulphone pyrolysis 893
BARAJAS R., voir FERNANDEZ-SANCHEZ C. 271
BARRY MAMADOU FOULA, voir GLATT H.—H. 639
BARRY MAMADOU FOULA, voir BACALOGLU ILSE 747
BEKÂROĞLU Ö., voir BIÇAK N. 405
BERDAN I. and I. SANDU, Complex compounds of T1(III) with organic heterocyclic ligands. III. Infrared absorption spectra (in French) 67
BERDAN I. and AL. CASCAVAL, A. SCORTEANU, Complex compounds of Co(II) with Schiff-base ligands (in French) 419
BHATNAGAR B. B., voir VARMA R. P. 305
BIÇAK N. and N. TAN, Ö. BEKÂROĞLU, A novel spectrophotometric method for determination of nitrite ions 405
BLAU B., voir EPPERLEIN J. 473
BLAU B., voir EPPERLEIN J. 685
BONCIOCAT N. and S. STERNBERG, T. VIȘAN, ADINA COTÂRTĂ, Electrode processes with interfacial generation of the electrochemical active species. I. The kinetic model and the equation of the current density 781
BORAU V., voir ARAMENDIA M. A. 17
BOZGA GR. and J. TOWFIGHI, O. FLOAREA, Optimal temperature profiles for propane pyrolysis in tubular reactors 87
BRÂNZOI V,. voir STERNBERG S. 111
BRÂNZOI V,. voir STERNBERG S. 775
BREZEANU M. and O. COSTIȘOR, Polynuclear coordination compounds containing vanadium-tin bond 143
— , voir ANDRUH M. 673
— , voir ILIE IOANA 803
— , voir ILIE IOANA 885
BRISSET JEAN-LOUIS, Thermodynamics of some iron complexes in water-pyridine mixtures 253

BUGEANU M. and V. EM. SAHINI, Aniline complexes with iodine acceptor 75
BURUIANĂ TINCA and A. CARACULACU, Synthesis and characterization of some 2,4'-dibenzyldiisocyanate ionic polymers. IV. Biological activity 809
BUTAN M., voir POP I. 283

CALU N. and N. FOCA, Complexes of Pd(II), Cu(II), Hg(I) and Hg(III) with 1-methyltriazol-diethylazoaniline (I) 59
CĂLUŞARU A., and M. APOSTOL, *REDOX* and *COLHOM* quantum transitions as basic components of chemical processes 25
CĂLUŞARU A., Mathematical foundation of chemical transformations on the basis of *REDOX* and *COLHOM* processes 921
CARACULACU A., voir BURUIANĂ TINCA 809
CARTIANU DAN, A study of the stability of realistic models of oscillating chemical reactions by using concepts derived from the rules for flow graphs 489
CAŞCAVAL AL., voir BERDAN I. 419
  — , and CILIANU BIBIAN ŞT., 2-Hydroxyketones. XX. New Mannich-Werner bases of 7-hydroxy-4-methyl-6- and S-propionylcoumarin 911
CECLAN RODICA, voir GHEORGHIU D. M. 83
CENAN M,. voir VLASSA M. 195
CHAUHAN R. S., voir PUROHIT D. N. 413
CHOI IL, voir BALABAN A. T. 377
CHIRALEU F., voir UNCUŢA C., ... 719
CILIANU BIBIAN STEFAN, voir CAŞCAVAL AL. 911
CIORĂNESCU ECAT., VOIR BANCIU M. 893
CÎMPEANU A., voir DOBRESCU V. 399
COLLERA O., voir GARCIA F. J. 385
CONSTANTINESCU DOINA, voir GHEORGHIU D. M. 83
CONSTANTINESCU MIRCEA, voir SURPĂŢEANU GH. 437
CONŢESCU C., voir PÂRVULESCU V. 3
CÖRMÖS D. C., voir MIOŞCU M. 455
CORNEA F., voir ZĂLARU F. 969
CORTÉS E., voit DAGNINO L. 371
COSTIŞOR O., voir BREZEANU M. 143
COTÂRŢĂ ADINA, voir BONCIOCAT N. 781
CRIŞAN D., voir NICOLESCU I. V. 993
  — , voir UDREA M. 1005
  — , voir UDREA M. 1013
CRUCEANU M., voir IACOMI F. 149
CRUZ R., voir GARCIA F. J. 385
CSUNDERLIK C. , voir GLATT H. H. 639
  — , voir GLATT H. H. 975

DAGNINO L. and E. CORTES, Ortoheffects of substituents in oximes, hydrazones and azines derived from benzaldehydes by electron impact 371
DARBIEU MARIE-HELENE and CHRISTINE RIPOLL, Biosynthesis of the vitamine B_{12} (in French) 897
DAVID V. and G. E. BAIULESCU, A UV/VIS spectrometric study of the reaction of the Pd(II)-*p*-nitrosodiphenylanine complex with carbon monoxide 603
  — , An informational representation of the spectral analytical systems as communication systems with data decoding 937
DOBRESCU A., voir VÎLCU R. 107
DOBRESCU V., voir ANDREI C. 53
  — , and G. ANDREI, A. CÎMPEANU, C. ANDREI, Some properties of linear low density polyethylene and branched low density polyethylene 399
DOCA N. and E. SEGAL, Dehydrogenation kinetics of low aliphatic alcohols on copper catalysts. IV. Analysis of structure — activity relationships 13
DOMENECH J. and MIRO J. Ionic B coefficients in the Jones-Dole viscosity equation of halide ions in aqueous formamide solutions 579
DONESCU A., voir WEINBERG J. 795
DRĂGHICI C., voir BANCIU M. 893
DUCA A., voir SURPĂŢEANU M. 325
DULVAC H., voir GLATT H. H. 975
DUMITRU T. and I. JULEAN, Z. SIMON, Kinetic investigation of basic zinc-carbonates decomposition : $2ZnCO_3 \cdot 3Zn(OH)_2$ (in German) 569

ELIAN M., voir UNCUȚA C. 719
— , voir BANCIU M. 893
EL-DIWANI H. I., voir HISHMAT O. H. 741
EL-NAGDY S. and A. A. EL-KHAMRY, M. A. SHAABAN, M. M. HABASHY, Synthesis and some reactions of 2-(α-benzoylaminostyryl)-3,1(4H)-benzoxazin-4-one and 3-amino-2-(α-benzoylaminostyryl)quinazolin-4(3H)-one 827
— , voir EL-KHAMRY A.M.A. 833
EL-KHAMRY A. A., voir EL-NAGDY S. 827
EL-KHAMRY ABDEL MOMEN A. and S. EL-NAGDY, M. E. SHABAN, Synthesis of 2-(2′-thenyl)-3,1-(4H)-benzoxazin-4-one and its reactions with different nucleophiles 833
EL-SAYED A. M., voir EL-SHAFEI A. K. 291
EL-SHAFEI A. K. and A.M.EL-SAYED, Studies on the nucleophilic reactivity of sulphur and nitrogen in 2-mercapto-4(3H)quinazolinone under solid-liquid phase transfer catalysis conditions 291
EL-SHAHAT M. F. voir M. M. ABDEL BADEI 875
ENCULESCU M., Hydraulic binders. I. Contribution to the processes of producing high-quality Portland and aluminous cements, noble and coloured lines and plasters out of wastes resulted from the chemical industry and other industries . . . 199
EPPERLEIN J. and B. BLAU, The UV-VIS—spectral behaviour of arylazo compounds. I. General remarks 473
— and B. BLAU, The UV-VIS—spectral behaviour of arylazo compounds. II The UV-VIS absorption spectra of 4-amino-substituted azobenzenes 685

FAHMY A. M., voir ALY M.M. 167
— and KH. M. HASSAN, A. A. KHALAF, R. A. AHMED, Synthesis of some new β-lactamas, 4-thiazolidinones and pyrazolines 755
FAID-ALLAH H. M., Dithiocarbamate series. Part II. Pyrrolidino- and indolinodithiocarbamate esters of possible antibacterial and antimicrobial activity 815
FERNANDEZ-SANCHEZ C. and M. T. GANDASEGUI, R. BARAJAS and J. M^{a}. MARINAS, The effect of using aluminium phosphate-γ-alumina and aluminium phosphate-silica on the synthesis of organic esters (in Spanish) 271
FILOTI G., voir ANDRUH M. 673
— , voir IOANA ILIE 885
FINȚA Z. and J. ZSAKÓ, CS. VÁRHELYI, Kinetics and mechanism of substitution reaction of complexes. LIX. Influence of pH upon the equation kinetics of iodo-aquo-bis-bimethylglyoximato-cobalt(III) 263
FLOAREA O., voir BOZGA GR. 87
FEY I., voir POP. I 283
FOCA N., voir CALU N. 59
FULEA O. ADRIAN, Chemical shift nonequivalence *versus* chemical shift equivalence of geminal diastereotopic groups in prochiral assemblies and Curie's principle of symmetry. I. General analysis 39

GABER M., voir MEGEED M. F. ABDEL 865
GĂBURICI M., voir SURPĂȚEANU M. 325
GANDASEGUI Mª T., voir FERNANDEZ—SANCHEZ C. 271
GARCIA F. J. and R. CRUZ, O. COLLERA, J. L. SANCHEZ, Mass spectrometry of diterpenic compounds with a glycol function at $C_{16}-C_{17}$ 385
GEANĂ D., voir LANDAUER O. 237
GHEORGHIU CONSTANȚA, voir RADU O. 677
GHEORGHIU M. D. and L. PÂRVULESCU, R. CECLAN, I. MANOLESCU, D. CONSTANTINESCU, C. FLOREA, M. STĂNESCU, A convenient synthesis for Moore's ketene precursors 83
— , voir UNCUȚA C. 719
— and F. OLTEANU, The stereochemistry of Olah's reduction of bicyclo [2.2.1] heptene derivatives. A proof for a concerted reaction mechanism? 753
— , voir IORDACHE F. 903
GLATT HANS—HORST and M. F. BARRY, C. CSUNDELIK, I. BACALOGLU, S. TIMOFEI, Imines of aminoazoles. IV. Kinetics and mechanism of benzylidene-aminoazoles hydrolysis (in German) 639
— , voir BACALOGLU ILSE 747
— and C. CSUNDERLIK, I. GLATT, HORIA DULVAC, V. SCOROBETE,

Syntheses of heterocycles using carbonic acid derivatives. XI. Reaction of *o*-formylarylcyanates with NH-heterocycles affording benzoxazine derivatives (in German) . . . 975
GLATT INGRID, voir GLATT H.-H . . . 234
GÖÇMEN AYTEN, voir SARAÇ, A. SEZAI . . . 555
GOTHARD A. FRANCISC, Predicting fluid phase equilibria by a model of equilibrium of interactions in restrained molecular systems . . . 331
GRANDCLAUDON P., voir SURPĂȚEANU G. . . . 437
GRECU NICOLETA, voir PÎRVULESCU V. . . . 3
GRECU N., voir NEGOIȚA N. . . . 189
GÜNAYDIN KERIMAN and ÖZTÜRK TURAN, Photoirradiation of 1-phenyl-cyclopentadecene-1 . . . 177

HABASHY M. M., voir EL-NAGDY S. . . . 827
HABIB O.M.O. and I.I.ABD EL-GAWAD, E. M. KANDEEI, D. S. BADAWY, Synthesis and reactions of some new 3-oxo-fluoren-2-carboxanilide derivatives . . . 445
— , voir HASSAN H. M. . . . 653
— and I. I. ABD EL-GAWAD, D. S. BADAWY, Synthesis and reactions of some new 5-arylidene-1-aryl-3-oxo-2-indane carboxanilide derivatives . . . 657
HAIDUC IONEL, voir SILAGHI-DUMITRESCU I. . . . 133
— , voir MIOSCU M. . . . 455
— , voir SILAGHI—DUMITRESCU I. . . . 851
HASSAN H. M. and O.M.O. HABIB, Condensation of *o*- and -*p*-phenylenediamine with some substituted 2-thiazolin-5-ones . . . 653
HASSAN KH. M., voit FAHMY A. M. . . . 755
HERDAN J. M., voir NEGOIȚA . . . 189
— , voir MUNTEANU I. . . . 467
HISHMAT O. H. and A. H. ABD EL RAHMAN, H. I. EL—DIWANI, SH. H. ABU—BAKR, Synthesis of substituted furobenzopyrones . . . 741
HODOȘAN F. and voir POP LIDIA . . . 635
HOGEA I., voir ANDREI C. . . . 53
HOLLA B. S. and B. KALLURAYA, K. R. SRIDHAR, Studies on nitrofuran heterocycles. Part. I Synthesis and antibacteria activity of 7H, 6-(5-nitro-2-furyl)--s-triazolo(3,4-b)-1,3,4-thiadiazines . . . 277

IACOMI F. and ELEONORA TRIF, EV. POPOVICI, A. VASILE, M. ALEXANDROAEI, M. CRUCEANU, GH. SINGUREL, Determination of the nature of iron (III) impurities in NaA zeolites . . . 149
IBRAHIM H. A., voir MEGEED F. ABDEI . . . 865
ILIE IOANA and M. BREZEANU, L. PATRON, E. SEGAL, Synthesis of nickel ferrite from polynuclear coordination compounds. Part II. Study of the wet ferritization process . . . 803
— and M. BREZEANU, L. PATRON, E. SEGAL, G. FILOTI, Synthesis of nickel ferrite from polynuclear coordination compounds. Part III. Structural data of $NiFe_2O_4$ obtained by the wet ferritization method . . . 885
IONESCU D., voir ZALARU F. . . . 969
IONESCU GH. S., voir JURCONI E. . . . 947
IORDACHE F. and M. DANILA, ANA SCHIKETANZ, M. GHEORGHIU, F. BADEA, The reaction of cyclohexa-3,5-diene-1,2-dicarboxylic acid derivatives with *para*-benzoquinone and azo compounds I. . . . 903
IORDACHE GH., voir N. NEGOIȚĂ . . . 189
IOVU M., voir VASILESCU ELIZA MANUELA . . . 483
ISSA R. M., voir MEGEED M. P. ABDEL . . . 865
IULIAN OLGA, voir LANDAUER O. . . . 237
IVANCIUC O., Chemical graph polynomials. 1. The polynomial description of generalized chemical graphs . . . 709
—, Topological and empirical models. I. The prediction of the Gibbs energies of formation for alkanes . . . 839

JAIN ALKA, voir BAJPAI U.D.N. . . . 629
JIMENEZ C., voir ARAMENDIA M. A. . . . 17
JINESCU V. A fundamental property of matter. Part 1 . . . 763
JONNALAGADDA S. B., voir DHIUNDU P. M. . . . 611

JULEAN ILIE, voir DUMITRU T. 569
JURCONI E. and GH. S. IONESCU. On the mechanism of some manganese (III) complex oxalates thermal decomposition 947

KALLURAYA B., voir HOLLA B. S. 277
KANDEEL E. M., voir HABIB O.M.O. 445
KHALAF F. A., voir FAHMY A. M. 755
KHARABA A. MOHAMED, voir NASSAR A.M.G. 525
KHATRI VINEETA, voir MITAL R. L. 463
KISSLING CRISTIAN, Method for determining the phase composition in multicomponent polyphasic systems 363
KREMPELS H., voir POP L. 635
KUMAR ARVIND, voir SHARMA J. 789

LABLACHE-COMBIER A., voir SURPATEANU GH. 437
LANDAUER O. and C. MATEESCU, O. IULIAN, D. GEANĂ, Experimental determination of liquid-vapour equilibrium curves and correlation by different activity models for the cyclohexane-monochlorocyclohexane and cyclohexane-water systems (in French) 237
LUCHIAN CRISTINA, voir SURPĂŢEANU GH. 437

MACHO M. P. ALVAREZ, Kinetics of oxidation of some disaccharides by chromic acid in perchloric acid medium (in Spanish) 171
— , A kinetic and mechanistic study of reduction of Cr(VI) by acetone in sulfuric acid medium (in Spanish) 857
MANOLESCU IOANA, voir GHEORGHIU D. M. 83
MARINAS J. M., voir ARAMENDIA M. A. 17
— , voir FERNANDEZ—SANCHEZ C. 271
MATEESCU A., voir STERNBERG S. 111
MATEESCU A. and D. MATEESCU, Studies on corrosion of lead acid battery grids with addition of Se, Sb and silver 595
MATEESCU, C., voir LANDAUER D. 237
MATEESCU D., voir MATEESCU A. 595
MEGHEA A., voir ZĂLARU F. 969
MEKAMER AMADAN, voir AHMED M. NOUR EL-DIN 183
MIOŞCU MARIA and IOVANCA HAIDUC, D. C. GÖRMÖS, JANA RUSU, Potentiometric determination of some semisynthetic penicilins and their parent compounds using a Cu^{2+} sensitive electrode 455
MIRO JOAN, voir J. DOMENECH 579
MITAL R. L. and POONAM TANEJA, VINEETA KHATRI, LALIT PHRAKASH, Studies in the synthesis of some new fluoro-substituted mesoionic heterocycles 463
MOSTAFA M. R., voir EL-NADER H. M. ABU 693
MUNTEAN ION and JEAN MICHEL HERDAN, GABRIELA VĂLEANU, IR analysis of amines, carboxylic acids, alcohols, phenols and mercaptans after derivatization with n-butylisocyanate 467

NASSAR AHMED M. G. and MOHAMED A. KHARABA, ABDEL—HAMID A. YOUSSEF, A correlation of the reactivity of some substituted phenoxide ions. 525
NEGOIŢĂ N. and J. M. HERDAN, N. GRECU, GH. IORDACHE, Transformations of aminic antioxidants in the inhibited oxidation of hydrocarbons 189
NICOLESCU ALA, voir NICOLESCU I. V. 993
— , voir UDREA M. 1005
—, voir UDREA M. 1013
— , voir UDREA M. 1021
— , voir UDREA M. 1031
NICOLESCU I. V., voir PÂRVULESCU V. 3
— , and MARIANA UDREA, ALA NICOLESCU, I. UDREA, D. CRIŞAN, Catalytically active aluminas from precursors obtained by supersaturation of reactants. I. Synthesis of precursors and reaction mechanisms 993
—, voir UDREA M. 1005
— , vor UDREA M. 1013

— , voir UDREA M. 1021
— , voir UDREA M 1031
— , voir PÂRVULESCU V. 1041
NIZAMUDDIN and D. N. PUROHIT, Infrared spectral studies of 3-hydroxy-3-methyl-1-phenyl-triazene derivatives 295

OGONOWSKI JAN, The influence of activators on activity of PbO/MgO catalyst in the reaction of oxidative dehydrodimerization of toluene 881
OLTEANU E., voir GHEORGHIU M. D. 753
ÖZTÜRK TURAN, voir GÜNAYDIN K. 177

PALAGHITA M. and D. RĂILEANU, Nenitzescu synthesis of 5-hydroxyindoles. III. A diazaheptalenedione from 3-aminocinnamic ester 953
PALIBRODA N., voir BANCIU M. 893
PÂRVULESCU I., voir GHEORGHIU D. M. 83
PÂRVULESCU V. and I. SĂNDULESCU, N. GRECU, C. CONȚESCU, I. V. NICOLESCU, Effect of palladium concentration on the state and activity of Pd/γ—Al_2O_3 catalysts 3
— and VIORICA PÂRVULESCU, I. V. NICOLESCU, I. SĂNDULESCU, Hydrogenation of styrene on bimetallic supported catalysts $Pd-Me/\gamma-Al_2O_3$ . . (Me = Mn,Fe, Co, Ni and Cu) 1041
PÂRVULESCU VIORICA, voir PÂRVULESCU VASILE 1041
PATI S. C. and A. KUMAR SAHU, Y. SRIRAMULU, Kinetics and mechanism of Ru(III) chloride-catalysed oxidation of benzaldehyde and substituted benzaldehydes by trichloroisocyanuric acid in acid medium 157
PATRON L., voir ILIE IOANA 803
— , voir ILIE IOANA 885
PERIȘANU ST., voir VÎLCU R. 351
PETRIDE H. and D. RĂILEANU, Mesoionic oxazolones. II. Unstable non-acylated compounds 729
PETROVANU MAGDA, voir SURPĂȚEANU GH. 437
PLĂVEȚI M., voir UNCUȚA C. 719
POP I. and I. CIUPE, M. BUTAN, L. TEREC, L. FEY, I. BALDEA, Quantitative dialkylation of aromatic amines under a minimum excess of alkylation agent . . 283
POP LIDIA and H. KREMPELS, F. HODOȘAN, Exo- and endohormones. XIII. Synthesis of Z-9-pentacosene 635
POPOVICI EV., voir IACOMI F. 149
PRAKASH LALIT, voir MITAL R. L. 463
PURDELA D., The Z dependence of nuclear diamagnetic shielding constants for free atoms 623
PURI B. K., voir SHARMA JYOTI 789
PUROHIT D. N., voir NIZAMUDDIN 295
— and R. S. CHAUHAN, Spectrophotometric studies of lanthanides with 3-hydroxy-3-phenyl-1-*o*-carboxy phenyltriazene 413

RADU O., As(III) — HCl — H_2O system. I. Homogeneous state 585
— and C. GHEORGHIU, As(III) — HCl—H_2O system. Part II. Solid-liquid state 677
RĂILEANU DAN, voir PETRIDE H. 729
— , voir PALAGHITA M. 953
RAMAKRISHNA K., voir G. V. SARADAMBA 547
RAJU K. N., voir SARADAMBA G. V. 547
RAO V. SURBA, voir SARADAMBA G. V. 547
RIPOLL C., voir DARBIEU M.-H. 987
RUSU JANA, voir MIOȘCU M. 455

SAHINI V. EM., voir BUGEANU M. 75
— , voir WEINBERG J. 795
SALAH ZAKI SOWELLIM, voir ABED NOSRAT MUSTAFA 393
SANCHEZ J.L., voir GARCIA F. J. 385
SANDU I., voir BERDAN I. 67
SĂNDULESCU IOAN, voir PÂRVULESCU VASILE 3
—, voir PÂRVULESCU VASILE 1041
SARAÇ A. SEZAI and AYTEN GÖÇMEN, Kinetics of the cerium (IV) oxidation of

malonic acid in H_2SO — $HClO_4$ media 555

ŞARADAMBA G. V. and K. RAMAKRISHNA, K. N. RAJU, P. V. SUBBA RAO, Kinetics of oxidation of thiourea by iron (III) in the presence of 2,2' — bipyridyl 547

SCHIKETANZ ANA, voir IORDACHE F. 903

SCHWARTZ ANIKÓ, voir R. SCHWARTZ 313

SCHWARTZ ROBERT and ANIKO SCHWARTZ, 17α-Substituted derivatives of B-nor-5-androstene-3β-ol-17-one and 5-androstene-3β-ol-17-one 313

SCOROBETE V., voir GLATT H. — H. 975

SCORŢEANU A., voir BERDAN I. 419

SEGAL E., voir DOCA N. 13

— , voir ILIE IOANA 803

— , voir ILIE IOANA 885

SHAABAN M.A., voir EL-NAGDY S. 827

SHABAN M.E., voir EL-KHAMRY A.M.A. 833

SHARMA JYOTI and ARVIND KUMAR, B. K. PURI, Polarographic study of manganese(II)-pyridine-thiocyanate system and theormodynamic parameters 789

SHIUNDU P. M. and S.B. JONNALAGADDA, A novel spectrophotometric method for the determination of peroxydisulphate ion using *o*-dianisidine-$S_2O_3^{2-}$ Cu(II) indicator reaction 611

SILAGHI-DUMITRESCU I. and I. HAIDUC, Linear *versus* bent bis(diphosphine) iminium cations. A molecular orbital discussion of the bonding in $H_3PNPH_3^+$ and related species 133

— and IONEL HAIDUC, Electronic structure and bonding in diamidoboron cations. A molecular orbital study of $[H_2NBNH_2]^+$ 851

SIMON ZENO, voir DUMITRU T. 569

SINGH ANURADHA, voir VARMA R.P. 305

SINGH GYANENDRA, voir AGARWAL R.K. 537

SINGUREL GH., voir IACOMI F. 149

SOWELLIM SALAH ZAKI, voir NOSRAT MUSTAFA ABED 393

SRIDHAR K. R., voir HOLLA B.S. 277

SRIRAMULU Y., voir PATI S.C. 157

STĂNESCU MICHAELA, voir GHEORGHIU D.M. 83

STERNBERG S. and A. MATEESCU, V. BRÂNZOI, L. APĂTEANU, Effect of phosphoric acid on the $PbSO_4/PbO$ electrode in sulphuric acid solutions 111

STERNBERG S. and V. BRÂNZOI, L. APĂTEANU, M. UNGUREANU, Polarization behaviour of the n-and p-type silicon in sulphuric acid solutions 775

—, voir BONCIOCAT N. 781

SURPĂŢEANU GH. and C. LUCHIAN, M. CONSTANTINESCU, M. PETROVANU, A. LABLACHE-COMBIER, PIERRE GRANDCLAUDON, Theoretical and experimental study of the cycloaddition between 4-(*p*-tolyl)-1,2,4-triazolium N-(*p*-nitrophenacylide) and methyl *trans*-cinnamate (in French) 437

—- voir SURPĂŢEANU M. 325

SURPĂŢEANU M. and A. DUCA, GH. SURPĂŢEANU, M. GĂBURICI, The potentiometric determination of mixtures of alkylphosphates, orthophosphoric and hydrochloric acids 325

TANEJA POONAM, voir MITAL R.L. 463

TENIOU A., voir ABDEL-MEGEED F. M. 981

TEREC L., voir POP I. 283

TIMOFEI SIMONA, voir GLATT H. — H. 639

TOWFIGHI JAFAR, voir BOZGA GR 87

TRIF E., voir IACOMI F. 149

TUTLANI D.R., voir AGARWAL S.K. 533

UDREA I., voir NICOLESCU I.V. 993

— , voir UDREA M. 1005

— , voir UDREA M. 1013

— , voir UDREA M. 1021

— , voir UDREA M. 1031

UDREA MARIANA, voir NICOLESCU I. V. 993

UDREA MARIANA and I. UDREA, ALA NICOLESCU, D. CRIŞAN, I. V. NICOLESCU, Catalytically active aluminas from precursors obtained by supersaturation of reactants. II. Textural and structural properties and their relation to the nature of precursors and the thermal treatment 1005

— and I. V. NICOLESCU, ALA NICOLESCU, I. UDREA, D. CRIŞAN, Catalytically active aluminas from precursors obtained by super saturation of reactants. III. The catalytic activity of aluminas in isomerization of cyclohexene test reaction 1013

UDREA MARIANA and I. UDREA, I. V. NICOLESCU, ALA NICOLESCU, Catalytically active aluminas from precursors obtained by supersaturation of reactants. IV. Kinetics of cyclohexene isomerization 1021

— and I. V. NICOLESCU, I. UDREA, ALA NICOLESCU, Catalytically active aluminas from precursors obtained by supersaturation of reactants. V. Adsorption of cyclohexene by gas chromatography 1031

UNCUŢA CORNELIA and M. D. GHEORGHIU F. CHIRALEU M. PLAVETI, M. ELIAN, ALEXANDRU T. BALABAN, Reaction of pyrylium salts with nucleophiles. XXI. Unexpected formation of 6,6-dimethyl-5-isopropyl-2,4-cyclohexadienylidene-1-imines from primary amines and 2,6-diisopropyl-pyrylium salts . 719

UNGUREANU M., voir STERNBERG S. 775

VĂLEANU G., voir MUNTEAN IOAN 467

VARHELYI GS., voir FINTA Z. 263

VARMA R. P. and B. B. BHATNAGAR, ANURADHA SINGH, Studies on physical properties of some organochloro pesticides in methanol 305

VASILE A., voir IACOMI F. 149

VASILESCU ELIZA-MANUELA and M. IOVU, D. SĂNDULESCU, Molecular compounds with some alkyl aryl ethers. II. Hydrogen bond complexes 483

VÎLCU R. and A. DOBRESCU, Calculation of higher order Onsager's coefficients for monomolecular reactions 107

— and ST. PERISANU, Estimation of monopolar gas solubilities in polar solvents 351

VIŞAN T., voir BONCIOCAT N. 781

VLASSA M. and M. CENAN, Alkylation of phenothiazine using solid-liquid phase transfer catalysis without solvent 195

WOLDAN M., Viscosity of some alkali halides in water-acetamide mixtures at 333.15 K 125

WEINBERG J. and A. DONESCU, V. EM. SAHINI, β-Lactam antibiotics II. Substituent effects on cephalosporins 795

YOUSSEF A. ABDEL-HAMID, voir NASSAR AHMED M. G. 525

ZĂLARU FLORICA and A. MEGHEA, D. IONESCU, F. CORNEA, Some new copper (II) bromocomplex compounds with imidazole derivatives 969

ZSAKO J., voir FINTA Z. 263

Revue Roumaine de Chimie, **33**, *11–12*, 1072–1076 (1988)

INDEX DES SUJETS

Acid hydrolysis of propionamide in methanol-water mixtures. Kinetics and mechanism of—. H. M.ABU EL-NADER and M. R. MOSTAFA 693

Activators on activity of Pb/Mg catalyst in the reaction of oxidative dehydrodimerization of toluene. The influence of —. JAN OGONOWSKI 881

Alkali halides in water-acetamide mixtures at 333.15 K. Viscosity of some — . M. WOLDAN. 125

Alkylation of phenothiazine using solid-liquid phase transfer catalysis without solvent. M. VLASSA and M. CENAN 195

2-Alkyl-7-benzo-coumaranones, Synthesis of —. R. AGARWAL and P. BEHADUR . . 917

Aminic antioxidants in the inhibited oxidation of hydrocarbons. Transformations of—. N. NEGOIȚA, J. M. HERDAN, N. GRECU and GH. IORDACHE 189

Aminoazoleimines V. Molecular orbital calculations in benzylidene-aminoazole series by the Mosp method. I. BACALOGLU, H. GLATT and M. F. BARRY (in German) 747

Aniline complexes with iodine acceptor. M. BUGEANU and V. EM. SAHINI 75

5-Arylidene-1-aryl-3-oxo-2-indane carboxanilide derivatives. Synthesis and reactions of some new —. O. M. O. HABIB, I.I I. ABD ELGAWAD and D. S. BADAWY . . 657

As(III) — HCl — H_2O system. I. Homogeneous state. O. RADU. 585

As(III) —HCl—H_2O system. Part II. Solid-liquid state. O. RADU and CONSTANTA GHEORGHIU 677

2-(α-Benzoylaminostyryl)-3,1(4H)-benzoxazin-4-one and 3-amino-2-(α-benzoylaminostyryl) quinazolin-4(3H)-one. Synthesis and some reactions of —.S. EL. NAGDY, A.A. A. EL-KHAMRY, M. A. SHAABAN and M. M. HABASHY 827

Biosynthesis of the vitamine B_{12} . . . M.-H. DARBIEU and C. RIPOLL (in French) . . . 987

Bis(isothiocyanato)tetrakis(4-benzoyl-pyridine)iron (II). On the electronic structure of-. M.A. G. FILOTI and M. BREZEANU 673

Book reviews . . . . . . 97, 217—221, 347—348, 427—433, 565—566, 669—670, 847—848, 1055—1060

Catalytically active aluminas from precursors obtained by supersaturation of reactants. I. Synthesis of precursors and reaction mechanism. I. V. NICOLESCU, M. UDREA A. NICOLESCU, I. UDREA and D. CRIȘAN 993

Catalytically active aluminas from precursors obtained by supersaturation of reactants. II. Textural and structural properties and their relation to the nature of precursors and the thermal treatment. M. UDREA, I. UDREA, A. NICOLESCU, D. CRIȘAN and I. V. NICOLESCU 1005

Catalytically active aluminas from precursors obtained by supersaturation of reactants. III. The catalytic activity of aluminas in isomerization of cyclohexene test reaction. M. UDREA, I. V. NICOLESCU, A. NICOLESCU, I. UDREA and D. CRISAN 1013

Catalytically active aluminas from precursors obtained by supersaturation of reactants. IV. Kinetics of cyclohexene isomerization. M. UDREA, I. UDREA, I. V. NICOLESCU and A. NICOLESCU 1021

Catalytically active aluminas from precursors obtained by supersaturation of reactants. V. Adsorption of cyclohexene by gas chromatography. M. UDREA, I. V. NICOLESCU I. UDREA and A NICOLESCU 1031

Catalytic activity of Pt/$AlPO_4$ and related systems I. Gas-phase hydrogenation of monoalkylbenzenes. M. A. ARAMENDIA, V. BORAU, C. JIMENEZ and J. M. MARINAS 17

Cerium(IV) oxidation of malonic acid in H_2SO_4-$HClO_4$ media. Kinetics of the—.A. SEZAI SARAÇ and A. GÖÇMEN 555

Charge-transfer complexes of benzanilides with π-acceptors. ABOUL-FETOUH E. MOURAD 617

Chemical graphs. Part 49. Open problems in the area of condensed polycyclic benzenoids : topological stereoisomers of coronoids and congeners. A. T. BALABAN 699

Chemical graph polynomials. 1. The polynomial description of generalized chemical graphs. O. IVANCIUC 709

Complex compounds of Co(II) with Schiff-base ligands. I. BERDAN, AL. CAŞCAVAL and A. SCORŢEANU (in French) 419

Complexes of Pd(II), Cu(II), Hg(I) and Hg(II) with 1-methyltriazol-diethylazoaniline (I). N. CALU and N. FOCA 59

3-Connected carbon net (infinite tridimensional lattice of sp^2-hybridized carbon atoms) and congeneric systems. On a —. A. T. BALABAN 359

Coordination compounds containing vanadium-tin bond. M. BREZEANU and O. COSTIŞOR 143

Copper (II) bromocomplex compounds with imidazole derivatives. Some new —. F. ZĂLARU, A. MEGHEA, D. IONESCU and F. CORNEA 969

Cr(III) and cobalt (III) complexes with terephthalic acid hydrazide Schiff bases. Synthesis and structural charcterization of —. SURESH K. AGARWAL and D. R. TUTLANI 533

Curie's principle of symmetry. Chemical shift nonequivalence *versus* chemical shift equivalence of geminal diastereotopic groups in prochiral assemblies ad I. General analysis A. O. FULEA 39

Cyanine dyes with their orbital energies. Correlation of reduction potentials of —. J. AHMAD and K. BRIAN ASTIN 321

Cyclohexa-3,5-diene-1,2-dicarboxylic acid derivatives with *para*-benzoquinone and azo compounds. The reaction of — . Part I. F. IORDACHE, M. DĂNILĂ, A. SCHIKETANZ, M. GHEORGHIU and F. BADEA 903

Dehydrogenation kinetics of low aliphatic alcohols on copper catalysts. IV. Analysis of structure — activity relationships. N. DOCA and E. SEGAL 13

Decomposition of basic zinc carbonates $2ZnCO_3 \cdot 3Zn(OH)_2$ (In German). D. TITA, I. JULEAN and Z. SIMON 569

Dependence of nuclear diamagnetic shielding constants for free atoms The Z. — D. PURDELA 623

Dialkylation of aromatic amines under a minimum excess of alkylation agent. Quantitative — . I. POP, I. CIUPE, M. BUTAN, L. TEREC, L. FEY and I. BALDEA 283

Diamidoboron cations. A molecular orbital study of $[H_2NBNH_2]^+$. Electronic structure and bonding in —. I. SILAGHI-DUMITRESCU and IONEL HAIDUC 851

Dibenzoylacetylene with N-alkyl nitrones, heteroaromatic-N-oxides, diazo and azoxy compounds. Reactions of —. A. M. NOUR EL-DIN, ABD EL-RAZAK M. TAWIK and R. MEKAMER 183

2,4-Dibenzyldiisocynate ionic polymers. Synthesis and characterization of some—. IV. Biological activity. T. BURUIANĂ and A. CARACULACU 809

Dithiocarbamate series. Part II. Pyrolidino- and indolinodithiocarbamate esters of possible antibacterial and antimicrobial activity. H. M. FAID-ALLAH 815

Electrode processes with interfacial generation of the electrochemical active species. I. The kinetic model and the equation of the current density. N. BONCIOCAT, S. STERNBERG, T. VIŞAN and. A. COTARŢĂ 781

Exo- and endohormones. XIII. Synthesis of Z-9-pentacosene. L. POP, H. KREMPLES and F. HODOŞAN 635

Fluoro-substituted mesoionic heterocycles. Studies in the synthesis of some new-. R. L. MITAL, P. TANEJA, V. KHATRI and L. PRAKASH 463

Fundamental property of matter. Part I. V. V. JINESCU 763

Furobenzopyrones. Synthesis of substituted. O. H. HISHMAT, A. H. ABD EL RAHMAN, H. I. EL-DIWANI and SH. M. ABU-BAKR 741

Heterocycles-syntheses using carbonic acid derivatives. XI. Reaction of *o*-formylarylcyanates with NH-heterocycles affording benzoxazine derivatives. H. H. GLATT, C. CSUNDERLIK, I. GLATT, H. DULVAC and V. SCOROBETE (in German) 975

Hydraulic binders. I. Contribution to the processes of producing high-quality Portland and aluminous cements, noble and coloured limes and plasters out of wastes resulted from the chemical industry and other industries. M. ENCULESCU 199

Higher order Onsager's coefficients for monomolecular reactions. Calculation of —. R. VÎLCU and A. DOBRESCU 107

Hydrogenation of styrene on bimetallic supported catalysts Pd-Me/γ-Al$_2$O$_3$(Me = Mn, Fe, Co, Ni and Cu). V. PÂRVULESCU, V. PÂRVULESCU, I. V. NICOLESCU and I. SĂNDULESCU 1041

2-Hydroxyketones. XX. New *Mannich-Werner* bases of 7-hydroxy-4-methyl-6- and 8-propionylcoumarin. Al. CAȘCAVAL and ST. CILIANU-BIBIAN 991

3-Hydroxy-3-methyl-1-phenyl-triazene derivatives. Infrared spectral studies of —. NIZAMUDDIN and D. N. PUROHIT 295

Imines of aminoazoles. IV. Kinetics and mechanism of benzylidene-aminoazoles hydrolysis. H. H. GLATT. M. F. BARRY, C. CSUNDERLIK, I. BACALOGLU and SIMONA TIMOFTEI (in German) 639

Informational representation of the spectral analytical systems as communication systems with data decoding. V. DAVID 937

Inorganic sulphur compounds by indirect spectrophotometric method using ferricyanide-thymolphthalein reagent and osmium tetroxide as a catalyst. Oxidative microdetermination of some —. M. M. ABDEL BADEI and M. F. EL-SHAHAT. 875

Ionic B coefficients in the Jones-Dole viscosity equation of halide ions in aqueous formamide solutions. J. DOMENECH and J. MIRO 579

IR analysis of amines, carboxylic acids, alcohols, phenols and mercaptans after derivatization with-*n*-butylisocyanate. I. MUNTEAN, J. M. HERDAN and G. VĂLEANU 467

Kinetics and mechanism of substitution reactions of complexes. LIX. Influence of pH upon the aquation kinetics of iodo-aquo-bis-dimethylglyoximato-cobalt (III). Z. FINTA, J. ZSAKÖ and CS. VARHELYI 263

β-Lactam antibiotics. II. Substituent effects on cephalosporins. J. WEINBERG, A. DONESCU and V. EM. SAHINI 795

β-Lactams, 4-thiazolidinones and pyrazolines. Synthesis of some new — . A. M. FAHMY, KH. M. HASSAN, A. A. KHALAF and R. A. AHMED. 755

Lanthanides with 3-hydroxy-3-phenyl-1-*o*-carboxy phenyltriazene. Spectrophotometric studies of —. D. N. PUROHIT and R. S. CHAUHAN 413

Lead acid battery grids with addition of Se, Sb and silver. Studies on corrosion of -A. MATEESCU and D. MATEESCU 595

Linear low density polyethylene and branched low density polyethylene. Some properties of —. V. DOBRESCU, G. ANDREI, A. CIMPEANU and C. ANDREI . . . 399

Linear *versus* bent bis(diphosphine)iminium cations. A molecular orbital discussion of the bonding in [H$_3$PNPH$_3$]$^+$ and related species. I. SILAGHI-DUMITRESCU and I. HAIDUC 133

Liquid-vapour equilibrium curves and correlation by different activity models for the cyclohexane-monochlorocyclohexane and cyclohexane-water systems. Experimental determination of—.O·LANDAUER, C. MATEESCU, O. IULIAN and D. GEANĂ 237

Manganese(II)-pyridine-thiocyanate system and thermodynamic parameters. Polarographic study of —. J. SHARMA, A. KUMAR and B. K. PURI 456

Mass spectral fragmentation pattern studies of tartaric acid hydrazide and some of its arylidene derivatives. M. F. ABDEL MEGEED, M. GABER, R. M. ISSA and H. A. IBRAHIM 865

Mass spectrometry of diterpenic compounds with a glycol function at C$_{16}$—C$_{17}$. F. J. GARCIA, R. CRUZ, O. COLLERA and J. L. SANCHEZ 385

Manganese (III) complex oxalates thermal decomposition. On the mechanism of some —. E. JURCONI and GH. S. IONESCU 947

Mathematical foundation of chemical transformations on the basis of REDOX and COLHOM processes. A. CĂLUȘARU 921

Mesoionic oxazolones. II. Unstable non-acylated compounds. H. PETRIDE and D. RĂILEANU 729

Mixtures of alkylphosphates, orthophosphoric and hydrochloric acids. The potentiometric determination of —. M. SURPĂȚEANU, A. DUCA, G. SURPĂȚEANU and M. GABURICI 325

Molecular compounds with some alkyl aryl ethers. II. Hydrogen bond complexes, E. M. VASILESCU, M. IOVU and SĂNDULESCU 438

Moore's Ketene precusors. A convenient synthesis for—. M. D. GHEORGHIU, L. PÂR-

VULESCU, R.CECLAN, I.MANOLESCU, D. CONSTANTINESCU, C. FLOREA and. M. STANESCU 83

Multicomponent polyphasic systems. Method for determining the phase composition in —. C. KISSLING 363

Nature of iron(III) impurities in NeA zeolites. Determination of the — . F. IACOMI, E. TRIF, Ev. POPOVICI, A. VASILE, M. ALEXANDROAIEI, M. CRUCEANU and GH. SINGUREL 149

Nenitzescu synthesis of 5-hydroxyindoles. III. A. diazaheptalenedione from 3-aminocinnamic ester, M. PALAGHITA and D. I. RĂILEANU 953

Nickel ferrite from polynuclear coordination compounds. Synthesis of —. Part II. Study of the wet ferritization process. I. ILIE, M. BREZEANU, L. PATRON and E. SEGAL 803

Nickel ferrite from polynuclear coordination compounds. Synthesis —. Part. III. Structural data of NiFe$_2$O$_4$ obtained by the wet ferritazation method. I. ILIE, M. BREZEANU, L. PATRON, E. SEGAL and S. FILOTI 885

Nitrite ions. A novel spectrophotometric method for determination of —. N. BIÇAK, N. TAN and Ö. BEKAROGLU 405

Nitrofuran heterocycles. Part I. Synthesis and antibacterial activity of 7H, 6-(5-nitro-2-furyl)-*s*-triazolo[3, 4-b]-1,3,4,-thiadiazines, B. S. HOLLA, B. KALLAURAYA and K. R. SRIDHAR 277

Nonpolar gas solubilities in polar solvents. R. VÎLCU and ST. PERIŞANU 351

B-nor-5-androstene-3β-ol-17-one and 5-androstene-3β-ol-17-one. 17α-Substituted derivatives of-. R. SCHWARTZ and A. SCHWARTZ 313

Nucleophilic reactivity of sulphur and nitrogen in 2-mercapto-4-(3H)quinazolinone under solid-liquid phase transfer catalysis conditions. Studies on the—. A. K. EL-SHAFEI 29 and A. EL-SAYED 291

Organochloro pesticides in methanol. Studies on physical properties of some—. R. P. VARMA, B. B. BHATNAGAR and A. SINGH 305

Ortho effects of substituents in oximes, hydrazones and azines derived from benzaldehydes by electron impact, L. DAGNINO and F. CORTES 371

Oscillating chemical reactions by using concepts, derived from the rules for flow graphs. A study of the stability of realistic models of —. DAN CARTIANU 489

Oxidation of some disaccharides by chromic acid in perchloric medium Kinetics of—. M. P. ALVAREZ MACHO (in Spanish) 171

3-Oxo-fluoren-2-carboxanilide derivates. Synthesis and reactions of some new—. O. M. O. HABIB, I. I. ABDEL-GAWAD, E. M. KANDEEL and S. BADAWY 445

Oxovanadium (IV) complexes of octamethyl-pyrophosphoramide and nonamethylimidodiphosphoramide. Synthesis and characterization of some—. R. K. AGARWA and G. SINGIL 537

Pd/γ—Al$_2$O$_3$ catalysts. Effect of palladium concentration on the state and activity of — . V. PÂRVULESCU, L. SĂNDULESCU, N. GRECU, C. CONŢESCU and I. V. NICOLESCU 3

Peroxydisulphate ion using *o*-dianisidine-S$_2$O$_3^{2-}$ —. Cu(II) indicator reaction. A novel spectrophotometric method for the determination of —. P. M. SHIUNDU and S. B. JONNALAGADDA 611

bis (9,10-Phenanthro) [*a*, *e*]cycloocta-1,5-diene by sulphone pyrolys. Synthesis of —. M. BANCIU A. BANCIU, M. ELIAN, C. DRĂGHICI, N. PALIBRODA and E. CIORĂNESCU 893

o-and *p*-Phenylenediamine with some substitued 2-thliazoln 5-ones. Condensation of —. H. M HASSAN and O.M.O. HABIB 653

Phenoxideions. A correlation of the reactivity of some substituted —. AHMED M. G. NASSAR, MOHAMED A. KHARABA and ABDEL-HAMID A. YOUSSED . . 525

Phosphonium ylides. VI. The reaction of fluorenylidenetriphenyl phosphoranes and-arsinane with quinisatins. L. S. BOULOS, EL. S. M. YAKOUT and M. M. SIDKY . 823

Phosphoric acid on the PbSO$_4$/PbO$_2$ electrode in sulphuric acid solutions. Effect of S. STERNBERG, A. MATEESCU, V. BRÂNZOI and L. APĂTEANU 111

Photochemical bromination of anilides by benzenehexabromide. M. M. ALY, I.M.A. AWAD and A. M. FAHMY 167

Photodegradation and photostabilization of ethylene-vinyl acetate copolymers. II. New facts which support the scheme of photodegradation mechanism. C. ANDREI, I. HOGEA and V. DOBRESCU 53

Photoirradiation of 1-phenylcyclopentadecene-1. K. GUNAYDIN and T. ÖZTÜRK . . 177

Polarization behaviour of the n- and p-type silicon in sulphuric acid solutions. S. STERNBERG, V. BRÂNZOI, L. APĂTEANU and M. UNGUREANU 775

Predicting fluid phase equilibria by a model of equilibrium of interaction in restrained molecular systems. F. A. GOTHARD. 331

Propane pyrolysis in tubular reactors. Optimal temperature profiles for —. G. BOZGA, J. TOWFIGHI and O. FLOAREA 87

Pyrylium salts with nucleophiles. XX. Synthesis of 4-(N-pyridinium)-4-dialkylaminoazobenzene and 4-(4-dialkylaminophenylazo)-4′-(N-pyridinium)-biphenyl derivatives. A. T. BALABAN 377

Pyrylium salts with nucleophiles. XXI. Unexpected formation of 6-6-dimeyl-5-isopropyl-2,4-cyclohexadienyliden-1-imines from primary amines and 2-6,diisopropyl-pyrylium salts. C. UNCUŢA, M. D. GHEORGHIU, F. CHIRALEU, M. PLĂVETI, M. ELIAN and A. T. BALABAN 719

R*edox* and *Colhom* quantum transitions as basic components of chemical processes. A. CĂLUŞARU and M. APOSTOL 25

Reduction of Cr (IV) by acetone in sulfuric acid medium A kinetic and mechanistic study of —. M. P. ALVAREZ MACHO (in Spanish) 857

Ru(III) chloride-catalysed oxidation of benzaldehyde and substituted benzaldehydes by trichloroisocyanuric acid in acid medium. Kinetics and mechanism of —. SUBAS C. PATI, ASHOK KUMAR SAHU and Y. SRIRAMULU 157

Semisynthetic penicillins and their parent compounds using a Cu^{2+} sensitive electrode. Potentiometric determination of some—: M. MIOŞCU, I. HAIDUC, D. C. CORNOS J. RUSU 455

Silver ion catalyzed redox polymerization of acrylamide. U.D.N. BAJPAI, A. JAIN and A. K. BAJPA 629

Spectra absorption . Complex compounds of Tl(II) with organic heterocyclic ligands. III Infrared- I. BERDAN and I. SANDU (in French).. 67

Square-planar — tetrahedral isomerism of complexes. Electronic spectra and magnetic moments of Ni(II) complexes synthesized with ligands from the class of substituted 1-methyl-2-carbothoxy-glyoxalynyl-(1)-phenylhydrazones-(2). A. C. BANCIU, . 225

Stereochemistry of Olah's reduction of bicyclo[2.2.1].heptene derivatives. A proof for a concerted reaction mechanism? M. D.GHEORGHIU and E. OLTEANU . . . 753

3-Substituted 4(3H)-quinazolinone and 4(3H)-quinazolinethione derivatives and related fused biheterocyclic ring systems. Synthesis of some new—.M. F. ABDEL-MEGEED and A. TENOIU 981

Synthesis of organic esters. The effect of using aluminium phosphate-γ-alumina and aluminium phosphate-silica on the —. C. FERNANDEZ-SACHEZ, M T. GANDASEGUI, R. BARAJAS and J. Mª. MARINAS (in Spanish) 271

Thermodynamics of some iron complexes in water-pyridine mixtures. J. L. BRISSET . . 253

2-(2′-Thenyl)-3,1-(4H)-benzoxazin-4-one and its reactions with different nucleophiles. ABDEL MOMEN A. EL-KHAMRY, S. EL-NAGDY and M. E. SHABAN . . . 833

Thiourea by iron(III) in the presence of 2.2′-bipyridyl. Kinetics of oxidation of —. G. V. SARADAMBA, K. RAMAKRISHNA, K. N. RAJU and P.V. SUBBA RAO . . . 547

Topological and empirical models. I. The prediction of the Gibbs energies of formation for alkanes. O. IVANCIUC 839

Unsaturated acyl isothiocyanates. Some reactions of —. N. M. ABED, A. GIELAGAMEY, SALAHZAKI SOWELLIM and ABDEL-FATTAH ALI HARB 393

UV-VIS—spectral behaviour of arylazo compounds. I. General remarks. J. EPPERLEIN and B. BLAU 473

UV-VIS—spectral behaviour of arylazo compounds. II. The UV-VIS absorption spectra of 4-amino-substituted azobenzones. J. EPPERLEIN and B. BLAU 685

UV-VIS spectrometric study of the reaction of the Pd(II)-*p*-nitrosodiphenylamine complex with carbon monoxide V. DAVID and G. E. BAIULESCU 603

THE PLASTICS PROCESSING ENTERPRISE, BUCHAREST

YOUR LONG-TERM PARTNER

The Plastics Processing Enterprise (IPMP) in Bucharest is one of the reprezentative units of the Romanian plastics industry. A modern unit for obtaining high-tech products, IPMP — Bucharest, due to the quality of its products, and to the readiness towards the requirements of its clients has ensured a constant, relatively large group of foreign clients, faithful to the supplier just because of the tight correlation between their requirements and the services offered.

At present IPMP — Bucharest has as steady clients companies from Holland, France, West Germany, England, U.S.A., Jugoslavia, Zaire, Egypt, Jordan, Ghana, USSR, etc. : companies which expressed positive remarks on the quality of the delivered products, the promptness in delivery and the flexibiliy towards the requirements of the client.

As traditional products offered by the company we mention :

- PVC granulates (for electrical insulation, for tubes and hoses, for shoe soles, for bottles, etc.) ;
- PVC tubes and pipes (for electrical insulation, irrigation, building industry, etc.) ;
- heavy duty polyethylene bags for fertilizers, cement, etc. ;
- bags made of high and low density polyethylene, for household use, for packing, etc. ;
- carrier bags with various paintings ;
- polyethylene sheeting for agriculture, building industry, etc. ;
- various household articles made of plastics.

The factory has achieved a good experience in assimilating and producing car spare parts, by assimilating and producing the Romanian passenger cars DACIA, ARO and OLTCIT as well as the trucks and buses of the ROMAN family.

The unit performs a steady research and design work and also assimilates and produces under own conception and with own tools or with the clients' drafts and tools injected spare parts or profiles (with or without metallic insertion), of any thermoplastic material. Likewise, the factory is able to produce plastic spare parts, injected or extruded for various uses as functional parts, multivalent decorative accessories for machines and tools.

The efforts for renewing the products and for widening the products in the processing program led to assimilating new products in the compound family as :

- ROMAMID — FS 10, 15, 20, 25, 30 — polyamides reinforced with fibreglass ;
- ROMALEN F0, F1, F2 – fireproof polypropylene corresponding to UL 94 fireproofing classes V0, V1, V2 ;
- ROMAMID G2, G4 – modified polyamides with graphite as additive ;
- ROMALEN R-Cu – polypropylene resistant to copper ;
- ROMALEN T-10, T-20, T-30, T-40 — polypropylene filled with talcum ;
- ROMALON FS-20, FS-25 — polycarbonates reinforced with fibreglass ;
- ROMAMID M2, M4 — polyamides modified with MOS2

We are sure that on joining the great family of the IPMP — Bucharest buyers, our products will assure satisfaction.

Come for testing, for proving a new way and variant and you'll stay for quality, promptness, competitivity and flexibility.

WE ARE WAITING FOR YOU !

DRAGASANI

THE PLASTICS PROCESSING ENTERPRISE
– DRĂGĂŞANI –

The Plastics Processing Enterprise in Drăgăşani, 721, Tudor Vladimirescu Blvd., telephone 948/12060, telex 48619, has in its production activity a wide range of products processed from PVC, namely :

- PVC granules for cable insulations with application in electric conduits, for 1, 2, 6 and 10 kV ;
- PVC granules for shoe-soles, in a wide variety of colours and different degrees of flexibility ;
- PVC pipes of the Bergman-Pantzer type for protection and insulation of cables in electric conduits, with application in building industry ;
- PVC pipes of light, heavy and medium-weight types, available in a wide range of applications for water supply in sanitary-engineering installations, for transportation and draining of liquids in agriculture, for transportation of corrosive liquids at chemical plants. The various types of pipes have diameters ranging from 20 to 400 mm and they are working at service pressures of 2.5 up to 10 atm. ;
- PVC fittings for pressure and draining pipes, of the following types : tee elbows, joints, sockets for joining PVC pipes ;
- hoods made from PVC foil, 4.5 by 15 m, for general purpose packagings and with application in agriculture.

The Plastics Processing Enterprise in Drăgăşani manufactures products both for internal consumption and for export.

The products are marketed by "DANUBIANA" Foreign Trade Company, in Bucharest, 10, Republicii Blvd., that ensures a constant relationship with its foreign partners.

THE PLASTICS PROCESSING ENTERPRISE -- FOCŞANI –

The Plastics Processing Enterprise in Focşani, 76, Bucureşti, Blvd., telephone 13900 ; 13901 ; 13902, telex 53275, is manufacturing plastic products from the following materials :

- polyvinyl chloride ;
- high and low density polyethylene ;
- polypropylene ;
- polystyrene ;

The products are marketed by "Danubiana" Foreign Trade Company, Bucharest, Romania. Applications of these materials in different industries include : **Flat sheets** manufactured by extrusion technology from rigid PVC having the following ranges of dimensions :

- width of 1,200 to 1,400 ± 10 mm ;
- length of 2,000±10 mm up to 3,000±10 mm ;
- thickness of 2 up to 8 mm ± 20% ;

The sheets have a good resistance to chemical agents ; at temperatures of 50°C they resist to acids in aqueous solution : 5% nitric acid, chlorine hydride 10% ; phosphoric acid 20% and 30% ; sulphuric acid 10—45%, mineral oils etc.

The sheets are suitable for the following applications : protection material for walls, in chemical industry ; material for ventilation pipes and chimney hoods in building and house-building industries ; another field of application is that of electrotechnics ; the sheets can easily be processed by different methods : cutting, holing, milling, welding.

Approximate price : 23,000 lei/ton.

High and Low Density Polyethylene Sheets having the following ranges of dimensions : length of 800 to 2,000 ± 20 mm ; width of 1,000 up to 1,200 ± 1 0mm ; thickness of 2 up to 8 mm ± 20%.

The sheets have good resistance to chemical agents, such as : concentrated chlorine hydride, sulphuric acid 50%, nitric acid 40%, sodium chloride 10%, ethyl alcohol, acetone, transformer oil etc.

These types of sheets are suitable for the following applications : filters, frames and ventilation pipes in chemical industry ; packagings and mechanical protection for electrical underground cables ; they can be easily processed.

Approximate price : 25,000 lei/ton.

Honeycomb Scheets are manufactured from high density polyethylene ; these types of sheets have the following dimensions : length of 2,000 ± 25 mm ; width of 1,200 ± 10 mm ; plate-thickness 3 to 8 ± 0.3 mm ; wall-thickness of 0.2 to 0.5 mm.

Major uses of these products include : replacements for corrugated cardboard, packaging plating, sound and thermal insulations.

Approximate price : 24,000 lei/ton.

High Density Polyethylene Pipes of 2 types :

- type 3 (medium) for pressures of 6 atm ;
- type 4 (heavy) for pressures of 10 atm ;

having the following ranges of dimensions : diameter of 16 to 110 mm, length of 6 m (for larger diameters) or rolled (with a diameter of 16 to 40 mm and length of 100 to 300 m).

The pipes are used as means of transport fo. liquids, chemical agents or protection for telephone cables ; they also find application in building industry, namely civil, industrial, cultural and in zootechnic engineering. .Black coloured pipes are used for outer installations, because they are not sensitive to UV light.

The rolled pipes with diameter of 16 to 25 find application in zootechnics (floor heating systems) and as component parts of solar screens.

Approximate price : 25,000 lei/ton.

INTREPRINDEREA Napochim

THE PLASTICS PROCESSING ENTERPRISE —"NAPOCHIM"— CLUJ-NAPOCA

The Plastics Processing Enterprise "NAPOCHIM" in Cluj-Napoca, 34, Someșului Street, has in its production activity a wide range of products and technologies, namely:

- plastic products obtained by different processes: injection, pressing, thermoforming, vacuum-thermoforming, extrusion, blowing and high-frequency welding.
- PVC rigid and semirigid plasticized foils obtained by calendering;
- PVC rugs and carpets with or without textile backing;
- rubber technical parts;
- items for dental techniques;
- glassware obtained by glass-blowing;
- other types of items.

The Plastics Processing Enterprise "NAPOCHIM" processes a large variety of materials.

- PVC
- general purpose and impact-modified polystyrene
- high and low density polyethylene;
- conventional and modified polyamides;
- polypropylene;
- polycarbonate;
- methyl polymethacrylate;
- thermosets.

The polymers that are processed by the above-mentioned technologies are suitable for various applications, such as items, parts and products of different shapes, types, dimensions and colours. Among the products offered there are:

- household goods (thermos flasks, table linens, basins, babytubs, pots pails, holds for plates and dishes);
- school and office supplies (rulers, squares, protractors, French curves, etc.);
- patterns for technical drawing (circles, ellipses, squares, triangles etc.);
- patterns for technical writing (Roman type and inclined letters of different dimensions);
- items, and technical parts for machine-building industry and with application in different fields of industry;
- PVC and polypropylene pressure fittings for fixed joining by soldering of for mixed joining (soldering and screwing);
- pressed and injected products from thermosets (technical and sanitary items, rosettes, stoppers, clamps etc.);
- vacuum — thermoformed items (plywoods for ceilings, tapestries);
- polyethylene and polypropylene extruded and blown items (flasks, canisters, cans of different shapes and capacities, tanks for brake-fluid and for fluids used to clean the wind-screen, floating spherical balls for distillation columns and for pickling baths etc.);
- shopping bags, bags and thin sacks made from polyethylene foil;
- PVC calendered products (plasticized foils of 0.08—0.7 mm thickness and width up to 1,500 mm; semirigid foils, rigid foils and plates; foils for hydroinsulations etc.);
- items made from PVC welded by high frequency (covers for books and handbooks; files, briefcases and foliocases for documents; hoods etc.);
- inflatable items from plasticized PVC foils (ring-shaped, lifebuouys, balls, toys, etc.);

Besides the above-mentioned plastics items and products, the Plastics Processing Enterprise "NAPOCHIM" also has in its manufacturing activity different types of chemical products, processed in small quantities, such as: items for dental techniques; rubber technical parts, glass-ware; molds and punching tools; various other products.

Here are the most important types of products:

Chemical products manufactured in small quantities:

- green chromium oxide 90...98% ;
- variously coloured putty of "MASTIC" type for tightening operations ;
- foils suitable for heat-transfer printing with application in mashine-building industry and air-industry ; in light industry and in poligraphy ;
- general purpose test-paper for pH (ranging from 1 to 10) and special types of test-paper (ranging from 0.5 to 5 ; from 5.5 to 9 and from 9 to 13) and in box-form (ranging from 0.5 to 13) ;
- NAPOACRIL L + S — suitable for accurate castings and mouldings ;
- sodium silicate in solid form ;
- kits for determinations of hardness of water ;
- sets for ionic detection ;

Products with application in dental techniques :

- dental cements ;
- materials for impression taking and for insulation ;
- dental polymers of the NACRIL type for false teeth and for sets of plates ;
- material for pattern making and suitable for packing casting paste ;
- insulation material ;
- grinding stones ;

Rubber technical parts :

- gaskets of various types and dimensions ;
- plates and wheel rims ;
- conveyor belts.

Glassware :

- products made from plain glass or multilayer glass (sets of glasses cans, vases, ash-trays, bowls etc) ;
- household glassware (lamp shades, plates, jars).

Other types of items :

- white or differently coloured chalk for school-supplies or with application in industry (chalk for forestry technics, for leather processing industry, for tailoring etc) ;
- blue ink for writing ;
- tapes for computing mashines and for typewriters ;
- detergent in paste form ;
- car washing shampoo — EXTRA type.

Moulds and dies.

The Plastics Processing Enterprise "NAPOCHIM" in Cluj-Napoca manufactures a wide variety of products both for internal consumption and for export. The products are at present delivered to a number of buyers from different countries, such as : USA, France, West Germany, China, USSR, Hungary, India etc. The products are marketed by different Romanian trade companies : DANUBIANA, ICECOOP, ILEXIM, TERRA.

It is worth mentioning that our enterprise is manufacturing, on terms of settled agreements, various other types of parts by injection technology, from any type of polymer or thermopolymer, with moulds delivered by the buyers of the products.

THE PLASTICS PROCESSING ENTERPRISE —SF. GHEORGHE—

The Plastics Processing Enterprise in Sf. Gheorghe, 1, Braşov Street telephone 923/11360, has in its production activity a range of products made from different types of plastics, namely :

a. Foils from high- and low-density polyethylene in the following shapes, colours and dimensions :

- tube shape, film ;
- natural colour (transparent) or differently coloured and printed in 1—4 colours ;
- foils made from low density polyethylene with width ranging from 400 to 1,000 mm and thickness from 30 to 100 microns ;
- foils made from high density polyethylene with width ranging from 400 to 1,000 mm and thickness from 20 to 40 microns ;

b. Sacks made from low density polyethylene, natural colour (transparent) or differently coloured, with or without side folds, having the following dimensions :

- length : 700 up to 1,200 mm ;
- width : 500 up to 800 mm ;
- tickness : 25 up to 100 microns ;

c. Bags from low and high density polyethylene, natural colour (transparent) or differently coloured, with or without side folds, printed in 1—4 colours, having the following dimensions :

- bags from low density polyethylene with thickness ranging from 20 to 60 microns ;
- bags from high density polyethylene with thickness ranging from 20 to 40 microns ;

The products that are manufactured in our enterprise are marketed by "DANUBIANA" Foreign Trade Company.

Our enterprise is well known among other processing factories of the same kind as a manufacturer of high-quality products, always ready to accomplish successfully the agreements concluded with its partners.

THE PLASTICS PROCESSING ENTERPRISE —TULCEA—

The Plastics Processing Enterprise in Tulcea, 7 Grădinarilor Street, has in its production activity the following range of products that can be delivered on Buyers' requests:

- Polypropylene woven sacks ;
- Polypropylene foil —printed
  —unprinted
- Polypropylene bags —printed
  —unprinted
- High and low-density polyethylene foil —printed
  —unprinted
- High and low-density polyethylene shopping bags —printed
  —unprinted
- Low density polyethylene thin sacks.

THE PLASTICS PROCESSING ENTERPRISE — BUZĂU —

The Plastics Processing Enterprise in Buzău, 132, Transilvaniei Street, telephone 13425, Telex 56227, manufactures a large variety of products, that may be classified into four main groups, according to the manufacturing technology :

A. semi-finished and finished plastic products ;
B. filters and filtering component parts ;
C. protection devices for the breathing passages ;
D. active carbon.

A. Semi-finished and Finished Plastic Products

The Plastics Processing Enterprise in Buzău manufactures products from : HDPE, LDPE, PVC in suspension, impact modified PP and PS, by different technologies such as : extrusion, extrusion-blowing, extrusion-granulating, sintering, injection, thermoforming.

A.1. Polyethylene Products

1. The Plastics Processing Enterprise in Buzău manufactures and delivers HDPE and LDPE sheets for a wide range of applications in agriculture, industry and other fields of activity.

   The PE foils may be clear or opaque, uncoloured or pigmented.

a. According to the application, there are manufactured four types of LDPE foils with width (in pipe-form) ranging from 150 to 6,500 mm :

- for packaging applications ;
- for general purposes ;
- for industrial bags ;
- covers for agriculture use ;

The following values of thickness are given for each type of foil : 0.025—0.045 mm ; 0.045—0.25 mm ; 0.25—0.32 mm ; 0.100—0.160 mm.

b. The HDPE foils have values of thickness ranging from 0.020 to 0.060 mm and width from 150 to 1.100 mm.

The PE sheets are delivered rolled on PVC cores ; the maximum weight of a roll is of 50 kg.

Our enterprise is also manufacturing :

- LDPE and HDPE sheets with flaps, for agriculture use (covers for crops of vegetables) ;
- LDPE sheets for insulating irrigation canals ; their width ranges from 750 to 3 000 mm and their thickness from 0.5 to 1 mm.

c. Coextruded LDPE and HDPE foils.

2. PE sheets with the following applications :

- packagings (bags, carrier bags, thin sacks, hoods) for different products (chemical products, food, clothes) or protection covers for pallets (containing construction materials, equipments etc.).

They may be unprinted or printed in one to six colours.

- thick sacks for chemical fertilizers of for other types of powders or granules : maximum load for each sack is of 50 kilos. They may be unprinted or printed in one or two colours.

3. The Plastics Processing Enterprise in Buzău also produces high load packagings (for capacities ranging from 20 to 1,000 litres) by means of technological process used only in this enterprise in Romania, namely rotational or static moulding (sintering) of LDPE powders.

These packagings may have different shapes and colours, their application including boats and objects for sanitary use, tanks and silos, cans and containers that are to be palletized. The material used for these applications — LDPE — is characterized by thermal stability between — 5 and + 60°C, good impact strength, stiffness, chemical resistance to almost all chemical substances and it is also a good electrical insulator ; in a word, it shows a unique combination of qualities.

It may be applied in food industry as it meets the requirements for food-contact use, approved by the Ministry of Public Health.

On Buyer's request, the range of the existing types and dimensions of products can be extended, either by manufacturing new products or by adjusting connecting pieces, valves and corks to the already existing products.

4. The Plastics Processing Enterprise in Buzău also manufactures and delivers HDPE rifled or punched pipes for draining water in agriculture, with a nominal diameter of 50, 65 or 80 mm.
5. Our enterprise manufactures and delivers LDPE slings, reinforced with thread of viscose cord, used to fasten the pallets containing bags or boxes, with a maximum weight of one ton.

A.2. Semi-finished and Finished Products Made from PVC in Suspension

Our enterprise manufactures and delivers granules, pipes and insulating tubes made from PVC.

Major applications of PVC granules include :
- primary or secondary electrical insulations for pipes or electric cables ;
- footwear and different component parts for footwear, such as soles, heel pieces, straps, welts ;
- construction materials, namely pressure pipes, fittings, handrails ;
- records.

Applications of PVC pipes include technological and sanitary-engineering installations, used as conveyers for drinking water, waste water or liquids that do not attack PVC, for irrigations or as chanels for cables.

The Plastics Processing Enterprise in Buzău also manufactures pipes with an outer diameter determined by the values of pressure of the conveyed fluid : simple pipes Type 1 (light) for 2.5 atm., Type 3 (medium) for 6 atm. and Type 4 (heavy) for 10 atm., the values of diameters range from 32 to 110, 16 to 160 and, respectively, from 16 to 110 mm ; and coupling pipes with ring, for pressure of 10 atm., with a diameter of 125 to 315.

The coupling pipes are provided with a rubber gasket to ensure a proper sealing. The gaskets are delivered together with the coupling pipes.

The insulating pipes made from PVC are used for protective applications of the pipe-lines of electric wirings with voltages up to 1,000 V or used to replace the metallic pipes of the Bergman or Pantzer type.

Our enterprise is manufacturing insulating tubes with a outer diameter of 16—50 mm.

A.3. The Plastics Processing Enterprise in Buzău manufactures packagings from impact-modified polystyrene sheets by thermoforming

These packagings are of different shapes and dimensions, according to the Buyer's requirements and they include : baskets, casseroles, cells, glasses, cases, stands and are used as containers for fruit, frozen food, dairy products, candies, drugs, spare parts for industry etc.

The material used for packaging in the food industry meets the requirements for food-contact use, approved by the Ministry of Public Health.

Thermal stability of the packagings made from impact-modified PS ranges from —10 to + 50°C.

A.4. Products Made from Polypropylene

1. Our enterprise manufactures and divers PP tapes, with a width of 13 mm and a thickness of 0.5 mm, used for fastening different packagings (packs, boxes).
2. We also manufacture and deliver PP woven sacks, with the following dimensions : 550 × 1,000 mm, 650 × 1,150 mm, used as packagings for different chemical products, both for internal consumption and for export.
3. Our enterprise manufactures strings and ropes from flat PP threads used for fastening, attaching or binding different products. Twisting technology is used for manufacturing strings with a diameter of 1.5—3.5 mm and ropes with a diameter of 6—14 m, that show a very good resistance.

B. Filters and Filtering Parts

The Plastics Processing Enterprise in Buzău is the largest manufacturer of filters and the filtering parts in Romania.

he filters and the filtering parts are used as mponent parts of the equipments and engines ade in Romania or imported, such as reasing and hydraulic devices of the industrial quipments or filtering devices for air and quid fuels (gasoline, gas oil). They are also sed as component parts of different auto-otive products: cars of DACIA OLTCIT, KODA, LADA, MOSKVICI type, trucks of AC, ROMAN, ARO and FIAT type, motor ractors and excavators.

he performances of the filtering elements are iven both by the dimension of the smallest article that will not pass through the device nd by the flow of the fluid that is filtered.

hese devices include: air-filtering elements, ith a filtering accuracy of 20—25 microns, for a maximum flow of 250 m^3/hr, oil-filtering arts, with a filtering accuracy of 5—8, 9—12, 0—15, 20—25 microns for flows ranging from up to 1,000 liters/min. and filtering parts for liquid fuels with an accuracy of 5—8 and 8—11 microns, for flows of 0.15 up to 6.25 liters/min.

C. Protection Devices for the Breathing Passages

- protection masks with free aspiration of fresh air for environments with toxic gases (chlorine, ammonia, phosgene, cyanic compounds, organic solvents, aerosols, sulphur dioxide, carbon oxide, hydrogen sulphide etc.);
- dust-masks;
- rescue apparatus for mines;
- masks used in painting industry.

D. Active Carbon

The Plastics Processing Enterprise in Buzău manufactures active carbon in granular form (used as degasolination agent for oil-well gases, as purifying agent for industrial waters, as retainer of the traces of oil from the compressed air), in coalbrick form (used as catalyst for cyanuril chloride synthesis), in powder form (used as decolourizing agent for glucose, lactose and molasses in solution, syrups and other types of solutions) and as purifying, decolourizing and deodorizing agent for chemical and pharmaceutical oils and greases, animal and vegetable fats).

The Plastics Processing Enterprise in Buzău can offer, on your request, the technical assistance of its specialist in order to satisfy as well as possible, the demands of your enterprises.

INDUSTRIALEXPORTIMPORT

Foreign Trade Company

A company with complete capability to assure :

- Design
- Engineering
- Manufacturing
- Supply
- Services
- Technical assistance
- Studies
- Know-how
- Technologies
- Erection works
- Training
- Procurement

EXPORTS AND IMPORTS :

- Oilfield equipment
- Mining equipment
- Complete plants and process equipment for the chemical, petrochemical, oil refining and food industry
- Industrial pumps as well as sanitary valves and fittings

EXPORTS :

- Drilling rigs
- Well servicing and workover rigs
- Rigs and accessories for geological, seismic, structural and water wells
- Portal cranes

COOPERATES :

With specialized companies in other countries for the performance of industrial projects and the development of technologies in the field of chemical, petrochemical, oil processing and food industry.

INDUSTRIALEXPORTIMPORT 79519-Bucharest, Romania Telex 10052 ; 10930
Phone : 11.89.05 ; 13.10.09 P.O.Box 22-105 ; 768

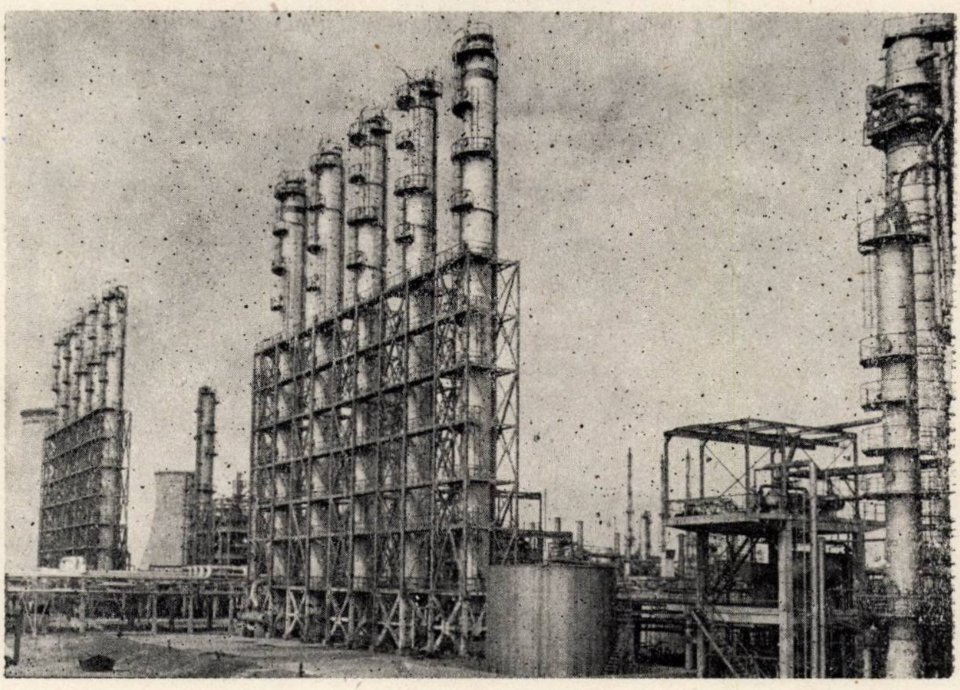

A NEW TECHNOLOGY FOR CATALYTIC HYDROFINING OF HEAVY PETROLEUM CUTS

I.C.I.T.P.R. Ploieşti (Institute of Research, Technological Engineering and Design for Refineries) has patented a catalytic hydrodesulphurization technology for reducing the content of sulphur, nitrogen and organo-metallic compounds of the vacuum distillate or vacuum distillate in admixture with products from destructive processes. The resulted product with a maximum content of 0.2% g sulphur and 0.02–0.05% g residual coke is the ideal feedstock for catalytic cracking.

A brief description of technology

The vacuum distillate as such or in admixture with gasoline and/or gasoil from destructive processes is mixed up with hydrogen rich gas, heated up to the reaction temperature by heat exchange with the reaction product and in an oven, then directed to the reaction system. The reactions of desulphurization up to 90%, denitrification up to 70%, saturation of olefinic compounds and reduction of organo-metallic compounds are carried out by contacting the feedstock with the catalytic bed, at a temperature and pressure adequate to the type of feed used and in the presence of hydrogen. The separation of light products (gas, light gasoline) from the reaction effluent is carried out in a high pressure separator and a stripping column.

The gas in the high pressure separator is desulphurated with MEA solution.

Institutul de Cercetări, Inginerie Tehnologică şi Proiectare
pentru Rafinării I.C.I.T.P.R.
Ploieşti—B-dul Republicii nr. 291 A—Cod 2000
Telefon 3.51.11—3.18.75
Telex 1.93.41

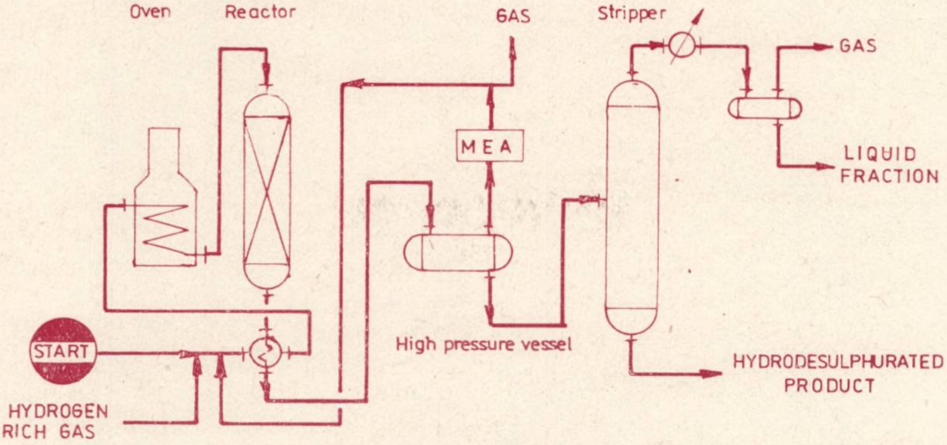

Flow—sheat of the I.C.I.T.P.R. technology for vacuum distillate hydrodesulphurization

Performance of the process

Feedstock, %g 97.45
Hydrogen gas, %g 2.55

Characteristics	Feedstock	Product
Density, d_{14}^{15}	0.88 to 0.91	0.88–0.910
Viscosity, cSt/50°	20 to 30	—
Chill point, °C	30 to 40	—
Sulphur, %	1.6 to 2.9	max.0.2
Residual coke, %g	0.04 to 0.5	0.02 to 0.05
Kindling temperature, °C	—	64 min.

Consumption of raw materials and utilities

Typical requirements per ton of raw material for a plant with a capacity of 1,200,000 t/year are

Electric power, kWh 24
Superheated steam (35 at) . . .0.04
Catalyst, kg 0.02
Catalyst life . . . . 2 years

Process implementation

The process has been applied on an industrial scale in Romania: two plants are now in operation, one plant is under construction.

ZAGOS MŰSZAKI INFORMÁ KÖZPONT ÉS KÖNYV 1327

NOTE POUR LES AUTEURS

La Revue Roumaine de Chimie publie des articles en anglais, français, russe, allemand ou espagnol. Les auteurs sont priés d'envoyer des articles et des comptes rendus inédits.

Les manuscrits seront dactylographiés à double interligne. La bibliographie, les tableaux et la légende des figures seront placés après le teste.

Si l'article fait partie d'une série numérotée, la partie précédente sera donnée comme première référence.

Chaque article sera précédé d'un résumé comprenant quinze lignes au maximum.

Les références bibliographiques dans le texte seront faites par des exposants sans parenthèses et paraîtront à la fin de l'ouvrage.

Les publications périodiques mentionnées dans la bibliographie seront présentées suivant les prescriptions internationales : le nom de l'auteur précédé de l'initiale du prénom, le titre du périodique abrége, conformément à « Chemical Abstracts » et souligné par une ligne, le numéro du tome indiqué par des chiffres arabes et souligné par deux lignes, suivi de la première page de l'article : à la fin, l'année de la parution sera placée entre parenthèses. Le numéro de la revue ne sera pas indiqué si les pages du volume sont numérotées consécutivement.

Les textes des livres ou traités inclueront : le nom des auteurs, précédé de l'initiale du prénom, le titre du livre entre guillemets et sans être souligné, le numéro du tome précédé par l'abréviation « vol. » (ou « Bd »), le numéro de l'édition, les éditions (the publisher), la localité de la parution du livre, l'année de la parution et la page de la référence précédée par l'abréviation « p » (ou « S »).

Les brevets seront indiqués comme suit : l'auteur ou la firme, le pays et le numéro du brevet, la date de la revue (*Chem. Abstr.*). Par ex. : M. Jones (to Union Carbide Co.) Brit. Pat. 610 238,2 Sept. 1959 : cf. *Chem. Abstr.*, **54**, 12808 (1960).

Si la référence n'a pas été lue en original, on indiquera aussi la revue de références consultée.

Les diagrammes seront tracés à l'encre de Chine sur papier calque. Les tableaux et les figures (en nombre strictement nécessaire), ainsi que les courbes dans les figures seront numérotés, par des chiffres arabes. Leur explication sera donnée dans la légende des figures. Prière de ne pas inscrire les mêmes données dans les tableaux et les figures. Chaque tableau aura un titre. On indiquera dans le texte la place approximative des tableaux et des figures. Les formules chimiques seront incluses dans le texte ; en outre, elle seront transcrites sur papier calque, à l'encre de Chine.

Les auteurs sont priés d'indiquer les caractères italiques (en soulignant les lettres au crayon), ainsi que tout autre caractère spécial : les préfixes *ortho*, *méta*, *para*, *cis*, *trans*, etc. seront soulignés pour indiquer leurs caractères italiques, et ne seront jamais écrits avec des majuscules.

Aucune correction à la main ne sera admise sur le manuscrit. Les corrections seront frappées à la machine. Les lettres grecques ou d'autres symboles spéciaux seront insérés à la main à l'encre clairement.

Le manuscrit sera signé par l'auteur.

Le titre courant aura 50 lettres au maximum.

L'entière responsabilité du contenu des articles appartient aux auteurs.

Sur demande on peut obtenir une note plus complète.

PRINTED IN ROMANIA

TRAVAUX PARUS AUX ÉDITIONS DE L'ACADÉMIE DE LA RÉPUBLIQUE SOCIALISTE DE ROUMANIE

ELENA CEAUŞESCU, **Răşini de hidrocarburi, vol. 1, 1988, 344 p.**
ELENA CEAUŞESCU, **Progrese în chimia şi tehnologia polimerilor, 1986, 466 p.**
ELENA CEAUŞESCU, **Forschungen im Bereich der Chimie und Technologie der Polymere, 1986, 444 p.**
ELENA CEAUŞESCU, **Cercetări în chimia şi tehnologia polimerilor, 1983, 520 p.**
ELENA CEAUŞESCU, **Noi cercetări în domeniul compuşilor macromoleculari, 1981, 536 p.**
ELENA CEAUŞESCU, **Polimerizarea stereospecifică a izoprenului, 1979, 307 p.**
ELENA CEAUŞESCU, **Research work on synthesis and characterization of macromolecular compounds. Contributions, 1974, 251 p.**
I. G. MURGULESCU, **Introducere în chimia fizică, Vol. I. 1. Atomi, molecule, legătură chimică, 1976, 560 p.**
I. G. MURGULESCU, V. EM. SAHINI, **Introducere în chimia fizică, Vol. I. 2. Structura şi proprietăţile moleculelor, 1979, 604 p.**
I. G. MURGULESCU, E. SEGAL, **Introducere în chimia fizică, Vol. II. 1. Teoria molecular-cinetică a materiei, 1978, 1056 p.**
I. G. MURGULESCU, TATIANA ONCESCU, E. SEGAL, **Introducere în chimia fizică, Vol. II. 2. Cinetică chimică şi cataliză, 1981, 1024 p.**
I. G. MURGULESCU, J. PĂUN, **Introducere în chimia fizică, Vol. I. 3. Nucleul atomic, reacţii nucleare, particule elementare, 1982, 606 p.**
I. G. MURGULESCU, RODICA VÎLCU, **Introducere în chimia fizică. Vol. III. Termodinamica chimică, 1982, 624 p.**
I. G. MURGULESCU, O. M. RADOVICI, **Introducere în chimia fizică. Vol. IV. Electrochimia, 1986, 410 p.**
CRISTOFOR I. SIMIONESCU, VALERIA GORDUZA, **Implicaţii bioenergetice ale coloranţilor, 1988, 208 p.**
R. VÎLCU, M. LECA, **Termodinamica polimerilor prin cromatografie de gaze, 1987, 238 p.**
I. ZUGRĂVESCU, M. PETROVANU, **Cicloadiţii 3+2 dipolare, 1987, 446 p.**
RAUL MIHAIL, ION GROZEANU, **Estimarea secvenţială aplicată sistemelor chimice, 1986, 406 p.**
M. BREZEANU, I. PATRON, M. ANDRUH, **Combinaţii complexe polinucleare şi aplicaţiile lor, 1986, 244 p.**
A. T. BALABAN et al., **Labelled Compounds and Radiopharmaceuticals Applied in Nuclear Medicine,** coédition avec John Wiley and Sons, 1986, 742 p.
D. PURDELA, **Nomenclatura chimiei organice — IUPAC, 1986, 451 p.**
PETRU BUDRUGEAC, **Probleme de chimie, 1986, 280 p.**
T. ONCESCU, S. G. IONESCU, **Conversie fotochimică şi stocare de energie, 1985, 272 p.**
V. DRĂGUŢAN, A. T. BALABAN, M. DIMONIE, **Olefin Metathesis and Ring-Opening Polymerization of Cyclo-Olefins,** coédition avec John Wiley and Sons, 1985, 544 p.
C. LITEANU, I. RÎCĂ, **Optimizarea proceselor analitice, 1985, 360 p.**
N. PERESCU, **Chimia extracţiei cu solvenţi şi aplicaţii, 1985, 212 p.**
V. E. SAHINI, M. HILLEBRAND, **Chimie cuantică în exemple şi aplicaţii, 1984, 378 p.**
GH. MARCU, **Chimia compuşilor coordinativi, 1984, 415 p.**
E. CORDOŞ, C. MANOLIU, **Spectrometria de absorbţie şi fluorescenţa atomică, 1984, 178 p.**
C. BODEA, **Tratat de biochimie vegetală, p. II, t. V, 1984, 438 p.**
N. AŞANDEI, A. GRIGORIU, **Chimia şi structura fibrelor, 1983, 395 p.**
N. IONESCU, M. CALDARARU, **Oxidarea catalitică a olefinelor inferioare, 1983, 178 p.**
C. CAŞCAVAL, **Studiul polimerilor prin piroliză şi cromatografie de gaze, 1983 220 p.**
C. I. SIMIONESCU, F. DANES, **Originea vieţii, 1983, 110 p.**
C. BODEA, **Tratat de biochimie vegetală, p. II, t. IV, 1982, 408 p.**
I. GĂLĂŢEANU, **Procese şi metode radiochimice în energetica nucleară, 1981, 234 p.**
CR. SIMIONESCU, VALERIA GORDUZA, **Polimeri biocompatibili şi biologic activi, 1980, 479 p.**
C. GH. MACAROVICI, **Analiza chimică cantitativă anorganică, 1979, 457 p.**
I. ZUGRĂVESCU, MAGDA PETROVANU, **N-ylid chemistry,** coédition avec McGraw-Hill International Book Company U.S.A., 1977, 396 p.

ISSN 0035 – 3930

I. P. INFORMAŢIA c. 2428

44 426

Lei 40